Institute of High Current Electronics SB RAS
Tomsk Scientific Center SB RAS
National Research Tomsk Polytechnic University
Tomsk Region Administration
P.N. Lebedev Physical Institute RAS
National Research Tomsk State University
Tomsk State University of Control Systems and Radioelectronics
Tomsk State University of Architecture and Building

8th International Congress on Energy Fluxes and Radiation Effects (EFRE 2022)

Abstracts

October 2–8, 2022

Tomsk, Russia

Tomsk 2022

General Chair of the Congress

Gennady Mesyats	Russian Academy of Sciences

Co-Chairmen of the Congress

Ilya Romanchenko	Institute of High Current Electronics SB RAS
Nikolay Kolachevsky	Lebedev Physical Institute RAS
Dmitry Sednev	National research Tomsk Polytechnic University
Alexey Markov	Tomsk Scientific Center SB RAS

Congress Program Chair

Alexander Batrakov	Institute of High Current Electronics SB RAS

Local Organizing Committee

Chairman	Maxim Vorobyov	Institute of High Current Electronics SB RAS, Tomsk, Russia
Co-Chairman	Valery Shklyaev	Institute of High Current Electronics SB RAS, Tomsk, Russia
	L. Avdeeva	Institute of High Current Electronics SB RAS, Tomsk, Russia
	V. Alexeenko	Institute of High Current Electronics SB RAS, Tomsk, Russia
	E. Chudinova	Institute of High Current Electronics SB RAS, Tomsk, Russia
	S. Doroshkevich	Institute of High Current Electronics SB RAS, Tomsk, Russia
	E. Dubrovskaya	Institute of High Current Electronics SB RAS, Tomsk, Russia
	D. Genin	Institute of High Current Electronics SB RAS, Tomsk, Russia
	O. Ivanova	Tomsk Scientific Center, SB RAS, Tomsk, Russia
	P. Kiziridi	Institute of High Current Electronics SB RAS, Tomsk, Russia
	S. Kondratiev	Institute of High Current Electronics SB RAS, Tomsk, Russia
	N. Labetskaya	Institute of High Current Electronics SB RAS, Tomsk, Russia
	K. Manabaev	National Research Tomsk Polytechnic University, Tomsk, Russia
	R. Minin	Tomsk Scientific Center, SB RAS, Tomsk, Russia
	O. Nozdrina	National Research Tomsk Polytechnic University, Tomsk, Russia
	S. Onischenko	Institute of High Current Electronics SB RAS, Tomsk, Russia
	E. Petrikova	Institute of High Current Electronics SB RAS, Tomsk, Russia
	N. Prokopenko	Institute of High Current Electronics SB RAS, Tomsk, Russia
	V. Ripenko	Institute of High Current Electronics SB RAS, Tomsk, Russia
	R. Sazonov	National Research Tomsk Polytechnic University, Tomsk, Russia
	A. Schneider	Institute of High Current Electronics SB RAS, Tomsk, Russia
	V. Shin	Institute of High Current Electronics SB RAS, Tomsk, Russia
	A. Shipilova	Institute of High Current Electronics SB RAS, Tomsk, Russia
	D. Sorokin	Institute of High Current Electronics SB RAS, Tomsk, Russia
	M. Syrtanov	National Research Tomsk Polytechnic University, Tomsk, Russia
	M. Tsventoukh	P.N. Lebedev Physical Institute RAS, Moscow, Russia

Conferences

22nd International Symposium on High-Current Electronics
16th International Conference on Modification of Materials with Particle Beams and Plasma Flows
20th International Conference on Radiation Physics and Chemistry of Condensed Matter
5th International Conference on New Materials and High Technologies

---

8th International Congress on Energy Fluxes and Radiation Effects (EFRE 2022) : Abstracts. — Tomsk : TPU Publishing House, 2022. — 582 p.

This book comprises the abstracts of the reports (presentations) for the oral and poster sessions of VIII International Congress on Energy Fluxes and Radiation Effects (EFRE 2022). The Congress will combine four International Conferences regularly hosted in Tomsk: International Symposium on High-Current Electronics, International Conference on Modification of Materials with Particle Beams and Plasma Flows, International Conference on Radiation Physics and Chemistry of Condensed Matter, and International Conference on New Materials and High Technologies. It will be a good platform for researchers to discuss a wide range of scientific, engineering, and technical problems in the fields of pulsed power technologies; ion and electron beams; high power microwaves; plasma and particle beam sources; modification of material properties; pulsed power applications in chemistry, biology, and medicine; physical and chemical nonlinear processes excited in inorganic dielectrics by particle and photon beams; physical principles of radiation-related and additive technologies; self-propagating high-temperature synthesis; and combustion waves in heterogeneous systems, synchrotron and neutron research.

ISBN 978-5-4387-1098-1

CONTENTS

Уважаемые участники конгресса EFRE-2022!

Несмотря на все сложности обстановки наш традиционный VIII Конгресс состоится в Томске и перед Вами книга абстрактов, включающая все тематики в том числе и новые.

Встреча учёных после длительных постковидных ограничений обещает быть насыщенной новыми идеями и разработками, которые продвинут наше перспективное научное направление «Энергетические потоки и радиационные воздействия».

Четыре мероприятия, которые будут проходить в рамках EFRE-2022: симпозиум по сильноточной электронике, конференции по модификации материалов пучками заряженных частиц и потоками плазмы, конференция по радиационной физике и химии конденсированных сред и конференция по новым материалам и высоким технологиям взаимодополняют и расширяют тематику исследований и разработок в области физики, техники и технологий по мощной импульсной энергетике, пучков заряженных частиц и плазменных потоков, генерации мощных потоков рентгена, микроволн и лазерного излучения, а также взаимодействия этих потоков с веществом в различных агрегатных состояниях, что актуально для разработки принципиально новых и модернизации традиционных технологий, модификации материалов и изделий для передовых отраслей промышленности, биологии, медицины и других применений, в которых так нуждается современное общество.

Важно, что наш Конгресс позволит наладить междисциплинарные связи и цепочки т.к. все мероприятия будут проходить компактно и будет возможность выбирать те из них, которые наиболее соответствуют решаемым учёными, разработчиками и технологами задач, зачастую носящими комплексный характер.

Участие в Конгрессе значительного количества молодых учёных позволит им не только приобрести опыт в популяризации своих достижений, но и установить научные связи на долгие годы вперёд.

Желаем всем участникам Конгресса плодотворной работы и успехов на непростом пути познаний и воплощения своих идей и разработок в реальную жизнь, что чрезвычайно важно в современном мире.

Председатель 22-го Симпозиума
по сильноточной электронике, академик Н.А.Ратахин

Plenary Session

NANOSECOND DISCHARGE IN AIR IN SUBMILLIMETER GAPS IN A UNIFORM ELECTRIC FIELD*

G. A. MESYATS[1], *I.V. VASENINA*[1]

[1]*P.N. Lebedev Physical Institute of the Russian Academy of Sciences, Moscow, Russia*

A pulsed nanosecond discharge in air at atmospheric pressure in a uniform electric field in the region of 10^6 V/cm is under investigation. The cathode-anode gap length reached fractions of a millimeter, and the gas pressure was atmospheric. Under such conditions, electrons runaway (RE) during the discharge. Such a discharge is referred to as nanosecond diffuse-channel (NDC). In such discharges, the critical length of the electron avalanche x_k is much smaller than the gap length, i.e., $x_k << d$. The greatest attention is paid to the discharge at d = 0.1 mm, when the overvoltage across the gap was 15. Due to careful processing of the cathode surface, one-electron discharge initiation was achieved. The initiating electron enters the discharge gap and ionizes air molecules due to REs.

During the discharge formation time of about 10^{-9} s, plasma accumulates. Upon reaching the critical value of the plasma density of the order of $n_k=10^4$ cm^3, a glow discharge (GD) begins. It leads to redistribution of the electric field to the plasma column and the cathode layer (CL). This redistribution lasts for a short time of the order of 10^{-11} s, which is called the commutation time. This beam occurs due to a rapid increase in the plasma density during the discharge. During this time, a beam of runaway electrons is formed in the number of $5\cdot10^{10}$ pieces, which, falling on the anode, leads to the formation of an X-ray pulse. Let us assume that the reduced electric field E_T/p in the CL obeys the scaling law and depends on j/p^2, where j is the current density at the cathode and p is the gas pressure. For a rough estimate, we use the formula

$$E_T / p = 1.1\ 10^5 \left(j / p^2 \right)^{0.6} \quad (1)$$

for nitrogen. It was obtained experimentally in the study of many discharges in the GD mode. For the used gap d=0.1 mm, the discharge current is equal to i=280 A, and the cathode surface area is $S=\pi D^2/4$=0.2 cm^2, where D is the cathode surface diameter. It is difficult to accurately determine the current density j, since it is not known what part of the cathode it occupies. If it occupies the entire surface, then $E_T=10^6$ V/cm, and if it takes only 10%, then $E_T=3.4\cdot10^6$ V/cm. It is known that when the electric field on the cathode is 10^6 V/cm or more, field emission (FE) from microprotrusions on the cathode surface takes place. Under the action of the FE current, an electric explosion of these microprotrusions occurs, which initiates a transition to explosive electron emission. This leads to the formation of explosive electron emission and the formation of a cathode spot and the transition of the discharge to the arc mode.

It should be noted that in the electric discharge in air we have considered, there are two types of runaway electrons. The first one is when runaway electrons participate in the process of discharge formation. The duration of this process with one-electron initiation is ~10^{-9} s. The second type is runaway electrons in the final stage of the discharge. They appear in the form of a beam with a duration of ~10^{-11} s with the number of electrons $5\cdot10^{10}$.

*This work was supported by the Russian Science Foundation (project No. 19-79-30086).

S5-O-019701

RUNAWAY ELECTRONS IN AN AIR GAP IN THE PRESENCE OF A MAGNETIC FIELD*

Y.I. MAMONTOV[1], G.A. MESYATS[2], K.A. SHARYPOV[1], V.G. SHPAK[1], S.A. SHUNAILOV[1], M.I. YALANDIN[1,2], N.M. ZUBAREV[1,2], O.V. ZUBAREVA[1]

[1]*Institute of Electrophysics UB RAS, Ekaterinburg, Russia*
[2]*Lebedev Physical Institute RAS, Moscow, Russia*

The study of runaway electrons (RAEs) in over-voltage gas gaps is relevant because of their role in fast breakdown development and applications for impact on objects, media excitation, generation of electromagnetic radiation, etc. The main disadvantage of this source of fast electrons is the divergence of the RAE flow due to the electric field distribution in the gap and particle scattering by gas molecules. For practical use, RAEs need to be focused in the paraxial region in order to increase the current density.

It has been recently shown [1] that the RAE flow divergence can be reduced by using an axial magnetic field in the gas diode with a tubular cathode. Moreover, the generated tubular RAE flow can be essentially compressed [2] by a nonuniform magnetic field increasing along the electron trajectories. However, two problems arise, which lead to extension of the RAE current pulse and, as a consequence, to a decrease in current density. The first problem is related to braking of particles and their partial reflection by the magnetic mirror. The second problem is that tubular RAE flow consists of adjoining jets whose emission from different regions of the cathode edge is not synchronous (this is a result of the time spread in the onset of field-emission from the cathode micro-protrusions). Therefore, to shorten the RAE bunch, it is expedient to switch to a pointed cathode placed into a strong uniform axial magnetic field. It can be expected that RAEs will start almost synchronously from the tip and then propagate along the lines of the guiding magnetic field.

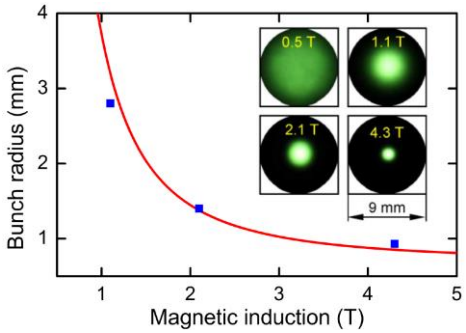

Fig.1. Dependence of the RAE bunch radius on the magnetic field (experimental data – blue squares; theory – red solid line). Insert: the corresponding glow of a luminescent screen.

In the present work, we have succeeded in applying this approach for spatiotemporal compression of the RAE flow. This made it possible for the first time to form RAE bunches of comparable radial and axial sizes of several mm. The maximal RAE current density (0.3–0.65 kA/cm^2) is effectively controlled by the magnetic field (1.1–4.3 T). The radial distribution of the RAE current density in the beam is experimentally determined, and the dependence of the RAE bunch radius on the magnitude of the applied magnetic field is found (Fig. 1). Our theoretical analysis shows that this dependence is due to two factors: the diffusion of RAEs across the magnetic field lines and a change of the character of RAE motion with a change in the Hall parameter β (the ratio of the electron gyrofrequency and the electron-molecule collision frequency). If β is relatively small, RAEs move predominantly along the electric field lines and their flow expands under conditions of an inhomogeneous electric field near the cathode tip. For large enough β, RAEs become magnetized and therefore propagate along the magnetic field lines. The results of the analysis are confirmed by numerical simulation of the RAE propagation by the Monte Carlo method.

REFERENCES

[1] G.A. Mesyats, K.A. Sharypov, V.G. Shpak et al., "Runaway electron flows in magnetized coaxial gas diodes," J. Phys.: Conf. Ser., vol. 2064, Article Number 012006, 2021.

[2] M.A. Gashkov, N.M. Zubarev, O.V. Zubareva et al., "Compression of a runaway electron flow in an air gap with a nonuniform magnetic field," JETP Lett., vol. 113, pp. 370–377, 2021.

* The work was supported in part the Russian Foundation for Basic Research under Projects 20-08-00249 and 20-08-00172.

C5-O-956402

4th GENERATION SYNCHROTRON RADIATION FACILITY SKIF: PROJECT DETAILS AND CURRENT STATUS *

V.I. BUKHTIYAROV[1], *E.B. LEVICHEV*[1,2]

[1]*Boreskov Institute of Catalysis SB RAS, Novosibirsk, Russia*
[2]*Boreskov Institute of Catalysis SB RAS, Koltsovo, Russia*

Synchrotron Radiation Facility SKIF is a new large-scale research infrastructure project currently underway in the Science City Koltsovo, 15 km apart from Novosibirsk. The 3 GeV electron storage ring designed by specialists from the Budker Institute of Nuclear Physics SB RAS will provide the record low emittance of 75 pm•rad by the date of scheduled commissioning in December, 2024.

The SRF SKIF will become a national-level multidisciplinary research and innovative center. Key directions of the scientific program to be deployed at the SRF SKIF will encompass biomedicine, green technologies in chemistry and energetics, advanced engineering materials and mechanical engineering technologies.

Presently, accelerator equipment is under production within two state contracts concluded between the Boreskov Institute of Catalysis SB RAS and the Budker Institute of Nuclear Physics SB RAS. The Titan2 Holding is responsible for the large-scale construction works on-site. The total budget of the project exceeds 47 billion Russian rubles.

The aerial view of the construction site as of summer 2022 is shown in Fig. 1. More than 30 specialized buildings with advanced engineering infrastructure will appear within several months.

Fig.1. Construction site of the Synchrotron Radiation Facility SKIF (as of summer 2022).

The present contribution gives a concise survey on technological parameters of the project and its potential scientific impact in the future. More information on the SRF SKIF project may be found elsewhere [1].

REFERENCES

[1] Tekhnologicheskaya infrastruktura Sibirskogo Koltsevogo Istochnika Fotonov SKIF, K.I. Shefer Ed., Novosibirsk: Boreskov Institute of Catalysis, 2022, 999 pages, ISBN 978-5-906376-40-4. Electronic resource https:// disk.yandex.ru/d/1SBhHph2rgbeBg [Technological Infrastructure of SRF SKIF, In russian].

* The work was supported by the Russian Ministry of Science and Higher Education of the Russian Federation within the Budget project for the Synchrotron Radiation Facility SKIF, Boreskov Institute of Catalysis SB RAS.

C5-O-047601

IN SITU INVESTIGATION Y-AL-O THERMAL BARRIER COATING *

E.L. VARDANYAN[1], A.YU. NAZAROV[1], K.N. RAMAZANOV[1], A.A. NIKOLAEV[1], A.N. SHMAKOV[2]

[1]Ufa state aviation technical university, Ufa, Russia
[2] Institute of High Current Electronics SB RAS, Tomsk, Russia

To increase the power and efficiency of gas turbine engines (GTE), it is necessary to increase the temperature of the gases in front of the GTE turbine. In this regard, it is necessary to protect the parts of the gas turbine engine from exposure to high temperatures and gas flow. To date, to protect GTE blades, multilayer coatings are traditionally used, which consist of an inner layer based on MeCrAlY or NiAlPt system and an outer thermal barrier layer based on ZrO2-Y2O3 [1, 2, 3]. But this coatings can't protect aviation parts at 1500 C. Therefore, investigation to create new thermal barrier coatings for higher temperatures.

The thermal barrier coating of the Y-Al-O system deposited by arc-pvd was studied by using synchrotron radiation. Coating based on the Y-Al-O system was deposited on molybdenum substrates from two single-component aluminum and yttrium cathodes. The phase stability of the coating when the sample was heated to 1500°C in vacuum was studied by using synchrotron radiation. The coating after deposition has an amorphous structure. This structure saved up to 1000°C, crystallization occurs when the temperature reaches 1160–1170 °C. Other phase transformations in the coating during heating wasn't observed . The qualitative phase composition of the coating was determined, and the microstresses in the coating were evaluated. The results demonstrate the absence of microstresses in the coating. Based on the results of the research, a fundamentally new method for the synthesis of thermal barrier coatings based on the Y-Al-O system was developed, in which coating consists of oxides YAlO3 (mainly), Y2O3 and YAl2 intermetallic compound. Obtained results may be applying for develop new Thermal Barrier coatings for perspective aviation engine.

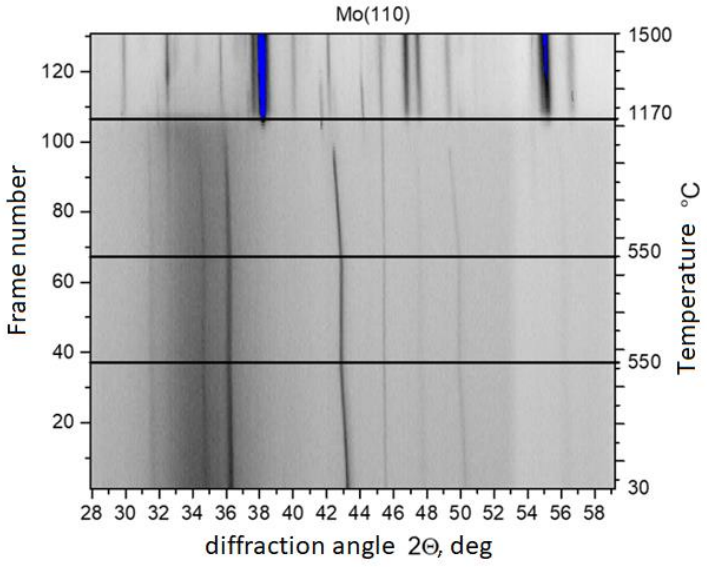

Fig.1. X-ray diffraction pattern of the YAlO sample in the representation of the projection of the intensity on the plane "diffraction angle-temperature".

REFERENCES

[1] *Riallant F.*, Cormier J., Longuet A., “High-Temperature Creep Degradation of the AM1/NiAlPt/EBPVD YSZ System” Metall Mater Trans A – 2014. V. 45. C. 351–360.

[2] *Kunal M.*, Luis N., Calvin M.D., “Thermal Barrier Coatings Overview: Design, Manufacturing, and Applications in High-Temperature Industries” Industrial & Engineering Chemistry Research – 2021. V.60. №.17. C. 6061-6077.

[3] *Zhang, C.*, Lv, P., Xia, H., Yang, Z., Konovalov, S., “The microstructure and properties of nanostructured Cr-Al alloying layer fabricated by high-current pulsed electron beam” Vacuum – 2019. V. 167. C. 263-270. *Alymov, M.I.*, Stolin, A.M., Bazhin, P.M. // Industrial Laboratory. Materials Diagnostics. - 2022, V. 88. №. 2. C. 40–48.

* This work was carried out with the financial support of Russian Federation represented by Ministry of Science and Higher Education (project No. 075-15-2021-1348).

C5-O-956101

COHERENT X-RAY OPTICS AND MICROSCOPY FOR ADVANCED MATERIAL RESEARCH APPLICATIONS

A. SNIGIREV

Immanuel Kant Baltic Federal University, 238300 Kaliningrad, Russia

With appearance of new Megascience facilities - fourth generation X-ray sources (synchrotrons and free-electron lasers) materials research will strongly benefit from the increased spectral brightness, small source size and divergence. New ultimate parameters of the beam provided by the diffraction-limited sources – new synchrotrons with the reduced horizontal emittance will open up unique opportunities to build up a new concept of X-ray diagnostics including diffraction, spectroscopy and microscopy techniques based on the beam transport and conditioning systems using in-line refractive optics [1]. The refractive optics can provide the various beam conditioning functions in the energy range from 3 to 200 keV: condensers, micro-radian collimators, low-band pass filters, high harmonics rejecters [2], and beam-shaping elements [3-4]. The implementation of the lens-based beam transport concept will significantly simplify the layout of new beamlines, easily expanding their microscopy capabilities in different fields including biomedical science [5-6] and material research under extreme conditions [7-10].

The versatile beam conditioning properties of refractive optics enable to develop and implement novel X-ray coherence-related techniques including Fourier optics [11-13] and interferometry [14-18]. Further development of phase contrast bright [19-24] and dark field microscopy [25] will benefit by recently proposed light and ultracompact objectives based on polymer and diamond microlenses made by 3D printing [26-27] and FIB technology [28].

All mentioned achievements and applications based on refractive optics are becoming especially relevant for the new SKIF synchrotron in Novosibirsk.

REFERENCES

[1] A. Snigirev, V. Kohn, I. Snigireva, B. Lengeler, *Nature*, **384,** 49, 1996.
[2] M. Polikarpov, I. Snigireva, A. Snigirev, *J. Synchrotron Rad.*, **21,** 484, 2014.
[3] D. Zverev, A. Barannikov, I. Snigireva, A. Snigirev, *Opt. Express*, **25**, 28469, 2017.
[4] D. Zverev, et al., *Optics Express*, **29**, 35038, 2021.
[5] M. W. Bowler, D. Nurizzo, R. Barrett, et al., *J. Synchrotron Rad.*, **22,** 1540, 2015.
[6] M. Polikarpov, et al., *Microsc. Microanal.* **24** (Suppl. 2), 384, 2018.
[7] N. Dubrovinskaia , L. Dubrovinsky, N. Solopova, et al., *Sci. Adv.*, **2,** e1600341, 2016.
[8] F. Wilhelm, G. Garbarino, J. Jacobs, et al., *High Pressure Research*, **36,** 445, 2016.
[9] A. Snigirev *et al*., *Microsc. Microanal.* **24** (Suppl. 2), 236, 2018).
[10] T. Fedotenko, et al., *Rev. Sci. Instrum*, **90**, 104501, 2019.
[11] P. Ershov, S. Kuznetsov, I. Snigireva et al., *Appl. Cryst*., **46, 1475,** 2013.
[12] D. V. Byelov, J.-M. Meijer, I. Snigireva et al., *RSC Advances*, **3**, 2013)
[13] A. Chumakov, et al., *J. Appl. Cryst*., **52**, 1095, 2019.
[14] A. Snigirev, I. Snigireva, M. Lyubomirskiy, et al., *Opt. express*, **22**, 25842, 2014.
[15] M. Lyubomirskiy, I. Snigireva, A. Snigirev, *Optics express*, **24**, 13679, 2016.
[16] M. Lyubomirskiy, I. Snigireva, V. Kohn, et al, *J. Synchrotron Rad*., **23**, 1104, 2016.
[17] S. Lyatun, et al., *J. Synchrotron Rad*., **26**, 1572, 2019.
[18] O. Konovalov, et al., *J. Synchrotron Rad.*, **26**, 1572, 2019.
[19] D. Zverev et al., *Microsc. Microanal*. **24** (Suppl. 2), 162, 2018.
[20] D. Zverev, et al., *Optics Express*, **28** (15), 21856, 2020.
[21] K. V. Falch, C. Detlefs, M. Di Michiel et al., *Appl. Phys. Lett.*, **109,** 054103, 2016.
[22] K. V. Falch, D. Casari, M. Di Michiel et al., *J. Mater. Sci*., **52,** 3437, 2017.
[23] K. V. Falch, M. Lyubomirskiy, D. Casari, et al., *Ultramicroscopy*, **184,** 267, 2018.
[24] I. Snigireva et al., *Microsc. Microanal.* **24** (Suppl. 2), 552, 2018.
[25] H. Simons, A. King, W. Ludwig et al., *Nature Communications*, **6**, 6098, 2015.
[26] A. K. Petrov, V. O. Bessonov, K. A. Abrashitova et al., *Optics Express*, **25**, 14173, 2017.
[27] A. Barannikov, et al., *J. Synchrotron Rad.*, **26** (2019) 714.
[28] P. Medvedskaya, et al., *Optics Express*, **28** (04), 4773, 2020

C3-O-953501

FOR THE 30TH ANNIVERSARY OF FERRY VATT

Ya. O. ZHELONKIN

Ferry Vatt LLC, Kazan, Russian Federation

The company's history starts in 1991 when a group of initiative employees of VAKUUMMASH Research Institute created Kvazar Company, later renamed as MP VATT [VATT small enterprise], and after that as FERRY VATT.

From the first days of operation, the company had orders for manufacturing various protective and decorative coating sputtering systems. Since 1993, the company has opened its coating application floor, which involved several round-the-clock operation systems. To date, our team has finished more than 150 unique projects and accumulated a wealth of experience in the development and manufacture of various vacuum equipment formalized in the form of 6 principal directions:

- Vacuum and plasma thin film and coating deposition technologies (PVD, CVD, PECVD, ALD, etc.);
- Miscellaneous material low-pressure radio-frequency (RF) plasma processing technologies (CCP, ICP);
- Composite material forming, and resin and lacquer impregnation vacuum equipment;
- Climate testing, space simulation and electric propulsion engine (EPE) testing systems;
- Miscellaneous vacuum furnaces;
- Special industrial and laboratory vacuum and plasma equipment (zone melting equipment, including single crystal zone melting equipment, vacuum melting systems).

Over the years, a hand-in-glove consolidated team has been created, ready to solve any tasks, including non-standard tasks. Our employees are graduates of the leading Russian vacuum and plasma technology departments of Kazan National Research Technological University and Bauman Moscow State Technical University. The highest skills of our team are confirmed by numerous scientific articles, diplomas and awards, as well as the choice of our Customers - state corporations, universities, research centers and manufacturing companies. The company is a regular participant and frequent winner of the International Exhibition of Vacuum Equipment VacuumTechExpo. The company is also experienced in dealing with foreign partners and customers – FERRY VATT systems are operated in 12 countries: Japan, China, Switzerland, Spain, Kuwait, Syria, Ukraine, Moldova, Belarus, Uzbekistan and Kazakhstan. The company's turnaround is cyclical, starting from the idea of implementation and design development to in-house manufacturing. FERRY VATT is proud of its past and looks forward to the future with confidence.

REFERENCES

[1] [1] Zhelonkin Ya O, Biktashev A A, Salikeev S I, Sungatullin I A and Zhelonkin O V 2019 Modern engineering tools for the development of new samples of vacuum process equipment // IOP Conf. Series: Journal of Physics: Conf. Series 1313 01206, doi:10.1088/

[2] [2] Glinkin V A, Biktashev A A and Murtazin R N 2014 Ustanovka dlya naneseniya prozrachnykh plenok oksida indiya magnetronnym metodom [Magnetron sputtering transparent indium oxide film application system] // Vestnik Kazanskogo tekhnologicheskogo universiteta [Bulletin of Kazan Technological University]. Vol. 17 No. 21. pp. 269-273.

[3] [3] Glinkin V A, Biktashev A A and Murtazin R N 2014 Vakuumnaya ustanovka dlya naneseniya pokrytiy metodom atomno-posloynogo osazhdeniya [Vacuum atomic layer deposition coating system]//Vestnik Kazanskogo tekhnologicheskogo universiteta [Bulletin of Kazan Technological University]. Vol. 17-No. 19. pp. 276-9.

[4] [4] Biktashev A A, Glinkin V A and Zhelonkin O V 2012 Promyshlennyye i issledovatel'skiye ustanovki dlya naneseniya nanostrukturnykh i nanorazmernykh pokrytiy [Industrial and research nanostructured and nanoscale coating systems]//Trudy seminara «Elektrovakuumnaya tekhnika i tekhnologiya» [Proceedings of the seminar "Electrovacuum technique and technology"]. Moscow: Moscow Power Engineering Institute of Bauman Moscow State Technical University, Pp. 157-161.

[5] [5] Biktashev A A. and Glinkin V A 2009 Novyye rossiyskiye vakuumnyye ustanovki dlya naneseniya tverdykh pokrytiy serii VATT [New Russian VATT-series vacuum hard coating systems] // Materialy IV mezhdunarodnoy nauchno-tekhnicheskoy konferentsii «Vakuumnaya tekhnika, materialy i tekhnologii» [Proceedings of the IV International Science and Technology Conference. "Vacuum technology, materials and technologies"]. Moscow: OMR. PRINT, pp. 50-56.

[6] [6] Biktashev A A, Zhelonkin O V, Glinkin V A and Lyapin A P 2006 Novoye pokoleniye vakuumnykh napylitel'nykh ustanovok ZAO "Ferry Vatt" [A new generation of Ferry Vatt vacuum sputtering systems] //Sbornik dokladov 7-y Mezhdunarodnoy konferentsii "Vakuumnyye nanotekhnologii i oborudovaniye" [Book of abstracts of the 7th International conference "Vacuum nanotechnologies and equipment"] Kharkiv: NSC KIPT, Kontrast Publishing House,

[7] [7] Biktashev A A, Zhelonkin O V, Burmistrov A V and Glinkin V A 2001 Oborudovaniye dlya naneseniya razlichnykh funktsional'nykh pokrytiy na steklo [Various functional glass coatings equipment] // Sbornik dokladov 4-go Mezhdunarodnogo simpoziuma "Vakuumnyye tekhnologii i oborudovaniye" [Book of theses of the 4th International Symposium "Vacuum Technologies and Equipment"]. Kharkiv: Kontrast Publishing House, 2001. – Pp. 337-338.

N1-O-036402

NEW PHYSICAL PHENOMENAS BEHIND SHS

A.A. GROMOV[1,2], *R.V. MININ*[3], *N. I. RADISHEVSKAYA*[3]

[1]*Moscow Polytechnic University, Moscow, Russia*
[2]*NUST MISiS, Moscow, Russia*
[3]*Tomsk Scientific Center SB RAS, Tomsk, Russia*

The problems of new physical effects appearance accompanied chemical combustion processes (SHS and analogues) were discussed. Those are soft X-ray irradiation, non-thermal routes of energy dissipation, and conditions of quasi-adiabatic combustion [1].

In the previous studies of Dr. A.I. Kirdyashkin's group [2, 3] and ours [4] it is shown that by thermites combustion, and especially for high-energy / high enthalpy ones, the local energy release could be higher than the theoretical ones assuming only chemical interaction. Calcium in noticeable concentrations was found in the solid combustion residues of Al-Fe_2O_3 thermites.

It has been found that during the synthesis of $MgAl_2O_4$ spinel by the SHS method in the (MgO-Al_2O_3-$Mg(NO_3)_2$ $6H_2O$)-Al system with boron additives (1-4 wt. %), diamond phase is formed in the synthesis products. The composition and structure of the final reagents were confirmed by XRD, SEM, equipped with an EDAX local X-ray microanalysis system. IR spectroscopic analysis confirmed the formation of carbon, which has a diamond-like lattice of lonsdaleite with aggregated nitrogen defects similar to the lattice of detonation diamonds. The emission spectrum of the radiation of the SHS process, obtained using a high-resolution spectrometer, showed that the composition of the evolved gases includes mainly hydrogen. Low-intensity lines of Al and O with various degrees of ionization and He are observed. It is shown that under certain conditions low-energy nuclear reactions (boron-proton reaction) occured in the high-speed SHS processes in the combustion wave. Due to the chemical inertness of $MgAl_2O_4$ to carbon at high temperatures, carbon formed during the boron-proton reaction is retained in the pores and intergranular space of the spinel. Based on the obtained experimental data, the most probable mechanism of carbon formation in the synthesis products was proposed [5].

REFERENCES

[1] S.B. Krivit and H.L. Jay, Nuclear energy encyclopedia: science, technology, and applications, vol. 5. John Wiley & Sons, 2011.

[2] A.I. Kirdyashkin, V.G. Salamatov, Yu.M. Maksimov, R.M. Gabbasov, É.A. Sosnin, V.F. Tarasenko, "X-ray radiation in self-propagating high-temperature synthesis processes", Combust. Explos. Shock Waves, vol. 44, no. 6, pp. 729-731, 2008.

[3] I.P. Borovinskaya, A.A. Gromov, E.A. Levashov, Yu.M. Maksimov, A.S. Mukasyan, A.S. and Rogachev, Concise Encyclopedia of Self-Propagating High-Temperature Synthesis. History, Theory, Technology, and Products, Elsevier Inc., 2017.

[4] A.A. Gromov, A.M. Gromov, E.M. Popenko, A.V. Sergienko, O.G. Sabinskaya, B. Raab, U. Taipel, "Formation of calcium in the products of iron oxide–aluminum thermite combustion in air", Russ. J. Phys. Chem., vol. 90, no. 9, pp. 2104–2106, 2016.

[5] N.I. Radishevskaya, O.K. Lepakova, A.Yu. Nazarova, O.V. Lvov, V.D. Kitler, R.M. Gabasov, R.V. Minin, "Characteristics of phase formation during combustion of the MgO-Al2O3-Mg(NO3)2·6H2O-Al-B system", Ceram. Int., [in press] 2022. doi.org/10.1016/j.ceramint.2022.01.279.

22nd International Symposium on High-Current Electronics

Chair	Nikolay RATAKHIN	Institute of High Current Electronics SB RAS, Tomsk, Russia
Co-Chair	Gennady REMNEV	National Research Tomsk Polytechnic University, Tomsk, Russia
Program Chair	Nikolay RATAKHIN	Institute of High Current Electronics SB RAS, Tomsk, Russia
Program Co-Chair	Gennady REMNEV	National Research Tomsk Polytechnic University, Tomsk, Russia

Program Committee

Efim OKS	Institute of High Current Electronics SB RAS, Tomsk, Russia
Alexander SHISHLOV	Institute of High Current Electronics SB RAS, Tomsk, Russia
Naum GINZBURG	Institute of Applied Physics RAS, Nizhny Novgorod, Russia
Gennady REMNEV	Institute of High-Technology Physics, TPU, Tomsk, Russia
Victor TARASENKO	Institute of High Current Electronics SB RAS, Tomsk, Russia
Vitaly ASTRELIN	Budker Institute of Nuclear Physics, Novosibirsk, Russia

International Advisory Committee

Stanislav CHAYKOVSKY	Institute of Electrophysics UB RAS, Ekaterinburg, Russia
Vasily GLUKHIKH	D.V. Efremov Scientific Research Institute of Electrophysical Apparatus, St. Petersburg, Russia
Evgenij GRABOVSKI	Troitsk Institute for Innovation and Fusion Research (TRINITI), Russia
Alexander KIM	Institute of High Current Electronics SB RAS, Tomsk, Russia
Francis LASSALLE	Centre d'Etudes de Gramat, Gramat, France
Alexander LITVAK	Institute of Applied Physics RAS, Nizhny Novgorod, Russia
Pavel LOGATCHOV	Institute of Nuclear Physics, Novosibirsk, Russia
Efim OKS	Institute of High Current Electronics SB RAS, Tomsk, Russia
Mikhail PETELIN	Institute of Applied Physics RAS, Nizhniy Novgorod, Russia
Nikolai RATAKHIN	Institute of High Current Electronics SB RAS, Tomsk, Russia
Vladislav ROSTOV	Institute of High Current Electronics SB RAS, Tomsk, Russia
Sergey RUKIN	Institute of Electrophysics UB RAS, Ekaterinburg, Russia
Marek SADOWSKI	Soltan Institute for Nuclear Studies, Warsaw, Poland
Victor SELEMIR	All-Russian Research Institute of Experimental Physics, FSUE RFNC – VNIIEF, Sarov, Russia
Edl SCHAMILOGLU	University of New Mexico, Albuquerque, USA
Valentin SMIRNOV	National Research Institute "Kurchatov Institute", Moscow, Russia
Valery SHPAK	Institute of Electrophysics UB RAS, Ekaterinburg, Russia
Victor TARASENKO	Institute of High Current Electronics SB RAS, Tomsk, Russia
Vasily USHAKOV	National Research Tomsk Polytechnic University, Tomsk, Russia
Yuriy USOV	National Research Tomsk Polytechnic University, Institute of Nuclear Physics, Tomsk, Russia
Mikhail YALANDIN	Institute of Electrophysics UB RAS, Ekaterinburg,

Conference topics

S1 Intense electron and ion beams
S2 Pinches, plasma focus and capillary discharge
S3 High power microwaves
S4 Pulsed power technology and applications
S5 Discharges with runaway electrons
S6 Numerical simulation in high current electronics

S1-O-000602

STABILIZATION OF THE BEAM CURRENT PULSE IN ELECTRON SOURCES WITH GRID PLASMA CATHODES*

M.S. VOROBYOV, N.N. KOVAL, P.V. MOSKVIN, V.I. SHIN, V.N. DEVYATKOV

Institute of High Current Electronics SB RAS, Tomsk, Russia

In electron sources with grid plasma emitters (GPE) and a plasma anode, the current in the accelerating gap I_0 is determined by several components [1–5] and can be written as:

$$I_0=\alpha\cdot I_d + I_{i2}\cdot[1+(1-\Gamma)\cdot\gamma_2 + \Gamma\cdot\gamma_1]$$

where $\alpha=I_{em}/I_d$ is the coefficient of electron extraction from the plasma emitter, equal to the ratio of the emission current I_{em} to the discharge current I_d; I_{i2} is the current of accelerated ions from the anode plasma; γ_2 is the coefficient of ion-electron emission from the metal during bombardment with accelerated ions of the emission electrode; γ_1 is the coefficient of ion-electron emission from the emission plasma due to ion-electronic processes in the plasma emitter; Γ is the effective geometric transparency of the emission electrode, which makes it possible to take into account the flow of ions that have passed through the grid of the emission electrode into the plasma emitter. In this case, the contribution of each term can be different depending on the specific type of electron source, the parameters of the generated electron beam, the geometry of the electrodes, their material, operating pressure, etc.

This work is devoted to methods for increasing the electrical strength of a high-voltage accelerating gap in electron sources with a GPE. First of all, the paper highlights the issues of stable generation of an electron beam under conditions of an uncontrolled increase in the current in the accelerating gap due to the ion component I_{i2}. Several methods have been proposed to reduce such instability, both by eliminating the positive feedback associated with an uncontrolled increase in the arc discharge current during its pulse, and by implementing several methods for introducing negative feedback (NFB) into the total current in the accelerating gap, which make it possible to level the factors, destabilizing the operation of electron sources on the example of a source with a GPE based on a low pressure arc. The use of any of the proposed methods for introducing beam current stabilization made it possible not only to increase the stability of the operation of several electron sources with GPE, but also to ensure greater repeatability and controllability of pulses, as well as to increase the integrated energy of the generated electron beams.

REFERENCES

[1] E. Oks. Plasma Cathode Electron Sources: Physics, Technology, Applications. WILEY-VCH. (2006). 171 p.

[2] S.P. Bugaev, Yu.E. Kreindel, P.M. Shcanin // Large-Cross-Section Electron Beams. – Moscow, Energoatomizdat, 1984 (in Russian)

[3] Vorobyov M.S., Moskvin P.V., Shin V.I., Koval N.N., Ashurova K.T., Doroshkevich S. Yu, Devyatkov V.N., Torba M.S., Levanisov V.A. Dynamic Power Control of a Submillisecond Pulsed Megawatt Electron Beam in a Source with a Plasma Cathode. Technical Physics Letters, 2021. DOI: 10.1134/S1063785021050291

[4] S.V. Grigoryev, V.T. Astrelin, V.N. Devjatkov, I.V. Kandaurov, N.N. Koval, A.V. Kozyrev, P.V. Moskvin, A.D. Teresov. “Generation of submillisecond electron beam in the diode with the grid plasma cathode and the plasma anode generated by the asymmetrical reflective discharge”. Proc. of 16th international symposium on high current electronics, 2010, PP. 19-22.

[5] N. N. Koval, V. N. Devyatkov, and M. S. Vorobyev. “Electron sources with plasma grid emitters: progress and prospects”, Russian Physics Journal, 2021, Vol. 63, No. 10, pp.1651-1660. DOI 10.1007/s11182-021-02219-3

* This work was supported by the Russian Science Foundation under grant No. 20-79-10015

S1-O-006402

OPERATION FEATURES AND EMISSION CHARACTERISTICS OF A CONSTRICTED ARC DISCHARGE FORMING EMISSION PLASMA IN A FOREVACUUM PLASMA-CATHODE SOURCE OF A PULSED ELECTRON BEAM*

A.V. KAZAKOV[1]

[1]*Tomsk State University of Control Systems and Radioelectronics, Tomsk, Russia*

A cathodic arc (an arc discharge with cathode spots) is rather often used to generate emission plasma in pulsed plasma-cathode electron beam sources [1, 2]. The cathodic arc provides high current and long pulse duration of the discharge current and accordingly of the electron beam current. On the other hand, the cathodic arc has some disadvantages caused by the chaotic movement and instabilities of cathode spots, and by formation of vapors and microdroplets of the cathode material during cathode spot operation. These disadvantages affect the characteristics and operation parameters of the plasma-cathode electron sources (e.g., it leads to decrease of electric strength of an accelerating gap). A constricted arc discharge is used to eliminate the disadvantages of the cathodic arc in the sources generating electron beams in the conventional gas pressure range of 10^{-4}–10^{-1} Pa [1, 2]. The forevacuum plasma-cathode electron sources, generating electron beams at higher pressures, operate in the isobaric mode, i.e., the pressures in the vacuum chamber and in the source are the same. Therefore, there is practically no pressure difference between the cathode and anode regions of the constricted arc discharge. This leads to specific features of the formation of the emission plasma by the constricted arc discharge in the forevacuum plasma-cathode electron source [3].

The aim of this work was to research operation features and emission characteristics of a constricted arc discharge forming emission plasma in a forevacuum plasma-cathode source that generates a pulsed electron beam at pressure of 3–20 Pa. In case of helium as working gas, the use of a metallic intermediate electrode with a constricting channel has not ensured stable operation of the constricted arc discharge with current more than 4 A and pulse duration longer than 15–20 μs due to the transition to the cascade operation mode. The cascade mode is discharge operation with cathode spots on the intermediate electrode, i.e., discharge consists of two serial cathodic arcs. The use of the intermediate electrode made of high-temperature ceramic has provided a rather stable current flow through the constricting channel. However, short spikes in the burning voltage of the constricted arc during a pulse have been observed. The amplitude of these spikes could reach several hundred volts. Voltage spikes in the discharge voltage are due to voltage fluctuations on the electric double layer near the constricting channel. Apparently, in case of the metallic intermediate electrode, these voltage spikes lead to an arc transition to the cascade operation mode. The ceramic intermediate electrode has also provided to increase a little maximum current and pulse duration of the constricted arc in case of using argon and nitrogen as working gases. Processes, occurring during the generation of the electron beam in the forevacuum pressure range, influence significantly on the constricted arc discharge. The maximum current and pulse duration of the constricted arc have increased in case of generation of the electron beam. An increase in these maximum parameters is provided by the back-streaming ion flow from the beam-produced plasma. Back-streaming ions penetrate into the discharge system of the plasma-cathode source through a mesh emission electrode and change the conditions for discharge operation. In particular, under the conditions of electron beam generation the probability of the transition of the constricted arc to the cascade operation mode has decreased. It was also found that length of an accelerating gap affects the maximum discharge parameters and the emission characteristics of the constricted arc. The efficiency of electron emission from arc plasma depends nonmonotonically on the length of the accelerating gap. The pulsed electron beam with energy up to 8 keV and current up to tens of amperes generated by the forevacuum plasma-cathode electron source based on the constricted arc has been obtained.

REFERENCES

[1] N.N. Koval, E.M. Oks, P.M. Schanin, Y.E. Kreindeland, and N.V. Gavrilov, “Broad beam electron sources with plasma cathodes,” Nucl. Instrum. Methods Phys. Res. A, Accel. Spectrom. Detect. Assoc. Equip., vol. 321, no. 3, pp. 417–428, October 1992,

[2] E. Oks, Plasma Cathode Electron Sources: Physics, Technology, Applications. Berlin, Germany: Wiley, 2006.

[3] A.V. Kazakov, A.V. Medovnik, E.M. Oks, and N.A. Panchenko, “Parameters and characteristics of a pulsed constricted arc discharge operating in a forevacuum-pressure plasma-cathode electron beam source,” Vacuum, vol. 186, Art. no. 110071, April 2021.

* The work was supported by the Russian Foundation for Basic Research (RFBR) under the Grant No. 20-08-00123.

S1-O-009601

DEVICE FOR ESTIMATION OF CURRENT AND ENERGY DENSITY DISTRIBUTION IN THE CROSS SECTION OF A PULSED SUBMICROSECOND ELECTRON BEAM *

M.A. SEREBRENNIKOV[1], *A.V. POLOSKOV*[1], *I.S. EGOROV*[1]

[1]*Tomsk Polytechnic University, Tomsk, Russia*

The research and practical application of electron beams [1–3] requires the measurement and control of the electron beam parameters in the area of its use. A sectioned calorimeter combined with a detector of the total electron beam current was developed for estimation of the charge and energy density distribution in the beam cross section.

The paper presents the features of the development, test results and description of the sectioned calorimeter modification, which collector is also the collector of the integral Faraday cup. The design of the device, its diagnostic and software equipment [4] make it possible to estimate the average kinetic energy of beam electrons in one measurement procedure.

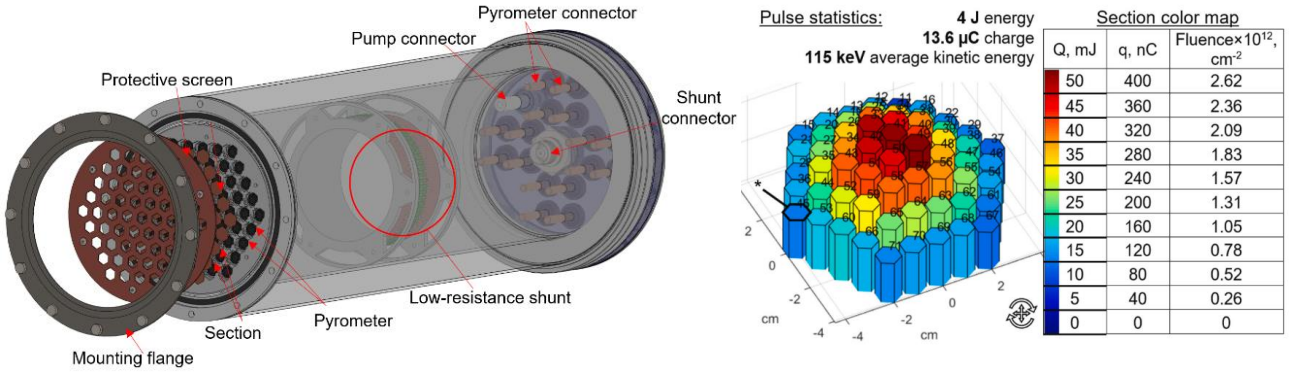

Fig.1. External view of the developed device without conductors (a) and measurement example of distribution of beam energy Q, charge q, and fluence across the calorimeter's collector (b) [5].

The calorimeter consists of a collector with isolated sections and an array of non-contact thermal sensors (pyrometers). The developed software controls the array of pyrometers and calculates the energy released in each section of the collector. The current detector monitors the total electron beam current through the electrical connection of each section to a low resistance shunt. The signal is detected by an oscilloscope to calculate the charge. Thus, the charge distribution is estimated in proportion to the energy distribution for a monoenergetic electron beam.

The set of the calorimeter characteristics makes it possible to measure the energy distribution in the cross section of pulsed electron beams with an electron kinetic energy of up to 700 keV, an energy density of up to 3.6 J/cm^2, and a total beam energy of up to 50 J/pulse. The design of the device allows measurements under various vacuum conditions: discrete with a separating membrane and with joint pumping; as well as under various beam transportation conditions: in gases and in vacuum (up to 10^{-5} Torr).

REFERENCES

[1] S. Korenev, The pulsed electron accelerator for applications, in: Dig. Tech. Pap. PPC-2003. 14th IEEE Int. Pulsed Power Conf. (IEEE Cat. No.03CH37472), IEEE, 2004: pp. 841–844. https://doi.org/10.1109/PPC.2003.1277940.

[2] I. Egorov, M. Serebrennikov, Y. Isakova, A. Poloskov, Sectioned calorimeter for quick diagnostic of the electron beam energy distribution, Nucl. Instruments Methods Phys. Res. A. 875 (2017) 132–136. https://doi.org/10.1016/j.nima.2017.09.002.

[3] I. Egorov, A. Poloskov, M. Serebrennikov, A. Isemberlinova, Research of Energy Density for Pulsed Electron Beam of Wide Electron Kinetic Energy Spectrum, Proc. - 2018 20th Int. Symp. High-Current Electron. ISHCE 2018. (2018) 27–30. https://doi.org/10.1109/ISHCE.2018.8521202.

[4] E. V. Adamov, M.A. Serebrennikov, I.S. Egorov, A.V. Poloskov, Registration, storage and conversion of readings from non-contact temperature sensors of a sectioned calorimeter for measuring parameters of a pulsed electron beam (in Russian), 2019665350, 2019.

[5] M. Serebrennikov, E. Adamov, A. Poloskov, X. Yu, I. Egorov, A calorimetric system for charge and kinetic energy characterizations of pulsed electron beams, Radiat. Meas. 143 (2021) 106569. https://doi.org/10.1016/j.radmeas.2021.106569.

* The authors are grateful to National Research Tomsk Polytechnic University (TPU, Russia) for technical support in a case of TPU development program. The work was conducted within the framework of the state assignment in the field of scientific activity: No. FSWW-2020-0008.

S1-O-016501

HIGH-CURRENT ELECTRON GUN WITH RADIALLY CONVERGING BEAM[i]

G.E. OZUR, P.P. KIZIRIDI, V.I. PETROV

Institute of High Current Electronics SB RAS, Tomsk, Russia

Low-energy (10–30 keV), high-current (up to 25 kA) electron beams (LHEB) are widely used for surface treatment of materials for several decades [1]. As a rule, such beams are produced in the guns with plasma anode and explosive-emission cathode. High energy density (up to 15 J/cm^2) and short pulse duration (2–4 μs) allow one to release beam energy in a thin (sub-micron or micron in thickness) surface layer providing its melting and even partial evaporation. Such effects provide the development of different promising technologies including surface alloying of sub-micron or micron range in thickness. Due to this, our LHEB-sources found wide applications both in physical experiment and in practice [2].

The present LHEB sources have a planar-axial geometry of electron gun and produce cylindrical beams transported along the guide magnetic field lines [1]. Plasma anode in such guns is formed with the use of high-current electron discharge in the space between the explosive-emission cathode and collector. At the same time, there are many tasks on irradiation of longitudinal cylindrical parts and it is better to use radially converging beams for these purposes [3]. For example, formation of protective coatings on the nuclear fuel elements made of Zr alloys or alloyed steels for prevention/deceleration from corrosion and high-temperature oxidation; increasing the lifetime of different cutting tools and dies. However, an essential defect of the «GESA» facilities described in [3] is relatively high accelerating voltage (up to 250 kV), that results in high cost of the equipment, decreases its reliability, pulse repetition rate (for «GESA» facilities it makes up 2 pulses/min). The absence of the sources of radially converging LHEB operating at voltages of tens of kV as well as good understanding of the physical processes in them determines an actuality of the proposed electron gun.

We proposed our recently developed new cathode assembly with multi-gap initiation of explosive emission by dielectric surface flashover [4] for the production of a radially converging beam (see Fig. 1). The present work is devoted to the research of electron gun with this new cathode assembly.

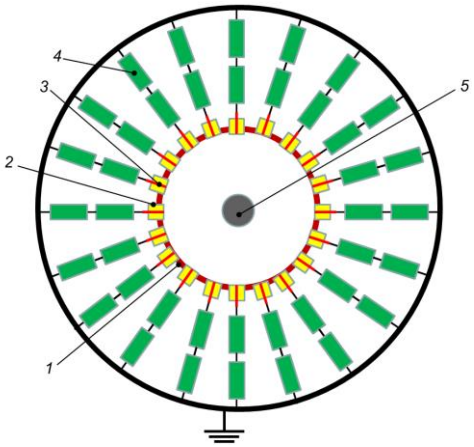

Fig. 1. Principal design of the gun with radially converging electron beam. *1* – explosive-emission cathode; *2* – ceramic tube; *3* – electrode (69 pcs); *4* – resistor TBO-2; *5* – anode (target).

REFERENCES

[1] G.E. Ozur and D.I. Proskurovsky, “Generation of Low-Energy High-Current Electron Beams in Plasma-Anode Electron Guns”, Plasma Physics Reports, vol. 44, No. 1, pp. 18–39, 2018. DOI: 10.1134/S1063780X18010130

[2] V.P. Rotshtein, D.I. Proskurovsky, G.E. Ozur, Yu.F. Ivanov. “Surface Modification of Metallic Materials with Low-Energy, High-Current Electron Beams”. – Novosibirsk (Russia): “Nauka”, 2019, 347 p. ISBN 978–5–02–038809–3

[3] V.I. Engelko, V.S. Kuznetsov, and Georg Mueller. Electron Source of Triode Type with Radial Converging Electron Flow for Irradiation of Cylindrical Targets // J. Applied Physics, 2009, vol. 105, 023305. DOI: 10.1063/1.2996286

[4] P.P. Kiziridi and G.E. Ozur. Cathode Assembly of a High-Current Electron Gun with Multichannel Initiation of Emission by Breakdown on the Surface of a Dielectric // Technical Physics Letters, 2020, Vol. 46, No. 8, pp. 775–778. DOI: 10.1134/S1063785020080088

[i] The work was supported by the Russian Science Foundation (grant No. 22-29-00070).

S1-O-021702

ANALYTICAL CROSS SECTION OF CHARGED PARTICLES SCATTERING UP TO RELATIVISTIC ENERGIES*

N. MEDVEDEV[1,2], A.E. VOLKOV[3,4,5]

[1] *Institute of Physics Czech Academy of Sciences, Prague, Czech Republic*
[2] *Institute of Plasma Physics Czech Academy of Sciences, Prague, Czech Republic*
[3] *P.N. Lebedev Physical Institute RAS, Moscow, Russia*
[4] *Joint Institute for Nuclear Research, Dubna, Russia*
[5] *NRC Kurchatov Institute, Moscow, Russia*

We derived a simple analytically solvable model for calculation of the differential and total inelastic cross sections, mean free paths, and energy losses of charged particles in solids beyond atomic approximation [1]. It is applicable from small up to relativistic incident energies (from 30-50 eV up to GeV in a case of an electron).

Within the linear response theory, the scattering cross section is defined by the complex dielectric function. We approximate this function with a set of delta-functional oscillators. The parameters of the oscillators can be obtained from the Drude-like oscillators using only optical data as an input. No ad-hoc correction terms are required. The approach enables us to avoid further approximations (such as close and distant collisions etc.) and to obtain a closed solution for the cross section.

Being analytically solvable, the model allows for very fast yet precise calculations, and thus can be efficiently implemented in any simulation tools, such as Monte Carlo models [2]. It also avoids the Bragg additivity rule of the atomic cross sections, and is well suitable for compounds. Application of the derived formulae greatly saves computational time of evaluation of cross sections with respect to the numerical integration required by other models.

We demonstrate that the derived expressions are in a very good agreement with other more complex numerical models and experimental data within a wide range of energies and targets (metals, semiconductors, insulators). For electrons and positrons, the range of applicability is from ~50 eV up to ~GeV (within the precision ~20% at the energy of ~10 GeV, and ~1% at ~MeV energies). For protons it is from ~100 keV to ~50 GeV, while for heavy ions it is from ~100 MeV to ~TeV, which covers a typical energy range of modern ion accelerators.

REFERENCES

[1] N. Medvedev, A.E. Volkov, Journal of Physics D: Applied Physics, 53 (2020) 235302; J. Phys. D: Appl. Phys. 55 (2022) 019501
[2] N. Medvedev, F. Akhmetov, R.A. Rymzhanov, R. Voronkov, A.E. Volkov, (2022) https://arxiv.org/abs/2201.08023

* AEV acknowledges support from the Russian Science Foundation (grant number №22-22-00676, https://rscf.ru/en/project/22-22-00676/).

S1-O-022701

EXCITATION OF SOLIDS UNDER THE HIGH-INTENSITY HEAVY ION BEAMS

S.A. GORBUNOV[1], *A.E. VOLKOV*[1,2,3]

[1] *P.N. Lebedev Physical Institute of the Russian Academy of Sciences, Leninskij pr., 53,119991 Moscow, Russia*
[2] *Joint Institute for Nuclear Research, Joliot-Curie 6, 141980 Dubna, Moscow Region, Russia;*
[3] *National Research Centre 'Kurchatov Institute', Kurchatov Sq. 1, 123182 Moscow, Russia;*

Designed high-intensity heavy ion accelerator facilities (e.g. HIAF, FAIR) will provide unique experimental conditions for investigation of unusual extreme matter states under intense ion beams [1, 2].

To study temporal nanometric inhomogeneities of target excitation at the initial stage of material excitation under such bunches, we developed a hybrid model, in which initial electronic excitation parameters are provided by Monte-Carlo code TREKIS [3]. This code supplies with radial distributions of the electrons concentration and their energy density up to 10fs, when the most part of ionization cascades finishes, and propagation of electrons changes from ballistic to diffusion one. We use microscopic kinetic approach [4] to describe subsequent joint electron-lattice kinetics. The dynamical structure formalism is applied to evaluate cross sections governing electron-lattice coupling [5]. Thermal diffusion approach describes spatial spreading of lattice excitation. We take Al_2O_3 for modeling, since the most part of blocks of this model was already built and well tested for this system [5].

We demonstrate spatial asymmetry of lattice relaxation caused by overlapping of excited areas as well as percolation threshold of the molten zone in the beam spot.

REFERENCES

[1] J.C.Yang, J.W.Xia, G.Q.Xiao, et al., "High Intensity heavy ion Accelerator Facility (HIAF) in China" Nucl. Instruments Methods Phys. Res. Sect. B Beam Interact. with Mater. Atoms., 317 (2013) 263

[2] T. Stöhlker, V. Bagnoud, K. Blaum, et al., "APPA at FAIR: From fundamental to applied research" Nucl. Instruments Methods Phys. Res. Sect. B Beam Interact. with Mater. Atoms., 365 (2015) 680

[3] N.A. Medvedev, R.A. Rymzhanov, A.E. Volkov, "Time-resolved electron kinetics in swift heavy ion irradiated solids" J. Phys. D. Appl. Phys. 48 (2015) 355303

[4] S.A. Gorbunov, N.A. Medvedev, P.N. Terekhin, A.E. Volkov, "The microscopic model of material excitation in swift heavy ion tracks" Phys. Status Solidi. 10 (2013) 697–700

[5] S.A. Gorbunov, N. Medvedev, R.A. Rymzhanov, A.E. Volkov, " Dependence of the kinetics of Al_2O_3 excitation in tracks of swift heavy ions on lattice temperature" Nucl. Instruments Methods Phys. Res. Sect. B Beam Interact. with Mater. Atoms. 435 (2018) 83–86

S1-O-024202

RING STRUCTURE OF ELECTRON-ION BEAMS EJECTED BY A PICOSECOND HIGH-CURRENT ELECTRON ACCELERATOR*

V.I.BARYSHNIKOV[1] and V.L.PAPERNY[2]

[1]Irkutsk State Transport University, Irkutsk, Russia
[2]Irkutsk State University, Irkutsk, Russia

The radial structure of electron-ion beams emitted by an electron accelerator with a discharge pulse of 200 ps duration, a voltage amplitude of 280 kV, and a current of about 5 kA was studied. An analysis of the shape of the beam imprints on the anode foil showed that, in addition to an intense central core several micrometers in size, the imprint contains several (3–5) concentric rings up to 150 μm in diameter. The color of the rings, which has an interference origin, was used to estimate the relative intensity of the ion tubes that form the peripheral structure of the beam.

* The work was supported by grant of the Russian Science Foundation No. 20-02-00322

S1-O-031103

MEASURING THE PARAMETERS OF EMISSION PLASMA IN ELECTRON SOURCE BASED ON ION-ELECTRON EMISSION *

S.YU. DOROSHKEVICH, V.A. LEVANISOV, I.V. LOPATIN, M.S. VOROBYOV, M.S. TORBA, S.S KOVALSKY, S.A SULAKSHIN

Institute of High Current Electronics SB RAS, 2/3 Akademichesky Ave., Tomsk, 634055, Russian Federation.

In electron sources with plasma emitters, which include sources based on ion-electron emission [1], the parameters of emission plasma affect the formation of ion-electron optics, the discharge current flow, the emission of charged particles into the accelerating gap, and, as a consequence, the electron beam generation [2]. That is why work is underway to measure the parameters of emission plasma and determine their dependence on the conditions of discharge and electron beam generation.

In this work, determination of the parameters of emission plasma was carried out in an electron source based on secondary ion-electron emission with the output of generated large cross section beam into the atmosphere [3,4]. The plasma ion emitter is formed by a self-sustained glow discharge with a hollow cathode and two thin-wire anodes. To determine the plasma parameters, we used a single cylindrical Langmuir probe with the possibility of moving inside the hollow cathode to measure the plasma concentration distribution in the region of glow discharge generation. Measurement and recording of probe bias voltage values and their corresponding current values was carried out by a specially designed automated measurement system. This measurement system captures points of the probe characteristic with a period of 20 μs, the maximum number of points stored in memory for a single measurement is 1000. To measure more points, the measurement system writes the data to the computer and repeats the measurement for 1000 more values. After measuring the required number of points, the system displays the obtained probe characteristic on the screen of a personal computer.

The following parameters of the emission plasma were obtained: plasma concentration ~ 10^8 cm^{-3}, electron temperature ~ 3 eV, plasma potential relative to the hollow cathode ~ 200 V. The measured plasma parameters in different modes of glow discharge generation will be used in modeling the ion-electron optics of the electron source.

References

[1] S.P. Bugaev, Yu.E. Kreindel and P.M. Schanin, Large cross section electron beams. Moscow: EAI, 1984 (in Russian).

[2] E.M. Oks, Plasma cathode electron sources: Physics, Technology, Applications. Wiley-VCH, 2006

[3] S.Yu. Doroshkevich, M. S. Vorobyov, M.S. Torba, N. N. Koval et al, “Efficiency of electron beam extraction to the atmosphere in an accelerator based on ion-electron emission” J. Phys.: Conf. Ser. vol. 2064, 012116, 2021

[4] S. Doroshkevich, S. Sulakshin, M.Vorobyov, N. Koval, A. Ekavyan and A.Chistyakov, “Electron accelerator based on ion-electron emission for generation of a wide-aperture beam”, IEEE2020, Proc. of 7th Int. Cong. on Energy Fluxes and Radiation Effects (EFRE) – 21st Int. Symp. on High-Current Electronics (Tomsk), pp. 42–45, 2020.

* The work was supported by the Russian Science Foundation (project No. 20-79-10015).

EXTRACTION INTO THE ATMOSPHERE OF A FOCUSED ELECTRON BEAM WITH AN ENERGY OF 2.5 MEV

E.V. DOMAROV, D.S.VOROBEV,N.K. KUKSANOV, R.A. SALIMOV, A.I. KORCHAGIN, S.N. FADEEV, V.G. CHEREPKOV, Y.I. GOLUBENKO, I.K. CHAKIN, M.G. GOLKOVSKY

Budker Institute of Nuclear Physics of Siberian Branch Russian Academy of Sciences, Novosibirsk, Russian Federation

For over 30 years, an extraction device has been successfully working in BINP at the ELV-6 accelerator to extract a focused beam of electrons into the atmosphere. The accelerating tube with permanent magnetic lenses was used in this installation. The design of these accelerator tubes with magnetic lenses is rather complicated. Recently, simpler design and high reliability accelerating tubes with big aperture is operating in ELV accelerators. For this reason, the problem number one at present is to develop the extraction device, capable of reliably working with serial accelerator tubes, of the ELV accelerator with power up to100 kW. We designed the optical scheme shown in Figure 1. The lens L1 is located directly at the lower end of the accelerating tube. Passing the lens L1, the beam is focused near the diaphragm D6 and increases to a diameter of ≤ 10 mm in the diaphragm D5. The walls of the chamber with diaphragms form the steps of the vacuum system. For passing the beam along the axis of the diaphragms, there are corrections coils C1 C2 C3. The diameter of diaphragm hole D1 is the most critical, because it determines the flow of gas that should be pumped out in the following steps of the vacuum system [1].

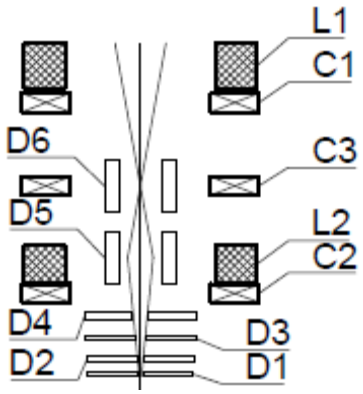

Fig.1. Optical diagram of the extractions device.

Measurements of the parameters of a high-power electron beam were carried out up to a power of 100 kW. Based on the data obtained, a new type of gas-dynamic extraction device was designed and pre-tested, which can efficiently output a focused electron beam to the atmosphere at the energy of 2,5 MeV and the beam current of 30 mA. In addition, this extraction device was tested at energy of 2.5 MeV and the beam current of 40 mA for a short time.

REFERENCES

[1] E.V. Domarov, D.S. Vorobyov, M.G. Golkovsky, Yu. I. Golubenko, A.I. Korchagin, N.K. Kuksanov, A.V. Lavrukhin, P.I. Nemytov, R.A. Salimov, A.V. Semenov, A.V. Sorokin,S.N. Fadeev, I.K. Chakin, V.G. Cherepkov, " Research of Parameters of the Powerful Electron Beam of Industrial Accelerator ELV," Sib. Jou. Phys., 2019, vol. 14, no. 2, p. 5–20.

AMPLITUDE MODULATION OF AN ELECTRON BEAM IN A PLASMA TRIODE*

V.I. SHIN, M.S. VOROBYOV, P.V. MOSKVIN, V.N. DEVYATKOV, V.V. YAKOVLEV

Institute of High Current Electronics SB RAS, Tomsk, Russia

The work is devoted to the generation of an electron beam in a triode-type electron source with a plasma cathode based on a low-pressure arc discharge [1]. The main purpose of the experiments was to demonstrate the possibility of controlling the beam current and, consequently, its power during a submillisecond pulse. In contrast to known analogs, in this work, the beam amplitude was controlled during a pulse up to 1 ms by applying a modulating voltage to the triode electrodes [2, 3].

The experiments were carried out on the SOLO facility [4, 5]. The scheme of the modernized facility is shown in Figure 1. To ignite the main arc discharge between cathode 2 and anode 3, an auxiliary discharge is used, initiated between the ignition electrode 1 and cathode 2. A redistributing electrode 4 is fixed in the center of anode 3. The redistributing electrode 4 is connected to anode 3 through resistors. A modulating voltage power supply has been developed to control the electron beam current. The modulating voltage is applied between the anode 3, the hole of which is covered with a fine grid 5, and the emission electrode 7, the hole in which is also covered with a fine grid 6. A constant accelerating voltage (up to 25 kV) is applied between the emission electrode 7 and the extraction electrode 8. The extraction electrode 8, drift tube 9 and collector 11 are at ground potential. The accelerated beam electrons are transported to the collector in the magnetic field of two coils 10, 12.

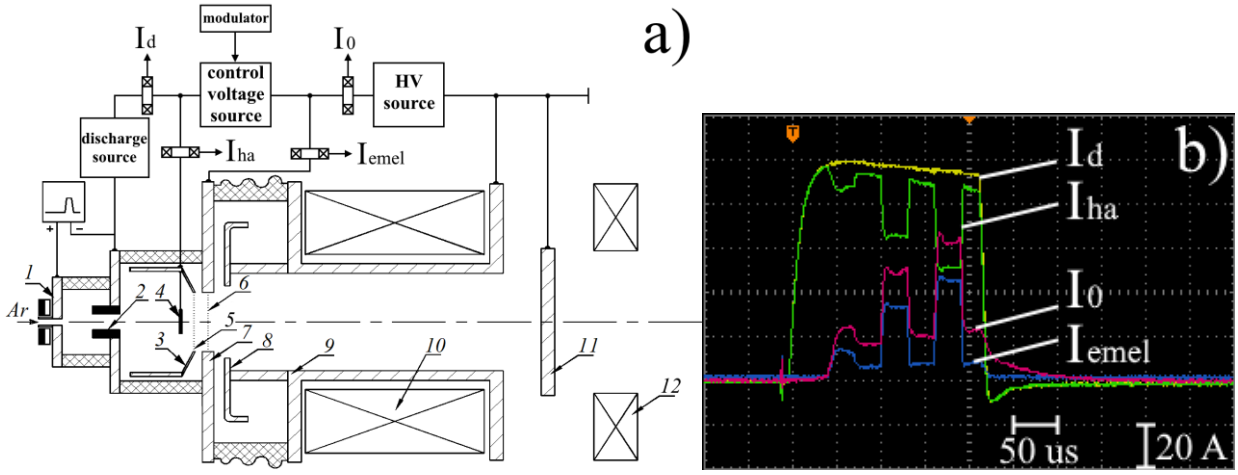

Fig.1. Scheme of electron source SOLO (a) and oscillogram of the main currents of the electron source (b): I_d – arc discharge current, I_{ha} – hollow anode current, I_{emel} – emission electrode current, I_0 – current in accelerating gap.

The dynamics of the main currents of the SOLO electron source, the switching coefficients of the discharge current, the coefficients of current extraction from the discharge are considered.

REFERENCES

[1] E. Oks, Plasma Cathode Electron Sources: Physics, Technology, Applications, WILEY-VCH, 2006.

[2] V.I. Gushenets, P.M. Schanin, "Submicrosecond Pulsed Electron Beam Formation in Electron Sources and Accelerators with Plasma Emitters," Russian Physics Journal, vol. 44, pp. 962–968, 2001.

[3] M.S. Vorobyov, P.V. Moskvin, V.I Shin, N.N. Koval, K.T. Ashurova, S.Yu. Doroshkevich, V.N. Devyatkov, M.S. Torba, V.A. Levanisov, "Dynamic Power Control of a Submillisecond Pulsed Megawatt Electron Beam in a Source with a Plasma Cathode," Technical Physics Letters, vol. 47, pp. 528–531, 2021.

[4] V.N. Devyatkov, N.N. Koval, P.M. Schanin, V.P. Grigoryev, and T.V. Koval, "Generation and propagation of high-current low-energy electron beams," Laser and Particle Beams, vol. 21, pp. 243-248, 2003.

[5] V.I. Shin, P.V. Moskvin, M.S. Vorobyev et al., "Increasing the Electrical Strength of the Accelerating Gap in an Electron Source with a Plasma Cathode," Instruments and Experimental Techniques, vol. 64, pp. 234–240, 2021.

* The work was supported by the Russian Science Foundation under grant No. 20-79-10015.

S1-O-051301

IRRADIATION EFFECT OF INTENSE PULSED ION BEAM ON (TiZrNbTaCr)C*

S.J. ZHANG[1,2,3,4]; L. CHEN[5]; A.V. STEPANOV[4]; O.P. LAPTEVA[4]; G.E. KHOLODNAYA[4]; X. YU[1,2,3]; M.F. XU[1,2,3]; Y.J. WANG[5]; G.E. REMNEV[1,4]; X.Y. LE[1,2,3]

[1] School of Physics, Beihang University, Beijing, 100191, PR China

[2] Beijing Advanced Innovation Center for Big Data-Based Precision Medicine, School of Medicine and Engineering, Beihang University, Key Laboratory of Big Data-Based Precision Medicine (Beihang University), Ministry of Industry and Information Technology, Beijing, 100191, PR China

[3] Beijing Key Laboratory of Advanced Nuclear Energy Materials and Physics, Beihang University, Beijing, 100191, PR China

[4] National Research Tomsk Polytechnic University, Tomsk, 634050, Russia

[5] School of Materials Science and Engineering, Harbin Institute of Technology, Harbin, 150001, China

Intense pulsed ion beam (IPIB), featured with pulsed high-power density, has been widely used in the modification of materials. The influence of IPIB irradiation on surface microstructure and phase structure of (TiZrNbTaCr)C ceramics was investigated in this work. Experiments were carried out using TEMP-4M accelerator with peak accelerating voltage, current density, and pulse duration (FWHM) of 220 kV, 150 A/cm^2, and 80 ns respectively. Atomic force microscope (AFM), scanning electron microscope pulse and Energy-dispersive X-ray spectroscopy (SEM+EDS), as well as X-ray diffraction (XRD) will be used to analyze the surface microstructure and phase structure of (TiZrNbTaCr)C ceramics under IPIB irradiation. The AFM images indicated that the grain size of (TiZrNbTaCr)C increased after IPIB irradiation which might improve the hardness and erosion resistance of material. The possible defects including micro-cracks and micro-craters caused by IPIB irradiation on surface will be analyzed according to SEM images. The influence of IPIB irradiation on elements distribution of samples will be analyzed based on EDS measurements. The phase structure stability of samples under IPIB irradiation will be analyzed by XRD and the lattice parameters, crystalline size, and micro-strain will be discussed as well. The evolution of surface structure and phase structure with pulse number will be summarized.

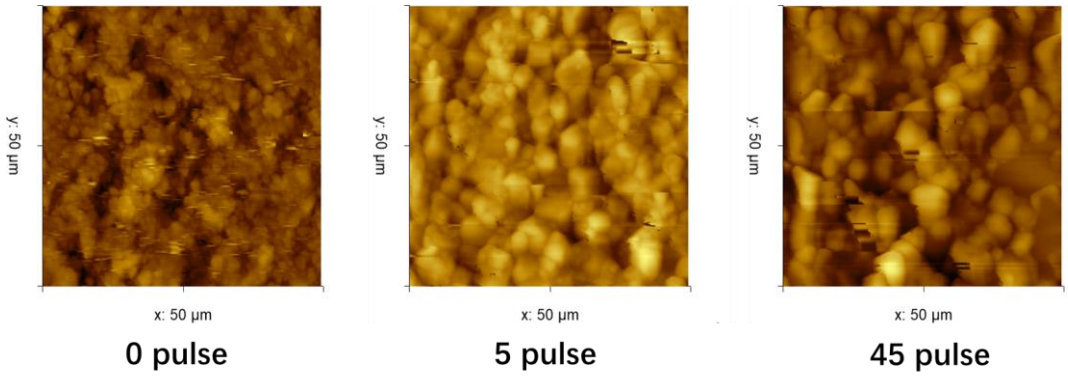

Fig.1. AFM images of original samples, and after 5 and 45 pulses IPIB irradiation

* The work was supported by National Natural Science Foundation of China by Grant No. 11875084 and 12075024. The authors are grateful to Mr. S. Pavlov from Tomsk Polytechnic University for his help in AFM measurement.

S1-P-016502

INFLUENCE OF THE PRESSURE AND KIND OF WORKING GAS ON THE HIGH-CURRENT ELECTRON GUN CHARACTERISTICS*

P.P. KIZIRIDI, G.E. OZUR

Institute of High Current Electronics SB RAS, Tomsk, Russia

The use of low-energy (up to 30 keV), high current (up to 25 kA) electron beams (LHEBs) is rather effective for the surface treatment and modification of metal products [1, 2] and has good prospects for further development. Usually, LHEB formation is carried out in a high-current gun with an explosive emission cathode and plasma anode based on a high-current reflective (Penning) discharge. Recently, we have proposed a new method for initiating explosive emission with resistively uncoupled arc plasma sources built in a disk cathode [3]. The new cathode unit, providing the initiation of explosive emission irrespectively from the acceleration gap length and fill medium, is a controlled device and can be used in an electron gun with a vacuum or a gas-filled diode without any plasma anode. The present work is devoted to the investigations of the influence of the pressure and kind of the working gas on the characteristics of high-current electron gun.

In the Fig. 1, the dependences of the beam pulse energy for the cases of argon, air and helium on gas pressure as well as for the case of vacuum diode at residual gas pressure (air) at 0.008 Pa are given. It is clear, that higher energy of the beam is achieved in the case of argon at pressure of 0.08–0.093 Pa. The decrease of the beam pulse energy at higher pressure is caused by a plasma-beam discharge in the gun which leads to a sharp decrease of the gun impedance and therefore the average kinetic energy of the beam electrons.

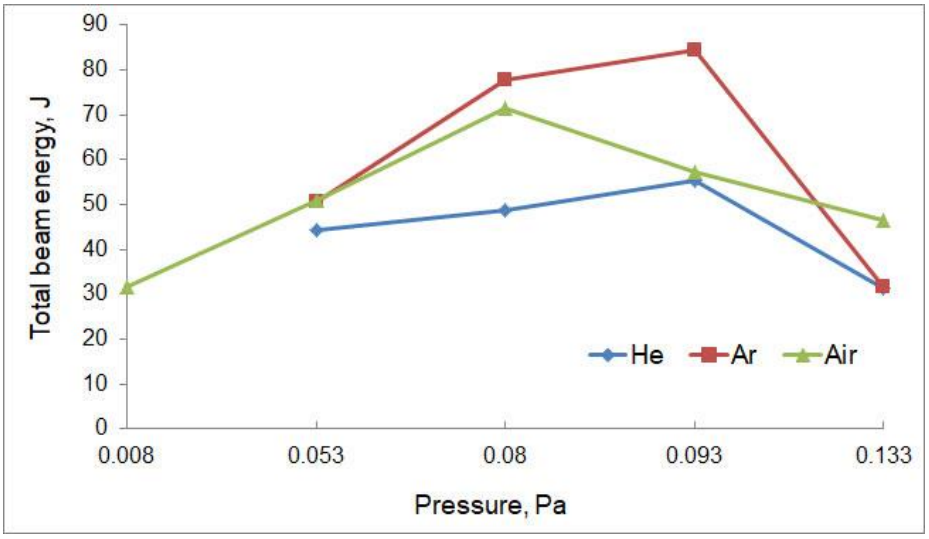

Fig.1. Beam current amplitude and total pulse energy in dependence on working gas pressure: argon (curve 1), air (2), and helium (3). Guide magnetic field – 0.1 T, acceleration voltage amplitude – 15 kV. The pressure values are given in an air equivalent.

Besides, the energy density distributions via the beam cross section obtained by a thermal imager have been studied.

REFERENCES

[1] V. P. Rotshtein, D. I. Proskurovsky, G. E. Ozur, Yu. F. Ivanov. "Surface Modification of Metallic Materials with Low-Energy, High-Current Electron Beams". – Novosibirsk (Russia): "Nauka", 2019, 347 p. ISBN 978–5–02–038809–3

[2] L. L. Meisner, V. P. Rotshtein, V. O. Semin, S. N. Meisner, A. B. Markov, E. V. Yakovlev, F. A. D'yachenko, A. A. Neiman, E. Yu. Gudimova, Microstructural Characterization and Properties of a Ti-Ta-Si-Ni Metallic Glass Surface Alloy Fabricated on a TiNi SMA Substrate by Additive Thin-Film Electron-Beam Method, Surface & Coatings Technology, 404 (2020), 12644, https://doi.org/10.1016/j.surfcoat.2020.126455

[3] P. P. Kiziridi, G. E. Ozur, Cathode Assembly of a High-Current Electron Gun with Multichannel Initiation of Emission by Breakdown on the Surface of a Dielectric, Technical Physics Letters 46 (2020), 775–778, doi: 10.1134/S1063785020080088

* The work was supported by Russian Ministry of Higher Education & Science (project No. FWRM-2021-0007).

S1-P-020602

INVESTIGATION OF THE CHARACTERISTICS OF AN INTENSE ION BEAM PROPAGATED OUTSIDE THE DIODE*

A.V.STEPANOV[1], I.N. PYATKOV[1], SHIJIAN ZHANG[2], E.N. STEPANOVA[1]

[1]National Research Tomsk Polytechnic University, Tomsk, Russian Federation
[2]School of Physics, Beihang University, Beijing, P.R. China

The transportation of an intense ion beam from the diode system [1] to the target has been studied. It was found that the angular ions divergence from the ideal (calculated) trajectory at the outer border of the beam, propagated outside the diode, was 10°. In this case, 26% of total beam energy was lost and the degree of positive beam charge compensation by electrons was 38%.

An approach for improving beam characteristics was proposed and studied [2, 3]. The ion beam was injected in the metal tube and due to the local divergence of ions the ion flux was partially closed on the inner tube wall. As a result, the ablation plasma was formed on the tube wall [4] and electrons entered into the ion beam. Thus, the full compensation of the beam space charge was provided.

The analysis of the radial profile of ion current showed that the drift tube provides an increase in the current density and beam energy in comparison with geometric focusing. Based on the data of the time-of-flight technique, the ion beam pulse had, as a rule, three peaks characteristic of the polyethylene coating of the anode. The first peak was corresponding to protons, the second and third ones - to singly and doubly ionized carbon ions. It was shown that the high density of ion current injected into the tube is mainly provided by protons. The relative content of protons in beam increased from 75.7% to 84.7%.

REFERENCES

[1] A.V. Stepanov, G.E. Remnev, “Influence of the configuration of the magnetic field of an ion diode on the parameters of an ion beam,” Instruments and Experimental Techniques, vol. 52 (4), 2009.

[2] X. Yu, S. Zhang, A.V. Stepanov, V.I. Shamanin, H. Zhong, G. Liang, M. Xu, N. Zhang, S. Kuang, J. Ren, X. Shang, S. Yan, G.E. Remnev, X. Le, “Focusing of intense pulsed ion beam by magnetically insulated diode for material research,” Surface and Coatings Technology, vol. 384, 2020.

[3] A.V. Stepanov, Haowen Zhong, Zhang Shijian, Mofei Xu, Xiaoyun Le, G. E. Remnev, “Study of the propagation of an intense ion beam to the target,” Vacuum, vol. 198, 2022.

[4] J.W. Poukey, S. Humphries, “Fast neutralization of ion beams in the presence of transverse magnetic fields,” Appl. Phys. Lett., vol. 33, 1978.

* The reported study was funded by RFBR and NSF, project number 21-53-53013 and was supported with the State Task in the Field of Scientific Activity FSWW-2020-0008.

S1-P-023601

PROPOGATION OF A PULSED ELECTRON BEAM IN GAS COMPOSITIONS OF CARBON-CONTAINING COMPOSITE NANOMATERIAL SYNTHESIS REAGENTS*

G.E. KHOLODNAYA, D.V. PONOMAREV, R.V. SAZONOV, M.A. SEREBRENNIKOV, O.P. LAPTEVA

Tomsk Polytechnic University, Tomsk, Russia

Carbon-containing composite nanomaterials are of great interest to researchers in chemistry, medicine, biology, and materials science. The physicochemical properties of nanomaterials depend on the synthesis method, on the composition of the mixture of initial reagents, on the synthesis temperature, and on the duration of the process [1]. To date, carbon-containing nanomaterials can be obtained by the sol-gel method [2]. The process is carried out at high temperatures, and the use of catalysts is also required, which shall be removed from the final product at the end of the process.

It seems promising to use the pulsed plasma-chemical method to synthesize nanomaterials. Efficient input of energy into the gas by a pulsed electron beam due to elementary processes of the first kind (collision ionization, dissociative electron attachment, etc.) significantly reduces the energy costs of the synthesis process. Investigation of the processes occurring during the interaction of pulsed electron beams with objects with a complex chemical composition, which are the key ones in technological processes, is topical.

The paper presents the results of comprehensive studies of the efficiency of the propagation of a pulsed electron beam in a mixture of gases: titanium tetrachloride (6 mmol) and hydrogen (18 mmol); titanium tetrachloride (6 mmol) and methane (18 mmol); titanium tetrachloride (6 mmol) and oxygen (36 mmol). The signified components are the initial reagents or products of plasma-chemical reactions of the synthesis process using pulsed electron beams.

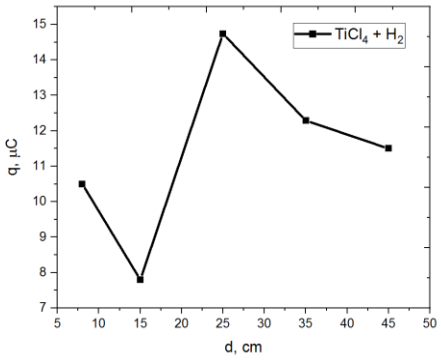

Fig.1. Dependence of an electron beam charge, having reached the collector of the Faraday cup, on the distance.

The investigations were carried out using a test bench including a TEA-500 pulsed electron accelerator, a drift chamber, and a sectioned cut-off calorimeter with a beam charge control function. The main characteristics of the electron beam are as follows: 60 ns half-amplitude pulse duration, up to 200 J pulse energy, and 5 cm beam diameter. During the experiments, the drift chamber was filled with the investigated gas, into which the electron beam was injected. Using a reverse current shunt, the charge of the electron beam was determined. The energy distribution over the beam cross section was measured using a sectioned calorimeter. The sectioned calorimeter with the beam charge control function was installed inside the mobile tube, which made it possible to perform measurements at a variable distance from the accelerator output window along the entire length of the drift chamber.

REFERENCES

[1] E. Costa, P. Zamora, and A. Zarbin, "Novel TiO_2/C nanocomposites: Synthesis, characterisation, and application as a photocatalyst for the degradation of organic pollutants," J. Colloid Interface Sci., vol.368, pp. 121–127, 2012.

[2] G. Kholodnaya, R. Sazonov, and D. Ponomarev, "TiO_2@C nanocomposites – from synthesis to application: A review". Fuller. Nanotub. Carbon Nanostructures," vol.29, issue 7, pp. 487-526, 2021.

* The research is supported by grant of the Russian Science Foundation (project No. 18-29-19020).

MEASUREMENTS OF THE ENERGY AND MASS-CHARGE COMPOSITION OF THE ION FLUX OF A VACUUM SPARK ON A TUNGSTEN CATHODE COATED WITH FUZZ NANOSTRUCTURES. *

I.L. MUZYUKIN,

Institute of Electrophysics UB RAS, 106 Amundsen Str., Ekaterinburg, 620016, Russia

The report is devoted to measurement of ion flow parameters of vacuum spark discharge with tungsten cathode, coated with FUZZ nanostructures.

A pulse of 20 kV, 50 ns was used. Distance cathode-anode 30-20 microns. Measurements were taken in 10 series of 100 pulses. For each position of the cathode, three series of 100 pulses were performed.

All components of the experimental setup are arranged coaxially, which makes it easier to find the optimal relative position of the spectrometer source and detector to obtain a spectrogram. The Thomson spectrometer has a circuit modified with respect to those previously used [1].

This design of the spectrometer differs from the previously used one by the presence of a plasma disruption system with additional acceleration of the ion component by 200 eV.

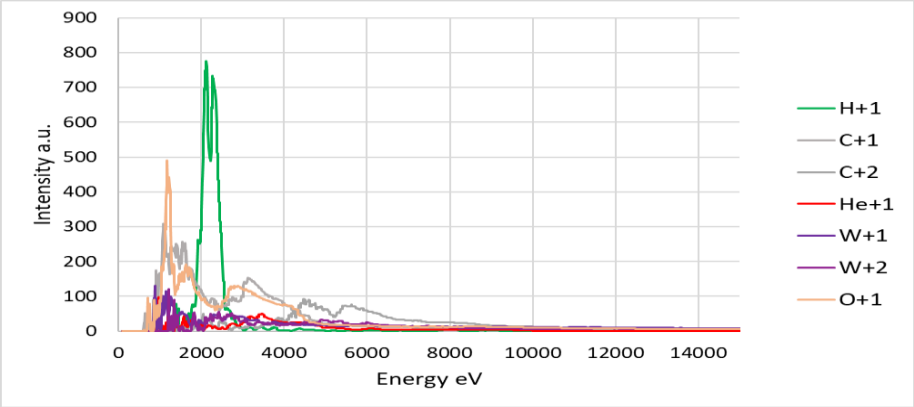

Fig.1. Energy spectra of the ion flux from the surface of tungsten coated with FUZZ for the first hundred pulses.

As a result of the measurements performed, it can be unambiguously indicated that during the first few tens of discharges on the FUZZ surface, the flow contains mainly hydrogen ions and impurities. Subsequently, the proportion of tungsten ions increases, while the proportion of hydrogen ions decreases to a few percent. The helium ion signal is present in almost all frames with a good ion signal. The energy spectra of the ions contain several local maxima in the range of 1000-6000 eV, which is several times less than the pulse amplitude at the anode, and, consequently, the energy of explosive electrons. When the cathode surface is cleaned from the coating, the proportion of fast hydrogen ions decreases, therefore, the velocity of the plasma boundary should drop by an order of magnitude from 10^8 cm/s to 10^7 cm/c.

REFERENCES

[1] Muzukin I.L . A Nanosecond Discharge Over a Dielectric Surface as a Method for Generation of Multicharged Plasma Plasma Science, IEEE Transactions 2005, vol. 33, № 5 Page(s): 1654 – 1657.

* The work was supported by the Russian Science Foundation (grant No. 20-19-00323).

S1-P-029301

ELECTRON BEAM SOURCE WITH A PLASMA ANODE AND THE BEAM OUTPUT TROUGH A FOIL WINDOW INTO THE ATMOSFERE *

E.N. ABDULLIN, G.F. BASOV

Institute of High Current Electronics SB RAS, Tomsk, Russia

Experiments were carried out to obtain electron beams of round or rectangular cross section up to 200 cm^2 in an electron beam source with an explosive emission cathode and a plasma anode at an accelerating voltage of 200 kV and the beams extraction through a foil window into the atmosphere. The electron beam current in the source was up to 2.5 kA, and the pulse duration was 5 μs. The beam energy estimated from the heating of the collector with a cross-section area of 74 cm^2 placed in the source behind the plasma anode was 650–850 J/pulse. The maximum beam energy extracted behind a grid with a geometric transparency of 80%, covered with an aluminum-magnesium foil 30-μm-thick, was up to 250–270 J/pulse. The power source was a Marx generator based on long lines, providing the obtaining of rectangular pulses at a constant arbitrary resistive load. Experiments have shown that the use of a plasma anode in an electron beam source with the use of a leading magnetic field makes it possible to increase the current and energy of the electron beam. At the same time, the presence of plasma in the interelectrode gap contributes to the appearance of low-energy electrons in the beam, which leads to a limitation of the energy output beyond the foil. One of the probable causes of energy losses during beam transportation in an electron beam source may be the development of the beam instability as a result of plasma-beam interaction. Data are obtained on the influence of the accelerating voltage and magnetic field on the beam energy.

* The work was supported by RFBR, Grant No. 18-48-700034 “r-a”

S1-P-029604

TESTING OF THE WATER SUPPLYING SYSTEM FOR THE CATHODE OF A VACUUM ELECTRON DIODE*

I.S. EGOROV[1], *M.A. SEREBRENNIKOV*[1], *A.V. POLOSKOV*[1],

[1]*Tomsk Polytechnic University, Tomsk, Russia*

An increase in the number of examples of the use of pulsed electron accelerators as sources of ionizing radiation stimulates the development of accelerator technology. One of the nodes that require the attention of researchers and developers of high-power pulsed accelerators is the electron emitter, the cathode. Research in this direction is being carried out both to improve the emission characteristics and to increase the lifetime and operational characteristics of the assembly. One of the original developments is the use of a liquid injected into the accelerating gap as a substance for plasma formation [1]. This work is devoted to testing the system of external liquid supply to the cathode of a vacuum electron diode. The change in the vacuum conditions in the diode during the injection of water is studied. The system is tested when a high voltage pulse is applied to the cathode. The values of water flow rates at which frostbite occurs by the injection system are established. Based on the research results, conclusions were made about the required characteristics of the liquid during injection into the accelerating gap of the vacuum electron diode of a pulsed submicrosecond accelerator.

REFERENCES

[1] I. Egorov, A. Poloskov, M. Serebrennikov, G. Remnev, Experimental demonstration of a single capillary, water-activated cathode for a sub-microsecond electron accelerator, Nuclear Instruments and Methods in Physics Research Section A: Accelerators, Spectrometers, Detectors and Associated Equipment. 943 (2019) 162459. doi:10.1016/j.nima.2019.162459.

* The authors are grateful to National Research Tomsk Polytechnic University (TPU, Russia) for technical support in a case of TPU development program. The work was conducted within the framework of the Russian Foundation for Basic Research: No. 20-02-00870.

S1-P-031001

DETERMINATION OF THE SPECTRUM OF A PULSED ION BEAM

A.I. PUSHKAREV

Tomsk Polytechnic University, Tomsk, 634050 Russia

An algorithm for calculating the energy spectrum of a pulsed ion beam generated by a direct-acting accelerator is presented. The ion spectrum is calculated using the oscillograms of the accelerating voltage, the experimental ion-current density, the one-dimensional Child–Langmuir (1D C–L) ratio, and the total current in the diode. The results of studying the ion spectrum generated by the TEMP-4M accelerator (250–300 kV, 150 ns) are presented. A good coincidence of the spectrum of ions that were calculated from the experimental ion-current density and 1D C–L equation is obtained. For ions whose energy is 95% of the total energy of the ion beam per pulse, the divergence between the spectra does not exceed 10% and is most significant in the region of low ion energies. The error in calculating the ion spectrum from the total current in the diode is much greater.

The ion spectrum from the experimental ion-current density was calculated for a small part (less than 5%) of the beam ions (local ion spectrum). The local ion spectrum was calculated in a similar way as the electron spectrum [1]. The full spectrum of ions per pulse was obtained by multiplying the local ion spectrum by the ratio of the total ion beam energy to the energy density at the point of measurement of the ion current density. The total beam energy was calculated by integrating the energy-density distribution over the beam cross section. The results of calculating the full spectrum of ions are shown in figure 1.

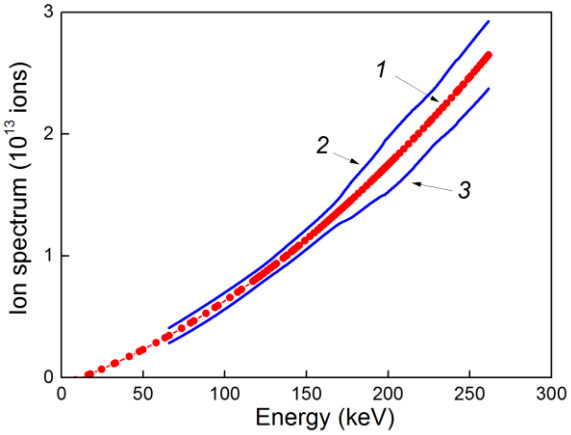

Fig.1. The full spectrum of ions generated by the diode per pulse (*1*), and the confidence interval taking the errors in the spectrum calculation into account (*2*, *3*)

Figure 1 shows the confidence interval for the full ion spectrum per pulse; it was determined taking the discrepancy of the spectra calculated from the experimental ion-current density and the 1D C–L ratio into account, as well as with consideration for the discrepancy of the local ion spectra over the ion beam cross section.

The total PIB energy that was calculated from the full spectrum of ions by summing (over the entire spectrum) the products of the number of ions with the energy E and their energy for the data presented in fig. 1 was 58 J. The total ion beam energy that was calculated by integrating the energy-density distribution over the beam cross section is 64 J. The calculation of the total ion beam energy from the ion spectrum gives underestimated values due to the contribution of fast atoms to the target heating.

The developed algorithm for calculating the energy spectrum of a pulsed ion beam that is generated by a direct-acting accelerator makes it possible to quickly control the beam spectrum with a small error during the target irradiation. To control the spectrum of ions, additional equipment and time-consuming processing of measurement results are not required.

REFERENCES

[1] A. Pushkarev, A. Prima, V. Ezhov, I. Miloichikova, E. Petrenko. “Determination of the pulsed electron beam spectrum by current and voltage oscillograms,” Laser and particle beams, article ID 881569, 2021.

S1-P-034803

INFLUENCE OF THE ACOUSTIC RESONANCE ON THE COLD PLASMA JET CHARACTERISTICS[1]

P.P. GUGIN, E.V. MILAKHINA, D.E. ZAKREVSKY

A. V. Rzhanov Institute of Semiconductor Physics SB RAS, Novosibirsk, Russia

Cold atmospheric pressure plasma jet is a current trend in modern science, technology and medicine. It is widely used in cosmetology, oncology and the food industry [1]. It consists of gas discharge pulses that form a streamer moving through a capillary into an open atmosphere at a pulse repetition rate of typically tens of kilohertz. The energy carried by the streamer is low enough to ensure that a target, such as a biological object, does not experience intense heating, causing the phenomenon to be called "cold". Despite its apparent simplicity, this type of discharge gives rise to a number of technical and scientific problems, so it is a relevant subject for research, both on the specific form of gas discharge and the phenomena associated with it [2,3].

Cold atmospheric pressure plasma jet exists in the open air, so it is possible to influence its characteristics by a large set of methods. One of these methods is to create conditions for acoustic resonance in the volume of the plasma gun and the gas supply fittings. The ignition of any gas discharge generates a shock wave in the environment. If the frequency of power pulses, and accordingly the generation of jets is matched to the length of the standing wave, which is formed in the volume of the installation, it is possible to have a significant influence on the intensity of the cold plasma jet, increasing or decreasing it.

The paper describes a study of the effect of acoustic resonance on the characteristics of a cold plasma jet. The frequency dependence of the current amplitude (fig. 1) carried by the jet is determined, in which the resonance peaks of intensity located at a multiple distance from each other are clearly visible. Experiments were carried out with helium and argon. An experiment was also carried out to tune the resonance to a given frequency by changing the length of the gas supply tube.

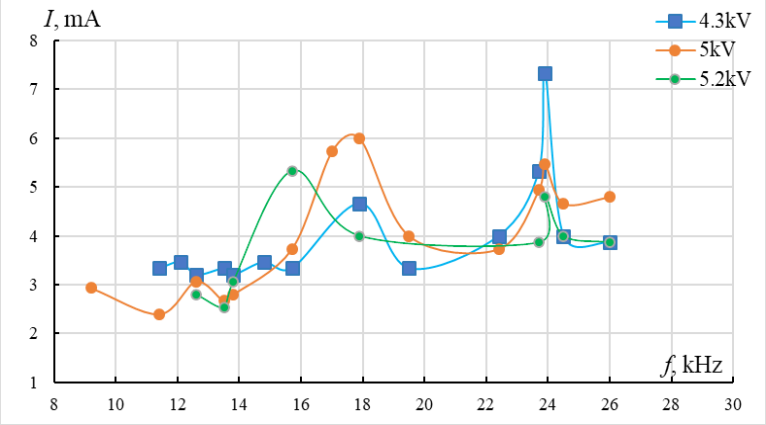

Fig.1. Jet current amplitude versus frequency at different voltages.

REFERENCES

[1] S Kalghatgi, D Dobrynin, G Fridman, M Cooper, G Nagaraj, L Peddinghaus, M Balasubramanian, K Barbee, A Brooks, V Vasilets, A Gutsol, A Fridman, G Friedman, "Applications of non thermal atmospheric pressure plasma in medicine" Plasma Assisted Decontamination of Biological and Chemical Agents. Springer, Dordrecht, 2008, pp.173-181.

[2] G. Fridman, G. Friedman, A. Gutsol, A. B. Shekhter, V. N. Vasilets, A. Fridman, "Applied Plasma Medicine" Plasma Processes and Polymers, vol. 5, pp. 503-533, 2015.

[3] I. Schweigert, Dm. Zakrevsky, P. Gugin et al. "Interaction of Cold Atmospheric Argon and Helium Plasma Jets with Bio-Target with Grounded Substrate BeneathGeneration peculiarities of cold atmospheric plasma jet in biomedical applications," Applied Sciences, vol. 9, p.4528, 2019.

1The work was supported by the Russian Science Foundation (project No. 22-49-08003).

S1-P-038101

DEVELOPMENT OF PHOTOINJECTOR IN IAP RAS*

A.V. AFANASIEV, I.V. BANDURKIN, A.M. GORBACHEV, K.V. MINEEV, N.Y. PESKOV, A.V. SAVILOV, A.A. VIKHAREV

Institute of Applied Physics, Nizhny Novgorod, Russia

Short dense electron bunches with a charge of 100 pC, duration up to 10 ps and a small spread of particle parameters obtained with a photocathode and accelerated up to MeV average energies can be used in such promising applications as generation of high-power short terahertz pulses of undulator or cyclotron radiation, Compton scattering of laser pulses, as well as injection into more energetic accelerators. A photoinjection complex is being created at the IAP RAS [1], in which a step-by-step acceleration of electrons up to energies of the order of 20 MeV should be realized while maintaining the normalized transverse emittance of bunches at a level of 1 mm mrad. The report describes the design of the accelerating and focusing systems of the accelerator and the development of new versions of the photocathode based on diamond films.

The first section of the accelerator is a classic version of a photoinjector with one-and-half-cell accelerating structure based on the symmetric TM π-mode. Powering the cavity from a 5 MW klystron at a frequency of 2.45 GHz provides an amplitude of the accelerating field at the cathode of about 70 MV/m and particle acceleration to an average energy of ~3.6 MeV. The design of the magnetic electron-optical system of the photoinjector includes a focusing system of the accelerating section consisting of a main solenoid with a field of about 0.25 T and a counter-cathode coil providing a zero magnetic field on the cathode surface. Such a system provides a regime of compensation for the space charge-related emittance [2] and focusing of the electron beam over a length of about 1 m.

For the second stage, a system of accelerating sections and focusing solenoids has been designed. Each accelerating section is a sequence of 6 coupled cells powered by a single microwave signal source at a frequency of 2.45 GHz. This frequency coincides with the operating frequency of the first stage of the photoinjector, which makes it possible to synchronize all final microwave amplifiers in both stages, feeding them through controlled phase shifters from one stable low-power continuous microwave signal source. The operating TM mode of the accelerating structure is a π-mode with antiphase field oscillations in neighboring cells. With a power supply signal of 5 MW, the amplitude of the accelerating field in the cavities is about 35 MV/m, which, according to calculations, provides an increase in the energy of relativistic particles of about 6.5 MeV over a length of one section of about 40 cm. The sequential arrangement of three such sections makes it possible to achieve an acceleration of 3.5 MeV photoinjection electron bunch up to an average energy of more than 20 MeV.

In parallel with the design of the accelerator, a study of photocathodes based on CVD diamond films is under way. Such cathodes can combine high quantum efficiency and insensitivity to vacuum quality [3, 4]. Investigations are carried out using a specially designed vacuum chamber, which makes it possible to register the electric charge emitted from the cathode surface under the action of laser radiation. According to preliminary results, the quantum efficiency of even a thin (several nm) diamond layer can exceed the quantum efficiency of a copper photocathode by several times, depending on the characteristics of the doping of the diamond.

REFERENCES

[1] A. A. Vikharev et al., “Development of Photoinjector Accelerator Complex at the Institute of Applied Physics of the Russian Academy of Sciences: Research Status and Prospects,” Radiophysics and Quantum Electronics, vol. 63, no. 5, pp. 430–439, 2020.

[2] B. E. Carlsten, “Space charge induced emittance compensation in high brightness photoinjectors,” Part. Accel., vol. 49, pp. 27–65, 1995.

[3] K. J. Pérez Quintero, S. Antipov, A. V. Sumant, C. Jing, and S. V. Baryshev, “High quantum efficiency ultrananocrystalline diamond photocathode for photoinjector applications,” Applied Physics Letters, vol. 105, no. 12, p. 123103, 2014.

[4] G. Chen, L. Spentzouris, C. Jing, M. Conde, G. Ha, W. Liu, J. Power, E. Wisniewski, A. V. Sumant, S. Antipov et al., “Demonstration of nitrogen-incorporated ultrananocrystalline diamond photocathodes in a RF gun environment,” Applied Physics Letters, vol. 117, no. 17, p. 171903, 2020.

* The work is supported by the Russian Science Foundation (grant #20-12-00378 for development of 3.5 MeV stage and photocathode studies and grant #21-72-30027 for development of 20 MeV stage).

S1-P-041101

PROMPT GAMMA AND NEUTRON SPECTROMETRY OF INTENSE NANOSECOND ION BUNCHES COLLECTIVELY ACCELERATED IN A LUCE DIODE

V.A. RYZHKOV, I.N.PYATKOV

National Research Tomsk Polytechnic University, Tomsk, Russian Federation

Instantaneous time-of-flight spectrometry of neutrons (nToF) and γ-spectrometry from nuclear reactions generated by nanosecond proton and ^{12}C ion bunches collectively accelerated in a Luce diode at a voltage across the diode of 250-300 kV has been thoroughly researched. A two-channel γ-spectrometer with time resolution of 2.5 ns enables a prompt control of number and energy of collectively accelerated protons in their separate bunches dumped into a sustainable and refractory B_4C target. Combination of nuclear reactions $^{10}B(p,\alpha\gamma)^7Be$, $^{12}C(p,\gamma)^{13}N$, and $^{11}B(p,\gamma)^{12}C$ was used to characterize the intense nanosecond (≤5 ns) proton bunches with energy and number per shot in excess of 500-750 keV and $6\cdot10^{14}$, respectively. The simultaneous control of signals from two organic scintillators shielded with lead layers of 1 and 7 cm was used to reliably separate contributions of the analytical reactions. The radioactivity of ^7Be and ^{13}N radionuclides produced in the reactions is measured with a conventional HP Ge detector to calibrate the prompt technique [1].

The threshold nuclear reactions $^{11}B(p,n)^{11}C$ and $^2H(^{12}C,n)^{13}N$ were used to perform nToF spectrometry of high-energy protons bunches (up to $3\cdot10^{11}$ per shot) with energy higher than 3.02 MeV [2] and ^{12}C ion bunches of $0.5\text{-}25\cdot10^{12}$ per shot and energy of 4-7 MeV [3]. The nToF spectrometry was also used to study the collective acceleration of deuterons [4] and helium-4 ions by use of nuclear reactions $^{10,11}B(d,n)^{11,12}C$, $^{12}C(d,n)^{13}N$ and $^{10,11}B(\alpha,n)^{13,14}N$, respectively.

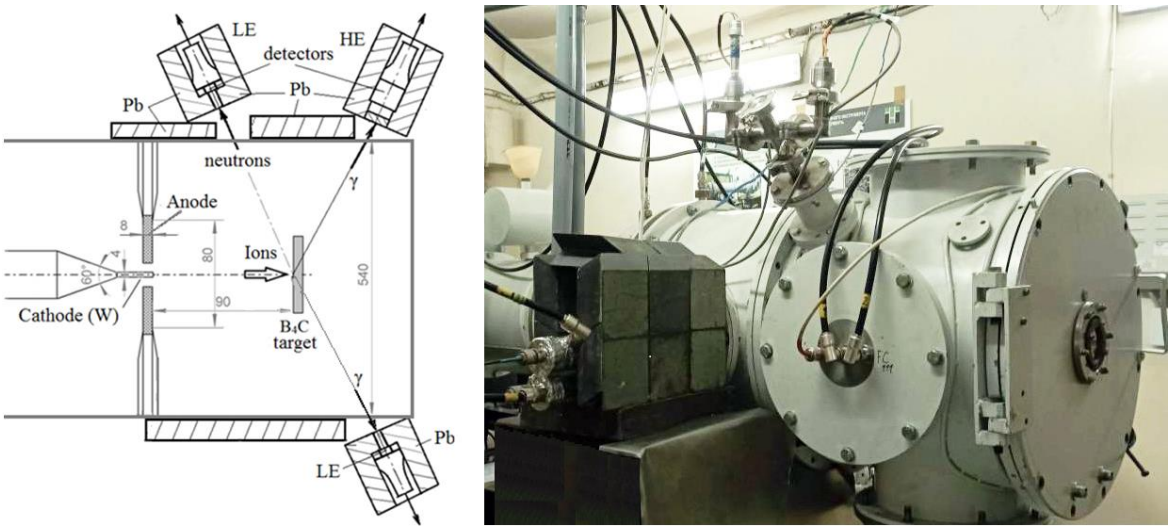

Fig.1. Scheme of registration of γ-rays and ToF neutrons from the threshold nuclear reaction $^{11}B(p,n)^{11}C$

This work was supported jointly by the Russian Foundation for Basic Research and Rosatom State Corporation in the framework of project no. 20-21-00025/20.

REFERENCES

[1] V.A.Ryzhkov, I.N.Pyatkov, G.E.Remnev, Time-resolved γ-spectrometer to promptly control number and energy of protons collectively accelerated as different bunches // Nuclear Instruments & Methods in Physics Research A, 998 (2021) 165190.

[2] V.A.Ryzhkov, I.N.Pyatkov, G.E.Remnev, Neutron time-of-flight spectrometry of high-energy proton bunches collectively accelerated in the Luce diode // Nuclear Instruments & Methods in Physics Research A, 1016 (2022) 166274.

[3] V.A.Ryzhkov, I.N.Pyatkov, G.E.Remnev, Selective determination of collectively accelerated ^{12}C ion bunches by neutron time-of-flight spectrometry //Submitted to Nuclear Instruments & Methods in Physics Research A

[4] V.A.Ryzhkov, I.N.Pyatkov, I.N.Kibler, M.V.Zhuravlev, G.E.Remnev, Comparison of collective acceleration of protons and deuterons in Luce diode with a polyethylene anode // Russian Physics Journal, 63/13 (2021) 151-155.

S1-P-044901

ELECTROSTATIC CUMULATION: A CONVINIENT RESEARCH INSTRUMENT TO OBTAIN MBAR PRESSURES IN SOLIDS

S. ANISHCHENKO[1], *V. BARYSHEVSKY*[1], *A. GURINOVICH*[1]

[1]*Research Institute for Nuclear Problems, Minsk 220030, Belarus*

Magnetic cumulation is not the sole phenomenon capable to produce high-dense electron beams in relativistic vacuum diodes. Electrostatic cumulation phenomenon also exists and reveals at much lower accelerating voltages in relativistic diodes with a ring-type cathode [1, 2]. A distinctive feature of electrostatic cumulation is quite low spread of electron energies in the produced high-dense beam. These circumstances give advantages to electrostatic cumulation phenomenon if the latter is considered as a convenient research instrument for high energy density physics.

Electrostatic cumulation was revealed during modeling of high-current accelerators [3] and confirmed experimentally [2]. The qualitative picture of electrostatic cumulation can be described as follows. In a relativistic vacuum diode, electron emission is most intense from the cathode's edges (Fig. 1). Let us consider electrons emitted from the inner edge. The Coulomb repulsion causes the charged particles to rush to the region free from the beam. As a result, the accelerated motion of electrons toward the anode comes alongside the radial motion to the cathode's symmetry axis. As a result, the high-current beam density increases multifold on the axis as compared to the average current density in the cathode-anode gap.

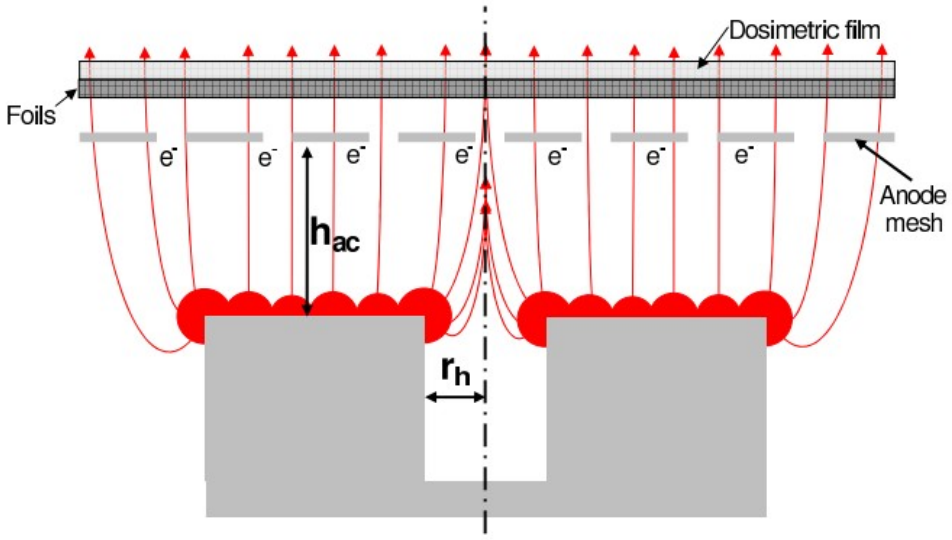

Fig.1. Electrostatic cumulation.

Electrostatically cumulated electron beam with an energy of 400 keV and a cross section of $3 \cdot 10^{-4}$ cm^2 is capable of delivering of 25 kJ/cm^3 of specific energy to a tungsten plate [4]. An increase in the accelerating potential up to several megavolts makes it possible to rise delivered specific energy by 1–2 orders of magnitude.

REFERENCES

[1] S. V. Anishchenko, V. G. Baryshevsky, and A. A. Gurinovich, “Electrostatic cumulation of high-current electron beams for terahertz sources,” Phys. Rev. Accel. Beams. Vol. 22, no. 043403, 2019.

[2] S. Anishchenko, V. Baryshevsky, A. Gurinovich, E. Gurinovich, E. Gurnevich, P. Molchanov, “Cumulation of high-current electron beams: theory and experiment,” IEEE Trans. Plasma Sci. Vol. 45, pp. 2739-2743, 2017.

[3] S. Anishchenko, A. Gurinovich, “Simulation of explosive emission and electron beam dynamics in a cathode-anode gap for cathode and anode optimization in an axial vircator,” Proc. 5th Euro-Asian Pulsed-Power Conf., Kumamto, Japan, P.~1-6, 2014.

[4] S. Anishchenko, V. Baryshevsky, A. Gurinovich, “Electrostatic cumulation: a convinient research instrument for high energy density physics,” The 48th IEEE International Conference on Plasma Science, Nevada, USA, 8O-C-05, 2021.

S1-P-049002

AUXILIARY DISCHARGE OF A WIDE APERTURE ELECTRON ACCELERATOR BASED ON ION-ELECTRON EMISSION*

A.A. GRISHKOV, M. S. VOROBYOV, S. Y. DOROSHKEVICH, V. A. SHKLYAEV

Institute of High Current Electronics SB RAS, Tomsk, Russian Federation

In this paper, the region of the auxiliary discharge of an electron accelerator based on a non-self-sustained high-voltage glow discharge is investigated. The paper presents the developed analytical model and the results of numerical simulation of an glow discharge, which plays the role of an auxiliary discharge and is used to generate plasma with subsequent extraction of ions into the main high-voltage gap.

In this glow discharge, two tungsten wires are the anode, and the cathode is the inner walls of the chamber. In the model, these discharge regions are considered as separate independent nodes, which are connected by a layer of conducting plasma that matches the boundary conditions. In this case, it is assumed that the Child-Langmuir conditions are satisfied for both the cathode and anode layers. The developed model, based on the representation of the auxiliary glow discharge as matched electron and ion diodes, makes it possible to estimate the range of possible voltages for each of the near-electrode layers and determine the plasma potential. Then this results was used in further simulation aimed at obtaining the maximum coefficient of electron beam extraction into the atmosphere.

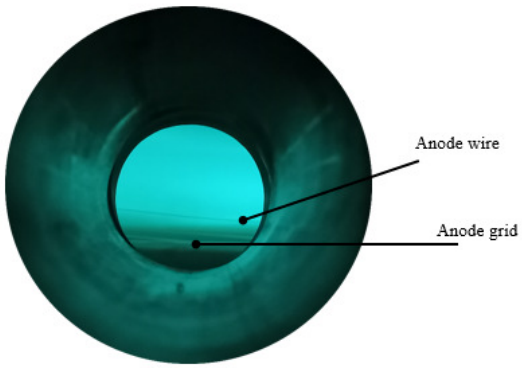

Fig. 1. Helium gas plasma of auxiliary discharge.

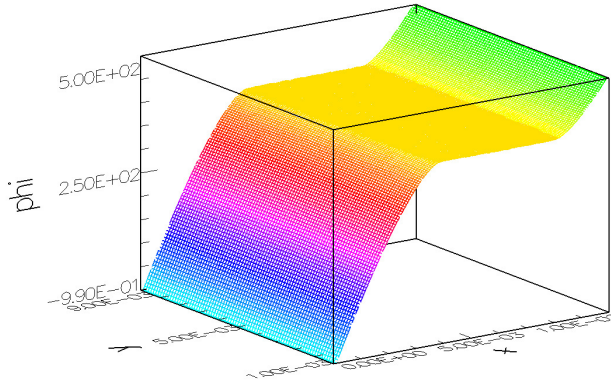

Fig. 2. Distribution of potential in the auxiliary discharge in “plane” model. Simulation with xoopic code.

Modeling was carried out using the codes KOBRA3-INP [1] and xoopic [2]. The calculation of the plasma potential and the parameters of the cathode and anode layers agree with the experimental results obtained by the probe method.

REFERENCES

[1] KOBRA3-INP, INP Wiesbaden, Junkernstr. 99, 65205 Wiebaden, Germany.

[2] Verboncoeur J. P., Langdon A. B., and Gladd N. T., An object-oriented electromagnetic PIC code, *Comput. Phys. Commun*. 87, 199 (1995).

* The work was carried out within the framework of the state assignment of the Ministry of Science and Higher Education of the Russian Federation on the topics FWRM-2021-0007.

S1-P-049004

SIMULATION OF A WIDE-APERTURE ELECTRON ACCELERATOR BASED ON ION-ELECTRON EMISSION IN REPETITIVELY PULSED MODE*

A. A. GRISHKOV, M. S. VOROBYOV, S. Y. DOROSHKEVICH, V. A. SHKLYAEV

Institute of High Current Electronics SB RAS, Tomsk, Russian Federation

The use of a modern elemental base makes it possible to create discharge power supplies in a repetitively pulsed mode with a pulse repetition rate at the level of a few to tens of kHz. However, due to the complex nature of the dependence of the power output factor on the control parameters, the high potential inherent in the transition from the continuous operation of the accelerator to the repetitively pulsed operation is difficult to study experimentally. The purpose of the work was to develop new and adapt existing numerical models and simulation codes for modeling the repetitively pulsed operation of an accelerator of this type, since such models have not yet been developed. The paper proposes analytical and numerical approaches to modeling the generation of an electron beam in a repetitively pulsed mode of a wide-aperture electron accelerator based on secondary ion-electron emission with a plasma emitter. With the help of well-known codes KOBRA3-INP [1], KARAT [2], xoopic [3] and the developed analytical approach, individual modes of accelerator operation are simulated. Qualitatively, the obtained experimental results are explained, which are in good agreement with the developed approach. Directions for further research and development of diagnostics are proposed.

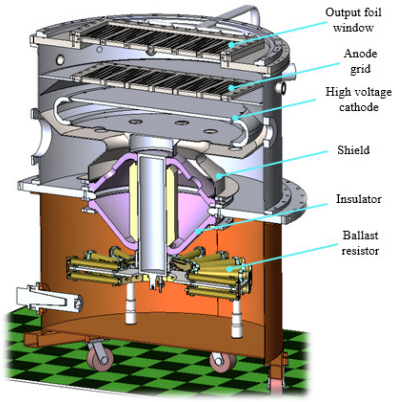

Fig. 1. Design of simulated wide-aperture electron accelerator based on ion-electron emission in repetitively pulsed mode. Electron energy: up to 150 keV, beam current 1–40 mA, current density 1–15 μA/cm^2.

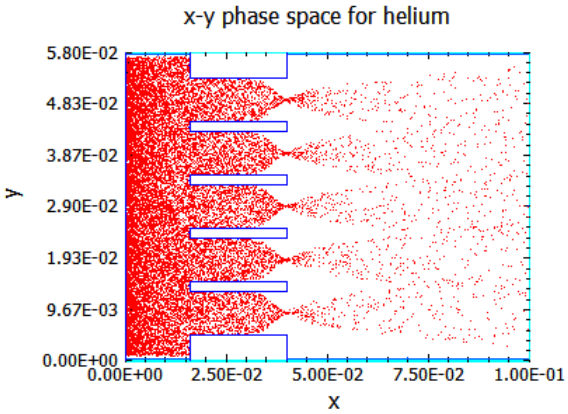

Fig. 2. Distribution of ion particles in the simulation in the five-slit approximation. Modeling with xoopic code.

Figure 1 shows a design of a wide-aperture electron accelerator, on which the experimental part of the work was carried out. Figure 2 shows instant distribution of ions in the computational domain. The computer simulation was done with the xoopic code. The emission boundary is set on the left boundary of the computational domain. The simulation was carried out taking into account the calculated parameters of the auxiliary discharge.

REFERENCES

[1] KOBRA3-INP, INP Wiesbaden, Junkernstr. 99, 65205 Wiebaden, Germany.

[2] V.P.Tarakanov, User's Manual for Code KARAT (Springfield: BRA), (1992).

[3] Verboncoeur J. P., Langdon A. B., and Gladd N. T., An object-oriented electromagnetic PIC code, *Comput. Phys. Commun*. 87, 199 (1995).

* The work was carried out within the framework of the state assignment of the Ministry of Science and Higher Education of the Russian Federation on the topics FWRM-2021-0007.

S2-O-007301

FAST SWITCHING OF MEGAAMPERE CURRENT TO THE LOAD*

S.A. SOROKIN

Institute of High Current Electronics SB RAS, 2/3 Akademichesky Ave., Tomsk 634055, Russia, s.sorokin@rambler.ru, +7(3822)491617

In experiments [1, 2, 3] on fast switching of the megaampere current to a foil liner or a solid metal rod 1–2 mm in diameter, the formation of a thin layer of hot (>100 eV) dense plasma was observed on the surface of the liner (rod). The process of switching the current to the load is accompanied by a powerful pulse of soft X-rays emitted from the surface of the load. The current switches to the load in 1-3 ns in the process of sweeping (pushing away from the load) by the magnetic field of the plasma, previously injected in the area of the load and the conical load holder. (Fig.1a). In the course of these experiments, the question arose of whether the formation of a surface plasma is the result of implosion onto the load surface of a part of the injected plasma swept by the current. To clarify this issue, test shots were made in this work with different configurations of the load area and the composition of the injected plasma.

In the first test, instead of a conical holder (Fig. 1a), a cylindrical holder (Fig. 1b) was used, i.e., a cathode configuration was used close to that used in the plasma focus [4]. In this configuration, after the swept plasma reaches the end of the cathode, it is possible (this occurs in the plasma focus) to implode the plasma onto the load surface. Upon transition to a cylindrical holder, the X-ray power from the surface of the aluminum liner decreased by several times. This result can be explained by the implosion of a portion of the injected plasma onto the liner surface. This plasma transfers the current even after its stagnation on the surface of the liner.

In the second test, a screen was used to eliminate the possibility of radial implosion of the injected plasma on the load (Fig. 1c). The presence of the screen eliminates the possibility of sweeping the injected plasma from the periphery to the load. The power and duration of the X-ray pulse, as well as the X-ray image of the load with and without a screen, practically coincided. This test confirms that the anode configuration (presence or absence of a shield) does not affect the result and the formation of a short X-ray pulse is due to the plasma pushing away from the load surface and the subsequent explosion of this surface.

A change in the elemental composition of the injected plasma also does not affect the radiative characteristics of the load.

Thus, the performed studies confirm that when plasma is injected into the load region with a conical holder, the plasma is pushed away from the load and the current is switched over to the surface of the load (liner or rod) in a few nanoseconds.

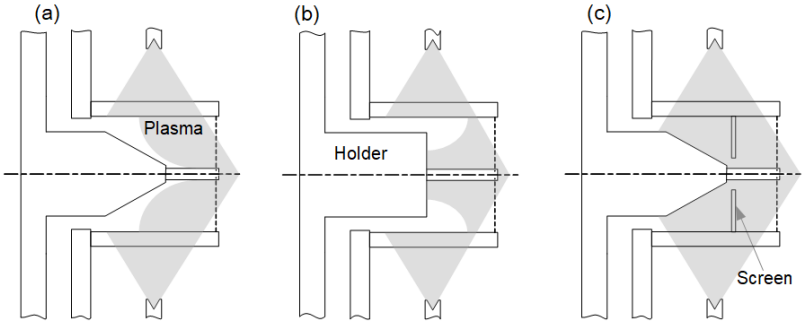

Fig. 1. Schematics of the load area with cone holder a), cylindrical holder b), cone holder and screen c).

REFERENCES

[1] *Sorokin S.A. //* Plasma Physics Reports. – 2017. – Volume 43. – № 5. Pages 542–546.
[2] *Sorokin S.A. //* Physics of Plasmas. – 2018. – Volume 25. – № 8. Pages 082704.
[3] *Sorokin S.A. //* Physics of Plasmas. – 2019. – Volume 26. – № 8. Pages 082706.
[4] *Mather J.W. and Bottoms P.J.* // Physics of Fluids. – 1968. Volume 11. – № 3. Page 611.

* This work was supported by the Russian Foundation for Basic Research (grant No. 18-08-00155).

S2-O-009807

LEAKAGE OF CURRENT FROM MITL WITH CERAMIC COATING CATHODE*

G.M.Oleinik[a], V.V.Aleksandrov[a], A.V.Branitskii[a], I.N.Frolov[a], E.V.Grabovskii[a], E.I.Predkova[a],O.B.Reshetnjak[a], and S.I.Tkachenko[a,b,c]

[a] *SRC RF TRINITI, Russia, Moscow Troitsk*
[b] *Moscow Institute of Physics and Technology (National Research University), Dolgoprudny, Moscow Region, Russia*
[c] *Joint Institute for High Temperatures, Russian Academy of Sciences, Moscow, 125412 Russia*

It was shown in [1] that the ceramic coating reduces the expansion of dense plasma from the surface of the MITL cathode. This made it possible to consider the coating of MITL cathodes with ceramics as protection against current leakage. The purpose of this work was to study the processes of current flow in MITL, in which the cathode is covered with ceramics. For this purpose, a 40mm short-circuited MITL was installed at the output of the eight-module installation of the Angara-5-1. The amplitude of the generator current reached 3 MA. The time of the current rise to the maximum was ~ 100 ns. With the help of loops, the currents were measured: flowing into the MITL, and at the end of the MITL.

Hollow stainless steel tube with a diameter of 3 mm and a wall thickness of 220 microns was used as the MITL cathode. The skin time of the current in the linear approximation (at low current amplitudes) is 16 ns, which is smaller than the duration of the current pulse. In a number of experiments, a ceramic tube with an inner diameter of 3 mm and an outer diameter of 5 mm was put on this tube.

An insulated conductor was located inside the cathode tube, which had contact with its inner surface and was used to measure the electric field strength on the inner surface of the tube. The MITL anode is made of stainless steel, its inner diameter is 20mm. The inductance of such a MITL is equal to 10 nHn. With the internal resistance of the generator of theAngara-5-1 installation 0.25 Ohms, the time of filling the MITL with a magnetic field is 40 ns, thus filling the MITL with a field occurs more than 2 times faster than the current reaches the amplitude value.

Based on the totality of the recorded information (electrical signals, laser shadow pictures and streak camera pictures), it can be argued that in the case when the MITL cathode was coated with ceramics, plasma formation on it occurs earlier than without such a coating. It is shown that, for our case of classical MITL, in which the cathode was located coaxially inside a cylindrical anode, just as in [2], in the case of coating the MITL cathode with ceramics, not all off the current entering the MITL flows to its end.

Numerical simulation of the processes occurring when a current with a linear density of up to 3 MA/cm is passed through a thick-walled tube with a wall thickness of 220 microns was carried out. A system of one-dimensional one-temperature magnetohydrodynamic equations was solved. To describe the properties of a real substance, wide-range semi-empirical equations of state [3] were used, taking into account phase transformations (melting and evaporation) and the possibility of realizing metastable states, as well as the dependence of transport coefficients (conductivity and heat capacity) on temperature [4, 5]. The numerical results are in good agreement with the measured value of the electric field strength on the inner surface of the tube.

[1] V.V. Aleksandrov, A.V.Branitskii, E. V. Grabovskii, A.N.Gribov, A.N. Gritsuk, V.D. Korolev, Ya.N. Laukhin, K.N. Mitrofanov, G. M.Oleinik, E.I. Predkova, A.A. Samokhin, V.P. Smirnov, I.N. Frolov, A. A. Samokhin, V. P. Smirnov, I. N. Frolov, and A. O. Shishlov, Plasma Phys. Rep. 46, 604 (2020). A. A. Samokhin, V. P. Smirnov, I. N. Frolov, and A.O. Shishlov. «Electric explosion of the carrier megaampere current of the surface» //Plasma Phys. Rep. 46, 604 (2020).

[2] S. S. Anan'ev , Yu. L. V. D. Korolev Bakshaev , A. V. Bartov , P. I. Blinov , S. A. Dan'ko , A. I. Zhuzhunashvili , E. D. Kazakov , Yu. G. Kalinin , A. S. Kingsep , V. D. Korolev , V. I. Mizhiritskii , V. P. Smirnov , S. I. Tkachenko , and A. S. Chernenko «Transportation Properties of a High-Current Magnetically Insulated Transmission Line and Dynamics of the Electrode Plasma» // Plasma Physics Reports, Vol. 34, No. 7, pp. 574–586, July 2008.

[3] Fortov V.E., Khishchenko K.V., Levashov P.R., Lomonosov I.V. Wide-range multi-phase equations of state for metals, Nucl. Instr. Meth. Phys. Res. A 415 (1998) 604.

[4] E. V. Grabovski, P. R. Levashov, G. M. Oleinik, C. L. Olson, P. V. Sasorov, V. P. Smirnov, S. I. Tkachenko, and K. V. Khishchenko Formation and Dynamics of Plasma Layers Formed on the Foil Surface under the Action of a High-Current Pulse. Plasma Physics Reports, 2006, Vol. 32, No. 9, pp. 718–728.

[5] H. Knoepfel, Pulsed High Magnetic fields (North-Holland, Amsterdam, 1970.

* This work was supported by the Russian Foundation for Basic Research (project no. 20-21-00082).

S2-O-011601

GENERATION OF AR K-SHELL RADIATION USING A HYBRID GAS PUFF WITH AN OUTER PLASMA SHELL. *

A.V. SHISHLOV, R.K. CHERDIZOV, V.A. KOKSHENEV, N.E. KURMAEV, S.A. VAGAITSEV

Institute of High Current Electronics SB RAS, Tomsk, Russia

In our work, we investigated a new type of load, a hybrid gas puff with an outer plasma shell, as a plasma radiation source for efficient production of K-shell radiation at microsecond implosion times. We used the hybrid load of the following type. The inner argon shell was actually a solid gas jet on the axis of the system with a diameter of 20 mm. An outer deuterium shell played a role of an implosion stabilizer and a current sharpener for the inner gas jet. The outer shell was formed at a diameter of 80 mm, extending outward to large initial radii. The falling profile of the gas density should ensure stable implosion of the gas puff for hundreds of nanoseconds while the generator current rose. The third component of the hybrid load was the outer plasma shell located at the diameter of 350 mm, which provided the initial conductivity and reduced the negative effects of the "cold start". The experiments have been carried out on the GIT-12 generator. The generator was operated in a microsecond mode that provides 4.7-MA current with the current rise time of 1.7 μs in a short-circuit load at a charging voltage of 50 kV.

The experiments showed that the hybrid gas puff with the outer plasma shell is capable to provide a stable Z-pinch compression at implosion times of 750-800 ns. The plasma column radiating in Ar K-shell lines had a typical diameter of 1-1.5 mm, and FWHM of the radiation pulse was in the range from 2.5 to 6 ns. The data on the Ar K-shell radiation power and yield were obtained for the Ar-D_2 gas puffs with different initial parameters. The experimental data were compared to the theoretical predictions of an expected K-shell yield at a certain current level in order to estimate the efficiency of a new type of K-shell plasma radiation source. The maximum Ar K-shell radiation power and yield observed in the experiments were 570 GW/cm and 1.6 kJ/cm at the peak implosion current of 2.9 MA and the implosion time of 780 ns. However, the efficiency of the plasma radiation source reached only 70%, i.e. the experimental K-shell radiation yield was still 30% lower in comparison with the theoretical predictions. Nevertheless, we consider this type of Z-pinch load as promising and plan to continue our research in this direction.

* The work was supported by Russian Science Foundation Project № 22-29-01554, https://rscf.ru/project/22-29-01554/

S2-O-019901

OPTIMIZATION OF DOUBLE SHELL HYBRID GAS-PUFF WITH OUTER PLASMA SHELL FOR EFFICIENT GENERATION OF K-SHELL RADIATION IN THE MICROSECOND IMPLOSION REGIME*

R.K. CHERDIZOV, A.V. SHISHLOV, V.A. KOKSHENEV, N.E. KURMAEV

Institute of High Current Electronics SB RAS, Tomsk, Russia

Studies of Z-pinch plasma as X-ray source were carried out on the GIT-12 generator (4.7 MA, 1.7 μs) in the IHCE SB RAS, Tomsk. The main purpose of the research was optimization of load parameters for efficient generation of the argon K-shell radiation in the microsecond implosion regime. A new type of a Z-pinch load, a hybrid gas-puff with an outer plasma shell, was tested. The inner argon shell is actually a solid gas jet on the axis of the system with a small initial diameter. An outer deuterium shell plays the role of an implosion stabilizer for the inner gas jet. The third component is the outer plasma shell, which provides the initial conductivity. The outer deuterium shell, together with the outer plasma shell, has proved its effectiveness in past experiments, providing stable implosion at times of the order of μs [1][2]. In these experiments, the diameter of the inner argon jet was 20 mm, the diameter of the annular deuterium shell was 81 mm, and the outer plasma shell was generated by 48 plasma guns located at the diameter of 350 mm. The experiments were carried out at constant parameters of the outer deuterium and plasma shells with varying parameters of the inner argon jet. An electromagnetic valve with separate volumes formed a hybrid gas-puff consisting of an annular outer shell and an inner central jet.

To increase the K-shell radiation yield, the following initial load parameters were changed: the mass of the gas-puff, the time of gas injection, and the transparency of the grids of the interelectrode gap. To study the dependence of the K-shell yield on the implosion dynamics, we analyzed the initial density profiles of the gas-puff [3], and B-dots data. The K-shell yield increased when the matter of the central argon jet did not propagate from the central region to the periphery. This was achieved by reducing the mass of argon jet, the injection time, and the absence of a grid under the central argon jet. As a result, K-shell radiation yield increased from 1.0 kJ/cm to 1.5 kJ/cm, and the power increased from 380 GW/cm to 535 GW/cm at a peak implosion current of 2.8 MA. This radiation yield is 70% of the theoretical yield at this current level, calculated by the two-level model [4]. Previously [5], for a double shell argon gas-puff with outer plasma shell (with cascade parameters jet/shell of 20/100 mm), the K-shell radiation yield was 60% of the theoretically expected yield for a current level of 3.1 MA, and the power reached 280 GW/cm. Thus, the hybrid gas-puff proved to be promising for a further increase in the yield of K-radiation in the microsecond implosion regime, which is the subject of our further investigations.

REFERENCES

[1] D. Klir et al., "Efficient neutron production from a novel configuration of deuterium gas-puff Z-pinch", Phys. Rev. Lett., 112, 095001, 2014.

[2] D. Klir et al., "Ion acceleration mechanism in mega-ampere gas-puff z-pinches", New J. Phys. 20 053064, 2018

[3] R.K. Cherdizov et al., "Effect of tailored density profiles on the stability of imploding Z-pinches at microsecond rise time megaampere currents", Plasma Phys. Control. Fusion 64 015011, 2022

[4] D.Mosher et al., "A two-level model for K-shell radiation scaling of the imploding Z-pinch plasma radiation source", IEEE Trans. Pl. Sci., vol. 26., No. 3, pp. 1052-1061, 1998.

[5] A.V. Shislov et al., "Generation of K-Shell Radiation of Noble Gases in the Microsecond Implosion Regime", Russ Phys J 62, 1243–1252, 2019

* The work was supported by the Russian Science Foundation under grant No. 22-29-01554.

S2-O-021501

A WIDEBAND PLASMA MODEL FOR METALS AT HIGH ENERGY DENSITIES*

N. B. VOLKOV, E. A. CHINGINA

Institute of Electrophysics UB RAS, Yekaterinburg, Russian Federation

The main objective the paper present is to develop the wideband plasma model of a metal at high energy densities (HED) on the basis of ideas expressed in [1-4].

Accounting mentioned above about HED and fact the melting specific heat of phase transition liquid – solid state is lower then that one for liquid-gas transition we will not differ liquid and solid state of matter .

We suppose the metal represents a mixture of two 'liquids': the ionic, consisting ion skeletons of identical weight occupying sites of a deformable lattice, and electronic, containing electrons of a continuous spectrum. The electron transitions between localized (discrete) and delocalized (continuous) states with total rate $\Gamma_e = \delta n_e / \delta t$ are taken in account in our model also. With the help of the approach developed by Andreev and Pushkarov [4] we deduced the two-liquid, two-temperature equations for describing the metal interaction with a pulse electromagnetic field within the framework of full Maxwell equations system in view of generation and recombination of the conduction electrons, and of their inertia. Expressions for electron and phonon transport in deformable crystal were obtained with the help of known methods solving of kinetic equations for phonons and conduction electrons.

In the case of slow electrophysical processes at high energy densities, one can ignore the displacement current and to use the one-liquid and one-temperature approximation. For this case, wideband expressions for the thermodynamic functions and electronic transport coefficients of aluminum are obtained. It is shown that the resulting equation of state for aluminum describes well the experimental Hugoniot adiabats known from the literature.

REFERENCES

[1] N.B. Volkov, "Plasma model for metal conductivity," Zhurnal Tekhicheskoi Fisiki, vol. 49, no. 9, pp. 2000-2002, September 1979.

[2] N.B. Volkov, A.Z. Nemirovsky, "The ionic composition of the non-ideal plasma produced by a metallic sphere isothermally expanding into vacuum," J. Phys. D: Appl. Phys., vol. 24, pp. 693–701, 1991.

[3] N.B. Volkov, E.A. Chingina, A.P. Yalovets, "Dynamical equations and transport coefficients for the metals at high pulse electromagnetic fields," J. Phys. Conf. Ser., vol. 774, art. no. 012147, 2016.

[4] A.F. Andreev, D.I. Pushkarov, "Dynamic equations of metals," Sov. Phys. JETP, vol. 62, no. 5, pp. 1087-1090, November 1985.

* The work was supported by the Russian Science Foundation under grant No. 22-29-20058.

S2-O-025301

ESTIMATIONS OF CRITICAL TEMPERATURE OF METALS FROM VACUUM ARC PLASMA PARAMETERS

M.M. TSVENTOUKH

Lebedev Physical Institute of Russian Academy of Sciences, Moscow, Russia

Vacuum arc cathode spot consists of ensemble of explosive electron emission pulses resembling the 'boiling' of metal surface. The plasma parameters of these splashes strongly vary in time and space within nanoseconds and micrometers, as can it be seen in experiments. However, there are some nearly invariant characteristic that depends on the element. In particular, the plasma expansion velocity vary in narrow range from about 5 to 20 km/s, and the average ions' charge vary from +1 to +3 for different metals. We have developed model for estimation of plasma parameters from parameters of the critical state of metal [1-3]. The model includes

(i) a Saha-like equation for the average charge of a weakly nonideal plasma,
(ii) two-temperature calculations with finite *e–i* relaxation rate, and
(iii) the current density evolution derived from a liquid-jet tearing model

Estimations for the ions kinetic energy and their average charge have been obtained

$$E_{kin} \approx 100\ T_{cr} \quad (1)$$

$$Z_{av} \approx 1 + T_{cr}/\mathrm{eV} \quad (2)$$

where T_{cr} – is the critical temperature of metal. Both estimations agree with typical experimental results for the T_{cr} values obtained by Fortov *et al* [4].

One may propose to evaluate critical temperature of metal T_{cr} and the corresponding cohesive energy $E_{coh} \approx 5\ T_{cr}$ from the experimentally measured vacuum arc plasma parameters – E_{kin} and Z_{av}.

It was found that the cathode voltage deviates from the ‘cohesive energy rule’ for Nb-Al composite and intermetallic cathodes [5]. Estimations by (1) and (2) from experimentally measured average charge and kinetic energy give T_{cr} and corresponding E_{coh} lower than that was calculated by DFT and USPEX in [5]. Values T_{cr} are close to that for Al for various cathode composition Nb/Al = ¼, ⅔, ¾. Deviation of character of cathode voltage from nearly linear dependence could be described by ‘cohesive energy rule’ with our new estimations of T_{cr} (and E_{coh}) from measurements of average ion charge and their kinetic energy by our model.

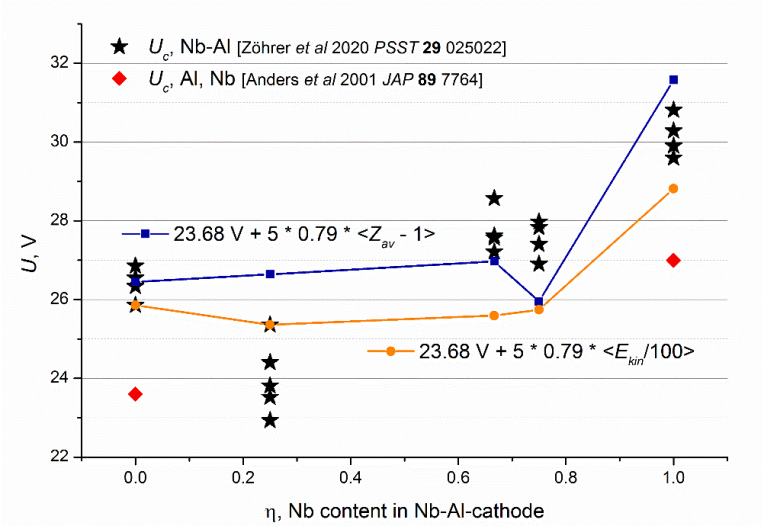

Measured cathode fall voltage values U_c for Nb-Al and estimations by average charge and kinetic energy of the vacuum arc plasma ions.

REFERENCES

[1] G. A. Mesyats and M. M. Tsventoukh 2015 *IEEE Trans. Plasma Sci.* **43** 3320
[2] M.M. Tsventoukh 2018 *Phys Plasmas* **25** 053504
[3] M.M. Tsventoukh 2021 *Phys. Plasmas* **28** 024501
[4] Fortov V.E., Dremin A.N., and Leont’ev A.A. 1975 *High Temp.* **13**(5) 984 [*Teplofiz. Vys. Temp.* **13**(5) 1072]
[5] Siegfried Zöhrer, Mehran Golizadeh, Nikola Koutná, David Holec, André Anders, and Robert Franz 2020 *Plasma Sources Sci. Technol.* **29** 025022

S2-O-033401

MODELING WAVEGUIDE FORMATION IN LASER-ASSISTED CAPILLARY DISCHARGES*

V.A. GASILOV, G.A. BAGDASAROV, N. SAVENKO

Keldysh Institute of Applied Mathematics (Russian Academy of Sciences), Moscow, Russia

A plasma-based acceleration scheme for particle acceleration by space charge wave was proposed by Y. Fainberg in 1956 [1]. Later on, plasma-based accelerators (PBA) were considered as an alternative for the conventional ones. PBAs use either intense laser pulses in the case of laser wake-field acceleration (LWFA) or charged particle beams passing through plasma in the case of plasma wake-field acceleration (PWFA). These acceleration approaches allow overcoming the most significant limitation in conventional accelerators - limited electric field gradient in radio frequency accelerating structures. Extreme LWFA accelerating gradients, demonstrated experimentally by different teams, offer a path towards a compact PBA needed in a broad variety of applications, including free-electron lasers (FEL). Comprehensive model of processes in a discharge capillary is required in order to obtain nominal parameters of a preformed plasma channel suitable for the laser wake-field acceleration [2]. We present 3D magnetohydrodynamics simulations of a hydrogen gas filling process and discharge plasma formation in a short square shape capillary with gas supply channels. Time evolution of the gas pressure and the plasma density in the capillary channel for a chosen discharge current profile is analyzed. Performed simulations provide distributions of the electric current, the magnetic field and the electron density along the whole channel, taking into account gas supply areas as well as areas outside of the capillary. Obtained results show that presence of gas supplies leads to the inhomogeneous plasma density distribution along the capillary channel which have to be taken into account for generating optimal laser-driven electron beam.

The computations were carried out using supercomputers K60 and K100 at KIAM RAS.

REFERENCES

[1] Ia. B. Fainberg, The use of plasma waveguides as accelerating structures in linear accelerators. In: CERN Symposium on High-Energy Accelerators and Pion Physics. Proceedings, 1st International Conference on High-Energy Accelerators, HEACC 1956, v.1-2 : CERN, Geneva, Switzerland, June 11-23, 1956, 84-90

[2] A. J. Gonsalves, K. Nakamura, J. Daniels, C. Benedetti, C. Pieronek, T. de Raadt, S. Steinke, J. Bin, S. S. Bulanov, J. van. Tilborg, C. G. R. Geddes, C. B. Schroeder, Cs. Toth, E. Esarey, K. Swanson, L. Fan-Chiang, G. Bagdasarov, N. Bobrova, V. Gasilov, P. Sasorov, W. P. Leemans, "Petawatt laser guiding and electron beam acceleration to 8 GeV in a laser-heated capillary discharge waveguide", Physical Review Letters 122, 084801 (2019)

* The work was supported by the Russian Science Foundation under grant No. 21-11-00362 https://rscf.ru/en/project/21-11-00362/.

S2-O-038701

THE PLASMA GENERATION ON COPPER AND DURALUMIN CONDUCTORS COATED WITH MOLYBDENUM OR BISMUTH *

N.A. LABETSKAYA[1], *I.M. DATSKO*[1], *S.A CHAIKOVSKY*[1,2], *V.A. VANKEVICH*[1], *V.I. ORESHKIN*[1]

[1]*Institute of High Current Electronics SB RAS, Tomsk, Russia*
[2]*Institute of Electrophysics UB RAS, Ekaterinburg, Russia*

The use of a double-layer structure of a conductor with an outer layer up to 100 μm thick, obtained by vacuum deposition, which has a lower conductivity, leads to a delay in the onset of plasma generation on its surface compared to a homogeneous conductor in fields with a maximum magnetic field induction of 200÷400 T [1,2]. In addition, the outer layer suppresses the development of plasma instabilities comparing to a homogeneous conductor [3]. Titanium or zirconium was usually used as the outer layer, and the main conductor was made of copper or duralumin.

Assuming such parameters as conductivity and mass of the ion of molybdenum and bismuth, these materials look quite promising. But the experiments on the MIG generator (current amplitude up to 2.5 MA, rise time 100 ns) show that the use of molybdenum and bismuth as the outer layer of double-layer conductors does not improve the results comparing to titanium and zirconium. Thus, when choosing a material of deposition as the outer layer for double-layer conductors, one should take into account both the features of the materials themselves and the methods of their deposition: adhesion, increased stresses in the material, the complexity of deposition of "thick" layers of tens of microns, etc.

REFERENCES

[1] I.M. Datsko, N.A. Labetskaya, S.A. Chaikovsky, V.V. Shugurov, "Skin electric explosion in double-layer conductors with a low-conductivity deposited layer", Technical Physics, vol.61, no.6, pp.855-859, 2016.

[2] I.M. Datsko, N.A. Labetskaya, S.A. Chaikovsky et al., "Delay in plasma generation on copper and duralumin conductors coated with titanium or zirconium", Journal of Physics: Conference Series, vol.1115, I.1, Article Number 022008, 2018.

[3] N.A. Labetskaya, S.A. Chaikovsky, I.M. Datsko et al., "Delayed large-scale instabilities on Ti-coated duralumin conductors", Journal of Physics: Conference Series, vol.946, I.1, Article Number 012135, 2018.

* The work was supported by RFBR and ROSATOM under grant No. 20-21-00036.

S2-O-043801

COMPACT TORUS COLLIDER

A.G.MOZGOVOY

Lebedev Physical Institute, Know How Ltd, Moscow, Russia

A compact torus or FRC is Field Reversed Configuration.is an axisymmetric configuration with a closed loop with a current in the plasma. The main advantage of such torus is the possibility of their acceleration and compression by an external magnetic field for use in inertial thermonuclear fusion, as well as in electric rocket thrusters or for collective ion acceleration. The main idea of a FRC collider in the formation of two torus with their subsequent acceleration towards each other.

Compact torus were obtained using theta-pinches at the Novosibirsk BINP, later at TRINITI, and the Sukhum Physicotechnical Institute. In the USA - in Livermore, Los Alamos. Currently, two private companies Tri Alpha Energy (rised 800 mil. $.+50 mil. $ from Rosnano) and Helion Energy (recieved 500 mil. $ in 2021) are conducting research on ICF using FRC. Their method of forming FRCs using theta-pinch is not effective - the current in a compact torus is always small, but it is promised to supply energy to the grid by 2024.

We have proposed a new method for formation of compact torus in inductive storage devices [1]. The energy of the magnetic field was accumulated in two inductors in the form of multi-start windings, such as an Archimedes spiral, placed on the end flanges of the vacuum chamber. Before the current maximum, plasma was injected into this volume and the current was forcibly cut off with exploding wires. When the current is cut off, a closed current loop arises in the plasma, capturing most of the magnetic flux (more than 70 percent) and storing the energy stored in the magnetic field. Two formed FRC with the same current direction begin to attract each other. When they collide, the plasma heats up and to flash of soft X-ray.

Seven independent capacitor banks and switches were used (a total of 60 capacitors, K-5-40, charging voltage 20-26 kV, energy storage up to 100 kJ)

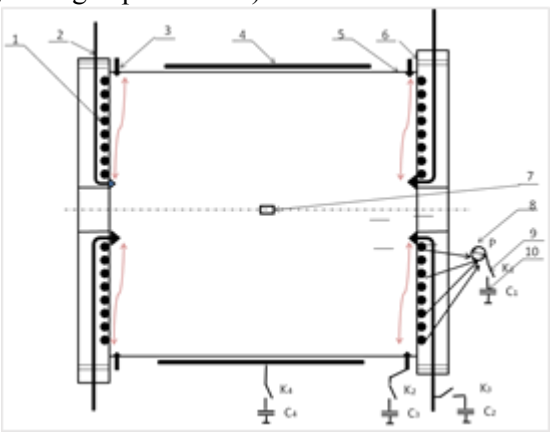

The current in the FRC, according to estimates, reached several tens of kiloamperes with a diameter of 30 cm. The plasma temperature at the collision site exceeded several keV and the duration of a soft X-ray pulse was about 1 microsecond, i.e. three orders of magnitude higher than in installations with a plasma focus and with a Z-pinch. 1 - inductive storage in the form of a 3-lead spiral, 2 - high-voltage electrodes (to create an azimuthal magnetic field), 3 - plasma guns, 4 - loops for radial plasma compression, 5 - vacuum chamber with a diameter of 300 mm, 6 - end flanges with inductive storage devices, 7 - magnetic field sensor in the center of the chamber, 8 - current breaker on exploding wires, 9 - K1-K4 switches (half shown) 10 - C1-C4 capacitor banks (half shown)

REFERENCES

[1] A. G. Mozgovoy, I. V. Romadanov, and S. V. Ryzhkov, Formation of a compact toroid for enhanced efficiency, Physics of Plasmas 21, 022501, 2014

S2-O-046201

STUDY OF PROCESSES OCCURRING IN POLYMERS TARGETS UNDER HIGH-ENERGY EXPOSURE *

O.G. OLKHOVSKAYA[1], *D.S. BOYKOV*[1], *V.A. GASILOV*[1], *E.D. KAZAKOV*[2], *S.I. TKACHENKO*[3], *A.R. SMIRNOVA*[2,3]

[1]*Keldysh Institute of Applied Mathematics of the Russian Academy of Sciences, Moscow, Russia*
[2]*National Research Center "Kurchatov Institute", Moscow, Russia*
[3]*Moscow Institute of Physics and Technology, Moscow, Russia*

Polymers and composites are often used as construction materials for aircraft, space, terrestrial transport, and many other industrial applications due to their high strength characteristics and relatively low weight of structures. The impact of powerful energy flows on polymer samples, for example, in experiments with relativistic electron beams, is one of the effective methods for analyzing the resistance of polymer materials to extreme loads. Experimental studies of short high intensity action on polymers usually are accompanied by numerical simulations. Modern tools of modeling thermomechanical effects during pulse loading of polymer samples allow study the details of wave structures as well as zones of material failures.

We studied the impact of a powerful relativistic electron beam on polymer targets at energy density up to 600 J/cm^2. Experiments were carried out on high current electron accelerator "Kalmar" at beam current up to 45 kA and electron energy up to 300 keV. Laser shadow streak image was used to visualize the dynamics of the passage of shock waves in transparent materials [1] and to record the plasma dynamics in the diode gap of the generator [2].

Three-dimensional numerical simulation of gasdynamic phenomena in the diode gap and elastoplastic phenomena that depend on them in the target material was performed using MARPLE3D [3] multiphysics software package. Our report concerns with the new technique designed for end-to-end modeling including hydrodynamic of heating and evaporation of the target under the action of the electron beam; evaporation of the cathode material and interaction of plasma streams in the diode gap; nonlinear wave processes leading to internal fractures and spalling phenomena in the target material. We use wide-range equation of state (semi-empirical QEOS model) [4] for the description of the liquid and solid phases of matter at low temperatures.

Appropriate modeling of this complex multiphysics problem is based on high resolution numerical methods as well as on high performance computing. The implemented computer models are verified by experimental data. Comparison of simulation results with experimental data are used to test the used models of volumetric fractures and spallations in brittle solids and validate wide-range equations of state. The developed software can be used for numerical stress-strain analysis of various structural units loaded by strong pulsed forces and/or energy fluxes.

The calculations were performed using supercomputers K-60 and K-100 in KIAM RAS.

REFERENCES

[1] Demidov, B.A., Kazakov, E.D., Kalinin, Y.G. *et al.* Application of Laser Shadow Streak Image for Studying the Dynamics of Shock Waves in Transparent Materials. *Instrum Exp Tech* **63,** 370–374 (2020). https://doi.org/10.1134/S0020441220030094

[2] Kazakov, E.D., Kalinin, Y.G., Krutikov, D.I. *et al.* Methods of Laser Shadow Photography with Recording by Streak Camera to Study Plasma Dynamics in the Diode of a Relativistic Electron Beam Generator. *Plasma Phys. Rep.* **47,** 803–813 (2021). https://doi.org/10.1134/S1063780X21080067

[3] Gasilov, V.A., Grushin, A.S., Ermakov, A.S. *et al.* Simulation of the Destruction of Polymer Materials under the Action of Intense Energy Flows. *Math Models Comput Simul* **11,** 198–208 (2019). https://doi.org/10.1134/S2070048219020066

[4] https://www.keldysh.ru/cgi/thermos/navigation.pl?en,home.

* The work was supported by the grant of the Russian Science Foundation, RSF № 21-11-00362, https://rscf.ru/project/21-11-00362/.

S2-O-048501

EVOLUTION OF MITL PARAMETERS DURING THE PASSAGE OF A POWERFUL CURRENT PULSE*

S.I.TKACHENKO [1,2,3], V.V.ALEKSANDROV [1], I.N.FROLOV [1], E.V.GRABOVSKY [1], K.M.MITROFANOV [1], YA.N.LAUKHIN [1], G.M.OLEINIK [1]

[1]*JSC SRC RF TRINITI, Moscow Troitsk, Russia*
[2]*Moscow Institute of Physics and Technology (National Research University), Dolgoprudny, Moscow Region, Russia*
[3]*Joint Institute for High Temperatures, Russian Academy of Sciences, Moscow, 125412 Russia*

When a submicrosecond current with a linear density of more than 1 MA/cm flows over MITL, a significant heating of the metal occurs, up to melting, evaporation, and ionization. In the experiments, a thick-walled tube made of stainless steel was used as a MITL model. To simulate the processes occurring in a thick-walled tube when a current with a high linear density is passed through it, numerical calculations were carried out. A system of one-dimensional one-temperature magnetohydrodynamic equations was solved (in [1], a similar problem was studied for thin-walled tubes – the wall thickness is less than the skinning thickness of the magnetic field).

To describe the properties of a real substance, wide-range semi-empirical equations of state [2] were used, taking into account phase transformations (melting and evaporation) and the possibility of realizing metastable states, as well as the dependence of transport properties (conductivity and heat capacity) on temperature [3, 4]. The parameters of the tube made of stainless steel and the time dependence of the current in numerical calculations were used those that were used in the experiments.

At different times, the distributions of pressure, temperature, substance density, and current density over the wall thickness of a tube with an outer diameter of 3 mm and a wall thickness of 220 μm were obtained. It can be seen that by the time of 100 ns, the current density is almost uniformly distributed over the thickness; the substance density decreased most of all at the outer boundary of the tube in the region where the temperature increased the most. By this moment, the substance of the tube from the outer boundary and slightly more than to the middle of its thickness is already in a liquid state; the remaining part near the inner boundary has not yet had time to melt to the end and is in a two-phase state of a solid–liquid.

The time for the melting wave to reach the inner surface of the tube is clearly seen in the time dependence of the resistive voltage calculated on the inner surface of the tube. The same voltage was measured in experiments; comparing them, it can be stated that the time of the melting wave reaching the surface of the inner boundary of the tube and its duration coincide in experiments and numerical calculations.

REFERENCES

[1] E. V. Grabovskii, P. R. Levashov, G. M. Oleinik, C. L. Olson, P. V. Sasorov, V. P. Smirnov, S. I. Tkachenko, and K. V. Khishchenko. Plasma Physics Reports, 2006, Vol. 32, No. 9, pp. 718–728.

[2] Fortov V.E., Khishchenko K.V., Levashov P.R., Lomonosov I.V. Wide-range multi-phase equations of state for metals, Nucl. Instr. Meth. Phys. Res. A 415 (1998) 604.

[3] E. V. Grabovski, P. R. Levashov, G. M. Oleinik, C. L. Olson, P. V. Sasorov, V. P. Smirnov, S. I. Tkachenko, and K. V. Khishchenko Formation and Dynamics of Plasma Layers Formed on the Foil Surface under the Action of a High-Current Pulse. Plasma Physics Reports, 2006, Vol. 32, No. 9, pp. 718–728.

[4] H. Knoepfel, Pulsed High Magnetic fields (North-Holland, Amsterdam, 1970.

* This work was supported by the Russian Foundation for Basic Research (project no. 20-21-00082)

S2-P-001403

TRIGGERING STABILITY OF THE COLD-CATHODE THYRATRON WITH A TRIGGER UNIT BASED ON FLASHOVER*

N.V. LANDL, Y.D. KOROLEV, V.G. GEYMAN, O.B. FRANTS, G.A. ARGUNOV, I.A. SHEMYAKIN

Institute of High Current Electronics SB RAS, Tomsk, Russia

Currently, high-current switching devices based on low-pressure hollow-cathode pulsed discharge (so-called pseudospark switches) are widely used [1-4]. The design and principle of operation of these switches are close to those of a classical hot-cathode hydrogen thyratrons. However, these devices do not have a hot cathode. Therefore, pseudospark switches are often called cold-cathode thyratrons or thyratrons with a grounded grid [3, 4].

As in the case of classical thyratrons, a range of operating pressures of the switch corresponds to the left branch of Paschen's curve. Under these conditions, the electron free path for ionization is much in excess of the electrode separation. For both self-breakdown of the main gap of the thyratron and for external discharge triggering a considerable pre-breakdown electron current is required [1, 3, 5]. For the case of external triggering, this current is provided due to a special trigger unit that is placed in the main cathode cavity. One type of trigger units is based a discharge over a dielectric or semiconductor surface or, in other words, based on a flashover [3, 4].

Any trigger unit is intended for plasma generation of trigger discharge inside the thyratron cathode cavity at a curtain instant of time. When a trigger unit based on discharge formation over the dielectric surface is used, trigger discharge plasma is generated due to the interception of surface discharge current to the main cathode cavity. In this report the results of investigation of the trigger unit based on discharge over the dielectric surface with the high value of dielectric permittivity are presented. Schematic of the experimental setup is shown in fig. 1. Experiments were carried out with the demountable single-gap thyratron with the external gas filling. Data on delay times to discharge initiation in the trigger unit, current interception to the main cathode cavity and breakdown in the thyratron main gap were obtained.

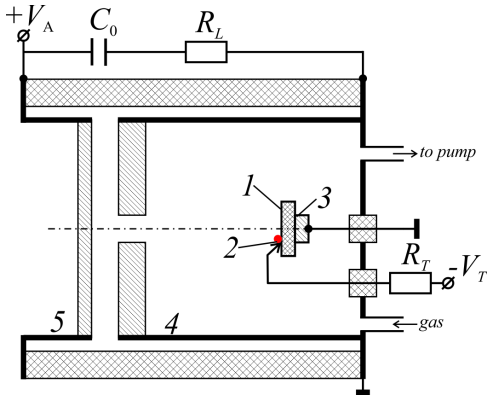

Fig.1. Schematic of the experimental setup. 1 – dielectric, 2 – multipoint contact, 3 – ground contact, 4 – main cathode cavity, 5 – main anode, V_A = 15 kV, R_L = 15 Ω, C_0 = 10 nF, R_T = (15 – 50) Ω, V_T = (2 – 8) kV.

REFERENCES

[1] Y.D. Korolev and N.N. Koval, "Low-pressure discharges with hollow cathode and hollow anode and their applications," J. Phys. D: Appl. Phys., vol.51, Article Number 323001, 2018.

[2] K Bergmann, M Muller, D Reichartz, W Neff and R Lebert, “Electrode phenomena and lifetime considerations in a radial multichannel pseudospark switch,” IEEE Trans. Plasma Sci., vol.28, pp. 1486-1490, 2000

[3] Y.D. Korolev, K. Frank, “Discharge formation processes and glow-to-arc transition in pseudospark switch,” IEEE Trans. Plasma Sci., vol.27, p.1525, 1999

[4] V.D. Bochkov, V.M. Dyagilev, V.G. Ushich, O.B. Frants, Y.D. Korolev, I.A. Shemyakin, K. Frank, “Sealed-off pseudospark switches for pulsed power applications (current status and prospects),” IEEE Trans. Plasma Sci., vol.29, no.5, pp. 802-808, 2001.

[5] Y.D. Korolev, N.V. Landl, V.G. Geyman, O.B. Frants, G.A. Argunov, A.V. Bolotov, “Role of Prebreakdown Currents in a Static Breakdown of a Two-Sectioned Cold-Cathode Thyratron, Russ.Phys.J., vol.62, No.7, pp.1269-1278, 2019

* This work was funded by RFBR according to the research project № 19-48-700023.

S2-P-003401

CONDUCTION CURRENT IN LOW-DENSITY PLASMA OPENING SWITCHES*

S.V. LOGINOV

Institute of High Current Electronics SB RAS, Tomsk, Russia

Recently [1], a new concept of conduction has been proposed for low-density plasma opening switches. The concept suggests that a unipolar ion layer is formed near the cathode as electrons leave it under the action of an electric field induced by magnetic field penetration into the plasma. The main aspects of this concept, being an alternative to that on the formation of a bipolar near-cathode space charge layer subject to unlimited cathode emissivity [2], are reduced to the following.

For a collisionless plasma, the magnetization time of electrons in a rising magnetic field is given by $\tau = (3mc / e\dot{B})^{1/2}$, where $\dot{B}$ is the field rise rate, m and e are the electron mass and charge, c is the velocity of light. The transport of current across a strong magnetic field is provided by electron drift in crossed magnetic and polarization electric fields. The polarization field results from charge separation during the motion of electrons in the current channel. As a result, the velocity of field penetration into a plasma of density n is given by $u = (\dot{B}c / 6\pi en)^{1/2}$, and the switch conduction current for this velocity by $I_c = (3\pi encr_c^2 \dot{B} l^2 / 2)^{1/2}$.

The paper presents a comparison of the derived relations with experimental data [3], showing that the conduction current behaves strictly as $I_c \propto n^{1/2}$ at a plasma density of about 10^{11} – 10^{14} cm^{-3} and field rise rate of about 0.3 – 4 kA/ns and that this behavior holds for any plasma bridge length. Attaining the same conduction current at different bridge lengths requires that nl^2 be constant. As the magnetic field rise rate varies, the conduction current behaves as $I_c \propto \dot{B}^{1/2}$. These results differ radically from what is predicted by the bipolar model [2]. Additionally, the paper presents arguments of why the axial current channel width varies nonmonotonically during a pulse and gives estimates of the electron temperature in plasma opening switches at different plasma densities and field rise rates.

REFERENCES

[1] S.V. Loginov, “Self-magnetic insulation in plasma opening switches”, J. Plasma Phys., vol.86, Article Number 905860609, 2020.

[2] P.F. Ottinger, S.A. Goldstein S.A., Meger R.A., “Theoretical modeling of the plasma erosion opening switch for inductive storage applications”, J. Appl. Phys., vol. 56, no. 3, pp. 635–648, August 1984.

[3] B.V. Weber, R.J. Commisso, G. Cooperstein et al., “Plasma erosion opening switch research at NRL”, IEEE Trans. Plasma Sci., vol. 15, no. 6, pp. 774–784, December 1987.

* The work was performed under State Assignment of the Ministry of Science and Higher Education of the Russian Federation (project No. FWRM-2021-0001).

S2-P-007302

TIME-RESOLVED MEASUREMENT OF THE TEMPERATURE OF A PINCHED DENSE PLASMA BY THE RATIO OF THE SIGNALS OF TWO X-RAY DIODES WITH DIFFERENT SPECTRAL RESPONSE *

S.A. SOROKIN

Institute of High Current Electronics SB RAS, 2/3 Akademichesky Ave., Tomsk 634055, Russia, s.sorokin@rambler.ru, +7(3822)491617

One of the most effective ways to create a hot dense plasma is the implosion of cylindrical shells (liners) by the current of a high-current generator. The density of energy and particles of the pinched plasma are largely determined by the implosion time (initial radial size) of the liner, which should be longer than the rise time of current through the liner. Due to the preliminary injection of plasma into the region of the liner load, the rise time of the current through the liner can be reduced to several nanoseconds, and the initial radius of the liner can be reduced to 1 mm or less [1,2]. This approach makes it possible to obtain a plasma column with a particle density higher than the particle density in a solid, and a plasma energy density of more than 10^8 J cm^{-3} already at a generator current of 1-2 MA. The spectrum of thermal X-ray emission from such a plasma can be close to the Planck spectrum, which makes it possible to determine the plasma temperature from the ratio of the signals of radiation sensors with different spectral responses. In this work, under the assumption of the Planck radiation spectrum, the temperature dependence of the signal ratio of two photoemission X-ray diodes (XRDs) with an aluminum photocathodes and polypropylene filters 10 μm and 20 μm thick is calculated (Fig.1). It can be seen that in the temperature range from 100 eV to 350 eV there is a strong dependence of the signal ratio on temperature. The calculation results were used to determine the temperature of the pinched plasma column, which is formed after the 2-MA implosion of liners about 1 mm in diameter, made of 2.5-μm thick aluminum foil. The temperature measured in this way during the evolution of the plasma after its first stagnation satisfactorily corresponds to the temperature estimate from the Bennett relation.

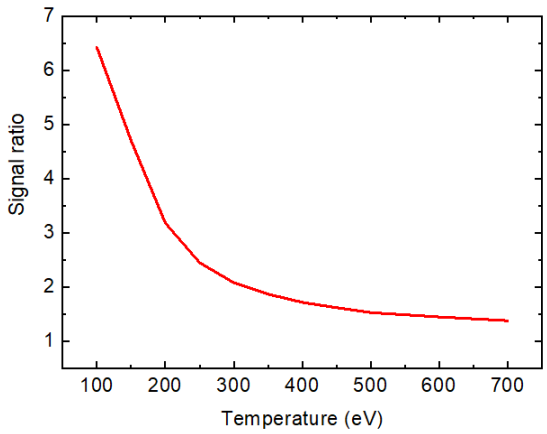

Fig. 1. Results of calculating (under the assumption of the Planck radiation spectrum) the temperature dependence of the signal ratio of two photoemission X-ray diodes (XRDs) with an aluminum photocathodes and polypropylene filters 10 μm and 20 μm thick.

REFERENCES

[1] *Sorokin S.A. //* Plasma Physics Reports. – 2017. – Volume 43. – № 5. Pages 542–546.
[2] *Sorokin S.A. //* Physics of Plasmas. – 2019. – Volume 26. – № 8. Pages 082706.

* This work was supported by the Russian Foundation for Basic Research (grant No. 18-08-00155).

S2-P-019601

SOME FEATURES OF CURRENT SHEET FUNCTIONING IN GAS-PLASMA SYSTEMS*

V.A. KOKSHENEV, A.V. SHISHLOV, R.K. CHERDIZOV

Institute of High Current Electronics SB RAS, Tomsk, Russia

The paper analyzes the results of experiments with argon/deuterium gas-puffs with an outer plasma shell. The dynamics and characteristics of the current sheet (CS) were studied using magnetic probes (*B-dot*) and optical diagnostics [1]. Measurements of the currents in the CS using *B-dot*, installed at different radii from the axis of the system, but at the same level relative to the cathode surface, show that there is a decrease in the amplitude of the current *B-dot* relative to the generator current *Ig* as the CS moves towards the center. The width of the current sheet decreases as one moves toward the axis with an increase in the average current density from units of kA/cm^2 to tens of kA/cm^2. Such high current densities cannot be explained by thermal, auto- or photoemissions. Obviously, a dense explosive emission plasma is formed on the cathode, which provides emission with a current density of tens of kA/cm^2. This high concentration plasma will expand into the interelectrode gap, and its front becomes the emitting cathode. A double layer is formed at the boundary between the dense cathode plasma and the injected anode plasma, as is the case in plasma opening switch.

When the cathode plasma expands into the interelectrode gap with a simultaneous increase in the magnetic field, it is possible to shift the emission boundary from the electrode into the plasma with shielding of part of the current in *B-dot*. This may be one of the reasons for the decrease in the current amplitude obtained by integrating the signal from magnetic probes near the pinch axis. An experiment with magnetic probes installed at different levels relative to the cathode plane confirms the possibility of such a scenario. On Fig. 1 shows a graph of the fraction of the probe current *IK*2 at a radius of 6 cm relative to the generator current *Ig* depending on the location of *B-dot* relative to the cathode grid.

The dynamics of the CS during the implosion of gas-puffs is the essence of the evolution of the near-cathode double layer and the current sheath formed by electrons injected from the cathode plasma. The acceleration of ions in a CS can only occur in an electric field. In our case, a self-consistent electric field arises in the CS due to the Hall effect and directed to the axis of the system: $E_r \sim j_z B_\varphi / en$. On the basis of optical diagnostics, the appearance of a glow on the axis of the system was registered at the moments when the front of the CS did not reach the center. Obviously, this is the registration of a shock wave front with a jump in density and temperature.

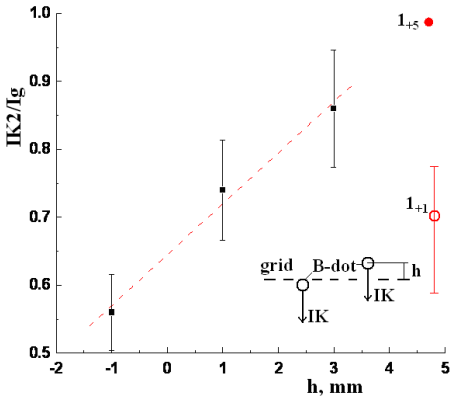

Fig.1. Graph of the dependence of the current fraction in the CS *IK*/*Ig* on the position of *B-dot* relative to the cathode plane h at a radius of 6 cm. Points 1_{+1} and 1_{+5} were obtained for *B-dot* at a radius of 3 cm in an experiment with an argon gas-puff with an outer plasma shell, 1_{+1} - standard position of the sensor (completely above the grid), 1_{+5} - the sensor is raised by 5 mm into the interelectrode gap (h = 5 mm).

REFERENCES

[1] V. Kokshenev, A. Rousskikh, A. Shishlov et al., "Formation and dynamics of the current sheath in the plasma shell of a Z-pinch in the microsecond implosion regime", 7th International Congress on Energy Fluxes and Radiation Effects (EFRE), Tomsk, Russia, pp. 217-221, 2020, doi: 10.1109/EFRE47760.2020.9241970.

* The work was supported by the Russian Science Foundation under grant No. 22-29-01554.

S2-P-019602

CHARACTERISTICS OF PLASMA JETS OF A HIGH-CURRENT VACUUM-ARC DISCHARGE*

V.A. KOKSHENEV, N.E. KURMAEV

Institute of High Current Electronics SB RAS, Tomsk, Russia

Plasma sources based on high-current discharges in vapors of aluminum electrode material initiated by breakdown along the surface of ceramics based on aluminum oxide are studied. Two geometries of discharge gaps with a corundum ceramic insert between the cathode and anode were tested. Option 1 - end, where the cathode, anode and the surface of the ceramic insert are in the same plane, option 2 - the cathode was inside the ceramic tube with an increase in the gap along the surface of the ceramic by 2-3 times. The capacitive storage provided the oscillatory regime of the discharge current with a period of ~5.7 μs. The discharge was initiated by a high-voltage breakdown over the surface of a ceramic insert between the electrodes. The current amplitude of the plasma gun was controlled both by the charging voltage (30–40 kV) and by the connection circuit [1].

The plasma flow velocity was measured by the time-of-flight technique using double probes with a reference electrode [1]. The flow velocity was measured by the time shift of the signal maximum from two probes. The figure shows a graph of the dependence of the plasma flow velocity on the amplitude of the vacuum arc current. It is found that with an increase in the discharge current, both the velocity and the concentration of the plasma jet increase for both variants of the discharge gap. The recorded decrease in the opening angle of the plasma jet with increasing current is obviously associated with an increase in the influence of the intrinsic magnetic field on the compression of the current-carrying plasma [2].

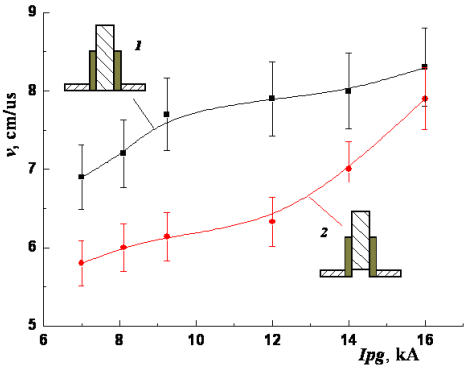

Fig.1. Зависимость скорости плазменного потока от разрядного тока. Dependence of the plasma flow velocity on the discharge current.

Large values of velocity for variant 1 can be associated with a more effective action of electrodynamic forces as the main mechanism for accelerating the current-carrying plasma along the axis of the system. If we assume that the velocity of the plasma bunch in the section between the discharge gap and the probes changes insignificantly, then the formation of a directed flow lags behind the onset of the current by ~ (200–300) ns. Due to the high thermal stability of the corundum dielectric insert, ceramic ablation is negligible. The plasma flow basically consists of ions of the electrode material with a significant proportion of ions of the cathode jet [2]. Plasma compression can be associated with the dynamic head of the convergent ion flow characteristic of the inertial regime. Estimation of the plasma concentration from the hydrodynamic model of a current-carrying jet gives the value $n \sim I^2/(M_i v^2) \sim (1\text{-}2)\cdot 10^{15}$ см$^{-3}$ for aluminum ions.

REFERENCES

[1] V.A. Kokshenev and N.E. Kurmaev, "Formation of plasma jets by a high-current discharge in metal vapor", J. Phys.: Conf. Ser. 2064 (2021) 012033 IOP Publishing doi:10.1088/1742-6596/2064/1/012033.

[2] V.I. Krasov, I.A. Krinberg, V.L. Paperny et al., "Acceleration of ions during the expansion into vacuum of a high-current cathode plasma jet", Tech. Phys. Letters., vol.33, № 22, pp. 1–8,2007.

* The work was performed under State Assignment of the Ministry of Science and Higher Education of the Russian Federation (project No. FWRM-2021-0001).

S2-P-023101

ELECTRICAL EXPLOSION OF FLAT COPPER CONDUCTORS IN CURRENT SKINNING MODE*

V.A. VAN'KEVICH[1], *I.M. DATSKO*[1], *N.A. LABETSKAYA*[1], *S.A. CHAIKOVSKY*[1, 2], *E.V. ORESHKIN*[3], *V.I. ORESHKIN*[1]

[1]*Institute of High Current Electronics of the Siberian Branch of the Russian Academy of Sciences, Akademichesky Avenue 2/3, Tomsk 634055, Russia*
[2]*Institute of Electrophysics of the Ural Branch of the Russian Academy of Sciences, Amundsen 106, Yekaterinburg 620016, Russia, UD, RAS, Yekaterinburg, Russia*
[3]*Lebedev Physical Institute, RAS, Moscow 119991, Russia*

Experimental studies of the explosion of flat copper conductors on the MIG facility at a current level of 2 MA passing through them and a current pulse rise time of 100 ns have been carried out. In these experiments, we have studied the electric explosion of flat conductors in the current skinning mode, and the propagation of a magnetic field nonlinear diffusion wave that occurs during such explosion. The magnitude of the magnetic field induction significantly exceeded the values required for the explosion of both plate surfaces in a symmetrical configuration. The conductor surface plasma formation was recorded by its glow in the visible range using a four-frame optical camera with an exposure time of 3 ns for each frame. The internal structure of the surface plasma at different times was studied with X-ray radiography with $h\nu > 0.8$ keV and an exposure time of 2-3 ns, which is formed in the X-pinch "hot spot". It has been shown that during the explosion in megagauss magnetic fields of flat conductors, the width of which (along the x-axis) is much greater than their thickness (along the y-axis), and the current flows in the direction of the z-axis, the plasma expansion along the x-axis is suppressed, and the conductor expands along the y-axis almost from the beginning of the current flow through it. In this case, large-scale instabilities develop on the foil edge, the appearance of which is similar to the instabilities that develop during the cylindrical conductors explosion. On the wide side of the plate along its longitudinal axis z, approximately 75 ns from the current beginning, a plasma channel is formed. Estimations, that were made taking into account the enhancement of the magnetic field at the foil edges showed that it takes about 70-80 ns for the propagation of magnetic field nonlinear diffusion wave from the foil edge to its center. Interpretation of the experimental results was carried out using radiation magnetohydrodynamic simulation (RMHD) of the flat conductor's explosion process. The performed magnetohydrodynamic calculations showed good agreement with the results of experiments on measuring the expansion rate along the y-axis from X-ray shadow patterns.

*The work was supported by the Russian Science Foundation (grant No. 20-19-00364).

S2-P-024801

DENSITY DISTRIBUTION OF THE NEAR-SURFACE SUBSTANCE AT THE INITIAL STAGE OF THE PLASMA FORMATION PROCESS DURING THE SKIN EXPLOSION OF CYLINDRICAL CONDUCTORS*

I.M. DATSKO[1], N.A. LABETSKAYA[1], S.A. CHAIKOVSKY[1, 2], V.A. VAN'KEVICH[1], V.I. ORESHKIN[1]

[1]Institute of High Current Electronics of the Siberian Branch of the Russian Academy of Sciences, Akademichesky Avenue 2/3, Tomsk 634055, Russia
[2]Institute of Electrophysics of the Ural Branch of the Russian Academy of Sciences, Amundsen 106, Yekaterinburg 620016, Russia, UD, RAS, Yekaterinburg, Russia

Plasma formation on the conductor surface is a key issue in terms of the energy imputed into the metal substance. For the magnetic field growth rates, which are characteristic for magnetically isolated transmission lines of multi-megaampere generators, this issue remains insufficiently studied. Therefore, the task of this work was to study the dynamics of plasma and its density on the metal surface at magnetic induction values up to 700 T and its growth rates of (2-7) T/ns. The experiments were carried out on a pulse-power MIG generator at a current amplitude of up to 2.5 MA and a rise time of 100 ns. The formation of plasma on the conductor surface was recorded by its glow in the visible range using a four-frame optical camera with an exposure time of 3 ns for each frame. In addition, vacuum photoemission diodes recorded the surface plasma reaching a temperature of more than 1 eV in the black body approximation. The surface plasma internal structure, the estimation of the substance density in it and its radial distribution were studied using X-ray radiography obtained by transmission with $h\nu > 0.8$ keV and an exposure time of 2-3 ns, which is formed in the "hot spot" X-pinch. According to the data of X-ray studies of the conductor's electric explosion, the distribution profile of the substance along its radius at various points in time was simulated by means of the developed calculation code using the Abel transformation. In the course of the experiments, the cylindrical conductor's electric explosion made of various materials and with various diameters was studied, which made it possible to study the formation of plasma at different magnetic field induction growth rates up to 7 T/ns. It is shown that current increase prompts the lighting up of "spots" on the cylindrical conductor surface, and they serve as sources of low-temperature and relatively low-density plasma, that is, they are centers of plasma formation. Subsequently, current channels develop in this plasma. The dependences of $\mu \cdot \rho$ on the conductor radius in the selected section of the X-ray radiography picture of its explosion are obtained. The value of the mass radiation absorption coefficient μ was determined from the X-ray transmission patterns of stepped filters made of the same conductor material as the exploding one. The dependences of the load substance ρ density on its radius at different moments of time from the current beginning are determined and plotted.

If the maximum field on the conductor surface is more than 600 T, which in our experiments was achieved with their initial diameter less than 1 mm, then for a duralumin conductor with an initial diameter of 0.95 mm in the visible range, its size increased at 104 ns up to 1.46 mm, and at 144 ns - up to 2.4 mm. In this case, density estimations of the substance that expanded by 65 μm to 80 ns relatively to the initial radius (that is, at a radius of 0.54 mm) are 0.17–0.19 g/cm^3, and at a radius of 0.5 mm from the axis, 0.45 g/cm^3. By 142 ns, a density of more than 0.15 g/cm^3 is reached at a radius of 0.7 mm, and at a radius of 1 mm, the substance density in the column is 0.01 g/cm^3. The streaks of instabilities at this time expand up to 700 μm from the initial conductor radius, and the density of matter in them is less than 0.01 g/cm^3. It can be concluded that the low density of matter at the boundary of the plasma column does not allow us to assume any significant fraction of the current carried by it.

*The work was supported by the Russian Science Foundation (grant No. 20-19-00364).

S2-P-033502

3D MODELING OF PARTIALLY IONIZED PLASMA INTERACTED WITH MAGNETIC FIELD[1]

Y.S. SHAROVA[1]

[1]*Keldysh Institute of Applied Mathematics, RAS, Moscow, Russia*

Plasma physics is a vast area of physics, which includes both fundamental aspects, such as, for example, astrophysics, and more applied ones: new compact plasma accelerators, compact powerful sources of X-ray and gamma radiation, new promising, practically inexhaustible sources of clean energy due to controlled thermonuclear fusion, compact ion sources for cancer therapy and isotope sources for nuclear medicine. Currently, studies of non-stationary and non-equilibrium processes in pulsed plasma created under the influence of high-intensity energy flows on matter are topical. Energy flows of multiterawatt and petawatt power levels are created, for example, in laboratory conditions, by electric pulse generators, as well as by short-pulse laser installations.

This paper presents a hydrodynamic model that considers ions and neutrals as separate fluids that interact with each other through collisional processes. In this case, the evolution of ions is determined by the system of magnetic hydrodynamics, and of neutrals - by ordinary, non-magnetic hydrodynamics. Such an approximation makes it possible to carry out simulations and study effects in a partially ionized plasma [1,2]. The code MARPLE3D (Keldysh Institute of Applied Mathematics, Russian Academy of Sciences), developed for solving problems of magnetic radiation gas dynamics on high-performance cluster-type computing systems, was used for simulation [3].

REFERENCES

[1] Y.S. Sharova, “MHD simulation of supernova remnant dynamics taking into account the neutral component of the plasma”, Matem. Mod., vol. 34, no. 1, pp. 47–58, 2022. https://doi.org/10.20948/mm-2022-01-04

[2] Y.S. Sharova, S.I. Glazyrin and V.A. Gasilov, “Study of the Influence of the Background Neutral Component on the Dynamics of the Envelope in Supernova Remnants”, Astron. Lett., vol. 47, pp. 746–753, March 2021. https://doi.org/10.1134/S1063773721110050

[3] G. A. Bagdasarov, A. S. Boldarev, V. A. Gasilov, et al., State Registration Certificate no. 2012660911 from December 30, 2012, Program for a Computer ‘‘MARPLE Software Package.’’

[1]The work was supported by the grants the Russian Science Foundation (project No. 21-11-00362).

S2-P-043201

ELECTRIC EXPLOSION OF MICROWIRES BY HIGH FREQUENCY CURRENT.*

V.I. ORESHKIN[1], *S.A. BARENGOLTS*[2], *E.V. ORESHKIN*[3]

[1] *Institute of High Current Electronics, RAS, Tomsk 634055, Russian Federation*
[2] *Prokhorov General Physics Institute, RAS, Moscow 119991, Russian Federation*[1]
[3] *Lebedev Physical Institute, RAS, Moscow 119991, Russian Federation*

In various accelerating structures operating at a high frequency, an important role is played by the mechanism of explosive emission [1]. Such a situation can be realized, for example, at the Compact Linear Collider (CLIC) [2], the development of which is being carried out within the framework of international cooperation. In the process of explosive emission, an electric explosion of metal microprotrusions occurs on the cathode surface, and the one formed during the explosion emits electrons. In this work, using magnetohydrodynamic calculations, the influence of the frequency of an electromagnetic pulse on the characteristics of an electric explosion is determined.

REFERENCES

[1] Mesyats, G. A. “Ecton or electron avalanche from metal,” Physics-Uspekhi, 38(6), 567. 1995

[2] Raubenheimer, T. O. et al. “A 3 TeV $ e^+ E^-$ Linear Collider Based on CLIC Technology,“No. CERN-2000-008, 2000.

* The work was supported part by RFBR and ROSATOM according to the research project No. 20-21-00036.

S2-P-046202

3D NUMERICAL SIMULATION OF WIRE-ARRAY Z-PINCHES *

O.G. OLKHOVSKAYA[1]

[1]*Keldysh Institute of Applied Mathematics of the Russian Academy of Sciences, Moscow, Russia*

Experiments at Angara 5-1 facility [1] on the current implosion of combined nested arrays [2] and single arrays of metalized dielectric fibers [3] have demonstrated stable and compact compression of the metal plasma. The presence of substances with a low rate of plasma ablation at the periphery of the arrays leads to suppression of the development of magnetic Rayleigh-Taylor instability in plasma at the axis of the array, as compared with the compression of the of single cylindrical wire arrays. As a result, stable and compact Z-pinches were formed, and SXR pulses with the amplitude of 5–7TW and the duration about 5ns were obtained.

The report is devoted to numerical simulation of implosion of combined arrays with various designs. The aim of the simulation is to explore the interaction of plasma flows and the magnetic field during the implosion of different types of wire arrays, determine the physical conditions for a shock wave region formation between the arrays, and help to control the time profile and amplitude of the resulting SXR pulse.

Three-dimensional numerical simulation is based on two-temperature radiative magnetic gasdynamic (RMHD) model with dissipation implemented in multiphysics program package MARPLE-3D [4]. The data on the equations of state and optical properties of matter were calculated using the THERMOS program [5]. For modeling combined arrays from various materials, the MARPLE-3D code has been upgraded to solve hydrodynamic problems for the flow of a multicomponent mixture. To describe the evaporation of wires under the action of a current, a semi-empirical model [6] is used, taking into account the experimental data on the plasma ablation rate [3]. Thus the process of non-stationary plasma generation of fibers and wires is reproduced adequately. Appropriate modeling of this complex multiphysics problem is based on high resolution numerical methods as well as on high performance computing. The implemented computer models are verified by experimental data.

The numerical simulation as a whole reproduces the main tendencies registered in experiments with combined arrays. The computations confirmed the experimentally found existence of an optimal configuration with an external array mass in the range 7–10μg/cm. Numerical simulation using 3D RMHD code made it possible to visualize the interaction of the plasma of the arrays, namely: the spreading of the plasma jets of the outer array as a result of their interaction with the magnetic field of the inner array and the formation of a quasi-homogeneous shell from the plasma of the outer cascade around the inner cascade. A comparison of the calculated values of the power and total energy of the SXR pulse with the experimental data was used to calibrate the RMHD code and the model of the matter properties.

The calculations were performed using supercomputers K-60 and K-100 in KIAM RAS.

REFERENCES

[1] https://www.triniti.ru/en/services/unikalnye-nauchnye-ustanovki/angara-5-1/

[2] Mitrofanov, K.N., Aleksandrov, V.V., Grabovski, E.V. *et al.* Study of Implosion of Combined Nested Arrays. *Plasma Phys. Rep.* **43,** 1147–1171 (2017). https://doi.org/10.1134/S1063780X17120042

[3] Mitrofanov, K.N., Aleksandrov, V.V., Gritsuk, A.N. *et al.* Specific features of implosion of metallized fiber arrays. *Plasma Phys. Rep.* **43,** 141–163 (2017). https://doi.org/10.1134/S1063780X17020106

[4] Aleksandrov V.V. et al. STUDY OF INTERACTION BETWEEN PLASMA FLOWS AND THE MAGNETIC FIELD AT THE IMPLOSION OF NESTED WIRE ARRAYS. Plasma Physics and Controlled Fusion. 2019. v. 61. N 3. p. 035009.

[5] https://www.keldysh.ru/cgi/thermos/navigation.pl?en,home.

[6] Aleksandrov, V.V., Branitskii, A.V., Volkov, G.S. *et al.* Dynamics of Heterogeneous Liners with Prolonged Plasma Creation. *Plasma Phys. Rep.* **27,** 89–109 (2001). https://doi.org/10.1134/1.1348487

* The work was supported by the grant of the Russian Science Foundation, RSF № 21-11-00362, https://rscf.ru/project/21-11-00362/.

S3-O-018201

RADIATION OF HIGH-POWER LINEARLY POLARIZED ULTRAWIDEBAND PULSES OF SUBNANOSECOND DURATION BY A HYBRID ANTENNA*

E.V. BALZOVSKY, Y.I. BUYANOV, A.M. EFREMOV, V.I. KOSHELEV, E.S. NEKRASOV, S.S. SMIRNOV

Institute of High Current Electronics SB RAS, Tomsk, Russia

A high-power source of ultrawideband (UWB) radiation with a hybrid antenna has been developed. The hybrid antenna is an offset reflector, in the focus of which there is an antenna array-feeder. The elements of the antenna array are combined antennas designed to be excited by bipolar pulses with a duration of 0.5 ns. The transverse dimensions of the antennas are 65×60 mm^2. The choice of the position of the antennas in the array based on numerical calculations is justified in the paper [1]. Figure 1 shows the position of the antennas in the array-feeder. The antennas are oriented the same way and have linear vertical polarization. The modes of operation of the hybrid antenna are implemented when the elements of the antenna array are synchronously excited by bipolar voltage pulses and when the elements of the array are excited with a time delay of 1 ns between pulses — the mode of the wave beam scanning. The combined antennas used in the work and their characteristics are given in the paper [2].

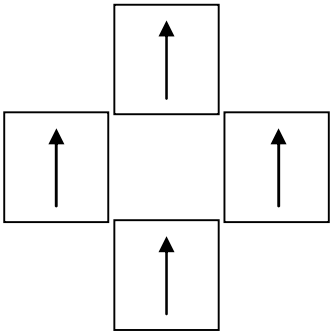

Fig.1. Position of antenna elements in the array-feeder.

Studies of radiation characteristics of a hybrid antenna at low and high voltages pulses have been carried out. Measurements at a low voltage level were carried out using a low-voltage bipolar pulse generator. The directivity characteristics of the hybrid antenna were measured in different operating modes. Measurements at high voltage were carried out using a four-channel generator of bipolar voltage pulses, which allows applying pulses with an amplitude of up to 65 kV to the input of each antenna element at a repetition rate of up to 100 Hz. In the mode of synchronous excitation of the array-feeder elements, high-power pulses of UWB radiation of a hybrid antenna were obtained. The product of the peak electric field strength at a distance (4.5 m) was at least 500 kV and at least 200 kV in the mode of discrete scanning by a wave beam with a time delay of 1 ns between high-voltage bipolar pulses at the pulse repetition frequencies up to 100 Hz.

REFERENCES

[1] Yu.I. Buyanov, E.V. Balzovsky, V.I. Koshelev, E.S. Nekrasov, "Radiation characteristics of an offset reflector antenna excited by a combined antenna array," Rus. Phys. J., vol. 62, no. 7, pp. 1214–1219, July 2019.

[2] E. Balzovsky, Y. Buyanov, V. Koshelev, E. Nekrasov, "Compact combined antenna for high-power ultrawideband radiation sources with subnanosecond pulse duration," Microw. Opt. Technol. Lett., vol. 63, pp. 2866–2869, July 2021.

* The work was supported by the Russian Foundation for Basic Research under grant No. 20-08-00529.

S3-O-020502

HIGH-POWER TERAHERTZ CHERENKOV RADIATION IN OVERSIZED SLOW-WAVE STRUCTURE*

V.A. CHAZOV, M.P. DEICHULY, V.I. KOSHELEV, A.A. PETKUN

Institute of High Current Electronics SB RAS, Tomsk, Russia

Cherenkov-type electronic vacuum devices seem to be promising sources of high-power terahertz (0.3–3 THz) radiation. To create small-sized sources of high-power radiation on a mobile platform, it is necessary to use high-current electron beams with electron energy of up to 500 keV. At present, in a Cherenkov surface wave oscillator [1], radiation pulses with a power of 2.1 MW have been obtained in the frequency range of 0.319–0.349 THz. In this case, a slow-wave structure has an oversize parameter (the ratio of the diameter to the radiation wavelength) of 6.8. In the experiments, the authors [1] used an annular electron beam with a current of I_b = 2.3–3.6 kA generated in a diode at a voltage of U_d = 350–480 kV in a magnetic field B = 3.1 T.

For numerical simulation of various Cherenkov devices with axial symmetry, we develop a 2.5D hybrid electromagnetic code consisting of two parts. The electrodynamic part of the code based on the scattering matrix method is used to study the resonant properties of oversized sectioned slow-wave structures. Examples of using the electrodynamic program, including in the sub-terahertz frequency range, can be found in [2, 3]. The second part of the code is developed based on the PIC-method and is used to simulate the interaction of a tubular electron beam with an electromagnetic field of pre-calculated resonant modes with a high quality factor.

In this paper, we present the first results of numerical simulation of a Cherenkov surface wave oscillator in the terahertz frequency range using the developed hybrid code. The interaction of a tubular electron beam and an electromagnetic field near the π-type of oscillations of TM_{01} mode was investigated. The model used the condition of ideal conductivity of the slow-wave structure surface, i.e., radiation losses in the metal [1, 4] were not taken into account. This is the subject of further work.

In the calculations, we used a slow-wave structure diameter of 40 mm with a period of rectangular diaphragms of 0.34 mm. The number of diaphragms is 40. The tubular electron beam with the leading edge duration of 0.5 ns and the current of 5 kA was injected into the slow-wave structure. The electron energy in the slow-wave structure was about 420 keV, which corresponded to the diode voltage of about 430 kV. The electron beam was transported in a uniform magnetic field B = 3 T. The average beam radius and the thickness varied in the calculations. The ratio of the slow-wave structure diameter to the radiation wavelength was about 50.

Two main longitudinal resonances of TM_{011} and TM_{012} modes with the frequencies of 0.3678 and 0.3658 THz and Q-factors of 2464 and 622, respectively, were found in the electrodynamic calculation. During the beam-field interaction, by the time moment of 1.5 ns from the pulse start, the longitudinal modes are synchronized at a frequency of 0.3662 THz. The radiation bandwidth is no higher than 0.04%. Total radiation power in forward and backward directions is equal approximately to 100 MW. Average electron losses of the beam for the period of diaphragms due of to deposition on the slow-wave structure surface are 0.015%.

REFERENCES

[1] J. Wang, G. Wang, D. Wang, S. Li, and P. Zheng, “A megawatt-level surface wave oscillator in Y-band with large oversized structure driven by annular relativistic electron beam,” Scientific Reports, vol. 8:6978, pp. 1–7, December 2018.

[2] V. A. Chazov, M. P. Deichuly, and V.I. Koshelev, “Resonance interactions of symmetric surface and bulk waves in oversized sectioned slow-wave structures,” Rus. Phys. J., vol. 63, no. 2, pp. 221–230, February 2020.

[3] V. Chazov, M. Deichuly, V. Koshelev, “ Resonance characteristics in oversized slow-wave structure of a multiwave Cherenkov generator with difraction reflectors in sub-THz frequency range,” Proc. 21th Int. Conf. on High Current Electronics (ISHCE), Tomsk, Russia, pp. 23–28, 2020.

[4] A. M. Malkin, I. Z. Zheleznov, A. S. Sergeev, and N. S. Ginzburg, “Quasi-optical theory of relativistic Cherenkov surface-wave oscillators with oversized cylindrical waveguides,” Pys. Plasmas, vol. 28, Art.no. 063102, June 2021.

* The work was supported by the Russian Science Foundation under grant No. 22-29-00063.

S3-O-023301

NUMERICAL SIMULATIONS AND DESIGN OF THE RESONATOR CHAMBER OF MICROWAVE-ASSISTED CVD REACTOR

E.V. BALZOVSKY, S.S. SMIRNOV

Institute of High Current Electronics SB RAS, Tomsk, Russia

One of the directions to obtain diamond films of high purity is a microwave-assisted plasma chemical reactor using chemical vapor deposition (CVD) synthesis [1-2]. It is possible to obtain diamond crystals and defect-free films using plasma heating near the substrate with powerful microwave radiation [3-4]. A careful approach is required when designing the excitation system of the resonator chamber from the microwave oscillation source. One of the most commonly used commercial plasma reactors is the cylindrical reactor, which uses a TM_{011} mode and an electrical type system with a disk-shaped probe. Microwave energy is injected through the bottom of the resonator.

The design of the resonator chamber is shown in Figure 1a. Modification of the upper part of the resonator made it possible to concentrate areas with maximum electric field strength directly near the substrate. The shape of the cavity *1* above the substrate is optimized. The tuning element is a movable piston above the substrate, which changes the size of the cavity *2* to find resonance. Quartz ring *3* is located between two flat surfaces away from the area of high plasma concentration.

Numerical modeling of field distribution in the cylindrical resonator using CST Studio Suite was performed to find the optimal design of chamber. In addition to the main mode TM_{011}, this resonator also contains secondary radial maxima, which are associated with simultaneous excitation of the TM_{021} and highest modes. The results of simulation of electric field strength distribution in the resonator at the input power of 1 kW are given in Figure 1b. Figure 1c shows the field distribution along the z-axis.

The optimal geometry of the disc-shaped resonator chamber is found. The maximum electric field strength in the vicinity of the substrate with the growing samples is achieved. To increase the stability of ignition of microwave discharge in the resonator chambers the movable piston is used. According to the simulation results the sample of the resonator chamber was machined and experimental studies were carried out. The power source is a magnetron of a microwave oven. The improvement of the magnetron consists of the using of the water cooling system. By powering the magnetron from a three-phase network, the obtained power in the load of at least 2.5 kW. Experimentally found steady-state plasma ignition modes at air pressures up to 10 Torr and plasma clot combustion at pressures of 30-80 Torr.

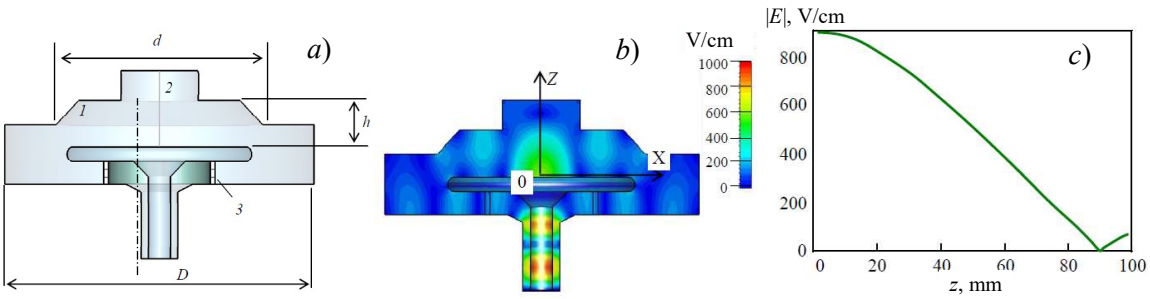

Figure 1 - Resonator chamber design (a); distribution of the electric field in the cross section of the resonator chamber (b) and distribution of the field along the z-axis at a power input of 1 kW (c).

REFERENCES

[1] A. Tallaire, J. Achard, F. Silva, O. Brinza, A. Gicquel, “Growth of large size diamond single crystals by plasma assisted chemical vapour deposition: Recent achievements and remaining challenges” Comptes Rendus Physique, vol. 14, no. 2-3, pp. 169–184, 2013.

[2] J. Weng, F. Liu, L. W. Xiong, J. H. Wang, Q. Sun, “Deposition of large area uniform diamond films by microwave plasma CVD”, Vacuum, vol. 147, pp. 134–142, 2018.

[3] X. J. Li, W. Z. Tang, S. W. Yu, S. K. Zhang, G. C. Chen, F. X. Lu, “Design of novel plasma reactor for diamond film deposition”, Diamond and Related Materials, vol. 20, no. 4, pp. 480–484, 2011.

[4] Y. Gu, J. Lu, T. Grotjohn, T. Schuelke, J. Asmussen, “Microwave plasma reactor design for high pressure and high power density diamond synthesis”, Diamond and Related Materials, vol. 24, pp. 210–214, 2012.

S3-O-028901

EFFICIENCY OF MODERATELY RELATIVISTIC RESONANT S-BAND BWO

P.V. MOLCHANOV, E.A. GURNEVICH

Institute for Nuclear Problems, Belarusian State University, Minsk, Belarus

The scheme of a resonant relativistic BWO was proposed by the Tomsk group of researchers [1, 2] for efficient generation of high-power microwave radiation in the S-band while maintaining relatively small structure length (only 2–4 λ). Due to the fact that this scheme implements effective conditions for the interaction of the beam with both the (-1st) spatial harmonic of the backward wave and the fundamental harmonic of the forward wave, a high generation efficiency (up to 30%) and record powers (above 5 GW) were achieved, both in simulations and experiments.

As far as can being found from publications, the scheme proposed in [1, 2] uses high-current relativistic electron beams with energies of 0.7–1.5 MeV and a strong guiding magnetic field (at least 1.5 T, typically 2–3 T). In this paper, we propose a variant of a resonant BWO that operates at more lower, moderately relativistic beam energies (400–550 keV) and at similar values of the guiding magnetic field (starting from 1.3 T). Compared to the original BWO geometry [2], in the the current investigated scheme, the length of the periodic structure is increased by 1 period (see figure 1 below). The main generation wavelength is about 8 cm.

Simulation and optimization of the proposed BWO were carried out in 2.5D particle-in-cell code XOOPIC [3]. A general view of the electrodynamic structure of the proposed BWO is shown in figure below. For optimization, the length of the insert between the cutoff-neck and the periodic structure, as well as the corrugation profiles of the slow wave structure were varied in the calculations. It is shown in the numerical simulation that for a beam energy of 500 keV and current of 6.25 kA, the average radiation power reaches 875 MW (28% efficiency). High generation efficiency is achieved in magnetic fields of 1.3 T and higher.

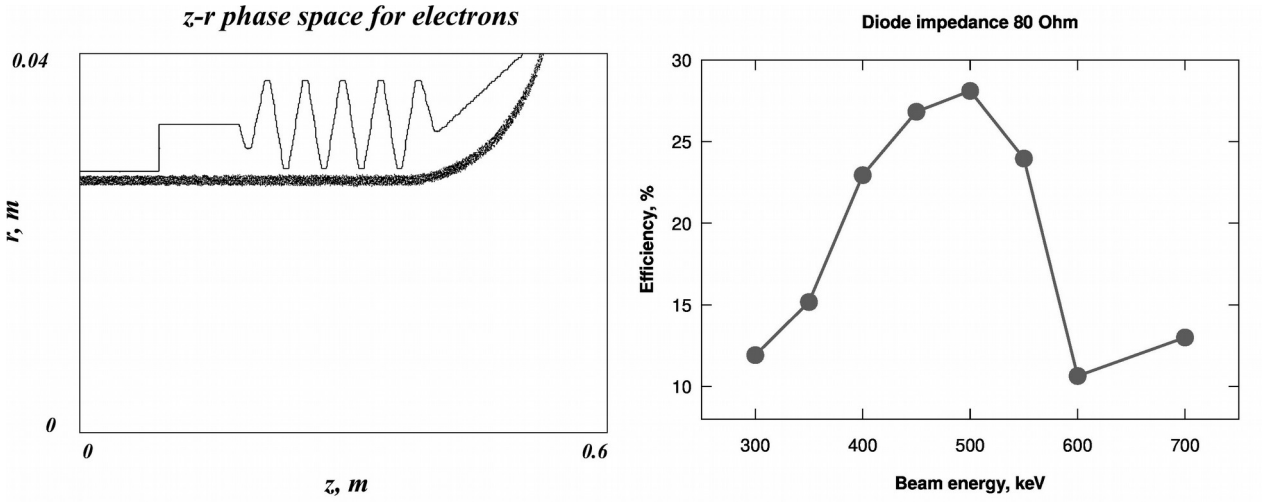

Fig.1. Geometry of the proposed resonant BWO in XOOPIC (left) and its efficiency as function of beam energy for beam impedance 80 Ohm (right).

REFERENCES

[1] S.A. Kitsanov, A.I. Klimov, S.D. Korovin et al., "Resonant Relativistic BWO in decimeter-wave band with peak power 5 GW", Lett. J. Tech. Phys. (Rus.), vol. 29, issue 19, p. 6, 2003.

[2] S.D. Polevin, S.D. Korovin, B.M. Kovalchuk et al., "Pulse lengthening of S-band resonant relativistic BWO", Proc. 13th Int. Symp. High Current Electron., p. 246, 2004.

[3] J.P. Verboncoeur, A.B. Langdon, N.T. Gladd, "An object-oriented electromagnetic PIC code," Comput. Phys. Commun., vol.87, Article Number 199, 1995.Phys. (Rus.), vol. 29, issue 19, p. 6, 2003.

S3-O-032701

POWERFUL LONG-PULSE FEL OSCILLATOR IN THE SUB-THZ/THZ RANGE: DEVELOPMENT AND TESTING OF AN ELECTRODYNAMIC SYSTEM *

N.YU. PESKOV[1,2], A.V. ARZHANNIKOV[2], V.I. BELOUSOV[1], N.S. GINZBURG[1,2], D.A. NIKIFOROV[2], YU.S. OPARINA[1,2], M.D. PROYAVIN[1], A.V. SAVILOV[1], E.S. SANDALOV[2], S.L. SINITSKY[2], V.YU. ZASLAVSKY[1]

[1]Federal Research Center Institute of Applied Physics of the Russian Academy of Sciences, Nizhny Novgorod, Russian Federation
[2]Budker Institute of Nuclear Physics of Siberian Branch Russian Academy of Sciences, Novosibirsk, Russian Federation

Development of a high-power long-pulse FEL operating from the sub-terahertz to the terahertz range was initiated in collaboration between the INP SB RAS (Novosibirsk) and the IAP RAS (Nizhny Novgorod) based on a new generation of linear induction accelerators "LIA 5" - 20 MeV / 2 kA / 200 ns. The goal of the project is to achieve a record sub-gigawatt power level and energy content in radiation pulses up to 10 – 100 J in the specified ranges. One of the key problems in the implementation of this FEL is the development of an electrodynamic system capable of providing stable narrow-band generation under conditions of significant oversized factor.

To ensure the current passage of an intense electron beam formed by the LIA through the FEL interaction space, the diameter of the system should be $Ø \geq 20$ mm, which is orders of magnitude greater than the radiation wavelength in the discussed ranges. To solve the problem of mode selection under these conditions, two main types of electrodynamic systems have been studied: (1) modified Bragg resonators and (2) quasi-optical Talbot resonators.

A distinctive feature of the modified Bragg resonators is the inclusion of quasi-cutoff waves in the feedback loop, which makes it possible to significantly improve their selective properties compared to conventional analogs. To operate in the range of 0.7 THz, structures of this type were developed with a diameter of $Ø \approx 20$ mm ($Ø/\lambda \sim 45$) and a length of about 5 cm, an axisymmetric corrugation with a period of 0.43 mm and a depth of 0.15 mm provided a feedback cycle $TE_{1,1} \leftrightarrow TE_{1,45} \leftrightarrow TE_{1,1}$. Three-dimensional modeling using the CST Microwave Studio software shows that even with such large transverse dimensions, the modified Bragg structures allow selective reflection of the operating wave with an efficiency of ~ 80 – 90 % in power. The performed “cold” electrodynamic tests confirm the simulation results and demonstrate the presence of effective narrow-band reflection in the calculated frequency range.

To carry out “cold” tests of an electrodynamic system of the second type, a model of a Talbot resonator was made with a diameter of 36 mm ($Ø/\lambda \sim 40$) and a length of about 80 cm for operation in a frequency range of about 0.3 THz. The mirrors located at the edges had a width of 4 mm; a coupling hole with diameter 2 mm was made on the output mirror (the position of the hole corresponded to the position of the calculated field maximum). The resonator was excited from the input side of the resonator by a $TE_{1,1}$ wave. According to the simulation, this wave is effectively transformed into the $TE_{1,7}$ wave, which is maximally represented in the supermode at the operating frequency. The detection of the output signal was carried out through the specified coupling hole. The simulation shows that at the frequency corresponding to the desired supermode, there should be a power peak at the coupling hole. In accordance with the simulation results, in the carried out "cold" tests, a well-defined peak of the detected output power at the calculated frequencies was observed, which thus confirmed the operability of this type of resonator.

* This work was supported by Russian Scientific Foundation (RSF), project 19-12-00212.

S3-O-032702

SUBGIGAWATT POWER LEVEL KA- AND W-BAND CHERENKOV OSCILLATORS WITH TWO-DIMENSIONAL PERIODIC SLOW-WAVE STRUCTURES *

V.YU. ZASLAVSKY, N.YU. PESKOV, E.B. ABUBAKIROV, A.A. VIKHAREV, N.S. GINZBURG, A.N. DENISENKO, A.M. MALKIN, M.D. PROYAVIN

Federal Research Center Institute of Applied Physics of the Russian Academy of Sciences, Nizhny Novgorod, Russian Federation

The original concept of powerful pulsed spatially-extended Cherenkov oscillators is being developed at the Institute of Applied Physics of the Russian Academy of Sciences (Nizhny Novgorod). A distinctive feature of the ongoing research is the use of high-current relativistic electron beams (REB) of tubular geometry, which allows increasing the total power of the oscillator by increasing one of its transverse dimensions while maintaining moderate current densities and electromagnetic field strengths. Under conditions of a large oversized factor, the spatial coherence of radiation is achieved by using two-dimensional (2D) distributed feedback (DFB). To implement 2D DFB, 2D Bragg structures are used, in which transverse wave flows synchronize the radiation of tubular REBs.

A spatially-extended Cherenkov-type surface wave oscillator (SWO) operating in the Ka-band is being developed on the basis of the "Sinus-6" high-current explosive-emission accelerator 0.5 MeV / 5 kA / 25 ns (IAP RAS), which forms oversized tubular electron beam with a diameter of about 40 mm. Oscillators of this type are characterized by deceleration of the main wave and provide a high impedance of electron-wave interaction. To operate in this frequency range, a 2D slow-wave structure (SWS) of cylindrical geometry with an average diameter of Ø = 44.3 mm (perimeter of about 16 wavelengths) and a length of about 16 cm was designed, having a 2D sinusoidal corrugation with a period of 7.75 mm, a depth of 3.5 mm and 16 azimuthal variations. The simulation of the SWO was carried out using the three-dimensional PIC code CST Studio Suite with parameters close to the experimental conditions. The simulation results demonstrate the establishment of a narrow-band oscillation regime with an output power of 0.4 - 0.5 GW and an electronic efficiency of ~ 25% at optimal parameters. The structure of the operating slow wave field has an azimuthally symmetric distribution and is a set of $TM_{0,n}$ – type modes of a cylindrical waveguide. In the initial experiments, in the calculated range of parameters, narrow-band radiation was registered at an operating frequency of about 32 GHz with an output power of ~ 0.2 – 0.3 GW. The radiation pattern of the output radiation, which was analyzed using a panel of neon lamps installed at different distances from the oscillator, was characterized by a pronounced minimum on the axis, which corresponded to the excitation of the calculated set of $TM_{0,n}$ – type modes. Currently, experiments are being carried out to optimize the configuration of the interaction space to achieve the calculated power.

To operate in the W-band (operating frequency ~ 75 GHz), the SWO was developed on the basis of the same electron beam formed by the "Sinus-6" accelerator. For this oscillator, a 2D SWS of cylindrical geometry was designed with an oversized factor Ø/λ ~ 10 (system perimeter ~ 30 wavelengths), a corrugation period of 3.59 mm, an azimuthal number of variations of 32, a corrugation depth of ~ 1 mm, and a total length of about 10 cm. The simulation demonstrated the establishment of a stable narrow-band generation regime with selective excitation of operating azimuthally symmetric wave at the calculated parameters. According to the simulation, the electronic efficiency of the oscillator is ~15 - 20%, and the expected output power level reaches ~ 0.3 – 0.35 GW. At present, a 2D periodic SWS of the W-band with the described geometry has been manufactured and the assembly of the oscillator has been completed. In the initial experiments, narrow-band radiation with a power level of ~ 0.2 GW was obtained in the calculated range of parameters. Experimental studies of this oscillator are currently in progress.

* The work is supported by Russian Federation program "Development of equipment, technologies and research in the field of atomic energy use in the Russian Federation for the period up to 2024" (IAP RAS Project No. 0030–2021-0027).

S3-O-032801

DEVELOPMENT OF HIGH-CURRENT RELATIVISTIC GYROTRON WITH TM-TYPE OPERATING MODE *

E.B. ABUBAKIROV[1], YU.YU. DANILOV[1], A.N. DENISENKO[1], A.N. LEONTYEV[1], R.M. ROZENTAL[1], V.P. TARAKANOV[2,3]

[1]*Institute of Applied Physics RAS, Nizhny Novgorod , Russia*
[2]*Moscow Engineering Physics Institute, Moscow, Russia*
[3]*Joint Institute for High Temperatures RAS, Moscow, Russia*

Currently, the development and experimental implementation of millimeter-wave microwave sources with a sub-gigawatt output power level is the subject of active research [1–3]. The use of gyrotrons for this purpose is of particular interest, since in cyclotron interaction there is no need to transport the electron flow close to the electrodynamic system surface, in contrast to Cherenkov devices. To achieve a sub-gigawatt output radiation power level, gyrotrons must be powered by relativistic helical electron beams formed by explosive emission cathodes. In this case, a significant problem is the selective excitation of the working oscillation on time scales of tens of nanoseconds, corresponding to the characteristic duration of the electron beam.

This report presents the results of the development and the first experimental tests of a high-current gyrotron with an operating frequency of 30 GHz with a new type of plate-type slitted cavity. Such a cavity provides a significant rarefaction of the mode spectrum due to a significant decrease in the quality factor of the TE-type modes while maintaining the quality factor of the TM-type modes. As a result, it becomes possible to operate in one of the TM-modes in the gyrotron.

The results of experimental studies of an electron-optical system based on a coaxial magnetically insulated diode and a kicker, which forms a beam with an energy of 500 keV, a current of up to 2 kA, and a pitch-ratio of about 1.0, are presented. Experimentally and within the framework of three-dimensional PIC-simulation, it was demonstrated that when using the classical scheme for constructing a gyrotron with separation of the beam formation space and the electron-wave interaction region, the problem of parasitic self-excitation arises in the beam formation section. Possible modifications of the gyrotron are proposed to solve this problem and achieve the expected output radiation power level.

Fig.1. Photos of the assembled gyrotron (a) and plate cavity (b).

REFERENCES

[1] B. Deng, J. He, J. Ling, L. Song, L. Wang, "Preliminary research of a V-band coaxial relativistic transit-time oscillator with traveling wave output structure" // Phys. Plasmas 28, 103103 (2021); doi: 10.1063/5.0060186.

[2] A. M. Malkin, A. E. Fedotov, V. Yu. Zaslavsky, S. E. Fil'chenkov, A. S. Sergeev, E. D. Egorova, and N. S. Ginzburg, "Relativistic sub-THz surface-wave oscillators with transverse Gaussian-like radiation output" // IEEE Electron Dev. Lett. 42, 751 (2021), doi: 10.1109/LED.2021.3067170.

[3] A.V. Palitsin, A.E. Fedotov, A.M. Malkin, V.Yu. Zaslavsky, M.B. Goykhman, A.V. Gromov, Yu.M. Guznov, A.N. Panin, Yu.V. Rodin, and N.S. Ginzburg, "Design of W-band Relativistic Surface-Wave Oscillator with Sheet Electron Beam" // IRMMW-THz 2021, doi: 10.1109/IRMMW-THz50926.2021.9567091.

* This work was supported by the Institute of Applied Physics of the Russian Academy of Sciences (IAP RAS) Project through the Program "Development of engineering, technology and scientific research in the field of atomic energy until 2024" under Grant 0030-2021-0027.

S3-O-033701

TERAHERTZ FREE ELECTRON LASER WITH AN ELECTRODYNAMIC SYSTEM BASED ON THE EXCITATION OF TALBOT-TYPE SUPERMODES*

Y.S. OPARINA, N.Y. PESKOV, A.V. SAVILOV, A.A. VIKHAREV

Institute of Applied Physics, Russian Academy of Sciences, Nizhny Novgorod, Russia

Currently, there is a growing interest in creating sources operating in the terahertz frequency range with high radiation power. The natural way to implement such a source is to use the radiation of a high-current relativistic electron beam. However, there are a number of problems associated with the generation of powerful coherent THz radiation in free electron masers based on relativistic electron beams. First of all, the application of the traditional approach (i.e., operating on one pre-selected cavity mode) to the THz frequency range faces natural difficulties. Obviously, the cavity in this case must be oversized; this is necessary for a number of reasons, namely, the transportation of a relativistic high-current beam, the problem of breakdown of the field of powerful radiation inside the cavity, ohmic heating of the walls of the resonator by powerful radiation, etc. However, in this situation, the spectrum of transverse modes of the microwave system becomes very dense, which makes it difficult to ensure selective excitation of one operating transverse mode. The second problem is the difficulty of providing selective single-mode feedback in a oversized system.

We describe an alternative concept of selective excitation of a operating oscillation in an electron maser with a oversized electrodynamic system powered by a high-current relativistic electron beam. The main idea is to abandon the excitation of a fixed resonator mode in favor of the excitation of a high-Q supermode formed by a fixed set of transverse modes of a oversized waveguide. Such a supermode can be formed inside a relatively simple cavity, which is a segment of a waveguide ending in two mirrors, as a result of the Talbot effect, namely, periodic reproduction of the transverse structure of a multimode wave field in a oversized waveguide [1].

Despite the complexity of multidimensional spatial structures of Talbot-type supermodes, the ideology that is used in describing the modes of conventional waveguides and resonators, namely decomposition by a set of orthogonal modes, can be applied to them to some extent. Although the formation of supermodes involves a large number of partial transverse modes, the number of supermodes with high Q-factor is limited by the fact that the diffraction Q-factor of a supermode decreases sharply with an increase in the supermode index. Thanks to this, even in very supersized systems, it is possible to ensure that only one lower supermodel remains in the system [2]. Apparently, this gives us a reason to talk about the unique selective properties of Talbot-type caviries.

As an example of the application of this approach, we will present simulations of a free electron laser powered by an electron beam of 10 MeV/2 kA /200 ns and based on the excitation of a Talbot-type supermode at a frequency close to 2 THz. This work is aimed at the experimental implementation of such a laser on a unique high-current accelerator developed at the Budker Institute of Nuclear Physics[3]. The report presents the results of our multi-wave modeling of electron-wave interaction in the space-time process of formation and amplification of a supermode in a oversized microwave system. The calculated electronic efficiency of this laser at the level of 5% corresponds to the gigawatt level of output power. A prototype cavity has been developed and tested in cold experiments.

REFERENCES

[1] Oparina Yu. S., Peskov N.Y., Savilov A.V., “Electron rf Oscillator Based on Self-Excitation of a Talbot-Type Supermode in an Oversized Cavity”, *Physical Review Applied*, vol. 12, p. 044070, 2019.

[2] Oparina Yu.S., Savilov A.V., Shchegolkov D.Yu., “Supermodes of oversized Talbot-type cavities”, *Journal of Applied Physics*, vol. 128, no. 11, p. 114502, 2020.

[3] Logachev P. V., Kuznetsov G.I., Korepanov A. A., Akimov A.V., Shiyankov S.V., Pavlov O.A., Starostenko D.A., Fat'Kin G.A., “LIU-2 linear induction accelerator,” *Instruments and Experimental Techniques*, vol. 56 (6), p. 672-679, 2013.

* The work was supported by Russian Science Foundation, grant 19-12-00212.

S3-O-034101

MICROWAVE GENERATORS WITH PASSIVE MODE-LOCKING*

N.S. GINZBURG, S.V. SAMSONOV, G.G. DENISOV, M.N. VILKOV, I.V. ZOTOVA, A.A. BOGDASHOV, I.G. GACHEV, A.S. SERGEEV, R.M. ROZENTAL

Institute of Applied Physics RAS, Nizhny Novgorod, Russia

Passive mode-locking as a method for generating periodic sequences of ultrashort optical pulses (USPs) is well known in laser physics [1]. This effect is achieved by incorporating a saturable absorber (nonlinear filter) into the laser resonator. The theoretical studies carried out [2-4] have shown the possibility of transferring the described method to microwave electronics. The key point for the development of electronic USP generators with passive mode-locking was the development of an absorber that should provide saturable absorption in the microwave range at a power level of tens and hundreds of kilowatts. For this purpose, it was proposed to use cyclotron resonant absorption of radiation by an initially rectilinear electron beam, when the absorption saturation is caused by the relativistic dependence of the gyrofrequency on the particle energy [3]. Based on the theoretical analysis, the two-section Ka-band USP generator has been developed which comprised a helical-waveguide gyro-TWT as an active unit (Fig. 1a). In good agreement with theoretical predictions, periodical trains of 0.4 ns pulses with peak power of 100 kW and repetition period of 2.5 ns were measured (Fig. 1b). Phase coherence of radiated pulses was demonstrated based on analysis of the auto-correlation function [4]. Performed experiments open essential new possibilities in generation of wide-band coherent radiation highly demanded for numerous applications.

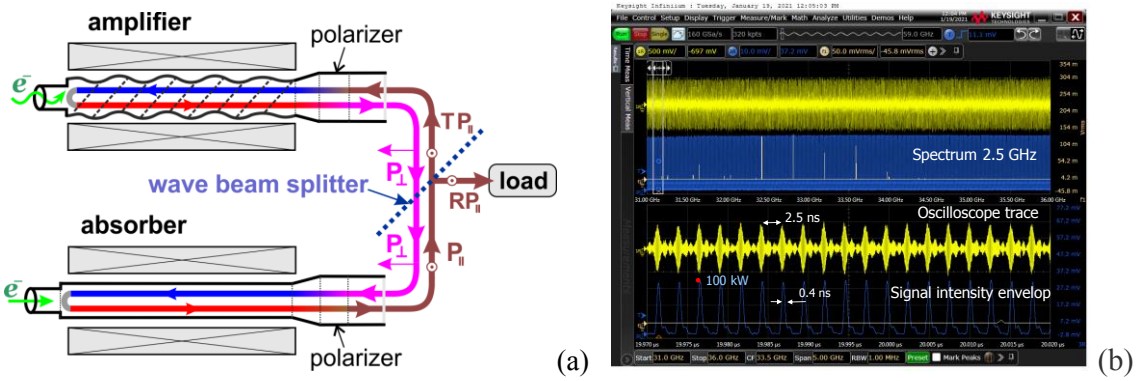

(a) (b)

Fig.1. (a) Principal scheme of a microwave mode-locked generator comprising a helical-waveguide gyro-TWT (amplifier) and a regular-waveguide saturable cyclotron resonance absorber (blue and red arrowed lines inside both tubes correspond to idle and active wave propagation, respectively. (b) Oscilloscope traces of recorded signal in the experiment.

REFERENCES

[1] U. Keller, “Recent developments in compact ultrafast lasers”, Nature, vol. 424, 831-838, August 2003.

[2] N.S. Ginzburg, G.G. Denisov, M.N. Vilkov, I.V. Zotova, A.S. Sergeev, “Generation of “gigantic” ultra-short microwave pulses based on passive mode-locking effect in electron oscillators with saturable absorber in the feedback loop”, Phys. Plasmas, vol. 23, no. 5, art.no. 050702, May 2016.

[3] N.S. Ginzburg, G.G. Denisov, M.N. Vilkov, A.S. Sergeev, S.V. Samsonov, A.M. Malkin, and I.V. Zotova, “Nonlinear cyclotron resonance absorber for a microwave subnanosecond pulse generator powered by a helical-waveguide gyrotron traveling-wave tube”, Phys. Rev. Appl., vol. 13, art.no. 044033, April 2020.

[4] N.S. Ginzburg, S.V. Samsonov, G.G. Denisov, M.N. Vilkov, I.V. Zotova, A.A. Bogdashov, I.G. Gachev, A.S. Sergeev, R.M. Rozental, “Ka-band 100-kW subnanosecond pulse generator mode-locked by a nonlinear cyclotron resonance absorber”, Phys. Rev. Applied, vol. 16, art.no. 054045, April 2021.

* The work was supported by the IAP RAS Contract No. 0030-2021-0027 (Program "Development of equipment, technologies and research in the field of atomic energy use in the Russian Federation for the period up to 2024").

S3-O-034602

DESIGN OF ONE-OCTAVE BANDWIDTH GYRO-BWO WITH ZIGZAG QUASI-OPTICAL TRANSMISSION LINE *

S.V. SAMSONOV, G.G. DENISOV, A.A. BOGDASHOV, I.G. GACHEV, M.V. KAMENSKIY, K.A. LESHCHEVA

Institute of Applied Physics RAS, Nizhniy Novgorod, Russia

A gyrotron backward-wave oscillator (gyro-BWO) is a type of cyclotron resonance maser (CRM), which differs from a gyrotron (the most developed version of CRM) by the potential for a much wider-band smooth oscillation frequency tuning (see e.g. [1], [2]). In conventional gyro-BWOs using a section of a smooth waveguide, the frequency tuning is, as a rule, piecewise with strong variations in the power and spatial structure of the output radiation [3]. In [4] we proposed a concept of a CRM, based on the use of an open quasi-optical (QO) mirror transmission line as a microwave circuit, in which a Gaussian wave beam is directed by mirrors along a zigzag trajectory, so that its periodic intersections with the electron beam occur at right angles (Fig.1). 3D Particle-In-Cell (PIC) simulations show that such a configuration is prospective for implementation of relatively high-power short-millimeter-wave amplifiers and oscillators with extremely wide frequency tunability.

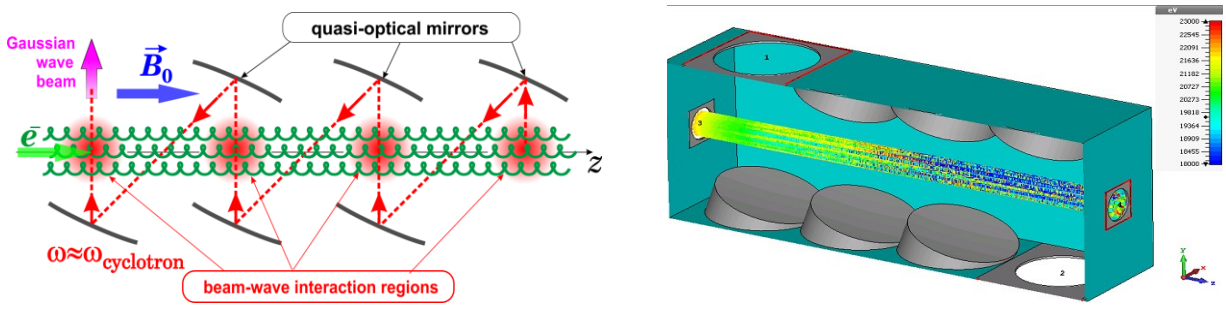

a) b)

Fig.1. Schematic layout (a) and CST model (b) of a gyro-BWO with 3-period zigzag QO transmission line.

In this paper, we present design of a proof-of-principle experiment on implementation of such a broadband frequency-tunable gyro-BWO. A general layout and results of computer modeling of major experimental components (interaction circuit, electron gun, output microwave system etc.) are discussed for a CW device using a cryomagnet with the B-field of 4-8 T. According to CST simulations, the designed gyro-BWO ensures output of nearly Gaussian wave beam of kilowatt power level at any predefined frequency within 107-215 GHz range.

REFERENCES

[1] M. Thumm, "State-of-the-art of high-power gyro-devices and free electron masers," J. Infr., Millim., THz Waves, vol. 41, no. 1, pp. 1–140, Jan. 2020.

[2] G. S. Nusinovich, Introduction to the Physics of Gyrotrons. Baltimore, MD, USA: Johns Hopkins Univ. Press, 2004.

[3] C.-H. Tsai et al., "Reflective gyrotron backward-wave oscillator with piecewise frequency tunability," IEEE Trans. Electron Devices, vol. 68, no. 1, pp. 324–329, Jan. 2021.

[4] S.V. Samsonov, G.G. Denisov, A.A. Bogdashov, I. G. Gachev "Cyclotron Resonance Maser with Zigzag Quasi-Optical Transmission Line: Concept and Modeling", IEEE Trans. Electron Dev., 2021, vol. 68, № 11, P. 5846-5850.

* The work was supported by the Russian Science Foundation under grant No. 21-19-00443, https://rscf.ru/project/21-19-00443/.

S3-O-034901

DEVELOPMENT OF W-BAND SHORT PULSE GENERATOR WITH PASSIVE MODE-LOCKING*

M.N. VILKOV, N.S. GINZBURG, I.V. ZOTOVA, A.S. SERGEEV

Institute of Applied Physics RAS, Nizhny Novgorod, Russia

In laser physics, a well-known method exists for production of ultrashort optical pulses (USP) based on the effect of passive mode-locking [1], which is achieved by incorporating a saturable absorber (nonlinear filter) into the laser resonator. The similar method of USP generation was experimentally realized recently in high-power microwave electronics in a two-section Ka-band oscillator [2-3] consisting of a gyro-TWT amplifier and a nonlinear cyclotron resonance absorber in the feedback loop. The amplifier operated at the second cyclotron harmonic while the absorber operated at the first harmonic. This seriously restricts the advancement of the above scheme of USP generator into the shorter (W or G) wavebands and its use in the applications like spectroscopy.

In this paper, we suggest an alternative scheme of W-band USP generator with passive mode-locking, which includes two gyro-TWT [4-5] sections with helical corrugation (Fig. 1a). One of them is used as an amplifying unit, while the other operates in the regime of nonlinear Kompfner absorption [6-7]. The regime of amplification or absorption in a gyro-TWT is achieved by adjusting the cyclotron resonance detuning. Both sections operate at the second cyclotron harmonics, which allows the required magnetic field to be reduced. According to simulations for W-band gyro-TWT with electron energy of 60 kW and current of 10 A, it is possible to generate periodical trains of pulses with the peak power of about 400 kW and 60 ps duration (Fig.1b-c).

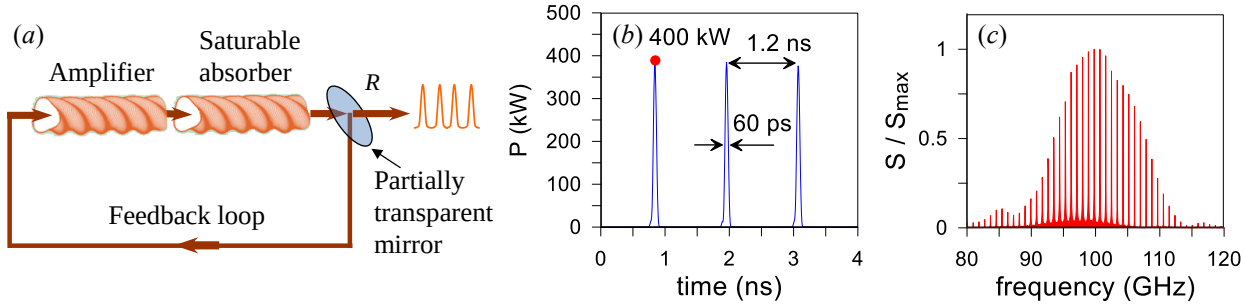

Fig.1. (a) scheme of a mode-locked microwave oscillator consisting of two coupled helical gyro-TWTs, (b) profiles of microwave pulses, and (c) radiation spectrum.

REFERENCES

[1] U. Keller, “Recent developments in compact ultrafast lasers”, Nature, vol. 424, 831-838, August 2003.

[2] N.S. Ginzburg, G.G. Denisov, M.N. Vilkov, A.S. Sergeev, S.V. Samsonov, A.M. Malkin, and I.V. Zotova, “Nonlinear cyclotron resonance absorber for a microwave subnanosecond pulse generator powered by a helical-waveguide gyrotron traveling-wave tube”, Phys. Rev. Appl., vol. 13, art.no. 044033, April 2020.

[3] N.S. Ginzburg, S.V. Samsonov, G.G. Denisov, M.N. Vilkov, I.V. Zotova, A.A. Bogdashov, I.G. Gachev, A.S. Sergeev, R.M. Rozental, “Ka-band 100-kW subnanosecond pulse generator mode-locked by a nonlinear cyclotron resonance absorber”, Phys. Rev. Applied, vol. 16, art.no. 054045, April 2021.

[4] S.V. Samsonov, G.G. Denisov, I.G. Gachev, A.A. Bogdashov, "CW operation of a W-band high-gain helical-waveguide gyrotron traveling-wave tube", IEEE Electron Device Lett., vol. 41, no. 5, pp. 773-776, May 2020.

[5] W. He, C.R. Donaldson, L. Zhang, K. Ronald, A.D.R. Phelps, A.W. Cross, "Broadband Amplification of Low-Terahertz Signals Using Axis-Encircling Electrons in a Helically Corrugated Interaction Region", Phys. Rev. Lett., vol. 119, art.no. 184801, October 2017.

[6] R. Kompfner, "On the operation of the traveling wave tube at low level", J. Brit. IRE, vol. 10, pp. 283-289, August-September 1950.

[7] C.S. Kou, K.R. Chu, D.B. McDermott, and N.C. Luhmann Jr., "Effective bandwidth and the Kompfner dip for cyclotron autoresonance maser amplifiers", Phys. Rev. E, vol. 51, pp. 642-648, January 1995.

* The work was supported by Grant of the President of the Russian Federation No. MK-4048.2022.1.2

S3-O-035004

INFLUENCE OF NON-RESONANT REFLECTION ON MODE COMPETITION IN A MEGAWATT-POWER GYROTRON*

YU.V.NOVOZHILOVA, V.L.BAKUNIN, G.G.DENISOV, A.N.KUFTIN, E.S.SEMENOV, A.S.ZUEV

Institute of Applied Physics RAS, Nizhny Novgorod, Russian Federation

Gyrotrons are well-known as the sources of the highest power in sub-THz and THz frequency bands. However, one of the main problems is achievement of single-mode oscillation with high efficiency and stable frequency, because modern gyrotrons operate at very high-order transversal modes with dense mode spectrum, where competition with spurious modes can be dangerous. One of the efficient ways is frequency locking by external signal, which has been deeply studied in the recent years, especially after the development of two-channel quasi-optical converter in IAP RAS [1]. The drawback of this method is that one needs special driver gyrotron with extremely high frequency stability and transmission line. The other way is using the reflections from gyrotron's output window in the gyrotron with quasi-optical converter [1] for "self-locking" and frequency stabilization. The effect of the reflected wave on the gyrotron radiation spectrum was studied in a number of papers [2-4].

In this work, we studied the possibility of stabilizing the operating mode frequency under the action of a reflected wave with a sufficiently large delay and in the presence of small harmonic variations of the accelerating voltage.

We consider the numerical model of 170-GHz megawatt-power level gyrotron. Such a gyrotron was developed in IAP RAS [1]. High-order operating mode TE28.12 competes with its sideband satellites TE27.12, TE29.12. In the case of free-running oscillation mode competition can significantly affect the operating mode and achievable efficiency. We assume that the window reflects at the frequency of operating mode.

Equations, describing multimode gyrotron with reflections from non-resonant load in the fixed longitudinal field structure approximation, are given in [4]. The operating current is chosen 45A, which is typical for MW-power gyrotrons. Operating mode TE28.12 has quality factor Q = 1300. The reflection coefficient is 0.35 amplitude-wise, the delay time is equal to 9 ns. Satellites TE27.12 and TE29.12 (Q = 1300) are not affected by reflection.

Our simulations show that reflection provides stabilization of the operating mode frequency at certain interval of magnetic field due to the sufficiently long delay time. The displacement of the reflector within the wavelength leads to a slight shift in the frequencies of stable states and the values of the magnetic field at which transitions between these states occur. Such changes in the radiation frequency depending on the magnetic field and on the distance to the reflector, which are typical for sufficiently large values of the delay time and reflection coefficient, are in agreement with the theory [4]. In the presence of small harmonic variations of the operating voltage, gyrotron with reflection on the operating mode demonstrates significantly smaller variations of the radiation frequency (more than an order of magnitude) than free-running gyrotron. A similar effect we observed at frequency locking of gyrotron by the external signal [5]. Also reflection expands oscillation zones of TE28.12 operating mode and significantly increases orbital efficiency compared to the free-running gyrotron.

REFERENCES

[1] A.V. Chirkov, G.G. Denisov, and A.N. Kuftin. "Perspective gyrotron with mode converter for co- and counter-rotation operating modes". Appl. Phys. Lett. 106, 263501, 2015.

[2] M.M. Melnikova, N.M. Ryskin. "Influence of reflections on mode-competition processes in a high-power multimode gyrotron". Phys. Plasmas **29**, 013104 (2022). https://doi.org/10.1063/5.0071210

[3] R.M. Rozental', I.V. Zotova, M.Y. Glyavin, et al. "Widening of the Frequency Tuning Bandwidth in a Subterahertz Gyrotron with an External Bragg Reflector". Radiophys Quantum El **63,** 363–370 (2020).

[4] Y.V. Novozhilova, G.G. Denisov, M.Yu. Glyavin, N.M. Ryskin, V.L. Bakunin, A.A. Bogdashov, M.M. Melnikova, and A.P. Fokin, "Gyrotron frequency stabilization under the influence of external monochromatic signal or wave reflected from the load: Review," Izv. Vyssh. Ucheb. Zaved. Prikladnaya Nelineynaya Dinamika 25 (1), 4-34, 2017 (in Russian).

[5] V.L. Bakunin, G.G. Denisov, Yu.V. Novozhilova. "Phase Locking of a Gyrotron with Low-Frequency Voltage and Current Fluctuations by an External Monochromatic Signal". Radiophys. Quantum El. **63**, 392-402 (2020). Authors, "Article title," Abbreviated Journal Title, vol. , no. , pp. , Month year .

* The work was supported by by the Russian Science Foundation (RSF) under Grant # 19-79-30071.

S3-O-038201

TRANSVERSE RADIATION INPUT AND OUTPUT FOR PLANAR RELATIVISTIC SURFACE-WAVE OSCILLATORS AND AMPLIFIERS*

A.E. FEDOTOV, A.M. MALKIN, V.YU. ZASLAVSKY, A.S. SERGEEV, AND N.S. GINZBURG

Institute of Applied Physics of the Russian Academy of Sciences, Nizhny Novgorod, Russia

The output power of relativistic high-current microwave sources decreases when operating frequency increases and transverse dimensions of the slow-wave structure (SWS) shrinks. To mitigate this power decline, the oversized slow-wave structures are needed so the problem of mode competition arises. Relativistic surface-wave oscillators are attractive devices for generation of multi-megawatt power at sub-terahertz waves, since a usage of evanescent operating mode provides ultimate mode selection at least in one transverse direction. However, evanescent nature of the operating wave brings a number of difficulties such as a scattering of the wave at the edges of the grating, a power leakage to the cathode, and high ohmic losses. All these issues hamper utilizing of the generated microwave radiation for the applications.

To organize the effective and practical radiation output in the relativistic high-power surface-wave oscillator, we recently proposed [1] to apply an additional diffraction grating with a period twice larger than the period of the main corrugation (Fig. 1). The similar method was studied earlier for low-voltage clinotron devices [2-4]. The main corrugation and the additional corrugation form the bi-periodic grating with the odd grooves being deeper than the even grooves. The auxiliary grating scatters the evanescent operating waves into the gaussian beam leaking in perpendicular direction to slow-wave structure. Produced gaussian output beam is suitable for applications. Besides, at sub-terahertz frequencies, the transverse energy extraction reduces the Ohmic losses drastically thus increasing the device efficiency. According to simulations, 150-GHz surface-wave oscillator based on sheet electron beam with voltage of 600 kV and current of 600 A can provide 90 MW of output power with 25 % efficiency.

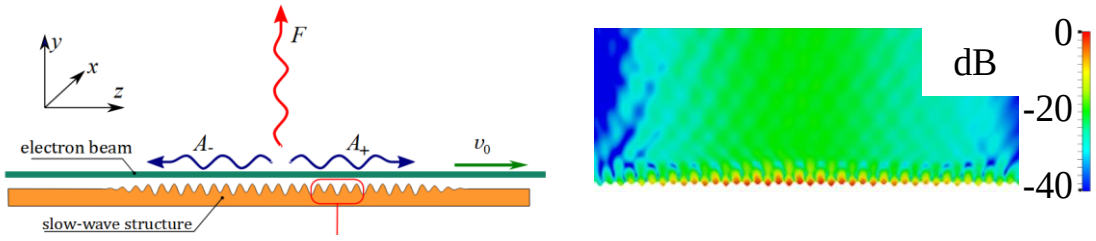

Fig.1. (Left panel) Surface-wave oscillator with transverse energy output (not in scale). Bi-periodic slow-wave structure driven by sheet electron beam provides coupling of surface wavebeams A_+ and A_- with transverse output wavebeam F. The odd grooves of the bi-periodic grating are deeper than the even grooves. (Right panel) PIC-code simulated pattern of the microwave magnetic field. Both the evanescent operating mode and the output gaussian beam are seen.

The same method could be used for power input in surface-wave amplifier as well [5]. In high-power extended interaction klystron exploiting open gratings as surface-wave cavities driven by a high-current sheet electron beam, additional corrugation provides in- and out-coupling of the radiation. Simulations based on both averaged quasi-optical model and PIC code demonstrate the feasibility of the 150 GHz amplifier with 20-40 MW output power in gaussian beam and 20-30 dB linear gain in 1% bandwidth.

REFERENCES

[1] A.M. Malkin, A.E. Fedotov, V.Yu. Zaslavsky, A.S. Sergeev, S.E. Fil'chenkov, E.D. Egorova, and N.S. Ginzburg, “Relativistic sub-terahertz surface-wave oscillators with transverse Gaussian-like radiation output.” // *IEEE Electron Device Letters*, vol. 42, No. 5, pp. 751-754, 2021.

[2] E.M. Khutoryan, A.N. Kuleshov, S.S. Ponomarenko, K.A. Lukin, Y. Tatematsu, M. Tani, “Efficient Excitation of Hybrid Modes in a THz Clinotron.” // *J. Infrared, Millimeter, and THz Waves*, vol. 42, pp. 671–683, 2021.

[3] E.M. Khutoryan, Yu.S. Kovshov, A.S. Likhachev, S.S. Ponomarenko, S.A. Kishko, K.A. Lukin, V.V. Zavertanniy, T.V. Kudinova, S.A. Vlasenko, A.N. Kuleshov, T. Idehara, “Excitation of Hybrid Space-Surface Waves in Clinotrons with Non-uniform Grating.” // *J. Infrared, Millimeter, and THz Waves*, vol.39, no.3, pp.236-249, 2018.

[4] S.S. Ponomarenko, A.A. Likhachev, S.A. Vlasenko, Y.S. Kovshov, V.V. Stoyanova, S.A. Kishko, E.M. Khutoryan, A.N. Kuleshov, K.A. Lukin, Y. Tatematsu, and M. Tani, “Traveling-Wave Amplification in a Circuit With Nonuniform Grating.” // *IEEE Transactions on Electron Devices*, vol. 68, no. 10, pp.5232-5237, 2021.

[5] N.S. Ginzburg, A.M. Malkin, V.Yu. Zaslavsky, A.E. Fedotov, and A.S. Sergeev, “Relativistic sub-THz surface-wave sheet-beam amplifier with transverse energy input and output.” // *IEEE Transactions on Electron Devices* , vol. 69, No. 2, pp. 759-762, 2022.

* The work was supported by Complex DETR Program as IAP RAS Project No. 0030–2021-0027.

S3-O-038301

INFLUENCE OF COULOMB FIELDS ON THE FORMATION OF EMITTANCE IN PHOTOGUNS

V.Ya. IVANOV

Budker Institute of Nuclear Physics, Novosibirsk, Russian Federation

The modern colliders require intensive high quality electron beams. The beam parameters for such projects, as SKEKB [1,2], FCC [3] or Super C-Tau factory [4] need the beam charge of a few nC (1-6.5 nC), the energy spread less than 1%, the normalized transverse emittance less than 20 mm-mrad, The DC electron guns with thermionic cathode allow to achieve the beams with such charges, but the low emittance and the energy spread are difficult to obtain with such guns. For example, when one uses S-band accelerating structures, the beam length has to be of a few millimeters, and to have the energy spread less than 1%. There is nothing wrong with that, since for FCC or Super C-Tau Factory the rms energy spread is about 0.1%, therefore the beam length should be less than 1 mm in this case. Thus, the DC guns with thermionic cathode need the bunching system, but the beam compressing with high quality can be a very difficult challenge.

In spite of the promising of the RF photoguns, there are a lot of challenges, which should be resolved. One of these is the high charge of the beam, and especially the effect of them on the beam emittance. Since 1985, when the first photogun was constructed at the Los Alamos laboratory, such sources have become more and more popular. Photoguns are promising sources of electron bunches with a small transverse emittance [5-9].

The performed theoretical analysis and numerical calculations give an idea of the emittance acquired by the bunch due to the influence of Coulomb fields when moving in the accelerating cavity of the photogun. The data obtained provide a relationship between the emittance not only with the geometric dimensions of the beam, but also with an arbitrary distribution of the space charge density in the bunch. It is shown that the output value of the bunch emittance is minimal for a compact (uniform) charge distribution and increases significantly when the charge is smeared for a normal distribution in the longitudinal and transverse directions. For a bunch in the form of a thin disk, the growth of the transverse component of the emittance is much greater than that for the longitudinal direction. In practice, the degree of smearing of the space charge is determined by the shape of the laser pulse that excites photoemission. The results of numerical simulation will further serve as the basis for comparing the degree of influence of the high-frequency field of the resonators and the Coulomb fields of the bunch on the total emittance of the beam at the output of the photogun. The analysis performed allows us to formulate a number of recommendations for the design of the photogun to compensate for the growth of the emittance.

REFERENCES

[1] T. Miura et al., Upgrade Status of Injector LINAC for SuperKEKB, in Proceedings of the IPAC'14, Dresden, Germany (2014), pp. 59-61.

[2] https://www-linac.kek.jp/linac-com/report/b2gm/linac-status-satoh-200622.pdf

[3] https://link.springer.com/content/pdf/10.1140/epjst/e2019-900045-4.pdf

[4] https://ctd.inp.nsk.su/c-tau/

[5] D. Nguyen, J. Lewellen, L. Duffy, RF Linac for High-Gain FEL. Photoinjectors/ US Particle Accelerator School, June 16-20, 2014.

[6] K.-J. Kim, RF and Space-Charge Effects in Laser-Driven RF Electron Gun, NIM A275 (1989) 201-218.

[7] T. Natsui, M. Yoshida, X. Zhou, Y. Ogawa, Quasi-traveling wave gun and beam commissioning for SuperKekb, Proc. Of IPAC2015, Richmond, VA, USA, PP. 1610-1612.

[8] H.Bluem, A. Todd, M. Cole et al. ELECTRON INJECTORS FOR NEXT GENERATION X-RAY SOURCES, SPIE 49 th Annual Mtg., Denver, CO, 206 August, 2004.

[9] D. H. Dowell, Sources of Emittance in RF Photocathode Injectors: Intrinsic emittance, space charge forces due to non-uniformities, RF, and solenoid effects, http://arxiv.org/abs/1610.01242.

S3-O-043301

ELECTROMAGNETIC PROPERTIES CHARACTERIZATION AND Q-FACTOR MEASUREMENTS OF NIOBIUM PROTOTYPES OF 325 MHZ COAXIAL HALF-WAVE RESONATOR

D. BYCHANOK[1,2] , A. SUKHOTSKI[1], S. HUSEU[1], S. MAKSIMENKO[1], M. GUSAROVA[3], M. LALAYAN[3], S. POLOZOV[3], A. SHVEDOV[4], S. YUREVICH[4], V. PETRAKOVSKY[4], A. POKROVSKY[4], V. ZALESKI[4], A. BUTENKO[5] AND E. SYRESIN[5]

[1]*Institute for Nuclear Problems of Belarusian State University, Minsk, Belarus.*
[2]*Tomsk State University, 36 Lenin Prospekt, Tomsk, Russia.*
[3]*National Research Nuclear University MEPhI , Moscow, Russia.*
[4]*Physical-Technical Institute, Minsk, Belarus.*
[5]*Joint Institute for Nuclear Research, Dubna, Russia.*

The results of experimental measurements of the electromagnetic properties of a niobium prototype of coaxial half-wave resonators (HWR) [1] operating at a frequency of 325 MHz for the Nuclotron-based Ion Collider fAcility (NICA) injector are presented and discussed.

The experiments were carried out in a test cryomodule [2] at room temperature and liquid nitrogen temperature. Various methods for measuring the Q-factor of the niobium prototype are compared and analyzed.

The presented results will be used for further development and fabrication of superconducting niobium resonators of a similar design for the NICA project.

REFERENCES

[1] D. Bychanok, A. Sukhotski, S. Huseu, E. Vasilevich, E. Gurnevich, G. Walynets, N. Liubetski, S. Maksimenko, A. Shvedov, V. Petrakovski, A. Pakrouski, S. Yurevich, Y. Tamashevich , M. Gusarova, M. Lalayan, S. Polozov, A. Butenko, E. Syresin, "Electromagnetic properties control during prototyping, fabrication and operation of low-β 325 MHz half-wave resonators" Journal of Physics D: Applied Physics, 54(25), 255502 doi:10.1088/1361-6463/abf168, (2021).

[2] D. Bychanok, S. Huseu, E.Vasilevich, A. Sukhotski, V. Bayev, S. Maksimenko, M. Gusarova, M. Lalayan, S. Polozov, A. Shvedov, S. Yurevich, V. Petrakovsky, A. Pokrovsky, D. Nikiforov, A. Butenko, E. Syresin "Design and characteristics of cryostat for testing of low-beta 325 MHz half-wave resonators", XXVII RUSSIAN PARTICLE ACCELERATOR CONFERENCE from 27 September to 1 October 2021.

S3-O-045201

DESIGN AND EXPERIMENTAL TESTING OF W-BAND PLANAR SURFACE-WAVE OSCILLATOR DRIVEN BY SHEET HIGH CURRENT RELATIVISTIC ELECTRON BEAM *

A.V. PALITSIN[1], V.YU. ZASLAVSKY[1], YU.V. RODIN[1], M.B. GOYKHMAN[1], A.V. GROMOV[1], YU.M. GUZNOV[1], A.N. PANIN[2], V.V. PARSHIN[1], A.M. MALKIN[1], N.S. GINZBURG[1]

[1] Institute of Applied Physics of the Russian Academy of Sciences, Nizhny Novgorod, Russia
[2] Institute for Physics of Microstructures of Russian Academy of Sciences, Nizhny Novgorod, Russia

In [1, 2] a surface-wave oscillator (SWO) of planar geometry have been described. In this configuration the use of a planar waveguide with one corrugated wall and open along the x axis (Fig. 1a) makes it possible to provide mode selection in two transverse coordinates. In this case using of sufficiently wide (on the wavelength scale) sheet relativistic electron beams can provide monochromatic radiation with a power of several tens of megawatts in the short-wavelength part of the millimeter range.

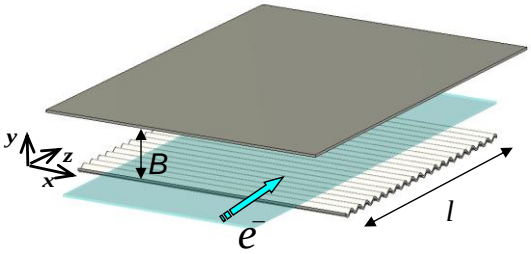

Fig.1. Schematic of the interaction space of SWO driven by a rectilinear sheet electron beam.

This paper is devoted to theoretical and experimental studies of W-band planar SWO. In simulation we use both the quasi-optical approach [2 – 5] and direct 3D PIC modeling. The research parameters were chosen close to the parameters of the experiments currently being carried out on the basis of the "SINUKI" accelerator (IAP RAS, N. Novgorod). The oscillator is designed for the operation frequency 75 GHz. The device is driven by 20 mm wide sheet electron beam with a thickness of 1 mm and current 1 kA and electron energy 0.7 MeV. A sinusoidal-profile grating with a period of 1.6 mm, a groove depth of 0.46 mm, and length of 20 periods was assumed. A modeling of the nonlinear dynamics showed that the use of an "open" electrodynamic structure with the transverse width of about 20 mm leads to the establishment of a stationary single-frequency π-mode regime with the output radiation power 40 MW.

In the experiment, the sheet electron beam was injected from a blade cathode and guided by uniform 3 T magnetic field. 1 kA sheet beam with transverse dimensions of 20 × 0.7 mm2 was obtained. The beam was aligned parallel to the grating surface in order to minimize the distance between the beam and grating, as well as to minimize the beam interception. The microwave generation with a frequency of about 75 GHz was registered by microwave detector; measured pulse duration was about 4 ns. The output power measured by the calorimetric method was about 25 MW which is in a satisfactory agreement with the theoretical predictions. The important specific of the experimental set-up is the use of high efficient side wall absorber for realization of open edge configuration.

REFERENCES

[1] A.E. Fedotov, P.B. Makhalov, "Transverse dynamics of a surface wave excited by a wide electron beam," Physics of Plasmas, vol. 19, p. 033103, 2012.

[2] N.S.Ginzburg, V.Y. Zaslavskii, A.M. Malkin, A.S. Sergeev, "Relativistic surface-wave oscillators with 1D and 2D periodic structures," Tech. Phys, vol. 57, pp. 1692–1705, 2012.

[3] N.S.Ginzburg, V.Y. Zaslavsky, A.M. Malkin, A.S. Sergeev, "Quasi-optical theory of relativistic surface-wave oscillators with one-dimensional and two-dimensional periodic planar structures," Physics of Plasmas, vol. 20, p. 113104, 2013

[4] [4] A.M. Malkin, V.Yu. Zaslavsky, I.V. Zheleznov, M.B. Goykhman, A.V. Gromov, A.V. Palitsin, A.S. Sergeev, A.E. Fedotov, P.B. Makhalov, N.S. Ginzburg, "Development of high-power millimeter-wave surface-wave generators based on relativistic ribbon electron beams," Radiophysics and quantum electronics, vol. 63, no. 5-6, pp. 458-468, May 2020.

[5] [5] A.V. Palitsin, A.E. Fedotov, A.M.Malkin, V.Yu. Zaslavsky, M.B. Goykhman, A.V. Gromov, Yu.M. Guznov, A.N. Panin, Yu.V. Rodin, N.S. Ginzburg "Design of W-band relativistic surface-wave oscillator with sheet electron beam," 2021 46th Int. Conf. on Infrared, Millimeter and Terahertz Waves (IRMMW-THz), pp. 1-2, 2021.

* The work is supported by Russian Federation program "Development of equipment, technologies and research in the field of atomic energy use in the Russian Federation for the period up to 2024" (IAP RAS Project No. 0030–2021-0027).

THERMAL LOSSES IN THE DIELECTRIC CASE OF THE ABSORBING LOAD OF LIQUID CALORIMETER IN MEASURING THE ENERGY OF HIGH-POWER MICROWAVE PULSES

A.I. KLIMOV, V.YU. KONEV

Institute of High Current Electronics SB RAS, Tomsk, Russia

Liquid calorimeters are successfully used to measure the energy of high-power microwave pulses [1]. The energy of the pulses is determined by measuring the increase in the volume of the working fluid based on ethyl alcohol, filling the volume of the absorbing load. An advantageous feature of these devices is their calibration, which is performed by applying an electrical pulse to an active load (calibration heater) located in the volume of the working fluid. An analysis of the thermal processes associated with the calibration of the calorimeters was carried out in [2]. The process of absorption of microwave pulse energy in the working fluid may be accompanied by the loss of part of the heat into the dielectric housing of the absorbing load and, thus, the underestimation of the measured energy. This work is devoted to the analysis of this undesirable effect. Using the results of solving the well-known problem of half-space cooling [3] in a flat approximation (Figure 1) without taking into account convection, analytical estimates of the heating of the polyethylene case of the absorbing load of the calorimeter were made.

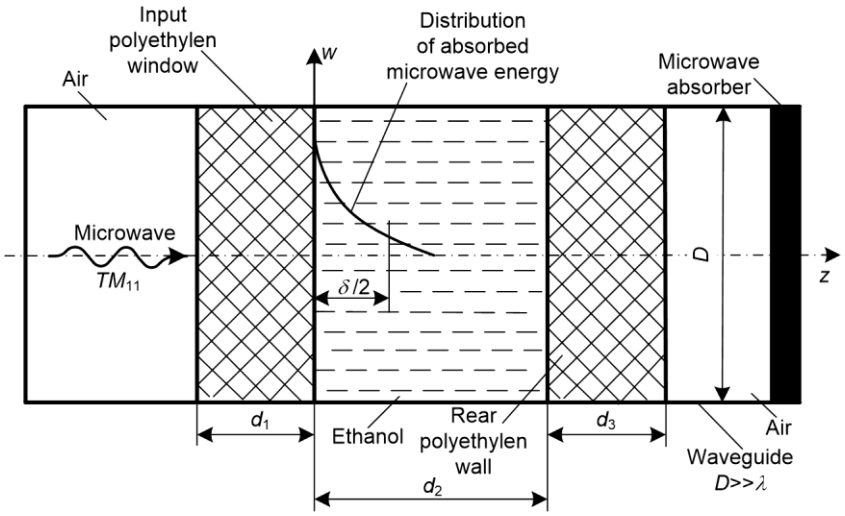

Fig. 1. Computational geometry of the problem.

The estimates show that the fraction of heat transferred from the alcohol to the dielectric increases with an increase in the carrier frequency of the microwave pulse and the duration of the measurement procedure. In the less favorable case, when the measurements are performed in the X-band, and the microwave energy is released mainly near the dielectric, the estimate of the underestimation of the measured microwave energy can reach tens of percent during the measurement time of 10 s. These results differ markedly from the experimental data. In order to more fully take into account the effects of heat transfer and more accurately determine the possible underestimation of the calorimeter readings, numerical simulations were performed.

REFERENCES

[1] A.I. Klimov, “Wide-aperture liquid calorimeters for measuring the energy of powerful microwave radiation pulses,” Rus. Phys. Journ., vol. 62, no. 7, pp. 1260–1268, July 2019.

[2] P.V. Priputnev, A.I. Klimov, and I.K. Kurkan, “On thermal processes in the calibration and control of liquid calorimeters for measuring the energy of high-power microwave pulses”, IOP Publ. Journ. Phys.: Conf. Ser., vol. 2094, Article Number 022066, 2021.

[3] D.V. Sivukhin, Obshchij kurs fiziki, T. 2, Termodinamika i molekulyarnaya fizika, Moskva, Nauka, 1990.

S3-P-016808

SCHEMES FOR RECORDING NANOSECOND HIGH-POWER MICROWAVE PULSES BY DETECTORS ON HOT CARRIERS

A.I.KLIMOV

Institute of High Current Electronics SB RAS, Tomsk, Russia

To detect nanosecond high-power microwave pulses [1], waveguide detectors [2–4] are used, based on the effect of a decrease in carrier mobility in a semiconductor upon absorption of microwave energy. The detectors use p-type Ge or n-type Si crystals. Examples of the two measurement schemes used are shown in Figures 1 and 2.

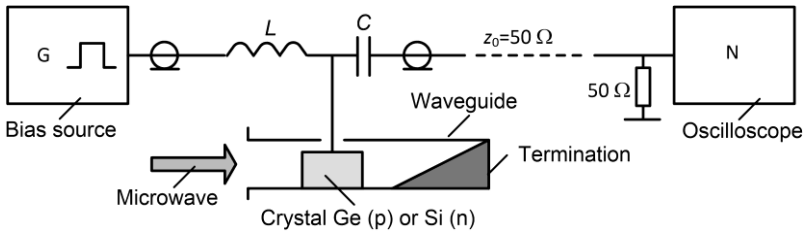

Fig. 1. Measurement scheme with a bias source next to the detector.

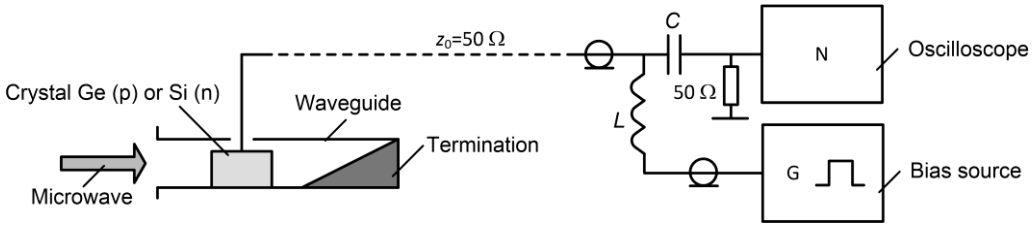

Fig. 2. Measurement scheme with remote bias source.

In both schemes, a bias voltage pulse with an amplitude U_0 and a duration significantly exceeding the duration of the microwave pulse is supplied to the crystal from the pulse generator through the inductance L. This voltage sets the steady current I_0 in the crystal and the initial resistance of the crystal R_0. When a microwave wave appears in the waveguide, the crystal resistance $R(t)$ increases, which is determined by the microwave power $P(t)$, which depends on time t. Under the condition $L / R(t) >> \tau$, where τ is the duration of the microwave pulse, the current through the crystal during the microwave pulse remains constant and equal to the initial value I_0. The output signal of the detector is determined by the registration circuit and depends on the voltage increase $\Delta U(t) = I_0[R(t) - R_0]$ on the crystal. In the scheme presented in Figure1, the bias source is close to the detector, and the bias signal at the cable input is suppressed by capacitance C. According to the conditions of the experiments, the useful signal is transmitted over a cable with a length usually exceeding the length of the signal in the cable to a remote oscilloscope for registration. This circuit corresponds to the detector calibration circuit. The only difference is that the microwave pulse in the calibration procedure is supplied from a special magnetron oscillator [4]. Therefore, the calibration corresponds to the measurement conditions in experiments with high-power microwave pulses. In the scheme presented in Figure 2, the bias source is removed from the detector by a cable length and is located next to the oscilloscope. The measurement conditions are different from the calibration conditions.

In this paper, the applicability of the calibration conditions (Figure 1) is analytically considered in this case as well.

REFERENCES

[1] J. Benford, J.A. Swegle, and E. Shamiloglu, High power microwaves, Oxford, Taylor & Francis Group, 2016.

[2] M. Dagys, Z. Kancleris, R. Simniskis, E. Schamiloglu, and F.J. Agee, “The Resistive Sensor: A device for high-power microwave pulsed measurements”, IEEE Ant. Prop. Mag., vol. 43, no 5, pp. 64–78. October 2001.

[3] V.I. Zelentsov, M.M. Ofitserov, M.D. Rayzer, and L.E. Tsopp, “Vysokochastotnye izmereniya v relyativistskoj elektronike”, Relyativistskaya vysokochastotnaya elektronika, Gor'kij, IPF AN SSSR, 1979, pp. 275–291.

[4] A.I. Klimov, Eksperimental'nye metody v sil'notochnoj elektronike, Tomsk, TPU, 2013.

S3-P-027601

DIFFRACTION OF A MONOPOLAR ELECTROMAGNETIC PULSE ON A SLIT

V.N. KORNIENKO [1], V.V. KULAGIN [1,2]

[1] Kotelnikov Institute of Radioengineering and Electronics RAS, Moscow, Russia
[2] Lomonosov Moscow State University, Moscow, Russia

A number of works published recently talk about the possibility of generating and emitting monopolar (or unipolar) electromagnetic pulses (MEMP) into free space [1,2]. Possible mechanisms for obtaining MEMP are considered. For example, the generation of MEMP is possible during the passage of a flat short bunch of relativistic electrons through an obliquely mounted conducting foil [3,4]. An electric discharge can be used for the radiation of a pair of solitary MEMP of opposite polarity in free space [5], etc.

Separately, there is the problem of managing of MEMP: its focus, change in the direction of distribution. To solve this problem, it is necessary, in particular, to consider the structure of the field formed during the passage of MEMP through a region of space containing inhomogeneities of a simple geometric shape.

This report presents the results obtained in a series of computational experiments, the purpose of which was to reveal the features of the spatiotemporal distribution of the diffraction field of a short MEMP with a flat front on a slit.

In Fig.1. the dependences of the diffraction field components on the longitudinal coordinate are shown at different times for two different polarizations of the incident pulse. In both cases, the field is bipolar, and for the TM polarization its profile is close to the profile of the time derivative of MEMP.

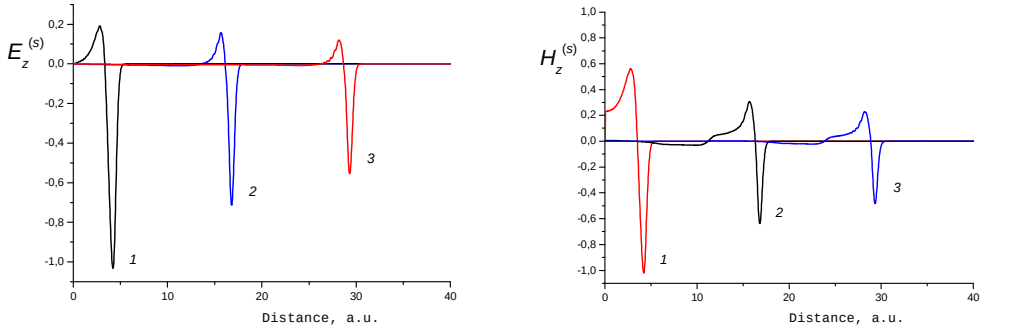

a) b)

Fig.1. Diffraction field on the axis of the system at different times (curves *1*,*2*,*3*). Case of *TE*- (a) and *TM*- (b) MEMP polarization.

It is shown that, for the considered cases, the MEMP diffraction field has a bipolar (or quasi-monopolar) form at distances comparable to the aperture size of the optical system, regardless of the polarization of the incident radiation.

REFERENCES

[1] R.M. Arkhipov, M.V. Arkhipov, N.N. Rosanov, “Unipolar light: existence, generation, propagation, and impact on microobjects” // Quantum Electronics. 2020. V.50. No 9. P.801.

[2] V.M. Fedorov, V.E. Ostashev, V.P. Tarakanov, A.V. Ul’yanov, “High power radiators of ultra-short electromagnetic quasi-unipolar pulses” // IOP Conf. Series: Journal of Physics: Conf. Series 830 (2017) 012020.

[3] Wu H.-C., Meyer-ter-Vehn J., “Giant half-cycle attosecond pulses” // Nature Photonics. 2012. V. 6. P. 304.

[4] Xu J., Shen B., Zhang X. et al., “Terawatt-scale optical half-cycle attosecond pulses” // Scientific Reports. 2018. V. 8. № 1. P.2669.

[5] V. N. Kornienko, D. R. Rumyanzev, V. A. Cherepenin., “Features of radiation of a pair of monopolar electromagnetic pulses into free space and the nature of their interaction with a model medium” // Journal of radio electronics [online journal]. 2017. №3. (http://jre.cplire.ru/jre/mar17/8/text.pdf) (in russian).

METALIZATION AND MANUFACTURING METAMATERIALS WITH 3D PRINTING TECHNOLOGY FOR VACUUM ELECTRON DEVICES*

A.B.DE ALLELUIA[1]

[1]*Power Microwaves and Photonics Laboratory, São Paulo, Brazil*

The design and fabrication of vacuum electron devices (VED) for high-power microwaves strongly depend on the manufacturing process. Due to the advance of additive manufacturing for 3D printers nowadays, it is possible to make devices with complex geometries using one machine only. The traditional manufacturing process in workshops is expensive because of many intermediate steps for fabrication, tools, and a significant amount of feedstock. The fabrication method based on the Fused Deposition Modeling (FDM) is the process that has presented the lowest cost to prototype from polymeric matrices.

This paper presents the process of manufacturing metamaterials through additive manufacturing with electroplating and sputtering metallization techniques. The figure 01 below illustrates the set of 02 complementary split-ring resonators for S band using a conductive polymer with resistances of 1.00 kΩ and 1.13 kΩ, respectively.

Figure 1- Split Rings printed with conductive material

Polymers with conductive properties are interesting to work as a seed layer in the material's metallization; however, high resistance and lack of material uniformity limit their application. Moreover, post-processing on the 3D printed material is necessary, and a conductive layer is applied. The results of this process and electroplating are in the figure 02.

Figure 2- Split rings printed and copper plated

After the metallization process, the initial surface resistance was reduced by up to 7E3 compared to the conductive polymer. The Sputtering process for 02 samples in figure 3 has a surface resistance of 0.2Ω and 0.68Ω, respectively. However, the deposition process was interrupted because of mechanical deformation that occurred in the samples.

Figure 3- Split rings printed copper plated with sputtering technique

The fabrication of split-ring resonators using 3D printers and metallization constitute an essential step in technological innovation for VED, allowing researchers to develop and manufacture complex geometries for metamaterials at a low cost quickly.

S3-P-031802

HIGH-GRADIENT ACCELERATION OF ELECTRON BEAM BY SUPERRADIATIVE MICROWAVE PULSE*

K.A. SHARYPOV[1], *N.S. GINZBURG*[2], *V.G. SHPAK*[1], *S.A. SHUNAILOV*[1], *M.I. YALANDIN*[1], *I.V. ZOTOVA*[2]
[1]*Institute of Electrophysics UB RAS, Ekaterinburg, Russia*
[2]*Institute of Applied Physics RAS, Nizhny Novgorod, Russia*

The prospect of high-gradient electron acceleration by microwave superradiance (SR) pulses is related to the fact that in the millimeter-wave band such pulses are shorter than 300 ps, and at low exposures of a strong microwave field, breakdowns of electrodynamic structures are delayed. For example, in a relativistic backward wave oscillator (BWO), it is possible to obtain Ka-band SR pulses with a power of 1–3 GW, although the microwave field strength on the wall of the slow-wave structure (SWS) exceeds 2 MV/cm [1, 2]. Apparently, at the edges of a resonant reflector located at the SWS entrance, many times larger fields arise. The report presents a model of acceleration of a paraxial electron beam in a low-Q "pill-box" cavity [3] pumped by Ka-band SR pulse.

An experimental scheme proposed in [4] is considered, where devices for SR generation and electron acceleration are combined in one block. Coaxial electron beams are used, which are formed from the cathodes powered by the same voltage pulse (-300 kV; 2 ns). The outer tubular beam is used to excite SR BWO, while the inner (paraxial) beam is accelerated. For its emission, a needle cathode is used, the axial position of which determines the beam current. In test experiments this current varied within 15-150 A. In the simulations by particle-in-cell method (KARAT code [5]), it reached ≈250 A. Since the SWS has an average diameter larger than the generation wavelength, it is possible to place a "pill-box" cavity with a central hole for introducing paraxial beam in front of the SWS entrance. The outer tubular beam passes in a narrow annular slot between the anode constriction before the SWS entrance, and the outer wall of the "pill-box" cavity. With that, a resonant reflector at the SWS entrance is not required. After "pill-box" pumping, the used SR pulse is output in the direction of external beam collector. Due to the gap between solenoid windings, magnetic field transporting the beams is profiled to drop external beam onto collector after the SWS. The area of paraxial beam registration by the current probe is located further than this collector.

At a magnetic field induction of ≈7 T in the SWS region, the simulated peak power of SR pulse at the "pill-box" cavity entrance reaches 1 GW. Acceleration effect for a paraxial beam is tracked in numerical simulations using a phase portrait of electron bunches. At the cavity pumping peak, a normalized electron momentum $p_z/mc \approx 4.5$ is reached, which corresponds to their kinetic energy of 1.85 MeV. Thus, a paraxial beam with initial energy of ≈250 keV has accelerated to 1.6 MeV. Since the depth of the "pill-box" cavity is 0.4 cm, the acceleration gradient turns out to be 400 MeV/m. An integral phase portrait of the accelerated beam separated by radius shows $p_z/mc \approx 5$ for paraxial particles at some instants, which corresponds to an energy of ≈ 2.1 MeV. However, this indicator does not refer to the particles at the "pill-box" exit, but to those localized along the SWS closer to the collector. In this additional acceleration, one can assume the influence of the non-synchronous interaction of paraxial bunches with z-field of SR wave (TM_{01}), which moves slower than the fast incidental electrons.

REFERENCES

[1] S.D. Korovin, G.A. Mesyats, V.V. Rostov et al., "Subnanosecond 1-GW Pulsed 38-GHz Radiation Source," Tech. Phys. Lett., vol. 30, no. 2, pp. 117–119, 2004.

[2] V. V. Rostov, I.V. Romanchenko, M.S. Pedos et al., "Superradiant Ka-band Cherenkov oscillator with 2-GW peak power," Phys. Plasmas, vol. 23, Article Number 093103, 2016.

[3] A. Vikharev, N. Ginzburg, S. Kuzikov et al., "Generation of Powerful Subterahertz Superradiance Pulses for High-Gradient Acceleration of Charged Particles," European Physical Journal Web of Conferences, vol. 195, Article Number 01023, 2018.

[4] M. I. Yalandin, A. A. Vikharev, I. V. Zotova et al., "Generation of Ka-Band Superradiant Pulses for High-Gradient Acceleration of Electrons in a Scheme with Two Coaxial Beams," In: Proc. of of 46th International Conference on Infrared, Millimeter and Terahertz Waves (IRMMW-THz), 29 Aug.-3 Sept. 2021, Chengdu, China, pp.1-1. https://doi.org/10.1109/IRMMW-THz50926.2021.9567202.

[5] V.P. Tarakanov, User's Manual for Code KARAT. Sprinfield, VA: Berkley Research. Associates, Inc. 1992.

* The work was supported by the Russian Science Foundation under grant No. 21-19-00260..

S3-P-032802

HIGH-CURRENT THZ-BAND GYROTRONS BASED ON AXIAL-SLIT CAVITIES*

YU. YU. DANILOV, A. N. LEONTYEV, A. M. MALKIN, R. M. ROZENTAL, D. YU. SHCHEGOLKOV
Institute of Applied Physics RAS, Nizhny Novgorod, Russia

At present, the prospects of generation high-power terahertz-band radiation are under intense investigation. For instance, in [1], a 330 GHz surface-wave oscillator was studied with output power exceeding 40 MW fed by an electron beam with an energy of 380 keV and a current of 2.2 кА. In [2], prospects for realization of 2 THz planar free electron lasers with a multi-MW power were discussed. Currently, gyrotrons are known to be the highest-power CW radiation sources in THz band, as they feature high mode selectivity allowing for use the highly oversized electrodynamical systems [3]. Gyrotrons fed by high-current relativistic beams can potentially be used as sources of high-power THz radiation. However, the selective excitation of the operating oscillation can constitute a significant problem in this case.

Here we propose a new type of high-selectivity resonators for high-current gyrotrons based on the coupling of modes with proportional azimuthal indexes and close eigenvalues. Based on the analytic approach and numerical simulations, we demonstrate that in an oversized cylindrical cavity with M axial slits, the coupling of the modes of regular waveguide with azimuthal indexes M and $2M$ can lead to formation of high-Q modes with small radial losses at the quasi-cutoff frequencies.

Simulations of electrodynamical properties of axial-slit cavities were conducted using the CST Microwave Studio software. As an example, Fig. 1a shows the cross section of a six slits cavity. The "internal" part of the eigenmode has six variation along the azimuth while the external has twelve (Fig.1b). Similar transverse structure can be obtained by arithmetic summation of the $TE_{6,4}$ and $TE_{12,2}$ mode fields (Fig.1c). Clearly, the "supermode" is based on the combination of the specified modes of the cylindrical waveguide coupled via axial slits.

We consider the cavities for $TE_{6,4}$+$TE_{12,2}$ mode combination in 300 GHz band and и $TE_{8,7}$+$TE_{16,4}$ mode combination in 500 GHz band. Using 3D PIC simulations at KARAT code [4], we show the possibility of development of gyrotrons with output power of up to 100 MW based on these cavities. We have also simulated the electron optics systems of high-current THz-band gyrotrons with an initially rectilinear electron beam pumped by a kicker and subsequent compression in rising magnetic field.

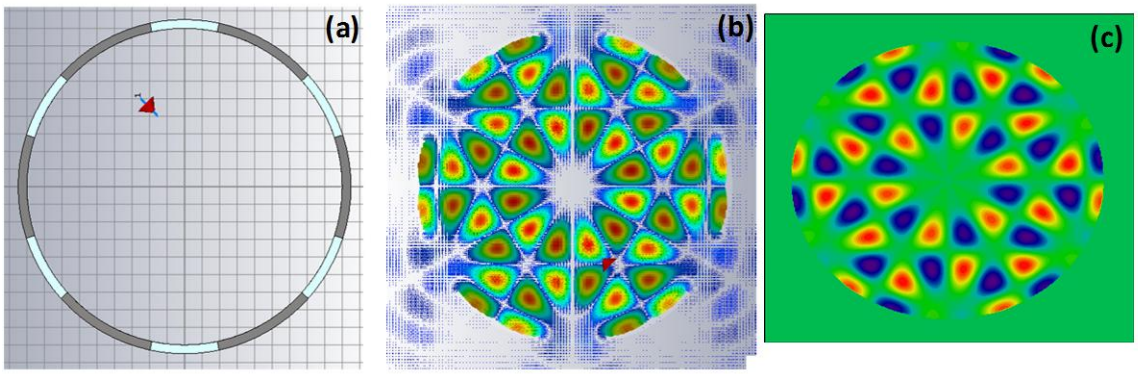

Fig.1. Cross section of a six slits cavity (a), transverse structure of the axial component of the microwave magnetic field in the case of "supermode" excitation (b), arithmetic sum of $TE_{6,4}$ and $TE_{12,2}$ transverse structures (c).

REFERENCES

[1] S. Li, J. Wang, D. Wang, "Relativistic Surface Wave Oscillator in Y-Band with Large Oversized Structures Modulated by Dual Reflectors," *Sci. Rep.* vol. 10, art.no. 336, January 2020, doi: 10.1038/s41598-019-55525-9

[2] A.V. Arzhannikov, N.S. Ginzburg, G.G. Denisov, P.V. Kalinin, N.Y. Peskov, A.S. Sergeev, S.L. Sinitskii, "A traveling-wave ring resonator with Bragg deflectors in a two-stage terahertz free-electron laser," *Tech Phys. Lett*, vol. 40, no.9, pp. 730-734, September 2014, doi: 10.1134/S1063785014090028

[3] M.Yu. Glyavin, G.G. Denisov, V.E. Zapevalov, M.A. Koshelev, M.Yu. Tretyakov, A.I. Tsvetkov, "High-power terahertz sources for spectroscopy and material diagnostics," *Physics-Uspekhi*, vol. 59, no. 6, pp. 595-604, doi: 10.3367/UFNe.2016.02.037801

[4] V.P. Tarakanov, "Code KARAT in simulations of power microwave sources including Cherenkov plasma devices, vircators, orotron, E-field sensor, calorimeter etc.," *Proc. EPJ Web Conf.*, 2017, vol. 149, art.no. 04024, doi: 10.1051/epjconf/20171490

* This work was supported by the Institute of Applied Physics of the Russian Academy of Sciences (IAP RAS) Project through the Program "Development of engineering, technology and scientific research in the field of atomic energy until 2024" under Grant 0030-2021-0027.

S3-P-033703

NONLINEAR AMPLIFICATION OF POWERFUL TERAHERTZ PULSEES BY ELECTRON BUNCHES*

A.V. SAVILOV, Y.S. OPARINA, D.D. KRYGINA

Institute of Applied Physics, Russian Academy of Sciences, Nizhny Novgorod, Russia

The effect of electron acceleration in the fields of wave pulses has been well studied [1,2]. In this work, we consider a possibility to "reverse" this problem and investigate the amplification of a short powerful terahertz-frequency-range wave pulse by a photo-injector electron bunch due to the deceleration (reflection) of electrons. In this process, the initial longitudinal velocities of electrons exceed the group velocity of the pulse. Naturally, this process should be realized in a media with the "proper" dispersion, so that the group velocity of the wave pulse is small enough. The electrons catch up with the pulse, and it reflects them, so that their final velocities become less than the group velocity of the wave packet. As a result, kinetic electron energy is passed to the wave.

Since this is a principally non-linear process, amplification of very powerful wave pulses is possible. We describe an amplifier based on a principally non-linear effect of reflection of a short high-current relativistic electron bunch from the powerful wave pulse. This is effective mechanism of energy extraction by the wave from particles, when parameters of the electron bunch (initial energy spread, bunch length and emittance) haven't significant influence on the efficiency of the electron-wave interaction. We describe two schemes of realization of this process. The first one is the amplification of high-power pulses due to the almost total braking in a waveguide under effect of the non-resonant pondermotive force (Fig. 1 a). Second, the amplification of weak pulses in a waveguide immersed in the undulator magnetic field is describes (Fig. 1 b); here, the undulator resonance provides an efficient electron-wave interaction.

Results of numerical simulations on the basis of the approach described elsewhere [3,4] demonstrate the possibility to provide nonlinear amplification of powerful wave pulses by at least in order of magnitude with efficiencies of the electron-wave interaction process at a level of 10 %. The amplification is accompanied by compression of wave pulses. Several examples of complicated dynamic of the nonlinear interaction between short electron bunches and powerful wave pulses will be given in the presentation.

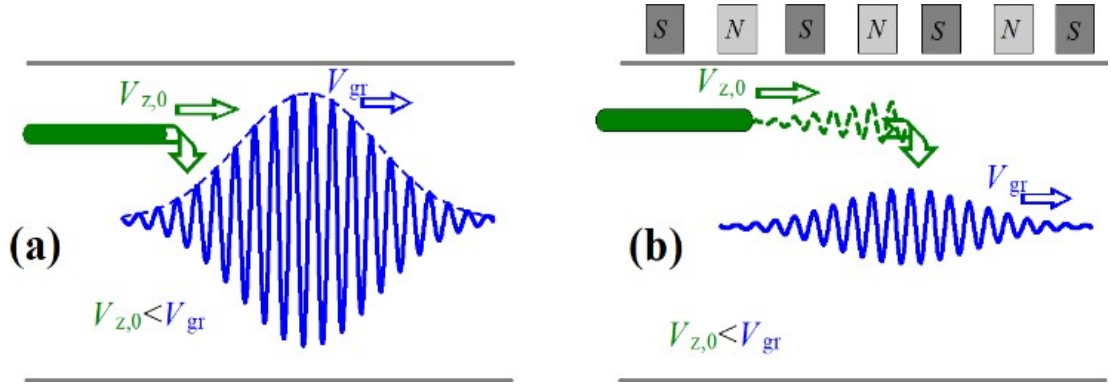

Fig.1. Non-resonant (a) and resonant (b) "reflection" of electron by a short powerful wave pulse.

REFERENCES

[1] Nanni E.A. et al. "Terahertz-driven linear electron acceleration", Nature Communications. vol. 6, p. 8486, 2015.

[2] T. Tajima and J.M. Dawson "Laser electron accelerator," Phys. Rev. Lett., vol. 43, pp. 267-270, 1979.

[3] I.V. Bandurkin, Y.S. Oparina, A.V.Savilov, "Super-radiative self-compression of photo-injector electron bunches," Appl. Phys. Letters, vol. 110, no. 26, p. 263508, 2017.

[4] Y.S. Oparina, A.V. Savilov, "Coherent super-radiative undulator emission of ultra-short THz wave pulses," Physics of Plasmas, vol. 28, no. 9, p. 093302, 2021.

* The work was supported by Russian Science Foundation (grant no. 21-72-30027).

S3-P-034601

SIMPLIFYED THEORY OF GYRO-BWO WITH ZIGZAG QUASI-OPTICAL MICROWAVE SYSTEM *

E.M. NOVAK, S.V. SAMSONOV, A.V. SAVILOV

Institute of Applied Physics RAS, Nizhniy Novgorod, Russia

Recently, a microwave system in the form of a quasi-optical transmission line was proposed for electron cyclotron sources of short-wavelength coherent electromagnetic radiation [1]. The system consists of focusing mirrors, which are periodically located along the longitudinal axis of coordinates and ensure the transportation of a Gaussian wave beam along a zigzag trajectory (Fig. 1). The operating electron beam propagates along the same axis, so that the electron beam intersects the wave beam periodically. Electron-wave cyclotron interaction occurs in regions where the wave propagates strictly across the electron beam, which leads to gyrotron-type electron-wave interaction with minimal sensitivity to the velocity spread of particles in the beam. 3D PIC modeling demonstrates the attractiveness of this "zigzag" cyclotron maser for realizing gyrotron backward wave oscillators (gyro-BWOs) operating in the sub-THz frequency range with an octave band of frequency tuning.

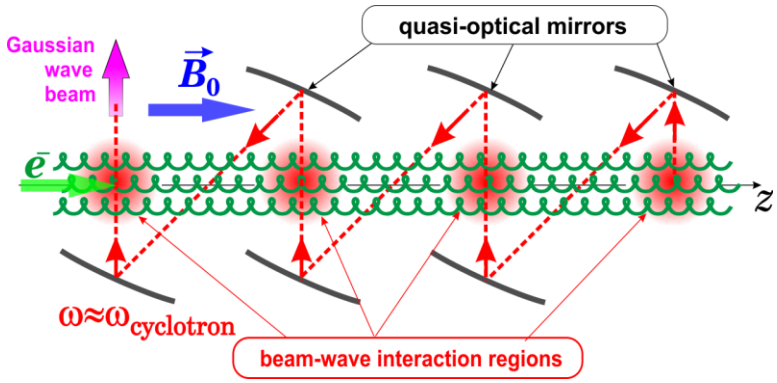

Fig.1. Schematic layout of a gyro-BWO with 3-period zigzag QO transmission line.

In this paper, we develop a quasi-analytical linear theory of such a gyro-BWO, as well as a simplified nonlinear space-time theory. These approaches explain the features of changing the operating frequency and output signal power in the process of broadband frequency tuning due to a change in the operating magnetic field. In particular, the complicated discrete-like nature of the dependence of the frequency of the excited wave on the cyclotron frequency with periodically occurring frequency “jumps” is explained, as well as various scenarios for changing the output power and generation frequency with a change in the external magnetic field or the initial energy of the particles. In addition, the nonlinear theory predicts the existence in this system of complex self-modulation regimes of generation, as well as regimes of superradiance of high-power short microwave pulses.

REFERENCES

[1] S.V. Samsonov, G.G. Denisov, A.A. Bogdashov, I. G. Gachev “Cyclotron Resonance Maser with Zigzag Quasi-Optical Transmission Line: Concept and Modeling”, IEEE Trans. Electron Dev., 2021, vol. 68, № 11, P. 5846-5850.

* The work was supported by the Russian Science Foundation under grant No. 21-19-00443, https://rscf.ru/project/21-19-00443/ .

S3-P-038102

SUB-TERAHERTZ GYROTRON BASED ON THE USE OF EXTERNAL FREQUENCY-TUNABLE MIRROR*

I.V. BANDURKIN, YU.K. KALYNOV, N.Y. PESKOV,

A.V. SAVILOV, I.V. OSHARIN, D.YU. SHCHEGOLKOV

Institute of Applied Physics, Russian Academy of Sciences, Nizhny Novgorod, Russia

For spectroscopic applications, compact sources of continuous coherent radiation of the sub-terahertz frequency range with relatively high (tens of Watts and higher) power are required. Important requirements for such sources are a narrow-band spectrum of the output radiation and, simultaneously, the possibility of smooth broadband frequency tuning, which would make it possible to obtain a spectral picture in a frequency band of at least a few percent. The most attractive sources for terahertz spectroscopy are gyrotrons (electron cyclotron masers based on selective excitation by weakly relativistic electron beams of high-Q quasi-critical modes of open cavities). However, the use of such operating modes in gyrotrons significantly limits the possibilities of frequency tuning.

We describe a project of a frequency-tunable sub-THz gyrotron. To ensure smooth broadband frequency tuning, we propose to implement a scheme based on excitation of different far-from-the-cutoff axial modes of an irregular cavity. The change of the operating mode provides the change of the operating frequency. The selective excitation of each of the modes is provided by reflecting part of the output signal from a narrow-band mirror, which is located outside the gyrotron window (that is, outside the vacuum zone) and "tuned" to the frequency of the excited mode (Fig. 1). The absence in an irregular cavity of high-Q modes that could be excited without external reflection is principally important. In this situation, the frequency of the excited mode is easily changed by mechanical change of the frequency of the external mirror (or even replacing one mirror with another).

The idea of the system shown in Fig. 1 arose after analyzing results of the experiment with a 30 keV/0.7A / 0.39 THz large-orbit CW gyrotron [1]. As a development of this work, we present a design and results of preliminary simulations of large-orbit gyrotrons at the fundamental (the frequency is close to 140 GHz) and the second (~280 GHz) cyclotron harmonics. Simulations predict selective excitation of different axial modes in a wide (~10%) frequency band with a relatively high efficiency of the electron-wave interaction (20-35%).

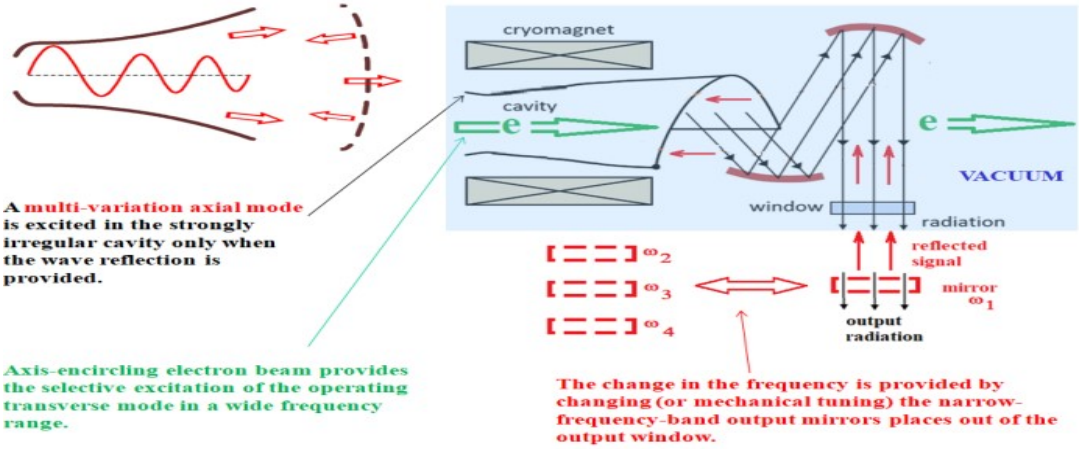

Fig.1. Schematic of the gyrotron with reflections of the excited wave from the external frequency-tunable mirror.

REFERENCES

[1] Yu.M. Guznov, Y.K. Kalynov, I.V. Osharin, A.V. Savilov, "Competition of Spurious Fundamental-Harmonic Oscillations in the Horn Section of a High-Harmonic Gyrotron," IEEE Trans. Electron Devices, vol. 69, p. 325, 2021.

* The work was supported the IAP RAS Program No. 0030-2021-0027.

S4-O-001004

TRIGGER CIRCUIT OPTIMIZATION OF THE OIL-INSULATED LTD CAVITY

V.M. ALEXEENKO[1], *A.A. KIM*[1], *V.A. SINEBRYUKHOV*[1], *S.S. KONDRATIEV*[1], *S.N. VOLKOV*[1],

[1]*IHCE SB RAS, Tomsk, Russian Federation*

The goal of this research was to reduce the number of external trigger pulses needed to trigger the LTD cavity with oil insulation. Previously the trigger circuit inside such cavity was a single wire O-ring which was connected to the switches of the cavity bricks via trigger resistors or coils. The minimum number of the external trigger cables connected to this O-ring was determined long time ago as 1 cable per 10 switches. It means, for example, that to trigger the switches of the cavity with ~30 bricks there must be at least 3 external trigger pulses.

In [1] a novel trigger system was presented for the cavity of 34 usual bricks and one internal trigger brick, which was triggered by only 1 external trigger pulse. In our tests similar trigger system was used but without the internal trigger brick. The external trigger pulse for our cavity of 16 bricks was generated by usual trigger generator. The cavity was loaded into matched load, and tested in more than 3000 shots, at a charge voltage of the cavity capacitors ±100 kV, dry air pressure in the switches 4 ata, and a charge voltage of the trigger generator 100 kV. In all these shots no any malfunction was observed.

Simulation has shown that up to 40 switches might be successfully triggered by one external trigger pulse not only in case the trigger system similar to [1] but without the internal trigger brick is used, but also in case of our previous trigger circuit consisting just of a simple wire O-ring. This last prediction was tested in experiment with our cavity of 16 bricks in 600 shots, at the charge voltage of the cavity capacitors ±100 kV, dry air pressure in the switches 4 ata, and a charge voltage of the trigger generator 100 kV. In these shots no any malfunction was observed also. The comparison of tests with similar to [1] and with our previous trigger circuit of just one wire O-ring has shown, that the jitter of the output pulse did not change, and the mean delay of the cavity firing reduced from ~58 ns to ~44 ns.

The results of this research, including simulation and tests, have shown that safe triggering of oil-insulated LTD cavity can be provided by using previous trigger circuit inside the cavity and 1 external trigger pulse, allowing to simplify considerable the trigger system presented in [1]. Previous requirement of 1 trigger cable per 10 switches can be reduced to less strict claim of 1 trigger cable per 16 switches, allowing to reduce at least 1.5 times the number of such cables needed for each LTD cavity.

REFERENCES

[1] Zhou Lin, Li Zhenghong, Wang Zhen et. al. Design of a 5-MA 100-ns linear-transformer-driver accelerator for wire array Z-pinch experiments// Phys. Rev. AB 19, 030401 (2016).

S4-O-002801

SURGE OF A HIGH-VOLTAGE PULSE IN THE TRIGGER SYSTEM OF A PSEUDOSPARK SWITCH DURING COMMUTATION*

G. A. ARGUNOV, N.V. LANDL, Y.D. KOROLEV, V.G. GEYMAN, O.B. FRANTS, V.O. NEKHOROSHEV

Institute of High Current Electronics SB RAS, Tomsk, Russia

High-current gas discharge commutators have always been of a keen interest in various fields of applications. Especial niche here have been occupied by cold cathode thyratrons, also known as pseudo-spark switches [1]. These devices showed exceptional triggering characteristics such as low jitter and low delay time to triggering along with a capability to commutate high currents up to several kA's at high anode voltage at a level of 40 kV and above [2].

Previously it has been shown that the trigger system is a crucial part, responsible for stability of triggering of the thyratrons [3]. To provide a nanosecond stability of triggering, it is necessary to achieve a stable formation of the pulse trigger discharge, which ignites in the trigger unit [3, 4]. Due to numerous trials and research, an optimal trigger unit of the thyratron has been developed [5, 6]. The new trigger unit provides a stable formation of the trigger discharge thus delivers a stable triggering of the switch.

There is a dark side of the new trigger unit. It generates a dense plasma during triggering and this plasma conducts a high electric potential from the anode into the trigger unit cavity, delivering a pulse of high voltage into the trigger system when triggering. This drawback may bring undesirable consequences in some sensitive applications.

In this work, we investigate opportunities to eliminate the high-voltage pulse, emerging in the trigger system during triggering of the thyratron. Different approaches have been applied toward investigation of the high-voltage pulse.

REFERENCES

[1] V.D. Bochkov, V.M. Dyagilev, V.G. Ushich, O.B. Frants, Y.D. Korolev, I.A. Shemyakin, K. Frank, "Sealed-off pseudospark switches for pulsed power applications (current status and prospects)," IEEE Trans. Plasma Sci., vol.29, no.5, pp. 802-808, 2001

[2] Y.D. Korolev, N.V. Landl, V.G. Geyman, A.V. Bolotov, V.S. Kasyanov, V.O. Nekhoroshev, S.S. Kovalsky, "Nanosecond Triggering for Sealed-Off Cold Cathode Thyratrons With a Trigger Unit Based on an Auxiliary Glow Discharge," IEEE Trans. Plasma Sci., vol.43, no.8, pp.2349-2353, 2015

[3] Y.D. Korolev, N.V. Landl, V.G. Geyman, O.B. Frants, I.A. Shemyakin, V.S. Kasyanov, and A.V. Bolotov, "Study of cold-cathode thyratron triggering stability at high anode voltages," Plasma Phys. Rep., vol. 44, pp. 112–120, 2018

[4] Y.D. Korolev, N.V. Landl, V.G. Geyman, G.A. Argunov, O.B. Frants, and A.V. Bolotov, "Methods of triggering for the cold-cathode thyratrons with a trigger system based on an auxiliary glow discharge," AIP Advances, vol. 9, 085326, 2019

[5] Y.D. Korolev, N.V. Landl, V.G. Geyman, O.B. Frants, "Hollow-cathode glow discharge in a trigger unit of pseudospark switch," Phys. Plasmas., vol.25, no.11, 13510, 2018

[6] N.V. Landl, Y.D. Korolev, V.G. Geyman, O.B. Frants, G.A. Argunov, A.V. Bolotov, A.V. Akiov, P.A. Bak, "Special Features of Parasitic Current Formation in a Sealed-Off Cold-Cathode Thyratron with Trigger Unit Based On an Auxiliary Glow Discharge" // Rus. Phys. J., vol.62, no.7, pp. 1279-1288, 2019

* This work was funded by RFBR according to the research project № 19-08-00326a

S4-O-005401

SURFACE IRRADIATION INSTALLATION BASED ON URT-0,5M ACCELERATOR *

S.YU. SOKOVNIN[1,2], M.E. BALEZIN[1]

[1] *Institute of Electrophysics UB RAS, Yekaterinburg, Russia*
[2]*Ural Federal University named after First President of Russia B.N. Yeltsin , Yekaterinburg, Russia*

A surface irradiation installation based on the URT-0,5M accelerator (~ 0.45 MeV, 1 kW) [1] that includes built-in radiation protection and a radiation-resistant conveyor of products under the beam was developed based on the peculiarities of application in industrial poultry farming [2].

The oil-filled tank of the accelerator, where a circuit of high voltage pulse generation is located, has detachable side coversfor ease of installation and maintenance. A vacuum diode is used for double-sided irradiation with a beam diameter of ~ 100 mm. The core of the pulse transformer is made of 1V-M magnetic conductors.

Built-in radiation protection is made of grade S3 lead, the thickness of the sheets (up to 36 mm) is based on the calculation, moreover, the dose limit allowed in the Russian Federation (20 mSv/year) is provided at a distance of 1 m from the beam axis during operation 2000 hours/year.

The radiation-resistant conveyor consists of a console and a conveyor. The console contains ED3100 frequency converter, which allows to adjust conveyor belt speed by setting frequency within the range from 1 to 50 cm/s.

All systems are operated and controlled from a personal computer connected to the control panel using a fiber-optic communication line up to 25 m long. The operating and control program installed on the laptop runs on Windows 7. Information on vacuum level, high voltage level, pulse generation and status of all sensors is supplied to control and monitoring program and recorded in a text file [3].

Tests of the installation showed that the resulting doses of the electron beam are sufficient for surface disinfection of eggs (~ 12 kGy) simultaneously on both sides at a rate of movement of egg cassettes of 3.1 cm/s, which provides a productivity of up to 5400 eggs/hour. Dosimetry showed that the designed protection provides the required level of safety.

REFERENCES

[1] S.Y. Sokovnin, M.E. Balezin, "Improving the Operating Characteristics of an УРТ-0.5 Accelerator", Instrum Exp Tech, vol. 48**,** pp. 392–396, 2005.

[2] S.Yu. Sokovnin, " An electron beam technology of surface disinfection of the packed egg", Food and Bioproducts Processing, vol. 127, pp. 276–281, 2021.

[3] M. A. Safonenko, S.V. Shcherbinin, "Control System of The Powerful Pulse Electron Accelerator", AIP Conference Proceedings, vol. 2313, 040020, 2020.

* The work was partially supported by RFBR, Russia and Sverdlovsk region, project number 20-48-660019 p_a..

S4-O-008301

TECHNOLOGICAL ASPECTS OF THE PRODUCTION OF SPARK GAP-SHARPENERS FOR VOLTAGE UP TO 500 KV

D.S. MAKHANKO

PLASMA, JSC Research Institute of Gas-Discharge Devices, Ryazan, Russia

The purpose of this work is to provide basic information about the manufacturing technology of sealed-off spark gaps-sharpeners in metal-ceramic design with hydrogen filling and pressures up to 120 atmospheres providing minimum geometric dimensions at voltages up to 500 kV, subnanosecond response times and a resource of at least $3x10^6$ inclusions in a given operating mode.

Uncontrolled spark gaps-sharpeners are one of the main elements of any high-voltage pulse generator designed to generate high-voltage pulses with amplitudes of hundreds of kilovolts and a leading edge duration of units and tenths of a nanoseconds. The fields of application of spark gaps-sharpeners as part of high-voltage pulse generators are portable X-ray machines, accelerator technology, sources of pumping gas-discharge lasers of superatmospheric pressure, electron-optical converters and photo recorders of pico- and femtosecond radiation processes.

This paper describes the relationship between the structural elements of the spark gap-sharpener and the electrical strength of the ceramic insulator to breakdowns on its surface, as well as the breakdown of the gap between the high-voltage output and the body of the spark gap.

To ensure high rates of switching characteristics in spark gap-sharpeners, hydrogen is used as a working medium at pressures up to 120 atmospheres. High pressure values impose very strict requirements on the mechanical strength of both individual components and the design of the spark gap-sharpener as a whole. It is also necessary to correctly select the electro-vacuum materials used, which ensure high mechanical strength and vacuum density of metal - ceramic junctions. It should be noted that the use of ceramic insulators imposes certain restrictions on their design, in particular in the form of a truncated cone.

The main technological process of soldering the cathode metal-ceramic unit using silver solder PSr 72, the process manufacturing the anode unit using the two-stage soldering method, and describes the filling and training of the spark gap-sharpener with electronegative gas to increase the electrical strength are given.

Soldering at elevated temperature according to the mode described in this work contributes to better wetting of the soldered surfaces with solder, its faster spreading and filling of the covering seams, and also provides capillary filling of the edge seams. With a sharp change in the soldering temperature, the solder in the edge joint begins to melt from the outside to the inside of the seam. Moving the molten solder from the outside to the inside of the seam significantly improves the structure of the seam and, as a result, the mechanical and thermal characteristics of the ceramic-metal connection.

A promising direction for improving the quality of manufactured spark gap-sharpeners and other complex structures of devices with simultaneous use of both edge and covering metal-ceramic and metal junctions is the use of the technology of soldering of metal-ceramic assemblies given in this article with a significant excess of the soldering temperature, the rate of temperature change and exposure during soldering, depending on the design features of the products. This method of manufacturing a gas-filled metal-ceramic spark gap-sharpener made it possible to ensure high reliability and tightness of the device. Additional training of high-voltage spark gap-sharpeners in SF_6 gas or its mixtures with inert gas and/or nitrogen can significantly increase the electrical strength of the spark gap-sharpeners.

The industrial production of a series of spark gap-sharpeners of the RO – 48, – 43, – 49, – 72 type has been mastered for operating voltages from 100 to 500 kV for use mainly in pulsed X-ray technology. Using the manufacturing method described in this work, the percentage of usable products increased to 95% during the mass production of spark gap-sharpeners.

Measurements of the switching characteristics of spark gaps were carried out on a stand, in which instead of an X-ray tube, were set low-inductive resistors of the TVO-60 type and a resistive current shunt with R=0.01 Ohms were installed. A constructive capacitive divider was used to register the temporary behavior of the voltage on the spark gap.

S4-O-008705

VISUALIZATION OF THE TEMPERATURE DISTRIBUTION IN A DBD-DRIVEN HELIUM ATMOSPHERIC PRESSURE PLASMA JET*

A.A. DYACHENKO, O.M. STEPANOVA, M.E. PINCHUK

Institute for Electrophysics and Electrical Power of the Russian Academy of Sciences, Saint-Petersburg, Russia

A helium plasma jet is often used in modern studies on plasma-bio interactions as a source of cold atmospheric plasmas [1]. Thermal control is a crucial factor for a plasma jet application, especially for the treatment of living tissues [2].

Here, a gas temperature field visualization of the DBD-driven helium plasma jet directed along upward vertical axis is presented. The plasma jet was generated by a dielectric-barrier discharge in a quartz tube with the inner diameter of 4.6 mm and the thickness of the wall of 1 mm. An electrode system consists from an inner electrode, a copper wire of 1.5 mm in diameter, located along the tube central line at the distance of 7.5 mm from the edge of the tube and an outer electrode, a copper foil strip of 5 mm wide, wrapped around the tube at the distance of 5 mm from its edge. A high-voltage tailoring signal was applied to the inner electrode with the peak-to-peak value of 4.6 kV and a duty cycle of ≈90%. The applied voltage waveform and additional details about the experimental set-up can be found in [3].

Helium flow rates were set 2, 4, 6 and 8 l/min as in the paper [4]. A transition from one-pass propagation to stepwise propagation of a guided streamer along the plasma jet was observed at varying the gas flow rate . So, here we specified the temperature conditions associated with the transition from one-pass mode to stepwise propagation of the guided streamer.

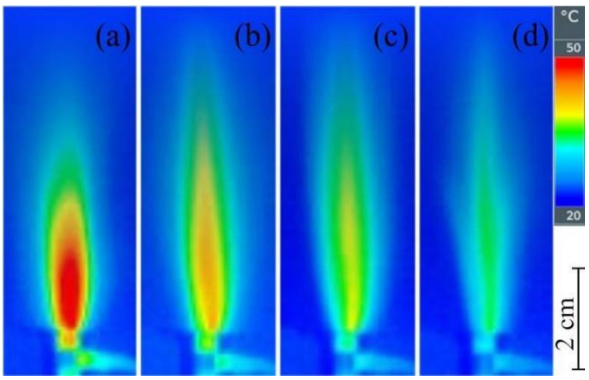

Fig.1. Temperature distribution in helium plasma jet at the gas flow rate of 2 **(a)**, 4 **(b)**, 6 **(c)** and 8 **(d)** l/min

The temperature field was visualized on a thin glazed paper sheet, placed along the axis of the jet, and measured with a thermal imager looked perpendicular at the sheet's surface. It was assumed that the temperature field qualitatively reflects the temperature distribution in the plasma jet. It has been experimentally determined that the temperature regime is set within two minutes. The temperature distribution patterns for different gas flow rates after 2.5 min are shown in Fig. 1. The temperature distribution obtained using the shadow method and temperatures obtained using thermocouples [5] coincides with those obtained using this technique.

REFERENCES

[1] S. Bekeschus et al. "White paper on plasma for medicine and hygiene: Future in plasma health sciences," Plasma Processes & Polymers, e1800033, doi:10.1002/ppap.201800033 (2018).

[2] Physics of Thermal Therapy: Fundamentals and Clinical Applications. Edited by Eduardo G. Moros, CRC Press:Taylor & Francis Group, (2013).

[3] M. Pinchuk et al. "Role of charge accumulation in guided streamer evolution in helium {DBD} plasma jets," Scientific Reports, 11, 17286, doi:10.1038/s41598-021-96468-4 (2021).

[4] M. Pinchuk et al. "Transition from one-pass mode to stepwise propagation of a guided streamer along a helium plasma jet," Applied Physics Letters, 119, 054103, doi:10.1063/5.0053672 (2021).

[5] O. Stepanova et al. "Temperature distribution in DBD-driven helium atmospheric pressure plasma jet measured by schlieren technique," XIII-FLTPD & I-FLTPS, Book of Abstracts, Bad Honnef, Germany: Ruhr University Bochum, p.16 (2019)

The study was financially supported by the Russian Science Foundation (project 22-29-01215, https://rscf.ru/en/project/22-29-01215/).

S4-O-014401

THE INFLUENCE OF DC PULSE CURRENT PATTERN ON THE DIFFERENT MATERIALS PROPERTIES OF SAMPLES OBTAINED BY SPARK PLASMA SINTERING

THET NAING SOE[1], I.M.MAKHADILOV[1], A. P. MALAKHINSKY[1], N.W.SOLIS PINARGOTE[1]

[1] "Moscow State Technological University "STANKIN" (MSTU "STANKIN"), Moscow, Russia

Spark Plasma sintering (SPS) is most advanced sintering technology that is progressively developed for the manufacture of nanostructured composites and gradient materials. This sintering method is based on a modified hot-pressing process in which an electric current is passed directly through the die and the material to be sintered rather than through an external heater. SPS is one of nanopowder consolidation methods, which apply a uniaxial pressure and thermal expansion between the raw powder and the matrix using high heating rates (from 100 to 1000 °C/min). The heating used for the sintering is meanly generated by Joule heating in a graphite matrix when a DC pulse current, created during the SPS process, crosses through them. Thanks to this, the thermal field in the sample is caused mostly by heat conduction from the matrix and others heating mechanisms as Joule heating, electrical discharges, and high-temperature plasma, associated with the electric current. The current is created by a DC pulse current generator, which can control the ON-OFF parameters of the DC pulses. Thereby, the use of pulse current during sintering promotes the appearance of spark discharges in the gap or at the point of contact between the material particles. The temperature in the spark discharge zones is in the order of about 1000 °C, which leads to local melting and/or evaporation of the raw material in very short periods of time. This leads the formation of a neck in the contact zones between the powder particles due to the mass transfer process during sintering [1,2,3]. For this reason, the study of the influence of the pulse current form on the mechanical properties of sintered samples is a very interesting field of research, which requires a lot of attention due to its practical application. Unfortunately, only few research groups are carried out investigations in this field, and they established some dependence for the sintering of specific materials under certain conditions. For instance, Xie et al [4], showed that the frequency is a factor that influences on the homogenous temperature distribution through sintering raw powder, but it has not influence on the sintered sample material properties. On the other hand, a pulsed DC current during sintering can generate very high heating and cooling rates, which enhance the diffusion mechanism of the raw material, which in turn permit the grain growth control process, and leads to a combined improvement of different material properties that include high-temperature strength and good mechanical properties such as density, toughness, flexural strength and good surface stability at the high-temperature environment [5].

REFERENCES

[1] D.B Kumar, B.S Babu, K.M Aravind Jerrin, N Joseph, A Jiss, “Review of Spark Plasma Sintering Process,” IOP Conf. Series: Mater. Sci. and Eng. 993 .2020.

[2] J. Fu, J. C. Brouwer, I. M. Richardson and M. J. M. Hermans, Effect of mechanical alloying and spark plasma sintering on the microstructure and mechanical properties of ODS Eurofer, Mater. and Des. 177, 2019.

[3] Z.H. Zhang, Z.F. Liu, J.F. Lu, X.B. Shen, F.C. Wang, Y.D. Wang, The sintering mechanism in spark plasma sintering- proof of the occurrence of spark discharge, Scr. Mater. 81 (2014) 56-59.

[4] Xie et al, O Ohashi, K Chiba, N Yamaguchi, M.H Song, K Furuya, T Noda, “Frequency effect on pulse electric current sintering process of pure alumina,” Mater. Sci. and Eng. A359, 384-390, 2003

[5] N Sahed, I Zafar, A Khalil, A.S Hakeem, A.A Nasser, T Laoui., Qutub A Al, R Kirchner, “Spark Plasma Sintering of Metals and Metal Matrix Nanocomposites: A Review,” Jour. of Nanomater. Vol 2012, 4 June 2012.

S4-O-017504

GAS DISCHARGE RM ION LASERS OPERATING AT HIGH PULSE REPETITION FREQUENCY*

M.A. LAVRUKHIN[1], *P.A. BOKHAN*[1], *P.P. GUGIN*[1], *I.M. ANANYEV*[2], *D.E. ZAKREVSKY*[1,2]

[1] *A. V. Rzhanov Institute of Semiconductor Physics SB RAS, Novosibirsk, Russia*
[2] *Novosibirsk State Technical University, Novosibirsk, Russia*

Pulsed gas discharge lasers on resonance-metastable (RM) transitions still remains in-demand devices due to their unique parameters, which include high gain coefficient, narrow line-width, large radiation pulse power, etc. [1]. Specific areas of their application include active optical systems, dermatology, micromachining and etc. In general lasers on RM atom transitions are more efficient and powerful than on the ion ones. However, this situation can be different in case of high pulse repetition frequency (PRF), because maximum of the average output power P_{av} for atom RM transitions is reached at lower values of PRF. For example, recently [2], for Ba^+ laser growth of P_{av} up to 60 kHz was demonstrated, meanwhile for the copper vapor laser maximum of the average output power lies in the range of ~ 10 - 30 kHz [1]. High PRF is important in active optical systems, because it determine temporal resolution. So, it is valuable to study other ion RM lasers operating at high PRF (100 kHz and more), as they may be more suitable for this distinct application. Also, a lot of ion RM transitions in UV spectrum range exists, which increases potential interest in the investigation of these lasers. Excitation of RM lasers at high PRF is complicated due to high prepulse electron concentration, which requires rapid voltage growth between the GDT electrodes in order to achieve preferable electron temperature for laser levels excitation. One of the possible solution is to use appropriate nanosecond switching devices, such as described in [3].

Two different active medium were investigated. In the first, lasing occurred on 4p $^2P^o_{3/2}$ - 3d $^2D_{5/2}$ (λ = 854.2 nm) and 4p $^2P^o_{1/2}$ - 3d $^2D_{3/2}$ (λ = 866.2 nm) RM-transitions in Ca^+. Second studied laser operated on $5d^{10}6p\ ^2P_{3/2}$ - $5d^96s^2\ ^2D_{5/2}$ RM-transition in mercury ion (λ = 398.4 nm). In case of Ca^+ laser gas discharge tube (GDT) was manufactured from BeO ceramics with inner diameter of 1.5 mm and length of 55 cm. The operating temperature of the active medium was maintained by an external heater. The studies were carried out using helium, neon or a mixture of helium and hydrogen as a buffer gas in the active medium of the laser. The lasers operated in the burst mode to perform the measurements while independently controlling the pumping power and the temperature of the GDT wall. Maximum measured average output power in the steady-state mode at PRF 100 kHz reached more than 5 W (Fig. 1), which is almost an order of magnitude higher than obtained in other studies [1].

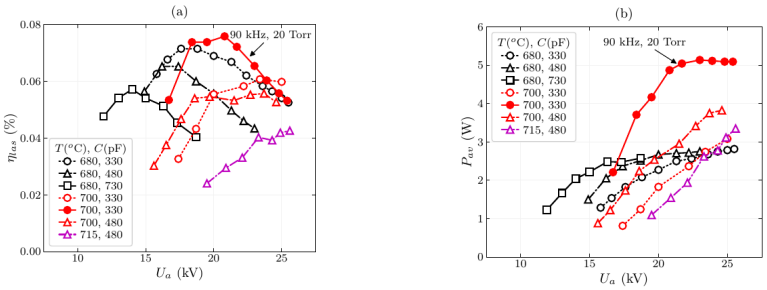

Fig.1. Dependences of the laser efficiency η (a) and average output power P_{av} (b) on the voltage amplitude U_a at the operating capacitance for different values of the operating capacitance C and GDT wall temperature T. Helium buffer gas pressure p equals 10 Torr and PRF f = 50 kHz, except for the curve with maximum values.

To investigate output parameters of UV Hg^+ laser two externally heated GDT with various inner diameters (5 and 12.5 mm) were constructed. Excitation circuit was modified in order to increase operating PRF up to 200 kHz. As the result lasing with radiation pulses duration of ~ 20 ns were obtained in burst operation mode.

REFERENCES

[1] Little C.E., “Metal vapour lasers : physics, engineering and applications”, Wiley-VCH, Chichester New York, 1999.

[2] Lavrukhin M.A., Bokhan P.A., Gugin P.P., Zakrevsky D.E., “Self-terminating barium ion laser at 614.2 nm”, Optics & Laser Technology, vol. 149, p. 107625, 2022.

[3] P.A. Bokhan, P.P. Gugin, D.E. Zakrevsky, M.A. Lavrukhin, “Frequency Characteristics of a Subnanosecond Plasma Switch”, Russian Physics Journal, vol. 62, № 11, p. 2059, 2020.

*The work was supported by the Russian Science Foundation (project No. 19-19-00069).

S4-O-021801

GENERATING ACOUSTIC VIBRATIONS IN THE AIR MEDIUM BY USING A GAS DISCHARGE EMITTER

D.A. DERUSOVA[1], V.O. NEKHOROSHEV[2], V.P. VAVILOV[1]

[1]Tomsk Polytechnic University, Tomsk, Russian Federation
[2] Institute of High Current Electronics SB RAS, Tomsk, Russian Federation

By using an atmospheric-pressure spark discharge, an apparatus and methodology for generating acoustic waves in the air medium were developed [1]. The gas discharge operation principle involves the forming of electric current pulses (t_p <1 μs) in the electrode system of the emitter while the storage capacitor discharges through the gas discharge plasma channel. This leads to the appearance wide range of acoustic vibrations, in the ambient air and, correspondingly, on the emitter surface. By using the scanning laser Doppler vibrometry technique [2-4] in the time mode, the damped vibrations of the emitter membrane were measured during discharge current flowing. A typical graph of vibrations magnitude in the center of the membrane is shown in fig. 1.

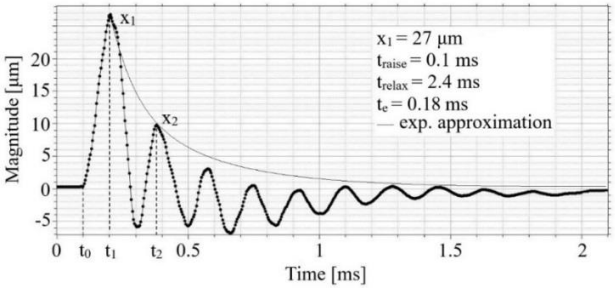

Fig.1. Vibrations of gas discharge emitter membrane excited by gas discharge electric pulse.

The evaluation of membrane vibrations showed that the amplitude of the first maximum of 1-mm aluminum membrane oscillations reached 27 μm in the case of a minimal inter-electrode gap of 5 mm. Typical relaxation time is 2.1 ms, therefore, in the particular experiment, the recording time at each scanned point was chosen to be under 4 ms. This allowed recording emitter vibrations with the pulse repetition rate up to 30 Hz. In general, the results above show that the grade of damping of the oscillating system was low and it can be corrected by changing damping characteristics in particular applications.

The amplitude-frequency spectrum of the proposed gas discharge emitter, as well as repeatability of the amplitude of vibrational displacement in the pulsed mode were analyzed. As a result, a non-stable character of vibrational displacement on the emitter membrane was demonstrated. The periodicity of measured is probably related to the physical processes in the gas discharge caused by variations of gap and plasma parameters.

The mean displacement value matches well the corresponding characteristic of classical piezoelectric and magnetostrictive transducers [5]. Moreover, the amplitude-frequency spectrum analysis shows that the emitter generates acoustic waves in the air in the total frequency range from 50 Hz to 100 kHz and can be used for non-destructive testing of composite materials. An example of using a gas discharge emitter in combination with SLDV for nondestructive testing of a hybrid flax/carbon fiber reinforced composite is presented to confirm the possibility of defect evaluation.

ACKNOWLEDGEMENT

This work was supported by Russian Science Foundation under grant no. 21-79-00169

REFERENCES

[1] D.A. Derusova, V.P. Vavilov, V.O. Nekhoroshev, V.Y. Shpil'noi, N.V. Druzhinin, "Features of Laser-Vibrometric Nondestructive Testing of Polymer Composite Materials Using Air-Coupled Ultrasonic Transducers," Rus. J. of NDT, vol. 57, no. 12, pp. 1060-1071, 2021.

[2] Solodov, D. Doring, G. Busse, "Air-coupled laser vibrometry: analysis and applications", Appl. Opt. 48, 33-37 (2009).

[3] Solodov, A. Dillenz, M. Kreutzbruck, "A new mode of acoustic NDT via resonant air-coupled emission", J. of Appl. Phys. 121, 245101 (2017)

[4] J. Segers, S. Hedayatrasa, E. Verboven, G. Poelman, W. Van Paepegem, M. Kersemans, "In-plane local defect resonances for efficient vibrothermography of impacted carbon fiber-reinforced polymers (CFRP) ," NDT and E Int., vol. 102, pp. 218 – 225, March 2019

[5] D.A. Derusova, V.P. Vavilov, N.V. Druzhinin, ect. "Investigating vibration characteristics of magnetostrictive transducers for air-coupled ultrasonic NDT of composites", NDT and E Int. 107, article number 102151 (2019)

S4-O-024702

THRUST CHARACTERISTICS OF MICRO PULSED PLASMA TRUSTER FOR NANOSATELLITES

P.S. MIKHAILOV, I.L. MUZYUKIN, A.D. MAKSIMOV

Institute of Electrophysics UB RAS, Yekaterinburg, Russian Federation

The paper deals with the development micro pulse plasma thruster. Currently, the number of launches of nano and micro satellites is growing [1]. This is facilitated by their low price and mass. For example, a 3U CubeSat is a satellite with sizes 30x10x10 cm and a mass of about 4 kg. At the moment, the majority of satellites are not equipped with a propulsion system. The presence of the thruster will help to expand the number of available missions and to prolong the life of the satellite [2].

The main principals of electrical propulsion systems are that stored electrical energy is converted into kinetic energy of propellant. This occurs during flashover on the dielectric surface (propellant). The resulting plasma has fairly high velocities. The thruster consists of 2 main parts: a high-voltage pulse generator and a discharge gap. A coaxial discharge gap with an anode-cathode distance of ~ 1 mm was used in experiments. The high-voltage pulse generator weighs about 60 g and operates from 5 volts and consumes 2-3 watts.

The main purpose of the work is to measure the thrust depending on the operating mode of the thruster. The first mode is when short high-voltage pulses (4-5 kV, 1-2 kHz) are directly applied to the discharge gap. The second, the voltage multiplier is connected to the output of the transformer (10 kV 60-120 Hz). The thrust was measured with a torsional pendulum, by measuring the oscillation amplitude of the pendulum after a series of impulses.

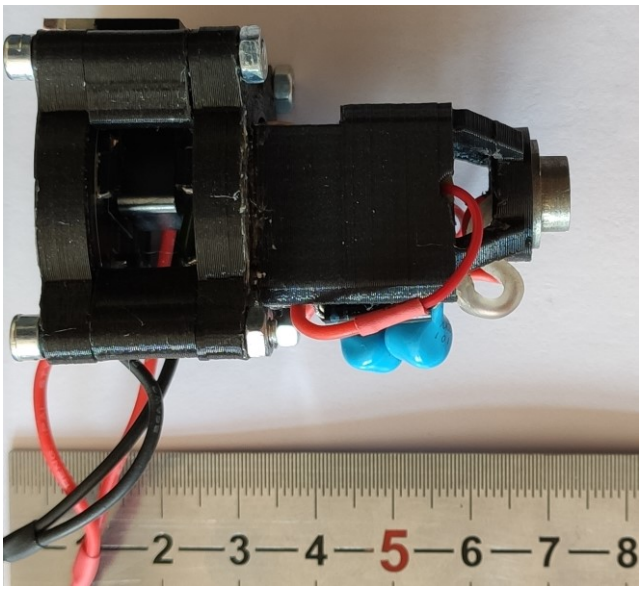

Fig.1. Photo of a thruster prototype.

REFERENCES

[1] D. O'Reilly, G. Herdrich, and D. F. Kavanagh, "Electric Propulsion Methods for Small Satellites: A Review," Aerospace, vol. 8, no. 1, p. 22, Jan. 2021.

[2] I. Levchenko, et al, "Perspectives, frontiers, and new horizons for plasma-based space electric propulsion", Physics of Plasmas vol. 27, Article Number 020601, Feb. 2020.

S4-O-026401

PLASMA INSTABILITY IN A LASER CONTROLLED HIGH-VOLTAGE SWITCH FOR RADAN TYPE ELECTRON ACCELERATOR *

A. I. LIPCHAK, N B VOLKOV, S. V. BARAKHVOSTOV, E. A. CHINGINA, I. S. TURMYSHEV

Institute of Electrophysics, Russian Academy of Science, Ural Branch, 106 Amundsen Street, Yekaterinburg 620016

The laser-induced gas breakdown [1] is widely used in high-pressure gas gaps with optical control [2, 3]. The stability of switch transition time to the conducting state is important both for commutation losses decrease and when it is necessary to fire up several devices simultaneously on a conjoint load. The most significant advantage of optical controlled switches in comparison with electrically triggered analogs is the isolation of control circuits from commutated ones. Despite decades of development, this determines the interest in the improvement of such switches even in the present time and the activity aimed at their development is underway now, in particular, new switches has been patented quite recently [4]. Thus the data we obtained earlier [5] could not be explained in frameworks on simple theoretical models [6]. Using this approach no one can explain the both the dependence of the delay time t_d vs gap voltage U (Figure 1) and its instability (jitter), since the initial laser plasma formation is not related to the voltage, i.e. the field strength in the spark gap, because it is determined by the laser pulse characteristics. Our analysis of the distribution of the axial electric field of the gap for different sizes of a laser plasma plume shows its dynamics is similar to that one of the ionization wave front in a cathode propagating streamer as a result of the transfer of resonance radiation along with associative ionization [7]. The processes on the ionization wave front seem to be determined mainly both by the absorption/excitation of gas atoms and the effects of a high-field domain (HDV) we propose.

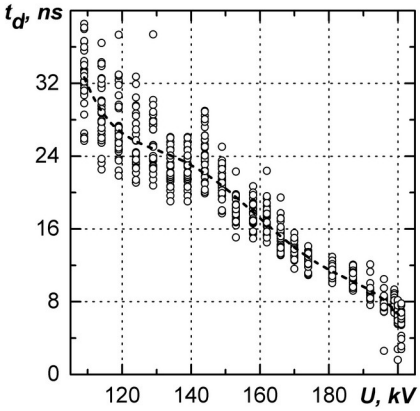

Fig.1. Switch on delay time vs gas gap voltage.

Within the framework of the model we developed the formation of HDF is studied both with and without accounting the effect of electron photoemission from the anode induced by laser radiation. It has been established the role of this electron photoemission plays a minor role in the formation of such HFD. Nevertheless, it has been found that this factor mainly affects the stability of the switching characteristics for devices of this type.

REFERENCES

[1] R. G. Meyerand, A. F. Haught, “Gas Breakdown at Optical Frequencies” Phys. Rev. Lett. vol. 11, no 9, pp. 401–402, November 1963.

[2] W. K. Pendleton, A. H. Guenther, “Investigation of a Laser Triggered Spark Gap”, Rev. Sci. Instrum., vol. 36, no. 11, pp. 1546–1550, November 1965.

[3] A. J. Alcock, M. C. Richardson, K. Leopold, “A Simple Laser-Triggered Spark Gap with Subnanosecond Risetime”, Rev. Sci. Instrum. vol. 41, no. 7, pp. 1028–1029, July 1970.

[4] S.Simpson, O. Johns, C. E. Rose, A. Yalin, C. Dumitrache, “Photonic-Crystal-Fiber-Delivered Laser-Triggered High-Voltage Gas Switch” Patent US No 10 687 412 16.06.2020

[5] A. I. Lipchak, S.V. Barakhvostov, “An Investigation of the Stability of Turning a High-Current Pulse Accelerator On with an Optical Control”, Instr. and Exp. Tech., vol. 64, no. 3, 376–380, July 2021

[6] G. A. Mesyats, M. I. Yalandin, “High-power picosecond electronics” Phys. Usp. vol. 48, no. 3, pp. 211–229, March 2005.

[7] E.D. Lozanskiy, O.B. Firsov, Teorija iskry [Theory of spark], Moscow, Atomizdat Publ., 1975. 272 p. (Rus)

* The work was supported by the Russian Science Foundation under grant No 22-29-20058.

S4-O-026701

EFFECT ON THE GAAS PARAMETERS OF A PHOTOCONDUCTING SEMICONDUCTOR SWITCH WITH A SILICON OXIDE LAYER WHEN SWITCHED BY 355-NM LASER RADIATION*

V.V. BARMIN, I.V. ROMANCHENKO, V.YU. KONEV

Institute of High Current Electronics SB RAS, Tomsk, Russia

The influence of the oxide layer of silicon deposited on the front side of a GaAs photoconductive semiconductor switch (PCSS) on its resistance in on–state has been discovered. The PCSS was switched by a laser pulse with a duration 5 ns and a wavelength of 355 nm from the back side of the PCSS. The effect is to reduce the required electric field for breakdown in the nonlinear mode and increase the resistance in the on-state. With an increase in the electric field applied to the PCSS with an oxide layer, an increase in resistance to a threshold value is observed, after which there is a sharp decrease to a value comparable to the resistances without an oxide layer.

* The work carried out within the state assignment of Ministry of Science and Higher Education of the Russian Federation (theme No.FWRM-2022-0002)

S4-O-027404

OPERATION OF MULTI-GIGAWATT MAGNETIC COMPRESSION LINES

S.N. TSYRANOV, S.N. RUKIN

Institute of Electrophysics UB RAS, Ekaterinburg, Russia

Non-linear transmission lines (NLTL) filled with saturated ferrite are used as solid-state sources of high-power microwave oscillations [1]. Application of a pulse magnetic field orthogonal to bias constant magnetic field in time less than the relaxation time, leads to the precession of the magnetic moment vector and generation of voltage oscillations across the NLTL output. Recently NLTLs also have been used to increase the peak power of picosecond unipolar pulses in the multi-gigawatt power range [2-3]. Such kind of NLTLs is called Magnetic Compression Line (MCL). Shortening the duration of the input voltage pulse made it possible to obtain only one oscillation at the line output instead of several oscillations. The highest peak power achieved with the MCL is 77 GW with the voltage amplitude of 1.93 MV and pulse duration of 105 ps [3].

In this paper, we numerically study the mechanism of MCL operation. The simulation was carried out using the Maxwell equations and the Landau-Lifshitz equation, which describe the dynamics of the electromagnetic field and magnetization, respectively. It has been found that the MCL regime is realized under the condition when the precession period of the magnetic moment is less than 2 T_0, where T_0 is the electromagnetic wave travel time between the inner and outer conductors of the line (2 T_0 is equal to the period of the H_{01} wave in coaxial line).

The formation of waves of the H_{01} type limits the width of the output pulse to a value close to $2\ T_0$. Several periods of precession are located within the output voltage pulse. Such a mode can be called a multiwave mode with a cutoff, in contrast to the classical mode [1], in which one period of precession corresponds to one period of voltage oscillations.

The studies have shown that the input pulse amplification in power has its maximum value when an input pulse width is around of 4 T_0. While moving along the MCL, the input pulse splits in two peaks and then the energy is redistributed in favor of the first peak [2]. This effect is due to the fact that several periods of precession are located within the first and second peaks, and their number and frequency change during the movement.

REFERENCES

[1] V. P. Gubanov, A. V. Gunin, O. B. Kovalchuk, V. O. Kutenkov, I. V. Romanchenko, V. V. Rostov, “Effective transformation of the energy of high-voltage pulses into high-frequency oscillations using a saturated-ferrite-loaded transmission line,” Technical Physics Letters, vol. 35, No 7, pp. 626-628, 2009.

[2] E. A. Alichkin, M. S. Pedos, A. V. Ponomarev, S. N. Rukin, S. P. Timoshenkov, and S. Y. Karelin, “Picosecond solid-state generator with a peak power of 50 GW,” Rev. Sci. Instrum., vol. 91, p. 104705, 2020.

[3] S. Rukin, A. Ponomarev, E. Alichkin, S. Timoshenkov, M. Pedos, and K. Sharypov, “Generation of Multi-Gigawatt Picosecond Pulses by Magnetic Compression Lines,” Proc. 7th Int. Congr. on Energy Fluxes and Radiation Effects (EFRE), Tomsk, Russia, pp. 92-97, 2020.

S4-O-039001

PICOSECOND PULSED POWER BASED ON SOS+MCL APPROACH

S.N. RUKIN

Institute of Electrophysics UB RAS, Yekaterinburg, Russia

Ferrite gyromagnetic nonlinear transmission lines (NLTLs) are used to convert the input video pulse into an output radiofrequency pulse, i.e. operate as a microwave generator [1, 2]. Typical frequency of the generated oscillations is in the range of units of GHz with a peak power of hundreds of MW. In the past several years, it has been shown that under certain conditions, NLTL can operate not as a microwave generator, but as an input pulse power amplifier. Lines operating in this mode were called MCLs (Magnetic Compression Lines). In combination with the solid state input pulse generator (SOS generator), such lines made it possible to implement the SOS+MCL approach for creating solid state picosecond pulsed power systems with a peak power of tens of GW [3–6].

This report presents an overview of the systems based on SOS+MCL approach and shows the last results achieved in this area.

REFERENCES

[1] V. P. Gubanov, A. V. Gunin, O. B. Kovalchuk, V. O. Kutenkov, I. V. Romanchenko, V. V. Rostov, “Effective transformation of the energy of high-voltage pulses into high-frequency oscillations using a saturated-ferrite-loaded transmission line,” Technical Physics Letters, vol. 35, No 7, pp. 626-628, 2009.

[2] I. V. Romanchenko, V. V. Rostov, A. V. Gunin, and V. Yu. Konev, “High power microwave beam steering based on gyromagnetic nonlinear transmission lines,” J. Appl. Phys., vol. 117, p. 214907, 2015.

[3] A. I. Gusev, M. S. Pedos, S. N. Rukin, and S. P. Timoshenkov, “Solid-state repetitive generator with a gyromagnetic nonlinear transmission line operating as a peak power amplifier,” Rev. Sci. Instrum., vol. 88, p. 074703, 2017.

[4] A. I. Gusev, M. S. Pedos, A. V. Ponomarev, S. N. Rukin, S. P. Timoshenkov, and S. N. Tsyranov, “A 30 GW subnanosecond solid-state pulsed power system based on generator with semiconductor opening switch and gyromagnetic nonlinear transmission lines,” Rev. Sci. Instrum., vol. 89, p. 094703, 2018.

[5] E. A. Alichkin, M. S. Pedos, A. V. Ponomarev, S. N. Rukin, S. P. Timoshenkov, and S. Y. Karelin, “Picosecond solid-state generator with a peak power of 50 GW,” Rev. Sci. Instrum., vol. 91, p. 104705, 2020.

[6] S. Rukin, A. Ponomarev, E. Alichkin, S. Timoshenkov, M. Pedos, and K. Sharypov, “Generation of multi-gigawatt picosecond pulses by magnetic compression lines,” Proc. 7th Int. Congr. on Energy Fluxes and Radiation Effects (EFRE), Tomsk, Russia, pp. 92-97, 2020.

S4-O-041801

PICOSECOND MULTI-GIGAWATT 4-STAGE MAGNETIC COMPRESSOR

M.S. PEDOS[1], *E.A. ALICHKIN*[1], *V.E. PATRAKOV*[1,2], *A.V. PONOMAREV*[1], *S.N. RUKIN*[1], *S.P. TIMOSHENKOV*[1], *S.N. TSYRANOV*[1]

[1]*Institute of Electrophysics UB RAS, Yekaterinburg, Russia*
[2]*Ural Federal University, Yekaterinburg, Russia*

Over last several years, the situation in the field of generating powerful picosecond pulses has changed drastically. It turned out that a gyromagnetic nonlinear transmission line (NLTL), containing ferrite rings set on the inner conductor of the line and magnetized by an external magnetic field, under certain conditions can operate not only as a microwave oscillator [1], but also as a peak power amplifier [2–4]. The essence of the approach is that the line operates in a magnetic compression mode (Magnetic Compression Line, MCL), which is realized at close values of the input pulse duration and the period of oscillations generated in the line. In this case, the main part of the input pulse energy is transmitted only to the first peak of the oscillations.

The most important features of the MCL approach are as follows. Firstly, it does not require the use of any switching elements – closing or opening switches. The amplification of the pulse in power and its compression in time occurs automatically during the passage of the pulse along the line. Secondly, the approach allows the use of several MCLs connected in series. Herewith, in each MCL power amplification close to twofold occurs. Third, being solid state devices, MCLs allow to create all-solid-state picosecond generators using a solid state driver of the input pulse. In particular, this is implemented in the SOS+MCL approach, when the input pulse from a solid-state generator with a semiconductor opening switch (SOS) is used.

In this paper, we present results of the study of a 4-stage magnetic compressor, which focuses on the operation of the fourth stage line, MCL4. The maximum electric and magnetic fields are realized in this line, and the output peak power reaches ~80 GW at a pulse duration of less than 100 ps. Issues of the influence of the transverse dimensions of the line on the output pulse parameters are discussed. The results of theoretical studies of the energy compression mechanism are presented, as well as the results of numerical simulation and their comparison with experimental data.

REFERENCES

[1] V. P. Gubanov, A. V. Gunin, O. B. Kovalchuk, V. O. Kutenkov, I. V. Romanchenko, V. V. Rostov, “Effective transformation of the energy of high-voltage pulses into high-frequency oscillations using a saturated-ferrite-loaded transmission line,” Technical Physics Letters, vol. 35, No 7, pp. 626-628, 2009.

[2] A. I. Gusev, M. S. Pedos, A. V. Ponomarev, S. N. Rukin, S. P. Timoshenkov, and S. N. Tsyranov, “A 30 GW subnanosecond solid-state pulsed power system based on generator with semiconductor opening switch and gyromagnetic nonlinear transmission lines,” Rev. Sci. Instrum., vol. 89, p. 094703, 2018.

[3] E. A. Alichkin, M. S. Pedos, A. V. Ponomarev, S. N. Rukin, S. P. Timoshenkov, and S. Y. Karelin, “Picosecond solid-state generator with a peak power of 50 GW,” Rev. Sci. Instrum., vol. 91, p. 104705, 2020.

[4] S. Rukin, A. Ponomarev, E. Alichkin, S. Timoshenkov, M. Pedos, and K. Sharypov, “Generation of multi-gigawatt picosecond pulses by magnetic compression lines,” Proc. 7th Int. Congr. on Energy Fluxes and Radiation Effects (EFRE), Tomsk, Russia, pp. 92-97, 2020.

S4-O-044201

AUTOMATED SYSTEM FOR MEASURING THE CURRENT DENSITY OF A WIDE-APERTURE BEAM EXTRACTED INTO THE ATMOSPHERE*

V.A. LEVANISOV, S.YU. DOROSHKEVICH, M.S. TORBA, M.S. VOROBYOV, S.A. SULAKSHIN

Institute of High Current Electronics SB RAS, Tomsk, Russia

Some applications of large electron beams require a low degree of current density inhomogeneity across the beam cross section. For example, when pumping electroionization lasers, the used beam should have a low degree of inhomogeneity of the current density distribution over the beam cross section, not exceeding 10% [1]. In this case, it becomes necessary to measure the current density distribution over the beam cross section and to search for ways to reduce its inhomogeneity [2, 3]. The work is devoted to the development of a system for measuring the current density of an electron beam extracted into the atmosphere and the analysis of the obtained results. The object of study is a wide-aperture electron accelerator based on ion-electron emission with a non-self-sustained high-voltage glow discharge with beam extraction into the atmosphere [4, 5]. The scheme for measuring the beam current density in the atmosphere is shown in Fig. 1.

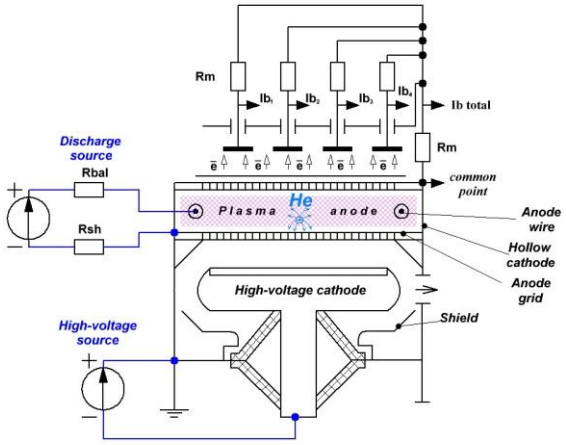

Fig.1. Scheme for measuring the beam current density.

A sectioned collector is installed on the output window of the electron accelerator, each section of which is connected to a measuring resistor. Measuring resistors from each collector plate are connected in one node. A measuring resistor is connected between this node and the common point to measure the total current. he electron beam reaching the collector plates creates a voltage drop across the measuring resistors, this voltage is applied to the inputs of analog multiplexers, which switch the voltage to the input of the analog-to-digital converter of the microcontroller.

An automated system for measuring the beam current density has been developed and created, which makes it possible to measure the beam current density over its cross section both in the direct current mode and in the repetitively pulsed mode with a beam generation frequency of tens of kilohertz.

REFERENCES

[1] M.A. Abroyan, S.L. Kosogorov, I.V. Nabokov, N.A. Uspensky, V.A. Chumisev, V.B. Shapiro, V.Ya. Shvedyuk “A system for real-time measurements of current-density distribution in low-energy electron beams with large cross sections” Instruments and Experimental Techniques. – 2007. – Vol. 50. – No 4. – P. 530-533.

[2] Ponomarev A.V., Pedos M.S., Mamontov U.I., Gusev A.I., Scherbinin S.V. “A system for measuring the current-density distribution of a completed pulsed corona discharge” Instruments and Experimental Techniques. – 2015. – Vol. 58. – No 4. – P. 499-504.

[3] M. S. Vorobyov, S.S. Kovalsky, N. N. Koval. “An Automated System for Measuring the Current Density of a Pulse–Periodic Electron Beam with a Large Cross Section” Instruments and Experimental Techniques, 2018, Vol. 61, No. 6, pp. 849–855.

[4] S.Yu. Doroshkevich, M. S. Vorobyov, M.S. Torba, N. N. Koval et al, “Efficiency of electron beam extraction to the atmosphere in an accelerator based on ion-electron emission” J. Phys.: Conf. Ser. vol. 2064, 012116, 2021

[5] S. Doroshkevich, S. Sulakshin, M.Vorobyov, N. Koval, A. Ekavyan and A.Chistyakov, “Electron accelerator based on ion-electron emission for generation of a wide-aperture beam”, IEEE2020, Proc. of 7th Int. Cong. on Energy Fluxes and Radiation Effects (EFRE) – 21st Int. Symp. on High-Current Electronics (Tomsk), pp. 42–45, 2020

* The work was supported by the Russian Science Foundation under grant No. 20-79-10015.

S4-O-044902

SIMULATION AND DESIGN OF HELICAL FCG WITH SIMULTANEOUS INITIATION OF EXPLOSION FROM BOTH LINER ENDS

S. ANISHCHENKO[1], P. BOGDANOVICH[1], A. GURINOVICH[1], D. LEONENKO[2]

[1]Research Institute for Nuclear Problems, Minsk 220030, Belarus
[2]Electrophysical laboratory, Minsk 220088, Belarus

The critical limitation for increasing FCG output appears due to limited velocity of detonation. The idea enabling to overcome this limitation by double-side ignition of the explosive charge in FCG liner was already discussed and tested by different authors [1, 2, 3]. The principal challenge in use of this idea is collision of counter-propagating detonation waves, which should be thoroughly described in order predict liner dynamics.

In contrast to the design considered in [1] we propose to use mirrored FCG inductors of equal length with load connecting point located in the middle. Simulation of helical FCG of this design with simultaneous initiation of explosion from both liner ends is presented.

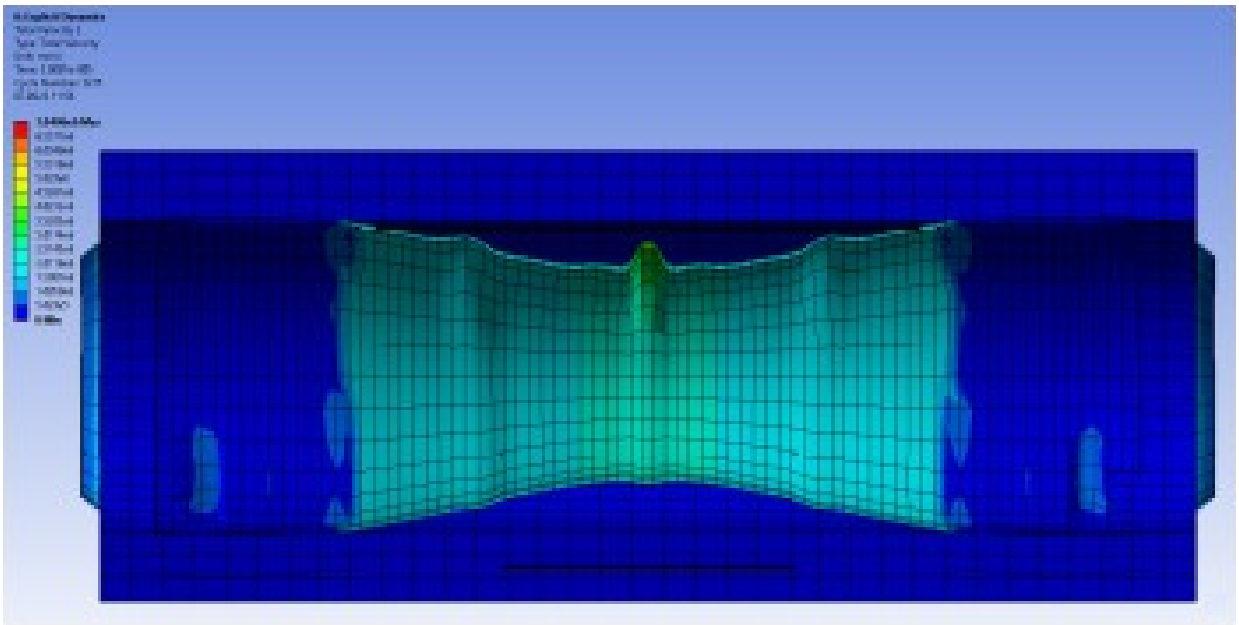

Fig.1. Snapshot of liner geometry after the collision of two detonation waves

Liner dynamics is considered separately in order to describe the geometry and velocity of liner wall at different operation stages. Power transmitted to the load is shown to be increased as compared to the helical FCG of the same length (volume) initiated from one end. Design approaches and solutions are considered to eliminate load damage, which could happen due to significant increase of liner expansion velocity in the area of two detonation waves collision (see Fig.1).

REFERENCES

[1] V.A. Demidov, “Limitations of the Fast Operation of Helical Magneto-Cumulative Generators,” IEEE Trans. Plasma Sci. Vol. 38, No. 8, P. 1780, 2010.

[2] Crawford J.C., Damerow R.A., “Explosively driven high-energy generators,” J. Appl. Phys. Vol. 39, No. 11, P. 5224 – 5231, 1968.

[3] A. C. Anastacio, C. Knock, “Radial blast prediction for high explosive cylinders initiated at both ends,” Propellants, Explosives, Pyrotechnics, Vol. 41, No. 4, P. 682 – 687, 2016.

S4-O-047901

POWERFUL HIGH-VOLTAGE PULSE GENERATOR OF NANOSECOND DOUBLE PULSES

M.V.ZHURAVLEV, A.A. BUKHARKIN, G.V.KURAPOV, A.C.YUDIN, S.U. DACKEVICH, E.U.BURKIN, V.V. SVERIDOV, G.E. REMNEV

Tomsk Polytechnic University, Tomsk, Russia

The paper presents the results of a study of the operating modes of a pulse generator of double pulses. The design of a powerful pulse generator is made on the basis of 2 pulse transformers, a single and a double forming line connected in series. In the single-pulse mode, a single forming line is used as a transmission line, and in the two-pulse mode of accelerator operation, as an additional pre-pulse generator with a voltage amplitude of up to 200 kV. The duration of the generated voltage pulses at half maximum in both modes depends on the type of dielectric used in the forming lines. For water, the duration is 60 ns with a Double Forming Line (DFL) energy reserve of 1155 J at a voltage of 400 kV, while for glycerin it is 40 ns and the DFL energy reserve is 580 J. The synchronization system for the operation of pulse transformers provides a wide range of adjustment of the pause between pulses. The minimum value of the pause between pulses, associated with the spread in the operation of spark gaps based on compressed gas forming lines and pulse transformers, was 50 ns. The results of the operation of the generator as part of a pulsed light ion accelerator, when the first pulse served to form plasma in a diode system, are discussed.

S4-O-049101

PULSED GENERATOR WITH PSEUDOSPARK SWITCH FOR SKIF BOOSTER RING KICKER'S POWER SUPPLY

A.V. AKIMOV[1,2], P.A. BAK[1], Y.D. KOROLEV[3], N.V. LANDL[3], V.D. BOCHKOV[4], D.V. BOCHKOV[4]

[1]*Budker Institute of Nuclear Physics of Siberian Branch Russian Academy of Sciences, Novosibirsk, Russia*
[2]*Novosibirsk State University, Novosibirsk, Russia*
[3]*Institute of High Current Electronics of Siberian Branch Russian Academy of Sciences, Tomsk, Russia*
[4]*Pulsed Technology Ltd., Ryazan, Russia*

SKIF is a synchrotron light source that is being built in Novosibirsk. For beam extraction from the booster ring the magnet kickers with a stable amplitude are used. To provide a required kicker's B-filed a pulsed generator has been developed, it is capable of producing into an inductive load a current up to 5 kA with 200 ns rise time and 300 ns pulse duration. A voltage at the generator's Pulse Forming Network could achieve 25 kV. A 50 kV, 10 kA TPI-type cold cathode thyratron, or Pseudospark Switch, is considered as a most convenient device for such application. One of the most important generator's parameters that should be achieved is an output current amplitude stability at a level of ±0.2 %. In this work it was shown that a gas-filled switch could influence on that parameter. To find the way to increase the stability the hot cathode TGI thyratrons and TPI Pseudospark Switches were tested. Also a new developed Pseudospark Switch without a high-emissivity cylinder [1] that is usually used to improve the auxiliary glow discharge characteristics has been examined.

The different driver schematics were applied to trigger the thyratrons. The driver can provide single or double trigger pulses going to one or two grids [2]. The best generator's output current stability was achieved while using a double pulse trigger of the auxiliary glow discharge thyratron's grid and a single-pulse trigger of the main grid. Also a lower thyratron's turn-on time jitter was observed while using such a driving principle. Special driver was applied for the pseudospark switch that was developed to exclude the high-emissivity cylinder. Such a switch is considered to be operated in a grounded grid mode. The test results of thyratrons and pseudospark switches taken in kicker's pulsed generator nominal operation are presented in the paper.

REFERENCES

[1] Yu. Korolev et al., "A sealed-off pseudospark switch with nanosecond stability of triggering", IEEE Trans. Electron Devices, vol. 68, no. 9, pp. 4692-4697, Sep. 2021.

[2] A. Akimov et al., "Application of TPI-Thyratrons in a Double-Pulse Mode Power Modulator with Inductive-Resistive Load", IEEE Trans. Dielectrics and Electrical Insulation, vol. 17, no 3, pp. 718-722, June 2010.

S4-O-052301

DECOMPOSITION OF SF_6 IN THE PLASMA MEDIUM OF AN ELECTRON BEAM*

HONGDA LI[1], S.A. SOSNOVSKIY[2], A.I. PUSHKAREV[3], V.I. SACHKOV[4], N.V. GOLOVKOV[5]

[1]*School of Equipment Engineering, Ph.D., professor, Shenyang Ligong University, Shenyang, China*
[2]*Candidate of Physical and Mathematical Sciences, Senior Researcher, National Research Tomsk State University, Tomsk, Russia*
[3]*Doctor of Physical and Mathematical Sciences, National Research Tomsk Polytechnic University, Tomsk, Russia*
[4]*Doctor of Chemical Sciences, National Research Tomsk State University, Tomsk, Russia*
[5]*Doctoral student, National Research Tomsk Polytechnic University, Tomsk, Russia*

Sulfur hexafluoride (SF_6) is commonly used as an etching/etching-aid gas in fabricating the submicrometer features of modern integrated circuits because it has a higher fluorine content than CF_4 but does not undergo polymerization. However, the destruction of SF_6 has attracted much interest because of the important environmental issues and the toxicity of sulfur compounds. Radio-frequency (RF) discharge plasma, which must be manipulated at low pressure, recently has become the most popular plasma technology used in the high-profit semiconductor industry, in both replicating patterns and depositing films. The discharge plasma can be manipulated at low substrate temperatures without changing its original properties and can replicate submicrometer patterns with anisotropic features. However, in the presence of an RF discharge, SF_6, acting as an etching/etching-aid gas, can be decomposed into lower fluorides of sulfur and can generate hazardous byproducts, such as S_2F_{10}, SO_2F_2, SOF_2, SOF_4, and SF_4. Particularly toxic is S_2F_{10}, which has an LC50. Because reducing or eliminating the toxicity of gaseous effluent from the RF discharge process is a serious concern.

In this work, plasmas in medium of an electron beam were used to decompose SF_6 [1-3]. The studies showed that in the conversion of sulfur hexafluoride plasma pulse the electron beam is realized effect. Mass spectrometric studies of the positive ion yield due to the electron impact ionization of sulfur hexafluoride molecules in the gas phase have been carried out. The exothermal reaction going is organized in the reactor volume. The oscillation-excited products of these reactions participate in the dissociation of initial halogenide molecules. The non-equilibrium plasma is formed due to the action of pulsed electron beam with the duration of not more than 10^{-9} s to the mixture of halogenides and gas-carrier. Nitrogen, hydrogen and oxygen are used as the gas-carrier. The processing of halogenides is performed by adding of diluent gas to the mixture of halogenide and gas-carrier up to the total pressure providing full absorption of nanosecond pulsed electron beam energy. The thermal dynamic modeling showed that in case of plasma of SF_6 and H_2 all the elements such as S, HF, H_2F_2 and SF_4 are stable products of decomposition of sulfur hexafluoride in the mixture with hydrogen. The calculations showed the possibility of condensed phase formation of sulfur monomer S, sulfur dimmer S2 and of other clusters. In our case, at the expense of dissociation of sulfur hexafluoride by electronic shock: $SF_6 + e \rightarrow S + 6F$ and dissociative adhesion of low-energy electrons: $SF_6 + e \rightarrow SF_6^- \rightarrow S + 6F$. The atomic fluorine is formed, which initiates reactions in a mixture with molecular hydrogen. The major reactions are: $H_2 + F = HF + H + 1{,}47$ eV. The energy which is released in the exothermic reaction can be spent for initial decomposition of sulfur hexafluoride. The technical result is in the fact that the energy-capacity of chemical element degradation to nanodispersed condition from its halogenide significantly decreases. The experiments are performed at the electron accelerator TEU-500. The parameters of electron beam are the following: electron energy is 400-500 keV, pulse duration at the half-height is 60 ns, frequency rate is up to 5 pulses per second, energy per pulsed is up to 200 J. The electron beam is injected to the closed reactor through the anode foil. The results allow one to define the range of the possible chemical compounds - reagents to carry out an efficient reaction, to determine the requirements to system and to chemical reactor, to estimate the efficiency of the technological process as a whole.

REFERENCES

[1] Parker RK, Anderson RE, Duncan CV. Plasma-induced field emission and the characteristics of high-current relativistic electron flow // Journal of Applied Physics. – 1974. – V. 4. – № 6. – P. 2463–2479.

[2] Mesyats GA. Pulsed Energy and Electronics. – M.: Nauka, 2004. (in Russian)

[3] Ezhov V.V., Vlasov V.A., Pushkarev A.I., Remnev G.E., Sosnovskiy S.A. Sulfur reductionfrom SF_6 by pulsed electronic beam // 8th Korea-Russia International Symposium on Science and Technology, Tomsk, 2004, v. 2, p. 212-215.

S4-P-001001

MULTICHANNEL HIGH-VOLTAGE PULSED GENERATORS FOR ELECTRO-DISCHARGE TECHNOLOGIES

V.M. ALEXEENKO[1], *A. A. ZHERLITSYN*[1], *S. S. KONDRATIEV*[1]

[1]*IHCE SB RAS, Tomsk, Russia*

We present here the design and test results of portable HV pulsed generators, designed for materials fragmentation, though some other technological applications are possible as well. The generator consists of a low-voltage block, high-voltage block and fragmentation chamber with 4 independent discharge channels. The low-voltage block of the generator, consisting of a primary capacitor bank (~330 μF) and a thyristor switch, stores pulse energy and transfers it to the HV block. The primary capacitor bank stores energy of 660 J at the maximum charging voltage of 2 kV. The HV block includes an HV pulsed step-up transformer, HV capacitive storage (12.5 nF per discharge channel), and two electrode gas switches. Air at atmospheric pressure is used for insulation of the generator and as the work medium of the gas switch.

Experimental tests of the generator consisted of the crushing[A1] of 4-layer printed circuit boards. Tests have shown that this generator circuit allows the implementation of four discharge channels simultaneously in the fragmentation chamber. The following technical parameters of the generator were achieved: output voltage up to 100 kV, voltage rise time of ~60 ns, current amplitude of ~5 kA per channel.

Comparison of the results of crushing in a single-channel and multichannel mode demonstrates that a multichannel generator allows both a reduction of the specific energy consumption and an increase in the productivity of the crushing process in proportion to the number of channels, without increasing the stored energy of the generator.

The work was performed with the support of the Russian Foundation for Basic Research (No. 18-29-24079 mk).

S4-P-004701

IMPROVING THE GENERATION CHARACTERISTICS OF A N2 LASER PUMPED BY A LONGITUDINAL DISCHARGE*

YU. N. PANCHENKO[1], I. N. KONOVALOV[1], A.V. PUCHIKIN[1], M.V. ANDREEV[1], E.V. GORLOV[2], V.I. ZHARKOV[2]

1 Institute of High Current Electronics SB RAS, Tomsk, Russia
2 V. E. Zuev Institute of Atmospheric Optics SB RAS, Tomsk*, Russia*

Many applications of UV laser radiation require high pulsed power, a narrow spectral line, and a high pulse repetition rate. In a number of cases, widely used semiconductor lasers do not meet the presented requirements. The most effective and simple solution in this case may be a nitrogen laser [1,2].

Thus, we present the results of a study of an N_2 laser with longitudinal pumping by a pulsed anomalous glow discharge. The possibility of bulk plasma formation at a maximum specific current density of 2.75 ± 0.25 kA/cm^2 and a specific pump power of more than 1 MW/cm^3 is shown. Preservation of a stable discharge structure was ensured by the automatic inclusion of preliminary ionization of the gas volume, due to the introduction of sharply inhomogeneous distortions in the electric field of the discharge gap. An LC inverter was used as a pump generator with storage capacitances of 11 nF and 5.6 nF and a discharge capacitance of 3.8 nF.

It is demonstrated that at a nitrogen pressure (purity 99.6%) P = 10 mbar, the pulse duration of the generated radiation corresponds to the duration of the pump pulse. At the charging voltage U_0 = 24 kV, the energy in the radiation pulse reached 1.3 ± 0.1 mJ with a duration at the half-intensity level up to 14 ± 2 ns, Fig.1.

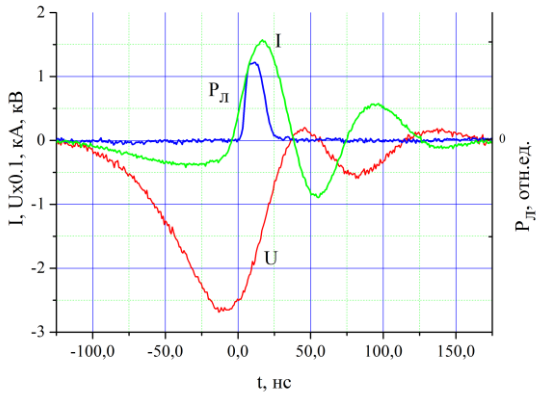

Fig.1. Oscillograms of the current I, voltage U on the discharge capacitance, and the time shape of the radiation pulse P_l.

The maximum peak power of the output beam was 80 kW. The generation of radiation developed near the inner wall of the discharge tube with an inner diameter of 9–12 mm, in a ring ~2.5 mm wide, and the cross section of the laser beam was 0.6 cm^2. The internal efficiency (relative to the energy stored in the discharge capacitance) was 0.11%. It is noted that when nitrogen was replaced in the discharge tube with atmospheric air (~78% N_2, ~21% O_2) at a pressure of 8 mbar and charging voltage U_0 = 24 kV, the energy in the radiation pulse was 0.6 mJ at a pulse duration t = 12 ns. Without a system for pumping a gaseous medium, in a repetitively pulsed mode of laser operation up to 10 Hz, a stable repeatability of the discharge and generation characteristics of the laser was maintained.

REFERENCES

[1] I. N. Konovalov, Yu. N. Panchenko, A. V. Puchikin, V. F. Losev, and S. M. Bobrovnikov, Izv. Physics. 2019. T. 62. № 9. C. 139.

[2] Yu. N. Panchenko, I. N. Konovalov, V. F. Losev, A. V. Puchikin. Nitrogen laser excited by a longitudinal electric discharge; Pat. No. 2664780; publ. 08/22/2018. - Bull. No. 24

* The work was supported by the Russian Science Foundation under grant No. 17-19-01229.

EFFECT OF ELECTRON IRRADIATION OF BARLEY SEEDS ON ENZYMATIC ACTIVITY AND DEVELOPMENT OF SPROUTS

N.N. LOY[1], E.A. KAZAKOVA[1], N.I. SANZHAROVA[1], D.D. BABINA[1], M.S. VOROBYEV[2]

[1]RIARAE, Obninsk, 249032, Kaluga region, Kiev highway, 109 km, Russia
[2]IHCE SB RAS, Tomsk, 634055, 2/3 Akademichesky Avenue, 2/3, Russia

Under extreme conditions, the most important mechanism of resistance is the activation of a multi-level biochemical system of antioxidant protection, which includes a large number of components. Among them, a special place is occupied by antioxidant enzymes as a component of the cell signaling system.

In laboratory experiments, the effect of pre-sowing irradiation of barley seeds with low-energy electronic radiation on the activity of antioxidant enzymes, seed qualities and disease incidence of sprouts was studied.

Studies were conducted on spring barley (*Hordeum vulgare* L.) of the Vladimir variety. The seeds were irradiated in the dose range of 1 to 5 kGy at a radiation dose rate of 500 Gy/imp. According to the methodology described in the article Loy, 2019 [1]. The activity of enzymes was determined by the method described in the article Bitarishvili, 2018 [2]. In addition, morphometric indicators of the development of sprouts and the incidence of their diseases were determined.

Analysis of the data obtained showed that no statistically significant differences in enzyme activity between control and irradiation were found. However, at a dose of 5 kGy, there is a noticeable tendency to increase the activity of two enzymes - guaiacol peroxidase and ascorbate peroxidase (Table 1).

Table 1 – Activity of catalase, guaiacol peroxidase, ascorbate peroxidase in control and irradiated barley seedlings

Dose	Activity, ME					
	CAT		POX		APX	
	M	Q1; Q3	M	Q1; Q3	M	Q1; Q3
0 kGy (control)	230.849	225.172; 241.571	0150	0105; 0152	2943	2759; 3.035
1 kGy	201.835	198.051; 280.046	0.060	0.056; 0.286	3.127	2.851; 3.587
3 kGy	208.142	207.511; 219.495	0.128	0.122; 0.259	2.943	2.207; 3.127
5 kGy	208.142	203.096; 217.603	0.372	0.244; 0.389	3.127	3.035; 3.679

Note: the data is in the format "Median (Q1; Q3)».

Irradiation of seeds in doses of 1 and 5 kGy had a stimulating effect on the length of the sprout by 1.1 times and the root by 1.25 and - 1.1 times, respectively.

Electron irradiation in doses of 3 and 5 kGy completely suppressed the development of fusarium (exciter *Fusarium* spp.) on 7-day sprouts of barley, at the same time stimulated the development of helminthosporiosis (exciter *Helminthosporium sativum* Pam.) – the degree of damage increased in variants with irradiation by 1.4-2.1 times, the prevalence of the disease by 1.4-1.7 times compared with unirradiated control.

Thus, it has been shown that low-energy electron irradiation of barley seeds before sowing affects the morphometric indicators of the development of sprouts, the defeat of their fungal diseases and, at the level of tendency, the enzymatic activity.

REFERENCES

[1] *Loy N.N., Sanzharova N.I., Gulina S.N., Vorobiyov M.S., Koval N.N., Doroshkevich S.Yu., Chizh T.V., Suslova O.V.* Influence of electronic irradiation on the affection of barley by root rot. IOP Conf. Series: Journal of Physics: Conf. Series **1393 (**2019) 012107 doi:10.1088/1742-6596/1393/1/012107

[2] *Bitarishvili S.V., Bondarenko V.S., Geraskin S.A.* Influence of γ-irradiation on the expression of genes encoding enzymes of abscisic acid metabolism in barley seed embryos // Ecological genetics. – 2018 – V. 16 – No 4 – P. 85–89.

PLASMA CHEMICAL REACTOR WARMING-UP

A.A. DYACHENKO[1], O.M. STEPANOVA[1], Y.A. KHOHLOVA[2], AND M.E. PINCHUK[1]

[1]1nstitute for Electrophysics and Electrical Power RAS, Saint-Petersburg, Russia
[2]National research Tomsk Polytechnic University, Tomsk, Russia

Plasma chemistry is a rapidly developing branch of industry. One of the most important parameters of the balance of chemical reactions is the temperature of working gas [1]. To achieve an operating mode, a reactor must be preheated.

In this work, the measuring technique of warming a plasma chemical reactor based on a dielectric barrier discharge is presented. The plasma temperature in the reaction volume was determined by analyzing the profile of the N_2 0-0 337.13 nm spectral band using the Massive OES software package [2].

The plasma reactor consists of a quartz tube with an inner diameter of 7.6 mm and a wall thickness of 1 mm, inside which a high-voltage electrode with a diameter of 4 mm is located. The outer ring electrode is grounded via the measuring capacitor. The reactor is powered by the 25 kHz sinusoidal voltage with the peak-to-peak value of 12 kV. The air with the humidity of 95±5% at a temperature of 20 ^{o}C was passed through the discharge cell at a flow rate of 0.2 liters per minute. Description of plasma reactor was presented in [3]. The radiation of the barrier-discharge plasma was collected by a quartz lens into the optical fiber and recorded using an MS-257 LOT Oriel spectrograph with an Andor CCD 420-UV-FK camera.

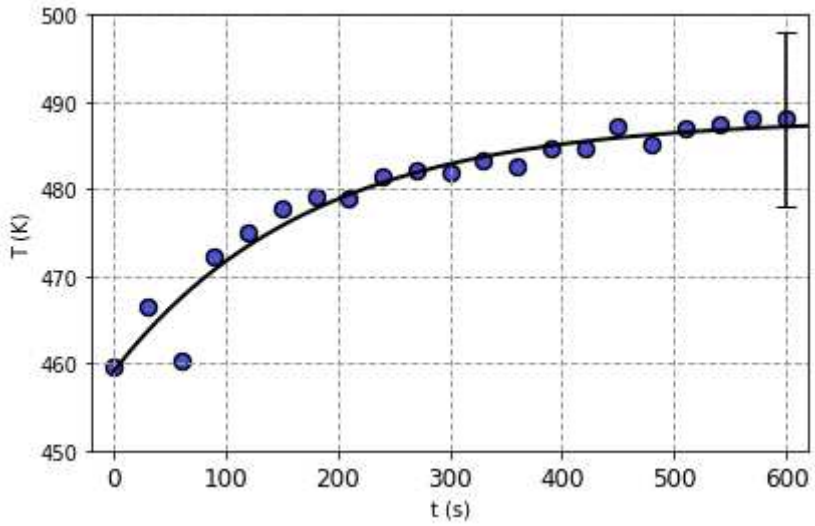

Fig.1. Rotational temperature for N_2 0-0 337.13 nm band vs time inside the reactor.

The time dependence of the rotational temperature of nitrogen molecules is shown in Fig. 1. The spectral determination of temperature corresponds to gas temperature inside the reactor. The rotational temperature obtained correlates with ozone and nitrogen oxides production.

REFERENCES

[1] L. S. POLAK, CHEMICAL PROCESSES IN LOW-TEMPERATURE PLASMAS, BOSTON: SPRINGER, 1966.

[2] J. VORÁČ, P. SYNEK, L. POTOČŇÁKOVÁ, J. HNILICA, AND V. KUDRLE, “DEDUCING ROTATIONAL QUANTUM-STATE DISTRIBUTIONS FROM OVERLAPPING MOLECULAR SPECTRA” PLASMA SOURCES SCI. TECHNOL., VOL. 26, NO 2, 025010, 2017.

[3] M. PINCHUK, D. SUBBOTIN, O. STEPANOVA, V. POPOV, AND V. SPODOBIN, “CO_2 -REFORMING OF METHANE BY DIELECTRIC BARRIER DISCHARGE,” PROC. 8TH INT. CONF. PLASMA PHYS. PLASMA TECHNOL. (PPPT). MINSK, BELARUS: KOVCHEG, PP. 446–448,2015.

S4-P-012701

COMPARISON OF THE EFFECTS OF EXPOSURE TO NANOSECOND PULSED MICROWAVES ON A BURN INJURY DEPENDING ON THE PULSE REPETITION FREQUENCY

A.V. SAMOYLOVA[1-3], A.A. GOSTYUKHINA[1,4], V.V. YARTSEV[2,3,4], S.S. EVSEEVA[3,4], V.M. MOCHALOVA[3], M.A. BOLSHAKOV[1,3], K.V. ZAITSEV[4], O.P. KUTENKOV[1], V.V. ROSTOV[1]

[1]*Institute of High-Current Electronics SB RAS, Tomsk, Russia*
[2]*Siberian state medical university, Tomsk, Russia*
[3]*National research Tomsk state university, Tomsk, Russia*
[4]*Siberian Federal Scientific Clinical Center (SFSCC) of the Federal Medical and Biological Agency (FMBA), Tomsk*

The problem of restoring skin after thermal damaging in humans is an urgent biomedical problem [1]. One of the promising ways to solve this problem is the creation of new recovery methods using high-frequency low-intensity electromagnetic factors. From this point of view, data on the wound healing effect of pulsed radio-frequency radiation [2, 3], as well as nanosecond pulsed electromagnetic radiation (RPMs) are of some interest. RPMs under certain parameters can stimulate the reparative regeneration of a full-layer skin wound in mice. According to some reports, the positive effects of wound healing using extremely high-frequency exposure are explained by a decrease in the intensity of inflammatory processes due to increased microcirculation in the wound site and adjacent tissues [4].

The experiment was performed using 30 mature male rats of the Wistar line (250-280 g). All animals were divided into three groups: control – animals with a burn of the III degree without exposure to electromagnetic radiation; experimental group 1 – animals that, after modeling a III degree burn were exposed to local burn wound effects with exposure to radiation with peak power flux density (pPFD) of 140 W/cm^2, with a pulse repetition rate of 8 Hz; experimental group 2 – animals that, after modeling a III degree burn were exposed to local burn wound effects with exposure to radiation with pPFD of 140 W/cm^2, with a pulse repetition rate of 13 Hz. Thermal burns were modeled according to the standard method. The pulsed laboratory generator based on the MI-505 magnetron was used as a source of nanosecond RPMs. Histological processing of the skin was carried out by standard methods. Statistical processing of the results was carried out according to standard procedures of mathematical statistics using the capabilities of the program Statistica 8.0 for Windows.

In the performed experiments, after thermal exposure in laboratory rats, a burn injury was formed, corresponding to a third-degree burn in humans. In the control group of animals not exposed to nanosecond RPM, a monotonous decrease in the area of burn wounds was recorded. The healing process proceeded gradually from days 1 to 32 of the study. It was accompanied by a long-term preservation of the scab, which completely fell off only on the 16th day of the experiment, and partial epithelialization was observed from the 28th day. In rats of experimental group 1, subjected to 4-fold local irradiation with RPM with an intensity of 140 W/cm^2 at a pulse repetition rate of 8 Hz, starting from the 19th day, a statistically significant decrease in the area of the wound was recorded compared to the control group. At the same time, the discharge of the formed scab began on the 12th day of the experiment, and epithelialization occurred by the 24th day with complete healing of burns in all animals by the 28th day. In rats from experimental group 2, irradiated with nanosecond RPMs with an intensity of 140 W/cm^2 at a pulse repetition rate of 13 Hz, by the 5th day of the study, a statistically significant decrease in the area of the wound was observed relative to both the control group and experimental group 1. However, a further decrease in the area of wounds in experimental group 2 was monotonous and did not differ significantly from that in the control group. The scab was fully formed and began to recede only on the 14th day of the experiment, and on the 28th day of the study, partial epithelization of the wounds was observed. Thus, a comparison of the obtained results allows us to state that nanosecond low-intensity RPMs 140 W/cm^2 accelerates wound healing processes. At the same time, the impact with a pulse repetition rate of 8 Hz turned out to be more effective compared to a pulse repetition frequency of 13 Hz. Histological analysis of rat skin showed an increase in the rate of wound healing due to the accelerated formation of granulation tissue, a decrease in the thickness of the eschar, and scarless healing.

References

[1] A.A. Alekseev, A.E. Bobrovnikov, “Contemporary technologies of local conservative treatment in patients with burns” // Annals of surgery. № 2. pp. 32–38. 2012.

[2] A.B. Gapeyev, “Study of the mechanisms of biological effects of low-intensity extremely high-frequency electromagnetic radiation: progress, problems and prospects” // Biomedical Radioelectronics. № 6. pp. 20-30. 2014.

[3] B. Strauch, C. Herman, R. Dabb et al., “Evidence-based use of pulsed electromagnetic field therapy in clinical plastic surgery” // Aesthet. Surg. J. № 29 (2). pp. 135–143. 2009.

[4] K.V. Lushnikov, A.B. Gapeev, Yu.V. Shumilina, et al., “Suppression of cell-mediated immune response and nonspecific inflammation on exposure to extremely high frequency electromagnetic radiation” // Biophysics.Vol. 38, № 5. pp. 918–925. 2003.

FORMATION OF BIPOLAR PULSES OF VARIOUS DURATIONS IN A CIRCUIT WITH ONE SPARK GAP*

A.M. EFREMOV, V.M. ALEXEENKO

Institute of High Current Electronics, Siberian Branch, Russian Academy of Sciences, 2/3 Akademichesky AvenueTomsk 634055, Russia, efremov@oit.hcei.tsc.ru

High-voltage bipolar nanosecond pulses are used to excite antenna arrays of electromagnetic UWB radiation. The spectrum of the emitted pulse depends on the duration of the bipolar pulse and can be expanded if the antenna array is synchronously excited by bipolar pulses of different durations. Works of this kind were carried out at the IHCE SB RAS. Four-channel formers were created in combinations with pulse durations of 0.5; 1; 2 and 3 ns [1–3]. The scheme for the formation of bipolar pulses was rather complicated in tuning: up to 9 spark gaps were used, located in 5 independent high-pressure gas volumes. This report proposes a new scheme for a four-channel bipolar pulse former with durations of 1 ns (2 channels) and 2 ns (2 channels). A significant difference from the above-mentioned four-channel former circuit is that only one high-pressure spark gap is used in the circuit. The advantages of the circuit are also the ease of setting the circuit, more stable amplitudes and durations of bipolar pulses, tight synchronization of pulses on the leading edges. The original scheme of the former and the experimental bipolar pulses are shown in Figure 1. The forming lines FL_1 - FL_8 were charged at a frequency of 100 Hz from the Sinus-160 generator. When the spark gap S was actuated in the transmission lines FL_9 - FL_{12}, loaded with matched loads R, bipolar pulses with durations of 1 and 2 ns with an amplitude of up to 90 kV were formed. Forming lines and a multichannel spark gap are located in a nitrogen atmosphere at a pressure of 40 atm. The output bipolar pulses were recorded by coupled-line dividers installed in the transmission lines. The electrical insulation of the transmission lines is SF_6 gas at a pressure of 4 atm.

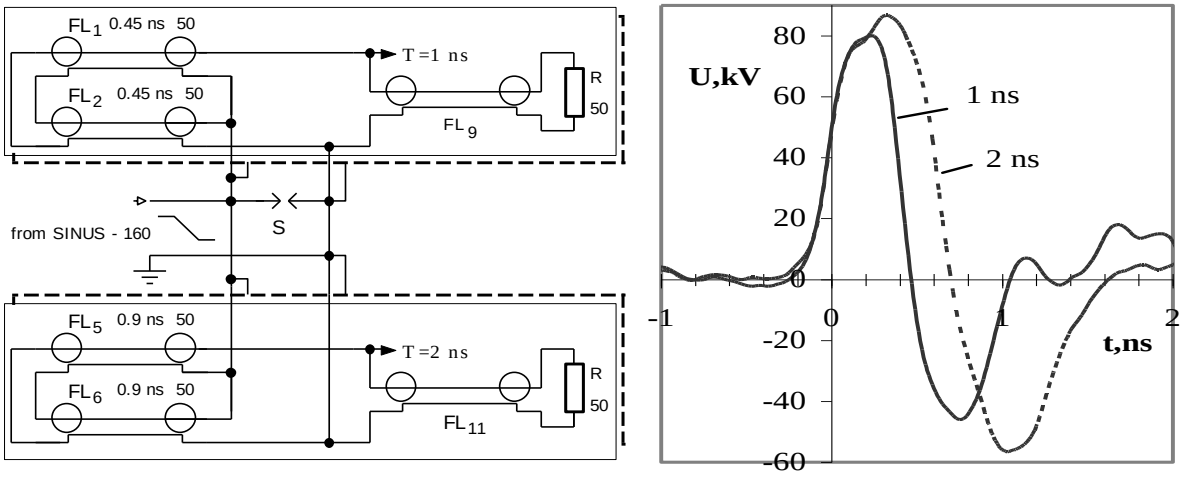

Fig.1. Schematic diagram of a four-channel shaper and experimental bipolar voltage pulses

REFERENCES

[1] A. M. Efremov, V. I. Koshelev, V. V. Plisko, and E. A. Sevostyanov, “A high-power synthesized ultrawideband radiation source,” Review of Scientific Instruments, 88, 094705, 2017.

[2] A. M. Efremov, V. I. Koshelev, V. V. Plisko, “Synthesis of electromagnetic pulses with different frequncy bands in free space,”Journal of communications and electronics, Vol 65, № 5, с. 480–494, 2020.

[3] A. M. Efremov, V. I. Koshelev, V. V. Plisko, and E. A. Sevostyanov. “A High-Power Source of Ultrawideband Pulses of Synthesized Radiation,” Instruments and Experimental Techniques, Vol. 62, No. 1, pp. 33–41, 2019.

* The work was supported by Russian Foundation for Basic Research, grant 20-08 -00093 A.

S4-P-017502

NANOSECOND SWITCHES BASED ON THE CAPILLARY DISCHARGE WITH HOLLOW CATHODE*

P.A. BOKHAN, P.P. GUGIN, M.A. LAVRUKHIN, D.E. ZAKREVSKY

A. V. Rzhanov Institute of Semiconductor Physics SB RAS, Novosibirsk, Russia

Capillary discharge applications include a wide range of areas, such as UV and X-ray sources, generation of high-voltage nanosecond pulses, etc. In a number of recent papers [1, 2] the unique ability of nanosecond switches based on capillary discharge to operate at high pulse repetition frequency (PRF) has been demonstrated. In burst operation mode, with optimization of external conductive shield around the capillary, PRF more than 100 kHz was achieved [3]. Such values make these switches promising for a number of applications, such as plasma processing, excitation of gas lasers, etc.

Nevertheless, the development of models of the considered type of the switch, capable to operate in the regular pulses mode at high PRF values (50-200 kHz and more) and high average switching power ~1-10 kW, is associated with a number of difficulties, caused by intensive heat dissipation inside the switch. In particular, it leads to a change in gas composition and pressure in the switch volume, which negatively affects the switching characteristics and lifetime of the device. One of the ways to mitigate this problem is the maximum simplification of structural parts of the switch, particularly the cathode node and capillary structure, with minimal deterioration of the switch operating parameters.

In most recent works devoted to the study of switching characteristics of the capillary discharge, a rather complicated discharge structure has been used as a plasma cathode. Particularly, it is due to the preionization of the cathode region in order to increase the switch efficiency. Nonetheless, it has been demonstrated in [4] that additional ionization does not play a significant role at PRF greater than 20 kHz. Regarding the capillary configuration, in [3] it was suggested that the process of formation of runaway electrons in the capillary region has a significant influence, which leads to a decrease in the degree of pulse compression and the maximum achievable PRF values. However, direct experiments demonstrating the influence of the capillary structure shape haven't been presented.

Comparative experimental studies of several switches with different capillary configurations were performed in this work. In all cases, a hollow cylindrical Ti cathode with an inner diameter of 2.6 cm and a length of 90 cm was used as a cathode node. In the side surface of the cylinder a rectangular hole was formed to which a capillary of rectangular cross section made of Al_2O_3 plates was attached. Studies were carried out using helium with pressure of 2-20 mbar as a working gas of the switch. To form high-voltage pulses on the operating capacitance primary generator with a PRF of up to 200 kHz in the burst operation mode was used.

REFERENCES

[1] P.A. Bokhan, P.P. Gugin, M.A. Lavrukhin, I.V. Schweigert, A.L. Alexandrov, D.E. Zakrevsky, “A high-voltage subnanosecond sharpener based on a combination of 'open' and capillary discharges”, J. Phys. D: Appl. Phys., vol. *51*, p. 364001, 2018.

[2] P.A. Bokhan, P.P. Gugin, D.E. Zakrevsky, M.A. Lavrukhin, “Frequency Characteristics of a Subnanosecond Plasma Switch”, Russian Physics Journal, Vol. 62, № 11, p. 2059, 2020.

[3] P.A. Bokhan, E.V. Belskaya, P.P. Gugin, M.A. Lavrukhin, D.E. Zakrevsky, I.V. Schweigert, “Investigation of the characteristics and mechanism of subnanosecond switching of a new type of plasmas switches. II switching devices based on a combination of ‘open’ and capillary discharges —eptrons”, Plasma Sources Science and Technology, vol. 29, p. 84001.

[4] P.A. Bokhan, M.A. Lavrukhin, D.E. Zakrevsky, “Influence of the cathode region preionization on the operating parameters of the eptron” Journal of Physics: Conference Series, vol. 2064, p. 12125, 2021.

*The work was supported by the Russian Science Foundation (project No. 19-19-00069).

S4-P-021901

NONEQUILIBRIUM PLASMA OF PULSED DISCHARGES FOR THE PURPOSE OF AIR PURIFICATION FROM TYPICAL VENTILATION EXHAUSTS OF POLYMER PRODUCTION*

I.E. FILATOV, V.V. UVARIN, D.L. KUZNETSOV

Institute of Electrophysics, UB, RAS, Yekaterinburg, Russia
e-mail: fil@iep.uran.ru

The production of polymer materials is one of the most important sources of air polluted with volatile organic compounds (VOCs). Technologies using nonequilibrium plasma (NP) of electric discharges of various types are promising for air purification from VOC vapors [1,2].

VOCs are: monomeric compounds used to produce polymers: butadiene, styrene, acrylonitrile, methyl methacrylate (MMA), acrylic ethers and many other compounds. As a rule, these are highly toxic compounds. They can be contaminated during transportation, during the polymerization reaction, during the processing of plastics, etc. Freshly prepared plastic contains a small amount of monomer, which pollutes the air. A significant amount of VOCs is formed during the heat treatment of plastics and during their recycling in order to obtain valuable chemical raw materials.

This paper presents the results of a study of the effect of pulsed corona discharge plasma on air containing volatile pyrolysis products of polymers of wide application: Polystyrene, polymethyl-methacrylate (MMA), ABS plastic, poly-olefins and rubber. Each of the polymer materials at a temperature of 300-600°C forms a variety of volatile products, the analysis of which was carried out by the GC/MS method. These are aliphatic and aromatic unsaturated compounds of various structures, including monomers. Each of these products has a different reactivity to plasma components and different toxicity. For the research, an installation with a plasma chemical reactor, in which a pulsed corona discharge with parameters: pulse duration of 40 ns, pulse repetition rate of 10 Hz, a voltage of 100 kV, and a current of up to 100 A, described in detail in [3], was used. The method of competing reactions developed by us [4] allows us to study the relative reactivity of each of the components most effectively.

It is shown that NP removes unsaturated and saturated aliphatic compounds more effectively, and aromatic compounds are removed less efficiently. The high reactivity of unsaturated compounds is due to their reaction with ozone [5,6].

The found dependencies will be useful in the development of new energy-efficient air purification technologies for the tasks of primary and secondary plastics processing.

REFERENCES

[1] J. Schnelle, R. Dunn, M. Ternes, R.F. Dunn, and M.E. Ternes. Air Pollution Control Technology Handbook, Second Edition. CRC Press, 2015.

[2] A.M. Vandenbroucke, R. Morent, N. De Geyter, and C. Leys. “Non-thermal plasmas for non-catalytic and catalytic VOC abatement”, J. Hazard. Mater., vol. 195, pp. 30-54, 2011.

[3] I.E. Filatov, V,V. Uvarin and D.L. Kuznetsov, "Estimation of qalitative and quantitative prameters of air cleaning by a pulsed corona discharge using multicomponent standard mixtures,"Technical Physics, vol.63, no.5, pp. 680–688, 2018.

[4] I.E. Filatov, V.V. Uvarin, V.V., Nikiforova, D.L. Kuznetsov, “Investigation of the relative reactivity of volatile organic compounds in the air plasma of a pulsed corona discharge by the method of competing reactions”, ,” J. Phys. Conf. Ser., vol. 2064, p. 012094, 2021.

[5] I.E. Filatov, V.V. Uvarin, D.L. Kuznetsov, “About the role of ozone in air purification from vapors of volatile organic compounds by pulsed discharges”. In *2020 7th International Congress on Energy Fluxes and Radiation Effects (EFRE)*, IEEE, pp. 322-37, 2020.

[6] I.E. Filatov, V.V. Uvarin, D.L. Kuznetsov, “Investigation of the relative reactivity of unsaturated volatile organic compounds in air under the action of pulsed corona discharge plasma”. In *2020 7th International Congress on Energy Fluxes and Radiation Effects (EFRE)*, IEEE, pp. 317-21, 2020.

* The work was supported in part by the RFBR Grant No. 20-08-00882 (methods) and RFBR & Sverdlovsk region, Grant No. 20-48-660062 r_a. (objects).

S4-P-027101

RLC-CIRCUIT PARAMETERS INFLUENCE ON ABLATION PULSED PLASMA THRUSTER PERFORMANCE*

D.K. FEDOROVA[1], *D.A. EGOSHIN*[1], *A.V. PAVLOV*[1], *V.D. TELEKH*[1]

[1]*Bauman Moscow State Technical University, Moscow, Russian Federation*

Nowadays CubeSat nanosatellites are widespread technology in space industry. Due to the low manufacturing and launch price, CubeSat is an attractive option for testing new technologies, for observation and etc. Sometimes a low-thrust propulsion system is required on these satellites for increasing lifetime and number of satellite abilities. Electric propulsion systems (EPS), which can generate thrust about 1 μN…10 mN fit this requirement the best [1].

However there are a number of restrictions on power supply, propulsion system volume and mass for CubeSats due to their small dimensions. Some EPS (for example, GIT or Hall thrusters) suffer from performance decrease and manufacturing complication at low powers. This raises satellite's price [2].

In this regard ablation pulsed plasma thruster (APPT) is considered as a promising propulsion system for nanosatellites. APPT operation is stable at low power supplies; this thruster uses solid dielectric material as propellant. This makes propellant supply system simple and propulsion system's price low.

APPT operation principle is mass acceleration by electromagnetic and gas dynamic forces. Mass flow with thermal velocities makes specific impulse low. So processes in APPT have to occur under optimal conditions in order to make most amount of mass accelerated by electromagnetic forces [3, 4]. One of the promising ways to organize optimal mass acceleration is matching energy distribution during the impulse.

Experimental and theoretical studies of ablation and acceleration processes matching with thruster performance parameters were carried out. Electrical parameters variation in RLC-circuit allows managing the decay factor and natural angular frequency in current and voltage oscillations. This can lead to circuit released power changing during the same time.

Since the determining resistance value in the circuit is the plasma resistance, an increase in the other elements resistance will lead to power release on the element with the highest resistance value. This will lead to the fact that less energy will be delivered to the plasma so the efficiency will decrease.

In this regard, energy storage capacity and circuit inductivity were varied for studying the current oscillation influence on thruster performance parameters. In each case current waveform data and impulse bit were measured. Impulse bit was measured by shooting method.

Measured data allows estimating impulse bit of the plasma filament contribution to the total impulse bit measured by shooting method. Based on experimental data, an assumption was made. It is assumed that most amount of plasma filament, which takes part in electromagnetic acceleration, left discharge channel during the first period.

REFERENCES

[1] D. O'Reilly, G. Herdrich, and D. F. Kavanagh. "Electric Propulsion Methods for Small Satellites: A Review" Aerospace 8, no. 1: 22. https://doi.org/10.3390/aerospace8010022.

[2] N.N. Antropov et al. "Novyy etap razvitiya ablyatsionnykh impul'snykh dvigatelei v NII PME", Vestnik FGUP «NPO im. S.A. Lavochkina», no. 5, pp. 30-40, 2011.

[3] Z. Zhang, W.Y.L. Ling, H. Tang et al. "A review of the characterization and optimization of ablative pulsed plasma thrusters," Rev. Mod. Plasma Phys. vol. 3, no. 5, 2019. https://doi.org/10.1007/s41614-019-0027-z10.2514/1.J056272.

[4] Wu, Zhiwen, Guorui Sun, Tiankun Huang, Xiangyang Liu, Kan Xie and Ning-fei Wang. "Optimization of the Energy Distribution in Ablative Pulsed Plasma Thrusters," AIAA Journal, vol. 56, no. 8, 2018.

* The presented results have been obtained at large-scale research facilities "Beam-M" of Bauman Moscow State Technical University following the government task by the Ministry of Education and Science of the Russian Federation (0705-2020-0046).

S4-P-035203

CONVERSION OF LC-CIRCUIT ENERGY INTO KINETIC ENERGY OF CURRENT-CARRYING METAL PLATE

A.V. KOZYREV, A.A. ZHERLITSYN

Institute of High Current Electronics SB RAS, Tomsk, Russian Federation

When conducting shock-wave experiments with metal plates accelerated to a speed of about 10 km/s, it is possible to use electric generators based on a capacitive energy storage. An analysis of the efficiency of energy transfer of a capacitive storage into the kinetic energy of a current-carrying plate (planar liner geometry) has been carried out.

The mathematical model included the equation for the current in the LC-circuit with a nonlinear load inductance and the 1-dimensional equation for the liner motion. It is shown that at a fixed dimensionless ratio, $\lambda_F = L_F/L_0$ (here, L_F is the final inductance of the liner, L_0 is the inductance of the electrical circuit), liner kinetic energy depends only on one dimensionless parameter u, which combines the parameters of the generator and the liner, and u is proportional to the initial charge of the capacitive storage. The results of a numerical calculation of the dimensionless ratio, S, of the final kinetic energy of the liner to the energy stored in the capacitive energy storage are shown in the figure 1. The dotted line shows the linear dependence of the points of maximum efficiency on the coordinate plane (u-S). The data shown make it possible to determine the optimal parameters of the capacitive storage for the given parameters of the liner, while it is necessary to ensure the lowest inductance of the electric circuit, L_0, since it determines the value of the key parameter λ_F.

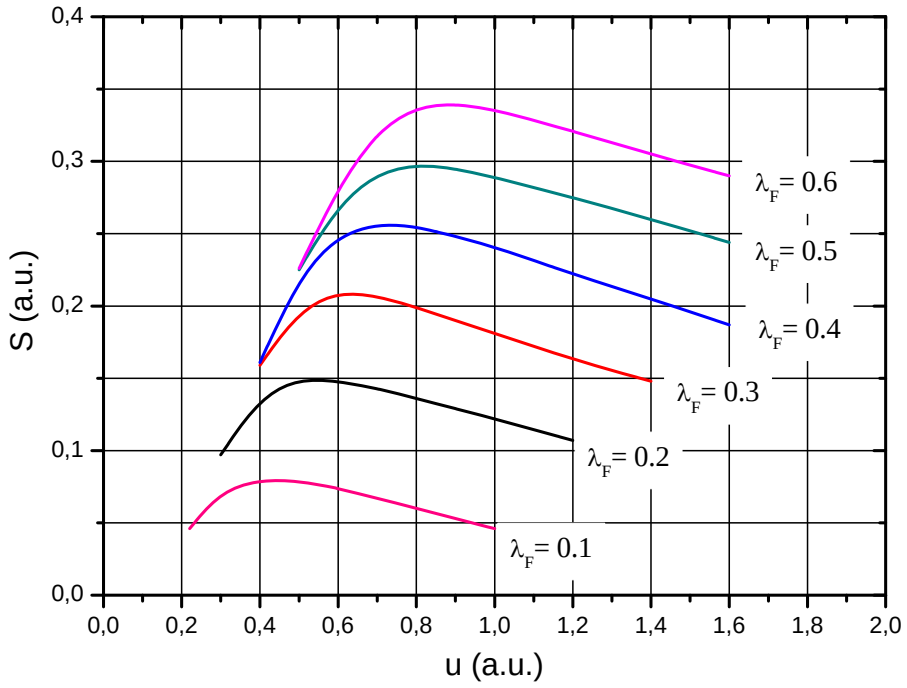

Fig.1. Dependences of the efficiency of energy transfer to the liner, S, versus the dimensionless parameter u for different dimensionless liner inductances λ_F .

PULSE POWER SUPPLY FOR PLASMA CATHODE LOW ENERGY PULSE ELECTRON SOURCE *

S.V. GRIGORYEV[1], V.O. OSKIRKO[1,2], A.P. PAVLOV[2], I.M. GONCHARENKO[1], P.V. MOSKVIN[1]

[1]Institute of High Current Electronics SB RAS, Tomsk, Russia
[2]OOO Prikladnaya Elektronika, Tomsk, Russia

Low-energy intense electron beams with a pulse duration of a few, tens and hundreds of microseconds are currently widely used for research on creating the scientific foundations of technologies in the field of surface modification of metal and metal-ceramic materials. The greatest number of studies were carried out with the use of electron sources in the pulse duration range of 1-4 μs. [1] or in the range of 20 - 300μs. [2, 3]. At the same time, the range 4–20 μs is of interest and remains unexplored at the moment.

The paper presents a description of a pulsed power supply for an arc discharge of a plasma cathode for a pulsed source of electrons with energies up to 25 keV. The source is suitable for powering the SOLO arc plasma cathode with an additional discharge initiation cell [4]. A feature of the developed switching power supply is the possibility of generating current pulses with an amplitude of up to 2000 A and a duration of 7 μs. The formation of short current pulses is ensured by the use of an isolating transformer with low stray inductance and a multi-channel thyristor pulse shaper. Fig. 1a shows the power supply circuit and Fig. 1b shows the waveforms of trigger pulse current for arc discharge initiation, as well as the pulses of the main arc supply channel.

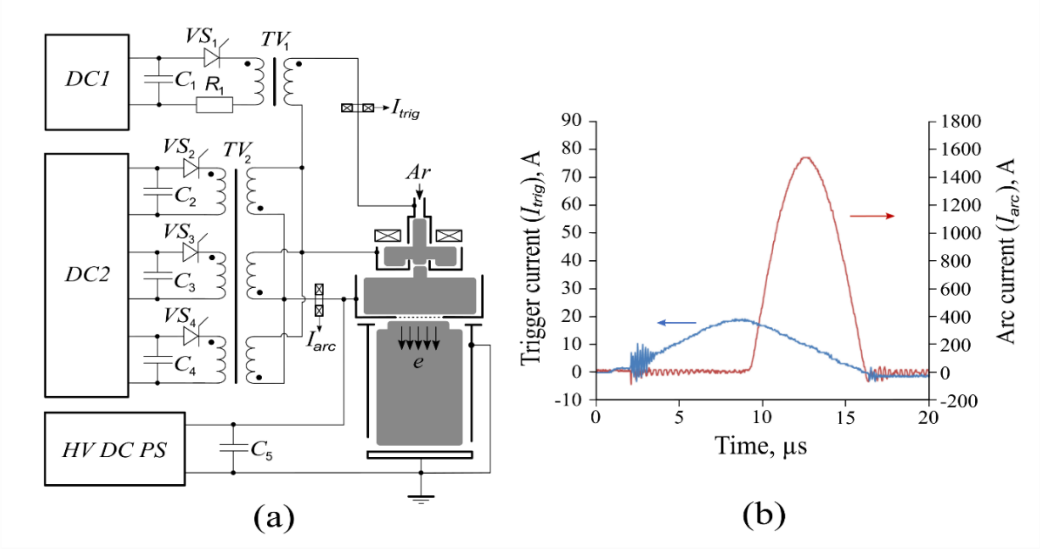

Fig.1. Scheme of high power supply for low energy pulse electron source (a) and typical output waveforms (b).

REFERENCES

[1] G.E. Ozur, D.I. Proskurovsky, "Generation of low-energy high-current electron beams in plasma-anode electron guns," Plasma Physics Reports, vol. 44, no. 1, pp 18-39, 2018.

[2] V.I. Engelko, G. Muelle, "Microsecond intense electron beams for industrial applications," IEEE Transactions on Plasma Science, vol. 41, no. 10, pp 2769-2773, 2013.

[3] V. N. Devyatkov, N.N. Koval, S.V. Grigoriev, A.D. Teresov "Equipment for pulsed thermal treatment of the surfaces of materials by a low-energy electron beam," High Temperature Material Processes: An International Quarterly of High-Technology Plasma Processes., vol. 17, no. 2-3, pp 187-194, 2013.

[4] V.N. Devyatkov et al. "Generation and propagation of high-current low-energy electron beams, ", Laser and Particle Beams, vol. 21, no. 2, pp 243-248, August 2003.

* The work was supported by RFBR and ROSATOM, project number 20-21-00111.

S4-P-036501

MODIFIED CAPACITOR-SWITCH ASSEMBLY FOR LTD GENERATORS OF PETAWATT POWER LEVEL*

D.V. RYBKA, A.D. LENSKIY, S.A VAGAYTSEV, E.A. VAGAYTSEV

Institute of High Current Electronics SB RAS, Tomsk, Russia

Currently, LTD-technology is positioned as a promising direction in the construction of high-current pulse installations of a new generation. The development of LTD-cavities, as a basic element of LTD-generators, is actively underway in the USA, China and Russia [1 - 9].

Most of the developments in this area are carried out using "bricks" based on high-voltage capacitors manufactured by GA, models No. 35473, No. 35479, No. 35462 with a nominal capacity (40-100) nF [10], or their analogues. But in [11], the authors presented a prototype of a capacitor-switch assembly (CSA) of a unique design with an output power level exceeding the existing values. In [12 - 14], it was proposed to use CSA to create compact LTD generators, and in [15, 16], technical requirements for CSA for use in LTD generators with a water transmission line of a petawatt power level were formulated.

This paper presents the design and results of resource tests of the CSA, which can be used as a basic LTD driver in electrophysical installations with an initial energy reserve of up to 50 MJ.

REFERENCES

[1] M. G. Mazarakis, W. E. Fowler, A. A. Kim et al., “High current, 0.5-MA, fast, 100-ns, linear transformer driver experiments.” Phys. Rev. ST Accel. Beams, vol 12, 2009, Art. no. 050401, doi: 10.1103/PhysRevSTAB.12.050401.

[2] J. R. Woodworth, W. E. Fowler, B. S. Stoltzfus et al., “Compact 810 kA linear transformer driver cavity.” Phys. Rev. ST Accel. Beams, vol. 14, 2011, Art. no. 040401, doi: 10.1103/PhysRevSTAB.14.040401.

[3] B. M. Kovalchuk, A. V. Kharlov, E. V. Kumpyak, and A. A. Zherlitsyn, “Pulse generators based on air-insulated linear-transformer-driver stages.” Phys. Rev. ST Accel.Beams vol.16, 2013, Art. no. 050401, doi: 10.1103/PhysRevSTAB.16.050401.

[4] W. A. Stygar, T. J. Awe, J. E. Bailey et al., “Conceptual designs of two petawatt-class pulsed-power accelerators for high-energy-density-physics experiments.” Phys. Rev. ST Accel. Beams, vol. 18, Nov. 2015, Art. no. 110401, doi: 10.1103/PhysRevSTAB.18.110401.

[5] L. Zhou, Z. Li, Z. Wang et al., “Design of a 5-MA 100-ns linear-transformer-driver accelerator for wire array Z-pinch experiments.” Phys. Rev.Accel. Beams vol.19, 2016, Art. no. 030401 doi: 10.1103/PhysRevAccelBeams.19.030401.

[6] J. D. Douglass, B. T. Hutsel, J. J. Leckbee et al., “100 GW linear transformer driver cavity: Design, simulations, and performance,” Phys. Rev. Accel. Beams, vol. 21, Dec. 2018, Art. no. 120401, doi: 10.1103/PhysRevAccelBeams.21.120401.

[7] R. D. McBride, W. A. Stygar, M .E. Cuneo et al., “A Primer on Pulsed Power and Linear Transformer Drivers for High Energy Density Physics Applications,” IEEE Trans. Plasma Sci., vol. 46, Nov. 2018, pp. 3928–3967, doi: 10.1109/TPS.2018.2870099

[8] L. Chen, W. Zou, L. Zhou, et al., “Development of a fusion-oriented pulsed power module,” Phys. Rev. Accel. Beams, vol. 22, 2019, Art. no. 030401, doi: 10.1103/PhysRevAccelBeams.22.030401.

[9] L. Chen, W Zou, J. Jiang, et al., “First results from a 760-GW linear transformer driver module for Z-pinch research.” Matter Radiat. Extremes, vol. 6, 2021, 045901 (2021); doi: 10.1063/5.0003346

[10] https://www.ga.com/capacitors/series-pds-pdss-fast-pulse-capacitors

[11] I. Lavrinovich, D. Molchanov and N. Zharova, “High-Power Capacitor-Switch Assemblies Rated at 100 ns.” 2018 20th Int. Symp. on High-Current Electronics (ISHCE), Tomsk, 2018, pp. 98–102, doi: 10.1109/ISHCE.2018.8521223.

[12] I. Lavrinovich, A. Artyomov, D. Molchanov and D. Rybka, "Compact LTD Stage Based on a New Capacitor-Switch Assembly." 2018 20th Int. Sym. on High-Current Electronics (ISHCE), Tomsk, 2018, pp. 103-106, doi: 10.1109/ISHCE.2018.8521210.

[13] I. Lavrinovich, S. Vagaytsev, A. Erfort et al., “New Type Capacitor-Switch Assembly for LTD Technology.” 2019 IEEE Pulsed Power and Plasma Science (PPPS), Orlando, FL, USA, 2019, pp. 1–4, doi: 10.1109/PPPS34859.2019.9009957.

[14] I. Lavrinovich, S. Vagaytsev, A. Erfort, et al., “Concept Designs of a Compact LTD Generator with a Pulse Rise Time of 100 ns.” 2019 IEEE Pulsed Power and Plasma Science (PPPS), Orlando, FL, USA, 2019, pp. 1–4, doi: 10.1109/PPPS34859.2019.9009657.

[15] I. Lavrinovich, D. Rybka, A. Lenskiy et al., "Architecture of a 100-ns LTD Generator Based on a New Type of Capacitor-Switch Assemblies." 2020 7th International Congress on Energy Fluxes and Radiation Effects (EFRE), 2020, pp. 297-301, doi: 10.1109/EFRE47760.2020.9241939.

[16] N. D. Zameroski, C. Anderson, H. Kirbie, et al., “Characterization of a 200-nF unipolar, high current, low inductance capacitor switch assembly.” Rev. Sci. Instrum. vol. 92, 2021, Art. no. 094710, doi: 10.1063/5.0047261.

* The research was funded by RFBR and Tomsk region, project number 19-48-700017.

S4-P-039301

METHOD FOR MEASURING VOLTAGE DROP ALONG A LOAD OF THE MIG PULSE POWER GENERATOR*

A.G. ROUSSKIKH, A.S. ZHIGALIN, V.I. ORESHKIN

Institute of High Current Electronics SB RAS, Tomsk, Russia

The work is devoted to development of a technique for measuring the voltage drop along a load of the pulse power generator MIG [1]. In the course of solving the problem posed, we tested various approaches to solving the problem of voltage measurement. The amplitude values of the voltage drop in the point of the voltage sensor location can be several hundred kilovolts with a rise time of about 80 ns. Voltage drop measurements are made in conditions of closely spaced current-carrying electrodes. The most reliable and adequate scheme that allows us to measure the voltage drop along the load is an inductive divider. The parameters and features of an inductive voltage divider developed and implemented in the course of this task are described.

REFERENCES

[1] I.E. Gorelchanik, A.F. Korostelev, V.K. Petin, N.A. Ratakhin, A.N. Shepelev, V.F. Fedushchak, S.V. Shlyakhtun, “High-power electron beam generator MIG,” 13th International Conference on High-Power Particle Beams, BEAMS 2000, pp. 172-175, 6220141, 2000.

* THE WORK WAS SUPPORTED BY THE RUSSIAN SCIENCE FOUNDATION UNDER GRANT NO. 20-19-00364

.

S4-P-039401

CALIBRATION TECHNIQUE FOR A SLEET STREAK SPECTROMETER UNDER THE CONDITIONS OF THE PULSE-POWER MIG GENERATOR*

A.S. ZHIGALIN, A.G. ROUSSKIKH, V.A. VANKEVICH, V.I. ORESHKIN

Institute of High Current Electronics SB RAS, Tomsk, Russia

The paper describes the method of spectral and temporal calibration of the Hamamatsu C10910 sleet streak spectrometer, carried out before experiments on the pulse-power MIG generator [1]. The design and principle of operation of a hydrogen flash lamp specially designed for spectral and temporal calibrations are described. Optical circuits for recording the spectrum of a hydrogen flash lamp and electrical circuits for synchronizing a streak camera with a pulse-power MIG generator are presented.

REFERENCES

[1] I.E. Gorelchanik, A.F. Korostelev, V.K. Petin, N.A. Ratakhin, A.N. Shepelev, V.F. Fedushchak, S.V. Shlyakhtun, “High-power electron beam generator MIG,” 13th International Conference on High-Power Particle Beams, BEAMS 2000, pp. 172-175, 6220141, 2000.

* THE WORK WAS SUPPORTED BY THE RUSSIAN SCIENCE FOUNDATION UNDER GRANT NO. 20-19-00364

A FIVE-CHANNEL TRIGGER SIGNALS AMPLIFIER*

A.P. ARTYOMOV[1], A.V. FEDUNIN[1], A.G. ROUSSKIKH[1], V.I. ORESHKIN[1,2]

[1] Institute of High Current Electronics SB RAS, Tomsk, Russia
[2] National Research Tomsk Polytechnic University, Tomsk, Russia

At present, plasma physics is actively investigating objects whose lifetime can be tens or even units of nanoseconds, for example, the electric explosion of conductors, Z- and X-pinches, and others [1-6]. It is often necessary to use additional high-voltage equipment to diagnose [1–3] or form [4-6] these objects in an experiment. Moreover, this equipment must be synchronized with the main generator with a jitter of less than ±10 ns.

High-voltage gas trigatrons are widely used as an intermediate stage for starting high-current pulse generators with an operating voltage of over 30 kV. They make it possible form voltage pulses with an amplitude of 15-20 kV and a rise time of less than 20 ns. Low-voltage multichannel trigger generators (TG) are often used as the primary trigger device, which form a pulse with an amplitude of up to 300 V. It is often impossible to provide an acceptable level of the triggering signal for a trigatrons spark gap directly from the TG. In this case, either a large trigatrons jitter is observed, or it does not start at all. In addition, in some cases it is necessary to increase the length of the cable between the TG and a trigatrons spark gap that leads to the attenuation of the trigger pulse. This can also negative effects on the trigatrons operation.

A five-channel trigger signal amplifier was developed to solve these problems. A voltage pulse with an amplitude of -1 kV is formed at the output of each channel. The amplifier was tested in operation with a high-voltage gas trigger, which formed a voltage pulse with an amplitude of -18 kV to start a pulse power generator. As a result of the tests, it was shown that the jitter at the output of the high-voltage gas trigger (-18 kV) did not exceed ±3 ns, and the jitter of the high-current generator was no more than ±10 ns.

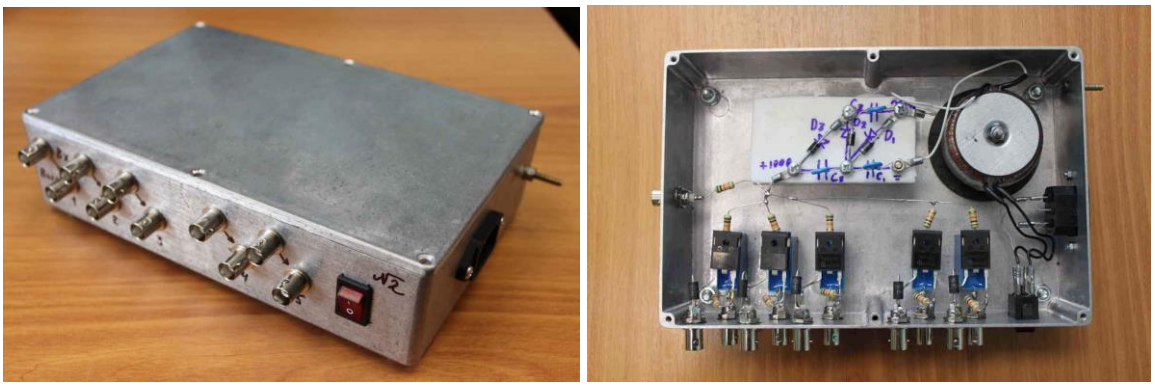

Fig.1. External and internal view of the five-channel trigger signal amplifier.

REFERENCES

[1] S.I. Tkachenko, V.M. Romanova, A.R. Mingaleev et al, “Study of plasma parameter’s distribution upon electrical wire explosion”, Eur. Phys. J. D, vol. 54, pp. 335–341, 2009.

[2] D.B. Sinars, T.A. Shelkovenko, S.A. Pikuz et al, “The effect of insulating coatings on exploding wire plasma formation”, Phys. Plasmas, vol. 7, pp. 429-432, 2000.

[3] R.B. Baksht, A.G. Rousskikh, A.S. Zhigalin, V.I. Oreshkin, and A.P. Artyomov, ”Stratification in Al and Cu foils exploded in vacuum”, Phys. Plasmas, vol. 22, 103521, 2015.

[4] A.G. Rousskikh, A.V. Shishlov, A.S. Zhigalin, *et al*, “Small-sized vacuum-arc-discharge x-ray radiograph,” Plasma Sources Sci. Technol., vol. 20, 035011, 2011.

[5] A.P. Artyomov, S.A. Chaikovsky, A.G. Rousskikh and A.V. Fedunin, “Soft x-ray source based on the point Z-pinch for pulse radiography”, Journ. of Phys.: Conf. Series, vol. 1556, 012083, 2020.

[6] R.K. Cherdizov, R.B. Baksht, V.A. Kokshenev et al, “Effect of tailored density profiles on the stability of imploding Z-pinches at microsecond rise time megaampere currents”, Plasma Phys. Control. Fusion, vol. 64, 015011, 2022.

* The work was supported by the Russian Science Foundation under grant No. 22-19-00686.

S4-P-040802

COMPACT PULSE POWER GENERATOR AS A SOURCE OF ENERGY FOR A PLASMA GUN*

A.P. ARTYOMOV[1], A.V. FEDUNIN[1], N.V. ZHAROVA[1], A.D. LENSKIY [1], A.G. ROUSSKIKH[1], D.V. RYBKA[1], V.I. ORESHKIN[1,2]

[1] Institute of High Current Electronics SB RAS, Tomsk, Russia
[2] National Research Tomsk Polytechnic University, Tomsk, Russia

Ten years ago, at the Institute of High Current Electronics SB RAS in Tomsk a new method for the formation of a reusable point source of soft X-rays was proposed as an alternative to the X-pinch. This method was called PZ-pinch (Point Z-pinch) [1, 2]. In contrast to the X-pinch, the plasma of the PZ-pinch is preliminarily produced and then injected into the high voltage gap of pulse power generator during the operation of a high-current arc discharge.

The work is devoted to a new compact pulse generator designed as a source of power for a plasma gun. It was designed and created to replace the pulsed generator based on the IK-50-3 capacitor (3 μF), which we used earlier. The IK-50-3 capacitor provided a current pulse with an amplitude of 70 kA and a current rise time of 1 μs when operating on an arc. Its operating voltage was 20 kV [2]. However, this capacitor has impressive weight (120 kg) and size (31x31x67 cm^3) parameters. In addition, the potential energy storage of the IK50-3 capacitor is excessive for plasma gun, which we use as part of a low-scale XPG-3 current generator to form PZ-pinch.

The new generator is based on a 1 μF capacitor-switch assembly (Fig. 1*a*) of our own design [3, 4]. The dimensions of the pulse generator are Ø30x30 cm, which is significantly smaller than its predecessor. The operating voltage of the new generator is 25 kV. It provides an arc current amplitude of 120 kA with a rise time of 500 ns. The external view of the generator is shown in fig. 1*b*. Experiments have shown that the power of the new generator is sufficient to form a bright point source of soft X-ray radiation based on the PZ-pinch in a wide range of linear pinch masses.

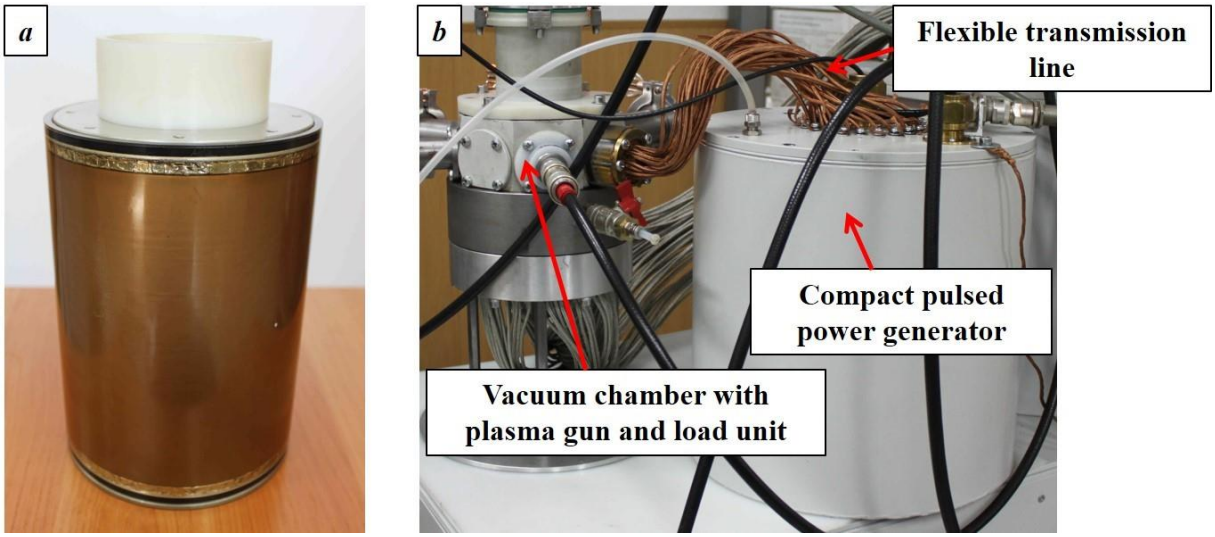

Fig.1. External view of the capacitor-switch assembly (*a*) and the compact pulse power generator (*b*).

REFERENCES

[1] A.G. Rousskikh, A.V. Shishlov, A.S. Zhigalin, *et al*, "Small-sized vacuum-arc-discharge x-ray radiograph," Plasma Sources Sci. Technol., vol. 20, 035011, 2011.

[2] A.P. Artyomov, S.A. Chaikovsky, A.G. Rousskikh and A.V. Fedunin, "Soft x-ray source based on the point Z-pinch for pulse radiography", Journ. of Phys.: Conf. Series, vol. 1556, 012083, 2020.

[3] S.A. Chaikovsky, A.P. Artyomov, N.V. Zharova *et al*, "Small-size high-current generators for x-ray backlighting", Russ. Phys. Journ., vol. 60, pp. 1408-1412, 2017.

[4] N.V. Zharova, N.A. Ratakhin, A.V. Saushkin, V.F. Fedushchak, and A.A. Erfort, "Fast energy output from a high-current pulsed capacitor by using a pseudospark gap", Instrum. Exp. Tech., vol. 49, pp. 384–387, 2006.

* The work was supported by the Russian Foundation for Basic Research under grant No. 19-48-700017.

S4-P-042404

STUDY OF URT-1M ACCELERATOR IN SUBMICROSECOND OPERATION

M.E. BALEZIN[1], *S.YU. SOKOVNIN*[1,2], *A.S. GERASIMOV*[1,2,]

[1] *Institute of Electrophysics UB RAS, Yekaterinburg, Russia*
[2]*Ural Federal University named after First President of Russia B.N. Yeltsin , Yekaterinburg, Russia*

In recent years, the concept of surface radiation sterilization (SRS) has been actively developing, the essence is the effect of an electron beam only on the surface layer of the object being irradiated. This approach is promising in many applications, such as the treatment of various food products: grains [1], eggs [2], lumped meat and feeds [3]. The main advantage of SRS is the ability to localize changes in the product in a narrow surface layer (tens to hundreds of microns), which is contaminated by various microorganisms. At the same time, the main part of the product is irradiated only by bremsstrahlung, the level of absorbed doses in which is tens of thousands less than on the surface. This allows to maintain not only the nutritional value of the main part of the product, but also the vital ability of seeds or eggs.

At the same time, the requirements for maximum electron energy for such accelerators are significantly reduced to 0.5 MeV, and the presence of low-energy electrons in the spectrum becomes useful. These electrons intensify the irradiation of the surface layers and reduce the output of bremsstrahlung, the only limitation being their high absorption in the output foil, and increase the thermal load on it.

The purpose of this work was to investigate the operation of the URT-1M [4] accelerator with a power system without SOS switch. The approaches used in the high-voltage pulse generation system of this accelerator allow generating a pulse with an amplitude of up to 500 kV, a duration of ~ 450 ns and a supply repetition rate up to 50 pps during discharge of the second circuit capacitor.

It was found that in this mode, an accelerator with a metal dielectric cathode works stably at a charging voltage of up to 35kV (accelerating ~ 350 kV). Further increase of voltage is limited by breakdown of through vacuum insulator with shielding of dielectric surface [5].

REFERENCES

http://www.fep.fraunhofer.de/en/Anwendungsfelder/Landwirtschaft.html

S.Yu. Sokovnin, " An electron beam technology of surface disinfection of the packed egg", Food and Bioproducts Processing, vol. 127, pp. 276–281, 2021.

R A Vazirov, S Yu Sokovnin, A S Krivonogova and A G Isaeva // Investigation of the effectiveness of antimicrobial treatment of poultry products by electrophysical methods / Journal of Physics: Conference Series 2064 (2021) 012084 doi:10.1088/1742-6596/2064/1/012084

S.Yu. Sokovnin, M.E. Balezin, Repetitive Nanosecond Electron Accelerators type URT-1 for radiation technology, Radiation Physics and Chemistry. V. 144, 2018, pp. 265-270. https://doi.org/10.1016/j.radphyschem.2017.08.023

Kotov, Yu.A., Rodionov, N.E., Sergienko, V.P., Sokovnin, S.Yu., Filatov, A.L., 1986.Vacuum insulator with shielded surface of dielectric. Prib. Tekh. Eksp. 2, 138–141.

PRODUCTION OF IRON OXIDE NANOPOWDERS BY RADIATION-CHEMICAL METHOD

M.E. BALEZIN[2], *S.YU.SOKOVNIN*[1,2]

[1]*Ural Federal University, Yekaterinburg, 620002, Russia*
[2]*Institute of Electrophysics, UB, RAS, Yekaterinburg, Russia*
e-mail: mk@iep.uran.ru

Were continued the studies of nanopowders (NP) of iron oxide produced by radiation-chemical method [1] at irradiation of iron sulfate solutions in water and iron nitrate in isopropyl alcohol on electron accelerator URT-0,5 [2].

With an increase in the concentration of iron sulfate in the solution, the specific surface area of the NP decreases, and the yield increases. For iron nitrate, with an increase in its concentration in solution, both the yield of NP and the specific surface area grow under irradiation under the same conditions (absorbed dose of 2.3 MGp at an accelerator frequency of 10 Hz).

Since the particles produced from the iron nitrate solutions are amorphous, they were annealed, followed by X-ray phase analysis. It has been found that these are hematite, Fe_2O_3 particles (unlike maghemite C, γ- $Fe_{21.33}O_{32}$ particles from iron sulfate). The specific surface area of the particles increases with the annealing temperature (from 2.4 nm at 400 ° C to > > 200 nm at 1200 ° C).

The produced NPs can be used to create promising upconversion materials for medicine based on them.

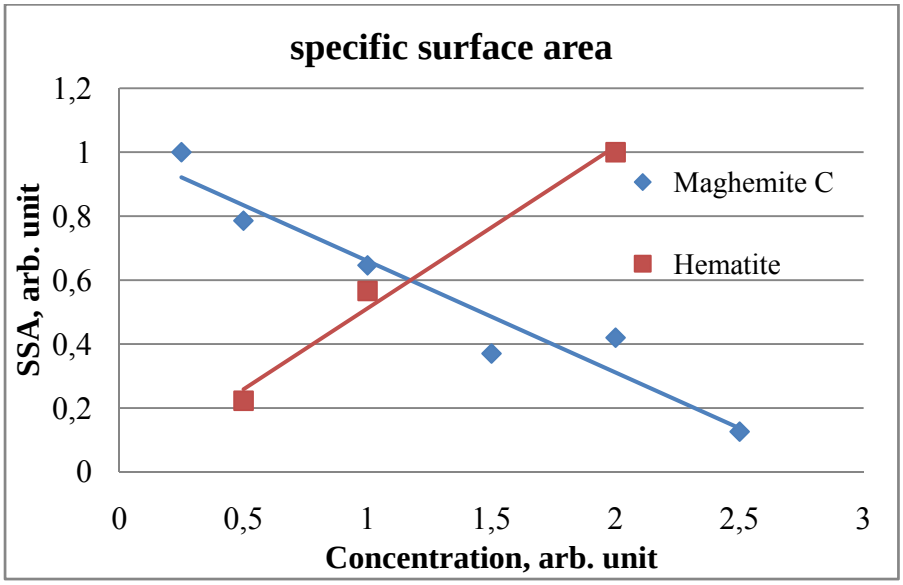

Fig.1. Specific surface of NP FeO at change of concentration in solution.

REFERENCES

[1] S. Yu. Sokovnin, M. Balezin, Production of nanopowders using nanosecond electron beam, Ferroelectrics, V: 436, 01, p. 108 - 111. DOI:10.1080/10584587.2012.731330

[2] Sokovnin, S.Y., Balezin, M.E. Improving the Operating Characteristics of an УРТ-0.5 Accelerator. *Instrum Exp Tech* **48,** 392–396 (2005). https://doi.org/10.1007/s10786-005-0068-0

S4-P-044601

LINEAR PULSE TRANSFORMER WITH PULSE REPETITION UP TO 5 HZ

V.M. ALEXEENKO[1], *A. A. ZHERLITSYN*[1], *S. S. KONDRATIEV*[1]

[1]*IHCE SB RAS, Tomsk, Russia*

A linear pulse transformer is successfully used for charging an intermediate storage (capacitance with water isolation or inductive) [1,2]. Compared with the more common Marx generators, the linear pulse transformers have some advantages: significantly less high-voltage isolation volume and simplified monitoring and maintenance of capacitors and switches of the storage. Article [3] showed the possibility of using a linear pulse transformer for applied tasks. However, in this case, it is necessary to implement the frequency mode of operation with acceptable stability.

This work presents the design and results of the study of a linear pulse transformer (the transformer below) with air insulation at atmospheric pressure. Distinctive features of this transformer are the frequency mode of operation, the absence of a liquid dielectric in the insulation of the transformer, the placement of a capacitive storage inside the case (inductor) and its direct connection to the primary loop without the use of high-voltage transmission cables. The capacity of the transformer storage is 150 nF, the charging voltage is up to 80 kV, and the stored energy is up to 480 J. The transformer allows about 60% of the stored energy to be transferred to a matched load (5–7 Ohm) in a characteristic time of about 1 μs. At a high-resistance load, the transformer generates a voltage pulse with a rise time of 100 ns and an amplitude close to twice the charging voltage. The increase in output voltage and power is realized by connecting several transformers in series. The experimental results are show possibility of the frequency mode of operation with a pulse repetition of 1–5 Hz and with output pulse jitter at the level of 20 ns.

The work was performed under State Assignment of the Ministry of Science and Higher Education of the Russian Federation (No. FWRM-2021-0001) and with the support of the Russian Foundation for Basic Research (No. 19-08-00115 a).

REFERENCES

[1] V. A. Vizir' et al. Prib. Tekh. Eksp., V.5, 1986.

[2] A. V. Luchinskii, et al. Russ. Phys. J., vol. 38, pp. 1246–1252, 1995 DOI:10.1007/BF00559385.

[3] D. Molchanov, et al., IEEE 21st PPC, 2017, pp. 1-4. DOI:10.1109/PPC.2017.8291167.

S4-P-045001

CONTROLLED PULSED INJECTION FOR HV GAS BLAST CIRCUIT BREAKERS

N.K. KURAKINA, E.N. TONKONOGOV, I.V. MURASHOV, R.I. ZHILIGOTOV, N.V. OBRAZTSOV

Peter the Greet St.Petersburg Polytechnic University, High School of Electrical Engineering, Saint-Petersburg, Russia

According to modern trends, the interrupting performance and reliability of modern HV gas blast circuit breakers (CB) should be increased. It becomes increasingly important with transition to SF6-free technologies [1]. The basic aim of the investigation is to improve the efficiency of arc quenching by increasing of interruption ability in CB with the same rated pressure and without drive parameter changing. Some disadvantages of the controlled switching [2] for modern CB are discussed.

A method of a short time gas pulse under high pressure - synchronous gas injection - is proposed in the study. It is developed with benefits and drawbacks of the controlled switching in mind. The synchronous gas injection should be introduced to the plasma region before current zero to reduce pre-zero arc conductivity, change the initial gas-dynamics characteristics (density, pressure, velocity, and mass flow rate), deform the arc thermal boundary layer, provide the turbulent mixing in the upstream region [3], and by doing so achieve necessary cooling-heating balance for successful arc extinguishing.

Performance of the suggested approach is investigated by numerical simulation and empirical relationships with a model arc quenching device. Air is conditionally taken as a gas medium. The research confirms the synchronous gas injection has a perspective to increase breaking capacity of circuit breakers in high voltage levels considering the limited power of the drives. Gas injection parameters in the vicinity of current zero are determined. Efficiency of the synchronous gas injection on the CB interruption ability is presented.

REFERENCES

[1] Franck C. M., Chachereau A., Pachin J., IEEE Electr Insul M (2021) 37, 1, 7-16.

[2] CIGRÉ Working Group A3.07, Controlled Switching of HV AC Circuit Breakers, CIGRÉ (2004), Paris.

[3] Kurakina N., Frolov V., Tonkonogov E., Plasma Physics and Technology (2019), 6(1), 43-46.

S4-P-045301

INVESTIGATION OF WIRES LAYOUT IN EXPLODING WIRE ARRAY

S. ANISHCHENKO[1], A. GURINOVICH[1], E. GURNEVICH[1], D. LEONENKO[2], A. ROUBA[1]

[1]Research Institute for Nuclear Problems, Minsk 220030, Belarus
[2]Electrophysical laboratory, Minsk 220088, Belarus

Exploding wires serving as opening switch for pulsed power applications are widely studied. Geometry of exploding wire array (EWA) could significantly influence on the output parameters of the switch, namely: the amplitude and duration of the produced pulse [1,2].

Compact EWA design could imply use of non-strait wires, for example, zigzag or helical installation [3]. High-voltage breakdown should be taken into account for a compact EWA, thus use of insulating gas should be considered as an option. According to multiple studies SF_6 looks to be the best choice for EWA. Experiments demonstrate possibility to keep the amplitude of the EWA-produced high-voltage pulse with twice as short array length with zigzag wires installation in pressurized SF_6. Simultaneous increase of pulse duration after switching to the load could reach 30% as compared to the pulse produced with straight wires exploded in air.

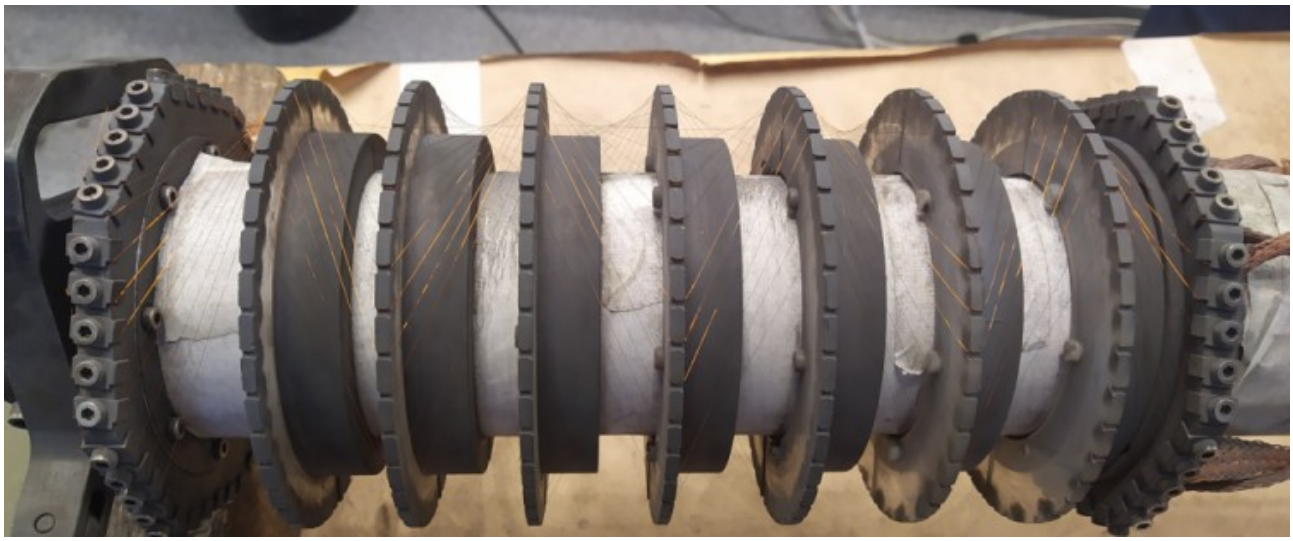

Fig.1. Exploding wire array with zigzag wires installation.

Wires damage is shown to be of high importance during installation. Any extra tension applied to wires could cause reducing of amplitude of high-voltage pulse as much as 15%.

REFERENCES

[1] G.A. Mesyatz, “Pulsed power,” Springer, Boston, MA, 2005.

[2] A.E. Borisevich, S.L. Cherkas, “Effect of the Conductor Radius on the Electric Explosion Dynamics: Magnetohydrodynamic Simulation,” Technical Physics. Vol. 57, No. 10, P. 1380–86, 2012.

[3] D. McCauley, D. Belt, J. Mankowski, J. Dickens, A. Neuber, and M. Kristiansen, “Electro-explosive fuse optimization for helical flux compression generator using a non-explosive test bed,” Proceedings of 16th IEEE International Pulsed Power Conference. 2007.

S4-P-046101

METHODOLOGY FOR CONDUCTING IN-PILE EXPERIMENTS TO STUDY SPECTRAL-TEMPORAL CHARACTERISTIC OF GAS MEDIA UPON EXCITATION BY THE $^{6}Li(n,\alpha)^{3}H$ NUCLEAR REACTION*

K.K. SAMARKHANOV[1], E.G. BATYRBEKOV[2], M.U. KHASENOV[1,3], YU.N. GORDIENKO[1], A.N. KOTLYAR[1], A.A. MILLER[1], V.K. TSKHE[1], YE.A. MARTYNENKO[1], Z.B. KOZHABAYEV[1]

[1] Institute of Atomic Energy Branch of the National Nuclear Center of the Republic of Kazakhstan, IAE NNC RK, Kurchatov, Kazakhstan
[2] National Nuclear Center of the Republic of Kazakhstan, NNC RK, Kurchatov, Kazakhstan
[3] School of Sciences and Humanities, Nazarbayev University, Nur-Sultan, Kazakhstan

The study of optical (laser and spontaneous) radiation from a nuclear-excited plasma, formed by the products of nuclear reactions is interesting for developing a method of energy output from a nuclear reactor by direct conversion of energy into light [1, 2]. The direct pumping of active media is carried out, as a rule, by the products of nuclear reactions with thermal neutrons of a nuclear reactor: $^{3}He(n,p)^{3}H$, $^{10}B(n,\alpha)^{7}Li$, $^{235}U(n,f)F$ or others. The laser-working medium must contain ^{235}U, ^{3}He or ^{10}B, or a compound with these isotopes is deposited on walls of the laser chamber. Less studied was $^{6}Li(n,\alpha)^{3}H$ nuclear reaction.

The National Nuclear Center of the Republic of Kazakhstan currently operates two research reactors: IVG.1M [3] and IGR [4]. The main results of a series of reactor experiments performed at the stationary reactor IVG.1M are given in [5-7]. Based on the experience of the in-pile experiments at the IVG.1M reactor and considering the specificity of experiments at the pulsed reactor IGR of a thermal neutron flux density up to $7 \cdot 10^{16}$ n/cm^{2}s, the principal scheme of the experimental setup and the methodology of in-pile experiments were developed. Experimental facility functionally consists of gas-vacuum system, optical radiation registration system, irradiation device with a lithium layer, and systems of registration and temperature control of the device housing. The design of the irradiation device (ID) was developed to conduct in-pile experiments at the IGR reactor. Irradiation device, coated with a lithium layer will be loaded into the central channel of the IGR reactor and filled with the test gas mixture. The light radiation will be outputted from reactor core using a fiber, then split into individual beams. Luminescence spectra will be recorded using the optical spectrometer. Spectral-temporal characteristics will be recorded using a monochromator, tuned to the wavelength of the investigated atomic transition, a photodiode and PMT.

Neutron-physical and thermal-physical calculations, using MCNP5 and Ansys Fluent software, respectively, were performed to justify the irradiation device design and safety conducting of in-pile experiments. The calculations were performed at a thermal power level of the IGR reactor equal to 1 GW and a pulse duration of 0.12 s. Based on the results of the performed neutron-physical calculations, the specific power of the energy release of the main elements of the ID design, as a result of neutron and gamma irradiation at the IGR reactor was determined. It was determined, with the IGR reactor power, equal to 1 GW, the total ratio of lithium energy release to energy release in the reactor is $8.23 \cdot 10^3$ W/g. Based on the results of the performed thermal-physical calculations, the temperature field of the experimental cell of the ID was determined.

REFERENCES

[1] S.P. Mel'nikov, A.N. Sizov, A.A. Sinyanskii, G. H. Miley, Lasers with Nuclear Pumping. Springer, New York, NY, USA, 2015.

[2] E. Batyrbekov, "Converting nuclear energy into the energy of coherent optical radiation," Laser and Particle Beams, vol. 31, no. 4, 2013.

[3] R.A. Irkimbekov, L.K. Zhagiparova, V.M. Kotov, A.D. Vurim, V.S. Gnyrya, "Neutronics Model of the IVG.1M Reactor: Development and Critical-State Verification," Atomic Energy, vol. 127, no 2, pp. 69–76, 2019.

[4] V. Vityuk, A. Vurim, "Method for determining the energy parameters in pulse reactor experiments," Annals of Nuclear Energy, vol. 127, 2019.

[5] E. Batyrbekov, M. Khasenov, Yu. Gordienko, K. Samarkhanov, Yu. Ponkratov, "Optical radiation from the sputtered species under gas excitation by the products of the 6Li(n,α)3H nuclear reaction," Journal of Luminescence, vol. 220, Article Number 116973, 2020.

[6] K. Samarkhanov, M. Khasenov, E. Batyrbekov, I. Kenzhina, Ye. Sapatayev, V. Bochkov, "Emission of Noble Gases Binary Mixtures under Excitation by the Products of the 6Li(n,α)3H Nuclear Reaction," Science and Technology of Nuclear Installations, vol. 2020, 2020.

[7] K. Samarkhanov, M. Khasenov, E. Batyrbekov, Yu. Gordienko, Yu. Baklanova, I. Kenzhina, Ye. Tulubayev, I. Karambayeva, "Optical radiation from sputtered species under excitation of ternary mixtures of noble gases by the $^{6}Li(n,\alpha)^{3}H$ nuclear reaction products," Eurasian Chemico-Technological Journal, vol. 23, no. 2, pp. 95–102, 2021.

* This work was supported by the Ministry of Energy of the Republic of Kazakhstan (Program "Development of nuclear energy in the Republic of Kazakhstan for 2021–2023 years"),

S4-P-046601

HIGH-VOLTAGE PULSE CAPACITOR VIK 120-0.04: DESIGN AND RESULTS OF RESOURCE TESTS*

L.A. DARIAN[1], A.D. LENSKIY[2], V.A. LOGUNOV[1], D.V. RYBKA[2]

[1]Federal State Unitary Enterprise "Russian Federal Nuclear Center - Zababakhin All-Russia Institute of Technical Physics", Snezhinsk, Chelyabinsk Region, Russia
[2]Institute of High Current Electronics SB RAS, Tomsk, Russia

The paper presents the results of resource tests of high-voltage pulse capacitors (VIK) with an operating voltage of 120 kV and a capacity of 0.04 uF. VIK is designed and manufactured on the basis of domestic technological and testing equipment as part of the implementation of the import substitution program. Aluminum foil of Russian production was used as capacitor plates. A combined paper-film insulation impregnated with vegetable oil was chosen as a dielectric. In the manufacture of capacitors, a scheme of "non-inductive" winding of sections was used, which made it possible to provide the required discharge characteristics for LTD-cavities of electrophysical installations. Thanks to the optimization of design parameters and winding technology, in particular the bending of the edge of the aluminum foil, it was possible to provide not only improved technical characteristics compared to foreign analogues of the VIK currently used, but also to increase the service life of the developed pulse capacitors.

* The work was funded in part by RFBR and Tomsk region, project number 19-48-700017.

S4-P-048901

SELF-TRIGGERING CIRCUIT FOR A PULSE THYRATRON SWITCH IN A PULSE VOLTAGE GENERATOR

A.S. YUDIN, S.M. MARTEMYANOV

National Research Tomsk Polytechnic University, Tomsk, Russian Federation

The paper describes the self-triggering circuit of the ТДИ4-200к/25СН thyratron [1], which operates as part of a pulse voltage generator based on a pulse transformer. Thyratrons of this series have a number of advantages. They allow one to switch pulsed currents up to 200 kA with a frequency of up to 300 pulses per second, do not require maintenance, are produced with an incandescent cathode and instant readiness. Also, if there are no strict requirements for the turn-on jitter, these thyratrons are not too demanding on the parameters of the trigger pulse.

The self-triggering circuit under consideration was initially developed for the EG350 pulse voltage generator [2], which used an eight-channel switch in a gas under pressure of the trigatron type as a main switch. We replaced the main switch with a thyratron and adapted the existing trigger circuit for it. The peculiarity of the proposed self-triggering circuit (Figure 1, (*STC*)) is its complete autonomy, automatic generation of a trigger pulse at the moment the maximum voltage value is reached on capacitor *C2*, as well as simplicity and reliability.

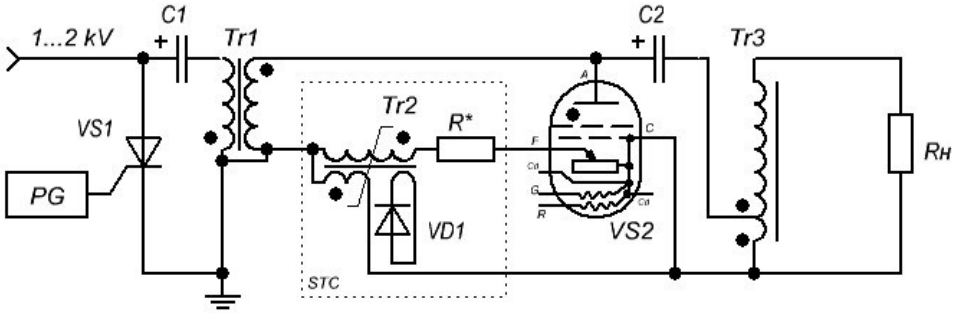

Fig.1. Schematic diagram of the pulse voltage generator: (*VS1*) ТБИ 253-1000-36 thyristor; (*VS2*) ТДИ4-200к/25СН thyratron; (*STC*) self-triggering circuit; (*Tr1*) pulse step-up transformer; (*Tr2*) peak transformer; (*Tr3*) pulse step-up autotransformer; (*VD1*) avalanche diode; (*R**) current limiting resistor; (*C1*) first stage capacitor; (*C2*) second stage capacitor.

REFERENCES

[1] http://pulsetech.ru

[2] Kanaev G. G., Kukhta V. R., Lopatin V. V., Nashlevsky A. V., Remnev G. E., Uemura K. High-voltage pulse generator for electric discharge technologies / Patent No. 2402873 dated October 27, 2010

ROCK CUTTING BY ELECTRIC PULSE METHOD

M.Yu. ZHURKOV, S.Yu. DATSKEVICH, M. V. ZHURAVLEV, A.S. YUDIN

National Research Tomsk Polytechnic University, Tomsk, Russian Federation

The work is devoted to the development of an electric pulse method for cutting rocks and other solid dielectric and semiconducting materials. Previously, we have shown the possibility of electric pulse cutting with a two-electrode moving system with a low energy of the pulse generator, which will make it possible to create a competitive electric cutter in comparison with mechanical and plasma [1].

Studies of cutting by electric pulsed discharges were carried out on a test laboratory facility, consisting of a source of high pulsed voltage, a two-rod electrode system placed in a tank with water ($\gamma \approx 300$ μS*cm), and an electromechanical reversible drive that moves the electrode system in the direction of the cut [2]. The removal of chipped rock from the treatment zone was carried out using a flushing system.

The main disadvantage of the pulsed voltage sources previously used in electric pulse cutting machines was that the pulse repetition rate of the generators (made according to the Marx scheme) is low and the destruction productivity and cutting speed were limited as a result.

In this work a generator based on a pulse transformer with a stored energy of up to 140 J, an output voltage of up to 160 kV, and a pulse repetition rate of up to 25 pulses/s was used for the first time as a source of high-voltage pulses. The generator circuit with slight differences is similar to that described in [3].

Fig.1. Photograph of a cut slit in granite.

On the experimental bench, slits were obtained in granite (Fig. 1) and sandstone with a total area of about 800 cm^2. The distance between the electrodes in the experiments with sandstone was 9 mm, with granite, 8.5 mm. The average depth of destruction in one pass of the electrode system was 6 mm. A sieve analysis of the granite sludge obtained during cutting was carried out, which showed that the proportion of “fine” sludge (less than 2.5 mm) exceeds 85%. This with such an interelectrode gap indicates overgrinding, most likely due to insufficient flushing performance, which reduces the productivity of the cutting [4].

Experiments have shown the possibility of using pulse generators with low energy and a high pulse repetition rate in the electric pulse cutting method, while the mechanical system for moving the electrodes and flushing performance needs to be improved to increase productivity.

REFERENCES

[1] V.F. Vazhov, M.Y. Zhurkov, V.V. Lopatin, V.M. Muratov, “Electric-Discharge Cutting of Rocks,” J. Min. Sc., vol. 44, no. 2, pp. 176–182, 2008.

[2] V.F. Vazhov, M.J. Zhurkov, V.M. Muratov, “Method for electric pulse destruction of rocks Patent, ” RU2232271, 2004.

[3] Kanaev G. G., Kukhta V. R., Lopatin V. V., Nashlevsky A. V., Remnev G. E., Uemura K. High-voltage pulse generator for electric discharge technologies / Patent No. 2402873 dated October 27, 2010.

[4] V.F. Vazhov, S.Y. Datskevich, V.M. Muratov, S.Y. Ryabchikov, “Grain size composition and distribution in drill cuttings in the electric impulse destruction of rocks,” J. Min. Sc, vol. 48, no. 1, pp. 103-109, 2012.

S4-P-050101

OBTAINING OF TIN OXIDE BY THE SPARK DISCHARGE METHOD, WITH A CONTROLLED AVERAGE PARTICLE SIZE

A.D.MAKSIMOV [1], I.V.BEKETOV [1,2], S.FARENBRUH [2],

[1]Institute of Electrophysics UB RAS, Yekaterinburg, Russian Federation
[2]Ural Federal University, Yekaterinburg, Russian Federation

Tin oxide was obtained on an experimental setup operating on the principle of the spark discharge method [1,2]. The operating parameters of the method were selected in such a way as to achieve different dispersity of the powders.

The main parameters affecting the dispersion of powders when using the spark discharge method are: the carrier gas flow rate, the energy introduced into the discharge, and the discharge repetition rate. Three electrodes made of tin with a purity of 99.9999% were used as the starting material.

In the work, a study was carried out to determine the most optimal parameters of the method, which provide relatively high productivity, as well as the ability to control the dispersion of the resulting tin oxide powders.

Several series of experiments were carried out to obtain the dependence of the dispersion of the obtained powders on the parameters of the installation. Changes were made to such parameters as: carrier gas flow rate, storage capacity, trigger pulse repetition rate. The range of variation of the carrier gas flow was from 20 to 60 l/min. The repetition rate of the trigger pulses varied based on the storage capacity. For a capacitance of 13.6 nF, the frequency change was from 100 to 400 Hz, at 100 nF from 20 to 60 Hz, respectively. The charging voltage of the capacitor and the size of the gap between the electrodes remained approximately at the same level in all series of experiments, 8-10 kV and 3-4 mm, respectively.

REFERENCES

[1] I.V.Beketov, A.V.Bagazeev, E.I.Azarkevich, A.D.Maksimov, A.I.Medvedev, A.I.Beketova, ” Installation for the production of nanopowders of metals and oxides by the spark discharge method and its testing”, Russian Physics Journal, Tomsk, T61, № 9/2, P166, 2018.

[2] A.D.Maksimov, I.V.Beketov, A.V.Bagazeev, E.I.Azarkevich, A.I.Medvedev, S.O.Cholah, A.M.Murzakaev, “Preparation of metal oxide nanopowders by the spark discharge method”, AIP Conference Proceedings, 2174, 020037, 2019.

S4-P-052101

COMPARISON OF THE DOSE-DEPTH DISTRIBUTION OF ELECTRON BEAMS WITH MONOENERGETIC AND COMPOSITE SPECTRA OF ELECTRON KINETIC ENERGIES*

I.S. EGOROV[1], *M.A. SEREBRENNIKOV*[1], *A.V. POLOSKOV*[1],

[1]*Tomsk Polytechnic University, Tomsk, Russia*

The development of high-voltage high-current pulsed circuitry stimulates the creation of pulsed particle accelerators with operational characteristics appropriate for practical use. At the same time, continuous sources of electron beams are the traditional basis for the radiation technologies development. The paper presents an analysis of the beam depth-energy distribution for a monoenergetic electron beam and for a beam with a composite electrons kinetic energy spectrum [1] in terms of their effective practical use. It was shown that for a number of applications that require beam exposure depth limiting while providing a minimum dose, the use of a beam with composite electrons kinetic energy spectrum is preferable. The research results can be used for electron beam processing modes selection in the radiation technologies development.

REFERENCES

[1] A. Poloskov, M. Serebrennikov, A. Isemberlinova, I. Egorov, Energy depth distribution of pulsed electron beam with wide electron kinetic energy spectrum for an aluminum target, Journal of Physics: Conference Series. 1393 (2019) 012115. doi:10.1088/1742-6596/1393/1/012115.

* The authors are grateful to National Research Tomsk Polytechnic University (TPU, Russia) for technical support in a case of TPU development program. The work was conducted within the framework of the state assignment in the field of scientific activity: No. FSWW-2020-0008.

OPTIMIZATION OF MODES OF THE ELECTRIC DISCHARGE GRINDING OF QUARTZ RAW

S.S. KONDRATIEV[1], A.A. ZHERLITSYN[1], V.M. ALEXEENKO[1], A. I. NEPOMNYASHCHIKH[2], A. P. ZHABOEDOV[2], V.S. ROMANOV[3]

[1]IHCE SB RAS, Tomsk, Russia
[2]Vinogradov Institute of Geochemistry SB RAS, Irkutsk, Russia
[3]ZAO «Kvartsevyye materialy», Irkutsk, Russia

One of the tasks of the technology for obtaining quartz concentrates is the grinding of quartz raw to a fraction of 100–300 μm [1]. Traditionally, mechanical crushing, thermal crushing (thermal softening) and abrasion are used for these purposes. As an alternative, an electric discharge grinding method is considered [1], in which the working tool is a channel of a high-current discharge in water, initiated by a high-voltage pulse. With this method, there are reasonable prerequisites for minimizing contamination and obtaining a relatively narrow fractional distribution of quartz concentrate.

In this work, various modes of operation of electric discharge grinding of quartz raw were studied in order to increase the yield of a fraction of 100–300 μm. The experiments were performed at a pulse repetition rate of 5 Hz on three submicrosecond repetitively pulsed generators with a high-voltage energy storage capacity of 8, 15, and 50 nF and an output voltage of 90 to 280 kV. East Sayan quartzite with an initial size of ~25 mm was used as the initial raw material. Table 1 shows the fractional distribution of the crushing products for modes characterized by an approximately equal total energy input. The maximum fraction yield of 100–250 μm was obtained at the level of 40% for the generator with a storage capacity of 8 nF and a charging voltage of 200 kV (mode 2 in Table 1). The yield of the overgrinding product is less than 21% in this mode. It is shown that the preliminary thermal crushing of the material is not required for effective electric discharge grinding of quartzites (mode 1 and 2 in Table 1).

Table 1. Comparison of different mode of operation of electric discharge grinding of quartz in a series of 1300 pulses.

	$C_{storage}$, nF	U_{charge}, kV	$E_{storage}$, J	I_{max}, kA	$T_{current}/4$, ns	Thermal crushing	Fraction 100–250 μm, %	Overgrinding, %
1	8	160	160	4.2	260	yes	42	25
2	8	200	160	4.2	260	no	40	21
3	15.4	160	197	9.6	370	no	36	28
4	49.9	90	202	26	450	no	7	6

A comparative analysis of the chemical and structural composition of the quartz raw and quartz concentrate with a fraction of 100-300 μm obtained both by usual mechanical abrasion and electric discharge grinding (mode 2 from Table 1) was performed. Microscopic studies on an OLIMPUS BX-51 optical microscope in transmitted light showed that quartz aggregates obtained by mechanical abrasion contain a large amount of fluid inclusions, while no fluid inclusions were found in grains obtained by electric discharge grinding.

REFERENCES

[1] L.Jung, High purity natural quartz. New. Jersey: Quartz Tehnology Inc., 1992.

[2] E. Dal Martello, S. Bernardis, R. B. Larsen, G. Tranell, M. Di Sabatino, L. Arnberg, “Electrical fragmentation as a novel route for the refinement of quartz raw materials for trace mineral impurities,” Powder technology, vol.224, 209-216, 2012.

S4-P-955701

FIELD TRIALS OF A PLANT FOR THE ELECTROPHYSICAL CONVERSION OF LOW-GRADE FOSSIL SOLID FUELS *

A.A. BUKHARKIN[1], *S.M. MARTEMYANOV*[1]

[1] *Federal State Autonomous Educational Institution for Higher Education National Research Tomsk Polytechnic University, Tomsk, Russia*

Electrophysical conversion [1] is a promising way to develop low-grade fossil solid fuels that are unprofitable for traditional mining methods. Wells are drilled directly at the deposit, electrodes are immersed in them. A high voltage is applied to the electrodes, which causes a conductive channel to form in the formation. A low voltage current is passed through this channel, which leads to local heating of the rock. As a result, the thermal conversion of the organic component of the fuel into gaseous and liquid products occurs. Tests of the described method in the field at the Bogatyr mine (Kazakhstan, Ekibastuz) showed its potential profitability and scalability.

The installation necessary for the implementation of such a conversion method should provide a high voltage at the initial stage during the formation of the channel. High voltage of lesser value, but more current for the intermediate stage of increasing the conductivity of the channel. And relatively high low voltage current directly at the conversion stage. The maximum voltage provided by the pilot plant was 100 kV, the maximum current was 400 A.

Two types of tests were carried out. The goal of the first was to carry out a long-term conversion with a stable debit. The interelectrode distance was 1 m. To form the channel, a voltage of up to 3 kV was required. The gas debit amounted to 3 n.cub.m./hour. In addition to this, about 10 liters of resin, similar to viscous oil, collected in the chipper. The purpose of the second type of test was to determine the potentially required voltage for a larger interelectrode distance. The distance between the wells was 6 m, and the voltage required to initiate the channel formation did not exceed 1.5 kV.

Among other things, according to the test results, it was concluded that optimization is necessary to transfer the installation to a pilot industrial scale. Firstly, the reduction of the maximum voltage and, accordingly, the cost and weight and size parameters. Secondly, changing the structure of the intermediate and high-current links to increase the resource of the equipment, reduce the time from channel formation to direct conversion, and increase the converted volume per cycle.

REFERENCES

[1] S. M. Martemyanov, A. A. Bukharkin, B. T. Ermagambet, Zh. M. Kasenova, “Field test of in-situ conversion of coal,” International Journal of Coal Preparation and Utilization, July 2021, DOI: 10.1080/19392699.2021.1957855

S5-O-000208

EFFECT OF IONIZATION WAVE VELOCITY ON VOLTAGE*

THEORY, SIMULATION, EXPERIMENT.

V.A. SHKLYAEV, A.A. GRISHKOV, S.YA. BELOMYTTSEV, D.V. BELOPLOTOV, D.A. SOROKIN

Institute of High Current Electronics SB RAS, Tomsk, Russia

Investigations of pulsed breakdown of a gas-filled gap with a highly inhomogeneous electric field have shown that a runaway electron beam (REB) is formed during the breakdown [1–3]. It was also shown that REB is formed at the initial stages of breakdown (stage of a sharp increase in the voltage pulse). The formation of REB leads to the multielectron breakdown initiation and the appearance of an ionization wave (IW). The velocity of IW movement varies widely depending on various parameters (geometry, amplitude and temporal characteristics of the voltage pulse, type and pressure of the gas) and can reach values comparable to the speed of light, which has been repeatedly shown in numerical simulations [4-7]. The so fast ionization wave rapidly changes the gap geometry such that displacement current comparable with the transmission line charging current arises [6] and the voltage across the gap and the line drops. The faster the ionization wave, the higher the displacement current. The voltage U_d in the transmission line depends on IW velocity v:

$$U_d = \frac{2U_0}{1+\frac{v}{c}}, \tag{1}$$

where U_0 is the voltage in the traveling wave, and c is the speed of light [6].

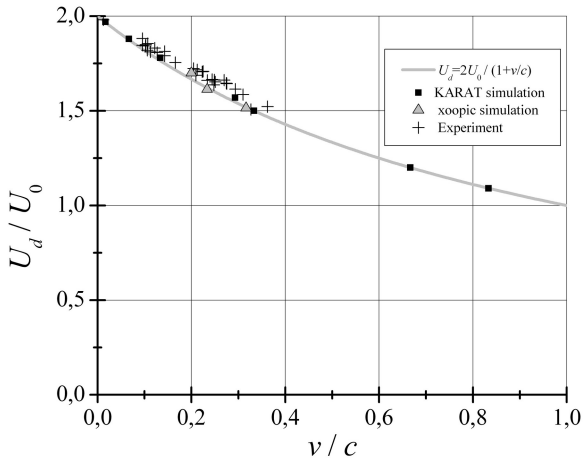

Fig.1. Transmission line voltage vs IW velocity according to theoretical (gray curve), simulation and experimental data (symbols).

Figure 1 demonstrates the behavior of voltage according to expression (1), results of numerical simulation [6] and experiments under different conditions.

REFERENCES

[1] Tarasenko V.F., Baksht E.Kh., Beloplotov D.V., Burachenko A.G., Lomaev M.I., and Sorokin D.A., Laser Part. Beams, vol. **34**, no. 4, pp. 748–763 (2016); doi: 10.1017/S0263034616000719

[2] V. A. Shklyaev, S. Ya. Belomyttsev, and V. V. Ryzhov, J. Appl. Phys., vol. **12**, 113303 (2012); doi: 10.1063/1.4768912

[3] VV Lisenkov, VA Shklyaev, Phys. Plasmas, vol. **22**, no. 11, 113507; doi: 10.1063/1.4935398

[4] Dmitry A. Sorokin, Dmitry V. Beloplotov, Victor F. Tarasenko, and Evgeni Kh. Baksht, Appl. Phys. Lett. **118**, 224101 (2021); doi:10.1063/5.0052686

[5] Naidis G.V, Tarasenko V.F., Babaeva N. Yu., Lomaev M.I., Plasma Sources Sci. Technol., vol. **27**, no.1, 013001 (2018); doi: 10.1088/1361-6595/aaa072

[6] S. Ya. Belomyttsev, A. A. Grishkov, V. A. Shklyaev, and V. V. Ryzhov, **123**, 043309 (2018); doi: 10.1063/1.500208820

[7] Abbas, M.F., Yuan, X.-C., Li, H.-W., Xue, J.-Y., Sun, A.-B. and Zhang, G.-J., High Voltage, Vol. **6**, no. 1, pp. 16-24. (2021); doi: 10.1049/hve2.12020

* The work was carried out within the framework of the state assignment of the Ministry of Science and Higher Education of the Russian Federation on the topics FWRM-2021-0007 and FWRM-2021-0014) as well as was funded by RFBR, project number 20-02-00733.

S5-O-000703

A SOURCE OF COLD ATMOSPHERIC-PRESSURE PLASMA*

D.A. SOROKIN, V.A. PANARIN, V.S. KUZNETSOV, E.A. SOSNIN, D.V. BELOPLOTOV, V.F. TARASENKO

Institute of High Current Electronics SB RAS, 2/3 Akademichesky Ave., Tomsk, 634055 Russia, SDmA-70@loi.hcei.tsc.ru

The problem of creating a source of non-equilibrium low-temperature plasma, formed upon excitation of the ambient air and having a temperature of the order of room one or slightly higher, continues to be extremely urgent. Despite the huge amount of research in this direction, such a plasma source has not been implemented yet. However, such a source is extremely promising from a practical point of view and can be used in various fields [1].

The study deals with the results of studies of the characteristics of a source of cold air plasma based on the relatively recently discovered phenomenon of the gas discharge physics – an apokampic discharge (Fig. 1a) [2]. Its formation is due to streamers propagating at a high speed from the bright branch (3 in Fig. 1a) of the pulse discharge channel (2 in Fig. 1a). It should be noted that this type of discharge can be considered as a laboratory model of the phenomena occurring in the upper atmosphere of our planet and not only, i.e. Transient Luminous Events such as blue jets, starters and red sprites [2].

A source design is proposed in which several apokamps are localized and stabilized at the center due to the gas flowing. Measurements of electronic, vibrational, rotational, and gas temperatures, as well as the reduced electric field strength in plasma in various zones of the discharge formed in this design were carried out by optical emission spectroscopy techniques [3]. It is shown that everywhere plasma is strongly non-equilibrium – there is a strong difference between the electronic temperature (several eV) and the temperature of heavy particles (hundreds to thousands of K, depending on the measurement zone). Thus, a cold air plasma source based on the apokampic discharge has been implemented (Fig. 1c).

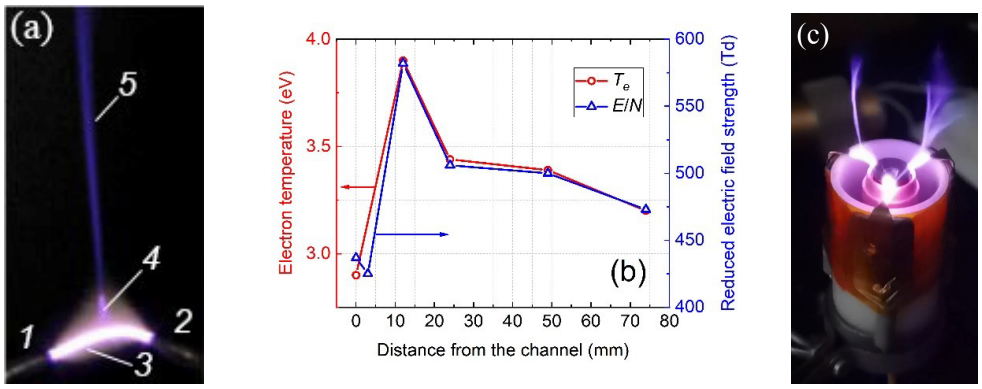

Fig.1. (a) Apokampic discharge. 1, 2 – electrodes; 3 – discharge channel; 4 – bright branch; 5 – plasma plume. (b) Electron temperature and reduced electric field strength at different distances from the main discharge channel (3 in Fig. 1a). (c) Multiapokampic atmospheric-pressure air plasma source.

REFERENCES

[1] I. Adamovich, S.D. Baalrud, A. Bogaerts et al., "The 2017 Plasma Roadmap: Low temperature plasma science and technology," J. Phys. D: Appl. Phys., Vol. 50, Article Number 323001, 2017. (DOI: 10.1088/1361-6463/aa76f5)

[2] E.A. Sosnin, N.Yu. Babaeva, V.Yu. Kozhevnikov et al., "Modeling of transient luminous events in Earth's middle atmosphere with apokamp discharge", Phys. Usp., Vol. 64, P. 191–210, 2021. (DOI: 10.3367/UFNe.2020.03.038735)

[3] H. Nassar, S. Pellerin, K. Musiol et al., "N_2^+/N_2 ratio and temperature measurements based on the first negative N_2^+ and second positive N_2 overlapped molecular emission spectra", J. Phys. D: Appl. Phys., Vol. 37, P. 1904–1916, 2004. (DOI: 10.1088/0022-3727/37/14/005)

* The reported study was performed within the framework of the State assignment of the IHCE SB RAS, project No. FWRM-2021-0014.

S5-O-012802

MAIN MODES OF CORONA DISCHARGE WITH CHANGING IN VOLTAGE POLARITY*

V.F. TARASENKO, E.KH. BAKSHT, N.P. VINOGRADOV, V.S. KUZNETSOV, V.A. PANARIN, V.S. SKAKUN

Institute of High Current Electronics SB RAS, Tomsk, 634055, Russia

Corona discharge is one of the most common self-discharge modes and is widely used in various fields. His research was carried out in many works and continues now [1-5]. This is due, in particular, to the presence of non-stationary regimes during the initiation of a corona discharge with both positive and negative polarity of the voltage on the electrode with a small radius of curvature [4].

This paper presents the results of studies of a corona discharge with a cathode or anode with a radius of curvature of ≈20 μm. The conditions for the initiation of the discharge and the transition from stationary to pulsed regimes are shown. On figure 1 shows photographs of a corona discharge in atmospheric air that illustrate different modes with negative and positive polarity of the needle.

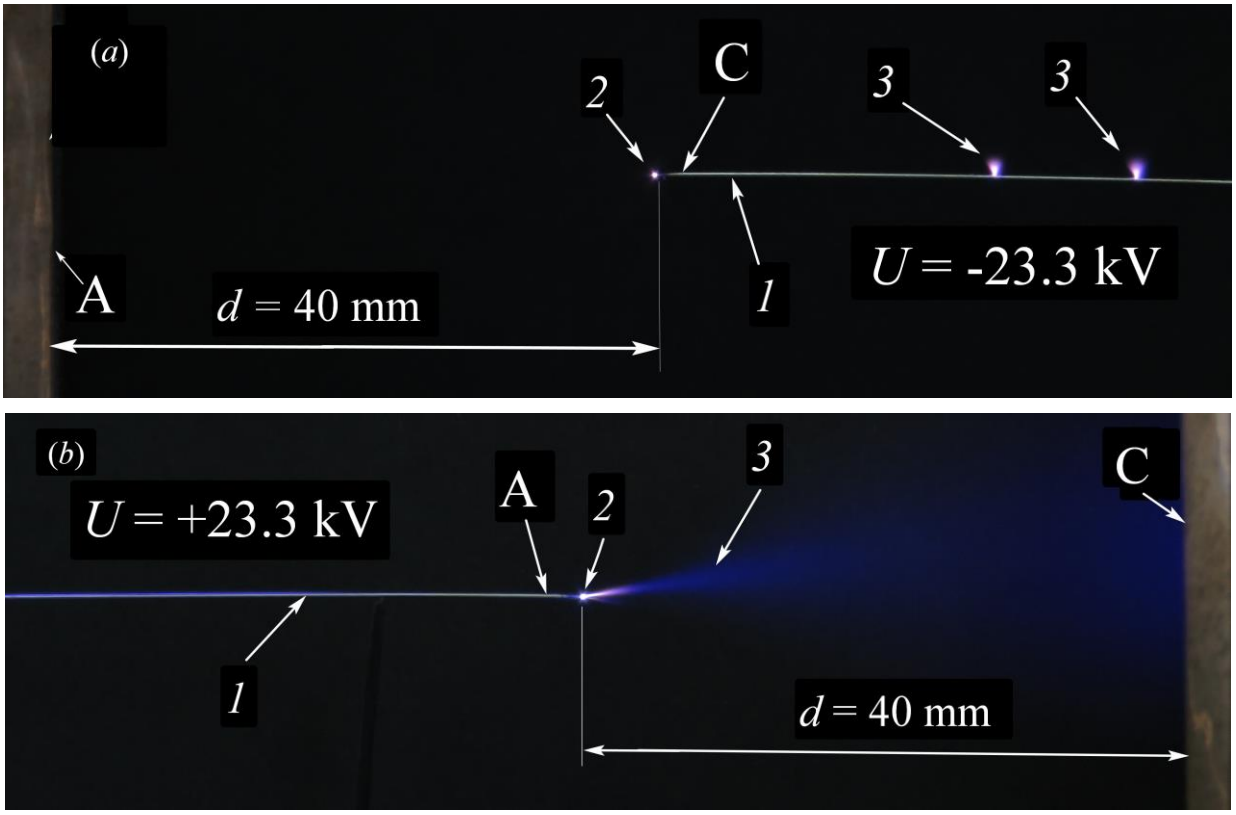

Fig.1. Photographs of the glow of a corona discharge, demonstrating different modes in a gap 40 mm long with negative (*a*) and positive polarity of the tip (*b*). *1* - needle, *2* - area of bright glow at the tip of the needle, *3* - plasma jets.

The minimum size of the luminous region near the tip, which had a spherical shape, in these conditions was ≈0.08 mm, and the length of the cylindrical jet from the positive tip with increasing voltage reached a flat electrode (d = 40 mm).

REFERENCES

[1] L.B. Loeb, Fundamental Processes of Electrical Discharges In Gases, New York, 1950.
[2] Y. S. Akishev, I. V. Kochetov, A. I. Loboiko, A. P. Napartovich, “Numerical simulations of Trichel pulses in a negative corona in air,” Plasma Physics Reports, vol. 28, no. 12, pp. 1049-1059, 2002.
[3] W. Liu, Z. Li, L. Zhao, Q. Zheng, C. Ma, “Study on formation mechanism of atmospheric pressure glow discharge air plasma jet,” Physics of Plasmas, vol. 25, no. 8, p.083505, 2018.
[4] V. F. Tarasenko, V. S. Kuznetsov, V. A. Panarin, V. S. Skakun, E. A. Sosnin, E. Kh. Baksht, “Role of streamers in the formation of a corona discharge in a highly nonuniform electric field,” JETP Letters, vol. 110, no. 1, pp. 85-89, 2019.
[5] M. Černák, T. Hoder, Z. Bonaventura, "Streamer breakdown: cathode spot formation, Trichel pulses and cathode-sheath instabilities," Plasma Sources Science and Technology, vol. 29, no. 1, p. 013001, 2019.

* This research was performed within the project of the Russian Science Foundation on grant # 22-29-00137.

S5-O-012803

PARAMETERS OF RUNAWAY ELECTRON BEAMS GENERATED IN ATMOSPHERIC PRESSURE AIR*

V.F. TARASENKO, D.V. BELOPLOTOV, E.KH. BAKSHT, M.I. LOMAEV, D.A. SOROKIN

Institute of High Current Electronics SB RAS, Tomsk, 634055, Russia

The study of runaway electron beams (RAEBs) generated during subnanosecond breakdown of air and other gases continues to attract great attention. In well-known works, the tasks were set to obtain the maximum amplitudes of the beam current, to determine the duration of REAB current pulses and electron energy, as well as to study the influence of the design of gas diodes, the shape and material of electrodes on the parameters of RAEBs. The parameters of RAEBs were measured in various gases in a wide pressure range. Much attention was paid to modeling the physical processes of the RAEB generation.

The purpose of this work is to systematize the experimental data on the parameters of RAEBs in air at atmospheric pressure obtained at the Institute of High Current Electronics SB RAS [1–5]. In particular, the effect of the anode design on the duration of RAEB current pulses was studied. Figure 1 shows the duration of RAEB current pulses recorded at various diameters of the hole in the anode (figure 1a) and at various cathodes (figure 1b).

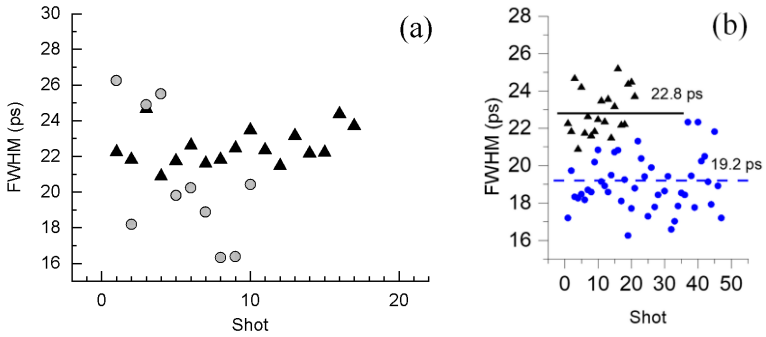

Fig.1. (a) FWHMs of RAEB current pulses recorded with anodes having different hole diameters: 1 (triangles) and 0.1 mm (squares). (b) Variation of FWHM of REAB current pulses from pulse to pulse (triangles - needle cathode, circles - cone cathode). GIN-55-1 generator (rise tine of 0.7ns, voltage pulse amplitude of ≈78 kV in the idle mode). Air pressure of ≈100 kPa.

The shortest RAEB current pulse was observed for a conical cathode (90°) through a 0.1-mm hole in the anode. It was experimentally found that to increase the number of electrons with energies exceeding eU_m, where e is the electron charge and U_m is the maximum voltage across the gap, spherical cathodes should be used. The highest amplitudes of RAEB current pulses were observed in a gas diode with a conical insulator. In addition, the cathode must have an extended edge with a small radius of curvature and must be made of stainless steel.

REFERENCES

[1] V. F. Tarasenko, E. Kh. Baksht, D. V. Beloplotov, A. G. Burachenko, D. A. Sorokin, M. I. Lomaev, “Generation and registration of runaway electron beams during the breakdown of highly overvoltaged gaps filled with dense gases,” Journal of Physics D: Applied Physics, vol. 51, no. 42, p. 424001, 2018.

[2] D. A. Sorokin, V. F. Tarasenko, C. Zhang, I. D. Kostyrya, J. Qiu, P. Yan, E. Kh. Baksht, T. Shao, “X-ray radiation and runaway electron beams generated during discharges in atmospheric-pressure air at rise times of voltage pulse of 500 and 50 ns,” Laser and Particle Beams, vol. 36, no. 2, pp. 186-194, 2018.

[3] D. V. Beloplotov, V. F. Tarasenko, V. A. Shklyaev, D. A. Sorokin, “Generation of runaway electrons in plasma after a breakdown of a gap with a sharply non-uniform electric field strength distribution,” Journal of Physics D: Applied Physics, vol. 54, no. 30, p. 304001, 2021.

[4] D. A. Sorokin, D. V. Beloplotov, V. F. Tarasenko, E. Kh. Baksht, “Main modes of runaway electron generation during a breakdown of high-pressure gases in an inhomogeneous electric field,” Applied Physics Letters, vol. 118, no. 22, p. 224101, 2021.

[5] D. V. Beloplotov, V. F. Tarasenko, D. A. Sorokin, V. A. Shklyaev, “Generation of Two Pulses of Runaway Electron Beam Current,” Technical Physics, vol. 66, no. 4, pp. 571-582, 2021.

* This research was supported by the Ministry of Science and Higher Education of the Russian Federation (agreement no. 075-15-2021-1026 of November 15, 2021).

S5-O-014002

SIMULATION IN LABORATORY EXPERIMENTS THE COLOR OF RED SPRITES*

N.P. VINOGRADOV, V.F. TARASENKO, E.KH. BAKSHT

Institute of High Current Electronics SB RAS, Tomsk, 634055, Russia

Currently, much attention is paid to the study of transient luminous events (TLEs) [1–3]. Many photographs are given in articles and on the Internet, see for example [4-6]. A large number of works are devoted to research on the properties of red sprites, blue jets and analogs of blue jets (starters, giant jets) and elves. In particular, experimental studies of laboratory discharges are being carried out, which in their properties correspond to the most common TLEs [7-9].

This work presents the results of studies of pulsed discharges in atmospheric air at pressures that correspond to those recorded at altitudes for the appearance of red sprites.

The figure 1 shows photographs of the design of electrodes and of light from different discharge modes with different pressures of air.

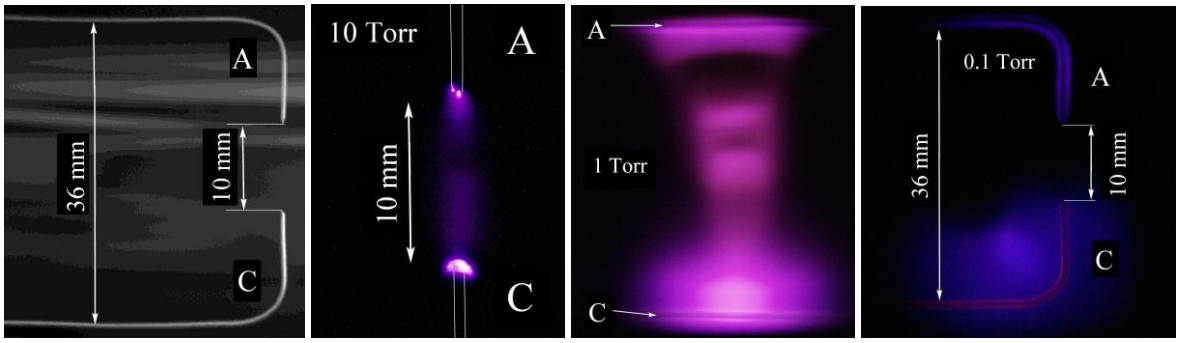

Fig.1. Photographs of the design of electrodes and light of the diffuse discharges in air with different pressures.

It has been established that the pressure range at which the emission of red sprites is recorded is much wider than with a glow discharge in laboratory experiments. For example, red sprites are observed at altitudes from 40 to 100 km, which roughly corresponds to air pressures from 10 to 0.001 Torr. Whereas the color of a pulsed discharge in air with pulse durations of a few to tens of microseconds had a pronounced red color only at a pressure of about 1 Torr.

The report will present data on the properties and color of various modes of pulsed discharges correspond to the most common TLEs. In particular, oscilloscope traces of voltage pulses and discharge currents, radiation spectra, and the dynamics of air breakdown development at pressures from 0.1 to 30 Torr will be presented.

REFERENCES

[1] D.D. Sentman, E.M. Wescott, “Red sprites and blue jets: Thunderstorm-excited optical emissions in the stratosphere, mesosphere, and ionosphere,” Physics of Plasmas, vol. 2, no. 6, pp. 2514-2522, 1995.

[2] V.P. Pasko, U.S. Inan, T.F. Bell, Y.N. Taranenko, “Sprites produced by quasi-electrostatic heating and ionization in the lower ionosphere,” J. Geophys. Res., vol. 102, pp. 4529–4561, 1997.

[3] Y.P. Raizer, G.M. Milikh, M.N. Shneider, “Streamer and leader-like processes in the upper atmosphere: Models of red sprites and blue jets,” J. Geophys. Res., vol. 115, p. A00E42, 2010.

[4] O. Chanrion, T. Neubert, A. Mogensen, Y. Yair, M. Stendel, R. Singh, D. Siingh, “Profuse activity of blue electrical discharges at the tops of thunderstorms,” Geophys. Res. Lett., vol. 44, pp. 496–503, 2017.

[5] A. Huang, G. Lu, J. Yue, W. Lyons, F. Lucena, F. Lyu, S.A. Cummer, W. Zhang, L. Xu, X. Xue, S. Xu, “Observations of red sprites above hurricane matthew,” Geophys. Res. Lett., vol. 45, pp. 13-158, 2018.

[6] Flickr.com. Available online: https://www.flickr.com/photos/frankie57pr/49610428072/ (accessed on 10 February 2022).

[7] F.J., Gordillo-Vázquez, A. Luque, M. Simek, “Spectrum of sprite halos,” J. Geophys. Res., vol. 116, p. A093919, 2011.

[8] V.F. Tarasenko, E.A. Sosnin, V.S. Skakun, V.A. Panarin, M.V. Trigub, G.S. Evtushenko, “Dynamics of apokamp-type atmospheric pressure plasma jets initiated in air by a repetitive pulsed discharge,” Physics of Plasmas, vol. 24, no. 4, p. 043514, 2017.

[9] E.A. Sosnin, N.Y. Babaeva, V. Y. Kozhevnikov, A. V. Kozyrev, G. V. Naidis, V. A. Panarin, V. S. Skakun, and V. F. Tarasenko, “Modeling of transient luminous events in Earth’s middle atmosphere with apokamp discharge,” Phys.-Uspekhi, vol. 64, no. 2, pp. 191–210, 2021.

* This research was supported by the Ministry of Science and Higher Education of the Russian Federation (agreement no. 075-15-2021-1026 of November 15, 2021).

S5-O-018402

FEATURES OF RECORDING DISCHARGE CURRENT PULSES AT ELECTRON BEAM GENERATION IN A HIGH-VOLTAGE NANOSECOND DISCHARGE IN VACUUM AND GAS DIODES*

M.I. LOMAEV[1,2]

[1]*Institute of High Current Electronics SB RAS, Tomsk, Russia*
[2]*National Research Tomsk State University, Tomsk, Russia*

From a practical point of view, the effect of cumulation (self-focusing) of an electron beam attracts, first of all, by the possibility of increasing the beam current density and, accordingly, increasing the power density in the cumulation zone. This can be used to generate highly ionized plasma and powerful X-rays, in the study of matter at elevated pressure and thermonuclear research [1], in the fields of radiation chemistry and solid state physics [2], to generate powerful radiation in the terahertz frequency range [3], luminescence excitation of artificial and synthetic crystals [4, 5] and in other applications. It was found that at currents of tens to hundreds of kA, the beam is focused by its own magnetic field [6]. At the same time, at currents not exceeding ~ 2 kA, beam focusing is treated differently. Thus, in the case of a vacuum diode with an annular graphite cathode, according to the developed model and experimental data, the relativistic electron beam is compressed due to the electrostatic repulsion of electrons emitted from the inner surface of the cathode [3]. The formation of a conductive plasma jet in a vacuum-pulsed discharge, consisting of several filaments with a diameter of ~ 50 μm and a current of ~ 1 kA in each of them, was reported in [7].

The purpose of this work was to study the effect of electron charge compensation on the self-focusing of an electron beam generated by a high-voltage nanosecond discharge in a nonuniform electric field in vacuum and gas diodes and to reveal the features of recording the discharge current under these conditions.

The results of the study indicate that, in addition to the effect of beam self-focusing, which realizes in the gas and vacuum diodes from the beginning of the beam current pulse, an additional self-focusing mechanism is activated in the gas diode several nanoseconds after the beginning of the pulse. The most probable reason for the additional self-focusing of the electron beam in a gas diode is the effect of compensation of the electron charge by the charge of positive ions arising as a result of gas ionization by beam electrons. The experimental data obtained and the result of the estimation of the characteristic time required to activate the charge compensation effect at a pressure of 0.2 Torr are close to each other.

It was found that the shape of the current pulse recorded by the current shunt under the conditions of electron beam generation during high-voltage nanosecond discharge in vacuum and gas diodes is determined by the influence of the reactive component of the voltage drop across the current shunt resistance.

REFERENCES

[1] A.C. Kolb, "Uses of intense electron beams, " IEEE Trans. Nucl. Sci. vol. 22. Issue 3. P. 956–961. 1967.

[2] High-energy Solid State Electronics. Ed. D.I. Weisburd, Novosibirsk, Nauka, 1982.

[3] S.V. Anishchenko, V.G. Baryshevsky, A.A. Gurinovich, "Electrostatic cumulation of high-current electron beams for terahertz sources", Physical review accelerators and beams. vol. 22. P. 043403. 2019.

[4] V.I. Solomonov, S.G. Mikhailov, Pulsed cathodoluminescence and its application to the analysis of condensed media, Ekaterinburg, Ural Branch of the Russian Academy of Sciences, 2003.

[5] D.A. Sorokin, A.G. Burachenko, D.V. Beloplotov, V.F. Tarasenko, E.Kh. Baksht, E.I. Lipatov, M.I. Lomaev, "Luminescence of crystals excited by a runaway electron beam and by excilamp radiation with a peak wavelength of 222nm," J. Appl. Phys. vol. 122. P. 154902. 2017.

[6] E.E. Tarumov, Obtaining and focusing of high-current relativistic electron beams in diodes. P.122 - 181. / In the book: Generation and focusing of high-current relativistic electron beams. Ed. L.I. Rudakov, Moscow, Energoatomizdat, 1990.

[7] V.I. Baryshnikov, V.L. Paperny, "On the electron temperature in the cathode plasma of a pulse vacuum discharge," J. Phys. D: Appl. Phys. vol. 28. P. 2519-2521. 12995.

*This research was supported by the Ministry of Science and Higher Education of the Russian Federation within Agreement no. 075-15-2021-1026 of November 15, 2021.

S5-O-018901

PULSE PLASMA-BEAM DISCHARGES WITH EXTENDED SLOT CATHODE AND THEIR TECHNOLOGICAL APPLICATIONS*

N.A. ASHURBEKOV[1], *M.Z. ZAKARYAEVA*[1,2], *K.O. IMINOV*[1], *K.M. RABADANOV*[1], *G.SH. SHAKHSINOV*[1]

[1]*Dagestan State University, Makhachkala, Russian Federation*
[2]*Institute of Physics, Dagestan Federal Research Center, Russian Academy of Sciences, Makhachkala, Russian Federation*

The results of studies of the kinetic processes of development of nanosecond discharges with an extended slot cathode in inert gases (He, Ne, and Ar) are presented. The block representation of the experimental setups is given in [1-4]. It is shown that, depending on the values of the parameters of the reduced electric field *E/N* and electron density, there are three different forms of functioning of a nanosecond discharge (a stratified discharge, a homogeneous volume discharge with a beam of electrons, and a high-current dense discharge with areas of cumulation of the electric field and charged particles). The main parameters of striations and boundaries of their formation in discharges with inert gases are determined. It is shown that in the presence of growing values of applied voltage in the gap, there appear high-energy electrons that destroy the spatial periodic structure of the discharge. The formation conditions, general regularities, and energy characteristics of high-energy electrons in transverse nanosecond discharges are established. It is shown that an unlimited discharge with a cathode with a rectangular cavity, where the beam current on the anode surface reaches up to 20% of the discharge current value, is optimal for generating electron beams.

It has been found that at high values of the applied external field, an area of uncompensated positive charge is formed along the center of the cavity in the cathode and at the exit from the cathode cavity, which leads to a change in the spatial structure of the discharge and the dynamics of ionization processes.

For the configuration of the discharge with an extended hollow cathode under consideration, the results of numerical simulation of the structure of ionization fronts during nanosecond gas breakdown are presented. The results of calculating the relaxation of the electron distribution function both inside the cathode cavity and between the electrodes are given. The possibility of using the two-term approximation in the calculation of the electron distribution function is analyzed.

The possibilities of using this type of discharge to create plasma reactors for precision plasma technologies for atomic layer etching of micro- and nanoelectronics materials are considered.

REFERENCES

[1] N.A. Ashurbekov, K.O. Iminov, O.V. Kobzev, V.S. Kobzeva, “Generation of high-energy electrons in a transverse slot-cathode nanosecond discharge at working gas medium pressures”, Tech. Phys., vol. 55, no. 8, pp. 1138–1144, 2010.

[2] N.A. Ashurbekov and K.O. Iminov, Generation of high-energy electrons in the nanosecond gas discharges with a hollow cathode Generation of Runaway Electron Beams and X-Rays in High Pressure Gases vol 1, ed V F Tarasenko. New York: Nova Publishers, 2016.

[3] N.A. Ashurbekov, K.O. Iminov, O.A. Popov, G.Sh. Shakhsinov, ”Current self-limitation in a transverse nanosecond discharge with a slotted cathode”, Plasma Sci. Technol., vol. 19, no. 3, p. 035401, 2017.

[4] N.A. Ashurbekov, K.O. Iminov, G.Sh. Shakhsinov, M.Z. Zakaryaeva, K.M. Rabadanov, “The dynamics of a nanosecond gas discharge development with an extended slot cathode in argon”, Plasma Sci. Technol., vol. 22, no. 12, p. 125403, 2020.

* This work was partially supported by a grant from the Russian Foundation for Basic Research No. 19-32-90179 and the project of the Ministry of Education and Science of Russia FZNZ-2020-0002.

S5-O-018902

THE INFLUENCE OF THE TYPE OF THE ELECTRON DISTRIBUTION FUNCTION ON THE PROPERTIES OF A NANOSECOND DISCHARGE IN EXTENDED SHIELDED TUBES WITH CYLINDRICAL HOLLOW ELECTRODES *

N.A. ASHURBEKOV[1], *K.O. IMINOV*[1], *G.SH. SHAKHSINOV*[1], *M.B. KURBANGADZHIEVA*[1,2], *K.M. RABADANOV*[1]

[1]*Dagestan State University, Makhachkala, Russian Federation*
[2]*Institute of Physics, Dagestan Federal Research Center, Russian Academy of Sciences, Makhachkala, Russian Federation*

The paper presents the results of experimental research on the properties of plasma of a nanosecond discharge in neon in an extended shielded discharge tube with cylindrical hollow electrodes.

The block representation of the experimental setup used in this work is given in [1, 2]. To generate a nanosecond gas discharge, a voltage pulse generator was used. It generated high-voltage pulses with adjustable amplitude up to 40 kV, with a voltage pulse rise time of 50–80 ns and a pulse repetition rate of up to 100 Hz [3].

The results of experimental studies of the dynamics of the formation of optical radiation from the discharge, the dynamics of the population of metastable states of neon atoms, the structures of ionization wave fronts, their propagation velocities, and the damping coefficients of ionization waves in the neon pressure range of 1-60 Torr are presented. Experimental studies of the structure of longitudinal and transverse plasma inhomogeneities in a discharge tube as a function of amplitudes of voltage pulses and gas pressure have been carried out.

Numerical modeling of the kinetics of ionization processes for the type of discharge under consideration has been performed. The results of numerical simulations of the plasma of a nanosecond discharge in neon are presented, taking into account the electron distribution function from the solution of the Boltzmann kinetic equation in the two-term approximation. To analyze the influence of the form of the electron distribution function on the dynamics of the formation of the spatial distribution of plasma parameters in the discharge configuration under study, numerical simulation was performed taking into account the processes of direct and stepwise ionization from $2p^6$, $2p^5 3s$, and $2p^5 3p$ electronic configurations of the neon atom. To solve this problem, a two-dimensional axisymmetric model whose geometry corresponded to the experimental setup was used. The kinetic and transport properties of the plasma were determined using the electron distribution function calculated from the solution of the Boltzmann kinetic equation in the classical two-term approximation.

The results of the experimental research and numerical simulation are compared.

REFERENCES

[1] N.A. Ashurbekov, K.O. Iminov, G.Sh. Shakhsinov, M.B. Kurbangadzhieva, K.M. Rabadanov, “Formation of asymmetric optical transmission spectra of a nanosecond discharge in extended shielded tubes upon resonant interaction of short laser pulses with excited neon atoms”, Proceedings of SPIE - XV International Conference on Pulsed Lasers and Laser Applications, vol. 12086, p. 1208617, December 2021.

[2] N.A. Ashurbekov, K.O. Iminov, M.B. Kurbangadzhieva, G.Sh. Shakhsinov, “Quantum-optical effects of resonant short laser pulse interaction with neon nanosecond discharge plasma in narrow shielded tubes”, Proceedings of SPIE - XIV International Conference on Pulsed Lasers and Laser Applications, vol. 11322, p. 113220H, December 2019.

[3] N.A. Ashurbekov, K.O. Iminov, G.S. Shakhsinov, A.R. Ramazanov, “The role of high-energy electrons during the formation of nonstationary optical emission and transmission spectra of plasma behind the edge of high-velocity ionization waves”, High Temperature, vol. 53, no. 5, pp. 627-37, 2015

* This work was partially supported by a grant from the Russian Foundation for Basic Research No. 20-32-90150 and the project of the Ministry of Education and Science of Russia FZNZ-2020-0002.

S5-O-019101

THE HISTORY AND STATE OF THE ART IN THE RESEARCH OF THE DC NEGATIVE CORONA

YU.S. AKISHEV

[1]SRC RF TRINITI, 108840, Moscow, Troitsk, Pushkovykh Str., 12, Russia
[2]NRNU MEPhI, 115409, Moscow, Kashirskoe shosse, 31, Russia

The subject of our talk is the unipolar negative corona in the air at atmospheric pressure. DC corona happens between the high voltage (HV) cathode of small size and the grounded anode of large size (see Fig.1).

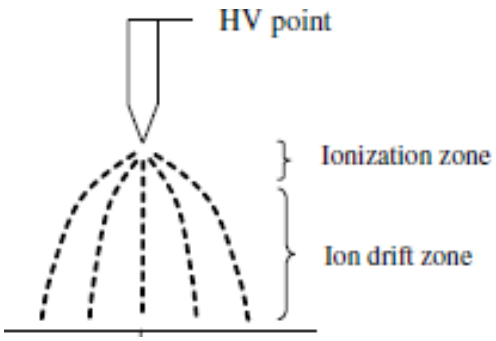

Fig.1. Sketch of corona structure.

Fig. 2. St. Elmo's fire.

Leonard Benedict Loeb (1891–1978)

The corona irradiance around sharp or pointed objects was known long before serious scientific research of this phenomenon. One of the well-known examples of the ancient observations of the corona is so-called St. Elmo's fire which appeared on ships at sea during thunderstorms (see Fig.2). A great contribution to systematic study and development of the physics of corona discharges was done by L. Loeb and his colleagues (see photo). They showed that the shape and size of corona glow depends on the cathode tip size (see Fig.3).

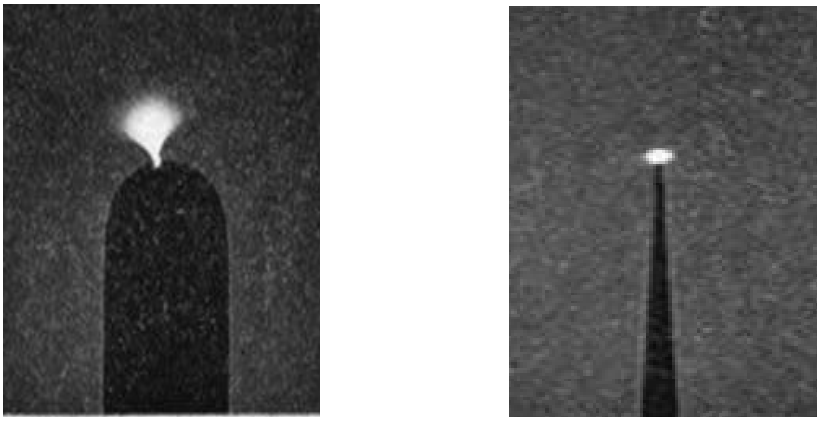

Fig.3. Typical images of corona glow on the cathodes of different diameters.
L. B. Loeb, Electrical Coronas, Univ. of California Press, Berkley, USA (1965)

The goal of this talk is to give a short review of the achievements and open questions in modern physics of a negative corona. Among the questions under review are the corona volt-ampere characteristics, the cathode processes, the ionic wind, the Trichel pulses, the transition of corona regime with a negative space charge into the glow discharge regime with a quasi-neutral plasma in the air gap at atmospheric pressure. Some review of practical applications of a negative corona will be given as well.

S5-O-020101

MODE TRANSITION OF NANOSECOND PULSED DISCHARGES FROM DIFFUSE TO MULTI-STREAMERS AND THE GUIDING EFFECT OF RUNAWAY ELECTRONS*

B. D. HUANG[1], *C. ZHANG*[1,2], *T. SHAO*[1,2]

[1] *Beijing International S&T Cooperation Base for Plasma Science and Energy Conversion, Institute of Electrical Engineering, Chinese Academy of Sciences, Beijing, China*
[2] *University of Chinese Academy of Sciences, Beijing, China*

Runaway electrons (RAEs) have been widely observed in nanosecond pulsed discharges (NPDs) and it is believed that RAEs have a big impact on the breakdown and propagation of NPDs and the formation of diffuse discharge at atmospheric pressure [1, 2]. Nevertheless, it is still desirable to explore how RAEs function on the pattern and mode of NPDs.

In this work, the role of RAEs on the mode transition of NPDs from diffuse to multi-streamers is investigated. NPD is driven by high-voltage (HV) pulses with a rise time of about 3 ns between blade-to-plate electrodes with a gap of ~ 1 cm, where the blade is the cathode with a width of ~ 4 cm. A beam collector with a rise time of about 50 ps and covered by a titanium foil with a thickness of 1 μm as electron energy filter (higher than 10 keV) is used to detect RAEs. By increasing the HV amplitude, the distribution of RAEs' amplitude also shifts to higher value, i.e., more RAE pulses with a larger amplitude are observed.

With intensified charge coupled device (ICCD) camera, single-shot discharge images are observed. It is observed that with a large HV amplitude (~ 30 kV), the NPD is initially in a diffuse mode near the blade (cathode). Later on, it branches and transfers into multi-streamers, which propagate synchronously toward the plate (anode). However, with a small HV amplitude (~ 10 kV), the NPD forms a short diffuse channel near the blade and cannot penetrate the gap.

Using particle-in-cell Monte-Carlo collision (PIC-MCC) simulation, a similar mode transition of diffuse to multi-streamers can be obtained with RAEs emitted from the cathode, as observed in discharge images. This mode transition cannot be reproduced without RAEs, i.e., the NPD rapidly turns into filamentary mode without RAEs in the PIC-MCC simulation. Furthermore, it is proved that the flux of RAEs controls the pre-ionization degree before the discharge is initiated and dictates the branching and non-uniformity degree of discharge during its propagation. With the distance from the cathode increasing, RAEs are depleted and the non-uniformity of the NPD develops. Assisted with the PIC-MCC simulation, it is proposed that an enhanced RAE emission would produce a large volume diffuse discharge at atmospheric pressure.

REFERENCES

[1] V. F. Tarasenko, "Runaway electrons in diffuse gas discharges," Plasma Sources Sci. Technol., vol. 29, no. 03, pp. 034001, 2020.

[2] B. D. Huang, C. Zhang, J. T. Qiu, X. Zhang, Y. J. Ding, T. Shao, "The dynamics of discharge propagation and x-ray generation in nanosecond pulsed fast ionisation wave in 5 mbar nitrogen," Plasma Sources Sci. Technol., vol. 28, no. 09, pp. 095001, 2019.

* This work was supported by the National Science Fund for Distinguished Young Scholars (Grant No. 51925703) and the National Natural Science Foundation of China (Grant No. 51907190).

S5-O-020201

FABRICATION AND CHARACTERISTICS OF GRADED-PERMITTIVITY TITANIA COATINGS*

F. KONG[1], *C. ZHANG*[1,2], *C. REN*[1], *T. SHAO*[1,2]

[1] *Beijing International S&T Cooperation Base for Plasma Science and Energy Conversion, Institute of Electrical Engineering, Chinese Academy of Sciences, Beijing, China*
[2] *University of Chinese Academy of Sciences, Beijing, China*

Nowadays, with the increase of the voltage level and capacity of electrical equipment (e.g., in power transmission grids or pulsed power devices, etc.), the electrical insulation often fails when high electric fields are generated [1]. Functionally graded materials (FGMs) exhibit unique properties and have application potential at extreme conditions [2-3]. Here, in order to improve the electrical insulation of conventional materials, a simple fabrication method of FGM with two-phase-interfaced, graded-permittivity titania (TiO_2) by an atmospheric pressure plasma deposition.

As shown in Fig.1, FGM structure is composed of rutile (ε_r=110) and anatase (ε_r=48) layers of TiO_2, as well as the original ceramic layer (ε_r=9). Meanwhile, the optimized deposition conditions of anatase and rutile layers of TiO_2 are determined, respectively. Compared with the original samples, the maximum electric field along the surface of FGM decreased by 66%, and the surface flashover voltage of FGM in vacuum is increased by 36%. Also, the insulating performances of FGM have long-term stability. The increase of surface flashover voltage results from the electric field relaxation effect caused by the gradient distribution of permittivity in the designed FGM [4]. Next, with further optimizing the FGM structure, it is expected to further improve the surface-insulating performance of FGM at industry-relevant scales, thereby nearing the real-world industrial applications of the novel interface-engineered materials in diverse fields. To this end, a movable jet array and continuous processing will need to be developed further to scale up the plasma processing and improve the processing efficiency.

REFERENCES

[1] H. C. Miller, “Flashover of insulators in vacuum: the last twenty years,” IEEE Trans. Dielectr. Electr. Insul. 22, 3641−3657, 2015.

[2] M. Naebe, K. Shirvanimoghaddam, “Functionally Graded Materials: a Review of Fabrication and Properties,” Appl. Mater. Today, 5, 223−245, 2016.

[3] N. Hayakawa, Y. Miyaji, H. Kojima, K. Kato, “Simulation on discharge inception voltage improvement of GIS spacer with permittivity graded materials (ε-FGM) using flexible mixture casting method,” IEEE Trans. Dielectr. Electr. Insul. 25, 1318−1323, 2018.

[4] F. Kong, M. Zhao, C. Zhang, C. Ren, K. Ostrikov, T. Shao, “Two-phase-interfaced, graded-permittivity titania electrical insulation by atmospheric-pressure plasmas,” ACS Applied Materials & Interfaces, 14, 1900-1909, 2022.

* The work was supported by the National Natural Science Foundation of China under contracts 51925703, 52177163, 52022096 and 52037004.

S5-O-020801

POWERFUL SOURCES OF VUV RADIATION BASED ON RUN-AWAY ELECTRON PREIONIZED DIFFUSE DISCHARGE*

V. KOZHEVNIKOV, A. N. PANCHENKO, V.F. TARASENKO

Institute of High Current Electronics SB RAS, Tomsk, Russia

The paper deals with the development of powerful sources of VUV emission on the base of diffuse discharge formed in non-uniform electric field by run-away electrons. The VUV radiation spectra of diffuse discharges in various high-pressure gas mixtures have been studied and the VUV radiation power has been measured, as well. Parameters of diffuse discharges in mixtures of rare gases with F_2 and in pure rare gases, CO, H_2 were investigated.

The discharge gap was consisted of two needles set at a distance of 4 mm or blade electrodes 30 cm length with a gap of 18 mm. To form the diffuse discharge, a GIN-55-01 generator was used, which forms a train of pulses with an amplitude in the incident wave up to 38 kV and a FWHM duration of $\tau_{0.5} \approx 0.7$ ns with a rise time of $\tau_{0.1–0.9} \approx 0.7$ ns or a RADAN-220 formed pulses wit an amplitude up to 250 kV with pulse duration of 2 ns (FWHM) at a matched load. Emission spectra in the range 120–540 nm were recorded with a VM-502 vacuum monochromator (Acton Researcher Corp.), while the radiation power was measured with a vacuum photodiode with copper cathode. The experimental equipment and measurement procedure is described in [1, 2].

It is shown that upon excitation of pure rare gases by a series of successive voltage pulses with a duration of 0.7 ns, arriving at an interval of 30 ns, the intensity of the second continuum radiation decreases to the second and subsequent voltage pulses, and increases in the afterglow. It is confirmed that in a pulsed diffuse discharge, the second continuum of rare gas dimers makes the largest contribution to the radiation energy of the diffuse discharge between two needles.

Sufficient homogeneity of diffuse discharges was found to makes it possible to use it as a source of excitation of lasers based on various gas mixtures at an elevated pressure. This is evidenced by the continuation of the VUV laser pulses during several current oscillations in the gap.

It was found that quite uniform diffuse discharge can be formed between long blade electrodes using a RADAN-220 generator. As a result powerful stimulated emission in the VUV range was obtained on ArF* (193 nm), F^*_2 (157 nm) and H_2 (≈160 nm) molecules. The total duration of the laser pulses at 157 and 193 nm is as long as 30 ns, while that at 160 nm did not exceed 5 ns. The radiation energy on F^*_2 molecules increased linearly with He-F_2 gas mixture pressure. The maximum radiation energy on F^*_2 molecules at He pressure of 8.5 atm is as high as 3 mJ. In this case, a further increase in the generation energy is possible. The electrical efficiency of the F^*_2 laser reached 0.15%, which corresponds to the parameters of F^*_2 lasers obtained upon excitation by a transverse discharge with UV preionization [3].

Stimolated emission was obtained in pure H_2 and He-H_2 mixture at pressures up to several atm. Maximal radiation energy on H_2 molecules was about 0.15mJ, which is second only to the results obtained in [4].

REFERENCES

[1] A.N. Panchenko, D.A. Sorokin, and V.F. Tarasenko "Gas lasers pumped by runaway electrons preionized diffuse discharge," Progress in Quantum Electronics, vol.76, Article number 100314, 2021.

[2] A.N. Panchenko, D.V. Beloplotov, V.V. Kozevnikov et.al., "Wide radiation bands of sub-nanosecond discharge plasma in xenon and inaccuracies in their measurements," IEEE Transact. Plasma Sci., vol. 49, p.1614–1620, 2021.

[3] V.V. Atezhev, S.K. Vartapetov, A.N. Zhukov, et.al., "Efficient excitation conditions for an electric-discharge F_2 laser, " *Quantum Electron*., vol.33, p.677–683, 2003.

[4] I. Knyazev; V. Letokhov; V. Movshev, "Efficient and practical hydrogen vacuum ultraviolet laser, " IEEE J. Quant. Electron., vol.11, no.10, p.805 – 817, 1975.

* This research was supported by the Ministry of Science and Higher Education of the Russian Federation (agreement no. 075-15-2021-1026 of November 15, 2021)..

S5-O-022602

GENERATION OF X-RAY QUANTS IN PULSED DISCHARGES OF ULTRA-HIGH PRESSURE*

YU.I. MAMONTOV[1], V.V. LISENKOV[1,2], I.V. UIMANOV[1]

[1]Institute of Electrophysics UB RAS, Yekaterinburg, Russia
[2]Ural Federal University, Yekaterinburg, Russia

Runaway electrons (RE) are known to be usually generated in a discharge gap at the breakdown stage of a discharge and provide pre-ionization of a gas medium. The volume pre-ionization leads to a decrease in the commutation time of a high-pressure diode [1] and the formation of a discharge in a volume form before the development of a spark channel [2,3]. In particular, in [4], a formation of a subnanosecond volume discharge was registered experimentally in nitrogen at a pressure of 6 atm. Wherein, the experimental conditions [1] were believed to be not sufficient for the development of the volume discharge stage observed. A simulation performed in [4,5] by means of the Monte-Carlo numerical model proved the possibility of the RE generation in the vicinity of cathode microprotrusions and the volume discharge initiation under the conditions described in [4,5]. Nevertheless, the simulation also showed that most of electrons initially accelerated near the cathode microprotrusions up to the energies of ~2-5 keV may impact a series of "catastrophic" collisions with scattering angles more than $\pi / 2$. These "catastrophic" collisions not only lead to thermalization of REs, but also have to provide generation of X-ray bremsstrahlung quants which may contribute significantly to the volume pre-ionization, as REs do. Moreover, for gas discharges of an ultra-high pressure (~10 atm and more), the X-ray pre-ionization might prevail over the electron impact ionization provided by REs because of a high collision frequency and a low runaway probability. Within the present paper, the Monte-Carlo approach was employed to calculate radiation energy losses of REs. Frequency of "catastrophic" collisions was determined. Limits of scattering angles and impact parameters within which the X-ray quant generation is possible were estimated. A bremsstrahlung quant spectrum was calculated.

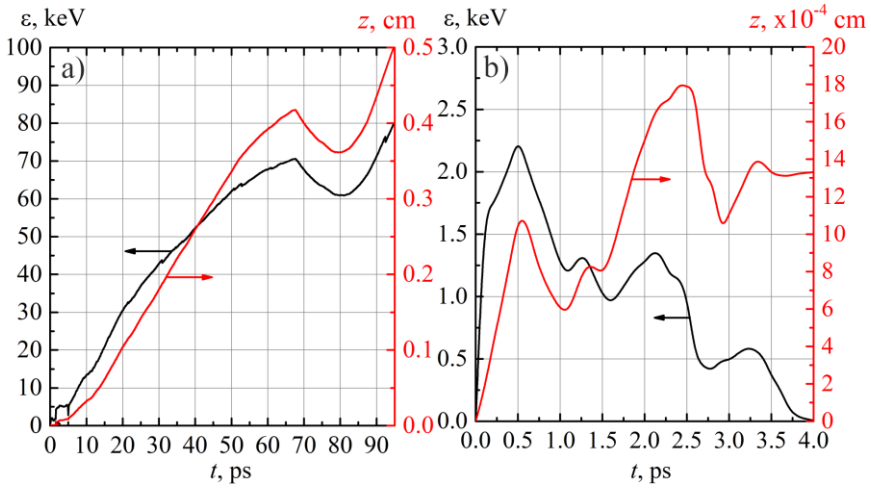

Fig.1. Two types electron motion through a discharge gap: a) – continuous accelerating, b) – deceleration and thermalization. Sharp changes in the electron motion direction along the z-axis correspond to "catastrophic" collisions. The discharge system considered is the same as in [4,5]: nitrogen at a pressure of 6 atm, the cathode-anode distance is 0.5 cm, average electric field strength is ~200 kV/cm.

REFERENCES

[1] G.A. Mesyats and M.I. Yalandin, "On the nature of picosecond runaway electron beams in air," IEEE Trans. on Plasma Sci., vol. 37, no. 6, pp. 785–789, May 2009.

[2] G.A. Mesyats and M.I. Yalandin, "Nanosecond volume discharge in air initiated by a picosecond runaway electron beam," Phys. Usp., vol. 62, pp. 699–703, July 2019.

[3] N.Yu. Babaeva, Ch. Zhang, J. Qiu, X. Hou, V.F. Tarasenko, and T. Shao, "The role of fast electrons in diffuse discharge formation: Monte Carlo simulation," Plasma Sources Sci. Technol., vol. 26, no. 8, 085008, August 2017.

[4] S.N. Ivanov, V.V. Lisenkov, and Y.I. Mamontov, "Streak investigations of the dynamics of subnanosecond discharge developing in nitrogen at a pressure of 6 atm with the participation of runaway electrons," Plasma Sources Sci. Technol., vol. 30, no. 7, 075021, July 2021.

[5] Y.I. Mamontov and V.V. Lisenkov, "Features of the electron avalanche formation process in a strongly inhomogeneous electric field under high overvoltages," J. Phys.: Conf. Ser., vol. 2064, 012020, Nov. 2021.

* The work was supported in part by the Russian Foundation for Basic Research under Projects No 20-08-00172 and No 20-38-90147.

S5-O-026303

PULSE GENERATORS FOR PUMPING LOW–PRESSURE NITROGEN LASERS AT PULSE REPETITION RATES UP TO 10 KHZ

B.A KOZLOV, I.V. LOGIN

Ryazan State Radio Engineering University, Ryazan, Russia

Effective excitation of nitrogen molecules in nitrogen lasers is carried out by direct electron impact at the breakdown stage [1,2]. For industrially produced nitrogen lasers with a discharge channel length of 350–500 mm, the breakdown voltage reaches 100 kV. In this case, the duration of the leading edge of voltage pulses does not exceed 100–120 nanoseconds.

At pulse repetition rates of units and tens of hertz, the formation of such pumping pulses is not very difficult. However, with an increase in the pulse repetition rate to 1 kHz or more, the formation of high–voltage pulses with the above parameters becomes a difficult task.

This work is devoted to the design of compact pulse generators for pumping low–pressure nitrogen lasers and their application for efficient energy input into the gas–discharge gap at the breakdown stage at pulse repetition rates up to 10 kHz.

Low–inductance pulse transformers were chosen as pulse generators. Such choice was due to the simplicity of design, compactness and the possibility of using only one high–current switch.

The following types of pulse transformers have been designed and tested:

– "traditional", in which the turns of the primary winding fit between the turns of the secondary winding. High–voltage wires of the VZM–04 brand with insulation from fluoroplastic tapes and electrical strength up to 20 kV were used as conductors. After their impregnation with transformer oil, the electrical strength increases up to 50 kV;

– "single-turn" [3]. In this version of the transformer, the primary and secondary windings were made of copper strips. The primary winding is one continuous turn, open in the upper part of the magnetic circuit;

– "cable" [4, 5]. The primary windings were segments of the outer sheath of the cable, the secondary winding was the central wire.

In all these pulse transformers, closed magnetic cores made of ferrite rings of the M1000NN brand (125x80x12 mm) were used. To determine the effect of overvoltage on the magnitude of the pumping discharge current and the energy introduced into the gas–discharge gap at the breakdown stage, multi–gap spark gap of the R–30M1 type operating at pulse repetition rates up to 5 kHz were connected in series with high–voltage outputs.

The results of the work carried out showed the following:

1. "Cable" pulse transformers provide the minimum duration of the leading edge of voltage pulses $\tau \approx 40$ nanoseconds and the current value in the gas–discharge gap of 1 kA at duration of ≈ 20–22 nanoseconds.

2. "Traditional" and "one–turn" pulse transformers make it possible to form high–voltage pulses with a leading edge duration of up to 50 nanoseconds and to pass currents up to 800 A through the discharge tube in 20–25 nanoseconds.

3. The use of multi–section spark gaps makes it possible to increase the breakdown voltage of the gas–discharge tube by ≈10 kV and provide the discharge current at a level of 1.2–1.4 kA. The duration of the discharge current at half maximum is 18–20 nanoseconds.

REFERENCES

[1] V.V. Kyun, V.G. Samorodov and Yu.M. Tokunov, "Pulse-periodical nitrogen lasers," Reviews of electronic engineering. Series 11. Laser technology and optoelectronics, 1989.

[2] A.N. Sviridov and Yu.D. Tropihin, “Kinetika generacii N2-lazera v impul'sno-periodicheskom rezhime (Generation kinetics of an N2 laser in a repetitively pulsed regime),” I. Teorija, Kvantovaja jelektronika, T.5, № 9, 1978, pp. 2015-2026. [in Russian]

[3] S.S. Vdovin, “Proektirovanie impul'snyh transformatorov (Design of pulse transformers),” 2 izd., L.: Jenergoatomizdat. Leningr. otd-nie, 1991. 208 p. [in Russian]

[4] G.A. Mesyac, A.S. Nasibov and V.V. Kremnev, “Formirovanie nanosekundnyh impul'sov vysokogo naprjazhenija (Formation of nanosecond high voltage pulses),” M., «Jenergija», 1970. [in Russian]

[5] G.A. Mesyac, “Impul'snaja jenergetika i jelektronika (Pulse Energy and Electronics),” M.: Nauka, 2004. 704 p. [in Russian]

S5-O-027901

STUDY ON PULSED PLASMA ENABLED CH_4 CONVERSION FOR THE PRODUCTION OF VALUED-ADDED CHEMICALS*

Y. GAO[1], L.G. DOU[1], J.C. L[1,3], J.W. LI[1], T. SHAO[1,2]

[1]Beijing International S&T Cooperation Base for Plasma Science and Energy Conversion, Institute of Electrical Engineering, Chinese Academy of Sciences, Beijing 100190, China
[2]University of Chinese Academy of Sciences, Beijing 100049, China
[3]Shandong Normal University, Jinan 250014, China

CH_4 is the raw material of carbon-based value-added chemicals and hydrogen carrier. Under the goal of carbon neutralization, it is an urgent need to develop environmental-friendly approaches of CH_4 conversion to platform chemicals at mild condition with high energy and resources utilization efficiency [1-2]. Herein, several highly adjustable pulsed power sources are employed to directly convert the CH_4 into H_2, C_2H_2, syngas and other platform chemicals by CH_4 non oxidation, reforming and partial oxidation processes. A generator characteristics-plasma properties-catalytic surface multiphase interface is proposed to regulate the target reaction pathway, furtherly revealing evolution of transient species and the responding mechanism between discharge and chemical reactions. In situ optical diagnosis, zero dimension kinetic modelling and in-line electrical measurements were used to obtain an integrated insights into the synergetic effect on electron-induced reaction and describe a panorama of plasma contributions. The gas products distribution is found to be highly correlated discharge mode and the pulsed parameters (rising/falling edge, pulse width). In the CH_4 non oxidation process, the highest CH_4 conversion of 91.2% and H_2 yield of 38.4% are achieved with energy efficiency of 44.3% by pulsed spark discharge. In the CH_4 reforming process, a shorter rising time is suggested to contribute both on conversion and energy efficiency.

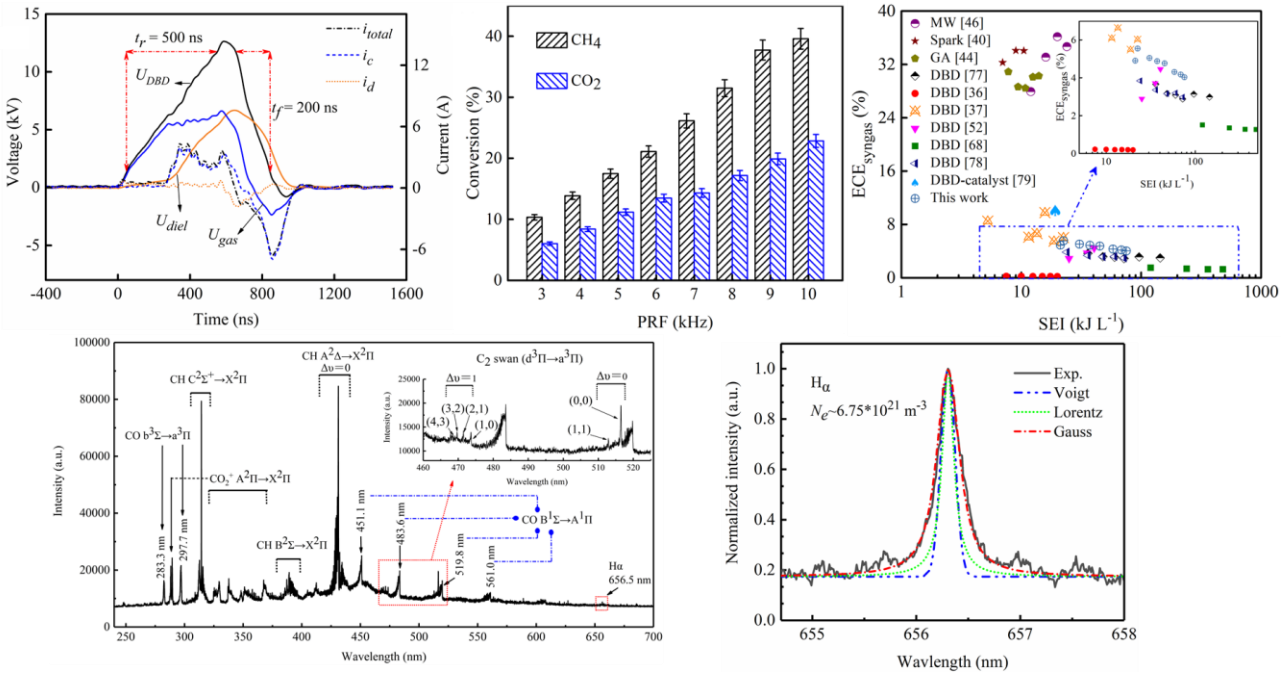

Fig.1. Pulsed plasma enabled CH_4/CO_2 reforming process.

REFERENCES

[1] X. Meng, X. Cui, N. P. Rajan, et al, "Direct methane conversion under mild condition by thermo-, electro-, or photocatalysis," Chem., vol.5, pp. 1–30, may 2019.

[2] G.K. Van, V.V. Galvita, G.B. Marin, "Making chemicals with electricity," Science. vol. 364, no.6442, pp. 734–735. May 2019.

* This work was supported by the National Key Research and Development Plan of China (Grant No. 2021YFE0114700) and National Science Fund for Distinguished Young Scholars (Grant No 51925703).

S5-O-029101

SUSTAINABLE NITROGEN FIXATION BY PULSED AIR DISCHARGE*

S. ZHANG[1], L.ZONG[1], X. ZENG[1,2], T. SHAO[1,2,*]

[1]Beijing International S&T Cooperation Base for Plasma Science and Energy Conversion, Institute of Electrical Engineering, Chinese Academy of Sciences 100190, China.
[2]University of Chinese Academy of Sciences, Beijing, 100049, China

Considering the increasing demand for fertilizers to support the global food supply, as well as the high-energy consumption and environmental concerns caused by industrial nitrogen fixation (i.e., Haber–Bosch process), there is a critical need to develop and integrate more sustainable, green-chemistry-based processes of nitrogen fixation. Energy-efficient and environmentally benign alternatives for NH_3 synthesis are urgently needed, especially the green-chemistry, light- or electricity-driven processes (*i.e.*, photo-catalysis, electro-catalysis, and non-thermal plasma (NTP)) using renewable energy (*i.e.*, solar and wind), to near the ultimate goal of zero carbon emissions [1].

As an electrically driven process, NTPs have been extensively investigated as an alternative for decentralized NO_x or ammonia production powered by renewable clean energy sources [2]. Emerging NTP-enabled nitrogen fixation processes are used to convert N_2/H_2 or N_2/H_2O directly to NH_3. On the other hand, the indirect approach involving plasma nitrogen oxidation ($N_2 \rightarrow NO_x$) and further catalytic reduction to ammonia ($NO_x \rightarrow NH_3$) have been proposed with the obtained energy efficiency of 4.6 MJ mol^{-1} NH_3, which is more than four times lower than the state-of-the-art plasma-enabled NH_3 synthesis from N_2 and H_2 with reasonable yields (>1 %) [3]. However, the issue of decoupling the challenges of molecular activation and product selectivity remains.

Recently, this work reveals the underlying reaction mechanisms for sustainable nitrogen fixation in nanosecond repetitive plasmas in spark discharges in the air by the combinatorial experiment, process diagnostics, and modeling investigations [4]. It is revealed that more than 50% of the generated NO originate from the chain reactions of O and N radicals with vibrationally excited N_2 and O_2 molecules ($O + N_2(\upsilon) \rightarrow NO + N$ and $N + O_2(\upsilon) \rightarrow NO + O$). Most NO_2 molecules are formed by further oxidation of NO species ($NO + O \rightarrow NO_2$). The presence of O and N spectral lines at the post-discharge stage further confirmed the important role of free-radical-chain reactions. These results provide new insights into sustainable and decentralized NO_x production.

It should be pointed out that the current energy cost of the plasma-based NO_x synthesis process is however still too high to be competitive with the electrolysis-based Haber–Bosch process combined with the Ostwald process, which will limit its large-scale industrialization [5]. Alternatively, we are now working on directly synthesizing compound fertilizer (*i.e.*, NO_x^- and trace metal ions) by pulsed air discharge to avoid the NH_3 synthesis pathways and testing their effects on pea seed's germination speed [6].

REFERENCES

[1] J. G. Chen, R. M. Crooks, L. C. Seefeldt, K. L. Bren, R. M. Bullock, M. Y. Darensbourg, P. L. Holland, B. Hoffman, M. J. Janik, A. K. Jones, M. G. Kanatzidis, P. King, K. M. Lancaster, S. V. Lymar, P. Pfromm, W. F. Schneider, and R. R. Schrock, "Beyond fossil fuel-driven nitrogen transformations," Science, vol. 360, no. 6391, 2018.

[2] T. Shao, R. Wang, C. Zhang, and P. Yan, "Atmospheric-pressure pulsed discharges and plasmas: Mechanism, characteristics and applications," High Voltage, vol. 3, no. 1, pp. 14-20, 2018.

[3] L. Li, C. Tang, X. Cui, Y. Zheng, X. Wang, H. Xu, S. Zhang, T. Shao, K. Davey, and S. Z. Qiao, "Efficient Nitrogen Fixation to Ammonia through Integration of Plasma Oxidation with Electrocatalytic Reduction," Angewandte Chemie - International Edition, vol. 60, no. 25, pp. 14131-14137, 2021.

[4] S. Zhang, L. Zong, X. Zeng, R. Zhou, Y. Liu, C. Zhang, J. Pan, P. J. Cullen, K. Ostrikov, and T. Shao, "Sustainable nitrogen fixation with nanosecond pulsed spark discharges: insights into free-radical-chain reactions," Green Chemistry, vol. 24, no. 4, pp. 1534-1544, 2022.

[5] K. H. R. Rouwenhorst, F. Jardali, A. Bogaerts, and L. Lefferts, "From the Birkeland-Eyde process towards energy-efficient plasma-based NO: X synthesis: A techno-economic analysis," Energy and Environmental Science, vol. 14, no. 5, pp. 2520-2534, 2021.

[6] X. Li, J. Luo, K. Han, X. Shi, Z. Ren, Y. Xi, Y. Ying, J. Ping, and Z. L. Wang, "Stimulation of ambient energy generated electric field on crop plant growth," Nature Food, vol. 3, pp. 133-142, 2022.

* The work was supported by the National Science Fund for Distinguished Young Scholars (Grant No. 51925703), the National Natural Science Foundation of China (Grant No. 52077205) and the Youth Innovation Promotion Association CAS (Grant No.2022136).

S5-O-033802

RUNAWAY ELECTRONS, DISPLACEMENT CURRENTS, AND DISCHARGE DEVELOPMENT IN A QUASI-HOMOGENEOUS ELECTRIC FIELD*

D.V. BELOPLOTOV, V.F. TARASENKO, D.A. SOROKIN

Institute of High Current Electronics SB RAS, Tomsk, Russia

Interest in the study of discharges in a homogeneous electric field is due to their use, for example, in switches. At the same time, such discharges are interested from a scientific point of view. In particular, it concerns the generation of runaway electrons (REs). They provide conditions for the ignition of the discharge in diffuse form. Thanks to the decades of intensive studies in this field, the conditions for the transition of electrons into runaway mode are defined [1–3]. However, specific processes in the discharge still require a detailed study. The success of such studies depends on progress in the development of measuring equipment and the emergence of new methods.

Experimental studies of the generation of REs during the formation of a nanosecond discharge in gaps with an electric field strength distribution close to homogeneous, filled with helium and nitrogen at different pressures, have been carried out. The experiments were carried out using high-speed recording methods (streak camera, four-channel ICCD camera), as well as using an original method based on measuring the displacement current caused by the appearance and formation of a streamer. This made it possible to study RE generation with reference to the dynamics of streamer development. It was possible for the first time in the experiment to accurately determine the instant of RE generation relative to the development of ionization waves in a flat gap filled with nitrogen at a pressure of 300 kPa.

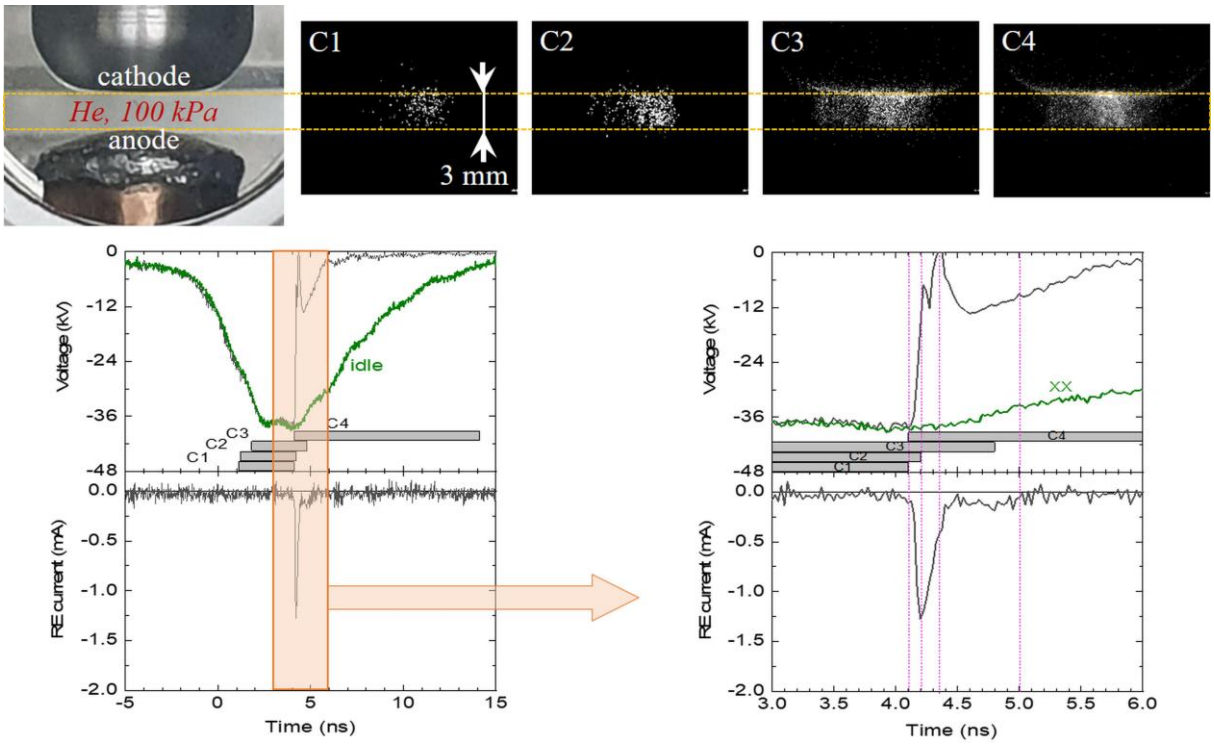

Fig.1. ICCD images of the discharge formation in helium at a pressure of 100 kPa and corresponding waveforms of voltage and runaway electron current. Rectangles show the exposure duration of the ICCD camera channels (C1–C4).

REFERENCES

[1] A.V. Gurevich, "On the theory of runaway electrons," Sov. Phys., vol.12, Article Number 904, 1961.

[2] L.P. Babich, High-energy phenomena in electric discharges in dense gases, Arlington, VA: Futurepast, 2003.

[3] V.F. Tarasenko, Runaway Electrons Preionized Diffuse Discharges, New York, Nova Science Publishers, Inc., 2014.

* The reported study was funded by RFBR, project number 20-02-00733

S5-O-034804

NANOSECOND PULSE BREAKDOWN IN NOBLE GASES[1]

P.A. BOKHAN[1], N.A. GLUBOKOV[2], P.P. GUGIN[1], M.A. LAVRUKHIN[1], D.E. ZAKREVSKY[1,2]

[1] Rzhanov Institute of Semiconductor Physics SB RAS, Novosibirsk, Russia
[2] Novosibirsk State Technical University, Novosibirsk, Russia

The breakdown phenomenon underlies the operation of the gas-discharge switching devices. In devices with a cold cathode in most cases the breakdown is due to the Townsend or streamer mechanisms, which are based on the development of electron avalanches from the initial/background electrons concentration. There is form of gas discharge in which such a geometry of the discharge gap is realized that processes outside the discharge gap behind the anode affect the mechanisms of emission and current development. In this so called "open" discharge in the discharge gap of ~ 0.1-10 mm the electrons are emitted under the influence of resonance radiation having the Doppler shift and generated by atoms which appears in the process of recharging of ions moving toward the cathode. A specific feature of such a discharge is insignificant multiplication of electrons in the discharge gap, so the discharge current is provided only by emission of electrons from the cathode and the external electric circuit. The breakdown characteristics in discharges of this type in form of dependences of current and delay of the discharge development on the voltage were investigated. The experiments were carried out in planar discharge cells consisting of circular *SiC* cathodes and two molybdenum grids used as anode and separated by 11 mm drift space. The length of the discharge gap was 7 mm. Such construction allowed studying the characteristics in two modes depending on the connection way: (i) - classical "open discharge" (OD), (ii) - "open discharge" with counter-propagating electron beams (ODCPEB). In the first case, the grid and cathode of one of the gaps were grounded through current shunts and acted as a collector. In the second case, the grids were grounded and the cathodes were supplied with the equal electric potential. Load resistance R_L = 33 Ω and discharge capacitance C = 100 pF. The Fig. 1 shows the dependences of *I(U)* in *He* (p_{He} = 20-100 Torr), *Ne* (p_{Ne}=1.5-25 Torr), and *Ar* (p_{Ar} = 0.5-4 Torr) in the ODCPEB mode as increasing curves, with *I(U)* weakly depending on *He* pressure.

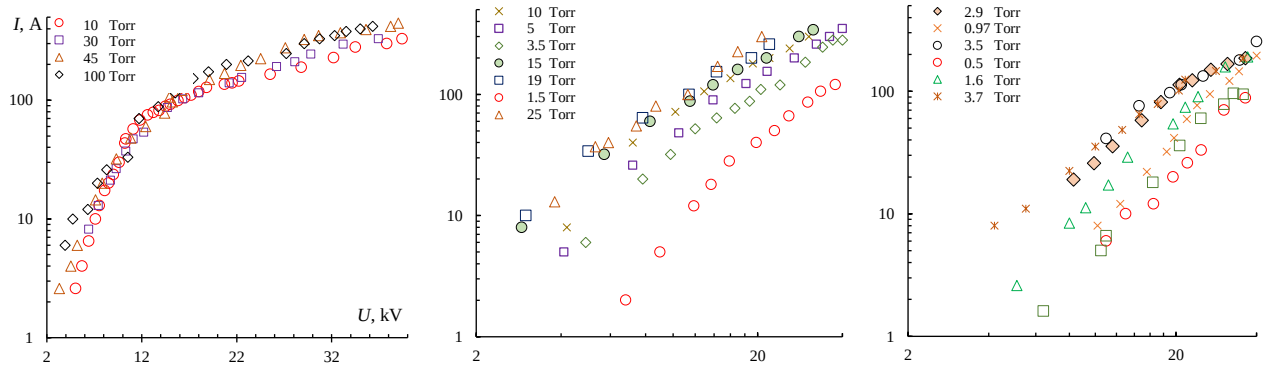

Fig.1. Dependences *I*(*U*): (*a*) - *He* (p_{He} = 20–100 Torr), (*b*) - *Ne* (p_{Ne}=1.5–25 Torr), (c) - *Ar* (p_{Ar}=0.5–4 Torr)

The dependences of the parameter $p \times \tau$ on E/p for different gases (τ is the delay time of the discharge development) shows that the discharge development in both types of studied discharges is characterized by higher E/N values than in case of the avalanche breakdown [1]. As pressure increases for each gas, the dependences converge, and in the *He-Ne-Ar* series, the heavier gas is characterized by higher values of τ. ODCEB in comparison with OD is characterized by significantly lower τ, associated with intensive generation of VUV radiation during the oscillations of electrons in the discharge gaps in the former, and the absence of them in the later. At increased values of the gas pressure (p_{He}=60 Torr) in case of *He*, when the decelerating length of beam electrons is less than drift space length and, electron oscillations are absent, current development rates in ODCPEB and OD are equalized and reach in *He* (p_{He}=100 Torr and U=36 kV $\tau \approx$0.3 ns).

REFERENCES

[1] P. Felsenthal, J.M. Proud “Nanosecond-pulse breakdown in gases”, Physical Review, vol. 139 n. 6A, pp. A1796, 1965.

[1] The work was supported by the Russian Science Foundation (project No. 19-19-00069).

S5-O-035202

PHYSICAL KINETICS OF RUNAWAY ELECTRONS DURING THE BREAKDOWN OF GAS-FILLED HIGH-PRESSURE GAPS

A.V. KOZYREV, V.YU. KOZHEVNIKOV, A.O. KOKOVIN, N.S. SEMENIUK

Institute of High Current Electronics SB RAS, Tomsk, Russian Federation

A high-voltage high-pressure discharge with runaway electrons has been intensively studied in recent years [1]. As a result, the level of understanding of the main processes in this phenomenon has increased significantly. If at first only the criterion of the generation of runaway electrons (exceeding the threshold field strength) was used, then the modern kinetic theory of this phenomenon does not need the concept of a threshold field.

The kinetic approach to describing electrons can be effectively integrated into the hydrodynamic theory of streamer breakdown of gas-discharge gaps. Advanced multi-fluid breakdown theory can describe in detail not only one-dimensional, but also two-dimensional discharge gap configurations. If a gap configuration has a direction of spatial symmetry (plane or axis of symmetry), then the kinetic method of describing an ensemble of electrons can be implemented along this direction. The hybrid method makes it possible to bring simplified theoretical models as close as possible to experimental conditions. In this paper, the advantages of the method will be demonstrated with some examples. Figure 1 shows an example of a hybrid simulation.

A complete kinetic approach, unfortunately, we can implement only within the framework of a 1D1V-dimensional model. But even these limited possibilities make a great contribution to our understanding of the key factors that determine the current, the pulse duration, and the energy spectrum of the runaway electron beam.

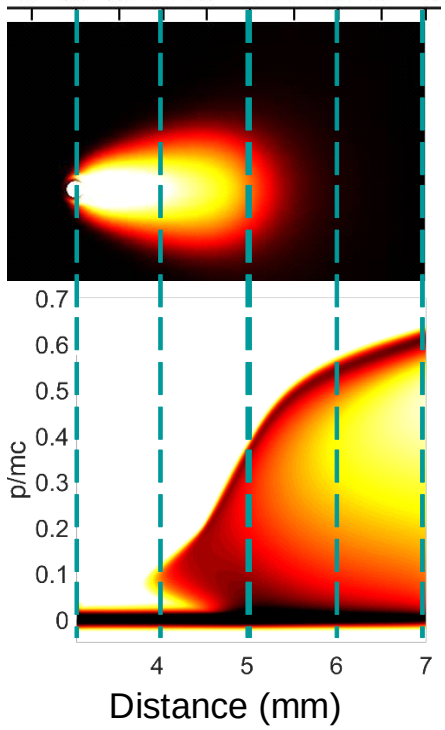

Fig.1. Instantaneous pattern of plasma number density distribution, $n(x,z)$ (top) and space-momentum distribution function of the electron ensemble, $f(z,p,t_0)$ (bottom) at time point of t_0=330 ps after applying a voltage pulse with amplitude of 140 kV to the 4 mm gap "200 μm diameter wire - plane anode" filled with nitrogen at 1 atm.

REFERENCES

[1] Generation of Runaway Electron Beams and X-Rays in High Pressure Gases. Volume 2: Processes and Applications / Edited by Victor F. Tarasenko. – USA, NY: Nova Science Publishers, 2016. – 331 p.

S5-O-039102

IMPURITY INFLUENCE ON THE V-I CHARACTERISTIC OF GLOW DISCHARGE*

P.A. BOKHAN[1], G.V. SHEVCHENKO[1,2], P.P. GUGIN[1], V.A. KIM[1], D.E. ZAKREVSKY[1,2]

[1] *Rzhanov Institute of Semiconductor Physics SB RAS, Novosibirsk, Russia*
[2] *Novosibirsk State Technical University, Novosibirsk, Russia*

High-voltage glow discharges in helium and other noble gases are find a variety of applications in various fields of science and technology. It is possible to allocate two directions on which the most intensive researches are carried out: generation of electron beams keV – range of energies and commutation of high-voltage pulses with subnanosecond rise front [1,2]. The transition to high voltages made it possible to obtain results previously unknown in the study of low-voltage discharges. One of the most unusual is the detection of S – shaped volt-ampere characteristics (V–I characteristics). For the first time they were registered as early as 1965 in the work [3], but up to 2002 [4] they were not obtained. In a series of subsequent papers [5,6 et al] it was shown that the S – shaped V–I characteristics are registered only in high frequency gases, both in the conventional glow discharge and in its special form of "open discharge".

In the present work, the influence of impurities on the V–I characteristic was investigated under different conditions from the [5,6] works. The discharge between a flat molybdenum cathode with an active area of 2cm^2 and a copper anode in the form of a Faraday cylinder was used. Simultaneously with the measurement of the V-I characteristic, the emission spectrum of the plasma in the interelectrode gap was recorded. Fig.1 shows the radiation spectrum from the helium discharge for 3 cases with the impurity content of 10^{-3}, 10^{-4} and less than 10^{-5} Torr. Fig.2 shows the corresponding V–I characteristics. It can be seen that the more polluted the helium, the higher the current, and the V–I characteristic becomes more rapid-growing. These changes are attributed to the transition of emission under the influence of energetic impurity ions formed by the recharge of helium ions on impurities and the acceleration of impurity ions in the region of which the potential drops to an energy comparable to the value of eU, where U is the applied voltage.

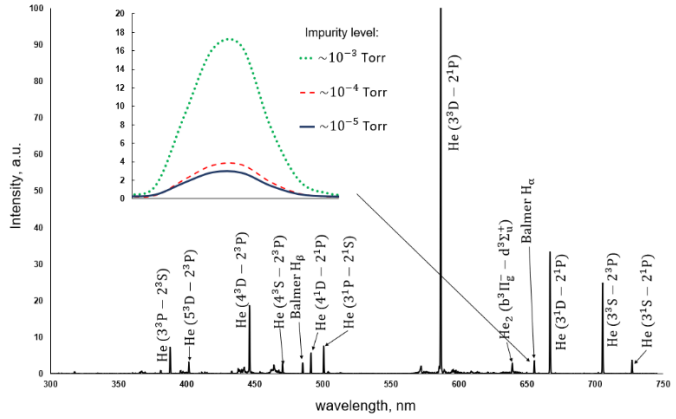

Fig. 1 Plasma spectrum at different impurity content

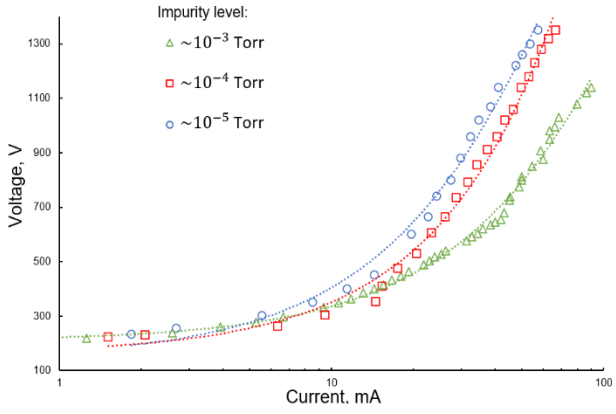

Fig. 2 V-I charateristics of the glow discharge at different impurity content

REFERENCES

[1] P.A. Bokhan, P.P. Gugin, M.A. Lavrukhin, D.E. Zakrevsky, I.V. Schweigert, A.L. Alexandrov “Investigation of the characteristics and mechanism of subnanosecond switching of a new type of plasma switches. I. Devices with counter-propagating electron beams—kivotrons”. *Plasma Sources Science and Technology*. vol. 29, pp. 084002, 2020.

[2] P.A. Bokhan, E.V.Belskaya, P.P. Gugin, M.A. Lavrukhin, D.E. Zakrevsky, I.V. Schweigert “Investigation of the characteristics and mechanism of subnanosecond switching of a new type of plasma switches. II. Switching devices based on a combination of ‘open’ and capillary discharges – eptrons”. *Plasma Sources Science and Technology*. vol. 29, pp. 084001, 2020.

[3] K.-B. Persson “Brush cathode plasma – a well-behaved plasma” J Appl. Phys. vol. 36, p3086, 1965.

[4] P.A.Bokhan, D.E.Zakrevsky, “Self-sustained photoelectron discharge” Appl. Phys. Lett, vol. 81, pp. 2526, 2002.

[5] P.A. Bokhan, P.P. Gugin, D.E. Zakrevsky, M.A. Lavrukhin, "Study of the properties of an anomalous glow discharge generating electron beams in helium, oxygen, and nitrogen", Plasma Physics Reports, vol. 45, p.1035, (2019).

[6] P.A. Bokhan, P.P. Gugin, D.E. Zakrevsky, V.A. Kim, M.A. Lavrukhin, "Switching of high-voltage pulses in devices based on open discharge in nitrogen and oxygen", Techn. Phys. Lett, vol. 46, p. 1020, (2020).

* The work was supported by the Russian Science Foundation (project No. 19-19-00069)

S5-O-040901

FORMATION OF WIDE STREAMERS IN AIR AND HELIUM: THE ROLE OF FAST ELECTRONS*

N.YU. BABAEVA[1], G.V. NAIDIS[1], V.F. TARASENKO[2]
[1]Joint Institute for High Temperatures RAS, Moscow 125412, Russia
[2]Institute of High Current Electronics SB RAS, Tomsk 634055, Russia

Experimental and computational studies of subnanosecond breakdown of atmospheric-pressure air in nonuniform electric fields revealed that the ionization waves have nearly spherical or conical shapes [1]. In this work, we discuss the results from the computational studies of nanosecond pulsed discharges in air and helium. The model, *nonPDPSIM*, used in this paper, is a two-dimensional code which is executed on unstructured numerical meshes. In the model, the kinetic Electron Monte Carlo Module integrates the trajectories of fast electrons. The energies of fast electrons are recorded to compute electron energy distributions (EEDs). From the EEDs, electron impact source functions and sources of secondary electrons are computed.

We demonstrate that wide and diffuse discharges can be formed due to fast electrons. The discharge is initiated near the cathode having a small radius of curvature and propagates towards the flat anode as shown in Fig. 1. Fast electrons are periodically emitted from the surface of the cathode during ion bombardment. The pulse has 2 ns duration, 0.2 ns rise and 0.2 ns fall time with a peak voltage -110 kV, the gap is 8.5 mm.

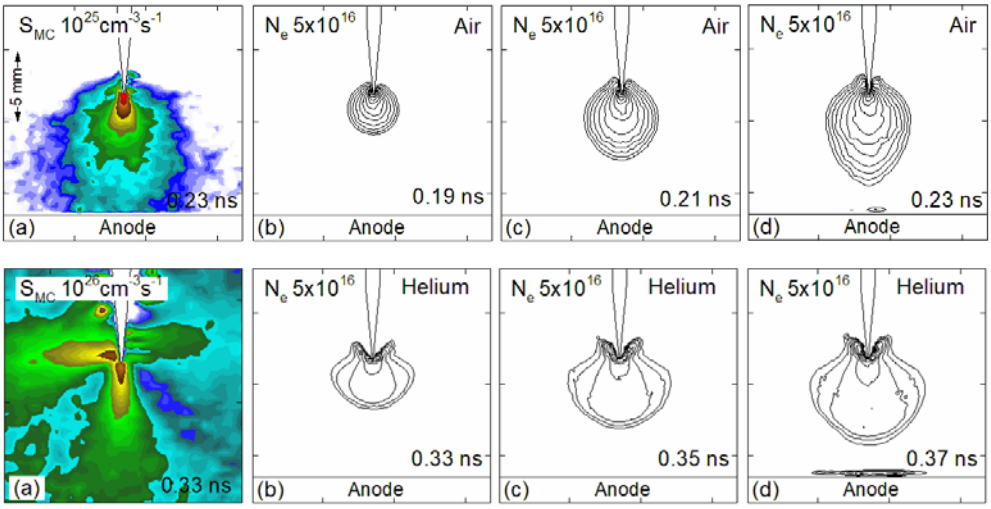

Fig.1. (a) Sources of fast electrons obtained from Monte Carlo simulations (plotted on 3 decades log scale); (b) to (d) Electron density at three successive time moments (plotted on 3 decades log scale). Maximum values are shown in each frame. The upper row of frames shows the development of a streamer in air, the bottom row – in helium.

The secondary electrons are emitted from the cathode surface as a beam of electrons with the typical energy of 4 eV for air and 16.6 eV for helium. These values correspond to the energy difference $I - 2W$. Here I = 12.1 eV is the ionization potential of oxygen molecules (O^+_2 is the most abundant ion) and I = 24.6 eV is the ionization potential for helium. W = 4 eV is the work function for a metal (copper) electrode. The process of secondary electron emission by ions (Auger neutralization) is discussed in detail in [2]. With more energetic beam electrons emitted from the cathode in helium, horizontal (as well as vertical) tracks of these electrons are observed (Fig. 1a, bottom row). This results in a wider streamer formation as compared to that in air. Note that air streamers calculated with account for fast beam electrons are also wider than conventional streamers (driven only by photoionization).

REFERENCES

[1] V. F. Tarasenko, G. V. Naidis, D. V. Beloplotov, I. D. Kostyrya, and N. Yu. Babaeva, “Formation of Wide Streamers during a Subnanosecond Discharge in Atmospheric-Pressure Air”, Plasma Physics Reports, vol. 44, No. 8, pp. 746–753, 2018.
[2] H. D. Hagstrum, “Theory of Auger ejection of electrons from metals by ions”, Phys. Rev., vol. 96, pp. 336–365, 1954.

* This research was supported by the Ministry of Science and Higher Education of the Russian Federation (agreement no. 075-15-2021-1026 of November 15, 2021).

S5-O-041001

INTENSE X-RAY, LOW- AND HIGH-FREQUENCY RADIO EMISSIONS TRIGGERED BY THE STREAMER FORMATION PROCESSES IN A HIGH-VOLTAGE DISCHARGE*

E. PARKEVICH[2], *A. KHIRIANOVA*[2], *T. KHIRIANOV*[2], *I. BAIDIN*[2], *K. SHPAKOV*[2],

A. RODIONOV[2], *YA. BOLOTOV*[1,2], *V. RYABOV*[2], *YU. KURILENKOV*[3], *A. OGINOV*[2]

[1]*Moscow Institute of Physics and Technology, Institutskiy Pereulok 9, Dolgoprudny, Moscow Region 141700, Russia*
[2]*P. N. Lebedev Physical Institute of the Russian Academy of Sciences, 53 Leninskiy Prospekt, Moscow 119991, Russia*
[3]*Joint Institute for High Temperatures, Russian Academy of Sciences, Izhorskaya str. 13/2, Moscow 125412, Russia*

The study is aimed at revealing the discharge breakdown processes that are able to emit broadband radio and x-ray emissions, as well as investigating the emission properties in detail. For a laboratory discharge initiated in a long air gap by a microsecond megavolt pulse, we for the first time simultaneously register wideband high-frequency (GHz) and low-frequency (MHz) microwave emissions together with hard x-rays (up to ~100 keV). When registering various electromagnetic emissions, we image the discharge morphology by employing a sCMOS gated intensified camera, with the camera gate being of ~55–60 ns. We thoroughly analyze the temporal relationship of the emissions, depending on the discharge evolution, and provide comprehensive data on the spectral and temporal characteristics of the LF- and HF-radio emissions during the discharge formation. We show that the intense development of the anode-directed streamers is accompanied only by the LF-radio emission (10–150 MHz), whereas the HF-radio emission (1–4 GHz) and x-rays appear within the discharge stage when a complex net of countless plasma channels forms and spans the entire discharge gap, see Fig. 1. The channel formation is closely related with the intense development and multiplication of multiple streamers, as well as starts after very fast development of the cathode-directed streamers. We directly show that the power of the LF-radio emission sharply increases almost synchronously with that of the HF-radio emission, whereas the onset of hard x-rays coincides with the appearance of the HF-radio emission. The HF-radio emission has a complex spectral and temporal structure and appears as multiple short (<1 ns) bursts characterized by various frequency components, existing in subnanosecond time intervals.

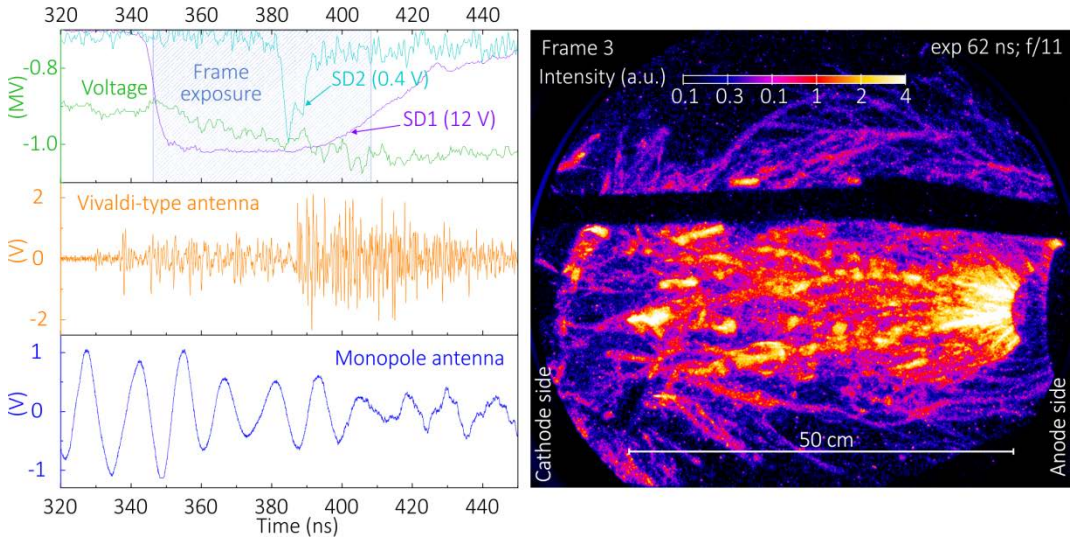

Fig.1. On the left: voltage waveform, x-ray signals (SD1: threshold energy 20 keV and SD2: threshold energy 100 keV), monopole (MHz) and Vivaldi-type (GHz) antenna signals obtained in a single discharge event. The detector signals are shown for the time period corresponding to the exposure of the frame presented on the right panel.

REFERENCES

[1] E.V. Parkevich, et al. Streamer formation processes trigger intense x-ray and high-frequency radio emissions in a high-voltage discharge. Submitted to Physical Review E. March, 2022.

* The work was supported by the Russian Science Foundation (grant no. 19-79-30086). The analysis of the microwave spectrums was funded by the grant of the Russian Foundation for Basic Research (no. 20-08-01156).

S5-P-000209

EXPERIMENTAL INVESTIGATION OF INFLUENCE OF IONIZATION WAVE VELOCITY ON VOLTAGE DROP DURING PULSED GAS BREAKDOWN*

V.A. SHKLYAEV, D.V. BELOPLOTOV, A.A. GRISHKOV, S.YA. BELOMYTTSEV, D.A. SOROKIN

Institute of High Current Electronics SB RAS, Tomsk, Russia

Previously experiments [1] have shown that the formation of both positive and negative streamers in a point-to-plane gap causes a voltage drop. The report presents the first experimental verification of our theoretical data [2-3] on the relation between the ionization wave velocity and the voltage dynamics during pulsed breakdowns in a highly inhomogeneous electric field.

The experimental setup consisted of nanosecond high-voltage generators, a high-voltage cable, a discharge chamber with a transmission line and a built-in capacitive voltage divider. The cathode was an Al foil twisted into a tube. A 4.5 cm long tube made of a twisted fluoroplastic film was put on the cathode to prevent the development of the ionization wave toward the side wall of the chamber. The grounded electrode was plane. The interelectrode distance was varied from 1 to 4 cm. The chamber was pumped out with a fore vacuum pump and then filled with air. The pressure was varied in the range of 4–100 Torr.

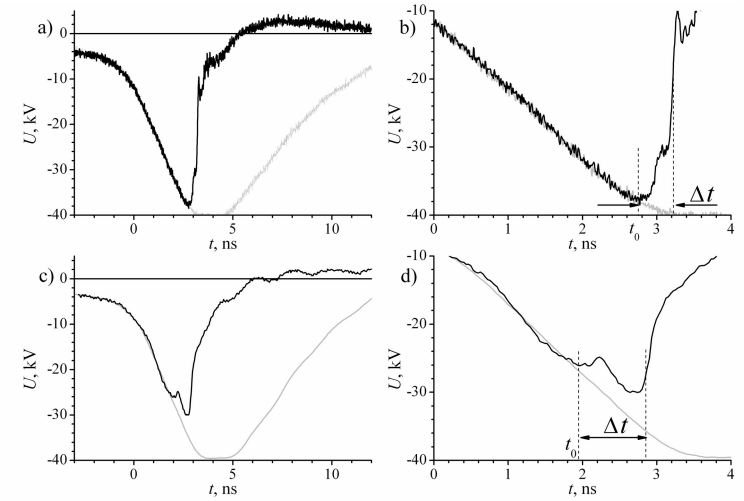

Fig. 1. Waveforms of voltage from capacitive voltage divider during discharge in air at a pressure of 10 Torr. Grey curve – idle mode, black curve – breakdown mode. Interelectrode distance is (a, b) 2 cm and (c, d) 4 cm.

Figure 1 shows typical waveforms of voltage from voltage divider recorded in the experiments. It is seen from Fig. 1b, d that at t_0 the voltage goes slightly below the voltage in idle mode. There is a short interval Δt of ionization wave propagation from cathode to anode. The voltage decreasing in the interval Δt can be explained by the displacement current comparable with the transmission line charging current arises. As the wave reaches the anode (grounded electrode), the voltage decreases sharply and a breakdown occurs. To estimate the ionization wave velocity, we can measure the time interval Δt.

REFERENCES

[1] Beloplotov D.V., Tarasenko V.F., Lomaev M.I., and Sorokin D.A., Experimental Determination of the Generation Moment of Runaway Electrons, IEEE Trans. Plasma Sci., vol. 47, no. 10, pp. 4521–4524 (2019) DOI: 10.1109/TPS.2019.2907998

[2] S. Ya. Belomyttsev, A. A. Grishkov, V. A. Shklyaev, and V. V. Ryzhov, Effect of the ionization wave velocity on the current and voltage of a gas-filled diode, *Journal of Applied Physics*, 123, 203302 (2018) DOI: 10.1063/1.5026030

[3] S. Ya. Belomyttsev, A. A. Grishkov, V. A. Shklyaev, and V. V. Ryzhov, Current in a pulsed gas breakdown at a highly inhomogeneous electric field, *Journal of Applied Physics*, 123, 043309 (2018); DOI: 10.1063/1.500208820

* The work was carried out within the framework of the state assignment of the Ministry of Science and Higher Education of the Russian Federation on the topics FWRM-2021-0007 and FWRM-2021-0014) as well as was funded by RFBR, project number 20-02-00733.

S5-P-000702

THE DYNAMICS OF A STREAMER IN A SHARPLY INHOMOGENEOUS ELECTRIC FIELD AND ITS INFLUENCE ON THE AMPLITUDE-TIME CHARACTERISTICS OF VOLTAGE AND CURRENT*

D.A. SOROKIN, D.V. BELOPLOTOV, V.F. TARASENKO

Institute of High Current Electronics SB RAS, 2/3 Akademichesky Ave., Tomsk, 634055 Russia, SDmA-70@loi.hcei.tsc.ru

Due to wide range of applications, nanosecond discharges in gases in sharply inhomogeneous electric fields have attracted the attention of researchers all over the world [1–2]. Therefore, it is extremely important to know what physical processes occur at the breakdown stage. The purpose was to find experimentally and study the relationship between the dynamics of the discharge formation and the amplitude-time characteristics of current and voltage.

The formation of a nanosecond discharge with the use of a Hamamatsu streak-camera and with simultaneously wideband (10 GHz) measurement of voltage and displacement current caused by a streamer in one pulse was studied (Fig. 1). Nanosecond voltage pulses of various amplitudes (16–27 kV) were applied across a point-to-plane gap (8.5 mm) filled with air at various pressures (13–200 kPa). It was found that as soon as a streamer appears in the vicinity of the pointed electrode the voltage across the gap drops. At the same time, a pre-breakdown current begins to flow. The magnitude of the pre-breakdown current, as well as the voltage drop, is determined by the rate of formation of dense plasma and, accordingly, by the rate of redistribution of the electric field in the gap. The streamer velocity determines the rise time and amplitude of the current. The higher the streamer velocity, the shorter the rise time and the higher the amplitude of the pre-breakdown current. The propagation of a backward and third ionization waves was observed both with the streak camera and by measuring the displacement current. As they propagate, the discharge current increases to its amplitude value.

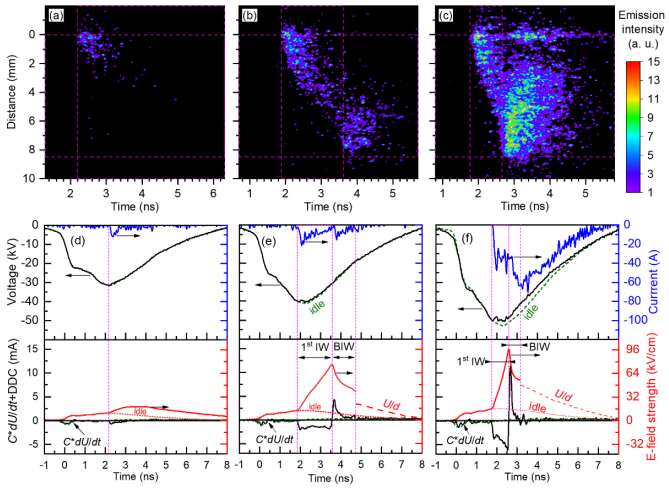

Fig.1. (a–c) Streak-images and (d–f) corresponding waveforms of voltage, current, displacement current ($C_{gap}dU/dt$ + Dynamic Displacement Current) measured with the collector placed behind the grounded grid electrode, and the electric field strength near the surface of the grounded electrode at various voltages across the gap. 1st IW – first ionization wave (streamer), BIW – backward ionization wave. Air at a pressure of 200 kPa.

REFERENCES

[1] A. Bourdon, F. Péchereau, F. Tholin, Z, Bonaventura, "Morphology of positive ionization waves in atmospheric pressure air: influence of electrode set-up geometry", J. Phys. D Appl. Phys., Vol. 54, Article Number 075204, 2021. (DOI: 10.1088/1361-6595/ac2be5)

[2] A. Brisset, P. Tardiveau, K. Gazeli et al., "Experimental study of the effect of water vapor on dynamics of a high electric field non-equilibrium diffuse discharge in air", J. Phys. D Appl. Phys., Vol. 54, Article Number 215204, 2021. (DOI: 10.1088/1361-6463/abe81e)

[3] V.F. Tarasenko (ed.), Runaway Elctron Preionized Diffuse Discharges, Nova Science Publishers, Inc. NY, USA, 2014.

* This research was supported by the MSHE of the Russian Federation within Agreement No. 075-15-2021-1026.

S5-P-001101

ELECTRIC EXPLOSION OF MICROWIRES BY HIGH FREQUENCY CURRENT.*

E.V. ORESHKIN[1]

[1] *Lebedev Physical Institute, RAS, Moscow 119991, Russian Federation*

In avalanches of runaway electrons, which are formed in high-altitude atmospheric discharges, the average electron energy is several megaelectronvolts. For such high-energy electrons, the loss of energy by bremsstrahlung is significant when they collide with gas atoms. The aim of this study was to evaluate the effect of bremsstrahlung on the exponential growth length of a runaway electron avalanche. It has been shown that taking account of the bremsstrahlung produced by the electrons of an avalanche gives corrections of no more than a few percent to the avalanche exponential growth length. The corrections are maximum for electric field strengths close to the threshold below which the avalanche electrons fail to become continuously accelerated. The effect of bremsstrahlung decreases with increasing electric field strength. The higher the atomic number of the gas in which an avalanche of runaway electrons propagates, the greater the corrections[1].

REFERENCES

[1] Oreshkin, E. «Effect of bremsstrahlung on the characteristic growth length of an avalanche of runaway electrons. Europhysics Letters», 136(1), 15001, 2022.

* This work was supported by a grant from the Foundation for the Development of Theoretical Physics and Mathematics "BASIS".

S5-P-014001

MODELING THE COLOR OF HIGH-ALTITUDE ATMOSPHERIC DISCHARGES USING A REPETITIVELY PULSED DISCHARGE IN AIR, NITROGEN AND ARGON*

N.P. VINOGRADOV, V.F. TARASENKO, E.KH. BAKSHT

Institute of High Current Electronics SB RAS, Tomsk, 634055, Russia

High-altitude electrical discharges in the Earth's atmosphere are studied by a large number of scientific groups [1, 2]. In scientific laboratories, these phenomena are modeled both experimentally and theoretically [1, 2, 3, 4]. However, the scientific community cannot find answers to some questions, such as the mechanism of the initiation of different TLEs and their influence on each other, as well as the nature of the color of the observed high-altitude electrical discharges.

In this work, the influence of the electrode material (aluminum and stainless steel) during the formation of mini jets on the color of a repetitively pulsed diffuse discharge in air, nitrogen, and argon is studied. The discharge was formed under the conditions of generation of runaway electrons in a nonuniform electric field with a cone-shaped and wire cathode and a plane anode.

As a result of the experiments, it was found that the similarity of the color of the mini jets, which are formed at the electrodes of aluminum and stainless steel, is closer to the emission of red sprites and blue jets, respectively, than the emission during a diffuse discharge without mini jets. At the same time, it was found that the color of the plasma changes due to the evaporation of the electrode material. There are photographs of discharges with aluminum and stainless steel electrodes in the figure 1.

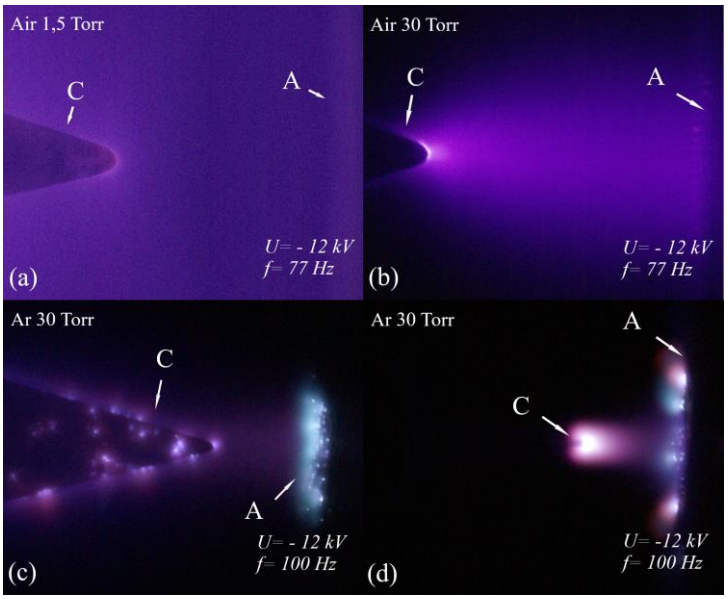

Fig.1. Photos of the discharge in air and argon. The gap length is d = 6 mm (a), 12 mm (b), 2 mm (c,d). Cathode – aluminum (a,b,c,d), anode – aluminum (a,b), anode – stainless steel (c,d).

According to obtained data, it can be assumed that metal vapors in the Earth's atmosphere, for example, due to small meteorites [5], affect the color of the TLEs.

REFERENCES

[1] D.D. Sentman, E.M. Wescott, “Red sprites and blue jets: Thunderstorm-excited optical emissions in the stratosphere, mesosphere, and ionosphere,” Physics of Plasmas, vol. 2, no. 6, pp. 2514-2522, 1995.

[2] V.P. Pasko, U.S. Inan, T.F. Bell, Y.N. Taranenko, “Sprites produced by quasi-electrostatic heating and ionization in the lower ionosphere,” J. Geophys. Res, vol. 102, pp. 4529–4561, 1997.

[3] S. Nnadih, M. Kosch, J. Mlynarczyk “Estimating the electron energy and the strength of the electric field within sprites using ground-based optical data observed over South African storms,” J. Atmos. Sol.-Terr. Phys., pp. 105760, 2021.

[4] E.A. Sosnin, N.Y. Babaeva, V.Y. Kozhevnikov, A.V. Kozyrev, G.V. Naidis, V.A. Panarin, V.S. Skakun, V.F. Tarasenko, “Modeling of transient luminous events in Earth's middle atmosphere with apokamp discharge,” Physics-Uspekhi, vol. 64, no, 6, pp. 191–210, 2021.

[5] J.M. Plane, G.J. Flynn, A. Määttänen, J.E. Moores, A.R. Poppe, J.D. Carrillo-Sanchez, C. Listowski, “Impacts of cosmic dust on planetary atmospheres and surfaces,” Space Science Reviews, vol. 214, no. 23, pp. 1-42, 2018.

* The reported study was performed within the framework of the State assignment of the IHCE SB RAS, project No. FWRM-2021-0014.

S5-P-014201

STUDY OF INTERMITTENT CORONA DISCHARG USING ICCD CAMERA*

E.KH. BAKSHT, V.F. TARASENKO, N.P. VINOGRADOV

Institute of High Current Electronics, 2/3 Akademichesky Ave., Tomsk 634055, Russia

Corona discharge is widely used in electrostatic precipitators, plasma-chemical systems for ozone synthesis and surface treatment, aerosol charging systems, and many other applications. Corona discharge can also be a negative factor, for example, in high-voltage gas insulation systems. Therefore, the research of the one is still relevant.

We have studied an intermittent corona discharge in atmospheric air at various voltages. Two electrode configurations were used to ignite the corona discharge: a single point and a point-plane. The discharge was photographed with an HSFC-PRO ICCD camera. Waveforms of the discharge current and voltage across the gap were recorded. We also studied the first current pulses that occur when a corona discharge was ignited when a gradual voltage increase at the potential electrode.

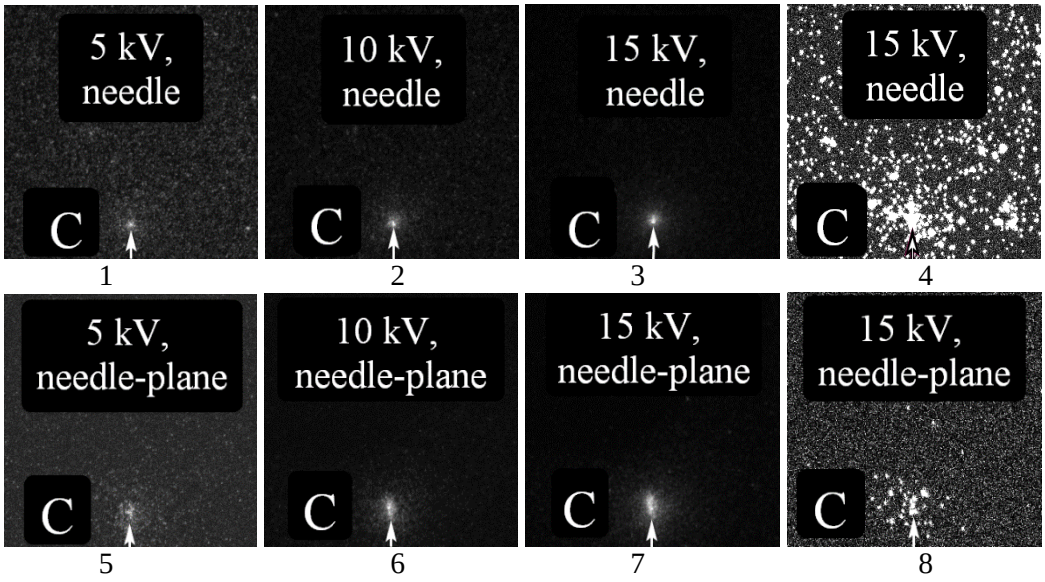

Fig.1. Photographs of the light emission of the negative corona discharge around a single point (1 – 4) and in the point-plane gap with d = 2 cm (5 – 8) in the atmospheric air, obtained by ICCD camera. The exposure time of one frame is 10 ms (1, 2, 3), 50 μs (4), 500 μs (5, 6, 7) and 1 μs (6). The radius of curvature of the needlepoint is 24 μm.

* The work was supported by the Russian Science Foundation, project #22-29-00137.

S5-P-014202

SUBNANOSECOND THREE-SECTION ELECTRON ACCELERATOR*

E.KH. BAKSHT, V.F. TARASENKO, S.B. ALEKSEEV

Institute of High Current Electronics, 2/3 Akademichesky Ave., Tomsk 634055, Russia

The design and test results of a subnanosecond accelerator are presented, in which three sections are used (a double forming line, a ferrite line and a line with variable wave resistance), as well as a gas-filled diode. The beam current amplitude of ~2.7 kA was recorded behind the anode foil at the pulse duration of ~370 ps (FWHM). The accelerator allowed studing Cherenkov radiation, as well as pulsed cathodoluminescence, in the samples made of KU-1 quartz glass, polymethyl methacrylate, and KBr.

* The work was performed in the framework of the State task for HCEI SB RAS, project # FWRM-2021-0014.

S5-P-019307

NUMERICAL STUDY ON THE EFFECT OF SECONDARY ELECTRON EMISSION PROCESS CONSIDERING THE SURFACE CHARGES ON THE ATMOSPHERIC PRESSURE DIELECTRIC BARRIER DISCHARGE*

JIAN WANG, DONG DAI

School of Electric Power, South China University of Technology, Guangzhou 510641, People's Republic of China

The ion-induced secondary electron emission (SEE) process is the fundamental physical process for low temperature plasmas[1, 2]. The surface charge on the dielectric plays an important role in the SEE process, thus influencing the dynamics of the plasma discharge[3]. In this work, compared to the previous model which simplifies the electronic structure and the parameter of surface charges, a more accurate method based on Auger neutralization and the density functional theory (DFT) model is applied to calculate the secondary electron emission coefficient (SEEC) of MgO with accumulated surface charge in the atmospheric pressure helium dielectric barrier discharge (DBD) with nitrogen impurities[4].Based on it, we explore the change of DBD spatiotemporal characteristics when the SEE is affected by the dielectric surface charges. The simulation results indicate that, the phase of discharge moment is advanced and the current amplitude illustrates the obvious reduction when the secondary electron emission process considering the dielectric surface charges. Furthermore, the result in the fluid model based on the accurate SEEC calculation method is compared with using the simplified SEEC calculation method[5]. It turns out that the model based on the simplified SEEC calculation method and the based on our accurate calculation of SEEC all illustrate the uniform discharge, our model shows the more uniform state and the lower electron density. Further analysis reveals that the surface charge influences the secondary electron emission rate on the dielectric surface, thus having an impact on the electron distribution and discharge uniformity. Enhancing the acknowledgment that the dielectric surface charge influences the dynamics of the plasma discharge, this study explores the relationship between the SEE on the surface charge and the evolution of the plasma characteristics with a more accurate theoretical method, and elucidate the impact of the SEE caused by the specific material on the plasma characteristics. It lays a theoretical foundation for further study about the physical process of DBD discharge in the future.

REFERENCES

[1] Haiyun Luo, Junkai Jiao, Kai Liu, Yang Yue, Xinxin Wang, "Characteristics of Shallow Traps in the Dielectric Surface and Their Effects on Diffuse Dielectric Barrier Discharge in Air," IEEE Transactions on Plasma Science, vol. 45, no. 4, pp. 749–753, December 2016.

[2] Gang-Hu Liu, Xiang-Yu Wang, Yong-Xin Liu, Jing-Yu Sun, You-Nian Wang, "Effects of secondary electron emission on plasma density and electron excitation dynamics in dual-frequency asymmetric capacitively coupled argon plasmas," Plasma Sources Sci Technol, vol. 27, no. 6, pp. 064004, June 2018.

[3] Congwei Yao, Sile Chen, Zhengshi Chang, Hai-Bao Mu, Guan-Jun Zhang, "Atmospheric pressure dielectric barrier discharge involving ion-induced secondary electron emission controlled by dielectric surface charges" J Phys D: Appl Phys, vol. 52, no. 45, pp. 455202, August 2019.

[4] HAGSTRUM H D, "Theory of Auger Neutralization of Ions at the Surface of a Diamond-Type Semiconductor" Physical Review, vol. 122, no. 1, pp. 83-113, April 1961.

[5] Shu Zhang, Guang-Yu Sun, Arnas Vol˙cokas, An-Bang Sun, Unveiling the role of dielectric trap states on capacitively coupled radio-frequency plasma discharge: dynamic charging behaviors" Plasma Sources Sci Technol, vol. 30, no. 5, pp. 055007, May 2021.

*This work is supported by the Key Program for International S&T Cooperation Projects of China (Grant No. 2021YFE0114700)

S5-P-019403

INFLUENCE OF DIFFERENT REPETITIVE UNIPOLAR NANOSECOND PULSE EXCITATIONS ON MULTIPLE-CURRENT-PULSE BEHAVIORS AND SPATIAL MODES IN AN ATMOSPHERIC HELIUM DIELECTRIC BARRIER DISCHARGE[¯]

JIANGPING XIAO[1], *DONG DAI*[1]

[1]*School of Electric Power, South China University of Technology, Guangzhou, People's Republic of China*

Dielectric barrier discharges (DBDs) has demonstrated promising application potential in many fields, including energy conversion , material processing, pollution control, and bio-medicine, etc [1,2]. By controlling operating parameters, DBDs driven by a nanosecond pulse (PDBDs) can display different spatiotemporal discharge characteristics, including multiple-current-pulse (MCP) behaviors and abundant spatial modes [3,4]. Therefore, studying the influence of operating application parameters on MCP phenomenon and putting forward the method to eliminate MCP phenomenon have always been an important research to improve the discharge uniformity of DBDs [5]. In our work, we report a systematic numerical study regarding the effect of different repetitive unipolar nanosecond pulse excitations on the MCP behaviors and spatial modes in an atmospheric helium dielectric barrier discharge by using one-dimensional fluid models. The results indicate that the MCP phenomenon exists in both rectangular pulse dielectric barrier discharge (RPDBD) and Gaussian pulse dielectric barrier discharge (GPDBD), and the behavior of MCP leads to axial electron density stratification. While with the same average input power, the MCPs discharge behavior of RPDBD and GPDBD are different, and the current pulse number of the total current in GPDBD is less than that in RPDBD. Further analysis reveals that the above-mentioned difference in MCP discharge performance is caused by the different rise rates of the two pulse voltages. Therefore, the performance of the MCP discharge behavior of the plasma can be affected by adjusting the pulse voltage rise rate, thereby improving the electron density axial distribution in the narrow pulse dielectric barrier discharge. The result of this work is expected to help realize discharge mode manipulation and discharge stabilization in industrial application scenarios.

REFERENCES

[1] Tao Shao, Ruixue Wang, Cheng Zhang, Ping Yan, "Atmospheric-pressure pulsed discharges and plasmas: mechanism, characteristics and applications," High Volt., vol. 3, no. 1, pp. 14–20, March 2018.

[2] Qiao Wang, Dong Dai, Wenjun Ning, Yuhui Zhang, "Atmospheric dielectric barrier discharge containing helium–air mixtures: the effect of dry air impurities on the spatial discharge behavior," J. Phys. D: Appl. Phys., vol. 54, no. 11, pp. 115203, January 2021.

[3] Bo Chen, Tuantao ,Zhang, Zhenyu Tan,Xinxin Song, "Study on multi-peak behavior of pulsed dielectric barrier discharges in atmospheric-pressure helium," Vacuum, vol. 86, no. 12, pp. 1992–1997, May 2012.

[4] Xiaoxi Duan, Feng He, Jiting Ouyang, "Uniformity of a dielectric barrier glow discharge: experiments and two-dimensional modeling," Plasma Sources Sci. Technol., vol. 21, no. 1, pp. 015008,January 2012.

[5] Yuhui Zhang, Wenjun Ning, Dong Dai, Qiao Wang, "Manipulating the discharge pulse number in an atmospheric helium dielectric barrier discharge with multiple current pulses per half cycle," Plasma Sources Sci. Technol., vol. 28, no. 10, pp. 104001, October 2019.

[¯] The work was supported by the Key Program for International S&T Cooperation Projects of China (Grant No. 2021YFE0114700).

S5-P-019502

CHARACTERISTICS OF STATIONARY NEGATIVE CORONA DISCHARGE*

A.O. KOKOVIN, A.V. KOZYREV, V.YU. KOZHEVNIKOV, N.S. SEMENIUK

Institute of High Current Electronics SB RAS, Tomsk, Russian Federation

Corona discharge is a specific type of self-sustained discharge. For its formation, it sufficient to apply high voltage to the electrode with a small radius of curvature. However, there is a range of applied voltage value, at which the corona discharge has an unstable mode [1]. Our previous work [2] has shown that the negative corona discharge in atmospheric-pressure air has four evolution stages including unstable mode, stationary glow and unstable-to-stationary transition. Characteristics of stationary mode is of interest for practical application. In this paper we investigate the characteristics of negative corona discharge's stationary mode and unstable-to-stationary transition.

Gas discharge model is based on the two-moment drift-diffusion hydrodynamic time-dependent model including two continuity equations for the electron component (density & mean energy) and a number of ion continuity equations. The transport equations are coupled to the Poisson's equation in order to consider the electric field self-consistently. The gas discharge diode represents the pin-to-plate structure with small radius of curvature. To take into account the most important reactions in atmospheric air (production of single charged ions, important conversion reactions, various electron energy losses) the simplified plasma-chemical reaction set is implemented in the model. The calculations are performed using the COMSOL Multiphysics software.

Numerical calculations have been shown that the stationary discharge structure consists of a positive space charge (mainly of N_2^+ and O_2^+ ions) layer with characteristic width of $r_{curv}/10$, where r_{curv} is curvature radius of the tip, and a plasma channel consisting mainly of O_2^- and O_4^+ ions. Electric field in plasma channel is almost uniform.

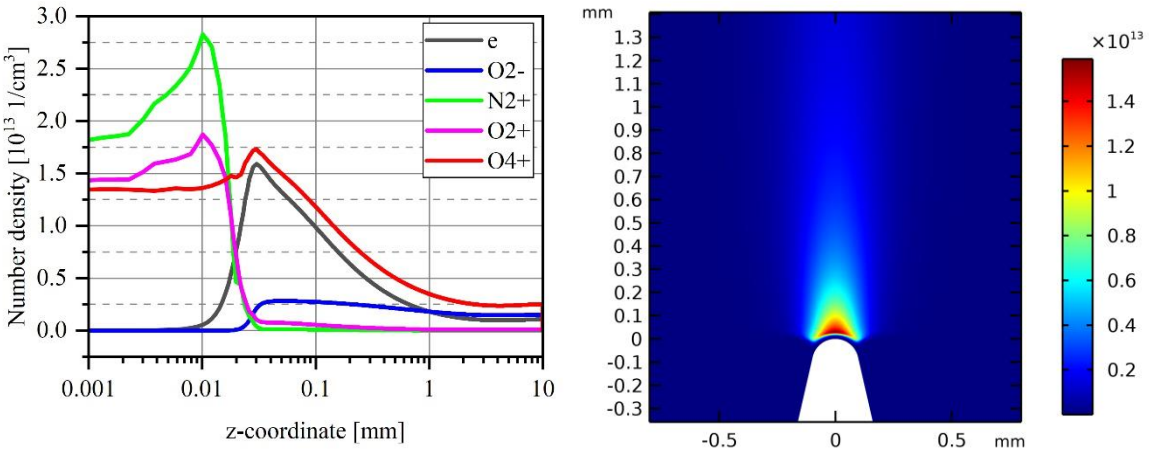

Fig.1. Plasma components number density at symmetry axis (left) and electron number density (right) distributions.

REFERENCES

[1] G.W. Trichel, "The mechanism of the negative point to plane corona near onset," Phys. Rev., vol. 54, pp. 1078, 1938.

[2] A.O. Kokovin, A.V. Kozyrev and V.Yu. Kozhevnikov, "Simulation of negative corona discharge in atmospheric air: from mode of Trichel pulses to stationary discharge", J. Phys. Conf. Ser., vol. 2064, 2021.

* The work was supported by the Russian Science Foundation under grant No. 22-29-00137.

S5-P-020803

UV AND VUV RADIATION OF RARE GASES AND NITROGEN IN DIFFUSE DISCHARGES, FORMED IN AN INHOMOGENEOUS ELECTRIC FIELD*

V.V. KOZHEVNIKOV[1,2], *A.N. PANCHENKO*[1], *V.F. TARASENKO*[1,2]

[1]*Institute of High Current Electronics SB RAS, Tomsk, Russia*
[2]*National Research Tomsk State University, Tomsk, Russia*

The development of high power VUV and UV spontaneous and stimulated radiation sources is an important task associated with the use of such sources in various scientific and industrial applications. In [1,2], studies of xenon radiation in diffuse discharges formed between two needles by voltage pulses of sub-nanosecond duration were carried out and it was confirmed that xenon dimers produces the highest radiation energy in the region of 120–800 nm.

The data obtained are consistent with the results of our previous work [3] and fundamentally differ from the spectral measurements described in [4, 5]. Besides, parameters of the spontaneous and stimulated emission on the nitrogen second positive system and the conditions in which the emission is observed in [5] is very different from the conditions under which this radiation has been usually produced [6, 7].

In this report we carry out additional studies of the VUV and UV emission of diffuse discharges formed by sub-nanosecond voltage pulses in rare gases and nitrogen. As a result, the optimal conditions for lasing on the second positive nitrogen system were determined and the data were obtained on of Ar_2* and Xe_2* emission both in diffuse and contracted discharges.

The results obtained are shown in Fig.1. It is seen that in a pulsed diffuse discharge, the second continuum of rare gas dimers Ar_2* and Xe^*_2 makes the largest contribution to the VUV radiation energy. In the case of N_2 only week VUV lines are evident, while emission on C-B band of N_2 and that of B-X band of CN are dominated in the UV and visible ranges. Powerful lasing at 337 nm was obtained only with 30 cm long blade electrodes.

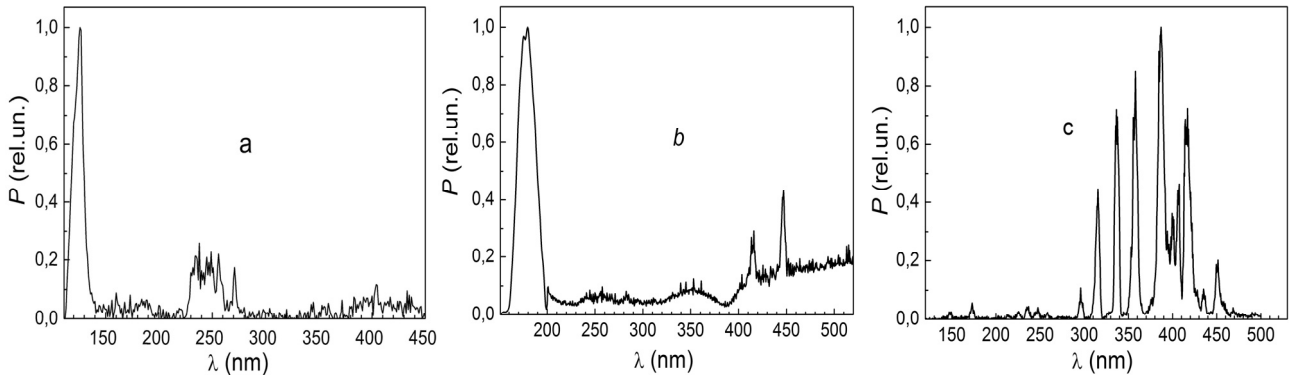

Fig.1. Spectra of diffuse discharges in Ar at 2 Atm (a), Xe at 3 Atm (b) and N_2 at 1 Atm (c). The discharge is formed between two needles by a series of successive voltage pulses with a duration of 0.7 ns, arriving at an interval of 30 ns

REFERENCES

[1] A.N. Panchenko, D.V.Beloplotov, V.V, Kozevnikov, et.al., "Wide emission bands of plasma of a sub-nanosecond discharge in xenon and inaccuracies in their measurements," IEEE Trans. Plasma Sci., vol. 49, no. 5, pp. 1614-1620, May 2021.

[2] A.N. Panchenko, D.V. Beloplotov, V.V. Kozhevnikov, et.al., "Emission of xenon in the spectral range of 120-800 nm upon excitation by diffuse and spark discharges," Quant. Electron., vol. 51, no. 7, pp. 649-654, July 2021.

[3] E.Kh. Baksht, M.I. Lomaev, D.V. Rybka, et.al., "Study of emission of a volume nanosecond discharge plasma in xenon, krypton and argon at high pressures,", Quant. Electron., vol. 36, no. 6, pp. 576-580, June 2006.

[4] V. Baryshnikov, V. Paperny, and A. Chernykh, "Small-sized nanosecond source of powerful wide-band VUV-UV radiation," Proc. Int. Congress on Energy Fluxes and Radiation Effects (EFRE), Tomsk, Russia, pp. 107-110, 2020.

[5] V.I. Baryshnikov, V.L. Paperny, "Picosecond high-current discharge pumping of gaseous media emitting VUV-UV," J. Physics: Conf. Ser., vol. 2064, Article Number 012008, Nov. 2021.

[6] H. Strohwald, H. Salzmann, "Picosecond uv laser pulses from gas discharges in pure nitrogen at pressures up to 6 atm," Appl. Phys. Lett., vol. 28, no. 5, pp. 272-274, March 1976.

[7] V.F. Tarasenko, A.N. Panchenko, D.V. Beloplotov, "Diffuse and volume discharges in high-pressure gas lasers pumped by transverse discharge (A Review)," Plasma Phys. Rep., vol. 46, no. 8. pp. 850–858, Aug. 2020.

* This research was supported by the Ministry of Science and Higher Education of the Russian Federation (agreement no. 075-15-2021-1026 of November 15, 2021).

S5-P-026202

PULSE-PERIODICAL VOLUME DISCHARGES IN CO2–LASER MIXTURES OF SUPERATMOSPHERIC PRESSURE

B.A KOZLOV[1], *D.S. MAKHANKO*[2]

[1]*Ryazan State Radio Engineering University, Ryazan, Russia*
[2]*PLASMA, JSC Research Institute of Gas-Discharge Devices, Ryazan, Russia*

At present, to solve many technological problems, pulses of laser radiation in the infrared range (9–10 μm) with a radiation energy of several tens of millijoules per pulse, a duration of less than 20 nanoseconds, and a maximum pulse repetition rate of up to 20 kHz are required [1].

Such parameters can only be realized at superatmospheric pressure CO2 lasers. The excitation of volume discharges of superatmospheric pressure at pulse repetition rates of units and tens of hertz does not present any particular difficulties. In the repetitively pulsed mode (FRPM $=10^2$–10^4 Hz), the formation of volume pumping discharges becomes a big problem.

The purpose of this work was to determine the conditions for the formation of volume pumping discharges in CO2 laser mixtures at a total pressure of up to 6 atmospheres at pulse repetition rates up to 2.5 kHz in a gap with geometric dimensions V=7.5x0.8x0.8 cm^3.

To initiate a volume discharge in the gap between profiled graphite electrodes, hard VUV radiation was used from a series of corona electrodes installed along the main gap with an interval of 1 cm.

The excitation of the auxiliary and volumetric discharges is carried out from two autonomous pulse generators based on pulse transformers with an adjustable delay between the start moments. If it was necessary to generate voltage pulses up to 160–180 kV, pulse generators were used based on a combination of a two–stage Marx generator and a pulse transformer with a low transformation ratio ($k \leq 4$) [2, 3]. In this case, it is possible to maintain the duration of the leading edge of the voltage pulse at the level of 70–100 nanoseconds and to carry out the breakdown of the gas–discharge gap at the amplitude value of the voltage pulse.

Pulsed hydrogen thyratrons of the TGI2–500/20 and TGI1–1000/25 types were used as switches.

Negative effects from residual voltages in the gas–discharge gap after the pumping current with their negative (relative to the pumping pulse) polarity were eliminated using damping circuits based on high-voltage vacuum diodes and low–inductance resistors [3].

The main results of the work:

1. For the formation of stable volume discharges in CO2–laser mixtures of superatmospheric pressure in the repetitively pulsed regime, it is expedient to make graphite electrodes and multiply the initial ionization level in the main gap.
2. The most efficient and damage–resistant sources of hard VUV radiation for preionization purposes are electrode structures for the formation of pulsed corona discharges.
3. The duration of the volume discharge current should not exceed 30 nanoseconds.
4. In CO2–laser mixtures CO2:N2:He=1:1:8 at a total pressure of up to 6 atmospheres at a pulse repetition rate of 2–2.5 kHz, the specific energy density W=100–150 $mJ \cdot cm^{-3} \cdot Atm^{-1}$ introduced into the volume discharge plasma has been achieved.

REFERENCES

[1] B.A. Kozlov, “TEA–CO2 laser with pulse repetition rates up to 5 kHz for technological applications,” Proceedings - 2016 International Conference Laser Optics, LO 2016. 2016. C. R220.

[2] B.A. Kozkov, V.I. Seredinov, S.A. Pyanchenkov and D.S. Makhanko, “High-voltage pulse generators for effective pumping of super-atmospheric pressure CO2-lasers,” Journal of Physics: Conference Series. The proceeding 14th International Conference "Gas Discharge Plasmas and Their Applications". Institute of High-Current Electronics of the Siberian Branch of the Russian Academy of Sciences. 2019. C. 012010.

[3] B.A. Kozlov and A.Ya. Payurov, "Super-atmospheric CO2 laser with pulse repetition rate up to 2 kHz," Proceedings of SPIE - The International Society for Optical Engineering. XIV International Conference on Pulsed Lasers and Laser Applications, AMPL 2019. 2019. C. 113220F.

S5-P-031801

PARAMETERS OF A PARAXIAL MAGNETIZED BUNCH OF RUNAWAY ELECTRONS*

K.A. SHARYPOV[1], *E.A. OSIPENKO*[1], *V.G. SHPAK*[1], *S.A. SHUNAILOV*[1], *M.I. YALANDIN*[1,2], *N.M. ZUBAREV*[1,2]
[1]*Institute of Electrophysics UB RAS, Ekaterinburg, Russia*
[2]*Lebedev Physical Institute RAS, Moscow, Russia*

It has been recently demonstrated [1] that the flux of run-away electrons (RAEs) in a short (6 mm) air gap with a sharp conical cathode represents a thin divergent layer with a duration of paraxial fraction of no more than 10 ps. Behind the anode collimator with a hole diameter of 1 mm, the current and current density achieve ≈ 200 mA and ≈ 25 A/cm^2, respectively. For excitation of optically active media, radiation effect onto materials, calibration measurements, etc., these parameters can be increased by applying a strong longitudinal magnetic field limiting the transverse dimension of the RAE flow. In this case, when using an extended gas gap, by increasing the distance and time of RAEs acceleration, selecting the instant of their emission and the rate of the voltage rise, electrons acquire an increased energy at the anode. This approach has been demonstrated to obtain magnetized tubular RAE flows [2, 3], and then a conical cathode 30 mm away from the anode was used [4]. This communication presents the methods for diagnosing of a dense paraxial magnetized RAE bunch, its spatiotemporal and energy characteristics.

The instant of RAE emission is estimated from the dispersion minimum for the "delay" between a variable trigger point of the oscilloscope at the front of accelerating voltage and the front of electron current pulse [5]. A collector sensor behind a thin anode foil is used to determine the width of the RAE bunch.. In a longitudinal magnetic field of 1 – 4 T, the change in the bunch radial size requires the use of collector with a diameter of ≈10 mm. The time response of such a sensor and its prototype with a collector diameter of 5 mm was compared [1]. Data are given on the change in the bunch characteristics (amplitude - front - duration of the current pulse at half-height) depending on the recording bandwidth of the oscilloscopes which reached 60 GHz. The data show that paraxial magnetized RAE bunch has the width on the order of 10 ps. After the drift of such a short bunch behind the anode foil, the electron energy distribution was constructed by time-of-flight method. These data do not contradict the presence of a high-energy component of the bunch which was also confirmed by the method of filters that cut off slow particles.

The RAE flow is visualized by the phosphor glow which is photographed with an open shutter. This gives approximate data on the transverse structure of the bunch, since the phosphor glow intensity from the current (charge) and electron energy is not calibrated. However, visualization is indispensable when alignment the electron bunch which is required to determine the charge distribution in the transversal cross section of the bunch using anode diaphragms with the holes of different diameters. Note we are talking about the charge, since the bunch width can be comparable to or less than the time the charge drains from the current probe collector. That is, for an open collector aperture and in the presence of a small diameter collimator, different current durations will be recorded. This circumstance was considered when obtaining the dependences of the bunch current density on radius for several values of a longitudinal magnetic field. For example, at an induction of ≈ 4 T, in a central part of the bunch (0.7 mm in diameter), the current density exceeded 0.6 kA/cm^2.

REFERENCES

[1] G.A. Mesyats, M.I. Yalandin, N.M. Zubarev et al., “How short is the runaway electron flow in an air electrode gap?,” Appl. Phys. Lett., vol. 116, Article Number 063501, 2020.

[2] G.A. Mesyats, K.A. Sharypov, V.G. Shpak et al., “Runaway electron flows in magnetized coaxial gas diodes,” J. Phys.: Conf. Ser., vol. 2064, Article Number 012006, 2021.

[3] G. Mesyats, V. Rostov, K. Sharypov et al. “Emission Features and Structure of an Electron Beam versus Gas Pressure and Magnetic Field in a Cold-Cathode Coaxial Diode,” Electronics, vol. 11, no.2, Article Number 248, 2022.

[4] G.A. Mesyats, E.A. Osipenko, K.A. Sharypov et al., “An ultra-short dense paraxial bunch of sub-relativistic runaway electrons,” IEEE Electron device Lett., doi: 10.1109/LED.2022.3155173

[5] M. I. Yalandin, A. G. Reutova, K. A. Sharypov et al. “Moment of Injection of Runaway Electrons at the Front of Accelerating Pulse in Air-Filled Diode with Inhomogeneous Field: From Instability to Determinacy,” Tech. Phys. Lett. 2010, vol. 36, no. 9, pp. 830–833, 2010.

* In the part of development and calibration of a fast-response e-bunch probe, the work was supported by the RSF under Project 21-19-00260..

S5-P-033803

QUASI-VOLUME IONIZATION AT THE FINAL STAGE OF STREAMER DEVELOPMENT IN A SHARPLY INHOMOGENEOUS ELECTRIC FIELD*

D.V. BELOPLOTOV, V.F. TARASENKO, D.A. SOROKIN

Institute of High Current Electronics SB RAS, Tomsk, Russia

Streamer discharges have been studied for a very long time [1, 2]. They are formed at high gas pressures, in particular at atmospheric pressure. Studies of the initial stage of nanosecond diffuse discharges in an inhomogeneous electric field by high-speed methods have shown that a large diameter streamer develops in the discharge gap. It was shown that the streamer velocity changes as it develops and is associated with a change in its diameter and a reduction in the distance to the opposite electrode [3]. It was found that in the final stage, the streamer velocity rises sharply. Uunder some conditions, the propagation velocity of the streamer front can reach practically the light speed [4]. In this work, we studied in the details this stage of the streamer development in air and nitrogen (to exclude the photoionization) at different pressures using a streak camera and an original technique based on measuring a displacement current caused by the streamer. Under these conditions, the initiation of the streamer occurred during the generation of runaway electron (RE) beam with a duration of tens of picoseconds. The waveforms of electrical parameters were accurately synchronized with the streak images. It is shown that REs are generated at the start of the ionization processes in the vicinity of the pointed electrode. The RE current is detected even if the streamer stops somewhere in the middle of the gap. It was found that a quasi-volume ionization (QVI) is observed at the final stage of streamer development. The size of the QVI region depends on the gas pressure. It is assumed that the reasons for the change in the nature of the breakdown are the development of a large-diameter streamer (on the order of the gap length) and the preliminary ionization of the gas by REs.

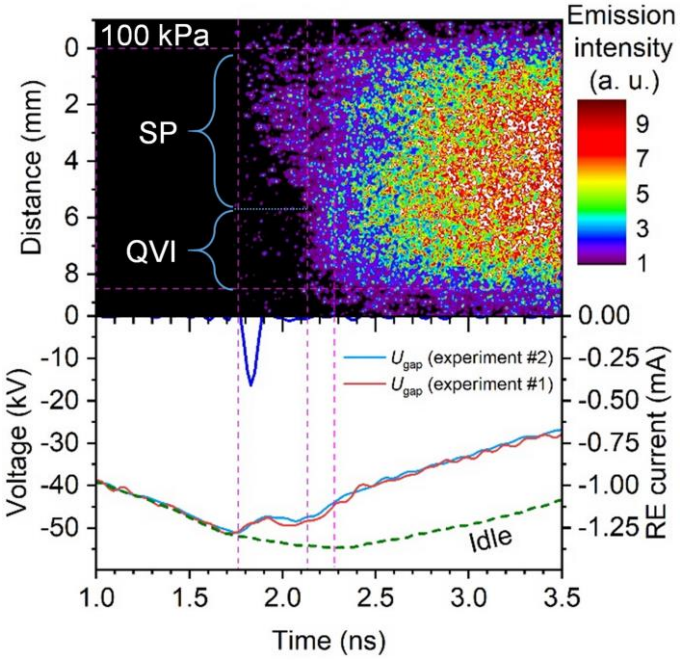

Fig.1. Streak-image of the discharge formation in nitrogen and corresponding waveforms of voltage and runaway electron current.

REFERENCES

[1] I. Langmuir, C.G. Found and A.F. Dittmer, "A new type of electric discharge: The streamer discharge," Science, vol.60, Article Number 392, 1924.

[2] Y.P. Raizer, Gas discharge physics, Berlin, Springer-Verlag, 1991.

[3] D.A. Sorokin, V.F. Tarasenko, D.V. Beloplotov et al., "Features of streamer formation in a sharply non-uniform electric field," J. Appl. Phys., vol.125, Article Number 143301, 2019.

[4] D.V. Beloplotov, D.A. Sorokin, M.I. Lomaev et al., "Formation of a Negative Streamer in a sharply nonuniform electric field and the time of generation of runaway electrons," Russ. Phys. J., vol.62, Article Number 1967, 2020.

* The work was supported by the Ministry of Science and Higher Education of the Russian Federation within Agreement no. 075-15-2021-1026

S5-P-034402

INVESTIGATION OF FEATURES OF AN ABNORMAL DISCHARGE, A HOLLOW CATHODE DISCHARGE, AND AN OPEN DISCHARGE FOR EXCITATION OF LASERS ON SELF-LIMITED TRANSITIONS

E.V. BELSKAYA, P.A. BOKHAN, P.P. GUGIN, D.E. ZAKREVSKY, T.A. ZIRENKO

Rzhanov Institute of Semiconductor Physics SB RAS, Novosibirsk, Russia

Different types of discharges are used to create population inversion in gas lasers: an abnormal glow discharge (AD), hollow cathode discharge (HCD), an open discharge (OD). In order to compare and determine the most effective type of discharge for excitation of lasers at self-terminated transitions, the operating ranges, achievable parameters and features of populating the metastable state of the helium atom as a test laser at a self-terminated transition were investigated.

The most efficient way to excite lasers at self-terminated transitions is to pump them with an electron beam due to the large value of the electron excitation cross section of the first resonant level, which is usually the upper laser level. The power of laser radiation is proportional to the pressure of the working gas, respectively, operation at high pressures is preferable.

All discharges are realized in cuvettes of close geometry: the active area is an open cylinder with diameter D=33 mm and length L=60 mm. In AD the electrodes are two steel rings with inner diameter D, with the distance between them equaled to L. In OD the cathode is a cylinder of silicon carbide with diameter D. As an anode in the OD a metal grid with a diameter of 27 mm was installed coaxially with the cathode. The cathode in HCD is a silicon carbide cylinder with diameter D, the anode is metal rings located at a distance of 12 mm on both sides of the cylindrical cathode.

Studies in the pulse mode of the current-voltage dependences at different helium pressures demonstrated the following features:

1) the volumetric, uniform character of the luminescence was observed at a significantly larger pressure range in the OD (up to 50 Tor) compared to the HCD and to the AD (up to 7 Tor).
2) the discharge current did not depend on the helium pressure in a wide pressure range $I \propto U^{\alpha}$ in OD and HCD. The current was determined by both gas pressure and voltage $I \propto U^{\alpha} p^{\beta}$ in AD. The dependence of the current only on the voltage at different pressures suggests that the mechanisms of electron generation differ from those in the anomalous discharge.

The relative magnitude of the metastable state (MS) occupancy of the helium atom as a test medium was investigated by recording the absorption in the discharge cuvettes of sample laser radiation at the self-terminated He transition ($2^1P_1^0 - 2^1S_0$) with λ=2.058 nm. Since the absorption of radiation occurs at the He ($2^1S_0 - 2^1P_1^0$) transition, the absorption coefficient, k, determined from the ratio of intensities of incoming and outgoing radiation: $\frac{I_{out}}{I_0} = e^{kL}$, is proportional to the population difference of the metastable He (2^1S_0) level (MS) and resonant one. It was obtained experimentally that the absorption coefficient and, consequently, the MS population observed in AD is much higher than in other types of discharge. It was obtained that the smallest MC population is observed in OD at the same excitation parameters of the cuvettes.

S5-P-041002

CORRELATION BETWEEN X-RAY, MICROWAVE, NEAR-ULTRAVIOLET, VISIBLE, AND IR EMISSIONS FROM A HIGH-VOLTAGE DISCHARGE IN A LONG AIR GAP*

E. PARKEVICH[2], *A. KHIRIANOVA*[2], *T. KHIRIANOV*[2], *I. BAIDIN*[2], *K. SHPAKOV*[2],

A. RODIONOV[2], *YA. BOLOTOV*[1,2], *V. RYABOV*[2], *YU. KURILENKOV*[3], *A. OGINOV*[2]

[1]*Moscow Institute of Physics and Technology, Institutskiy Pereulok 9, Dolgoprudny, Moscow Region 141700, Russia*
[2]*P. N. Lebedev Physical Institute of the Russian Academy of Sciences, 53 Leninskiy Prospekt, Moscow 119991, Russia*
[3]*Joint Institute for High Temperatures, Russian Academy of Sciences, Izhorskaya str. 13/2, Moscow 125412, Russia*

The study is focused on obtaining new data in the field of electromagnetic emissions produced by laboratory discharges and revealing the mechanisms of the intense x-ray and microwave emissions. We investigate the development of a laboratory discharge initiated in a ~50 cm air gap by applying a ~1 MV pulse (negative polarity) with a ~1 μs duration and a rise time of about several hundred nanoseconds. The discharge formation is accompanied by hard x-ray (~10 keV–1.5 MeV), low- (~10–100 MHz) and high- (~1–6 GHz) frequency radio, near-ultraviolet (~300–400 nm), visible (within ~450–600 nm), and IR (>700 nm) emissions which we register in the experiments together with the short-exposure images of the discharge glow, employing a sCMOS gated intensified camera (with the gate of ~55–60 ns). We discuss the temporal and spectral characteristics of the detected emissions, as well as investigate their correlation with the evolution of the discharge morphology. The energy spectra of x-ray flashes and their anisotropy are presented as well.

We show that the appearance of an initial cathode corona and propagating streamers coincides with the instant the intense near-ultraviolet emission starts. It is established that the streamer propagation towards the anode is accompanied by LF-radio emissions only. The intense x-ray and high-frequency radio emissions can appear almost synchronously in the discharge but only when a complex net of countless plasma channels forms and spans the entire discharge gap. The channel formation is closely related with the intense development of multiple streamers triggered after very fast formation of the cathode-directed streamers. Within the x-ray and microwave generation, multiple streamers develop from the electrodes and, probably, inside the discharge bulk, but without any leader formation which starts later after the instant the x-ray and microwave emissions vanish. Intense visible and IR emissions are registered only after the gap breakdown. The discharge formation turned out to have a step-wise character that correlates with temporal grouping x-ray and HF-radio bursts. We discover a complex spectral and temporal structure of the HF-radio emission. This type of the electromagnetic emission appears as multiple bursts, with their durations and the delay between neighboring bursts both being shorter than 1 ns. By employing the developed techniques for obtaining data on the spectral and temporal characteristics of HF-radio emissions, we find that a single burst of the HF-radio emission appears as a complex temporal process driven by the superposition of many subprocesses, characterized by different durations and frequencies. Indeed, the higher the frequency describing the microwave burst is, the shorter the time interval is related with this frequency.

Our findings provide a comprehensive temporal map of the electromagnetic emissions produced by a high-voltage discharge. The study and data obtained can be helpful in developing consistent models describing the mechanisms of the high-energy and microwave emissions in both laboratory and atmospheric discharges.

REFERENCES

[1] E.V. Parkevich, et al. Streamer formation processes trigger intense x-ray and high-frequency radio emissions in a high-voltage discharge. Submitted to Physical Review E. March, 2022.

* The work was supported by the Russian Science Foundation (grant no. 19-79-30086). The analysis of the microwave spectrums was funded by the grant of the Russian Foundation for Basic Research (no. 20-08-01156).

S5-P-041703

ATMOSPHERIC PRESSURE GAS DISCHARGE EXCITED BY NANOSECOND PULSES AT 100 KHZ [1]

P.A. BOKHAN[1], N.A. GLUBOKOV[2], P.P. GUGIN[1], M.A. LAVRUKHIN[1], E.V. MILAKHINA[1,2], D.E. ZAKREVSKY[1,2]

[1] *Rzhanov Institute of Semiconductor Physics SB RAS, Novosibirsk, Russia*
[2] *Novosibirsk State Technical University, Novosibirsk, Russia*

Studies of atmospheric pressure gas discharges were carried out in order to create gas-discharge high-energy devices (reactors) for dissociation of complex gaseous chemical compounds and neutralization of environmentally harmful volatile compounds. The idea was to use the physical and technical capabilities of new developed switching devices (eptrons) to generate high-voltage (up to 50 kV) short pulses (10–30 ns) with nanosecond edge (1-2 ns), capable to function at high pulse repetition frequencies (up to $f \sim 100$ kHz) to study the conditions of volume current flow in gases up to atmospheric pressure.

Two types of the cells were used in the experiments. In the first one a 5 mm discharge gap was formed by a cathode made of $BaTiO_3$ or SiC ceramics and a metal anode in the form of a ball with diameter of 26 mm. Another one had a planar design with two discharge gaps separated by a drift space, in which one-directional or counter-propagating electron beams could be formed. A gas-discharge switch (eptron) with an additional pulsed pre-ionizing discharge between cathodes and additional grid electrodes was used for rapid voltage rise. Power supply provided pulses up to 40 kV with leading edge up to 1 ns on the active load. The experiments were carried out in the burst operation mode with a burst repetition frequency of 5 Hz and a pulse repetition frequency in the burst of 1-100 kHz.

In the first cell pure helium at $p_{He} = 1$ atm was used as operating gas. At excitation parameters U= 20–25 kV and f = 1–20 kHz the discharge had an non-homogeneous form and represented a stable set of separate plasma channels. Increasing the frequency f and the number of pulses in the burst up to 200 led to the fact that from f > 50 kHz up to the maximum f = 100 kHz the discharge was spatially uniform. Decreasing of the discharge capacity led to the uniform mode of the current flow in the whole investigated range of pulse repetition frequencies $f \approx$ 10-100 kHz. Fig.1 shows photos of the discharge glow for the helium pressure p_{He} in the range of 20-1000 mbar. Typical oscillograms of U and I pulses are shown in Fig. 2. It can be seen that for $U = 20$ kV the voltage pulse edge is ~ 2 ns, current $I \sim 250$ A (rise rate 25A/ns), and I increases with increasing gas pressure.

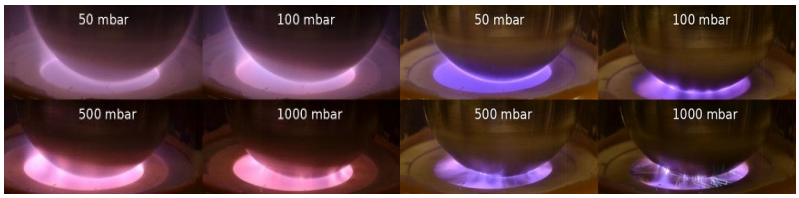

Fig.1 Photographs of discharge glow at different pressures of helium (a), nitrogen (b).

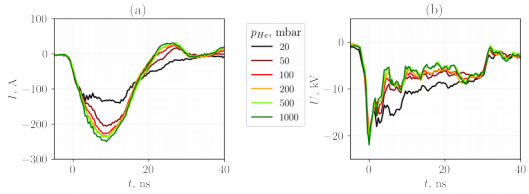

Fig.2 Oscillograms of current (a) and voltage (b) at different nitrogen pressures

Similar experiments with nitrogen as operating gas demonstrated the homogeneous form of the discharge up to 100 mbar with the following stochastic nature of the gas discharge, with I weakly depending on the gas pressure. The oscillograms of U and I during electrode short-circuiting and in the case of discharge show that the short-circuiting current is more than 2 times higher than the discharge current, which indicates the absence of the discharge spark phase.

The experiments in the second cell demonstrated that spatially homogeneous discharge in air is stable up to p ≈ 0.5 atm for the case when one acceleration gap is used (one-directional electron beam). In case of applying 2 acceleration gaps (counter-propagating electron beams), the discharge is stable up to p = 1 atm. At $f = 90$ kHz, stable discharge burning was achieved with average power during the burst of 3.5 kW, which corresponds to input power per unit volume ~18 kW/cm^3.

[1] The work was supported by the Russian Science Foundation (project No. 19-19-00069).

S5-P-049301

THE FEATURES AND INSTABILITIES OF PLASMA MICROSTRUCTURES OCCURING AT AN EARLY STAGE OF AIR DISCHARGE FORMATION NEAR THE SURFACE OF THE POINT ELECTRODE.

A.I.KHIRIANOVA[1], T.F. KHIRIANOV[1], E.V.PARKEVICH[1]

[1]The Lebedev Physical Institute of the Russian Academy of Sciences, Moscow, Russian Federation

When registering an object by interferometry, the phase raid of the probing radiation is restored both in the frame with the object under study, in our case an air discharge, and in a similar frame without an object, in our case the electrode interval before the discharge occurs. The difference between the two-dimensional phase raid maps with and without the object forms a phase raid map on the object under study. For the most significant one-dimensional slices of the obtained map, using the inverse Abel equation, the density of the object is restored, assuming the symmetry of the one-dimensional slice. In order to improve the accuracy of determining the phase raid in the frame, regardless of the distance from the lines of intensity extremes, the processing of the original frame was carried out in accordance with the algorithm until the unambiguous correspondence of the brightness of each point of the frame to the phase raid in it was established [1].

In the electrode gap, 1-3 ns after the beginning of the development of the discharge in the near-cathode region, a phase object of spherical geometry is registered, with a center on the surface of the electrode (the center of the sphere coincides with the border of the shadow of the cathode tip with an accuracy of 3 μm) and a radius of 35-60 μm. The surface of the sphere is formed by a constant phase line. Perpendicular to the spherical surface, as a rule, 1-3 filaments with a diameter of 15-30 μm develop, further propagating in the direction of the anode. The application of the inverse Abel transformation to the phase raid slices on the sphere and filaments shows that these objects coincide in density in the adjoining zones with an accuracy of 25% and are 1-3e19 cm-3. These data lead us to the assumption that at the initial stage of the development of the discharge, cathode emission occurs, forming a spherical expanding plasma object, from the surface of which, due to instabilities, dense plasma filaments develop.

The study was supported by the grant of the Russian Foundation for Basic Research (no. 20-08-01156).

REFERENCES

[1] Gurov I., Volkov M. ”Evaluation of complicated fringe patterns by the nonlinear data-dependent fringe processing method”. IEEE Cat. No. 04CH37510, Vol. 2, p. 1333–1337 , 2004.

S5-P-049601

ULTRA-WIDEBAND RADIO INTERFEROMETRY FOR MAPPING THE SOURCES OF THE MICROWAVE FLASHES IN THE GHZ FREQUENCY RANGE

I.S. BAIDIN, A.V. OGINOV, E.V. PARKEVICH, K.V. SHPAKOV

P.N.Lebedev Physical Institute RAS, Moscow, Russian Federation

The paper presents the results of ultra-wideband radio interferometry performed for the first time using 3 Vivaldi coplanar type antennas operating in the 1-6 GHz band. The system has been tested on an atmospheric high-current laboratory spark discharge channel in the long gap (~ 60 cm). The high voltage generator can generate electrical pulses with voltage magnitude up to 1.2 MV and current up to 12 kA. The antennas are located at a distance of 3-4 m from the discharge gap and register microwave radiation in various projections. The microwave radiation observed in the initial stage of discharge (before the main current flows) has the character of multiple short bursts. For the first time, localization of these flashes was carried out not only in time, but also in space using correlation analysis of signals from antennas. The features of the geometry used and the characteristics of the recording equipment make it possible to localize the sources of microwave flashes with an accuracy of 6 cm. A map of the observed microwave radiation is constructed. It can be noted that the most intense and well-correlated flashes of microwave radiation come from the near-cathode and near-anode discharge zones at a distance of about 10 cm from the electrodes. The observed effects are in good agreement with the theoretical assumptions and serve as a reliable basis for further research in this area.

The work was partially supported by the RFBR grant 20-08-01156 A

REFERENCES

[1] Baidin, I.S., Rodionov, A.A., Oginov, A.V. et al. LOCALIZATION OF RADIO EMISSION SOURCE IN THE INITIAL PHASE OF THE SPARK DISCHARGE. Bull. Lebedev Phys. Inst. 48, 349–352 (2021). https://doi.org/10.3103/S1068335621110038

[2] Байдин И.С., Огинов А.В., Паркевич Е.В. Сверхширокополосная антенна для регистрации радиоизлучения в начальной фазе высоковольтного лабораторного атмосферного разряда. ЖТФ Т. 91, Вып.12, с. 1910-1915 (2021) DOI: 10.21883/JTF.2021.12.51756.12-21

[3] Montanyà, J., Fabró, F., March, V., van der Velde, O., Solà, G., Romero, D., & Argemí, O. (2015). X-rays and microwave RF power from high voltage laboratory sparks. Journal of Atmospheric and Solar-Terrestrial Physics, 136, 94-97.

S6-O-005101

STUDY OF DIFFUSION HIGH MAGNETIC FIELDS INTO PLANE AND CYLINDRICAL CONDUCTORS*

P.A. RUSSKIKH

Institute of Electrophysics UB of RAS, Ekaterinburg, Russia

Diffusion of high magnetic field has been studying since the last century. It has a number of applications: electromagnetic acceleration of solids, electromagnetic energy transport through vacuum transmission lines, and compressing metal shells with single-turn solenoids (inductors). The main problem of latter is low durability as they are used in highly strain conditions. High pulsed magnetic fields with an amplitude of 50 T and a half-wave duration of 5-20 microseconds cause strong heating of the surface, thermomechanical stresses, deformations and finally breakdown. A possible solution was suggested in [1], where the author without considering thermal effects showed that in the material with resistivity decaying exponentially by depth Joule heating diminishes remarkably. Detailed analysis of how gradient resistivity of the material influences on possible durability is the aim of the current work.

Simulation was carried out in both plane and cylindrical one-dimensional geometries. Corresponding magnetic diffusion equations coupled with heat flux equations were solved. Mechanics processes were described with Hooke's law and yield criterion von Mises. Temperature dependence of resistance and tensile strength were approximated by linear function. Spatial resistivity was assumed as three parameters function. The first parameter is the ratio of the surface and bulk resistance ρ^*/ρ_{bulk}, the second is depth of modified layer x_c and the third N_γ is sharpness of the profile. Sharpness determines whether profile is close to exponential or to step form. Other parameters of the material were assumed constant. The magnetic field at the inner boundary of the specimen was set as a decreasing sine. The amplitude of the magnetic field at the inner boundary B_{th} that does not result in plastic deformation at the cooling stage was used as a criterion for estimating durability.

The simulation shows that under the same impact material in the radial geometry, especially with small inner radius, has lower B_{th}, since current and Joule heating concentrate at the inner surface. Therefore, the smaller radius of the specimen the resistive material at the surface must be to shift destructive impact into the depth and distribute it. The influence of the main parameters of the material on B_{th} was studied as well. The temperature at which plastic deformation occurs was obtained analytically for cylindrical and plane geometries.

REFERENCES

[1] G.A. Shneerson, Fields and transients in equipment superstrong currents, Leningrad: Energoizdat Publ., 1981.

* The work was supported by RFBR grants No. 20-58-00029 and No. 20-21-00050.

S6-O-005202

MODELING OF PLASMA DYNAMICS PARAMETERS OF MAGNETOPLASMA COMPRESSOR*

V.V. KUZENOV, S.V. RYZHKOV, N.V. BATRAK, N.G. KOPALEISHVILI

Bauman Moscow State Technical University, 2 Baumanskaya Street, 5, 1, Moscow, 105005, Russia, E-mail: svryzhkov@bmstu.ru, +7(499)263-65-70

The prospect of using magnetoplasma compressor (MPC) in compact radiation sources and pulsed plasma jets to reduce their mass and size characteristics, the formulation of ways to improve their physical and technical characteristics and control the integral output of broadband radiation is justified by a large number of publications [1-5]. High velocity jets formed by magneto plasma compressor can be used for fusion devices, aeronautics, mechanical and power engineering systems [7-12]. Thermal modeling of radiation-magneto plasma dynamic processes of powerful electric discharge sources is presented.

The paper contains a mathematical model of MPC discharges in gases for a wide range of changes in the main parameters and the surrounding gas environment. This model is based on a nonstationary axisymmetric two dimensional system of equations for viscous one-temperature radiation plasma dynamics. The numerical solution of the nonstationary two dimensional radiation gas dynamic model developed in the work is based on the method of splitting into physical processes and spatial directions. The developed computational code uses a multi-block multigrid technology for calculations on nonorthogonal structured grids. On the basis of the performed computational studies, quantitative data were obtained on the modes, structures, and plasma dynamics of the end type MPC for the transient power - power mode of the MPC discharge in gas [13-19].

REFERENCES

[1] *Shanenkov I.I., Sivkov A.A., Ivashutenko A.S., et al.* // Journal of Alloys and Compounds. – 2019. – V. 774. – P. 637-645.
[2] *Kuzenov V.V., Ryzhkov S.V., Starostin A.V.* // Russian Physics Journal. – 2019. – Vol. 62.
[3] *Ryzhkov S.V., Kuzenov V.V.* // ZAMP. – 2019. – Vol. 70. – P. 46.
[4] *Kuzenov V.V., Ryzhkov S.V.* // Laser Physics. – 2019. – Vol. 29. – P. 096001.
[5] *Kuzenov V.V., Ryzhkov S.V.* // Journal of Physics: Conference Series. – 2017. – V. 815. – P. 012024.
[6] *Ryzhkov S.V., Kuzenov V.V.* // International Journal of Heat and Mass Transfer. – 2019. – Vol. 132. – P. 587-592.
[7] *Kuzenov V.V., Ryzhkov S.V.* // Applied Physics. – 2014. – No. 3. – P. 26-30.
[8] *Ryzhkov S.V.* // Prikladnaia Fizika. – 2010. – No. 1. – P. 47-54.
[9] *Kuzenov V.V., Ryzhkov S.V.* // Physics of Plasmas. – 2019. – Vol. 26. – P. 092704.
[10] *Kuzenov V.V., Ryzhkov S.V.* // Journal of Physics: Conference Series. – 2017. – V. 830. – P. 012124.
[11] *Kuzenov V.V., Ryzhkov S.V., Frolko P.A.* // Journal of Physics: Conference Series. – 2017. – V. 830. – P. 012049.
[12] *Chirkov A.Yu., Ryzhkov S.V., Bagryansky P.A., Anikeev A.V.* // Plasma Physics Reports. – 2012. – V. 38. – P. 1025-1031.
[13] *Kuzenov V.V., Ryzhkov S.V.* // Journal of Enhanced Heat Transfer. – 2018. – V. 25 (2). – P. 181-193.
[14] *Kuzenov V.V., Ryzhkov S.V.* // Physics of Atomic Nuclei. – 2018. – Vol. 81, No. 10. – P. 1460-1464.
[15] *Ryzhkov S.V., Chirkov A.Yu.* Alternative Fusion Fuels and Systems. – 2019. – CRC Press, Taylor & Francis Group. – 200 p.
[16] *Kuzenov V.V., Ryzhkov S.V.* // High Temperature. – 2021. – V. 59.
[17] *Kuzenov V.V., Ryzhkov S.V.* // Physica Scripta. – 2021. – V. 96. – P. 125613.
[18] *Kozlov A.N.* // Contrib. Plasma Phys. – 2020. – V. 60. – P. e201900174.
[19] *Kuzenov V.V., Ryzhkov S.V., Gavrilova A.Yu. et al.* // High Temperature Material Processes. 2014. – V. 18. Iss. 1-2. P. 119-130.

* The work was partially supported by the Russian Ministry of Science and Higher Education (Project No. 0705-2020-0044).

S6-O-006701

ON THE INFLUENCE OF ELASTIC SCATTERING COLLISIONS ON THE FORMATION OF THE INITIAL STAGE OF VACUUM BREAKDOWN*

V.Y. KOZHEVNIKOV[1], A.V. KOZYREV[1], A.O. KOKOVIN[1], N.S. SEMENIUK[1]

[1]Institute of High Current Electronics, Tomsk, Russia

The discovery of explosive electron emission posed a number of actual problems for theoretical and experimental plasma physics [1]. One of the fundamental problems is directly related to the study of fast processes at the initial stage of vacuum gap breakdown. An extensive explosive electron emission experimental base allows to unequivocally state that the cathode plasma expansion from the cathode to the anode occurs with high velocities of about $\sim 2 \cdot 10^6$ cm/s, which significantly exceeds typical thermal velocities of initial explosion plasma components [2]. If we consider the cathode plasma as a whole, then the question arises: what exactly leads to the positive metal ions accelerations from the cathode towards anode? This phenomenon is known also as an “anomalous” ions transport [3].

In a number of researches, it was shown that "anomalous" ions acceleration is caused by the electrodynamic forces. This explanation is called an electric potential "hump" hypothesis [4]. However, some other reasons can potentially contribute to "anomalous" ions acceleration that are not related to electrodynamics [4]. In particular, it is believed that electron-ion and ion-ion elastic scattering collisions provide the directed velocity to ions in order to move towards anode.

In the paper [5], it was shown for the first time based on a self-consistent kinetic model of a multicomponent plasma that the "anomalous" ion dynamics is accomplished by the appearance of a nonstationary electric potential “hump”, which leads to a continuous acceleration of ions towards anode. In addition, it was shown that this process is essentially collisionless. In further papers (e.g. [6]) the same mechanism was also observed with respect to a multi-component cathode plasma. Thus, it is argued that non-electrodynamic processes play a secondary role or simply insignificant during the cathode plasma expansion into the gap. In the present work, the contribution of ion-ion collisions to the "anomalous" character of ion acceleration and the overall current transfer at the initial stage of vacuum breakdown formation is elucidated.

In this paper, we include elastic collisions between ions in previous collisionless kinetic model in the form of collision integral in BGK approximation. This model’s improvement allows to elucidate the collisional effects between ions on the overall picture of the initial stage of vacuum breakdown development.

REFERENCES

[1] G. A. Mesyats and D. I. Proskurovsky, “Pulsed Electrical Discharge in Vacuum,” 1989.

[2] E. A. Litvinov, G. A. Mesyats, and D. I. Proskurovskiĭ, “Field emission and explosive electron emission processes in vacuum discharges,” Soviet Physics Uspekhi, vol. 26, no. 2, pp. 138–159, Feb. 1983.

[3] A. A. Plyutto, "Acceleration of positive ions in expansion of the plasma in vacuum," Zhur. Eksp. Teor. Fiz. (USSR), vol. 39, pp. 1589-1592

[4] A. Anders, “Ion energies in vacuum arcs: A critical review of data and theories leading to traveling potential humps,” 2014 International Symposium on Discharges and Electrical Insulation in Vacuum (ISDEIV), Sep. 2014.

[5] V. Y. Kozhevnikov, A. V. Kozyrev, and A. O. Kokovin, “The problem of ‘anomalous’ ion transport in high-current vacuum discharges,” Journal of Physics: Conference Series, vol. 2064, no. 1, p. 012025, Nov. 2021.

[6] V. Kozhevnikov, A. Kozyrev, A. Kokovin, and N. Semeniuk, “The Electrodynamic Mechanism of Collisionless Multicomponent Plasma Expansion in Vacuum Discharges: From Estimates to Kinetic Theory,” Energies, vol. 14, no. 22, p. 7608, Nov. 2021.

* The work was carried out within the framework of the state assignment of the Ministry of Science and Higher Education of the Russian Federation on the topics FWRM-2021-0007, FWRM-2021-0014.

S6-O-006702

A QUASINEUTRAL EXPANSION OF PLASMA BUNCH INTO VACUUM: BEYOND THE "PLASMA APPROXIMATION"*

V.Y. KOZHEVNIKOV[1], *A.V. KOZYREV*[1], *A.O. KOKOVIN*[1]

[1]*Institute of High Current Electronics, Tomsk, Russia*

"The plasma approximation" is known to be applicable to low-frequency and steady-state phenomenon, popular among plasma scientists in various fields [1]. Sometimes more appropriable term is used here "the plasma condition" [2], i.e. the number of electrons in a Debye sphere is large enough to effect charge shielding. But the utilizing it leads to inconsistencies in the equation of motion and prevents a proper, field-theoretic treatment of a condensed matter in the plasma state. This circumstance takes place due to the fact that if the plasma reaches a quasi-neutral state $n_e \approx n_i$, its space charge is approximately equal to zero $\rho \approx 0$. According to Poisson equation this leads to $\boldsymbol{E} = 0$. But the "plasma approximation" states that $\boldsymbol{E} \neq 0$ and the electric field can be found elsewise [1]. Such a separation of the initially consistent solution of plasma and field equations in the most cases leads to ambiguous multivalued interpretation of the electric field definition. That is the main methodological drawback of the "plasma approximation".

One of the fundamental problems where the "plasma approximation" seems to be the most appropriate choice is the problem of a spatially inhomogeneous quasi-neutral bunch expansion of dense plasma into a vacuum gap. The process in this case is essentially nonstationary. It is accompanied by considerable cooling of electrons and therefore the study of this process requires special approaches. The analytical investigations of this problem have been carried out both in terms of phenomenological hydrodynamic [4] and kinetic models [5].

This paper is aimed to clarify the details of a two-component plasma bunch expansion into free space by numerically solving the system of Poisson-Vlasov equations. Its main purpose is to show the features of this process without using the "plasma approximation". For simplicity, but without loss of generality, we solve the problem of plasma expansion in a one-dimensional Cartesian spatial configuration. The calculation results are compared with the exact solutions of the Vlasov equations with the "plasma approximation" taken from paper [5].

REFERENCES

[1] F. F. Chen, Introduction to Plasma Physics and Controlled Fusion: Springer, 1984, ISBN 0306413329

[2] K. Nishikawa and M. Wakatani, Plasma Physics: Basic Theory with Fusion Applications: Springer, 2000

[3] A.V. Gurevich, L.V. Pariskaya, and L. P. Pitaievskii, "Self-similar motion of rarefied plasma," Sov. Phys. JETP 22, 449, 1966

[4] C. Sack and H. Schamel, "Plasma expansion into vacuum — A hydrodynamic approach," Physics Reports, vol. 156, no. 6, pp. 311–395, Dec. 1987.

[5] D. S. Dorozhkina and V. E. Semenov, "Exact Solution of Vlasov Equations for Quasineutral Expansion of Plasma Bunch into Vacuum," Physical Review Letters, vol. 81, no. 13, pp. 2691–2694, Sep. 1998.

* The work was carried out within the framework of the state assignment of the Ministry of Science and Higher Education of the Russian Federation on the topics FWRM-2021-0007, FWRM-2021-0014.

S6-O-010005

NUMERICAL SIMULATION OF INDIVIDUAL CELL OF THE ELECTRON BEAM SOURCE WITH A PLASMA CATHODE

V.T. ASTRELIN[1], *I.V. KANDAUROV*[1], *V.P. TARAKANOV*[2]

[1]*Budker Institute of Nuclear Physics SB RAS, Novosibirsk, Russia*
[2]*Joint Institute for High Temperatures, Moscow, Russia*

Investigations on the formation of an electron beam in a source with a plasma cathode [1] were recently carried out at the INP SB RAS. A source with a multiaperture diode EOS was used to generate the beam.

Previous experimental and theoretical studies of plasma emitters of electrons [2] made it possible to obtain a qualitative and semi-quantitative physical picture of the processes for different emission regimes. The use of numerical simulation for the quantitative calculation of plasma emission sources of electron beams was difficult due to the lack of codes adequate to the problem. In most cases, simulations are performed using programs for calculating ion beams in the positron simulation mode [3, 4, etc.]. These, as well as existing codes for modeling electron sources, for example [5, 6] assume that electron emission occurs from an open plasma boundary. But, as a rule, in beam sources used for applications, plasma emitters operate in the regime of layer emission stabilization [2, p.46]. This mode was generally not considered in numerical simulation codes. Therefore, it seems necessary to check the applicability of any of the available universal codes for modeling these modes.

For this purpose, the KARAT code developed on the basis of the "particles in cells" (PIC) method [7] is considered. The steady state problem is solved for the formation of electron and ion flows in the plasma emitter of an electron beam source [1]. The main problem in formulating the problem was the lack of data on the parameters of the real emission plasma. Therefore, the parameters used in the model are typical for such emitters. At the first stage, the analysis of the obtained physical picture was carried out – the structure of the potential and fluxes of the plasma components during the formation of the electron beam. Two regimes of emitter operation are demonstrated: the regime of layer emission limitation and the regime of a partially open plasma boundary. Quantitative dependences of the beam characteristics on the source parameters are obtained. Conclusions are drawn about the scope of this code.

REFERENCES

[1] V. V. Kurkuchekov, V. T. Astrelin, A. P. Avrorov et al. "Novel Injector of Intense Long Pulse Electron Beam for Linear Plasma Devices," Fus. Sci. and Techn., vol. 63, no.1T. pp. 292-294, 2013.

[2] E. M. Oks, "Electron Sources with Plasma Cathode: Physics, Technics, Applications," Tomsk, STL publ. House, 2005. (In Russian)

[3] Jack E. Boers, "PBGUNS: A digital computer program for the simulation of electron and ion beams on a PC," International Conference on Plasma Sciences (ICOPS), IEEE, p. 213, 1993.

[4] P. Spadtke, C. Muhle, "Simulation of ion extraction and beam transport," Rev. Sci. Instr., vol. 71, no. 2, p. 820-825, 02B108, 2000.

[5] O. N. Petrovich, V. A. Gruzdev, "Code ELIS for Numerical Simulation EOS PIEL," Advances of Applied Physics, vol. 2, no. 5, pp.79-85, 2012. (In Russian)

[6] V. T. Astrelin, "Features of solving a plasma emission electronics problems in CAD POISSON-2," Advances of Applied Physics, vol. 1, no. 5, pp.571-573, 2013. (In Russian)

[7] V. P. Tarakanov, "Versatile Electromagnetic Code KARAT," in Mathematical Simulation: Problems and Results, Eds. by I. M. Makarov, O. M. Belocserkovskiy, Moscow, Nauka, Russia, pp.456-476, 2003. (In Russian)

S6-O-012201

INVESTIGATION OF NEAR CATHODE GLOW DISCHARGE PLASMA IN HELIUM AND ITS APPLICATION IN GAS ANALYSIS

A.I. SAIFUTDINOV

Kazan national Research Technical University named after A.N.Tupolev - KAI, Kazan, Russia

The paper is devoted to investigations of the non-local negative glow (NG) plasma of a glow discharge in helium at low and high pressures.

The first part of the report presents the results of measurements of the electron energy distribution function (EEDF) using a Langmuir probe at low pressures. It is shown that the temperature of the main group of electrons in the NG plasma is low and amounts to fractions of an eV. The formation of narrow peaks in the fast part of the EEDF from fast electrons produced in the reactions of Penning ionization of impurities of air molecules by metastable helium atoms is demonstrated.

In the second part of the report, the possibility of using a wall probe to measure the fast part of the EEDF in a non-local near-cathode plasma at medium and high pressures is substantiated and a formula is obtained that relates the electron current density per probe to the spectrum of fast electrons [1]. The results of registration of air impurities in helium in a discharge structure with flat electrodes at medium pressures and in a discharge with microhollow electrodes at atmospheric pressure are presented. It is shown that in microdischarges with a hollow cathode, by limiting the outer part of the cathode, it is possible to achieve that the wall electrode is located directly in the negative glow region with a low electron temperature in a larger range of discharge currents, while simultaneously increasing the sensitivity in determining the spectra of fast electrons from the Penning ionization of impurities by metastable atoms of helium [2].

The third part of the report demonstrates the possibility of detecting impurities of complex molecules: hydrocarbons, alcohols, ammonia in the near-cathode plasma of a glow discharge in helium at low pressures [3].

In the fourth part of the report, a self-consistent hybrid model of a near cathode negative glow plasma is formulated, including the Boltzmann kinetic equation, written in the f_0-f_1 approximation in the variables «spatial coordinate - kinetic energy», and systems of one-dimensional drift- diffusion equations for a positive ion, excited atoms, as well as the Poisson equation to determine the self-consistent electric field in plasma. Numerical experiments were carried out for helium and argon at low pressures. Numerical experiments have shown satisfactory agreement with the experimental results on the temperature of the main group of electrons and the concentration of charged particles. At the same time, it was shown that the results of numerical calculations in modeling the near-cathode negative glow plasma differ significantly from the results of numerical calculations carried out in the framework of the extended fluid description with the Maxwellian EEDF and with the EEDF obtained in the framework of the iterative solution of the local kinetic equation with a system of fluid equations. Additionally, numerical calculations were carried out on the formation of narrow peaks on the EEDF and on the differential flux from fast electrons produced as a result of Penning ionization reactions of metastable helium atoms of methane impurities and radicals. The minimum impurity concentrations that can be detected by plasma electron spectroscopy have been determined.

REFERENCES

[1] Chengxun Yuan, A.A. Kudryavtsev, A.I. Saifutdinov, et al., "Determining the spectrum of Penning electrons by current to a wall probe in nonlocal negative glow plasma," Physics of Plasmas 25, 104501, 2018.

[2] Saifutdinov A.I., Sysoev S.S. Diagnostics and comparative analyzes of plasma parameters in micro hollow cathode discharges with an open and covered external surface of cathode in helium using an additional electrode," PSST, 30 (1), № 017001, 2021

[3] Zhou C.,Yao J.,Saifutdinov et al. "Use of plasma electron spectroscopy method to detect hydrocarbons, alcohols, and ammonia in nonlocal plasma of short glow discharge," PSST, 30(11), 117001, 2021.

* Theoretical research was supported by a grant from the Foundation for the Development of Theoretical Physics and Mathematics "BASIS", project No. 21-1-3-53-1.

S6-O-012202

* NUMERICAL STUDY OF DIRECT CURRENT ATMOSPHERIC PRESSURE DISCHARGE: FROM GLOW TO ARC DISCHARGE IN ATOMIC AND MOLECULAR GASES *

A.I. SAIFUTDINOV

Kazan national Research Technical University named after A.N.Tupolev - KAI, Kazan, Russia

. In the presented work, a self-consistent physical and mathematical model of direct current gas discharges is formulated, which in a unified way describes the processes occurring in the discharge gap and electrodes [1-3]. The model is based on equations for an extended fluid description of processes in a gas-discharge plasma, taking into account secondary and thermionic or thermofield emission from the cathode, heat balance equations for electrodes that describe the distribution of temperature fields in them, continuity equations for the current density in the electrodes, and an equation for an external electric circuit. Within the framework of the formulated model, numerical studies were carried out in 1D and 2D approximations on the formation of parameters of direct current discharges in atomic and molecular gases of atmospheric pressure in a wide range of currents.

As a result of numerical experiments, for one-dimensional geometry, the dependence of the voltage drop across the discharge on the current density was obtained, and for the two-dimensional geometry, the current-voltage characteristic (CVC) of the discharge, which reproduces the formation of glow, transition from glow to arc, and arc modes of direct current discharges in argon and nitrogen. The distributions of the main mechanisms of electrode heating are presented, as well as the values of their temperatures at the boundary with the discharge, depending on the current density. It is shown that in a discharge with refractory (tungsten and graphite) electrodes, an arc discharge is formed with a diffuse current spot completely covering the cathode surface. In a discharge with copper (non-refractory) electrodes, supported by thermionic field emission, an arc discharge is formed with a contracted current spot on the cathode. For various DC discharge modes, the distributions of plasma parameters are presented: the concentrations of charged and excited particles, the intensity and potential, the temperature of electrons and neutral particles, and also the vibrational temperature.

In addition, a study was made of the effect of electrode material evaporation on the distributions of the main plasma parameters in arc discharges of atmospheric pressure in argon with graphite (refractory) electrodes and copper (non-refractory) electrodes. In addition to plasma-chemical processes in argon [1], for a discharge with graphite electrodes, a fairly detailed set of plasma-chemical reactions was compiled, taking into account the formation of neutral carbon particles C, C_2, C_3, their ions C^+, C_2^+, C_3^+ and excited states C*, C_2*, C_3* . For a discharge with copper electrodes, a set of elementary processes with the participation of copper atoms was taken into account, taken from [4], in which processes with the formation of atomic copper ions were taken into account. As a result of numerical experiments, it is shown that when the critical value of the current density is reached, an abrupt change in the plasma parameters is observed: on the current-voltage characteristic of the discharge and on the dependences of the charged particle concentrations averaged over the gas-discharge gap on the current density. A transition is observed from an arc discharge in an argon atmosphere to an arc in carbon vapor or copper vapor.

REFERENCES

[1] Saifutdinov, A.I., Fairushin, I.I. & Kashapov, N.F. Analysis of various scenarios of the behavior of voltage–current characteristics of direct-current microdischarges at atmospheric pressure. Jetp Lett. 104, 180–185 (2016)

[2] Saifutdinov A.I. Unified simulation of different modes in atmospheric pressure DC discharges in nitrogen // (2021) Journal of Applied Physics, 129 (9), no. 093302.A. I. Saifutdinov *J. Appl. Phys*. **129**, 093302 (2021).

[3] Saifutdinov A.I., Timerkaev B.A., Saifutdinova A.A. Features of Transient Processes in DC Microdischarges in Molecular Gases: From a Glow Discharge to an Arc Discharge with a Unfree or Free Cathode Regime // (2020) JETP Letters, 112 (7), pp. 405-412.

[4] M. Baeva *et all. J. Phys. D: Appl. Phys.* **54** 025203 (2021).

* Theoretical research was supported by a grant from the Foundation for the Development of Theoretical Physics and Mathematics "BASIS", project No. 21-1-3-53-1.

S6-O-023901

COMPUTER SIMULATION OF ATOMIC EMISSION SPECTRA IN ALTERNATING ELECTRIC FIELDS

E.V. KORYUKINA

National Research Tomsk State University, Tomsk, Russia

The interest in studying the influence of alternating electric fields on atomic emission spectra results from the necessity of solving many theoretical and practical problems of atomic spectroscopy, gas discharge physics and plasma diagnostics.

Theoretical methods based on non-stationary perturbation theory were developed for calculating atomic emission spectra in laser fields at the end of previous century. By the present time, a lot of other excitation sources (in particular, electrodeless high-frequency discharge lamps, light-emitting diodes, superpower lasers, and so on) have appeared. These sources generate electric fields with parameters essentially different from those of optical lasers. Perturbation theory, by virtue of its limitations, is not always suitable for calculating atomic spectra excited by electric fields of the above-mentioned sources.

In the present work, a theoretical approach is suggested for calculating the emission spectra of atoms in an alternating electric field. This approach, based on the numerical solution of the non-stationary Schrцdinger equation, is free from limitations of perturbation theory and suitable for calculations of atomic emission spectra in alternating electric fields with the parameters changing in wide ranges. The algorithm of the suggested method is implemented in a special software package written in FORTRAN and Maple [1].

The results of computer simulations obtained in the framework of the suggested approach have allowed us: (1) to study the dependences of the AC Stark effect on the electric field strength and frequency; (2) to reveal regularities in the behavior of the transition probabilities in the electric field; (3) to analyze the reasons for an increase in the intensity of spectral lines and their quenching in the electric field; (4) to investigate the mechanisms of the formation of the spectral line profiles in the electric field.

The theoretical regularities established in this work have been obtained for the first time. They are of interest both from a theoretical point of view and in solving practical problems of plasma diagnostics, magnetic reconnection, and other branches of physics where spectroscopic methods are used to study the influence of alternating electric fields on the properties of the object under study. In addition, the established regularities can be used to develop new excitation sources with required characteristics and to search for the optimal operating mode of existing sources.

REFERENCES

[1] E.V. Koryukina, "Software package StarkD for calculating atomic emission spectra in an alternating electric field," J. Phys.: Conf. Series, vol. 1141, Article Number 012053, 2018.

S6-O-029605

COMPUTATION OF OUTPUT PARAMETERS OF A SUBMICROSECOND ELECTRON ACCELERATOR*

I.S. EGOROV[1], *M.A. SEREBRENNIKOV*[1], *A.V. POLOSKOV*[1],

[1]*Tomsk Polytechnic University, Tomsk, Russia*

The development of complex systems computational models makes possible the evaluation of their various operation mods with minimal time and resources investment. Including the determination of the system operating parameters ranges, in which their characteristics correspond to the desired ones. This paper presents a submicrosecond electron accelerator computation made in the Multisim electrical process simulation program. The accelerator [1] is based on a high-voltage pulse generator according to the scheme of a high-voltage energy storage device, a pulse transformer, and a vacuum electron diode with an explosive emission cathode. The paper describes the applied methods and approaches of simulation development, the limitations and simplifications used, as well as the simulation error estimation. Based on the created computation, the output electrical parameters of the accelerator were analyzed depending on the amount of stored energy and the parameters of the diode system. The diode system model was verified in the previous studies [2]. The obtained research results can be used in the development of new exemplars of high-voltage pulse technology and for tuning existing accelerators.

REFERENCES

[1] A. Poloskov, I. Egorov, A. Nashilevskiy, V. Ezhov, E. Smolyanskiy, M. Serebrennikov, G. Remnev, Submicrosecond electron accelerator based on pulsed transformer, Nuclear Instruments and Methods in Physics Research Section A: Accelerators, Spectrometers, Detectors and Associated Equipment. 969 (2020) 163951. doi:10.1016/j.nima.2020.163951.

[2] I. Egorov, A. Poloskov, G. Remnev, Computation of the impedance of a vacuum electron diode with emission current delay, Nuclear Instruments and Methods in Physics Research Section A: Accelerators, Spectrometers, Detectors and Associated Equipment. 921 (2019) 68–70. doi:10.1016/j.nima.2018.12.008.

* The authors are grateful to National Research Tomsk Polytechnic University (TPU, Russia) for technical support in a case of TPU development program. The work was conducted within the framework of the state assignment in the field of scientific activity: No. FSWW-2020-0008.

S6-P-001402

MODEL OF THE PLASMA EXTENSION IN THE TRIGGER UNIT OF THE COLD-CATHODE THYRATRON BASED ON FLASHOVER*

N.V. LANDL, N.S. SEMENIUK, Y.D. KOROLEV, O.B. FRANTS, A.V. KOZYREV, G.A. ARGUNOV

Institute of High Current Electronics SB RAS, Tomsk, Russia

Currently, high-current switching devices based on low-pressure hollow-cathode pulsed discharge (so-called pseudospark switches) are widely used [1-4]. The design and principle of operation of these switches are close to those of a classical hot-cathode hydrogen thyratrons. As in the case of classical thyratrons, a range of operating pressures of the switch corresponds to the left branch of Paschen's curve. For both self-breakdown of the main gap of the thyratron and for external discharge triggering a considerable pre-breakdown electron current is required [1, 3, 5]. For the case of external triggering, this current is provided due to a special trigger unit that is placed in the main cathode cavity. One type of trigger units is based a discharge over a dielectric or semiconductor surface or, in other words, based on a flashover [3, 4].

Any trigger unit is intended for plasma generation of trigger discharge inside the thyratron cathode cavity at a curtain instant of time. When a trigger unit based on discharge formation over the dielectric surface is used, trigger discharge plasma is generated due to the interception of surface discharge current to the main cathode cavity. The delay time of current interception depends on a plasma extension velocity from the cathode spot to the hollow-cathode surface.

In this report we used origin theoretical model to describe the plasma extension and compare obtained results with the experiment. We used one-dimensional kinetic simulation of electron and ion transport and multiplication (based on the Boltzmann kinetic equations) in a self-consistent electric field after electron injection from the cathode surface. The 1D1V Boltzmann equations take into account the electron impact ionization, elastic electron scattering, and resonant ion recharging [6].

REFERENCES

[1] Y.D. Korolev and N.N. Koval, "Low-pressure discharges with hollow cathode and hollow anode and their applications," J. Phys. D: Appl. Phys., vol.51, Article Number 323001, 2018.

[2] K Bergmann, M Muller, D Reichartz, W Neff and R Lebert, “Electrode phenomena and lifetime considerations in a radial multichannel pseudospark switch,” IEEE Trans. Plasma Sci., vol.28, pp. 1486-1490, 2000

[3] Y.D. Korolev, K. Frank, “Discharge formation processes and glow-to-arc transition in pseudospark switch,” IEEE Trans. Plasma Sci., vol.27, p.1525, 1999

[4] V.D. Bochkov, V.M. Dyagilev, V.G. Ushich, O.B. Frants, Y.D. Korolev, I.A. Shemyakin, K. Frank, “Sealed-off pseudospark switches for pulsed power applications (current status and prospects),” IEEE Trans. Plasma Sci., vol.29, no.5, pp. 802-808, 2001.

[5] Y.D. Korolev, N.V. Landl, V.G. Geyman, O.B. Frants, G.A. Argunov, A.V. Bolotov, “Role of Prebreakdown Currents in a Static Breakdown of a Two-Sectioned Cold-Cathode Thyratron, Russ.Phys.J., vol.62, No.7, pp.1269-1278, 2019.

[6] A.V. Kozyrev, V.Y. Kozhevnikov, and N.S. Semeniuk, ” Kinetic theory of high-voltage low-pressure gas discharge with electron initiation on a cathode in a planar gap,” Plasma Sources Sci. Technol.., vol.29, No.12, art number 125023 (8pp), 2020.

* This work was funded by RFBR according to the research project № 19-48-700023.

S6-P-017001

COMPUTER SIMULATION OF MULTI-GIGAWATT MAGNETIC COMPRESSION LINES

V.E. PATRAKOV[1,2], *S.N. RUKIN*[1]

[1]*Institute of Electrophysics UB RAS, Yekaterinburg, Russia*
[2]*Ural Federal University, Yekaterinburg, Russia*

Non-linear transmission lines (NLTL) filled with saturated ferrite are promising solid-state sources of high-power microwave radiation. At present such gyromagnetic NLTLs can provide microwave generation in GHz range with typical pulsed RF power on the order of 100 MW [1]. The main principle of generation of these high-power microwave oscillations is the precession of the magnetization vector $\boldsymbol{M}$ around the lines of the effective magnetic field (the sum of driver pulse $\boldsymbol{H}$-field and external bias $\boldsymbol{H}$-field). This precession induces voltage across NLTL conductors and thus leads to pulse transformation and to the generation of oscillations.

In recent years NLTLs also have been utilized to increase the peak power of unipolar pulses in the multi-gigawatt power range [2-4]. This NLTL type is called Magnetic Compression Line (MCL). To date, the highest reported pulse power achieved with the MCL approach is 77 GW at 48-Ohm load, with the pulse amplitude of 1.93 MV and pulse duration of 105 ps (FWHM) [4]. The device uses a semiconductor opening switch (SOS) generator as the input pulse driver, and four consecutive MCL stages as power amplifiers, thus making the generator an extension of all solid-state pulsed power approach.

In this study, a numerical model of MCL operation was created and tested. The electrodynamic part of the model is described by Maxwell's equations reduced to one $\boldsymbol{A}$-potential-dependent equation, i.e., the "full-wave" formulation. The precession of magnetization vector $\boldsymbol{M}$ is described by Landau-Lifshitz-Gilbert equation. The resulting coupled system is solved using COMSOL Multiphysics numerical modeling software [5]. System geometry can be specified in 2D-axisymmetric or full 3D definition. The model also accounts for the nonlinearity of ferrite magnetization by adding non-linear relative permeability μ_r.

The model shows good agreement with existing experimental data [3] in amplitude, overall shape, and delay of the main peaks of the output pulse (figure 1). Optimal ferrite filling length can be determined, and field distribution in the line cross-section can be analyzed. The created model allows to design and analyze MCL power amplification systems, as well as microwave NLTL systems.

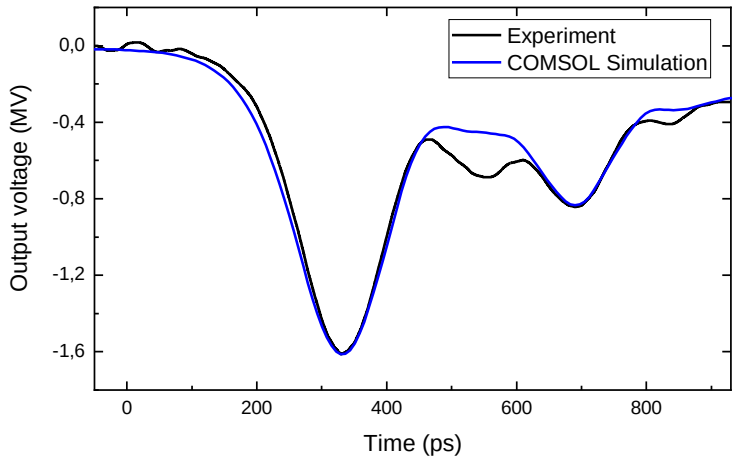

Fig.1. Comparison of experimental output pulse waveform [3] and simulated output pulse waveform for third MCL stage

REFERENCES

[1] I. V. Romanchenko, M. R. Ulmaskulov, K. A. Sharypov, S. A. Shunailov, V. G. Shpak, M. I. Yalandin, M. S. Pedos, S. N. Rukin, V. Yu. Konev, and V. V. Rostov, "Four channel high power RF source with beam steering based on gyromagnetic nonlinear transmission lines," Rev. Sci. Instrum., vol. 88, p. 054703, 2017.

[2] A. I. Gusev, M. S. Pedos, A. V. Ponomarev, S. N. Rukin, S. P. Timoshenkov, and S. N. Tsyranov, "A 30 GW subnanosecond solid-state pulsed power system based on generator with semiconductor opening switch and gyromagnetic nonlinear transmission lines," Rev. Sci. Instrum., vol. 89, p. 094703, 2018.

[3] E. A. Alichkin, M. S. Pedos, A. V. Ponomarev, S. N. Rukin, S. P. Timoshenkov, and S. Y. Karelin, "Picosecond solid-state generator with a peak power of 50 GW," Rev. Sci. Instrum., vol. 91, p. 104705, 2020.

[4] S. Rukin, A. Ponomarev, E. Alichkin, S. Timoshenkov, M. Pedos, and K. Sharypov, "Generation of Multi-Gigawatt Picosecond Pulses by Magnetic Compression Lines," Proc. 7th Int. Congr. on Energy Fluxes and Radiation Effects (EFRE), Tomsk, Russia, pp. 92-97, 2020.

[5] "COMSOL Multiphysics Reference Manual 5.4", COMSOL AB, Stockholm, Sweden, 2018.

S6-P-021101

2D KINETIC MODELING OF PLASMA JET IN EXTERNAL MAGNETIC FIELD

D.L. SHMELEV[1], I.V. UIMANOV[1], S.A. BARENGOLTS[2], M.M. TSVENTOUKH[3]

[1]Institute of Electrophysics, UB, RAS, Ekaterinburg, Russia
[2]Prokhorov General Physics Institute, RAS, Moscow, Russia
[3]Lebedev Physical Institute, RAS, Moscow, Russia

Numerical particle-in-cell and Monte Carla simulations were carried out to study the effect of an external axial magnetic field on a plasma jet flowing from a cathode spot of a vacuum arc. A plasma jet carrying a current of 1 A from a cathode spot with a radius of 5 μm was studied. The calculated domain had a size of 22X60 μm. The range of variation of the external axial magnetic field was 1–2.5 T. An increase in the magnetic field predictably leads to compression of the plasma jet (Fig.1). The difference from previous calculations using various quasi-neutral approximations (for example, [1]) is that, in kinetic simulation, a positive space charge is accumulated in the outer layers of the plasma jet.

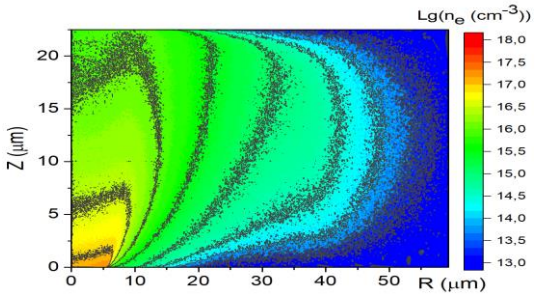

Fig.1. Electron density. External axial magnetic field – 2 T.

Fig. 2 shows the distributions of the electron and ion current densities from the plasma to the cathode. It can be seen that the electron current dominates near the cathode spot, while the ion current dominates in the outer regions. With an increase in the external magnetic field, the area dominated by the electron current shrinks, and the ion current density increases. In the region where the ion current predominates, the mechanism of charging and subsequent breakdown of dielectric films, leading to the ignition of a new cathode spot [2], is possible. If this mechanism works, then it is obvious that the probability of the appearance of a new cathode spot should increase with increasing magnetic field.

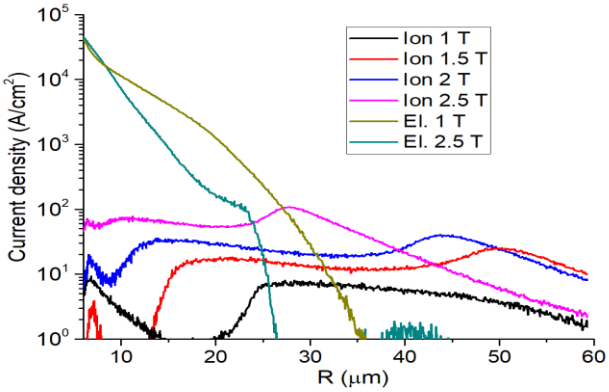

Fig.2. Distributions of electron and ion current to cathode at different magnetic field.

REFERENCES

[1] D.L. Shmelev, V.I. Uimanov and L. Wang, “Numerical simulation of low-current vacuum arc in strong axial magnetic field taking into account the generation of secondary plasma”, Proc. 4th International Conference on Electric Power Equipment- Switching Technology (Xi'an; China), , pp. 642-646, 2017.

[2] M. M. Tsventoukh, S. A. Barengolts, V. G. Mesyats, D. L. Shmelev, “Retrograde motion of cathode spots of the first type in a tangential magnetic field,” *Tech. Phys. Lett.*, vol. 39, pp. 933–937, 2013.

S6-P-021102

NUMERICAL MODEL OF HIGH CURRENT PLASMA SOURCE

D.L. SHMELEV[1], S.A CHAIKOVSKY[1], I.V. UIMANOV[1], V.I. ORESHKIN[2], A.G. ROUSSKIKH[2]

[1]Institute of Electrophysics, UB, RAS, Ekaterinburg, Russia
[2]Institute of High Current Electronics, SB, RAS, Tomsk, Russia

Recently, in experiments on the implosion of plasma Z-pinches, a plasma source with an annular anode similar to the source shown in Fig.1 [1, 2] was used to create a plasma liner. The current passed through such a source can reach hundreds of kiloamperes. Radiographic measurements of the mass of the plasma liner (Fig. 2) show that the mass flow from the source corresponds to a specific erosion in the source on the order of milligrams per Coulomb. This is about a hundred times greater than the cathodic erosion typical of a conventional vacuum arc. Obviously, the discharge burning in the considered source cannot be a classical vacuum arc.

To investigate possible erosion mechanisms, a simplified 2D CFD source model with aluminum electrodes and a sinusoidal current pulse with an amplitude of 325 kA was created. It was found that after 0.2 μs intense evaporation followed by ionization occurs from the entire cathode and anode surfaces into the gap. Moreover, the anode makes the main contribution to the erosion. Plasma radiation makes a significant contribution to the heating of electrodes. Comparison of the calculated mass of the liner with the experiment is shown in Fig. 2. It can be seen that the calculation qualitatively coincides with the experimental results.

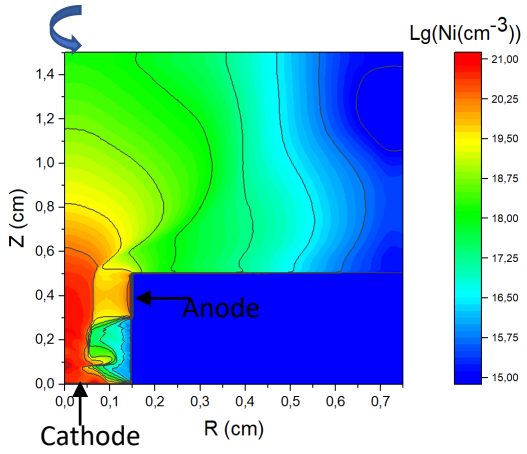

Fig.1. Plasma density distribution at 0.6 ms.

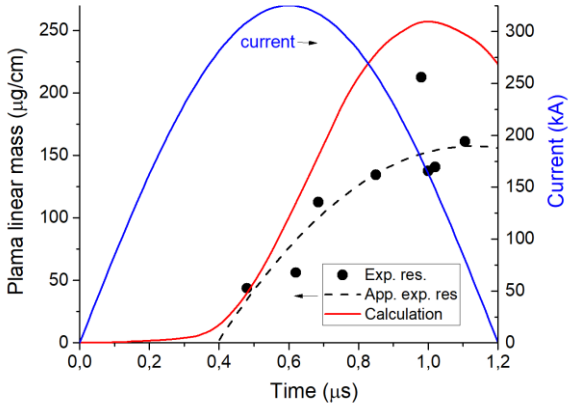

Fig.2. Arc current and plasma mass. Points – experimental results, dushed curve – approximation of experimental results, red solid curve – calculation results.

REFERENCES

[1] D.L. Shmelev, A.S. Zhigalin, S.A. Chaikovsky, V.I. Oreshkin, A.G. Rousskikh, "Formation of double shell during implosion of plasma metal puff Z-pinches. Physics of Plasmas", 27(9), 092708, 2020.

[2] R. K. Cherdizov, R. B. Baksht, V. A. Kokshenev, V. I. Oreshkin, A. G. Rousskikh, A. V. Shishlov, D. L. Shmelev, A. S. Zhigalin, "Effect of tailored density profiles on the stability of imploding Z-pinches at microsecond rise time megaampere currents", Plasma Physics and Controlled Fusion, 64(1), 015011, 2022

S6-P-021201

DEPENDENCE OF THE OSCILLATIONS FREQUENCY IN A NONLINEAR TRANSMISSION LINE WITH SATURATED FERRITE ON MAGNETIC FIELDS AND LINE DIMENSIONS

O.O. MUTYLIN[1], P.V. PRIPUTNEV[1], I.V. ROMANCHENKO[1], V.P. TARAKANOV[1,2,3]

[1]Institute of high current electronics SB RAS, Tomsk, Russian federation
[2]Joint Institute for High Temperatures, Moscow, Russian Federation
[3]National Research Nuclear University MEPhI, Moscow, Russian Federation

The study and development of nonlinear transmission lines (NLTLs) has been going on for several decades. Initially, NLTLs were used for high-voltage pulse sharpening. The best results have been achieved in ferrite-filled lines [1]. The use of lines with saturated ferrite filling made it possible to increase the voltage rise rate and obtain rise times of tens of picoseconds [2]. The results of further studies have shown that in NLTL with saturated ferrite, it is possible to efficiently excite high-frequency oscillations with central frequency of a few GHz at power level of hundreds of MW [3].

In the course of experiments on the excitation of high-frequency oscillations in the NLTL with saturated ferrite, it was shown that the frequency of the excited oscillations in the line depends on the strength of the magnetic fields in which the process of pulsed magnetization reversal of the ferrite filling occurs. It was found that an increase in the frequency of the excited oscillations corresponds to an increase in the azimuthal component of the magnetic field strength, while the frequency decreases with an increase in the strength of the longitudinal magnetic field saturating ferrite. However, to date, it is not possible to determine all the factors that affect the frequencies of excited oscillations in an NLTL, since today there is no analytical model for describing this process that considers non-TEM modes, and experimental study is too expensive.

The solution to this problem can be the use of numerical simulation to conduct a numerical experiment on the process of excitation of oscillations in the NLTL [4,5]. This work is devoted to the determination of the main factors affecting the frequency of excited oscillations in the NLTL with saturated ferrite. The influence of the magnetic field strengths, the coefficient of ferrite transverse filling, and the transverse dimensions of the line on the frequency and efficiency of the excited oscillations was studied.

REFERENCES

[1] J.E. Dolan, H.R. Bolton, A.J. Shapland, “Development of ferrite line pulse sharpeners”, proc. IEEE Int. Pul. Pow. Conf., pp. 795-798, Jun. 1993.

[2] M.R. Ulmaskulov, S.A. Shunailov, K.A. Sharypov, M.I. Yalandin, “Modification of high-voltage pulse waveform by the spiral and core-transformer fierrite-filled lines”, IEEE trans. Plas. Sci., vol. 45, no. 10, pp. 2707-2714, Oct. 2017.

[3] V.V. Rostov, N.M. Bykov, D.N. Bykov, A.I. Klimov, O.B. Kovalchuk, I.V. Romanchenko, “Generation of subgigawatt RF pulses in nonlinear transmission lines”, IEEE Trans. Plasma Sci., vol. 38, no. 10, pp. 2681-2685, Oct 2010

[4] V.P. Tarakanov, “Multipurpose electromagnetic code KARAT”, Math. Mod.”: prob. and res., pp. 456-476, 2003.

[5] P.V. Priputnev, I.V. Romanchenko, V.P. Tarakanov, I.V. Pegel “2-D and 3-D numerical simmulation of ferrite loaded coaxial transmission lines”, 2020 7th International Congress on Energy Fluxes and Radiation Effects (EFRE), Sep. 2020.

S6-P-022601

MODEL OF ELECTRON EMISSION FROM EXPANDING EXPLOSIVE EMISSION PLASMA FRONT*

YU.I. MAMONTOV[1], *I.V. UIMANOV*[1]

[1]*Institute of Electrophysics UB RAS, Yekaterinburg, Russia*

The 1D-3V PIC-MCC (1 dimension – 3 velocities Particle-in-Cell with Monte-Carlo collisions) self-consistent spherical-symmetric model was developed to investigate numerically dynamics of electrons emitted from an expanding explosive plasma front. The model describes a process of the virtual cathode formation within the nearest vicinity of the plasma front for fixed values of a plasma density and a voltage U between the front and an outer boundary of a calculation grid. This boundary was considered as an anode of the model; respectively, the plasma was assumed to be a cathode. U was varied from 0 V up to 1000 V. A radius r of the plasma front was in the range of 10 μm – 1 cm. An initial plasma density N_{pl0} was 10^{21} cm^{-3} [1,2]. The plasma density N_{pl} near the emitting front was assumed to decrease as r^{-2}. An emission current density J_{em} was determined as $J_{em} = eN_{pl} < V_t >$, where e is an elementary charge, $< V_t >$ is an average thermal velocity of electrons in plasma. For plasma emitted electrons, the Maxwellian energy distribution function was assumed to be valid [1,2]. The near-front plasma temperature T_{pl} was in the range of 1 eV – 3 eV. As a result of simulations, the dependencies of the current density J_{an} of plasma emission electrons near the anode on U, T_{pl}, and N_{pl} were obtained. In addition, the virtual cathode height U_{vc} was calculated for various simulation conditions. The effect of the electron beam self-closing was demonstrated. The limitations of the model caused by the electric field penetration in plasma were determined.

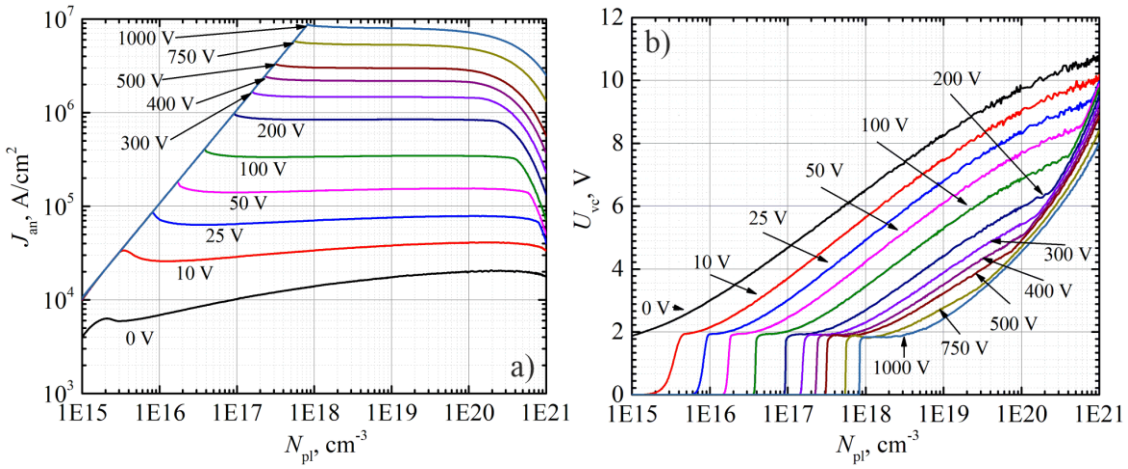

Fig.1. a) – anode current density J_{an} for various plasma density and voltage applied, b) – virtual cathode height U_{vc} for various plasma density and voltage applied. For a) and b), plasma temperature is 1 eV.

REFERENCES

[1] G.A. Mesyats and D.I. Proskurovsky, Pulsed Electrical Discharge in Vacuum. Berlin, Germany: Springer, 1989.

[2] G.A. Mesyats, Cathode Phenomena in a Vacuum Discharge: The Breakdown, the Spark and the Arc. Moscow, Russia: Nauka, 2000.

* The work was supported in part by the Russian Foundation for Basic Research under Project No 20-38-90147.

S6-P-023902

A THEORETICAL STUDY OF THE INFLUENCE OF ALTERNATING ELECTRIC FIELDS ON THE FORMATION OF LINE PROFILES IN ARGON EMISSION SPECTRA

E.V. KORYUKINA

National Research Tomsk State University, Tomsk, Russia

Atomic spectroscopy methods are widely used for diagnostics of processes taking place in plasma. The plasma parameters such as the electron density and temperature of atoms can be estimated from profiles of the spectral lines emitted by plasma. The electric field is one of the most important factors that form the line profiles in atomic emission spectra. Calculating the Stark profiles and their convolutions with the Doppler ones for atomic spectral lines in alternating electric fields is very complicated problem in modern physics.

To solve this problem, we propose the unified theoretical approach based on the numerical solution of the non-stationary Schrцdinger equation. This approach is free from limitations of perturbation theory and is valid in wide ranges of the electric field strength and frequency. The algorithm of the suggested method is implemented in a special software package written in FORTRAN and Maple.

Within the framework of this approach, we succeeded in analyzing the influence of changes in the electric field strength and frequency on the spectral line profiles and on the shift direction of the spectral lines of the Ar atom in the electric field. In addition, a computer simulation within the framework of the suggested approach made it possible to estimate the contribution of the electric field to the processes of quenching of spectral lines and increasing their intensity.

As an illustration of potentialities of the proposed approach, Fig. 1 shows the shift of the $6d[1/2]_1$-$4p[1/2]_1$ spectral line of the Ar atom with an increase in the electric field strength and splitting of this line into the Stark components in the electric field (the electric field frequency is 10^5 MHz).

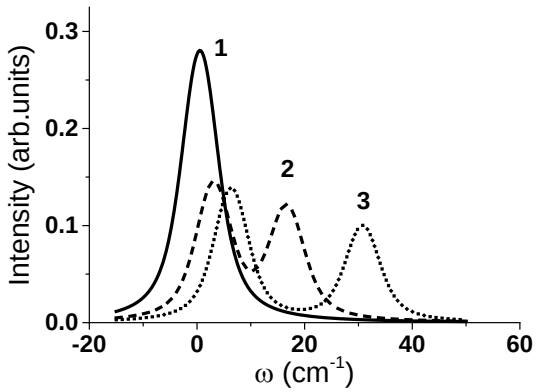

Fig.1. Evolution of the $6d[1/2]_1$–$4p[1/2]_1$ spectral line in the electric field:

1 – F=20 kV/cm,
2 – F=80 kV/cm,
3 – F=120 kV/cm.

These theoretical results are interesting from a theoretical viewpoint, and they have practical applications in plasma spectroscopy, laser physics, and in studying magnetic reconnection. Finally, the results obtained are useful for searching optimal operation modes of existing excitation sources and for constructing new devices.

S6-P-028801

THE DEVELOPMENT OF HYDRODYNAMIC AND THERMAL INSTABILITIES IN A LIQUID METAL JETS IN THE CATHODE SPOT OF A VACUUM ARC*

I.V. UIMANOV[1], *G.A. MESYATS*[1,2]

[1]*Institute of Electrophysics, UB, RAS, Yekaterinburg, Russia*
[2]*Lebedev Physical Institute, RAS, Moscow, Russia*

e-mail: uimanov@iep.uran.ru

The explosion of the liquid metal jets is considered to be the basic mechanism of the birth of new cathode spot cells [1-4]. In this work a two-dimensional axisymmetric model has been developed to describe the formation of a liquid metal jet, the droplet pinch-off and temperature runaway in the droplet-jet neck during melt splashing from the cathode crater in a vacuum arc. The development of hydrodynamic and thermal instabilities has been self-consistent simulated in a copper current-carrying liquid metal jet in the "inertial" mode of the melt splashing (see Fig. 1). In this case, a jet with a longitudinal velocity gradient is formed and the droplet-jet neck becomes unstable due to the action of capillary forces (Rayleigh–Plateau instability). As a result, the neck radius decreases rapidly and the droplet splits off. In a current-carrying jet, this process is accompanied by a strong increase in the current density in the neck and its rapid heating due to the Joule effect to a critical temperature at certain values of current from the cathode spot plasma. It is shown that the heating process has the nature of a temperature runaway and, accordingly, can lead to its electric explosion. Assuming a constant current density on the jet surface, its minimum "explosion" value was calculated depending on the diameter, velocity and initial temperature of the jet. It is shown that for craters and jets of low-current arcs this density does not exceed 10^7 A/cm^2 and, accordingly, can be provided by the ion current from the plasma of the cathode spot.

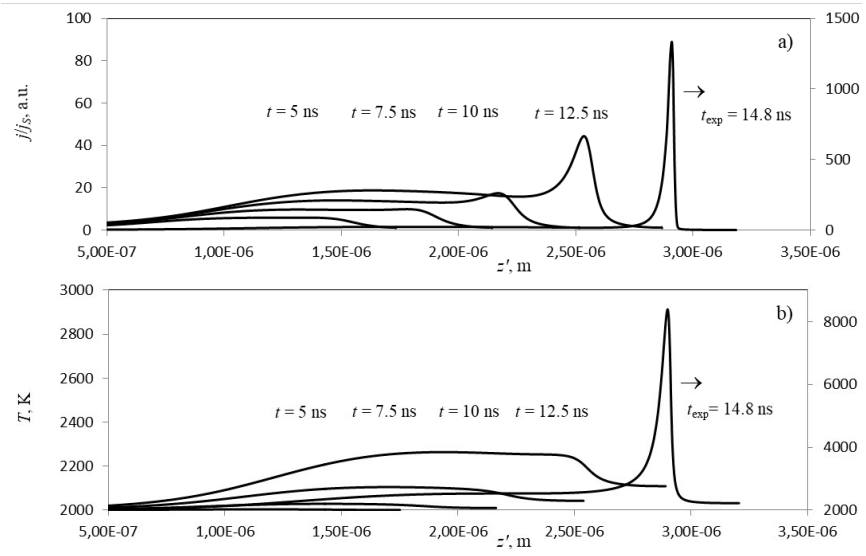

Fig. 1. Temporal evolution of the current density a) and temperature b) distributions along the jet.

REFERENCES

[1] G A Mesyats and D I Proskurovsky, Pulsed Electrical Discharge in Vacuum, Berlin: Springer, 1989, pp. 110–114.

[2] G A Mesyats, Cathode Phenomena in a Vacuum Discharge: The Breakdown, the Spark and the Arc, Nauka, Moscow, 2000. pp. 167–170.

[3] G A Mesyats, JETP Lett., vol. 60, pp. 593–596, April 1994.

[4] E A Litvinov, G A Mesyats, A G Parfenov and A I Fedosov, Zh. Tekh. Fiz., vol. 55, p. 2270, May 1985.

S6-P-028802

MODELING OF PREBREAKDOWN PHENOMENA IN THE CATHODE MICROPROTRUSION, TAKING INTO ACCOUNT THE MELT MOVEMENT

I.V. UIMANOV[1], D. L. SHMELEV[1] AND S. A. BARENGOLTS[2,3]

[1]Institute of Electrophysics, UB, RAS, Yekaterinburg, Russia
[2]Prokhorov General Physics Institute, RAS, Moscow, Russia
[3]Lebedev Physical Institute, RAS, Moscow, Russia

The explosion of the cathode microprotrusions due to heating by emission current is considered to be the basic mechanism of the vacuum DC [1,2] and RF [3-6] breakdown. However, in these approaches, the consideration of prebreakdown processes did not take into account the dynamics of the microprotrusion shape after melting. In this work the development of hydrodynamic and thermal instabilities after melting has been self-consistent simulated in a copper cathode microprotrusion exposed to RF electromagnetic field within the two-dimensional axisymmetric model. The model includes a self-consistent calculation of the electric field strength and emission characteristics on the "emission" half-wave of the RF field within the PIC method, calculation of current density and temperature distributions in the microprotrusion. From the moment the melt appears in the top part of the microprotrusion, the model describes the movement of the liquid phase under the action of forces from the electric field (Maxvell stress) and surface tension forces. Within the framework of this model, modeling of the development of hydrodynamic and thermal instabilities for a microprotrusion with an initial electric field enhancement factor $\beta \sim 86$ in a microwave wave with a strength amplitude of 250 MV/m and a frequency of 10 GHz was carried out. The dynamics of microprotrusion heating and the change in the microprotrusion shape after melting are shown in Fig. 1 and Fig. 2, respectively.

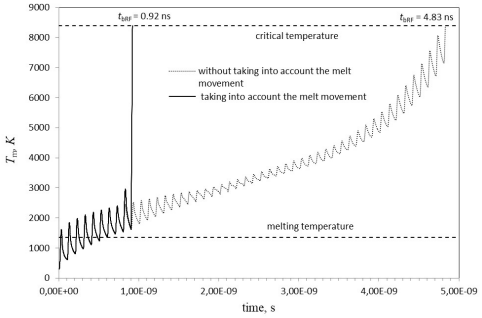

Fig. 1. Dynamics of the heating of microprotrusion with $\beta \sim 86$ to the critical temperature in an RF field of amplitude 250 MV/m and frequency 10 GHz.

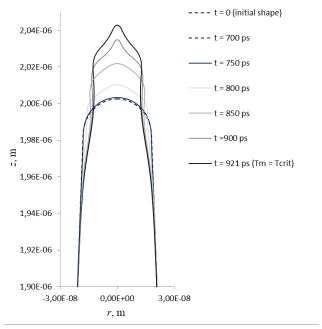

Fig. 2. Dynamics of the microprotrusion shape after melting.

Based on the results obtained (see Fig. 1), it is shown that the time for the development of thermal instability (explosion delay time) during stretching and sharpening of a microprotrusion in the molten state is significantly lower than in the case of an unchanged microprotrusion shape. This is due to the fact that after melting, the top of the microprotrusion in the electric field begins to stretch and become sharp. This leads to an increase in the electric field strength and electron emission current density.

REFERENCES

[1] G A Mesyats and D I Proskurovsky, Pulsed Electrical Discharge in Vacuum, Berlin: Springer, 1989.

[2] G A Mesyats, Cathode Phenomena in a Vacuum Discharge: The Breakdown, the Spark and the Arc, Nauka, Moscow, 2000. pp. 42–53.

[3] S. A. Barengolts, M. Y. Kreindel, and E. A. Litvinov, "Initiation of explosive electron emission in microwave fields," IEEE Trans. Plasma Sci., vol. 26, no. 3, pp. 252–255, Jun. 1998.

[4] S. A. Barengolts et al., "Mechanism of vacuum breakdown in radio-frequency accelerating structures," Phys. Rev. Accel. Beams, vol. 21, no. 6, Jun. 2018, Art. no. 061004.

[5] Barengolts S A, Uimanov I V and Shmelev D L, "Prebreakdown Processes in a Metal Surface Microprotrusion Exposed to an RF Electromagnetic Field", IEEE Trans. Plasma Sci., vol. 47, pp. 3400–3405, 2019.

[6] I V Uimanov, D L Shmelev and S A Barengolts, "Effect of electrode temperature on radiofrequency vacuum breakdown characteristics", J. Phys. D: Appl. Phys. 54 (2021) 065205. https://doi.org/10.1088/1361-6463/abc213.

* The work was supported by the Russian Science Foundation (Grant Nos. 20-19-00323).

S6-P-048201

MODELING OF LUCE DIODE*

A.O. URAZBAYEV[1], *I. PYATKOV*[1], *M V ZHURAVLEV*,

[1]*Tomsk Polytechnic University, Tomsk, Russia*

The goal of this work is to simulate process in Luce diode by means of PIC code WARP. We used geometry of real experiments. The anode was a needle 4 mm in diameter with a rounded end. A conducting toroid with an inner aperture 6 mm in diameter was modeled as a cathode and the end of the needle was leveled with the outer surface of the anode. A potential of 250 KEV was applied to the end of the needle

During the modeling, electrons and hydrogen ions were placed at the end of the needle. The number of injected electrons was choose to obtain a current of 15kA, approximately the current we had in the experiments.

The simulation showed that the current is modulated in amplitude, which was already observed in the simulation of vircators [2]. This modulation was observed at area about several centimeters from the end of the needle.

The needle almost immediately absorbed most of the ions, but some of them accelerated away from the needle, reaching a speed of 5e6 meters per second and energy of 200 KEV. Spuriously, they continued to accelerate even at a distance of several centimeters from the end of the needle (Figure 1)

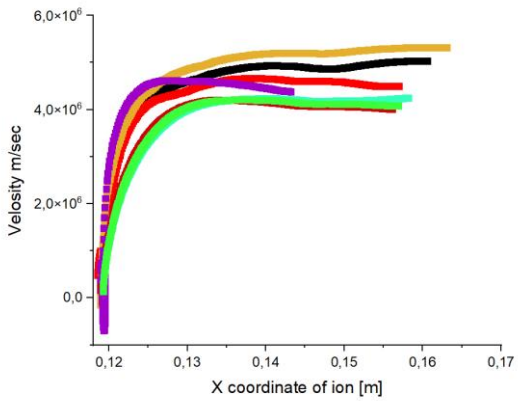

Figure 1. Movement of ions along the x-axis from the speed of the ion. Y axis is speed of ions. X =12 cm is the end of the needle of the Luce diode..

Note that the acceleration occurs in the absence of any accelerating potentials, moreover, it goes in the opposite direction from the potential. We assume that the driving force of ion acceleration in this case is the ponderomotive force. Acceleration occurs in the direction of a weak field, electron clouds lead to the appearance of an oscillating field, which are key factors for the appearance of ponderomotive forces. Ponderomotive force is not related to potentials directly. Therefore, it can be reason why energy of ions can be greater than accelerating potential.

REFERENCES

[1] Determination of Energy and Fluences of Protons Collectively Accelerated in a Luce Diode Accelerator, Ryzhkov, V.A., Remnev,. (2019) Technical Physics Letters, 45 (7), pp. 718-720

[2] 3-D PIC Numerical Investigations of a Novel Concept of Multistage Axial Vircator for Enhanced Microwave Generation; S Champeaux, P Gouard, Ieee Transactions On Plasma Science, Vol. 43, No. 11, November 2015

* The work was supported by…All acknowledgments should be written as footnotes (EFRE Footnote style): 8 pt, justified alignment, spacing 0 pt before and 10 pt after paragraphs, single line spacing.

16th International Conference on Modification of Materials with Particle Beams and Plasma Flows

Chair	Nikolai KOVAL	Institute of High Current Electronics, Tomsk, Russia
Co-Chair	Valery KRIVOBOKOV	Institute of Physics and Technology, TPU, Tomsk, Russia
Program Chair	Nikolai KOVAL	Institute of High Current Electronics, Tomsk, Russia

Program Committee

Vladimir DENISOV	Institute of High Current Electronics SB RAS, Tomsk, Russia
Valery KRIVOBOKOV	National Research Tomsk Polytechnic University, Tomsk, Russia
Yuri IVANOV	Institute of High Current Electronics SB RAS, Tomsk, Russia
Yuri AKHMADEEV	Institute of High Current Electronics SB RAS, Tomsk, Russia
Yan ZUBAVICHUS	Synchrotron Radiation Facility SKIF, Novosibirsk, Russia
Irina KURZINA	National Research Tomsk State University, Tomsk, Russia

International Advisory Committee

Andre ANDERS	Leibniz Institute of Surface Engineering (IOM), Leipzig, Germany
Valiantsin ASTASHYNSKI	State Scientific Institution «A.V. Luikov Heat and Mass Transfer Institute of the National Academy of Sciences of Belarus», Minsk, Belarus
Massimiliano BESTETTI	Politecnico di Milano, Milan, Italy
Ian BROWN	on retired from Lawrence Berkeley National Laboratories, USA
Oleg DOLMATOV	National Research Tomsk Polytechnic University, Tomsk, Russia
Viktor DRAGUNOV	National Research University "Moscow Power Engineering Institute", Moscow, Russia
Igor GARKUSHA	National Science Center Kharkov Institute of Physics and Technology, Kharkov, Ukraine
Nikolai GAVRILOV	Institute of Electrophysics UB RAS, Ekaterinburg, Russia
Yuri IVANOV	Institute of High Current Electronics SB RAS, Tomsk, Russia
Kairat KADYRZHANOV	L.N. Gumilyov Eurasian National University, Astana, Kazakhstan
Alexander KOROTAEV	National Research Tomsk State University, Tomsk, Russia
Jindrich MUSIL	University of West Bohemia, Plzen, Czech Republic
Efim OKS	State University of Control Systems and Radioelectronics, Institute of High Current Electronics SB RAS, Tomsk, Russia
Kamil RAMAZANOV	Ufa State Aviation Technical University, Ufa, Russia
Timothy RENK	Sandia National Laboratories, Albuquerque, New Mexico, USA
Alexander RYABCHIKOV	National Research Tomsk Polytechnic University, Tomsk, Russia
Alexander SEMENOV	Institute of Physical Material Science SB RAS, Ulan-Ude, Russia
Yuriy SHARKEEV	Institute of Strength Physics and Materials Science SB RAS, Tomsk, Russia
Vyacheslav SHULOV	National Research University "Moscow Aviation Institute", Moscow, Russia
Yang SI-ZE	Institute of Physics, Chinese Academy of Sciences, Beijing, China
Anatoly SMYSLOV	Ufa State Aviation Technical University, Russia
Kensuke UEMURA	ITAC Ltd., Takarazuka, Japan
Vladimir UGLOV	Belarusian State University, Minsk, Belarus
Alexander YALOVETS	South Ural State University, Chelyabinsk, Russia
Georgi YUSHKOV	Institute of High Current Electronics SB RAS, Tomsk, Russia
Vitaly ZALESSKY	Physical-Technical Institute, Minsk, Belarus
Vladimir DENISOV	Institute of High Current Electronics SB RAS, Tomsk, Russia
Yuri AKHMADEEV	Institute of High Current Electronics SB RAS, Tomsk, Russia
Roman SURMENEV	National Research Tomsk Polytechnic University, Tomsk, Russia
Andrey LIDER	National Research Tomsk Polytechnic University, Tomsk, Russia
Sergey LAZAREV	Deutsches Elektronen-Synchrotron DESY, Hamburg, Germany

Conference topics

C1 Beam and plasma sources
C2 Fundamentals of modification processes
C3 Modification of material properties
C4 Coatings deposition
C5 Synchrotron and neutron research in materials science
C6 Beam-plasma engineering of SMART-materials

C1-O-002001

CLEANING SYSTEM FOR DIELECTRIC SUBSTRATES

S. A. TRIFONOV[1]

[1] JCS "D.V.Efremov Institute of Electrophysical Apparatus", Saint-Petersburg, Russia

The main disadvantage of ionic surface cleaning methods before the metallization process in microelectronics production is that, in order to obtain an effective result, the substrates are exposed to high-energy ion flows. During long-term treatment, a potential arises on the surface that is comparable to the energy of ions, which contributes to the breakdown of thin dielectric substrates, as well as the formation of defects associated with the action of charges. A decrease in the ion current inevitably leads to a deterioration in the quality of product preparation and a decrease in the adhesion strength of the coating. For this tasks of finish cleaning of the substrate dielectrical material and surface activation before the coating process an ion-plasma source basis of a controlled gas-discharge was developed (Fig. 1).To organize the movement of charged particles generated in the gas discharge in the direction of the cathode (neutralizer) an external magnetic field generated by a solenoid is used.

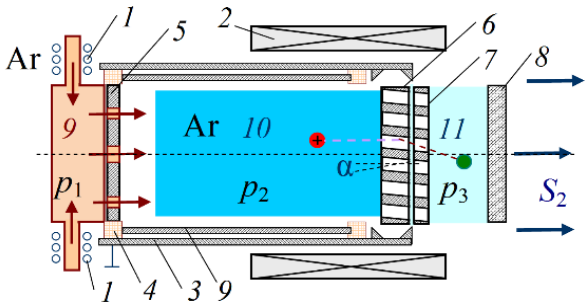

Fig. 1. Design of a controlled gas-discharge source.

Electrical scheme of the developed source consists of a cathode (neutralizer) *6*, anode *3* and a supplementary electrode *9*. The anode is grounded and on the supplementary electrode a floating potential is set. Supply system of a working gas (argon) consists of a prior warm-up device *1* and a gas distributor *5*. The latter provides the alignment distribution of the gas atoms in the discharge existence zone, which occupies the inner volume of the source *10*.

The major part of the fast atoms stream that bombards the surface of the processed dielectric is formed as a result of the recharge of the high-energy ions due to the reflection from the walls of the output channels in the cathode *6*. To organize the movement of charged particles which are generated in the gas discharge in the direction of the cathode (neutralizer) *6* an external magnetic field generated by a solenoid *2* is used.

In the presence in the source volume of a working gas and under condition that a negative potential is set on the main cathode a gas discharge which occupies the inner volume of the source *10* is ignited. In this discharge positively charged ions are generated that are later accelerated by a cathode voltage drop. Neutralization of ions occurs generally due to their reflection from the main cathode *6*, but a minor part of charged particles is neutralized due to a resonant charge exchange. A fast directed stream of working gas atoms is formed as a result of both types of neutralization.

Received results showed that the minimum (optimal) operating pressure for the developed source $p_{1\ min}$ = 1…2 Pa. For higher pressures the ignition voltage is less than 800 V and with increasing pressure it slowly falls. The source allows modification of the dielectric surfaces by their bombardment with a flux of neutral particles with energies from tens of electronvolts to a few kiloelectronvolts.

REFERENCES

[1] Yu.P. Maishev, S.L. Shevchuk, and V.P. Kudrya, “Generation of fast neutral beams based on closed drift ion sources”, Russian Microelectronics, vol. 43, no. 5, pp. 345-351, 2014.

[2] A.S. Fadeev, A.S. Talanov, D.K. Kostrin, S.A. Trifonov, A.A. Lisenkov, and V.D. Goncharov, “Cleaning of the dielectric surfaces using a controlled gas-discharge source of fast neutral particles”, Journal of Physics: Conference Series, vol. 872, p. 012021, 2017.

[3] V.T. Barchenko and N.A. Babinov, “Ions neutralization by reflection from solid target surface”, Journal of Physics: Conference Series, vol. 479, p. 012008, 2013.

[4] M.L. Vinogradov, D.K. Kostrin, V.V. Smelova, S.A. Trifonov, and A.A. Lisenkov, “Technology for producing new wear-resistant coatings in the plasma of a vacuum-arc discharge”, Proceedings of the 2016 IEEE North West Russia Section Young Researchers in Electrical and Electronic Engineering Conference, pp. 729-730, 2016.

[5] V.P. Kudrya and Yu.P. Maishev, “Calculation of the flow capacity of a gas channel in the sources of beams of fast neutral particles by means of the Monte-Carlo method”, Russian Microelectronics, vol. 42, no. 3, pp. 184-188, 2013.

C1-O-002401

ELECTRICAL CHARACTERISTICS OF A HOT-TARGET HIPIMS DISCHARGE IN REACTIVE O_2/AR AND N_2/AR ENVIRONMENTS*

A.S. ISAKOVA[1], D.V. KOLODKO[1,2], V.YU. LISENKOV[1], A.V. KAZIEV[1], G.I. RYKUNOV[1], A.V. TUMARKIN[1]

[1]National Research Nuclear University MEPhI (Moscow Engineering Physics Institute), Moscow, Russia
[2]Fryazino Branch of Kotel'nikov Institute of Radio Engineering and Electronics RAS, Fryazino, Russia

A high-current pulsed magnetron discharge in a reactive (oxygen- or nitrogen-containing) medium with a thermally insulated target is a promising and currently little-studied type of gas discharge, which can be used to obtain high-quality oxide and nitride coatings at rates significantly higher than those in classical magnetron sputtering systems. To adequately describe the entire variety of processes occurring on a target in this regime, the numerical model of the thermal state of the target [1] and the nonstationary model of reactive film deposition in pulsed sputtering systems with a high discharge current density (more than 10 A/cm^2) can be considered [2]. For the development of these models, it is necessary to experimentally study a high-current pulsed reactive magnetron discharge with target evaporation and to determine the dependences of its parameters on the flow of the reactive gas into the vacuum chamber.

In this work, we study the effects introduced by adding a reaction gas (O_2 and N_2) to a magnetron discharge with a thermally insulated target from the point of view of its electrical parameters. The dependences of the current-voltage characteristics and the shapes of the current and voltage pulses of a high-current pulsed magnetron discharge on the reaction gas flow are studied.

To form the discharge, an APEL-M-5HPP-1200 power supply with a maximum average power of 5 kW was used. We analyzed the voltage and current waveforms recorded at various pulse duration of 50–500 μs, frequency of 1 kHz and for reactive gas flow rates 0–1.80 l/h. The voltage and current waveforms exhibit a transition into unstable mode with increasing the reactive gas flow and pulse duration. In this mode, in power-regulation regime of the power supply, the pulses follow certain recurring patterns characterized by the current oscillations in a wide range from several to tens of amps.

REFERENCES

[1] A.V. Kaziev, D.V. Kolodko, N.S. Sergeev, “Properties of millisecond-scale modulated pulsed power magnetron discharge applied for reactive sputtering of zirconia,” Plasma Sources Sci. Technol., vol. 30, Article Number 055002, 2021.

[2] A.V. Kaziev, D.V. Kolodko, A.V. Tumarkin et al., “Comparison of thermal properties of a hot target magnetron operated in DC and long HIPIMS modes,” Surf. Coat. Technol., vol. 409, Article Number 126889, 2021.

* The work was supported by the Russian Science Foundation under grant No. 18-79-10242.

C1-O-002402

PLASMA PARAMETERS OF A PULSED HIGH-CURRENT LOW-VOLTAGE NON-SPUTTERING MAGNETRON DISCHARGE IN LIGHT GASES*

A.V. KAZIEV[1,2], D.V. KOLODKO[2], N.P. ORLOV[1]

[1]National Research Nuclear University MEPhI (Moscow Engineering Physics Institute), Moscow, Russia
[2]Fryazino Branch of Kotel'nikov Institute of Radio Engineering and Electronics RAS, Fryazino, Russia

Nowadays, a lot of practical applications—such as material etching; electric propulsion (plasma thrusters); material testing under high thermal and plasma loads—demand having efficient sources of highly ionized metal-free plasma. It could be convenient to utilize commercially available high-power impulse magnetron sputtering (HiPIMS [1]) technique for this purpose. However, originally HiPIMS is being used for coating deposition and thus in its conventional form is not suitable for generating plasma free of metal species. The usage of light working gas (hydrogen or helium) can significantly reduce the sputtering effects and turn this type of discharge into highly efficient generator of metal-free plasmas.

Depending on operating conditions (including pulse duration), it is possible to transform long HiPIMS regime (L-HiPIMS) into the non-sputtering low-voltage mode at the same power level. This mode is known as non-sputtering magnetron discharge (NSMD) [2–4]. Introducing hydrogen or helium into NSMD might result in high density plasma generation with extremely low cathode material erosion rate.

In this study, the operation of millisecond-scale non-sputtering discharge in hydrogen and helium has been examined. The pulse duration was around 1 ms, and the maximum pulse power was around 80 kW. The plasma parameters were monitored with an electric probe. The optical emission spectra from plasma were recorded synchronously with each pulse by AvaSpec ULS2048 spectrometer. Typical waveforms of discharge voltage and current together with probe current are presented in Fig. 1.

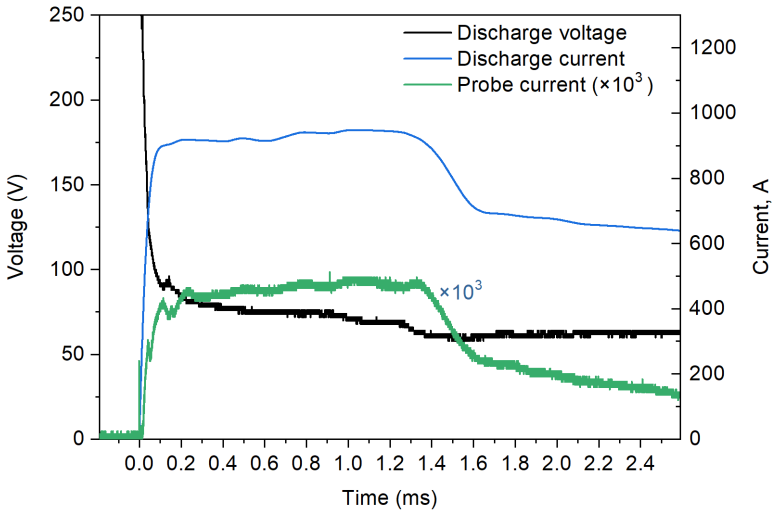

Fig.1. Discharge current and voltage traces together with probe current waveform (H_2, 2 Torr).

The use of the pulsed non-sputtering modes in hydrogen and helium enables achieving non-constricted plasmas with high density and no traces of optical emission lines corresponding to the species of cathode or anode materials.

REFERENCES

[1] J.T. Gudmundsson, N. Brenning, D. Lundin, U. Helmersson, "High power impulse magnetron sputtering discharge," J. Vac. Sci. Technol. A, Vol. 30, Article Number 030801, 2012.

[2] G.V. Khodachenko, D.V. Mozgrin, I.K. Fetisov, T.V. Stepanova, "Nonsputtering impulse magnetron discharge," Plasma Phys. Rep., Vol. 38, P. 71–78, 2012.

[3] A.V. Kaziev, "Cathode sheath processes in a non-sputtering magnetron discharge," Vacuum, Vol. 158, P. 191–194, 2018.

[4] T.J. Sommerer, S.C. Aceto, J.F. Trotter et al. "Operating modes of a magnetized cold cathode plasma in helium 50–6400 mTorr," J. Phys. D: Appl. Phys., Vol. 52, Article Number 435202, 2019.

* The work was supported by the grant of the Russian Federation President (MK-4445.2022.4).

C1-O-003002

CHARACTERISTIC OF PLASMA JETS FORMED AT THE BASIS OF GLOW DISCHARGE IN THE FLOWS OF ARGON AND AIR *

V.O. NEKHOROSHEV, N.V. LANDL, Y.D. KOROLEV

Institute of High Current Electronics SB RAS, Tomsk, Russia

Currently, plasma jets formed at the basis of the atmospheric-pressure discharges are attracting increasable attention [1, 2, 4]. Typical examples of gas discharge systems used for obtaining discharge in a gas flow and plasma jet are so-called plasmatron and "Gliding arc" [1–3]. The electrodes of plasmatron are configured to allowing the carrier gas to flow through the discharge region [2, 3]. Thus, the flow of heated and weakly ionized gas, so-called "plasma jet", forms in the plasmatron outlet [1–5].

The paper deals with the investigation of atmospheric-pressure gliding glow discharges and characterizing the properties of plasma jets, formed at the basis of that discharges. One of the features in proposed experimental setup is using an additional electrode for plasma jet electrical diagnostics (fig. 1).

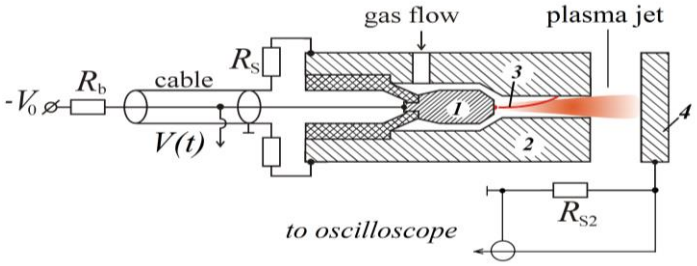

Fig.1. Simplified circuit of experimental plasma jet setup, based on non-steady state plasmatron. 1 – cathode, 2 – anode, 3 – gas discharge channel, 4 – additional electrode for plasma jet diagnostics, $V(t)$ – discharge burning voltage, V_0 – power supply voltage, R_b – ballast resistor, R_S, R_{S2} – shunt resistors for current measurement.

The discharges in argon flow and in airflow for coaxial plasmatron and gliding arc-type electrodes have been investigated using oscillography methods and CCD camera photography. Waveforms of discharge current and current through the plasma jet at the coaxial plasmatron outlet using the system of diagnostic electrodes are obtained. The gas temperature in the plasma jets are measured using thermocouple. The analysis compares the results on the discharge behavior and their effect on the jet parameters in argon and in the airflow.

The obtained data allow to concluding that the electrical current flowing through the jet volume forms due to electrons that can drifted from the discharge plasma region. Based on experimental data, the estimated value of the electron density in the jet is (10^7–10^9) cm^{-3} for air and up to 10^{12} cm^{-3} for argon. At such value of electron density, the electric field in plasma jet volume is weakly distort by the space charge of electrons and this can lead to the current self-limitation effect. It shown that the jet current magnitude determined by the flow rate and type of carrier gas, the discharge channel position and strongly depends from the parameters of the gas discharge in the plasmatron.

REFERENCES

[1] Y. D. Korolev, "Low-current discharge plasma jets in a gas flow. Application of plasma jets," Russ. J. Gen. Chem., vol. 85, no. 5, pp. 1311–1125, May 2015.

[2] Y. S. Akishev, "Non-thermal plasma at atmospheric pressure and its opportunities for applications," Izv. Vyssh. Ucheb. Zaved., Khim. Khim. Tekhnol., vol. 62, no. 8, pp. 20–62, August 2019.

[3] Y. D. Korolev, V. O. Nekhoroshev, O. B. Frants, N. V. Landl, A. I. Suslov, and A. V. Bolotov, "Features of the current sustainment in a low-current discharge in airflow," Plasma Chem. Plasma Process., vol. 39, no. 6, pp. 1519–1532, November 2019.

[4] V. Gamaleev, N. Iwata, M. Hiramatsu, and M. Ito, "Tuning of operational parameters for effective production of nitric oxide using an ambient air rotating glow discharge jet," Jpn. J. Appl. Phys., vol. 59, no. SHHF04, July 2020.

[5] K. P. Savkin, E. Oks, G. Yushkov, and Y. Ivanov, "A low-current atmospheric pressure discharge generating atomic magnesium fluxes," J. Appl. Phys. vol. 127, no. 21, p. 213303, June 2020.

* The work was supported by Russian Science Foundation, project № 22-29-00703.

C1-O-004101

INCREASING THE ELECTRICAL STRENGTH OF THE ACCELERATING SYSTEM OF A SMALL-SIZED ION ACCELERATOR

I.A. KANSHIN

Dukhov Automatics Research Institute (VNIIA), 22 Suschevskaya Ul., Moscow 127055, Russia, ilia.kanshin2011@yandex.ru, phone.: 89267930525

When developing small-sized linear accelerators, the design of which includes the Penning ion source and the accelerating system [1, 2], special attention is paid to the device electrical strength. Its decrease is mainly due to the fact that "secondary" processes occur in the accelerator's accelerating system when a negative voltage is applied to the accelerating electrode. One of them is the deposition of the accelerating system insulator inner surface by the products of the ion beam interaction with accelerating system electrodes [3]. In this case, a conductive layer is formed on insulator inner surface. It contributes to the insulator surface breakdown [3]. Another process is the electron emission from the accelerating system areas with an increased local electric field strength: "triple" junctions [4], the negative electrode edges, having a small radius of curvature. The avalanche-like movement of electrons emitted from the "triple" junctions also leads to a decrease in the electrical strength of the accelerator's accelerating system.

This work is devoted to the study of the effect of insulator inner surface deposition on the accelerating system electrical strength, as well as "triple" junctions and negative electrodes edges having a small radius of curvature. To do this, first, a trajectory analysis was carried out in the accelerating system to identify the causes of deposition formation [5]. After that, calculations of electric fields in the accelerating system were performed, which made it possible to identify areas with a local increase in the electric field strength (Fig. 1).

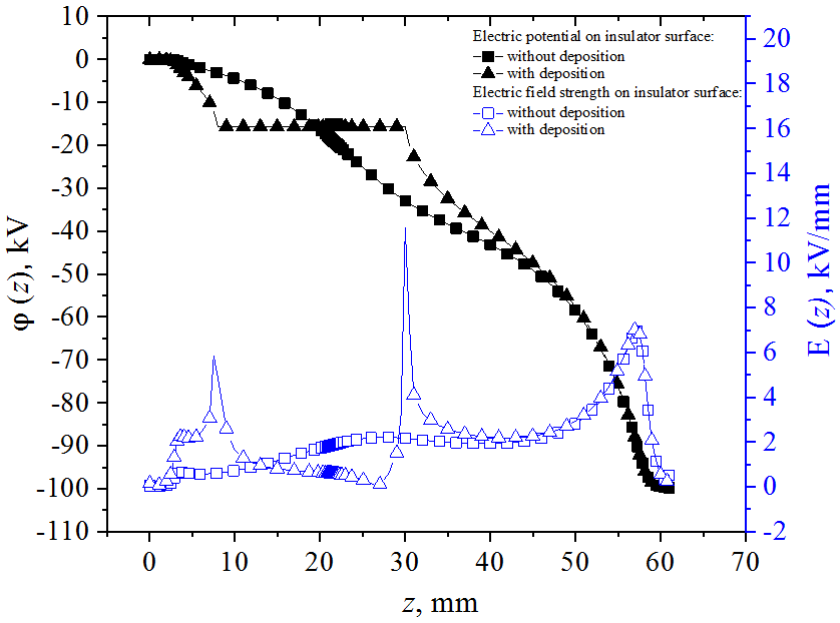

Fig. 1. The potential and the electric field strength modulus dependences near the insulator inner surface in the absence and presence of deposition

REFERENCES

[1] N.V. Mamedov, D.E. Prokhorovich, D.I. Yurkov, I.A. Kanshin, A.A. Solodovnikov, D.V. Kolodko, and I.A. Sorokin, "Measurements of the Ion-Beam Current Distribution over a Target Surface under a High Bias Potential", Instruments and Experimental Techniques., vol. 61, no. 4, pp. 530–537, 2018, DOI: 10.1134/S0020441218030223.

[2] N.V. Mamedov, N.N. Shchitov, and I.A. Kan'shin, "An Experimental Apparatus for Penning Ion Source Research", Instruments and Experimental Techniques, vol. 59, no. 6, pp. 870–878, 2016, DOI: 10.1134/S002044121606004X.

[3] I.A. Kanshin and A.A. Solodovnikov, "Measuring the Emittance of a Charged-Particle Beam in a Small Linear Accelerator", Instruments and Experimental Techniques, vol. 63, no. 3, pp. 319–328, 2020, DOI: 10.1134/S0020441220030112.

[4] Karthik Reddy Venna. "A Simulation Analysis to Improve the Dielectric Strength Inside High Voltage Vacuum Interrupters", p. 114, 2015.

[5] I.A. Kanshin "Trajectory Analysis of the Corpuscular Flow Extracted from a Small-Sized Linear Accelerator Plasma Source", Published in: 2020 7th International Congress on Energy Fluxes and Radiation Effects (EFRE). 978-1-7281-2685-2/20/$31.00 ©2020. IEEE. DOI: 10.1109/EFRE47760.2020.9241976. pp. 474-478

C1-O-008401

APPLICATION OF AN ELECTRON BEAM GENERATED BY A FORE-VACUUM PLASMA SOURCE TO INITIATE A NON-SELF-SUSTAINED GLOW DISCHARGE IN LONG NARROW METAL TUBES*

I.YU. BAKEEV

Tomsk state university of control systems and radioelectronics, Tomsk, Russia

Ion-plasma processing methods have found wide application for the tasks of surface cleaning, coating deposition and modification of the near-surface layer of dielectric and metallic materials for various purposes [1].

Ion-plasma treatment of the internal surfaces of narrow extended cavities with a transverse size of several millimeters requires a joint solution of the problems of plasma penetration into the cavity and ensuring its uniformity along the entire length of the cavity. Many works [2-4] have been devoted to solving the problem of ion-plasma treatment of the inner surface of tubular products.

One way to facilitate the generation of plasma in narrow extended cavities is the injection of electrons into the cavity to initiate non-self-sustained glow discharge [4]. However, the use of a focused electron beam generated at elevated pressures of the working gas [5] as an ionization source inside the cavity will provide great opportunities for controlling the processes of initiation and burning of a non-self-sustained discharge in a narrow extended cavity.

The paper presents the results of a study of the propagation processes and geometric dimensions of a focused electron beam generated at elevated pressures in the fore vacuum range. The processes of propagation of a focused electron beam during its passage through a narrow extended metal tube were studied. The conditions for the initiation of a non-self-sustained glow discharge in a narrow extended metal tube, initiated by injection of a focused electron beam into the tube, are studied. The results of studying the influence of the parameters of a focused electron beam and working gas on the filling of a narrow extended tube with non-self-sustained discharge plasma are presented. Presented in fig. 1 photographs show the dynamics of ignition and the distribution of the discharge in the tube.

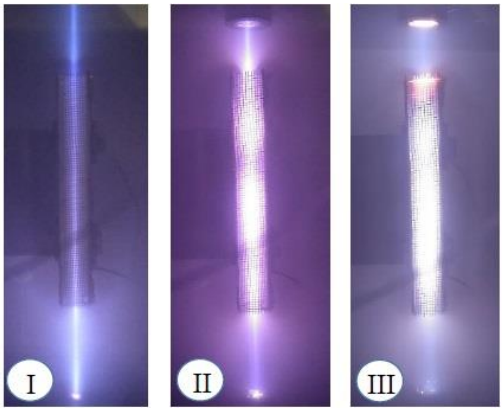

Fig.1. Photographs of the glow of the electron beam and the discharge in the tube for various beam currents Ib: I - 7 mA; II - 18 mA; III - 24 mA. Length of the tube - 15 cm, internal diameter – 12 mm.

REFERENCES

[1] R.J, Shul and S.J. Pearton, Handbook of advanced plasma processing techniques, Springer Science & Business Media, 2011.

[2] S.C. Kwon, S.C. Kwon, M.J. Park, W.S. Baek and G.H. Lee, "Geometric effect of ion nitriding on the nitride growth behavior in hollow tube," Journal of Materials Engineering and Performance, Vo.l. 1, No. 3, P. 353-358, 1992.

[3] Y.V. Borisyuk, D.V. Mozgrin, N.M. Oreshnikova, M.M. Berdnikova. and A.A. Pisarev. "Nitriding of internal cylindrical surfaces in abnormal glow discharge." Journal of Surface Investigation: X-ray, Synchrotron and Neutron Techniques, Vol. 12, No. 3, P. 603-606, 2018.

[4] D.Y. Ignatov, I.V. Lopatin, V.V. Denisov, N.N. Koval and Y.H. Ahmadeev, "Generation of Plasma in Non-Self-Sustained Glow Discharge With Hollow Cathode for Nitriding Inner Surfaces of Elongated and Complex Shaped Cavities." IEEE Transactions on Plasma Science, Vol. 48, No. 6, P. 2050-2059, 2020.

[5] I.Y. Bakeev, A.S. Klimov, E.M. Oks and A.A. Zenin, "Generation of high-power-density electron beams by a forevacuum-pressure plasma-cathode electron source." Plasma Sources Science and Technology, Vol. 27, No. 7, Article Number 075002, 2018.

* The work was supported by the Russian Science Foundation in the framework of Project No. 21-79-10217, https://rscf.ru/project/21-79-10217/.

C1-O-015201

SIMULATION OF THE ION BEAM MOVEMENT & ELECTRODES SPUTTERING IN MINIATURE LINEAR ACCELERATOR

I.A. KANSHIN[1], N.V. MAMEDOV[1,2], A.A. SOLODOVNIKOV[1], N.E. EFIMOV[2], A. S. ROHMANENKOV[1]

[1]Dukhov Automatics Research Institute (VNIIA), 22 Suschevskaya Ul., Moscow 127055, Russia
[2]National Research Nuclear University MEPhI, Kashirskoest., 31, Moscow, Russia, 115409

Miniature linear accelerators (MLA) are widely applied in various fields of science and technology [1,2]. Traditional MLA consists of a Penning ion source (PIS), an ion-optical system (IOS) and a neutron-generating target. One of the main reasons for failure of MLA is the decrease in the electric strength of the high-voltage insulator. During prolonged operation deposition metal layer on high-voltage insulator inner surface is formed due to IOS electrodes sputtering. When a certain critical thickness of the conductive metal layer is formed on the insulator between the accelerating electrode and the focusing electrodes, a high-voltage breakdown is provoked [3].

In this paper, the main sources of deposited particles are identified using three steps of numerical simulations:

1. ion beam trajectory analysis in Comsol Multiphysics [4],
2. simulations of surface sputtering by BCA codes SRIM [5], SDTrimSP [6],and SCATTER [7,8]
3. sputtered particles trajectory analysis in Comsol Multiphysics.

To determine the electrode sputtering areas, additional processes of ion beam interaction with the residual gas during its transportation to the IOS was considered. Simulation results were compared with experimental dates. Experimental data were obtained by digitizing MLA photos which were taken during operation by usage of the ImageJ software [9].

REFERENCES

[1] V. Vladivoj, *14 MeV Neutrons. Physics and Applications*, CRC Press Taylor & Francis Group, New York (2016),

[2] *Neutron Generators for Analytical Purposes* In IAEA Radiation Technology Reports No. 1. Vienna: International Atomic Energy Agency, 2012. 145 pp. ISBN 978-92-0-125110-7.

[3] I.A. Kanshin and A.A. Solodovnikov // Instruments and Experimental Techniques, 2020, Vol. 63, No. 3, pp. 315–324

[4] www.comsol.com

[5] www.srim.org

[6] Eckstein, W., Dohmen, R., Mutzke, A., & Schneider, R. (2007). *SDTrimSP: A Monte-Carlo Code for Calculating Collision Phenomena in Randomized Targets* (IPP 12/3). Garching: Max-Planck-InstitutfürPlasmaphysik.

[7] V.A. Kurnaev, Trifonov N.N., Drozdov M.N., Salashchenko N.N. // Vacuum 56, (2000), p. 253-255, doi.org/10.1016/S0042-207X(00)00136-6

[8] N.N.Trifonov, *Interaction of hydrogen ions of thermonuclear energies with thin layers of matter*, Cand. Sci. (Phys.–Math.) Dissertation, Moscow: Natl. Res. Nucl. Univ.MEPhI, 2002 (in Russian).

[9] www.imagej.net

C1-O-015801

PLASMA GENERATION IN THE GAS CAVITIES DURING DISCHARGE IN SALINE SOLUTION*

Y.D. KOROLEV, V.S. KASYANOV, I.A. SHEMYAKIN, A.V. BOLOTOV, N.V. LANDL, V.O. NEKHOROSHEV

Institute of High Current Electronics SB RAS, Tomsk, Russia

The paper deals with the investigation of the pulsed discharge in saline solution (30 g of NaCl per litre) between the point electrode *3*, whose diameter is 1.4 mm and length is 7.5 mm, and the return electrode *4*. The capacitance C_0 = 40 μF is discharged via the interelectrode gap by means of switch *S*. The gap resistance in the initial condition is R_0 = 12 Ω. When the voltage pulse is applied to the gap, the gas cavities in the form of microbubbles appear in a vicinity of the point electrode due to the process of boiling. These microbubbles merge with each other thus forming a macrobubble similar to that shown in Fig. 1.

According to the generally accepted approach, the gas discharge can appear if only the surface of the active electrode is completely covered by the vapor cavity [1–3]. Then the electrode becomes shielded from the bulk of solution so that the whole voltage is applied to the gas cavity. If this voltage is sufficient to provide breakdown in the narrowest place, the gas-discharge plasma arises. Such a case is realized in our experimental conditions when the initial voltage at the gap reaches a critical value $V_0 = V_{cr}$ = 1000 V.

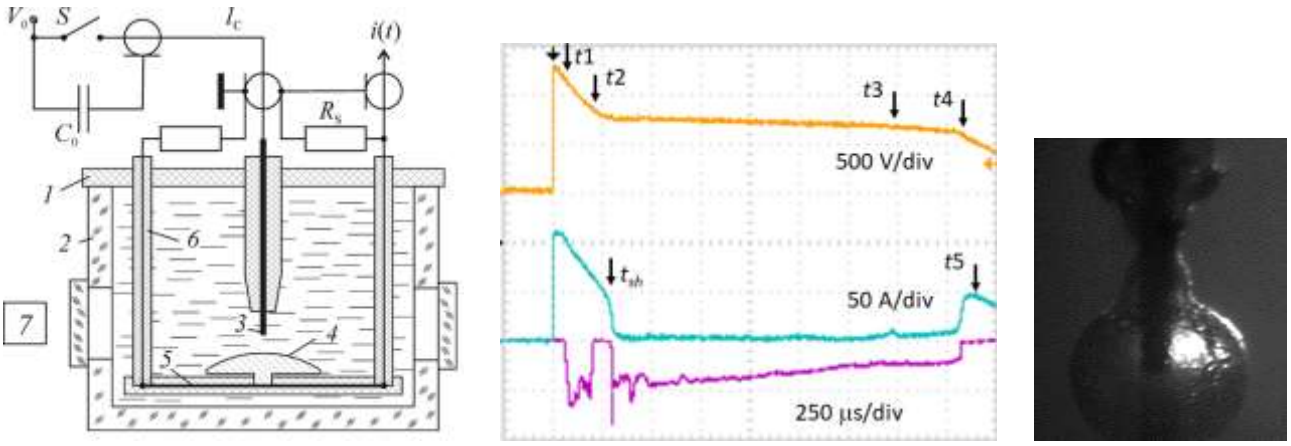

Fig.1. Experimental arrangement, the waveforms of voltage, current and PMT signal jointly with the photograph of macrobubble.

This paper demonstrates that the discharge is able to be initiated even if the active electrode is not covered by the vapor cavity completely. This situation is characteristic of the conditions when the initial voltage V_0 exceeds the critical value. The statement is illustrated by the waveforms in Fig. 1. It is seen that at the instant t_{sh} = 275 μs the current decreases abruptly i.e. the macrobubble prevents the current passage in the gap. The PMT signal shows the availability of a low-current glow-type discharge inside the macrobubble. Nevertheless, we can also observe the PMT signal starting from the instant $t1$ = 50 μs when there is no the complete electrode shielding. The discharge arises in the thin gas layer at the tip of the active electrode. After a time interval of 150 μs to the instant t2 = 200 μs, the discharge disappears since the voltage decreases to $V(t2)$ = 850 V, and this voltage is not sufficient for discharge sustaining.

One more effect, which is observed in the experiment, is the sharp destroying of the macrobubble and cleaning of the electrode surface from the gas cavities. The process of destroying begins at the instant t4 = 2075 μs. The solution enters in the direct contact with the electrode surface, which leads to a fast increase in the gap current. To the instant $t5$ = 2150 μs the gap resistance acquires the initial value R_0 = 12 Ω.

REFERENCES

[1] L. Schaper, W.G. Graham, K. R. Stalder, "Vapour layer formation by electrical discharges through electrically conducting liquids—Modelling and experiment," Plasma Sources Sci. Technol., vol.20, Article Number 034003, 2011.

[2] Y.D. Korolev, I.A. Shemyakin, V.S. Kasyanov, V.G. Geyman, A.V. Bolotov, V.O. Nekhoroshev, "Development of discharge in a saline solution at near-threshold voltages", Plasma Phys. Rep., vol.44, no.6, pp. 581–587, 2018.

[3] Y.D. Korolev, I.A. Shemyakin, V.S. Kasyanov, V.G. Geyman, N.V. Landl, A.V. Bolotov, "Transient processes during an initial stage of breakdown in saline solution," J. Appl. Phys., vol. 129, Article Number 043304, 2021.

* The work was supported by the Ministry of Science and Higher Education of the Russian Federation (FWRM-2021-0007).

C1-O-018103

INVESTIGATION OF THE TARGET HEATING UNDER THE COLD PLASMA JET INFLUENCE *

P.P. GUGIN[1], E.V. MILAKHINA[1,2], I.V. SCHWEIGERT[3], S.A. VAGAPOV[3], D.E. ZAKREVSKY[1,2]

[1]Rzhanov Institute of Semiconductor Physics SB RAS, Novosibirsk, Russia
[2]Novosibirsk State Technical University, Novosibirsk, Russia
[3]Khristianovich Institute of Theoretical and Applied Mechanics SB RAS, Novosibirsk, Russia

Currently, the field of medicine investigating the plasma formations influence on biological targets is actively developing. In most biomedical investigations conducted to study the effects caused by the plasma influence on biological targets, a cold plasma jets sources of atmospheric pressure are used [1]. The plasma jet is a sequence of streamers that are initiated by applying, for example, a sinusoidal voltage to the electrodes and propagating along the gas flow. Increasing the plasma jet power makes it possible to improve the efficiency of the plasma jet interaction with biological targets, since an increase in the energy contribution leads to an acceleration of plasma-chemical reactions [2]. In this case, heating of living tissues occurs, which can cause local burns and, subsequently, the destruction of protein compounds in cells. The investigation of the heating temperature of the target under the action of a cold plasma jet was made. A ceramic Al_2O_3 plate placed on a grounded electrode was used as a target, and the temperature in the interaction area with the jet was measured. It is shown that in certain operation modes the target temperature can exceed 50 ℃, which is unacceptable for affecting biological objects (for example, T = 60 ℃ at υ = 9 L/min, f = 13 kHz, U = 6 kV).

Comparative studies of target heating under various conditions under the action of a plasma jet were carried out: generation of a plasma jet in helium *He* with preliminary gas cooling (Fig. 1*a*, f = 13 kHz); generation of a plasma jet in a gas mixture of helium *He* and oxygen *O* (Fig. 1*b* helium flow rate *He* υ = 9 L/min, f = 13 kHz); generation of a plasma jet with limited current pulse duration (f = 25 kHz, υ = 4.5 L/min).

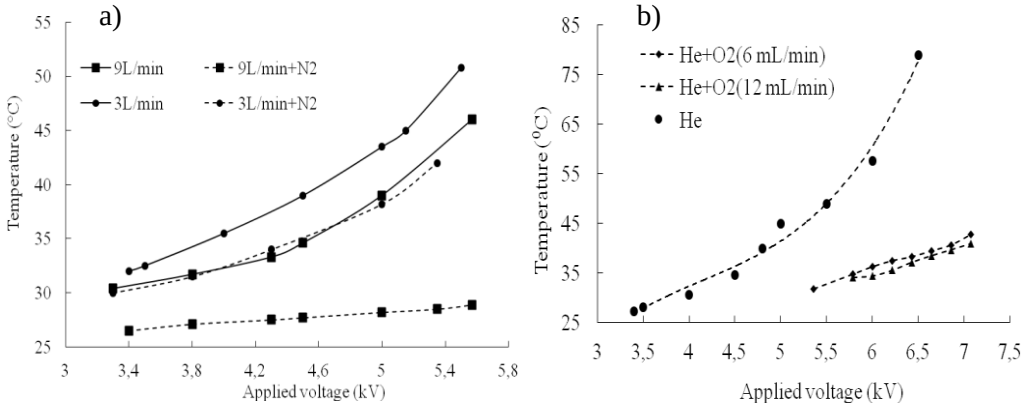

Fig.1. Reduction of target heating in the interaction zone.

Lowering the target temperature with the use of preliminary cooling of the gas pumped through the gas-discharge cell makes it possible to lower the temperature in the interaction zone to ~43%. An increase in the concentration of oxygen-containing radicals leads to a significant decrease in target heating. The effect was also observed with an increase in the rate of oxygen O_2 pumping through the gas-discharge cell. The oxygen O_2 supply into the body of the gas-discharge cell at a rate of 1.5-9 mL/min with helium *He* υ = 3-12 L/min makes it possible to reduce surface heating by ~25–50% under other comparable exposure conditions. The current pulse duration is one of the main factors affecting the temperature in the area where the plasma jet affects the target. By limiting the pulse duration, the target temperature decreased by ~20%.

Thus, the application of the developed techniques for reducing target heating makes it possible to use high-energy operation modes in biomedical research.

REFERENCES

[1] L. Lin, M. Keidar, "A map of control for cold atmospheric plasma jets: From physical mechanisms to optimizations," Appl. Phys. Rev., vol. 8, pp. 011306, January 2021.

[2] I. Schweigert, Dm. Zakrevsky, P. Gugin, E. Yelak, E. Golubitskaya, O. Troitskaya and O. Koval "Interaction of Cold Atmospheric Argon and Helium Plasma Jets with Bio-Target with Grounded Substrate Beneath," Appl. Sci., vol. 9, p. 4528, September 2019.

* The work was supported by Russian Science Foundation, research project No. 22-49-08003.

C1-O-024901

EXPERIMENTS ON THE INTERACTION OF A HIGH-ENERGY PLASMA FLOW WITH A GAS JET AND A SOLID-STATE TARGET*

D.A. TOPORKOV[1,3], V.V. GAVRILOV[1], A.M. ZHITLUKHIN[1], D.A. BURMISTROV[1,5], S.D. LIDZHIGORIAEV[1,3], V.A.KOSTYUSHIN[1], I.M. POZNYAK[1,3], A.V. PUSHINA[1,4], S.A. PIKUZ[2,4], S.N. RYAZANTSEV[2,4], I.YU. SKOBELEV[2,4]

[1]*SRC RF Troitsk Institute for Innovation and Fusion Research, Moscow, Russia*
[2]*Joint Institute for High Temperature RAS, Moscow, Russia*
[3]*NIU Moscow Institute of Physics and Technology, Moscow, Russia*
[4]*NIU Moscow Engineering Physics Institute, Moscow, Russia*
[5]*NIU Moscow Power Engineering Institute, Moscow, Russia*

The interaction of a powerful plasma flow with a pulsed gas jet and a tungsten target was investigated. Study is carried out within the framework of a project to develop high-power line X-ray sources based on pulsed plasma accelerators. The results obtained may also be of interest for solving some applied problems, such as the development of a dissipative ITER divertor and technologies for purposeful modification of surface layers of solid-state materials.

The plasma flows with a velocity of $(4\div6) \times 10^7$ cm/s and energy content of ≈ 50 kJ was produced by the pulsed electrodynamics plasma gun at MK-200 (TRINITI) facility. Hydrogen, nitrogen and neon were used as the supply gas for the plasma gun. The plasma flow moved in a vacuum chamber with a magnetic field of ≤ 2 T induction. The supersonic gas jet of nitrogen/ neon was guided by a flat Laval nozzle along the surface of the tungsten target. The density in the gas stream reached 10^{17}cm^{-3} with a jet thickness of ≈ 5 cm and a width of ≈ 15 cm. The 120 mm × 140 mm tungsten target was located at 10/20/200 mm from the central plane of the gas jet, depending on the conditions of the experiment.

The EUV&SXR images of the plasma flow interaction with the jet and target were taken using a multi-framing MCP camera. The transmission grating spectrometer was used for recording emission spectra in the wavelength range 1-70 nm with a spatial and temporal resolution. Photodiodes measured absolute power of target plasma radiation. Set of thermocouples made it possible to record the energy absorbed by the tungsten target.

The result of the experiments is a large amount of data obtained with spectral, temporal and spatial resolution, the subsequent processing of which made it possible to draw important conclusions. It was found that jet-forming gases nitrogen and neon were ionized up to the He-like state and the Li-like state correspondingly. In particular, numerical modeling of the recorded spectra in the case of the hydrogen plasma flow and the nitrogen gas jet gives the value of plasma electron temperatures in the range of 40÷50 eV, and in the case of a neon gas jet, it can reach 70÷100 eV. Information was also obtained on the power of the radiation, its spectral and spatial distribution for targets various combinations (the tungsten target with no gas jet, and the tungsten target with nitrogen or neon jets) and plasma flow composition (hydrogen, nitrogen, neon).

An important feature of the hydrogen/nitrogen/neon plasma flow impact on the tungsten target with no gas jet is that the target plasma radiation contains mainly spectral lines of tungsten. In the case of the hydrogen plasma exposure, the tungsten vapor propagates to a distance of more 6 cm from the surface towards the plasma flow along the longitudinal magnetic field, as for non-hydrogen plasma, fewer 2 cm.

The results of the non-hydrogen (nitrogen/neon) plasma impact on the gas jet and the tungsten target are presented as well. In these experiments tungsten vapor also did not travel more than 2 cm from the tungsten target surface and the emission contained spectral lines of the gas jet, rather than the plasma flow.

*The work was supported by the Russian Foundation for Basic Research (Projects No. 18-29-21013 and No. 20-21-00153).

C1-O-025401

THE SYSTEM OF PLASMA-ASSISTED RF - APPLYING COATINGS FROM POWDER DIELECTRIC MATERIALS*

I.I. AZHAZHA, V.V. SHUGUROV

Institute of High Current Electronics SB RAS, Tomsk, Russia
E-mail: chieftainhawk00@gmail.com

This paper presents the results of the development and study of the system of plasma-assisted RF application of dielectric coatings from powder materials. The system (Fig. 1) consists of a target with a diameter of 200 mm with a powder material from which covers and a gas plasma generator "Pink" are applied. The system reduces the coating pressure to significantly increase the coating rate and allows you to control the properties of the coatings of the plasma assistation during the deposition process. Studies were carried out at the installation of electron-ion-plasma engineering of the complex surface "Complex" developed in the laboratory of plasma emission electronics IHCE SB RAS.

The operating modes of the system were investigated and the dependence of the ion current density was removed on the samples from the power of the RF discharge in the Ar and Ar + N_2 atmosphere. All data were removed for 7 values of the current of the discharge of the plasma generator I_p = 5, 10, 15, 20, 30, 40, 50 A. for these values, the dependences of the current density from the RF power and the discharge voltage from the RF power were constructed.

Trial processes of deposition of the coating $AlMgB_{14}$ (BAM) were carried out. Substrates - Samples (VK8 alloy and steel R6M5) were pre-cleaned in an ultrasonic bath, were fixed on the substrate and placed in the chamber. The second phase of purification was purified in the gas discharge of the plasma generator for 15 minutes at a current of discharge 30 A, the displacement supplied to the samples was -990 V, with a duty of 75%. After cleaning, the samples unfolded to the target attached to the RF-current, AlMgB composition. The inclusion of the RF of the generator and the matching device was filled with 300 W power to warm up the target and its expansion. When pressure is set, the power rises to 700 W, so that the discharge burning voltage was about 1 kV. The displacement for samples was established about 100 V with a duty capacity of 50%. The process adjustment was carried out by changing the reflected RF power and flow current of the plasma generator.

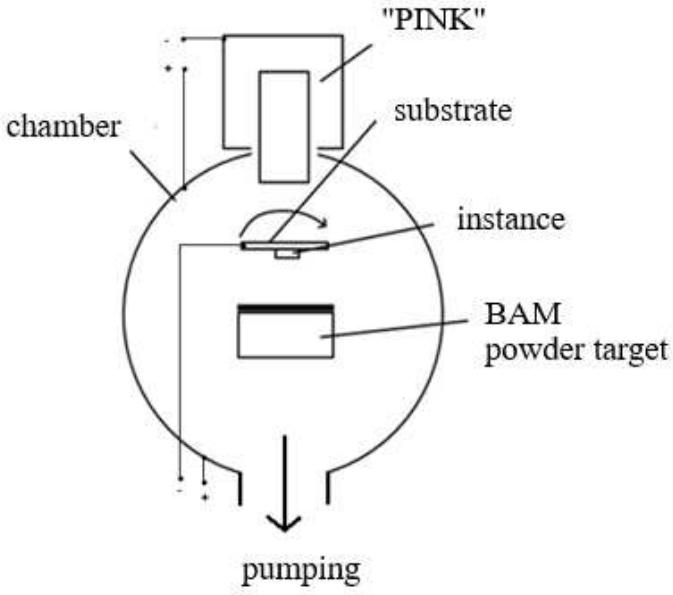

Fig.1. Scheme of experiment.

BAM coatings with a thickness of up to 3 μm were obtained with a precipitation rate of ~ 1.3 μm / hour.

* The work was supported by RSF project No. 19-19-00183.

C1-O-028101

THE APPLICATION OF THE PD-BA COATING IN THE PENNING ION SOURCE

A.G. SADILKIN, N.N. SCHITOV

Dukhov Research Institute of Automatics, Russian Federation, Moscow

The method to improve service characteristics of the gas-filled electrovacuum devices, based on the Pd-Ba coating of the Penning ion source, is described. This improvement is achieved due to the rise of the atomic ion fraction in the extracted beam as well as to the fall of the discharge potential. The first effect may be explained by the Pd catalytic properties, whereas the second – by the adding of the emission active doping (Ba). The improved service characteristics data are exemplified.

C1-O-029901

NUMERICAL STUDY OF THE EXTINGUISHING PHENOMENA IN THE PULSED MODULATED INDUCTION THERMAL PLASMA TORCH

LONG MIAO, MINGQING NIE, YURI M GRISHIN, RUOYU HAN, ZIHAO HE, ZHENGXI ZHU, NINGFEI WANG

School of Aerospace Engineering, Beijing Institute of Technology, Beijing, China

In this work, a two-dimensional unsteady laminar model is developed to simulate the transient process of the pulse-modulated induction thermal plasma. A standard PL-50 type induction thermal plasma torch is considered in the model, and the generator frequency is 3MHz, the coil current is set in the range of 100-200A. The critical current is studied to determine the waveform to ensure that a smaller current can be used to sustain a stable discharge. Special attention is paid to investigate two different vortex pattern: Benard and toroidal vortex in induction thermal plasma torch under different inject tube diameter, central gas flow rate, shimmer current level and duty factor.

C1-O-030501

ELECTRIC ARC HYDROGEN PRODUCTION FROM NATURAL GAS AND GAS CONDENSATES

S.D. POPOV[1], V.E. POPOV[1], D.I. SUBBOTIN[1], A.V. SUROV[1], E.O SERBA[1], A.V. NIKONOV[1], GH.V. NAKONECHNY[1], V.A. SPODOBIN[1]

[1] Institute for Electrophysics and Electric Power of the Russian Academy of Sciences (IEE RAS), St. Petersburg, Russia

In the 21st century, the role of alternative energy and, especially, hydrogen energy is growing significantly. The main methods for producing hydrogen are steam catalytic reforming of natural gas [1] and electrolysis of water [2]. Steam reforming is a large-scale production, however, it has significant disadvantages: a high carbon footprint, incomplete methane conversion, and heating of steam to high temperatures [3]. At the same time, electrolysis has low productivity and high energy consumption [4].

At present, a number of methods for obtaining hydrogen from hydrocarbons by plasma pyrolysis are proposed [5, 6]. However, these methods are severely limited by the productivity of the facilities and the period of their continuous operation. Features of power sources and the design of plasma devices significantly affect the efficiency of the overall process. At the same time, plasma methods ensure the creation of small local production facilities. Such plants can meet the demand for hydrogen for the production of small-scale chemical products.

The report discusses a plasma-chemical facility for the pyrolysis of natural gas and light hydrocarbons. It consists of a high-voltage AC plasma torch, a plasma-chemical reactor, a plasma torch power supply system, a system for supplying reagents and analyzing reaction products.

The plasma torch consists of three water-cooled arc channels with end copper electrodes [7]. The plasma torch has two zones for the supply of plasma-forming media. A shielding gas (argon) is supplied to the near-electrode zone, and hydrocarbons are supplied to the electric arc burning zone. Thus, the electrode insulators are protected from the ingress of electrically conductive graphitized soot into them. The power of the plasma torch depends on the flow rates of plasma-forming media and the value of the electric current regulated by the power source.

The plasma-chemical reactor is a hollow lined cylinder equipped with pressure sensors, high-temperature thermocouples, and sampling probes [8]. The content of solid particles in the produced products was determined gravimetrically using a thimble quartz filter. The composition of the gas phase was determined with a calibrated quadrupole mass spectrometer.

Four experiments were carried out with natural gas and propane-butane fraction. The conversion of hydrocarbons primarily depended on the temperature in the plasma-chemical reactor. When the reactor was preheated, the conversion of methane increased from 65% to 75%, and the conversion of the propane-butane fraction increased from 75% to 85%. The analysis showed that the produced carbon black consists of two fractions with different properties: graphite (70%) and polyaromatic hydrocarbons (30%). Also traces of iron (up to 0.07% wt.) and other metals were found in the carbon black. This indicates the erosion of the metal walls of the plasma torch during its operation.

Thus, it can be concluded that the plasma pyrolysis of hydrocarbons can be used to produce hydrogen and carbon black. To accomplish this task, it is necessary to combine efforts in the development of high-power high-voltage plasma torches and their integration into the renewable energy system.

REFERENCES

[1] S. A. Ghoneim, R. A. El-Salamony, S. A. El-Temtamy, “World Journal of Engineering and Technology,” Review on Innovative Catalytic Reforming of Natural Gas to Syngas, vol. 4, no 1, pp. 116-139, 2016.

[2] M. M. Rashid, M. K. Al Mesfer, H Naseem, “Hydrogen Production by Water Electrolysis: A Review of Alkaline Water Electrolysis, PEM Water Electrolysis and High Temperature Water Electrolysis,” IJEAT, vol. 4, Is. 3, 2015.

[3] H. Zhang, Z. Sun, Y. H. Hu, “Steam reforming of methane: Current states of catalyst design and process upgrading,” Renewable and Sustainable Energy Reviews, vol. 149, pp. 111330-111353, 2021.

[4] M. Eyvaz, Advances In Hydrogen Generation Technologies, London: IntechOpen, 2018.

[5] A. Górska, K. Krawczyk, S. Jodzis, K. Schmidt-Szałowski, “Non-oxidative methane coupling using Cu/ZnO/Al2O3 catalyst in DBD,” Fuel, vol. 90, Is. 5, pp. 1946-1952, 2011.

[6] Morgan, N. N. Hydrogen Production from Methane Through Pulsed DC Plasma,” Plasma Chemistry and Plasma Processing, vol. 37, Is. 5, pp. 1375-1392, 2017.

[7] A.V. Surov, S.D.Popov, V.E.Popov, D.I.Subbotin, E.O.Serba, V.A.Spodobin, Gh.V.Nakonechny, A.V.Pavlov,“ Multi-gas AC plasma torches for gasification of organic substances,” Fuel, vol. 203, pp. 1007-1014, 2017.

[8] P. G. Rutberg, V. A. Kuznetsov, V. E. Popov, S. D. Popov, A. V. Surov, D. I. Subbotin, A. N. Bratsev,“ Conversion of methane by CO2 + H2O + CH4 plasma,” Applied Energy, vol. 148, pp. 159-168, 2015.

C1-O-030601

PLASMA OSCILLATIONS INFLUENCE ON ION-FLUX PROPAGATION IN SEPARATOR LAPLACE 1*

V.S. SMIRNOV[1], *S. KISLENKO*[2,1], *G. LIZIAKIN*[2,1], *A. GAVRIKOV*[2,1]

[1] *Moscow Institute of Physics and Technology (State University), Moscow, Russia*
[2] *Joint Institute for High Temperatures of the Russian Academy of Sciences, Moscow, Russia*

We propose a numerical model for ion beam mass-separation in plasma. The model parameters are based on an experimental setup Laplace 1 for spent nuclear fuel mass separation [1]. We use Particle-in-cell method with Monte-Carlo collisions to simulate background plasma [2]. Gyrokinetic model for electron component is used to boost calculations [3]. Ion component motion is simulated with a classical Boris scheme [4]. The ion flux propagation in a background plasma is simulated in a single-particle approximation. We investigate oscillations of background plasma obtained via numerical model. They are in a good agreement with experimental results. We obtain the results on the ion separation in a background plasma and study the impact of plasma oscillations on a quality of ion separation.
This study was supported by the Russian Science Foundation № 21-19-00716, https://rscf.ru/en/project/21-19-00716/.

REFERENCES

[1] G. Liziakin, N. Antonov, V. S. Smirnov, R. Timirkhanov, A. Oiler, R. Usmanov, A. Melnikov, N. Vorona, S. Kislenko, A. Gavrikov, V. P. Smirnov, “Plasma mass separation in configuration with potential well,” J. Phys. D. Appl. Phys., vol. 54, no. 41, pp. 414005, July 2021.

[2] G. D. Liziakin, A. V. Gavrikov, Y. A. Murzaev, R. A. Usmanov, and V. P. Smirnov, “Particle-in-cell charged-particle simulations, plus Monte Carlo collisions with neutral atoms, PIC-MCC,” EEE Transactions on Plasma Science, vol. 19, no. 2, pp. 65-85, April 1991.

[3] A. H. Boozer, “Plasma Confinement,” Encyclopedia of Physical Science and Technology, vol. 13, pp. 1, 1992.

[4] H. Qin, S. Zhang, J. Xiao, J. Liu, Y. Sun, and W. M. Tang, “Why is Boris algorithm so good?,” Physics of Plasmas, vol. 20, no. 8, pp. 084503, May 2013.

* The work was supported by the Russian Science Foundation № 21-19-00716, https://rscf.ru/en/project/21-19-00716/.

C1-O-030802

PLASMA PARAMETERS OF PULSED PLANAR MAGNETRON DISCHARGE WITH ELECTRON INJECTION FROM VACUUM ARC*

M.V. SHANDRIKOV[1], *A.A.CHERKASOV*[1], *V.P.FROLOVA*[1,2], *A.V.VIZIR*[1], *E.M. OKS*[1,2]

[1] *Institute of High Current Electronics SB RAS, 2/3 Akademichesky ave., Tomsk, Russia, 634055*

[2] *Tomsk State University of Control Systems and Radioelectronics, 40 Lenin ave., Tomsk, 634050, Russia.*

A discharge system based on a planar magnetron with a central electron injection from a vacuum-arc discharge plasma is studied in detail. The experiments were carried out on a copper target. The operating pressure varied in the range of 0.5-3 mTorr. The pulse current of the magnetron discharge was 10-30 A (50÷250 μs).The change in the ratio of gas and metal ions in the magnetron plasma is shown depending of supplying the working gas and the type of discharge used as an electron emitter. The effect of the electron injection and a reflector electrode on the radial uniformity of the magnetron plasma is investigated. The excitation conditions of rotational inhomogeneity in the magnetron's racetrack region and its linear velocity are determined. The electron temperature was measured depending on the operation mode of magnetron discharge.

* The work was supported by the RSF Grant 21-19-00136.

C1-O-031701

MULTIARC GRID PLASMA EMITTER BASED ON AN ARC DISCHARGE FOR GENERATING A RADIALLY CONVERGING ELECTRON BEAM

M.S. TORBA, M.S. VOROBYOV, N.N. KOVAL, V.V. EZHOV, S.YU. DOROSHKEVICH, S.A. SULAKSHIN

Institute of High Current Electronics, Tomsk, Russian Federation

The promise of using electron sources with a plasma cathode based on a low-pressure arc discharge with grid/layer stabilization of the emission plasma boundary, and a plasma anode with an open plasma boundary, has been repeatedly demonstrated for surface modification of various materials and products, leading to a multiple improvement in the functional properties of their surface, modifications of the surface of materials that are unattainable by other means, which clearly confirms the need for further development and implementation of equipment of this class. However, the complexity of the shape of most processed products hinders the introduction of such equipment in a specific technological process. That is why in this work we study a grid plasma emitter for generating a radially converging electron beam, suitable for modifying the surface of products not only cylindrical, but also of a more complex shape (for example, processing stents) [1,2].

Thus, this paper describes the design of a grid plasma emitter based on a low-pressure (~10-2 Pa) multi-arc discharge for generating a radially converging submillisecond electron beam [3,4]. The developed and created power supply system based on inductive energy storage devices makes it possible to generate arc discharge current pulses of submillisecond duration with an amplitude of up to 200 A. The conducted studies of the generation of emission plasma allow us to assert that this method of generating an electron beam is promising for scientific and industrial purposes when processing products of complex shape, or generating microwave radiation.

REFERENCES

[1] V. E. Gromov, F. Y. Ivanov, S. V. Vorobiev, and S. V. Konovalov, Fatigue of Steels Modified by High Intensity Electron Beams. Cambridge, U.K., 2015, p. 272.

[2] E. Oks, Plasma Cathode Electron Sources: Physics, Technology, Applications. Hoboken, NJ, USA: Wiley, 2006, p. 171.

[3] Koval. N.N., Grigoryev S.V., Devyatkov V.N., et al. // IEEE Trans. Plasma Sci. -2009. – V.37.- No. 10. – P.1890-1896.

[4] Vorobyov M.S., Gamermaister S.A., Devyatkov V.N., et al. // Tech. Phys. Lett. – 2014. –V.40.-No.6.-P.526-528.

C1-O-035601

PIGIS' PULSE FIELDS MODULATION

N.N. SCHITOV

Dukhov Automatics Research Institute (VNIIA), 22 Suschevskaya Ul., Moscow 127055, Russia, nschitov@mail.ru, phone.: 89160820555

The investigations' onset of pulsed fields influence on Penning ion sources (PIGIS) in pulse or frequency regimes was described in [1, 2]. This modulation was carried out by pulse fields generated by the storage capacitance discharge through flat spiral antennas being cathodes of a Penning cell in H_2. In [1] experiments were carried out with Al wire coils. In [2] all PIGIS electrodes including anode were fabricated from metalized ceramics with lathe cut grooves. The number of possible fields' combinations (mutual direction etc) rose up to 9 in [2]. However, this technology – diamond lathe cutting – is far from perfect or actual. For instance, it is impossible to make the twin or double antennas [1] this way. Laser grooves cutting or chemical etching through mask are much more attractive. The next step discharge construction with laser cut grooves is actually in progress.

To complete the research the funnel-shaped coils made of Al wire as in [1] are investigated. In [3] is shown that the magnetic field distribution may improve the current pulse time characteristics, decrease discharge current and increase the extraction coefficient. In the case of funnel-shaped coils the magnetic field's axial component maximum is drift to the center of the Penning cell so that changing the funnel cone half-angle one may superpose it with the ionization coefficient maximum. The gas discharge becomes "combined" – the hollow cathode and the Penning ones. Besides, the existence of cell axe's length dependence in such antennas leads to the appearance of curl axial electric fields absent in the case of the flat one. Finally, the radial components of the funnel-shaped coils are significantly higher near cathodes than that of the flat ones. It means that the asymmetry relative to polarity is higher for the formers. It may be useful from the ion's extraction point of view.

The last discussed aspect of pulsed fields' modulation concerns the discharge key's (vacuum lightning arresters) location [1, 2]. In experiments described earlier it was mounted just between the storage capacitance connected with grounded cathodes and the power supply so that the stationary PIGIS' electric field distribution took place during the whole discharge period. But when cathodes are isolated by the key from a ground all electrodes are equipotential at the initial moment that is no fields exist. During the capacitance discharge the gas discharge's form turns out from the TCP (transformer coupled plasma) one into the Penning one due to the cathode's potential drop through discharge. In this case the pulsed magnetic field is in phase synchronism with the storage capacitance discharge whereas the azimuthally curl electric field changes its sign twice during the period.

Total pulse fields generated in the gas discharge chamber during the store capacitor discharge are calculated. Using these calculations electrons trajectories and correspondingly ionization probabilities are estimated for various fields' directions' combinations. These estimates are compared with the experimental results carried out in the experimental unit described in detail in [1], still slightly changed.

REFERENCES

[1] N N Schitov 2019 J. Phys.: Conf. Ser. **1393** 012053. doi:10.1088/1742-6596/1393/1/012053
[2] N N Schitov *2020* 7th International Congress on Energy Fluxes and Radiation Effects (EFRE-2020 online): Abstracts.— Tomsk: Publishing House of IAO SB RAS, 2020. — 98 p.
[3] N V Mamedov et al *Plasma Sources Sci. Technol.* **29** (2020) 025001

This work was partly supported by Russian Foundation for Basic Research under grant #12-02-13513 – ofi_m_RA.

C1-O-037201

LOW TEMPERATURE PLASMA JET OPTIMIZATION FOR CANCER TREATMENT

I. SCHWEIGERT[1], *D. ZAKREVSKY*[2,3], *E. MILAKHINA*[2,3], *P. GUGIN*[3]

M. BIRUKOV[4] *AND O. KOVAL*[4,5]

[1] Khristianovich Institute of Theoretical and Applied Mechanics, Novosibirsk, Russia
[2]A.V. Rzhanov Institute of Semiconductor Physics, 630090 Novosibirsk, Russia
[3]Novosibirsk State Technical University, 630090 Novosibirsk, Russia;
[4]Institute of Chemical Biology and Fundamental Medicine, Novosibirsk, Russia;
[5]Department of Molecular Biology, Novosibirsk State University, Novosibirsk, Russia

Recently the low temperature atmospheric pressure plasma jets (CAPS) are widely used for the inhibition of the solid tumor growth, and in particularly with a combination with nanoparticles [1]. In this work, to maximize the effect of the CAPJ treatment on the different cancer cell lines, the optimization of the plasma jet device was done for the sinusoidal and positive pulsed voltage discharge initiation. The different modes of discharge operation were analyzed in the experiment and fluid model numerical simulations. The efficacy of chosen regimes was confirmed in our bio experiments with cancer cell lines (A549, MX7, A431 etc). The viability of the cancer cells was analyzed with MTT assay 24 hours after the CAPJ exposure. It was shown that the viability of cancer cell depends on the choice of the mode of the discharge operation. In physical experiment and simulations, the optimization of CAPS regimes was done with an analysis of the self-organization of voltage – streamer propagation frequencies, which sets the total effect of the bio target treatment [2,3]. In fact, an increase of the voltage amplitude and frequency causes a nonmonotonic increase of the plasma-target interaction. The temperature of the zone of CAPJ contact with the target can rapidly increase and burn the bio tissue. So the safety conditions should be monitored. We also study the dynamics of the NPs penetration on the cancer cells in vitro and the effect of nanoparticle presence inside the cells on their viability after CAPS treatment. In Figure 1, the plasma device, simulation domain and mouse treatment with CAPJ are shown.

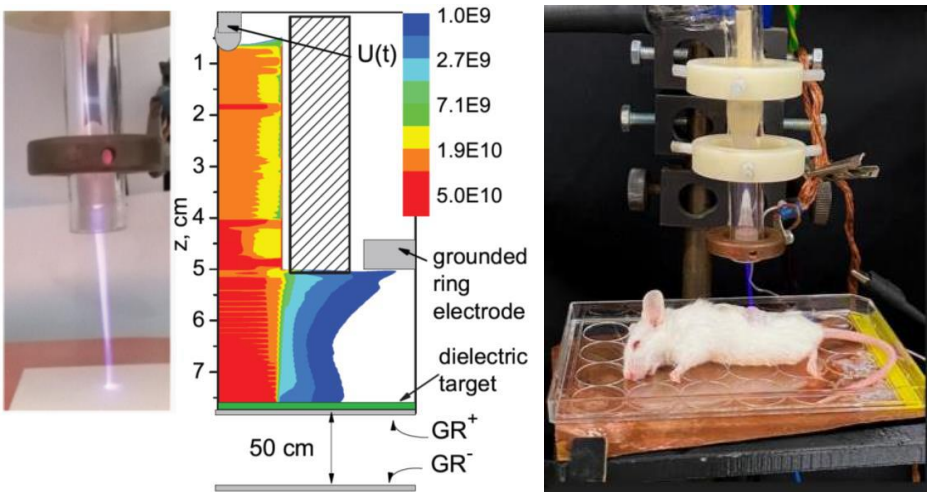

Fig.1. Experimental device and fluid model calculation domain with the ion density distribution when the streamer touches the dielectric target, GR+ and GR− correspond to the cases with the grounded electrode beneath the target and the grounded electrode 50 cm apart from the target. Sleeping mouse with tumor during CAPJ treatment.

REFERENCES

[1] Kong MG, Keidar M, Ostrikov K: Plasmas meet nanoparticles—where synergies can advance the frontier of medicine. Journal of Physics D: Applied Physics 2011, 44(17):174018.doi:10.1088/0022-3727/44/17/174018

[2] I. Schweigert, A. Alexandrov, D. Zakrevsky, *Plasma Sources Sci. Technol.* 29 12LT02 (2020)

[3] I.Schweigert, D. Zakrevsky, E. Milakhina, P. Gugin, M. Biryukov, E. Patrakova, O. Koval Grounded electrode beneath dielectric target or cancer cells enhances impact of cold atmospheric plasma jet. Plasma Physics and Controlled Fusion, 2022 *Plasma Phys. Control. Fusion* 64 044015

The authors gratefully acknowledge financial support from Russian Science Foundation, grant N 22-49-08003.

C1-O-039701

ELV-15 – NEW ACCELERATOR FOR INDUSTRIAL APPLICATIONS

D.S. VOROBEV, E.V. DOMAROV, M.G. GOLKOVSKII, Y.I. GOLUBENKO, A.I. KORCHAGIN,

D.A. KOGUT. N.K. KUKSANOV, R.A. SALIMOV, A.V. SEMENOV, S.N. FADEEV,

V.G. CHEREPKOV, A.V. LAVRUKHIN.

Budker Institute of Nuclear Physics, Novosibirsk, Russia

Budker Institute of Nuclear Physics produces high power electron beam accelerators for industrial application. These accelerators have the name “ELV”. Flexible (because of the possibility of completing with different under beam systems) and reliable ELV accelerators found wide applications in industries. The family of the ELV accelerators covers the energy range from 0.3 to 3 MeV, and beam current up to 130 mA of beam current, with power up to 100 kW. Special versions of ELV accelerators allows to obtain 400 kW of power with a maximum beam current of 0.4A. Over 200 accelerators were delivered and installed by now. Even for the last three years, under the significant influence of COVID-19, we had delivered 17 accelerators to our customers. For 2022, the same amount is in the queue.

New accelerators of the ELV type are also being developed. Last version is “ELV-15” accelerator[1]. The energy range is up to 3.0 MeV and the beam power is up to 100 kW. It is shown on Fig.1. It has all features of ELV accelerators:

- High electron beam power in wide energy range;
- High efficiency of electron beam (70-80%), which important for long term operation;
- High stability of electron beam parameters;
- Extra-long lifetime and high reliability: 24/7 mode of operation.

At present time accelerator was assembled, tested and delivered to China. Increasing the energy up to 3 MeV expands the possibilities of industrial application. It allows to increase the thickness of treated material and cable insulation. There are many requests for the new accelerator.

Additionally, it can operate as X-ray generator. The smaller conversion coefficient for 3 MeV can be compensated the higher beam power and efficiency from electricity to beam. So, it produce same amount of X-rays in comparison with 7.5 MeV accelerator and same consumption power.

During designing of new accelerator we had taken into mind the experience of previous models, changing of electrical and electronic components simultaneously with possibilities to exchange of elements and systems new and old machines.

Fig.1. Accelerating tube inside of primary windings of ELV-15 accelerator.

[1] N.K. Kuksanov, D.S. Vorobev, R.A. Salimov, S.N. Fadeev. “The High Voltage Source for the ELV-15 Accelerator”. Siberian Journal of Physics, 2022, vol. 17, no. 1, pp. 23–33.

C1-O-042601

PROCESSING OF MATERIALS WITH ARC PLASMA TORCHES WITH THERMOCHEMICAL CATHODES *

A.S. ANSHAKOV, P.V. DOMAROV, V.A. FALEEV

Kutateladze Institute of Thermophysics SB RAS, Novosibirsk, Russia

Despite the variety of design schemes of electric arc plasma torches, there is always a need for low-power plasma devices (10–50 kW) for heating air and other oxygen-containing media, for example, in the technologies of plasma cutting of metals, plasma spraying, for modifying surfaces and synthesizing various materials. In this case, thermochemical composite cathodes are widely used (Fig. 1). The electron emitter in such cathodes is zirconium or hafnium inserts soldered or pressed into a water-cooled copper body.

The thermochemical cathode is essentially a thermionic cathode, and got its name due to the fact that in air the high-temperature surface of the zirconium (hafnium) insert chemically interacts with nitrogen and oxygen, forming an oxonitride film with good emission properties, electrical conductivity and thermal stability. The resulting film reliably protects the zirconium (hafnium) insert from further oxidation, which ensures the operation of the cathode in air.

On fig. Figure 1 shows the location of a single Hf or Zr insert (Fig. 1a) with a diameter dk and depth Δ l = 3 mm and a recess δ of the insert and modified with four Hf inserts to increase the electrode life (Fig. 1b). The latter differs from the cathode with a single thermal insert in that, in addition to the central insert, three more radial rods are pressed into the copper body at intervals of 120°. The diameter of the central insert is dk = 2.45 mm, the side inserts are 1.6 mm.

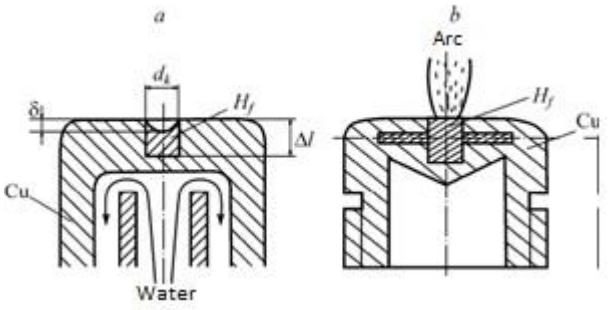

Fig.1. Schemes of thermochemical cathodes

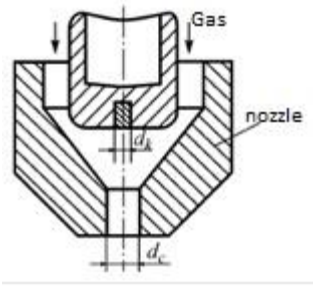

Fig.2. Nozzle chamber of the PVR-402 plasma torch.

On fig. Figure 2 shows the axisymmetric placement of the cathode assembly in the plasma torch for air-plasma cutting of metals (dc = 3.6 mm).

The studies carried out by other authors made it possible to establish the general regularities of the parameters of thermochemical cathodes in terms of current density, heat fluxes, specific erosion, optimization of the insert diameter dk with respect to current, incl. depending on the method of embedding the Hf insert into the copper holder. Despite the significant scatter of experimental data, the specific erosion of thermochemical cathodes has an almost linear dependence on the arc current and amounts to 10 – 11 – 10 – 10 kg/C. At low discharge currents (I ≤ 200 - 300 A), their continuous operation resource reaches several tens of hours.

It is shown that the deepening δ grows with time at a constant current value. The rate of destruction of the cathode in time is uneven. The depth of development of the thermochemical cathode, as well as the tungsten cathode, has an optimum in terms of the diameter of the insert.

On the basis of thermochemical cathodes, highly efficient electric arc plasma torches for cutting metals (Fig. 2), spraying powder materials EDP-167, and heating gas EDP-104 with a power of 10–50 kW have been created. More details about them will be discussed in the article (report).

* This work was carried out under state contract with IT SB RAS (№ 121031800229-1).

C1-O-043402

DIFFUSE VACUUM ARC DISCHARGE WITH HEATED CATHODE MADE OF MIXTURE OF CERAMIC AND METAL POWDERS*

R.A. USMANOV, A.D. MELNIKOV, V.P. POLISTCHOOK

Joint Institute for High Temperatures RAS, Moscow, Russia

We present results of an experimental study of a plasma flow parameters generated by a vacuum arc discharge with heated cathode made of mixture of ceramic and metal powders. The discharge existed in a diffuse mode of cathode current attachment [1]. The diffuse mode was characterized by relatively low values of cathode current density (10-100 A/cm^2), absence of significant voltage oscillations and stable glow of plasma formation (Fig. 1).

The experiments were carried out in vacuum chamber with residual gas pressure less than 10 mPa. The cathode was presented by a mixture of powders of cerium dioxide (CeO_2) and chromium (Cr). The cathode mixture was placed in a molybdenum crucible, under which an electron beam heater (EBH) was situated. The mixture was tentatively sintered in vacuum at a temperature of the crucible of 1500 C for an hour. At a temperature of 1900 C the breakdown of the discharge gap was initiated. The molybdenum plate with centered hole of 14 mm in diameter for plasma outflow was used as an anode of the arc. The length of the discharge gap was about 30 mm. EBH allowed us to vary the crucible temperature at fixed arc current that caused significant changes of the discharge parameters, in particular, a voltage drop of the discharge gap.

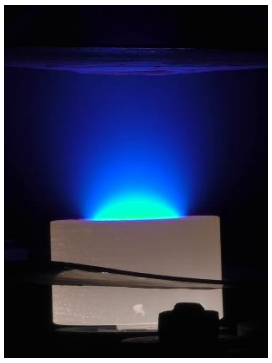

Fig.1. Photo of the diffuse vacuum arc discharge on mixture cathode of CeO_2 and Cr powders.

The dependencies of heat fluxes coming from plasma into the cathode on arc current and power of EBH were studied. The data on mean charge of the arc plasma flow, ion energies and ion composition obtained by time-of-flight mass spectroscopy method [2] were obtained. It was shown that chromium is a main source of the plasma forming medium when cerium dioxide is a main source of electrons of thermionic emission. The comparison of the arc discharge parameters on mixture cathode with arcs on monocomponent cathodes of Cr [3] and CeO_2 [4] was performed.

Obtained results can be useful in designing of stabile plasma sources of multicomponent condensed substances for wide range of applications from deposition of composite coatings to plasma mass separation [5].

REFERENCES

[1] V.P. Polishchuk, R.A. Usmanov, A.D. Melnikov et al., “Vacuum Arcs with Diffuse Cathode Attachment (Review),” High Temp., vol. 58, pp. 476-494, 2020.

[2] A.D. Melnikov, R.A. Usmanov, R.Kh. Amirov et al., “Study of the Ion Composition of the Diffuse Vacuum Arc on a Hot Cathode by the Time-of-Flight Method,” Plasma Phys. Rep., vol. 46, pp. 611-616, 2020.

[3] V.M. Batenin, I.I. klimovskii, V.P. Polistchook et al., “A Stationary Vacuum Arc with a Diffuse Spot on a Nonemitting Chrome Cathode,” High Temp., vol. 41, pp. 586-593, 2003.

[4] R.A. Usmanov, R.Kh. Amirov, A.V. Gavrikov et al., “Diffuse vacuum arc on cerium dioxide hot cathode,” Phis. Plasmas, vol. 25, Article Number 063524, 2018.

[5] G.D. Liziakin, N.N. Antonov, V.S. Smirnov et al., “Plasma mass separation in configuration with potential well,” J. Phys. D.: Appl. Phys., vol. 54, Article Number 414005, 2021.

* The work was supported by the Russian Science Foundation under grant No. 21-72-00077 (https://rscf.ru/en/project/21-72-00077/).

C1-O-047001

INFLUENCE OF MAGNETIC FIELD INDUCTION ON THE ENERGY OF IONS AND INJECTION PROCESSES OF IONIZED FLOWS OF WORKING SUBSTANCES IN A PLASMA MASS SEPARATOR*

ANTONOV N.N.[1], *VETROVA S.B.* [1,2], *USMANOV R.A.* [1], *LIZIAKIN G.D.* [1],

VOLKOV L.S. [1,2], *MELNIKOV A.D.* [1], *GAVRIKOV A.V* [1], *SMIRNOV V.P.*[1]

[1] *Joint Institute for High Temperatures of the Russian Academy of Sciences, Moscow, Russian Federation*
[2] *Moscow Institute of Physics and Technology, Dolgoprudny, Russian Federation*

The concept of plasma mass separation of substances in a configuration with a potential well [1] implies the development of specialized plasma sources [2]. The conversion of condensed matter into a low-temperature plasma flow and its further injection into the separation chamber is a crucial stage that largely determines the efficiency of the technological process. It is especially important if the aim of the concept is the separation of spent nuclear fuel (SNF).

Figure 1 shows a scheme of the created device. The mixture of working substances is placed in a molybdenum crucible. At this stage, silver and lead are used as model substances, which simulate the "light" and "heavy" components of SNF, respectively. The crucible is heated up to 1000-1450°C by the induction method. The substance in the form of vapor enters the discharge gap and is ionized. The generated plasma penetrates into the separation chamber along the magnetic field lines (magnetic induction 1400 G) through the cavity in the anode.

As part of the study, the following plasma parameters were measured: plasma density, source productivity or ion saturation current, optical emission spectra, energy spectrum of ions of working substances depending on the value of the magnetic field induction (0-1400 G). The characteristic FWHM of the energy distribution is 7-15 V. The average energy varies from 14 eV to 22 eV.

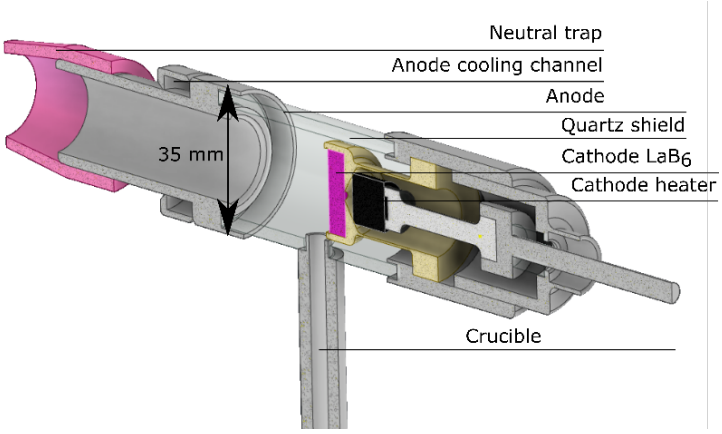

Fig.1. Scheme of the plasma source of model substances.

A productivity rate of the source of 20 g/h was reached, which corresponds to an ion current of 2.6 A at the discharge current of 120 A. With these parameters, the current-voltage characteristic is growing. The plasma concentration at the outlet of the source is about 10^{12} cm^{-3}.

The possibility of switching from one working substance to another with diverse saturated vapor pressure while maintaining the working potential difference between the cathode and the anode has been experimentally demonstrated.

REFERENCES

[1] G Liziakin, N Antonov, V S Smirnov, R Timirkhanov, A Oiler, R Usmanov, A Melnikov, N Vorona, S Kislenko, A Gavrikov, V P Smirnov "Plasma mass separation in configuration with potential well", J. Phys. D: Appl. Phys. V. 54, N. 41, 414005, 2021;

[2] V. P. Polishchuk, R. A. Usmanov, A. D. Melnikov, N. A. Vorona, I. M. Yartsev, R. Kh. Amirov, A. V. Gavrikov, G. D. Liziakin, I. S. Samoylov, V. P. Smirnov & N. N. Antonov "Vacuum Arcs with Diffuse Cathode Attachment (Review) ", High Temperature, V. 58, pp. 476–494, 2020;

[3] V. S. Smirnov, R. O. Egorov, S. A. Kislenko, N. N. Antonov, V. P. Smirnov, and A. V. Gavrikov "Simulation of ion flux of actinides and uranium fission products in the plasma separator with a potential well", Physics of Plasmas, V. 27, 113503, 2020;

* The work was supported by a Russian Federation President grant (MK-5652.2021.1.2).

C1-O-047902

COLLECTIVE ACCELERATION OF LIGHT IONS IN A PLASMA FILLED DIODE WITH A POINTED CATHODE

M.V.ZHURAVLEV, A.O.URAZBAEV, A.A. BUKHARKIN, I.N.PYATKOV, V.A. RYZHKOV, G.V.KURAPOV, G.E. REMNEV

Tomsk Polytechnic University, Tomsk, Russia

The results of the collective acceleration of light ions, protons and deuterons, in the Plutto / Luce diode system are presented [1-2]. The diode system is a pointed cathode and an anode plate with a central hole in the region of which a plasma cloud is formed due to the ionization by a pulsed electron beam of gas preliminarily injected into the anode region after the gas valve has been actuated. The minimum valve response time has been achieved as low as 20 μs. The gas concentration was controlled by the delay time of the accelerator operation with respect to the valve opening time. We also used a 2-pulse generator operation mode, in which it was the first high-voltage nanosecond voltage pulse that provided gas ionization. The diode current was 20 kA at the pulse duration of 60 ns at an accelerating voltage of up to 400 kV. The dependences of the efficiency of acceleration of light ions on the gas density and, accordingly, the plasma density in the region of the diode system, the size of the diode gap are obtained. The parameters of the ion beam were determined using electrophysical and nuclear-physical methods of analysis [3].

REFERENCES

[1] Ion Acceleration in Electron Beams, A.A. Plyutto,. (Saratov, 2007).

[2] J. S. Luce, H. Sahlin, and N. R. Crites, IEEE Trans. Nucl. Sci. 20, 336 (1973)

[3] Determination of Energy and Fluences of Protons Collectively Accelerated in a Luce Diode Accelerator, Ryzhkov, V.A., Remnev,. (2019) Technical Physics Letters, 45 (7), pp. 718-720

C1-O-950301

A HIGH-VOLTAGE AC PLASMA TORCH: COMPUTATIONAL STUDY*

A.V. SUROV[1], *N.V. OBRAZTSOV*[2,1], *A.A HVATOV*[1], *M.A. MASLYAEV*[1], *N.Y. BYKOV*[1]

[1] *ITMO University, Saint-Petersburg, Russian Federation*
[2] *Peter the Great St. Petersburg Polytechnic University, Saint-Petersburg, Russian Federation*

In modern technologies, the function of a plasma torch is not limited to increasing the enthalpy of the working gas for its subsequent use in a plasma-chemical reactor. When using multi-species gaseous mixture, chemical reactions occur in electric discharge chambers and in the jet. The processes occurring in electric arc systems are non-stationary even when DC is used [1]. In AC devices [2] this is further enhanced by a periodically changing release of energy. The design features of plasma generators significantly complicate the diagnosis of physical parameters. Comprehensive research involves the use of computer simulation and validation based on available experimental data.

Significant differences in the shapes of arc column in the channels and outside for high voltage plasma torch with rod electrodes were noted in [3]. To study processes in powerful plasma torch with hollow electrodes [4] shown in Fig.1, it is also important to consider the processes in the vicinity of electrodes.

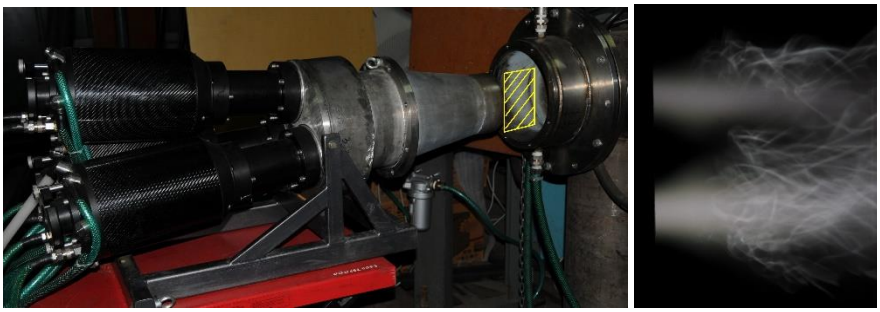

Fig.1. Photo of a powerful high-voltage plasma torch by IEE RAS (left) and arc columns at the outlet of the channels (right). The arc shooting area in the photo of the plasma torch is marked in yellow.

Computation of time-dependent flow for simplified linear axial configuration of the arc without considering near-electrode processes using a supercomputer takes several days. To reduce the complexity and resource for the more complicated case, an approach is proposed that involves the hybrid computational model. In it, the movement of the electric arc spot is described by a differential equation, restored by the generative design method [5] from experimental data. Data on the movement of an electric arc for various conditions were obtained in the laboratories of the IEE RAS. The arc spot motion equation complements the non-stationary 3-D model of the gas flow in the channels and in the jet of the plasma torch. The results of applying the hybrid modelling approach to solving a non-stationary problem describing the operation of a high-voltage plasma torch are presented in the report.

REFERENCES

[1] J.Mostaghimi, M.I.Boulos, “Thermal Plasma Sources: How Well are They Adopted to Process Needs?”, Plasma Chem. Plasma Process. 35, 421–436, 2015. https://doi.org/10.1007/s11090-015-9616-y.

[2] L.Fulcheri, F. Fabry, S. Takali, V. Rohani, “Three-Phase AC Arc Plasma Systems: A Review”, Plasma Chem. Plasma Process. 35, 565–585 2015. https://doi.org/10.1007/s11090-015-9619-8.

[3] A.V. Surov, S.D.Popov, V.E.Popov, D.I.Subbotin, E.O.Serba, V.A.Spodobin, Gh.V.Nakonechny, A.V.Pavlov, “Multi-gas AC plasma torches for gasification of organic substances”, Fuel, vol. 203, pp. 1007-1014, 2017.

[4] P.G. Rutberg, G. V. Nakonechny, A. V. Pavlov, S.D. Popov, E.O. Serba, A. V. Surov, “AC plasma torch with a H2O/CO2/ CH4 mix as the working gas for methane reforming”, J. Phys. D. Appl. Phys. 48, (2015).

[5] M. Maslyaev, A. Hvatov, A. V. Kalyuzhnaya, Partial differential equations discovery with EPDE framework: application for real and synthetic data, J. Comp. Sci., 101345, 2021.

* This research is financially supported by The Russian Science Foundation, Agreement No. 21-11-00296, https://rscf.ru/en/project/21-11-00296/.
The authors thank the Institute for Electrophysics and Electric Power of Russian Academy of Sciences (IEE RAS, St. Petersburg) and partially Peter the Great St. Petersburg Polytechnic University for the data provided.

C1-P-001601

DESIGN AND OPERATING CHARACTERISTICS OF HOLLOW CATHODE PLASMA ELECTRON GUN WITH NON-SELF-SUSTAINING HIGH-VOLTAGE GLOW DISCHARGE.*

V.I. GUSHENETS[1], *A.S. BUGAEV*[1], *E.M. OKS*[1,2]

[1]*Institute of High Current Electronics SB RAS, Tomsk, Russia*
[2]*Tomsk State university of Control System and Radioelectronics Tomsk, Russia*

In this report, the design and performance of pulsed electron sources (electron guns) are described. The discharge mechanism of the source is based on non-self-sustaining high-voltage glow discharge. The electron guns can be divided into two main types: secondary electron emission type (Fig. 1a) with flat cathode and plasma electron generation (hollow cathode plasma source) type (Fig. 1b). In the last electron gun type, the plasma that generates inside the hollow cathode acts as an electron beam source. Electrons emitted by the cathodes (being bombarded by ions) are accelerated by a voltage drop (Uacc) of several tens of thousands volts.

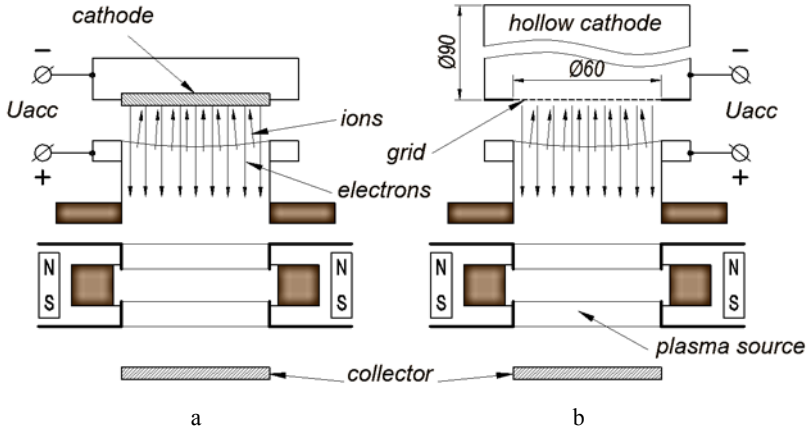

Fig.1. Schematic diagrams of the electron sources

The anode plasma acts as an ions ranging in beam current up to 1.5 A in pulse mode accelerated towards the cathode. The plasma is created by a toroidal plasma generator built according to the scheme of a plasma thruster with closed electron drift and a short acceleration zone (an anode layer). The working gas pressure has a strong effect on the anode plasma generator operation - determining the generator discharge current (and hence the ion beam current) and the duration of the discharge current pulse. Argon, nitrogen, and air were used as a operational gas. The pulse mode of the electron gun operation is implemented due to the pulse mode of the plasma anode generator.

It was shown in experimental studies the electron beam current increases by more than one and a half times for the hollow cathode type of electron gun compared to the current for the flat cathode. Under certain experimental conditions, the formation of a pre-modulated electron beam with a frequency of up to 20 MHz was observed in the hollow cathode type gun. The maximum electron beam current for the hollow cathode type was 10 A with a pulse duration about 250 μs and the high-voltage drop up to 35 kV.

* The work was supported by FWRM-2021-0006 (0291-2021-0006).

C1-P-002501

STUDYING OF PARAMETERS OF MIDDLE FREQUENCY PULSE ATMOSPHERIC PRESSURE DISCHARGE IN ARGON

K.P. SAVKIN[1], E.M. OKS[1,2], G.YU. YUSHKOV[1], A.S. BUGAEV[1], A.G. NIKOLAEV[1], M.V. SHANDRIKOV[1]

[1]Institute of High Current Electronics SB RAS, Tomsk, Russia
[2]Tomsk State University of Control System and Radioelectronics, Tomsk, Russia

In this work, we studied a low-current discharge (up to 1 A) at atmospheric pressure in the pulsed power supply mode with a frequency of 20 to 100 kHz in an argon flow with a flow rate of up to 3 L/s. An increase in the pulse repetition rate leads to a decrease in the discharge initiation voltage and has little effect on the burning voltage (Fig. 1). This experimental fact is based on the assumption of an increase in the concentration of the residual plasma and excited argon and nitrogen molecules in the intervals between pulses. This assumption, in turn, is confirmed by the results of studying the optical emission of the discharge plasma.

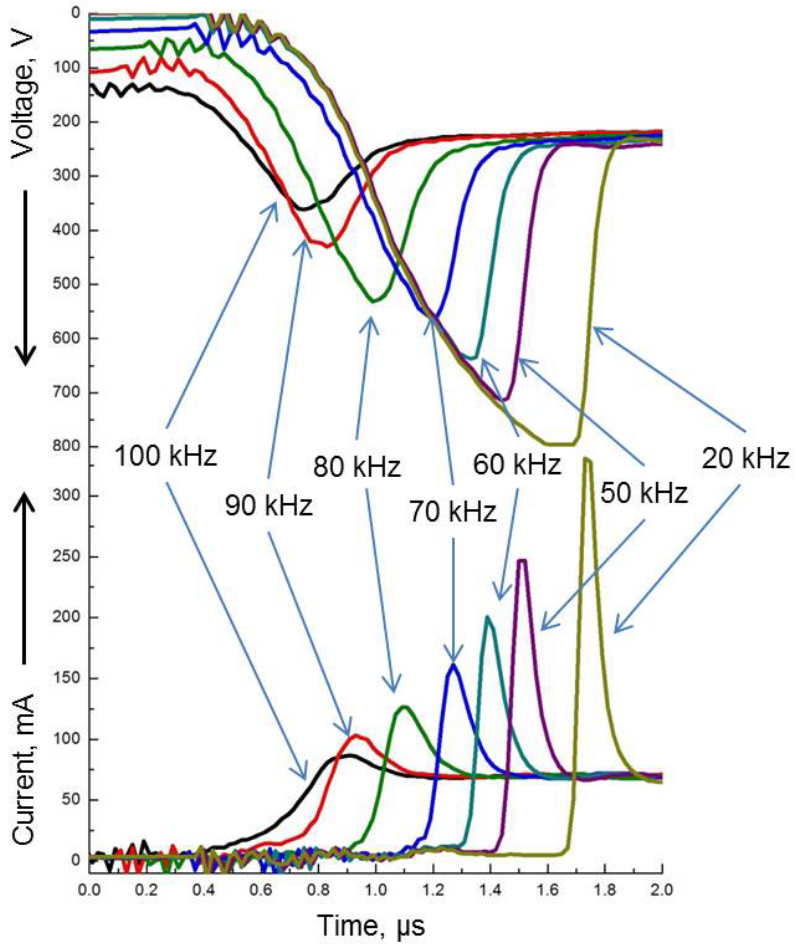

Fig.1. Waveforms of peak voltage and current at the moment of ignition of the discharge pulse.

C1-P-002503

GENERATION OF PLASMA FLOWS WITH A HIGH CONTENT OF METAL PARTICLES IN ATMOSPHERIC PRESSURE GLOW DISCHARGE *

K.P. SAVKIN[1], D.A. SOROKIN[1], E.M. OKS[1,2], A.G. NIKOLAEV[1], M.V. SHANDRIKOV[1], A.S. BUGAEV[1], V.I. GUSHENETS[1]

[1]*Institute of High Current Electronics SB RAS, Tomsk, Russia*
[2]*Tomsk State University of Control System and Radioelectronics, Tomsk, Russia*

The paper presents the results of studying the features of the operation of an atmospheric pressure glow discharge at currents below the threshold for switching to the arc mode, but providing efficient generation of plasma flows with a high content of the metal component. The limitation of the discharge current is due to the desire to improve the quality of the erosion products of the electrodes of the discharge system by reducing the geometric dimensions of their particles in order to achieve ultrafine properties of powder materials obtained under atmospheric pressure conditions.

* The research was supported by RSF (project No. 22-19-00265).

C1-P-003003

GENERATION OF NITROGEN OXIDES MOLECULES IN THE PLASMA OF ATMOSPHERIC PRESSURE GLOW DISCHARGE IN AIRFLOW*

V.O. NEKHOROSHEV, N.V. LANDL, Y.D. KOROLEV, G. A. ARGUNOV

Institute of High Current Electronics SB RAS, Tomsk, Russia

The paper deals with the investigations of nitrogen oxide production in a column area of low-current glow-type discharge in airflow at atmospheric pressure. When the gas flows through the discharge plasma area, a luminous region, which is often referred to as a plasma jet, forms at the outlet of electrode system [1–4]. The jet contains the charged and chemically activated particles, so a great variety of the jets applications can be provided [1–6]. The special attention is payed to the biomedical applications [2, 5, 6], since the nitrogen oxides and the other active particles are available in the jet. For example, nitric monoxide is used in inhalation therapy as far as it has a relaxing effect on the blood vessels and for disinfection of wounds and skin wound healing [5, 6].

The electrode configuration of proposed gas discharge system (fig 1.) correspond to the non-steady-state coaxial plasmatron described in [1, 4].

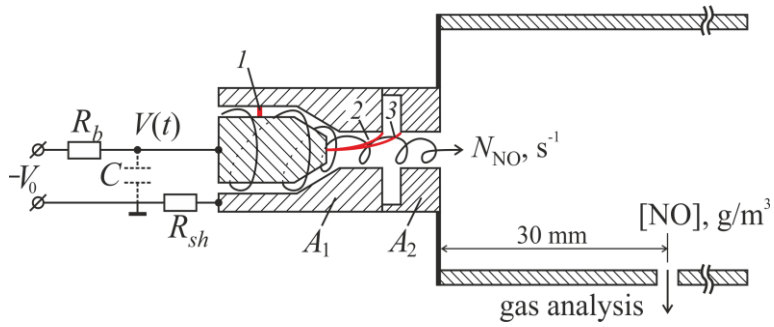

Fig. 1. Simplified circuit of experimental setup for NO_x production based on non-steady state plasmatron. 1 – position of the first breakdown, 2, 3 – schematic positions of positive column of glow discharge, A_1, A_2 – anodes of plasmatron, $V(t)$ – discharge burning voltage, V_0 – power supply voltage, R_b – ballast resistor, R_{sh} – shunt resistor for current measurement.

The glow-like discharge in plasmatron have been investigated using oscillography and CCD camera photography. The waveforms of the discharge burning voltage and the discharge current are obtained. The concentration of NO_x molecules in the produced gas flow are measured using gas analysis system.

It is shown, that the positive column of discharge in a gas flow is sustained in a constricted mode with a typical current density from 50 to 120 A/cm^2 and with the electron density up to 2×10^{14} cm^{-3}. The gas temperature in the plasma column of glow discharge is estimated as (3000–3600) K. In spite of a rather high gas temperature, the plasma is still nonequilibrium. The main channel of the nitric oxide production is associated with the interaction of vibrational excited nitrogen with atomic oxygen. The described conditions provide a total production rate of NO and NO_2 molecules from the plasma column up to $N_{NO} = 3\times10^{19}$ 1/s with the average energetic cost per one molecule of about 50 eV and less.

REFERENCES

[1] Y. D. Korolev, “Low-current discharge plasma jets in a gas flow. Application of plasma jets,” Russ. J. Gen. Chem., vol. 85, no. 5, pp. 1311–1125, May 2015.

[2] A. Dickenson, N. Britun, A. Nikiforov, C. Leys, M. I. Hasan, J. L. Walsh, “The generation and transport of reactive nitrogen species from a low temperature atmospheric pressure air plasma source,” Phys. Chem. Chemical Phys., vol. 20, no. 45, pp. 28499–28510, October 2018.

[3] Y. S. Akishev, “Non-thermal plasma at atmospheric pressure and its opportunities for applications,” Izv. Vyssh. Ucheb. Zaved., Khim. Khim. Tekhnol., vol. 62, no. 8, pp. 20–62, August 2019.

[4] Y. D. Korolev, V. O. Nekhoroshev, O. B. Frants, N. V. Landl, A. I. Suslov, V. G. Geyman, “Nonsteady-state processes in a low-current discharge in airflow and formation of a plasma jet,” J. Phys. Commun., vol. 3, no. 8, Article Number 085002, August 2019.

[5] V. N. Vasilets, “Plasmachemical generation of nitric oxides in air plasmas for medical applications,” Izv. Vyssh. Ucheb. Zaved., Khim. Khim. Tekhnol. vol. 62, no. 5, pp. 4–13, May 2019.

[6] V. P. Demkin, S. V. Melnichuk, O. V. Demkin, H. Kingma, R. Van de Berg, “Spectroscopic studies of non-thermal plasma jet at atmospheric pressure formed in low-current nonsteady-state plasmatron for biomedical applications,” Phys. Plasmas, vol. 23, no. 4, Article Number 043509, February 2016.

* The work was supported by Russian Science Foundation, project № 22-29-00703

C1-P-007101

INVESTIGATION OF THE GENERATION PROCESSES OF MULTIPLY CHARGED HEAVY METAL IONS IN VACUUM ARC PLASMA*

A.G. NIKOLAEV[1], V.P. FROLOVA[1,2], E.M. OKS[1,2], G.YU. YUSHKOV[1]

[1] Institute of High Current Electronics SB RAS, 2/3 Academichesky Ave., Tomsk, 634055, Russia,
Email: nik@opee.hcei.tsc.ru, phone: +7(3822)-491776
[2]Tomsk State University of Control Systems and Radioelectronics, 40 Lenin Ave., Tomsk, 634050, Russia

In a vacuum arc operating at an arc current pulse amplitude of hundreds of amperes, a pulse duration of more than tens of microseconds, and at a residual gas pressure of 10^{-4} Pa, without special measures to increase the charge states of the ions, the average charge of the plasma ions of the cathode material and, accordingly, the formed based on the ion beam, ranges from 1+ for carbon to 3+ for heavy metals. A further increase in the charge states of the vacuum arc plasma ions makes it possible to increase the ion energy in the extracted beam without a corresponding increase in the accelerating voltage. This expands the technological capabilities of ion sources in solving problems of ion-beam modification of surface properties.

The charge states of the ions can be significantly increased in the case of a vacuum arc with a short pulse duration. Previously [1], we showed that the use of such a discharge with a pulse duration of a few microseconds and a kiloampere current range makes it possible to obtain the 19+ charge state for bismuth ions at an average charge state of 17+ ions. This report presents a study of the processes of generation of multiply charged heavy metal ions on the example of a tantalum cathode. The duration of the arc current pulse was further reduced to a submicrosecond level with a corresponding increase in the current and discharge power. As a result, record charge states for tantalum were obtained up to 13+ at a record average charge of tantalum ions 11+.

REFERENCES

[1] G. Yu. Yushkov, V. P. Frolova, A. G. Nikolaev, E. M. Oks, “High-charge-state ion beam generation in a high-current pulsed vacuum arc source,” IEEE Transactions on Plasma Science, vol. 47, pp. 3586-3589, August 2019.

* The work was supported by the Russian Science Foundation under grant No. 22-29-00118.

C1-P-009101

MAGNETRON SPUTTERING WITH A HEATED BORON TARGET *

A.G. NIKOLAEV[1], V.P. FROLOVA[1,2], E.M. OKS[1,2], G.YU. YUSHKOV[1]

[1] Institute of High Current Electronics SB RAS, 2/3 Academichesky Ave., Tomsk, 634055, Russia,
Email: nik@opee.hcei.tsc.ru, phone: +7(3822)-491776
[2]Tomsk State University of Control Systems and Radioelectronics, 40 Lenin Ave., Tomsk, 634050, Russia

Interest in obtaining boron-based coatings is determined by the prospects of their use for goals of modifying the surface properties of a wide range of parts and equipment. Boron-based coatings potentially have high resistant to mechanical wear, corrosion, significant thermal stability, and a low friction coefficient. In this work, we consider the equipment for the implementation of plasma method for the deposition of thin boron-based films on the surface. This is a magnetron sputtering with a crystalline boron target heated in the discharge. The design, the principle of operation, and the characteristics of a planar magnetron sputter with pure boron target are presented. A feature of this device is the use of a thermally insulated target (cathode) made from pure crystalline boron, which was heated to provide electrical conductivity sufficient for the stable functioning of the magnetron discharge, by an auxiliary low-current discharge. This makes it possible to realize in the magnetron a DC mode as well as a pulsed self-sputtering mode, in which boron ions in the discharge plasma dominate over the ions of the working gas. The properties of the resulting boron-based coatings have been measured and discussed.

* The work was supported by the Russian Science Foundation under grant No. 22-29-00381.

C1-P-009102

VACUUM ARC PLASMA DECAY AFTER INTERRUPTION OF THE DISCHARGE CURRENT*

G.YU. YUSHKOV[1], E.M. OKS[1,2], A.G. NIKOLAEV[1], V.P. FROLOVA[1,2], AND K.P. SAVKIN[1]

[1]*Institute of High Current Electronics SB RAS, Tomsk, Russia*
[2]*Tomsk State University of Control Systems and Radioelectronics*

The decay processes of vacuum arc discharge plasma with cathodes based on copper *Cu* and chromium *Cr* have been studied. As the main experimental approaches, the method of breaking the discharge current and measuring the emission current of charged particles from the plasma to the collector under a floating potential was used. Thus, it was shown that during arcing, the collector current is determined predominantly by more mobile electrons. The interruption of the arc current led to the appearance of an ion current in the collector circuit. The presence of an axial magnetic field in the discharge gap led to the appearance of a nonmonotonic decay of the ion current pulse, which consisted in the appearance of a second current peak. The time interval between the peaks also depended on the magnetic field induction. Based on these results, the mechanism of the influence of a magnetic field on plasma confinement in the interelectrode space of a vacuum-arc discharge system is considered.

* This work was supported by state assignment projects FWRM-2021-0006.

C1-P-009301

STUDY OF THE STRUCTURAL-PHASE STATE OF SIALON OBTAINED BY SYNTHESIS UNDER THE INFLUENCE OF LOW-TEMPERATURE PLASMA ENERGY

V.A. VLASOV[1], A.A. KLOPOTOV[1], K.A. BEZUKHOV[1], N.N. GOLOBOKOV,[2] M.S. SYRTANOV[3],

S.A. BUINOVSKII[4], G.G. VOLOKITIN[1]

[1]Tomsky State University of Architecture and Building, Tomsk, Russia
[2]Tomsk branch of the Institute of structural Macrokinetics SB RAS, Tomsk, Russia
[3]National Research Tomsk Polytechnic University, Tomsk, Russia
[4]Seversk Technological Institute NRNU, MEPI, Tomsk, Russia

Sialons appertain to the class of ceramic materials with excellent high-temperature properties and high mechanical properties. These properties contribute to their wide application in many areas of industry: automobile engines, gas turbine blades, high-performance bearings, etc.

About 10 types of four-component sialons with crystal structures are known. The main and widely used are α-, *β*- and O'-SiAlON [1]. Non-stoichiometric composition β–SiAlON described by the formula $Si_{6-\varepsilon}Al_{1+\varepsilon}O_{1+\delta}N_{8-\delta}$. Here δ and ε characterize deviations from stoichiometry within the limits of $1\leq\varepsilon\leq3.2$ and $1\leq\delta\leq4.2$. With a lack of nitrogen in the compound, anions N^{3-} have two possibilities: 1) create vacancies on the nitrogen sublattice; 2) anions O^{2-} infiltrate the nodes on the nitrogen sublattice. A similar situation exists metal nodes on cationic sublattices Al and Si. As a result, β-SiAlON have a wide area of homogeneity and this compound is isostructural to a two-component compound β-Si_3N_4. α-SiAlON is a compound, which already contains four formula units β-Si_3N_4, and is described by the formula $Me_\varepsilon Si_{12-(\varepsilon+\delta)}Al_\varepsilon O_\delta N_{16-\delta}$ (Me≡ metal ion). It is known that the phase transition between the two types of SiAlON satisfies the conditions [2]: α- SiAlON+O_2→β-SiAlON and β-SiAlON+N_2→α-SiAlON. The physical and mechanical properties of these two types of sialon differ significantly.

In [3] data on the study of mullite synthesis by means of thermal influence of plasma beam are given. Application of plasma energy is also possible for the synthesis of other high-temperature ceramics.

The aim of this work was to study the structural-phase composition of the synthesis products obtained by plasma-chemical synthesis of SiAlON.

For the experiment, mixtures were prepared from which briquettes were formed followed by heat treatment in an oven at 400 C° for 30 minutes. Two reaction mixtures are used for the synthesis of SiAlON by the plasma chemical method: SiAlON-I: β-Si_3N_4+AlN+H_4N_2CO+Na_2SiO_3; SiAlON-II: β-Si_3N_4+AlN+H_4N_2CO+Na_2SiO_3+Re (Fe, Co) (where Re=Nd, Pr, La).

High-temperature exposure to the sample was carried out in a plasma jet obtained in a plasma generator of the VPR-410 NPP type. Plasma generator power P =30 kW with specific heat flow $q=2{,}3\times10^6$ W/m^2. The plasma gas was nitrogen.

During the interaction of a low-temperature plasma jet with a mass-average temperature T = 6100÷7300 K with sample material compounds with different crystal structures are formed in the heat-affected zone within tens of seconds. A feature of SiAlON formation is the strong dependence of solid-phase reactions on the movement of point defects in the high-temperature fields created by the plasma jet. Because the reactivity of solids depends significantly on non-stoichiometry. As a result, this property was well manifested in the reactions solid-solid, solid-gas in our experiment.

X-ray diffraction analysis showed that the main phase is the compound β- SiAlON (Si_5AlON_7 space group $P6_3$). Also found traces of the original compounds β-Si_3N_4 and AlN compounds. In addition to the crystal phases, a halo belonging to the X-ray amorphous phase is fixed on diffractogram. Introduction of metallic powder into the charge REM-Fe(Co) led to the formation of additional lines on the diffractograms, which are α-SiAlON.

REFERENCES

[1] *C.B. Carter, M.G. Norton, Ceramic Materials Science and Engineering, Springer New York Heidelberg Dordrecht London, 2013.*
[2] *M.H Lewis, A.R. Bhatti, R.J. Lumby, B.J. North, «The microstructure of sintered Si-Al-ON ceramics», Mater Sci, vol.15, pp. 103-113,1980.*
[3] *V.A. Vlasov, A.A. Klopotov, Y.A. Abzaev, V.I. Vereshchagin, R.E Gafarov, V.V. Shehovtsov , N.N. Golobokov , K.A. Bezukhov, O.G. Volokitin «Mullit Synthesized by DC Arc Plasma » 15th International Conference on Modification of Materials with Particle Beams and Plasma Flows, Tomsk, Russia, pp. 756-759, 2020.*

*The work was supported by the state assignment of the Ministry of Science and Higher Education of the Russian Federation (project number FEMN-2020-0004).

C1-P-012101

INVESTIGATION OF THE PLASMA PARAMETERS OF A NON-SELF-SUSTAINED GLOW DISCHARGE INSIDE HOLLOW CATHODES OF DIFFERENT SHAPES

D.YU. IGNATOV[1]

[1]*Institute of High Current Electronics, Tomsk, Russia*
e-mail: danilabay29@ya.ru

To generate low-temperature plasma in a vacuum chamber or inside a hollow cathode at low pressures, a hollow cylindrical cathode is widely used. In contrast to discharges with flat cathodes, a discharge with a hollow cathode makes it possible to obtain plasma with a higher concentration.

A two-discharge system for plasma generation inside a long hollow cathode is proposed. In such a system, the main non-self-sustained glow discharge generates a dense plasma inside the hollow cathode, and the auxiliary discharge with a combined incandescent and hollow cathode is a source of additional electrons that are injected through a grid installed at the end face of the main discharge hollow cathode. The main discharge burns at pressure up to 1 Pa, voltage from 100 V to 500 V and current up to 10 A.

The plasma parameters were measured using double cylindrical probes mounted along the hollow cathode. The scheme of experiments to study the parameters of the plasma of a non-self-sustained glow discharge with a straight hollow cathode is described in detail in [1]. This work is a continuation of the study of plasma parameters inside a long hollow cathode and shows the influence of the shape of the hollow on the parameters of the generated plasma.

REFERENCES

[1] D. Yu. Ignatov, S. S. Kovalsky, V. V. Denisov, I. V. Lopatin, and N. N. Koval, “Influence of the discharge burning conditions on distributions of the parameters of plasma generated in a non-self-sustaining glow discharge inside a hollow cathode,” Russian Physics Journal, Vol. 64, No. 11, pp 2170 – 2176, March, 2022.

C1-P-014602

PARTIAL DISCHARGE EMISSION CHARACTERISTICS IN THE UV RANGE

Y.A. YAKOVLEV[1], N.B. KALYASKAROV[1], N.R. ZHOLMAGAMBETOV[1], L.A. ZINOVYEV[2], U.B. ARKABAEV[1], I.R. GALIMYANOV[1]
[1]Karaganda technical university, Karaganda, Kazakhstan
[2]Karaganda Buketov university, Karaganda, Kazakhstan

This work is a continuation of the research described in [1].

The dependence of the energy characteristics of partial discharge radiation in the UV range on the discharge conditions was studied.

The plasmatron, in which the discharge was carried out, was powered from a pulsed RC generator, the scheme of which is also given in [1]. A plug spark without a top electrode was used as a plasmatron, diameter of the central electrode 2 mm, value of the discharge gap δ = 3 mm. The space 10 mm deep between the central electrode and the outer electrode was filled with 1.5% NaCl solution. During the experiments, the polarity of the central electrode (CE) was changed. To register UV radiation, we used a combined instrument "TKA-PKM" series designed to measure the energy illuminance (E, mW/m^2) in three spectral regions: 200...280 nm (UV-C zone), 280...315 nm (UV-B zone) and 315...400 nm (UV-A zone). The instrument also displays the calculated parameters: the maximum (peak) value of energy illuminance E_{max} and energy exposure in the corresponding spectral regions. Switching from one part of the spectrum to another is done by changing the receiving optical heads. Since the duration of discharge is 10^{-3} s, and the time constant of the device is equal to 1 s, to get the real values of illumination, we recalculated the readings of the device by the formula, $E_{(calc)}=(t_2/t_1)E_{(meas)}$, where t_2 is the double time constant (the reaction time to flash appearance and to its extinction was considered), t_1 is the time of the discharge existence [1]. Since the measuring heads have a limited angle of view (10°), they were located at such a distance (0.09 m), that the radiating region completely falls into this angle.

Measurements of the energy illuminance were performed for discharges occurring at different values of the voltage U, applied to the discharge gap. The polarity of the applied voltage was also changed. As the value of the applied voltage increased, the type of discharge changed. An incomplete partial discharge turned into a completed discharge, which was accompanied by a bright flash. In the course of the experiments, no UV radiation was detected in the course of an incomplete partial discharge, most likely due to its low intensity. Also UV radiation in the region of 200-280 nm was not registered due to its absorption by the atmosphere.

The data obtained during the experiments are shown in Table 1

Table 1 - Peak values of energy illumination in the UV range during a completed partial discharge

Polarity of the CE	Spectral region, nm	U, V	$E_{max(meas)}$, mW/m^2	$E_{max(calc)}$, mW/m^2
minus	315-400	675	5,56	11120
minus	280-315	675	9,18	18360
plus	315-400	630	8,36	16720
plus	315-400	900	6,06	12120
plus	280-315	600	29,5	59000
plus	280-315	900	23,3	46600

As you can see the UV radiation is mainly concentrated in the 280-315 nm range

REFERENCES

[1] E A Yakovlev et al 2021 J. Phys.: Conf. Ser. 2064 012038

C1-P-018301

HIGH-INTENSITY ION BEAMS WITH SUBMILLISECOND DURATION FOR SYNERGISTIC OF ION IMPLANTATION AND ENERGY IMPACT ON THE SURFACE

A.I. RYABCHIKOV, D.O. SIVIN, S.V. DEKTYAREV

National Research Tomsk Polytechnic University, Tomsk, Russia

The development of methods to modify materials based on the synergistic high-intensity implantation and simultaneous energy impact on the ion-doped layer involves using the pulsed and repetitively-pulsed beams of metal and gas ion beams with micro-submillisecond duration with high pulsed power density. The paper presents the results of experimental studies on the formation of pulsed and repetitively-pulsed high-intensity beams of titanium ions with a pulse duration from 150 to 500 μs. The plasma flow was generated by a vacuum arc discharge. To obtain ion beams with a power density in the range from several tens to several hundreds of kilowatts per square centimeter, ballistic focusing of ions was used using an extracting grid electrode in the form of a part of a sphere. Implementing the "solar eclipse" effect excluded the possibility of direct passage of macroparticles, explosive emission products in the cathode spot from the cathode's working surface into the focused beam region into the geometric focus of the ballistic focusing system. The features of the forming the high-power repetitively-pulsed beams of titanium ions were studied using both the ion source "Rainbow 5" and the plasma immersion approach, when the focusing system was immersed in a titanium plasma flow and a negative bias potential was applied to it. Data are presented on the influence of the ion beam space charge neutralization processes at current densities from fractions to several amperes per square centimeter on the efficiency of the ion beam's transport and focusing at accelerating voltages from 10 to 40 kV.

C1-P-018603

DETERMINATION OF ION BEAM ENERGY SPATIAL DISTRIBUTION USING A CALORIMETRIC METHOD WITH A NON-CONTACT TEMPERATURE MEASUREMENT *

A.I. RYABCHIKOV[1], V.O. NEKHOROSHEV[2], A.I. IVANOVA[1]

[1]National Research Tomsk Polytechnic University, Lenin Avenue 30, Tomsk, 634050, Russia
[2] Institute of High Current Electronics,Siberian Branch, Russian Academy of Sciences, 2/3 Akademichesky Avenue, Tomsk 634055, Russia

Currently, plasma technologies based on the use of ion beams are being investigated due to the broad prospects of practical application [1-3]. For example, ion beams are used for ion etching, surface properties modification, ion implantation, etc. The development of a method based on the synergy of repetitively-pulsed high-intensity ion implantation and energy impact on the surface [4] requires the development of methods for measuring the dynamic characteristics of the ion beam and thermal fields of the irradiated target. In the case of plasma-immersion formation of submillisecond ion beams of high pulsed power, the problem of non-contact measurement of parameters is especially topical.

The paper deals with the results of experimental determination of ion beam energy spatial distribution using a calorimetric method with a non-contact temperature measurement. The simplified circuit of proposed experimental setup for diagnostic of ion beam showed on the figure 1.

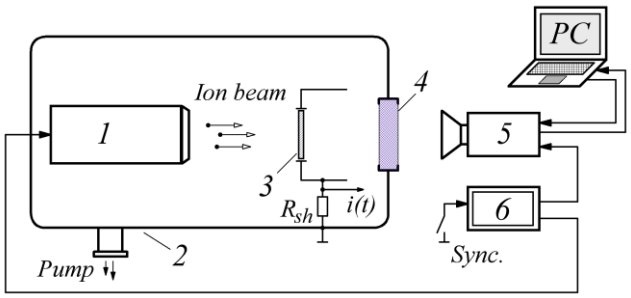

Fig. 1. Simplified circuit of experimental setup for of ion beam energy spatial distribution measurement. 1 – vacuum-arc ion source, 2 – vacuum chamber, 3 – collector, 4 – infrared window, 5 – IR-camera, 6 – synchronization device, Rsh – shunt resistor for beam current flows to the collector measurement.

The ion source 1 based on vacuum-arc discharge is described in detail in [4,5]. The ballistically focused beam of titanium ions with an energy up to 30 keV and pulse duration about 300 μs was directed at the collector 4 made from thin titanium foil. The temporal evolution of collector surface temperature (thermogram) measured by the infrared camera 5. As a result of the interpretation of the data obtained during the IR camera image processing the temperature rise of the collector surface was measured. Then knowing an collector thermal properties is able to estimate ion beam energy spatial distribution by using the calorimetric method. The shunt resistor and oscilloscope are used for beam current flows to the collector measurement. In the experiments, the thermogram of the ion beam trace on the collector surface has been obtained. It is shown that at an accelerating voltage of 30 kV a diameter of beam thermal trace on the collector is 5...7 mm and an energy density reaches 2.7 J/cm^2.

REFERENCES

[1] Y. D. Korolev, “Low-current discharge plasma jets in a gas flow. Application of plasma jets,” Russ. J. Gen. Chem., vol. 85, no. 5, pp. 1311–1125, May 2015.

[2] A. Dickenson, N. Britun, A. Nikiforov, C. Leys, M. I. Hasan, J. L. Walsh, “The generation and transport of reactive nitrogen species from a low temperature atmospheric pressure air plasma source,” Phys. Chem. Chemical Phys., vol. 20, no. 45, pp. 28499–28510, October 2018.

[3] Y. D. Korolev, V. O. Nekhoroshev, O. B. Frants, N. V. Landl, A. I. Suslov, V. G. Geyman, “Nonsteady-state processes in a low-current discharge in airflow and formation of a plasma jet,” J. Phys. Commun., vol. 3, no. 8, Article Number 085002, August 2019.

[4] A.I. Ryabchikov, “High-intensity implantation with an ion beam's energy impact on materials,” IEEE Transactions on Plasma Science, vol. 49, no. 9, pp. 2529-2534, September 2021.

* The work was supported by the Russian Science Foundation (grant No. 22-19-00051)

C1-P-019702

CONICAL STRUCTURES ON THE SURFACE OF A LIQUID WITH SURFACE IONIC CONDUCTIVITY: THE SPACE CHARGE EFFECT*

M.A. BELYAEV[1], N.M. ZUBAREV[1,2], O.V. ZUBAREVA[1]

[1]*Institute of Electrophysics UB RAS, Ekaterinburg, Russia*
[2]*Lebedev Physical Institute RAS, Moscow, Russia*

The free surface of liquids is unstable in a sufficiently strong external electric field. As a result, quasi-stationary conical structures (cone-shaped cusps) can be formed on the surface. Such structures are a source of charged particles (ions or drops), which determines the practical interest in their study. For the case of a perfectly conducting liquid, these structures were described in the classical work of Taylor [1]. It was established that the cone apex half-angle is equal to 49.3^0 and the electric field strength near the apex follows the scaling law $E \sim R^{-1/2}$, where R is the distance from the singular point. This result was generalized to the case of an ideal dielectric liquid in [2]. The influence of the space charge of the droplets emanating from the apex of the conducting liquid cone was considered in [3]. It is remarkable that the electric field in the spray region also obeys Taylor's $R^{-1/2}$ law. Recently, it was shown that this scaling also remains valid if the surface ion current is taken into account [4-6].

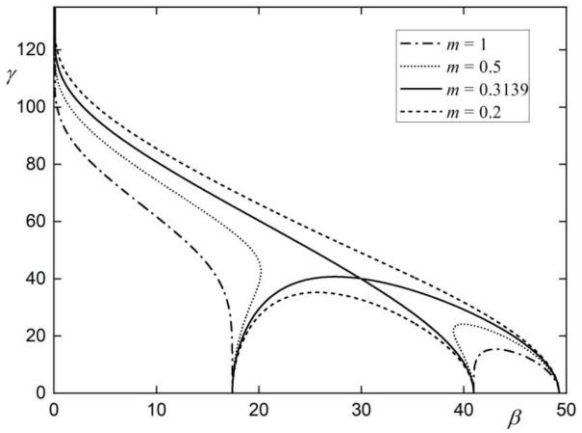

Fig.1. Relations between half-angles β and γ for $\varepsilon = 25$ and different $m = 0.2, 0.31, 0.5, 1.0$.

In the present work, combining approaches developed in [1-6], we consider the conical formation on the surface of a liquid with surface ionic conductivity in an external electric field. Ions move over the cone surface towards the apex, and charged droplets (or ions also) emanating from the cone apex drift through the surrounding gas medium. The exact solution for the electric field distribution near the cone apex is found taking into account the influence of both the space charge of droplets and the surface charge of ions. The obtained solution allows us to determine the relation between the cone and spray half-angles (β and γ) and such parameters as the dielectric constant of the liquid (ε) and the carrier mobility ratio (m). This relation turned out to be quite sophisticated; it contains many different branches: see examples in Fig. 1. Also, the current-angle dependencies for the system were found.

REFERENCES

[1] G.I. Taylor, "Disintegration of water drops in an electric field," Proc. R. Soc. London, Ser. A, vol. 280, pp. 383–397, 1964.

[2] A. Ramos and A. Castellanos, "Conical points in liquid-liquid interfaces subjected to electric fields," Phys. Lett. A, vol. 184, pp. 268–272, 1994.

[3] J.F. De La Mora, "The effect of charge emission from electrified liquid cones," J. Fluid Mech., vol. 243, pp. 561–574, 1992.

[4] A.V. Subbotin, "Electrohydrodynamics of cones on the surface of a liquid," JETP Lett., vol. 100, pp. 657–661, 2015.

[5] M.A. Belyaev, N.M. Zubarev, and O.V. Zubareva, "Saturation current of a stationary cone-shaped singularity on the surface of a liquid with ionic conduction in an electric field," Tech. Phys. Lett., vol. 45, pp. 395–397, 2019.

[6] M.A. Belyaev, N.M. Zubarev, and O.V. Zubareva, "Space-charge-limited current through conical formations on the surface of a liquid with ionic conductivity," J. Electrostat., vol. 107, Article Number 103478, 2020.

* The work was supported in part the Russian Foundation for Basic Research under Project 20-08-00172.

C1-P-021302

NUMERICAL SIMULATION OF THE FEATURES AND REGULARITIES OF THE HIGH-POWER DENSITY ION BEAM FORMATION*

A.I. RYABCHIKOV[1], *V.P. TARAKANOV* [2]

[1]*National Research Tomsk Polytechnic University, Lenin Avenue 30, Tomsk, 634050, Russia*
[2] *National Research Nuclear University MEPhI – Moscow Engineering Physics Institute, Kashirskoe shosse 31, Moscow 115409, Russia*

The development of methods for modifying materials based on the synergistic of high-intensity implantation and simultaneous energy exposure is intended at creating deep ion-doped layers. For this purpose, it is proposed to use pulsed and repetitively-pulsed beams of metal and gas ions of micro-submillisecond duration with a high-pulsed power density. The paper presents the results of numerical simulation of forming the pulsed and repetitively-pulsed high-intensity ion beams. Simulations were performed using the Karat code [1]. The ballistic focusing of heavy ions was studied at injection current densities from 0.1 to 3 A. The influence of the ion current density, accelerating voltage, ion charge composition, and conditions for neutralizing the beam space charge on the transport and focusing of a high-power ion beam has been studied. The conditions for the appearance of a virtual anode have been determined and studied. It has been found that for long durations of ion beam formation at low pressures of the residual atmosphere, multiple appearance and disappearance of a virtual anode are possible. The possibility of ballistic ion beam formation with a pulse density of hundreds of kilowatts per square centimetre has been shown.

REFERENCES

[1] V.P. Tarakanov, User's Manual for Code KARAT, Berkeley Research Associates Inc, Va: Springfield, 1992.

* The work was supported by the Russian Science Foundation (grant No. 22-19-00051)

C1-P-022503

THE GRIDLESS GENERATION SYSTEM OF A LOW-ENERGY ION BEAM BASED ON A GLOW DISCHARGE WITH A HOLLOW CATHODE AND EXTERNAL ELECTRON INJECTION

*

I.V. LOPATIN, YU.H. AKHMADEEV, A.E. PETROV

Institute of High Current Electronics, Siberian Branch, Russian Academy of Sciences (IHCE SB RAS), Tomsk, Russia

An ion beam generation system based on a glow discharge with a hollow cathode and external electron injection has been developed (Fig. 1). The system is supposed for ion beam deposition of coatings based on aluminum, including its oxide. The system makes it possible to generate an ion flux with controlled energy up to 150 eV. A feature of the system is the absence of a structural element that acts as a stopper for the plasma boundary. The plasma boundary is limited by the formation of a double electrostatic layer between the plasma of the main and auxiliary discharges. The PINK device was used as an auxiliary discharge plasma generator [1]. The double electrostatic layer was localized near the emission window, through which the counter-reciprocal emission of electrons and ions was carried out. The main characteristics of the main and auxiliary discharges are studied depending on the conditions of their combustion. It is shown that the operating pressure range of the system is from 0.1 to 1 Pa, the main discharge current is a few Amperes. The possibility of controlling the potential difference on the electrostatic double layer by changing the burning voltage of the main glow discharge with a hollow cathode and external electron injection is also shown.

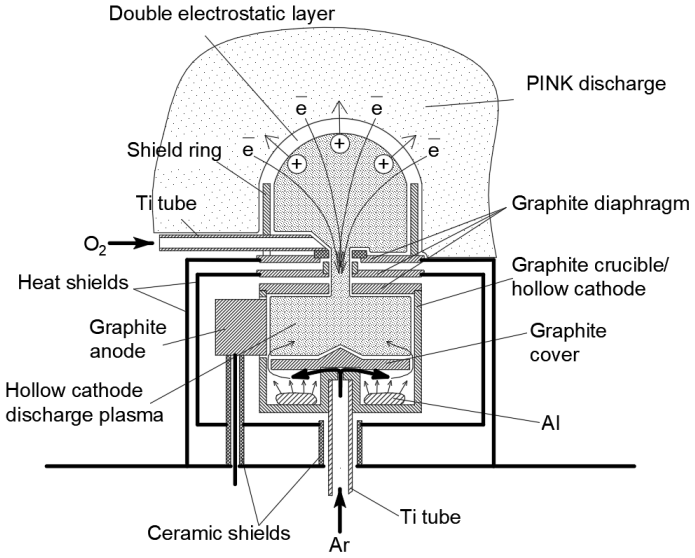

Fig.1. Schematic diagram of a gridless ion beam generation system.

REFERENCES

[1] Lopatin I. V., Akhmadeev Yu. H., Koval N. N. Effect of thermionic cathode heating current self-magnetic field on gaseous plasma generator characteristics // Review of Scientific Instruments, 86, 103301, 2015.

* The work was supported by RFBR and ROSATOM, project number 20-21-00111.

C1-P-023701

A NON-EQUAL GAP DISTANCE DIELECTRIC BARRIER DISCHARGE: BETWEEN SPIRAL-SHAPE AND CYLINDER-SHAPE ELECTRODES*

S. JIN[1], *X. LU*[1], *Z. LI*[1], *X. LEI*[1]

[1]*Huazhong University of Science and Technology, Wuhan, China*

A non-equal gap distance DBD between a spiral-shape electrode and a cylinder-shape electrode is reported. A spiral-shape air plasma is generated when a nanosecond pulse voltage is applied to the two electrodes. The smaller the pitch of the spiral-shape electrode is, the more diffuse of the air plasma appears. The discharge current has a pulse width of more than 400 ns, which is much longer than that of ordinary DBDs in air. According to the high speed photographs of the plasma captured by an ICCD camera, the discharge first ignites at the position where the gap distance is smallest, then it propagates continuously along the spiral electrode with the increase of gap distance at a speed of about 10^6 m/s, which is at least one order faster than the propagation speed of plasma bullet in noble gas. Both optical emission spectrum method and electric field induced second harmonic (E-FISH) method are employed for measurement of the electric field at different locations. The obtained electric field from both methods have good agreement and are in the range of 60-105 kV/cm depending on the gap distance of the locations, which is much higher than the breakdown voltage of air under direct current (DC) voltage.

REFERENCES

[1] A. Fridman, A. Chirokov, A. Gutsol, “Non-thermal atmospheric pressure discharges,” J. Phys. D Appl. Phys., vol. 38, 2005.

[2] K. K. Ostrikov, U. Cvelbar, A. B. Murphy, “Plasma nanoscience: setting directions, tackling grand challenges,” J. Phys. D Appl. Phys., vol. 44, 2011.

[3] G. V. Naidis, et al, “Dynamics and structure of nonthermal atmospheric-pressure air plasma jets: experiment and simulation,” IEEE Trans. Plasma Sci., vol. 44, 2016.

[4] M. Laroussi, D. B. Graves, M. Keidar, “Special issue on plasma medicine,” Plasma Med. Sci., vol. 2, 2018.

[5] M. Laroussi, “Plasma medicine: a brief introduction,” Plasma., vol. 1, 2018.

[6] Z. Chen, X. Cheng, L. Lin, M. Keidar, “Cold atmospheric plasma discharged in water and its potential use in cancer therapy,” J. Phys. D: Appl. Phys., vol. 50, 2017.

[7] N. Y. Babaeva, G. Naidis, “Modeling of plasmas for biomedicine Trends Biotechnol,” Trends in biotechnology., vol. 36, 2018.

[8] S. Jin, Z. Li, Y. Xian, “A non‐equal gap distance dielectric barrier discharge: Between cone‐shape and cylinder‐shape electrodes,” High Voltage, vol. 7, 2022.

[9] Z. Li, S. Jin, Y. Xian, “A non-equal gap distance dielectric barrier discharge: between a wedge-shaped and a plane-shaped electrode,” Plasma Sources Science and Technology, vol. 30, 2021.

* The work was supported by the National Key Research and Development Program of China (Grant No. 2021YFE0114700) and National Natural Science Foundation of China (Grant Nos. 52130701 and 51977096).

C1-P-023801

AN ATMOSPHERIC PRESSURE GLOW DISCHARGE IN AIR STABILIZED BY A MAGNETIC FIELD AND ITS APPLICATION ON NITROGEN FIXATION*

Z. LI[1], *X. LU*[1], *S. JIN*[1], *X. LEI*[1]

[1] *Huazhong University of Science and Technology, Wuhan, People's Republic of China*

An atmospheric pressure glow discharge in air stabilized by a magnetic field is reported. The plasma is fixed at a position when the direction of the Lorentz force and the direction of the air flow is opposite. The effects of the applied voltage, the magnetic field and the air flow rate on the plasma characteristics, including the electrical characteristics, the dynamics of the discharge, the electron density, the reduced electric field, and the rotational and vibrational temperature of the plasma, are studied. For applied voltage of 6.5kV, air flow rate of 2L min^{-1}, and magnetic field of 0.11T, the discharge is under direct current (DC) discharge mode with discharge voltage (V_{dis}) and discharge current (I_{dis}) of 1.2kV and 49.7mA, respectively. The rotational and vibrational temperature is about 3420K and 4550K respectively. The electron density is on the order of $10^{14}cm^{-3}$ and the reduced electric field of plasma is about 36.9 Td, which is favorable for vibrational excitation of N_2 to promote the production of NO_x. Because the plasma is fixed at a position, all the gas has to pass the plasma region and treated by the plasma when they are flowing, which is not the case for traditional gliding arc discharge where only a little percentage of gas is actually treated by the plasma. The energy cost of NO_x production for the plasma stabilized by magnetic field of 0.19T is about 2.65MJ mol^{-1}, which is 41% lower than the traditional gliding arc (GA) discharge. Besides, if the direction of the magnetic field is reversed, although the plasma appears in much larger region, the energy cost of NO_x production is much higher than the case of traditional GA discharge.

REFERENCES

[1] S. Gangoli, A. Gutsol, A. Fridman, "A non-equilibrium plasma source: Magnetically stabilized gliding arc discharge: I. Design and diagnostics", Plasma Sources Sci. Technol. Vol. 19, 065003, 2010.

[2] W. Wang, B. Patil, S. Heijkers, V. Hessel, A. Bogaerts, "Nitrogen fixation by gliding arc plasma: Better insight by chemical kinetics modelling", ChemSusChem, vol. 10, pp. 2145–2157, 2017.

[3] B. Patil, F. Peeters, G. Rooij, J. Medrano, J. Lang, Q. Wang, V. Hessel, "Plasma assisted nitrogen oxide production from air: Using pulsed powered gliding arc reactor for a containerized plant", AIChE Journal, vol. 64, pp. 526-537, 2018.

[4] X. Pei, D. Gidon, Y. Yang, Z. Xiong, D. Graves, "Reducing energy cost of NOx production in air plasmas", Chemical Engineering Journal, vol. 362, pp. 217–228, 2019.

[5] F. Jardali, S. Alphen, J. Creel, H. Eshtehardi, M. Axelsson, R. Ingels, R. Snydersb, A. Bogaerts, "NOx production in a rotating gliding arc plasma: Potential avenue for sustainable nitrogen fixation", Green Chem. Vol. 23, pp. 1748–1757, 2021.

[6] X. Lei, H. Cheng, L. Nie, Y. Xian, X. Lu, "Plasma-catalytic NOx production in a three-level coupled rotating electrodes air plasma combined with nano-sized TiO_2", J. Phys. D: Appl. Phys. Vol. 55, 115201, 2022.

[7] Y. Raizer, Gas discharge physics, Berlin: Springer, 1991.

[8] E. Vervloessem, M. Aghaei, F. Jardali, N. Hafezkhiabani, A. Bogaerts, "Plasma-based N2 fixation into NOx: Insights from modeling toward optimum yields and energy costs in a gliding arc plasmatron", ACS Sustainable Chem. Eng. Vol. 8, pp. 9711−9720, 2020

[9] S. Kelly, A. Bogaerts, "Nitrogen fixation in an electrode-free microwave plasma", Joule, vol. 5, pp. 1–25, 2021

[10] S. Djurovic, N. Konjevic, "On the use of non-hydrogenic spectral lines for low electron density and high pressure plasma diagnostics", Plasma Sources Sci. Technol. vol. 18, 035011, 2009

* The work was supported by the National Key Research and Development Program of China (Grant No. 2021YFE0114700) and National Natural Science Foundation of China (Grant Nos. 52130701 and 51977096)

C1-P-024401

NITROGEN FIXATION AS NO_X ENABLED BY A THREE-LEVEL COUPLED ROTATING ELECTRODES AIR PLASMA COMBINED WITH NANO-SIZED TIO_2

X. LEI[1], X. LU[1], S. JIN[1], Z. LI[1]

[1]State Key Lab of Advanced Electromagnetic Engineering and Technology, School of Electronic and Electrical Engineering, Huazhong University of Science and Technology, Wuhan, Hubei, People's Republic of China

A novel three-level coupled rotating electrodes air plasma with nano-sized TiO_2 photocatalysts is developed for evaluation of nitrogen fixation. Factors influencing NO_x concentration and energy cost, including gas flow rates, N_2 fractions, relative humidity levels, blade numbers at each rotating electrode and rotating speed, are examined. Gas flow rates prove to have no effect on the rotational temperature of N_2 337.1 nm and the emission intensities of N_2^+ and N_2, but specific energy input (SEI) and species' residence time can be shorter with higher air flow rates, resulting in lower NO_x concentration and energy cost. The addition of H_2O also has a positive effect on both NO_x concentration and energy cost. Optical emission spectrum (OES) shows that air + H_2O plasma has stronger 336 nm (NH) and 309 nm (OH) emission lines than air plasma, indicating that NH and OH are the key species in NO_x enhancement. Final results show that the exceptional synergistic effect between TiO_2 and three-level coupled rotating electrodes air plasma significantly increases the NO_x concentration by 68.32% (from 4952 to 8335 ppm) and reduces the energy cost by 40.55% (from 2.91 to 1.73 MJ mol^{-1}) at gas flow rate of 12 l min^{-1} and relative humidity level of 12%, which beats the ideal thermodynamic energy limit ~2.5 MJ mol^{-1} for the thermal gas-phase process. A possible mechanism for enhanced NO_x production with TiO_2 is discussed: Highly energetic electrons in plasma contribute to the formations of the electron–hole pairs and oxygen vacancy (V_o) on the TiO_2 catalyst surface, which may facilitate the dissociative adsorption of O_2 molecules to form superoxide radical groups (like O_2^-) and H_2O molecules to form surface hydroxyl groups (like OH·), and thus, improving energy efficiency.

C1-P-024506

PRECISION PROCESSING OF MICROTOOLS WITH BEAMS OF FAST ATOMS OBTAINED IN PLASMA BY ACCELERATING ITS IONS AND THEIR CHARGE EXCHANGE COLLISIONS*

E.S. MUSTOFAEV, A.S. METEL, Y.A. MELNIK

Moscow State University of Technology, 1 Vadkovsky lane, Moscow 127055, Russian Federation

The wear-resistant coatings can appreciably improve efficiency of cutting tools. However, the cutting edge radii of micro cutters can grow by 2–2.5 times after the coating deposition, and it does not allow a stable cutting process. Micro cutters are small and have a lower ability to resist bending. Therefore, it is impossible to increase the thickness of the cut chips, because bending can result in destruction of the tool.

To solve the problem a layer should be removed from the tool surface its thickness exceeding the thickness of the wear-resistant coating deposited afterwards. The surface layer removal was carried out using a grid immersed in the glow discharge plasma filling a vacuum chamber (Fig. 1). The grid is fastened to a feedthrough and can be negatively biased to 5 kV. There is inside the chamber a rotating holder for micro end mills by Cerin (IT) with the working part diameter amounting to 3 mm and length of 12 mm.

At an argon pressure in the chamber $p \sim 0.3$ Pa, an increase in the voltage between the anode and the chamber to several hundred volts results in a glow discharge with a current in the anode circuit I_a up to 4 A and a discharge voltage of U_d = 400–500 V [1]. The transparency of 20-cm-diameter concave grid with a surface curvature radius of 20 cm amounts to ~ 80%. Under negative voltage of 5 kV, it is surrounded by a space charge sheath. The ions accelerated from the plasma pass through the grid holes. Due to collisions in the sheath with gas molecules, they turns into fast neutral atoms sputtering the rotating end mill.

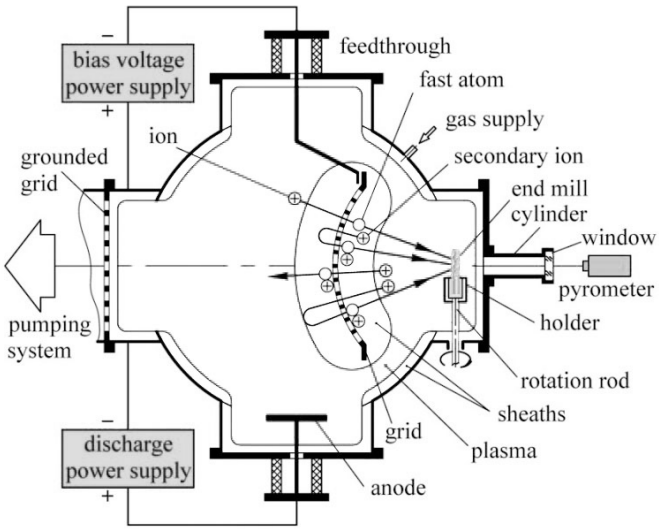

Fig.1. Scheme of a concentrated beam generation by a grid immersed in plasma

Measurements of the cutting edge radius R using an optical measuring system MikroCAD premium+ manufactured by GFMesstechnik GmbH showed that during a three-hour-long processing it diminished from the initial R ~ 11 μm to R ~ 4 μm. After the end mill processing, a 3-μm-thick wear-resistant coating was deposited on its surface using a Platit π 311 system manufactured by Platit (Switzerland). The deposited diamond-like coating (DLC) was a two-layer composition: an adhesive sublayer based on a complex nitride (CrAlSi)N and a wear-resistant DLC layer. The cutting edge radius of coated end mill amounted to 7 μm. Hence, the sharpening of micro tools with a fast atom beam makes it possible to avoid blunting of their cutting edges caused by an increase in their radii after the coating deposition.

REFERENCES

[1] A.S. Metel, S.N. Grigoriev, Y.A. Melnik, V.V. Panin, "Filling the vacuum chamber of a technological system with homogeneous plasma using a stationary glow discharge", Plasma Phys. Rep., vol. 35, no. 12. pp. 1058–1067, 2009.

* The work was supported by the Russian Science Foundation under grant No. 20-19-00620.

C1-P-024507

REMOVAL OF DEFECTIVE SURFACE LAYERS FROM CUTTING CERAMIC INSERTS BY FAST ARGON ATOMS BEFORE DEPOSITION OF WEAR-RESISTANT COATINGS*

E.S. MUSTOFAEV, A.S. METEL, M.A. VOLOSOVA, Y.A. MELNIK, E.A.OSTRIKOV

Moscow State University of Technology, 1 Vadkovsky lane, Moscow 127055, Russian Federation

Deposition of wear-resistant coatings on hard alloy tools ensures high operational stability and increase wear resistance by three times, even when machining hard-to-machine titanium and nickel alloys. Ceramic cutting inserts can be operated at high cutting speed unattainable for tools made of hard alloy. However, it is impossible to fully realize the potential of wear-resistant coatings on ceramic inserts. Because they undergo diamond sharpening and after that the insert surface is replete with shallow scratches, deep grooves profiled with single diamond grains and caverns with a depth up to 5 μm. The coatings effectiveness can be ensured only after removal from the insert surface of the defective layer with a thickness exceeding 5 μm.

To deposit wear-resistant TiAlN coatings on round cutting inserts with a diameter of 19.05 mm and a height of 7.9 mm made of dielectric AS500 ceramic an experimental system was used, which comprises a source of fast neutral atoms [1-3], two planar magnetrons and a rotation system for eight inserts. The inserts are fastened thereon in a vertical line. Each insert is placed on its individual holder fastened to one of the eight parallel axes. The angle of the axes relative to trajectories of fast atoms is 45 degrees (Fig. 1).

The beam of fast atoms is produced using a grid composed of twenty parallel 150-mm-long, 300-mm-wide and 0.5-mm-thick titanium plates. The power supply allows regulation of the negative bias voltage on the grid from zero to 5 kV. Ions accelerated from the plasma emitter enter the gaps between the grid plates. They touch the plates and turn into fast atoms. As sections of the grid plates facing towards the plasma emitter are shaped as segments of a 50-cm-radius circle, trajectories of the fast atoms are directed to the center of this circle. Therefore, the width of the fast atom beam is decreasing from 30 cm near the plasma emitter to 2.5 cm near the rotating cutting inserts. The flux density of fast argon atoms and the rate of cutting plates etching increase in this case by a factor of 30/2.5 = 12.

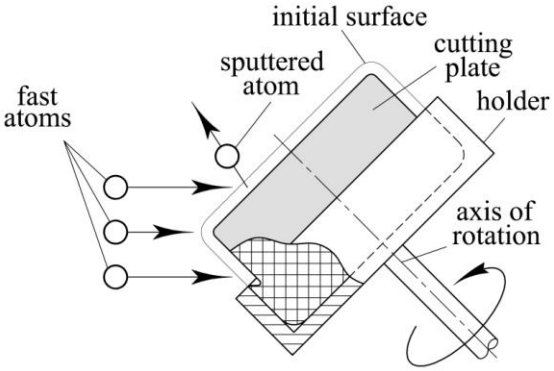

Fig.1. Schematic of etching a ceramic cutting plate with fast argon atoms.

At the equal angles of incidence to the front and back surfaces of the cutting wedge amounting to 45 degrees, two-hour-long etching of cutting inserts provides removal of a 10-μm-thick surface layer of the hard-to-sputter ceramic. As a result the cutting edge radius of the insert diminished from R ~ 20 μm to R ~ 10 μm. Wear-resistant TiAlN coatings deposited after the etching increase wear resistance of the cutting inserts by not less than 1.7 times and significantly increase the processing stability.

REFERENCES

[1] S. Grigoriev, Y. Melnik, A. Metel, “Broad fast neutral molecule beam sources for industrial scale beam-assisted deposition,” Surf. Coat. Technol. vol. 156, pp. 44–49, 2002.

[2] A. Metel, S. Grigoriev, Yu. Melnik, V. Panin, V. Prudnikov, “Cutting tools nitriding in plasma produced by a fast neutral molecule beam”, Jap. J. Appl. Phys., vol. 50, no. 8, 08JG04, 2011.

[3] S. Grigoriev, Y. Melnik, A. Metel, M. Volosova, “Focused beams of fast neutral atoms in glow discharge plasma”, J. Appl. Phys., vol.121, 223302, 2017.

* The work was supported by the state assignment of the Ministry of Science and Higher Education of the Russian Federation, project No FSFS-2021-0006.

C1-P-024601

MULLITE FILIFORM CRYSTALS PRODUCED BY THE PLASMA MELTING METHOD*

V.V. SHEKHOVTSOV, R.E. GAFAROV, N.K. SKRIPNIKOVA, O.G. VOLOKITIN

Tomsk State University of Architecture and Building, TSUAB, Tomsk, Russia

Mullite has excellent heat-resistant and strength properties, which allows it to be widely used in the production of various refractory materials. Mullite is rare in nature, and the main difficulty associated with the synthesis of mullite is the need to use high temperatures to start the process of mullite formation [1–3]. This problem can be solved by arc-discharge plasma, in the flow of which the temperature varies from 1700 K to 18000 K.

In this work, a mixture of aluminum oxide and kaolin from the Zhuravliny Log deposit was used to obtain mullite ceramics. Plasma melting was carried out on an electroplasma stand [4]. The schematic diagram consists of a plasma torch with a remote arc discharge (nozzle diameter 4 mm) installed at a distance of 60 mm from the base of the graphite crucible. Graphite crucible parameters: height 55 mm, diameter 15 mm, wall thickness 3 mm. The melting of the 7 g material took place within 30 seconds at: current strength 100 A, voltage 110 V, plasma gas flow rate 14 nl/min (air). On fig. 1 shows an electron image (*a*) of the surface of the resulting melt product and an EDX spectrum (*b*).

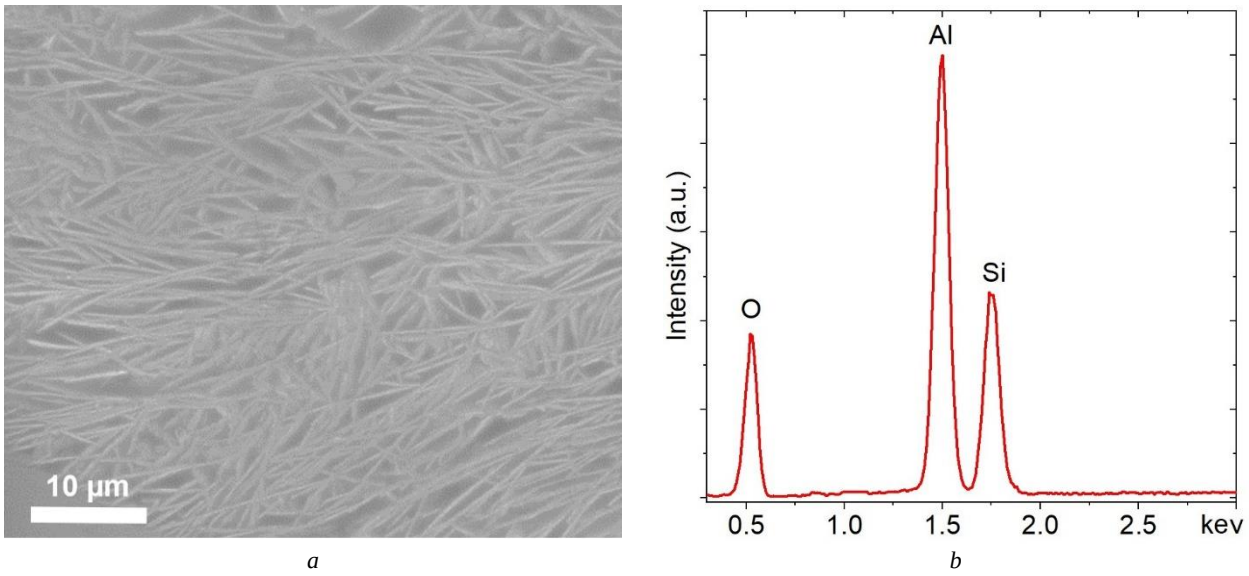

a *b*

Fig.1. Morphology of the surface of the melting product: *a* – TEM images at a magnification of 6000 times; *b* – EDX spectrum.

As can be seen (fig.1, *a*) the surface morphology is represented by branched system of filiform crystals. The filaments are ~1–2 μm in diameter, and their length does not exceed ~40 μm. The formation of weakly anisotropic filaments is carried out according to the vapor-liquid-solid phase mechanism as a result of moderate heat removal. Analysis of the EDX spectrum (Fig. 1, *b*) showed that the condition 3:2 – Al_2O_3:SiO_2 is satisfied, which is typical for the $3Al_2O_32SiO_2$ mullite phase. Thus, the work shows the possibility of obtaining filiform mullite ceramics by plasma melting of natural materials.

REFERENCES

[1] C. Shin, S. –H. Oh, J. –H. Choi, K. –T. Hwang, K. –S. Han, S. –J. Oh, J. –H. Kim, "Synthesis of porous ceramic with well-developed mullite whiskers in system of Al_2O_3–Kaolin–MoO_3," Journal of Materials Research and Technology, vol. 15, pp. 1457–1466, 2021.

[2] M. Romero, I. Padilla, M. Contreras, A. López-delgado, "Mullite-based ceramics from mining waste: A review," Minerals, vol. 11/3, no. 332, pp. 1–39, 2021.

[3] R. E. Gafarov, V. V. Shekhovtsov, O. G. Volokitin, "Synthesis of mullite from aluminosilicate raw materials in a thermal plasma flow," 15th Int. Conf. Gas Discharge Plasmas and Their Applications (GDP), Ekaterinburg, Russia, p. 180, 2021.

[4] V. V. Shekhovtsov, O. G. Volokitin, G. G. Volokitin, N.K. Skripnikova, R.E. Gafarov, N.A. Tsvetkov, "Efficiency of thermal plasma treatment of aluminosilicate particles," Key Engineering Materials, vol. 769, pp. 23–28, 2018.

* The work was carried out with the support of the state task of the Ministry of Science and Higher Education of the Russian Federation FEMN–2020–0004 and grant President of the Russian Federation MK–66.2022.4.

C1-P-025703

INVESTIGATION OF THE CHARGE STATE VARIATION OF SN IONS IN THE PLASMA OF LOW-CURRENT VACUUM ARC ON A TIN CATHODE*

YU. A. ZEMSKOV, I.V. UIMANOV

Institute of Electrophysics UB RAS, Yekaterinburg, Russia

Investigations of variation of the ion charge composition in low current vacuum arc plasma have both theoretical and practical importance. In a fundamental physics area, data of the investigations help to develop a model of plasma generation by cathode explosive emission centers in vacuum discharges. And for practical applications, it is useful to find a range of applicability for the classical data [1] about the charge composition of ions in the vacuum arc plasma, which were obtained in current ranges of tens and hundreds of amperes.

A decrease in the average charge of the ions of the cathode material with a decrease in the vacuum arc current was noted by several researchers. We studied this effect in detail for copper cathodes in the course of several experiments at various parameters. Also, this effect was confirmed for composite cathodes made of CuCr material and for refractory cathodes using molybdenum as an example. In the course of this study, a tin cathode was chosen as the object. This material differs significantly from the materials mentioned above, both in terms of thermophysical properties and the charge composition of ions in vacuum arc plasma at currents above 100 A. According to classical data, the average charge of tin ions in the vacuum arcs is 1.53, while for copper and chromium this parameter exceeds 2, and for molybdenum it exceeds 3. The charge composition was studied using a Thomson spectrometer with automatic signal recording and digital data processing. The arc discharge was feed by a generator based on an LC line with a quasi-rectangular pulse shape. The arc current was varied in the range from 2 to 125 A. The behavior of the charge composition of the ions of the cathode material in the case of a tin cathode differed significantly from the previously studied materials. The general observation was, that instead of a decrease in the average charge of ions with the arc current, an increase in this parameter was found. In the arc plasma at low currents, the fraction of Sn^{3+} ions increased. In the low-current range Sn^{4+} ions also appeared, and the fraction of the ions increased with current decrease too, while at discharge currents above 40 A the signal of the Sn^{4+} ions was not noticeable against the noise background at all.

REFERENCES

[1] A. Anders, "Ion charge state distributions of vacuum arc plasmas: The origin of species," Physical Review E, 1997, vol. 55, pp. 969-981.

* The work was supported in part by RFBR Grant No. 19-08-00783.

C1-P-027701

PLASMA REACTOR FOR MATERIAL SYNTHESIS AND WASTE RECYCLING*

ZH. BOLATOVA[1], A.YA. PAK[1], A. A. GUMOVSKAYA[1], P.V. POVALYAEV[2], R.S. MARTYNOV[1], K.B. LARIONOV[2]

[1]Tomsk Polytechnic University, Tomsk, Russia
[2]T.F. Gorbachev Kuzbass State Technical University, Kemerovo, Russia

In the modern world, a huge amount of waste of various origins is accumulated: municipal solid waste, industrial waste and organic waste [1]. Separate types of waste can be processed in various ways, such as thermochemical method (combustion, gasification, pyrolysis) and biochemical (anaerobic digestion) [2]. There is a group of plasma methods for waste disposal, the advantages of which can be considered: the possibility of achieving high temperatures and heating rates [3]. The main disadvantage is the relative complexity of the design of plasma reactors, their cost and the high energy intensity of the waste recycling process [4]. In this regard, the issue of simplifying the design of plasma reactors and increasing their energy and resource efficiency is topical. One of the approaches for improving such reactors is the use of air as the initial working gaseous atmosphere [5]. This approach makes it possible to reduce the weight and dimensions of arc reactors; allows to abandon the vacuum circuit as part of the installation, which further reduces the energy intensity of the waste processing process.

In the course of the research, an atmospheric arc plasma reactor was created [6], its automation system was developed, and software was written for it [7]. The reactor contains a power source with a working direct current up to 200 A, electrodes - an anode and a cathode in the form of rods; a working non-sealed graphite chamber in the form of a glass, in the walls of which holes are made, into which the electrodes of the discharge circuit are inserted. The system for recording electrical parameters includes a two-channel digital oscilloscope, a Hall sensor and a potentiometer-type voltage divider.

The created arc reactor was tested in the processes of recycling various wastes: plastics, rubber tires, broken glass, ash and slag waste.

The peculiarity of the created reactor is the use of atmospheric air as a working gaseous atmosphere. At the same time, the synthesis products are gaseous products (namely, methane, hydrogen, CO and CO_2 gases), which shield the reaction zone from atmospheric oxygen, preventing oxidative processes; this also enables to synthesis of various materials, in particular, carbon nanostructures in the process of waste disposal. Preliminary calculation and experimental data show the possibility of reducing the energy intensity of the waste processing process by eliminating the vacuum circuit and the vacuum pump by about 10 times compared to direct analogues. At present, the created reactor and the methodology for working on it are implemented on a laboratory level. Further research will focus on recycling other types of waste and scaling up.

REFERENCES

[1] T.F.McGowan, Waste to Energy Conversion Technology Woodhead Publishing Series in Energy, USA: TMTS Associates, Inc., 2013.
[2] F. Zhang,Y. Zhao, D. Wang, M. Yan, J. Zhang, P. Zhang “Current technologies for plastic waste treatment: A review,” J. of Clean. Produc., vol. 282, no. 124523, February 2021.
[3] E. Gomez, D.A. Rani, C.R. Cheeseman, D. Deegan, M. Wise, A.R. Boccaccini, “Thermal plasma technology for the treatment of wastes: a critical review,” J. Hazard. Mater., vol. 161, pp. 614–626, January 2009.
[4] J. Zhao, Y. Su, Z. Yang, L. Wei, Y. Wang, Y. Zhang, “Arc synthesis of double-walled carbon nanotubes in low pressure air and their superior field emission properties,” Carbon N. Y., vol. 58, pp. 92– 98, July 2013.
[5] N. Arora, N.N. Sharma, Arc discharge synthesis of carbon nanotubes: Comprehensive review, Diam. Relat. Mater., 50, pp. 135-150, November 2014.
[6] R.S. Martynov, A.Ya. Pak, G. Ya. Mamontov, Ustrojstvo dlya polucheniya poroshka na osnove karbida bora [Device for obtaining powder based on boron carbide]. Patent RF, no. 2700596, 2019.
[7] P.V. Povalyaev, A.Ya. Pak, Upravlenie sistemoj pozicionirovaniya elektrodov i registraciya parametrov rabochego rezhima dugovogo reaktora postoyannogo toka [Controlling the electrode positioning system and recording the parameters of the operating mode of the DC arc reactor]. Certificate of state registration of computer programs RF, no. 2022611637, 2022.

* The work was supported financially in accordance with an additional agreement on the provision of subsidies from the federal budget for financial support for the implementation of the state task for the provision of public services (internal number 075-ГZ/X4141/687/3).

C1-P-030502

THE PRODUCTION OF CALCIUM NITRATE BY THE AIR HIGH-VOLTAGE AC PLASMA TORCH

S.D. POPOV[1], V.E. POPOV[1], D.I. SUBBOTIN[1], A.V. SUROV[1], E.O SERBA[1], A.V. NIKONOV[1], GH.V. NAKONECHNY[1], V.A. SPODOBIN[1]

[1] Institute for Electrophysics and Electric Power of the Russian Academy of Sciences (IEE RAS), St. Petersburg, Russia

At present, the main methods for obtaining nitrogen fertilizers are synthesis from nitric acid and ammonia [1]. Both of these substances are produced using hydrogen in a catalytic chemical process. Due to the instability of hydrocarbon prices, the cost of producing nitrogen fertilizers can vary significantly over time. At the same time, political tension significantly complicates the functioning of the nitrogen fertilizer market.

In most cases, the production of nitrogen fertilizers is highly localized due to high capital costs and high productivity of existing chemical facilities [2]. Obviously, it is necessary to create local industries, taking into account regional factors: the need for fertilizers, the availability of chemical and electrical resources, seasonality in the use of fertilizers, etc.

At the beginning of the 20th century, facilities were created for the production of nitrogen oxides from the air by the electric arc method. The Haber method replaced the previous method due to its high performance and relatively low cost. At present, with the development of alternative energy, it is possible to create installations for electric arc synthesis, taking into account the functioning of alternative energy power plants, which makes it possible to use it in the local production of nitrogen fertilizers [3].

The proposed solution is based on a high-voltage AC plasma torch operating in air and a mixture of nitrogen and oxygen (1:1 mol.). This plasma torch has a high thermal efficiency of up to 95% and an operating life of the electrode unit up to 2000 h [4].

It has been experimentally established that a plasma-chemical installation with a high-voltage plasma torch makes it possible to obtain product gas with a nitrogen oxide concentration of up to 3.5 wt%. (predominantly nitrogen monoxide). The application of this method for the synthesis of nitrogen oxides for the production of calcium nitrate ($Ca(NO_3)_3$) was evaluated. The sequence of stages is as follows: 1. synthesis of nitrogen monoxide from air; 2. production of nitrogen dioxide by catalytic oxidation; 3. absorption of nitrogen dioxide by calcium hydroxide and further oxidation to nitrates. The enthalpy of the air plasma generated by the plasma torch is 6.12 MJ/kg.

Table - Energy consumption for obtaining synthesis products

Substance	Yield, kg/kg of air	Energy costs	
		MJ/kg	kW·h/kg
Nitrogen monoxide (NO)	0,035	174,86	48,57
Nitrogen dioxide (NO_2)	0,051	114,04	31,68
Nitric acid (HNO_3)	0,074	83,24	23,12
Calcium nitrate ($Ca(NO_3)_3$)	0,191	31,98	8,88

The table shows that the energy costs for obtaining calcium nitrate are quite large and approach the cost of its production by traditional methods. Thus, the further use of electric arc synthesis of nitrogen oxides for the production of nitrogen fertilizers is advisable for local use in relatively large farms with complex fertilizer logistics.

REFERENCES

[1] K. Jones, The Chemistry of Nitrogen, Oxford: Pergamon Press, 1975.

[2] M. Park, The Fertilizer Industry, Cambridge: Woodhead Publishing, 2001.

[3] N. Cherkasov, A.O. Ibhadon, P.Fitzpatrick.“ A review of the existing and alternative methods for greener nitrogen fixation,” Chemical Engineering and Processing: Process Intensification, vol. 90, pp. 24-33, 2015.

[4] A.V. Surov, S.D.Popov, V.E.Popov, D.I.Subbotin, E.O.Serba, V.A.Spodobin, Gh.V.Nakonechny, A.V.Pavlov,“ Multi-gas AC plasma torches for gasification of organic substances,” Fuel, vol. 203, pp. 1007-1014, 2017.

C1-P-034403

INVESTIGATION OF COLD PLASMA JET GENERATION PROCESS UNDER EXCITATION BY UNIPOLAR POSITIVE PULSES *

A.S. BOROVIKOVA[1], P.P. GUGIN[2], E.V. MILAKHINA[1,2], D.E. ZAKREVSKY[1,2]

[1]Novosibirsk State Technical University, Novosibirsk, Russia
[2]Rzhanov Institute of Semiconductor Physics SB RAS, Novosibirsk, Russia

A modern trend in the development of plasma medicine is the impact of plasma formations, in particular atmospheric pressure plasma jets, on biological targets of various nature. In the area of plasma structure distribution and the interaction area with the target, charged particles cause chemical reactions. As a result, there is an increase in the radical concentration containing oxygen and nitrogen, which affects the current processes inside the cells [1].

The course of chemical reactions in the interaction area with biological targets depends on the contact frequency of the surface with a plasma jet. Earlier, in [2], it was shown that each positive half-cycle of the applied sinusoidal voltage initiates a streamer inside the dielectric channel, but outside the discharge zone, the streamer propagation is prevented by the bulk plasma formation accumulated from previous cycles. Such phenomena depend on the conditions in the nozzle–target gap and is determined by the ratio of the plasma density formed in the streamer head and the residual plasma density above the target surface. Thus, the current frequency reaching the target f_I does not coincide with the frequency of the applied voltage f_U.

In the present work, the plasma jet generation upon excitation by unipolar positive pulses at frequency f_U = 1-40 kHz, applied amplitude voltage 2-6 kV was studied. The operation modes of a plasma jet excited by unipolar positive pulses were studied and determined modes, which provided the coincidence of the current contact frequency f_I and the frequency of the applied voltage f_U. The fundamental difference between the excitation nature of the discharge by pulsed or sinusoidal voltages was the time of the voltage rise τ. With pulsed excitation, the rise time was τ = 3 μs; with sinusoidal excitation was τ = 5 μs. The investigation of plasma jet generation upon excitation by unipolar positive pulses with different leading edge durations τ = 3 μs (Fig. 1*a*) and τ = 10 μs (Fig. 1*b*) demonstrated that excitation by pulses with a leading edge τ = 3 μs ($f_U \approx$ 22 kHz, U = 5 kV) provides the condition for the frequency ratio $f_I = f_U$, and at τ = 10 μs ($f_U \approx$ 22 kHz, U = 5 kV) the frequency ratio is $f_I = f_U/2$.

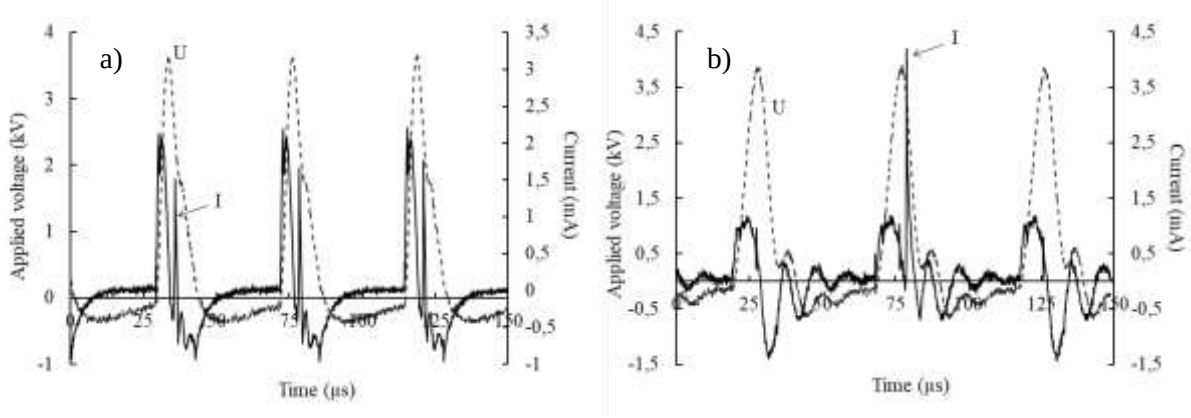

Fig.1. Oscillogram of current and voltage with different duration of the leading edge

REFERENCES

[1] L. Lin, M. Keidar, "A map of control for cold atmospheric plasma jets: From physical mechanisms to optimizations," Appl. Phys. Rev., vol. 8, pp. 011306, January 2021.

[2] I. Schweigert, A. Alexandrov, Dm. Zakrevsky, "Self-organization of touching-target current with AC voltage in atmospheric pressure plasma jet for medical application parameters," Plasma Sourc. Sci. Tech., vol. 29, pp. 12LT02, 2020.

* The work was supported by Russian Science Foundation, research project No. 19-19-00255.

C1-P-036302

EXPERIMENTAL STUDY OF THE PROPERTIES OF A MICROWAVE DISCHARGE WITH DIELECTRIC BARRIER CONFIGURATION*

V.N. TIKHONOV [1], *S.N. ANTIPOV* [2], *M.KH. GADZHIEV* [2], *S.A. GORBATOV* [1], *I.A. IVANOV* [1], *A.V. TIKHONOV* [1]

[1] *Russian Institute of Radiology and Agroecology, Obninsk, Russian Federation*
[2] *Joint Institute for High Temperatures of RAS, Moscow, Russian Federation*

Broad prospects for the use of non-thermal atmospheric pressure plasma (NTAP) are associated with its huge potential for unique technological capabilities in the creation of new products and technologies [1-3]. This article presents the results of an experimental study of the parameters of the microwave NTAP source, which combines the characteristics of a dielectric barrier discharge and a non-thermal plasma jet [4, 5].

Studies of the formation processes, as well as the structure and dynamics of a microwave dielectric barrier discharge of atmospheric pressure excited in an argon flow have been carried out by the high-speed video filming. Thermocouple and thermal imaging measurements of the temperature profiles of the plasma jet formed in argon flow behind the discharge tube outlet have been made. Measurements and analysis of emission spectra of the discharge in the region of the argon plasma jet have been carried out. In the emission spectra of the plasma, molecular bands of N_2, OH, and atomic lines of Ar are observed (see Figure 1 on the left). Figure 1 on the right shows a thermogram of a heat spot on aluminum foil placed across the plasma flow at a distance of 30 mm from the discharge tube nozzle.

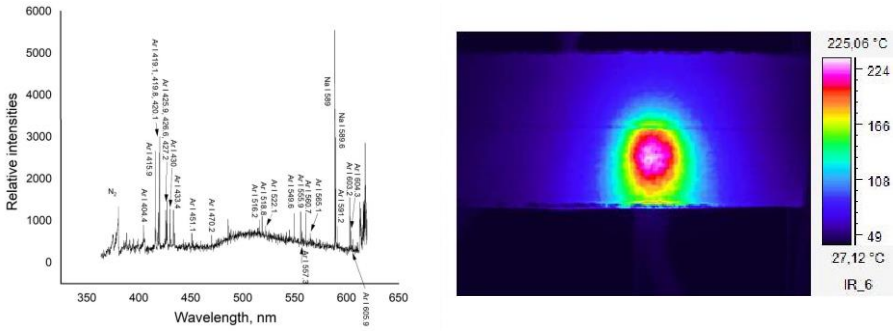

Fig.1. Emission spectrum of the microwave DBD argon plasma jet in the wavelength range 350-650 nm (left). Thermogram of a heat spot on aluminum foil placed across the plasma jet (right).

To measure the temperature by the contact method, we used an open fast-response chromel-copel thermocouple of the L type. The thermocouple was fixed with a special holder on a positioning table with a micrometer feed along the axis of the discharge tube. A quartz tube with an outer diameter of 8 mm and a wall thickness of 1 mm was used as the discharge chamber. The tube was located in such a way that the cut of its exit hole coincided with the plane of the outer surface of the narrow wall of the waveguide. The measurements were carried out at a microwave generator power of 600 W for two flow rates of the working gas (argon), 15 and 30 L/min. Under these conditions, at a distance of 12 mm from the nozzle, the measured jet temperature was 350 and 260 degrees Celsius, respectively. At an argon flow rate of 10 L/min, the length of the visible (luminous) part of the plasma jet was about 26 mm. Modification of heat-sensitive surfaces by treating with such DBD-discharge plasma jets opens new possibilities for development of novel materials.

REFERENCES

[1] V. Nehra, A. Kumar, H.K. Dwivedi, "Atmospheric Non-Thermal Plasma Sources," International Journal of Engineering, vol. 2, no. 1, pp. 53-68, 2008.

[2] N.N. Misra, O. Schlüter, P.J. Cullen, Cold plasma in food and agriculture: fundamentals and applications. London, United Kingdom: Academic Press, 2016.

[3] Z. Gan, X. Feng, Y. Hou, A. Sun, and R. Wang, "Cold plasma jet with dielectric barrier configuration: Investigating its effect on the cell membrane of E. coli and S. cerevisiae and its impact on the quality of chokeberry juice," LWT, vol. 136, 110223, 2021.

[4] V.N. Tikhonov, I.A. Ivanov, A.V. Tikhonov, "A new type of non-thermal atmospheric pressure plasma source," J. Phys. Conf. Ser., vol. 1393, 2019.

[5] V.N. Tikhonov, S.A. Gorbatov, I.A. Ivanov, A.V. Tikhonov, "A new type of non-thermal atmospheric pressure plasma source based on a waveguide bridge," J.Phys. Conf. Ser. vol. 2064, 2021.

* The work was supported by the Russian Foundation for Basic Research (project No. 20-08-00894).

C1-P-046401

A COMPACT SETUP FOR LASER-INDUCED DESORPTION SPECTROSCOPY IN BACKGROUND RF PLASMA*

G.I. RYKUNOV[1,2], A.V. KAZIEV[1], A.I. ALIEVA[1], D.V. KOLODKO[1,3], M.M. KHARKOV[1], YU.M. GASPARYAN[1], N.S. SERGEEV[1]

[1]National Research Nuclear University MEPhI (Moscow Engineering Physics Institute), Moscow, Russia
[2]MIREA – Russian Technological University, Moscow, Russia
[3]Fryazino Branch of Kotel'nikov Institute of Radio Engineering and Electronics RAS, Fryazino, Russia

Development of remote control methods for diagnosing the content of hydrogen and its isotopes in the fusion-relevant materials is an important direction of plasma-surface interaction studies. There has recently been a renewed interest in laser techniques combined with optical spectroscopy for the local measurement and removal of hydrogen particles from materials, including laser-induced breakdown spectroscopy (LIBS), laser-induced ablation spectroscopy (LIAS) and laser-induced desorption spectroscopy (LIDS) [1]. Such methods can be realized and studied in a setup that meets the following requirements: 1) it should be a compact device; 2) it should incorporate laser source for surface diagnostics; 3) it should be suitable for implementation of spectroscopic measurements of species ejected from surface under laser exposure. The latter can be more effectively done in presence of a background diffuse plasma.

We have recently developed and built a wide-application compact device with radiofrequency (RF) inductively coupled plasma (ICP), and here we report equipping it with the millisecond-pulse laser and studying its characteristics. The high peak power that can be achieved on a sample surface with short laser pulse together with ICP plasma environment enable exciting the laser-desorbed material species for further spectroscopic analysis. It is important to use a laser with intensity less than that required for ablation, in order to analyze the material without damaging the surface. The scheme of the diagnostic setup is shown in Fig. 1.

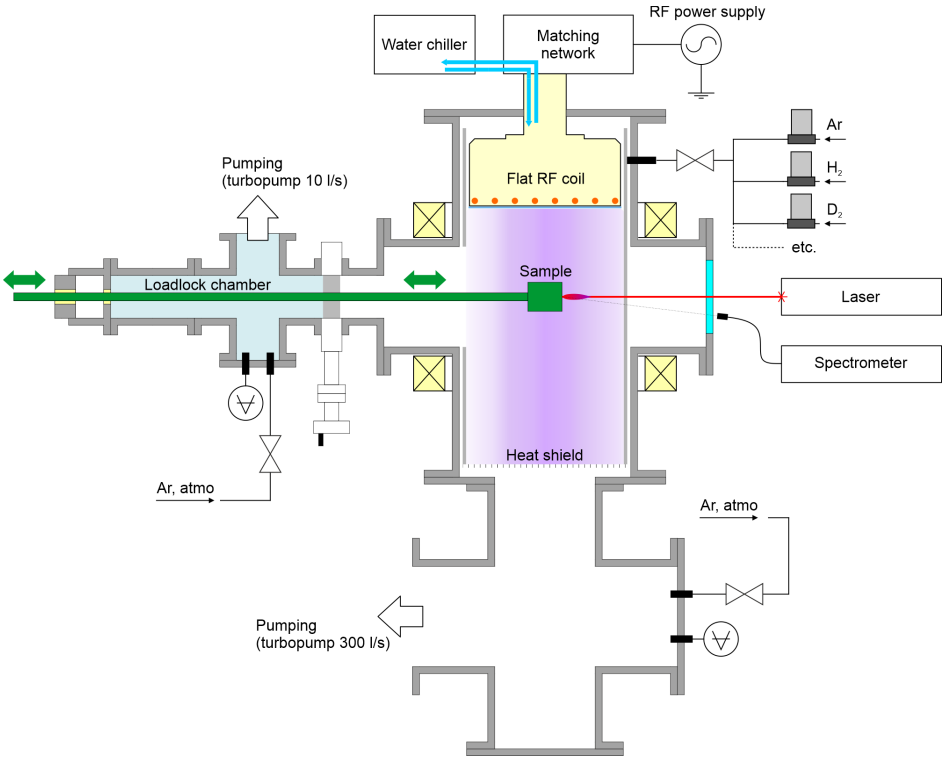

Fig.1. Diagnostic setup scheme.

REFERENCES

[1] J.H. Yu, M.J. Baldwin, M.J. Simmonds, A. Založnik, "Time-resolved laser-induced desorption spectroscopy (LIDS) for quantified in-situ hydrogen isotope retention measurement and removal from plasma facing materials," Rev. Sci. Instrum., Vol. 90, Article Number 073502, 2019.

* The work was supported by the Ministry of Science and Higher Education of the Russian Federation (project no. 0723-2020-0043).

C1-P-050502

PLASMA GENERATION IN AN ARC DISCHARGE WITH A CATHODE SPOT AND A NON-SELF-SUSTAINED DISCHARGE WITH A HOT ANODE*

V.V. SHUGUROV, I.I. AZHAZHA, N.A. PROKOPENKO

Institute of High Current Electronics SB RAS
E-mail: shugurov@inbox.ru

The paper presents the results of a study of plasma generation during the simultaneous operation of an arc metal evaporator and a PINK plasma generator with a hot evaporated anode made of boron powder. This discharge system makes it possible to obtain coatings from borides of various metals.

The plasma concentration, electron temperature, and ion current density, and their dependence on the operating modes of the discharge system, as well as their influence on the properties, structure, and composition of the modified substrate layer, were studied by the probe method.

* The work was supported by RSF project No. 19-19-00183.

C1-P-907801

ROLE OF ELECTRONS OF PLASMA AND ELECTRON BEAM IN GENERATION OF BEAM-PRODUCED PLASMA IN MEDIUM VACUUM*

A.V. TYUNKOV, YU.G. YUSHKOV, D.B. ZOLOTUKHIN,

Tomsk State University of Control Systems and Radioelectronics, Tomsk, Russia

We discuss here the results of experimental studies aimed at revealing the role of low-energy electrons of plasma and high-energy electrons of energetic electron beam in the generation of beam-produced plasma in the fore-vacuum pressure range. Our main research instrument was RGA-300, the residual atmosphere quadrupole mass analyzer which ionizer was replaced by an ion-optical system described in details in [1].

The idea of the experiment was to inject different inert gases – argon and helium – in equal concentrations as a working mixture. During the process of generation of beam plasma, the mass spectrum of ions in such plasma was monitored, and the ratio of densities of argon to helium ions was recorded. This experimental ratio was compared with theoretical estimates of the ratio of the ionization probabilities P_{Ar}/P_{He} for the mentioned gases. The plasma electrons temperature was assumed to be 1.5 eV with the Maxwellian distribution function [2, 3]. For the beam electrons, it was assumed that their energy is completely dissipated during sequential acts of working and residual gas ionization.

According to theoretical estimations, the ratio P_{Ar}/P_{He} equals to 2058 in case of ionization by plasma electrons only, while for the ionization by energetic electron beam this ratio becomes equal to 5.54. Experimental ratio of densities of argon to helium ions was 5.8.

Therefore, we can conclude that the main contribution to plasma generation in medium vacuum make high-energy beam electrons not plasma electrons. However, the small contribution of plasma electrons can be significant during the ionization of alkali metal vapors with a low potential and a maximum ionization cross section.

REFERENCES

[1] D. B. Zolotukhin, A. V. Tyunkov, Y. G. Yushkov, E. M. Oks “Modified quadrupole mass analyzer RGA-100 for beam plasma research in forevacuum pressure range,” Review of Scientific Instruments, vol. 86. No 12. pp. 123301. 2015.

[2] D. B. Zolotukhin, V. A. Burdovitsin, E. M. Oks, A. V. Tyunkov, Yu. G. Yushkov “On the influence of electron-beam metal evaporation on parameters of beam plasma in medium vacuum,” Physics of Plasmas, vol. 26. No 5. pp. 053512. 2019.

[3] D. B. Zolotukhin, E. M. Oks, A. V. Tyunkov, Y. G. Yushkov “Deposition of dielectric films on silicon using a fore-vacuum plasma electron source,” Review of Scientific Instruments, vol. 87. No 6. pp. 063302. 2016.

*The work was supported by the Russian Science Foundation (grant #21-79-10035)

C1-P-950302

TIME-RESOLVED SPECTRAL DIAGNOSTICS OF A HIGH-VOLTAGE PLASMA TORCH

A.V. SUROV[1], A.A. DYACHENKO[1], I.L. IOV [2], A.V. NIKONOV[1], G.V. NAKONECHNY[1], E.O. SERBA[1], M.E. PINCHUK[1], S.D. POPOV[1], V.A. SPODOBIN[1], D.I. SUBBOTIN[1]

[1] Institute for Electrophysics and Electric Power, Saint-Petersburg, Russian Federation
[2] Saint Petersburg State University, Saint-Petersburg, Russian Federation

Electric arc generators of thermal plasma are promising tools for creating plasma technologies that are in demand for solving global issues. Among the current technologies: pyrolysis of hydrocarbons to produce hydrogen [1], reforming to produce synthesis gas [2], gasification of municipal waste to produce energy, production of clean materials [3]. Powerful AC plasma torches [4, 5] are well suited for industrial applications. High requirements for the reliability of plasma torches determine the need for their improvement. Therefore, it is necessary to have knowledge about the processes occurring in the electric discharge chamber and at the outlet of plasma torch. This determines the relevance of complex research. Experimental data are of interest not only for understanding a particular process under study but are also necessary for validation of computational models.

High-temperature gas flow with high gradients of parameters is formed in the limited space of the electric discharge chamber of a high-voltage plasma torch. At the same time, the processes are non-stationary in nature, assuming periodic changes in parameters. This is due to the time-varying release of energy from AC power source.

Previously, time-averaged temperature distribution profiles were obtained at the outlet of the channel of a high-voltage air plasma torch [6]. This report presents new data on the change in the temperature profile with a change in the phase of the arc discharge current of a high-voltage plasma torch (Fig.1).

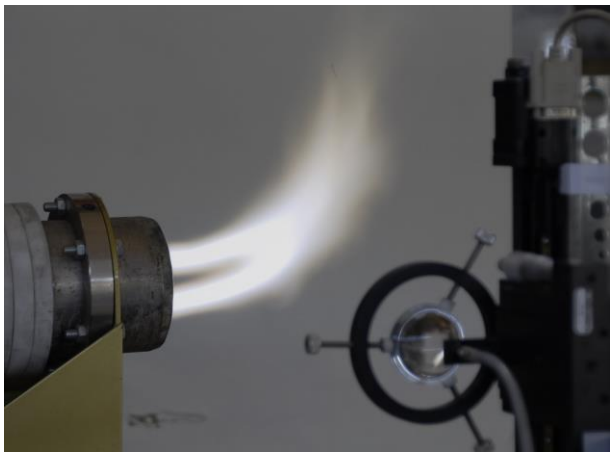

Fig.1. The arc column at the outlet of the channels of the high-voltage plasma torch.

Temperature profiles were obtained by the copper emission spectra. Spatial scanning was provided automatically synchronously with the shooting, the minimum allowable step was 5 microns. The exposure was about 1 ms when synchronized at the set values of the current amplitude. The power of the plasma torch was 6.5 kW at RMS voltage of 1.2 kV with an air flowrate of 1.0 g/s. On the axis of the plasma torch channel, the temperature during the period of current change varies in the range from 5000 to 5500 K.

REFERENCES

[1] N. N. Morgan, “Hydrogen Production from Methane Through Pulsed DC Plasma”, Plasma Chemistry and Plasma Processing, vol. 37, Is. 5, pp. 1375-1392, 2017.

[2] P. G. Rutberg, V. A. Kuznetsov, V. E. Popov, S. D. Popov, A. V. Surov, D. I. Subbotin, A. N. Bratsev,“ Conversion of methane by CO2 + H2O + CH4 plasma,” Applied Energy, vol. 148, pp. 159-168, 2015.

[3] V.E. Kison, A.S. Mustafaev, V.S. Sukhomlinov, “Development of a new plasma technology for producing pure white corundum”, Scientific and Technical Journal of Information Technologies, Mechanics and Optics, 21(3), pp. 380-385, 2021.

[4] L. Fulcheri, F. Fabry, S. Takali, V. Rohani “Three-phase AC arc plasma systems: a review”, Plasma Chem Plasma Proc, 35, 565–85, 2015

[5] A.V. Surov, S.D.Popov, V.E.Popov, D.I.Subbotin, E.O.Serba, V.A.Spodobin, Gh.V.Nakonechny, A.V.Pavlov,“ Multi-gas AC plasma torches for gasification of organic substances,” Fuel, vol. 203, pp. 1007-1014, 2017.

[6] Rutberg FG, Pavlov AV, Popov SD, Sakov AI, Serba EO, Spodobin VA, Surov AV., “Spectral measurements of the gas and electron temperatures in the flame of a single-phase AC plasma generato”r, High Temp., 47(2), pp.175–80, 2009.

R4-P-950401

SIMULATION OF THE EXTRACTION SYSTEM OF A LABORATORY ECR ION SOURCE*

K.E. PRYANISHNIKOV, D.N. SELESNEV, A.B. ZARUBIN, N.N. VINOGRADSKY, S.V. BARABIN, P.A. FEDIN, T.V. KULEVOY

NRC "Kurchatov Institute", Moscow, Russia

At the NRC "Kurchatov Institute" work is underway to study the radiation resistance on heavy ion beams. Simulation experiments on heavy ion beams makes enables a preliminary radiation resistance express analysis for specimens of structural materials for nuclear and thermonuclear reactors during few hours rather than years in the research reactor. A two-beam facility is under development for these irradiation experiments. HIPr is used to accelerate heavy ions Fe^{+2} and forming defects in the material similar to neutron ones. An electrostatic accelerator implants hydrogen and helium ions into material specimens, thereby simulating the products of nuclear reactions.

The ECR ion source [1] is designed for an electrostatic ion accelerator. The scheme of the ECR ion source is shown in Figure 1. The source includes a 2.46 GHz magnetron, a rectangular waveguide 72 * 34 mm passing into a discharge chamber with a length of 580 mm. Accelerating voltage 25 kV.

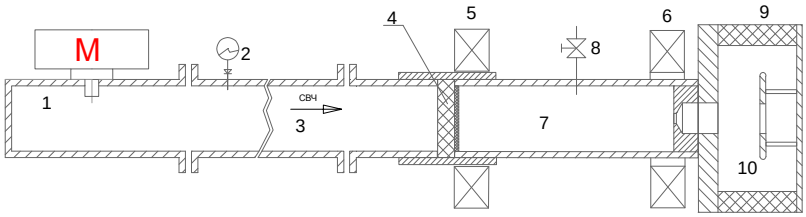

Fig.1. Scheme of a laboratory ECR ion source: 1-section with a magnetron; 2-diode detector; 3-measuring section; 4-high-frequency vacuum window; 5-magnetic coil No.1; 6-magnetic coil No.2; 7-discharge chamber; 8-gas input; 9-high-voltage insulator; 10-vacuum chamber with ion extraction system.

New beam formation system for the ECR ion source is being developed using the Kobra3-INP program to improve the beam parameters [2]. To adjust KOBRA3-INP initial parameters, the beam parameters from the current design of the ECR ion source were measured. The total beam current of the laboratory ECR ion source was measured using a Faraday cup. The emittance was measured by the "pepper-pot" method [3]. The model of existing extraction optics geometry was developed in Kobra3-INP. The parameters of the transverse temperature and longitudinal energy of gas ions were determined during the development of the model. The model will be used to develop the extraction system for the final version of the ECR source.

The report presents the results of developing a model of existing extraction system ECR ion source and preliminary results for a new extraction system.

REFERENCES

[1] D. N. Selesnev, A. B. Zarubin, V. G. Kuzmichev, T. V. Kulevoy "ECR source of light ions" Proceedings of scientific papers VII International Conference Laplas-2021, Moscow, pp. 382-383, 2021.

[2] Spädtke P. Model for the description of ion beam extraction from electron cyclotron resonance ion sources //Review of Scientific Instruments. – 2010. – Т. 81. – №. 2. – С. 02B725.

[3] S. V. Barabin, D. N. Selesnev, A. Y. Lukashin, P. R. Zenkevich, N. N. Vinogradsky "Method for characterizing an ECR ion source using a pepper-pot emittance meter" Proceedings of scientific papers VIII International Conference Laplas-2022, Moscow, p. 317, 2022.

* This work was supported by the Russian Science Foundation, project no. 22-29-01279. The equipment of the KAMIKS Shared Access Center (https://ckp-rf.ru/ckp/502001/) at the National Research Center "Kurchatov Institute" was used.

C2-O-008902

VIBROACOUSTIC MONITORING FEATURES OF RADIATION-BEAM TECHNOLOGIES BY THE CASE STUDY OF LASER, ELECTRICAL DISCHARGE, AND ELECTRON-BEAM MACHINING[1]

M.P. KOZOCHKIN, A.A. OKUNKOVA, S.V. FEDOROV[1,]

[1]*Department of High-Efficiency Processing Technologies, Moscow State University of Technology «STANKIN», Moscow, Russia*

Modern trends in the development of technologies suggest the presence of automatic monitoring systems to control the flow of manufacturing processes and provide information about deviations of the current conditions from the optimal modes, warn about developing defects and emergencies. Simultaneously, there is a multiplicity of approaches to the algorithms for diagnosing and selecting diagnostic parameters.

But there is not enough information about monitoring methods implemented in processes related to radiation-beam technologies (RBT), based on the impact on the product's surface by concentrated heat flows of energy with a high-power density. For example, such technologies include exposure to plasma jets, laser radiation, electron or ion beams. A feature of this technologies is similar processes: the transfer of thermal energy, heating of the volume, the development of melting, evaporation, ionization and vapor expansion during evaporation, cooling after the end of the energy impact. These processes accompanied by phase transformations and chemical reactions that cause changes in the volume of matter and, as a result, by the release of vibroacoustic energy that propagates through the flexible system of technological equipment in the frequency range up to 50 kHz. This range is characterized by a lower attenuation rate when transmitting over long distances. The use of relatively low-frequency ranges is essential for monitoring processes in places where the installation of vibration measuring equipment near the high-intensity treatment zone is impossible.

It experimentally shown that the amplitudes of the vibroacoustic (VA) signal accompanying the RBT processes increase with the increasing power density and process performance. It shown that this relationship is inherent in a wide range of frequencies of the VA signal, but the rate of change of these parameters with a change in the intensity of the thermal effect is different for different frequency ranges. From a comparison of experimental data and data from literature sources, it assumed that the accelerated growth of the high-frequency components of the VA signal with an increase in the intensity of the energy flow is associated with the activation of the processes of volumetric boiling and evaporation the processed material.

The K_f parameter introduced as the ratio of the effective amplitudes of the low-frequency and high-frequency ranges of the VA signal to monitor the results of the impact on the material by high-energy energy flows in the direction of vaporization. It shown that the tendency to decrease the K_f parameter shows an increase in the proportion of the substance evaporated and in the boiling stage during laser treatment.

Experimental studies have allowed us to establish that with an increase in the concentration of erosion products during electric discharge machining (EDM), the intensity of the energy flow generated by the discharge current decreases. Part of the energy spent on the destruction of the particles of the products of erosion. This phenomenon increases the size of the energy impact area and, accordingly, reduces the power density. As a result, the proportion of vaporization and release of the material into the working fluid decreases and reflected in the increase in the K_f parameter. Control of the K_f parameter allows to indicate the short-circuit moment at EDM with a free electrode to increase the productivity and reliability of the technological process. This fact fits into the general scheme of the relationship of the K_f parameter with the intensity of the high-energy impact on materials during RBT.

Monitoring of electron-beam alloying processes can allow evaluating the performance of the operation in real-time by monitoring the parameters of the VA signals, introducing the necessary correction of processing modes, and even optimizing them. Monitoring of the K_f parameter makes it possible to estimate the proportion of the substance in the state of volumetric boiling and evaporation, to select rational treatment modes, not allowing excessive evaporation of the applied coating, but providing the necessary intensity of the impact power to trigger the necessary chemical reactions.

1 These studies were carried out with the financial support of the Ministry of Science and Higher Education of the Russian Federation as part of the assignment in the field of scientific activity (project No. FSFS-2021-0003).

C2-O-022702

ATOMISTIC MODEL OF WET CHEMICAL ETCHING OF SWIFT HEAVY ION TRACKS

S.A. GORBUNOV[1], *R.A. RYMZHANOV*[2,3], *A.E. VOLKOV*[1,2,4]
[1]*P.N. Lebedev Physical Institute of the Russian Academy of Sciences, Leninskij pr., 53,119991 Moscow, Russia*
[2]*Joint Institute for Nuclear Research, Joliot-Curie 6, 141980 Dubna, Moscow Region, Russia;*
[3] *The Institute of Nuclear Physics, Ibragimov St. 1, 050032 Almaty, Kazakhstan;*
[4]*National Research Centre 'Kurchatov Institute', Kurchatov Sq. 1, 123182 Moscow, Russia;*

Combination of the swift heavy ion (SHI) irradiation and wet chemical etching is widely applied technology for manufacturing of nano- microstructures: nanopores, nanowires, polymer filters, nano- and micro-diaphragms [1]. The technique is also used for registration of tracks of heaviest galactic cosmic rays nuclei [2] in meteorites and satellite detectors.

Despite of widespread interest to the etching treatment of SHI tracks, etching models face crucial difficulties with description of temporal evolution of pores, especially in anisotropic crystals. For example, etching of tracks of ions with the same dE/dx, but with different velocities may result in a different etched pore shapes [3], which can not be predicted before irradiation & etching experiments in current state of art.

This motivated us to develop an atomistic model of wet chemical etching. In this scheme Monte-Carlo code TREKIS [4] describing electronic excitation in SHI track is combined with MD simulations of subsequent relaxation of the lattice [5]. Application of these models provide initial conditions for transition state theory based algorithm of sequential removal of atoms from etching surface.

We applied this approach to SHI track etching in crystalline olivine (Mg_2SiO_4). We demonstrate dependence of etched pore shape on various crystallographic orientations. The model describes a transition of a rounded pore resulting from cylindrical symmetry of structural damage in SHI track into the polygonal shape.

REFERENCES

[1] F.F. Komarov, " Nano- and microstructuring of solids by swift heavy ions" Physics-Uspekhi, 60 (2017) 435–471

[2] V. Alexeev, A. Bagulya, V. Alexeev, et al., "Charge spectrum of heavy and superheavy components of galactic cosmic rays: results of the olimpiya experiment" Astrophys. J. 829 (2016) 120

[3] M. Lang, K. Voss, R. Neumann, et al., "Influence of ion velocity on the track morphology in dark mica" GSI Sci. Rep. 3 (2006) 343

[4] N.A. Medvedev, R.A. Rymzhanov, A.E. Volkov, "Time-resolved electron kinetics in swift heavy ion irradiated solids" J. Phys. D. Appl. Phys. 48 (2015) 355303

[5] A.P. Thompson, H.M. Aktulga, R. Berger, et al., " LAMMPS - a flexible simulation tool for particle-based materials modeling at the atomic, meso, and continuum scales" Comput. Phys. Commun. 271 (2022) 108171

C2-O-025801

INVESTIGATION OF MATERIALS LIGHT EROSION BY SHORT-WAVE RADIATION*

A.V. PAVLOV, YU.YU. PROTASOV, V.D. TELEKH, T.S. SHCHEPANUK

Bauman Moscow State Technical University, Educational and Scientific Center of Photon Energy
2nd Bauman str., 5, Moscow, 105005

This study suggests the plasmodynamic structures parameters diagnostic and quantitative description technique. These structures arise due to the exposure on various samples (metals and polymers) by the broadband (from visible to VUV range) high-power (with a radiation flux up to of $\approx 10^6$ W·cm^{-2}) radiation from the high-current plasma accelerator – magnetic plasma compressor (MPC) of erosion type. Peculiarity of the method is that information about the processes was obtained as a result of limited series of experiments (practically, a single one). As a result, it is possible to determine both the parameters of the generated gas flows (pressure, density in the shock-compressed layer, etc.) and the thermodynamic parameters inside the plasma (pressure, temperature, and concentrations).

The processes occurring on the surface and in the near-surface vapor-plasma layer when exposed to VUV radiation on different materials understanding is relevant for the creation and optimization of different plasma energy devices (ablative pulsed plasma accelerators, plasmodynamic sources of ultraviolet and soft X-rays, radiation surface strengthening, photochemical installations, etc.) where information is needed on the distribution of heat fields and energy flows arising from the operation of such devices. This explains the interest in these studies.

High-current plasma discharge – the plasma dynamic discharge of magnetic plasma compressor (MPC) of erosion type was used as radiation source. In MPC plasmodynamic heating of electric discharge plasma is carried out as a result of shock-wave thermalization of directed kinetic energy of high-speed flow of dense radiating plasma at its braking in gas medium. The buffer gas simultaneously acts as a filter for the harsh component of the radiating plasma emission spectrum [1, 2]. As a consequence, since the rise times of the light pulses are determined only by the time profile of the hydrodynamic energy flow of the plasma jet in the braking zone, it is possible to significantly differ from the characteristic discharge times in the electrical circuit, which allows to form powerful pulses of VUV radiation with steep leading edge.

Samples in the form of bars with dimensions of 30 mm by 50 mm and thickness of 10 mm were installed with a long side along the discharge at near discharge zone. Thus, the near-to-discharge end of the target received 2-2.5 times more energy than the far one. This made it possible to register significantly different dynamics of vapor-plasma flow disperse when moving from one edge of the target to the other [3].

For visualization of shock waves (SW) and other expansion zones of vapor-plasma flow in external gas with large concentration gradients, two-exposure laser holographic interferometry with visualization of large optical fields and the Toepler method in the light field mode were used [4].

The processing of interferograms, together with the analysis of other data of the experiment, allows to find the distribution of parameters in the plasma layer above the target surface. It has been found that the maximum energy absorption is inside the plasma layer. Spatial distribution of the parameters (temperature, pressure and concentrations of electrons and ions) is defined with the assumption of local thermodynamic equilibrium. The obtained results are discussed.

REFERENCES

[1] "Radiative Plasmodynamics" vol. 1, ed Yu S Protasov. Moscow: Energoatomizdat, 1991

[2] A.V. Pavlov, Y.Y. Protasov, V.D. Telekh, T.S. Shchepanuk "Experimental research of dynamics and macrostructure of light erosion radiative plasmodynamic discharges," J. Phys.: Conference Series, vol. 830, № 1, Article Number 012062, 2017

[3] A.V. Pavlov, Y.Y. Protasov, V.D. Telekh, T.S. Shchepanuk "Investigation of the dynamics of expansion of the near-surface light erosion plasma formed during the evaporation of a material by broadband high-brightness radiation," J. Phys.: Conf. Ser., vol. 1393 № 1, Article Number 012019, 2019

[4] A.V. Pavlov, Y.Y. Protasov, V.D. Telekh, T.S. Shchepanuk "Laser holographic interferometry of short ultraviolet radiation with high power density interaction with condensed matters," Scientific Visualization, vol. 11, № 3, P. 111-125, 2019

* The reported study was funded following the government task 0705-2020-0046 by the Russian Ministry of Education and Science and has been performed at large-scale research facilities "Beam-M" of Bauman Moscow State Technical University.

C2-O-034301

FEATURES OF THE ACTION OF A HIGH-POWER ION BEAM ON POLYETHYLENE TEREPHTHALATE

V.S. KOVIVCHAK

Dostoevsky Omsk State University, Omsk, Russia
Omsk Scientific Center SB RAS, Omsk, Russia

The modification of the surface properties of polymers, transformation of their surface layers into nanostructured carbon under the action of a high-power ion beam (HPIB) of nanosecond duration are of great interest, both from a scientific and practical point of view. The high temperatures resulting from such exposure lead to melting, intensive evaporation and decomposition of polymer materials. For most polymers, under such influence, intense pore formation is observed in the surface layer.

The features of the action of HPIB on a widely used polymer - polyethylene terephthalate (PET) have been investigated. The samples were irradiated at the Temp accelerator with a proton-carbon beam (30% H^+ +70% C^+, E ~ 200 keV, j ≤ 150 A/cm^2, τ=60 ns) with varying ion current density and the number of irradiation pulses.

It has been established that HPIB irradiation leads to the formation of various surface formations on the PET surface having an internal periodic structure with a characteristic size of ~ 20 μm. At the same time, the formation of surface pores (primarily closed or semi-open) is minimal compared to other previously irradiated polymer materials. Multiple (>10 pulses) HPIB irradiation leads to the formation on the PET surface of a complex system of periodic protrusions of a solidified polymer melt with a period of ~ 150 μm. The height of the protrusions is up to 80 μm and the average diameter is ~ 35 μm.

Possible mechanisms of the formation of PET morphology under the action of HPIB are considered taking into account the peculiarities of the thermo-physical characteristics of PET.

C2-O-047203

MODELING OF REACTIVE SPUTTERING AND EVAPORATION IN A HOT-TARGET MAGNETRON DISCHARGE*

S.M. SOROKIN[1], D.V. KOLODKO[1,2], A.V. KAZIEV[1], V.YU. LISENKOV[1], A.V. TUMARKIN[1]

[1]National Research Nuclear University MEPhI (Moscow Engineering Physics Institute), Moscow, Russia
[2] Fryazino Branch of Kotelnikov Institute of Radio Engineering and Electronics, RAS, Fryazino, Russia

The processes of obtaining oxide and nitride coatings in magnetron sputtering systems are associated with known effects of a complex nonlinear and often unstable behavior of the deposition rate and film stoichiometry depending on the reactive gas flow. Controllability and productivity of such processes can be largely improved through modification of existing technologies and the development of new approaches. In particular, one can find evidences of a positive effect that a high temperature of a magnetron target has on the stability of the characteristics of the reactive sputtering process [1]. On the other hand, a number of scientific groups have been actively studying reactive deposition of oxides and nitrides in the high-power pulsed magnetron discharges (see e. g. [2] and references therein), and have found favorable effects of high-power pulses on the controllability of the process.

In the present work, we theoretically consider the joint influence of hot-target effects and the pulsed nature of the discharge on the state of the target surface. We enhance the previously modified time-dependent Berg model [3] by taking into account the evaporation of target material as well as the influence of target temperature on the rate of chemical reactions on its surface. The system of equations describes the state of the target in terms of poisoned area fractions θ_1 and θ_2, where index 1 corresponds to the monoatomic surface layer, and index 2 — to the layer beneath the surface (sub-surface layer). The processes of chemisorption on target surface, sputtering of reactive gas atoms from target, implantation of reactive gas ions to the sub-surface layer, material evaporation, and transfer between the layers are considered. A separate equation connects the atomic fluxes of reactive gas associated with target and substrate surfaces with the volumetric characteristics, such as gas injection rate and pumping speed. The equations are solved numerically for the conditions relevant to the experimental hot-target magnetron setup. The results are then discussed in connection with the experimental observations of magnetron discharge with hot Cu, Cr, and Si targets in O_2/Ar and N_2/Ar environments.

REFERENCES

[1] V.V. Karzin, A.E. Komlev, K.I. Karapets, N.K. Lebedev, “Simulation of heating of the target during high-power impulse magnetron sputtering,” Surf. Coat. Technol., Vol. 334, P. 269–273, 2018.

[2] K. Strijckmans, F. Moens, D. Depla, “Perspective: Is there a hysteresis during reactive High Power Impulse Magnetron Sputtering (R-HiPIMS)?” J. Appl. Phys., Vol. 121, Article Number 080901, 2017.

[3] A.V. Kaziev, D.V. Kolodko, N.S. Sergeev, “Properties of millisecond-scale modulated pulsed power magnetron discharge applied for reactive sputtering of zirconia,” Plasma Sources Sci. Technol., Vol. 30, Article Number 055002, 2021.

[4] A.A. Barybin and V.I. Shapovalov, “Nonisothermal chemical model of reactive sputtering,” J. Appl. Phys., Vol. 101, Article Number 054905, 2007.

* The work was supported by the Russian Science Foundation under grant No. 18-79-10242.

C2-P-002601

NON-METALLIC ULTRA-DISPERSED POWDER OBTAINED IN THERMAL PLASMA*

V.V. SHEKHOVTSOV

Tomsk State University of Architecture and Building, TSUAB, Tomsk, Russia

The synthesis and study of nanosized refractory oxide powders today is an urgent problem in predicting the characteristics of materials obtained on their basis. To date, the most capacious market for the production of nanosized powder is the production of silicon dioxide SiO_2. This nanosized powder has found its application in the production of structural materials [1] and coatings [2]. A wide material base for the production of nano-sized SiO_2 can be natural raw materials enriched with silicon dioxide over 75 wt. %, for example quartz sands and concentrates based on it.

To obtain oxide nanopowder SiO_2, quartz sand (QS) was used - Tugan deposit, Tomsk, Russia. Silicon dioxide content ~ 97 wt. %. The synthesis of nanopowder was carried out in a plasma-chemical reactor [3, 4], including: an electric-arc plasmatron (cathode) with an outlet nozzle section of 8 mm; water-cooled cylindrical chamber (h = 150 mm, r = 75 mm), at the base of which a graphite anode is installed; system for supplying a plasma-forming gas (compressed air) and cooling liquid to heat-stressed elements; power supply with adjustable amperage from 5 to 160 A. The operating parameters during the experiments corresponded to: current strength 150 A, voltage 110 V, plasma-forming gas flow rate 20 l/min, thermal efficiency 78%. The calculated mass-average temperature of the generated plasma reaches 5400 K.

According to TEM data (electron microscope Philips CM 30), it was found that the obtained SiO_2 nanopowder in the initial state mainly consists of spherical particles of polydisperse composition (Fig. 2).

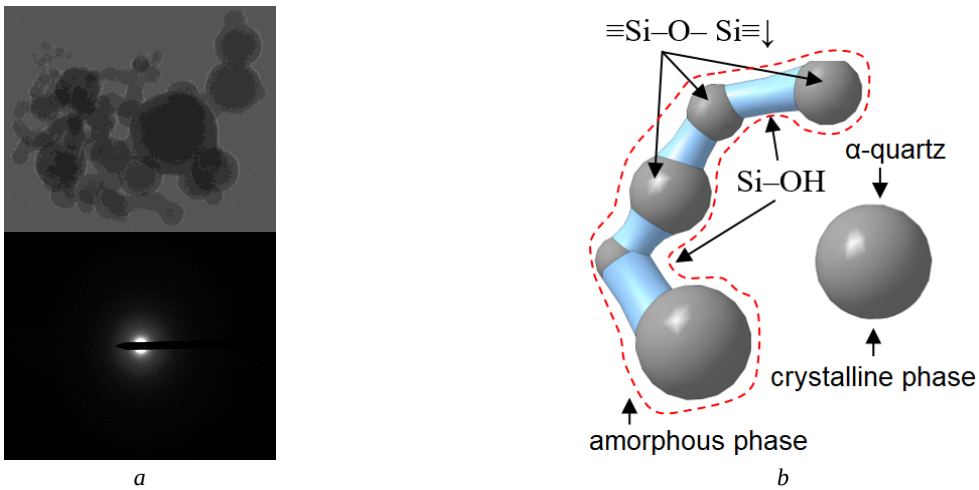

a *b*

Fig.1. Morphology of ultrafine SiO2 particles: a - TEM images; b – physical model

The particle diameter is in the range from 10 to 150 nm, while there are single particles with a diameter of 500 nm. Of the morphological features, we note the presence of rounded-oval, ellipsoidal and welded particles, while there are no pronounced contact zones (see Fig. 2). These features are typical for particles less than 80 nm. Particles ~ 500 nm in diameter are crystallized and correspond to high-temperature α-quartz.

REFERENCES

[1] J. Yang, W. She, W. Zuo, K. lyu, Q. Zhang, “Rational application of nano-SiO_2 in cement paste incorporated with silane: Counterbalancing and synergistic effects,” Cement and Concrete Composites, vol. 118, pp. 3169 – 3181, 2021.

[2] Q. Ma, N. Izu, Y. Masuda, “High orderly nano-silica assembly and its application in synthesizing TiO_2/SiO_2 bilayer films,” Surface and Coatings Technology, vol. 345, pp. 22–30, 2018.

[3] V.V. Shekhovtsov, N.K. Skripnikova, O.G. Volokitin, “Phase transitions in SiO_2 nanopowder synthesized by electric arc plasma,” IEEE Transactions on Plasma Science, vol. 49, no. 9, pp. 2618 – 2623, 2021.

[4] V.V. Shekhovtsov, O.G. Volokitin, “Перспективы использования низкотемпературной плазмы в строительстве и архитектуре,” Физ. и хим. стекла, Т. 44/3, pp. 324 – 327, 2018.

* The work was supported by grant from the President of the Russian Federation No. MK-66.2022.4.

C2-P-018602

SIMULATION OF TEMPERATURE FIELDS IN TARGETS AT COMBINATION OF REPETITIVELY-PULSED HIGH-INTENSITY ION IMPLANTATION AND ENERGY IMPACT ON A SURFACE*

A.I. IVANOVA, D.O. SIVIN, G.A. BLEYKHER, O.S. KORNEVA

National Research Tomsk Polytechnic University, Lenin Avenue 30, Tomsk, 634050, Russia

Methods to modify surface and near-surface layers of materials and coatings by ion beams are used in many fields of science and technology.

The method of high-intensity implantation by high-power density ion beams with submillisecond duration involves significant pulsed heating of the irradiated target's near-surface layer, followed by its rapid cooling due to heat transfer into the material due to thermal conductivity and the implementation of repetitively-pulsed radiation-enhanced diffusion of atoms to depths exceeding the projective ion range. Using the numerical simulation, this work studies the dynamics of changes in temperature fields in targets under single-pulse and repetitively-pulsed exposure to submillisecond titanium and aluminum ion beams with a pulsed power density up to 50 kW/cm^2. When simulating, two target materials (aluminum and titanium) are used, differing significantly in their characteristics. The conditions are determined under which the temperature in the ion-doped layer will correspond to the conditions of radiation-stimulated diffusion of the implanted element, and the temperature in the matrix material will not deteriorate its microstructure and properties.

* The work was supported by the Russian Science Foundation (grant No. 22-19-00051)

C2-P-025702

VARIATION OF THE ION CHARGE STATE IN THE PLASMA FLOW DURING THE REPEATING MICROSECOND VACUUM ARC DISCHARGE WITH THE W-FUZZ CATHODE*

YU. A. ZEMSKOV, YU.I. MAMONTOV, I.V. UIMANOV

Institute of Electrophysics UB RAS, Yekaterinburg, Russia

The "W fuzz" nanostructure, which is a harmful effect in the operation of thermonuclear installations, has been widely studied over the past decade. One of the aspects of the study is the electrophysical properties of this nanostructure, in particular, the fundamental properties of its behavior in vacuum discharges. Thus, it was shown [1] that the average charge of tungsten ions in the plasma of a vacuum arc on a “fuzz”-nanostructured cathode surface differs significantly from the average charge of tungsten ions in the absence of nanostructured formations. The average charge in the case of the presence of "fuzz" layer was noticeably lower than without it. In addition, it was shown that the average charge of tungsten ions increases as the sample surface is eroded by repeated discharges. In this work, an attempt was made to confirm and clarify the data of [1]. For this aim, a short arc discharges up to 10 μs were chosen with purpose to provide greater detail in measurements of the evolution of the charge composition of the arc plasma as the nanostructured layer was destroyed. The Thomson spectrometer with automatic signal recording and digital data analysis was used as an analytical instrument. The arc on the "W-fuzz" sample was initiated more than 350 times. The results demonstrate an increase in the average charge of tungsten ions with the erosion of the sample surface. However, in this experiment, contrary to the results of [1] it was not possible to achieve the ion flow parameters equal to parameters for tungsten samples without fuzz-nanostructure. In addition, the detailing of erosion using short arcs made it possible to record a very noticeable spread in plasma parameters from discharge to discharge (± 0.5 units for the value of the average charge of tungsten ions). These features can be explained by the incomplete destruction of the nanostructured layer in the region accessible to arc plasma. This effect is apparently possible in case of the short arcing on the large sample.

REFERENCES

[1] S.A. Barengolts et al, “Dynamics of the changes in the parameters of the arc plasma during the destruction of a heliuminduced tungsten fuzz by arc pulses”, 2020, Nucl. Fusion **60** 044001.

* The work was supported by the Russian Science Foundation (grant No. 20-19-00323).

C2-P-028502

EXPERIMENTAL RESEARCH AND COMPARATIVE ANALYSIS OF PERSPECTIVE MPPT PROPELLANTS EVAPORATION BY UV-VUV RADIATION*

E.O. CHEBYKIN[1], D.K.FEDOROVA[1], A.V. PAVLOV[1], YU.YU. PROTASOV[1], T.S. SHCHEPANUK[1], V.D. TELEKH[1]

[1] Bauman Moscow State Technical University, Moscow, Russia

A serious increase in the number of CubeSat satellites launches is noticed over the last five years [1]. This type of spacecrafts are simple to manufacture and cheap to launch. This advantages provide solutions to various problems. Many publications on micro propulsion systems proves that this topic became highly relevant. Electric propulsion (EP) is suitable for CubeSat. Ablative pulsed plasma thruster (APPT) is highlighted because for its low manufacturing price and simple design [2].

APPT are performed with polymer propellant. The pulsed discharge vaporizes part of the polymer. Radiation energy (UV and visible range) from the plasma formation heats and vaporizes the propellant. Ionized and accelerated by Lorentz force vapor of propellant creates thrust.

Investigation of the broadband high-brightness radiation interaction on the polymers is necessary to optimize the characteristics and the processes in operation of the microAPPT. There is no complete and acknowledged model of the ablation process despite the fact that polymers light erosion research has been going on for more than fifty years [3]. In this regard, the experimental study of polymers evaporation under the action of broadband radiation becomes even more topical.

We performed experiments of light erosion (including the vacuum UV range) of different polymers, that can be used as propellants of APPT. This work presents determination of plasma parameters of microAPPT's promising propellants: PTFE, polyamide-6, acrylic glass, etc.

The source of radiation was an erosive type discharge of the magnetoplasma compressor (MPC), which is similar to the APPT discharge [4]. Usage of different gases with MPC discharge makes it possible to control the spectral composition of the radiation. So does the distance from the sample to the emitter for the radiation energy coming to the sample. The discharge radiation heats, evaporates and ionizes the sample vapor. It expands and realizes the "plasma piston" model, compressing the layer of background gas above the sample surface.

Diagnostics of evaporation processes was performed by schlieren photography and the method of double-exposure laser holographic interferometry [5]. Interferograms and schlieren photographs processing made it possible to determine the studied materials dynamics of evaporation and ionization. It is a necessary step for choosing the optimal propellant for microAPPT.

The obtained results are discussed.

REFERENCES

[1] O'Reilly, D.; Herdrich, G.; Kavanagh, D.F. Electric Methods for Small Satellites: A Review. Aerospace 2021, 8, 22. https://doi.org/10.3390/aerospace8010022

[2] Popov G.A. and Antropov N.N. Ablative PPT. New quality, new perspectives. 2006. Acta Astronautica. 59 175 https://doi.org/10.1016/j.actaastro.2006.02.009

[3] Lippert, T. (2005), Interaction of Photons with Polymers: From Surface Modification to Ablation. Plasma Processes Polym. 2: 525-546. https://doi.org/10.1002/ppap.200500036

[4] Protasov Yu.S, Protasov Y.Y, Telekh V.D, Shchepanyuk T.S. Plasmadynamic light sources of high spectral brightness and shock waves generators. 2014. Enciclopedia of Low Temperature Plasma. Vol IX-4. Plasma aerodynamics. Moscow: Yanus-K. P. 383-436 [in Russian]

[5] A.V. Pavlov, Yu.Yu. Protasov, V.D. Telekh, T.S. Shchepanuk. Laser holographic interferometry of short ultraviolet radiation with high power density interaction with condensed metters (2019). Scientific Visualization 11.3: 111 - 125, DOI: 10.26583/sv.11.3.10

* The presented results have been obtained at large-scale research facilities "Beam-M" of Bauman Moscow State Technical University. The reported study was funded by RFBR and ROSATOM (No.20-21-00087)

C2-P-030201

ULTRAFAST NONTHERMAL PHASE TRANSITIONS IN COMPOUND INSULATORS BY EXTREME ELECTRONIC EXCITATIONS

R.A. VORONKOV [1], N. MEDVEDEV[2,3], A.E. VOLKOV[1]

[1]P. N. Lebedev Physical Institute RAS, Moscow, Russia
[2]Institute of Physics, Czech Academy of Sciences, Czech Republic
[3]Institute of Plasma Physics, Czech Academy of Sciences, Czech Republic
roman.a.voronkov@gmail.com

Irradiation of solids with swift heavy ions (SHI) or free-electron laser beams (FEL) highly excites the electronic system of a target. Subsequent energy transfer to the target lattice may lead to structural changes in the irradiated solid. However, electron density modifications induce changes in the interatomic potential even at subpicosecond timescales, before the cooling of the electronic system. With a sufficient level of excitation, various kinds of responses can occur in the crystal structure of the material, including the so-called nonthermal melting of its lattice (ultrafast disordering without a significant increase of the ionic temperature [1]) as well as changes in the band structure.

We apply the density functional theory-based molecular dynamics (DFT-MD) to study an effect of the modified interatomic potential caused by extreme excitation of the electronic system (T_e ~ 1-10 eV) on nonthermal instability in various insulators and semiconductors. We demonstrate a creation of a superionic state in Al_2O_3 – an exotic state with a coexistence of nonthermaly melted oxygen sublattice and a crystalline aluminum one [2].

In Y_2O_3 and NaCl nonthermal amorphization occurs, whereas in TiO_2 a transition into a new crystalline phase is predicted.

We also show that instability of the band gap depends on a level of the bond ionicity of a material [3]. In covalent and mixed-bonded materials, the band gap significantly shrinks or even collapses within characteristic times of the electronic system cooling after an SHI irradiation. Although nonthermal melting is highly improbable to occur in a single SHI track [4], even slight atomic displacements contribute to overall lattice damage and cause significant electronic structure changes (e.g., the band gap shrinkage) affecting electron-lattice coupling in SHI track. Considering that described effects are even more important at high intensity beams expected at GSI-FAIR facilities, we conclude that nonthermal changes should be taken into account in theoretical models of SHI tracks formation.

REFERENCES

[1] N. Medvedev, V. Tkachenko, V. Lipp, Z. Li, and B. Ziaja, 4open 1, 3 (2018).

[2] R. A. Voronkov, N. Medvedev, and A. E. Volkov, Phys. Status Solidi - Rapid Res. Lett. 14, 1900641 (2020).

[3] R. A. Voronkov, N. Medvedev, and A. E. Volkov, Sci. Reports 2020 101 10, 1 (2020).

[4] R. A. Voronkov, N. Medvedev, R. A. Rymzhanov, and A. E. Volkov, Nucl. Instruments Methods Phys. Res. Sect. B Beam Interact. with Mater. Atoms 435, 87 (2018).

C2-P-936201

THE INFLUENCE OF PULSED ELECTRON BEAM IRRADIATION ON THE STATE OF ZRN COATING/SILUMIN SUBSTRATE SYSTEMS*

P.V. MOSKVIN[1], *N.N. KOVAL*[1], *T.V. KOVAL*[2], *O.V. KRYSINA*[1], *YU.F. IVANOV*[1], *A.D. TERESOV*[1], *MY KIM AN TRAN*[3], *N.A. PROKOPENKO*[1], *E.A. PETRIKOVA*[1]

[1]*Institute of High Current Electronics SB RAS, Tomsk, Russia*
[2]*Tomsk Polytechnic University, Tomsk, Russia*
[3]*Ton Duc Thang University, Ho Chi Minh City, Vietnam*

A eutectic silumin was subjected to a combined treatment, including the deposition of a ZrN coating on a silumin substrate and the treatment of the coating/substrate system with a pulsed electron beam of submillisecond duration. Examination of thin transverse sections of the ZrN-coated silumin performed after electron beam treatment revealed an extended melt zone, the thickness of which was 30–55 μm for all samples. In the melt zone of the samples with coatings of thickness 0.5–2 μm irradiated with five electron beam pulses, a partial immersion of the coating into the bulk substrate to a depth of 45 μm was observed. Local measurements of the temperature in the electron beam treatment zone, numerical modeling of the fast heating (within 150 μs) and solidification of the melt under the action of an intense heat source were carried out for the action of experimental electron beam pulses (1.8×10^9 W/cm^2) on the bare and the ZrN-coated silumin. It was found that when the coating thickness was increased from 0.5 to 2 μm, the rise rate of the surface temperature increased from 6×10^7 to 9×10^7 K/s and the maximum temperature during the pulse rise increased from 760 to 1070°C (fig. 1). The melt depth was no more than 57 μm. The speed of the melt front during the pulse was 3×10^5 μm/s. The numerical simulation has shown that the eutectic temperature was not achieved at depths over 55 μm. Comparing numerical calculations and measurements of the surface temperature of materials subjected to electron beam treatment, it is possible to elucidate the dynamics of the temperature field and melt depth in order to attain predetermined properties of materials upon electron beam treatment. It should be emphasized that the pulsed electron beam with unique parameters we used made it possible not only to trace in detail the dynamics of changes in the temperature of the molten surface layer of a ZrN-coated silumin sample, but also to produce a rather extended (tens of micrometers) modified structure. According to preliminary estimates, such a modified structure of the surface layer of a product made of silumin should significantly improve its operational properties. The results obtained are important for the development of technology for pulsed electron beam modification of the structure and surface properties of silumin products used in modern industry.

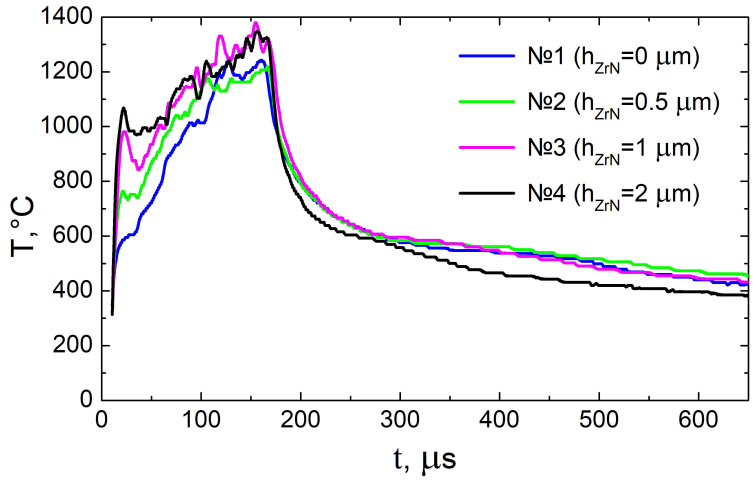

Fig.1. Time variations of the local surface temperature during electron beam treatment for the bare and ZrN-coated silumin sample (experiment).

* This research was funded by the Ministry of Science and Higher Education of the Russian Federation (FWRM-2021-0006); by the Russian Foundation for Basic Research and ROSATOM according to the research project № 20-21-00111.

C2-P-956001

STUDY OF THE INFLUENCE OF PLASTIC DEFORMATION OF THE HSS M2 SURFACE ON ION-PLASMA NITRIDING IN THE GLOW DISCHARGE*

R.K. VAFIN, A.V. ASYLBAEV[1], D.V. MAMONTOV[1], I.D. SKLIZKOV[1]

Ufa State Aviation Technical University, Ufa, Russian Federation
[1] alexander.aslb@gmail.com

This paper examines the influence of plastic deformation of the HSS M2 surface on the characteristics of the hardened layer after ion-plasma nitriding in the glow discharge.

It is known that diffusion of atoms in metals is greatly influenced by various structural defects - deviations of the lattice structure from the ideal one [1]. As the structural defects increase, the diffusion rate in the metal increases. However, along with structural defects, diffusion is also affected by the size of the metal grain: the finer the grain, the higher the diffusion rate [2, 3]. Therefore, to increase the diffusion rate in metals, methods of plastic deformation have recently become increasingly widespread. One of these methods is the method of intense plastic deformation by torsion, which consists in deformation of metal by two simultaneously acting forces: compression and torsion (Fig. 1a).

In the study it was found that the plastic deformation of the steel surface increases the rate of nitrogen diffusion deep into the material, due to an increase in dislocation density and the formation of microdefects, due to a highly refined grain-like ultrafine grain structure. It was also found that the plastic deformation of the steel surface before ion-plasma nitriding leads to a 2-fold increase in the thickness of the hardened layer HSS M2, due to an increase in surface free energy, which contributes to increased adsorption of the saturation element and the formation of nitrides in the near-surface layer of nitrided material.

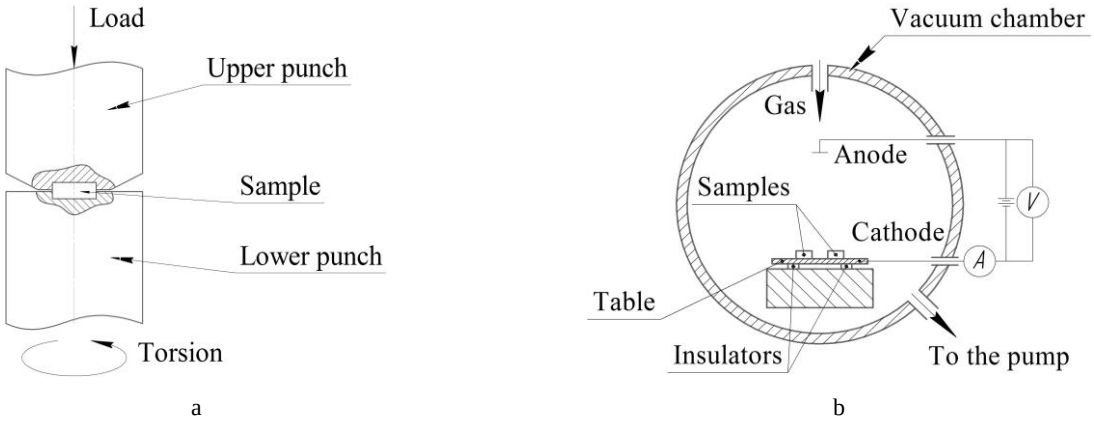

Fig.1. Process schemes: a - severe plastic deformation by torsion, b - ion-plasma nitriding in a glow discharge.

REFERENCES

[1] Bokshtejn B. S., Diffusion in metals, Moscow: Metallurgy, 1978.

[2] Valiev R. Z., Zhilyaev A. P. and Langdon T. G., Bulk nanostructured materials. Fundamental and Applications, Hoboken: Wiley/TMS, 2014.

[3] Valiev R. Z. and Aleksandrov I. V., Nanostrukturnye materialy, poluchennye intensivnoj plasticheskoj deformaciej, España: Universidad Complutense de Madrid, 2000.

* The work was supported by a grant in the form of subsidies in science from the budget of the Republic of Bashkortostan for state support of young scientists - postgraduate students and candidates of science (theme: AT-TM-04-21-GB).

C3-O-005301

COMPLEX MODIFICATION OF STAINLESS HIGH-ALLOY STEEL - STRUCTURE AND PROPERTIES *

YU.F. IVANOV, E.A. PETRIKOVA, A.D. TERESOV, O.S. TOLKACHOV, I.V. LOPATIN

Institute of High Current Electronics SB RAS, Tomsk, Russia

Modification of the steel 310 (Fe-0.2C-23Cr-18Ni) surface layer was carried out by the pulsed electron-beam treatment ("SOLO" setup) methods [1, 2]. It is shown that with an increase in the energy density of the electron beam, an increase in microhardness (from 1.7 GPa in the initial state to 2.4 GPa after irradiation at 30 J/cm^2) and wear parameter (from 1.9*10^{-4} mm^3/N*m at 10 J/cm^2 up to 5.2*10^{-4} mm^3/N*m at 30 J/cm^2) of the specimen's surface layer. The steel wear parameter before irradiation is 4.9*10^{-4} mm^3/N*m.

Nitriding was carried out ("QUINTA" setup) of steel 310 specimens previously irradiated with a pulsed electron beam in a low-pressure gas discharge plasma by two methods: by heating the samples with plasma ions (hereinafter, method 1) [3] and by heating the samples with plasma electrons (hereinafter, method 2) [4].

It is shown that during nitriding according to method 1, the maximum microhardness, 19 GPa (exceeds the hardness of steel before modification by 11.2 times and the hardness of steel after irradiation with an electron beam by 8 times), and the minimum wear parameter, k = 0.7 * 10^{-6} mm^3/N*m (more than 700 times less than the steel wear parameter before modification and more than 750 times less than the steel wear parameter after electron beam irradiation) are observed on specimens irradiated at an electron beam energy density of 30 J/cm^2, 200 μs , 3 imp. and subsequent nitriding at a temperature of 520^{0}C for 3 hours.

The thickness of the hardened layer is 40 μm. It has been established that the specimens that demonstrated the highest values of hardness and wear resistance have the maximum (90.6%) content of nitride phases (chromium and iron nitrides) in the surface layer.

The elion method of nitriding (method 2) leads to close (nitriding at 450^{0}C, 3 hours) or lower (nitriding at 520^{0}C, 3 hours and 600^{0}C, 5 hours) values of the steel surface layer microhardness, in relation to nitriding by the method one. During tribological tests, it was found that after nitriding at a temperature of 450^{0}C, 3 hours and 600^{0}C, 5 hours, the wear resistance of steel specimens modified according to method 1 is higher than the wear resistance of steel after nitriding according to method 2. Nitriding at a temperature of 520^{0}C, 3 hours leads to better results when using method 2, namely, the wear resistance of steel samples modified according to method 1 is lower than the wear resistance of steel after nitriding according to method 2 by 2.9 (E_S = 10 J/cm^2) and 1.2 times (E_S = 30 J/cm^2). It has been established that nitriding (method 2) at 450^{0}C and 520^{0}C temperatures for 3 hours of specimens previously irradiated with an electron beam (10 J/cm2, 200 μs, 3 pulses) is accompanied by the formation of a ceramic layer containing only iron and chromium nitrides. For the first time, during electron-ion-plasma nitriding (method 2), the phenomenon of blistering was discovered - the formation of bubbles on the surface of the material. It has been established, in the study of specimen's fracture surface previously irradiated with an electron beam and subjected to nitriding by two methods, that the destruction of steel surface layer nitriding according to method 1 proceeds mainly through a viscous mechanism; the destruction of the steel surface layer nitriding according to method 2 proceeds mainly by the quasi-brittle mechanism.

REFERENCES

[1] S.V. Grigoriev, N.N. Koval, V.N. Devjatkov, A.D. Teresov, «The automated installation for surface modification of metal and ceramic-metal materials and products by intensive pulse sub-millisecond electron beam», Proc. 9th Intern. Conf. on Modification of Materials with Particle Beams and Plasma Flows. – Tomsk, 2008.

[2] V. Rotshtein, Yu. Ivanov, A. Markov, «Surface treatment of materials with lowenergy, high-current electron beams», Materials surface processing by directed energy techniques / ed. by Y. Pauleau. – Elsevier, Ch. 6, 2006.

[3] I.V. Lopatin, Yu.H. Akhmadeev, N.N. Koval, E.A. Petrikova, «AISI 5140 steel nitriding in a plasma of a non-self-sustaining arc discharge with a thermionic cathode under the pulse action of ions», IOP Conf. Series: Journal of Physics: Conf. Series, 1115, 032042, 2018.

[4] Yu. Ivanov, I. Lopatin, Yu. Denisova, E. Petrikova, O. Tolkachev, «Elion method of nitriding of high-chromium stainless steel: Structure and properties», Proceedings - 2020 7th International Congress on Energy Fluxes and Radiation Effects, EFRE, 2020.

* *The research was funded by RFBR and Tomsk region, project number 19-48-700010».*

C3-O-007201

NICKEL-BASED SUPERALLOY, RELATION BETWEEN NON-LINEAR ULTRASOUND AND MICROSTRACTURE CHANGES DUE TO CREEP DAMAGES

Yutaka ISHII[1], Kuniaki ISHIHARA[1], Toshihiro OHTANI[1], Takayuki SAKAKIBARA [2], Masayuki KAMAYA[3], Yuutarou OHTA[4], and Keiji KUBUSIRO[4]

[1] *Shonan institute of technology, Fujisawa, Japan*
[2] *Chuo Spring Co., LTD, Miyosi, Japan*
[3] *INSS, Mikatagun, Japan*
[4] *IHI Coporation, Yokohama, Japan*

Nickel-based superalloy, Inconel® 718, has high temperature strength effected by γ″(Ni_3Nb) phase at approximately 973 [K]. Inconel 718 was determined that the γ″ phase disappearance lead to the creep destruction. In the study, we applied the nonlinear ultrasonic method for evaluation the creep damages and the microstructural degradation in γ″ phase for Inconel 718 test pieces at the evaluated temperature 973 [k]. The nonlinear ultrasonic shows the possibility to becoming the primary means of characterizing creep in the metals [1, 2], because it is to probe the change of dislocation structure during the creep. Its sensitivity to microstructural evolutions during the creep is often higher than that of linear properties. We analyzed the relation between the microstructural change and the propagation of nonlinear acoustic characterizations three-wave interacting [3], with the electromagnetic acoustic resonance (EMAR) [4] throughout the creep life, and nonlinearly relations change in dislocation density. This was supported with X-ray diffraction, EBSD [5] and SEM images.

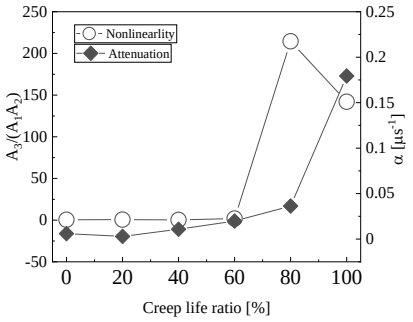

Fig.1. Propagation of attenuation coefficient α, and, the nonlinearity with three-wave interaction at the creep life. (1,253[k], 200[MPa])

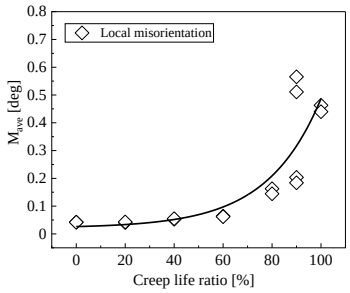

Fig.2. Miss-orientation average analysis by EBSD

Fig.1 shows the propagation of the nonlinearity in three-wave-interaction, ultrasonic attenuation, α; nonlinearlity rise dramaticaly and rapidly from 60[%] of the creep life ratio. After the peak, the nonlinearlity decrease near the rupture. Propagations of α shows the gradually increase of the 60 [%] of creep life. α increases sharply until the rupture. Fig.2 shows EBSD measurement of local miss-orientation average (M_L).M_L show the increases rapidly from 60[%] of the creep life.

This phenomenon shows nonlinearity, and α, M_L as creep progress related to the microstructure changes, especially, to the dislocation mobility during the creep life.

SEM images shows δ phase appearance at 60[%] of the creep life. This phenomenon is Coarsening of γ″ phase during the creep damages.

Assessment of the advanced creep damage and microstructural changes of the metals may potentially facilitate by the nonlinear acoustics measurement with EMAR. In future, we may have any prospect due to Energy Reflection.

REFERENCES

[1] K.Y. Jhang, “Nonlinear ultrasonic technique for nondestructive assessment of micro damage in material : a review”, Int. J. Precis. Eng. Manuf, Vol.10, No.1, pp.123-135, 2009.

[2] T. Ohtani, H. Ogi, and M. Hirao “Noncontact Evaluation of Surface-Wave Nonlinearity for Creep Damage in Cr–Mo–V Steel” Jpn J. Appl. Phys. 48. 07GD02-1. 2009.

[3] G. L. Jones, and D. R. Kobett, “Interaction of elastic waves in an isotropic solid” J. Acoust. Soc. Am., Vol.35, No.1, pp.5-10. 1963.

[4] M. Hirao and H. Ogi, H. EMATs for science and industry: nondestructive ultrasonic measurements, Kluwer Academic Publishers: Boston 2003.

[5] M. Kamaya, A. J. Wilkinson, and J. M. Titchmarsh, “Quantification of plastic strain of stainless steel and Nickel alloy byelectron backscatter diffraction", *Mcta Materialia*, Vol. 54, pp. 539-548. 2006.

C3-O-007601

SURFACE NANOSTRUCTURING OF KTP CRYSTAL BY CLUSTER ION BOMBARDMENT*

I.V. NIKOLAEV, N.G. KOROBEISHCHIKOV

Department of Applied Physics, Novosibirsk State University, Novosibirsk, Russian Federation

The periodic nanostructures on the surface of various materials can lead to unique anisotropy of properties: optical activity, conductivity, adhesion, wetting, etc. [1, 2]. Previously, it was shown that the ion beam bombardment of the surface at oblique angles of incidence can be used as one of the methods of self-organizing nanostructuring [3, 4]. In the comparison with the monomer ion beam, the nonsize-selected beam of cluster ions has high intensity and cluster impact on a target leads to minimum subsurface damage [5–7].

Earlier, we have experimentally studied the influence of angles of cluster incidence on nanostructure formation on the surface of potassium titanyl phosphate (KTP) single crystals [8]. In this work, the features of surface nanostructuring of KTP surface by argon cluster ions with the different energy per cluster atom, ion fluence have been studied. To study the characteristics of the periodic nanostructures, we used the atomic force microscope (AFM) Ntegra Prima HD. Figure 1 shows the AFM images of KTP surface before and after cluster ion bombardment with the kinetic cluster energy E = 6.5 keV and mean cluster size N_{mean} = 600 atoms at the scan sizes of 2×2 μm^2 with a resolution of 1024×1024 pixels.

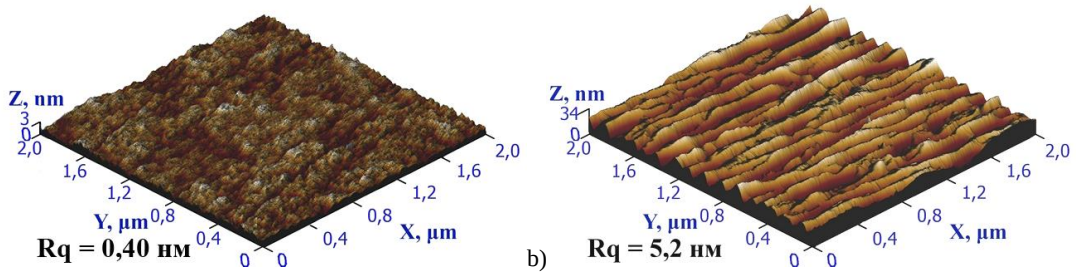

Fig.1. 3D AFM images of the KTP surface: a) as-prepared, b) after the cluster ion bombardment.

The characteristics of self-organizing nanostructures, the etching rates and sputtering yields for KTP single crystals in a wide range of energy per atom in the argon cluster (E/N_{mean} = 10–110 eV/atom) have been determined. A comparison has been made of the nanostructures formed at the same mass fluxes, but at different parameters of cluster ions. The dynamics of changes in the parameters of nanostructures depending on the ion fluence are demonstrated.

REFERENCES

[1] K. Pohl, M.C. Bartelt, J. de la Figuera, N.C. Bartelt, J. Hrbek, R.Q. Hwang, "Identifying the forces responsible for self-organization of nanostructures at crystal surfaces," Nature, vol. 397, pp. 238-241, 1999.

[2] S. Tawfick, M. De Volder, D. Copic, S.J. Park, C.R. Oliver, E.S. Polsen, M.J. Roberts, and A.J. Hart, "Engineering of Micro- and Nanostructured Surfaces with Anisotropic Geometries and Properties," Advanced materials, vol. 24, no. 13, pp.1628-1674, 2012.

[3] B. Ziberi, F. Frost, T. Höche, B. Rauschenbach, "Ion-induced self-organized dot and ripple patterns on Si surfaces," Vacuum, vol. 81, pp. 155-159, 2006.

[4] M. Engler, S. Macko, F. Frost, and T. Michely, "Evolution of ion beam induced patterns on Si(001)," Phys. Rev. B., vol. 89, Article No. 245412, 2014.

[5] I. Yamada, J. Matsuo, N. Toyoda, T. Aoki, T. Seki, "Progress and applications of cluster ion beam technology," Cur. Opin.Sol. State and Mat. Sci., vol. 19, pp. 12-18, 2015.

[6] A. E. Ieshkin, K. D. Kushkina, D. S. Kireev, Yu. A. Ermakov, and V. S. Chernysh, "Polishing superhard material surfaces with gas-cluster ion beams," Tech. Phys. Lett., vol. 43, no. 1, pp. 95–97, 2017.

[7] N. G. Korobeishchikov, I. V. Nikolaev, M. A. Roenko, and V. V. Atuchin, "Precise sputtering of silicon dioxide by argon cluster ion beams," Appl. Phys. A, vol. 124, Article Number 833, 2018.

[8] I. V. Nikolaev, and N. G. Korobeishchikov, "Influence of the Parameters of Cluster Ions on the Formation of Nanostructures on the KTP Surface," Applied Nano, vol. 2, pp. 25–30, 2021.

* The work was supported by the Russian Science Foundation under grant No. 21-19-00046.

C3-O-011701

INFLUENCE OF IRRADIATION BY AN INTENSE PULSE ELECTRON BEAM ON THE MECHANICAL PROPERTIES OF THE COMPOSITE MATERIAL "FILM (Ti)/(SILUMIN AK5M2) SUBSTRATE"

Yu.F. IVANOV[1], *A.A. KLOPOTOV*[2], *D.V. ZAGULYAEV*[3], *A.M. USTINOV*[2], *A.D. TERESOV*[1], *N.A. PROKOPENKO*[1], *Yu.A. ABZAEV*[1], *V.D. KLOPOTOV*[4]

[1]*Institute of High Current Electronics SB RAS, Tomsk, Russia*
[2]*Tomsk State University of Architecture and Building, Tomsk, Russia*
[3]*Siberian State University of Industry, Novokuznezk, Russia*
[4]*National Research Tomsk Polytechnic University, Tomsk, Russia*
e-mail: klopotov@tpu.ru

Alloys based on Al-Si (silumins) are widely used in Russian and foreign industries. A significant disadvantage of silumins is increased fragility. One of the methods for improving the mechanical properties is the modification of the alloy surface by concentrated energy flows. This paper presents the results of studies of the mechanical properties of AK5M2 silumin samples, the surface layer of which is modified by irradiating the “film (Ti)/(AK5M2) substrate” system with a pulsed electron beam.

Under conditions of uniaxial tension of flat proportional samples in the initial state and samples with a modified surface, deformation curves were obtained in the stress-strain coordinates (Fig. 1). The deformation was carried out on an INSTRON 3386 testing machine. The evolution of deformation fields during testing was recorded using a VIC-3D optical measuring system. The deposition of a Ti film 0.7 μm thick on silumin samples was carried out on a KVINTA setup. The samples were irradiated with a pulsed electron beam using a SOLO setup (30 J/cm2, 200 μs, 3 pulses).

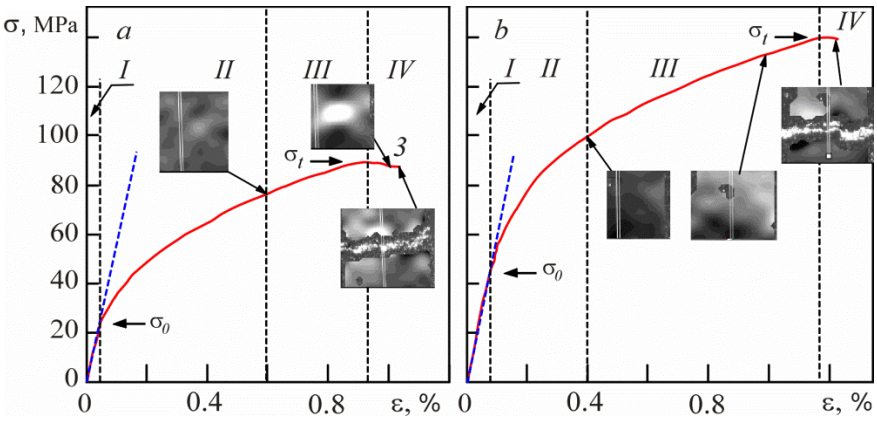

Rice. Fig. 1. Diagrams of deformation of samples of AK5M2 silumin under uniaxial tension: a - initial state; b - composite material "film (Ti)/(silumin AK5M2) substrate", irradiated with a pulsed electron beam. The insets show fragments of the distributions of deformation fields on the surface of the samples.

On the deformation curves, four stages of deformation can be distinguished: I - the stage of elastic deformation; II and III - hardening stages with a parabolic functional dependence of the form with different values of the coefficients θ and n:

$$\sigma = \sigma_0 + \theta\varepsilon^n \quad (1)$$

where σ_0 – yield point; $\theta(\varepsilon)=d\sigma/d\varepsilon$–strain hardening factor; $n<1$ – strain hardening index. Stage IV - the stage of sample pre-fracture. The numerical values of the parameters from equation (1) for the original and modified samples are given in the table. From the given data it can be seen that the modification of the surface layer of samples of silumin brand AK5M2 led to an increase in the strength and plastic properties of the material

Table. Parameters characterizing the strength properties of AK5M2 silumin

Sample	σ_0, MPa	σ_t, MPa	n_{II} на стадии II	n_{III} на стадии III
Initial	24±3	90±15	0.49±0.02	0.31±0.02
Modified	45±3	140±15	0.49±0.02	0.31±0.02

This work was supported by a grant from the Russian Science Foundation (project no. 19-79-10059).

C3-O-015701

SURFACE MODIFICATION USING A-C:H:SIO$_X$ FILMS

A.S. GRENADYOROV[1], *A.A. SOLOVYEV*[1], *M.O. ZHULKOV*[1,2], *D.A. SIROTA*[1,2], *A.M. CHERNYAVSKIY*[1,2], *V.V. MALASHCHENKO*[1,3], *L.S. LITVINOVA*[3], *O.G. KHAZIAKHMATOVA*[3], *N.D. GAZATOVA*[3], *I.A. KHLUSOV*[3,4]

[1] *Institute of High Current Electronics SB RAS, 634055 Tomsk, Russia*
[2] *E. Meshalkin National Medical Research Center of Ministry of Health of Russian Federation, 630055 Novosibirsk, Russia*
[3] *Immanuel Kant Baltic Federal University, 236016 Kaliningrad, Russia*
[4] *Siberian State Medical University, 634050 Tomsk, Russia*

One type of diamond-like carbon materials is a-C:H:SiO_x coatings, also called diamond-like nanocomposites (DLN), SiO_x-doped DLC. Such coatings have low internal stresses (less than 1 GPa), hardness in the range of 10÷20 GPa, low friction coefficient and low wear rate [1-3]. Due to the presence of silicon and its compounds (SiO_x) in the structure, the biocompatibility of a-C:H:SiO_x coatings with the human biological environment is improved [4].

The plasma-assisted chemical vapor deposition in a mixture of argon and polyphenylmethylsiloxyloxane vapors was used for coating deposition. The method is described in detail in our previous works [5, 6]. Titanium alloy (Ti-6Al-4V) and stainless steel AISI 316L samples were used as substrates.

It has been shown that deposition of a-C:H:SiO_x coatings leads to improvement of mechanical and tribological properties of materials surface. In particular, after deposition of a-C:H:SiO_x coatings on titanium, titanium alloys and stainless steel its surface hardness increases more than 2-4 times, friction coefficient decreases more than 6 times, and wear rate decreases by two orders of magnitude [7, 8].

It has been established that a-C:H:SiO_x films had low thrombogenicity and are not cytotoxicity for mononuclear leukocytes of human blood (hBMNCs). In addition, a-C:H:SiO_x film leads to decreased concentrations of the proinflammatory cytokines IL-17 and TNF-a as well as the chemokines IL-8, RANTES, MCP-1 (MCAF) in 24-h in vitro culture of hBMNCs. This suggests a potential anti-inflammatory effect of the studied coating and the possibility of its medical application in the field of cardiovascular surgery. The dependence of the concentration of proinflammatory cytokines and chemokines on the a-C:H:SiO_x film thickness correlating with the surface wettability and electrostatic surface potential was established. It was shown that a-C:H:SiO_x film deposition contributed to increasing the corrosion resistance of Ti-6Al-4V samples in 0.5M NaCl and PBS solutions (corrosion rate decreased up to 10^{-6} mm/year). The results of 5-week biodegradation in 0.9% sodium chloride solution demonstrated minimal salt deposition on the surface of samples coated a-C:H:SiO_x film.

*This research was supported by the grant of the Russian Science Foundation, project No. 19-19-00186.

REFERENCES

[1] Mingwen Bai, Liuquan Yang, Jiayu Li, Lun Luo, Shikuan Sun, Beverley Inkson, “Mechanical and tribological properties of Si and W doped diamond like carbon (DLC) under dry reciprocating sliding conditions” Wear, vol. 484-485, Article ID 204046, 2021.

[2] M. Toyonaga, T. Hasebe, S. Maegawa, T. Matsumoto, A. Hotta, T. Suzuki, “The property of adhesion and biocompatibility of silicon and fluorine doped diamond-like carbon films”, Diamond and Related Materials, vol. 119, Article ID 108558, 2021.

[3] J. Wang, J. Pu, G. Zhang, L. Wang, “Tailoring the structure and property of silicon-doped diamond-like carbon films by controlling the silicon content”, Surface & Coatings Technology, vol. 235, pp. 326-332, 2013.

[4] S. Meskinis and A. Tamuleviciene, “Structure, Properties and Applications of Diamond Like Nanocomposite (SiOx Containing DLC) Films: A Review”, Materials science, vol. 17, no. 4, pp. 358-370, 2011.

[5] A.S. Grenadyorov, M.O. Zhulkov, A.A. Solovyev, K.V. Oskomov, V.A. Semenov, A.M. Chernyavskiy, D.A. Sirota, N.A. Karmadonova, V.V. Malashchenko, L.S. Litvinova, O.G. Khaziakhmatova, N.D. Gazatova, I.A. Khlusov, “Surface characterization and biological assessment of corrosion resistant a-C:H:SiO_x PACVD coating for Ti-6Al-4 V alloy”, Materials Science & Engineering C, vol. 123, Article ID 112002, 2021.

[6] A.S. Grenadyorov, A.A. Solovyev, K.V. Oskomov, V.O. Oskirko, V.A. Semenov, “Thermal stability of anti-reflective and protective a-C:H:SiO_x coating for infrared optics”, Applied Surface Science, vol. 510, Article ID 145433, 2020.

[7] A.S. Grenadyorov, A.A. Solovyev, K.V. Oskomov, S.A. Onischenko, A.M. Chernyavskiy, M.O. Zhulkov, V.V. Kaichev, “Modifying the surface of a titanium alloy with an electron beam and a-C:H:SiOx coating deposition to reduce hemolysis in cardiac assist devices”, Surface and Coatings Technology, vol. 381, 125113, 2020.

[8] A.S. Grenadyorov, V.O. Oskirko, A.A. Solovyev, K.V. Oskomov, I.A. Khlusov, “Wear and Corrosion Resistance of a-C:H:SiOx Coating on Medical 316L Stainless Steel”, Journal of Materials Engineering and Performance, vol. 30, pp. 1099-1109, 2021.

C3-O-017802

PHASE TRANSFORMATIONS UNDER THERMAL TREATMENT IN Al-12%Si-Zr SYSTEM WITH METASTABLE STRUCTURE SYNTHESIZED BY COMPRESSION PLASMA FLOWS IMPACT

N.N. CHERENDA[1], N.V. BIBIK[1], V.M. ASTASHYNSKI[2], A.M. KUZMITSKI[2]

[1]Belarusian State University, Minsk, Belarus
[2]A.V.Lyikov Heat and Mass Transfer Institute of the National Academy of Sciences of Belarus, Minsk, Belarus

Mixing of a "coating/substrate" system by ion, electron, plasma and laser beams allows alloying the substrate material with the coating elements. This process is of special interest in producing nonequilibrium, immiscible and metastable compounds. The use of such a technique for materials treatment leads to formation of surface layers with improved properties. At the same time metastable structure of the modified layer may be not effective for materials working at the high temperature. Thus, investigation of the effect of thermal treatment on the structure, phase composition and properties of Al-12%Si alloy surface layer alloyed with Zr atoms under compression plasma flows impact on Zr/Al-12%Si system was the main aim of this work.

Al-12%Si alloy was the research object. Before compression plasma flows (CPF) treatment Zr coating with the thickness of 2 μm was deposited on the alloy surface using the vacuum arc vapor deposition technique. CPF were obtained in nitrogen atmosphere using a gas-discharge magneto-plasma compressor of compact geometry. Structure, element and phase composition of the surface layer were characterized by the X-ray diffraction analysis, scanning electron microscopy and energy-dispersive X-ray microanalysis. Vickers microhardness measurement was also carried out. Annealing in air in the temperature range of 450-550^{o}C and period of 0.5-10 hours was carried out to investigate modified layers structure and properties stability.

The findings showed that CPF treatment of the Zr/Al-12%Si system led to the formation of surface Al-Si layer with the thickness up to 65 μm containing metastable $(Al,Si)_3Zr$ compound with a tetragonal $D0_{22}$ crystal lattice (so called τ_1 phase in Al-Si-Zr system). The minimal size of τ_1 phase precipitates was 200 nm. The lattice parameters of τ_1 phase were decreasing with the growth of the energy absorbed (Q) by the surface layer during plasma impact: from a=0,3890 nm and c=0,8806 nm at Q=15 J/cm^2 to a=0,3873nm and c=0,8791 nm at Q= 35 J/cm^2 (a=0,3903 nm and c=0,9008 nm - in Al_2SiZr standard). Besides that formation of supersaturated Al(Si, Zr) solid solution was observed.

Annealing of alloyed sample at 450^{o}C resulted in partial disintegration of supersaturated Al(Si,Zr) solid solution and formation of Al_3Zr (after 0.5 annealing hour) and $ZrSi_2$ (after 2 annealing hours) phases. Increase of annealing time at this temperature also led to Si atoms release from τ_1 phase precipitates and increase of τ_1 lattice parameters up to a=0,3890nm and c=0,8931 nm (after 10 annealing hours).

Further increase of annealing temperature up to 500^{o}C led to the change of τ_1 precipitates shape from dendritic-like to equiaxial.

Increase of annealing temperature up to 550^{o}C provided more substantial phase transformations in the alloyed layer just after 0.5 hour. In particular, dissolution of most of τ_1 phase precipitates and formation of plate-like $ZrSi_2$ precipitates was observed.

Increase of annealing temperature and time was accompanied by microhardness decrease.

The mechanisms and the reasons of the observed effects are discussed.

C3-O-024201

OPTICAL ABSORPTION OF RADIATION DEFECTS IN ALKALI-HALIDE CRYSTALS IMPLANTED MAGNESIUM AND SILVER IONS*

V.L. PAPERNY[1], *N.A. IVANOV*[2], *S.A. NEBOGIN*[2], *L.I. BRYUKVINA*[3], *R.A. AVVAKUMOV*[2], *S.N. CHELISHKOV*[2]

[1]*Irkutsk State University, Irkutsk, Russia*
[2]*Irkutsk National Research Technical University, Irkutsk, Russia*
[3]*Irkutsk Branch of Institute of Laser Physics of the SB RAS, Irkutsk, Russia*

This work presents the results of a research of the properties, structure, and formation mechanisms of metallic magnesium and silver nanoparticles obtained by ion implantation in LiF, NaCl, KCl, and KBr crystals. The crystals were irradiated with a pulsed beam of accelerated Mg ions with an average energy of ~ 80 keV and an average current density of 4 μA/cm^2. Dose range was from 2.2×10^{16} to 7.5×10^{16} ion/cm^2.

Nanoparticles were formed in a thin crystalline layer (~60–100 nm) along with color centers. The relevance of this topic is confirmed by the fact that metal nanoparticles produce optical effects, such as, for example, giant Raman scattering of molecules and plasmon-enhanced luminescence [1], which are promising for the development of various nanotechnologies.

It was noted that the luminescence intensity of color centers with λ_{max}=640 nm in implanted layers was more than 10^3 times higher than that in heavily γ-irradiated LiF:Mg crystals [1, 2].

The absorption spectra of NaCl, KCl, and KBr alkali halide crystals implanted with magnesium ions are shown in Fig.1. The nature of the centers responsible for the band ~ 320 nm in the spectrum of NaCl, KCl, and KBr crystals can be finally established by experiments on thermal annealing and optical bleaching.

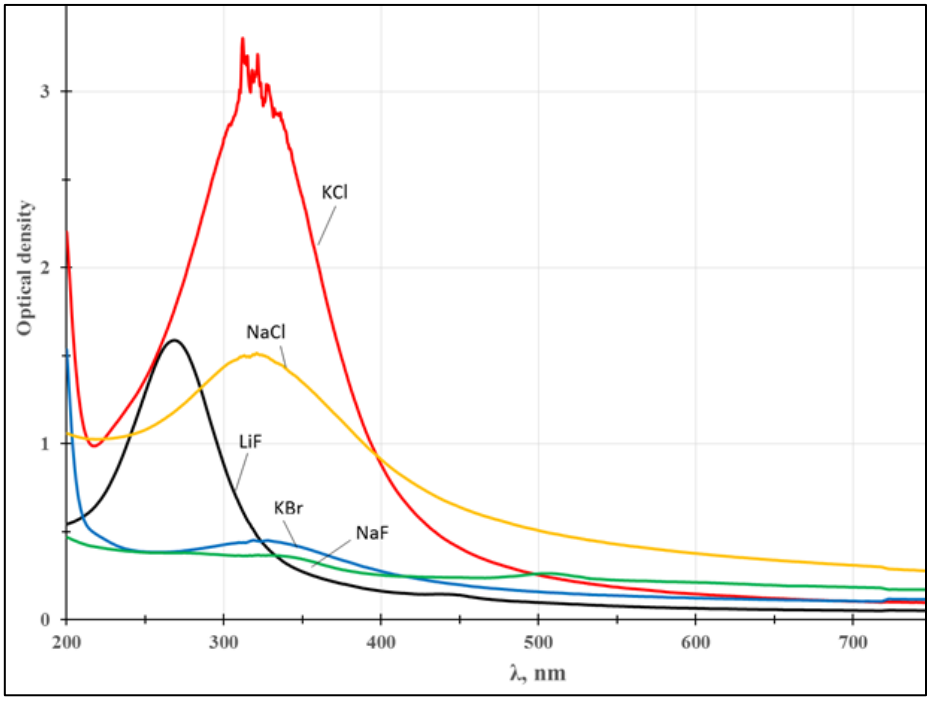

Fig.1. Absorbance spectra of alkali-halide crystals after magnesium ions implantation.

A comparison of the optical properties of crystals implanted with magnesium and silver ions shows a significant superiority of the optical characteristics in the case of implantation with magnesium ions.

REFERENCES

[1] S.F. Nebogin, N.A. Ivanov, L.I. Bryukvina, N.V. Shipitsin, A.E. Rzhechitski, V.L. Papernyi, “Photoluminescence of magnesium-associated color centers in LiF crystals implanted with magnesium ions,” PNFA, vol. 29, pp. 36-41, February 2018.

[2] L. Bryukvina, N. Ivanov, S. Nebogin, “Relationships between lithium and sodium nanoparticles and color centers formation in LiF and NaF crystals with hydroxide and magnesium ions impurities,” J. Phys. Chem. Sol., vol. 120, pp. 133-139, April 2018.

* The work was supported by grant of the Russian Science Foundation No. 20-02-00322 and grant No. FZZS-2021-0007 of scientific and educational center “Baikal”

C3-O-024701

MEASUREMENTS OF VACUUM ARC THRESHOLD CURRENT FOR W FUZZ*

P.S. MIKHAILOV, I.L. MUZYUKIN, YU.I. MAMONTOV, I.V. UIMANOV, YU.A. ZEMSKOV

Institute of Electrophysics UB RAS, Yekaterinburg, Russian Federation

The interaction of plasma with the surface is a key factor for the realization of magnetic confinement fusion. Experiments on the interaction of plasma and tungsten walls were carried out on linear accelerators and tokamaks. As a result of the interaction of helium plasma with the walls, nanostructures are formed, called "fuzz" [1,2].

This work is devoted to the study of the vacuum arc for a tungsten cathode with a nanostructured surface. Tungsten cathodes were thin metal plates with sides of 16 x 13 mm. Several cathodes were used with different exposure times to helium plasma (1-8 hours). The trigger method for ignition of a vacuum arc was used. For this purpose, a trigger electrode was placed between the anode and cathode. High voltage pulse (500 ns; 15 - 25 kV; ~ 3.5 A) was applied to trigger electrode to start vacuum arc. The anode was a tungsten wire placed parallel to the cathode surface. In this experiment, the vacuum arc was powered by anode RC circuit charged to 200 V. The arcing current was measured by a low inductive shunt.

As a result, the distribution of the threshold currents was obtained. The threshold current value is much lower than for ordinary tungsten.

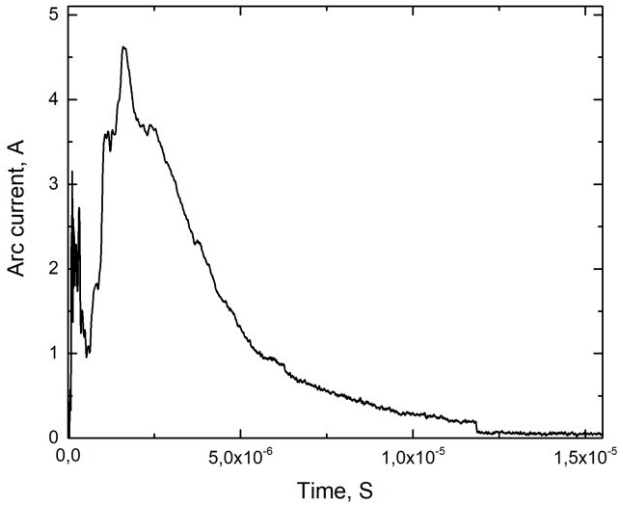

Fig.1. Typical waveform of arc current.

REFERENCES

[1] S. Takamura, N. Ohno, D. Nishijima, and S. Kajita, “Formation of nanostructured tungsten with arborescent shape due to helium plasma irradiation,” Plasma Fusion Res., Rapid Commun., vol. 1, p. 051, Sep. 2006.

[2] S. Kajita, W. Sakaguchi, N. Ohno, N. Yoshida, and T. Saeki, “Formation process of tungsten nanostructure by the exposure to helium plasma under fusion relevant plasma conditions,” Nucl. Fusion, 49, no. 9, p. 095005, Aug. 2009.

* The work was supported by the Russian Science Foundation (grant No. 20-19-00323).

C3-O-025001

THE FEATURES OF AN ARC DISCHARGE BURNING ON A TUNGSTEN CATHODE COATED WITH FUZZ NANOSTRUCTURES. *

P.S. MIKHAILOV, I.L. MUZYUKIN, YU.I. MAMONTOV, YU.A. ZEMSKOV, I.V. UIMANOV

Institute of Electrophysics UB RAS, 106 Amundsen Str., Ekaterinburg, 620016, Russia

Complex investigations of vacuum discharge with FUZZ coated tungsten cathode were done. The waveforms of vacuum arc current, interelectrode voltage drop and plasma luminescence were stored and analysed. The cathode spot erosion traces were obtained for small current short discharges.

It was found that the vacuum arc on the FUZZ cathode significantly more unstable. The discharge current and interelectrode voltage drop can arbitrarily change the burning modes. Sometimes the discharge become high voltage small current discharge with the discharge parameters close to glow discharge ones. This low current mode can be suddenly changed to the high current low voltage mode. The vacuum arc on the FUZZ cathode does not have the threshold current which is essential property of the vacuum arc discharge on the clean tungsten cathode.

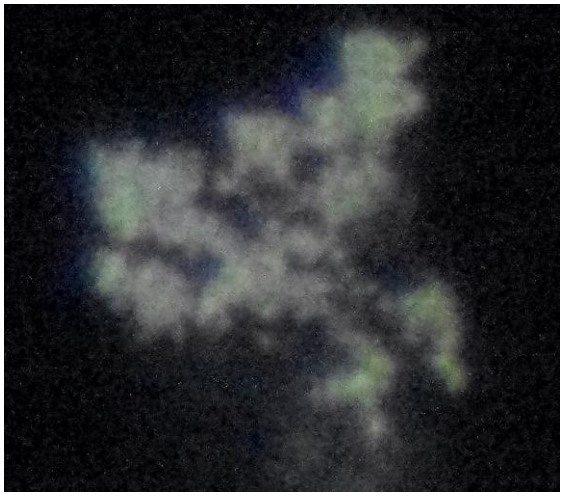

Fig.1. The erosion traces leaved by five low current short-term discharges (10mks,4A)

The erosion traces on the cathode surface show the fractal nature of the cathode spots on the FUZZ coating. There are no traces of the second type of cathode spot well-defined craters. The erosion traces look like a chaotically melted surface. The more discharges were burn on the place the larger erosion traces area. It was established that the short-term discharges could not clean the area around a ignition point. The cathode spot usually burns on the FUZZ coating at the end of discharge.

* The work was supported by the Russian Science Foundation (grant No. 20-19-00323).

C3-O-026902

EFFECT OF PULSED ION BEAM IRRADIATION ON THE STRUCTURAL AND PHASE STATE AND MECHANICAL PROPERTIES OF ZIRCONIUM ZR-2.5NB ALLOY*

E.N. STEPANOVA[1], G.P. GRABOVETSKAYA[2], A.V. STEPANOV[1], KRUGLYAKOV M.A.[1]

[1]National Research Tomsk Polytechnic University, Tomsk, Russia
[2] Institute of Strength Physics and Materials Science SB RAS, Tomsk, Russia

Recently, processing methods associated with the use of charged particle beams are often used to improve the performance of metals and alloys and create protective coatings. In the process of electron and ion beam exposure accumulation of defects, formation of metastable phases and nanocrystalline structure are observed in the subsurface layer of metal polycrystals [1–2]. In this case, the presence of hydrogen in the material can significantly affect the structure formed in the subsurface layer. The surface structure, which has a high defect density and contains metastable phases, can have a considerable effect on the properties of materials.

In this work, the effect of irradiation with a pulsed beam of carbon ions on the structural and phase state and mechanical properties of hydride-forming alloys of the Zr-Nb-H system was studied.

Zirconium Zr-2.5Nb alloy with a hydrogen content of 0.002 and 0.19 wt.% (hereinafter, Zr-2.5Nb and Zr-2.5Nb-0.19H alloys) was used as a material for the study. To assess the effect of irradiation on the structure and properties, the samples were irradiated with a pulsed beam of carbon ions with the TEMP accelerator [3]. The peak energy of carbon ions was 200 keV, the ion current density was 100 A/cm^2, and the duration of the ion current pulse was 200 ns. The ratio of H^+/C^{n+} ions in the beam was 20%/80%.

In the initial state in the Zr-2.5Nb alloy, particles of the Nb_β phase are observed in the bulk and at the grain boundaries. The volume fraction of particles determined by the standard grid method in optical images of the alloy structure is 3–4%. At the same time, according to the data of X-ray diffraction analysis, in the initial state, the alloy contains only the Zr_α phase, which is due to the low volume fraction of the secondary phase and the presence of a crystallographic texture in the Zr_α phase.

Hydrogenation of the alloy to a hydrogen concentration of 0.19 wt.% does not lead to any noticeable structural changes. However, according to the data of X-ray diffraction analysis, the phase composition of the alloy changes as a result of hydrogenation. In addition to the main Zr_α phase, the Nb_β phase appears in the Zr-2.5Nb-0.19H alloy and precipitations of ZrH and ZrH_2 hydrides are also observed. In this case, the texture in the Zr_α phase is preserved.

As a result of irradiation with a pulsed beam of carbon ions, an insignificant number of shallow craters are observed on the surface of Zr-2.5Nb and Zr-2.5Nb-0.19H alloys. In this case, the phase composition of the alloy also changes: in addition to the Zr_α phase with the texture preserved as a result of irradiation, precipitates of the Zr_β phase appear in the alloy. At the same time, in a hydrogenated alloy, irradiation leads to more significant changes in the phase composition. In addition to the main Zr_α phase with an unchanged crystallographic texture, the Zr_β phase also appears in the alloy, the volume fraction of the Nb_β phase decreases, and the ZrH_2 hydride precipitates are completely dissolved.

Microhardness measurements for the samples in various states have shown that hydrogenation, as well as irradiation with a pulsed beam of carbon ions, results in the considerable changes in microhardness. Thus, in the initial state, the microhardness of the Zr-2.5Nb alloy samples is (130±7) HV, and after hydrogenation this value rises by 1.3 times, up to (166±7) HV. After irradiation, the values of microhardness for the Zr-2.5Nb and Zr-2.5Nb-0.19H samples are (145±7) HV and (202±7) HV, respectively.

REFERENCES

[1] N. Pushilina, E. Stepanova, A. Stepanov, M. Syrtanov, “Surface modification of the EBM Ti-6Al-4V alloy by pulsed ion beam,” *Metals*, vol. 11, 512, 2021.

[2] I. P. Mishin, G. P. Grabovetskaya, E. N. Stepanova, R. S. Laptev, A. D. Teresov, “Hydrogen effect on the defect structure formation in the Zr-1 wt.% Nb alloy under pulsed electron beam irradiation,” Rus. Phys. J., vol. 62, no. 5, pp. 854-860, September 2019.

[3] A. V. Stepanov, V. I. Shamanin, G. E. Remnev, “The study of operation modes of the self-magnetically insulated ion diode,” Rev. Sci. Instrum., vol. 90, 033302, 2019.

* The work was funded by the Russian Foundation for Basic Research, research project No. 21-53-53013.

C3-O-029401

PULSED E-BEAM IRRADIATION TO MODULATE DRUG RELEASE FROM FIBERS*

A.A. VOLOKHOV [1,2], *D.V. PONOMAREV* [1], *I.A. KURZINA* [2], *S.I. TVERDOKHLEBOV* [1]

[1] *Tomsk Polytechnic University, Tomsk, Russian Federation*
[2] *Tomsk State University, Tomsk, Russian Federation*

Drug-loaded electrospun fibers have been an object of interest for several decades now. Possibility of a steady, controlled drug release combined with extracellular matrix features have made them widely investigated topic of research.

Synthetic biodegradable polymers are the most used sources for drug-loaded fiber production. Their advantages are: accessibility, high mechanical strength, predictable chemical interactions with body fluids and low immunogenecy. High molecular weight polymers are easier to process via electrospinning. However, high molecular weigh of the polymer could affect drug release rate.

Several material modification methods are shown to modulate drug release dynamics [1]. We have previously demonstrated how electron-beam irradiation of electrospun drug-loaded scaffolds can increase drug release rate [2,3]. In this work we present results of the study of the drug release kinetic parameters and overall material properties dependance on the absorbed irradiation dose.

Poly(ε - caprolactone) scaffolds with an incorporated chloramphenicol were the object of the research. Pulsed e-beam irradiation with doses 0, 25, 50 and 75 kGy were applied. Irradiation leads to changes in the molecular wight of the polymer and its crystallinity. Drug release profiles also change after modification. It has been demonstrated that the observed effects are dose and drug concentration dependent.

REFERENCES

[1] A.A. Volokhova, D.A. Fedorishin, A.O. Khvastunova, T.I. Spiridonova, A.I. Kozelskaya, J. Kzhyshkowska, S.I. Tverdokhlebov, I. Kurzina, Reactive Magnetron Plasma Modification of Electrospun PLLA Scaffolds with Incorporated Chloramphenicol for Controlled Drug Release. Polymers, vol. 14, 2022.

[2] A. A. Volokhova, V. L. Kudryavtseva, T. I. Spiridonova, I. Kolesnik, S. I. Goreninskii, R. V. Sazonov, G. E. Remnev, S. I. Tverdokhlebov "Controlled drug release from electrospun PCL non-woven scaffolds via multi-layering and e-beam treatment," Mater. Today Commun., vol. 26, 2021.

[3] A.A. Rakina, T.I. Spriridonova, V.L. Kudryavtseva, I.M. Kolesniik, R.V. Sazonov, G. E. Remnev, S.I. Tverdokhlebov. Ibuprofen controlled release from E-beam treated polycaprolactone electrospun scaffolds. Jour. of Phys.: Conf. Ser., vol. 1115, n. 3, p. 032051, November 2018

* This research was supported by the TPU development program - Priority 2030 (Project No. Priority-2030-NIP/IZ-011-0000-2022).

C3-O-030002

STRUCTURE CHANGES IN SEVERAL METALS AFTER THEIR LASER TREATING IN DIFFERENT CONDITIONS

A.YU. IVANOV, E.A.KARPOVICH, A.L. SITKEVICH, N.G.VALKO, S.V. VASILIEV

Grodno State University, Osheshko, 22, Grodno, 230023, Belarus, ion_ne@mail.ru, (0152)610098

The radiation of the GOR-100M ruby laser (λ = 0.694 mm) operating in the free oscillation regime (pulse duration ~1.2 mc) passed through the focusing system and was directed onto the surface of metal (Ti, Cd, Cu, In) sample. Both mono-lens and two-lens systems were used for focusing of laser radiation. This avoided to form an image of a diaphragm on the surface of irradiated sample as a spot with the sharp borders. During the experiments a spot diameter was varied from 1 to 3 mm. This avoided to vary the flux density of laser radiation q from 10^4 to 10^6 W cm^{-2}. The energy of the laser pulses varied from 5 to 50 J. The samples were treated from one and from both sides.

For determination of structure changes in metal samples (continuous polycrystalline) having in equilibrium state the cubic side-centered crystalline grid before and after action of laser radiation we used X-ray difractometer DRON-2.0. Radiation K_α-line from the tube with copper anticathode filtered by standard nickel filter on wavelength 154,050 pm was used in the difractometer.

Calculation of temperature changes after action on the target of each pick of free oscillation pulse was also fulfilled.

During interaction of laser radiation with matter a number of changes in the treated sample can take place: changes of chemical composition of matter, phase transitions, defects of new types appearance, increase of already existing defects concentration, changes of inter-crystalline planes properties.

For the titanium samples treated by laser radiation with the flux density of radiation q ~ $5\cdot10^4$ W cm^{-2} splitting of correlation function maxima was not observed. However the width of X-ray difractograms was essentially changed. This effect testifies the considerable growth of crystalline grid defects concentration in the irradiated zone. Micro-hardness of titanium samples in the irradiated zones also considerably increased. The calculations show that after treating of titanium sample by laser radiation with the flux density q ~ $5\cdot10^5$ W cm^{-2} number of crystalline elementary cells were subjected to the transformation from the cubic side-centered to the distorted (having a form of parallelepiped, different from the cub) can reach 50 %.

For copper samples irradiated by laser beam with the flux density of radiation q ~ $5\cdot10^5$ W cm^{-2} not only erosion but even splitting of the first maximum of correlation function was observed. It testifies to the transformation of the matter crystalline structure after its laser treating. In the irradiated zone the form of the crystalline elementary cell was changed from the cubic side-centered to the distorted (having a form of parallelepiped, different from the cub). Micro-hardness of metal samples in the irradiated zones considerably (30 % and even more) increased. It is also to be mentioned that after treating of copper sample by laser radiation with the flux density enough for the melting of metal in the irradiated zone (q > 10^6 W cm^{-2}) any changes of X-ray difractograms were not observed and micro-hardness of metal samples in the irradiated zones slightly decreased.

Estimation of the height of the first maxima of correlation functions before and after laser treating of copper samples permitted us to discover that 83 % of crystalline elementary cells were subjected to the transformation from the cubic side-centered to the distorted (having a form of parallelepiped, different from the cub). These data are in good consent with the results of calculations (~ 80 % of total number of the crystalline elementary cells).

C3-O-030301

OXIDATION BEHAVIOR OF METALS TREATED WITH COMPRESSION PLASMA FLOWS

V.I. SHYMANSKI[1], V.V SHEVELEVA[1], V.M. ASTASHYNSKI[2], A.M. KUZMITSKI[2]

[1]*Belarusian State University, Minsk, Belarus*
[2]*A.V. Luikov Heat and Mass Transfer Institute of National Academy of Science of Belarus, Minsk, Belarus*

Modification of different metals and its alloys with plasma flows and charged particles beams is widely used for improvement the physical properties and exploiting parameters. The pulse mode of interaction between the plasma flow or particle beam with the metal target is used. Taking into account both the short time of the pulse (not more than several hundred microseconds) and quite high energy density (several tens J/cm^2), just the surface layer of the material is subjected to the modification of structure and phase composition. Many published works demonstrate the increase in hardness, wear resistance after the treatment. Other interesting and practically important problem connecting to investigation of oxidation resistance of the modified structures. Indeed, a lot materials work at elevated temperature that are much higher than room one and oxygen diffusion occurs very fast. Due to diffusion of oxygen atoms an oxide layer grows on the surface and the physical properties of the material degrade. So, the main aim of the present work is to find the main peculiarities of oxidation process in refractory metals subjected to compression plasma flows impact.

The samples of commercial pure titanium, zirconium and tungsten were subjected to compression plasma flows (CPF) which were generated in magnetoplasma compressor of compact geometry. The plasma impact was made in pulsed mode with a pulse duration of 100 μs. The samples were treated with plasma flows in the nitrogen residual atmosphere. The energy parameters of the plasma flows provided the absorbed energy density enough for melting of the surface layer. After this, the samples were placed in the furnace for annealing in open air atmosphere at temperatures 500 – 800 °C.

The plasma impact melts the surface layer with a thickness of several micrometers and more. Due to high cooling rate of the melt the grain structure of the solidified layers is characterized with a small size of the grains. The oxidation process of the untreated samples shows the formation a set of oxide phases – TiO_2 (rutile) for titanium, ZrO_2 (monoclinic type) for zirconium and volatile oxide WO_3 for tungsten. According to the well-known diffusion law the amount of the oxide phases increases with the annealing time. The appearance of the oxide phase was found by means of X-ay diffraction method. The treated samples demonstrate the decrease in the diffraction signals from oxide phases after the oxidation at the same condition. Moreover, the time of beginning of oxide growth also increases, i.e. it requires more time for oxide film growth. The measurement of mass gain of the samples after the oxidation shows very weak difference between the treated and untreated samples. It means, the absolute amount of oxygen atoms penetrated inside the surface layer doesn't depend of the plasma impact. Nevertheless, the small grain size increases the density of the grain boundaries which can work as ways for enhancement diffusion. The rate of the diffusion rises and prevent the surface layer from the oxygen accumulation and distortion of the lattice for phase transformation.

Additional alloying of the samples with other elements during the plasma flows impact producing the solid solutions with distorted crystal lattice. In this case the oxidation process goes more slowly as the internal stress decelerated the diffusion of oxygen,

The main results of the works show the promising approach of compression plasma flows influence on materials preventing them from oxidation at elevated temperatures.

C3-O-033101

COMPLEX ION-PLASMA SURFACE TREATMENT OF DIE STEEL*

A.A. LEONOV, YU.A. DENISOVA, V.V. DENISOV, M.V. SAVCHUK, V.N. TISHCHENKO

Institute of High Current Electronics SB RAS, Tomsk, Russia

The paper presents the evolution patterns of the tribological and mechanical properties of nitrided layers and nitride coatings on the surface of Cr12MoV die steel, created by the methods of ion-plasma nitriding, plasma-assisted electric arc depositing, and a combination of these methods, and also determines the optimal and efficient modes of ion-plasma treatment of die steel, which increase its wear resistance and hardness.

As a material for the study we used Cr12MoV die steel (1.45–1.65 wt.% C; 11–12.5 wt.% Cr; 0.4–0.6 wt.% Mo; 0.15–0.3 wt.% V). The samples were subjected to three types of ion-plasma treatment: 1 – nitriding; 2 – deposition of coatings, 3 – combined treatment, including nitriding and subsequent deposition of coatings. Die steel was nitrided in glow discharge plasma with a hollow cathode. High purity nitrogen and a mixture of Ar+N_2 gases were used as the working gas. Determination of the effect of nitrogen content in the nitrogen-argon gas mixture on the properties of the nitrided layer was carried out at the same pressure of 1 Pa for the following values of the nitrogen content in the working mixture: 100, 50, 25 and 10 %. The temperature of the samples during nitriding was 520 °C, the nitriding time was 3 h. The coatings were deposited using a plasma-assisted electric arc method on a modernized NNV 6.6-I1 device. To generate a metal plasma flow, two arc evaporators with cylindrical cathodes 80 mm in diameter made of Ti grade VT1-0 and Cr (99.8 %) were used. The source of gas plasma with a hot and hollow cathode "PINK" was used for heating steel samples and their preliminary cleaning, as well as for additional gas ionization and assistance in the deposition of coatings. All coatings were deposited at a substrate bias voltage (–) of 150 V, a substrate temperature of 390–400 °C in a nitrogen-argon gas mixture (90 % (N_2) and 10 % (Ar)) at a pressure of 0.6 Pa. Single-layer coatings of the (Ti, Cr)N system were deposited, in which the Cr content was varied by changing the current of the chromium electric arc evaporator (40, 60, 80, 100 A). Multi-layer CrN/TiN coatings, in which the thickness of each layer and the number of layers (500 nm for 8 layers, 250 nm for 16 layers, and 125 nm for 32 layers) were varied, were deposited at electric arc evaporator currents of 80 A (Ti) and 90 A (Cr). During combined treatment, nitriding was carried out in two modes: 1 – N_2 gas at a pressure of 1 Pa (samples had a "white" nitride layer) and 2 – a mixture of gases 50 % N_2 and 50 % Ar at a total pressure of 0.25 Pa (samples without nitride layer). The constant parameters in the nitriding processes were: substrate bias voltage (–) 600 V, substrate temperature 520 °C, and nitriding time 3 h. Before coating deposition, the nitrided samples were polished. The deposition of coatings on polished, nitrided samples was carried out by a plasma-assisted electric arc method using the best deposition modes in terms of tribological properties, namely, deposition of a CrN coating, a single-layer TiCrN (80/80) coating, and 32-layer CrN/TiN coating. Tribotechnical tests were carried out on a Tribotechnic tribometer under dry friction conditions with reciprocating movement of the sample relative to a counterbody in the form of an Al_2O_3 ball 6 mm in diameter. Nitriding of Cr12MoV steel in glow discharge plasma makes it possible to increase the wear resistance of the material by two orders of magnitude. The lowest wear coefficient was observed for the composition of the gas mixture N_2 (10 %) + Ar (90 %), in which there is no "white" nitride layer. The nitride layer, the main phase of which is ε-$Fe_{2-3}N$, is very brittle and during wear it breaks down and begins to act as an abrasive. It has been established that single-layer TiCrN coatings have a rather low coefficient of friction, on the order of 0.13-0.14. The most wear-resistant TiCrN coating is formed at electric arc evaporator currents of 80 A (Ti) and 80 A (Cr) and has a wear coefficient of 3.8×10^{-7} $mm^3/N*m$, because in this coating, the main phase is (Ti, Cr)N, a phase with a face-centered cubic lattice of the NaCl type. It is shown that changing the architecture of multilayer coatings by reducing the thickness of the layers makes it possible to smoothly reduce the wear coefficient and friction coefficient to the values of 6.8×10^{-7} $mm^3/N*m$ and 0.28, respectively, characteristic of 32-layer CrN/TiN coating. With combined treatment, coatings deposited on steel in the initial state and after nitriding (with and without a nitride layer) have similar values of the wear coefficient. However, the results of the scratch test unequivocally show that the coatings on the nitrided layer have a significantly higher resistance to destruction, and combined processing is most appropriate in cases where high loads are applied to the surface of the stamping tool.

* The work was carried out within the framework of the state task of the Ministry of Science and Higher Education of the Russian Federation on topic No. FWRM-2022-0001.

C3-O-035901

UNIFORM ION DOPING OF NUCLEAR MATERIALS FOR SUBSEQUENT TEM STUDIES

D.A. KOMAROVA, A.S. SOHATSKY, A.I. KRYLOV, S.V. MITROFANOV

Joint Institute for Nuclear Research, Dubna, Russian Federation

During an operation of nuclear reactors there is doping of fuel materials and construction materials in the active core by nuclear reaction products. These products are mainly atoms of noble gases (e. g. Kr, Xe, He). The atoms are insoluble in most materials. They strive for segregation on structure defects. Such behavior leads to irreversible degradation of mechanical properties of the materials. The degradation is observed in the form of high-temperature embrittlement, creep, fatigue changes, swelling [1-4]. The radiation swelling is the main factor limiting time of exploitation for construction nodes and active core details in nuclear reactors [1]. Structure researches of materials doped by noble gases atoms are carried out with usage of transmission electron microscopy (TEM). Such studies are widely used for estimation of materials radiation resistance.

As an alternative of difficult and expensive experiments using research nuclear reactors, it is possible to apply ion implantation [5]. However, the main problem of ion implantation is a complexity of getting required concentration of the doping impurity in a sample volume. Nowadays in Flerov Laboratory of Nuclear Reactions of Joint Institute for Nuclear Research a principle of uniform ion doping is developed. The principle is applied to material samples before further structure researches by TEM. As the base of the method is an idea of uniform scanning of ion zone stopping across the depth in target substance. For realization of the method, a construction of the target node was developed and made. In this construction a rotating target is irradiated. The rotation velocity changes across giving functional dependence versus rotation angle. Based on the theoretical calculation a software for control of target rotation and measure devices was created.

Nowadays the uniform ion doping experiments are carried out at EG-5 accelerator (Frank Laboratory of Neutron Physics, JINR) using helium beams (He^+) with the energy of 2.5 – 4 MeV for irradiation of metal samples.

REFERENCES

[1] A. S. Sohatsky, T. V. Nguen, V. A. Skuratov, I. A. Bobrikov, J. H. O'Connell, J. Neethling, M.Zdorovets, "To a question of temperature driven gas swelling in helium doped ferritic alloys", JNM, vol. 533, May 2020.

[2] H. Ullmaier, "The influence of helium on the bulk properties of fusion reactor structural materials", Nucl. Fusion, vol. 24, 1984.

[3] H. Ullmaier, "Helium in fusion materials: high temperature embrittlement", J. Nucl. Mater, vol. 133&134, pp. 100-104, 1985.

[4] H. Ullmaier, J. Chen, "Low temperature tensile properties of steels containing high concentrations of helium", J. Nucl. Mater., vol. 33, pp. 186-194, 1969.

[5] A. G. Zaluzhnyy, Yu. N. Sokurski, V. N. Tebus, Helium in reactor materials, Moscow: Energoatomizdat, 1988.

C3-O-045601

EFFECT OF IRRADIATION WITH A PULSED ION BEAM ON THE MORPHOLOGY, STRUCTURE, AND CHEMICAL STATE OF SURFACE LAYERS OF TUNGSTEN-FREE HARD ALLOYS

A.M. BADAMSHIN

Omsk state technical university, Omsk, Russia

Titanium carbide-based tungsten-free hard alloys (TFHA) are an inexpensive alternative to traditional hard alloys. One of the promising methods for modifying the structure and properties of hard alloy materials is their irradiation with pulsed energy flows: ions and electrons of micro- and nanosecond duration. There are works [1,2] in which a significant positive effect of these types of impact on the performance properties of tools made of traditional hard alloys based on WC. However, the study of the influence of various modes of ion modification on the change in the composition and properties of TFHA has not been studied enough, but is of great scientific and practical interest. In this paper, we study the influence of the impact of a pulsed ion beam (PiB) of nanosecond duration on the change in the morphology, structure and chemical state of TFHA of the "TiC-TiNi" system. The samples were irradiated at the «Temp» accelerator with a proton-carbon beam (30% H^+ and 70% C^+). The particle energy E was ≈250 keV. The duration of the irradiation pulse is $\tau \approx 60$ ns., beam current density ≈ 150 A/cm^2.

On fig. 1 shows the Ti_2p XPS spectra of the TFHA composition of 50% TiC-50% TiNi in the initial state (a) and after irradiation to one PIB pulse (b).

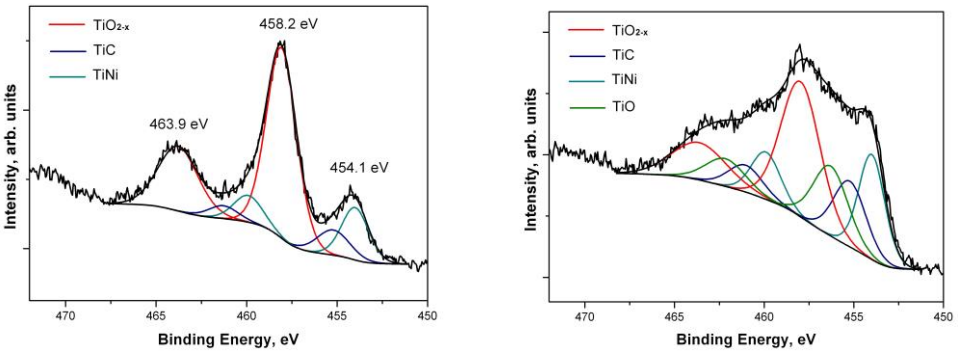

Fig.1. XPS Ti_2p spectra TFHA 50% TiC – 50% TiNi: (a) – initial, (b) – irradiated sample

In the initial state, the spectrum of titanium Ti_2p consists of three component, maximum which are located on the binding energies: 458.2 eV, 455.2 eV and 454.1 eV. They correspond to defective nonstoichiometric oxide TiO_{2-X}, titanium carbide TiC, and titanium in the metallic state Ti^0, respectively [3]. In the spectrum of the irradiated sample, the intensity of the components corresponding to metallic titanium in the composition of the TiNi binder and titanium carbide TiC increases significantly. Formation of Ti-C bonds can proceed with the participation of the reaction of adsorbed free carbon on the surface of the sample and metallic titanium, as part of the TiNi binder, as a result of high-temperature beam exposure.

The impact of PIB leads to a significant melting of the surface of the TFHA "TiC-TiNi". On the basis of experimental studies, it has been established that this type of irradiation leads to an increase in the microhardness of the studied TFHA by ~ 20% and the resistance of samples to gas corrosion at high temperatures. The results obtained in the work can be used in the development of technological processes for the surface modification of titanium-based hard alloys.

REFERENCES

[1] V.V. Uglov, A.K. Kuleshov, G.E. Remnev, M.S. Saltymakov, V.M. Astashinsky "Modification of T15K6 hard alloy by powerful pulsed ion beams and compression plasma flows," Izv. Vuz. Porosh. Metal. i Fun. coat. no. 3, pp. 63-68, 2011.

[2] S.N. Povoroznyuk, K.N. Poleshchenkov, G.A. Vershinin, P.V. Orlov "Variation of surface properties of hard alloys exposed to ion beams of various intensity," Surf. Inv.: X-Ray, Synch. and Neutr. Techn. Vol. 15, no. 5, pp. 791-796, 2000.

[3] A.M. Badamshin, S.N. Nesov, V.S. Kovivchak, S.N. Povoroznuyk, V.V. Akimov "The Influence of Ion Irradiation on the Morphology and Elemental and Chemical Composition of Surface Layers of Tungsten-Free Hard Alloys, " Tech. phys. let.. Vol. 47, no. 3, pp. 757-760, 2021.

C3-O-046803

THERMAL STABILITY OF THE STRUCTURAL-PHASE STATE OF THE MODIFIED LAYER OF HYPEREUTECTIC SILUMIN SPECIMEN

E.A. PETRIKOVA, YU.F. IVANOV, A.D. TERESOV, M.E. RYGINA

Institute of High Current Electronics SB RAS, Tomsk, Russia

The aim of the work is to develop methods and approaches to significantly improve the strength (microhardness) and tribological (wear rate and friction coefficient) characteristics of hypereutectic silumin (Al-22-24% Si) by creating hardened surface layers as a result of irradiation with a pulsed electron beam of the “film (ZrTiCu) / (hypereutectic silumin) substrate".

The thermal stability of the structural-phase state of a modified specimens layer of a hypereutectic silumin by a pulsed electron beam was studied under annealing conditions (200^0C and 400^0C for 2 and 4 hours) in an argon atmosphere at a residual pressure of 0.1 Pa.

It has been established that exposure of hypereutectic specimens, treated by a pulsed electron beam (25 J/cm^2, 200 μs, 3 pulses), at a temperature of 200^0C for 2 and 4 hours, does not lead to the destruction of the high-speed cellular crystallization structure and intensive decomposition of the solid solution based on aluminum with the formation of silicon and intermetallic compounds nanosized particles.

Exposure of silumin specimens irradiated with a pulsed electron beam (25 J/cm^2, 200 μs, 3 pulses) at a temperature of 400^0C for 4 hours led to partial destruction of the structure of cellular crystallization and growth of cells, as well as an increase in the size of particles of the second phase located at the boundaries of the cells.

C3-O-050001

GIANT RADIATION-DYNAMIC EFFECTS DURING CORPUSCULAR IRRADIATION AND THEIR PRACTICAL USE FOR ION-BEAM MODIFICATION OF THE PROPERTIES OF METALS AND ALLOYS

V.V. OVCHINNIKOV[1]

[1]*Institute of Electrophysics, Ural Branch of Russian Academy of Sciences, Yekaterinburg, Russia*

Nanoscale dynamic effects and processes in metals and alloys are considered for cascade-forming types of irradiations by heavy ions, neutrons, and fission fragments. The role of these processes is beyond the scope of classical radiation physics of condensed matter.

The sources of shock-wave effects studied and used in practice are the regions of passage of dense cascades of atomic displacements, r ~ 5 nm, thermalized over times of the order of one trillionth of a second (thermal spikes) with gigantic temperatures and thermal pressures in these regions (T = 3000-6000 K, P = 5-40 GPa), which are sources of powerful elastic and shock post-cascade waves. Shock-wave effects must be taken into account for cascade-forming types of irradiation, along with purely migration processes involving radiation defects, which are considered by classical radiation physics.

A theory of self-propagating (theoretically over unlimited distances) structural-phase transformations in metastable media initiated by ion bombardment has been developed.

In practice, this ensures: 1) an increase in the zone of action of penetrating radiation on materials by at least 3-5 orders of magnitude, in particular, the depth of action of accelerated ions (with energies of tens and hundreds of keV) up to several mm or more with projective ranges R_p of such ions in substance within only 0.01-1 μm; 2) lowering the temperature of initiated transformations by tens and hundreds of degrees compared to similar thermally activated processes; 3) an increase in the rate of migration of atoms by several orders of magnitude in comparison with thermally and radiation-stimulated processes.

The report considers examples of radiation-induced processes (structural-phase and intraphase transformations) in metals and alloys with changes in electrical, magnetic, mechanical, resource, and other characteristics.

Practical applications concern the modification of the properties of functional materials. Namely, the modes of ion-beam processing are proposed, providing: zero value of the TCR of high-resistance alloys for precision resistors of the Fe-Pd-Au system (in the range of T=300-700 K). As a result of joint work with scientific and technical organizations and industrial enterprises, a decrease in watt losses for magnetization reversal was achieved (from 5 to 35%) for strips of transformer steels and nanocrystalline tapes made of magnetically soft materials (a patent was received).

A technology has been developed for multiply accelerated cold radiation annealing of sheets and profiles of industrial aluminum alloys (together with Kamensk Uralsky Metallurgical Works (KUMZ)) by beams of accelerated Ar^+ ions (E = 20-40 keV) for 5-30 s at 150-200 K temperatures, providing a 2-3-fold reduction in labor intensity and energy intensity of the process, instead of a long 2-6 hours of standard intermediate furnace annealing. There is a patent for the method of ion-beam processing and an act of approbation at JSC KUMZ with a recommendation to use the process as a breakthrough industrial technology.

It has been established that the irradiation of hot-pressed and aged profiles from alloys D16 (Al-Cu-Mg) and B95 (Al-Zn-Mg-Cu) for several seconds with small (10^{15}-10^{16} cm^{-2}) fluences of Ar^+ ions (E = 20 keV) increases their plasticity. At the same time, the resource during standard tests at loads of the order of $0.3\sigma_u$ (measured by the number of cycles before failure) increases for these alloys, respectively, by 2.4 and 5 times (from several hundred thousand to a million cycles and more).

Rapid (within a few seconds) processes of formation in alloys of phases depleted and multiply enriched in chemical elements during ion bombardment at temperatures much lower than the activation threshold for thermal diffusion have been discovered, which are of fundamental interest. The emerging near-equilibrium states cannot be obtained by any other means. This makes it possible to detect theoretically predicted as well as unknown low-temperature phases (which are "things in themselves") with unknown properties.

Based on the analysis of the emission spectra of targets made of Al, Fe, W, Zr, and other metals, for the first time, measured the temperatures of the above-mentioned thermal peaks and estimated the thermal pressures. The substantiation of a unified fractal structure of cascades of atomic displacements in a given target is given, regardless of the nature and energy of cascade-forming radiation, which is the basis for the legitimacy of simulation studies of the radiation resistance of reactor materials.

C3-O-051901

NON-SPHERICAL PLASMONIC COPPER NANOPARTICLES IN A TRANSPARENT $MGAL_2O_4$ CERAMIC MATRIX

A.SH. VAGAPOV [1], A.N.KIRYAKOV [1], A.F. ZATSEPIN [1], B.L. OKSENGENDLER [1,2,3], N.V. GAVRILOV [4]

[1]*Ural Federal University, Yekaterinburg, Russia*
[2]*Institute of Materials Science NPO "Physics-Sun" AS RUz, Tashkent, Uzbekistan*
[3]*Institute of Ion-Plasma and Laser Technologies AS RUz, Tashkent, Uzbekistan*
[4]*Institute of Electrophysics UB RAS, Yekaterinburg, Russia*

Plasmonic nanostructures attract high attention due to their promising ability to enhance the physicochemical effects of various devices and sensors [1]. At the micro level LSPR effect can be controlled by setting the required form to plasmonic nanoparticles. Promising plasmonic nanostructures for photonic and optoelectronic devices are copper core-shell nanoparticles. In a solid possible controllable growth of plasmonic nanoparticles in spinel matrix was induced by the method of ion implantation of glasses and radiation-resistant monocrystals of $MgAl_2O_4$ [2]. The aim of this work is to study the optical characteristics of plasmonic nanoparticles formed during spinel ion implantation.

We chose transparent nanocrystalline $MgAl_2O_4$ ceramics as a radiation-resistant material for ion-implantation. Plasmonic copper nanoparticles synthesized by pulsed ion implantation with the synthesis parameters: ion type is Cu^{2+}; working atmosphere is Ar; implantation dose is 1×10^{17} cm^{-2}; accelerating voltage of ions is 30 kV; pulse time is 0.4 ms; discharge current is 60 A. The bombardment was perpendicular to the sample surface.

We analyzed the dependence of the polarization plane of transmitted radiation on the sample rotation angle. Irradiation of plasmon particles with polarized light resolves the SPR band to two maxima (fig. 1a). Two-mode structure of SPR band and its dependence on sample rotation angle and the polarizer position show that the particles have an ellipsoidal shape, and these modes are characteristic for the major and minor axes of the ellipsoid [1]. The two-mode structure of the LSPR band in the polarized optical absorption spectra indicates that the particles in the sample are oriented not chaotically, but co-directionally. Figure 1b shows the approximate orientation of the particles. Additionally, we calculated optical characteristics of plasmonic nanoparticles with the finite element method the, as well as the calculation of the electric field strength near an ensemble of codirectional plasmonic nanoparticles

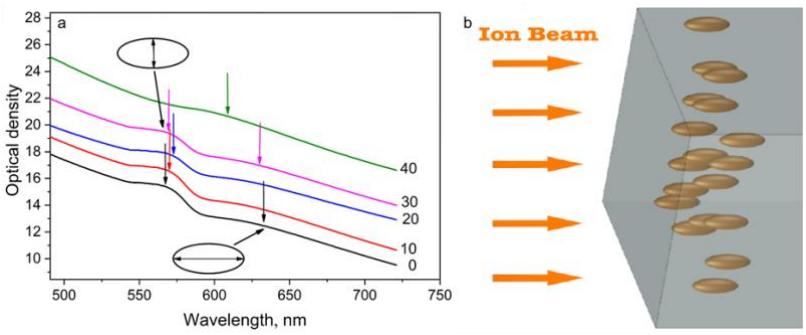

Fig.1. Optical absorption spectra in polarized light (a), approximate orientation of particles formed during implantation (b)

The sensitivity of plasmons to polarized light causes the appearance of microstresses as a result of the coincidence of the polarization planes with the direction of the major and minor axes of the ellipsoid. A conceptual model has been developed for the formation of nonspherical nanostructures as a result of highly nonequilibrium impacts.

REFERENCES

[1] P. Khan, G. Brennan, J. Lillis, S.A Tofail, N. Liu, C. Silien, "Characterisation and manipulation of polarisation response in plasmonic and magneto-plasmonic nanostructures and metamaterials," Symmetry (Basel)., vol.12, no. 8, pp. 1365, 2020

[2] A.F. Zatsepin, A.N.Kiryakov, D.A. Zatsepin, N.V Gavrilov, B.L. Oksengendler, "Ion-beam synthesis of copper nanoparticles in transparent ceramics of aluminum-magnesium spinel." Vacuum., vol. 175, pp. 109243, 2020

C3-P-000901

COMBINED TREATMENT OF ELECTRODES AS A MEANS OF INCREASING THE ELECTRICAL STRENGTH OF VACUUM INSULATION

S.A. ONISCHENKO[1], *E.V. YAKOVLEV*[1], *E.V. NEFEDTSEV*[1], *G.E. OZUR*[1]

[1]*Institute of High Current Electronics, Tomsk, Russia*

One of the methods for increasing the electrical strength of vacuum insulation is the preliminary polishing of the electrodes with a low-energy high-current electron beam (LEHCEB) [1]. A specially selected mode allows us to evaporate or dissolve a significant part of the foreign inclusions in the near-surface volume of the electrode, and make the surface itself smooth. Such treatment allows to increase the pulsed electrical strength of millimeter vacuum gaps to values exceeding 1 MV/cm. However, these values remain more than an order of magnitude less than the theoretically achievable limit which due to the onset of intense field emission from a smooth and chemically pure homogeneous metal surface. A probable reason for this limitation is residual dielectric or semiconductor inclusions fixed in the matrix of the substance, creating triple points on which the electric field is concentrated.

Earlier, we pointed out the possibility of selective removal of the initial surface inclusions by separate short-pulse conditioning of stainless steel electrodes under plasma [2]. After finishing treatment the conditioned electrodes by the LEHCEB, the results were contradictory. Despite the fact that the average value of the pulsed electrical strength of the vacuum gaps practically did not change, the spread of this value increased so much that individual vacuum gaps showed record high values close to 2 MV/cm. This indicated the possibility of further work to improve the quality of vacuum insulation. Based on the short-pulse plasma conditioning method developed in [2], in this paper, additional actions were taken to stabilize the pulsed electrical strength of vacuum gaps at relatively high levels close to 2 MV/cm.

REFERENCES

[1] A.Batrakov, D.Nazarov, G.Ozur, S.Popov, D.Proskurovsky, and V.Rotshtein. IEEE Trans. Dielectr. Electr. Insul., V. 4, pp. 857–862, 1997.

[2] E.V. Nefedtsev, S.A. Onischenko, G.E. Ozur, D.I. Proskurovsky, “Improvement of Electrical Insulation in Vacuum by Comprehensive Treatment of Electrodes under Plasma”, Proc. of 28th International Symposium on Discharges and Electrical Insulation in Vacuum (ISDEIV), pp.97-100, 2018.

C3-P-000902

FORMATION OF SURFACE AMORPHOUS ALLOYS FOR IMPROVING THE ELECTRICAL STRENGTH OF METALLIC ELECTRODES

S.A. ONISCHENKO[1], *E.V. YAKOVLEV*[1], *E.V. NEFEDTSEV*[1]

[1]*Institute of High Current Electronics, Tomsk, Russia*

The initiation of electric breakdown of vacuum gaps is usually associated with geometrical and/or chemical nonuniformities of the electrode surface having high emissive activity: microprotrusions, pores, micro- and nano-particles, dielectrical or semi-conductive films, secondary phase inclusions [1]. In the conditions of using modern methods of materials surface cleaning [2], the factor of electrical strength limitation of vacuum gaps should be sought not only on the surface, but also inside surface layer of electrode material. Recent theories indicate that the initiators of the vacuum breakdown may be defects of crystal structure of electrode material, most likely the dislocations [3].

In this work a possibility of the electrical insulation improvement in vacuum by formation of amorphous alloys on the metallic electrodes surfaces has been studied. It is assumed that the polishing of the electrodes with a low-energy high-current electron beam in a specially selected mode will allow us to evaporate or dissolve a significant part of the foreign inclusions in the near-surface volume of the electrode and make the surface itself smooth. The use of amorphous alloys will avoid the factors of electrical strength limitation connected with defects of the crystal structure of the electrode material.

REFERENCES

[1] Edited by Latham R., High-VoltageVacuum Insulation. Basic Concepts and Technological Practice, London: Academic Press, 568 p, 1995.

[2] G. E. Ozur, D. I. Proskurovsky, V. P. Rotshtein, and A. B. Markov, "Production and application of low-energy high-current electron beams" Laser Part. Beams 21(2), pp 157-174, 2003.

[3] E. Z. Engelberg, A. B. Yashar, Y. Ashkenazy, M. Assaf, and I. Popov, "Theory of electric field breakdown nucleation due to mobile dislocations", *Phys. Rev. Accel. Beams,* vol.22, pp. 083501-(1-16), 2019.

C3-P-002602

SYNTHESIS OF CERAMICS BASED ON SPINELS IN ELECTRIC ARC PLASMA*

V.V. SHEKHOVTSOV, N.K. SKRIPNIKOVA

Tomsk State University of Architecture and Building, TSUAB, Tomsk, Russia

This paper presents the results of an experimental evaluation of the use of thermal plasma energy for the synthesis of ceramic samples based on spinels. Electric arc plasma torch was used as source of thermal energy, which made it possible to realize the complete synthesis of homogeneous melting products in terms of chemical composition. Analysis of the microstructure and phase composition was carried out to identify the key factors influencing the processes formation the microstructure of ceramics by the plasma melting method.

The following materials were chosen as the starting material for the synthesis of spinel-based ceramic samples: boehmite γ-AlO(OH), quartz sand β-SiO_2, magnesite $MgCO_3$. The component composition of the prepared charge corresponded to 30/10/60 wt. %. The prepared mixture was granulated to a fraction of agglomerates of 3–5 mm. An aqueous solution of sodium silicate Na2O(SiO_2)n with a concentration of 8% was used as a binder. The melting of the prepared samples was carried out on an experimental stand, including: electric arc plasma torch with remote discharge, nozzle diameter 5 mm; graphite crucible *h*=55, *d*=35, δ=3 mm; source of power CUT 160. The operating parameters of the plasma torch during the experiments corresponded to: current strength 100 A; voltage 120 V, thermal efficiency 87%, plasma gas flow rate 15 nl/min, exposure time 30 s.

Fig. 1, *a* shows diagram of the experimental stand. Fig. 1, *b* electronic images of the surface obtained melt product.

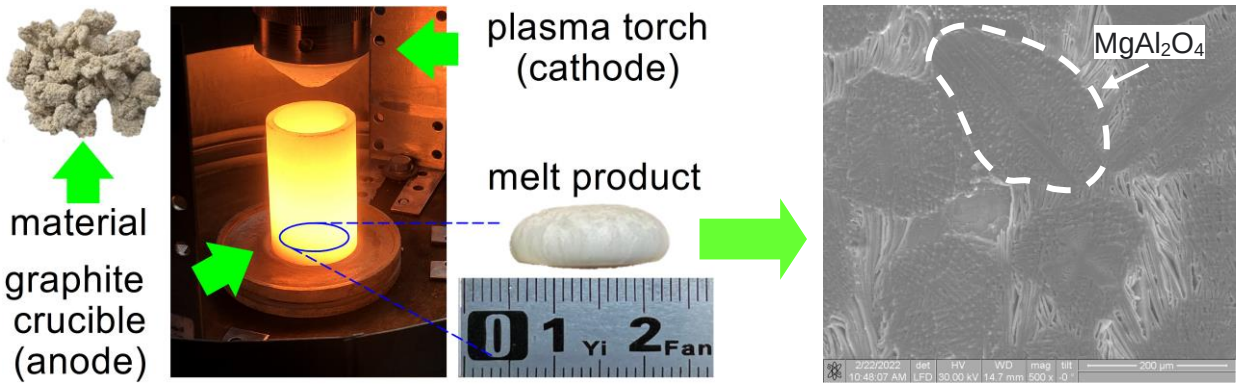

a *b*

Fig. 1. *a* – scheme of the process synthesis of ceramic samples based on spinels;
b – electronic image of the sample surface x500

As can be observed (fig. 1, *b*) the surface morphology of the synthesized spinel-based ceramic sample is represented by clear separation of grains by connected fibers. The shape of the grains is close to oval, and the structure has dendritic structure. According to the XRD results, the products are characterized by crystalline phase $MgAl_2O_4$. The main intensity of the diffraction peaks is at 2θ = 36.8, 44.8, 65.2°; no other impurities were found. Obviously, the grains are the centers of $MgAl_2O_4$ nucleation. Thus, in the work of showing the possibility of using electric arc plasma in the synthesis of ceramic samples based on spinels based on natural materials.

REFERENCES

[1] Nguyen M., Sokolář R., "Corrosion Resistance of Novel Fly Ash–Based Forsterite–Spinel Refractory Ceramics," Materials, vol. 15, no. 4, 1363, 2022.

[2] Pappas J.M., Dong X., "Comparative study of filament-fed and blown powder-based laser additive manufacturing for transparent magnesium aluminate spinel ceramics," Journal of Laser Applications, vol. 33, no. 4, 042037, 2021.

[3] Volokitin O.G., Shekhovtsov V.V., "Prospects of Application of Low-Temperature Plasma in Construction and Architecture," Glass Physics and Chemistry, vol. 44, no. (3), pp. 251-253, 2018.

[4] Volokitin O.G., Shekhovtsov V.V., Maslov E.A., "Plasma treatment technology for silicate melt used in mineral fiber production," Advanced Materials Research, vol. 880, pp. 233-236, 2014.

* The work was carried out with the support of the state task of the Ministry of Science and Higher Education of the Russian Federation FEMN-2020-0004 and grant President of the Russian Federation MK-66.2022.4.

C3-P-004001

HIGH-VOLTAGE NANOSECOND PULSES AND DIELECTRIC BARRIER DISCHARGE IN AIR CONSEQUENCES ON PHYSICOCHEMICAL PROPERTIES OF NATURAL ILMENITE*

I.Zh. BUNIN, N.E. ANASHKINA

Institute of Comprehensive Exploitation of Mineral Resources of the Russian Academy of Science, IPKON RAN, Moscow, Russia

Ilmenite ($FeO{\times}TiO_2$ or $FeTiO_3$) and rutile (TiO_2) are the main mineral resources to beneficiation in titanium (TiO_2) content for subsequent hydrometallurgy. Gravity and magnetic separation, flotation are often combined to the separation of ilmenite and rutile from gangues. For ilmenite, there are many pretreatment methods to improve its flotability, such as the surface dissolution, roasting, oxidation, introducing ions, attrition-scrubbing raw ores, and microwave irradiation. In this paper we present the results of experimental studies on the impact of two types of nonequilibrium electrical discharges (high-power electromagnetic pulse (HPEMP) and dielectric barrier discharges (DBD) in air at atmospheric pressure) have on the surface morphology, microhardness, and physicochemical properties of natural ilmenite (Juina deposit of Brazil).

With the HPEMP effect, the duration of high-voltage nanosecond pulses was 4–10 ns. Pulse amplitude U~25–30 kV; strength of the electric field in the 5 mm interelectrode gap, $E{\sim}10^7$ $V{\times}m^{-1}$; rate of pulse repetition f=100 Hz. Electrode voltage in the cell of the barrier discharge generator, 20 kV; pulse duration, 8 μs; duration of a pulse leading edge, ~300 ns; rate of pulse repetition, 16 kHz; length of interelectrode gap, ~5 mm. The duration of sample treatment varied in the range t_{treat}=10–150 s. Infrared spectra (FTIR) of ilmenite were recorded throughout the region of 4000–400 cm^{-1} (spectral resolution, 4–6 cm^{-1}) using a Nicolet-380 spectrometer equipped with a special Smart Diffuse Reflectance accessory. Morphology, defects, and elementary composition of new micro- and nanoformations on mineral surface of ilmenite particles have been investigated using methods of Scanning Electronic Microscopy, X-ray Spectral Microanalysis (SEM–EDX) and Confocal Laser Scanning Microscopy (CLSM). The mineral's microhardness was determined according to Vickers (HV, MPa) using the standard he procedure and a PMT-3M microhardness tester. The load on the indenter was 100 g, and the period of loading was 10–15 s.

Extended fragmented traces of streamer discharges with a complex discrete internal structure formed on the surfaces of ilmenite particles as a result of brief (t_{treat}=10–30 s) nonthermal HPEMP treatments (Fig. 1a). When the duration of electrical pulse treatment was extended, ilmenite microhardness fell monotonically from ~670 MPa in the initial state to ~520 MPa (t_{treat}=150 s). The relative drop in microhardness ΔHV_{max} was ~22.4%. The morphological changes in the mineral surface due to the DBD effect were related to the formation of erosive microcraters and paths (Fig. 1b) that resembled microstructural features of the imprints (autographs) of current channels of high-voltage microsecond spark discharge. The ilmenite's microhardness fell monotonically (from 670 MPa in the initial state to 590 MPa at t_{treat}=150 s, ΔHV_{max} was ~12%). Advantages are shown of using brief energy (HPEMP and DBD) treatments (t_{treat}=10–30 s) to modify the chemical structure of surfaces of ilmenite and its physicochemical properties (contact angle, and electrokinetic potential) in order to improve the efficiency of processing complex titanium ores.

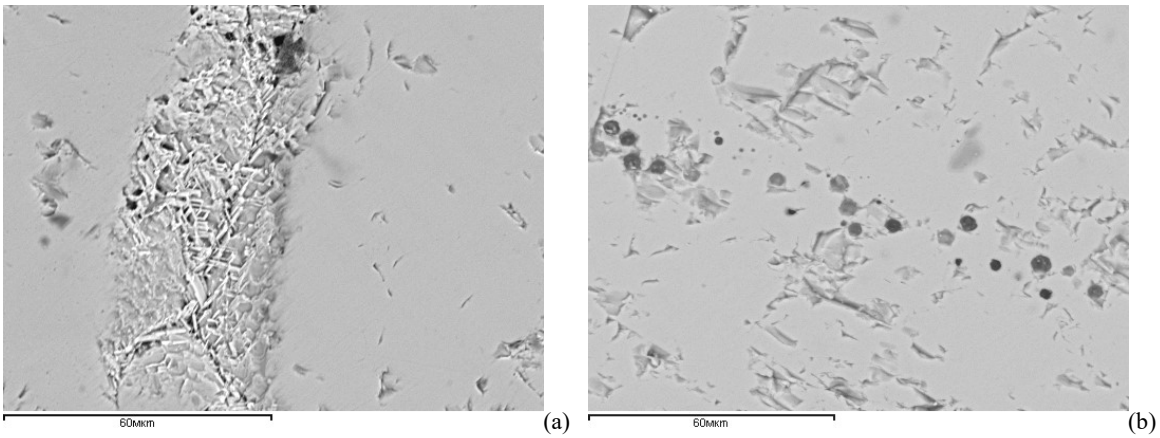

Fig.1. SEM-images of ilmenite surface as a result of (a) HPEMP and (b) DBD treatment (t_{treat}=50 s). SEM; scales 60 μm.

* The work was supported by the President of the Russian Federation under contract number NSh–7608.2016.5 (academician V.A. Chanturiya's scientific school).

C3-P-004202

THE EFFECT OF HEATING ON THE CHARGE NEUTRALIZATION OF Al_2O_3-ZrO_2 CERAMICS DURING ELECTRON BEAM SINTERING IN THE FOREVACUUM PRESSURE RANGE*

A.S. KLIMOV[1], *I.YU. BAKEEV*[1], *A.S. DOLGOVA*[1], *A.A. ZENIN*[1]

[1] *Tomsk State University of Control Systems and Radioelectronics, 40 Lenin ave., Tomsk, 634050, Russia*

Ceramic composites based on aluminum oxide and zirconium dioxide are used in conditions of high thermal and mechanical loads. The Al_2O_3-based material is highly corrosion resistant, resistant to most organic and inorganic acids and salts. The main disadvantage of this material is low crack resistance in a number of structural ceramics. To eliminate this disadvantage, an additive of zirconium dioxide (ZrO_2) is used, which has high hardness, corrosion resistance, and high crack resistance among ceramic materials. By combining the two components ZrO_2 and Al_2O_3, solid and durable Al_2O_3-ZrO_2 ceramics are obtained. Due to the contribution of highly solid Al_2O_3, the phases of zirconium oxide are stabilized.

Currently, there are many ways of sintering Al_2O_3-ZrO_2 composite. One of the most novel methods that allows sintering in a short time is electron beam sintering in the forevacuum pressure region. When irradiating nonconducting ceramic materials at working gas pressures of several tens of pascals, the charging of the surface is reduced due to the plasma generated by the electron beam. In addition, as it was shown earlier, when the ceramic is heated, its electrical conductivity increases, which also helps to reduce the charge on its surface [1]. There have been no detailed studies of this phenomenon to date, which served as the subject of this study. Figure 1 shows the dependence of the current flowing through Al_2O_3-ZrO_2 ceramics when it is irradiated with an electron beam. A composite consisting of 75% (wt.) Al_2O_3 and 25% (wt.) ZrO_2 was used as a target.

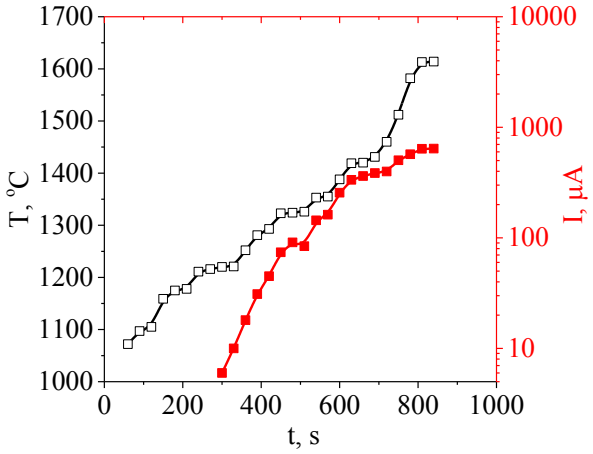

Fig.1. The dependence of temperature and current flowing through Al_2O_3-ZrO_2 ceramics during its sintering.

It can be seen that during electron-beam irradiation of the composite, the current through the sample increases with increasing temperature. The increase in current is due to an increase in the electrical conductivity of ceramics and can lead to additional heating of ceramic grains due to the flowing current. Such heating helps to reduce the sintering time of ceramics. The simulation of the current flow showed that the current value also depends on the composition of the ceramics.

REFERENCES

[1] A.S. Klimov, V.A. Burdovitsin, A.A. Zenin, E.M. Oks, O.L. Khasanov, E.S. Dvilis, A.O. Khasanov, «Specific features of the charge neutralization of silicon carbide in sintering by electron beam in the forevacuum range of pressures», Technical Physics Letters, vol. 41(8), pp. 747-749, 2015.

* The work was supported by Council on Grants of the President of the Russian Federation under the project MD-754.2021.4.

C3-P-005001

SURFACE TOPOGRAPHY AND ELEMENTAL COMPOSITION OF CRATERS ON THE SURFACE OF TANTALUM

A.B. LIGACHEV[1], G.V. POTEMKIN[2], M.V. ZHIDKOV[3], Y.R. KOLOBOV[3], S.K. PAVLOV[2], V.L. TARBOKOV[2], G.E. REMNEV[2]

[1]Prokhorov General Physics Institute of the Russian Academy of Sciences, Moscow, Russia
[2]Tomsk Polytechnic University, Tomsk, Russia
[3]Institute of Problems of Chemical Physics of RAS, Chernogolovka, Russia

The structure of the crater formed on the surface of tantalum after the impact of high power pulsed ion beam (HPPIB) (carbon ions C^{n+}, accelerating voltage 250 kV, pulse energy density 2.6-3 J/cm^2 , current density 130-150 A/cm^2) was studied by scanning electron microscopy.

After exposure to three pulses, cracks form on the surface along the direction of deformation of tantalum. Also round-shaped microcraters with a diameter of 2-5 microns form on the surface. The relief of the modified surface is smoothed out. After exposure to 10 pulses, the size of craters increases to a diameter of 20-30 microns.

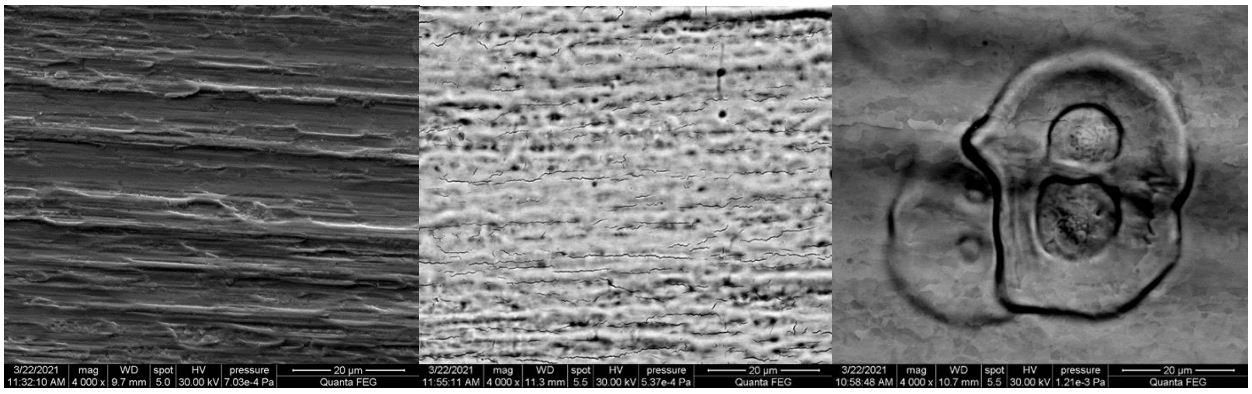

a b c

Fig.1. Top-view topography of the surface of samples of tantalum before (a) and after 3 (b) and 10 (c) pulses of HPPIB processing at F=2.6 - 3 J/cm^2.

C3-P-005701

HEAT TRANSFER ESTIMATION DURING LASER-ASSISTED METAL-INDUCED CRYSTALLIZATION OF AMORPHOUS SILICON FILMS*

L.D. VOLKOVOYNOVA[1], *I.O. KOZHEVNIKOV*[1], *A.M. PAVLOV*[1], *A.A. SERDOBINTSEV*[1], *A.V. STARODUBOV*[1,2]

[1]*Saratov State University, Saratov, Russia*
[2]*Saratov Branch, V.A. Kotel'nikov Institute of Radio Engineering and Electronics RAS, Saratov, Russia*

Elaboration of new methods of polycrystalline silicon films formation on low-melting substrates is of great interest today [1]. Using of such substrates (glass or plastic) has two main advantages: decrease of the end product cost and extension of the possible application toward wearable devices. An original approach to amorphous silicon film crystallization on glass [2] and polyimide [3] substrates was developed by our group. This approach using common fiber 1064 nm laser and thin metal layer for laser power absorption on the top of the a-Si film to be crystallized. Applying Al or Ni as a metal for absorption layer the temperature of c-Si formation can be lowered due to metal-induced crystallization mechanism [4]. This work is devoted to developing of simple estimation approach of heat energy transferring to amorphous silicon layer and underlying substrate during laser-assisted metal induced crystallization.

We considered a simple static case of heat distribution between metal absorption layer and amorphous silicon film. Estimation was done for 1000 nm thick a-Si film with 300 nm Al absorption layer. Laser processing parameters were the following: beam diameter 20 μm, pulse power 0.2, 0.4 and 0.6 W and the laser scanning rate was varied from 25 to 250 mm/s. To take into account speed variation the laser fluence was calculated according with the work [5]. Taking into account material constants for Si and Al and the laser processing parameters it is possible to evaluate a maximum laser scanning rate for Al layer completely evaporized that is near 200 mm/s. Decreasing the scanning rate leads to increase of excessive heat energy transferred to a-Si film. Dependence of excessive energy vs. scanning speed for three levels of pulse power is shown oh Figure 1.

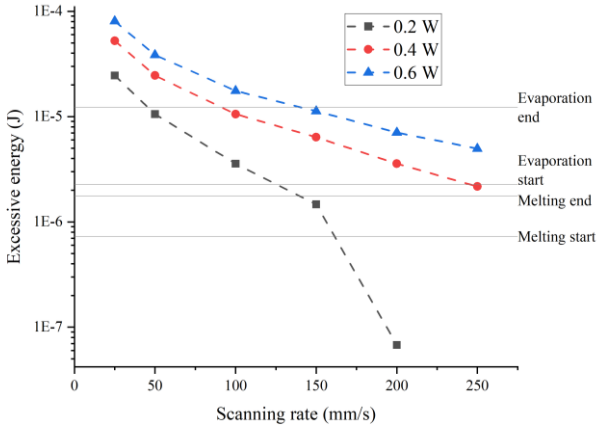

Figure 1. Excessive heat transferred to a-Si film for varied scanning rate and pulse power

It can be concluded that optimal crystallization conditions are 0.2 W pulse power and 150-200 mm/s scanning rate. The a-Si film start to melt but its evaporation is not occurred yet.

REFERENCES

[1] N. Vouroutzis, J. Stoemenos, N. Frangis, G.Z. Radnóczi, D. Knez, F. Hofer, B. Pécz, Structural characterization of poly-Si Films crystallized by Ni Metal Induced Lateral Crystallization, Sci. Rep. 9 (2019) 1–8. https://doi.org/10.1038/s41598-019-39503-9.

[2] A.A. Serdobintsev, I.O. Kozhevnikov, A. V. Starodubov, P. V. Ryabukho, V. V. Galushka, A.M. Pavlov, Scalable Approach for Amorphous Thin Silicon Films Near-IR Laser-Induced Crystallization Using Nickel Absorption Layer, Phys. Status Solidi. 216 (2019) 1800964. https://doi.org/10.1002/pssa.201800964.

[3] A.A. Serdobintsev, V.A. Luzanov, I.O. Kozhevnikov, P. V. Ryabukho, D.M. Mitin, D.N. Bratashov, A. V. Starodubov, A.M. Pavlov, Thin amorphous silicon films crystallization upon flexible substrates, J. Phys. Conf. Ser. 1400 (2019) 055034. https://doi.org/10.1088/1742-6596/1400/5/055034.

[4] Z. Wang, L.P.H. Jeurgens, E.J. Mittemeijer, eds., Metal-Induced Crystallization, Taylor & Francis Group, LLC, Boca Raton, 2015.

[5] I. Rasulov, I. Kozhevnikov, A. Serdobintsev, V. Atkin, A. Zakharevich, A. Starodubov, Study of the ablation regimes of thin copper films on dielectric substrates by nanoseconds laser pulses, in: V.L. Derbov (Ed.), Saratov Fall Meet. 2020 Laser Physics, Photonic Technol. Mol. Model., SPIE, 2021: p. 42. https://doi.org/10.1117/12.2591042.

* The work was supported by the Russian Foundation for Basic Research under grant No. 20-07-00929.

C3-P-006201

MODELING OF THERMAL FIELDS DURING LASER ALLOYING WITH NITROGEN OF THE SURFACE OF STRUCTURAL STEELS*

R.S. ESIPOV, A.A. ARSENTIY, E.A. TYAPUNOVA, A.V. ASYLBAEV

[1]*Ufa State Aviation Technical University, Ufa, Russian Federation*
email

It is known that to increase the duration of the surfaces of machine parts and mechanisms, hardening chemical-thermal treatment is used. Recently, laser surface treatment of metals and alloys has been expanding. With this treatment, the temperature effect and its duration are important factors that determine the result of the treatment. This paper presents a computer model that makes it possible to determine and predict temperature fields on the surface of a sample during laser pulsed processing. The paper considered a two-dimensional problem of modeling thermal fields and thermal cycle. The calculations were carried out using the COMSOL Multiphysics®.

On Fig. 1. shows the direction of heat fluxes arising on a sample with dimensions of 4 × 4 × 1.5 mm. Where Q_1 is the heat flux from the pulsed laser source and directed to surface 2, Q_2 are heat losses from convective heat exchange between the environment and the body, directed from surfaces 1, 2 and 3, Q_3 are heat losses from radiation directed from surfaces 1, 2 and 3. Surface 4 is assumed to be isolated.

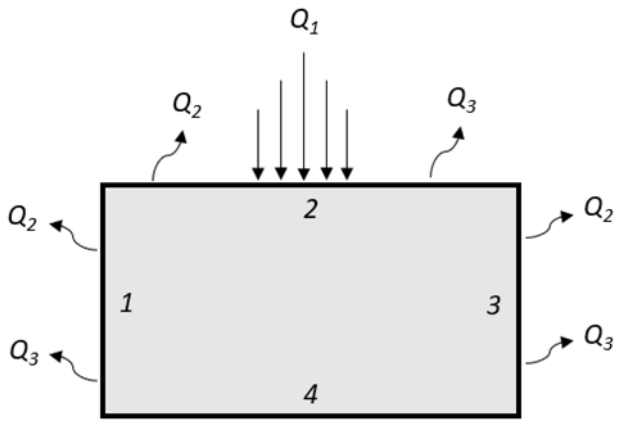

Fig.1. Two-dimensional calculation scheme of the thermal model.

This article presents a two-dimensional computer model of thermal processes when a material is heated by a stationary laser beam in a pulsed mode, which makes it possible to predict and study thermal cycles for various technological processing parameters. In addition, the developed model makes it possible to calculate thermal cycles and fields at different sample depths.

The obtained results of the calculation make it possible to determine the optimal technological modes that are relevant for chemical-thermal and heat treatment without melting the surface of metals and alloy.

REFERENCES

[1] P. Shaaf, “Laser nitriding of metals,” Progress in materials science, vol. 47, no. 1, pp. 1-161, 2002 .

[2] D. Höche, J. Kaspar, P. Schaaf, “Laser nitriding and carburization of materials,” Laser Surface Engineering, pp. 33–58, 2015.

[3] N. Maharjan, W. Zhou, Y. Zhou, Y. Guan and N. Wu, “Comparative study of laser surface hardening of 50CrMo4 steel using continuous-wave laser and pulsed lasers with ms, ns, ps and fs pulse duration,” Surface and Coatings Technology, vol. 366, pp. 311–320, 2019.

[4] D. Deng, H. Murakawa, “Numerical simulation of temperature field and residual stress in multi-pass welds in stainless steel pipe and comparison with experimental measurements,” Computational materials science, vol. 37, no. 3, pp. 269–277, 2006.

* The work was supported by Grant of the President of the Russian Federation» no. MC-2024.2022.4.

C3-P-007401

ON THE DYNAMICS OF THE CURRENT FLOWING THROUGH A SAMPLE OF ALUMINUM OXIDE CERAMICS WITH TITANIUM DURING ELECTRON BEAM SINTERING

A.A. ZENIN, I.YU. BAKEEV*, A.A. KLIMOV*, E.M. OKS***

** Tomsk State University of Control Systems and Radioelectronics,*
Russia, Tomsk, 40 Lenina ave., 634050
*** Institute of High Current Electronics SB RAS, 2/3 Academichesky Ave., Tomsk, 634055, Russia*

Trends in the development of modern technologies require the development of new and improvement of existing composite materials, both organic and inorganic. One of the promising materials from the point of view of technology are various composites based on a matrix of alumina ceramics [1]. The physical and mechanical properties of finished products depend both on the initial composition of the compacted mixture and on the technology of its further sintering. Plasma electron-beam technologies developed at the TUSUR Department of Physics make it possible to treat conductive and non-conductive materials [2]. One of the areas of work of this research team is the electron-beam sintering of ceramics [3]. This work is devoted to the study of current flow through a sample of alumina ceramics with the addition of 10% titanium.

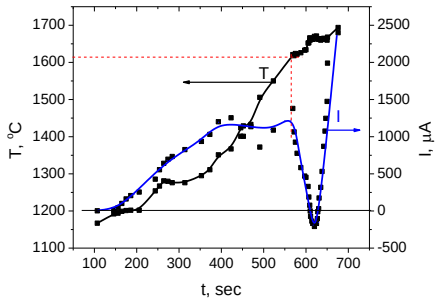

Fig. 1. Dynamics of changes in the flowing current through the sample during electron-beam sintering of aluminum oxide ceramics with titanium depending on temperature

Several characteristic areas can be clearly distinguished from the graph presented in Fig. 1. So, at temperatures of the surface of the sintered sample from 1200 to 1350 ℃, a monotonous increase in the current flowing through the sample is observed, while the current reaches about 1000 μA. With a further increase in the sample temperature in the range of 1400-1630 ℃, the current growth stops. However, when a certain critical temperature value of 1630-1640 ℃ is exceeded, a sharp decrease in current is observed down to a change in polarity, and upon subsequent heating, the current again increases to the previous values and even higher. Such dynamics of the current flow, namely, the observed current drop through the sample, can be explained by the thermionic emission of titanium on the surface of the compact. With the subsequent evaporation of titanium, the current returns to its original values.

The work on electron beam formation was partly supported by the grant from the Ministry of Science and Higher Education of the Russian Federation within the framework of the 2021 competition "Creation of new laboratories, including under the guidance of young promising researchers" of the national project "Science and Universities" FEWM-2021-0013, whereas investigation of the current passing through the samples was supported by Council on Grants of the President of the Russian Federation under the project MD-754.2021.4.

REFERENCES

[1] Richerson, W. Modern Ceramic Engineering, Properties: Processing and Use in Design. – London: CRC Press. –2020. – 803 p.

[2] *Oks, E. Plasma Cathode Electron Sources: Physics, Technology, Applications / E. Oks. – Weinheim : Wiley - VCH Verlag GmbH & CO. KGaA, 2006. – 171 p. – ISBN 978-3-527-40634-0. – DOI 10.1002/9783527609413.*

[3] *Burdovitsin V.A, Klimov A.S, Oks E.M, // On the possibility of electron-beam processing of dielectrics using a fore-vacuum plasma electron source.// TECHNICAL PHYSICS LETTERS Volume: 35 Issue: 6 Pages: 511-513 Published: JUN 2009.*

C3-P-012501

EVOLUTION OF THE STRUCTURE AND PROPERTIES OF AISI 1020 STEEL SUBJECTED TO "ELION" NITRIDING IN A LOW-PRESSURE GAS DISCHARGE PLASMA*

YU.H. AKHMADEEV, I.V. LOPATIN, YU.F. IVANOV, E.A. PETRIKOVA, M.E. RYGINA

Institute of High Current Electronics SB RAS, Tomsk, Russia

The nitriding technique for steel AISI 1020 with electron plasma component sample heating has been developed. A nitriding regime for 500 μm thick hardened layer formation has been revealed (Fig. 1). The steel surface layer microhardness increasing with an increasing in the nitriding temperature is shown that correlates with the relative content of the nitride phase. The maximum microhardness value in nitriding temperature range from 450 to 600°C was fixed at a temperature of 520°C in the near-surface layer at a depth of ≈10 μm. The steel wear resistance was established as depending on the nitrogen atoms concentration in the crystal lattice of α-Fe. The micropores in the steel surface layer nitrided at 520°C is shown to contributes the material wear increasing under dry friction conditions.

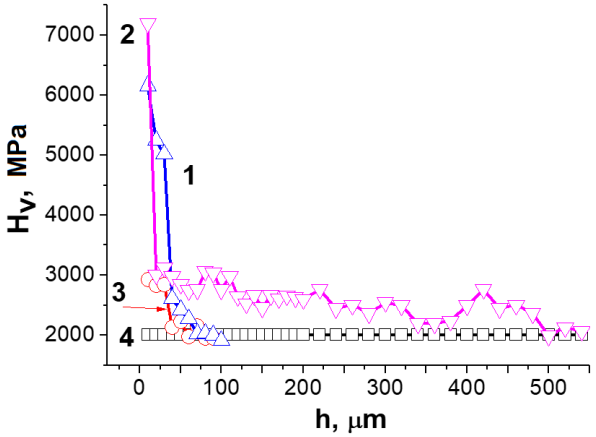

Fig.1. Microhardness profiles of AISI 1020 steel samples subjected to nitriding at temperatures of 600°C (curve 1), 520°C (curve 2), and 450°C (curve 3); curve 4 - AISI 1020 steel in the initial state

Nitriding of AISI 1020 steel samples was carried out in the “elion” mode, which provides efficient heating of the processed samples by the electronic component of the plasma.

It has been established (using X-ray microanalysis) that the nitrogen concentration in the surface layer of steel varies nonmonotonically, reaching a minimum value of 13.5 at. % at a nitriding temperature of 520 °C. It is shown that after steel nitriding at temperatures of 520°C and 600°C, the main phase (85 and 93 wt. %) of the surface layer of the samples is iron nitride of composition Fe4N; at a lower temperature, the main phase (97 wt. %) is a solid solution based on α-iron.

It has been found that the microhardness of the surface layer of steel increases with an increase in the nitriding temperature and depends in a correlated manner on the relative content of the nitride phase. It is shown that the maximum value of microhardness at nitriding temperatures of 450 °C and 600 °C is fixed on the nitriding surface; at a temperature of 520 °C - in the subsurface layer at a depth of ≈10 μm. The greatest thickness of the hardened layer (up to 500 μm) is achieved after nitriding at 520°C. It has been established that steel samples nitrided at 520°C are characterized by relatively high wear values, which is primarily due to the presence of micropores that contribute to material embrittlement.

* The reported study was supported by RFBR and ROSATOM, project number 20-21-00111.

C3-P-017602

IMPROVEMENT PROPERTIES OF PROTECTIVE COATINGS ON ZIRCONIUM ALLOYS AND AUSTENITIC STAINLESS STEELS BY PRE-TREATMENT WITH HIGH-INTENSE PULSED ION BEAMS*

V.A. TARBOKOV[1], *M.S. SLOBODYAN*[2], *S.K. PAVLOV*[1], *E.A. SMOLYANSKIY*[1], *D.G. KROTKEVICH*[1], *V.A. RYZHKOV*[1], *V.V. UGLOV*[3], *G.E. REMNEV*[1]

[1]*Tomsk Polytehcnic University, Tomsk, Russia*
[2] *Tomsk Scientific Center of the Siberian Branch of the Russian Academy of Sciences, Tomsk, Russia*
[3]*Belarusian State University, Minsk, Belarus*

We have investigated the effect of pre-treatment of metal substrates with a high-intense pulsed ion beam (HIPIB) on functional properties of subsequently deposited protective coatings. Austenitic stainless steel and the Zr-1%Nb alloy have been studied, which are widely used in the nuclear industry as a structural material for fuel assemblies. The following irradiation parameters have been applied: the accelerating voltage of 200kV, pulse duration of 90ns, and the energy density per pulse of 1.5J/cm^2. After irradiation, coatings of both Fe-Cr-Al and Al-Si-N systems have been deposited by magnetron sputtering. Then, both normal and loss-of-coolant accident (LOCA) conditions for water-cooled nuclear reactors are simulated. In the first way, radiation damage was modeled using protons accelerated to 400keV at a current density of 0.667μA/cm^2 and a fluence of $2.25 \cdot 10^{16}$ proton/cm^2. The second modeling method was the hydrogenation of samples in hydrogen (purity 99.999%) at a temperature of 360°C and a pressure of 2 atm. for 80 minutes. After irradiating the coatings with protons or saturating them with hydrogen, high-temperature oxidation of the samples was carried out in air and steam at a temperature of 1000ºC for 180 seconds. Finally, the oxidized samples have been studied by scratch tests and subsequent investigations using scanning electron microscopy in order to understand the effect of the pre-treatment procedure.

The results of testing samples for resistance to high-temperature oxidation have showed that the HIPIB treatment of the surfaces of both stainless steel and zirconium alloy has reduced their weight gain. In addition, the HIPIB pre-treatment of the stainless-steel surface has enhanced adhesion of both Fe-Cr-Al and Al-Si-N coatings under the simulated normal and LOCA conditions.

* The work was supported by RFBR and ROSATOM, project number 20-21-00025.

The research was carried out using the equipment of the Centers for Sharing Use ‘Nanotech’ of the ISPMS SB RAS and the ‘Nanomaterials and Nanotechnologies’ of Tomsk Polytechnic University

C3-P-017803

SYNTHESIS OF TI-6AL-4V SURFACE LAYER ALLOYED WITH Ag BY COMBINED ION-PLASMA TREATMENT

A.V. BASALAI[1], *N.N.CHERENDA*[2], *A.YU. ISOBELLO*[1],

A.P. LASKOVNEV[1], *V.V. UGLOV*[2], *V.M. ASTASHYNSKI*[3], *A.M. KUZMITSKI*[3]

[1] *State Scientific Institution "The Physical Technical Institute" of the National Academy of sciences of Belarus, Minsk, Belarus*
[2]*Belarusian State University, Minsk, Belarus,*
[3]*A.V.Lyikov Heat and Mass Transfer Institute of the National Academy of sciences of Belarus, Minsk, Belarus*

Titanium alloys (in particularly Ti-6Al-4V) are widely used in the manufacture of medical implants. It is widely accepted that post-operative implant-related infections are associated with biofilm, dense extracellular polymeric substances produced by adherent microbial aggregates [1]. One of the widely adopted strategies is to incorporate antimicrobial agents into the implants. Common methods for improving the antibacterial properties of the implants surface include plasma spray, magnetron sputtering, microarc oxidization [2], etc. It is known that Ag atoms are effective as a broad-spectrum bactericide even against drug-resistant strains [1, 3]. Thus improvement of antibacterial properties can be achieved by additional surface alloying of the Ti-6Al-4V alloy with argentum atoms.

The formation of a titanium-based surface alloy containing argentum was carried out by preliminary deposition of a argentum coating with a thickness of ~ 2 μm on samples of the Ti-6Al-4V alloy by the method of vacuum cathode-arc deposition and subsequent exposure to compression plasma flows (CPF). The samples were processed by three pulses of CPF generated in the nitrogen atmosphere. Energy density absorbed by the surface was varied from 26 to 43 J/cm^2 per pulse. The surface morphology of the samples was studied using scanning electron microscopy. The elemental composition of the samples was determined by X-ray spectral microanalysis (X-ray microanalysis) using Oxford X-ray detector coupled to a scanning electron microscope. The phase composition was investigated by X-ray diffraction analysis.

It has been established that the impact of the CPF on the Ag/Ti-6Al-4V system led to the formation a surface titanium layer alloyed by aluminum, vanadium, and silver with a uniform distribution of elements. The findings showed that plasma treatment resulted in the formation of α-Ti solid solution containing alloying elements in the surface layer and δ-TiN on the surface. The surface nitride film had a dendritic structure in all processing modes, which is associated with crystallization under conditions of a high cooling rate. The phase and elemental composition of the formed surface alloy depended on the energy absorbed by the surface layer. Growth of the energy absorbed by the surface led to decrease of silver concentration (from 20 to 7 wt.%).

The mechanisms and the reasons of the observed effects were discussed.

REFERENCES

[1] W. R. Fordham, S. Redmond, A. Westerland, E.G. Cortes, C.Walker, C. Gallagher, C.J. Medina, F. Waecther, C. Lunk, R. F. Ostrum, G. A. Caputo, J. D. Hettinger, R. R. Krchnavek, "Silver as a Bactericidal Coating for Biomedical Implants", Surface & Coatings Technology, vol 253, pp. 52-57, 2014.

[2] Sh. Maharubin, Yi. Hu, D. Sooriyaarachchi, W. Cong, G. Z. Tan, "Laser engineered net shaping of antimicrobial and biocompatible titanium-silver alloys" Mat. Science & Engineering, vol. 105, pp. 110-118, 2019.

[3] Z. Lei, "Antibacterial activities and biocompatibilities of Ti-Ag alloys prepared by spark plasma sintering and acid etching", Materials Science & Engineering, vol. 92, pp. 121‑131, 2018.

C3-P-017901

EFFECT OF TREATMENT WITH FAST ARGON ATOM BEAMS ON THE FRACTURE RESISTANCE OF THE SURFACE LAYER OF OXIDE AND NITRIDE TOOL CERAMICS*

M.A. VOLOSOVA[1], *A.E. SELEZNEV*[1]

[1]*Moscow State Technological University "STANKIN", Moscow, Russia*

The purpose of this study is to investigate the effect of fast argon atom beam treatment at gas pressure 0.1 Pa, discharge current 2 A and accelerating voltage 4 keV on the fracture resistance of the surface layer of tool ceramics – Al_2O_3/TiC and SiAlON. The particles beam treatment technology was developed to remove the defect layer that is always formed when diamond grinding ceramic cutting inserts. Grinding is necessary for sharpening cutting edges and is the finishing stage of the manufacturing process. The formation of a distinctive defect layer often leads to an intensification of the cutting edge fracture process of ceramic inserts during the machining. It may be assumed that effective removal of the defect layer significantly increases the fracture resistance of the surface layer of ceramic specimens near the cutting edge. Commercially available round ceramic inserts with a diameter of 19.05 mm and a height of 7.9 mm were used for the experiments. The particles beam treatment was carried out for 2 hours. At the selected treatment conditions the thickness of the removed defective layer differed for the investigated tool ceramics and amounted to: for SiAlON - 10 μm; for Al_2O_3/TiC - 12 μm. The SEM-images of the surface layer of the tool ceramics - initial (1) and after particles beam treatment (2) presented in Fig. 1 illustrate the changes involved.

Fracture resistance of tool ceramics (original and after particles beam treatment) was measured according to an original technique. Using a QNESS Q30 automatic micro-hardness tester, a diamond indenter was forcefully pushed onto the surface layer of round ceramic inserts near the cutting edge (Fig. 2).

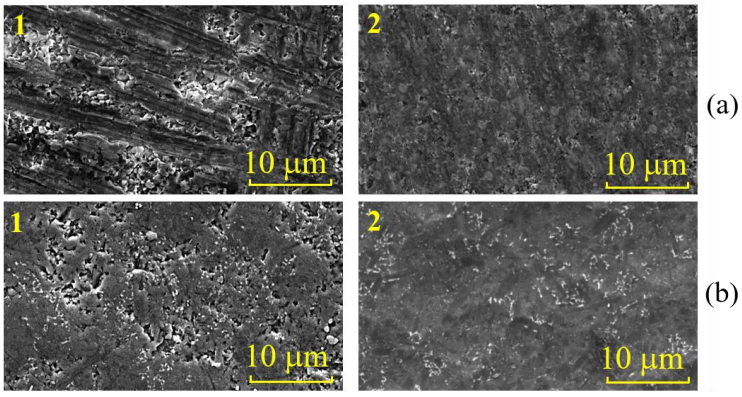

Fig.1. SEM-images of the surface of Al2O3 (a) and SiAlON (b) ceramics.

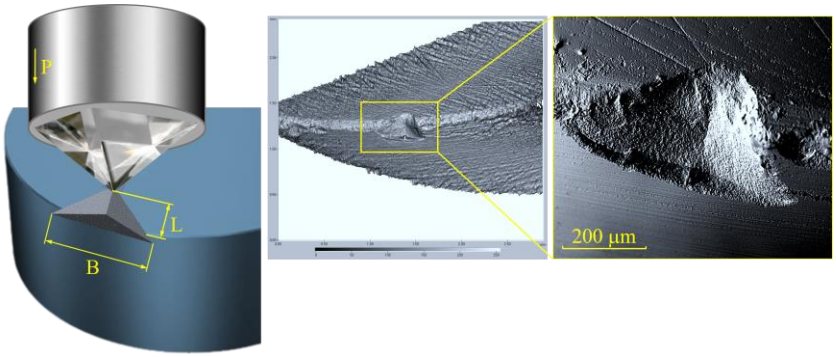

Fig.2. Technique for measuring the fracture resistance of tool ceramics.

The results of experimental investigations showed that the proposed technology of fast argon atom beam treatment significantly increases the critical load at which the area at the cutting edge is fractured. In the case of identical loads on ceramic specimens, the size of the spalling area is significantly reduced.

* This work was supported financially by the Ministry of Science and Higher Education of the Russian Federation (project No 0707-2020-0025).

C3-P-018001

COMPOSITION OF CATALYTIC LAYERS PREPARED BY ION BEAM ASSISTED DEPOSITION OF DYSPROSIUM AND PLATINUM FROM A PULSED ARC DISCHARGE PLASMA ONTO CARBON CATALYSTS CARRIERS [1]

V.V. POPLAVSKY, A.V. DOROZHKO, V.G. MATYS

Belarusian State Technological University, Minsk, Belarus, e-mail: vasily.poplav@tut.by

The aim of this work is to study the composition of the catalytic layers prepared on special carbon carriers of catalysts in the process of ion beam assisted deposition from plasma generated in metal vapors of a vacuum arc discharge, platinum as the main catalytic metal and dysprosium as an activating additive.

As substrates for the preparation of the studied layers we used special carbon materials: Toray Carbon Fiber Paper TGP-H-060 T and AVCarb® Carbon Fiber Paper, which are used as material of diffusion layers of the membrane electrode assemblies for low temperature fuel cells with a polymer membrane electrolyte. The plasma produced in metal vapors of a low-voltage vacuum arc discharge between two metal electrodes at their periodic contact was used to preparation surface catalytic layers by ion beam assisted deposition (IBAD) of dysprosium and platinum onto carbon fiber catalysts carriers. Formation of layers in IBAD mode, by means of the deposition of metal and mixing of precipitating layer with the substrate by accelerated (U = 5 kV) ions of the same metal, was carried out. Investigation of the composition of prepared layers was carried out by EDX, SEM, RBS and WD-XRF methods.

According to EDX (Fig. 1), RBS (Fig. 2) and XRF data, the atoms of deposited metals (Pt, Dy), carrier components (C, and F in the case of Toray Carbon Fiber Paper TGP-H-060 T hydrophobized with Teflon), and oxygen as an impurity is included in the composition of the layers. At the same time, the surfaces contain deposited metals inclusions with sizes of the order of a micrometer (Fig. 1), which arise from the precipitation of metal droplets from the arc discharge of the ion source. The distribution of oxygen over the surface correlates with the distribution of dysprosium (Fig. 1), which may indicate the formation of rare earth metal oxide.

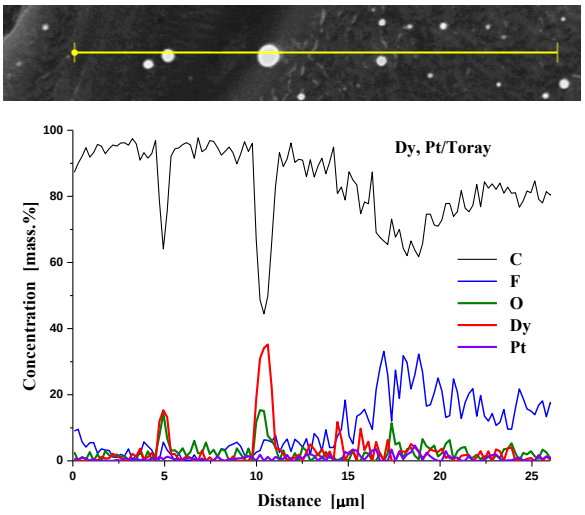

Fig. 1. Distribution of atoms of elements across the scanning line over the surface of Toray Carbon Fiber Paper TGP-H-060 T carrier with layer formed by the IBAD of dysprosium and platinum according EDX analysis.

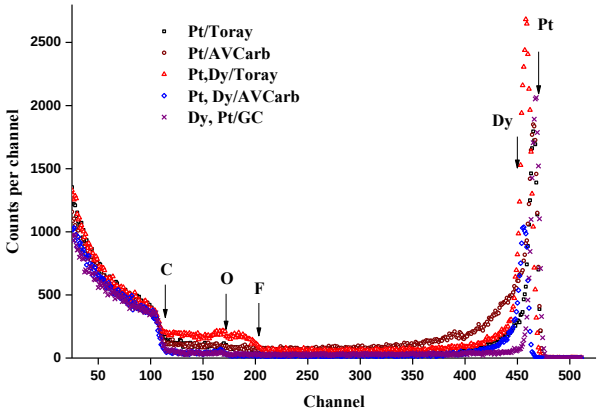

Fig. 2. RBS spectra of ^{4}He ions scattered by atomic nuclei of elements that make up layers obtained by IBAD of metals on Toray Carbon Fiber Paper TGP-H-060 T and AVCarb® Carbon Fiber Paper P500 T carriers, and dense carbon material – glassy carbon (GC).

The thickness of the prepared layers is ~50 nm; content of each of deposited metal atoms in the layers – ~(1–2) × 10^{16} cm^{-2}. In the maximum distribution located near the surface, the concentration of each of the deposited metals is about several atomic percent.

In the process of IBAD of metals in the proposed mode, ionic mixing of all components of the layer being formed takes place. Electrocatalysts with the prepared layers are active in the oxidation of methanol and ethanol reactions, which are the basis of the principle of operation of low-temperature fuel cells.

[1] The work was supported by the Republic of Belarus state research program "Materials science, new materials and technologies".

C3-P-018002

COMPOSITION AND PROPERTIES OF PROTECTIVE LAYERS FORMED BY ION-PLASMA TREATMENT OF TITANIUM ALLOY[1]

V.V. POPLAVSKY[1], A.V. DOROZHKO[1], V.G. MATYS[1], I.L. POBOL[2], I.P. SMIAGLIKOV[2]

[1]Belarusian State Technological University, Minsk, Belarus, e-mail: vasily.poplav@tut.by
[2]Physical-Technical Institute of the National Academy of Sciences of Belarus, Minsk, Belarus

In this paper we investigated the possibility of obtaining chromium-containing layers on the surface of a BT1-0 titanium alloy using ion-plasma deposition, which contribute to increasing the resistance of the material to electrochemical corrosion. Titanium alloys can be used as a material for the manufacture of current collectors of fuel cells. In fuel cells of direct methanol and ethanol oxidation (DMFC and DEFC) the ion exchange membrane Nafion is used as an electrolyte, which is a fluorocarbon polymer containing sulfogroups. Under the operating conditions of the fuel cell, the surfaces of current collectors in contact with the membrane electrode assembly are subjected to electrochemical corrosion due to the high aggressiveness of the medium containing SO_4^- и F^- anions.

Chromium-containing layers on samples of titanium BT1-0 and current collectors made of it were obtained by two methods: ion-plasma deposition and ion beam assisted deposition. Ion-plasma formation of coatings was carried out by deposition from cathode arc erosion plasma generated by an arc source with a chromium cathode in a nitrogen medium – to obtain coatings from chromium nitride and carbon dioxide – to obtain coatings from chromium oxycarbide. The formation of surface layers using ion beam assisted deposition (IBAD) technology was carried out by deposition of chromium, as well as chromium and tin from a vacuum electric arc discharge plasma in a mode in which accelerated (U = 10 kV) ions of the deposited metal are used as assisting the deposition process.

The microstructure and composition of the obtained layers were studied using SEM, EDX and RBS (Fig. 1) methods. The corrosion resistance of titanium alloys with a surface modified in ion-plasma treatment processes to electrochemical corrosion in a solution of 1 M H_2SO_4 + 2×10^{-6} M HF at a temperature of 70–80°C, modeling the operating conditions of current collectors of fuel cells with a polymer membrane electrolyte Nafion is investigated (Fig. 2).

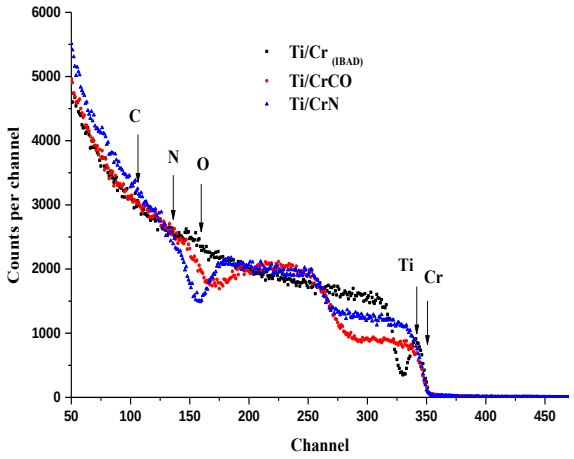

Fig. 1. RBS spectra of ^{4}He ions scattered by atomic nuclei of elements that make up titanium surfaces with layers formed by: chromium IBAD (Ti/$Cr_{(IBAD)}$); ion-plasma deposition of chromium oxycarbide (Ti/CrCO) and chromium nitride (Ti/CrN).

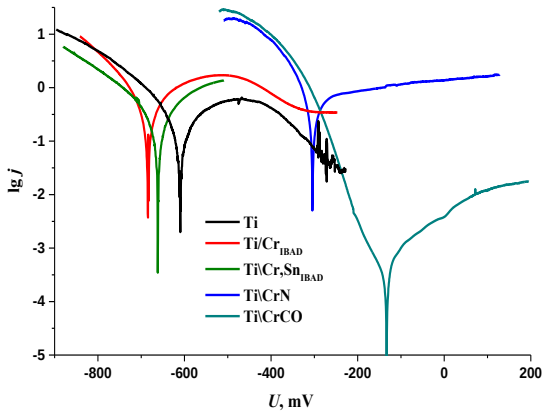

Fig. 2. Polarization curves of the investigated titanium samples in 1 M H_2SO_4 + 2×10^{-6} M HF solution.

IBAD of metals from vacuum arc discharge plasma ensures the formation of nanosice multicomponent layers and is characterized by one-stage operation, it does not lead to a significant increase in corrosion resistance, which may be due to the low chromium content and the small (~30 nm) thickness of the layers. A significant (by more than two orders of magnitude) decrease in the corrosion current density occurs for titanium with a coating formed by ion-plasma deposition of chromium oxycarbide (Ti\CrCO).

[1] The work was supported by the Republic of Belarus state research program “Materials science, new materials and technologies”.

C3-P-018303

HIGH-INTENSITY IMPLANTATION OF LOW-ENERGY ALUMINUM IONS UNDER CONDITIONS OF TITANIUM ION SPUTTERING COMPENSATION*

A.I. RYABCHIKOV, D.O. SIVIN, A.I. IVANOVA O.S. KORNEVA, D.O. VAKHRUSHEV

National Research Tomsk Polytechnic University, Tomsk, Russia

Developing the method of low-energy high-intensity implantation of gas and metal ions into various materials has shown that, in addition to the forming the ion-doped layers with thicknesses of tens and hundreds of micrometers, the new possibilities to modify the surfaces of parts have appeared. These possibilities were previously not available for traditional beam ion implantation.

This work studies the possibility to modify the inner surface of holes with focused low-energy high-intensity metal ions beams. An axially symmetric system of plasma immersion extraction and ballistic focusing ensured the ion beam formation. The impact of the ion beam on the inner surface was carried out in the beam defocusing area.

The study considered the impact of an aluminum ion beam with an average energy of 3 keV on the inner surface of a GRADE-2 titanium pipe with a diameter of 25 mm. The beams were formed from the continuous vacuum-arc discharge plasma with a repetition rate of 40 kHz and a pulse duration of 10 μs.

It has been established that the mutual sputtered material deposition on opposite sides of the hole leads to self-compensation of ion sputtering in axially symmetric holes. The ion sputtering suppression leads to an increase in the ion-doped layer thickness. As a result of ion beam impact on the inner surface of a titanium tube, there were obtained the layers containing titanium aluminide crystallites with a thickness of more than 7.5 μm with a maximum aluminum concentration of more than 25 at.%.

The impact of a high-intensity ion beam in the zone of its defocusing leads to an uneven distribution of the dopant along the length of the lateral surface of the hole. There is also a gradual decrease in the diffusion depth of implanted atoms with distance from the beam focus. The work shows the possibility of a significant improvement in the uniformity of aluminum distribution along the hole inner surface due to the reciprocating movement of the specimen relative to the focal plane of the beam.

The work considers some features of the treating the inner surface of a through and closed hole on one side of the so-called glass.

* The work was carried out with the financial support of the Ministry of Education and Science of the Russian Federation (grant FSWW-2020-0008).

C3-P-020704

STUDY OF THE INFLUENCE OF A POWERFUL PULSED ION BEAM ON TITANIUM DEEPLY-DOPED WITH ALUMINUM*

A.I. RYABCHIKOV[1], O.S. KORNEVA[1], D.O.SIVIN[1], A.I.IVANOVA[1], A.A. CHERNYSHEV[2], V.A. TARBOKOV[1]

[1]National Research Tomsk Polytechnic University, Lenin Avenue 30, Tomsk, 634050, Russia
[2]National Research Tomsk State University, Lenin Avenue 36, Tomsk, 634050, Russia

The work studies the impact of high-intensity implantation of aluminum ions and the subsequent impact of a powerful pulsed ion beam on the microstructure and properties of titanium. The high-intensity aluminum ion beam formation was carried out using a method based on plasma-immersion extraction of ions from the free boundary of a vacuum-arc plasma, their acceleration in a high-voltage sheath layer, followed by ballistic focusing. Specimens of titanium were implanted for one hour at a temperature of 900°C with an irradiation fluence of 10^{21} ions/cm^2. Layers with a thickness of about 150 μm were obtained. The energy impact was carried out by a powerful ion beam with an ion current density on the target of 100 A/cm^2. The paper presents data on changes in the elemental composition, surface morphology, and microstructure of ion-doped and energy-modified layers. It has been established that the additional energy impact on the ion-implanted layer of a powerful pulsed beam improves wear resistance by 10 times. The synergistic of high-intensity ion implantation of aluminum and the energy impact of a pulsed ion beam improves the wear resistance of titanium by eighteen folds.

* The work was supported by the Russian Science Foundation (grant No. 22-19-00051)

C3-P-020705

REPETITIVELY-PULSED NITROGEN IMPLANTATION IN TITANIUM BY A HIGH-POWER DENSITY ION BEAM*

A.I. RYABCHIKOV, O.S.KORNEVA, D.O.SIVIN

National Research Tomsk Polytechnic University, Lenin Avenue 30, Tomsk, 634050, Russia

The paper presents the results of studies of the features and regularities of high-intensity nitrogen ion implantation in titanium using high-power density repetitively-pulsed beams. It has been shown that the method of low-energy high-intensity nitrogen ion implantation at current densities of 180, 140, 60, and 10 mA/cm^2 makes it possible to obtain wide ion-doped layers in titanium. The regularities of changes in both thickness and elemental composition of ion-doped layers depending on the ion current density have been established. It has been established that at ion current densities from 60 to 180 mA/cm^2, a wide diffusion layer is observed. With an increase in the ion current density, an increase in the nitrogen concentration in the diffusion layer is observed. Using X-ray diffraction analysis, it was found that the modified near-surface layer of titanium contains two phases – δ-TiNx and TiN0.3. A change in the crystal lattice period and the volume fraction of δ-phase depending on the ion current density has been noted. Transmission electron microscopy data are presented showing that the modified layers at a depth of 10 μm consist of α-Ti, in the volume of which the nanosized particles of δ-TiN crystallize. The average size these particles is 15.4 nm. The regularities of changes in the ion-doped layer microhardness depending on the ion implantation modes are discussed.

* The work was supported by the Russian Science Foundation (grant No. 22-19-00051)

C3-P-022502

ELION NITRIDING OF AISI 1020 AND AISI 5140 STRUCTURAL STEELS*

I V. LOPATIN, YU H. AKHMADEEV, E.A. PETRIKOVA, M.E. RYGINA, YU.F. IVANOV

Institute of High Current Electronics, Siberian Branch, Russian Academy of Sciences (IHCE SB RAS), Tomsk, Russia

Nitriding of steels AISI 1020 and AISI 5140 was carried out under conditions of exposure of samples to both the ion and electron components of the gas discharge plasma, realizing the "elion" process [1]. This made it possible to control the temperature of the nitriding process without changing the current density of the incident ions and their energy. A nitriding regime has been revealed that makes it possible to form a hardened layer up to 500 and 240 μm thick, respectively. It is shown that the microhardness of the surface layer of steel increases with an increase in the nitriding temperature. It was found that in the nitriding temperature range from 450 to 600°C, the maximum value of microhardness for both steels is fixed at a temperature of 520°C in the near-surface layer at a depth of ≈10 μm. It has been established that the wear resistance of steel is determined by the concentration of nitrogen atoms in the α-Fe crystal lattice. It is shown that the studied steels are subject to different morphological transformations during nitriding under the same conditions.

REFERENCES

[1] Lopatin, I.V., Akhmadeev, Yu.H., Kovalsky, S.S., Ignatov, D.Yu. Arc discharges operation in elion mode // Journal of Physics: Conference Series, 2064(1), 012029, 2021.

* The work was supported by RFBR and ROSATOM, project number 20-21-00111.

C3-P-022901

SYNTHESIS OF THE TIN-CU COMPOSITE LAYERS ON ALLOY T15K6 BY METHOD OF VACUUM-ARC EVAPORATION AND MAGNETRON SPUTTERING*

D.B-D. TSYRENOV[1], A.P. SEMENOV[1], I.A. SEMENOVA[1], M.A. MOKEEV[1]

[1]Institute of Physical Materials Science SB RAS, Ulan-Ude, Russia

The processes of TiN synthesis in Cu vapors appear promising for the synthesis of composite nanostructured TiN–Cu coatings [1]. In this paper, we consider the structure, phase and elemental composition, microhardness of composite TiN-Cu layers on the T16K6 alloy obtained at different values of the arc current, magnetron discharge current, and working gas pressure. The deposition of the composite layers was carried out on a modernized installation with a vacuum arc evaporator and a planar magnetron [2].

TiN-Cu coatings were deposited in copper vapor in the mode of titanium evaporation in argon and nitrogen-containing plasma, dissociation of molecular nitrogen N2 - 2N, and chemical reaction of Ti and N. Samples of alloy T15K6, 18x18 mm in size and 5 mm thick, were used as substrates. For a more efficient sputtering of the magnetron target, a gas mixer was used, in which nitrogen and argon were mixed in different proportions. The proportion of argon ranged from 20% to 50% of the total volume of the working gas. X-ray phase analysis (XRD) was performed on a Phaser 2D Bruker diffractometer (Cukα - radiation). The microstructure of the layers was investigated on a METAM PB-22 microscope. By means a JSM-6510LV JEOL electron microscope with a system of microanalysis INCA Energy 350 Oxford Instruments by scanning electron microscopy and X-ray spectral microanalysis were carried out the study of the surface and determination of the elemental composition. The microhardness of the formed layers was determined using a PMT-3 microhardness meter. X-ray phase analysis was performed according to which the samples contained TiN phases with different crystal lattice and volume fraction. In addition, reflections of copper reflections were recorded, the intensity of which was very low intensity. According to the data of X-ray spectral microanalysis, the content of Ti, N and Cu in various concentrations was detected. The concentration of these elements varies and depends on the deposition conditions. In addition to the main elements, in the coating was found a negligible content of aluminum, tungsten and oxygen.

The thickness of the TiN layers and the TiN-Cu composite ranged from 2-3 microns to 5-8 microns depending on the deposition time. Figure 1 shows a microimage of T15K6 alloy sample with the deposited TiN-Cu layer.

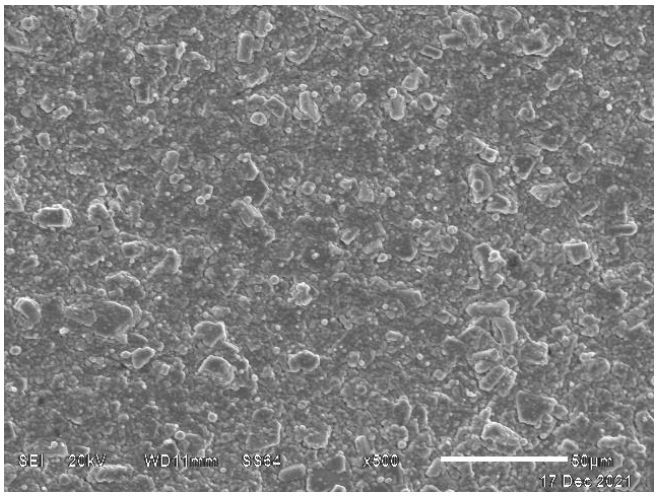

Fig.1. The surface of TiN-Cu layer deposited on the T15K6 alloy.

REFERENCES

[1] He J.L., Setsuhara Y., Shimizu I., Miyake S. // Surface and Coatings Technology. 2001. V. 137. P. 38–42.

[2] A.P. Semenov, D.B-D. Tsyrenov, I.A. Semenova // Instruments and Experimental Techniques. 2017. Vol. 60. №6. Pages 892-895.

* The work was supported by the State Job of the Ministry of Science and Education of the Russian Federation (topic no. 0270-2021-0001)

C3-P-024002

FORMATION OF A BORON-BASED PROTECTIVE COATING ON THE SURFACE OF D2 DIE STEEL BY ELECTRON BEAM PROCESSING*

A.S. MILONOV, D.E. DASHEEV

Institute of Physical Materials Science SB RAS, Ulan-Ude, Russia

To improve the performance properties of steels of various grades, various methods of surface treatment of the material are used. Boriding technology occupies not the last place among the common methods. The essence of the technology is to saturate the surface layer of the metal with boron and iron compounds FeB and Fe2B. When boriding by the traditional method, hard boride layers are obtained, but along with high hardness, borides are quite brittle and prone to chipping. In this work to reduce the brittleness of the layers, we studied the saturation of the D2 steel surface with boron under the action of continuous electron beams in vacuum. We have considered the effect of alloying elements on FeB and Fe_2B boride layers.

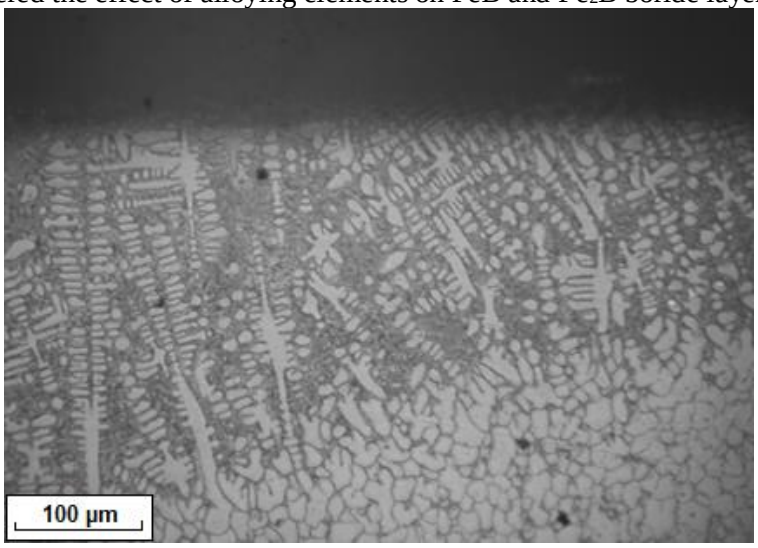

Fig. 1. Boride layer on D2 steel

We investigated the microstructure (Fig. 1) and microhardness (Fig. 2) of the obtained layers. The hardness of D2 steel is 256 HV. The hardness of the boride layer reaches up to 900 HV, and the hardness of the base up to 400 HV. From this we can conclude that the steel itself is hardened by an electron beam.

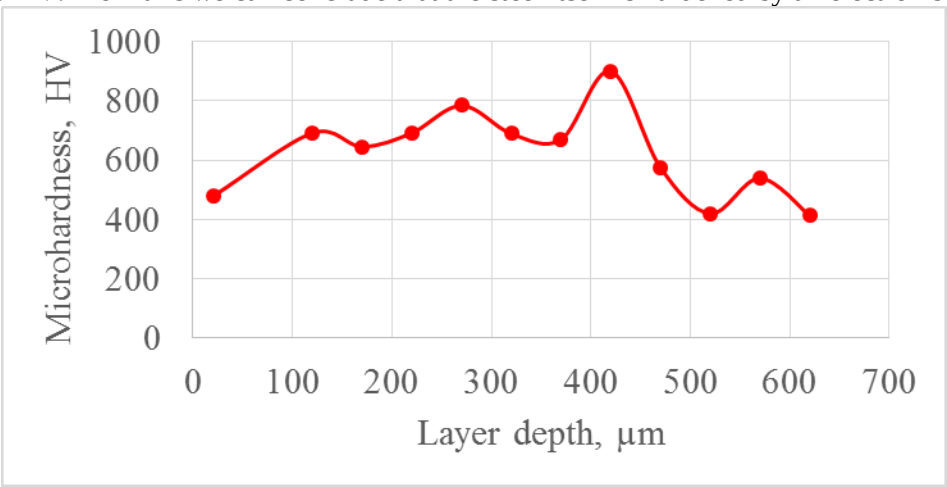

Fig. 2. Microhardness of the boride layer on D2 steel

The results obtained give us the opportunity to consider the use of electron beam boriding of die tool steels in production.

* The work was carried out with the financial support of the state task of the Ministry of Science and Higher Education of the Russian Federation, topic No. 0270-2021-0001

C3-P-034001

CHEMICAL INTERACTION OF THE PARTICLES BEAM WITH THE TARGET MATERIAL*

E.S. PARFENOVA[1], A.G. KNYAZEVA[1,2]

[1]Institute of Strength Physics and Materials Science of Siberian Branch of Russian Academy of Sciences, Tomsk, Russia
[2]Tomsk Polytechnic University, Tomsk, Russia

The different methods of surface treatment of metals with charged particle beams are widely used in order to improve hardness, wear resistance and resistance to chemical attack. Various physical and chemical processes arise after the interaction of particles beam with the target. And these phenomena interact with each other and influence the final result. For example, heating, stress field formation, composition changes, defect generation and migration, formation of new compounds and phases and etc. Only theoretical research allows us to study each such process separately from the others. It is impossible to do it experimentally.

The purpose of this work consists in numerical investigation the co-propagation of elastic mechanical waves and implanted particles, taking into account their chemical interaction with the treated material. The mathematical model takes into account the finite relaxation times of the heat and mass fluxes. Also the thermal conductivity equation and balance equation for the introduced component take into account the heat source/loss due to the chemical reaction and the impurity loss due to the formation of the chemical compound, respectively.

The process of interaction of the charged particle beam with the target surface can be described within the framework of the thermoelastic diffusion theory, taking into account the nonlinear effects associated with the dependence of the diffusion coefficient and the chemical reaction rate on the composition and temperature. In addition, the model is modified for the different number of reactions occurring in the surface layer during processing. We assume that the deformations, velocities and accelerations are small. We consider the particle beam to be uniformly distributed along the treated surface, so we can limit the study by a one-dimensional problem. The case of uniaxial loading under the experimental conditions is realized. The detailed derivation of the equations can be found in [1, 2].

The example of the problem solution for different time moments is shown in Figure 1. The target material is Ni, the introduced material is Al. Time of action of a single sinusoidal pulse is 0.05. Figure 1 shows the distributions for times comparable to the pulse action time.

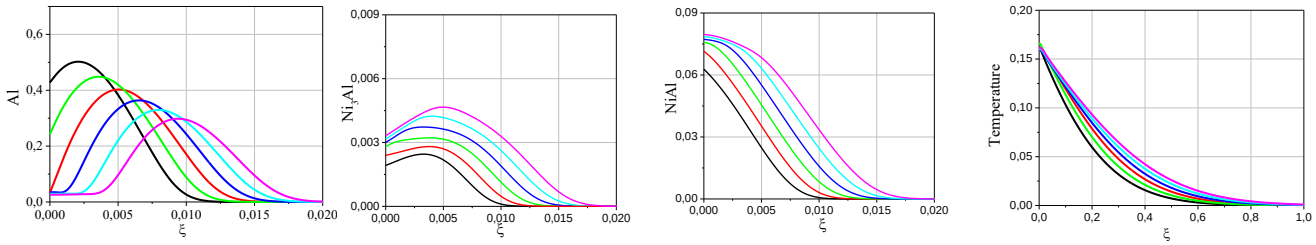

Fig.1. The results of solving a coupled problem: distribution of introduced material concentration (Al), mass content of the first reaction product (Ni_3Al), mass content of the second reaction product (NiAl) and temperature. Time moments are: 1 – 0.04; 2 – 0.045; 3 – 0.05; 4 – 0.055; 5 – 0.06; 6 – 0.65.

It can be seen that diffusion waves propagate much slower than heat wave. The rate of the chemical reaction increases obviously due to an increase in temperature and concentration of the introduced material. Chemical reactions also occur at times longer than the pulse time. As the temperature and implanted material concentration allow its. Because reactions with heat release are considered, then after the pulse stops, the temperature at the left boundary does not decrease and increases for a time.

REFERENCES

[1] A.G. Knyazeva, E.S. Parfenova, “Nonlinear coupled model of surface treatment by a particle beam taking into account the formation of a new phase”, J. Appl. Mech. Tech. Phys., vol. 62, no. 4, pp. 633–641, 2021. DOI: 10.1134/S002189442104012X.

[2] E.S. Parfenova, A.G. Knyazeva, “The influence of chemical reaction parameters on the interaction of thermal, diffusion and mechanical waves under surface treatment by a particle beam”, Comp. Continuum Mech., vol. 14, no. 1, pp. 77-90, 2021. DOI:10.7242/1999-6691/2021.14.1.7.

* The work was supported by the Russian Foundation for Basic Research and the Rosatom state corporation (Grant No. 20-21-00064 Rosatom).

C3-P-035401

ANORTHITE CERAMICS PRODUCED WITH PLASMA TECHNOLOGY

V.V. SHEKHOVTSOV, M.A. SEMENOVYKH, N.K. SKRIPNIKOVA

Tomsk State University of Architecture and Building, TSUAB, Tomsk, Russia

Today, obtaining anorthite ceramics using plasma technologies is an urgent task, as there is an increase in construction volumes and new conditions for building materials and high-quality products. With the help of plasma technologies, today it is possible to obtain a high-quality material with the necessary properties, both physical-mechanical and physicochemical [1, 2].

The following materials were used in this work: lime (CaO), quartz sand (SiO_2) and alumina (Al_2O_3). These oxides are the main ones in the production of ceramic products. They determine the properties and nature of the resulting material.

To obtain anorthite ceramics, the component compositions were selected based on the state diagram [3]. These powder compositions are suitable for the formation of anorthite, as they fall into the field of its crystallization. The component composition is represented by a composition consisting of CaO - 20 wt. %, Al_2O_3 – 37 wt. %, SiO_2 – 43 wt. %.

The scheme of the plasma installation consists of a plasma torch with a remote arc discharge (nozzle diameter 4 mm) installed at a distance of 60 mm from the base of the graphite crucible. Graphite crucible parameters: height 55 mm, diameter 15 mm, wall thickness 3 mm. Melting of 7 g of the material occurred within 30 seconds at: current strength 100 A, voltage 110 V, plasma gas flow rate 14 nl/min (air).

According to this technology, the composition of the component charge was thermally processed. After that, the resulting melt was processed into powder and its phase composition was studied. The obtained data were compared with the data of the original component charge. The resulting radiographs are shown in Fig. 1.

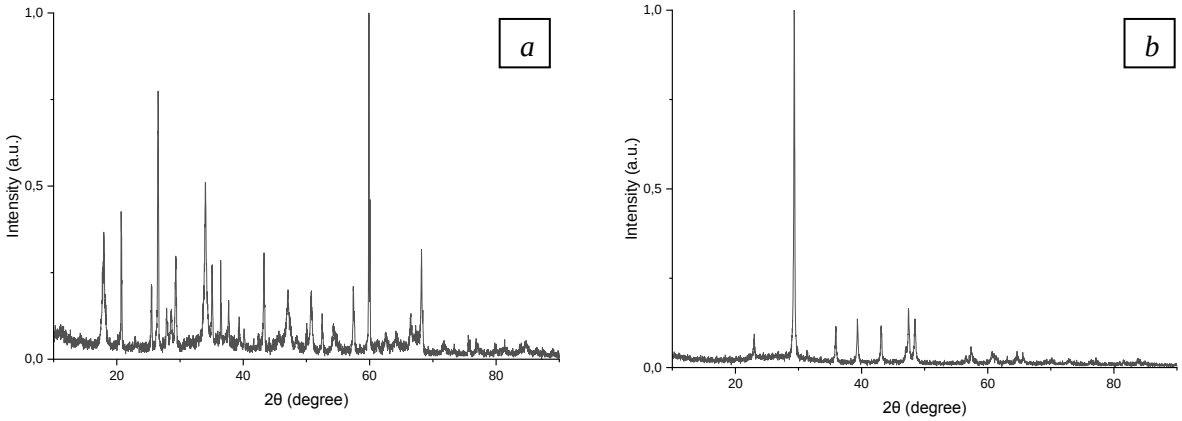

Fig.1. X-ray diffraction patterns of samples: a – component charge; b - melting product

As can be seen from the figure, the obtained X-ray patterns indicate that the phase composition of the component charge (Fig. 1, a) is represented by the phases SiO_2 (d = 0.433; 0.336; 0.263; 0.256;), Al_2O_3 (d = 0.349; 0.154 nm), $CaCO_3$ (d = 0.304; 0.256 nm), as well as some aluminosilicate compounds. The melting product is represented by SiO_2 (d = 0285; 0.229 nm), $CaO{\cdot}Al_2O_3{\cdot}2SiO_2$ (d = 0.170; 0.141; 0.139; 0.121; 0.113 nm).

Thus, the conducted studies have shown the possibility of forming anorthite ceramics using the plasma firing technology.

The work was carried out with the support of the state task of the Ministry of Science and Higher Education of the Russian Federation FEMN-2020-0004 and grant President of the Russian Federation MK-66.2022.4.

REFERENCES

[1] N. Skripnikova, G. Volokitin, M. Semenovykh, V. Shekhovtsov “Features of synthesis of clink minerals under conditions of high-concentrated heat flows”, 7th International Congress on Energy Fluxes and Radiation Effects (EFRE 2020), pp. 769-772, 2020.

[2] Shekhovtsov V., Volokitin O., Skripnikova N., Volokitin G., Semenovykh M. “Thermal plasma in construction industry” IOP Conference Series: Earth and Environmental Science, vol. 688, pp. 012010, 2021.

[3] Shekhovtsov V.V., Skripnikova N.K., Semenovykh M.A., Volokitin O.G. “Anorthite-containing building ceramic using metallurgical sludge waste”, Glass and Ceramics, vol. 78, no. 5-6, pp. 237-241, 2021.

C3-P-035402

STRUCTURAL FEATURES OF NATURAL MAGNESITE PROCESSED BY LOW-TEMPERATURE PLASMA

V.V. SHEKHOVTSOV, M.A. SEMENOVYKH, N.K. SKRIPNIKOVA

Tomsk State University of Architecture and Building, TSUAB, Tomsk, Russia

Today, obtaining anorthite ceramics using plasma technologies is an urgent task, as there is an increase in construction volumes and new requirements are imposed on building materials and products. With the help of plasma technologies, today it is possible to obtain high-quality material with the necessary properties, both physical-mechanical and physicochemical [1, 2]. From the point of view of the parametric characteristics and structural properties of MgO, it is worth noting the work [3], which emphasizes the use of periclase in the experimental physics of minerals, since its data on pressure-volume-temperature (P–V–T) can be applied to X-ray studies of heated solids. bodies under pressure using tungsten.

The purpose of this work is to evaluate the influence of the temperature factor on the structural and phase changes in natural magnesite ($MgCO_3$) under traditional (1173 K) and ultrahigh (6500 K) heating. Phase quantification plays an important role in the development of phase diagrams, understanding the behavior of MgO under non-environmental conditions, and developing possible applications based on it.

Magnesite $Mg(CO_3)$ was used as the object of study. The average oxide composition is presented (wt %): MgO ~ 46.26; CaO ~ 0.56; SiO_2 ~ 1.50; R_2O_3 ~ 1.51; Δmf ~ 50.24. Cylindrical specimens 35 mm in diameter and 10 mm high were fabricated on the basis of a fraction with a particle size of up to 80 μm. A 10% aqueous solution of liquid glass (Na_2O+SiO_2) was used as a binder. Plasma treatment of the fabricated samples was carried out on an experimental bench [4]. Experimental conditions: current strength 220 A, voltage 130 V, flow rate of plasma-forming gas (air) 0.7 g/s, distance to the sample from the nozzle exit 50 mm, exposure time 3 min. Using the heat flow calorimetric method [5], the mass average plasma temperature at the nozzle exit was 6500 K. The fabricated samples were subjected to a combined approach, including structural-phase analysis using a Shimadzu XRD 7000S, and differential thermal analysis using a TG/DSC analyzer STA 409 PC, NETZSCH.

Qualitative phase analysis of samples M-1173 and M-6500 showed that in both cases the MgO phase of variable composition 0494-MgO, 0495-MgO and 6458-MgO, 6751-MgO is formed. The change in the parameters is insignificant, but in the case of sample treatment at a temperature of 1173 K, the parameters decrease, and at a temperature of 6500 K, on the contrary, they increase. The gratings are stable, the fraction of individual phases in the integrated intensity is 64.91, 35.09 and 71.64, 28.29, respectively. The agreement criteria turned out to be high and equal to R_{wp}=6.6; 11.7%. A complete analysis of the parameters of the etalon lattices, as well as the refined values by the Rietveld method, are presented in Table. one.

As a result of the research, it was found that the main phases of the studied states are the standards $MgCO_3$, MgO in hexagonal and cubic forms. It follows from the analysis of the triplet diagram that $MgCO_3$ is stable with respect to separation into MgO, C, O, and CO_2 phases in the initial state. At the same time, the microstructure of the original sample after isothermal exposure to 1173 K is characterized by acute-angled grains of MgO, the boundaries of the adjoining particles are clearly separated, at the same time, when considering the structure of the surface of the melting product, rounded grains of a prismatic shape are observed, in some areas, sheath-like cellular-dendritic crystals were found on the surface of the grains plagioclase.

The work was carried out with the support of the state task of the Ministry of Science and Higher Education of the Russian Federation FEMN-2020-0004 and grant President of the Russian Federation MK-66.2022.4.

REFERENCES

[1] V. Leonov, G. Afonina, V. Demkin “Preparation of Porous Periclase Ceramic”, Refractories and Industrial Ceramics, vol. 56., pp. 486–489, 2016.

[2] K. Li, F. Zhao, X.Liu, et al “Fabrication of porous forsterite-spinel-periclase ceramics by transient liquid phase diffusion process for high-temperature thermal isolation” Ceramics International, vol. 48, no. 2, pp. 2330–2336, 2022

[3] L. Dubrovinsky, S. Saxena “Thermal Expansion of Periclase (MgO) and Tungsten (W) to Melting Temperatures”, Physics and Chemistry of Minerals, vol. 24, pp. 547–550, 1997.

[4] V. Vlasov, V. Shekhovtsov, O. Volokitin et al. The use of low-temperature plasma to obtain ash microspheres, Izvestiya Vysshikh Uchebnykh Zavedenii. Physics, vol. 61,no. 4(724), pp. 92-98, 2018.

[5] Nalivaiko V. I., Chubakov P. A., Pokrovsky A. N. et al. Small-sized spectrometer for emission analysis of low-temperature plasma flows, Thermophysics and Aeromechanics, vol. 14, no. 2, pp. 257–267, 2007.

C3-P-037702

THE EFFECT OF ANNEALING IN AIR ON THE PHYSICOCHEMICAL PROPERTIES OF CEF3 NANOPARTICLES PRODUCED BY PULSED ELECTRON EVAPORATION

V. G. ILVES[1], O. A. MALOVA[1,2], A. M. MURZAKAEV [1,2], T. R. SULTANOVA [2], S. Y. SOKOVNIN[1,2], M. A. UIMIN [2,3], M. V. ULITKO [2], M. G. ZUEV[2,4]

[1]*Institute of Electrophysics, UB RAS, Yekaterinburg, Russia*
[2]*Ural Federal University, Yekaterinburg, Russia*
[3]*M.N. Mikheev Institute of Metal Physics, UB RAS, Yekaterinburg, Russia*
[4]*Institute of Solid State Chemistry UB RAS, Yekaterinburg, Russia*

The present work continues to investigate the physicochemical characteristics of cerium fluoride nanopowder (NP) produced (Fig.1) using the method of pulsed electron beam evaporation in vacuum [1]. The resulting NP was isothermally annealed in air at the temperature of 200, 300 and 500 ° C for 30 minutes. Further, the properties of annealed NPs were evaluated using XRD, HRTEM, DSC-TG, photo and cathodoluminescence, magnetic measurements on Faraday scales. The degree of cytotoxicity of not annealed NP CeF_3 to cell cultures was determined. XRD showed that the cubic phase CeO_2 formed in NP CeF_3 after annealing at the temperature of 500 ° C. Cathodoluminescence was not excited, both in the initial NP and in annealed NP. The intensity of photoluminescence of NP CeF_3 decreased non-monotonically with an increase in the annealing temperature, the appearance of the oxide phase CeO_2 led to an increase in the intensity of photoluminescence.

The paramagnetic response of the NP decreased after annealing at the temperature of 500 °. The addition of not annealed NP CeF_3 to tumor culture HeLa and non-neoplastic Vero culture resulted in a 20-35% reduction in cell viability at all NP concentrations in the aqueous suspension (0.1, 05, 1.0 mg/ml). The obtained data show the low cytotoxicity of NP CeF_3 to tumor and non-tumor cells. Annealing of the NP CeF_3 at low temperatures (200 and 300 ° C) led to an improvement in the textural parameters of the not annealed NP, almost tripling the size and volume of the pores, with a slight decrease in the specific surface area of the NP, from 62 m^2/g in the not annealed NP to 44.5 m^2/g after annealing at 300 ° C. Improved texture parameters indicate the prospect of using CeF_3 as a nanocontainer to deliver various dosage forms in biomedicine.

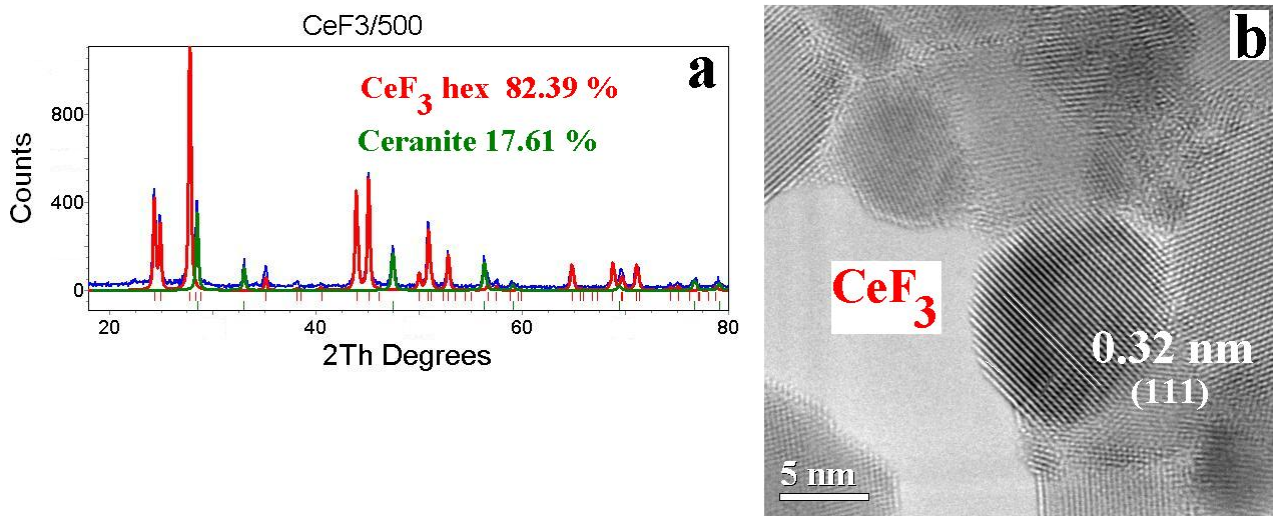

Fig.1. (a) XRD pattern NP CeF_3 annealed in air at the temperature 500 °C, (b) HRTEME image initial CeF_3 NP .

REFERENCES

[1] V. G. Ilves, S. Yu Sokovnin, M. A. Uimin, "Properties of cerium (III) fluoride nanopowder obtained by pulsed electron beam evaporation" J. Fluor. Chem., vol. 253, no. , pp. 109921(7), January 2022.

C3-P-039801

ON THE FUNDAMENTAL BASIS OF MEASURING THE MICROHARDNESS OF MICRO-ARC OXIDE COATINGS

P.E. GOLUBKOV, E.A. PECHERSKAYA, T.O. ZINCHENKO, A.V. VOLIK, G.V. KOZLOV, A.E. SHEPELEVA

Penza State University, Penza, Russia

Currently, the development of information-measuring control systems for technological processes, including micro-arc oxidation, is actively developing. The most advanced of them make it possible to indirectly measure the thickness of micro-arc oxide coatings during their formation. And it is quite understandable: firstly, the coating thickness is the simplest non-electrical parameter in terms of measurement, which can easily be experimentally verified; secondly, measurement of the coating thickness provides an additional opportunity to automate the MAO process, in particular, to turn off the process current source when the coating reaches the required thickness. However, for most areas of MAO coatings application, the microhardness of the coatings rather than the thickness is of decisive importance. It is the microhardness, or rather, the content of crystalline oxides, that determines the outstanding coatings properties: high wear resistance and heat resistance, chemical stability and electrical strength. In this regard, the measurement of the crystalline oxides content in the coating being formed is of increased scientific and practical interest.

It is known that the MAO coating acquires its unique properties as a result of not only electrochemical but also plasma processes. Therefore, the mathematical model underlying the measurement method must also take into account all these phenomena. According to [1], there is currently no unified fundamental theory of plasma electrolysis, but there are significant scientific works that reveal certain aspects of the coatings formation [2, 3]. In particular, the monograph [4] describes the physicochemical foundations of micro-arc oxidation, in contrast to microplasma processes in detail. Thus, the purpose of this work is to establish the initial positions, on the basis of which a generalized mathematical model of the micro-arc oxidation process can be developed.

The following considerations can be taken as a starting point for the development of this model. The coatings microhardness is determined by the crystalline oxide content in the coating, which depends on the temperature in the micro-arc discharges channel according to the Kolmogorov-Johnson-Mehl-Avrami equation. This temperature is determined by the microdischarges power, which largely depends on the applied energy impact in the form of high-voltage process current pulses. The main idea of the work is to determine the relationship between the current pulses parameters and the temperature in the micro-arc discharges channel by modeling the physical phenomena that accompany the coating formation process. It can be done by calculating the microdischarges power according to the law of energy conservation, based on the total power supplied to the galvanic cell, which is calculated theoretically from the process current waveform or determined experimentally based on the results of measuring the instantaneous current and voltage values.

The work results can be used in the selection of technological parameters of the micro-arc oxidation process in order to increase its efficiency and the formed coatings quality.

REFERENCES

[1] T.W. Clyne and S.C. Troughton, “A review of recent work on discharge characteristics during plasma electrolytic oxidation of various metals,” Int. Mater. Reviews, pp. 1-36, 2018.

[2] A.B. Rogov, A. Matthews, A. Yerokhin, “Role of cathodic current in plasma electrolytic oxidation of Al: A quantitative approach to in-situ evaluation of cathodically induced effects,” Electrochimica Acta, vol. 317, pp. 221-231, 2019.

[3] V.R. Aubakirova, V.V. Astanin, A.V. Butorin, E.V. Parfenov, “Modelling the electromagnetic field of an electrolyzer during plasma electrolytic oxidation,” Proc. Int. Conf. on Electrotechnical Complexes and Systems (ICOECS 2021), Ufa, Russia, pp. 111-115, 2021.

[4] A.I. Mamaev, V.A. Mamaeva, V.N. Borikov, T.I. Dorofeeva, Formation of nanostructured nonmetallic inorganic coatings by localization of high-energy flows at the phase interface, Tomsk: Publishing House of Tomsk University, 2010.

[5] E.A. Pecherskaya, P.E. Golubkov, D.V. Artamonov, O.A. Melnikov, O.V. Karpanin, T.O. Zinchenko, “Intelligent technology of oxide layer formation by micro-arc oxidation,” IEEE Transactions on Plasma Science, 49(9), pp. 2613–2617, 2021.

C3-P-040501

HIGH-ENERGY EXCITATION OF Zn_2SiO_4 NANOPARTICLES LUMINESCENCE IN ION-IMPLANTED SILICA*

A.F. ZATSEPIN[1], *E.A. BUNTOV*[1], *V.A. PUSTOVAROV*[1]

[1]*Ural Federal University, Ekaterinburg, Mira st., 19, 620002, Russia*

Zinc-implanted silica films and glasses constitute a popular research topic due to different types of nanoparticles formed within oxide before and after thermal annealing [1, 2]. A nanocrystalline α-Zn_2SiO_4 phase formation in silica glass subsurface layer was observed under pulsed zinc ion implantation and annealing [3]. However, the mechanism of bright green photoluminescence (PL) for such a structure is still a matter of debate having hypotheses of either intrinsic defect or uncontrolled impurity as emission center.

In present study the photoluminescence (PL) and high-energy synchrotron (UV-Vacuum UV) excitation spectra of willemite nanophases formed in glassy and thin-film SiO_2 matrices by means of ion implantation and 900-1000 °C annealing. Pure willemite ceramics is used as reference [3].

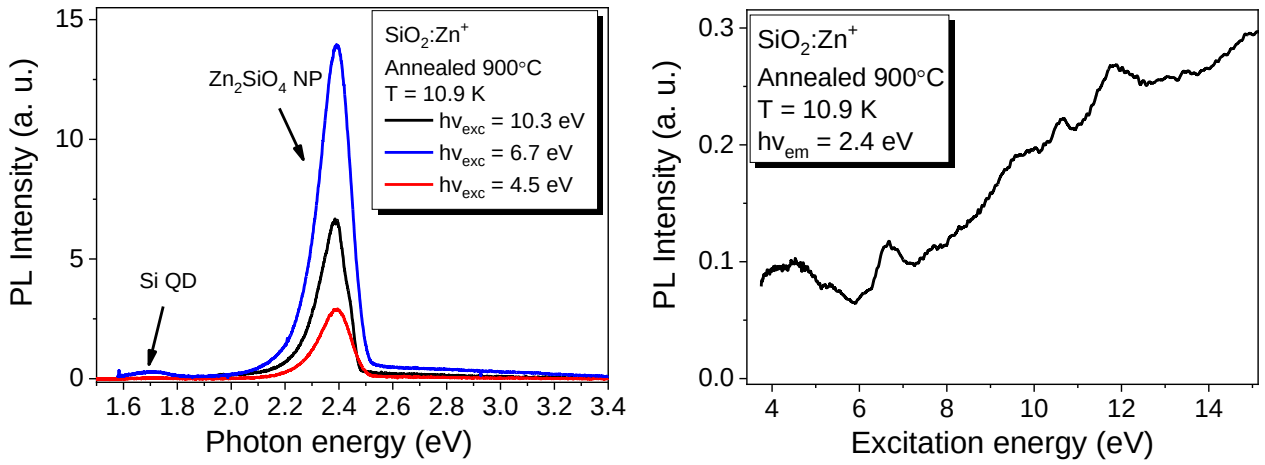

Fig.1. Low-temperature photoluminescence (left) and PL excitation spectra of the silica samples implanted with Zn^+ ions.

Silicon and willemite particles were detected by the characteristic PL bands at 1.7 eV and 2.4 eV, respectively (Fig. 1, left). Green and yellow light emission observed is associated with point defects inside α- and β-Zn_2SiO_4 nanoparticles. The electronic states of point defects are localized to dimensions much smaller than the nanocrystal size, so the PL band positions are similar to that of bulk willemite [4]. Different PL excitation mechanisms were distinguished for implanted silica, including energy transfer from free and self-trapped excitons showing up as the VUV PLE bands in the 10 eV – 12 eV region (Fig.1, right). The results obtained may be used to tailor the luminescent properties of the Zn-containing oxide nanocomposite in wide temperature range.

REFERENCES

[1] Khramov, E.V., Privezentsev, V.V., Palagushkin, A.N., Shcherbachev, K.D., Tabachkova, N.Y. "XAFS and TEM Investigation of Nanocluster Formation in $^{64}Zn^+$ Ion-Implanted and Thermo-Oxidized SiO_2 Film" Journal of Electronic Materials, 49 (12), pp. 7343-7348, 2020.

[2] Czarnacka, K., Koltunowicz, T.N., Makhavikou, M., Parkhomenko, I., Komarov, F.F. "Electrical and optical properties of SiO2 thin layers implanted with Zn ions" Acta Physica Polonica A, 136 (2), pp. 274-277, 2019.

[3] A. Zatsepin, E. Buntov, N. Gavrilov, and H.-J. Fitting, "Ion-beam synthesis and thermal behaviour of luminescent Zn_2SiO_4 nanoparticles in silica glasses and films" Phys. Status Solidi B 253, No. 11, pp. 2180–2184, 2016.

[4] A. Zatsepin, E. Buntov, V. Kortov et al. "Willemite photoluminescence in Zn-implanted silica glasses" Phys. Stat. Sol. C, 12, 1355–1358, 2015.

* This work was supported by the Russian Science Foundation project No. 21-12-00392.

C3-P-041404

MULTILAYER CORROSION-RESISTANT CERAMIC-METAL COATINGS (METAL/NITRIDE CERAMICS/ METAL/OXIDE CERAMICS) ON STAINLESS STEEL OBTAINED BY MAGNETRON SPUTTERING*

M.S. DOROFEEVA[1], T.A. GUBAIDULINA[2], T.I. DOROFEEVA[2], V.P. SERGEEV[2]

[1]Tomsk state University, Tomsk, Russia
[2] Institute of Strength Physics and Materials Sciences of Siberian Branch of Russian Academy of Sciences, Tomsk, Russia

During long-term operation in aggressive conditions (sea water and mechanical stress) stainless steel products require additional protection. A corrosion-resistant coating with enhanced physical and mechanical characteristics provides such protection. The coating may have a different composition, and the methods of formation may be different.

In this work, multilayer cermet coatings (Metal/nitride ceramics/ Metal/oxide ceramics) with increased corrosion resistance were obtained. The metal layer is presented in the form of the nickel layer, which makes it possible to minimize the arising stresses at the substrate–coating interface. Nickel is easily passivated in air and under the action of strong oxidizing agents, which can lead to corrosion resistance, but only if the coating is absolutely continuous. Nitride ceramics layer is presented in the form of silicon aluminum nitride, which is characterized by high hardness and wear resistance. It does not interact with most inorganic acids, but penetration of solvent ions along the grain boundaries to the substrate is possible if the coating structure is inhomogeneous. The outer layer of oxide ceramics is silicon alumina, consisting of silicon oxides and aluminum oxides, which are characterized by high hardness and corrosion resistance. In our case, this layer seals all previous layers, preventing the penetration of solvent ions, in particular, oxygen ions and, especially, chlorine ions, through the intercrystalline space.

Coatings are formed in one cycle under a changing gas atmosphere (argon, nitrogen, oxygen) using magnetron sputtering in a UVN-05MD "KVANT" vacuum unit equipped with two magnetrons. The thickness of the metal layer is about 0.5 μm, the nitride and oxide layers are about 2-2.5 μm. The resulting coating is gray with a mirror sheen (Figure 1).

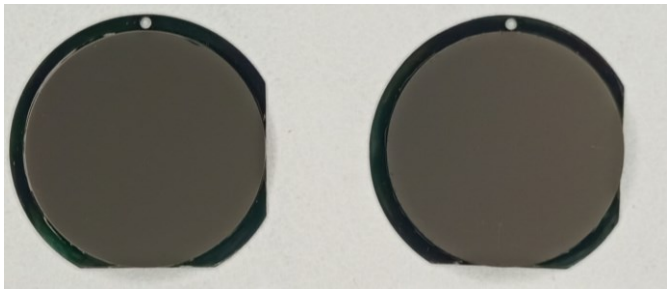

Fig.1. The photos of samples with multilayer metal-ceramic coating (Metal/nitride ceramics/ Metal/oxide ceramics) on stainless steel obtained by magnetron sputtering.

In the study of the cross section of the obtained coatings on a transmission microscope, it was revealed that metallic nickel has a fine-crystalline structure. The second layer has a nanocrystalline structure and contains the AlN phase. The outer layer is amorphous. During accelerated corrosion tests in a sea salt solution, the resulting coatings showed a decrease in the corrosion rate by several times. The corrosion rate was estimated using the Tafel equation.

Thus, the multilayer cermet coatings (Metal/nitride ceramics/ Metal/oxide ceramics) obtained by magnetron sputtering on stainless steel acquired the properties of each of the layers, and a synergistic effect appeared. In addition, the layering created several barriers to the diffusion of chloride ions from the environment. The thinness of these layers increased the elasticity of the final coated material.

* The work was performed as per to the State research task for ISPMS SB RAS, project FWRW-2021-0003.

C3-P-045002

ELECTRO-EROSION RESISTANCE OF DIFFERENT ELECTRODES MATERIALS FOR PLASMA GENERATORS[1]

IU.V. MURASHOV, N.K. KURAKINA, N.V. OBRAZTSOV, R.I. ZHILIGOTOV

Peter the Greet St.Petersburg Polytechnic University, High School of Electrical Engineering, Saint-Petersburg, Russia

Electrodes are the most important components of electrical devices operating at high temperatures (such as arc discharge). Such devices include plasma torches [1-3], different types of circuit breakers, lightning protection devices and many others. Therefore, the study of erosion issues is one of the most important and relevant task at the moment [4-5].

The experimental results of the hollow electrodes erosion resistance taking into account a pilot arc re-ignition during plasma torches operating, are presented in the study. A high voltage alternating current oscillator is used to simulate an initial process instability. The electrical circuit of the experimental setup with a pulsed discharge current up to 2 kA with time parameter 8/250 and a follow current of 800 A at industrial frequency is described. Four electrodes materials of tungsten (W), iron (Fe), copper (Cu), copper with a sprayed nickel+iron powder (Cu-Ni-Fe) are investigated. X-ray patterns of the different electrode surfaces are demonstrated after 4-9 pulses and one pulse with follow current impacts. The electric charge is calculated by integrating the obtained discharge current to assess the erosion coefficient. The following decreasing order of the electrical erosion resistance is determined: W – Fe – Cu-Ni-Fe – Cu.

REFERENCES

[1] A A Kadyrov et al 2021 J. Phys.: Conf. Ser. 1753 012019

[2] D. V. Ivanov and S. G. Zverev, "Mathematical Simulation of Processes in Air ICP/RF Plasma Torch for High-Power Applications," in IEEE Transactions on Plasma Science, vol. 48, no. 2, pp. 338-342, Feb. 2020.

[3] Irina Kumkova, Nikita Obraztsov, Victor Popov, and Dmitry Subbotin, "Plasma technology based on high-voltage AC plasma torch", AIP Conference Proceedings 2179, 020022 (2019)

[4] P. G. Derevyankin, V. Ya. Frolov and S. L. Gorchakov, "Analysis of Erosion Processes of Electrical Contacts Manufactured by Plasma Spraying Technology," 2020 IEEE Conference of Russian Young Researchers in Electrical and Electronic Engineering (EIConRus), 2020, pp. 622-625

[5] Budin, A.V., Pinchuk, M.E. Kurakina, N.K. Erosion Characteristics of Copper-Based Composite Electrodes in an Electric Arc of Variable Length with Transverse Gas Blowing. Tech. Phys. Lett. 44, 808–810 (2018)

1 The work was supported by the Russian Science Foundation under grant No. 22-29-20223

C3-P-047702

PLASMA THERMAL CYCLIC NITRIDING OF TITANIUM ALLOYS

I.V. KANDAROV[1], A. A. NIKOLAEV[2], E. L. VARDANYAN[2], A. YU. NAZAROV[2], K.N. RAMAZANOV[2]

[1] Tekhnopark AT, Ufa, Russia
[2] Ufa State Aviation Technical University, Ufa, Russia

Today nitriding is one of the effective methods of surface hardening of titanium alloys and steels [1]. However, in the temperature range of 450-550 °C, the process is carried out at long dwell times due to the low rate of nitrogen diffusion deep into the material. The diffusion rate can be significantly increased by various methods of intensifying the process by applying magnetic fields and installing special technological screens, which complicates the design of facilities. Also, the creation of ultrafine grained (UFG) structure by surface plastic deformation methods allows to increase the diffusion rate [2,3]. One of the easy ways to intensify the nitriding process is thermal cycling [4]. The idea of this method is to accelerate the diffusion kinetics by changing the duration of the surface saturation stage and internal nitrogen diffusion deep into the material. With traditional continuous nitriding, the nitride zone grows considerably with increasing dwell time, resulting in slower diffusion. This disadvantage of the process can be eliminated by using the thermocyclic method, thus speeding up nitrogen diffusion.

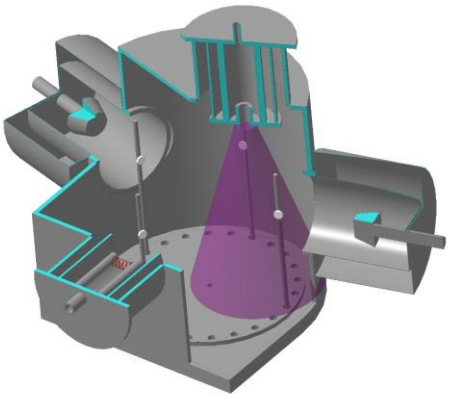

Fig.1. Scheme of thermocyclic nitriding.

In this work, the effect of changing the duration of the nitrogen saturation phase of the surface at different positions of the samples with respect to the plasma source was investigated. To establish the patterns, the roughness before and after nitriding, surface microhardness, and microstructure were examined and comparative tribological tests were performed.

REFERENCES

[1] Li, C. X., & Bell, T. // Corrosion Science. – 2004. – Vol. 46. – №6 . p. 1527-1547.
[2] Brokman, A., Dothan, F., & Tuler, F. // Materials Science and Engineering. – 1979. – Vol. 40. – №2 . p. 261-263.
[3] Brokman, A., & Tuler, F. R. // Journal of Applied Physics. – 2018. – Vol. 52. – №1. p. 468-471
[4] Nalimov Y. S. et al. //Strength of Materials. – 2020. – Vol. 52. – №. 2. – p. 262-267.

C3-P-048002

HOT-TARGET HIPIMS DEPOSITION OF W-FUZZ LAYERS*

M.M. KHARKOV, M.S. KUKUSHKINA, A.V. KAZIEV, O.V. OGORODNIKOVA

National Research Nuclear University MEPhI (Moscow Engineering Physics Institute), Moscow, Russia

Nanostructuring of tungsten surface under the exposure to helium ion fluxes has been studied by a number of scientific groups since 2007 [1]. This effect was examined mainly in the context of helium accumulation, and the growth mechanism of such structures on the surface was investigated. In present work, porous tungsten coatings were deposited by magnetron deposition in He environment. The deposition was carried out in the HiPIMS mode with a frequency of 1 kHz and a pulse duration of 300 μs. The tungsten target was thermally insulated from the water-cooled cathode The working gas was helium. The pressure of the working gas was varied in the range $2–6\times10^{-2}$ Torr. The average discharge power was 1.5 kW. A bias voltage was applied to the sample. The sample temperature was measured with a thermocouple in a separate experiment. The sample temperature was varied by changing the distance between the sample and the target.

Since it takes some time for the sample temperature to reach the stable value, the fracture of coating reveals different stages of fuzzy structure growth depending on temperature (Fig. 1b). The thickness of the coating depends on the temperature of the sample during deposition—the lower the temperature, the denser the coating, the smaller the thickness (Fig. 1a). However, in the range 900–1200 K, a dendritic structure of the coating with various heights is formed. The sizes of individual fibers are from 10 to 100 nm. With a further increase in temperature, the fibers are enlarged into separate ribbon formations with a width of several microns (Fig. 1c).

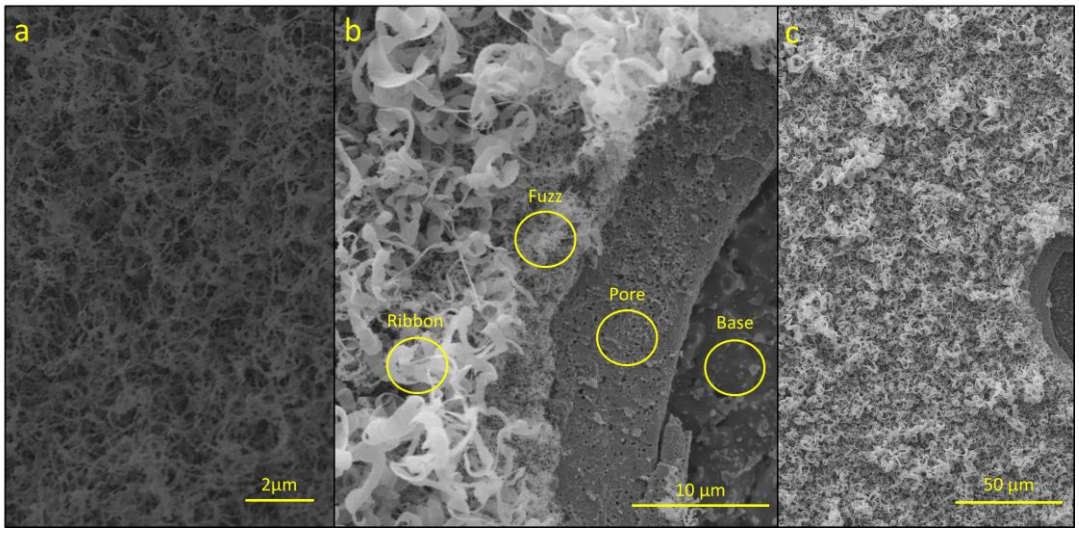

Fig.1. The structured coating deposited by HIPIMS method. a – classic tungsten-fuzz, b – different stages of fuzzy structure growth depending on temperature, c – separate ribbon formations of coating.

Such formations have not been previously reported in the literature devoted to the studies of tungsten structuring under the exposure to helium flux bombardment. Moreover, a number of works have shown that when He irradiation takes place at temperatures above 1200–1300 K, dendritic structures are not formed, and the surface remains smooth [2].

REFERENCES

[1] S. Kajita , S. Takamura , N. Ohno et al., "Sub-ms laser pulse irradiation on tungsten target damaged by exposure to helium plasma", Nucl. Fusion 47 (2007) 1358–1366 .

[2] Yunfeng Wu, Lu Liu, Bing Lu, Weiyuan Ni, Dongping Liu, "W nano-fuzzes: A metastable state formed due to large-flux Heþ irradiation at an elevated temperature" Journal of Nuclear Materials 482 (2016) 294e299

* The work was supported by the Russian Science Foundation under grant No. 20-12-00203.

C3-P-948701

OPTIMIZATION OF THE PRELIMINARY ELECTRON-ION-PLASMA TREATMENT OF THE SILUMIN SURFACE LAYER BEFORE NITRIDE COATING DEPOSITION*

N.A. PROKOPENKO, O.V. KRYSINA, A.D. TERESOV, M.E. RYGINA, E.A. PETRIKOVA

Institute of High Current Electronics SB RAS, Tomsk, Russia

The purpose of this work is to reveal the effect of an additional stage of electron-ion-plasma surface treatment (electron-beam treatment, ion-plasma etching, sublayer deposition) on the adhesion strength, wear resistance, and physical and technical properties of the coating/substrate system. The selection of optimal modes for pre-treatment of the surface of silumin samples was carried out on installations included in the list of unique scientific installations of the Russian Federation (https://ckp-rf.ru/usu/434216/?sphrase_id=9096861). To reduce roughness, heal pores, and increase the uniformity of the composition of the surface of silumin samples, a SOLO vacuum electron-beam installation was used. In order to clean the surface from possible contaminants, remove the oxidized surface layer, heat the sample, and activate the surface for better adhesion of the formed coating to the substrate, preliminary ion-plasma etching of the surface of the samples was carried out. To improve the adhesion of nitride coatings to the substrate, a thin sublayer from the group of transition metals (Ti, Cr, Mo, Zr) was deposited. Experiments on the ion effect on the surface of materials were carried out on an automated vacuum ion-plasma installation QUINTA. The following binary systems of transition metal nitrides were taken as model wear-resistant coatings: TiN, CrN, MoN, ZrN.

The following diagnostic equipment and techniques were used to test the coated samples. The thickness of the coatings was controlled on a Calotest CAT-S-0000 instrument (CSEM, Switzerland) by the Calotest method using images of spherical sections. Transverse cleavages and the surface of the coatings were studied by scanning electron microscopy (SEM) using a Philips SEM-515 electron microscope with an EDAX ECON IV microanalyzer (Netherlands). The hardness (HV) of the “coating/substrate” system was measured on a PMT-3 instrument. Tribological studies were carried out using a tribometer Pin on Disc and Oscillating TRIBOtester (TRIBOtechnic, France) in the "ball-disk" geometry. Adhesion strength was tested on a Micro-Scratch Tester MST-S-AX-0000. The crystal structure, phase composition, and crystal lattice deformation of the coatings were identified by X-ray diffraction on a Shimadzu XRD-6000 diffractometer (Japan).

Based on the results of the work done, the following conclusions were drawn:

1) To increase the adhesion of the "nitride coating/substrate" system and its wear resistance, where the binary systems TiN, ZrN, CrN, MoN act as a coating, it is rational to use the preliminary stages of electron-ion-plasma processing, such as ion-plasma etching in gas arc discharge plasma with heated and hollow cathodes, deposition of a metal sublayer (≈100 nm) and submillisecond pulsed electron-beam action.

2) When choosing the modes of preliminary electron-beam processing in order to improve the adhesion, mechanical and tribological properties of the "nitride coating/silumin substrate" system, it is rational to choose the number of exposure pulses of 15 or more, the duration of exposure is ≈150 μs, the energy density of the electron beam is 25-30 J/cm^2 .

3) High-cycle (at least 2 cycles) electronic processing leads to a significant increase in the hardness and wear resistance of the "nitride coating/silumin substrate" system.

* The work was funded by RFBR and ROSATOM, project number 20-21-00111 and under State Assignment of the Ministry of Science and Higher Education of the Russian Federation (project No. FWRM-2021-0006).

C4-O-003702

DRILLING OF TITANIUM ALLOY USING A CARBIDE TOOL WITH ANTIFRICTION COATINGS[1]

THET OO, G.V. OGANYAN, E.Yu. KROPOTKINA

Department of High-Efficiency Processing Technologies, Moscow State University of Technology «STANKIN», Moscow, Russia

Among the problems encountered in the processing of titanium alloys, in particular, during drilling, additional difficulties are associated with their low thermal conductivity. Since the heat released during the cutting process is distributed rather slowly over the workpiece, the expansion of the metal leads to pressure on the tool. Chips actively stick to it, the coefficient of friction increases, additional heat is released. The high temperature and its unfavorable distribution in the cutting tool significantly reduce the cutting time before the tool change.

To increase the durability of the tool, wear-resistant coatings are used everywhere and quite successfully. Moreover, modern coatings can be considered as wear-resistant complexes designed taking into account the working conditions of the tool. The three- to five-fold effect of increasing durability in the processing of carbon steels has already become normally. However, when processing titanium alloys, an increase of 50-70% can be considered a success.

From classical works in the field of the theory of cutting materials, it is known that the power of heat sources during shaping largely depends on the friction forces on the working surfaces of the tool. Consequently, their coating efficiency will largely depend on the ability to reduce the frictional interaction on the contact pads, of course, while maintaining heat resistance. Here, additional antifriction coatings can provide some help, which can be applied by a variety of methods.

Diamond-like carbon coatings (DLC) have pronounced advantages over nitride and oxide coatings in terms of providing a reduced coefficient of friction on the working surfaces of the tool. However, the use of DLC coatings for cutting tools in the conditions of processing difficult-to-process alloys is limited by their relatively low temperature resistance. However, modern DLC coatings remain undervalued, they have certain prospects in increasing the cutting ability of the tool when cutting titanium alloys.

Another interesting way to reduce friction is the technology of epilaming, which is based on the use of surfactants in fluorocarbon easily evaporating solvents. Such solutions (epilams), in particular the composition 6SFC-180-05, are applied to the surface and after evaporation form a thin film up to 100 nm thick. Modern compositions are quite capable of working in a zone of sufficiently high temperatures.

New experimental results on the evaluation of the cutting ability of carbide drills with coatings of group (CrTiAlSi)N and additionally applied antifriction coatings, as well as the establishment of the influence of such coatings on the condition of the workpiece surface can be a step towards expanding the areas of technological application of such coatings and their implementation based on new technical solutions.

1 This work was supported financially by the Ministry of Science and Higher Education of the Russian Federation (project No 0707-2020-0025)

C4-O-009703

ELECTRON-BEAM DEPOSITION OF THIN FILMS WITH COMBINED PROTECTIVE AND MAGNETIC PROPERTIES BY FORE-VACUUM ELECTRON SOURCES*

D.B. ZOLOTUKHIN[1], *YU.G. YUSHKOV, A.V. TYUNKOV, V.P. FROLOVA*[1,2]

[1]*Tomsk State University of Control Systems and Radioelectronics, Tomsk, Russia*
[2]*Institute of High Current Electronics, Tomsk, Russia*

Deposition and characterization of the coatings that combine protective and functional properties is an interesting and relevant task at the interface of modern particle accelerator physics, low-temperature plasma, and materials science [1]. Practical importance of the research of such coatings for engineering sciences is justified by the combination of electrical, magnetic and mechanical characteristics of such coatings. For example, the coatings with higher electrical and heat resistance would have less losses to the eddy currents but heightened mechanical properties (hardness, wear resistance, impact resistance) and, undoubtedly, will be widely used in radio electronics, radio engineering, and the development of absorbing radio protection for unmanned aerial vehicles.

In this work, as the main method for formation of such coatings, we propose to use electron-beam deposition from multi-component beam plasma generated in a medium vacuum (1-100 Pa) [2].

The proposed method seems to be promising since it implies the rapid and controllable electron-beam evaporation of the target followed by layer-by-layer deposition of the coatings with desired properties. This should provide the necessary combination of magnetic and electrical characteristics of the deposited coatings, with their uniformity and high mechanical strength.

This work presents the results of studying of an example of such coatings: a two-layer thin coating with an iron-based functional layer and a protective outer layer based on alumina ceramics.

REFERENCES

[1] S. Abdul, T. Judit, F. Ilona, M. Nikoletta, “Functional thin films and nanostructures for sensors,” Micro and Nano Technologies, vol. 1, pp. 485-519, 2018.

[2] E.M. Oks, Plasma Cathode Electron Sources: Physics, Technology, Applications, New York: Wiley, 2006.

* The work on the methodology for research of magnetic properties of the films was supported by the Grant of the President of the Russian Federation for the Young Scientists (МК-1399.2022.4). The research on surface properties of the films was supported by the Russian Foundation for Basic Research (grant #20-08-00370).

C4-O-010405

INCREASE PHOTOCELL EFFICIENCY PASSIVATION OF SILICON SURFACE BY A TRANSPARENT CONDUCTIVE COATING BASED ON TIN OXIDE

Z. S. KAZHIYEV, D. O. MURZALINOV

Al-Farabi Kazakh National University, Almaty, Kazakhstan

Texturing silicon wafers is an effective way to reduce internal light reflection. Passivation of surface by deposition of thin films reduces the probability of charge recombination on dangling bonds. A transparent conductive coating based on SnO2 obtained by the sol-gel method, due to the mild conditions of solution chemistry, provides the formation of a film without appearance of other tin oxides [1,2].

The purpose of this work was to determine the modes of applying a tin oxide coating on the textured surface of silicon wafers to increase the absorption of the sample.

The initial substrate had different surface defects, which is associated with different treatment times in acids during texturization and etching. Samples: A-56 – an untextured silicon, T-46 – with uneven distribution of pyramids, T-30 –with uniform distribution of pyramids on the surface.

Equally important is the dependence of the optical parameters on the number of applied coating films. It can be seen from the spectra of Fig. 1 that with an increase the number of layers from 5-15 for the T-30 sample, the absorption coefficient increases, while the reflection decreases, and the light transmission remains almost unchanged. In this case, the probability of the formation of electron-hole pairs increases. It is noticeable that when applying 15 layers, the maximum increase in the absorption coefficient occurs, then this parameter decreases. A similar trend is noticeable when measuring resistivity. Further increase in the number of applied layers (more than 20) will increase the absorption of light.

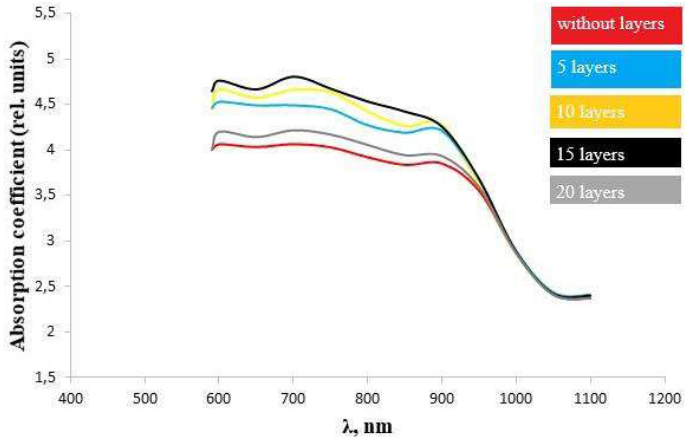

Fig.1. Optical characteristics depending on the number of applied coating layers (Sample T-30)

Changes in the specific surface area of the sample effects on the absorption of light. Analysis by adsorption and desorption methods allow to estimate this parameter. The coating of 5 and 10 layers is deposited on the surface of the plate in the form of separate spherical and filamentous formations. Thus, the surface already developed by texturing increases its inhomogeneity. It is known that such a surface absorbs lighter than a smooth surface. To reduce light reflection, surface morphology textured with coating particles. The reason increasing light absorption at T-30 sample is applying from 5 to 15 coating layers increased the specific surface area (Fig. 2). A further decrease in the absorption coefficient is associated with a decrease in the surface area.

REFERENCES

[1] Matthias Batzill, Ulrike Diebold 2005 The surface and materials science of tin oxide// Progress in Surface Science. 2005.V.79. P.49-53

[2] Mukhamedshina D.M., Mit' K.A., Beisenkhanov N.B., Dmitriyeva E.A., Valitova I.V. Influence of plasma treatments on the microstructure and electrophysical properties of SnOx thin films synthesized by magnetron sputtering and sol-gel technique //Journal of Materials Science-Materials in Electronics. 2008. V.19. P. S382-S387.

C4-O-010406

REDUCE THE SURFACE RESISTANCE OF SILICON SURFACE BY A TRANSPARENT CONDUCTIVE COATING BASED ON TIN OXIDE

Z.S. KAZHIYEV, D.O. MURZALINOV

Al-Farabi Kazakh National University, Almaty, Kazakhstan

Texturing silicon solar cells helps improve their light absorption and reduces reflection. By texturing solar cells, the path length of light through the cells is increased and the light is trapped more efficiently.

The purpose of this work was to determine the modes of applying a tin oxide coating on the textured surface of silicon wafers to reduce the surface resistance of the sample.

The initial substrate had different surface defects, which is associated with different treatment times in acids during texturization and etching. Samples: A-56 – an untextured silicon, T-46 – with uneven distribution of pyramids, T-30 –with uniform distribution of pyramids on the surface.

Coating with 5 layers of SnO_2, the dangling bonds of A-56 sample react with particles of the film-forming system and lose their activity (Fig. 1). At the same time, the resistance drops. Further increasing the number of layers also reduces the number of dangling bonds and surface resistance.

As a result of increased defectiveness in T-46 coated with 5 layers of SnO2 leads to an increase in resistance. 10 coats were applied, which results in a reduction of resistance. When 15 layers applied the wafer surface is completely passivated, and then, at 20 layers the resistance does not change significantly. A similar picture occurs for T-30 sample. 15 layers of tin oxide is enough to completely passivate the silicon wafers surface

Comparing the graphs, it is noticeable when 5 layers are coated, the greatest increase in resistance occurs for T-30 sample. Due to the processing time of wafers etching and texturization in acids is the longest. Therefore, the most effective removal of the damaged layer formed when cutting the wafers.

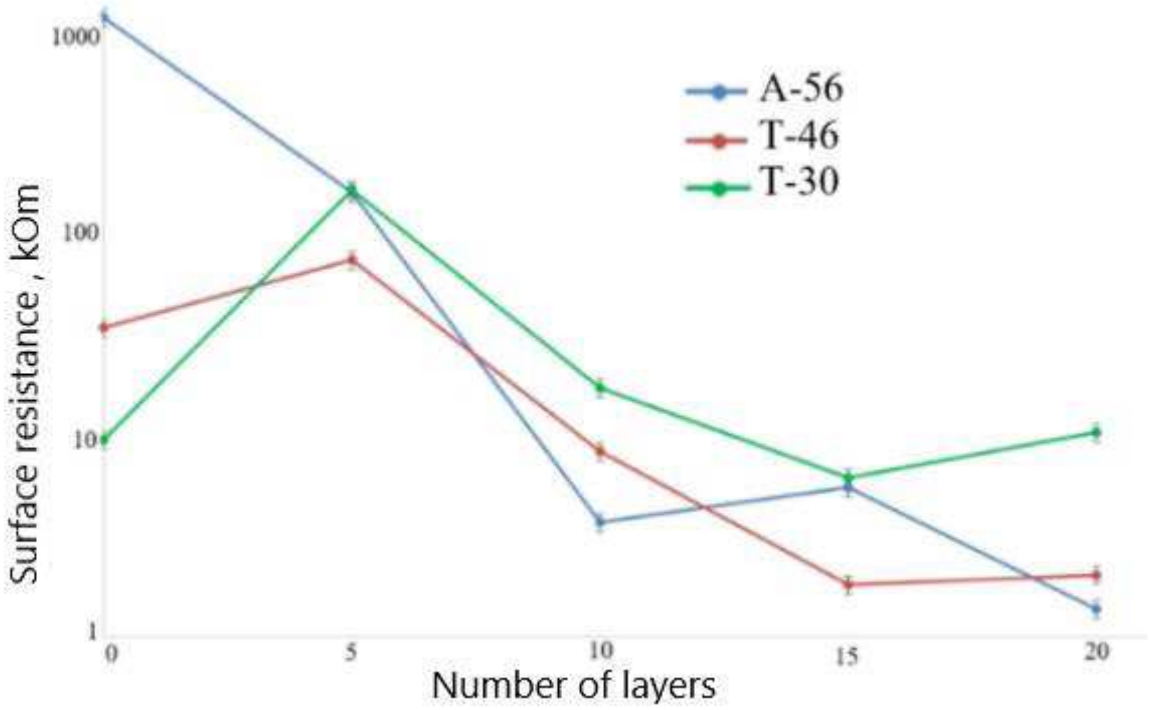

Fig.1. Dependence of resistivity on the number of applied coating layers.

Thus, the deposition of 15 layers is a critical point in the measurement of optical parameters, specific surface area, and resistivity for the samples under study.

REFERENCES

[1] Matthias Batzill, Ulrike Diebold 2005 The surface and materials science of tin oxide// Progress in Surface Science. 2005.V.79. P.49-53

[2] Mukhamedshina D.M., Mit' K.A., Beisenkhanov N.B., Dmitriyeva E.A., Valitova I.V. Influence of plasma treatments on the microstructure and electrophysical properties of SnOx thin films synthesized by magnetron sputtering and sol-gel technique //Journal of Materials Science-Materials in Electronics. 2008. V.19. P. S382-S387.

C4-O-018701

HIGH-RATE SYNTHESIS OF LiPON THIN FILMS BY THERMAL EVAPORATION OF Li_3PO_4 IN A NITROGEN PLASMA*

A.S. KAMENETSKIKH[1], *N.V. GAVRILOV*[1], *P.V. TRETNIKOV*[1], *A.A. ERSHOV*[1]

[1]*Institute of Electrophysics of the UB of RAS, Yekaterinburg, Russia*

Thin films of the LiPON ionic electrolyte are promising for the creation of all-solid-state lithium-ion microbatteries. However, the most common magnetron method of these films deposition has a low productivity. To increase the rate of synthesis of thin LiPON films, we used the method of lithium orthophosphate evaporation in a nitrogen arc plasma. It was shown that anodic evaporation of Li_3PO_4 in high-current arc is accompanied by intense decomposition of Li_3PO_4 vapor, which leads to an increase in the concentration of free lithium atoms both in the arc plasma and in the bulk of the film. The high diffusion mobility of lithium atoms in the film and its interaction with free oxygen atoms that arise when they are replaced by nitrogen in the LiPON structure promote the formation and the rapid growth in the growing film of inclusions with a composition different from that of LiPON. This effect makes it difficult to obtain single-phase LiPON films with a uniform microstructure and degrades the ionic conductivity of the films. A method was proposed for indirect heating of a crucible with Li_3PO_4, which reduces the interaction of the nitrogen arc plasma with dense vapor near the melt surface. The results of measuring the elemental composition of the films and their microstructure are presented. Reducing the degree of vapor decomposition allowed for higher Li_3PO_4 evaporation rate and obtain LiPON films with ionic conductivity up to $2 \cdot 10^{-6}$ S/cm at a film deposition rate of up to 10 nm/min.

* The studies were carried out in part with the financial support of Russian Federation represented by Ministry of Science and Higher Education (project No. 075-15-2021-1348) within the framework of event No. 2.1.13.

C4-O-022801

DEPOSITION OF AL_2O_3 IN HIPIMS AND ARC MIXED-MODE*

V.O. OSKIRKO[1,2], A.N. ZAKHAROV[1], I.M. GONCHARENKO[1], V.A. SEMENOV[1], M.I. AZHGIKHIN[1,2], A.A. SOLOVYEV[1]

[1]Institute of High Current Electronics, 2/3 Akademicheskii Ave., Tomsk, 634055, Russia
[2]OOO Prikladnaya Elektronika, 15-80 Akademicheskii Ave., Tomsk, 634055, Russia, oskirkovo@gmail.com, 8(3822)491651

Mixed-mode HIPIMS and ARC is a combined method of coating deposition, which is implemented in high-current pulsed operating regimes of magnetron sputtering system [1,2]. After the threshold current is reached, the magnetron discharge transits to an arc discharge, and the lifetime of the electric arc is controlled by the pulse duration. Combining the technology of pulsed magnetron sputtering with an arc makes it possible to provide a high level of ion impact on the substrate and increase productivity. This work is devoted to the study of Al_2O_3 coating deposition processes in mixed-mode. Fig. 1 shows a schematic of the experimental setup and oscillograms of the discharge current pulses, voltage, and the ion current pulses on a substrate in mixed-mode. During the magnetron discharge process, a discharge voltage of approximately 600 V is provided. At the moment of arc formation, the discharge voltage quickly drops to about 100 V and is maintained until the transistor of the high current pulse former is turned off. During this time, the current has time to grow up to 500 A, and the ion current to the substrate located at a distance of 100 mm reaches 6 A. It was found that when operating in the "poisoned" mode, the initiation of an arc discharge can occur during each pulse if the current density on the target surface reaches 0.4–0.6 A/cm^2. The results of a comparison of mixed-mode with MF magnetron sputtering show that in mixed-mode a higher average ion current density on the substrate is provided along with the coating deposition rate and radiation intensity of plasma increasing.

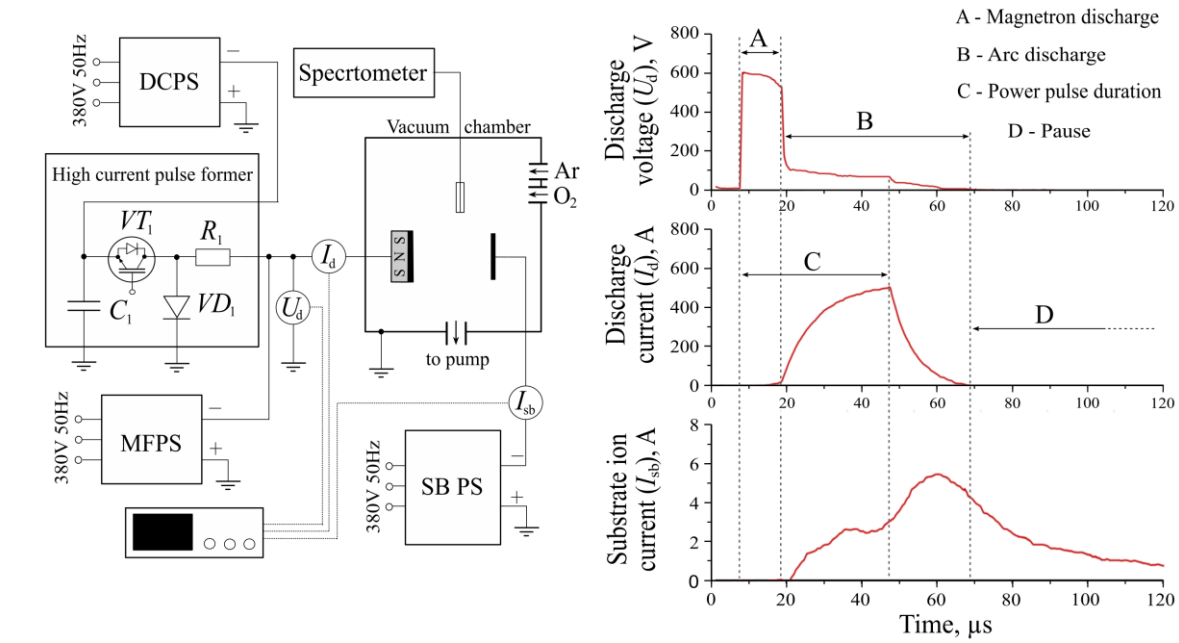

Fig. 1. a) Scheme of the experimental setup for the study of mixed-mode HIPIMS and ARC; b) oscillograms of the discharge current pulses, voltage, and the ion current pulses on a substrate.

REFERENCES

[1] *M. Tucker et al.* // Journal of Applied Physics. – 2016. – V. 119, 155303.
[2] *M. Lattemann et al.* // Diamond & Related Materials. – 2011. – V. 20, pp. 68–74.

* This work was carried out with the financial support of Russian Science Foundation (project No.22-29-00627, https://rscf.ru/project/22-29-00627/).

C4-O-023502

DIAGNOSTICS OF A LOW-PRESSURE ARC PLASMA (N_2, 0.1-1 PA) IN THE MODE OF ALUMINUM ANODIC EVAPORATION*

A.A. ERSHOV[1], *N.V. GAVRILOV*[1], *A.S. KAMENETSKIKH*[1], *D.R. EMLIN*[1]

[1]*Institute of Electrophysics of the UB of RAS, Yekaterinburg, Russia*

The use of an arc with a thermionic cathode burning in vapors of the anode material for the coating deposition provides high deposition rates, a controlled level of ion assistance, and the absence of microdroplets characteristic of a cathode arc. The use for this purpose of a low-pressure arc with a self-heating hollow cathode makes it possible to use an active gaseous medium for the synthesis of binary coatings, for example, nitride or oxide coatings. The rate of deposition of such coatings, their structure, and properties depend on such parameters of the discharge plasma as the plasma density and its electron temperature, the anode potential drop, the mass composition of the plasma, the degree of vapor ionization, and the degree of reactive gas dissociation. In this work, to diagnose the discharge plasma, probe diagnostics and optical emission spectroscopy were used. The results of measurements obtained in wide ranges of discharge current (5-30 A), reactive gas pressure (N_2, 0.1-1 Pa), and evaporation rate of Al ($(2 – 8)*10^{-8}$ g/cm^2 s) are presented. It has been shown by optical actinometry that the creation of dense counter flows of nitrogen and fast electrons in the narrowing of the discharge gap ensures an increase in the degree of N_2 dissociation up to 30%.

* The studies were carried out in part with the financial support of Russian Federation represented by Ministry of Science and Higher Education (project No. 075-15-2021-1348) within the framework of event No. 2.1.12.

C4-O-030401

DUAL MAGNETRON SPUTTERING WITH HOT TARGETS TO DEPOSITION CR COATINGS ONTO ZR ALLOY*

D.V. SIDELEV, V.A. GRUDININ

Tomsk Polytechnical University, Tomsk, Russia

Nowadays, a one of crucial problem of nuclear fuel elements is oxidation of fuel cladding under normal operation and accidental conditions. At present, the problems of swelling of fuel elements and its embrittlement can be solved by limiting the period of usage of fuel elements in the core of a nuclear reactor. However, the fast zirconium oxidation in water vapor under accidental conditions, for example in the case of loss of coolant accident (LOCA), can lead to destruction of nuclear fuel cladding. This problem can be solved by increasing the resistance of the surface of zirconium fuel cladding to oxidation. The most promising solution seems to be the protective chromium coating which can increase a coping time for emergency situation.

The several papers showed that chromium coating is able to prevent oxidation of the zirconium cladding at 1200 °C up to 5000 s [1-3]. However, it is necessary to significant increase the deposition rate of Cr coatings taking into account the geometry of the nuclear fuel cladding as well as the high number of zirconium claddings required annually for nuclear power plants.

This paper is devoted to show the possibility to use of dual magnetron sputtering systems with hot target to deposit Cr coatings on Zr alloy. The paper considers the dependences of deposition rate, structural properties of Cr coatings *vs.* target power density of dual magnetron.

REFERENCES

[1] D.V. Sidelev, S.E. Ruchkin, M.S. Syrtanov, E.B. Kashkarov, I.A. Shelepov, A.G. Malgin, K.K. Polunin, K.V. Stoykov, A.A. Mokrushin, " Protective Cr coatings with CrN/Cr multilayers for zirconium fuel claddings", Surf. Coat. Technol., vol. 433, № 128131, 2022.

[2] J.-C. Brachet, E. Rouesne, J. Ribis, T. Guilbert, S. Urvoy, G. Nony, C. Toffolon-Masclet, M. Le Saux, N. Chaabane, H. Palancher, A. David, J. Bischoff, J. Augereau, E. Pouillier, "High temperature steam oxidation of chromium-coated zirconium-based alloys: Kinetics and process", Corrosion Science, vol. 167, №108537, 2020.

[3] J.-C. Brachet, I. Idarraga-Trujillo, M. Le Flem, M. Le Saux, V. Vandenberghe, S. Urvoy, E. Rouesne, T. Guilbert, C. Toffolon-Masclet, M. Tupin, C. Phalippou, F. Lomello, F. Schuster, A. Billard, G. Velisa, C. Ducros, F. Sanchette, "Early studies on Cr-Coated Zircaloy-4 as enhanced accident tolerant nuclear fuel claddings for light water reactors", J. Nucl. Mater., vol. 517, p. 268-285, 2019.

* The work was supported by Grant of the President of the Russian Federation (project №МК-3570.2022.4).

C4-O-031901

THE STRUCTURE AND MECHANICALP ROPERTIES OF IMPACT COATING BASED ON Zr-Re-N*

M.V. FEDORISCHEVA[1], M.P. KALASHNIKOV[1,2], A.V.VORONOV[1], V.P. SERGEEV[1,2]

[1]*Institute of Strength Physics and Materials Science SB RAS, Tomsk, Russia*
[2]*National Research Tomsk Polytechnic University, Tomsk, Russia*

In outer space, there is a continuous bombardment of the spacecraft surface by small solid particles which have a transverse size of about 0.1-100 microns, and move at high speeds of 5-50 km / sec. As a result, many small craters and scratches are formed on the surface of the optical elements, in particular the windows. With a sufficiently long stay in open space, a strong erosion of the glass surface occurs, which significantly worsens the characteristics of the windows. This leads to a change in the optical, electrical, mechanical, and other characteristics of optical elements [1], which affects the performance of a spacecraft as a whole.

One of the possible ways to protect the windows is to apply protective coatings on their surface, which have a high resistance to shock loads [1-2]. In this work, coatings based on Re-Zr-N obtained by pulsed magnetron deposition were used to protect glass elements of a spacecraft from mechanical damage arising from the impact of micrometeoroids. The analysis of the structure and the properties revealed that various contents of argon in the argon-nitrogen gas mixture during deposition had a significant effect on the microhardness of the coating and the adhesion between the coating and the substrate [3,4].

In this connection, the purpose of this work is to investigate the effect of the argon content in the argon-nitrogen gas mixture under pulsed magnetron deposition on the microstructure, phase composition, and the mechanical properties of the coatings on the basis of the Zr-Re-N system.

The results of studies of the microstructure, phase composition, physical and mechanical properties of the Zr-Re-N coatings with a thickness of 5 μm on quartz glass substrates produced by pulsed magnetron deposition are presented. The X-ray, high-resolution transmission and electron microscopy (HRTEM) as well as nanoindentation methods were used to investigate their phase configurations, nanostructures and mechanical behaviors in order to investigate their dependences on the argon content.

It was established the method of magnetron deposition, Zr-Re-N coatings on the surface of quartz glass have been obtained with a gradient structure close to the amorphous one. Depending on the amount of argon in the mixture of gases (nitrogen and argon), the degree of crystallinity of the coating changes. In addition, a change in the ratio of nitrogen and argon affects the elemental composition of the coating. The composition of the coating with an argon content of 80% is close to Re2-Zr-N and a coating with an argon content of 60% to Re1.4- Zr- N. The protective coatings of the Zr-Re-N system with an argon content of 80% have a higher hardness compared to these with 60 and 70% of argon in the gas mixture.

REFERENCES

[1] E. Lewin, D. Loch, A. Montagne et al., “Comparison of Al–Si–N nanocomposite coatings deposited by HIPIMS and DC magnetron sputtering,” Surf. Coat. Technol. Vol. 232, pp. 680–689, 2013.

[2] Sergeev V., Psakhie S., Chubik P., et al., “Magnetron sputtering of Si-Al-N nanocomposite coatings on quartz glasses for protection against impacts of high speed microparticles” Vacuum,” vol. 143. Pp. 454-457, 2017.

[3] N. Panich, P. Wangyao, S. Hannongbua, P. Sricharoenchai and Y. Sun, “Effect of argon-nitrogen mixing gas during magnetron sputtering on titanium interlayer deposition with tIb2 coatings on high speed steel, Rev. Adv. Mater. Sci. vol.16, pp.80-87, 2007.

[4] Y.H. Lu a,*, J.P. Wangb, Y.G. Shen, “Effect of N content on phase configuration, nanostructure and mechanical behaviors in Ti–Cx–Ny thin films”, Applied Surface Science, vol. 255, pp. 7858-7863, 2009.

* This research was performed under the government statement of work for ISPMS Project No FWRW-2021-0010. TEM and X-ray investigation were performed by “Innovation Centre for Nanomaterials and Nanotechnologies” of the National Research Tomsk Polytechnic University.

C4-O-037801

TAILORING OF OPTICAL, MECHANICAL AND SURFACE PROPERTIES OF HIGH-ENTROPY CERAMIC THIN FILMS*

A.S. MITULINSKY[1], *S. P. ZENKIN*[1], *S.A. LINNIK*[1], *A.V. GAYDAYCHUK*[1]

[1]*Tomsk Polytechnic University, Tomsk, Russia*

Materials with a combination of high hydrophobicity, enhanced mechanical properties (hardness, toughness) and thermal stability find a various application in industry.

The group of the low-electronegativity metals oxides exhibit the hydrophobic effect. It is possible to enhance the mechanical properties of this group of ceramics without a weakening of the hydrophobic effect [1]. Several methods of the mechanical properties enhancement can be used for non-polymer thin films. One of the most promising is the entropy stabilization. High entropy alloys are surpassing traditional alloys and compounds in thermal stability and mechanical properties, making them potential high performance constructive and functional materials.

In order to create a robust transparent hydrophobic ceramic for the selection of the high entropy oxide (HEO) composition we used the combination of three material properties: a high melting temperature of the oxide, the lowest enthalpy of formation (or minimum Gibbs free energy per mole O_2) and low electronegativity of the base element. Resulted group of the selected oxides was taken as HfO_2, ZrO_2, Y_2O_3 and CeO_2, excluding radioactive ThO_2 and PuO_2 and toxic BeO.

In this work we performed a series of experiments devoted to change in optical, mechanical and surface properties depending on the Hf-Zr-Ce-Y-O thin film composition. The magnetrons were powered by high power impulse magnetron sputtering (HiPIMS) power supply.

$Hf_4Zr_4CeY_2O_{21}$ shows up to three times higher hardness compared to binary $HfZrO_4$ oxide and up to 50% higher hardness compared to cubic ZrO_2 and HfO_2 due to the solid solution hardening effect. Equimolar film exhibit a high transmittance >85% and high hydrophobicity with the water contact angle ≈ 106°. Variation of the elemental composition in Hf-Zr-Ce-Y-O is allows to simultaneously tune mechanical and wetting properties for the optimum configuration depending on the application.

REFERENCES

[1] J. Musil, S. Zenkin, Š. Kos, R. Čerstvý, S. Haviar, “Flexible hydrophobic ZrN nitride films,” Vacuum, vol. 131, pp. 34-38, September 2016.

* The work was supported by RFBR, project number 19-29-13034. The thin films growth equipment was created with the support by Tomsk Polytechnic University development programs.

C4-O-040502

ACCELERATED MOLECULAR SIMULATIONS OF THE LINEAR-CHAINED CARBON SYNTHESIS ON SILICON SUBSTRATE*

E.A. BUNTOV[1], *A.I. MATITSEV*[1], *K.P. ARSLANOV*[1]

[1] *Ural Federal University, Yekaterinburg, Russia*

Linear chain carbon (LCC) is a one-dimensional allotrope of carbon, which has a number of unique optical and electronic properties that make it a promising material for electronic applications. The LCC was first synthesized several decades ago [1] and has already found several applications due to its unique properties. However, the synthesis of linear-chain carbon is still a complex technological challenge. The cause of this problem is the extreme instability and reactivity of carbon chains.

The aim of this work is to study the synthesis of carbon chains on the surface of silicon using molecular dynamics. During the work, a simulation of the deposition of various carbon molecules and clusters (C_2, C_2H, C_2H_2, CH, C_4H_2, C_6H_2) on the silicon surface was performed (Fig. 1, left). Simulation was implemented using three methods of hybrid molecular dynamics [2]: subtractive, force-based and electrostatic. All methods show similar results when modeling a short molecule while for long molecules (C_4H_2 and C_6H_2), only advanced QM/MM methods predict mechanisms of destruction (Fig 1, right).

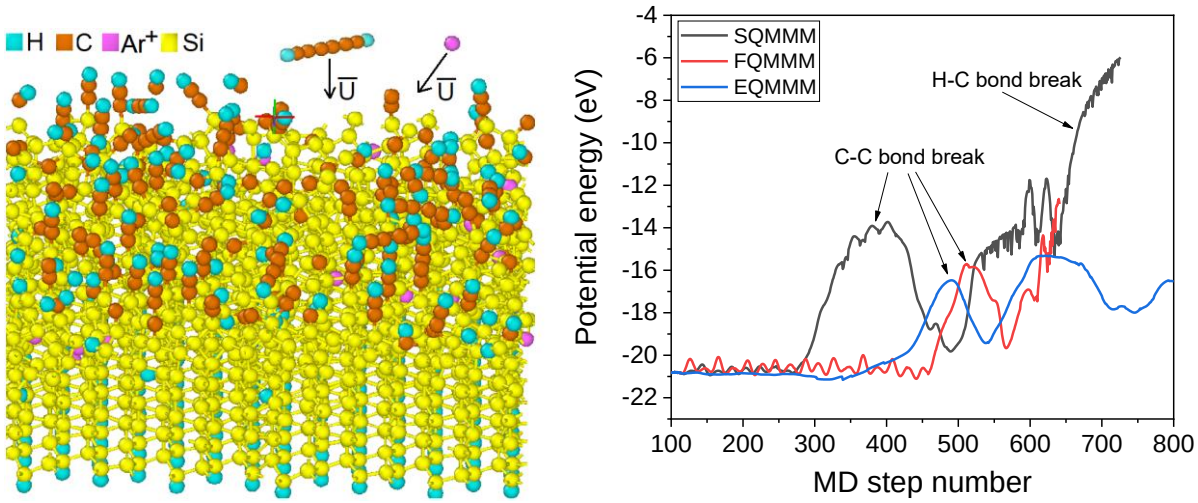

Fig.1. Structural model of the LCC plasma synthesis process (left) and energy profiles for different hybrid MD simulations (right).

The system under study has many metastable states difficult to achieve by conventional MD. In practical terms, metastability means that a system, when modeled by molecular dynamics, is likely to be in only one probability maximum for a long time. A possible way to solve this problem is to fill the free energy minima of metastable states in a controlled way, which allows the system to explore all states [3]. One of the methods for implementing this solution is metadynamics. In [4], the effect of bombardment by argon ions with different energies, bombardment angles, and flux densities on film growth was studied using the classical molecular dynamics method in the LAMMPS program to obtain linear chain carbon. However, the simulation time was not enough for significant film growth. In this work, further modeling was carried out to test the optimal conditions for the synthesis of chain structures. In order to accelerate their growth and increase the time scale of modeling, a complex of methods, including metadynamics, was used.

REFERENCES

[1] Matitsev A.I., Buntov E.A., Zatsepin A.F. “Intrinsic and extrinsic bands in optical spectra of linear-chained carbon films on sodium and potassium chloride substrates”, Optical Materials 115, p. 111021, 2021.

[2] Pezeshki S., Lin H. Recent Developments in QM/MM Methods towards Open-Boundary Multi-Scale Simulations, Molecular Simulation 41, 2014, pp. 1-22.T. V. Koval, Le Hu Dung, “Investigation of plasma generation and current transmission of an intense low-energy electron beam,” Izv. Vyssh. Uchebn. Zaved. Fiz., vol. 57, no. 3/2, pp. 118–121, 2014.

[3] G. Bussi, A. Laio, “Using metadynamics to explore complex free-energy landscapes”, J. Nature Reviews Physics 2, 200–212, 2020.

[4] E. Buntov, K. Arslanov, “A structural criterion for simulation of optimalion-stimulated plasma growth of chained carbon” J. Plasma Process Polym. 19, 1, 2100135, 2022.

* This work was supported by the Ministry of Science and Higher Education of Russian Federation (Project FEUZ-2020-0059).

C4-O-047204

MASS-RESOLVED SPECTROMETRY OF ION FLUX FROM HOT-TARGET REACTIVE HIPIMS DISCHARGE WITH CU, CR, AND SI TARGETS*

D.V. KOLODKO[1,2], A.V. KAZIEV[2], D.G. AGEYCHENKOV[2], A.V. TUMARKIN[2], M.M. KHARKOV[2]

[1]Fryazino Branch of Kotel'nikov Institute of Radio Engineering and Electronics RAS, Fryazino, Russia
[2]National Research Nuclear University MEPhI (Moscow Engineering Physics Institute), Moscow, Russia

High-power pulsed magnetrons enable obtaining denser and stronger coatings as compared to conventional low-ionization DC magnetrons. The use of pulsed magnetron discharges in reactive modes is a promising method for obtaining optical and structural coatings of complex composition. As a rule, working with reactive gases significantly reduces the target sputtering rate and, as a consequence, the rate of coating deposition. The use of a magnetron with a hot target could overcome this drawback, but the specifics of reactive HiPIMS discharges operated with hot targets have not been studied well. Among the most valuable characteristics are the parameters of the ion fluxes ejected from discharge region that eventually arrive at the substrate surface and contribute to the coating growth.

Our work is devoted to the study of the composition of ion fluxes from hot-target reactive HiPIMS discharge. Experiments were carried out for thermally insulated Cu, Cr, and Si targets. These materials are known for their comparatively high vapor pressure and the possibility of sustaining magnetron discharge exclusively in target vapors [1]. The HiPIMS discharge was operated in O_2/Ar mixtures for Cu and Si targets, and in N_2/Ar mixture for Cr target. For these target/gas pairs, the component composition of ion fluxes from plasma was measured by a custom magnetic mass-analyzer as a function of the reactive gas flow. An example of mass spectrum is shown in Fig. 1.

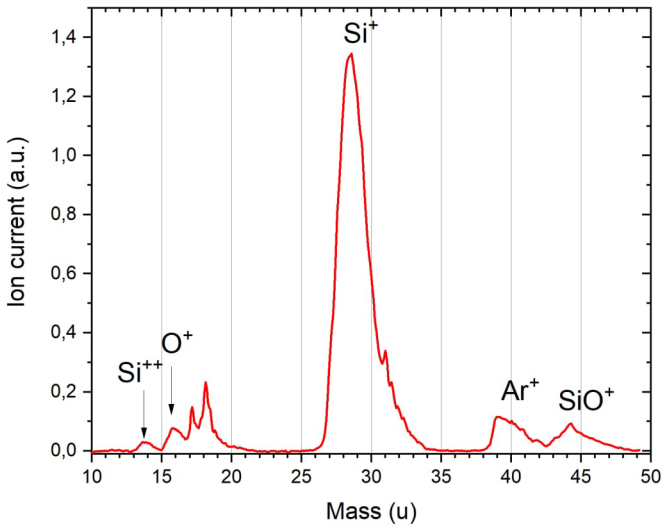

Fig.1. Mass spectrum of ion flux from HiPIMS discharge on Si target in O_2/Ar.

In the experiments, sharp changes in the ratio of fluxes of different ions were observed once the injected reactive gas flow exceeded certain levels. Nevertheless, in the HiPIMS mode, the dominant fraction of the ions are those of the target material.

Specifically, for Si/O_2 case, it is worth noting that the evaporation rate of the oxide is significantly higher than that of pure silicon. This significantly increases the rate of Si_xO_y coating deposition, which is therefore grown not only by the oxidation of the deposited silicon, but also by the deposition of the evaporated oxide. This is observed in the mass spectra of the ion flux where SiO^+ ions are clearly present.

REFERENCES

[1] A.V. Kaziev, K.A. Leonova, M.M. Kharkov et al., "Current–voltage characteristics of an impulse magnetron discharge in target material vapor," J. Phys.: Conf. Ser., Vol. 1686, Article Number 012019, 2020.

* The work was supported by the Russian Science Foundation under grant No. 18-79-10242.

C4-O-047602

DEPOSITION OF TI_2ALC MAX PHASE BY CATHODIC ARC DEPOSITION (ARC-PVD)

A.A.MASLOV[1], *A.YU.NAZAROV*[1], *E.L. VARDANYAN*[1], *K.N. RAMAZANOV*[1]

[1]*Ufa State Aviation Technical University, Ufa, Russia*
e-mail: alexey.maslov2011@gmail.com

In late 1990s the term MAX phases was coined and determined as new family of nitrides and carbides with chemical formula $M_{n+1}AX_n$, where n=1…3, M is an early transitional metal, A is an A-group element, and X is carbon or nitrogen. MAX phases have interesting properties both in bulk form and in thin film coating form. One of prospective methods to synthesize MAX phase thin film is a cathodic arc deposition due to its relatively high deposition rate compared to magnetron sputtering. Ti_3AlC_2 and especially Ti_2AlC are promising MAX phases in terms of high-temperature applications due to formation of stable α-Al_2O_3, therefore a technology of these phases synthesis is important for exploration.

In this work Ti_2AlC was a desired MAX phase for thin film deposition. There are 2 ways to evaporate and deposit Ti and Al: using 2 elemental targets made from pure titanium and aluminum and using one Ti-Al target. In some works, it was shown that deposition from 2 different targets are more preferably due to possibility to use optimal evaporation mode for each element. It is also known that the following annealing can significantly improve formation of desired MAX phase in coating. Therefore, in current work reactive Arc-PVD technology with 2 cathodes was used. After deposition some samples were annealed in vacuum at 800 ^{O}C with 30 minutes' step at 550 ^{O}C. Chamber atmosphere consisted of C_2H_2/Ar mixture which was supplied through hollow-cathode plasma generator.

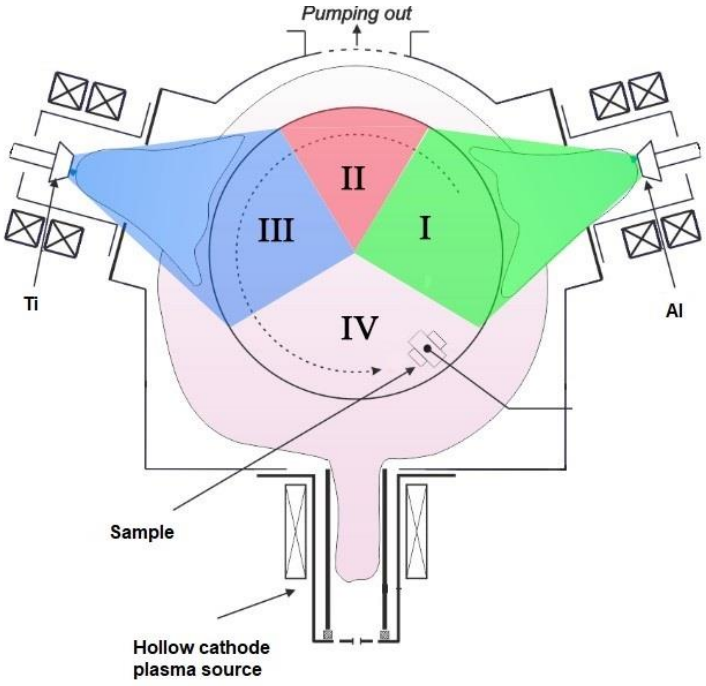

Fig.1. Deposition scheme

Current results demonstrate that amount of Ti_2AlC phase in coating is not 100%, but following annealing improves MAX phase formation, as it was described before. A promising planned way to improve formation of Ti2AlC MAX phase is the use of 2 plasma sources (hollow cathode and heated cathode sources) to improve reactive atmosphere ionization and to increase substrate temperature.

REFERENCES

[1] Eklund P. et al. The Mn+ 1AXn phases: Materials science and thin-film processing //Thin Solid Films. – 2010. – Т. 518. – №. 8. – С. 1851-1878. Mahmoudi Z. et al. Synthesis of Ti2AlC & Ti3AlC2 MAX phases by Arc-PVD using Ti–Al target in C2H2/Ar gas mixture and subsequent annealing //Ceramics International. – 2020. – Т. 46. – №. 4. – С. 4968-4975.

[2] Berger O. The correlation between structure, multifunctional properties and application of PVD MAX phase coatings. Part I. Texture and room temperature properties //Surface Engineering. – 2020. – Т. 36. – №. 3. – С. 225-267.

C4-O-047701

WEAR-RESISTANT FUNCTIONALLY GRADED COATINGS AND SURFACE LAYERS

A. A. NIKOLAEV, E. L. VARDANYAN, A. YU. NAZAROV,A.G. STOTSKIY, G.S. DYAKONOV, V.R. MUKHAMADEEV

Ufa State Aviation Technical University, Ufa, Russia

In the majority of cases of contact interaction, the most loaded part of the workpiece are the surface layers, which experience the highest loads and are subject to considerable wear. This problem is especially clearly marked in titanium alloys and in most cases is the only factor limiting their application. One of the most promising ways to improve the performance properties of materials is the creation of surface and near-surface wear-resistant layers. Application of special, in particular combined, coatings on the surfaces of parts often gives significantly better protection of the surface of the part. Industrial technologies for obtaining multilayer and adaptive coatings (with some properties varying in thickness) are of particular importance [1]. The presence of gradient structure in surface layers allows to obtain new, higher operational properties of products [2,3]. Application of functionally gradient coatings (FGC) allows to combine high adhesive and cohesive properties with high surface hardness, wear resistance, corrosion resistance, thereby obtaining products with unique characteristics. In terms of production costs, relatively simple methods of plasma and gas-dynamic spraying in the formation of FGC are the most attractive. The gradient of properties in the coating applied by one method is created by changing the composition of the sprayed material or the spraying conditions. In spite of the obvious progress in the field of FGP formation in recent years and the significant growth of research, theoretical research and development of formation principles remain insufficient.

In this paper proposed a method of forming FGC, which includes the following operations: ion cleaning of the surface and heating the sample in argon plasma, the application of nitride forming elements (nitride coating) on the surface and low-temperature (≤550 º C) nitriding in high density plasma. As a result, surface layers with greater hardness were obtained compared to the nitrided layers.

REFERENCES

[1] Abitbol G., Ramones J., York T., Journal of Gas Discharges (2004), **4,** 591–601. Cao X. et al. Surface and Coatings Technology (2019), **365**,. 214-221.

[2] Kozlov E. V., Glezer A. M., Gromov V. E., Izvestiya RAN. Series Physical (2003), **67(10)**, 1374.

[3] Krishna B. V. et al., Acta biomaterialia (2008), **4(3)**, 697-706.

C4-O-048101

INFLUENCE OF THE RATIO OF REACTION GASES IN MIXTURE DURING THE DEPOSITION TIAL SYSTEM COATING ON THE DURABILITY OF THE METAL-CUTTING TOOL [1]

A.YU. NAZAROV, E.L. VARDANYAN, V.R. MUKHAMADIEV, A.A. MASLOV, A.A. NIKOLAEV

Ufa state aviation technical university, Ufa, Russia

The purpose of this work is to develop new way to increase the tool life of metal-cutting tools by deposition coating the TiAl system in a mixture of three reaction gases. Among the existing principles for creating functional coatings, the most promising is the concept of multicomponent coatings. Such coatings can satisfy a range of often conflicting requirements. Using this concept, it is possible to create a coating in which compounds of various functional purposes are synthesized in one layer, providing the maximum reduction in tool wear intensity under various machining conditions.

In the conditions of the development of engineering and technology leads to an increase in the share of newly developed special materials with higher properties - heat-resistant and superalloys, composite materials. The mechanical processing of such materials with existing metal-cutting tools is associated with great difficulties [1,2]. High temperatures in the cutting zone, high strength and anisotropy of properties cause rapid tool wear or damage. To solve this problem, various solutions are used, from the development of new cutting tool materials to special hardening methods. One of which is the application of a wear-resistant coating [3,4].

Researches of microhardness, coefficient of friction, chemical and phase composition of the coating, sclerometric studies were carried out and describe in this paper. Investigations of coating wear during turning steel 45x have been carried out. Regularities of the influence of the concentration of the reaction gas of nitrogen, oxygen and acetylene in the composition of the gas mixture on the durability of the metal-cutting tool are obtained.

The results obtained make it possible to compare laboratory studies and production tests, which help develop a promising technology for applying coatings to metal-cutting tools.

REFERENCES

[1] Sousa, V.F.C.; Da Silva, F.J.G.; Pinto, G.F.; Baptista, A.; Alexandre, R. «Characteristics and Wear Mechanisms of TiAlN-Based Coatings for Machining Applications: A Comprehensive Review». Metals 2021, 11, 260.

[2] Gautam, R. K. S., Nautiyal, H., Tyagi, R., and Ranjan, V. "Tribological Characterization of TiAlC Nanostructured Coatings Deposited by DC Pulse Magnetron Sputtering." ASME. J. Tribol. August 2022; 144(8).

[3] S.N. Chen, Y.M. Zhao, Y.F. Zhang, L. Chen, B. Liao, X. Zhang, X.P. Ouyang, «Influence of carbon content on the structure and tribocorrosion properties of TiAlCN/TiAlN/TiAl multilayer composite coatings»,Surface and Coatings Technology,Volume 411,2021.

[4] Shtanskii, D.V., Bondarev, A.V., Kiryukhantsev-Korneev, F.V. et al. «Nanocomposite Antifriction Coatings for Innovative Tribotechnical Systems». Met Sci Heat Treat 57, 443–448, 2015.

[1] The work was supported by the grant of the President of the Russian Federation for state support of young Russian scientists - MK-4991.2022.4.

C4-O-048102

INVESTIGATION OF A CERAMIC COATING OF ALUMINUM OXIDE OBTAINED BY VACUUM-ARC DEPOSITION[1]

A.YU. NAZAROV, E.L. VARDANYAN, A.A. TULINA, E.A. KORZNIKOVA

Ufa state aviation technical university, Ufa, Russia

Surface wear of cutting tools is determined by the predominant influence of adhesive and diffusion processes. Operating the cutting edge at a small constant cutting cross section does not destroy the substrate. In this case, tool resistance is determined by the characteristics of the tool surface, namely the protective coating. The dominant factor that leads to dullness of the cutting edge in this case is the thermal impact, the value of which is determined by the cutting speed.

Achieving new physico-mechanical properties is possible due to chemical and physical effects. It is known that oxide coatings (Al_2O_3, SiO_2, TiO_2, ZrO_2, B_2O_3, HfO_2, SeO_2, etc.) have a number of properties not inherent in metal and other types of coatings - low thermal conductivity, chemical inertness, wear resistance. The majority of oxides have high melting point, hardness and wear resistance. They are the most universal under operating conditions and can be used as corrosion-resistant, heat-resistant, heat-proof, electrical insulating and wear-resistant. The most effective is the coating, which includes aluminum oxide. To obtain coatings from aluminum oxide, the method of CVD is used more often, but this method is not widespread due to the fact that the temperature of deposition on these units is 1050 °C, the CVD method is used to obtain metastable modifications of Al_2O_3 because the transition temperature of θ-Al_2O_3 to less porous and harder α-Al_2O_3 is 1200 °C [3].

The purpose of this work is to study the physical and mechanical properties and structural-phase coating of caps based on aluminum oxide. An alumina ceramic coating is applied to study the wear of the carbide. Microhardness, adhesion strength, coating thickness, coating phase composition were investigated on the obtained samples. Results of researches expand knowledge about physical and mechanical properties of ceramic coverings of aluminum oxide deposited their plasma of vacuum arc discharge.

REFERENCES

[1] D. Loktev, and E. Yamashkin. "Main types of wear-resistant coatings" Nanoindustry vol. 5, pp. 24-31, 2007.

[2] M. Maximov. "Wear-resistant coatings as the driving force behind innovative processes in tool material technology and modern metalworking." NanoWeek, № 106, 13 – 19 April 2010.

[3] Chaly V.P. "Metal hydroxides." Naukova dumka, p.160, 1972.

[4] Zaycev A.N.., Yagopolski A.G., Alexandrova Yu.P. " Evaluation of the influence of structure and chemical composition of plasma-sprayed coatings on their adhesion and tribotechnical properties", vol.12, p.657, 2014

[5] Pogrebnyak A.D., Ilyashenko M.V., Bratushka S.N., Ponaryadov V.V., Erdybaeva N.K. "Physico-mechanical properties of ceramic and metal-ceramic coatings applied by plasma detonation method." FIP, vol. 4, № 1-2, pp. 48-72, 2006.

[1] The study was carried out with the financial support of the Ministry of Science and Higher Education of the Russian Federation within the framework of the state task of the Federal State Budgetary Educational Institution of Higher Education "UGATU" (agreement No. 075-03-2022-318 / 1) youth research laboratory of the REC "Metals and Alloys under Extreme Impacts"

C4-O-048401

DEPOSITION OF TRANSPARENT CONDUCTIVE AZO FILMS ON MEDIUM-SIZED GLASS AND POLYMER SUBSTRATES

D.G. AGEYCHENKOV[1], A.V. KAZIEV[1], D.V. KOLODKO[1,2]

[1]National Research Nuclear University MEPhI (Moscow Engineering Physics Institute), Moscow, Russia
[2]Fryazino Branch of Kotel'nikov Institute of Radio Engineering and Electronics RAS, Fryazino, Russia

AZO transparent conductive coatings are one of the alternatives to ITO-based coatings with the closest possible optical and electrical properties [1]. Importantly, they do not contain rare and toxic elements that makes the usage of AZO-based transparent conductive coatings advantageous. In this study, thin layers of AZO (up to 2 μm) were deposited on medium-sized substrates. The substrate materials were silicon glass, acrylic, and polycarbonate. The deposition was carried out using a Pinch Magneto series magnetron [2].

Coatings were deposited by sputtering a sintered ceramic target AZO (98% ZnO:2% Al_2O_3) in DC power mode. The magnetron used for deposition was unbalanced, that resulted in significant flux of ions falling on the substrate. In order to mitigate the ion flux, the deposition was carried out at a sufficiently high pressure of 1 Torr. It has been experimentally shown that this pressure is optimal and makes it possible to achieve AZO films with electrical resistivity of ~ 4×10^{-6} Ω×m, while maintaining transparency in the optical range of 76%. The obtained mass spectra showed a correlation between the decrease in the ion flux and an increase in pressure.

Due to the design features of the sample table, the substrate is practically thermally insulated in vacuum. For acrylic samples, this leads to cracking of the coatings when the energy load exceeds 150 W×h. For polycarbonate samples, it was possible to achieve good resistivity and optical transparency (~ 6×10^{-6} Ω×m; 76% transparency) at an energy load of less than 300 W×h.

REFERENCES

[1] D.J. Rogers, F.H. Teherani, V.E. Sandana, M. Razeghi “ZnO thin films and nanostructures for emerging optoelectronic applications,” Proceedings of SPIE - The International Society for Optical Engineering, Vol. 7605, Article Number 76050K, 2010.

[2] A.V. Kaziev, D.G. Ageychenkov, A.V. Tumarkin, D.V. Kolodko, N.S. Sergeev, M.M. Kharkov, K.A. Leonova “Ion current optimization in a magnetron with tunable magnetic field configuration,” J. Phys: Conf. Ser. Vol. 2064, Article Number 012061, 2021.

C4-O-049803

RF AND DC MAGNETRON SPUTTERING METHODS for DEPOSITION of BIOINERT and BIOACTIVE COATINGS

YU.P. SHRKEEV[1,2], K.A. PROSOLOV[1], M.E. KONISHCHEV[2], K.E. EVDOKIMOV[2], A.D. BADARAEV[2], S.I. TVERDOKHLEBOV[2]

[1]Institute of Strength Physics and Materials Science of SB RAS, 2/4, pr. Academicheskii, Tomsk, 634055, Russia, konstprosolov@gmail.com, +7-961-888-58-33
2 National Research Tomsk Polytechnic University,30, Lenin Avenue, Tomsk, 634050, Russia

Surface modification of implants is a rapidly developing multidisciplinary field that combines expertise of materials science and healthcare professionals. Improvement of implants in terms of their biocompatibility, hemocompatibility, antibacterial properties, osteointegration and osteoinduction are the main topics of research. These properties are crucial to ensure desirable biological response to the newly implanted material, in the manner that the cells, which are adhered to the surface of such scaffolds can function in a way that is similar to physiological conditions or help to prevent possible complications.

Physical vapor deposition (PVD) of thin films, allowing the deposition of multicomponent coatings, has been available for some years. An emerging method for bioactive coating deposition in the field of PVD is radiofrequency (RF) magnetron sputtering method [1]. Magnetron sputtering is widely used in the formation of coatings for various applications. The continuous interest of scientists for this method is due to the possibility of modifying the coating structure and its physicochemical properties by variation of the deposition parameters. There is a significant interest in radiofrequency (RF) magnetron sputtering of bioactive calcium phosphate thin films. This method allows deposition of CaP coatings with a high level of adhesion to substrate. In the light of demand for antibacterial coatings, hydroxyapatite is frequently substituted by ions of Zn, Cu, and Ag [2]. Zinc ions, for example, are well-known not only for its antibacterial properties, but it also acts as an inhibitor of crystal growth. It is essential trace element for tissue regeneration [3]. An RF magnetron sputtering of Zn- or Cu-substituted hydroxyapatite allow to deposit antibacterial calcium phosphate coatings that not only improve osteointegration, but act as a protecting layer that could alter the degradation rate of the substrate and induce local antibacterial effect.

On the other hand, binary and ternary titanium compounds (oxides and oxynitrides) standalone among other coatings due to their high bio- and hemocompatibility. This is especially true for cardiovascular implants. The titanium oxynitride film, deposited using reactive magnetron sputtering, combines the properties of two components: titanium oxide and nitrogen oxide (NO). Modification of deposition parameters such as substrate bias, working gas, deposition pressure, allow to change the structure and properties of deposited layers.

Moreover, the magnetron sputtering method has been used to modify different scaffolds from bioinert polymers, ceramics and metallic alloys. The magnetron co-sputtering method with using of copper and titanium targets in an argon atmosphere is applied to modify the PCL scaffolds surface for improvement of osseointegration and antibacterial properties.

REFERENCES

[1] Prosolov, K. A., Lastovka, V. V., Belyavskaya, O. A., Lychagin, D. V., Schmidt, J., Sharkeev, Y. P. “Tailoring the surface morphology and the crystallinity state of Cu-and Zn-substituted hydroxyapatites on Ti and Mg-based alloys”, Materials, vol.19, no.13, pp. 1-20, October 2020.

[2] Noda I., Miyaji F., Ando Y., Miyamoto H., Shimazaki T., Yonekura Y., Miyazaki M., Mawatari M. and Hotokebuchi T. “Next Generation Antibacterial Hydroxyapatite Coating: Antibacterial Activity of Ag Ions in Serum”, Bioceram. Dev. Appl., vol. 1, no. 3, pp. 1-3, December 2011.

[3] Graziani V., Fosca M., Egorov A. A., Zobkov Y. V., Fedotov A. Y., Baranchikov A. E., Ortenzi M., Caminiti R., Komlev V. S. and Rau J. V. “Zinc-releasing calcium phosphate cements for bone substitute materials”, Ceram. Int., vol. 42, no. 15, pp. 17310-17316, November 2016.

[4]

C4-O-051001

INFLUENCE OF DEPOSITION TECHNOLOGICAL PARAMETERS COATINGS OF THE YALO SYSTEM BY THE METHOD OF VACUUM-ARC ON THE STRUCTURE AND PHASE COMPOSITION OF THE COATING.*

K.N. RAMAZANOV, A.YU. NAZAROV, E.L. VARDANYAN, A. M. KHUSAINOVA

Ufa state aviation technical university, Ufa, Russia

The paper deals with the development of simulation methods as applied to low-pressure discharges with extremely high reduced electric fields *E*/*p* for which it is problematic to correctly describe the ionization processes in classical electron avalanches. In some conditions, the electron free path for ionization can compare with the interelectrode gap width such that the notion of electron avalanches becomes inapplicable at all. Typical examples are discharges in so-called pseudo-spark switches and in electron and ion plasma sources [1].

Increase the temperature of the gases in front of the GTE turbine is necessary to improve the power and efficiency of gas turbine engines (GTE). In this regard, it is necessary to protect GTE parts from exposure to high temperatures and gas flow. Thermal barrier coatings based on ZrO_2-Y_2O_3 are used to protect the temperature drop of the blades [1, 2, 3, 4].

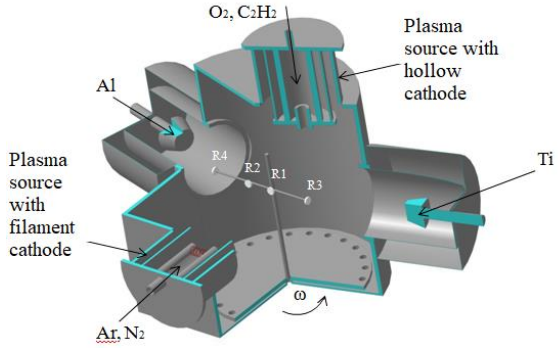

Fig. 1. Experimental installation NNV-6,6 I1.

Currently, a widely used material for thermal barrier coatings (TBCs) was zirconium dioxide, partially stabilized with yttrium, i.e. ≈8 wt. % Y_2O_3 (8YSZ) [6, 7, 8]. But recent works presented that yttrium aluminates are promising materials for TBC due to their excellent stability at high temperatures, as well as mechanical and thermal properties [5,6]. At high temperatures, yttrium aluminum garnet (i.e., $Y_3Al_5O_{12}$, YAG) is stable as Al_2O_3 [5], which used for Ni-based superalloys as a thermally grown oxide layer. Besides YAG, $Y_4Al_2O_9$(YAM) is also a stable compound in the YAlO system.

In this paper describe the effect of technological parameters of coating the YAlO system on phase and chemical composition. Regularities of the influence of the concentration of yttrium and aluminum on the phase composition of the coating are obtained. Heat-resistance of developed coating was studied.

REFERENCES

[1] Riallant F., Cormier J., Longuet A., «High-Temperature Creep Degradation of the AM1/NiAlPt/EBPVD YSZ System», Metall Mater Trans A – 2014. V. 45. C. 351–360.

[2] Kunal M., Luis N., Calvin M.D., «Thermal Barrier Coatings Overview: Design, Manufacturing, and Applications in High-Temperature Industries», Industrial & Engineering Chemistry Research – 2021. V.60. №.17. C. 6061-6077.

[3] Zhang, C., Lv, P., Xia, H., Yang, Z., Konovalov, S., «The microstructure and properties of nanostructured Cr-Al alloying layer fabricated by high-current pulsed electron beam», Vacuum – 2019. V. 167. C. 263-270..

[4] Alymov, M.I., Stolin, A.M., Bazhin, P.M., « Investigation of the structure and properties of protective coatings produced by the method of electric spar alloying with shs electrodes (review)», Industrial Laboratory. Materials Diagnostics. - 2022, V. 88. №. 2. C. 40–48.

[5] Bin L, Yuchen L, Changhua Z., «Advances on strategies for searching for next generation thermal barrier coating materials», Journal of Materials Science & Technology. – 2019.V. 35. № 5. C 833-851.

[6] Uwe S., Christoph L., Klaus F., Some recent trends in research and technology of advanced thermal barrier coatings», Aerospace Science and Technology. - 2003. V.7. №.1. C. 73-80.

[7] Clarke D., Oechsner M., Padture N., «Thermal-barrier coatings for more efficient gas-turbine engines», MRS Bulletin - 2012. V.37. №.10., C. 891-898.

[8] Padture N., «Advanced structural ceramics in aerospace propulsion», Nature Mater. - 2016. V. 15. C. 804-809.

* The work was supported by the Russian Science Foundation under grant No. 22-19-20119.

C4-O-051003

INVESTIGATION OF THE OXIDATION OF TI-AL AND AL-CR COATINGS DEPOSITED BY VACUUM-ARC DEPOSITION [1]

K.N. RAMAZANOV, A.YU. NAZAROV, E.L. VARDANYAN, A.A. TULINA, A. M. KHUSAINOVA

Ufa state aviation technical university, Ufa, Russia

The development of the aircraft engine industry leads to the fact that more and more new materials are being developed and introduced - carbon-free heat-resistant alloys and intermetallic alloys. However, to ensure the long-term performance of parts made from these materials under conditions of high-temperature oxidation, it is necessary to develop special protective coatings that prevent damage to the surface of the parts. If for nickel-based superalloys there are currently solutions for protection against high-temperature oxidation, then research work is only underway for intermetallic alloys.

The purpose of this work is to search and study new heat-resistant coatings for intermetallic alloys for protection against high-temperature oxidation. To date, intermetallic alloys of the TiAl system are a promising material for the development of heat-resistant alloys used for the manufacture of parts for aircraft engines and gas turbine power plants.

In this work, coatings of the TiAl and AlCr systems with a monolayer and gradient structure were studied. The phase and chemical composition of the initial coatings have been studied. After high-temperature tests, the mass gain was studied depending on the holding time, the phase composition, the chemical composition in depth, and the mechanism of coating oxidation.

REFERENCES

[1] C. Leyens, M. Peters, W.A. Kaysser., «Intermetallic Ti-Al coatings for protection of titanium alloys: oxidation and mechanical behavior», Surfacce and Coatings Technology 94-95 (1997) 34-40.

[2] Zhenyu L. , Guodong W., «Improvement of oxidation resistance of _-TiAl At 800 and 900 ◦C in air by TiAl2 coatings», Materials Science and Engineering A 397 (2005) 50–55.

[3] Takumi N. , Takeshi I., Shigenari H., Toshio N., « Two-step Cr and Al diffusion coating on TiAl at high temperatures», ntermetallics 11 (2003) 225–235.

[4] Braun, R., Fröhlich, M., Leyens C., "Oxidation behaviour of TiAl-based intermetallic coatings on γ-TiAl alloys" International Journal of Materials Research, vol. 101, no. 5, 2010, pp. 637-647.

[5] Xinfeng L., Chuiyi M., Xiantao X., Xiujie H., Canyu W., «Effect of Al content on high-temperature oxidation behavior and failure mechanism of CrAl-coated Zircaloy», Corrosion Science, Volume 192, 021.

[1] The work was supported by the Russian Science Foundation under grant No. 22-29-01463.

C4-O-900801

SYNTHESIS OF MULTILAYERED COATINGS BY VACUUM-ARC PLASMA-ASSISTED METHOD*

O.V. KRYSINA, YU.F. IVANOV, O.S. TOLKACHEV, E.A. PETRIKOVA

Institute of High Current Electronics SB RAS, Tomsk, Russia

The vacuum-arc synthesis of PVD coatings with multilayer structure has been described. Few methods have been considered. There are gas changing, the use of few arc evaporators with substrate holder rotating, the use of gas plasma generator, and etc. The feature of new low-inertia deposition method is the use of a gas plasma source based on a non-self-sustained arc discharge with thermionic and hollow cathodes. The coatings were synthesized by the vacuum-arc method in a QUINTA automated ion-plasma set-up (IHCE, Tomsk, Russia). Its description is detailed elsewhere [1]. The examples of multilayered coatings deposited by low-inertia method are presented. The systems of multilayer coating were based on Mo, Nb, Zr, Al, Ti and their nitrides. The properties, structure, elemental and phase compositions were detailed investigated. The thickness of one layer of multilayered coatings varied in the range of few to hundreds nanometers. It is shown that selected method characterized by low inertia, which would make it possible to achieve a high reproducibility of the composition and thickness of multi-layer coatings, which would naturally improve their functional properties.

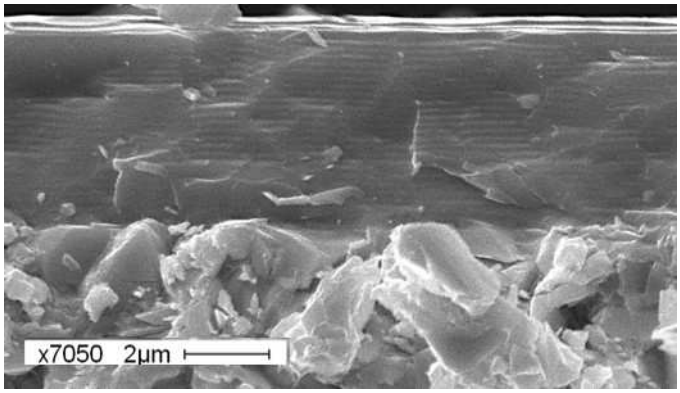

Fig.1. Typical SEM image of multilayered coatings with the 100-nm thickness of layer.

REFERENCES

[1] V.V. Shugurov, N.N. Koval, O.V. Krysina, N.A. Prokopenko, "QUINTA equipment for ion-plasma modification of materials and products surface and vacuum arc plasma-assisted deposition of coatings," IOP Conf. Ser.: J. Phys.: Conf. Ser., vol. 1393, pp. 12131 (1−10), 2019.

*This work was carried out with the financial support of Russian Federation represented by Ministry of Science and Higher Education (project No. 075-15-2021-1348) within the framework of event No. 2.1.5, 2.1.17, 2.1.20.

C4-P-003303

ELECTRON-BEAM DEPOSITION OF COMPOSITE COATINGS BASED ON METAL AND CERAMICS*

A.S. KLIMOV[1], E.M. OKS[1,2], A.V. TYUNKOV[1], YU.G. YUSHKOV[1], D.B. ZOLOTUKHIN[1]

[1]Tomsk State University of Control Systems and Radioelectronics, Tomsk, Russia
[2]Institute of High Current Electronics, Tomsk, Russia

Composite coatings consisting of two or more components combined to form a layered or mixed structure are an established feature for enhancing the parameters and characteristics of materials [1]. To date, one of the most promising composites for obtaining wear-resistant and corrosion-resistant plasma coatings that increase the durability and reliability of starting materials, are composites that consist of a metal-ceramic matrix [2]. Such coatings can be obtained by various mechanical, chemical, and modern high-performance beam-plasma methods [3]. Among all beam-plasma deposition methods, electron-beam evaporation and vapor deposition of the evaporated material on products has the highest deposition rates that ensure the formation of a coating with desired characteristics [4]. At the same time, the evaporation of dielectric materials including ceramics, by an electron beam is very difficult and inefficient; this problem is successfully solved with the use of fore-vacuum plasma electron sources [5].

The paper presents the results of experimental studies of the processes of obtaining plasma with ceramic and metal particles and coatings deposited from such plasma on metal substrates.

Evaporated ceramic-metal targets were fabricated from nanopowder of alumina ceramics sintered in the process of electron-beam exposure with different proportions of metal. The mass-to-charge composition of a multicomponent plasma formed during the evaporation of sintered targets has been studied, metal-ceramic coatings have been obtained, and their characteristics have been studied.

REFERENCES

[1] Winnicki, M. Advanced Functional Metal-Ceramic and Ceramic Coatings Deposited by Low-Pressure Cold Spraying: A Review. Coatings 2021, 11, 1044.

[2] X. Shan, L.Q. Wei, X.M. Zhang, W.H. Li, W.X. Tang, Y. Liu, J. Tong, S.F. Ye, Y.F. Chen, A protective ceramic coating to improve oxidation and thermal shock resistance on CrMn alloy at elevated temperatures, Ceram. Int. 41 (2015) 4706-4713.

[3] Chen Song. New preparation of ceramic coatings by low-pressure plasma spray. Materials Science [cond-mat.mtrl-sci]. Université Bourgogne Franche-Comté, 2018. English. ffNNT : 2018UBFCA009ff. fftel-01876692f.

[4] Yushkov, Yury G., Efim M. Oks, Andrey V. Tyunkov, and Denis B. Zolotukhin. 2022. "Electron-Beam Synthesis of Dielectric Coatings Using Forevacuum Plasma Electron Sources (Review)" Coatings 12, no. 1: 82.

[5] Alumina coating deposition by electron-beam evaporation of ceramic using a forevacuum plasma-cathode electron source / Y. G. Yushkov, E. M. Oks, A. V. Tyunkov, D. B. Zolotukhin // Ceramics International. – 2019. – Vol. 45. – No 8. – P. 9782-9787.

* The work was supported by the Grant of the Ministry of Education and Science of the Russian Federation, Project FEWM-2020-0038.

C4-P-003304

RESEARCH OF PROCESSES OF ELECTRON-BEAM DEPOSITION OF BORON-CONTAINING COATINGS IN FORE-VACUUM PRESSURE RANGE *

A.V. TYUNKOV[1], YU.G. YUSHKOV[1,2], D.B. ZOLOTUKHIN[1,2]

[1]Tomsk State University of Control Systems and Radioelectronics, Tomsk, Russia
[2]Institute of High Current Electronics, Tomsk, Russia

Boron plasma is widely used in the generation of accelerated ion beams for the technology of boron implantation into semiconductor wafers for the creation of element base of microelectronics and dielectric protective coatings [1-2]. The novelty of the ongoing research is based on the use of unique equipment and original approaches based on electron-beam evaporation of a solid target made of pure boron with low electrical conductivity [3]. It is the low conductivity of pure boron under normal conditions that prevents the use of a target made of this material for focusing an electron beam to heat it. The originality of the approach for the generation of boron plasma in relation to the creation of coatings, in this case, lies in the use of a fore-vacuum electron source operating at an elevated gas pressure of 10 Pa, at which the surface charge of the electron beam on the target is neutralized by ions from dense beam plasma. This provides the possibility of heating, evaporation and ionization of the solid-state target material made of pure boron.

This work presents the results of studying the characteristics of electron-beam evaporation of boron and the parameters of the beam plasma of boron, including the mass-charge composition of ions, the spatial distributions of vapors of the evaporated target, the deposition rates and the main characteristics of the coatings.

REFERENCES

[1] Walther S. Characterization of a Bernas ion source for multiply charged ion implantation // Review of Scientific Instruments, 1994, V. 65, p. 1307 - 1309.

[2] Deposition of boron-containing coatings by electron-beam evaporation of boron-containing targets / Y. G. Yushkov, E. M. Oks, A. V. Tyunkov [et al.] // Ceramics International. – 2020. – Vol. 46. – No 4. – P. 4519-4525.

[3] Alumina coating deposition by electron-beam evaporation of ceramic using a forevacuum plasma-cathode electron source / Y. G. Yushkov, E. M. Oks, A. V. Tyunkov, D. B. Zolotukhin // Ceramics International. – 2019. – Vol. 45. – No 8. – P. 9782-9787.

* The work was supported by grant of the Russian Science Foundation (project № 22-29-00381).

C4-P-004201

ELECTRON BEAM DEPOSITION OF CERAMICS ON POLYPROPYLENE IN THE FOREVACUUM PRESSURE RANGE*

A.S. KLIMOV[1], *I.YU. BAKEEV*[1], *V.T. TRAN*[1], *A.A. ZENIN*[1]

[1] *Tomsk State University of Control Systems and Radioelectronics, 40 Lenin ave,. Tomsk, 634050, Russia*

Currently, polymers are widely used in many areas of industry. This is possible due to the many advantages over other materials. In particular, polymers are relatively easier to produce, cheaper, easier to use materials with high insulating properties. However, they have disadvantages due to their structural properties (lower hardness and durability, weak adhesion), insufficient gloss [1]. To solve this problem, the application of protective metal or ceramic coatings on the surface of polymers is practiced [2, 3].

At present, electron beam evaporation is recognized as one of the best methods that provides a set of necessary coating properties in combination with a high deposition rate and processability of operations. This paper presents a study of thermal heating modes of polymer substrates located at different distances to the evaporated ceramic target. A forevacuum plasma electronic source was used to vaporize ceramics [4]. The peculiarity of the source is the possibility of direct processing of non-conductive materials, in particular glass, ceramics, polymers [5]. The ceramic target made of aluminum oxide was heated to the evaporation temperature and the evaporation products were sprayed onto polymer substrates. The dependences of the coating growth rate on the deposition time, target temperature and distance to the polymer substrate are obtained. As a result, coatings with a thickness of up to 0.1 microns were obtained. The prospects of electron beam evaporation of ceramics for coating polypropylene are shown.

REFERENCES

[1] Y. El-Ghoul, F.M. Alminderej, F.M. Alsubaie, R. Alrasheed, N.H. Almousa, «Recent Advances in Functional Polymer Materials for Energy, Water, and Biomedical Applications: A Review», Polymers, vol. 13, pp. 4327, 2021. https://doi.org/10.3390/polym13244327.

[2] S. Ayrault, A. Chateauminois, J. P. Soulier, D. Tréheux, A.B. Vannes, «Deposition of a ceramic coating on a thermoplastic polymer by atmospheric plasma and laser cladding», Surface and Coatings Technology, vol. 79(1-3), pp. 119–130, 1996.

[3] A. Ganesan, M. Yamada, M. Fukumoto, «Cold Spray Coating Deposition Mechanism on the Thermoplastic and Thermosetting Polymer Substrates», Echnical Physics Letters, vol. 22(8), pp. 1275–1282, 2003.

[4] A.S. Klimov, I.Yu. Bakeev, E.M. Oks, A.A. Zenin, «Forevacuum plasma source of continuous electron beam», Laser Part Beams, vol. 37(2), p. 203-8, 2019.

[5] A.A. Zenin, I.Y. Bakeev, Y.A. Burachevskii, A.S. Klimov, E.M. Oks «Electron beam focusing features in a plasma electron source under forevacuum pressures», Technical Physics Letters, vol. 42, №7, pp. 712-714, 2016.

* The work on the study of coating parameters was supported by the grant from the Ministry of Science and Higher Education of the Russian Federation within the framework of the 2021 competition FEWM-2021-0013. The part reported study on electron beam coating of polymers was funded by RFBR according to the research project №20-38-90184.

C4-P-005302

SURFACE HIGH SPEED STAINLESS STEEL ALLOYING WITH COPPER *

Yu.F. IVANOV, E.A. PETRIKOVA, A.D. TERESOV, N.A. PROKOPENKO, M.S. PETYUKEVICH

Institute of High Current Electronics SB RAS, Tomsk, Russia

The using copper as an alloying element, the addition of which in small concentrations to low-carbon steel instead of expensive elements - niobium, titanium and vanadium, leads to the appearance of high corrosion and mechanical characteristics associated with the formation of Fe-Cu precipitates in the bulk of the material [1-3]. It has been established that these precipitates are nanosized particles of a saturated (more than 1% at.) solid solution of copper in iron, while in the equilibrium state the maximum solubility of copper in iron does not exceed 0.38% at. In this case, one should speak about the properties of the material as a function of near-surface transition states. Nanosized copper-enriched particles in α-Fe formed during cooling provide high ductility and fracture toughness and cause dispersion strengthening of the steel.

The formation of the "film (Cu)/(steel 321) substrate" system was carried out on the QUINTA installation [4] by sputtering copper films 0.5 μm thick onto steel specimens. High-speed alloying of steel with copper was carried out by irradiating the "film (Cu)/(steel 321) substrate" system with a pulsed electron beam using a SOLO setup [4]. The irradiation mode corresponded to the liquid-phase alloying of the steel surface layer with copper.

Studies performed by scanning electron microscopy showed that at an electron beam pulse duration of 50 μs (15 J/cm^2, 15 pulses, 0.3 s^{-1}) a nanocrystalline structure with a crystallite size of (80-120) nm is formed on the specimen's surface. At an electron beam pulse duration of 200 μs (30 J/cm^2, 15 pulses, 0.3 s^{-1}), regions with a lamellar structure are formed on the specimens surface. A structure of cellular crystallization is observed in the bulk of the plates. The cell sizes vary within (0.58-0.81) μm. X-ray microanalysis revealed a decrease (more than 4 times) in the concentration of copper in the steel surface layer with an increase in the duration of exposure to the electron beam from 50 μs to 200 μs.

Using X-ray phase analysis methods, it was shown that at an electron beam pulse duration of 50 μs, a solid solution of copper in a crystal lattice based on γ-Fe and a $Fe_{0.5}Cu_{0.5}$ phase with a bcc crystal lattice are formed in the surface layer. With an increase in the pulse duration to 200 μs, a two-phase structure is formed in the surface layer - γ-Fe and a phase of $Fe_{0.7}Cu_{0.3}$ composition, which has an fcc crystal lattice.

Cu as a separate phase is not detected. An increase in the electron beam pulse duration from 50 μs to 200 μs leads to an increase in the crystal lattice parameter of γ-Fe from 0.35191 nm to 0.35300 nm. Taking into account the ratio of the sizes of the atomic radii of Fe (R(Fe) = 0.126 nm) and Cu (R(Cu) = 0.128 nm), we can conclude that the process of replacing iron atoms in the crystal lattice of the γ-phase by copper atoms increases with an increase in the duration of the electron beam pulse, which leads to an increase in the lattice parameter.

Thus, a two-stage mechanism of solid solution decomposition in the "film (Cu) / (steel 321) substrate" system irradiated with a pulsed electron beam was revealed, as a result of the performed studies. At an electron beam treatment duration of 50 μs, the formation of nanosized particles of the $Fe_{0.5}Cu_{0.5}$ phase, which has a bcc crystal lattice, is observed. With an increase in the duration of exposure to the electron beam to 200 μs, the formation of $Fe_{0.7}Cu_{0.3}$ composition phase, which has an fcc crystal lattice, is recorded in the steel surface layer.

REFERENCES

[1] L.A. Dreval. «Thermodynamic properties of liquid alloys of copper and iron with chromium, cobalt and nickel», Abstract of the dissertation of Cand. chem. Sciences. Kiev: Kiev National University, 2011.

[2] Yu.N. Gornostyrev, I.N. Karkin, L.E. Karkina, «Interaction of dislocations with nanoscale precipitates of the metastable phase and dispersion strengthening of the Fe-Cu alloy», Solid State Physics, V.53, No. 7, 2011.

[3] S.N. Saltykov, A.M. Hoviv, A.A. Maksimenko, «On the issue of polymorphic modifications of iron in a thin-film state», Journal of Inorganic Chemistry, V. 56, No. 3, 2011.

[4] S.V. Grigoriev, N.N. Koval, V.N. Devjatkov, A.D. Teresov, «The automated installation for surface modification of metal and ceramic-metal materials and products by intensive pulse sub-millisecond electron beam», Proc. 9th Intern. Conf. on Modification of Materials with Particle Beams and Plasma Flows. – Tomsk, 2008.

* *The work was supported by the Ministry of Science and Higher Education of the Russian Federation (Number: FWRM-2021-0006).*

C4-P-005501

INFLUENCE OF CARBON CATHODE PLASMA PARAMETERS ON THE STRUCTURE AND PROPERTIES OF THE DEPOSITED COATINGS

Y.M LIU[1,2], *X.H. JIANG*[1], D.G. PILIPTSOU[1,2], A.V. ROGACHEV[1,2]

[1]*International Chinese-Belorussian Scientific laboratory on Vacuum-Plasma Technology, Nanjing University of Science and Technology, Nanjing, China*
[2] *Francisk Skorina Gomel State University, Gomel, Belarus*

The interest in carbon coatings (ta-C) stems from their unique optical, electrophysical, and mechanical properties [1, 2]. Energy, carbon ion flux density, presence of carbon microparticles in the flux, incidence angle and substrate temperature are among the most important parameters determining the structure of carbon-carbon bonds and, consequently, the properties of coatings deposited from pulsed cathode plasma [3, 4]. The influence of these parameters on the structure and properties of the coatings is largely related to the nonequilibrium nature of pulsed plasma flow generation, the course of intensive energy exchange between ions in the flow, which leads to changes in the phase composition and properties of the coatings [4]. The effect of the carbon plasma pulse repetition rate on the ratio of sp^3/sp^2 bonds, hardness, optical properties and the band gap width during the deposition of the composite ta-C coatings is particularly noticeable, since in this case there is a change in the mass ratio of individual ingredients in the flows entering the substrate surface. When evaluating the possible causes that determine the change in the properties of coatings, it is necessary to consider the interaction peculiarities between carbon ions directly in the pulse, the change in the charge state and energy of the particles at the leading and trailing edges of the pulse when they move from the generation zone to the substrate surface. One of the most effective methods of forming a given charge and energy structure of the pulse is to change its duration and particle energy at different stages of plasma discharge generation.

This work aims to establish the influence of energy and time parameters of the discharge on the phase composition, structure and mechanical properties of the resulting carbon coatings. The equipment has been developed that allows forming ta-C coatings by eroding a carbon cathode with a pulsed discharge having two zones that differ in voltage. At the same time, it is possible to control temporal (pulse duration, pulse repetition frequency) and energy (pulse energy and its distribution) parameters of a pulsed cathode-arc discharge. Changing these parameters makes it possible to regulate the energy and density of the ion flux during the evaporation of the graphite cathode, as well as to provide the required thermal load on the substrate. The influence of the operation modes of the pulsed carbon plasma generator on the phase composition and mechanical properties of the carbon coatings has been established. It has been shown that the highest sp^3-phase content and, consequently, hardness, the lowest roughness, a more homogeneous structure of the surface layer, are achieved by creating a high-current pulsed arc discharge between the graphite cathode and the anode, at the leading edge of which the voltage value exceeds significantly the value at the trailing edge. It has been demonstrated that the change in the energy of evaporated carbon particles at the stage of their generation and in the transfer process affects the nature of deposition and determines its dependence on the distance to the substrate: near the evaporation zone, deposition is performed from a pulse flow, at larger distances - from a quasi-homogeneous flow. The optimal values of the duration and frequency of pulses have been determined, at which the maximum physical and mechanical properties are achieved.

The research findings are of interest when developing technological processes for creating new functional coatings based on amorphous carbon.

REFERENCES

[1] B Zhou, D.G. Piliptsou, X. Jiang, A.V. Rogachev, A.S. Rudenkov, E.A. Kulesh “Structure and mechanical properties of Ni and Cr binary doped amorphous carbon coatings deposited by magnetron sputtering and pulse cathodic arc“, Thin Solid Films, 701, 137942, March, 2020.

[2] A.S. Chaus, X.H. Jiang, P. Pokorný, D.G. Piliptsou, A.V. Rogachev “Improving the mechanical property of amorphous carbon films by silicon doping“, Diam. & Rel. Mater., 82,137–142, January 2018.

[3] S. Chepkasov, A. Zolkin, D. Piliptsou, M. Khomyakov, E. Maksimovskii, “The Effect of the Substrate Spatial Orientation on The Properties of Amorphous Carbon Coatings Deposited from Pulse Plasma Flows“ / / Proc. 21th Int. Conf. on High Current Electronics (ISHCE), Tomsk, Russia, pp. . 856-862, 2020

[4] D.G. Piliptsou, A.S. Rudenkov, P.A. Luchnikov, A.V. Rogachev, Jiang Xiao Hong, Zhou Bing, Composite carbon coatings deposited from cathode pulse plasma, Moscow: Radiotekhnika, 2020

C4-P-009701

PLANAR MAGNETRON WITH ELECTRON INJECTION AND REFLECTING ELECTRODE: A RESEARCH APPROACH USING NUMERICAL SIMULATION*

D.B. ZOLOTUKHIN[1]

[1]*Institute of High Current Electronics, Tomsk, Russia*

A high-current planar magnetron is an effective tool for high-quality thin films deposition in high vacuum conditions [1]. The planar magnetron working pressure can be shifted to the lower limit by injection into the main discharge domain the flow of accelerated electrons with independently-adjusted current and energy. According to experiments and numerical simulations [2], the positive effect of the injected auxiliary electrons is mainly caused by the additional independent ionization of residual gas and sputtered target vapor resulting in higher discharge currents, lower discharge voltages, and lower operational pressures. Initial experimental efforts have demonstrated that further improvement of performance of planar magnetron with electron injection can be realized by introducing the additional negatively-biased electrode placed in front of the cathode (target) with the purpose to reflect the stream of the injected electrons, prevent them to escape the plasma-generating discharge volume and finally enhance the degree of utilization of their energy.

This work is dedicated to the numerical study of the physical processes in a planar magnetron with electron injection and reflecting electrode. The research is focused mainly on the revealing the effects of the reflecting electrode parameters on the discharge parameters of the magnetron as well as on the mass-to-charge composition of the ions generating in such configuration.

REFERENCES

[1] Shandrikov M.V., Bugaev A.S., Oks E.M., Ostanin A.G., Vizir A.V., Yushkov G.Yu., “Effect of electron injection on the parameters of a pulsed planar magnetron,” Vacuum, vol. 159, pp. 200, 2019.

[2] D.B. Zolotukhin, “Numerical modeling of discharge characteristics of a planar magnetron with injection of electrons from auxiliary discharge”, Journal of Physics: Conference Series, 2022 (in press).

* The work was supported by the Russian Science Foundation (grant No. 21-19-00136).

C4-P-015702

ENERGY FLUX TO THE SUBSTRATE IN THE PROCESS OF PULSED DUAL MAGNETRON DEPOSITION OF TIALN FILMS*

A.S. GRENADYOROV[1,2], *A.N. ZAKHAROV*[1], *V.O. OSKIRKO*[1,2], *I.M. GONCHARENKO*[1], *A.P. PAVLOV*[1,2], *A.A. SOLOVYEV*[1]

[1]*Institute of High Current Electronics SB RAS, 2/3 Akademicheskii Ave., Tomsk, 634055, Russia*
[2]*Applied Electronics, LLC, 15-80 Akademicheskii Ave., Tomsk, 634055, Russia*

Functional TiAlN coatings are now widely used in industry. Compared to TiN, they are more resistant to oxidation and have increased hardness and heat resistance. To obtain TiAlN coatings, various deposition methods are used, in particular chemical vapor deposition, vacuum arc deposition, ion plating and so on [1]. The paper presents the results of using a dual magnetron sputtering system with metal targets (Al and Ti) to obtain TiAlN films in a mixture of Ar and N_2. The power supply of the sputtering system has a wide range of regulation of frequency, pulse duration, as well as high values of pulsed current and voltage. The schematic diagram of the vacuum installation is shown in Fig. 1. The results of studying the influence of the frequency and duty cycle of pulses on the ion current density on the substrate, the coating deposition rate and the energy flux density on the substrate under a floating potential or at a bias potential of -100 V are presented. It is known that when thin films are deposited, their stoichiometry, structure, and morphology strongly depend on the energy flux to the substrate [2, 3]. During the experiments, the total energy flux density on the substrate was measured, which depends on duty cycle and pulsing frequency. Figure 2 shows the dependences of total energy flux density on the frequency of voltage pulses for a substrate at floating potential and at a -100 V bias potential. The substrate was located at a distance of 10 cm from the magnetron targets. The total discharge power was 1.75 kW (1 kW for Ti targets, 0.75 kW for Al targets). It is shown that as the voltage pulse frequency decreases from 30 kHz to 3 kHz while maintaining their duration (20 μs), the part of energy delivered to the substrate due to ion bombardment increases from 40 to 65%. Also, the pulse frequency effects on mechanical properties (hardness H, plasticity index H/E and resistance to plastic deformation H^3/E^2) of TiAlN coatings due to changes in the elemental and phase composition. The optimal value of the pulse repetition frequency is found, at which high values of these parameters are achieved.

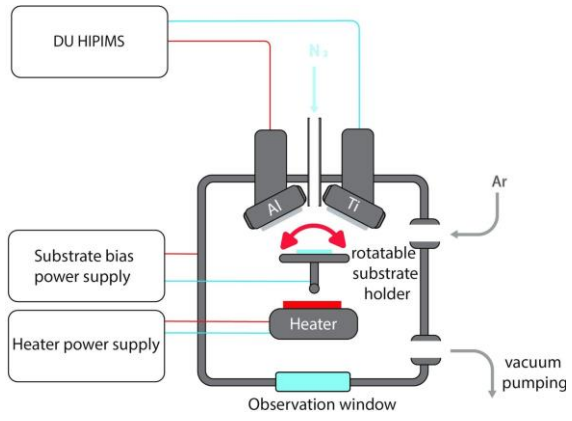

Fig. 1. The schematic diagram of the vacuum installation

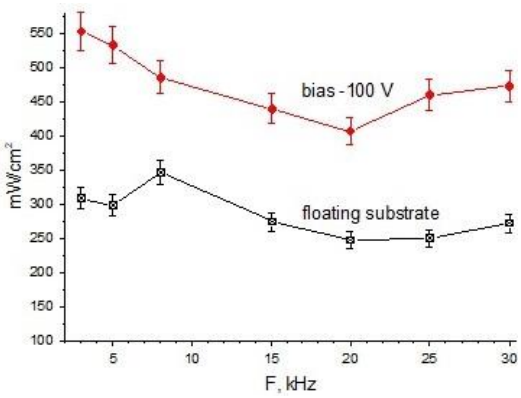

Fig. 2. The energy flux density on floating substrate and substrate at a -100 V bias potential

REFERENCES

[1] G.Kim, S. Lee, J.Hahn, "Properties of TiAlN coatings synthesized by closed-field unbalanced magnetron sputtering," Surf. Coat. Technol., vol. 193, no.1-3, pp.213-218, 2005.
[2] H. Deutsch, H. Kersten, A. Rutscher, "Basic mechanism in plasma etching," Contrib. Plasma Phys., vol. 29, pp. 263–284, 1989.
[3] I. Hussla, K. Enke, H. Grundwald, G. Lorenz, H. Stoll, "In situ silicon-wafer temperature measurements during RF argon-ion plasma etching via fluoroptic thermometry," J. Phys. D. Appl. Phys., vol. 20, pp. 880-896, 1987.

* The work was supported by the Ministry of Science and Higher Education of the Russian Federation (project No. 075-15-2021-1348, event No. 1.1.3).

C4-P-018702

EFFECT OF ION ASSISTANCE PARAMETERS ON THE PROPERTIES OF Ir COATINGS DEPOSITED BY MAGNETRON SPUTTERING

A.S. KAMENETSKIKH[1], *N.V. GAVRILOV*[1]

[1]*Institute of Electrophysics of the UB of RAS, Yekaterinburg, Russia*

Iridium coatings were deposited on Ni substrates by magnetron sputtering with ion assistance in the plasma of a low-energy electron beam. The influence of the parameters of the ion flux on the microstructure, the intrinsic stresses, and the adhesion of the coating is investigated. It is shown that deposition of a coating with a dense microstructure at a low homologous temperature (~0.15) is provided under the optimal ratio of the ion current density to Ir flux ~0.5 and the ion energy ~150 eV. The coatings deposited in the optimal mode are characterized by microdistortions of the crystal lattice of ~0.9% and have a predominant crystallite orientation (111), which is a favorable factor for providing corrosion protection. A low level of intrinsic stresses (~0.5 GPa) and a high adhesion strength of the coatings (the value of the critical load at nanoindentation is more than 3000 mN) have been achieved.

C4-P-020901

INFLUENCE OF ALUMINUM IMPLANTATION ON THE STRUCTURAL-PHASE STATE AND HARDENING OF ULTRAFINE GRAINED TITANIUM

NIKONENKO A.V.[1], *POPOVA N.A.*[2], *NIKONENKO E.L.*[2,3], *KYRZINA I.A.*[4]

[1] *Tomsk State University of Control Systems and Radioelectronics, Tomsk, Russia*
[2] *Tomsk State University of Architecture and Bilding, Tomsk, Russia*
[3] *National Research Tomsk State Polytechnic University Tomsk, Russia*
[4] *National Research Tomsk State University, Tomsk Russia*

Ion implantation of ultrafine grained (UFG) α-titanium (average grain size – 0.2 μm) was performed on the MEVVA-V.RU ion source at a temperature of 623K, accelerating voltage of 50 kV, ion beam current density of 6.5 mA/cm^2, distance 60 cm from the ion-optic system. The irradiation dose was 1×10^{18} ions/cm^2, the irradiation time was 5.25 h. The microstructure and phase composition were studied using an EM-125 transmission electron microscope at an accelerating voltage of 120 kV. The microstructure and phase composition of implanted titanium were studied in the area of modified layer at a depth of 50 – 70 nm from the irradiated surface.

The structural-phase state of α-Ti surface layers in the UFG state was investigated. It has been established that as a result of UFG-titanium irradiation with aluminum ions a polyphase implanted layer is formed on the basis of -titanium grains containing aluminide, oxide and carbide phases. Namely: 1) α-Ti grains having a BCC crystal lattice (spatial group Im3m), having a lamellar shape and located along the boundaries of α-Ti grains; 2) Ti3Al phase, an ordered phase with superstructure D019 and spatial group P63/mmc, having GPU crystalline, formed as lamellar precipitations along the boundaries of α-Ti grains; 3) $TiAl_3$ phase, an ordered phase with D022 superstructure, possessing a DSP crystal lattice with spatial group I4/mmm and localizing as rounded particles in triple junctions and along α-Ti grain boundaries; 4) particles of titanium carbide (TiC) having HCC crystal lattice (spatial group Fm3m), located inside alpha-Ti grains and having rounded shape; 5) inclusions of titanium oxide TiO_2 (otherwise brukite) having orthorhombic crystal lattice (spatial group Pbca), located on the boundaries and inside alpha-Ti grains on dislocations and having rounded shape.

Under ion implantation, the restructuring of the titanium matrix is observed – implantation leads to a decrease in the longitudinal grain size of α-Ti (from 1.9 μm to 0.7 μm), while the grain anisotropy factor decreases by 3 times.

The strength components included in the yield strength have been calculated. It is shown that implantation leads not only to a significant change in the structural-phase state of the material, but also to an additional hardening of almost 2.5 times. The contribution of individual strengthening mechanisms to the total hardening of the alloy is estimated: $\Delta\sigma_n$ - dislocation friction stress in the α-Ti crystal lattice; $\Delta\sigma_h$ - hardening of the α-Ti-based solid solution by atoms of alloying elements (Al, C, O); $\Delta\sigma_l$ - hardening by "forest" dislocations; $\Delta\sigma_D$ - hardening by long-range stress fields; $\Delta\sigma_{OR}$ - material hardening by incoherent particles when dislocations bypass them by the Orovan mechanism; $\Delta\sigma_H$ - hardening due to grain boundaries. It is shown that the share of the contribution is not equal. And the contribution of each of these mechanisms is different. Nevertheless, the main contribution to the total hardening after implantation is made by $\Delta\sigma_{Or}$.

This work was supported by RFBR No. 19-08-01041 and the Tomsk State University Development Program (Priority-2030)

C4-P-021601

INFLUENCE OF THE ACTIVATION CONDITIONS OF THE VAPOR-GAS MEDIUM ON THE PROPERTIES OF TISICN COATINGS*

Y.A. BRYUKHANOVA, A.I. MENSHAKOV, A.I. MEDVEDEV, A.S. KAIGORODOV

Institute of Electrophysics UB RAS, Yekaterinburg, Russia

The results of the study of the effect of the discharge current, composition and activation method of the vapor-gas mixture on the characteristics of TiSiCN coatings obtained by anodic evaporation of titanium and decomposition of hexamethyldisilazane in a hollow cathode arc discharge are presented. Figure 1 shows the electrode scheme of experimental facility. Nanocomposite coatings consisting of an amorphous phase based on SiCN with embedded nanocrystals TiN, TiC and TiCN were obtained. It is shown that an increase in the discharge current in the range of 10-50 A leads to a decrease in the hardness of nanocomposite coatings and deterioration of their adhesion, which can be explained by an increase in the proportion of the amorphous phase as a result of an increase in the decomposition degree of the precursor.

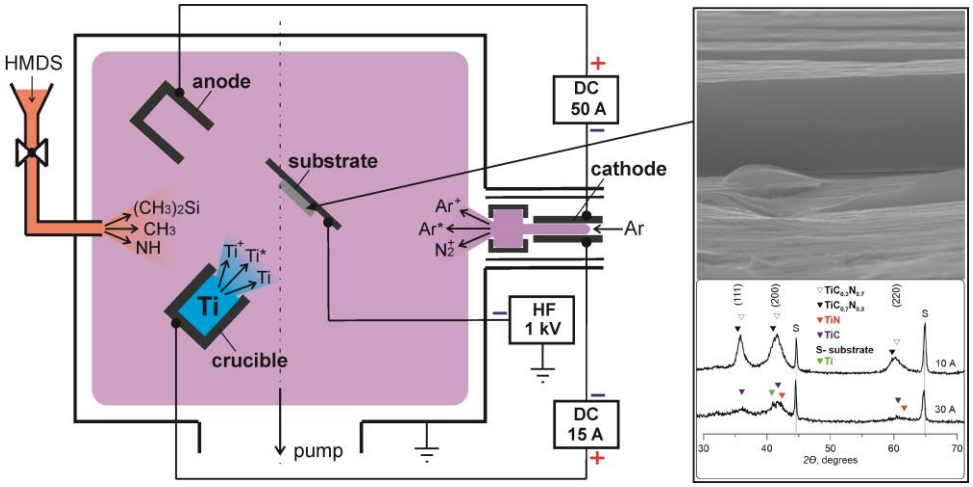

Fig.1. Electrode scheme of experimental facility

The experimental setup is based on a gas discharge system with a self-heating hollow cathode cylinder made of TiN powder. In this work, the discharge is used to ionize gases and decompose vapors of the organosilicon precursor, to heat the crucible and vaporize titanium using two independent sections of the anode (cooled hollow anode, uncooled anode - crucible).

* The work was supported by the Russian Science Foundation under grant No. 20-79-10059.

C4-P-022802

MAGNETRON SPUTTERING WITH HIGH POWER SUBMICROSECOND PULSES*

V.O. OSKIRKO[1,2], A.N. ZAKHAROV[1], A.P. PAVLOV[1,2], V.A. SEMENOV[1], S.V. RABOTKIN[1]

[1]Institute of High Current Electronics, 2/3 Akademicheskii Ave., Tomsk, 634055, Russia
[2]OOO Prikladnaya Elektronika, 15-80 Akademicheskii Ave., Tomsk, 634055, Russia, oskirkovo@gmail.com, 8(3822)491651

Ultra-short HIPIMS is a type of high power pulse magnetron sputtering technology, in which the pulse duration is 4-10 μs, while the discharge pulse power can reach several tens or hundreds of kW. Due to the use of short pulses, it is possible to reduce the number of electrical arcs and increase the deposition rate, while maintaining a high ionization rate of the sputtered material [1, 2]. We have previously shown that reducing the pulse duration to 5-7 μs leads to an increase in the average ion current density to a substrate [3]. This paper presents the results of experiments in which the duration of discharge current pulses during high power pulse magnetron sputtering of copper was reduced to 2 μs. Figure 1 shows the oscillograms of discharge current and voltage pulses in the submicrosecond pulses mode (s-HIPIMS). Due to the high pulsed voltage (1500 V) and the low inductance of the generator, the discharge current has time to increase to 300 A within 2 μs, while the pulsed power density on the target exceeds 5 kW/cm^2. Table 1 presents the results that allow comparing the s-HIPIMS mode with the DCMS and HIPIMS with a longer pulse duration modes. As in the case of HIPIMS, the deposition rate in s-HIPIMS mode is significantly reduced compared to DC. However, s-HIPIMS mode provides a significantly higher ion current density to a substrate compared to the DCMS and HIPIMS. The paper considers the possible causes of the observed ion current growth in the case of submicrosecond pulses.

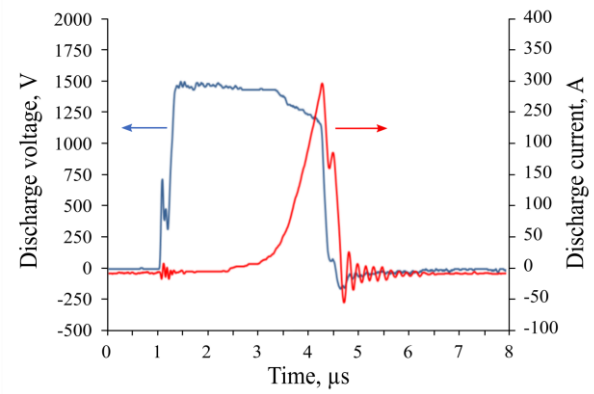

Fig. 1. Discharge current and voltage pulses in the s-HIPIMS mode

Table 1. Parameters of sputtering processes.

Mode	DCMS	HIPIMS	s-HIPIMS
Pulse voltage, V	372	871	1400
Average current, A	2.7	1.2	0.7
Average power, kW		1000	
Peak pulse current, A	-	200	350
Pulse frequency, kHz	-	1.7	7.0
Voltage pulse duration, μs	-	20	3
Current pulse duration, μs	-	15	2
Deposition rate, nm/s	302	24	31
Average ion substrate current, mA/cm2	0.7	1.0	6.5

REFERENCES

[1] *V. Tiron et al.* // Coatings. – 2020. – V. 10(7), 633
[2] *S. Konstantinidis et al.* // Journal of Applied Physics. – 2006. – V. 99, 013307.
[3] *V. Oskirko et al.* // 7th International Congress EFRE. – 2020. – pp. 822-926.

* This work was supported by the government contract of the Institute of High Current Electronics SB RAS (FWRM-2021-0006).

C4-P-024101

FEATURES OF HIGH-RATE DEPOSITION OF CRN_X COATINGS USING MAGNETRON SPUTTERING OF A HOT CROMIUM TARGET*

G.A. BLEYKHER, V.A. GRUDININ, D.V. SIDELEV, V.P. KRIVOBOKOV

Tomsk Polytechnic University, Tomsk, Russia

Our previous studies have shown that the use of a hot chromium target undergoing sublimation can significantly increase the deposition rate of chromium coatings during the operation of magnetron sputtering systems [1, 2]. This circumstance was used for the synthesis of coatings based on chromium-nitrogen compounds, which are of great interest for various industries. It seems that in this case it will be possible to significantly increase the productivity of applying such coatings to the surface of products.

A new scheme for the synthesis of CrN_x films in an atmosphere of argon and nitrogen during the operation of a magnetron sputtering system has been developed and implemented in experiments. Its specifics are as follows. The inlet of argon and nitrogen is carried out separately in the space of the vacuum chamber. A magnetron with a hot chromium target operates in a metallic mode and creates a flow of atomic chromium particles on the substrate. To increase the reactivity of nitrogen, an assisting radio-frequency inductively coupled plasma (RF-ICP) source is used. The regions of the RF-ICP discharge and the nitrogen flow into the chamber are combined and are significantly distant from the region of the magnetron discharge localization. Experiments have shown that this technique reduces the flow of nitrogen particles to the surface of the magnetron target (i.e., prevents its "poisoning") and provides conditions for intensive dissociation and ionization of nitrogen, which are necessary for the synthesis of chromium nitride on the substrate surface.

The effect of target heating on the functioning of the magnetron discharge is investigated. It is shown that under these conditions there is practically no hysteresis in the behavior of current and voltage depending on the rate of nitrogen flow into the chamber. Analysis of the target substance after a series of experiments showed the absence of chromium and nitrogen compounds in it. The contribution of the sublimation of the chromium target to the increase in the deposition rate of the chromium and CrN_x coating with the increase in the magnetron power is revealed experimentally and by calculations. It has been shown that the dependence of the deposition rate on the magnetron power density is a nonlinearly increasing function of over 18 W/cm^2, and in the range from 18 to 28 W/cm^2 the target sublimation enables an increase in the deposition productivity by a factor from 2 to 12 compared with the cooled target sputtering under the same experimental conditions.

The elemental and structural-phase composition of the coatings deposited using the planetary rotation of substrates has been studied depending on a magnetron power density. It has been found that with an intense sublimation on the chromium target surface, the coatings have an inhomogeneous elemental and structural-phase composition. In addition, an alternation of chromium layers with a low content of chromium nitride and layers that mainly consist of chromium nitride has been determined.

The working parameters that most significantly affect the mechanical properties of the formed coatings are revealed. The important role of the type of power supply, the configuration of the magnetic field and the power of the RF-ICP source in providing high hardness and wear resistance characteristics is shown.

REFERENCES

[1] D.V. Sidelev, G.A. Bleykher, V.P. Krivobokov, Z. Koishybayeva, “High-rate magnetron sputtering with hot target”, Surf. Coat. Technol., V. 308, pp. 168-173, 2016.

[2] G.A. Bleykher, D.V. Sidelev, V.A. Grudinin, V.P. Krivobokov, M. Bestetti, “Surface erosion of hot Cr target and deposition rates of Cr coatings in high power pulsed magnetron sputtering”, Surf. Coat. Technol., V. 354, pp. 161-169, 2018.

* The work was supported by Fondazione Cariplo (project №2020.1156 «Cutting tools regeneration by means of innovative vacuum plasma technologies»).

C4-P-025501

HIGH-RATE DEPOSITION OF COPPER OXIDE COATINGS USING MAGNETRON SPUTTERING OPERATED IN A METALLIC MODE*

E.D. VORONINA, V.A. GRUDININ, G.A. BLEYKHER, D.V. SIDELEV

Tomsk Polytechnic University, Tomsk, Russia

Coatings based on copper oxides (CuO_x) are of great interest due to high demand in many technological applications. For example, high absorption coefficient, good electrical conductivity and low cost make CuO_x films excellent material candidates for solar absorbers and p-n diodes [1, 2]. Nowadays, a lot of coating methods, such as sol-gel process, pulsed laser deposition and magnetron reactive sputtering, are used. The latter method has the wide application due to high quantity of control parameters and low cost of coating deposition. However, the presence of reactive gases in a vacuum chamber can lead to forming a thin layer of chemical compound (e.g., CuO_x) on target surface. It can induce change of the emission characteristics of the target surface in reactive atmosphere [3]. To solve this problem, we propose to separate the processes of target sputtering and coating condensation using separated supply of gases (Ar and O_2) and applying additional plasma source for dissociation and ionization of reactive gas near the substrate.

This study is aimed to determine the influence of process variables (oxygen flow, discharge power density and substrate rotation rate) on deposition rate and structure properties of CuO_x coatings deposited by magnetron sputtering in a metallic mode.

In this study the vacuum plasma of the Weinberg Research Center of Tomsk Polytechnic University was used. The scheme of the system is described in [4].

According to XRD study, CuO and Cu_2O phases and no Cu phase were identified in the deposited coatings. The intensities of CuO (110) and CuO (220) are noticeably higher for the coating which was deposited using a discharge power of 1 kW than that of 2 kW (Fig. 1). The sample obtained at O_2 flow rate of 27 sccm has Cu_2O (111) phase. The last results show that the phase composition of the copper oxide coatings can be controlled by changing the O_2 flow rate as well as the discharge power applied to the copper target.

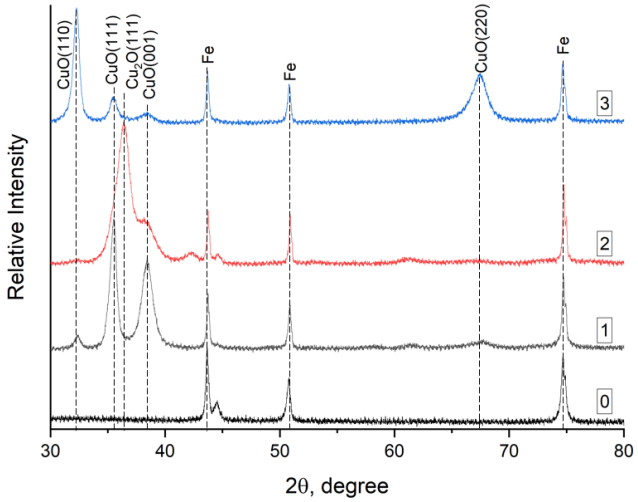

Fig. 1. XRD patterns of CuO_x coatings obtained at different discharge power and oxygen flow: 0 – uncoated substrate; 1 – 2 kW and 54 sccm of O_2; 2 – 2 kW and 27 sccm of O_2; 3 – 1 kW and 20 sccm of O_2.

Next deposition experiments demonstrated the role of the substrate rotation rate on the structural properties of copper oxide coatings, when magnetron sputtering in a metallic mode was used to deposit CuO_x coatings.

REFERENCES

[1] Absike H. et al. “Synthesis of CuO thin films based on Taguchi design for solar absorber”, Optical Materials, vol. 118, August 2021.

[2] P. Venkateswari, P. Thirunavukkarasu, M. Ramamurthy, M. Balaji, J. Chandrasekaran, “Optimization and characterization of CuO thin films for P–N junction diode application by JNSP technique”, Optik, vol. 140, pp. 476-484, 2017.

[3] E.V. Berlin, N.N. Koval, L.A. Seidman, Plasma chemical-thermal treatment of the surface of steel parts, Moscow: Technosphere, 2012.

[4] V. A. Grudinin, D. V. Sidelev, G. A. Bleykher, Y.N. Yuriev, V. P. Krivobokov, E. V. Berlin, S. Weiß, “Hot target magnetron sputtering enhanced by RF-ICP source for CrNx coatings deposition”, Vacuum, vol. 191, 2021.

* This study was supported by Russian Science Foundation (project №22-29-01173).

C4-P-025601

STRUCTURAL AND FUNCTIONAL PROPERTIES OF CHROMIUM COATINGS DEPOSITED BY HIGH-RATE MAGNETRON SPUTTERING EHNAHCED BY RF-ICP SOURCE*

A.A. BONDAR[1], V.A. GRUDININ[1], G.A. BLEYKHER[1], D.V. SIDELEV[1]

[1]Tomsk Polytechnic University, Tomsk, Russia

Nowadays, magnetron sputtering techniques are of great interest for deposition of coatings with a wide range of structural and functional properties. A one pf the main disadvantages of magnetron sputtering is relatively low deposition rate (it is about 10-20 nm/s even for metal coatings). The deposition rate of coatings can be increased using an additional mechanism of target erosion (sublimation or evaporation) [1]. However, it becomes more difficult to tailor and control the properties of coatings due to the fact that the flux of evaporated (sublimated) particles has an extremely low kinetic energy (0.1-0.3 eV). To increase the averaged kinetic energy of particles, high-power pulsed power sources can be used. Moreover, an additional discharge plasma source can be applied to increase the ionization degree of the erosion particle flux. The present study is devoted to investigate the role of an external plasma source on the structural and functional properties of chromium coatings obtained by high-rate magnetron sputtering.

The chromium coatings were obtained using different discharge power density and with coating thickness (1, 3 and 5 μm). For this purpose, a high-power pulsed power supply in oscillating mode (DOMS) was used. In addition to it, a radio-frequency (13.56 MHz) plasma generator (RPG-128) was used as the external plasma source. X-ray diffraction (XRD, Shimadzu XRD-7000S with a CuKα accelerating tube) was used to study the crystal structure of the Cr coatings. Coating thickness was determined using a Calotest instrument (CSEM, Switzerland) and a scanning electron microscope (Quanta 200 3D). The hardness of the Cr coatings was measured using the Oliver-Farr method (Nanohardness Tester 2, CSM). The corrosion resistance of the Cr coatings on AISI 321 substrate was studied in a 3.5 wt.% NaCl solution using a P-45X potentiostat-galvanostat (Electrochemical Instruments, Russia).

It was found that the use of the external (additional) plasma source (RPG-128) allow to tailor the functional characteristics of the obtained Cr films. The hardness of 1 μm-thick Cr coatings are varied from 4 to 18 GPa depending on the power density. Typical hardness of Cr coatings obtained by magnetron sputtering is usually in a range of 7-11 GPa [2]. The hardness at the maximum power density (44 W/cm2) is 4 GPa, when the erosion particle flux is mainly formed by sublimation. It is typical for chromium films produced by a resistive evaporation [3]. So, the functional properties of the Cr films can have the parameters close to the films obtained by magnetron sputtering at low power density and to conventional magnetron sputtering at high power density.

REFERENCES

[1] V.A. Grudinin, D.V. Sidelev, G.A. Bleykher, Y.N. Yuriev, V.P. Krivobokov, E.V. Berlin, V. Yu Grigoriev, A. Obrosov, S. Weiß, “Hot target magnetron sputtering enhanced by RF-ICP source for CrNx coatings deposition”, Vacuum, V. 191, № 110400, 2021.

[2] J. Lin, J.J. Moore, W.D. Sproul, B. Mishra, Z. Wu, “Modulated pulse power sputtered chromium coatings”, Thin Solid Films, V. 518, Issue 5, pp. 1566–1570, 2009.

[3] S. Kataria, S. Goyal, S. Dash, A.K. Tyagi, “Nanomechanical characterization of thermally evaporated Cr thin films — FE analysis of the substrate effect”, Thin Solid Films, V. 519, Issue 1, pp. 312–318, 2010.

* The work was supported by Fondazione Cariplo (project №2020.1156 «Cutting tools regeneration by means of innovative vacuum plasma technologies»).

C4-P-027201

STUDY OF PHASE FORMATION IN LAYERED SYSTEM BE-FE

A.K. ZHUBAEV[1], K.YE. ABILKAYR[1], S.K. YEREZHEPOVA[1], YE.A. KANTARBAY[2]

[1]Zhubanov Aktobe Regional University, Aktobe, Kazakhstan
[2]International IT University, Almaty, Kazakhstan

The Fe-Be system was chosen as a model for further consideration of the stainless steel–beryllium system, which is a promising reactor material. The regions of existence of phases on the Fe-Be phase diagram, slightly varying with temperature (except for a solid solution of Beryllium in Iron α-Fe(Be)) in the temperature range 500÷1000°C and a wide two-phase region α-Fe(Be)+$FeBe_2$ [1] made it a convenient model system.

The two-layer system Be(2 μm)–Fe(10 μm) was obtained by magnetron sputtering of Beryllium onto prepared armco-Iron foils. Sequential thermal annealing in vacuum was carried out at a temperature of 720°C. Figure 1 shows the spectrum of the layered system after 10 hours of annealing. The dotted line shows the spectrum of ^{57}Fe nuclei in α-Fe. It can be seen that the experimental spectrum is a sextet with widened lines. At the same time, no additional lines are observed. Consequently, we can talk about the formation of a solid solution of Be atoms in α-Fe. In [2], it was revealed that the substitution of 1 Iron atom with a Beryllium atom in the nearest environment of the central Iron atom of an elementary cell in the α-Fe lattice leads to a decrease in the hyperfine field by 23.4 kOe. Figure 1 shows the positions of the sextet lines corresponding to ^{57}Fe atoms without Be atoms in the nearest environment (H_0), with one (H_1) and two (H_2) Be atoms.

Using the MSTools software package [3], the Mossbauer spectra of phases present on the equilibrium diagram of Fe-Be binary system were modeled according to the [4] method. In this case, the parameters of the Mossbauer phase spectra from [5] were used.

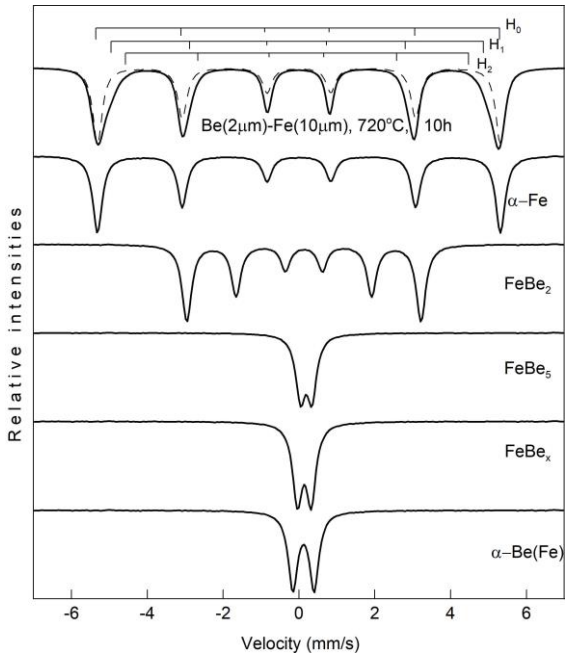

Fig.1. Mossbauer spectrum of Layered system Be-Fe and the simulated spectra of Fe-Be system's phases

As a result of the studies of thermally induced phase formation with a layered Be(2 μm)-Fe(10 μm) system after annealing at 720°C, the formation of a solid solution of α-Fe(Be) was revealed. The Mossbauer spectra of various phases of the Fe-Be binary system were modeled.

REFERENCES

[1] N.P. Lyakishev, Diagrams of the State of Double Metal Systems. Moscow: Mashinostroenie, 1997.
[2] K. Yagisava, Phys. Stat. Sol. (a), vol.18, p.589, 1973.
[3] V.S. Rusakov, Mossbauer spectroscopy of locally inhomogeneous systems. Almaty, 2000.
[4] A.K. Zhubaev, T.S. Mukhanbetzhan and S.K. Yerezhepova, IOP Conf. Series: Journal of Physics: Conf. Series, 1281, 012097, 2019.
[5] K. Ohta, J. of Appl. Phys., vol.39, no 4, p.2123, 1968.

C4-P-030801

THE EFFECT OF OPERATING PRESSURE ON THE PROPERTIES OF COPPER FILMS AT MAGNETRON DEPOSITION*

M.V.SHANDRIKOV, A.S.BUGAEV, A.A. CHERKASOV, V.I.GUSHENETS

[1]*Institute of High Curren Electronics SB RAS, 2/3 Akademicheskiy Ave., Tomsk, Russia, 634055*

The effect of operating pressure and additional electron injection during magnetron deposition on the properties of copper films in the range of extremely low operating pressure (low than 0.1 Pa) is investigated. The planar magnetron with a copper target with a diameter of 125 mm was used. The power of the magnetron discharge was 500 W in continuous mode. The effect of the reflector electrode on plasma uniformity, deposition rate and radial uniformity of films is shown. The measurements of the mass-to-charge composition and plasma concentration at the deposition regimes were carried out.

* The reported study was funded by RFBR according to the research project No 19-48-700003.

C4-P-041403

MULTILAYER CORROSION-RESISTANT CERAMIC-METAL COATINGS (METAL/NITRIDE CERAMICS/ METAL/OXIDE CERAMICS) ON STAINLESS STEEL OBTAINED BY MAGNETRON SPUTTERING*

M.S. DOROFEEVA[1], *T.A. GUBAIDULINA*[2], *T.I. DOROFEEVA*[2], *V.P. SERGEEV*[2]

[1]*Tomsk state University, Tomsk, Russia*
[2] *Institute of Strength Physics and Materials Sciences of the Siberian Branch of the Russian Academy of Science, Tomsk, Russia*

During long-term operation in aggressive conditions (sea water and mechanical stress) stainless steel products require additional protection. A corrosion-resistant coating with enhanced physical and mechanical characteristics provides such protection. The coating may have a different composition, and the methods of formation may be different.

In this work, multilayer cermet coatings (Metal/nitride ceramics/ Metal/oxide ceramics) with increased corrosion resistance were obtained. The metal layer is presented in the form of the nickel layer, which makes it possible to minimize the arising stresses at the substrate–coating interface. Nickel is easily passivated in air and under the action of strong oxidizing agents, which can lead to corrosion resistance, but only if the coating is absolutely continuous. Nitride ceramics layer is presented in the form of silicon aluminum nitride, which is characterized by high hardness and wear resistance. It does not interact with most inorganic acids, but penetration of solvent ions along the grain boundaries to the substrate is possible if the coating structure is inhomogeneous. The outer layer of oxide ceramics is silicon alumina, consisting of silicon oxides and aluminum oxides, which are characterized by high hardness and corrosion resistance. In our case, this layer seals all previous layers, preventing the penetration of solvent ions, in particular, oxygen ions and, especially, chlorine ions, through the intercrystalline space.

Coatings are formed in one cycle under a changing gas atmosphere (argon, nitrogen, oxygen) using magnetron sputtering in a UVN-05MD "KVANT" vacuum unit equipped with two magnetrons. The thickness of the metal layer is about 0.5 μm, the nitride and oxide layers are about 2-2.5 μm. The resulting coating is gray with a mirror sheen (Figure 1).

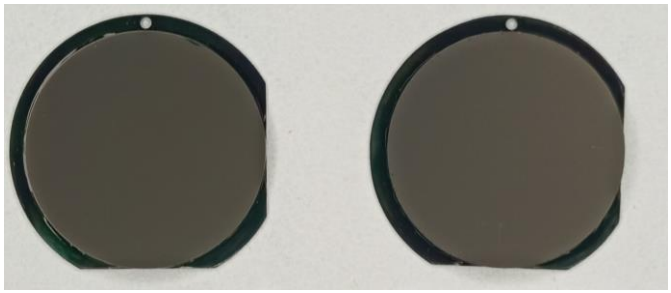

Fig.1. The photos of samples with multilayer metal-ceramic coating (Metal/nitride ceramics/ Metal/oxide ceramics) on stainless steel obtained by magnetron sputtering.

In the study of the cross section of the obtained coatings on a transmission microscope, it was revealed that metallic nickel has a fine-crystalline structure. The second layer has a nanocrystalline structure and contains the AlN phase. The outer layer is amorphous. During accelerated corrosion tests in a sea salt solution, the resulting coatings showed a decrease in the corrosion rate by several times. The corrosion rate was estimated using the Tafel equation.

Thus, the multilayer cermet coatings (Metal/nitride ceramics/ Metal/oxide ceramics) obtained by magnetron sputtering on stainless steel acquired the properties of each of the layers, and a synergistic effect appeared. In addition, the layering created several barriers to the diffusion of chloride ions from the environment. The thinness of these layers increased the elasticity of the final coated material.

* The work was performed as per to the State research task for ISPMS SB RAS, project FWRW-2021-0003.

C4-P-048001

PREPARATION OF COPPER OXIDE FILMS ON ALUMINA BY A HOT-TARGET HIPIMS PROCESS*

V.YU. LISENKOV[1], A.V. KAZIEV[1], D.V. KOLODKO[1,2], D.G. AGEYCHENKOV[1], A.V. TUMARKIN[1], M.M. KHARKOV[1], M.S. KUKUSHKINA[1]

[1]National Research Nuclear University MEPhI (Moscow Engineering Physics Institute), Moscow, Russia
[2]Fryazino Branch of Kotel'nikov Institute of Radio Engineering and Electronics RAS, Fryazino, Russia

One of the basic processes in production of electronic devices is the metallization of dielectric substrates, and particularly, preparation of ceramic print circuit boards (PCBs). There are various methods suitable for applying a conductive copper layer to a dielectric substrate. These include active metal brazing (AMB), cold gas-dynamic spraying (CGS), direct bonded copper (DBC) lamination, and a number of thick-film and thin-film vacuum technologies. The usage of plasma deposition methods for ceramic metallization is limited, mainly due to the relatively low productivity. However, in some applications, for example, when it is necessary to metallize substrates of complex topology, plasma methods might outperform popular mass production technologies in terms of quality and efficiency.

To improve adhesion of comparatively thick (more than 20 μm) magnetron deposited copper coatings, a dedicated intermediate layer of Cu_xO_y can be introduced between the substrate and the film. Here, we report the results of Cu_xO_y deposition on alumina substrates in a hot-target HiPIMS discharge.

The experiments were carried out in a magnetron deposition facility with thermally insulated copper target [1, 2]. To form the discharge, an APEL-M-5HPP-1200 power supply was used. Initially, the magnetron was separated from the substrate by a shutter. In the beginning of the process, the target was heated and melted by a HiPIMS discharge in Ar, at 0.5 Pa pressure. Then desirable O_2 flow was set, while Ar flow was set to zero. The shutter was opened, and the oxide deposition was performed. Cu_xO_y films with thicknesses 1–6 μm were prepared. Their structure was studied with scanning electron microscope, and the composition was measured by EDS and XRD methods. The results showed growth of CuO and Cu_2O films. The correlations between deposition parameters and coating characteristics are discussed.

REFERENCES

[1] A.V. Kaziev, A.V. Tumarkin, K.A. Leonova et al., "Discharge parameters and plasma characterization in a dc magnetron with liquid Cu target," Vacuum, Vol. 156, P. 48–54, 2018.

[2] A.V. Kaziev, D.V. Kolodko, A.V. Tumarkin et al., "Comparison of thermal properties of a hot target magnetron operated in DC and long HIPIMS modes," Surf. Coat. Technol., vol. 409, Article Number 126889, 2021.

* The work was supported by the Russian Science Foundation under grant No. 18-79-10242.

C4-P-050503

ELECTRON-ION-PLASMA METHOD FOR FORMING NANOSTRUCTURED MULTILAYER COATINGS ON THE EXAMPLE OF THE TI-B SYSTEM *

V.V. SHUGUROV, N.A. PROKOPENKO, E.A. PETRIKOVA, Yu.F. IVANOV, O.S. TOLKACHOV, O.V. KRYSINA

Institute of High Current Electronics SB RAS, Tomsk, Russia

Boron (its nuclide is 10B) is characterized by a high effective thermal neutron capture cross section ($3 \cdot 10^{-25}$ m^2) [1]. Therefore, pure boron, its alloys, and salt solutions are used as neutron-absorbing materials in the manufacture of control rods for nuclear reactors that slow down or stop fission reactions [2]. Boron is also often used as an alloying element in steels used in the manufacture of containers for storing spent nuclear fuel [3, 4].

The aim of this work is to develop an electron-ion-plasma method for the formation of multilayer nanostructured boron-containing coatings using the Ti-B system as an example.

The process of formation of nanostructured multilayer coatings was carried out on the "COMPLEX" installation [5]. Studies of the structure, phase and elemental composition of the film/substrate system were carried out using scanning (SEM 515 Philips device) and transmission diffraction (JEM-2100F JEOL device) electron microscopy, X-ray diffraction analysis (Shimadzu XRD-6000 diffractometer). The mechanical properties of the films were determined by measuring the microhardness (DUH-211S instrument (Shimadzu, Japan), indenter load 10 mN).

It has been established that the coating is multilayer and is in the amorphous-crystalline state (Fig. 1). Ti-B film microhardness 51.0 GPa (standard deviation 7.8 GPa), Young's modulus obtained by microhardness determination 360 GPa.

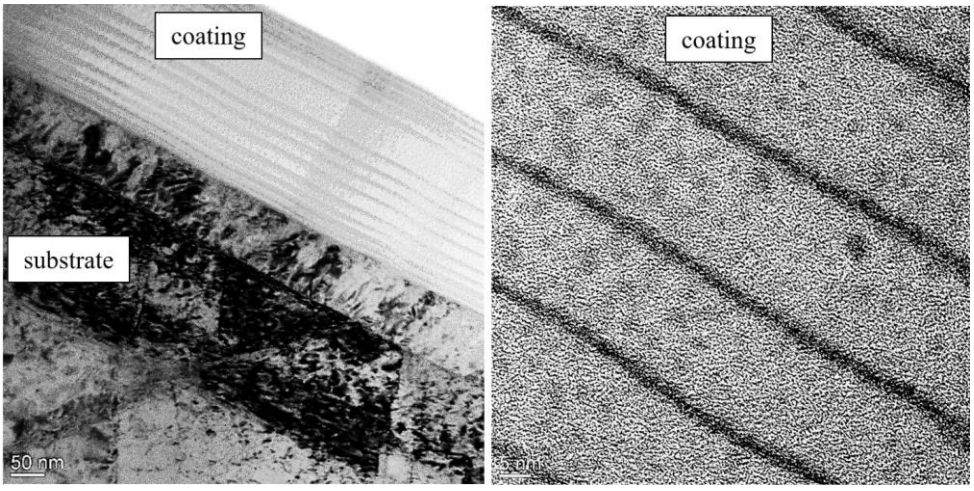

Pic. 1. Electron microscopic image of the structure of the Ti-B coating formed on steel AISI321.

REFERENCES

[1] V. A. Palekha and A. A. Getman. Boron. Properties and application in nuclear power // Casting and metallurgy. - 2017. - 3 (88). - S. 91-94.

[2] Risovany V.D., Zakharov A.V., Klochkov E.P., Guseva T.M. Boron in nuclear technology. - Dmitrovgrad: FSPU SSC RF RIAR, 2003 - 345 p.

[3] Churyumov A.Y., Khomutov M.G., Tsar'kov A.A., Pozdnyakov A.V., Solonin A.N., Efimov V.M., Mukhanov E.L. Study of the structure and mechanical properties of corrosion-resistant steel with a high concentration of boron at elevated temperatures // Phys. Met. Metallogr. 2014. Vol. 115. No. 8. P. 809 – 813.

[4] Shulga A.V. A comparative study of the mechanical properties and the behavior of carbon and boron in stainless steel cladding tubes fabricated by PM HIP and traditional technologies // J. Nucl. Mater. 2013. Vol. 434. No. 1-3. P. 133 – 140.

[5] N. N. Koval, Yu. F. Ivanov, V. N. Devyatkov, V. V. Shugurov, A. D. Teresov, and E. A. Development of a complex electron-ion-plasma method for modifying the surface of materials and products. Izv. universities. Physics. - 2020. - vol. 53, no. 10. - pp. 174-183.

* The work was supported by the Russian Science Foundation (Project No. 19-19-00183).

C5-O-007003

ATOMIC-ELECTRONIC STRUCTURE OF M(SALEN) COMPLEXES: STUDY USING SYNCHROTRON RADIATION*

P.M. KORUSENKO, A.V. VERESHCHAGIN, O.V. LEVIN, D.V. SIVKOV, O.V. PETROVA AND A.S. VINOGRADOV

St. Petersburg State University, Saint Petersburg, Russia

Functional polymeric materials obtained by the electrochemical polymerization of transition metal complexes with salen-type ligands [M(Salen)] (M=Ni, Co, Cu) (Fig. 1) are actively studied due to the prospects of their application as new energy storage electrodes [1]. Despite a significant amount of research on the atomic and electronic structure as well as properties of electroconductive redox poly-[M(Salen)] polymers, there is no single point of view on the mechanism of polymerization of monomer molecules. There are two main models: (i) monomers are connected to each other through a carbon-carbon bond (Fig. 1b); (ii) individual fragments are bound to each other by donor-acceptor and intermolecular interactions (Fig. 1c). The difference in approaches to describing the nature of the electrochemical activity of polymers also lies in the fact that two types are considered as positions for redox reactions - metal cations or ligand atoms [2]. At the same time, the mechanism of redox reactions in these complexes is also not fully understood. Thus, for the purposeful development of methods for the synthesis of these polymers and their successful practical application, detailed knowledge of the chemical (charge) state of metal atoms in monomers and their changes in poly-[M(Salen)] polymers in various (oxidized or reduced) states, and also of the role of 3d electrons of the metal atom in the formation of the electronic structure of these complexes are required. This information can be obtained using modern methods of X-ray spectroscopy (X-ray Photoelectron Spectroscopy – XPS and Near Edge X-ray Absorption Fine Structure – NEXAFS) with synchrotron radiation (SR). Unfortunately, X-ray spectral studies of M(Salen) complexes are currently extremely limited, which makes this study relevant.

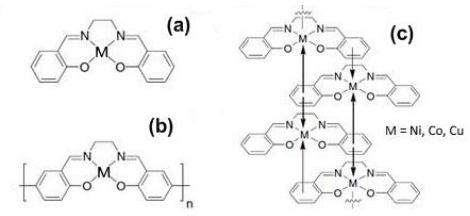

Fig.1. The polymerization scheme of the monomer [M(Salen)] (a) due to the linkage of the phenyl rings of the ligands of neighboring complexes (b); due to the linkage of the metal cation of one monomeric complex to the phenyl ring of another (c).

In this work, using the equipment of RGBL (BESSY II, Berlin: Germany) and K6.5.(KISI-Kurchatov, Moscow: Russia) SR beamlines, we studied the local atomic and electronic structure of [M(Salen)] complexes by NEXAFS and XPS. The M(Salen) monomers powders were synthesized according to the known method [3]. Layers of monomeric complexes for XPS and NEXAFS were obtained *in-situ* under vacuum conditions by thermal evaporation of the [M(Salen)] powders and their deposition onto Pt plates. Poly-[M(Salen)] samples were prepared *ex-situ* by electrochemical polymerization from a monomer solution in an electrolyte in the form of polymer layers on pure Pt plates.

As a result of the studies carried out, information was obtained on the distribution of electron density and the charge (chemical) state of M (Ni, Co, Cu) and ligand (O, N, and C) atoms, as well as on their changes upon replacement of the M3d atom for poly-[M(Salen)] in comparison with monomers [M(Salen)]. In addition, data was obtained on the chemical state of electrolyte ion atoms absorbed by the poly-[M(Salen)] films. The obtained information made it possible to determine the mechanism of polymerization of monomers [M(Salen)].

REFERENCES

[1] T.A. Skotheim, R.L. Elsenbaumer, J. R. Reynolds, Handbook of Conducting Polymers, 2nd Ed. New York: Marcel Dekker, 1998.

[2] O. V. Levin, M. P. Karushev, et al., "Charge transfer processes on electrodes modified by polymer films of metal complexes with Schiff bases", Electrochim. Acta, vol. 109, pp. 153–161, 2013.

[3] R. H. Holm, G. W. Everett and A. Chakravorty, "Metal Complexes of Schiff Bases and B-Ketoamines", Prog. Inorg. Chem., vol. 7, pp. 83–214, 2007.

* The work was supported by Russian Science Foundation (grant No. 21-72-10029).

C5-O-013805

SIMULATIONS OF THERMAL LOADS ON OPTICAL ELEMENTS OF THE "FAST PROCESSES" BEAMLINE AT THE SYNCHROTRON RADIATION FACILITY SKIF

A.A. STUDENNIKOV[1], I.A. RUBTSOV[1], E.R. PRUUEL[2], K.E. KUPER[1], YA.V. ZUBAVICHUS[1], A.V. BUKHTIYAROV[1]

[1]Synchrotron Radiation Facility SKIF Boreskov Institute of Catalysis SB RAS, Koltsovo, Russia
[2]Lavrentyev Institute of Hydrodynamics SB RAS, Novosibirsk, Russia
a.a.studennikov@srf-skif.ru

Studies of fast processes, including real-time monitoring of substances and engineering materials under conditions of dynamic and pulsed loading of various types, constitute one of the promising application areas of modern synchrotron radiation (SR) sources. To implement such techniques, a high X-ray power density is required, since exposure times as fast as fractions of nanoseconds are typical for such experiments. Therefore, high-power synchrotron radiation sources (i.e., wigglers or undulators) are needed. The 1-3 "Fast processes" beamline of the Synchrotron Radiation Facility SKIF, which is currently under construction, is among a few dedicated appropriate instruments worldwide. It will utilize hard X-ray radiation from a superconducting wiggler with the total thermal power of 40 kW. According to the beamline optical scheme, a large fraction of the radiation will be absorbed by a massive fixed mask made of copper under active water cooling, and only a fractional power of 12 kW will hit first X-ray filters and vacuum-tight windows located downstream. In order to ensure safe operating conditions for all heat-loaded elements exposed directly to hard X-rays, it is necessary to perform detailed numerical simulation of heat transfer processes therein.

In the present work, results of numerical simulations of heat transfer process within X-ray filters (made of either beryllium, diamond, or pyrolytic graphite) are given. Temperature fields within the filters under realistic operating conditions were reconstructed using the Ansys Fluent environment. Based on the simulations, the optimum parameters of required cooling system were identified.

C5-O-045701

HIGH-TEMPERATURE OXIDATION OF CR/MO COATED ZR-1NB ALLOY*

M.S. SYRTANOV, E.B. KASHKAROV, A.V. ABDULMENOVA, D.V. SIDELEV

Tomsk Polytechnic University, Tomsk, Russia

Currently, zirconium-based alloys are widely used in nuclear power industry for manufacturing fuel claddings and other structural elements of pressurized water reactor (PWR) due to their low thermal neutron capture cross-section, high corrosion and radiation resistance and acceptable mechanical properties [1–3]. Nevertheless, severe oxidation of zirconium alloys under possible high-temperature (HT) accidental conditions such as loss of coolant accident (LOCA) can cause a loss of claddings integrity and their destruction [4]. One of the possible method to protect zirconium alloy is coating deposition. Up to date, the most promising material considered as a protective coating for zirconium-based alloy claddings is chromium. However, Cr-Zr interdiffusion can occur at the coating/alloy interface at HT, that leads to the formation of Cr-Zr eutectic phase with a melting point of 1332 °C [5]. As a result of Cr-Zr interdiffusion, the Cr2Zr intermetallic layer forms at the Cr-Zr interface, which lead to accelerated oxidation of the zirconium alloy. One way to solve this problem is to develop a new type of Cr-based protective coating with a barrier sublayer that can prevent Cr-Zr interdiffusion. In the present work Mo was deposited by magnetron sputtering as a diffusion barrier layer. The high-temperature oxidation and interdiffusion behavior of Cr coatings with a Mo sublayer were investigated in the paper.

Cr (8 μm)/Mo (3 μm)- and Cr (8 μm)-coated Zr-1Nb alloys were oxidized in air at 1100 °C during 15-60 min. According to SEM, XRD and optical microscopy it was established that a 3 μm-thick barrier Mo layer can limit Cr-Zr interdiffusion under high-temperature oxidation. The phase composition of the Cr/Mo-coated Zr alloy after oxidation consists of the Cr2O3, α-Cr and Cr_3Mo phases. In situ XRD under linear heating up to 1250 °C with a heating rate of 50 °C/min shows Mo_2Zr phase formation at the Mo/Zr interface. The thickness of residual Cr after 60 minutes of oxidation is greater in Cr/Mo-coated Zr alloy (~5 μm) compared to single-layer Cr-coated sample (~3.5 μm). The thickness of the Cr-Mo and Mo-Zr interdiffusion layers is equal to ~2 and 20 μm after 60 min HT oxidation, respectively. The thickness of outer oxide Cr2O3 layer after HT oxidation of Cr- and Cr/Mo-coated Zr alloy samples are similar indicating that the Mo sublayer has no significant effect on oxidation resistance of outer Cr layer. However, enhanced oxidation of the Mo-Zr layer can cause local oxidation of the coated Zr alloy samples when oxygen will penetrate up to Mo layer/Zr alloy interface. It was established that the weight gains depend on the coating type. The single-layer Cr coatings demonstrate better oxidation resistance that Cr/Mo. The weight gains reduces by ~3 times compared to Cr/Mo coating. This is due to the uncoated area oxidation of the samples. A thin layer of Mo and Cr remained beneath the oxidation zone of the Zr alloy since oxygen contacted with these regions. This can indicate on predominant oxidation of Mo-Zr layer compared with other systems.

REFERENCES

[1] I. Charit and N. Murty, " Creep behavior of niobium-modified zirconium alloys," J. Nucl. Mater., no. 51, pp. 354–363, 2008.

[2] J. Yang, M. Steinbrück, C. Tang et al., " Review on chromium coated zirconium alloy accident tolerant fuel cladding," J. Alloys Compd., vol. 895, no. 162450, pp. 1-23, 2022.

[3] D.V. Sidelev, M.S. Syrtanov, S.E. Ruchkin et al., " Protection of Zr Alloy under High-Temperature Air Oxidation: A Multilayer Coating Approach," Coatings, vol. 11(2), no. 227, pp. 1–14, 2021.

[4] S.J. Zinkle, K.A. Terrani, J.C. Gehin et al., " Accident tolerant fuels for LWRs: A perspective," J. Nucl. Mater., vol. 448, no. 1-3, pp. 374-379, 2014.

[5] J. Ko, J.W. Kim, H.W. Min et al., " Review of Manufacturing Technologies for Coated Accident Tolerant Fuel Cladding," J. Nucl. Mater., vol. 561, no. 153562, pp. 1-24, 2022.

* The research was funded by Russian Science Foundation (grant No. 21-79-00175).

C5-O-912601

ON THE PROGRESS OF THE ACTIVITIES OF PROJECT «IN SITU METHODS FOR SYNCHROTRON INVESTIGATIONS OF MULTILAYER FUNCTIONAL STRUCTURES WITH UNIQUE PARAMETERS AND PROPERTIES CREATED BY BEAM-PLASMA SURFACE ENGINEERING » [1]

V.V. DENISOV, N.N. KOVAL, N.A. RATAKHIN, A.N. SHMAKOV, A.D. TERESOV

Institute of High Current Electronics SB RAS, 2/3 Akademichesky ave., Tomsk, 634055, Russia, e-mail: denisov@opee.hcei.tsc.ru, Tel.+7(3822)492683

Accelerating the process of creating of new materials with unique properties is possible only by combining the efforts of scientific, educational and industrial organizations, as well as using tools that contribute to solving fundamental problems facing both the scientific community of Russia and the whole world. It is known that in most cases of using materials in extreme conditions, it is the surface that determines their functional properties and, as a result, the service life of products as a whole. A multiple reduction in the time of development and implementation of new materials, methods and equipment for their production on the territory of the Russian Federation is possible with the use of the most modern methods and techniques of synchrotron research.

A consortium consisting of such organizations as HCEI SB RAS, INP SB RAS, ISPMS SB RAS, TSC SB RAS, Tomsk universities - TPU, TSU, TUSUR, IEP UD RAS, as well as the Ufa State Aviation Technical University and the industry enterprise "Technopark-AT", since October 2021, have been implementing a project on the topic "In situ methods of synchrotron investigations of multilayer functional structures with unique parameters and properties created by beam-plasma surface engineering" within the framework of the Federal Scientific and Technical program for the development of synchrotron and neutron research and research infrastructure for 2019 - 2027".

The objectives of the project are related to each other and, in accordance with Direction 1 "Synchrotron and neutron research (development) in the field of materials science for the development of high-tech production technologies", are focused on creating infrastructure and developing methods for synchrotron and neutron research of structural and functional materials.

The report provides information on the progress of the project, including the most important scientific results obtained using synchrotron radiation, a description of the infrastructure facilities being created for synchrotron research, as well as the progress of the educational component of the project.

1The work was carried out with the financial support of the Russian Federation represented by the Ministry of Science and Higher Education (project № 075-15-2021-1348) within the framework of the events № 1.2.1, 1.2.2 and 1.2.5.

C5-O-952601

ON THE CREATION AND PROSPECTS OF THE SCIENTIFIC RESEARCH CENTER «TOMSK COMPETENCE CENTER IN THE FIELD OF BEAM-PLASMA ENGINEERING AND SYNCHROTRON RESEARCH»*

A.D. TERESOV, V.V. DENISOV, N.A. RATAKHIN, N.N. KOVAL

Institute of high current electronics SB RAS, Tomsk, Russia

As part of the implementation of Agreement No. 075-15-2021-1348 dated October 5, 2021, concluded between the Institute of High Current Electronics SB RAS and the Ministry of Science and Higher Education of the Russian Federation, the Scientific Research Center «Tomsk Center of Competence in the Field of Beam-Plasma Engineering and Synchrotron Research» (SRC TCC) was created as part of the network synchrotron and neutron research infrastructure in the Russian Federation. SRC TCC was established as a structural subdivision of the HCEI SB RAS to carry out scientific-methodological, scientific and educational activities in the field of synchrotron and neutron research and to provide organizational and methodological support for work in the field of beam-plasma surface engineering, carried out by research departments of the HCEI SB RAS and third-party organizations. The main functions of the SRC TCC are:

- accumulation of data and knowledge in the field of synchrotron research, obtained by scientific groups participating in the activities of the SRC TCC, and their distribution among the participants;
- implementation of own scientific research in the field of methods of using synchrotron radiation for surface engineering;
- in the field of educational activities of the SRC TCC - assistance in the implementation of educational programs for the training and retraining of personnel by higher professional education organizations that have licenses to carry out educational activities, including programs for the training of scientific personnel in graduate school;
- development of the procedure and conditions for the use of methods and equipment of SRC TCC;
- repair and maintenance of high-tech equipment of SRC TCC;
- coordination of teams of scientific and educational institutions to carry out activities aimed at the development and creation of the station «Surface» of the resource sharing center «SKIF» (Koltsovo).

At the moment, a new unique vacuum electron-ion-plasma installation (VEIPS-1) is being created for the SRC TCC, equipped with sources of gas and metal plasma, electron beams, which allows to carry out the processes of forming layers and coatings in a wide range of operating parameters, to diagnose generated plasma, and, most importantly, to prepare specimens and test the methodology for in situ studies of the processes of formation of layers on the surface of materials by X-ray diffraction using synchrotron radiation before its implementation at the VEPP-3 station (Siberian Center for Synchrotron and Terahertz Radiation, Novosibirsk).

*This work was carried out with the financial support of the Russian Federation represented by the Ministry of Science and Higher Education (project No 075-15-2021-1348) within the framework of event No. 1.2.5.

C5-O-953701

VACUUM ELECTRON-ION-PLASMA STAND FOR IN SITU STUDIES OF THE MATERIAL SURFACE USING SYNCHROTRON RADIATION [1]

S.S. KOVALSKY, V.V. DENISOV, E.V. OSTROVERKHOV, N.N. KOVAL, A.N. SHMAKOV, A.D. TERESOV, M.V. SAVCHUK

Institute of High Current Electronics SB RAS, 2/3 Akademichesky ave., Tomsk, 634055, Russia, e-mail: kovalskiy_ss@bptvac.ru, Tel.+7(3822)492683

The report presents a description of a laboratory variant of a vacuum electron-ion-plasma stand (hereinafter VEIPS), designed to study the surface of samples by X-ray phase analysis of coatings obtained by beam-plasma surface engineering methods, in the process of their synthesis in situ mode using synchrotron radiation.

VEIPS can be equipped with gas and metal plasma sources, sources of electron beams and allows you to carry out the formation processes of layers and coatings in a wide range of operating parameters, to diagnose the parameters and composition of the generated plasma, and to monitor the processes of formation of layers on the surface of materials using X-ray diffraction in real time using synchrotron radiation. VEIPS implements the possibilities for determining the dependences between the plasma parameters, the conditions of its effect on the material surface and the properties of the formed surface using the methods of in situ synchrotron studies.

At this stand, it is planned to study the layer formation processes of ceramic single-layer and multilayer structures synthesized by methods of plasma-assisted cathode-arc vapor deposition, magnetron sputtering and by the method of reactive anode evaporation in a low-pressure arc discharge. It is assumed that the main tasks concerning the development and improvement of synchrotron research methods and the determination of the patterns of multilayer coatings phase formation will be carried out at the VEPP-3 synchrotron radiation source located at the Institute of nuclear physics SB RAS.

[1] The work was carried out with the financial support of the Russian Federation represented by the Ministry of Science and Higher Education (project № 075-15-2021-1348) within the framework of the event № 1.2.1.

C5-P-002201

COMPARATIVE ANALYSIS OF REACTOR RITM-200 AND KLT-40S BY DURATION OF NUCLEAR FUEL CAMPAIGNS*

S. ALHASSAN[1], *S.V BELIAVSKII*[1], *V.N NESTEROV*[1]

[1]*NATIONAL RESEARCH TOMSK POLYTECHNIC UNIVERSITY, TOMSK, RUSSIA.*

ABSTRACT

An essential parameter that justifies the interest in nuclear power reactors is the length of the fuel campaign. Floating nuclear power plants (FNPP) have proven to be a solution to bridging the developmental gap between urban and remote areas in terms of providing electricity and district heating. This article seeks to compare the reactors RITM-200 and KLT-40S in terms of their fuel performance. The Th - U fuel cycle is considered in the calculations. A spectra of neutron flux densities of both reactors was analyzed for (U^{238} + U^{235})O_2 and (Th^{232} + U^{233})O_2 fuel dispersion. The calculation of the fuel lifetime of both reactors revealed RITM-200 as superior reactor with about 1,100 effective days in fuel lifetime. From the calculations, the optimal diameter of the KLT-40S is 6.2 mm which is the same as the design value. For RITM-200 however, the optimal diameter of 7.5 mm is higher than the design value of 6.9 mm.

INTRODUCTION

For a variety of reasons, the Russians begun the research and development of a range of small power reactors from the late 1950's [1]. After about 30 years, the focus changed to the provision of electricity and district heating to remote and hard-to reach areas. The multipurpose and co-generational activities of these floating nuclear power plants (FNPP) have generated enormous attention.

USING THE ITERATIVE ALGORITHM IN SOLVING THE MULTIGROUP NEUTRON DIFFUSION EQUATION

The spectra of neutron flux were evaluated for both RITM-200 and KLT-40S reactors with the aid of the diffusion equation below in an iterative manner [7, 8]:

$$-D^i B_i^2 \phi^i - \Sigma_a^i \phi^i - \sum_{k=i+1}^{I} \Sigma_R^{i\to k} \phi^i + \sum_{k=1}^{i-1} \Sigma_R^{k\to i} \phi^k + \varepsilon^i \sum_{k=1}^{I} \nu_f^k \Sigma_f^k \phi^k = 0 \qquad (1)$$

$$\sigma_n = \sigma_n(293.6) \cdot \frac{\sqrt{\pi}}{2} \cdot \sqrt{\frac{293.6}{T_{\text{n.g.}}}} \cdot f_n \qquad (2)$$

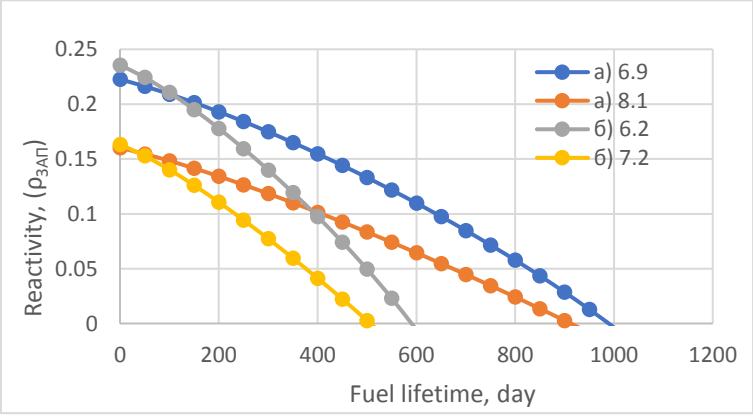

Fig. 2. Change in K_{eff} with time for $^{235}U+^{238}U$ at radii а) 6.9 & а) 8.1 for RITM-200 and б) 6.2 б) 7.2 for KLT-40S.

REFERENCES

[1] V. Sidorenko, "The history of Atomic Energy of the Soviet Union and Russia", Vol. 5. IzdAT, 2004.

[2] W.J.F. Standring, M. Dowdall, I. Amundsen, P. Strand, "Floating nuclear power plants: Potential implications for radioactive pollution of the northern marine environment", Marine Pollution Bulletin 58, pp. 174 – 178, 2009.

[3] V. Belyayev, K. Leontyev, "Reactor out of sea. Nuclear Engineering International 49 (594), pp. 18 – 20, 2004.

C5-P-007102

DEPOSITION AND PROPERTIES OF THIN BORON FILMS USING A PLANAR MAGNETRON*

A.G. NIKOLAEV[1], *A.S. BUGAEV*[1], *V.I. GUSHENETS*[1], *E.M. OKS*[1,2]

[1] *Institute of High Current Electronics SB RAS, 2/3 Academichesky Ave., Tomsk, 634055, Russia,*
Email: nik@opee.hcei.tsc.ru, phone: +7(3822)-491776
[2]*Tomsk State University of Control Systems and Radioelectronics, 40 Lenin Ave., Tomsk, 634050, Russia*

Boron thin films on the surface of metal substrates were obtained using planar magnetron sputtering with a pure boron target. Under normal conditions, boron has a high electrical resistance and ignition of a magnetron discharge with a boron target is impossible. However, since boron is a semiconductor, its resistance decreases as temperature increases. Thus, at the temperature of a boron target heated to 500 C or higher, the ignition of a stable magnetron discharge is already possible. We used a planar magnetron with a boron target heated in a DC discharge with a current of up to 50 mA at an argon and nitrogen pressure of 1 mTorr. Since the boron target was thermally insulated and the magnetron discharge voltage was about 600–700 V, the discharge power was about 30 W. At this power, the target did not crack due to thermal expansion, but it was sufficient to heat the target to an electrically conducting state. At the above discharge parameters, the deposition rate of boron coatings at a distance of 5 cm from a magnetron target of 5.1 cm in diameter was about 150 nm/h. Thin films of boron up to 1 μm thick were obtained and their surface morphology was studied. Structural-phase analysis of boron films was carry out at the "Anomalous Scattering Station" of channel #2 by synchrotron radiation from the electron storage ring VEPP-3 of the Siberian Center for Synchrotron and Terahertz Radiation of the Budker Institute of Nuclear Physics SB RAS. The boron film deposition techniques, as well as the properties of the films have been discussed.

* This work was carried out with the financial support of the Russian Federation represented by the Ministry of Science and Higher Education (project No. 075-15-2021-1348) within the framework of event No. 2.1.6.

C5-P-012502

FORMATION AND PROPERTIES OF MULTILAYER FILMS OF HIGH-ENTROPY ALLOYS BY ION-PLASMA METHODS*

YU.H. AKHMADEEV, YU.F. IVANOV, N.N. KOVAL, V.V. SHUGUROV, E.A. PETRIKOVA, O.V. KRYSINA, N.A. PROKOPENKO, I.I. AZHAZHA

Institute of High Current Electronics SB RAS, Tomsk, Russia

Comparative experiments were carried out on the formation of films of high-entropy alloys (HEA) by vacuum deposition with simultaneous independent evaporation of cathodes of several elements, as well as vacuum-arc evaporation using a multicomponent cathode (Fig. 1). It is shown that varying the discharge current of electric-arc evaporators during the formation of HEA from several cathodes makes it possible to change the elemental composition of HEA films over a wide range. It has been established that the formed films are single-phase materials with a nanocrystalline structure. The microhardness of the films depends on the concentration of chemical elements.

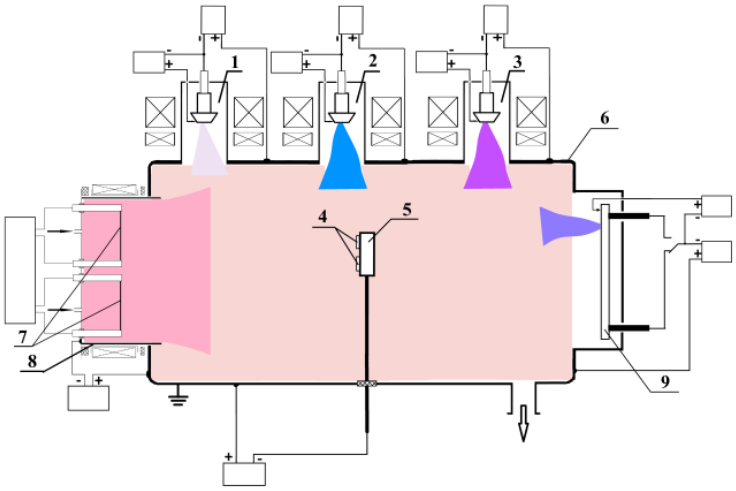

Fig.1. Scheme of the experiment for obtaining HEA films.

The samples of HEA films for X-ray phase analysis (XPA) were studied using the synchrotron radiation of the VEPP-3 electron storage ring as part of the Center for Collective Use of the SCST on the basis of the UNU "VEPP-4 Complex - VEPP-2000" at the Institute of Nuclear Physics of the Siberian Branch of the Russian Academy of Sciences. The phase composition and parameters of the crystal structure are revealed.

* The work was carried out with the financial support of the Russian Federation represented by the Ministry of Science and Higher Education (project no. 075-15-2021-1348) within the framework of measures no. 2.1.5, 2.1.17 and 2.1.20.

C5-P-032501

INVESTIGATION OF LANTHANUM STRONTIUM COBALTITE THIN FILMS USING SYNCHROTRON RADIATION*

A.A. SOLOVYEV1[1], *A.V. SHIPILOVA*[1], *S.V. RABOTKIN*[1], *E.A. SMOLYANSKIY*[2], *A.N. SHMAKOV*[3]

[1] *Institute of High Current Electronics SB RAS, Tomsk, Russia*
[2] *Tomsk Polytechnic University, Tomsk, Russia*
[3] *Budker Institute of Nuclear Physics SB RAS, Novosibirsk, Russia*

Lanthanum Strontium Cobaltite (LSC) is a highly conductive perovskite material that is often used as a cathode material in Solid Oxide Fuel Cells (SOFCs) [1]. In this study, $La_{0.6}Sr_{0.4}CoO_{3-\delta}$ (LSC) thin films were obtained by pulsed DC magnetron sputtering of the LSC target in $Ar+O_2$ atmosphere. X-ray diffraction analysis of the LSC films was conducted for the synchrotron radiation beam during thermal annealing at different temperatures up to 1300 °C. The phase composition and structure of the films were determined using X-ray diffraction and scanning electron microscopy, respectively. Anode-supported solid oxide fuel cells with bi-layered thin-film yttria-stabilized zirconia (YSZ) / gadolinium-doped ceria (GDC) electrolyte and an LSC thin film cathode were fabricated. Polarization curves were measured in the temperature range from 600 to 800 °C. The effect of annealing temperature on the crystalline structure of the LSC films and the characteristics of SOFCs was investigated.

REFERENCES

[1] K. Develos-Bagarinao, T. Ishiyama, H. Kishimoto, H. Shimada, K. Yamaji, "Nanoengineering of cathode layers for solid oxide fuel cells to achieve superior power densities," Nat. Commun., vol. 12, 3979, June 2021.

[2] H. Uchida, S. Arisaka, M. Watanabe, "High Performance Electrode for Medium-Temperature Solid Oxide Fuel Cells La(Sr)CoO_3 Cathode with Ceria Interlayer on Zirconia Electrolyte," Electrochem. Solid-State Lett., vol. 2, no. 9, pp. 428-430, 1999.

* The work was supported by the Ministry of Science and Higher Education of the Russian Federation (project No. 075-15-2021-1348, event No. 2.1.1)

C5-P-033102

INVESTIGATION OF RESISTANCE TO HIGH-TEMPERATURE OXIDATION AND STABILITY OF THE STRUCTURAL-PHASE STATE OF CRALN COATINGS BY X-RAY DIFFRACTION ANALYSIS USING SYNCHROTRON RADIATION*

A.A. LEONOV, YU.A. DENISOVA, V.V. DENISOV, M.V. SAVCHUK, V.N. TISHCHENKO

Institute of High Current Electronics SB RAS, Tomsk, Russia

The method of X-ray diffraction analysis using synchrotron radiation (Novosibirsk, Budker Institute of Nuclear Physics, Siberian Branch of the Russian Academy of Sciences) was used to study the resistance to high-temperature oxidation and the stability of the structural-phase state of ceramic coatings based on chromium and aluminum nitrides in the temperature range 30÷1300 °C. The source of synchrotron radiation was the VEPP-3 electron storage ring. The study was carried out using a high-temperature X-ray camera HTK-2000, a position-sensitive single-coordinate detector OD-3M-350, software - a program for processing measurement results Fityk v.1.3.1. The studies were carried out for the following experimental conditions: operating wavelength λ=0.172 nm, range of diffraction angles 2Θ: 28-59 degrees, sample heating rate 10 °C/min.

The processes of deposition of CrAlN coatings by the cathode-arc plasma-assisted method was carried out on an NNV6.6-I1 facility equipped with two electric arc evaporators with a cathode diameter of 80 mm and an additional “PINK” gas plasma source.

The results of studies of CrN/AlN coatings formed under conditions when metal plasma flows were mixed in the area of the substrate or were separated by a metal screen (layer-by-layer deposition) for heat resistance showed that these coatings behave similarly when heated in air. The critical temperatures differ slightly. The CrN/AlN coatings consist of chromium aluminum nitride, metallic aluminum is present. During heating, a change in the unit cell parameters of chromium-aluminum nitride and metallic aluminum is observed, indicating the mutual dissolution of the components; this process continues up to a temperature of ~725-730 °C, after which the reflections of aluminum disappear, and the reflections of chromium-aluminum nitride show only a shift due to thermal expansion. Chromium-aluminum nitride retains thermal stability up to a temperature of ~1110-1115 °C (~1075-1080 °C - with layer-by-layer deposition), after which the coating begins to oxidize, the reflections of chromium-aluminum nitride disappear at a temperature of ~1235-1240 °C (~1255-1260 °C with layer-by-layer spraying) (Fig. 1A and 1B).

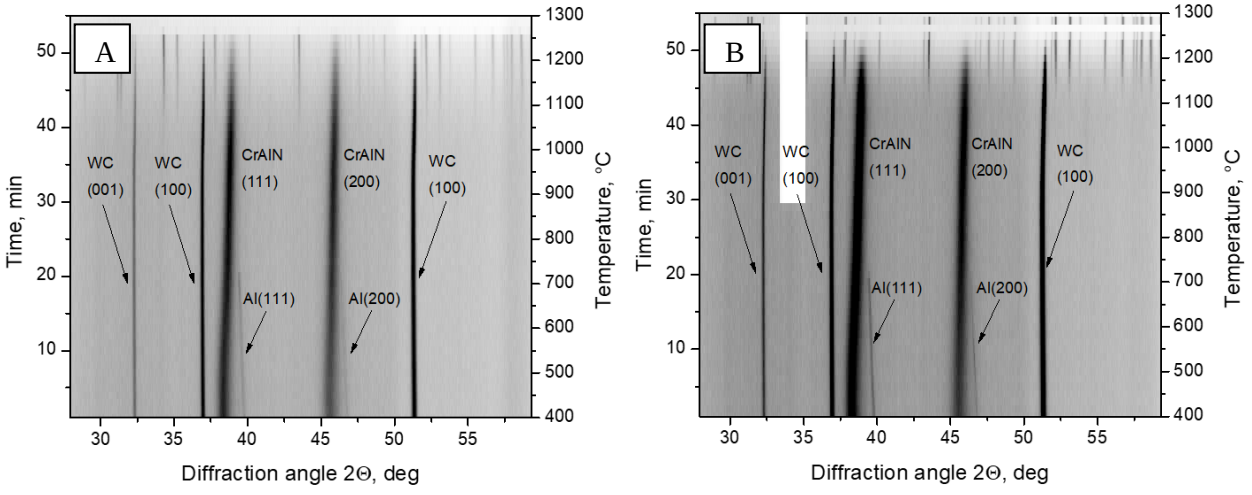

Fig.1. Full set of X-ray diffraction patterns of CrN/AlN (12rpm, screen - A) and CrN/AlN (12rpm, no screen - B) coatings during heating from room temperature to 1300 °C in air in projection view intensity on the plane "angle of diffraction - temperature"

* The work was carried out with the financial support of the Russian Federation represented by the Ministry of Science and Higher Education (project no. 075-15-2021-1348) as part of activity no. 2.1.15.

C5-P-041601

MEASUREMENT OF THE DYNAMICS OF THE EJECTION OF WOLFRAM MICROPARTICLES BY THE SR AND PDV METHODS

K.V. NOVOSELOV[1], *K.A. TEN*[2]

[1]*NSU, Novosibirsk, Russia*
[2]*LIH SB RAS, Novosibirsk, Russia*

Studies of the shockwave loading effects on various materials have revealed an effect known as ejection. The essence of this effect is the formation of a flux (cloud) of micro- and nanoparticles when a strong shock wave emerges on a free surface. When the rarefaction wave interacts with the roughness of the material surface, instabilities develop, leading to the formation of microjets that decay into an ejecta flow. Experimental studies of a rarefied high-speed ejecta flow represent a complex scientific and technical problem.

The paper presents the results of an experimental study of an ejecta flow from tungsten microparticles accelerated by a shock wave. Using the synchrotron radiation technique, the intensity distributions of the X-ray shadow from the particle cloud were obtained. Calibration was carried out and the calculation of the mass distribution of tungsten ejection was calculated using the obtained data. Simultaneously in experiments that employ PDV method, the velocity of the microparticles cloud and the velocity of the tantalum foil were measured with the indicator foil method. The measured foil velocity was used to calculate the mass distribution of the incident dust cloud. Differences in the data obtained are presented in this paper.

C5-P-046801

STRUCTURE AND PROPERTIES OF MULTILAYER CERMET FILMS PRODUCED BY THE ION-PLASMA METHOD*

E.A. PETRIKOVA, N.A. PROKOPENKO, V.V. SHUGUROV, YU.F. IVANOV, O.S. TOLKACHOV, N.N. KOVAL', YU.H. AKHMADEEV, O.V. KRYSINA

Institute of High Current Electronics SB RAS, Tomsk, Russia

Ceramic-metal films based on a high-entropy alloy (HEA) were formed using the vacuum-arc plasma-assisted deposition method on the «KVINTA» setup («UNIQUUM» complex, included in the unique scientific setups catalogue of the Russian Federation, http://ckp-rf. ru/usu/434216/), the design and operation of which are described in detail in [1, 2]. Cathodes made of chromium, molybdenum, niobium, as well as a composite cathode of (50% Ti-50% Al) composition were used for deposition. The chromium cathode was mounted on extended arc evaporator DP400, the niobium cathode - on a DI80 arc evaporator, and the composite Ti-Al and molybdenum cathodes were mounted on DI100 arc evaporators. After installing the specimens on the tooling, the vacuum chamber was evacuated to a pressure of $5 \cdot 10^{-3}$ Pa. Then, argon was injected to a pressure of 0.3 Pa, the extended gas plasma generator «PINK-P» was turned on, and ion-plasma cleaning of the specimen surface took place. After cleaning, the metal plasma generators were simultaneously turned on, which ensured the generation of a multicomponent gas-metal plasma. The formation of the coating was carried out in a mixture of argon and nitrogen gases in equal proportions, the pressure was 0.3 Pa. After the deposition was completed, the specimens were cooled in a vacuum chamber to a temperature below 100°C.

Studies of the phase composition of the ceramic-metal high-entropy coating formed on the WC-8%Co hard alloy, performed by X-ray diffraction analysis, showed that the coating is an X-ray amorphous material.

Using transmission electron diffraction microscopy, it was established that HEA cermet films are a multilayer material. The multilayer nature of the films is revealed at two scale micro- and nano - levels. At the microscale level, the thickness of the dark contrast layers is 0.21 μm, and that of the light contrast layer is 0.19 μm. Each of these layers has a layered substructure at the nanoscale level. The substructure thickness of dark layers is ≈20 nm, light layers is ≈12 nm.

The results of X-ray microanalysis show that the layers of both levels differ in elemental composition. Layers enriched in nitrogen, chromium, and aluminum are revealed at the microscale level. The layers enriched in nitrogen are depleted in chromium and aluminum atoms. Layers enriched in aluminum and layers enriched in chromium, molybdenum, and niobium are revealed at the nanoscale level. Titanium atoms are located quasi-uniformly in the HEA film.

Microhardness (measurements were carried out at an indenter load of 0.5 N) of a high-entropy alloy ceramic-metal film deposited on a WC-8%Co hard alloy substrate is 27.0 GPa (exceeds the hardness of the HEA metal film by 1.8 times), Young's modulus is 176 GPa (exceeds Young's modulus of the HEA metal film by 1.6 times).

The wear parameter (the value inversely proportional to the wear resistance) of the high-entropy alloy cermet film deposited on the WC-8%Co hard alloy substrate is 6.4 10^{-6} mm^3/N m (the wear parameter of the HEA metal film is 23 times less); the friction coefficient of the ceramic-metal film of the high-entropy alloy is 0.20 (the friction coefficient of the HEA metal film is 3.3 times less).

REFERENCES

[1] Shugurov V.V. Koval N.N., Krysina O.V., and Prokopenko N.A. // J. Phys.: Conf. Ser. – 2019. – V. 1393. – P. 012131.

[2] Krysina O.V., Koval N.N., Kovalsky S.S., Shugurov V.V., et al. // Vacuum. – 2021. – V. 187. – P. 110123.

* The work was carried out with the financial support of the Russian Federation represented by the Ministry of Science and Higher Education (Project № 075-15-2021-1348)

C5-P-048702

ION-PLASMA METHOD FOR FORMING MULTILAYER CERAMIC HARD COATINGS*

N.A. PROKOPENKO, V.V. SHUGUROV, Yu.F. IVANOV, E.A. PETRIKOVA, O.S. TOLKACHOV, N.N. KOVAL, Yu.K. AKHMADEEV, O.V. KRYSINA

Institute of High Current Electronics SB RAS, Tomsk, Russia

A method for vacuum-arc plasma-assisted deposition of ceramic hard coatings based on high-entropy alloy (HEA) nitrides has been developed. The scheme of the experiment on the deposition of HEA coatings is shown in fig. 1.

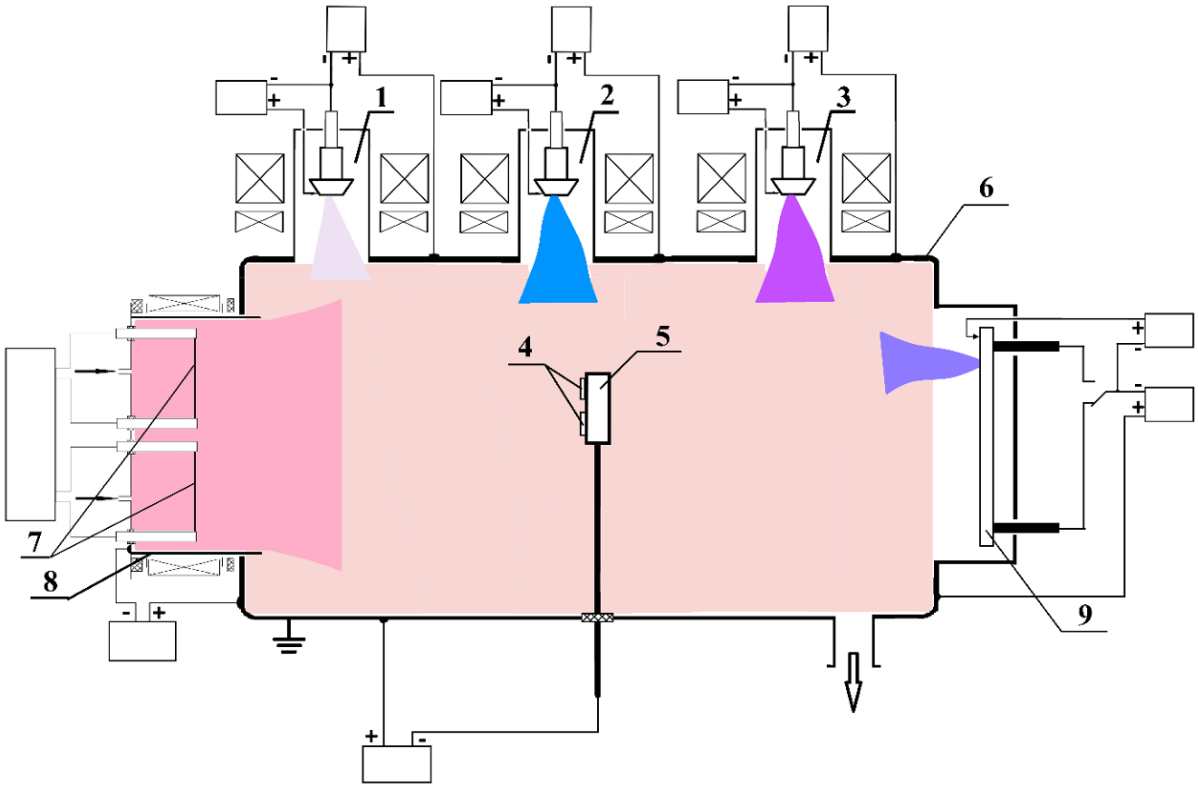

Fig. 1. Scheme of the experiment on obtaining HEA-hard coatings: 1 – DI100 arc evaporator with Mo cathode, 2 – DI80 arc evaporator with Nb cathode, 3 – DI100 arc evaporator with Ti-Al cathode, 4 – samples, 5 – substrate holder, 6 – vacuum chamber, 7 – heated cathodes, 8 – PINK-P gas plasma generator, 9 – DP400 arc evaporator with Cr cathode.

After fixing the samples on the substrate holder, the vacuum chamber was evacuated by a turbomolecular pump to a limiting pressure of $5 \cdot 10^{-3}$ Pa. Then, argon was injected to a pressure of 0.3 Pa, an extended gas plasma generator "PINK-P" with an output aperture of 40 × 400 mm was turned on, and ion-plasma cleaning of the surface of the samples took place. After cleaning, a mixture of gases (argon + nitrogen, pressure 0.3 Pa) was injected in different proportions and all metal plasma generators were turned on simultaneously, which ensured the generation of a sufficiently homogeneous in volume (± no worse than 20% of the average density value) multicomponent gas-metal plasma and HEA coverage growth. After the deposition was completed, the samples were cooled in a vacuum chamber to a temperature below 100°C and removed for examination. Optimal modes of application of ceramic coatings of HEA are revealed; the radial distribution of the ion current density from the plasma, the deposition rate, and the elemental composition of the coatings are determined. The elemental and phase composition, the defective substructure of ceramic coatings have been studied, the microhardness, wear resistance and friction coefficient have been determined.

* The work was carried out with the financial support of the Russian Federation represented by the Ministry of Science and Higher Education (project no. 075-15-2021-1348) within the framework of measures no. 2.1.5, 2.1.17 and 2.1.20.

C5-P-052802

STRESS EVOLUTION IN NICOFECRMN AND NICOFECR HIGH ENTROPY ALLOYS IRRADIATED BY HELIUM AND KRYPTON IONS

I.A. IVANOV[1,2], V.V. UGLOV[3], M.M. BELOV[3], S.V. ZLOTSKI[3], K. JIN[4], N.A. STEPANJUK[3], A.E. RYSKULOV[1], A.L. KOZLOVSKIY[1,2], M.V. KOLOBERDIN[1,2], A.E. KURAKHMEDOV[1], A.D. SAPAR[1]

[1]Institute of Nuclear Physics, Nur-Sultan, Kazakhstan
[2]L.N. Gumilyov Eurasian National University, Nur-sultan, Kazakhstan
[3]Belarusian State University, Minsk, Belarus
[4]Beijing Institute of Technology, Beijing, China

The operating environments envisaged for advanced nuclear reactors create significant challenges for structural materials due to a higher neutron flux, a more corrosive environment and higher operating temperatures [1]. It is therefore of interest to explore new alloy designs outside the paradigms of conventional steels, to meet these material requirements. High entropy alloys (HEAs) represent a new class of alloys that have the potential to replace conventional alloys in structural applications. Typically, they consist of four or five alloying elements in close to equiatomic concentrations. It is believed that maximizing the configuration entropy of HEAs promotes the formation of a single-phase disordered solid solution instead of the formation of complex intermetallic or second phases; as a result, the alloy has a simple microstructure with improved properties compared to traditional alloys. Numerous studies have shown that high-entropy alloys have a high elastic limit, wear, creep, and thermal and radiation resistance [2].

Multicomponent high entropy alloys NiCoFeCrMn and NiCoFeCr were synthesized using high-purity metals (>99.9%) by arc melting followed by homogenization. Then annealing was carried out for 24h and 72h at a temperature of 1150ºC with cold rolling up to 85 % reduction in thickness.

Ion implantation of alloys was carried out on a DC-60 heavy ion accelerator (Nur-Sultan) separately with He (40 keV, 2×10^{17} cm^{-2}) and Kr (280 keV, 5×10^{15} cm^{-2}) ions.

The X-ray diffraction analysis showed that a single-phase solid solution with a FCC lattice is formed in all samples. The results of scanning electron microscopy and X-ray energy dispersive analysis confirm the formation of homogeneous equiatomic multicomponent solid solutions, the grain size in the NiCoFeCrMn and NiCoFeCr alloys was about 80-100 μm. It was revealed that internal stresses in the NiCoFeCrMn and NiCoFeCr alloys are tensile and are about 68 and 125 MPa, respectively.

It was found that irradiation with helium and krypton ions leads to the formation of compressive stresses. At the same time, the stress level in samples irradiated with helium (-288 and -192 MPa for NiCoFeCrMn and NiCoFeCr alloys, respectively) exceeds the values for samples irradiated with krypton ions (-17 and -6 MPa for NiCoFeCrMn and NiCoFeCr alloys, respectively).

X-ray studies of the distribution of internal stresses and dislocation density in the NiCoFeCr alloy irradiated with helium and krypton ions over depth were carried out. The studies were carried out in the geometry of a small angle of incidence of the X-ray beam using the $\sin^2\psi$ and Williamson-Hall methods. It was found that the distribution of macrostress values in the NiCoFeCr alloy has two maxima corresponding to -250 MPa at a depth of 100±25 nm and -530 MPa at a depth of 255±25 nm. The results obtained are consistent with the SRIM data. According to calculations, the maximum radiation damage (dpa) corresponds to a depth of 125 nm, and the maximum of the implanted helium peak corresponds to a depth of 164 nm. The discrepancy in depth for the second maximum is mainly due to the swelling of the alloy during helium implantation.

It was found that the increase in the dislocation density in the irradiated NiCoFeCr alloy compared to the non-irradiated alloy is 3.5×10^{12} cm^{-2} and remains constant in depth up to 150 nm, and then decreases in 3 times.

The paper discusses the mechanisms of radiation defect formation in high entropy alloys, the influence of the type of ions and radiation damage on the formation of radiation defects, and their influence on the level of internal stresses.

REFERENCES

[1] S.J. Zinkle, G. Was, «Materials challenges in nuclear energy», Acta Mater., vol.61, Article Number 735, 2013.

[2] W. Zhang, P.K. Liaw, Y. Zhang, «High-entropy alumino-silicides: a novel class of high-entropy ceramics», Sci. China Mater., vol.61, Article Number 2, 2018.

C5-P-934201

SYNTHESIS OF MULTICOMPONENT FECRAL SURFACE ALLOY ON A ZIRCONIUM SUBSTRATE USING BY LOW-ENERGY HIGH-CURRENT ELECTRON BEAM*

E.V. YAKOVLEV, E.A. PESTEREV, V.I. PETROV, A.B. MARKOV

Institute of High Current Electronics SB RAS, Tomsk, Russia

Zirconium-based alloys have served the nuclear industry for several decades due to their unique set of properties [1]. Under normal use, zirconium alloys form a protective layer of zirconium oxide against corrosion. However, at high temperatures, which can occur under accident conditions, zirconium alloys exhibit poor oxidation kinetics [2, 3]. The replacement of the Zr coating with an alternative coating that is resistant to oxidation has generated considerable interest since the accident at the Fukushima Daiichi nuclear power plant [4]. However, the complete replacement of Zr is a difficult task, since it will entail major changes in the design of the reactor core due to different mechanical and neutronic properties. Moreover, large-scale production of fuel claddings from alternative materials is a long-term proposal. An alternative approach is to coat the Zr with an oxidation resistant coating, which will increase the resistance to accidents and minimize the effect on neutron transparency. FeCrAl has been proposed as a coating material due to its excellent oxidation resistance and thermal stability [5, 6]. Al in alloys can form a stable layer of aluminum oxide. The oxidation rate of FeCrAl is at least two orders of magnitude lower than that of Zr [7].

In this work, we used the RITM-SP electron-beam setup with an explosive emission cathode and a plasma-filled diode generating a low-energy high-current electron beam (LEHCEB) [8]. This machine is equipped with a magnetron sputtering system that allows the formation of multicomponent surfacealloys. The surface alloy was formed by the co-deposition of Fe, Cr, and Al on a Zr substrate and subsequent irradiation with LEHCEB.

The surface FeCrAl alloy was studied and analyzed by X-ray phase analysis using synchrotron radiation of the VEPP-3 electron storage ring as part of the Central Collective Use Center of the SCST based on the UNU "VEPP-4 Complex - VEPP-2000" at the INP SB RAS. The morphology of the surface and cross section is considered. The elemental composition was analyzed.

REFERENCES

[1] V. Azhazha, B. Borts, I. Butenko, V. Voevodin et al., Zirconium-Niobium alloys for NPP, Alushta, Ukraine, 2012.

[2] J.C. Brachet, E. Rouesne, J. Ribis et. al., "High temperature steam oxidation of chromium-coated zirconium-based alloys: Kinetics and process," Corros. Sci., vol. 167, Article Number 108537, 2020.

[3] K.A. Terrani, S.J. Zinkle, L.L. Snead, "Advanced oxidation-resistant iron-based alloys for LWR fuel cladding," J. Nucl. Mater. vol. 448, pp. 420–435, 2014.

[4] M. Kennas, H. Kim, J. G. Gigex et. al., "Radiation response of FeCrAl-coated Zircaloy-4," J. Nucl. Mater, vol. 536, Article Number 152175, 2020.

[5] B.A. Pint, K.A. Terrani, Y. Yamamoto, L.L. Snead, Material selection for accident tolerant fuel cladding, Metall. Mater. Trans. 2E, pp 190-196, 2015.

[6] B.R. Maier, B.L. Garcia-Diaz, B. Hauch, L.C. Olson, R.L. Sindelar, K. Sridharan Cold spray deposition of Ti2AlC coatings for improved nuclear fuel cladding, J. Nucl. Mater. 466, pp 712-717, 2015.

[7] L.J. Ott, K. Robb, D. Wang, Preliminary assessment of accident-tolerant fuels on LWR performance during normal operation and under DB and BDB accident conditions, J. Nucl. Mater. 448, pp 520-533, 2014.

[8] A.B Markov, A.V. Mikov, G.E. Ozu, A.G. Padei, Instrum. and Experim. Tech., vol. 54, pp. 862-866, 2011.

* The work was supported by the Ministry of Science and Higher Education of the Russian Federation (project No 075-15-2021-1348).

C6-O-007904

STRUCTURE AND PROPERTIES OF GLASSY SURFACE LAYERS OF TINI SUBSTRATE FABRICATED THROUGH HIGH-DOSE ION IMPLANTATION*

V.O. SEMIN[1,3], *L.L. MEISNER*[1], *E.M. OKS*[2], *K.P. SAVKIN*[2], *A.D. PLETNEV*[3], *A.V. GERASKEVICH*[4]

[1]*Institute of Strength Physics and Materials Science SB RAS, Tomsk, Russian Federation*
[2]*Institute of High Current Electronics SB RAS, Tomsk, Russian Federation*
[3]*National Research Tomsk State University, Tomsk, Russian Federation*
[4]*National Research Tomsk Polytechnic University, Tomsk, Russian Federation*

TiNi shape memory alloys (SMAs) are known to be smart materials utilized for fabrication of tiny medical instruments for small invasive surgery. This is due to the fact that TiNi SMA exhibits thermoelastic martensitic transformations, and its mechanical behavior is similar to the mechanical response of biological tissues. However, the issue of the assessment of biodegradation and corrosion properties of these alloys in the physiological environment is still under debate because release of toxic nickel ions could initiate inflammatory processes. Therefore, the formation of ultrastable oxide layers on the TiNi alloy surface, which prevents the nickel release into the biological environment, is an extremely urgent task. The method of ion implantation has a great potential for modifying the phase and chemical composition of TiNi SMAs [1–3] in order to improve corrosion properties and biocompatibility. In the current study, the approach of synthesis of barrier oxide layers on TiNi surface through ion-beam implantation of titanium was performed, and the detailed characterization of structure and electrochemical properties of the modified surface layers was given by means of high-resolution TEM/SEM and modern electrochemical methods.

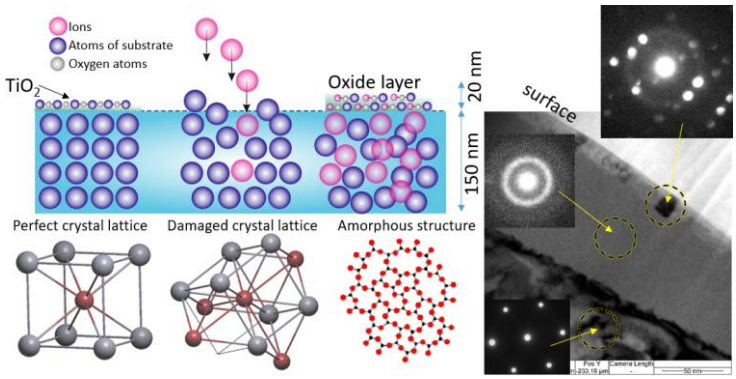

Fig.1. Scheme of ion implantation process of the TiNi alloy, leading to glass transition of a thin (up to 100 nm) surface layer. TEM images of the structure of the surface layer of the TiNi alloy after high-dose ($D=1\cdot10^{17}$ ion/cm^2) implantation with titanium.

The ion implantation of TiNi by titanium ions was carried out in the Laboratory of Plasma Sources (Institute of High Current Electronics, Tomsk) using a vacuum-arc ion source MEVVA-V.RU with a voltage of 30 kV, residual vacuum of $2\cdot10^{-4}$ Pa, at a pulse repetition rate of 10 Hz and an ion current density of 4.5 mA/cm^2. Material characterization was done in the center for the collective use «Nanotech» (Institute of Strength Physics and Materials Science, Tomsk).

The results (Fig. 1) have shown that ion implantation leads to the glass formation of a thin (100 nm) upper surface layer of TiNi substrate, when the dose of irradiation reaches $D=1\cdot10^{17}$ ion/cm^2. The nano-beam diffraction patterns indicate on the formation of a mixture of brookite TiO_2 and cubic TiO oxide phases on the sample surface. Data on corrosion properties (corrosion current, corrosion potential, breakdown potential, polarization resistance) demonstrate the advantage of ion implantation for improving the corrosion resistance.

REFERENCES

[1] Korotaev A. D. Amorphization of metals by ion implantation and ion mixing / A. D. Korotaev, A. N. Tyumentsev // FTT. - 1994. - No. 8. - P. 3-30.

[2] L.L. Meisner et al., The surface layers structure of differently oriented single titanium nickelide crystals subjected to ion implantation, Vacuum. – 2016. – Vol. 129. – P. 126-129.

[3] S.L. Girsova, T.M. Poletika, L.L. Meisner, E.Yu. Schmidt, The gradient structure of the NiTi surface layers subjected to tantalum ion beam alloying, J. Phys.: Conf. Ser. – 2017. – Vol. 830. – P. 012096.

* The work was supported by Government research assignment for ISPMS SB RAS, project FWRW-2021-0003.

C6-O-007905

RESIDUAL STRESS IN THE TINI SMART-MATERIAL AFTER ADDITIVE THIN-FILM ELECTRON-BEAM SYNTHESIS OF TI-NI-TA-SI SURFACE ALLOY*

M.G. OSTAPENKO[1], F.A. D'YACHENKO[1], A.A. NEIMAN[1], V.O. SEMIN[1], L.L. MEISNER[1]

[1]Institute of Strength Physics and Materials Science of Siberian Branch Russian Academy of Sciences, Tomsk, Russia

It is known that NiTi SMART-materials have shape memory effect and super-elasticity features. These materials are widely used in biomedicine (surgical stents, catheters) [1, 2] and industry (aerospace drives, sensors, seals) [3, 4]. The key issue responsible for degradation of functional properties of TiNi during operation is residual stresses arising from the sample processing and surface treatments. Recently, a novel method of surface modification of TiNi alloys has been proposed using an additive thin-film electron-beam synthesis of surface alloy [5].

The purpose of this work is X-ray diffraction examination of residual stresses formed in the near-surface layer of TiNi substrate after additive thin-film electron-beam synthesis of Ti-Ni-Ta-Si surface alloys.

The initial specimens at room temperature possess a three-phase mixture: a B2 phase (~85 vol.%), a Ti_2Ni phase (~10 vol.%) and a Ti_3Ni_4 phase (~5 vol.%). The magnetron co-deposition was performed through simultaneous sputtering of three targets {Ti, Ta, Si} on the surface of TiNi substrate to obey the composition $Ti_{60}Ta_{30}Si_{10}$ (at. %). For magnetron sputtering, we used cathodes made of pure elements Ti (99.95 wt. %), Ta (99.95 wt. %), and Si (99.95 wt. %) (Girmet, Russia). The deposition time was chosen in order to deposit a ~100 nm thick film on the surface of TiNi substrate. An additional post electron-beam treatment was employed with an energy density E_s = 1.7 J/cm^2 and pulse number n = 10. Formation of surface alloy on TiNi substrates and additional post electron-beam treatment was carried out in a single vacuum cycle on the modified setup "RITM-SP" (Microsplav Ltd., Russia) [6].

In this work, the fabricated Ti-Ni-Ta-Si surface alloys possess a multi-layered structure consisting of outer glassy layer and adjacent sublayers of TiNi substrate: eutectic B2+Ti_3Ni_4, martensitic R/B19' and heat-affected zone. The detailed XRD, TEM/EDS analysis revealed formation of two isostructural B2 phases with different lattice parameters, chemical compositions and microstructure. Changes of B2 lattice parameters are closely related with variation of chemical composition and residual elastic stresses of the first kind. The XRD determination of residual stresses in the as-cast samples has shown that compression stresses in the direction perpendicular to the irradiated surface reach a value of –350 MPa. Post electron-beam treatment results in decreasing of compression stress value down to –270 MPa. Based on the microstructural characterization, the step-by-step scenario of formation and evolution of residual stress fields after the synthesis of surface alloy and post electron-beam treatment of TiNi substrates is given.

REFERENCES

[1] M. H. Elahinia, et al. "Manufacturing and processing of NiTi implants: A review", Prog. Mater. Sci., vol. 57 (5), pp. 911-946, 2012.

[2] K. P. Zhu, et al. "Development and Application of Biomedical Ti Alloys Abroad", Rare Metal Materials and Engineering, vol. 41 (11), pp. 2058-2063, 2012.

[3] V. Torra, et al. "Civil Engineering Applications: Specific Properties of NiTi Thick Wires and Their Damping Capabilities, A Review", Shape Memory and Superelasticity, vol. 3 (4), pp. 403-413, 2017.

[4] N. Gangil, et al. "Towards applications, processing and advancements in shape memory alloy and its composites", Journal of Manufacturing Processes, vol. 59, pp.205-222, 2020.

[5] L. L. Meisner, et al. "Microstructural characterization of Ti-Ta-based surface alloy fabricated on TiNi SMA by additive pulsed electron-beam melting of film/substrate system", Journal of Alloys and Compounds, vol. 730 (Supplement C), pp. 376-385, 2018.

[6] G.E. Ozur, D.I. Proskurovsky, "Generation of low-energy high-current electron beams in plasma-anode electron guns", Plasma Phys. Rep., vol. 44 (1), pp. 18–39, 2018.

* The work was supported by the Government research assignment for ISPMS SB RAS, project FWRW 2021-0003.

C6-O-023001

MECHANISMS FOR IMPROVING THE FATIGUE LIFE OF TINI ALLOYS ASSOCIATED WITH ELECTRON-BEAM SURFACE MODIFICATION *

L.L. MEISNER, S.N. MEISNER
Institute of Strength Physics and Materials Science SB RAS, Tomsk, Russia

The study results of the influence of surface electron-beam treatments on the fatigue characteristics of an TiNi shape memory alloy (SMA) are presented in the report. Surface melting modes were used for processing by a pulsed low-energy high-current electron beam (LEHCEB) with electron energy densities E_S = 1.5, 2.7, and 3.7 J/cm^2 at different numbers of pulses n = 5 and 15. Cyclic tensile tests were carried out in the low-cycle fatigue mode on a servo-hydraulic testing machine Biss UTM 150 (Biss, India) with cycle asymmetry R=0.1 at a maximum load of 160 MPa and a frequency of 20 Hz. The study of the fatigue fracture surfaces of the LEHCEB's modified TiNi substrates was carried out with use a scanning electron microscope (SEM) EVO 50 (Zeiss, Germany).

It is shown that LEHCEB treatment of the TiNi surface led to an increase in the fatigue life of TiNi substrates by almost 1.5-2 times, compared with non-irradiated TiNi substrates, which is due to the effective cleaning of sample surfaces using LEHCEBs from particles/inclusions, as the main sources of fatigue microcracks on the surface. The highest result is observed after LEHCEB treatments at E_S = 1.5 and 3.7 J/cm^2 with the number of pulses n = 5, which is due to the formation of residual compressive stresses in the modified surface layer, which prevent the initiation of defects from the surface of the sample and their propagation into the internal volume.

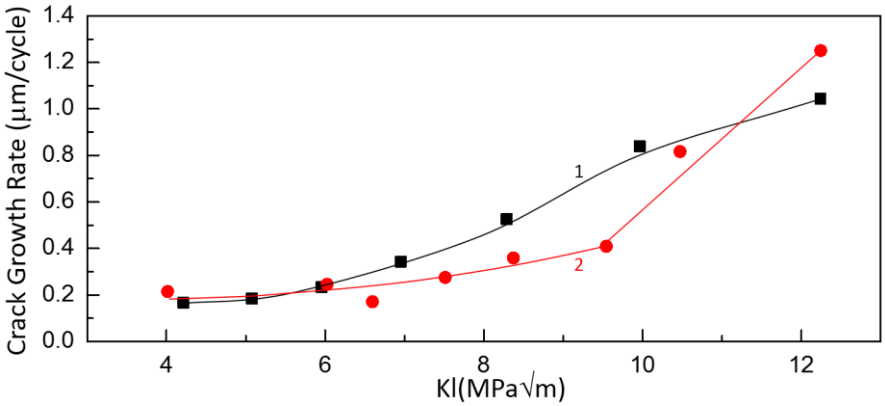

Fig.1. Dependences of fatigue crack growth rates on the maximum stress intensity factor before (1) and after (2) LEHCEB treatments of TiNi substrates.

Regularities of formation and propagation of fatigue cracks before and after LEHCEB treatment of TiNi substrates are studied. The influence of these treatments on the fatigue crack growth rates are estimated. It was found that LEHCEB modification leads to an increase in the average number of cycles <Nstart> of the beginning of fatigue crack formation by more than $\Delta N \approx 2000$. More over the fatigue crack growth rate in irradiated TiNi substrates at the first stages of formation and propagation of a fatigue crack is 4–10 times lower than this rate in non-irradiated samples. At the same time, the stages of critical destruction and the sizes of fracture zones before and after LEHCEB irradiation differ little from each other.

The conclusion is substantiated that LEHCEB surface modification plays a critical role in the first stages of the process of fatigue accumulation of defects, effectively preventing the onset of this process. The main reasons for this result are the structure of the modified layer and the residual stresses inside it and below, to a depth of ~100 μm, induced by LEHCEB treatment.

* The work was supported by the Russian Science Foundation under grant No. 22-29-00047.

C6-O-033604

INFLUENCE OF HELIUM ION IRRADIATION ON THE STRESS EVOLUTION IN NC-ZRN/A-ZRCU MULTILAYERD FILMS

V.V. UGLOV[1], S.V. ZLOTSKI[1], G. ABADIAS[2], I.S. VEREMEI[1]

[1]*Belarusian State University, Minsk, Belarus*
[2]*Institut Pprime, CNRS-Université de Poitiers- ENSMA, France*

Nowadays the development of new radiation-resistant materials is a crucial problem that is especially urgent for fission/fusion industry, aerospace application, etc. wherein objects are exposed to strong irradiation with ions, neutrons, electrons. So irradiation with light ions due to nuclear collisions can induce a higher ratio of point defects (e.g. vacancies and interstitials) produced relative to defect clusters (e.g. He bubbles) in metallic crystals [1]. This in turn remarkably degrades the performance of structural materials in advanced fission/fusion reactors, which must be significantly improved to extend the reliability and efficiency [2, 3].

For this, it is necessary to create materials with a large amount of sinks for point defects, such as dislocations, grain boundaries, and interphase boundaries [4]. Multilayer systems are promising for research, since interlayer boundaries can affect the elimination of radiation defects [5]. They have significant interfacial regions that can act as stable defect absorbers.

Multilayer films nc-ZrN/a-ZrCu with different Cu concentration (from 44.6 to 73.8 at.%) and thickness of amorphous layer ZrCu (5 and 10 nm) were formed at 300°C by reactive magnetron sputtering in a high vacuum chamber (base pressure $<10^{-5}$ Pa) equipped with three confocal targets and a cryogenic pump (max. 500 l/s). A constant bias voltage of -60 V was applied to the substrate during deposition, while the substrate was rotated at 15 rpm throughout the whole deposition to ensure an equal deposition rate across the substrate area. nc-ZrN/a-ZrCu multilayer films with different Cu content and thickness of ZrN and ZrCu elementary layers have been investigated. The Cu content in the ZrCu layers was varied by changing the DC power supply of the Cu target, from 40 to 52 W, and the DC power supply of Zr target, from 88 up to 294 W.

Ion implantation of multilayer films was carried out with He^{2+} ions with energy of 40 keV on a DC-60 heavy ion accelerator at fluences from 5.0×10^{16} to 1.1×10^{18} cm^{-2}. The energetic parameters of implantation were chosen so as the implanted He distribution depth did not exceed the film thickness, as calculated using the SRIM-2012 code.

X-ray diffraction and transmission electron microscopy (TEM) studies of multilayer films after deposition have shown that the films consist of alternating layers of nanocrystalline ZrN and amorphous a-ZrCu. The formation of horizontal continuous layers with flat and sharp interfaces was revealed.

Studies of stresses in multilayer films have shown that they are compressive and vary from -2 to -4 GPa depending on the thickness of the ZrCu layer and the Cu concentration in it. It has been found that irradiation with helium ions leads to a decrease in the level of compressive stresses. In this case, for multilayer films with an amorphous layer thickness of 5 nm at a dose of more than 9.0×10^{18} cm^{-2}, the stresses decrease to zero and become tensile. The decrease in the stress level is mainly associated with the effects of radiation erosion of multilayer films. The change in compressive stresses in multilayer films upon irradiation with helium ions is consistent with the TEM data. Microscopic studies revealed curvature of crystalline and amorphous layers in the area of implantation of helium ions.

In the paper discusses the mechanisms of changes in internal stresses after implantation of helium ions, as well as the influence of copper concentration in the amorphous layer, its thickness and radiation dose on the level of these stresses.

REFERENCES

[1] M.J. Demkowicz, D. Bhattacharyya, I. Usov et al., «The effect of excess atomic volume on He bubble formation at fcc–bcc interfaces», Appl. Phys. Lett., vol.97, Article Number 161903, 2010.

[2] M.J. Demkowicz, A. Misra, A. Caro, «The role of interface structure in controlling high helium concentrations», Curr. Opin. Solid State Mater. Sci., vol.16, Article Number 101, 2012.

[3] Z. Jiao, G.S. Was, «The role of irradiated microstructure in the localized deformation of austenitic stainless steels», J. Nucl. Mater., vol. 407, Article Number 34, 2010.

[4] R.E. Baumer, M.J. Demkowicz, «Radiation response of amorphous metal alloys: Subcascades, thermal spikes and super-quenched zones», Acta Mater., vol.83, Article Number 419, 2015.

[5] Xinghang Zhang, Khalid Hattar, Youxing Chen et al., «Radiation damage in nanostructured materials», Prog.Mat. Sc., vol.96, Article Number, 217, 2018.

C6-O-952201

DEPOSITING OF MULTILAYER MULTICOMPONENT COATINGS TO INCREASE THE LIFETIME OF CUTTING TOOLS*

M.V.SAVCHUK[1], V.V. DENISOV[1], YU.A. DENISOVA[1], A.A. LEONOV[1], V.N. TISCHENKO[1], A.B. SKOSYRSKY[2], V.M. SAVOSTIKOV[1]

[1]*Institute of High Current Electronics SB RAS, Tomsk, Russia*
[2]*National Research Tomsk State University, Tomsk, Russia*
e-mail: mixail96@bk.ru

In this paper, the physicomechanical and tribotechnical properties of multicomponent TiB/TiBN and TiCrB/TiCrBN coating systems are investigated to reduce the wear of the material surface.

Coating deposition is carried out by combining of method of ion-plasma nitriding and vacuum-arc plasma-assisted deposition of functional coatings. As a result of the experiments, the values of microhardness and nanohardness of the deposited coatings were obtained. Tribotechnical tests were also carried out.

In the course of the work, tests of cutting tools with multilayer coatings of TiB/TiBN and TiCrB/TiCrBN systems were carried out.

According to the test results, the wear resistance of the TiCrB/TiCrBN coated cutting tool increased by four times. At the same time, the coefficient of friction with the addition of chromium in the film decreased from 0,5 to 0,2.

* The work was carried out with the financial support of the Russian Federation represented by the Ministry of Science and Higher Education (project № 075-15-2021-1348) within the framework of even № 1.1.14.

C6-P-010701

EFFECT OF LOW-TEMPERATURE PLASMA NON-SELF-SUSTAINED DISCHARGE ON CHEMICAL COMPOSITION AND MORPHOLOGY OF POLYLACTIC ACID SURFACE *

O. A. LAPUT[1], I. V. VASENINA[2], YU. H. AKHMADEEV[3], I.A. KURZINA[1]

[1]Tomsk State University, Tomsk, Russia
[2]P.N. Lebedev Physical Institute, Moscow, Russia
[3]Institute of High Current Electronics SB RAS, Tomsk, Russia

The effect of argon flow non-self-sustained discharge plasma treatment on surface physicochemical properties of biocompatible scaffolds based on polylactic acid (PLA) was investigated. The PLA-based scaffolds were obtained by electrospinning on the Nanon-01 facility [1]. The plasma treatment conditions were following: the plasma gas – argon; the amplitude of discharge current – 5-10 A; working pressure – 0.3 Pa; exposure time – 5÷28 min. Surface modification by low-temperature plasma is used for alteration of the structure and physicochemical properties of PLA-based scaffolds, such as chemical compound, phase state, roughness etc.

X-ray diffraction analysis (XRD) before and after plasma treatment reveals diffraction patterns containing two distinct peaks at 2θ= 25,3°, 29,3°, corresponding to the crystallographic planes with indexes (015) and (216) [2]. After modification of PLA surface by low-temperature argon plasma, the main diffraction lines appeared: 2θ= 16.7°; 19.2°, corresponding to crystallographic planes with indices (110)/(200) and (203), that indicates the presence of α-shaped crystals (rhombic crystal lattice). The degree of crystallinity (χ_C) increases with increasing exposure time of plasma treatment. The enhance of χ_C was established from 28% (initial PLA) to the maximum value of 68% after 28 minutes of plasma treatment. The increasing of the degree of crystallinity indicates the orderliness of the PLA macromolecules packing. The non-self-sustained discharge plasma treatment of PLA surface leads to the increasing of carbonyl group band intensity, corresponding to the α-form of the PLA crystal structure, which indicates the destruction of polymer bonds.

According to the results by AFM spectroscopy, the roughness R_a is increased from 5 to 248 nm for plasma-treated scaffolds. It was found that roughness depends on the degree of crystallinity (Fig. 1). Increasing the scaffolds surface roughness submit a second-order polynomial law: $R_a = -15.429\ \chi_C^2 + 118.77\ \chi_C - 87.4$, while the approximation reliability coefficient $R^2 = 0.9612$. Increasing the surface roughness improves the adhesion and proliferation of cells on PLA surface.

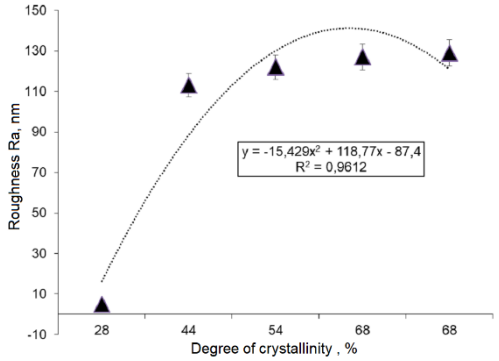

Fig.1. The dependence of the modified scaffolds PLA surface roughness from the degree of crystallinity

To sum up, argon flow non-self-sustained discharge plasma treatment is an effective technique for surface physicochemical property modification of biocompatible scaffolds based on PLA.

REFERENCES

[1] Laput OA, Ochered'ko AN, Vasenina IV, Yan Ch, Goroshkina UV, Ivonin IV (2020) Effect of low-temperature plasma barrier discharge on elemental composition and wettability of polylactic acid surface. AIP Conf Proc 2310:020179-1-020179–4.

[2] O. A. Laput, I. V. Vasenina, V. V. Botvin, I. A. Kurzina, Surface modification of polylactic acid by ion, electron beams and low-temperature plasma: a review // *J Mater Sci*. - 2022.

[3] Devyatkov V.N., Ivanov Yu.F., Krysina O.V., Koval N.N., Petrikova E.A., Shugurov V.V. Equipment and processes of vacuum electron-ion plasma surface engineering // Vacuum. – V. 143. – 2017. – P. 464-472.

* This work was supported the Tomsk State University Development Program (Priority-2030).

C6-P-018801

THE PROCESS OF MAO COATING FORMATION AT THE COATING-SURFACE INTERFACE*

A.I. KONDRATENKO, P.I. BUTYAGIN, I.A. EKIMOVA, S.S. ARBUZOVA, A.V. BOLSHANIN

MANEL JSC
Vysotskogo St. 25, Bldg. 12, 634040, Tomsk, Russia, Tel. (3822) 60-65-90, manel@manel.ru

Aluminum is one of the most promising and widely used materials in many industries. Aluminum alloy parts have low weight and high thermal conductivity relative to steel and cast iron. The disadvantages of aluminum products are low wear resistance, high coefficient of linear thermal expansion, irregularity and high porosity of the oxide film. The surface modification of aluminum parts allows improving their properties [1, 2, 3].

The method of micro-arc oxidation (MAO) allows modifying the surface and producing protective coatings on aluminum, titanium, magnesium, zirconium, tantalum, neobium and their alloys. The coatings have an increased adhesion ability, high hardness, corrosion resistance, resistance to aggressive media, and insulating properties. This method (MAO) consists in modification of product surface by microplasma discharges and formation of protective ceramic coating at the metal-electrolyte interface, consisting of oxide forms of substrate metal and electrolyte elements. It is possible to obtain coatings up to 400 μm thickness, using the MAO method [4, 5].

The study of the metal-MAO coating interface obtained at different technological parameters will help to study the coating formation processes in more detail, as well as to consider the influence of electrical parameters on the properties of MAO coatings.

MAO coatings were formed in the anodic mode by the MANEL technology on aluminum samples (D16 and AMg3 alloys), ø50 mm and h = 2 mm, in the electrolyte "Manel-B" (pH = 6) using a pulse power supply ARCCOR III (EleSy Company) at voltage 600 V, pulse duration from 20 to 200 μs and frequency from 70 to 300 Hz. There were implemented 6 technological modes and were obtained 2 samples for each mode. At the beginning of MAO process, a transition layer of metal-coating with a thickness of 5-20 μm was formed. Then the external thickness of the coating was increased up to 30-40 μm, the average formation speed depended on the parameters of the power source and ranged from 0.125 to 32 μm/min.

The samples were dried in a drying box at 100°C after MAO treatment. The surface roughness of MAO-coating was measured using TR220 roughness meter, elasticity was evaluated using an Eriksen method, and impact resistance was determined using a Constanta U2-M device.

Cross-sections were made from the samples obtained using a Buehler polishing system to study the metal-coating interface. The surface morphology and the cross-sectional microstructure of the coatings were characterized by scanning electron microscopy (SEM, Quanta 200 3D), microhardness was evaluated by Shimadzu DUH-211S dynamic ultra micro hardness tester; the film thickness was measured by Positector 6000 vortex thickness meter.

The paper presents the quantitative distribution of elements at the metal-MAO-coating interface. It was obseved that the microhardness values near the metal-MAO coating interface depend on a coating composition. On the other hand, technological parameters such as pulse duration and pulse frequency influence on distribution elements in the coating.

It is shown the MAO coating has the lowest values of the formation rate and surface roughness at low values of the pulse duration and pulse frequency. Increasing these parameters leads to MAO coating growth rate and surface roughness growth.

REFERENCES

[1] E.A. Pechyorskaya, P.E. Golubkov, O.V. Karpanin, D.V. Artamonov, M.I. Safronov, A.V. Pechyorsky, "Study of the effect of technological parameters of the micro-arc oxidation process on the properties of oxide coatings," Izvestiya vuzov. Electronics, Penza, Russia, pp. 363-369, 2019.

[2] Dong Yuting, Liu Zhiyang, Ma Guofeng, The research progress on micro-arc oxidation of aluminum alloy, Conference Series: Materials Science and Engineering, vol. 729, Shenzhen, China, pp. 12, 2019.

[3] Qingjun Zhu, Binbin Zhang, Xia Zhao and Binbin Wang, Binary Additives Enhance Micro Arc Oxidation Coating on 6061Al Alloy with Improved Anti-Corrosion Property, Coatings, vol.10, no 2, pp 11, February 2020.

[4] Frank Simchen, Maximilian Sieber, Alexander Kopp and Thomas Lampke, Introduction to Plasma Electrolytic Oxidation-An Overview of the Process and Applications, Coatings, vol.10, no 7, pp 19, July 2020.

[5] Lingqin Xia,1 Jianmin Han,1 Joseph P. Domblesky,2 Zhiyong Yang,1 and Weijing Li, Investigation of the Scanning Microarc Oxidation Process, Advances in Materials Science and Engineering, vol. 2017, pp. 12, June 2017.

* The work was supported by…All acknowledgments should be written as footnotes (EFRE Footnote style): 8 pt, justified alignment, spacing 0 pt before and 10 pt after paragraphs, single line spacing.

20th International Conference on Radiation Physics and Chemistry of Condensed Matter

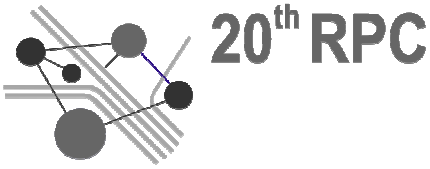

Chair	Elena POLISADOVA	National Research Tomsk Polytechnic University, Tomsk, Russia
Program Chair	Elena POLISADOVA	National Research Tomsk Polytechnic University, Tomsk, Russia

Program Committee

Anna KARNAUKHOVA	National Research Tomsk Polytechnic University, Tomsk, Russia
Vladimir OLESHKO	National Research Tomsk Polytechnic University, Tomsk, Russia
Sergey STEPANOV	National Research Tomsk Polytechnic University, Tomsk, Russia
Victor LISITSYN	National Research Tomsk Polytechnic University, Tomsk, Russia

International Advisory Committee

Albert ASHRYATOV	Ogarev Mordovia State University, Saransk, Russia
Boris ADUEV	Institute of Coal-chemistry and Material Science of the Siberian Branch of the RAS, Kemerovo, Russia
Habibula ABDULLIN	Al Farabi Kazakh National University, National Nanotechnology Laboratory of Open Type, Almaty, Kazakhstan
Abdirash AKILBEKOV	L.N. Gumilyov Eurasian National University, Astana, Kazakhstan
Gennady BONDARENKO	National Research University Higher School of Economics, Moscow, Russia
Flyura DJURABEKOVA	Helsingin Yliopisto, Helsinki, Finland
Boris KALIN	National Research Nuclear University MEPhI, Moscow, Russia
Mustafa KIDIBAEV	Kyrgyz National Academy of Sciences, Bishkek, Kyrgyzstan
Evgenij KOTOMIN	Max Planck Institute for Solid State Research, Stuttgart, Germany
Anatoly KUPCHISHIN	Abai Kazakh National Pedagogical University, Almaty, Kazakhstan
Aleksandr LUSHCHIK	Institute of Physics, University of Tartu, Tartu, Estonia
Sergey NIKIFOROV	Ural Federal University, Ekaterinburg, Russia
Hosam OTHMAN	Minufiya University, Department of Physics, Shebin el Kom, Egypt
Anatoli POPOV	Institute of Solid State Physics, University of Latvia, Riga, Latvia
Stanislav SHANDAROV	National Research Tomsk Polytechnic University, Tomsk, Russia
Han TAO	Research Institute for New Materials Technology, Chongqing University of Arts and Sciences, Chongqing, China
Yurij ZAKHAROV	Kemerovo State University, Kemerovo, Russia
Vladimir ZARKO	Voevodsky Institute of Chemical Kinetics and Combustion, Novosibirsk, Russia
Maxim ZDOROVETS	Institute of Nuclear Physics' Astana branch of the Republic of Kazakhstan
Evgenij MARTYNOVITCH	Institute of Laser Physics of the Siberian Branch of the RAS, Irkutsk, Russia
Vadim KRIGER	Kemerovo State University, Kemerovo, Russia
Ilya WEINSTEIN	Ural Federal University, NANOTECH Center, Ekaterinburg, Russia
Aleksandr NEPOMNYASHCHIKH	A.P. Vinogradov Institute of Geochemistry of the Siberian Branch of the RAS, Irkutsk, Russia

Conference topics

R1 Luminescence: processes, luminescence centers, scintillators and luminophores, application
R2 Non-linear physicochemical processes under severe energetic impact: breakdown, facture, explosion, etc.
R3 Physical principles of radiation and photonic technologies
R4 Radiation defects: structure, formation, properties
R5 Methods, instruments and equipment for physicochemical studies

R1-O-008001

INTRINSIC AND DOPANT-DRIVEN LUMINESCENCE IN $LiMgPO_4$*

M.O. KALINKIN[1], *V.G. ZUBKOV*[1], *D.A. AKULOV*[1], *N.I. MEDVEDEVA*[1], *R.M. ABASHEV*[2], *A.I. SURDO*[2], *D.G. KELLERMAN*[1]
[1]*Institute of Solid State Chemistry UrB RAS, Ekaterinburg, Russia*
[2]*Institute of Metal Physics UrB RAS, Ekaterinburg, Russia*

Nowadays, lithium–magnesium phosphate with an olivine structure is of special importance for radiation dosimetry applications, which is mainly due to chemical and thermal stability as well as ease of synthesis and low cost of the material. $LiMgPO_4$ turned out to be suitable for both optically (OSL) and thermally (TSL) stimulated luminescence [1].

In this work, we consider in detail peculiarities of photo-, radio-, and thermoluminescence in pure and doped Li-Mg phosphate with different morphology and synthesized using various methods. It is shown that, other things being equal, the smaller the specific surface of the powder sample, the higher the optical yield. Thus, undoped $LiMgPO_4$ with the best characteristics was obtained by melting and following quenching. To understand the nature of surface and bulk point defects that can act as traps and luminescence centers, the ESR method was applied. We determined the energy of defects using *ab initio* calculations and UV-viz spectroscopy.

Although pure $LiMgPO_4$ accumulates energy under ionizing irradiation and keeps it for a long time, to significantly enhance the dosimetric response, the presence of rare earth ions is required. A series of $LiMgPO_4:RE^{3+}$ phosphors was synthesized by the conventional solid-state method. It has been shown that all rare earths can be divided into two groups: Sm, Gd, Tb, Dy, Eu and Tm manifest themselves in RL and TSL spectra by the appearance of a characteristic set of lines reflecting the luminescence of rare earth elements as a result of f–f transitions from an excited state to a lower one, while Er, Pr, Yb, Ce, Ho, and Nd only greatly enhance the two-humped RL and TSL spectra of the phosphate matrix (Fig.1). The discovered effect was attributed to non-radiative energy transfer [2] from some RE^{3+} ions to matrix defects with energies close to the energies of upper radiation levels of these RE^{3+}. Regardless of the dopant, all irradiated samples exhibit thermoluminescence at temperatures of 100–300 ^{0}C, which significantly exceeds that of pure $LiMgPO_4$ in intensity. The best and almost similar characteristics are demonstrated by $LiMgPO_4$:Er and $LiMgPO_4$:Tb despite the fact that terbium in $LiMgPO_4$:Tb acts as a TSL activator and erbium is a sensitizer, enhancing the stimulated luminescence of the matrix.

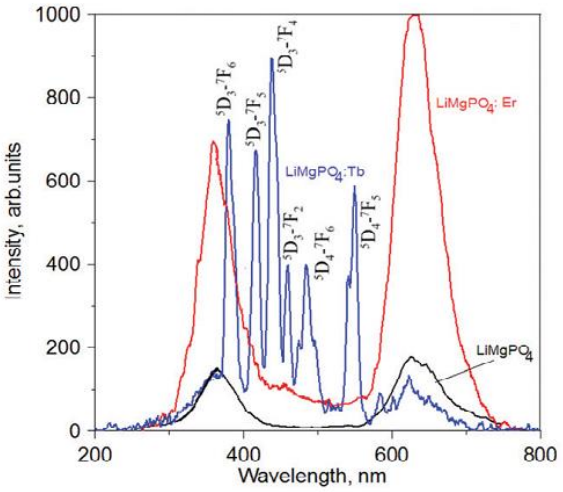

Fig.1. RL spectra of LiMgPO4, LiMgPO4:Er and LiMgPO4:Tb.

REFERENCES

[1] B. Dhabekar, S.N. Menon, E.A. Raja, et al., "LiMgPO4:Tb,B – A new sensitive OSL phosphor for dosimetry", Nucl. Instr. Methods Phys. B, vol. 269, pp. 1844–1848, 2011.

[2] T. Förster, "Transfer mechanisms of electronic excitation",. Discuss. Faraday Soc. vol.27, pp.7-17.

* The work was supported by the Russian Science Foundation under grant No. 20-13-00121.

R1-O-010301

THE LASER CREATION OF THIN LUMINESCENT-ACTIVE SENSITIVE LAYERS ON THE CORUNDUM SURFACE*

ABASHEV R.M.[1,2], *VOLOSHIN A.M.*[1], *SURDO A.I.*[1,2], *MILMAN I.I.*[1,2]

[1]*M.N. Mikheev Institute of Metal Physics of Ural Branch of Russian Academy of Sciences, Yekaterinburg, Russia*
[2]*Ural Federal University, Yekaterinburg, Russia*

Skin dosimetry requires the creation of luminescent detectors with a thin sensitive layer with a mass thickness of 5 mg/cm^2. The linear thickness of such a layer in corundum-based detectors is ~12 μm. To achieve this goal, we proposed in [1] to use laser treatment of specially prepared detectors based on single-crystal corundum. A scanning laser pulse beam with a wavelength of 10.6 μm was used to melt the surface and form a thin sensitive layer in the detectors with a thickness of ~12-15 μm. As a result of this treatment the responses of optically and thermally stimulated luminescence (OSL and TSL) from the thin layers of such detectors became proportional to the radiation dose. However, their OSL and TSL responses (sensitivity) were insufficient. To increase sensitivity of the detectors we have studied the dependences of the OSL and TSL responses (S_{OSL} and S_{TSL}) on the energy (E_{pulse}) delivered by focused laser beam in one pulse, on the pulse frequency (f), on the velocity (v) and the density of scanning (DPI – dots per inch). The change in the structure of the surface layer was monitored microscopically.

Fig. 1 shows micrographs of the surface of samples laser-treated at E_{pulse} = 14 mJ (a) and 38 mJ (b). As can be seen, with increasing E_{pulse}, the surface area with a modified structure increases. At $E_{pulse} \geq 68$ mJ, the entire surface is covered with similar structural elements. Moreover, at $E_{pulse} \geq 102$ mJ cracks is appeared in the volume of the samples and the samples begin to split. Fig. 2 shows the $S_{OSL}(E_{pulse})$ dependency. It can be seen that in the E_{pulse} range from 14 to 68 mJ the value S_{OSL} increases and next at $E_{pulse} > 68$ mJ it reaches saturation. The $S_{TSL}(E_{pulse})$ dependency has a similar form. Further, at E_{pulse} = 68 mJ, the dependences of S_{OSL} and S_{TSL} on v, f and DPI were investigated.

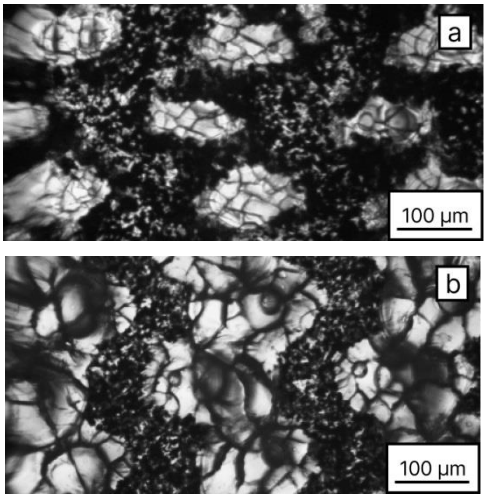

Fig.1. Micrographs of the surface of samples laser-treated at E_{pulse} 14 mJ (a) and 38 mJ (b).

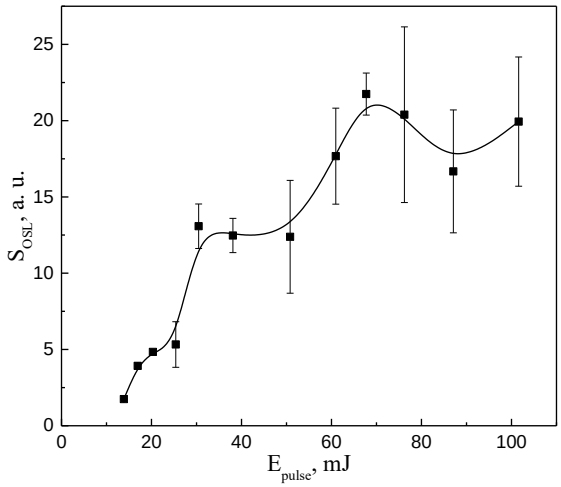

Fig.2. The $S_{OSL}(E_{pulse})$ dependency of samples IR laser treated at 100 pulses per inch, 250 dots per inch and irradiated with 20 mSv β-radiation.

As a result, the optimal laser scanning mode for creating thin sensitive layers of skin detectors based on corundum with maximum OSL and TSL responses was found. The detectors with such a sensitive layer fully meet the requirements of NRB-99/2009 [2] in thickness, energy and dose ranges for photon and β-radiation.

REFERENCES

[1] Milman I.I., Surdo A.I., Abashev R.M. "Method for obtaining thin-layer ionizing radiation detectors for skin and eye dosimetry", Patent RF, no.2747599.

[2] Radiation Safety Standards (NRB–99/2009). Moscow, 2009.

* The work was supported by the state assignment of Ministry of Science and Higher Education of the Russian Federation (theme "Expertise" No. AAAA-A19-119062590007-2), supported in part by RFBR (project No. 20-48-660045).

R1-O-013102

LUMINESCENCE OF DYE AFTER EXPOSURE TO ELECTRON BEAM RADIATION*

E.N. BOCHARNIKOVA[1], O.N. TCHAIKOVSKAYA[1,2], S.A. CHAYKOVSKY[2], V.I. SOLOMONOV[2],

A.S. MAKAROVA[2], G.V. MAYER[1], V.V. OSIPOV[2]

[1] National Research Tomsk State University, Tomsk, Russia
[2] Institute of Electrophysics of the Ural Division of the Russian Academy of Sciences, Yekaterinburg, Russia

Wastewater containing emissions from textile production poses an environmental hazard due to the refractory carcinogenic nature of dyes. Crystal violet (CV) is a typical triphenylmethane dye, is toxic to living organisms and is a mutagenic and mitotic poison. We know that the CV molecule is of interest for scientific research in the field of nonlinear properties, its interaction with ferroelectric crystals leads to outstanding optical properties and is of great interest because of its potential use in displays and electro-optical devices. The chemical coagulation process can intelligently remove dyes from wastewater, but it will generate a large amount of secondary waste. Activated carbon processes can remove dyes in aqueous solution efficiently but activated carbon and post-treatment of spent carbon are costly. There are a few research works devoted to the study of wastewater treatment from dyes using photolytic oxidation (TiO_2/UV, ZnO/UV, H_2O_2/UV, Fe^{2+}/H_2O_2/UV). UV radiation can destroy organic pollutants, including crystal violet, through direct and indirect photolysis. An analysis of the rate constant of CV had been reduced in water under the action of KrCl and XeBr excilamp radiation shows that under the action of XeBr radiation, the efficiency of CV degradation without additives in water is low and amounts to only 2%. The addition of hydrogen peroxide (1:1) reduces the concentration of CV in solutions, the conversion is already 93% under the action of KrCl [1]. The HPLC data of the irradiated solutions for 60 min showed that, in addition to the CV residue, the solution also contains its phototransformation products. The report presents the results of measuring the luminescence of the ambient air and aqueous solutions of CV when they are irradiated with a high-current pulsed electron beam with an average energy of Ee=170 keV and a duration of 2 ns, formed by the RADAN-303 accelerator [2]. The CV concentration in water was 0.05 mM (Fig. 1). Experimental studies were carried out in air at room temperature. The time-integrated emission spectrum in the range 200÷850 nm was recorded by two multichannel photodetectors with sensitivity ranges 200÷400 and 400÷850 nm. The absorption spectra of the CV after exposure to an electron beam were recorded on a two-beam Shimadzu UV-1700 spectrophotometer in the region of 200÷800 nm. It is shown that under such an impact, the dissolved CF is transformed, which is accompanied by a weakening of the air spectral lines during CV degradation with an increase in the number of irradiation pulses. The report discusses the mechanism and efficiency of CV transformations in water under the action of an electron beam.

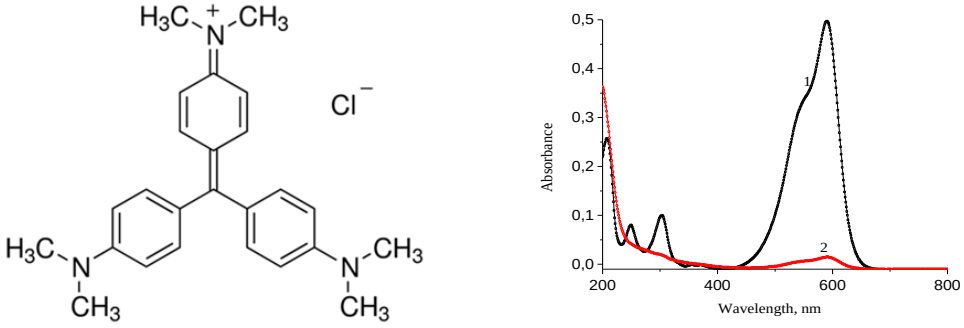

Fig.1. The structure of crystalline violet and the absorption spectrum of CV in water: before (1) and after exposure to an electron beam of 1600 pulses (2).

REFERENCES

[1] M. Gómez, M.D. Murcia, E. Gomez, S. Ortega, A. Sanchez, O.N. Tchaikovskaya, N.G. Bryantseva, "Modelling and experimental checking of the influence of substrate concentration on the first order kinetic constant in photo-processes," Journal of Environmental Management, no. 3, vol. 183, pp. 818–825, 2016.

[2] V.I. Solomonov, A.V. Spirina, M.P. Popov, O.A. Kaigorodova, "Luminescent signs of precious beryl deposits," Journal of Optical Technology, no. 8, vol. 83, pp. 494–497, 2016.

* The work was performed within the framework of the State Assignment of the Ministry of Education and Science of the Russian Federation (Project No. 0721-2020-0033).

R1-O-015401

POLYVALENCE STATES AND ANTI-SITE DEFECTS OF IRON IONS IN $MgAl_2O_4$ OPTICAL NANOCERAMICS*

A.N.KIRYAKOV[1], *A.F.ZATSEPIN*[1], *V.V.OSIPOV*[2]

[1]*Ural Federal University, Yekaterinburg, Russia*
[2]*Institute of Electrophysics Ural Division of Russian Academy of Science, Yekaterinburg, Russia*

Optical ceramics are promising media for doping with a wide spectrum of impurity ions with an unfilled d shell. Of particular interest are ions that are fundamentally capable of providing optical transitions with the emission of photons in the IR range. At the same time, to create a material that provides the necessary optical characteristics in the IR range, it is necessary to implement a number of factors in the matrix, such as a wide transmission range in the infrared region, chemical and mechanical resistance.

In this work, optically transparent aluminum-magnesium spinel nanoceramics were chosen as a solid-state matrix for doping. $MgAl_2O_4$ is an optimal candidate due to the wide range of optical transmission ($\lambda \sim 0.16 – 6.6$ μm) and the presence of two types of cationic sublattices providing both divalent and trivalent cationic states. Iron ions were chosen to modify the optical properties in the IR range. It is known that divalent iron ions localized in close-packed oxygen structures of the tetrahedra type provide splitting of the ground 5D term into the $5T^2$ ground and 5E excited states, the transition energy between which lies in the IR range. The purpose of this work is to study the optical characteristics of transparent $MgAl_2O_4$ nanoceramics doped with iron ions.

Optical nanoceramics were synthesized by sintering a compact made from monodispersed spinel and Fe_2O_3 nanopowders. Optical reflection and absorption spectroscopy methods have been used to establish a set of excited states associated with both Fe^{2+} and Fe^{3+} impurity ions. A shift of the excited states of the Fe^{2+} ions to the region of high energies, due to their localization in defective positions, has been found. Strong absorption in the UV spectral region is associated with the presence of both impurity Fe^{3+} ions and intrinsic optically active centers of the F and F^+ - type. An analysis of the photoluminescent spectra indicates the presence of at least two types of impurity Fe^{3+} ions with different spectral and kinetic characteristics. New bands were also found in the PL spectra of spinel, associated with the localization of impurity Fe^{3+} ions in the tetrahedral sites of the crystal lattice. The photoluminescence intensity of Fe^{3+} ions undergoes strong concentration quenching as the impurity iron increases from 0.04 Fe% to 2 Fe%, while the sample itself becomes opaque in the visible spectral range.

Thus, it has been shown that as a result of the modification of the optical characteristics of the aluminum-magnesium spinel with iron ions, polyvalent optically active Fe centers are formed, localized both in normal and defect positions.

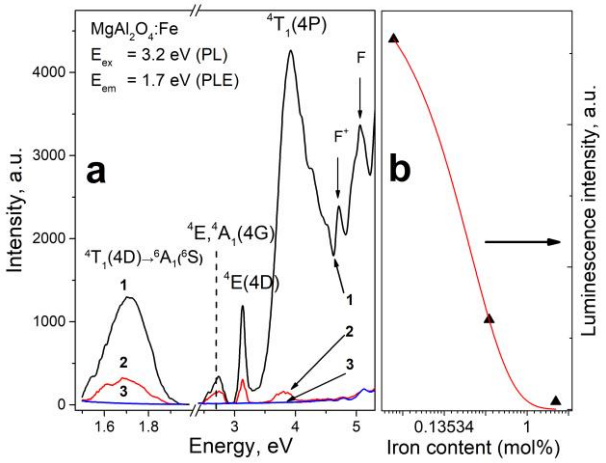

Fig.1. Spectra of Fe^{3+} ions PL and PLE - a. Iron content is 0.04, 0.4, 2 % for 1, 2 and 3 on picture. A concentration quenching is shown at - b.

* The work was supported by RFBR grants № 20-42-660012 and № 20-08-00054. A.F.Z. thanks Russian Scientific Foundation (Grant № 21-12-00392)

R1-O-022101

PHOTOLUMINESCENCE OF HIGH ENERGY ION IRRADIATED MAGNESIUM ALUMINATE SPINEL SINGLE CRYSTALS*

M.B. MAMATOVA[1,2,3], *V.A. SKURATOV*[1,4,5], *A. OLEJNICZAK*[1,6], *A.V. MAZANIK*[7], *N.M. KAZYUCHITS*[7], *N.S. KIRILKIN*[1], *A.K. DAULETBEKOVA*[2], *S.G. GINIYATOVA*[2], *A.T. AKYLBEKOV*[2]

[1]*Joint Institute for Nuclear Research, Dubna, Moscow Region, Russia*
[2]*L.N. Gumilyov Eurasian National University, Nur-Sultan, Kazakhstan*
[3]*The Institute of Nuclear Physics, Almaty, Kazakhstan*
[4]*National Research Nuclear University MEPhI, Moscow, Russia*
[5]*"Dubna" State University, Dubna, Moscow Region, Russia*
[6]*Nicolaus Copernicus University, Torun, Poland*
[7]*Belarusian State University, Minsk, Belarus*

Magnesium Aluminate spinel ($MgAl_2O_4$) is one of the most promising material for optical applications at nuclear-power facilities, laser technology and dosimetry, due to its high resistance to radiation damage, thermal stability and transparency in a wide spectral range. There are some experimental studies devoted to the structural disorders in $MgAl_2O_4$ irradiated with fast fission neutrons, high-energy electrons and protons [1-3]. However, information about radiation defects caused by swift heavy ions in this material has been lacking, particularly in the range of high ionization energy losses. In the present work, a swift heavy ion irradiation-induced defects in $MgAl_2O_4$ single crystals have been studied using photoluminescence spectroscopy technique.

Samples were irradiated with high energy Ar (46 MeV), Kr (107 MeV), Xe (150 MeV) and Bi (710 MeV) ions in the fluence range of 10^{10}-10^{13} cm^{-2} at IC-100 and U-400 cyclotrons in Flerov Laboratory of Nuclear Reactions JINR (Dubna, Russia). The PL measurements were performed in two experimental geometries: standard ($\lambda_{exc.}$ = 355 nm) using Shamrock SR303i spectrometer and confocal ($\lambda_{exc.}$ = 355 nm, 445 nm, 473 nm and 532 nm) using confocal microscope Ntegra Spectra NT-MDT at room temperature.

It was found that the PL spectra from intact $MgAl_2O_4$ contain emission bands of Cr^{3+} (1.8 eV) and Mn^{2+} (2.4 and 1.6 eV) impurities. Irradiation of $MgAl_2O_4$ crystals by high-energy heavy ions causes the appearance a broad luminescence band at 2.48–3.1 eV (standard geometry) with a three-peak structure, which is similar to MgO crystals [4], and an intense non-elementary bands around 1.55-3.1 eV (confocal system) under 355 nm, 445 nm, 473 nm and 532 nm excitation wavelengths. Intensities of these bands increase with the ion fluence up to 10^{12} cm^{-2}. The analysis of the PL spectra obtained in standard geometry allowed us to assume that the radiation-induced defects created in the track region are surrounded predominantly by Mg and O ions. In confocal geometry, upon different energy of excitation, the PL spectra of samples have been demonstrated the similar spectral shapes (emission bands), which have been tentatively ascribed to some of impurity centers in different charge states.

REFERENCES

[1] E. Feldbach, I. Kudryavtseva, K. Mizohata, G. Prieditis, J. Raisanen, E. Shablonin, A. Lushchik "Optical characteristics of virgin and proton-irradiated ceramics of magnesium aluminate spinel," Opt. Mater. (Amst). Elsevier, vol. 96 , no. P. 109308, pp. 1-7 , August 2019 .

[2] A. Lushchik, E. Feldbach, E.A. Kotomin, I. Kudryavtseva, V.N. Kuzovkov, A.I. Popov, V. Seeman, E. Shablonin, "Distinctive features of diffusion-controlled radiation defact recombination in stoichiometric magnesium aluminate spinel single crystals and transparent polycrystalline ceramics," Sci. Rep. Springer US, vol. 10, no. 1, pp. 1–9, 2020.

[3] V. Seeman, E. Feldbach, T. Karner, A. Maaroos, N. Mironova-Ulmane, A.I. Popov, E. Shablonin, E. Vasil'chenko, "Fast-neutron-induced and as-grown structural defects in magnesium aluminate spinel crystals with different stoichiometry," Opt. Mater. (Amst). Elsevier, vol. 91 , no. 0925-3467, pp. 42-49 , March 2019 .

[4] Y. Uenaka, T. Uchino, "Photoexcitation, trapping, and recombination processes of the F-type centers in lasing MgO microcrystals," Phys. Rev. B, vol. 83 , no. 195108, pp. 1-15 , May 2011 .

* The work was supported by Ministry of Education and Science of the Republic of Kazakhstan, grant No AP 09259669.

R1-O-028301

CHERENKOV LIGHT PRODUCED BY THE 5.7-MEV ELECTRON BEAM IN DIAMOND AND SAPPHIRE CRYSTALS *

A.P. POTYLITSYN[1], A.V. VUKOLOV[1], M.V. SHEVELEV[1], S.R. UGLOV[1], B.A. ALEKSEEV[1], A.G. BURACHENKO[2], Y.M. CHEREPENNIKOV[1], S.K PAVLOV[1]

[1]Tomsk Polytechnic University, Tomsk, Russia
[2]Institute of High Current Electronics SB RAS, Tomsk, Russia

Cherenkov effect is well-known phenomenon and finds a broad application in physics including beam diagnostics. The ability to separate Cherenkov and luminescence light in detector based on crystal is critical to develop the new generation of optical techniques in low energy beam diagnostics [1, 2]. In this report we demonstrate the first experimental results on detection of Cherenkov light from the 5.7 MeV electron beam passing through synthetic diamond and sapphire crystal. The measurements have been carried out at TPU microtron [2]. The oblique incidence allows extracting Cherenkov light at a right angle with respect to the electron beam [3]. Thus, we have measured the dependence of Cherenkov radiation intensity on the crystal rotation angle employing the silicon photomultiplier (MicroSC/FC model) for fixed observation angle. Measured amplitude-time characteristics of radiation indicate that Cherenkov and luminescent light possess different glow times for sapphire crystal, while for synthetic diamond these times are comparable. The special optical scheme consisting of filter and polarizer allows us to separate Cherenkov and luminescence light. The experimentally obtained dependences have good agreement with theoretical curves computed by the polarization currents approach [4]. The proposed scheme for detection of Cherenkov light will be used to develop a new method for measurement of the ion beam energy at NICA facility (JINR, Dubna, Russia) [5].

REFERENCES

[1] L. Jakuboski et al, "Measurement of high-energy electrons by means of a Cherenkov detector in ISTTOK tokamak", Radiat. Meas., vol.45, pp 1014-1019, 2010.

[2] A.V. Vukolov, A.I. Novokshonov, A.P. Potylitsyn and S.R. Uglov, "Diagnostics of electron beam beasd on Cherenkov radiation in a optical fiber", Russ. Phys. J., vol. 59, pp.1681-1685, 2016.

[3] Y. Takabayshi, E.I. Fiks, Y.L. Pivovarov, "First studies of 500-nm Cherenkov radiation from 255-MeV electrons in a diamond crystal", Phys. Lett. A., vol. 379, pp.1032-1035, 2015.

[4] A.P. Potylitsyn and S.Y. Gogolev, "Vavilov-Cherenkov radiation in an inclined dielectric plate and violation of azimuthal symmetry", Phys. Part. Nucl. Lett., vol. 16, pp.127, 2019.

[5] A. Baldin, "Applied research at the LHEP accelerator complex", JINST, vol. 15, Article Number C06051, 2020.

* The work was supported by the Russian Science Foundation under grant No. Приоритет-2030-НИП/ИЗ-005-0000-2030.

R1-O-032601

TSL OF ZIRCONIUM DIOXIDE CERAMICS IRRADIATED WITH FAST IONS *

A. DAULETBEKOVA[1], S. NIKIFOROV[2], S. ZVONAREV[2], D. ANANCHENKO[2], A. ZHUNUSBEKOV[1], Z. BAIMUKHANO1[3], A. AKILBEKOV[1], G. AKHMETOVA-ABDIK[1]

[1] L.N. Gumilyov Eurasian National University, Nur-Sultan, Kazakhstan
[2] Ural Federal University, Yekaterinburg, Russia

ZrO_2 (band gap 5.0-5.5 eV) is considered today one of the most important materials used in modern measuring technology, nanoelectronics and photonics. It has a significant luminescence yield, high reflectance, low phonon energy, and high thermal and chemical stability. Phosphors based on ZrO_2 are used for the manufacture of oxygen sensors, biological sensors, laser technology devices, optoelectronic devices, UV and ionizing radiation dosimeters, scintillators, high-energy radiation visualization devices, etc. For these applications, an important task is to ensure the stability of the luminescent properties of the material when exposed to various types of radiation. This problem is especially relevant when using ZrO_2-based devices in military and space technology, as well as in the nuclear industry.

In present work ZrO_2 compacts were studied. Compacts were formed by cold uniaxial pressing in the range of (900-1500) kgf/cm of nanostructured zirconium dioxide powder produced by the plasma chemical method (sample type 1 and 2), ultra-dispersed ZrO_2 powder (sample type 3). The samples were irradiated with 200 MeV Xe and 4.8 MeV N ions in fluence range (10^{10}- 10^{14}) cm^{-2} at cyclotron DC-60 (Nur-Sultan, Kazakhstan). Thermoluminescence (TL) properties of ZrO_2 compacts were investigated to determine the possibility of their use for dosimetry of pulsed electron beams (130 keV, 2 ns). The virgin and ion-beam-irradiated (Xe and N) compacts were irradiated with a test dose of 5 kGy pulsed electron beam. TL was measured in the linear heating mode at a rate of 2 K/s in the spectral range of 200-600 nm. TL curves of the virgin and irradiated compacts showed two TL peaks at 330-430 K and 430-550 K. The peak at 430-550 K is most intense in the nonirradiated sample. The greatest change in the TL intensity of this peak occurs in the sample irradiated with N ions: 2 to 3 times reduction. The kinetic parameters of the TL peak at 430-550 K (kinetic order b, activation energy E, and frequency factor S) were determined from the analysis of the TL curves.

The greatest changes in the kinetic parameters compared to the unirradiated compacts are observed in the samples irradiated with N ions. This samples are characterized by an order of kinetics close to 1 (b = 1.1), indicating that the probability of trap recapture of charge carriers is low.

* The work was supported by grant of the Ministry of Education and Science of the Republic of Kazakhstan AP09260057 «Люминесценция и радиационная стойкость синтезированных при различных условиях микро и наноструктурированных компактов и керамик на основе ZrO_2»

R1-O-036901

THERMALLY ACTIVATED LUMINESCENCE SPECTROSCOPY OF TRAPS IN DOSIMETRIC ULTRAFINE Al_2O_3-BeO CERAMICS

S.V. NIKIFOROV, M.F. GERASIMOV, T.V. STANG, D.V. ANANCHENKO

Ural Federal University, Yekaterinburg, Russia

At present, high-dose (more than 100 Gy) ionizing radiation is widely used in radiation technologies and scientific research. It is promising to use thermoluminescence (TL) dosimetry methods for registering high-dose radiation. One of the promising materials to detect high absorbed doses is ultrafine ceramics based on Al_2O_3-BeO [1]. This material was obtained by high-temperature vacuum annealing of nanostructured Al_2O_3 compacts in BeO crucibles in the presence of carbon [2]. We found that the TL of the dosimetric peak at 525 K of the studied Al_2O_3-BeO ceramics is not described by the simplest two-level model, but is due to the energy depth distribution of traps [1]. So far, evidence for the presence of the energy distribution of traps in the material under study has been obtained only under TL stimulation in the linear heating mode. Thereby it is of interest to study the TL kinetics with other methods of thermally activated spectroscopy (TAS); in particular, by using the analysis of isothermal decay curves [3] and fractional glow (FG) [4].

The aim of this work is to study TL of Al_2O_3-BeO ceramics by various TAS methods and to construct a kinetic model that takes into account the energy distribution of the traps and most fully describes the whole complex of TL properties of the material under study.

The samples used in this work were tablets 1 mm in thick and 5 mm in diameter. The technique of synthesizing ceramics had been described earlier [2]. To excite TL, the samples were irradiated at room temperature with a pulsed electron beam (60 A/cm^2, 2 ns) from the RADAN EXPERT accelerator with electron energy of 130 keV. The radiation dose was 15 kGy. TL was measured in three modes of TAS (linear heating at a rate of 2 K/s, isothermal heating and FG, the parameters of which were identical to those used in [4]).

An anomalous behavior of the TL isothermal decay curves of the dosimetric peak at 525 K in the temperature ranges of 423–463 K and 523–623 K was revealed, which consists in a decreasing decay rate with an increasing isothermal holding temperature. In the temperature range of 463–523 K, no anomalous behavior of the curves was observed. Analytical approximation of the TL decay curves, as well as the results of the Tm-Tstop and initial rise methods [5], make it possible to unambiguously reveal the presence of the energy distribution of traps responsible for the dosimetric peak. This conclusion is also confirmed by the presence of a temperature dependence of the trap activation energy in the indicated peak obtained by the FG method.

Based on the results of computer simulation of the charge transfer processes by solving systems of differential kinetic equations, it is shown that the observed features of the TL of the studied material, in particular, the anomalous behavior of the isothermal decay curves, are caused by the simultaneous emptying of several traps, whose distribution of activation energies has a form similar to the exponential one. The paper also discusses possible physical reasons for the appearance of the complex energy spectrum of the TL peak traps at 525 K.

REFERENCES

[1] S.V. Nikiforov, I.G. Avdyushin, D.V. Ananchenko, A.N. Kiryakov, A.F. Nikiforov, “Thermoluminescence of new Al_2O_3-BeO ceramics after exposure to high radiation doses,” Appl. Radiat. Isot., vol. 141, pp. 15-20, 2018.

[2] I.G. Avdyushin, S.V. Nikiforov, A.N. Kiryakov, A.F. Nikiforov, “Luminescence of new Al_2O_3-BeO ceramics: Influence of the preparation method,” AIP Conf. Proc. 2015, Article Number 020004, 2018.

[3] G. Kitis, G.S. Polymeris, I.K. Sfampa, M. Prokic, N. Meric, V. Pagonis, “Prompt isothermal decay of thermoluminescence in MgB4O7:Dy,Na and LiB4O7:Cu,In dosimeters,” Radiat. Meas., vol. 84, pp. 15-25, 2016.

[4] I.A. Tale, “Trap spectroscopy by the fractional glow technique,” Phys. Status Solidi (a), vol. 66, no. 1, pp. 65-75, 1981.

[5] R. Chen and V. Pagonis, Thermally and optically stimulated luminescence: A simulation approach. Chichester: Wiley, 2011.

R1-O-037401

PHOTOLUMINESCENCE OF OXYGEN CENTRES IN LITHIUM FLUORIDE CRYSTALS WITH METAL IMPURITIES

GUANGHUI GE, V.I. KOREPANOV

National Research Tomsk Polytechnic University, Tomsk, Russia

Multivalent metal impurities, in the form of oxides, are known to be injected into LiF crystals. Different forms of luminescent oxygen centers, including those with scintillation properties, can be created. The nature of the injected metal type's influence on centre structure, and also the regularity of LiF-Me scintillator emission characteristics fluctuation, are undetermined.

In the present study the results of luminescence properties of LiF-Fe_2O_3, LiF-TiO_2 and LiF-WO_3 crystals under selective photo-excitation in the range of 200 ... 350 nm (impurity absorption) at temperatures of 80 ... 300 K. A Cary Eclipse spectro-fluorimeter was used for the investigations.

It has been established that photo-excitation in the range of 4.0...6.0 eV causes the formation of two photo-luminescence bands (PLBs) with similar but distinct maximum and half-width values in all crystal types. Parameters of the bands in the studied crystals at 80 K are given in the table. The characteristics of LiF-Fe_2O_3 band 1 are identical to those of (O^{2-}-Va^{+})-center.

Crystal	Maximum band 1	Maximum band 2	Half-width band 1	Half-width band 2
LiF-Fe_2O_3	3.10 ±0,04 eV	2.60 ±0,04 eV	0.7 ±0,05 eV	0.68 ±0,05 eV
LiF-TiO_2	3.00 ±0,04 eV	2.60 ±0,04 eV	0.58 ±0,05 eV	0.58 ±0,05 eV
LiF-WO_3	2.93 ±0,04 eV	2.55 ±0,04 eV	0.54 ±0,05 eV	0.48 ±0,05 eV

Luminescence excitation bands (LE) were studied and determined. Their number depends on the type of metal: in LiF-Fe_2O_3 - 2; in LiF-TiO_2 - 3; in LiF-WO_3 - 4. The parameters of the bands in LiF-Fe_2O_3 are close to the parameters of the first (beginning with the high-energy) two bands in LiF-TiO_2, while the parameters of the bands in LiF-TiO_2 are close to the parameters of the first three bands in LiF-WO_3. The ratio of the PL band intensities depends on the excitation band and the temperature of the crystal. Examples of PL and LE spectra are shown in Figures 1 and 2.

The analysis of kinetic curves of PL attenuation under excitation in the range of 3.0....6.2 eV, and regularities of luminescence attenuation parameters in the temperature range 80...300 K, showed similar parameters and characteristics of PL and LE spectra for all crystals.

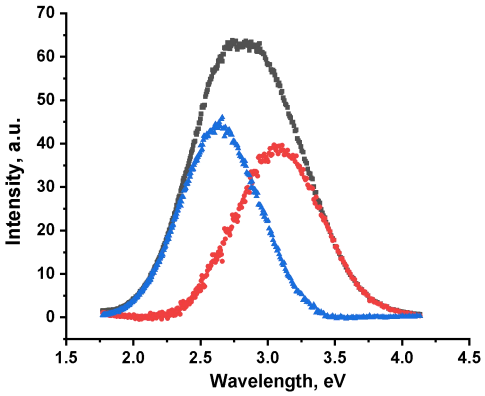

Fig.1. PL spectra of LiF-TiO_2 at 300K with excitation in the region of 230nm.

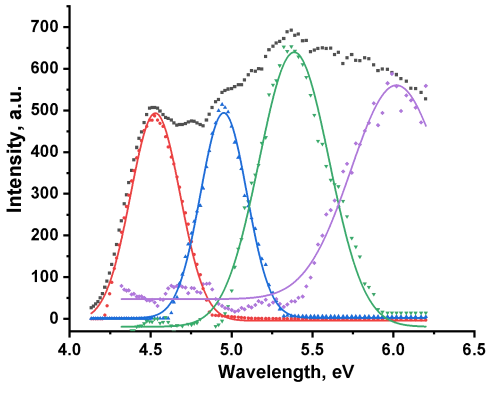

Fig. 2. LE spectra of LiF-WO_3 at 300K with luminescence monitoring in the 430nm region.

According to the research, all types of luminescence centres in all crystals contain a fragment of (O^{2-}-Va^{+})-center perturbed to different degrees by impurities, i.e. (O^{2-}-Va^{+}). The number of possible luminous center configurations is governed by the configuration of defects created to compensate for the excess charge of injected metal and is dependent on the type of injected metal. The metal's purpose is limited to facilitating the introduction of an oxygen center into the LiF crystal.

R1-O-044502

STRUCTURAL PROPERTIES SYNTHESIZED MAGNESIUM ALUMINATE SPINEL DOPED WITH CERIUM AND ERBIUM

E. F. POLISADOVA, N.D. TRAN

National Research Tomsk Polytechnic University, Tomsk, Russian Federation

In this study, we investigated the structural properties of magnesium aluminate spinel (MAS) doped with some rare earth elements such as cerium and erbium synthesized by radiation method [1]. The crystal structure, crystallinity, and phase of the obtained synthesized MAS were investigated by X-ray diffraction (XRD-7000S diffractometer, Shimadzu, Japan) equipped with CuKα (λ = 0,15406 nm) radiation. Result have shown that, the synthesized MAS have cubic structure and are in crystalline spinel $MgAl_2O_4$ and periclase MgO phase (fig. 1.). The clear diffraction peaks demonstrate the good crystallinity of the synthesized MAS. The weak peaks of phase MgO and no peaks related to aluminum oxides indicate the rather high purity of the obtained MAS.

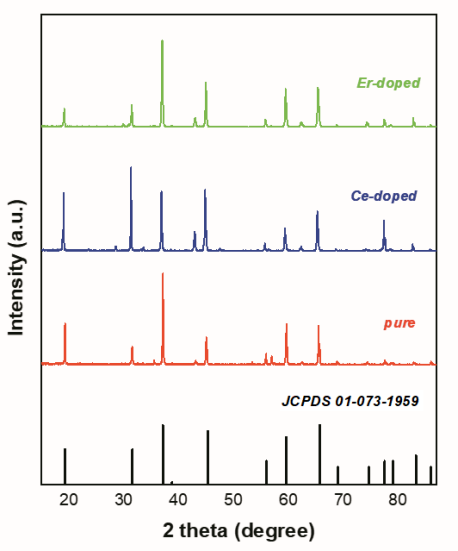

Fig.1. Experimental diffraction pattern (XRD) of obtained samples.

Calculation of parameters characterizing the crystal structure of the samples has been performed. The lattice constant of samples MAS pure, with Ce-doped and with Er-doped is 8.042 Å, 8.078 Å and 8.063 Å respectively. This result is also equivalent to standard card JCDPS 01-073-1959 (a = b = c = 8,05 Å). The change in crystal size in different samples is due to the substitution of ions Al^{3+} by ions Ce^{3+} and Er^{3+} at the octahedral position in the spinel. The larger the radius of ion, the larger the lattice constant. The radius of ion Ce^{3+} (1.14 Å) is larger than that of ion Er^{3+} (1.03 Å) and ion Al^{3+} (0.53 Å), so the lattice constant of the Ce-doped sample is the largest and the pure sample is the smallest. The average crystallites size of samples MAS pure, with Ce-doped and with Er-doped is 32.06, 32.89 and 34.78 respectively. The average crystal sizes of the spinel samples synthesized by radiation method are also similar to those synthesized by the published common methods. The replacement of ions Al^{3+} with rare earth ions not only changes the lattice constant, but also creates lattice defects, thereby reducing the crystallinity of the synthesized sample [2]. This explains the crystallinity calculation results of the synthesized MAS samples, the crystallinity of samples MAS pure, with Ce-doped and with Er-doped is 87.7%, 70.2% and 77.3%, respectively.

From the results of calculating the structural properties of synthesized MAS by X-ray diffraction method, it is shown that the synthesis of samples MAS pure as well as some doped rare earth elements such as Ce and Er by radiation method was performed successfully. This is the premise for the synthesis of samples MAS doped with transition metal elements and other rare earth elements by radiation method to create samples with suitable thermal and optical properties for different applications.

REFERENCES

[1] V M Lisitsyn, M G Golkovsky, D A Musakhanov, A T Tulegenova, Kh A Abdullin and M B Aitzhanov “YAG based phosphors, synthesized in a field of radiation”, IOP Conf. Series: Journal of Physics: Conf. Series, vol 1115, p. 052007, 2018.

[2] Li T, Wu J, Xiao X, Zhang B, Hu Z, Zhou J, Yang P, Chen X, Wang B, Huang L, “Band gap engineering of MnO_2 through in situ Al-doping for applicable pseudocapacitors”, RSC Adv., vol. 6, pp. 13914-13919, 2016.

R1-O-051801

OPTICAL SPECTROSCOPY OF NONLINEAR $YAl_3(BO_3)_4$: Mn CRYSTAL*

A.D. MOLCHANOVA[1], *K.N. BOLDYREV*[1], *L.N. BEZMATERNYKH*[2]

[1]*Institute of Spectroscopy, Russian Academy of Sciences, Moscow, Troitsk*
[2]*Kirensky Institute of Physics SB RAS*

Complex orthoborates of rare earth (RE) elements and trivalent cations are described by the general formula $RM_3(BO_3)_4$, where R = Y, La – Lu, M = Al, Ga, Cr, Mn, Fe, and crystallize into the structure of the huntite mineral $CaMg_3(CO_3)_4$. Crystals are of considerable interest as nonlinear optical, magnetoelectric, luminescent, and laser materials.

Among them, yttrium-aluminum borates $YAl_3(BO_3)_4$ are known phosphors in the case of partial replacement of Y^{3+} ions by rare earth ions. $YAl_3(BO_3)4:Eu^{3+}$ under UV excitation exhibits red luminescence, close in chromaticity coordinates to the parameters of the ideal commercial $Y_2O_3:Eu^{3+}$ phosphor. $YAl_3(BO_3)4:Eu^{3+}/Tb^{3+}$ is an environmentally friendly material for a white LED, which is advantageous in terms of its intensity, luminescence power, and cost [1]. Under UV excitation in $YAl_3(BO_3)_4:Sm^{3+}$ and $YAl_3(BO_3)_4:Tm^{3+}$, reddish-orange and blue radiation was obtained, respectively [2, 3].

In [4], the authors obtained the luminescence spectra of $YAl_3(BO_3)_4$ doped with manganese. The obtained spectra (in particular, three narrow lines in the region of 680 nm) are characteristic of Mn^{4+}, but further analysis is required to better understand the manganese valence in this compound and its optical spectra.

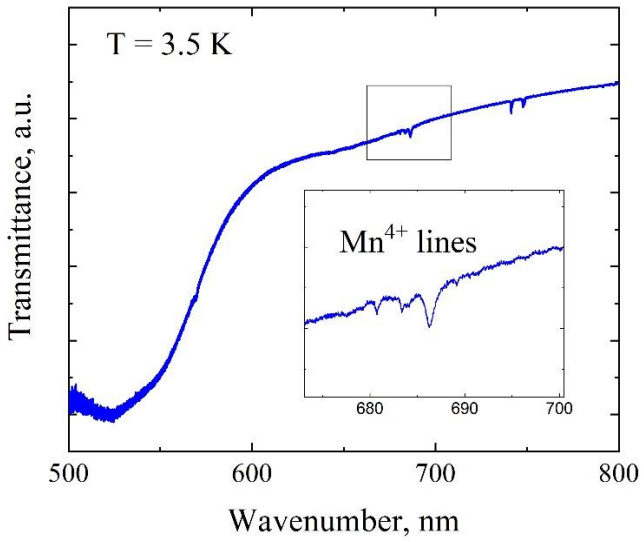

Fig.1. Transmission spectrum of $YAl_3(BO_3)_4$: Mn at T = 3.5 K.

In the present work, the luminescence spectra were recorded in a wide temperature range and at different pump wavelengths. Additionally, high-resolution low-temperature transmission spectra (up to 0.1 cm^{-1}) were measured in which three Mn^{4+} lines were also observed at frequencies around 680 nm (Fig. 1). An analysis of the obtained spectroscopic data made it possible to make an assumption about the energy structure of the electron shells of the Mn^{4+} and Mn^{2+} ions in $YAl_3(BO_3)_4$:Mn manganese.

REFERENCES

[1] Reddy, G.V.L., Moorthy L.R., Chengaiah T., Jamalaiah B.C., "Multi-color emission tunability and energy transfer studies of $YAl_3(BO_3)_4:Eu^{3+}/Tb^{3+}$ phosphors", Ceramics International vol. 40, no 2, pp. 3399-3410, 2014.

[2] Bajaj N.S., Koparkar K.A., Nagpure P.A., Omanwar S.K., "Red and blue emitting borate phosphor excited by near Ultraviolet Light", J. Opt-UK, vol. 46, pp. 91-94, 2017.

[3] Jamalaiah, B.C.; Jayasimhadri, M.; Reddy G.V.L., "Blue emitting $YAl_3(BO_3)_4:Tm^{3+}$ single-phase phosphors under UV excitation", Phys. Chem. Glasses,.vol. 57, pp. 68-70, April 2016.

[4] Aleksandrovsky, A.S.; Gudim, I.A.; Krylov, Temerov V.L., "Luminescence of yttrium aluminum borate single crystals doped with manganese", Physics of the Solid State, vol. 49, pp.1695-1699, September 2007.

* The work was supported by Russian Science Foundation, Grant № 21-72-00134

R1-P-013501

DISTRIBUTION IN THE MATERIAL OF THE ABSORBED ENERGY OF A SPACE-LIMITED BEAM FLOW OF HIGH-ENERGY ELECTRONS

D.A.MUSSAKHANOV[1], *V.M.LISITSYN*[2]

[1]*L.N.Gumilyov Eurasian National University, Nur-Sultan, Kazakhstan*
[2]*National Research Tomsk Polytechnic University, Tomsk, Russian Federation*

When passing through a substance, electrons with energies up to 5 MeV lose their energy mainly to ionization. The cross section for the interaction of electrons with atoms of a substance depends on their energy, and their trajectory of their movement changes during the interaction. Therefore, the distribution of absorbed energy in matter has a complex character. Even more difficult is the energy distribution under the action of a spatially limited electron beam. Part of the energy is transferred outside the beam, and the energy is also redistributed in the plane perpendicular to the beam axis.

The distribution of absorbed energy in the target determines the nature of the processes stimulated by radiation in matter. If these processes have a linear dependence on the flux power density, then with an increase in the absorbed dose, proportional changes in the structure and properties in the irradiated substance are observed. In the case when the processes stimulated by radiation are non-linear depending on the power density, one can expect the manifestation of unusual processes that determine the result of radiation treatment. Such effects have been found, for example, in the synthesis of refractory luminescent ceramics based on metal fluorides and oxides [1, 2]. Above certain thresholds, the effects associated with the ionization of matter and active processes between short-lived radiolysis products become dominant.

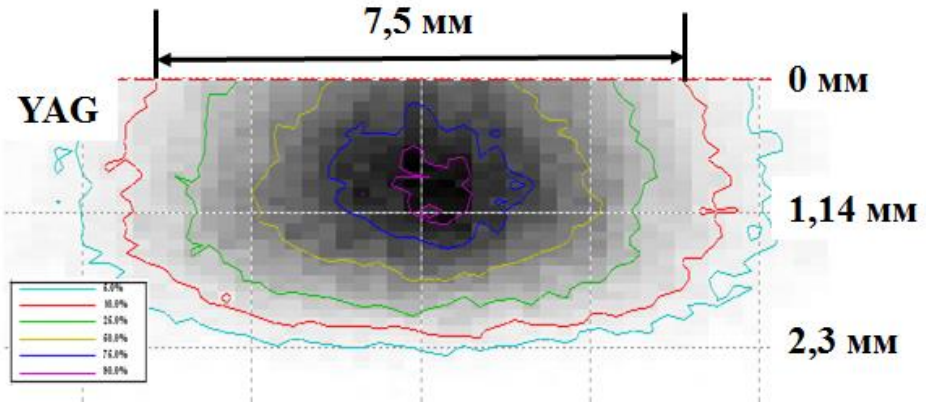

Fig.1. Energy Loss Distribution of an Electron Flow with E=2.0 MeV in YAG

We have calculated the energy losses of electrons with energies of 1.4 – 2.5 MeV in materials based on YAG, FSGM using Monte Carlo methods. Beams of streams of such electrons were used for the radiative synthesis of these materials. The beams had a Gaussian flux density distribution in cross section with a diameter near the surface of the irradiated charge of 7.5 mm. An example of the results of calculating energy losses is shown in the figure. The distribution of energy losses has the form of a curve with a maximum in sections parallel and perpendicular to the direction of the incident electron flow. The maximum energy of the electron beam with an energy of 1.4 MeV is absorbed in a region with a diameter of ≈4 mm in a cross section perpendicular to the direction of electron beam incidence and at a path depth of 1.5–2.0 mm. The highest energy loss density is inside the substance. Obviously, one should expect the manifestation of such a non-uniform distribution of the absorbed energy in matter in the processes of radiative synthesis.

With an increase in the electron energy, the region with the highest flux energy loss density increases in a disproportionate manner to the electron energy. The density of the generated electronic excitations in the irradiated region depends nonlinearly on the energy of the electrons. This effect must be taken into account when choosing the mode of radiation synthesis of dielectric materials.

REFERENCES

[1] V. M. Lisitsyn, L. A. Lisitsyna, M. G. Golkovskii, D. A. Musakhanov and A. V. Ermolaev. “Formation of luminescing high temperature ceramics upon exposure to powerful high energy electron flux” Russian Physics Journal, vol. 63, no. 9, pp. 1615-1621, January, 2021.
[2] V. M. Lisitsyn, L. A. Lisitsyna, A. V. Ermolaev, D. A. Musakhanov, M. G. Golkovskii. “Optical Ceramics Synthesis in the Field of a Powerful Radiation Flux” Russian Physics Journal, vol. 64, pp. 1067–1073, 2021.

R1-P-016601

LUMINESCENCE OF TUNGSTEN-ACTIVATED CERAMICS BASED ON MAGNESIUM AND BARIUM FLUORIDES

A.V. STRELKOVA[1], A.M. ZHUNUSBEKOV[2] , L.A. LISITSYNA[2]

[1] L.N.Gumilyov Eurasian National University, Nur-Sultan, Kazakhstan
[2] FGBOU VO "TGASU", NRU TPU, Tomsk, Russia

Polyvalent ions are effective activators in materials based on metal fluorides. However, the introduction of such ions into the lattice is a great difficulty. It is especially difficult to introduce multivalent ions, for example, W, U, which cannot be incorporated into the lattice without coactivators. During synthesis, such ions form volatile compounds, which are removed from the reactor. A promising method for obtaining activated materials based on metal fluorides is the radiation synthesis method, in which the formation of a lattice from mixtures occurs predominantly with the participation of highly excited radiolysis products.

We have completed a series of works on the synthesis and study of tungsten-activated materials based on alkaline earth metal fluorides with different lattice structures BaF_2, MgF_2, $BaMgF_4$. Synthesis was carried out by direct action of an electron beam with an energy of 1.4 MeV and a flux density of 18–23 kW/cm^2 on a charge of stoichiometric composition with 1 wt% WO_3. The resulting ceramic samples had a structure characteristic of that obtained by traditional methods. The entry of W was controlled by luminescent methods. The excitation and luminescence spectra of ceramic samples synthesized from mixtures were measured. The ceramic samples were crushed mechanically, and the excitation and luminescence spectra of the powders were measured using a CM2203 SOLAR spectrometer. Examples of the results of measurements of the PL of the samples are shown in the figure.

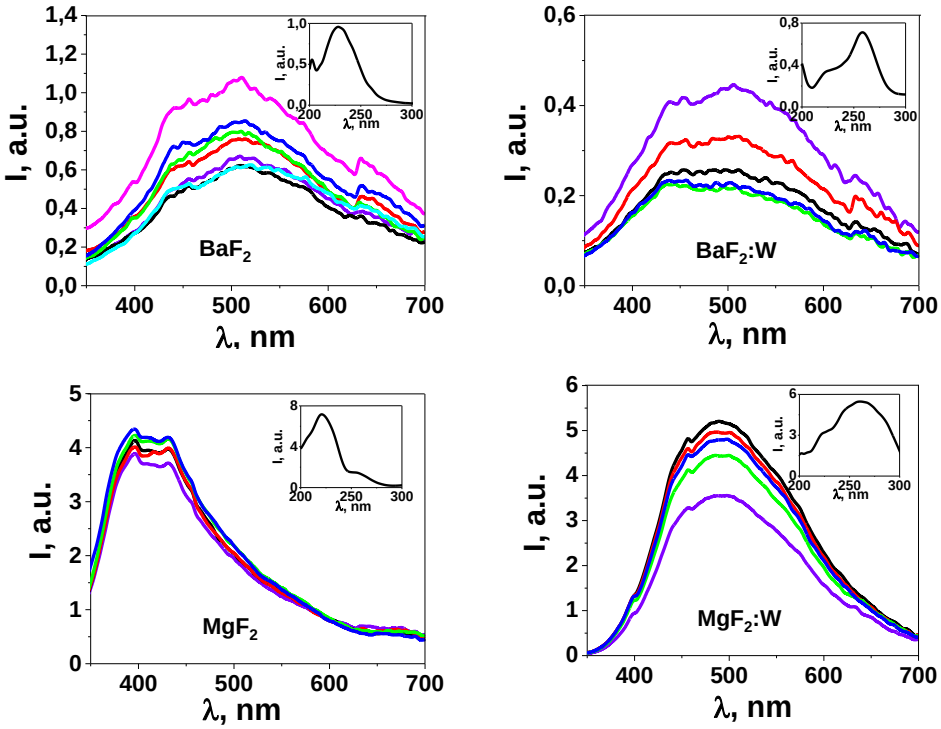

Fig.1. Spectra of luminescence and excitation of samples BaF_2, BaF_2+WO_3 , MgF_2, MgF_2+WO_3.

Similar results were also obtained for the $Ba_xMg_{2-x}F_4$ systems. It can be seen from the obtained results that the excitation spectra of the samples prepared from the mixture containing and not containing tungsten differ. The luminescence spectra also differ. Consequently, tungsten is introduced into the lattice during radiation synthesis in the absence of additional substances in the charge.

The reason for the possibility of introducing W into the lattice is a significantly different set of processes during radiative synthesis from those occurring during thermal synthesis.

REFERENCES

V.M. Lisitsyn, M.G. Golkovskii, L.A. Lisitsyna, A.K. Dauletbekova, D.A.Musakhanov, V.A. Vaganov, A.T. Tulegenova, Zh.T. Karipbayev, "MgF2–Based Luminescing Ceramics," Russian Physics Journal, V.61, Issue 10, P. 1908–1913, 2019

R1-P-016702

ELECTRON-HOLE TRAPPING CENTERS IN UV-IRRADIATED $Na_2SO_4 - Mn$ AND $K_2SO_4 - Mn$

T.N. NURAKHMETOV, A.M. ZHUNUSBEKOV, A.ZH. KAINARBAY, D.H. DAURENBEKOV, D.A.TOLEKOV, B.M. SADYKOVA, K. B. ZHANGYLYSSOV, T.T. ALIBAY, R.K.SHAMIEVA, A.E.AQZHALBEKOVA.

L.N.Gumilyov Eurasian National University, Nur-Sultan. Kazakhstan

Alkali metal sulfates activated by transition metals, which have an unfilled d-shell, are used in laser technology and as detectors for various radiations. In an irradiated $K_2SO_4 - Mn$ crystal at temperature of 80 K, a broad peak of thermally stimulated luminescence (TSL) at 120–190 K was found. The light sum under the low-temperature TSL peak at 120–190 K in irradiated $K_2SO_4 - Mn$ is several times greater than the light sum under the TSL peak at 190–200 K in pure K_2SO_4under the same conditions.

It is assumed that the increase in the light sum under the TSL peak of 120-190 K in $K_2SO_4 - Mn$ is associated with an increase in the concentration of self-trapped holes SO_4^-. Self-localized holes are formed in this crystal in addition to the electronic Mn^+– trapping centers.

Thus, in $Na_2SO_4 - Mn$ and $K_2SO_4 - Mn$ crystals, impurity electron-hole trapping centers are effectively created as a result of the localization of electrons with Mn^{2+}impurities.

We have investigated the nature of emission center and recombination emission at trapping centers in $K_2SO_4 - Mn^{2+}$and $Na_2SO_4 - Mn^{2+}$ crystals. When irradiated with ultraviolet photons with an energy of 5.9-6.2 eV, recombination emission was detected in these crystals at 1.82-1.84 eV for the $Na_2SO_4 - Mn$ crystal and 1.95-1.97 eV for the $K_2SO_4 - Mn$.

The detected emissions at 1.82-1.84 eV for the $Na_2SO_4 - Mn$ crystal are excited in the spectral range 3.34 eV and 3.56 eV, 3.08 eV and 2.79 eV and 2.41 eV at 80 K and 300 K. Similar emissions of 1.95-1.97 eV for the $K_2SO_4 - Mn$ crystal are excited in the spectral range 3.33 eV, 3.52 eV, 2.79 eV and 3.08 eV and 2.39 eV at 80 K and 300 K.

The emission of the Mn^{2+} ion in the Na_2SO_4 and K_2SO_4 matrices is assumed to be excited in three spectral groups slightly different for the two crystals. Similar results were obtained by the authors of [1] for a $ZnS - Mn$ piezoelectric crystal. According to the authors' [1] assumption, the first high-energy excitation band is associated with emission center transitions in the Mn^{2+}ion located in the main interstitial positions. The remaining two groups of excitation bands are connected by the formation of electron-hole trapping centers near the vacancy of the Zn ion or its location in the interstitial.

Our experimental results are interpreted as follows: During irradiation with UV photons, electron-hole pairs are created. The electron-hole pair transfers energy to impurities, and excitations of Mn^{2+}impurities are observed at 3.34 eV and 3.56 eV, followed by Mn^{2+}emissions in both crystals.

It is well known that electrons are well trapped by Mn^{2+}impurities according to the reaction $Mn^{2+} + e^- \rightarrow Mn^+$ and impurity electron-hole trapping centers of two types $Mn^+ - SO_4^-$depending on the positions of the impurity in the lattice Na_2SO_4 and K_2SO_4. The observed phosphorescence for two crystals at 2.79 eV and 2.39-2.41 eV confirms our assumptions about the formation of impurity trapping centers. The correlation between impurity trapping centers and intrinsic $SO_4^{3-} - SO_4^-$- trapping centers for pure K_2SO_4 and Na_2SO_4 crystals is discussed.

REFERENCES

[1] Yu. Yu. Bacherikov[1], A. G. Zhuk[1], S.V. Optasyuk[1], O. B. Okhrimenko[1], K. D. Kardashov[2], S. V. Kozitskiy[3], "The factors influencing luminescent properties of ZnS:Mn obtained by the method of one-stage synthesis," Semiconductor Physics. Quantum Electronics & Optoelectronics, 2012. V. 15, N 3, P. 239-246.

* The work was supported by the Science Committee of Ministry of Education and Science Republic of Kazakhstan grants IRN AP09259303

R1-P-028701

LUMINESCENT AROMATIC HYDROCARBONS OF ZAGLY PETROLEUM OF THE APSHERON PENINSULA OF AZERBAIJAN

U.J.Yolchuyeva[1], R.A.Japharova[1], A.F.Alieva[1], F.N.Alimardanova[2]

[1]Institute of Petrochemical Processes, Azerbaijan National Academy of Sciences, 30, Khojaly Ave., AZ1025, Baku, Azerbaijan
[2]Xazar University, School of Science and Engineering department, Mahsati Str.41, AZ1096, Baku, Azerbaijan

E-mail. u.jeyhunzade@gmail.com

Oil and petroleum products are a rich source of hydrocarbons, the study of the hydrocarbon composition of new deposits allows the discovery of new hydrocarbons, which can provide a number of industries (petrochemical and oil refining, pharmaceuticals, etc.) with corresponding cheap hydrocarbons. For example, the production of quality oil products by the oil industry is highly dependent on the quality of the raw materials supplied to the oil refining industry; aromatic-based heavy oil fractions are used to produce petroleum phosphors, etc. In this regard, at the Institute of Petrochemical Processes of the National Academy of Sciences of Azerbaijan, the composition of natural oil is currently being comprehensively studied using modern highly sensitive instruments (UV, IR, NMR, chromato-mass spectroscopy, luminescence, etc.) hydrocarbon compounds are determined, their physico-chemical and spectral-luminescent properties are studied and proposed for application in the corresponding industries.

In this work, the physicochemical and spectral-luminescent properties of Zagly natural oil are studied. Oil consists of paraffin-naphtha, aromatic hydrocarbons, and also contains resins and asphaltenes. Physical and chemical indicators are given in the table:

Substance name	Reflection coefficient, n_d^{20}	Density ρ_4^{20}, кг/м^3	Yield of components relative to oil, %
Paraffin-naphtha	1,4685	859,7	40,5
1st group aromatics	1,5074	892,1	15,3
1st group aromatics	1,5480	932,1	4,5
1st group aromatics	1,5790	972,2	7,8
1st group aromatics	1,6011	1043,6	18,7
Resin	-	1065,2	11,6
Asphalten	-	-	1,6

Since the petroleum substance is a dispersed system of complex composition, in order to improve the accuracy of spectral studies, Zagli's well oil was separated by liquid adsorption chromatography (GOST 11244-76) method into separate components and the structural-group composition of aromatic hydrocarbons was studied: mono (benzene-11.7; 23.1; 24.3; 7.1%), bi- (naphthalene-12.8; 17.1; 18.3; 30.1%) and tricyclic (anthracene-1.1; 1.1; 1.3; 2.7% and phenanthrene-10.9; 14.1; 15.4; 24.6%) hydrocarbons. It has been established that as the concentration of solutions increases, the UV spectra shift to the long-wavelength region of the spectrum, and even in group IV, the "red" edge of the spectrum reaches > 500 nm.

Using the methods of luminescent excitation and luminescence, it was found that, despite the presence of mono-, bi- and tricyclic aromatic hydrocarbons in components I-IV gr. AH of this oil, them the ratio varies by components and if in I-III gr. AH the main luminescent glow in the components is provided by tricyclic aromatic hydrocarbons (TAH) and their substituted compounds, then in component IV gr. AH, photoluminescence is provided by both polycyclic bicyclic aromatic hydrocarbons (BAH) and TAH. Based on the results obtained, it can be concluded that, despite the absorption of light quanta in oil components by individual hydrocarbons (benzene, naphthalene, phenanthrene, anthracene and their substituted ones), there is energy transfer between hydrocarbons and it occurs from a low molecular weight to a higher molecular weight hydrocarbon ($h\nu_{benzene} \rightarrow h\nu_{naphtha} \rightarrow h\nu_{phenanthrene} \rightarrow h\nu_{anthracene}$) and finally, an intense luminescent glow is observed, corresponding to a higher molecular weight hydrocarbon: TAH (I - III group AH), BAH and TAH (I-IV group AH).

Component IV gr. AH oil Zagly can be offered in the production of phosphors for the detection of microdefects in the field of fluorescent color flaw detection [1, 2].

REFERENCES

[1] Yolchuyeva U, Jafarova R, Khamiyev M, Vakhshouri AR, Khamiyeva G, "Investigation of photochemical conversion processes in aromatic hydrocarbons of Balakhani oil", J. Pet. Sci. Eng. vol. 196, 2021 doi.org/10.1016/j.petrol.2020.108089

[2] Yolchuyeva U, Japharova R, Vakhshouri AR, Khamiyev M, Salmanova Ch, Khamiyeva G,"Photochemical investigation of aromatic hydrocarbons of Balakhani crude oil as petroleum luminophores", Appl Petrochem Res10, 2020, p.139–148 doi.org/10.1007/s13203-020-00253-9

R1-P-035802

LUMINESCENCE CONTROL OF LED HETEROSTRUCTURES GROWN BY METHOD METALORGANIC VAPOR PHASE EPITAXY ON SAPPHIRE

ZIXUAN LI, VLADIMIR I. OLESHKO, LYUDMILA V. VOROBJEVA

The National Research Tomsk Polytechnic University，Tomsk，Russia

Recently, GaN-based semiconductor heterostructures are one of the most promising optoelectronic materials [1, 2]. However, obtaining high-quality structures is accompanied by a series of difficulties. Uncontrollable impurities, intrinsic defects and dislocations formed in the crystal lattice during the growth process have a significant impact on the properties of layers and heterostructures. Therefore, the successful development of modern optoelectronics is realized by creating technologies, which can cultivate highly advanced semiconductor heterostructures. As we all know, luminescence diagnosis can control the degree of stoichiometry, the existence of impurities and defects, and determine whether the structure is suitable for manufacturing light sources [3 - 8].

Objective to study the luminescence characteristics of GaN / InGaN epitaxial layer grown by metalorganic vapor phase epitaxy on sapphire. These structures were formed in different laboratories. The excitation of luminescence inspection is realized by two methods: high current electron beam (HCEB) and nitrogen laser (λ = 337.1 nm, τ = 10 ns). The effective energy of electrons in HCEB ~ 250 keV spectrum, and the pulse duration is 15 ns. The energy density of the electron beam ranges from 0.002 J / cm^2 to 0.2 J / cm^2. The pulsed cathodoluminescence (PCL) and pulsed photoluminescence (PPL) spectra of the samples were measured at 300 K. The time resolution (~ 15 ns) spectra were recorded by the measurement system based on diffraction monochromator (MDR) - 23, photoelectric electronic multiplier PMT-84 and computer related oscilloscope Tektronix DPO 3034. The integral (pulse time) spectra of PCL and PPL stimulated spontaneously were measured by optical fiber spectrometer AvaSpec-ULS2048CL-EVO-RS.

The spectral dynamics of spontaneous PCL and PPL GaN / InGaN quantum wells are explained in the donor receptor recombination model.

It was found that the stimulus PCL spectra measured in the same sample but in different local areas were different. The change of the maximum position of the forced radiation band of GaN / InGaN quantum wells is observed in the range of 2.81 – 2.83 eV, which may be due to the change of the composition of quantum pits in different heterostructure regions.

REFERENCES

[1] Туркин.А, “Обзор развития технологии полупроводниковых гетероструктур на основе нитрида галлия (GaN),” Полупроводниковая светотехника, № 6, С.6-9, 2011.

[2] В.В.Лундин, А.Е. Николаев, А.В. Сахаров, Е.Е. Заварин,С.О. Усов, В.С. Сизов, А.Л. З акгейм, А.Е. Черняков, А.Ф. Цацульников, “Высокоэффективные InGaN/GaN/AlGaN светодиоды с короткопериодной InGaN/GaN сверхрешеткой для диапазона 530−560 nm,” Письма в ЖТФ, Т. 36, № 22, С, 89–95, 2010.

[3] С.Г.Горина, Ли Цзысюань, А.В.Сычева, “Время-разрешенная люминесцентная спектроскопия эпитаксиальных слоев GaN, выращенных на подложках Al_2O_3,” Современные техника и технологии : сборник докладов XX Международной научно-практической конференции студентов, аспирантов и молодых ученых, Томск, Россия, С.103-104, 2014.

[4] Andrianov, V.Yu. Nekrasov, N.M. Shmidt, E.E. Zavarin, A.S. Usikov, N.N. Zinov’ev, M.N. Tkachuk, “Low-temperature time-resolved photoluminescence in InGaN/GaN quantum wells,” Физика и техника полупроводников, Т, 36, № 22, С,679-684, 2002.

[5] Домрачева, Я. В. и др, “Исследование многослойных светодиодных гетероструктур на основе InGaN/GaN методами рентгеноспектрального микроанализа и катодолюминесценции,” Поверхность. Рентгеновские, синхротронные и нейтронные исследования. № 8. С. 10-15, 2009.

[6] V. I. Oleshko, S. G. Gorina, S. V. Lazarev, V. V. Lopatin, “Effect of dislocation density on exciton luminescence intensity of GaN epitaxial layers,” Изв. вузов. Физика, Т. 57, № 12/3, С. 62-65, 2014.

[7] В. И. Олешко, С. Г. Горина, В. И. Корепанов, В. М. Лисицын, И. А. Прудаев, О. П. Толбанов, “Люминесценция тонкопленочных светодиодных структур при возбуждении сильноточным электронным пучком,” Изв. вузов. Физика. Т. 56, № 1, С. 55-58, 2013.

[8] В. И. Олешко, С. Г. Горина, В. И. Корепанов, В. М. Лисицын, И. А. Прудаев, О. П. Толбанов, “Суперлюминесценция светодиодных гетероструктур при возбуждении сильноточным электронным пучком,” Изв. вузов. Физика. Т. 56, № ½, С. 175-177,2013.

R1-P-037701

LUMINESCENCE OF COMPACTS FROM MIXTURES OF NANO AND MICRO CALCIUM FLUORIDE POWDERS

V.G. ILVES[1], *S.YU. SOKOVNIN*[1,2], *S.V. ZAYATS*[1], *M.G. ZUEV*[3]

[1]*Institute of Electrophysics, Ural Branch, Russian Academy of Sciences, Yekaterinburg, Russia*
[2]*Ural Federal University Named after the first President of Russia B.N. Yeltsin, Yekaterinburg, Russia*
[3]*Institute of Solid State Chemistry, Ural Branch, Russian Academy of Sciences, Yekaterinburg, Russia*

There were carried out the studies of pulsed cathodoluminescent (PCL) and photoluminescent (PL) properties of compacts made by static (SP) and magnetic-pulse (MPP) pressing from mechanical mixtures of micro and nano calcium fluoride powders. The mixtures contained commercial powder (TU 6-09-2412-84) and nanopowder (NP) CaF_2 (NP produced by pulsed electronic evaporation at the installation NANOBEAM-2 in vacuum [1]) at powder weight ratios: 10: 0.125 -10: 1. Was shown the effect of the concentration of the CaF_2 nanoadditive, the pressing temperature and the preliminary annealing of the nanoadditive on the density of compacts. Presence of nanoparticles of Ca at NP, strong defective structure and high porosity of NP had strong impact on luminescent characteristics of the compacts made both of clean NP CaF_2 and from their mixes. Annealing of the initial NP at a temperature of 400 °C made it possible to achieve the same density of compacts of pure micropowders and nanopowders (89% of the theoretical density) using the MPP method with heating. The maximum density of compacts from mixtures of powders of different dispersity did not exceed 78% of the theoretical density. The main factor that influenced the morphology of PCL spectra of all compacts, without exception, was the compaction temperature (425 °C) in the MPP method. The blue peak (434 nm) is associated with an impurity oxygen vacuum in the nanocrystalline CaF_2 lattice and was found in the photoluminescence spectra of compacts from NP annealed at 400 ° C. The morphology of the PL spectra is more sensitive to the influence of various factors (concentration of the nanoadditive, pressing method, pressing pressure, etc.) in comparison with the morphology of the PCL spectra. Is given the study of the density and transparency of ceramics from the above compacts after annealing the compacts in vacuum at a temperature of 1000 °C.

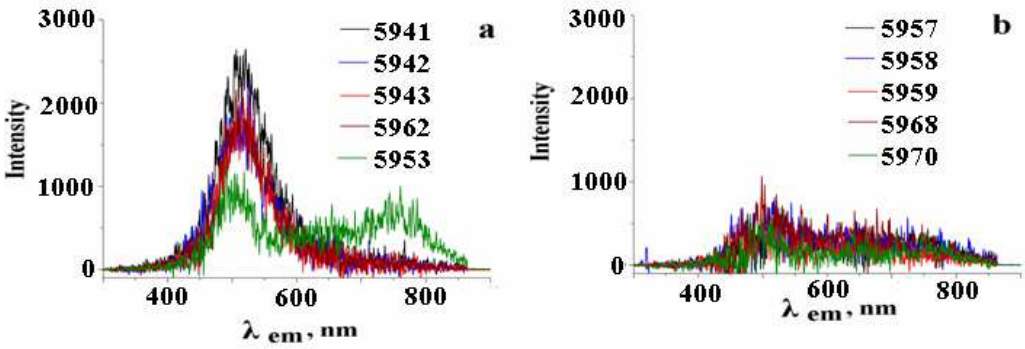

Fig.1. PCL spectra of the compacts from commercial micron powder (a) and nanopowder (b) CaF_2 . 5941-5943 и 5957-5959- static pressing, 5962, 5953 and 5968 and 5970- magnetic-pulse pressing.

REFERENCES

[1] V. G. Ilves, S. Yu. Sokovnin, M. A. Zuev, M. A. Uimin, M. Rähn, J. Kozlova, V. Sammelselg, “Effect of Annealing on Structural, Textural, Thermal, Magnetic and Luminescence Properties of Calcium Fluoride Nanoparticles,” Phys. Sol. State, vol.61 , no. 11, pp.2000-2217 , November 2019.

R1-P-043001

RADIATION SYNTHESIS OF CERAMICS BASED ON $ZnWO_4$, $MgWO_4$

L.A. LISITSYNA[1], Z.T. KARIPBAYEV[2], V. M. LISITSYN[3]

[1]Tomsk State University of Architecture and Building, Tomsk, Russia
[2] L. N. Gumilyov Eurasian National University, Nur-Sultan, the Republic of Kazakhstan
[3] National Research Tomsk Polytechnic University, Tomsk, Russia

The multicomponent materials based on metal oxides are among the most future advanced scintillators [1, 2]. The synthesis of dopant-free self-activating materials is complicated, difficult to monitor and requires high temperatures and pressure. In [3, 4], for the first time, synthesis of YAG based phosphors and doped ceramics, based on alkaline earth metal fluorides, was realized under the action of a high-energy electron flow in air at 300 K.

This presentation reports on the synthesis of $ZnWO_4$ and $MgWO_4$ ceramics on air at 300 K under irradiation with 1.4 MeV electrons which the power density flux varied in the range of 18–23 kW/cm^2. We used an ELV-6 electron accelerator created at the G. I. Budker Institute of Nuclear Physics of the SB RAS.

It should be noted that the difference in the melting temperatures of the charge components: 1975 (ZnO), 1473 (WO_3) and 2825 °K (MgO), was not an obstacle to the realization of the synthesis process.

High density of an ionization initiates the processes far from equilibrium unattainable with traditional synthesis methods: modification of an interionic interaction, destruction of the short-range order, creation of multiple types of the disordering, including complexes of intrinsic defects of various sizes, types, charges, creation conditions for evaporation and coagulation of atoms, defects, for the forming of new chemical compounds. The formation from such radiation chaos of a new crystalline phase of $ZnWO_4$ or $MgWO_4$ for a time not exceeding 1 s indicates at the extraordinary efficiency of the radiation-initiated processes of structure ordering as well.

Density of as-prepared charge was about of 1.8–1.6 g/cm^3. The synthesized ceramic samples were plates about 4 mm thick with a vitreous surface limited crucible dimension (Fig.1(on the left)).

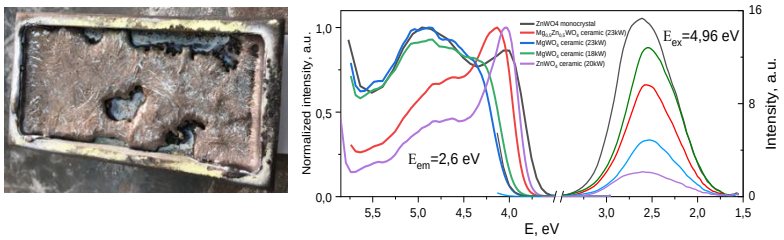

Fig.1. (Left) Photographs of the $ZnWO_4$ ceramic sample after synthesis in a massive copper crucible. (Right) Spectra of an excitation and photoluminescence at 300 K of the $ZnWO_4$ monocrystal and the samples of the different synthesized ceramics subjected to mechanical crushing.

The first studies of synthesized ceramics have been carried out. Figure 1 (on the right) shows the excitation and luminescence spectra of a single crystal of ZnWO4 and different types of synthesized ceramics. The similarity of the emission spectra in crystal and ceramic samples is obvious: peak positions of emission bands and the values of the FWHM are in restricted ranges of 2.6 –2.5 eV and 0.7– 0.6 eV, respectively. Similarity of excitation spectra also occurs.

In the paper will be also presented the radioluminescence and XRD patterns of the synthesized ceramics samples.

REFERENCES

[1] H. Kraus, V.B. Mikhilik, Y. Ramachers, D. Day, K.B. Hutton, J.Telfer. “Feasibility study of a ZnWO4 scintillators for exploiting materials signature in cryogenic WIMP dark matter searches”. Phys. Lett. B V. 610, P. 37-44, 2005

[2] M. Nikl, V.V. Laguta, A. Vedda. “Complex oxide scintillators: Material defects and scintillation performance”. Phys. Stat. Sol. (b) V. 245, P. 1701-1722, 2008

[3] V M Lisitsyn, M G Golkovsky, D A Musakhanov, A T Tulegenova, Kh A Abdullin and M B Aitzhanov “YAG based phosphors, synthesized in a field of radiation”, IOP Conf. Series: Journal of Physics: Conf. Series,V. 1115, P. 052007, 2018.

[4] V.M. Lisitsyn, M.G. Golkovskii, L.A. Lisitsyna, A.K. Dauletbekova, D.A.Musakhanov, V.A. Vaganov, A.T. Tulegenova, Zh.T. Karipbayev, “MgF2–Based Luminescing Ceramics,” Russian Physics Journal, V.61, Issue 10, P. 1908–1913, 2019

R1-P-044401

Tb^{3+} AND Eu^{3+}-DOPED QUATERNARY GARNETS AS PHOSPHORS FOR HIGH-BRIGHT CATHODOLUMINESCENCE-BASED LIGHT SOURCES*

D. TAVRUNOV[1], *G. DOSOVITSKIY*[3,4], *M. KORZHIK*[2,3], *V. DUBOV*[3,4], *V. SMYSLOVA*[3,4], *P. KARPUK*[3,4], *E. GORDIENKO*[3,4], *D. KUZNETSOVA*[3,4], *V. RETIVOV*[3,4], *V. PUSTOVAROV*[1]

[1]*Ural Federal University, Yekaterinburg, Russia*
[2]*Institute for Nuclear Problems, Belarus State University, Minsk, Belarus*
[3]*National Research Center "Kurchatov Institute", Moscow, Russia*
[4]*NRC "Kurchatov Institute" – IREA, Moscow, Russia*

Scintillators might be the pool of materials for choosing prospective phosphors with high radiation tolerance for application in cathodoluminescence (CL) light sources. In particular, radiation hard cerium-doped garnet-type single crystals are currently being successfully developed as scintillators for high-energy physics applications [1-3]. Quaternary garnets $(Gd,Y)_3Ga_3Al_2O_{12}$ (GYAGG) doped and codoped with Eu^{3+}, Tb^{3+} were fabricated as transparent and translucent ceramics by hot pressing to develop long-wavelength phosphors for high-brightness CL sources. The technique for obtaining ceramics is described in Ref. [1, 2]. The CL light yield of Tb-doped GYAGG ceramics at high-intensity electron beam excitation is shown to be more than twice as high as that of the conventional phosphor YAG:Ce, whereas codoping with Eu^{3+} allows to redshift the chromaticity.

In the present work, luminescence spectroscopic properties of GYAGG ceramics doped with Tb^{3+} and Eu^{3+} ions upon UV-, X-ray and cathode-ray excitation have been studied. In addition to observe behavior of defect-related luminescence, ceramics were irradiated with fast electrons (E = 10 MeV) from linear electron accelerator in UrFU, Yekaterinburg. A studies of the pulse CL decay kinetics show efficient non-radiative energy transfer between rare-earth ions $Tb^{3+} \rightarrow Eu^{3+}$ or $Tb^{3+} \rightarrow$ defects. Energy transfer is observed both from the $^5D_3$ level and from the $^5D_4$ level of the Tb^{3+} ion, and the energy transfer rate depends on the Eu^{3+} acceptor concentration. Forming point defects are produced by impact mechanism – elastic collisions. The luminescence spectra and decay kinetics of pulsed CL for some studied ceramics are shown in Fig. 1. The characteristic decay time and the type of electronic transitions are indicated.

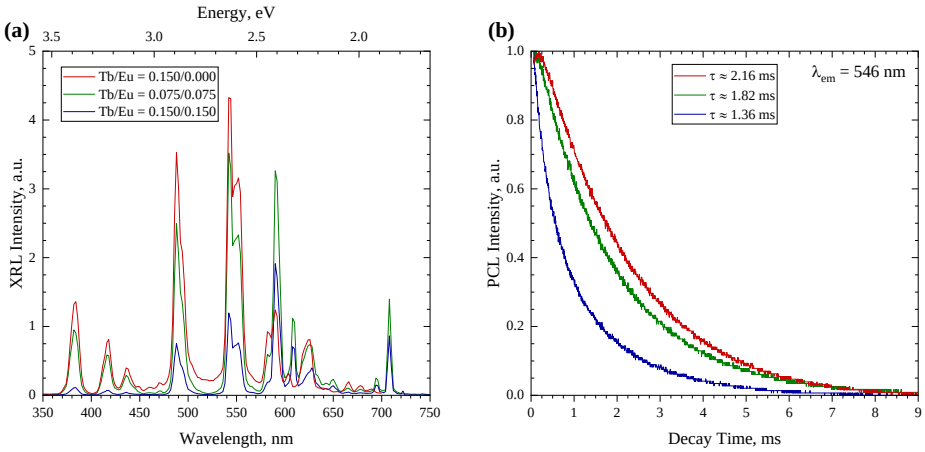

Fig. 1. X-ray excited luminescence spectra (a) and PCL decay kinetics (b) of GYAGG ceramics doped with Tb^{3+} and Eu^{3+} ions

REFERENCES

[1] M. Korzhik, A. Borisevich, A. Fedorov, E. Gordienko, P. Karpyuk, V. Dubov, P. Sokolov, A. Mikhlin, G. Dosovitskiy, V. Mechninsky, D. Kozlov, V. Uglov, "The scintillation mechanisms in Ce and Tb doped $(Gd_xY_{1-x})Al_2Ga_3O_{12}$ quaternary garnet structure crystalline ceramics", J. of Luminescence, vol. 234, p. 117933, January 2021.

[2] M. Korzhik, V. Alenkov, O. Buzanov, G. Dosovitsky, A. Fedorov, D. Kozlov, V. Mechinsky, S. Nargelas, G. Tamulaitis, A. Vaitkevicius, "Engineering of a new single-crystal multi-ionic fast and high-light-yield scintillation material $(Gd_{0.5}–Y_{0.5})_3Al_2Ga_3O_{12}$:Ce,Mg", CrystEngComm, vol. 22, no. 14, pp. 2502-2506, March 2020.

[3] M. Korzhik, A.Bondarau, G. Dosovitskiy, V. Dubov, E. Gordienko, I.Kamenskikh, P. Karpuk, D. Kazlou, D. Kuznetsova, V. Smyslova, V. Mechinsky, V.Retivov, V. Pustovarov, E. Talochka, D. Tavrunov, E.Tishchenko, A.Vasil'ev, "Scintillation mechanism in compositionally disordered $(Gd,Lu)_3Al_2Ga_3O_{12}$ crystalline scintillation material doped with Ce", J. of Luminescence, 2022. (In press).

* The work was partially supported by the Ministry of Science and Higher Education of the Russian Federation through the basic part of the government mandate, project No. FEUZ-2020-0060.

R1-P-047101

LUMINESCENCE OF MALTODEXTRIN-COATED CERIUM OXIDE NANOPARTICLES DOPED WITH RARE EARTH ELEMENTS

N.Y. OFITSEROVA, A.V..MYSHKINA, V.A.PUSTOVAROV, I.N.BAZHUKOVA

Ural Federal University, Yekaterinburg, Russia

Nanocrystalline cerium oxide CeO_2 is a promising object for various applications, including biomedical issues [1-3]. Physicochemical properties of cerium oxide change during the transition to the nanoscale state. This is assumed to be related to changes in material electronic structure, oxygen vacancies formation due to increasing the proportion of atoms located on the particle surface and, consequently, change in the oxygen nonstoichiometry. The appearance of oxygen vacancies leads to the reduction of Ce^{4+} ions on the nanoparticle surface to the Ce^{3+} state. Such oxygen nonstoichiometry correlates with the catalytic activity of cerium oxide nanoparticles and is responsible for their unique biological activity [2]. Modifying the degree of CeO2 surface oxidation and increasing the number of oxygen vacancies can be carried out by doping with trivalent rare earth (RE) metals [3]. We assume that this modification will lead to a change in the optical properties of the material. The purpose of this work is to study the luminescent properties of RE-doped cerium oxide nanocrystals.

CeO_2 nanoparticles with maltodextrin coating and doped with Er^{3+} and Sm3+ ions were produced by the deposition method according to the procedure presented in [4]. The photoluminescence (PL) emission and PL excitation spectra were recorded with a 400 W deuterium discharge lamp (DDS-400), two the double-prism DMR-4 type monochromators and a R6358-10 (Hamamatsu) type photomultiplier tube (PMT). The optical absorption spectra were recorded with a Helios Alpha spectrophotometer (λ = 190–1000 nm) equipped with the Vision 32 software.

Figure 1 shows the PL emission and PL excitation spectra of undoped maltodextrin-coated CeO_2 nanoparticles. The PL spectrum is presented by a wide intensive band with a maximum of 3.1 eV and a weak band at 2.5 eV. The band at 3.1 eV is probably due to radiative transitions in the Ce^{3+} ion from the relaxed lower 5d-excited state to the ground 4f state. The weak band at 2.5 eV nm could be associated with the emission of defects related to the oxygen vacancies [3]. The PL spectra of RE-doped CeO2 nanoparticles consist of characteristic emission bands related to radiative transitions in Er^{3+} и Sm^{3+} ions

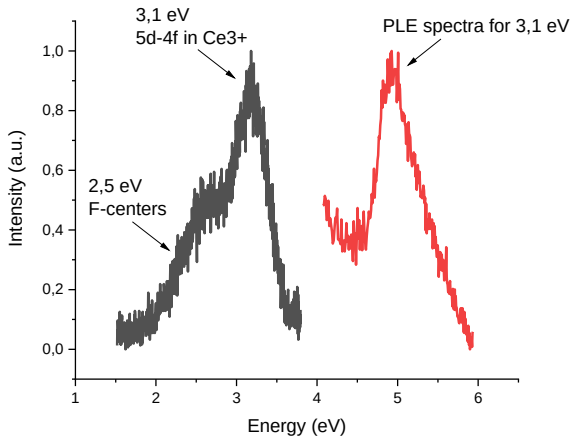

Fig.1. PL emission and PL excitation spectra of pure maltodextrin-coated CeO2 nanoparticles.

REFERENCES

[1] K. R. B. Singh, V. Nayak, T. Sarkar et al., "Cerium oxide nanoparticles: properties, biosynthesis and biomedical application," RSC advances., vol.10, Article Number 45, pp. 27194-27214, 2020.

[2] I. N. Bazhukova, S.Y. Sokovnin, V. Ilves et al., "Luminescence and optical properties of cerium oxide nanoparticles," Optical Materials., vol.92, pp. 136-142, 2019.

[3] G. Vinothkumar, S. Rengaraj, P. Arunkumar et al., "Ionic radii and concentration dependency of RE3+ (Eu3+, Nd3+, Pr3+, and La3+)-doped cerium oxide nanoparticles for enhanced multienzyme-mimetic and hydroxyl radical scavenging activity," The Journal of Physical Chemistry C., vol.123, Article Number 1, pp. 541-553, 2018.

[4] E.O. Baksheev, M.O. Pronina, M.A. Mashkovtsev et al., "Synthesis and study physicochemical properties of nanocrystalline ceria," AIP Conference Proceedings., vol.2174, Article Number 1, pp. 020156, 2019.

R1-P-047401

LUMINESCENCE CHARACTERISTICS OF ZnWO4 CRYSTALS IRRADIATED WITH 19.2 MEV CARBON IONS *

BAKYTKYZY A.[1], DAULETBEKOVA A.K[1]., POPOV A.I.[1,2], KARIPBAYEV ZH.T.,[1] LISITSYN V.M.[3], ZDOROVETS M.V.[1]

[1] *L.N.Gumilyov Eurasian National University, Nur-Sultan, Kazakhstan*
[2] *Institute of Solid State Physics, University of Latvia, Riga, Latvia*
[3] *National Research Tomsk Polytechnic University, Tomsk, Russian Federation*

$ZnWO_4$ is part of a family of metal tungstates that have a high potential for applications in various fields such as scintillators, laser hosts, acoustics, and photocatalysts [1, 2]. $ZnWO_4$ is attractive to researchers due to its unique combination of physical and chemical properties, including molecular and electronic versatility, reactivity, and stability. Zinc tungstate single crystals are unique materials for recording rare processes.

Irradiation of ZnWO4 single crystals with carbon ions with an energy of 19.2 MeV was carried out at the DC-60 accelerator (Nur Sultan, Kazakhstan) with fluences $F_1=4x10^{12}$, $F_2=1x10^{13}$, $F_3=3.3x10^{13}$, $F_4=1x10^{14}$ nucleon/cm^2. Using the SRIM-2013 code [3], the path length, as well as the electronic and nuclear energy losses for the carbon ion in the $ZnWO_4$ crystal, were calculated. The path length of a carbon ion in a single crystal was R = 10 μm. Photoluminescence was measured with a Solar CM2203 fluorometer. When excited by photons with a wavelength of 260 nm, all irradiated crystals luminesced with a maximum of 480 nm with a FWHM of 0.76 eV, for an unirradiated sample 0.72 eV (Fig.1.). The luminescence light yield decreases exponentially with fluence. For fluence F_1, the decrease in light output is 2 times, for F_2 - 3.1 times, for F_3 - 5.6 times, F_4 - 7 times. The results obtained are explained by taking into account that under the action of ion irradiation, the formation of point defects and the shift of the optical absorption edge occur.

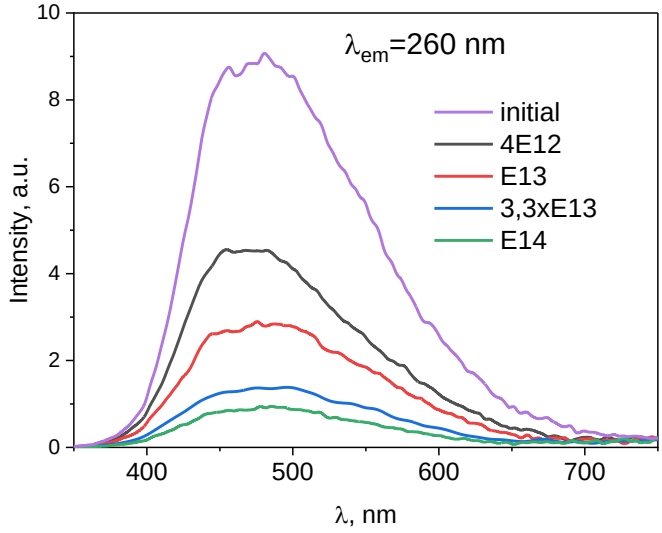

Fig.1. Luminescence spectra of unirradiated and carbon-irradiated $ZnWO_4$ crystals.

REFERENCES

[1] Huang G., Zhang C. and Zhu Y. ZnWO4 photocatalyst with high activity for degradation of organic contaminants // J. Alloy. Comp. - 2007. – Vol. 432(1-2). - P. 269–276.

[2] Pullar R. C., Farrah S. and Alford N. M. MgWO4, ZnWO4, NiWO4 and CoWO4 microwave dielectric ceramics // J. Eur. Ceram. Soc. - 2007. - Vol. 27(2-3). - P. 1059–1063.

[3] Nicklaus E. Optical Properties of Some Alkaline Earth Halides//Phys. Status Solidi a. Vol. 53. 1979. P. 217.

R1-P-047802

LUMINESCENCE OF INTRINSIC DEFECTS IN POLYCRYSTALLINE ZnO

N.L ALUKER

Kemerovo State University, Kemerovo, Russia,
Russia Federal Research Center of Coal and Coal Chemistry, SB RAS ,Kemerovo, Russia

The luminescence of undoped ZnO powders at room temperature has been studied. Photoluminescence was studied upon excitation by microsecond pulses from the region of interband transitions and the region of exciton absorption in the reflection scheme.

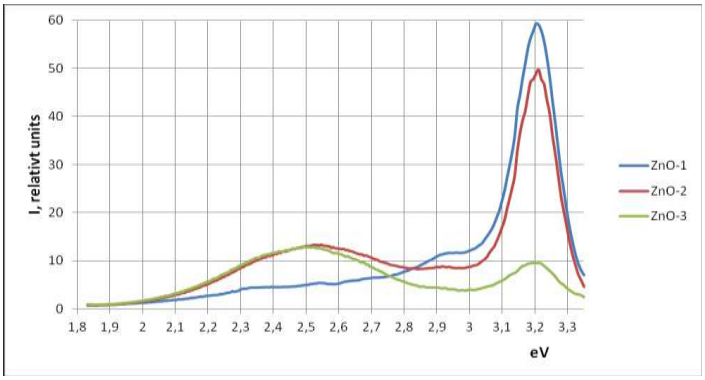

Fig.1. Luminescence of Samples with Different Contents of Growth F Centers.

The luminescence spectra exhibit two regions characteristic of ZnO: a short-wavelength region (~3.2 eV), associated in the literature with exciton luminescence, and a long-wavelength region, due to the presence of growth structural and impurity defects [1–3]. The observed long-wavelength luminescence is divided into components with different luminescence durations, and several components that form broad long-wavelength luminescence are identified. It is formed by at least three stripes. Fast luminescence (≤1 μs ~2.52 eV), long luminescence (≤500 μs ~2.69 eV). The longer wavelength component ≤2.32 eV, which is less reproducible for different samples, falls over times ≤100 μs. The yields of "exciton" luminescence and long-wavelength luminescence depend differently on the intensity of the exciting light. At very low intensities, only high-yield UV luminescence is observed, which decreases with increasing light pulse intensity. At medium intensities, there is a segment of the decrease in UV luminescence along with an increase in long-wavelength luminescence (competing processes). Subsequently, a slight increase in the luminescence yield is observed in both bands.

A comparison of the experimentally observed luminescence with calculations of the energy of the main defects led us to the conclusion that, for a consistent explanation of luminescence in undoped zinc oxide at room temperature, it is sufficient to consider the participation of only anionic sublattice defects in the process. In this case, it is necessary to assume the possibility of the coexistence of free and self-trapped excitons in ZnO. For self-trapping of a free exciton, there must be a small barrier that can be overcome at kT and limits self-trapping at low temperatures. The UV band (~3.2 eV) and the band at 2.52 eV are associated with the radiative decay of excitons in a regular lattice or at shallow traps (for example, F++ centers). The broad, long duration luminescence ~2.69 eV is determined by the triplet transition of the excited F center.

Luminescence associated with growth defects of the cationic sublattice is likely to manifest itself in powders with an excess of Zn in the region of 2.95 eV.

To implement the transitions associated with the charge exchange of the F-center, it is necessary to assume that the excited singlet state (F)* is in the conduction band, and the triplet state has a level in the band gap.

REFERENCES

[1] Ü. Özgür, Ya. I. Alivov, C. Liu, A. Teke, M. A. Reshchikov, S. Doğan, V. Avrutin, S.-J. Cho, and H. Morkoз. A comprehensive review of ZnO materials and devices / U.Ozgur [et al.] // J. Appl. Phys.– 2005, – Vol. 98. – P. 041301.

[2] Janotti A. Oxygen vacancies in ZnO / A. Janotti, C.G. Van de Walle // Appl. Phys. Lett. – 2005.– Vol. 87, – P. 122102.

[3] Meyer B.K., Alves H., Hofmann D.M., Kriegseis W., Forster D., Bertram F., Christen J., Hofmann A., Straβburg M., Dworzak M., Haboeck U., Rodina A.V. Bound exciton and donor-acceptor pair recombinations in ZnO // Phys. Status Solidi. B. 2004. V. 241. P. 231–260.

R1-P-049901

STRUCTURE AND LUMINESCENCE OF YAG:CE, GD, GA CERAMICS SYNTHESIZED RADIATION ASSISTED METHOD

ZHILGILDINOV ZH. S.[1], LISITSYN V.M.[2], KARIPBAYEV ZH.T.[1], TULEOV A.[1], MUSSAKHANOV D.A.[1]

[1]L.N. Gumilyov Eurasian National University, Nur-Sultan, Kazakhstan
[2]National Research Tomsk Polytechnic University, Tomsk, Russian Federation

YAG:Ce phosphor is the most common in the manufacture of white LEDs [1-3], materials based on YAG are used as scintillation, dosimetric, active media. They are used in the form of powders, films, ceramics, single crystals, composites. The synthesis of YAG:Ce materials of any morphology is difficult, since the formation of the main structure, yttrium aluminum garnet, is realized at temperatures above 1700 oC. Therefore, the existing technologies are constantly being improved and new technologies are being searched for.

The work shows the possibility of radiation synthesis based on YAG:Ce ceramics. Ceramic samples of various compositions were synthesized with the following charge content: $Y_3Al_5O_{12}$: Al_2O_3 (40%) + Y_2O_3(54) + Ce_2O_3 (1%)+ Ga_2O_3(2.5%) +Gd_2O_3 (2.5%). Synthesis was carried out by sintering samples from oxide powders in the field of high-energy electron flux. The lattice structure of synthesized samples of YAG:Ce and YAGG:Ce ceramics was compared with standards. The measured diffraction patterns are in good agreement with the standard ones.

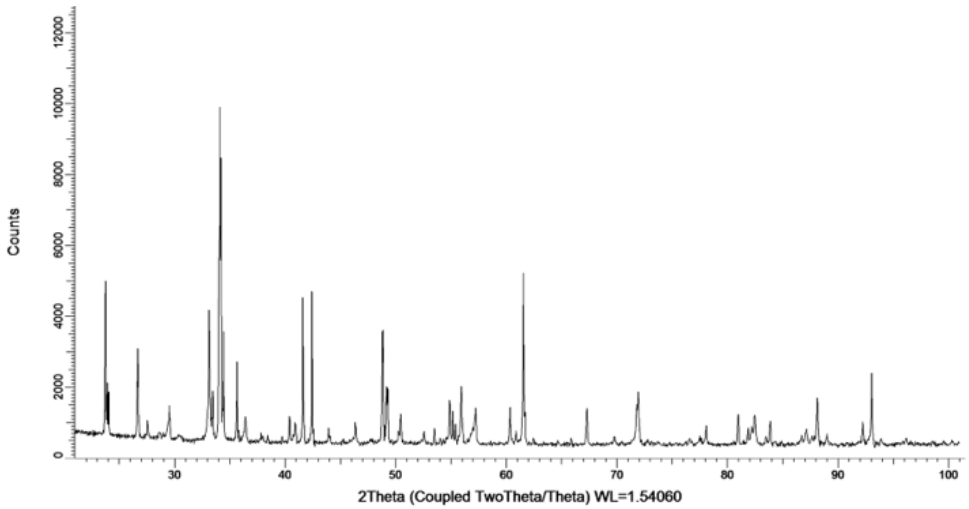

Fig. 1. X-ray diffraction pattern of synthesized YAGG:Ce ceramics

The results of studying the luminescence excitation spectra of the synthesized samples are presented. The excitation spectra of all samples exhibit two bands at 340 and ~460 nm due to $^4F_{5/2} \rightarrow {}^5D_0$, $^5D_1$ in Ce^{3+} activator ions. Through the action of a powerful radiation flux on the charge, it is possible to form luminescent ceramics based on YAG:Ce with characteristics similar to those known for YAG:Ce phosphors.

REFERENCES

[1] George, N.C.; Denault, K.A.; Seshadri, R. Phosphors for solid-state white lighting. Annu. Rev. Mater. Res. 2013. 43, 481–501.

[2] Narukawa, Y.; Ichikawa, M.; Sanga, D.; Sano, M.; Mukai, T. White light emitting diodes with super-high luminous efficacy. J. Physics D - Applied Physics. 2010, 43, 354002.

[3] Qiao, J.; Zhao, J.; Liu, Q.; Xia, Z. Recent advances in solid-state LED phosphors with thermally stable luminescence. J. of Rare Earths. 2019, 37, 6, 565–572.

* The work was carried out within the framework of the grant AP08052050 of the Ministry of Education and Science of the Republic of Kazakhstan. This research was supported by Tomsk Polytechnic University CE Program.

R1-P-051601

THE ROLE OF INTRINSIC DEFECTS IN OPTICAL PROPERTIES OF β-Ga_2O_3 CRYSTAL. AB INITIO STUDIES.

A. Usseinov[1], Zh. Koishybayeva[1], A. Platonenko[2], A. Akilbekov[1], Y. Suchikova[3], F. Abuova[1], A.I. Popov[2] and M. Zdorovets[1,4]

[1]*L.N. Gumilyov Eurasian National University, 2 Satpaeva Str., Nur-Sultan, Kazakhstan*
[2]*Institute of Solid State Physics, University of Latvia, 8 Kengaraga Str., Riga LV1063, Latvia*
[3]*Berdyansk State Pedagogical University, 4, Schmidta St., Berdiansk, Ukraine*
[4]*Department of Intelligent Information Technologies, Ural Federal University, 620075 Yekaterinburg, Russia*

Gallium oxide (β-Ga_2O_3) is emerging as a viable candidate for certain classes of power electronics, solar blind UV photodetectors, solar cells, and sensors with capabilities beyond existing technologies due to its large bandgap [1-5].

Currently, the lack of understanding and control of the unintentional *n*-type conductivity of β-Ga_2O_3 still inhibits its applications. As with many other oxides, this conductivity has historically been attributed to the presence of oxygen vacancies V_O, largely based on the correlation between conductivity and oxygen partial pressure in annealing environments. Calculations have offered insight into the migration mechanisms and the relative energies of oxygen vacancies in the inequivalent sites of the monoclinic structure but only minimal information about the charge states and ionization energies.

So, we report results of the *ab initio* LCAO calculations of optical charge transition levels of native and impurity defects in Ga_2O_3 crystal. As impurity the atomic hydrogen in interstitial and oxygen vacancy positions (H_i and H_O) has been considered. We used hybrid DFT method (B3PW exchange-correlation functional) as incorporated into the CRYSTAL computer code [6] using the supercell model and linear combination of atomic orbitals (LCAO) basis set. These computational set provide good approximation of basic properties of pure Ga_2O_3, in particular mach better prediction of direct bandgap than standard GGA functionals (4.58 eV vs 2.3 eV) that comparable with experimental value of 4.9 eV [7].

Formation energies E_f are key quantities from which we can derive impurity and defect concentrations, stability of different charge states, and the related electronic transition levels. Errors due to spurious electrostatic interactions in the finite-sized cells were corrected using the scheme proposed by Leslie and Gillan [8] and by Makov and Payne [9].

As results we suggest that V_O acts as a deep donor with transition levels more than 1 eV and cannot contribute to n-type conductivity. Moreover, formation energy of V_O is high enough excludes high concentration of these defects in crystal. On the other hand, we find that hydrogen impurity can be easily incorporate to crystal due its low formation energy and migration barrier. The calculated transition states of hydrogen both in vacancy and interstitial positions indicate its shallow donor character. Thus, the presence of hydrogen in Ga_2O_3 crystal good explains persistence n-type conductivity. Our calculated results are fully consistent with other computational studies [10 and references therein].

[1] G. Yang, S. Jang, F. Ren, S. J. Pearton, and J. Kim, Influence of High-Energy Proton Irradiation on β-Ga_2O_3 Nanobelt Field-Effect Transistors, ACS Appl. Mater. Interfaces, Vol 9, pp. 4047-40476 (2017)
[2] S. Oh, M.A. Mastro, M.J. Tadjer and J. Kim, Solar-blind metal-semiconductor-metal photodetectors based on an exfoliated β-Ga_2O_3 micro-flake, ECS J. Solid State Sci.Technol. Vol. 6, pp. Q79-Q83 (2017)
[3] Z. Cheng, M. Hanke, P. Vogt, O. Bierwagen, and A. Trampertless, Phase formation and strain relaxation of Ga_2O_3 on c-plane and a-plane sapphire substrates as studied by synchrotron-based x-ray diffraction, Appl. Phys. Lett., Vol. 111, pp. 162104(1-4) (2017).
[4] S. W. Kaun, F. Wu, and J. S. Speck, β-$(Al_xGa_{1-x})_2O_3/Ga_2O_3$ (010) heterostructures grown on β-Ga_2O_3 (010) substrates by plasma-assisted molecular beam epitaxy, J. Vac. Sci. Technol. A, Vol. 33, 041508(1-9) (2015)
[5] M. Ogita, K. Higo, Y. Nakanishi, and Y. Hatanaka, Ga_2O_3 thin film for oxygen sensor at high temperature, Appl. Surf. Sci., Vol. 175/176, 721-725 (2001)
[6] R. Dovesi, V.R. Saunders, R. Roetti, R. Orlando, C.M. Zicovich-Wilson, F. Pascale, B. Civalleri, K. Doll, N.M. Harrison, I.J. Bush, P. D'Arco and M. Llunell *CRYSTAL14 User's Manual* University of Torino, Torino (2014)
[7] M. Orita, H. Ohta, M. Hirano, and H. Hosono, Deep ultraviolet transparent conductive β-Ga2O3 thin film. Appl. Phys. Lett., Vol.77, pp. 4166-4168(2000)
[8] M. Leslie and M. J. Gillan, The energy and elastic dipole tensor of defects in ionic crystals calculated by the supercell method. J. Phys. C, Vol. 18, 973-982 (1985)
[9] G. Makov and M.C. Payne Periodic boundary conditions in ab initio calculations, Phys. Rev. B., Vol. 51(7), pp. 4014-4022 (1995).
[10] J. B. Varley, J. R. Weber, A. Janotti, and C. G. Van de Walle. Oxygen vacancies and donor impurities in β-Ga2O3, Appl. Phys. Lett., Vol. 97, pp. 142106(1-3) (2010)

COMPARATIVE INVESTIGATION OF THE PLASTIC MATERIALS RESPONSE TO THE HIGH-CURRENT ELECTRON BEAM OF THE KLMAR FACILITY IMPACT*

E.D. KAZAKOV[1,3], *M.YU. ORLOV*[1], *D.N. SADOVNICHII*[2], *M.G. STRIZHAKOV*[1], *K.YU. SHEREMET'EV*[2]

[1]*National Research Center "Kurchatov institute", Moscow, Russia*
[2]*The Federal center for dual-use technologies "Soyuz", Dzerzhinskii ,Moscow region Russia*
[3]*National Research University "MPEI", Moscow, Russia*

At present, using high-power electron beams, the features of the destruction of metals [1], polymers [2], and composite materials [3] have been studied in sufficient detail. However, the behavior of polymer gels, using the example of igdantin, showed an interesting feature - under the powerful electron beam with an energy of more than 1 MeV impact, the decisive role in their destruction is played not by shock-wave, but by radiation-thermal processes [4].

This paper presents the results of a study of the Kalmar accelerator high-current electron beam impact on igdantin and low molecular weight nitrile butadiene rubber SKN-18-KTR, which has a rare network of chemical bonds between rubber macromolecules formed by quinol ether. The materials are similar in mechanical and physical properties, but differ in chemical structure. Peak electron energy was up to 350 keV.

The methodological features of carrying out experiments on the Kalmar setup (current up to 40 kA, voltage up to 350 keV, pulse duration ≈ 100 ns) are presented in [5]. The region of interaction between the beam and the target was determined from X-ray images obtained with a pinhole camera. Plasma expansion from the cathode and sample surfaces was studied by laser shadow probing. Before and after irradiation, the samples were weighed, which made it possible to estimate the weight loss during irradiation.

It is shown that, at a beam energy of less than 600 J, the destruction of igdantin begins to a depth significantly exceeding the electron range, while nitrile rubber withstands a load of more than 700 J without significant damage (Fig. 1). The absorbed dose distribution was estimated using the Monte Carlo methods. Qualitative differences in the destruction of the gel and low molecular weight rubber in the range of incident beam energies up to 800 J are found, and the obtained experimental dependences of the rate of expansion of the irradiated surface are discussed.

Fig.1. A sample of igdantin (left) and rubber (right) after exposure to an electron beam with an energy of 580-600 J.

REFERENCES

[1] Boiko V. I., Valyaev A. N., Pogrebnyak A. D. "Metal modification by high-power pulsed particle beams" Phys. -Usp., vol. 42, no. 11, pp. 1139–1166, 1999

[2] Demidov B.A., Kazakov E.D., Kurilo A.A. "Experimental evaluation of the spallation strengh of polymeric targets" Problems of Atomic Science and Technology, Ser. Thermonuclear Fusion. 2017. V. 40. № 2. P. 73-77.

[3] B. A. Demidov, D. I. Krutikov, E. D. Kazakov et al "The study of fiberglass reinforced with carbon nanotubes destruction under a high-current electron beam impact" 7th International Congress on Energy Fluxes and Radiation Effects (EFRE), Tomsk, Russia, pp. 874-877, 2020.

[4] G.I. Dolgachev, E.D. Kazakov, Yu.G. Kalinin et al "Research of igdantine destruction under high-current beam ofelectrons with energy more than 1 MeV" Journal of Physics: Conference Series 1115(3),032003, 2018.

[5] E.D. Kazakov, Yu.G. Kalinin, D.I. Krutikovet al, "Methods of Laser Shadow Photography with Recording by Streak Camera to Study Plasma Dynamics in the Diode of a Relativistic Electron Beam Generator", Plasma Physics Reports., vol. 47, no. 8, pp. 803–8013, 2021.

* The work was supported by NRC "Kurchatov institute" (order № 3026 dated 25.11.2021).

R2-O-029801

IGNITION OF BROWN COAL BY LASER PULSES IN THE Q-SWITCHED MODE *

B.P. ADUEV, D.R. NURMUKHAMETOV, YA.V. KRAFT, Z.R. ISMAGILOV

Federal Research Center for Coal and Coal Chemistry SB RAS, Kemerovo, Russia

In [1], the ignition of brown coal with a particle size of $d \leq 100$ μm and a bulk density of $\rho = 0.5$ g/cm^3 by laser pulses operating in the free-running mode ($\tau_i = 120$ μs) was studied. Three different stages have been determined, differing in the ignition threshold H_{cr} and the time of luminescence onset. The ignition thresholds of the corresponding stages are $H_{cr}^{(1)} = 0.47$ J/cm^2, $H_{cr}^{(2)} = 1.95$ J/cm^2 and $H_{cr}^{(3)} = 2.6$ J/cm^2. At $H = H_{cr}^{(1)}$ the glow duration practically repeats the pulse duration and the glow is associated with the heating of the particle surface up to T~3000 K [1]. When $H_{cr}^{(2)}$ is reached, along with the glow during the laser pulse, the flame glow above the sample is observed in the time interval ~ 1 – 10 ms, associated with the release and ignition of volatile substances. In the spectral range of 350–750 nm, the glow of a CO flame, excited H_2 and H_2O molecules was identified [9]. At $H = H_{cr}^{(3)}$ along with the first two glows, a flame glow is observed in the time interval of 50 – 150 ms, associated with the combustion of the coke residue at a temperature of T~1800 K [1].

Laser pulses of nanosecond duration have practically not been used to study the ignition mechanism, although the results of such experiments can contribute to the study of the primary processes of interaction of coals with an oxidizer. This paper presents the first results of studies of the impact of laser pulses of a neodymium laser operating in the Q-switched mode on brown coal particles ($d \leq 63$ μm).

When nanosecond laser pulses are applied to brown coal pellets with a density of 1 g/cm^3 (particle size 63 μm), two stages are distinguished. At the first stage, during the pulse, volatile substances are released, evaporation, vaporization, and non-linear multiplication of luminescence centers occur. The ignition threshold at this stage is $H_{cr}^{(1)} = 0.2$ J/cm^2. The second stage includes the first one and the ignition of the coke residue, the ignition threshold of which is $H_{cr}^{(2)} = 3.5$ J/cm^2. In the luminescence kinetics at $H > H_{cr}^{(1)}$ two components are distinguished: a singlet luminescence with a duration of ~ 20 ns and a second luminescence component observed in the microsecond range, which decays according to the second-order kinetics. At $H > H_{cr}^{(2)}$ ~200 μs after the laser pulse, as a result of chemical reactions, the coke residue ignites and burns in the time interval of 200 – 1000 μs. The amplitude of the flame glow during the excitation pulse increases nonlinearly with increasing energy density, which indicates the avalanche nature of the process of formation of glow centers.

REFERENCES

[1] B. P. Aduev et al., "Spectral-Kinetic Characteristics of Laser Ignition of Pulverized Brown Coal," Opt. Spectrosc., vol. 125, no. 2, pp. 293–299, Aug. 2018.

* This work was carried out within the framework of a state contract at the Federal Research Center for Coal and Coal Chemistry, Siberian Branch, Russian Academy of Sciences (project no. 121031500513-4) using the equipment of the Center for Collective Use of the Federal Research Center for Coal and Coal Chemistry, Siberian Branch, Russian Academy of Sciences.

R2-O-031601

LUMINESCENCE OF COALS EXCITED BY A PULSED ELECTRON BEAM *

I.YU. LISKOV, B.P. ADUEV, G.M. BELOKUROV, Z.R. ISMAGILOV

Federal Research Center for Coal and Coal Chemistry SB RAS, Kemerovo, Russia

The purpose of this work is to study the spectral and amplitude-temporal characteristics of the luminescence of coals from the Kuznetsk Basin when excited by a nanosecond electron beam. The experiments were carried out at a temperature of T = 300 K. As objects of study, samples of coals of the following grades DG (long-flame gas) and K (coconut) were used [1]. Before carrying out, tablets of the corresponding grade of coal with a size of Ø17x4 mm were made. The density of the samples was 1.35 g/cm^3.

To measure the spectral and amplitude-temporal characteristics of the luminescence of the samples, an experimental complex was used, which was described in detail in [2]. A GIN-600 electron accelerator with an effective electron energy of 240 keV, a pulse duration of $\tau \approx 25$ ns, and an energy density of 20 J/cm^2 output to the sample was used as a source of sample luminescence excitation. The spectral range recorded during irradiation with a single pulse is 350-650 nm. The amplitude-time characteristics of the glow for all the studied grades of coals have the same character.

At this stage, we can give the following interpretation of the observed amplitude-time dependences of the glow. It is known that during the excitation of nonmetallic compounds by an electron beam, electron–hole pairs are generated at the first stage (in the case of coals, these can be free electrons and positively charged radicals). Some electrons are born near the genetic partner and quickly recombine with it through an excited state with the emission of luminescence quanta already during the irradiation pulse. Some of the electrons go a considerable distance from the genetic partner. In this case, diffusion of charged particles must be present to meet and recombine, which can lead to an observed increase in the luminescence intensity over a time of ~50 – 100 nm. The decrease in luminescence in the simplest case is associated with intracenter luminescence decay.

To study the mechanism of migration and dissipation of the energy introduced by the electron beam, more detailed studies are needed, for example, the measurement of the temperature dependence of the spectral-kinetic characteristics of the luminescence of samples. Measurements of this kind are of great interest and can provide information on chemical reactions in coals that occur under the action of a pulsed electron beam, and require a separate work.

In the luminescence spectra, a significant number of narrow bands can be distinguished, which are superimposed on a wide luminescence band. We have identified the bands. In all the studied coals, luminescence was found under the action of an electron beam, associated with a number of PAHs, most of which are carcinogens.

The experiments carried out showed that the luminescence arising upon excitation by a nanosecond electron beam has a luminescent nature with an increase in intensity in the time interval of 50–100 ns and a decrease over a time of 500 ns. In the luminescence spectra, the wide band is superimposed by a number of narrow bands associated with the luminescence of polycyclic aromatic hydrocarbons in the composition of the studied coals. The proposed method for detecting PAHs can be used as an express method for determining the presence of PAHs in coals and other organic objects.

REFERENCES

[1] B. P. Aduev, D. R. Nurmukhametov, Y. V. Kraft, and Z. R. Ismagilov, “Glow Spectral Characteristics of the Hard Coal Particles Surface during the Action of Laser Pulses in the Free Generation Mode,” Opt. Spectrosc., vol. 128, no. 12, pp. 2008–2014, Dec. 2020.

[2] B. P. Aduev, G. M. Belokurov, S. S. Grechin, and I. Y. Liskov, “Spectrokinetic characteristics of light emission from pentaerythritol tetranitrate single crystals detonating under the action of a high-current electron beam,” Russ. J. Phys. Chem. B, vol. 10, no. 5, pp. 796–800, Sep. 2016.

* This work was carried out within the framework of a state contract at the Federal Research Center for Coal and Coal Chemistry, Siberian Branch, Russian Academy of Sciences (project no. 121031500513-4) using the equipment of the Center for Collective Use of the Federal Research Center for Coal and Coal Chemistry, Siberian Branch, Russian Academy of Sciences.

R2-O-033001

INVESTIGATION OF THE COMPOSITION OF GASEOUS PRODUCTS OF LASER COAL OXIDATION BY MASS SPECTROMETRY

YA.V. KRAFT, V.D. VOLKOV, D.R. NURMUKHAMETOV, B.P. ADUEV, Z.R. ISMAGILOV

Federal Research Center for Coal and Coal Chemistry SB RAS, Kemerovo, Russia

At present, the issue of the negative impact of coal combustion products on the environment is acute. A large number of works are aimed at improving the combustion efficiency of coal fuel, and the possibility of using coal as a raw material for obtaining clean gaseous fuels, such as hydrogen, is also being considered.

In [5], three stages of the process of ignition and combustion of a coal particle were determined: as a result of the action of laser radiation, the coal particle is heated and the subsequent development of thermochemical reactions in the sample, then the release and ignition of various volatile substances, as well as the combustion of the non-volatile residue of the coal particle. In addition, each stage has a pronounced threshold character. In [6], studies of the thermal decomposition of brown coal under the influence of pulsed laser radiation in an inert medium were carried out. Using the method of mass spectroscopy, the following gaseous pyrolysis products were detected: H2, CH4, H2O, CO, and CO2. It was found that the concentration of hydrogen in the composition of gaseous pyrolysis products increases with increasing energy density in the pulse, while the concentration of carbon dioxide and water vapor, on the contrary, decreases. The concentrations of CO and CH4 remain constant. The yield of combustible gases increases linearly with an increase in the energy density of laser radiation.

In this work, mass spectroscopy was used to study the molecular composition of gaseous products of laser oxidation of coals of five different grades: long-flame (L), lean sintering (OS), weakly sintering (SS), lean (T), and anthracite (A) in air. The coals were ground in a ball mill. The resulting coal particles were subjected to dispersion through a vibrating sieve with a mesh size of 63 μm. Next, by pressing in a mold, tableted samples were obtained with a thickness of 2.5 mm, a diameter of 6.2 mm, and a weight of 70 mg. The source of laser radiation was a neodymium YAG:Nd3+ laser operating in the free-running mode at a wavelength of 1064 nm, with a pulse duration of 120 μs and a pulse repetition rate of 6 Hz. The diameter of the laser beam coincided with the diameter of the pelletized sample for complete radiation coverage of the sample surface. The samples were placed in an experimental sealed chamber filled with air. Laser radiation pulses were used, which are characterized by the following parameters: laser radiation pulse energy 438 mJ, energy density 1.5 J/cm2, pulse power 3.7 kW, pulse power density 12.7 kW/cm2. Gas sampling from the chamber was carried out continuously using a capillary, which was connected to a gas analyzer. An analysis of the experimentally obtained mass spectra made it possible to establish the presence of the following oxidation products: H2, CH4, H2O, CO, CO2.

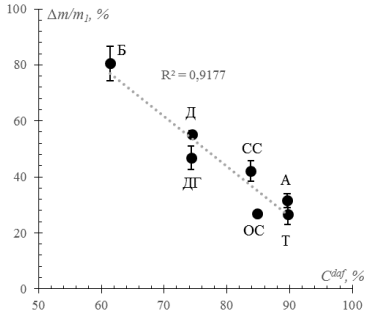

Fig.1. Dependence of the proportion of reacted coal samples on the atomic ratio of oxygen to carbon

On fig. 1 shows the dependence of the proportion of reacted coal samples on the carbon content. With an increase in the carbon content, the proportion of the reacted coal sample decreases.

REFERENCES

[1] B. P. Aduev et al., “Spectral-Kinetic Characteristics of Laser Ignition of Pulverized Brown Coal,” Opt. Spectrosc., vol. 125, no. 2, pp. 293–299, Aug. 2018.

[2] [1] Y. V. Kraft, D. R. Nurmukhametov, B. P. Aduev, and Z. R. Ismagilov, “Pyrolysis of kaichak lignite under the laser radiation exposure,” Vestn. Kuzbass State Tech. Univ., vol. 133, no. 3, pp. 5–15, 2019, doi: 10.26730/1999-4125-2019-3-5-15.

R2-O-045801

RELATION BETWEEN OPTICAL CHARACTERISTICS OF AP/AL MIXTURE AND SENSITIVITY TO LASER RADIATION

E.V. FORAT[1], *V.P. TSIPILEV*[1], *A.N. YAKOVLEV*[2]

[1]*National Research Tomsk Polytechnic University, Tomsk, Russia*
[2]*Kuzbass State Technical University, Kemerovo, Russia*

Ammonium perchlorate (AP) and aluminum are the main components of modern solid propellants, but their mixture is capable of burning and exploding on its own [1]. In addition, the AP/Al mixture is a convenient model object for studying the behavior of metallized double-base energetic materials (EM).

Previously, we studied the behavior of a AP/nanosized Al mixture (60:40 mass fraction) under the action of millisecond Nd-laser radiation [2–4]. It was found that the ignition threshold of confined mixture samples into PMMA capsule was much higher in comparison with open samples [5]. Such behavior is not characteristic of gasified EMs. This paper presents the results of studying the optical characteristics of both individual components and the mixture itself. It is shown that with an increase in the Al mass concentration, the optical properties of the mixture change radically. For concentrations less than ~5% of the Al content, the scattering properties of AP predominate, and at high concentrations, the optical properties are completely determined by the properties of Al. This conclusion is confirmed by the performed optical measurements and the results of numerical simulation by the Monte Carlo method.

Based on the obtained absorption and scattering coefficients, the problem of heating a mixture sample under the action of a laser pulse is solved by the method of finite differences. It is shown that at the absorption index of the mixture $\mu \approx 10^4$ cm^{-1}, heating occurs in a thin near-surface layer, which contributes to significant heat loss through the surface into the covering material.

REFERENCE

[1] A.A. Shevchenko, A.Y. Dolgoborodov, V.G. Kirilenko, M.A. Brazhnikov, "Detonation velocity of mechanically activated mixtures of ammonium perchlorate and aluminum," Combust., Explos. Shock Waves, vol. 53, no. 4, pp. 461-470, 2017.
[2] V.V. Medvedev, E.V. Forat, V.P. Tsipilev, A.N. Yakovlev, "The effect of aluminum particles dispersity on characteristics of ammonium perchlorate—aluminum composition laser ignition," J. Phys.: Conf. Ser., vol. 830, no. 1, pp. 012-146, April 2017.
[3] E. Forat, V. Medvedev, V. Tsipilev, A. Yakovlev, "The influence of aluminum and ammonium perchlorate dispersion on characteristics of the laser ignition," Sci. Technol. Energ. Mater., vol. 79, no. 5-6, pp. 186-188, 2018.
[4] V. Medvedev, V. Tsipilev, E. Forat, "Effect of ammonium perchlorate and aluminum composition density on characteristics of laser ignition," Propellants, Explos., Pyrotech., vol. 43, no. 2, pp. 122-125, 2018.
[5] V. Tsipilev, E. Forat, V. Medvedev, A. Yakovlev, V. Vavilov, V. Shiryaev, "Laser Ignition of Ammonium Perchlorate/Aluminum Composition Confined into PMMA Capsule," Propellants, Explos., Pyrotech., vol. 47, no. 3, 2022.

R2-O-045901

ELECTRICAL NATURE OF THE HOT SPOTS FORMATION IN PRESSED POWDERS OF ENERGETIC AND INERT MATERIALS UNDER LASER IRRADIATION

V.P. TSIPILEV[1], V.I. OLESHKO[1], A.N. YAKOVLEV[2], E.V. FORAT[1], N.A. ALEKSEEV[1]

[1]National Research Tomsk Polytechnic University, Tomsk, Russia
[2]Kuzbass State Technical University, Kemerovo, Russia

The question of the initiation mechanisms of the explosive decomposition reaction under laser excitation is one of the main questions in the energetic materials explosion physics. Currently two main models concerning the mechanism of explosion excitation are considered: non-thermal (chain) [1] and thermal [2-4]. The thermal micro hot-spot model is a well-established model for the energetic materials initiation by an external impulse. The hot spots are created due to the interaction of laser radiation with optical inhomogeneities (impurities and defects of various nature). However, the mechanism of hot spots formation under laser irradiation remains undefined by now.

In this work we study the mechanism of hot spots formation in pressed samples of energetic and inert materials by the first harmonic radiation of a Nd laser. Dependences of the luminescence intensity of these materials on the energy density of the laser pulse on the samples surface were obtained in the range from 10^{-3} to 10 J/cm^2. In this case, the luminescence intensity increases by nine orders of magnitude. An analysis of these dependences allows us to conclude that in the range of laser radiation energy densities from 1 to 30 mJ/cm^2, hot spots are formed as a result of optical (electrical) micro breakdown in the vicinity of absorbing inhomogeneities contained in the studied materials. In the range from 1 to 10 J/cm^2, the well-known mechanism of optical macro breakdown occurs with the formation of a plasma jet, surface destruction, and a characteristic "click" sound. The kinetic, spectral and spatial characteristics of the hot spots glow of energetic (PETN, PETN with soot and Al additives, ammonium perchlorate with aluminum) and inert (magnesium and titanium oxides, sugar) materials have been studied. Photographs of hot spots under a single and multi-pulse exposure are given. A conclusion is made about the optical (electrical) mechanism of initiation of energetic materials.

REFERENCES

[1] B.P. Aduev, E.D. Aluker, G.M. Belokurov, A.N. Drobchik, Y.A. Zakharov, A.G. Krechetov, A.Y. Mitrofanov, "Preexplosion phenomena in heavy metal azides," Combust., Explos. Shock Waves, vol. 36, no. 5, pp. 622-632, 2000.

[2] E.I. Aleksandrov, A.G. Voznyuk, "Initiation of lead azide with laser radiation," Combust., Explos. Shock Waves, vol. 14, no. 4, pp. 480-484, 1978.

[3] E.I. Aleksandrov, O.B. Sidonskii, V.P. Tsipilev, "Influence of combustion in the vicinity of absorbing inclusions on the laser ignition of a condensed medium," Combust., Explos. Shock Waves, vol. 27, no. 3, pp. 267-272, 1991.

[4] V.I. Tarzhanov, A.D. Zinchenko, V.I. Sdobnov, B.B. Tokarev, A.I. Pogrebov, A.A. Volkova, "Laser initiation of PETN," Combust., Explos. Shock Waves, vol. 32, no. 4, pp. 454-459, 1996.

R2-P-001901

ELECTROPHYSICAL PROCESSES IN ELECTRIC DISCHARGE REACTOR DETERMINED BY GEOMETRIC TRANSFORMATION OF ELECTRODE SYSTEM

S.A. GLOTOV, S.V. MELENTIEV, V.A. LITVINOVA, N.M. KONDRATIEVA

Tomsk State University of Architecture and Civil Engineering, Tomsk, Russian Federation

Consideration of the issues of destruction of the electrode systems of electric discharge reactors is of great theoretical and practical importance. The main element in the structural diagram of an electric discharge installation is an electric discharge reactor, in which final useful work is performed, for example, the synthesis of materials, the shaping of sheet metal, the emulsification of immiscible liquids, etc. [1,2].

The issues of destruction of the current conductor of a low-voltage electrode by its electrical erosion are considered. At present, the mechanism of destruction of electrode systems has been elucidated [3,4,5]. Erosion of the active element of the low-voltage electrode is caused by thermal action. There are four sources of thermal energy [5]: heat supplied to the electrode due to the bombardment of its surface with electrons (or ions); heat from flowing current; heat supplied to the electrode from radiation according to the Stephen-Boltzmann law; heat transferred to the electrode by the plasma jet. It has been established that the heat flux from the plasma jet leakage is one to three orders of magnitude greater than from all other heat sources and is the main cause of electrode destruction.

The paper considers the electrical erosion of an electrode located in a reactor filled with tap water. The source of pulsed energy is a generator of pulsed currents with a stored energy of 1.8 kJ. The pulse repetition rate is 1.5 Hz. The active element of the electrode is made of high-alloy steel 12X18H10T. The electrode was exposed to 10800 pulses, which corresponded to the operation of the installation for two hours. Figure 1 shows the active element of the electrode after exposure to electrical discharges.

Fig 1. The active element of the electrode after exposure to electrical discharges

The erosion crater looks like a semi-ellipsoid with a depth of about 10 mm. In the process of further erosion, the semi-ellipsoid tends to degenerate into the shape of a hemispheroid. It should be noted that an electric discharge in a liquid is accompanied by the appearance of cavitation processes, which are as powerful a source of perturbation as shock waves. Drawing an analogy with studies [6], we can draw an important conclusion from a practical point of view: an erosion crater in the form of a semi-ellipsoid or hemispheroid makes it possible to form cavitation phenomena in the depth of the treated liquid and thereby activate a larger volume of liquid.

USED BOOKS

[1] L.A. Yutkin, Electrohydraulic effect and its application in industry, L: Mashinostroenie, 1986.
[2] P.P. Malyushevsky, Fundamentals of discharge-pulse technology, Kyiv: Naukova Dumka, 1983.
[3] Gordienko P.S., Verkhoturov A.D., Dostovalov V.A., Zhevtun I.G., Panin E.S., Konevtsov L.A., Shabalin I.A., “Electrophysical model erosion of electrodes under pulsed energy exposure”, “Electronic processing of materials”, volume 47, number 3, pp. 15-27, 2011.
[4] V.I. Kurets, A.F. Usov, V.A. Zuckerman. Electropulse disintegration of materials. Apatity: Kolsk Scientific Center, 2002.
[5] Stepanyan, V.P.. Intensification of the process of extraction of biologically active compounds from plant raw materials by electric pulsed discharges: abstract of dissertation ... Candidate of Technical Sciences. -Tambov, 2000.-16s.
[6] Vinnikov D.V., Ozerov A.N., Yuferov V.B., Sakun A.V., Korytchenko K.V., Mesenko A.P., “Experimental study of an electric discharge in a liquid created between electrodes with a conical recess”, “Electrical engineering and electromechanics”, number 3, pp. 55-60, 2013.

DESTRUCTION OF THE INSULATOR OF THE HIGH VOLTAGE ELECTRODE OF THE ELECTRIC DISCHARGE REACTOR

S.A. GLOTOV, S.A. LARIONOV, S.V MELENTIEV, V.A. LITVINOVA, N.M. KONDRATIEV

Tomsk State University of Architecture and Civil Engineering, Tomsk, Russian Federation

An integral part of the electric discharge reactor is a high-voltage electrode, which in the simplest version is a current conductor enclosed in an insulating sheath. The electrode experiences significant loads of various kinds - thermal, mechanical and electrical, often acting simultaneously. The intensity of the impact on the electrode depends on many factors: the energy of single pulses; the environment in which the electrode operates; reactor material; reactor volume, etc.

The most important case. from the point of view of the resistance of the electrode insulator, is the operation of the electrode in a limited space, calculated in units of cubic decimeters. Under such conditions, significant pressures arise (if the working medium is represented by a liquid), reaching hundreds of MPa [1]. Such pressures arise, among other things, as a result of wave processes accompanied by reflections from the walls of the reactor and other elements located in the zone of action of the electric discharge. In addition, the flowing pulsed currents can reach tens of kA, causing heating of the insulator until it melts. As a result, it is required to protect the electrode insulator from damaging effects.

The paper considers the destruction of the electrode insulator by the type of melting, mechanical crack and electrical erosion. In contrast to the destruction of the current lead, the destruction of the insulator is catastrophic (instantaneous) in nature, when these destructions lead to a rapid loss of electrode performance. Known solutions [2,3,4] to protect the electrode insulator from destruction are not universal for all conditions of its operation.

Figure 1 shows three main cases of destruction of the electrode insulator. Destruction of the insulator by individual types may occur, and sometimes with their simultaneous development.

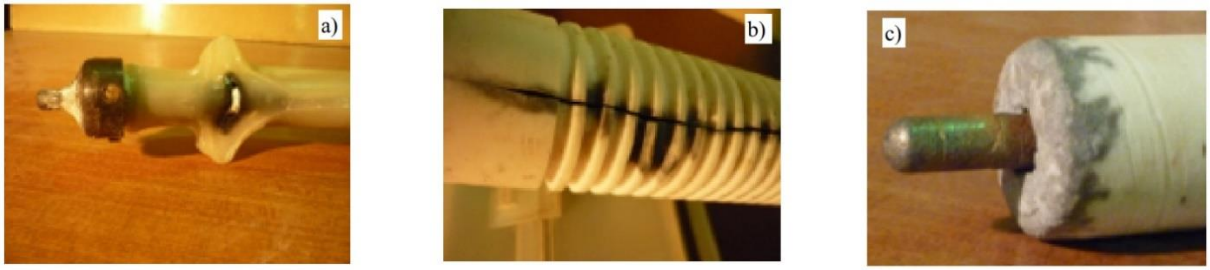

Fig 1. Types of destruction of the high-voltage electrode insulator
a) melting of the insulator, b) mechanical destruction of the insulator, c) electrical erosion of the insulator

Most often, materials such as polyethylene, caprolon, fluoroplast, fiberglass, which have a high resistance to deformation, are used to insulate the current conductor of the electrode. They, in addition to good insulating properties, must have significant mechanical characteristics. This requirement is due to the need to use insulators, including as a structural material. When choosing an insulator material, one must be guided by the specific conditions under which the high-voltage electrode will operate. For example, if the insulator operates under thermal stress, it is recommended to use a PTFE insulator. If significant mechanical loads will act, then the use of fiberglass is recommended. It should be noted that fiberglass and fluoroplast have little resistance to electrical erosion. Sometimes an effective method of dealing with mechanical loads is the constructive solution of the insulator in the zone of high mechanical loads, when the insulator is made in a streamlined shape.

USED BOOKS

[1] [1] B.V. Meriin L.A., Electrohydraulic processing of machine-building products L.: Mashinostroyeniye, Leningrad. department, 1985.
[2] [2] E.V. Krivitsky, Dynamics of electric explosion in a liquid. Kyiv: Nauk.dumka, 1986.
[3] [3] Nadis, I.B. Development of electrode systems for electrohydraulic installations: Abstract of the thesis. Candidate of Technical Sciences - M., 1983.- 19s.
[4] [4] Baranov, A.N. Development of high-voltage electrodes for electropulse utilization of reinforced concrete and drilling of holes. Abstract of the thesis Candidate of Technical Sciences - Tomsk., 1992.- 24s

R2-P-022203

INFLUENCE OF CHARACTERISTIC DIMENSIONS OF NTO AND HNS IN CUBIC SHAPE ON THE CRITICAL TEMPERATURE OF A THERMAL EXPLOSION*

A. V. KHANEFT[1,2], E. S. GALAKTIONOVA[1]

[1]*Kemerovo State University, Kemerovo, Russia*
[2]*National Research Tomsk Polytechnic University, Tomsk, Russia*

The paper analyzes the experimental data provided in [1] on the thermal explosion of low-sensitive explosives (EM) in the form of a cube: NTO and HNS. The ignition criterion of EM is generally defined by the expression:

$$\varphi(\mathrm{Bi})\,\delta_{cu}^{*} = l^2\,\frac{\rho QZ}{\lambda}\,\frac{E}{RT_s^{*2}}\exp\left(-\frac{E}{RT_s^{*}}\right), \qquad (1)$$

where T_s^* – is the surface temperature of the EM; l – характерный размер куба. Critical number for the cube $\delta_{cu}^{*} = 3\pi^2/\mathrm{e} = 2{,}72$ [2]. Function $\varphi(\mathrm{Bi})$ can be calculated in the following way [3]:

$$\varphi(\mathrm{Bi}) = \frac{\mathrm{Bi}}{2}\left(\sqrt{\mathrm{Bi}^2+4}-\mathrm{Bi}\right)\exp\left(\frac{\sqrt{\mathrm{Bi}^2+4}-\mathrm{Bi}-2}{\mathrm{Bi}}\right). \qquad (2)$$

From (1) we have an equation for determining the activation energy of the stationary rate of exothermic decomposition of EM:

$$E = 2R\,\frac{T_{S1}^{*}T_{S2}^{*}}{T_{S1}^{*}-T_{S2}^{*}}\left\{\ln\left(\frac{l_2T_{S1}^{*}}{l_1T_{S2}^{*}}\right)+\frac{1}{2}\ln\left[\frac{\varphi(\mathrm{Bi}_1)}{\varphi(\mathrm{Bi}_2)}\right]\right\}, \qquad (3)$$

where T_{S1}^{*}, T_{S2}^{*} – critical ignition temperatures of EM at characteristic cube sizes l_1 and l_2 accordingly. At $\mathrm{Bi} >> 1$, the second term in (3) ~ 0. Results of calculations of activation energies and parameter ratios $\rho QZ/\lambda$ for NTO and HNS are shown in the table.

EM	NTO	HNS
E, kJ/mol	165,621	170,386
$\rho QZ/\lambda$, K/m^2	$18{,}847\times10^{22}$	$1{,}099\times10^{22}$

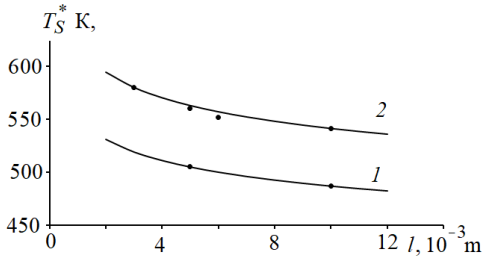

Dependence of the critical ignition temperature of cube-shaped explosives on its characteristic size: 1 – NTO, 2 – HNS (points – experiment [1], lines – calculation)

The critical ignition temperatures of EM were calculated using equation (1). As can be seen from the figure, the calculation results are in good agreement with the experiment [1]. In addition, we solved the heat conduction equation with Arrhenius nonlinearity. The calculation results agree with the critical ignition temperatures of NTO and HNS.

REFERENCES

[1] Krause G. Volume-Dependent Self-Ignition Temperatures for Explosive Materials. Propellants, Explosves, Pyrotechnics. Vol. 37, 107-115, 2012.
[2] Khaneft A. Determination of the Critical Temperature of Self-Ignition of Explosives from the Stability Analysis of the Thermal Conductivity Equation. Propellants, Explosives, Pyrotechnics. Vol. 46, No 3. P. 368-377, 2021.
[3] Barzykin V. V., Merzhanov A. G. The boundary objective in the theory of a thermal explosion. Dokl. Akad. Nauk SSSR. Vol. 120, No 6, 1271-1273, 1958.

* This work was supported by the Russian Science Foundation [grant number 18-13-00031].

R3-O-018401

RADIATION SOURCE WITH INCREASED VIRUCIDAL EFFICIENCY BASED ON A MIXTURE OF HELIUM WITH IODINE VAPOR*

M.I. LOMAEV[1,2], V.F. TARASENKO[1], V.S. KUZNETSOV[1]

[1]Institute of High Current Electronics SB RAS, Tomsk, Russia
[2]National Research Tomsk State University, Tomsk, Russia

Currently there are various sources of spontaneous emission in the UV and VUV spectral regions, which are widely used in science and technology. One of the most important applications in the context of the covid-19 pandemic is UV-inactivation of pathogens, including coronavirus [1]. The most efficient sources in this spectral region are excilamps - gas-discharge sources of spontaneous radiation in the UV and VUV regions of the spectrum, based on the nonequilibrium radiation of exciplex and excimer molecules [2]. From the point of view of coronavirus inactivation, the most promising are KrCl- and KrBr-excilamps (peak wavelengths of the main radiation bands are 222 nm and 206 nm, respectively), whose radiation is both effective for coronavirus inactivation and minimally dangerous for human skin and eyes [3]. At the same time, these excilamps have additional bands in the range of 225–300 nm, the radiation of which damages DNA molecules with high efficiency [4]. Therefore, the search for other efficient sources of radiation in the region of 200–225 nm is very important. At the same time, an additional important condition is the absence of intense lines or bands in the emission spectrum of the radiation source in the spectral region of 230–350 nm in order to exclude damage to DNA molecules during irradiation of human skin or eyes.

One of the options for creating a radiation source in this region of the spectrum, effective in terms of inactivation of the SARS-CoV-2 coronovirus, is a gas discharge lamp emitting at the iodine atom line with a wavelength of 206.16 nm. The advantage of this lamp compared to the KrCl-excilamp is that the absorption coefficient of DNA and protein molecules that make up bacteria and viruses at a wavelength of 206.16 nm is more than 2 times higher than the absorption coefficient at a wavelength of 222 nm. This provides a greater bactericidal/virucidal efficiency of the iodine lamp radiation, including during the inactivation of the coronovirus [4].

The aim of this work is to study the amplitude-time, energy, and spectral characteristics of an iodine vapor lamp, based on iodine vapor excited by a low-pressure capacitive discharge, which is promising from the point of view of developing a radiation source with increased virucidal efficiency for UV-disinfection of a human environment contaminated by pathogenic microorganisms, including the SARS-CoV-2 coronavirus. When performing the work, a comparison was made of the radiative characteristics of iodine vapors and their mixtures with inert gases. The light source under study based on iodine vapor can compensate for the lack of spontaneous emission sources in the spectral range of 200-220 nm.

REFERENCES

[1] H. Kitagawa, T. Nomura, T. Nazmul, K. Omori, N. Shigemoto, T. Sakaguchi, H. Ohge, "Effectiveness of 222-nm ultraviolet light on disinfecting SARS- CoV- 2 surface contamination," American Journal of Infection Control. vol. 49. Issue 3. P. 299-301. 2021.

[2] A.M. Boichenko, M.I. Lomaev, A.N. Panchenko, E.A. Sosnin, V.F. Tarasenko, The ultroviolet and vacuum-ultroviolet excilamps: physics, technology and applications, Tomsk, STT, 2011.

[3] M. Buonanno, D. Welch, D.J. Brenner, "Exposure of human skin models to KrCl excimer lamps: The impact of optical filtering," Photochemistry and Photobiology. vol. 97. P. 517-523. 2021.

[4] M. Hessling, R. Haag, N. Sieber, P. Vatter, "The impact of far-UVC radiation (200–230 nm) on pathogens, cells, skin, and eyes – a collection and analysis of a hundred years of data," GMS Hygiene and Infection Control. vol. 16. P. 1-17. 2021.

*This research was supported by the Ministry of Science and Higher Education of the Russian Federation within Agreement no. 075-15-2021-1026 of November 15, 2021.

R3-O-021701

NONTHERMAL MECHANISM RESOLVED A PARADOX OF SLOW ELECTRON-PHONON COUPLING VS. FAST ION TRACK HEATING*

N. MEDVEDEV[1,2], A.E. VOLKOV[3,4,5]

[1] *Institute of Physics Czech Academy of Sciences, Prague, Czech Republic*
[2] *Institute of Plasma Physics Czech Academy of Sciences, Prague, Czech Republic*
[3] *P.N. Lebedev Physical Institute RAS, Moscow, Russia*
[4] *Joint Institute for Nuclear Research, Dubna, Russia*
[5] *NRC Kurchatov Institute, Moscow, Russia*

For over two decades, there has been a puzzling discrepancy between slow electron-phonon coupling and creation of tracks swift heavy ions (SHI) decelerated in the electronic stopping regime. Due to fast cooling down of excited electrons (less than 100fs), track formation requires extremely fast energy transfer from the excited electrons to atoms [1]. In contrast, laser-irradiation experiments measured much too slow electron-phonon energy exchange rate, which is supported by various calculations [2]. This paradox lead to a widespread use of electron-phonon coupling as a fitting parameter in calculations of SHI track creation.

We resolve this contradiction noticing that electron-phonon coupling is not the sole mechanism of energy exchange between electrons and atoms in solids. Heating of electrons alters potential energy surface of atoms. Appearing forces due to modification of the interatomic potential accelerate atoms increasing their kinetic energy (”nonthermal heating”) [2]. This nonthermal mechanism may be extremely fast, significantly faster than the electron-phonon coupling. At high deposited doses it may even lead to ultrafast nonthermal structure transformations.

It suggests that the estimates of the ”electron-phonon coupling parameter” extracted from the data on SHI track sizes with help of the two-temperature (inelastic thermal spike) model do not reflect the electron-phonon coupling per se, but must be interpreted as a quantity reflecting the nonthermal heating of atoms (with a contribution of phononic and non-phononic elastic scattering of hot electrons and valence holes) [2]. This notion reconciles the much debated problem of extremely fast atomic heating in swift ion impacts (at hundred femtosecond timescales) with slow electron-phonon coupling (acting at picosecond timescales).

Our results suggest that the nonthermal heating of atoms is a universal effect in nonmetallic crystalline materials under ultrafast energy deposition, and thus must be taken into account in appropriate models and interpretation of experiments [2].

REFERENCES

[1] [A.E. Volkov, V.A. Borodin, Nucl. Instruments Methods Phys. Res. B. 146 (1998) 137–141

[2] [N. Medvedev, A.E. Volkov, (2021) https://arxiv.org/abs/2109.04401v1

* AEV acknowledges support from the Russian Science Foundation (grant number №22-22-00676, https://rscf.ru/en/project/22-22-00676/).

R3-O-953201

RADIATION SYNTHESIS OF REFRACTORY OPTICAL CERAMICS

V. LISITSYN

National Research Tomsk Polytechnic University Tomsk, Russia

Radiation technology for synthesis of refractory optical ceramics, which we first implemented [1, 2], fundamentally differs from conventionally used technologies. For synthesis, a mixture of stoichiometric composition required to obtain the desired phase was exposed to direct powerful electron flux with energy of 1.4 MeV and flux density of 15–23 kW/cm^2 using the ELV-6 accelerator (Institute of Nuclear Physics SB RAS). Radiation synthesis was performed with high efficiency within less than 1 s using radiation energy and mixture materials with no additives or any other materials used to promote synthesis. We obtained samples of luminescent ceramics based on YAG and YAGG doped with Ce and modified by Gd and Ga based on alkaline earth metal fluorides doped by tungsten. The luminescent properties of the samples (luminescence and excitation spectra, decay times) correspond to those known for phosphors, ceramics, and crystals of appropriate compositions fabricated by other synthesis techniques.

It was found that ceramics is synthesized in the radiation field at similar power densities above 15 kW/cm^2 from materials with significantly different melting points: from 1260 °C (MgF_2) to 2410 °C (Y_2O_3). A powerful radiation flux induces effective mixing of the base components of the mixture and dopants, their composition elements.

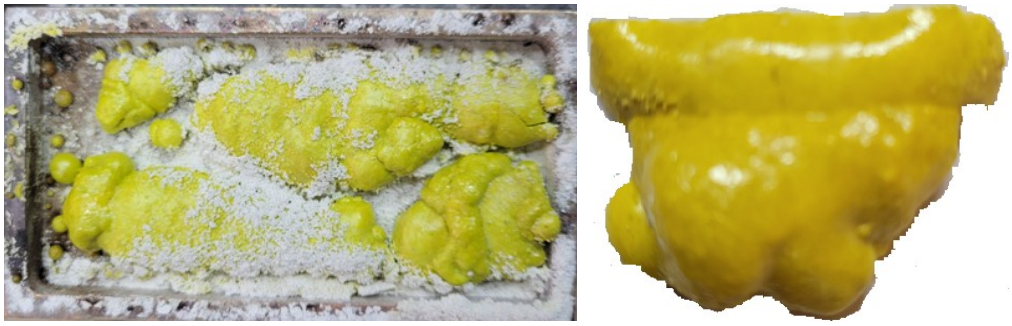

Fig.1 Photos of samples.

The cause of very high efficiency of radiative synthesis is largely incomprehensible. It is assumed that power densities of radiation fluxes used in the study increase ionization density of materials. Within the synthesis period, radiation creates a number of electronic excitations comparable to the number of lattice sites in the irradiated area. The electronic excitation decay causes formation of a high concentration of active radiolysis products, their interaction, and formation of new phases. Decomposition occurs at high temperatures and, hence, with an extremely high yield.

The report is supposed to show the main patterns revealed in synthesis of materials based on metal oxides and fluorides to formulate the basic ideas about the totality of processes occurring in dielectric materials in the field of powerful hard radiation fluxes.

REFERENCES

[1] V M Lisitsyn, M G Golkovsky, D A Musakhanov, A T Tulegenova, Kh A Abdullin and M B Aitzhanov “YAG based phosphors, synthesized in a field of radiation”, IOP Conf. Series: Journal of Physics: Conf. Series,V. 1115, P. 052007, 2018.

[2] V.M. Lisitsyn, M.G. Golkovskii, L.A. Lisitsyna, A.K. Dauletbekova, D.A.Musakhanov, V.A. Vaganov, A.T. Tulegenova, Zh.T. Karipbayev, “MgF2–Based Luminescing Ceramics,” Russian Physics Journal, V.61, Issue 10, P. 1908–1913, 2019

R3-P-013603

OUTCOME COMPARISON OF TREATMENT OF BRAIN METASTASES IN HYPOFRACTIONATION AND STAGED RADIOSURGERY

A.V. SHILENKO[1], V.V. KRASNYUK[2], D.A. BUTOVSKAYA[2], K.O. STAVITSKAYA[2]

[1]Novosibirsk State University, Novosibirsk, Russia
[2]Medical and Diagnostic Center of the Sergey Berezin International Institute of Biological Systems, Novosibirsk, Russia

Oncological diseases are among the most common diseases in the world, from which, according to The Global Cancer Observatory, more than 9.9 million people died in 2020. The characteristic features of cancer are rapid cell division, the ability to penetrate into surrounding tissues, as well as metastasize to other organs. Brain metastases occur in 20-40% of cancer patients [1]. The main methods of treatment are neurosurgical intervention, radiation therapy, and stereotactic radiosurgery is actively developing [2-3]. The advantage of radiosurgery is non-invasiveness, the effectiveness of exposure to foci and the low probability of radiation reactions after treatment. However, in patients with a tumor volume exceeding 3 centimeters in diameter, with radiosurgical doses (>18 Gy), the risk of post-radiation complications are subsequently high, therefore radiosurgical methods of hypofractionation and staged radiosurgery are increasingly used. The research included a group of patients (9 people) who underwent treatment by the method of trained radiosurgery and a group of patients (14 people) who underwent hypofractionation. The median age of patients at the time of the 1st PC session or HF was 56 years (range 37-82 years), the median KPS was 75% (range 50-90%). The study groups were dominated by patients with MGM breast cancer – 36% patients. Significantly less often the source of MGM was: lung cancer - 18% of patients, gastrointestinal cancer - 18% of patients, melanoma - 9% of patients, uterine cancer - 9% of patients, kidney and bladder cancer - 5% of patients. In a 1 case, the metastases were a manifestation of primary multiple cancer - 5%. The clinical study was conducted at the Leksell Gamma Knife Icon installation (Stockholm, Sweden). The summed dose was in the range from 16 to 30 Gy.

The purpose of our study was to study and compare the results of the use of hypofractionation methods and staged radiosurgery for brain metastases. Changes in the volume of tumors 1 month after treatment by hypofractionation or staged radiosurgery are shown in Figure 1.

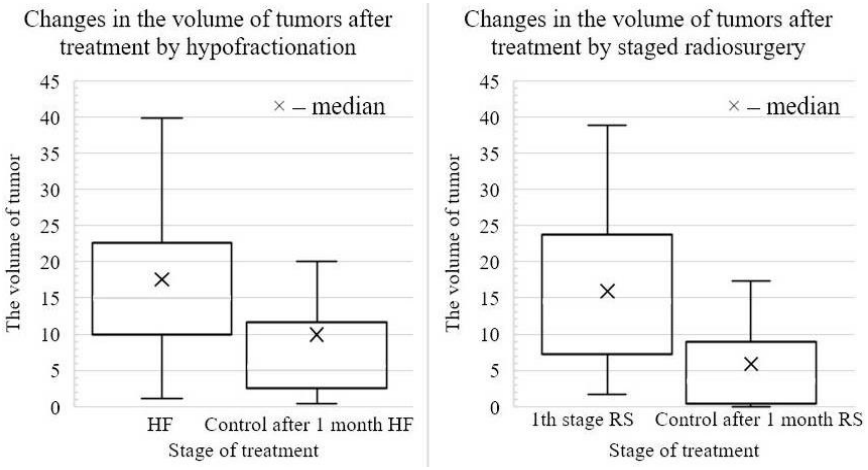

Fig.1. Changes in the volume of tumors after treatment by hypofractionation or staged radiosurgery.

The work shows that the trained radiosurgery provides satisfactory indicators of local control and is comparable to the hypofractive method of treatment of large intracranial metastases in the absence of the possibility of surgical removal.

REFERENCES

[1] J.S. Barnholtz-Sloan, A.E. Sloan, R.E. Sawaya, at al, "Incidence proportions of brain metastases in patients diagnosed (1973 to 2001) in the Metropolitan Detroit Cancer surveillance System", J. Clin. Oncol., vol. 22 , no. 14, pp. 2865–2872, July 2004.

[2] V.N. Kornienko, I.N. Pronin, Diagnostic neuroradiology. Volume 1, Moscow: Institute named after Burdenko, 2008.

[3] I.K. Osinov, A.V. Golanov, S.M. Banov, A.E. Artemenkova, V.V. Kostyuchenko, A.V. Dalechina, "Interned radiosurgery in the treatment of patients with metastatic brain damage", The Russian Journal of Neurosurgery, vol. 23, no. 1, pp. 26-37, April 2021.

R3-P-027302

THE ESTABLISHMENT OF RELATIVE BIOLOGICAL EFFECTIVENESS OF CARBON ION RADIATION IN ZEBRAFISH TESTES *

HONG ZHANG[1], *HONGYAN LI*[1]

1Institute of Modern Physics, Chinese Academy of Sciences, Lanzhou, China

With the development of nuclear technology, the risk of exposure to ionizing radiation (IR) becomes greater during radiotherapy used by carbon ions, the release of multiple radioisotopes following nuclear accidents, and the high-energy ions encountered during space missions [1]. Thus, the development of methods to reveal the harmful mechanism of IR is necessary. The process of spermatogenesis involves multiple spermatogenic cells in the testis, which is one of the most radiosensitive organs [2]. Radiation can induce necrosis, autophagy, apoptosis, premature senescence, and accelerated or delayed differentiation in germ cells, leading to cell death. We have shown that high linear energy transfer (LET) ions can seriously damage mouse testis and induce apoptosis of spermatogenic cells [3]. This process directly involves mitochondria since mitochondrial pathways appear to regulate heavy ion radiation (HIR) -induced apoptosis in spermatogenic cells [3]. This study compared the relative biological effectiveness (RBE) of carbon ion radiation (CIR) and X-ray irradiation in zebrafish testes at 7 days after irradiation. The logarithmic dose-response curves for the percentage of testes weight are shown in Fig. 1. At 7 days after irradiation, the X-ray dose for 50% reduction of testes weight was 13.2, the CIR dose for 50% reduction of testes weight was 8.86, the RBE of CIR in zebrafish testes was calculated as 1.48. From the dose-dependent curve, when testes weight was reduced to 70%, the dose of CIR was 3.8 Gy. Coincidentally, 4 Gy is commonly used as a high dose single-fraction. Although such a dose can increase long-term survival in childhood cancer patients, it increases the risk of infertility. Therefore, we chose 4 Gy as a single-fraction of high dose in radiotherapy or to simulate the one-off high dose or long−term accumulation of radiation under radiation environment.

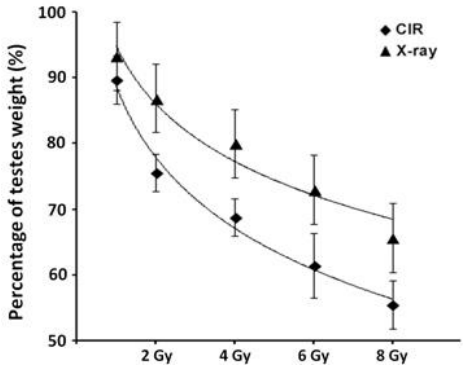

Fig.1. The RBE of CIR in zebrafish testes and the different biological effect in testicular cells apoptosis between X-ray and CIR.

REFERENCES

[1] C. Zeitlin , D. M. Hassler , F. A. Cucinotta , B. Ehresmann, R. F. Wimmer-Schweingruber, D. E. Brinza, S. Kang S, G. Weigle, S. Böttcher, E. Böhm, S. Burmeister, J. Guo, J. Köhler, C. Martin, A. Posner, S. Rafkin, G. Reitz, "Measurements of energetic particle radiation in transit to Mars on the Mars Science Laboratory," Science. vol. 340, no. 6136, pp. 1080-1084, May 2013.

[2] S. Khan, J. S. Adhikari, M. A. Rizvi, N. K. Chaudhury, "Radioprotective potential of melatonin against ^{60}Co γ-ray-induced testicular injury in male C57BL/6 mice," J Biomed Sci. vol. 24, no. 1, Jul 2015.

[3] H. Li, B. Wang, H. Zhang, T. Katsube, Y. Xie, L. Gan, "Apoptosis Induction by Iron Radiation via Inhibition of Autophagy in Trp53+/- Mouse Testes: Is Chronic Restraint-Induced Stress a Modifying Factor?," Int J Biol Sci. vol. 14, no. 9, pp. 1109-1121, Jun 2018.

* The work was supported by the Ministry of Science and Technology National Key R&D project (SQ2018YFE020524).

R3-P-908801

CREATION OF ZNSE NANOCLUSTERS IN A SILICON DIOXIDE TRACK TEMPLATE ON SILICON

A.D. AKYLBEKOVA, A.K. DAULETBEKOVA, Z.K. BAIMUKHANOV1, A.T.AKILBEKOV

[1]Eurasian National University named after L.N. Gumilyov, Nur-Sultan, Kazakhstan

In this work, we study the formation of zinc selenide nanocrystals during chemical deposition into a-SiO_2/Si-n track template. The relevance of the study is related to the production of new nanoclusters using track templates. One of the methods for obtaining nanoclusters is template synthesis. Template synthesis is a relatively simple and easy procedure, thanks to which the fabrication of rather complex nanomaterials has become available to almost any laboratory [1].

For the first time, zinc selenide nanocrystals were obtained by chemical precipitation in an aqueous alkaline medium using sodium selenosulfate as a source of Se ions. The deposition was carried out at a temperature of t = 75^0C for 40 min. The morphology was observed using scanning electron microscopy, and the crystalline phase was studied using X-ray diffraction analysis. Figure 1 shows the template surfaces after chemical deposition of ZnSe. SEM images of the study showed that most of the pores of the template are filled and the chemical precipitation method is excellent for growing with controlled morphology and a high degree of order. It has been established that the filling of nanopores depends on the temperature and deposition time (Fig. 1).

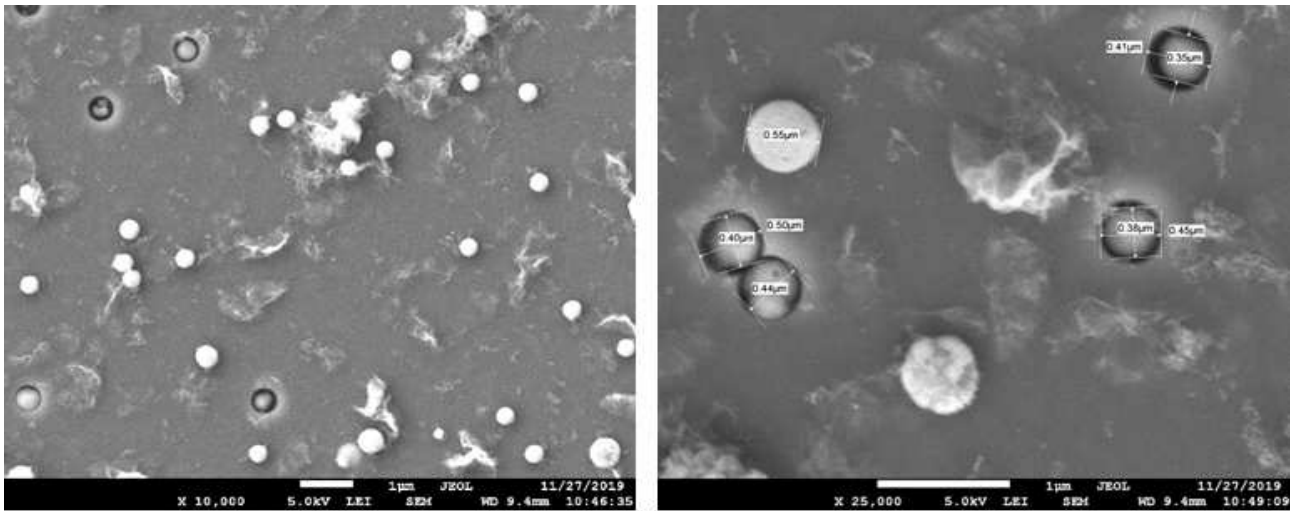

Fig.1. SEM images of the surface after CD of ZnSe for 40 min, at a temperature of t = 75^0C, on average, the nanopore diameter is from 410 nm to 550 nm..

To confirm the obtained ZnSe phase by X-ray diffraction analysis, we performed elemental analysis on a TM3030 scanning electron microscope.

The crystalline phase of the sample is a cubic structure (sphalerite) with space group F-43m. The unit cell parameters are: a = 5.592081 Å and corresponds with the results of other works. The unit cell parameters obtained by us coincide with the literature data [2]. Thus, in this work, the structural, morphological, and electronic properties of ZnSe nanocrystals of zinc selenide, obtained for the first time by chemical deposition into a-SiO_2/Si-n track templates, have been studied and characterized.

REFERENCES

[1] P. Ugo, L.M. Moretto, “Template deposition of metals”, Handbook of Electrochemistry, pp. 678-709, 2007.

[2] A. Continenza, S. Massidda, A. J. Freeman, "Structural and electronic properties of bulk ZnSe", Phys. Rev. B 38, p.12996, 1988.

R3-P-914301

PRE-SOWING STIMULATION OF POTATO WITH UVB RADIATION OF XeCl-EXCILAMP*

A.G. BURACHENKO[1], E.A. SOSNIN[1,2], I.A. VICTOROVA[3], Yu.V. CHUDINOVA[3], L.V. LUASHEVA[4]

[1]Institute of High-Current Electronics SB RAS, Tomsk, Russia
[2]National Research Tomsk State University, Tomsk, Russia
[3]Siberian Research Institute of Agriculture and Peat – a Branch of Federal State Budgetary Institution, Tomsk, Russia
[4]Northern Trans-Ural State Agricultural University, Tyumen, Russia

In modern plant science are relevant search for ways of seeds dormancy breaking to obtain earlier and good sprouts, laying the basis for increasing the yield, obtaining early and high-quality products. Currently, it has been established that various physical factors, such as plasma, gamma radiation, microwave fields, as well as optical radiation in optimal doses can stimulate seed germination and plant development [1, 2]. In particular, a lot of research is devoted to ultraviolet radiation effect on plants [3].

The UVB spectrum range (290-320 nm) action on plants is scantily known. In our works [4, 5] it was found that UVB radiation *subdoses* has a stimulating effect on a variety of crops during pre-sowing seed treatment. Independent studies (see review [6]) confirm our data.

The aim of current work is to study the growth and development of potato tubers ("Gala" cultivar) when treated with subdoses of UV-B radiation (option 1). In another variant, the tubers were additionally treated with a plant growth stimulator «Humophyte» (option 2). Planting and cultivation of plants was carried out in the field in the Kravtsovskoye farm (Tomsk district of Tomsk, Russian Federation).

It was found that the maximum yield was obtained in option 2. This is 429 c/ha, which is 139 c/ha more than the control variant and 100 c/ha compared to option 1. It is shown that experimental potato plants sprang earlier, accelerated growth was observed, and an increase in leave assimilating surface. These effects are most pronounced in option 2. The report also provides data on the nutritional parameters of tubers from the resulting crop and their infection with various pathogens.

Based on the data obtained, a conclusion is made about the prospects of using UVB radiation XeCl-excilamps for pre-sowing stimulation of potatoes, including in combination with plant growth enhancers.

REFERENCES

[1] T. Ohta, M. Shiratani, M. Hori, “Current status and future prospect of agricultural applications using atmospheric-pressure plasma technologies,” Plasma Process. Polym. vol. 15, no. 2, 201700073, 2018.

[2] S. S. Araújo, S. Paparella, D. Dondi, A. Bentivoglio, D. Carbonera, A. Balestrazzi, “Physical Methods for Seed Invigoration: Advantages and Challenges in Seed Technology,” Front. Plant Sci., vol. 7, 646, 2016.

[3] D. Thomas, T. T. Jos, T. Puthur, “UV radiation priming: A means of amplifying the inherent potential for abiotic stress tolerance in crop plants,” Environmental and Experimental Botany, vol. 138, no. 6, pp. 57□66, 2017.

[4] E. A. Sosnin, Y. V. Chudinova, I. A. Victorova, I. I. Volotko, “Application of excilamps in agriculture and animal breeding (review),” Proc. SPIE : XII International Conference on Atomic and Molecular Pulsed Lasers, vol. 9810, 98101K, 2015.

[5] E. A. Sosnin, P. A. Gol'tsova, Y. V. Chudinova, L. V. Lyasheva, V. A. Panarin, I. A. Prok, V. S. Skakun, I. A. Viktorova, T. P. Astaphyrova, “Photoregulation of agricultural plants growth and development by XeCl-excilamp,” Proc. SPIE : XIV International Conference on Pulsed Lasers and Laser Applications, vol. 11322, 1132226, 2019.

[6] M. Schreiner, J. Martínez-Abaigar, J. Glaab, M. Jansen, “UV-B Induced Secondary Plant Metabolites: Potential benefits for plant and human health,” Optik & Photonik, 2014, no. 2, pp. 34□37, 2014.

* The studies were performed in the framework of the State Task for IHCE SB RAS, project # FWRM-2021-0014.

MAGNETIZATION STUDY OF LI-ZN FERRITE SYNTHESIZED BY AN ELECTRON BEAM*

S.A. GHYNGAZOV[1], *E.N. LYSENKO*[1], *V.A. VLASOV*[1], *A.P. SURZHIKOV*[1], *M.V. KOROBEYNIKOV*[2]

[1]*National Research Tomsk Polytechnic University, Tomsk, Russia*
[2]*Budker Institute of Nuclear Physics SB RAS, Novosibirsk, Russia*

In this work, the magnetization of lithium-zinc ferrite synthesized under the conditions of electron beam heating of a powdered and compacted Fe_2O_3-Li_2CO_3-ZnO mixture was studied. For the synthesis of samples, an ILU-6 pulsed electron accelerator located at the Budker Institute of Nuclear Physics of Siberian Branch Russian Academy of Sciences was used [1]. The samples were heated by a 2.4 MeV high-energy electrons beam to synthesis temperatures of 600, 700, 750 °C and kept at these temperatures for up to 120 minutes. To establish the radiation effects arising during electron beam synthesis, another part of samples was obtained using traditional thermal annealing in a laboratory furnace under the same conditions.

The magnetization of the synthesized ferrite was studied in two ways, including measurements of the specific saturation magnetization (σ_S) using a magnetometer and thermomagnetometric measurements using a thermal analyzer. The latter, based on thermogravimetry in a magnetic field, makes it possible to analyze magnetic phase transitions in samples and determine their Curie temperature [2]. The data obtained from the results of measuring the specific magnetization of the samples are shown in Fig. 1.

a **b**

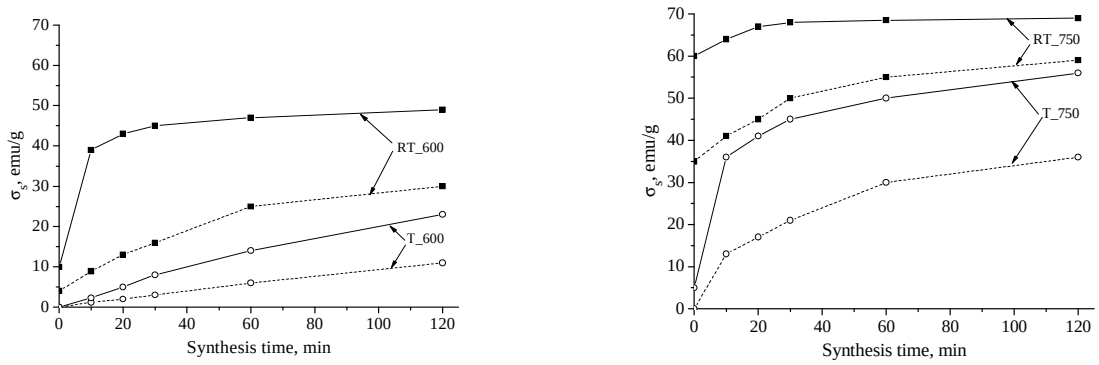

Fig. 1. Kinetic dependences of the specific magnetization of Li-Zi ferrite synthesized using an electron beam (RT) and thermal annealing (T) at a synthesis temperature of 600 (a) and 750 (b) °C: lines - compacted samples; dotted lines - powdered samples

The results obtained showed that the specific magnetization in the RT-synthesized samples significantly exceed the values of σ_S in the samples obtained by thermal annealing at the same temperature and time of synthesis. The results also revealed a higher degree of specific magnetization of compacted samples compared to powdered samples, which indicates a higher content of the spinel magnetic phase in the synthesized compacts.

Thus, it was found that the ferrite formation rate depends both on the heating method and on the density of the mixture. The specific magnetization for sample obtained from compacted mixture and RT-synthesized at 750 °C for 120 min is close to the nominal values of σ_S for Li-Zi ferrites, which indicates high content of ferrite in the synthesized samples.

Thus, measurements of the specific magnetization revealed the radiation effect of the accelerated formation of spinel magnetic phases during heating of ferrite mixtures by a beam of high-energy electrons. This conclusion is confirmed by thermomagnetometric and XRD data [3].

REFERENCES

[1] E.N. Lysenko, E.V. Nikolaev, V.A. Vlasov, A.P. Surzhikov, "Technological scheme for lithium-substituted ferrite production under complex high-energy impact," Nucl. Instr. Meth. B, vol. 474, pp. 49-56, 2020.

[2] A.L. Astafyev , E.N. Lysenko, A.P. Surzhikov, "Thermomagnetometric analysis of lithium ferrites," J. Therm. Anal. Calorim., vol.136, pp. 441-445, 2019.

[3] E.N. Lysenko, V.A. Vlasov, A.P. Surzhikov, A.I. Kupchishin, "Kinetic Study of Lithium–Zinc Ferrite Synthesis under Electron Beam Heating Conditions," Inorganic Materials: Applied Research, vol.13(2), pp. 494–500, 2022.

* The work was supported by the Russian Science Foundation under grant No. 22-19-00183.

R3-P-955102

INFLUENCE OF ADDITIVES ON SINTERING OF POWDER COMPACTS OF PARTIALLY STABILIZED ZIRCONIUM DIOXIDE*

S.A. GHYNGAZOV, E.N. LYSENKO, A.P. SURZHIKOV, I.P. VASILIEV

National Research Tomsk Polytechnic University, Tomsk, Russia

The study of powder sintering at low pressing densities up to bulk density is important for the manufacture of ceramic products by 3D printing. In this regard, a special role should be given to the use of the technique of doping powders with various fusible additives, which facilitate the process of interparticle interaction during heating. It is assumed that the role of additives will be extremely important in the development of 3D printing by radiation-thermal heating, in particular, by an electron beam [1]. To develop technological methods for sintering powders at bulk density, it is important to study the effect of additives and pressing pressure on the sintering of powder compacts.

The paper considers the influence of additives in the amount of not more than 5% on the processes of compaction of powdered ceramic masses during compaction by the method of uniaxial pressing at various pressures and subsequent sintering in a resistance furnace. The starting materials were powders of partially stabilized zirconia obtained by the sol-gel method (TOSOH, Japan) and by the plasma-chemical method (Siberian Chemical Plant). Polyvinyl alcohol, bismuth oxide, carbon were used as additives. A study was made of the influence of the type (Fig. 1), additive concentration (Fig. 2) and pressing pressure on the characteristics of sintered ceramics. It has been established that small amounts of additives do not worsen the properties of sintered ceramics, and sometimes even improve them.

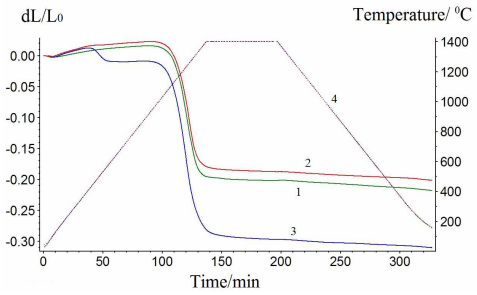

Fig.1. Influence of carbon concentration on densification of zirconium ceramics. 1 - no additive. 2 - 1% carbon. 3 - 5% carbon. 4 - temperature program.

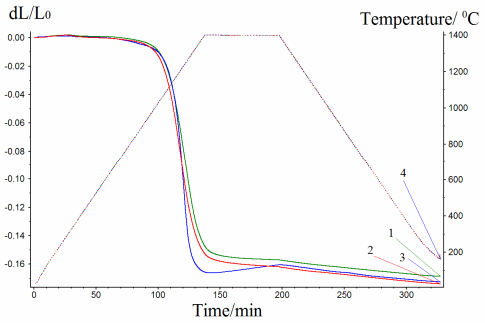

Fig.2. Influence of additive type on densification of zirconium ceramics.1 - without additive. 2 - addition of 1% PVA. 3 - addition of bismuth oxide 1%. 4 - temperature program.

The report also presents the results of a study of the mechanical properties of ceramics with and without additives.

REFERENCES

[1] V.K.V. Pasagada, N.Yang and C. Xu, "Electron beam sintering (EBS) process for Ultra-High Temperature Ceramics (UHTCs) and the comparison with traditional UHTC sintering and metal Electron Beam Melting (EBM) processes," Ceramics International, vol. 48(7), P. 10174-10186, 2022.

* The work was supported by the Russian Science Foundation under grant No. 22-19-00183.

R4-O-002101

FORMATION PROCESSES OF DISK-SHAPED CLUSTERS IN CHAOTIC SYSTEMS

G.A. MELNIKOV, N.M. IGNATENKO, A.S. GROMKOV

Southwest State University (SWSU), Kursk, Russia

The process of self-organization of particles with chaotic motion into a cluster system begins with a situation that randomly arises as a result of fluctuations, when two particles are at a distance equal to the distance of the minimum potential energy of interaction between two particles, but the binding energy is not enough to form their bound state [1, 2]. In this case, the appearance of the third particle at a distance exceeding the distance between the close pair leads to the appearance of the Efimov effect (Fig. 1).

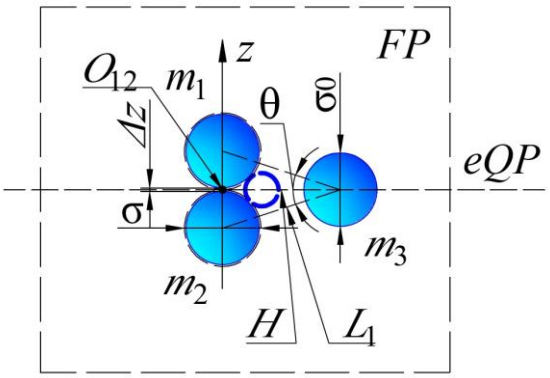

Fig.1. The Efimov effect in a three-particle cluster with the arrangement of particles according to the rule of the "golden" triangle in the model of absolutely hard spheres.

The diameter of one of the two interacting particles σ (in the dimer) and the distance to the third disturbing particle L_1 will be determined based on the properties of the "golden" triangle [3, 4]:

$$L_1 = \frac{\sigma}{2\sin\frac{\theta}{2}} = \Phi \cdot \sigma\,, \qquad (1)$$

where θ is the "golden" angle, Φ = 1.6180339… is the value of the "golden" proportion ("golden" ratio).

In the equatorial plane of the disk-shaped cluster, a centrally symmetric system is formed with the center at the center of mass of the dimer and circular formations of densely packed absolutely hard spheres. Such formations in the equatorial plane are characteristic of the structure of planar clusters (2D clusters), which have recently been actively studied [5].

In the structure of a disk-shaped cluster as an independent physical object, the formation of a nano-sized potential region in the form of a toroid is possible. When such clusters are irradiated with proton-ion beams, a toroidal quantum dot is formed into their structure [6].

REFERENCES

[1] V. Efimov, “Energy levels of three resonantly interacting particles,” Nucl. Phys. A, vol. 210, pp. 157–188, 1973.

[2] P. Naidon, S. Endo, “Efimov Physics: a review,” arXiv:1610.09805v2 [quant], 7 Apr 2017.

[3] The Fibonacci Association:http://www.mscs.dal.ca/Fibonacci/.

[4] The Fibonacci Quarterly: http://www.fq.math.ca/.

[5] G.A. Melnikov, “Clusters of Fibonacci in the structure of condensed medium,” Izv. Vyssh. Uchebn. Zaved. Fiz., vol. 61, no. 9-2 (729), pp. 207–210, June 2018.

[6] Y. Chiu, Li-Wei Huang, Ching-Ming Wei, Chia-Seng Chang, T. Tsong, “Magic numbers of atoms in surface-supported planar clusters,” Phys. Rev. Lett., vol. 97, p. 165504, 2006.

[7] G.A. Melnikov, N.M. Ignatenko, A.S. Gromkov, "Quantum dots in structure of quasicrystalline systems," Journal of Physics: Conference Series, vol. 1347, pp. 012031(6pp), 2019.

R4-O-009001

NANOSTRUCTURE OF OXIDE DISPERSION-STRENGTHENED STEELS AND ITS REARRANGEMENT UNDER ION IRRADIATION

KLAUZ A.V.[1,2], KHOMICH A.A. [1,2], BOGACHEV A.A. [1,2], NIKITIN A.A. [1,2], ZALUZHNYI A.G. [1,2], ROGOZHKIN S.V. [1,2]

[1] *National Research Center "Kurchatov Institute", Moscow, Russian Federation*
[2] *National Research Nuclear University MEPhI (Moscow Engineering Physics Institute), Moscow, Russian Federation*

Dispersion-strengthened oxide steels are prominent potential core materials for the next generation of fast-neutron reactors as well as perspective thermonuclear reactors. These steels are expected to withstand radiation loads up to damaging doses of around 200 dpa at irradiation temperatures of 400-700°C. Such loads can be withstood by materials due to being reinforced by small oxide particles which create barriers for dislocation movement as well as pining grain boundaries.

Production method of powder metallurgy allows for size and composition optimization of small inclusions, which leads to an increase of mechanical properties and radiation stability of affected steels. Mechanical properties of ODS steels significantly depend on characteristics of the nanostructure: the size and spatial distribution of dispersed inclusions and nanoscale clusters. These particles provide a significant increase in the creep strength, being effective barriers for dislocation motion.

The aim of this work was to study the initial state of the ODS steel samples with different alloying systems as well as conducting studies for irradiated samples to observe stability of inclusions and of the entire microstructure. Irradiated samples were obtained through ion beam irradiation, since it is considered that these types of defects (as well as their size and number density) caused by neutron bombardment from the nuclear reaction to be closely reproduced with the ion beam experiments.

To analyze the evolution of oxide inclusion and cluster distribution in the material during irradiation, simulation experiments were carried using Fe^{2+} ion irradiation at 5.6 MeV using samples of multiple ODS steels: KAERI 10Cr ODS, KP-3 ODS and Eurofer ODS.

Irradiation with doses of 3, 6 and 30 dpa at 350 °C was used to analyze low-temperature radiation embrittlement and its effects on material nanostructure. Additionally, studied steels were irradiated up to 100 dpa at 500 °C in order to analyze the oxide inclusion stability at enhanced temperatures of high dose irradiation.

The study of initial and irradiated materials was carried out using modern ultramicroscopy methods: transmission electron microscopy (TEM) and atom probe tomography (APT). This combination of techniques allowed for study of both small and large inclusions (oxide particles and clusters) as well as the analysis of their chemical composition.

The local nanochemical APT analysis showed the presence of high density of clusters with sizes of 2–5 nm. In all the steels studied, the clusters were enriched in Cr, Y, and O atoms. In Eurofer ODS steel, clusters also contained V atoms; there were Ti atoms in clusters in 10Cr ODS and KP-3 ODS steels, while clusters in KP-3 ODS steel also contained Al atoms.

The analysis after irradiation showed dissolution of both larger oxides and clusters. At 350 °C this effect was most prominent for ODS KP-3 with clusters that were no longer detectable at 30 dpa. As for Eurofer ODS, it had the most stable clusters and oxide particles when irradiated to 30 dpa.

The dissolution effect was even more prominent at 100 dpa and 500 °C. Which allowed us to determine which steels are more appropriate for nuclear core applications since oxide particles play a key role in radiation stability under operational conditions.

R4-O-009904

AB-INITIO CALCULATIONS OF ELECTRONIC PROPERTIES OF β-Ga_2O_3 OWN DEFECTS

ZH. KOISHYBAYEVA[1], A. AKILBEKOV[1], A. USSEINOV[1]

[1]Faculty of Physics and Technical Sciences, L.N. Gumilyov Eurasian National University,
Nur-Sultan, Kazakhstan

Gallium oxide is known in the scientific community for its unique electrical and optical properties. Due to its wide bandgap (~5.0 eV), it is of interest to scientists as a promising material in various fields of power electronics, optoelectronics, and photonics. [1, 2, 3].

The reflection spectrum [4] was calculated in the work for the direction of the electric vector E parallel to the b axis (E||b) (Fig. 1). It can be seen in the figure that the calculated IR reflections of the wave vector q⊥(100) and E||b are comparable with the experimental data [5], and the IR reflections of the wave vector of the other direction q⊥ (-201) and E||b are comparable with work [6]. In the work [6], pure TO phonons with Au symmetry are also observed.

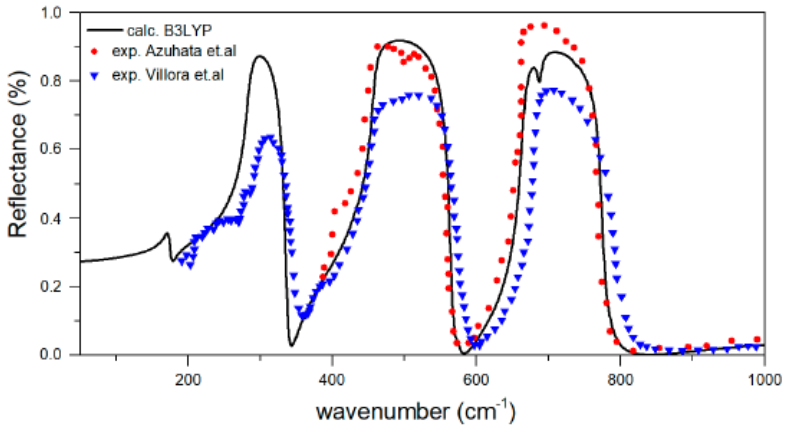

Figure 1. Estimated IR reflectance for the wave vector q⊥(100) and a specific direction of the electric vector E||b. Experimental data are presented for comparison. [5, 6]

Oxygen vacancies of gallium oxide are deep donors, since its transition levels are 1 eV below the minimum of the conduction band, and gallium vacancies are deep acceptors with empty levels that are located more than 0.7 eV above the valence band and rather lower than the donor level. [7]

Due to the fact that oxygen vacancies can easily donate their electrons to gallium vacancies, the energy of formation of oxygen vacancies decreases as the number of donors in the crystal decreases. In parallel with this process, an increase in the energy of formation of acceptors occurs, which leads to a decrease in the energy of formations of donors. Ultimately, this leads to an energy balance between the two processes and results in a constant concentration of native donors and acceptors. [7]

We assume that the observed n-type conductivity in β-Ga_2O_3 crystals can be caused by light doping of a donor impurity during crystal growth, such as hydrogen. Our calculations also show that gallium vacancies cannot be involved in p-type conductivity in β-Ga_2O_3. Because all types of gallium vacancies with different charge states are located above the valence band by more than 0.7 eV.

REFERENCES

[1] Higashiwaki M., Sasaki K., Kuramata A., Masui T., Yamakoshi S., "Gallium oxide (Ga_2O_3) metal-semiconductor field-effect transistors on single-crystal β-Ga_2O_3 (010) substrates", Appl. Phys. Lett., vol. 100, 2012

[2] Pearton S.J., Yang J., Cary P.H., Ren F., Kim J., Tadjer M.J., Mastro M.A. "A review of Ga_2O_3 materials, processing, and devices", Appl. Phys. Rev., vol. 5, 2018

[3] Zhang, J., Shi J., Qi D.-C., Chen L., Zhang K.H.L., "Recent progress on the electronic structure, defect, and doping properties of Ga_2O_3.", APL Mater., vol. 8, 2020

[4] Demichelis R., Suto H., Noël Y., Sogawa H., Naoi T., Koike C., Chihara H.;, Shimobayashi N., Ferrabone M., Dovesi R., "The infrared spectrum of ortho-enstatite from reflectance experiments and first-principle simulations", Mon. Not. R. Astron. Soc., vol. 420, 2012, pp. 147–154

[5] Víllora E.G., Morioka Y., Atou T., Sugawara T., Kikuchi M., Fukuda T., "Infrared reflectance and electrical conductivity of β-Ga_2O_3", Phys. Status Solidi Appl. Res., vol. 193, 2002, pp. 187–195

[6] Azuhata T., Shimada K., "Polar phonons in β-Ga_2O_3 studied by IR reflectance spectroscopy and first-principle calculations", Appl. Phys. Express, vol. 10, 2017

[7] Abay Usseinov , Zhanymgul Koishybayeva , Alexander Platonenko , Vladimir Pankratov , Yana Suchikova, Abdirash Akilbekov, Maxim Zdorovets, Juris Purans, Anatoli I. Popov, "Vacancy Defects in Ga_2O_3: First-Principles Calculations of Electronic Structure", Materials, vol. 14, 2021

R4-O-015101

EFFECT OF γ-n-PULSE ON AlGaAs LEDs*

F.F. ZHAMALDINOV[1], *A.V. GRADOBOEV*[1], *K.N. ORLOVA*[3], *A.V. SIMONOVA*[3]

[1]*National Research Tomsk Polytechnic University, Tomsk, Russian Federation*
[2]*National Research Nuclear University MEPhI, Moscow, Russian Federation*
[3]*Scientific and Engineering Centre for Nuclear and Radiation Safety, Moscow, Russian Federation*

The results of studying the effect of a γ-n-pulse on IR LEDs based on AlGaAs heterostructures are presented. The LEDs were tested in active and passive power modes. During the irradiation of LEDs in the active power mode after exposure to a γ-n - pulse (indicate *D* gamma and neutron flux), the LED radiation power is restored by *ΔP*. The regularity of LED power decrease in active and passive power supply modes is determined. It has been suggested that the restoration of the radiation power *ΔP* during irradiation with a γ-n-pulse in the active power supply mode of the LED is due to radiation-stimulated and/or electrically stimulated annealing of local mechanical stresses in the LED.

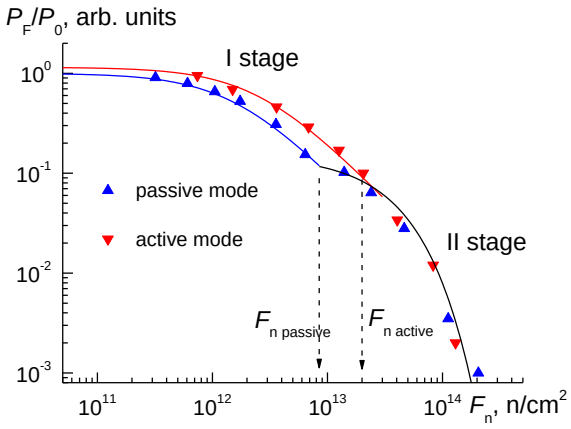

Fig.1. Variation of LED emission power (of 50 mA operating current) when exposed to γ-n-pulse in active and passive power modes: symbols – measurement results; lines – determined regularities (1-3); stage I, stage II – common stages of radiation power reduction; $F_{n\ passive}$ $F_{n\ active}$ – threshold values of neutron fluences at the boundary between selected stages for the respective irradiation modes

REFERENCES

[1] C. Claeus, E. Simoen "Radiation effects in advanced semiconductor materials and devices," Springer Series in Materials Science, vol. 57, p.351, 2002.

[2] V.N. Brudny, V.V Peshev, A.P. Surjikov "Radiation-induced defects formation in electric fields: gallium arsenide, indium phosphide," Novosibirsk: Nauka, p. 136, 2001.

[3] V.M. Ardyshev, A.A Verigin., Yu.Yu. Kryuchkov, A.P. Mamontov, I.P. Chernoc "Thermal annealing of defects in gallium arsenide irradiated by sulphur ions," Physics and Technology of Semiconductors, vol. 18, issue 2, pp.316–318, 1984.

[4] A.V. Gradoboev, K.N. Orlova, A.V. Simonova "The fast neutron irradiation influence on the AlGaAs IR-LEDs reliability," Microelectronics Reliability, vol. 65, pp.55-59, 2016

[5] A.V. Gradoboev, K.N. Orlova"Radiation Model Light Emitting Diodes Based on AlGaInP Heterostructures with Multiple Quantum Wells," Advanced Material Research, vol. 880, pp. 237-241, 2016

[6] A.V. Gradoboev, V.V. Sednev, A.V. Simonova, F.F. Zhamaldinov "Influence of long-term operation on the resistance of LEDs to irradiation gamma-quanta," 7th International Congress on Energy Fluxes and Radiation Effects (EFRE-2020 online): Abstracts, Tomsk: Publishing House of IAO SB RAS, p. 451, 2020.

[7] A.V. Gradoboev, E.P. Tesleva "Local Mechanical Stress relaxation of in Gunn Diodes irradiation by protons," IOP Confer. Series: Journal of Physics: Conf. Series 830, p. 9 , 2017.

* The work was supported by the Tomsk Polytechnic University Development Program.

R4-O-016301

OPTICAL EFFECTS AND TRACKS IN BAFBR CRYSTALS IRRADIATED WITH FAST KRYPTON IONS.

D. KENBAYEV[1], A. DAULETBEKOVA[1], E. F. POLISADOVA[2], A. I. POPOV[3], A. AKILBEKOV[1], ZH. KARIPBAYEV[1], M. ZDODROVETS[4,5], V. YU. YAKOVLEV[2]

[1]*L. N. Gumilyov Eurasian National University, Nur-Sultan, Kazakhstan*
[2]*Tomsk Polytechnic University, Tomsk, Russia*
[3]*Institute of Solid State Physics, University of Latvia, Riga, Latvia*
[4]*Astana branch of Institute of Nuclear Physics, Nur-Sultan, Kazakhstan*
[5]*Ural Federal University, Yekaterinburg, Russia*

In this work using photoluminescence (PL), X-Ray excited optical luminescence (XEOL), pulsed cathodoluminesence (PCL), optical absorption (OA), Raman spectroscopy (RS) and atomic force microscopy (AFM) the radiation damage and degradation of BaFBr crystals irradiated with 147 MeV ^{84}Kr ions to fluences (10^{10}-10^{14}) ion/cm^2 were investigated. BaFBr crystals were grown by the Steber method in a graphite crucible in a helium-fluoride atmosphere using stoichiometric mixtures of $BaBr_2$ and BaF_2. The effect of the oxygen impurity, which is present in the studied crystals, is also considered. In the spectra of PL and XEOL detected bands associated with oxygen impurity placing the halide sites. In the XEOL spectrum, except for the emission band associated with oxygen impurity the luminescence band of a self-trapped exciton is also observed. The quenching and shift of the PL and XEOL maximum with increasing fluence is due to the overlapping of tracks and aggregation of defects. Electronic and hole aggregate color centers arise mainly in the bromide sublattice. High irradiation doses lead to crystal degradation. In the process of recording the spectra of PCL in the region of 2-4 eV, a change in the intensity of the glow was observed both in the microsecond and nanosecond ranges. The absorption bands found in the ultraviolet region at 4.2 eV are attributed to the exciton emission of Br^- [1].

REFERENCES

[1] E A Radzhabov and A V Egranov, “Exciton emission in BaFBr and BaFCl crystals,” J. Phys. Condens. Matter, vol. 6, pp. 5639-5645, 1994.

R4-O-021401

SWIFT HEAVY ION TRACKS IN NANOCRYSTALLINE Y4Al2O9 AND Y2Ti2O7*

A.K. MUTALI[1,2,3], *A. IBRAYEVA*[2,4], *A. JANSE VAN VUUREN*[4], *J. O'CONNELL*[4], *E. KORNEEVA*[3], *A. SOHATSKY*[3], *R. RYMZHANOV*[2,3], *V. SKURATOV*[3,5,6], *M. ZDOROVETS*[2,7], *L. ALEKSEEVA*[8]

[1] *L.N. Gumilyov Eurasian National University, Nur-Sultan, Kazakhstan*
[2] *Institute of Nuclear Physics, Almaty, Kazakhstan*
[3] *Flerov Laboratory of Nuclear Research, Joint Institute for Nuclear Research, Dubna, Russia*
[4] *Centre for HRTEM, Nelson Mandela University, Port Elizabeth, South Africa*
[5] *National Research Nuclear University MEPhI, Moscow, Russia*
[6] *Dubna State University, Dubna, Russia*
[7] *Ural Federal University, Ekaterinburg, Russia*
[8] *Physico-Technical Research Institute, Lobachevsky State University of Nizhny Novgorod, Nizhny Novgorod, Russia*

Radiation stability of Y-Al-O and Y-Ti-O compounds which are key ingredients in oxide dispersion strengthened (ODS) steels as promise materials for nuclear applications, is a subject of extensive irradiation testing with various radiation sources. Most corresponding literature data focus on radiation damage produced by neutron and charged particle radiation in elastic collisions and much less is known about defects formed via relaxation of dense electronic excitations associated with high-energy, heavy ion irradiation. As known, (Y,Ti) and (Y,Al) nanooxides may retain crystallinity up to very high damage doses, sometimes more than 100 dpa [1]. At the same time, certain types of precipitates such as Y-Ti-O, may be easily amorphized by heavy ions of fission fragment energies via the formation of amorphous latent tracks produced by heavy ions of fission fragment energies at relatively low ion fluences of about 10^{13} cm^{-2} [2–4]. Contrary, $Y_4Al_2O_9$ (YAM) nanoparticles have demonstrated much higher resistance to dense electronic excitations effects that stimulates further research. This work is aimed at comparative high-resolution transmission electron microscopy (HRTEM) examination of Xe and Bi ion track parameters in both isolated and non-isolated (embedded into ferrite matrix) $Y_4Al_2O_9$ (YAM) and $Y_2Ti_2O_7$ nanoparticles.

The samples were irradiated with swift Bi and Xe ions with energies ranging from 148 to 714 MeV at electronic stopping powers from 2 to 35 keV/nm at the IC-100, U-400 and DC-60 cyclotrons at FLNR JINR (Dubna, Russia) and Astana Branch of Institute of Nuclear Physics (Nur-Sultan, Kazakhstan). The ion fluence corresponded to the "individual tracks" regime was 5×10^{11} cm^{-2}. Structural analysis was performed using Talos™ F200i S/TEM and JEOL ARM-200F TEM operating at 200 kV.

As was found, the track diameter in isolated nanoparticles of yttrium titanate for close levels of electron energy losses is much larger than in the same nanoparticles embedded in a metal (ferrite) matrix [3, 4]. Latent tracks in YAM have been revealed in isolated particles only alloy starting from the threshold energy loss 6.2 keV/nm [5]. It is suggested that different structural response of isolated and non-isolated nano-oxides as well parameters of the track regions is largely determined by peculiarities of the heat transfer processes in the nanostructured materials.

REFERENCES

[1] J.P. Wharry, M.J. Swenson, K.H. Yano, "A review of the irradiation and future directions," J. Nucl. Mater., vol. 486, pp. 11–20, 2017.

[2] I. Monnet, C. Grygiel, M.L. Lescoat, J. Ribis, "Amorphization of oxides in ODS steels/materials by electronic stopping power," J. Nucl. Mater., vol. 424, pp. 12–16, 2012.

[3] V.A. Skuratov, V.V. Uglov, J. O'Connell, A.S. Sohatsky, J.H. Neethling, S.V. Rogozhkin, "Radiation stability of the ODS alloys against swift heavy ion impact," J. Nucl. Mater., vol. 442 (1–3), pp. 449–457, 2013.

[4] V.A. Skuratov, A.S. Sohatsky, J.H. O'Connell, K. Kornieieva, A.A. Nikitina, V.V. Uglov, J.H. Neethling, V.S. Ageev, "Latent tracks of swift heavy ions in $Cr_{23}C_6$ and Y-Ti-O nanoparticles in ODS alloys," J. Nucl. Instr. Meth. B, vol. 374, pp. 102–106, 2016.

[5] A. Ibrayeva, A. Mutali, J. O'Connell, A. Janse van Vuuren, E. Korneeva, A. Sohatsky, R. Rymzhanov, V. Skuratov, L. Alekseeva, I. Ivanov, "Swift heavy ion tracks in nanocrystalline $Y_4Al_2O_9$," J. Nucl. Mater. Energy, vol. 30, pp. 101-106, 2022.

* The work was supported by the Ministry of Education and Science of the Republic of Kazakhstan (grant No AP09058081)

R4-O-026001

Investigation of the population degree of atomic orbitals near impurity O and C atoms in the Si29H36 cluster

M.Yu. Tashmetov, Sh.M. Mahkamov, F.T. Umarova, A.B. Normurodov, N.T. Sulaymanov.

Instite of Nuclear Physics of AN UzR, 100214 Tashkent, Uzbekistan. sulaymon@inp.uz

The influence of oxygen and carbon on the electrophysical properties, characteristics and structural parameters of silicon is well studied. However, the cumulative effect of these impurities, especially with the noticeable influence of dimensional quantum phenomena during the transition to nano-scales, has not been sufficiently elucidated. This work is devoted to the study of changes in the population of electronic orbitals in the defect region and the effect of these changes on the main energy characteristics of the Si29H36 silicon nano-cluster containing impurity atoms O and C in volume using the computer simulation method.

To determine the contribution of an impurity defect to changes in the population of atomic orbitals and their effect on energy characteristics, the parameters of Si29H36, Si29COH36, Si28VOCH36 clusters were calculated using the ORCA4 software package [1].

Calculations performed to optimize the structural parameters and energy characteristics of Si29H36 and Si28OCH36 nano-particles by computer modeling showed a decrease in the symmetry group and simultaneous formation of Si-C and Si-O defects near the central T_d position (Table 1). In nano-particles, the formation of defects and changes in energy characteristics occur due to external, primarily radiation exposure. As the results of our calculations show, the formation of a vacancy does not yet lead to a decrease in symmetry, but due to population deviations around the local defect region, a global redistribution of covalent electrons occurs throughout the cluster and a partial transition to d-orbitals occurs in Si atoms. This ensures the stabilization of Si-O and Si-C bonds.

Thus, computer modeling and analysis of the results of calculations of the populations of atomic orbitals show that the simultaneous introduction of O and C atoms into the central coordination sphere of the Si29H36 cluster leads to the formation of defects with a decrease in symmetry, the stabilization of which occurs by the redistribution of electrons in the region of their formation. At the same time, the binding energies of R_{Si-O} and R_{Si-C} are greater than the binding energy of R_{O-C}, i.e. in this case, two types of defects are formed inside the cluster − Si-O and Si-C, although the electro-negativity of both O and C is greater than Si. The combined influence of the matrix atoms (i.e., Si atoms) and the effect of radiation leads to equilibrium with the redistribution of electrons involved in the formation of bonds and rearrangement of the electronic structure in the defective region.

Table.1. Energy parameters of Si29H36 nanoparticles and nano-particles formed by the introduction of impurity atoms O and C near the central T_d node.

nano-particle	Z_s	Z_d	E_g (eV)	nano-particle	Z_s	Z_d	E_g (eV)
$Si_{28}VH_{36}$	-	-	-4.7040	$Si_{29}H_{36}$	+	-	-5.1394
$Si_{28}VC_sH_{36}$	-	-	-3.5854	$Si_{28}C_sH_{36}$	-	-	-5.0552
$Si_{28}VOH_{36}$	-	-	-5.0214	$Si_{28}OH_{36}$	-	+	-3.0075
$Si_{28}VOCH_{36}$	-	+	-4.8250	$Si_{28}OCH_{36}$	-	-	-2.4277

Note: *C*s - atom C replaces 1-atom Si at the central T_d node; *Zs* - the charge of the surface of the nano-particle, *Zd* - the charge of the defect formation area inside the nano-particle, *Eg* - the width of the band gap.

REFERENCES

[1] Frank Neese. Software update: the ORCA program system, version 4.0, 17 July 2017.

R4-O-026101

INFLUENCE OF ELECTRON IRRADIATION ON THE ELECTROPHYSICAL PARAMETERS OF SILICON DOPED WITH COBALT

*Tashmetov M.Yu., Makhkamov Sh., Tillaev T.S., Erdonov M.N., Saidov R.P., *Kholmedov Kh.M.*

Institute of Nuclear Physics, AS RU, 1 Khuroson str., 100214, Tashkent, Uzbekistan phone: +998 (71) 289-36-53; e-mail: erdonov@inp.uz
**Tashkent Al-Khwarizmi University of Information Technologies, 10 Amir Timur str., 100084, Tashkent, Uzbekistan, phone: +998 (71) 238-64-89.*

The paper presents the results of studies of doped single-crystal silicon irradiated with electrons with an energy of 4 meV in the fluence range of $10^{14} \div 10^{16}$ cm^{-2} depending on the concentration of introduced cobalt and the effect of induced radiation defects on the electrical parameters Si<Co>.

Silicon wafers of KEF grade of n-type conductivity with resistivity from 2 to 6 Ohm cm, dislocation density of $\sim 10^{14}$ cm^{-2}, and oxygen content of $5 \cdot 10^{17}$ cm^{-3} were used as the starting material. Diffusion of Co was carried out from a metal layer deposited in vacuum to the cleaned surface of the Si plates at temperatures of 1050÷1250 ^{0}C for 8÷10 hours. Comparison of electrophysical parameters of control and doped silicon samples after diffusion at 1250 ^{0}C showed that the values of resistivity (ρ) increase by 2÷3 times, and the concentration of free charge carriers also decreases within the specified limits. Such a change in the electrical parameters allows us to state that the admixture of in cobalt n-Si mainly exhibits acceptor properties and not amphoteric [1] and leads to compensation of the main current carriers.

The solubility of Co in Si was determined by neutron activation analysis, and the positions of deep centers in Si<Co> were determined from the Hall coefficient. At the same time, it was found that the total concentration of cobalt in the indicated temperature range varies within $9 \cdot 10^{14}$ cm^{-3} to $1 \cdot 10^{16}$ cm^{-3}, and the electrically active concentration is $4 \cdot 10^{13}$ cm^{-3} to $3 \cdot 10^{14}$ cm^{-3}, due to the capture of electrons deep centers located in the upper half of the band gap with ionization energies E_c-0.41 eV and E_c-0.53 eV.

To study the radiation degradation of the Si<Co> parameters, reference and doped samples were irradiated at an electron accelerator "Electronics U-003" at a flux density of $5 \bullet 10^{11}$ cm^{-2}. The temperature of the samples during irradiation did not exceed 40 ^{0}C.

It has been established that irradiation with electrons with an energy of 4 meV in the specified fluence range leads to a change in the values of ρ and the rate of removal of the current carrier concentration (n_e) both in the doped and in the control samples. In Si<Co> samples, the degradation efficiency is determined by the concentration of the electrically active cobalt center. Its increase in samples leads to an increase in the efficiency of degradation of electrophysical parameters compared to the reference control samples. Comparison of the degradation coefficients ρ and ne ($K_{\rho(ne)}$) at the same doses of electron irradiation 10^{16} cm^{-2} has shown that an increase in the concentration of electrically active Co centers from 4×10^{13} cm^{-3} to 3×10^{14} cm^{-3} leads to an increase in the value of $K_{\rho(ne)}$ by 1.3 times, and in comparison with undoped samples by 3 times, i.e. doping silicon with cobalt leads to a decrease in the radiation resistance of the electrophysical parameters of silicon, and not to an increase, as shown in [2]. The mechanism has been proposed for the occurrence of quasi-chemical reactions due to radiative decay of electrically inactive complex states of cobalt in a Si-Co solid solution with the subsequent formation of acceptor centers in the silicon interstices [1], which is indicated by an increase in the concentration of deep centers of cobalt after irradiation with electrons and an increase in their concentration with dose irradiation.

REFERENCES

[1] Фистул В.И. Атомы легирующих примесей в полупроводниках. М. физмат. 2004. 432 с.
[2] Бахадырханов М. К., Зайнабидинов С. З., Тешабоев А.Т. Взаимодействие атомов глубоких примесей с радиационными дефектами при γ-облучении // ФТП, 1977. – Т.11. вып.2, С.285-289.

R4-O-027001

WAVEGUIDE MICROMODIFICATIONS INDUCED BY MULTI-PULSE FILAMENTATION IN LiF CRYSTAL *

A.V. KUZNETSOV[1], V.O. KOMPANETS[2], S.V. CHEKALIN[2], A.E. DORMIDONOV[2] AND V.P. KANDIDOV[2,3]

[1]*Irkutsk Branch of Institute of Laser Physics, Siberian Branch, Russian Academy of Sciences, Irkutsk, Russia;*
[2]*Institute of Spectroscopy, Russian Academy of Sciences, Troitsk, Moscow, Russia;*
[3]*Department of Physics, M.V. Lomonosov Moscow State University, Moscow, Russia*

Lithium fluoride (LiF) is a unique material for studying the process of femtosecond laser filamentation due to the formation of stable fluorescent color centers (CCs), such as F_2 and F_3^+ CCs, in irradiated areas [1-3]. Using LiF, it is possible to experimentally study fluorescent tracks of both single-pulse and multi-pulse filamentation. One of the experimentally observed facts is the elongation of the tracks in LiF during multi-pulse filamentation [4,5]. This work is devoted to the study of the nature of this phenomenon and the development of a mathematical model that reproduces the observed modification of LiF.

The developed model takes into account two channels of CCs formation: excitonic and electron-hole channels. The relative contributions of these channels depend on the accumulated CCs density. This model describes modification of the refractive index in colored areas of LiF crystal. Each subsequent laser pulse propagates in a medium modified by all previous pulses.

The model was used to simulate a waveguide structure evolution during multi-pulse filamentation at a wavelength of 3 μm, located in the spectral region of anomalous group velocity dispersion. Results of the simulation qualitatively reproduce the experimentally recorded elongation of the fluorescent tracks of filamentation during femtosecond laser irradiation.

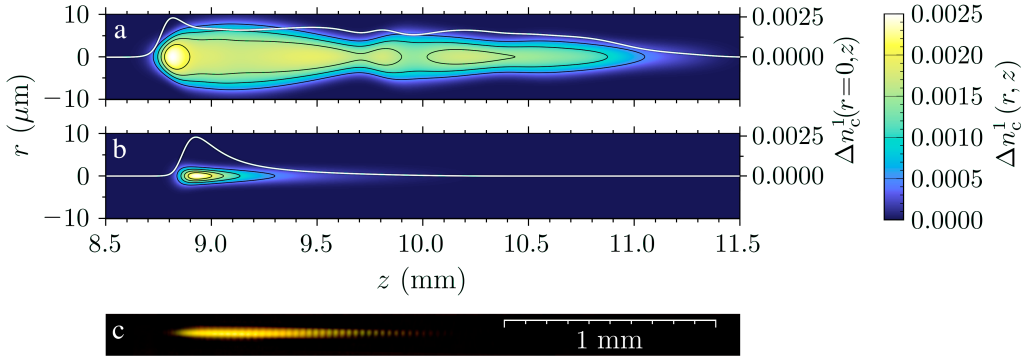

Fig.1. Spatial distribution of CCs density induced in LiF by single laser pulse: result of simulation with electron-hole channel of CC formation (a), simulation with excitonic channel only (b), experimental picture (c).

REFERENCES

[1] L.C. Courrol et al., Laser Physics, 16, 331 (2006).
[2] E.F. Martynovich et al., Opt. Spectrosc., 105, 348 (2008).
[3] A.V. Kuznetsov et al., Quantum Electron., 46, 379 (2016).
[4] E.F. Martynovich et al., Quantum Electron., 43, 463 (2013).
[5] S.V. Chekalin, V.O. Kompanets, Opt. Spectrosc., 127, 88 (2019).

* This work was supported by the Russian Science Foundation, project N 18-12-00422, and the Basic Research Plan of the Russian Academy of Sciences for the period up to 2025, project N 0243-2021-0004.

R4-O-028401

SIMULATION OF ION TRACK FORMATION IN POLYETHYLENE

P. BABAEV[1], N. MEDVEDEV[2,3], R. RYMZHANOV [4,5], F. AKHMETOV[6], S. GORBUNOV[1] AND A.E. VOLKOV[1]

[1]P.N. Lebedev Physical Institute of the Russian Academy of Sciences, Leninskij pr., 53,119991 Moscow, Russia
[2]Institute of Physics, Czech Academy of Sciences, Na Slovance 2, 182 21 Prague 8, Czech Republic
[3]Institute of Plasma Physics, Czech Academy of Sciences, Za Slovankou 3, 182 00 Prague 8, Czech Republic
[4]Flerov Laboratory of Nuclear Research, Joint Institute for Nuclear Research, Dubna, Russia
[5]Institute of Nuclear Physics, Almaty, Kazakhstan
[6]Industrial Focus Group XUV Optics, MESA+ Institute for Nanotechnology, University of Twente, Drienerlolaan 5, 7522 NB Enschede, The Netherlands

Our model of polymer damaging by swift heavy ions (SHI) combines Monte-Carlo (MC) code TREKIS [1], describing electronic and lattice excitations, with all-atom reactive molecular dynamics (MD) for atomic response. The simulation traces structure transformations, chemical bond creation/rupture and new molecular species emergence in ion tracks. Polyethylene (PE) serves as a prototypical system for model validation.

Crystalline 20 nm × 20 nm × 5 nm PE supercell with ~3×106 atoms was created by Moltemplate tool [2] and modelled using AIREBO-M [3] force field in MD simulation. Crystalline sample was melted and treated by Charge-Implicit ReaxFF force field [4] to produce an amorphous supercell. All MD simulations were performed in LAMMPS package [5].

We apply MC code TREKIS to get an initial radial energy distribution in the atomic system. Then, this distribution is converted into velocities of atoms in cylindrical layers surrounding the ion trajectory. The Berendsen thermostat at 300 K was employed at the borders of the simulation box.

A comparison of the simulation results with experimental track shapes and diameters [6] shows a reasonable agreement. Elliptic shape of tracks stretching is observed in both, the simulation and an experiment. Evolution of chemical bonds in tracks are also tracked during the track kinetics. The simulation provides atomic resolution of track structure and traced chemical species emerging in PE targets irradiated with SHIs. The results can be used for development of track etching models.

REFERENCES

[1] N. Medvedev, F. Akhmetov, R.A. Rymzhanov, R. Voronkov, A.E. Volkov, Https://Arxiv.Org/Abs/2201.08023v1. 53 (2022) 119991.
[2] A.I. Jewett, D. Stelter, J. Lambert, S.M. Saladi, O.M. Roscioni, M. Ricci, et al., J. Mol. Biol. 433 (2021) 166841.
[3] T.C. O'Connor, J. Andzelm, M.O. Robbins, J. Chem. Phys. 142 (2015).
[4] M. Kański, D. Maciazek, Z. Postawa, C.M. Ashraf, A.C.T. Van Duin, B.J. Garrison, J. Phys. Chem. Lett. 9 (2018) 359–363.
[5] A.P. Thompson, H.M. Aktulga, R. Berger, D.S. Bolintineanu, W.M. Brown, P.S. Crozier, et al., Comput. Phys. Commun. 271 (2022) 108171.
[6] J. Vetter, G.H. Michler, I. Naumann, Radiat. Eff. Defects Solids. 143 (1998) 273–286.

R4-O-029201

LASER COLORATION METHOD IN THE STUDY OF CEP EFFECT ON A SINGLE-CYCLE LIGHT BULLET IN LITHIUM FLUORIDE*

E.D. ZALOZNAYA[1,2,3], *A.E. DORMIDONOV*[1,2], *V.O. KOMPANETS*[2], *S.V. CHEKALIN*[2], *V.P. KANDIDOV*[2,3]

[1]*Dukhov Automatics Research Institute, Moscow, Russia*
[2]*Institute of Spectroscopy, Russian Academy of Sciences, Troitsk, Moscow, Russia*
[3]*Lomonosov Moscow State University, Faculty of Physics, Moscow, Russia*

The filamentation of femtosecond laser pulses under anomalous group velocity dispersion condition is accompanied by the formation of extremely compressed wave packets - light bullets [1], the duration of which is about one period of optical oscillations [2]. Spatiotemporal and energy characteristics of the formed light bullet periodically change during its propagation due to the continuously changing relation between the phases of the carrier wave and its envelope (carrier-envelope phase, CEP). This significantly affects the efficiency of the nonlinear optical interaction of the light bullet with the medium [3]. Consistent experimental study of the effect of CEP on the dynamics of a light bullet is possible only with the use of the laser coloration method [4] in a single-pulse mode.

The report presents the results of a study of the CEP effect on the characteristics of tracks of color centers generated in LiF by a high-intensity light bullet. Experimental registration was carried out in the single-pulse exposure mode, which allowed avoiding errors associated with fluctuations in radiation parameters from pulse to pulse. Analyzing the luminescence of structures induced in LiF by a light bullet at different wavelengths, a periodic modulation of the density of color centers was recorded in the direction of pulse propagation. The modulation depth of the luminescence profiles increases with increasing wavelength (Fig. 1).

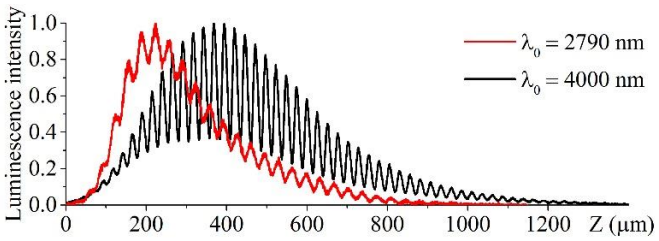

Fig.1. Experimentally measured luminescence profiles on the axis of tracks of color centers induced in LiF by a light bullet at wavelengths (red curve) 2790 nm, (black curve) 4000 nm.

Numerically, by solving the unidirectional pulse propagation equation describing the formation and nonlinear optical interaction of a light bullet with LiF, we found that due to the CEP effect, the electric field strength of a light bullet periodically oscillates during its propagation [3], which leads to a periodic change in the rate of color centers generation and, as a consequence, to modulation of their density along pulse propagation direction. At that, the period of induced structures decreases with an increase in the carrier wavelength due to a change in the ratio between the group and phase velocities of the pulse, and the modulation depth, on the contrary, increases, and is determined by the duration of the light bullet.

The results obtained make it possible to predict the effect of the wavelength of a light bullet on its nonlinear optical effect on a transparent dielectric. This can be used in the currently promising fields of ultrafast metrology and micromodification of materials.

REFERENCES

[1] V.P. Kandidov, E.D. Zaloznaya, A.E. Dormidonov, V.O. Kompanets, S.V. Chekalin, “Light bullets in transparent dielectrics”, Quantum Electronics, vol. 52, no. 3, pp. 233, 2022.

[2] M. Durand, A. Jarnac, A. Houard, Y. Liu, S. Grabielle, N. Forget, A. Durécu, A. Couairon, and A. Mysyrowicz, “Self-guided propagation of ultrashort laser pulses in the anomalous dispersion region of transparent solids: A new regime of filamentation”, Phys. Rev. Lett., vol. 110, pp. 115003, 2013.

[3] E.D. Zaloznaya, V.O. Kompanets, A.D. Savvin, A.E. Dormidonov, S.V. Chekalin, V.P. Kandidov, “Carrier-envelope phase of a light bullet”, arXiv:2201.04357, 2022.

[4] S.V. Chekalin, V.O. Kompanets, “A method of laser coloration in experiments on filamentation of individual impulses and the formation of a light bullet in a homogeneous transparent dielectrics”, Opt. Spektrosc., vol. 127, no. 1, pp. 88, 2019.

* The work was supported by Russian Science Foundation (project no. 18-12-00422). E.D. Zaloznaya acknowledges Theoretical Physics and Mathematics Advancement Foundation “BASIS" for the financial support.

R4-O-031202

POSITRON ANNIHILATION ANALYSIS OF NANOSIZED METAL COATINGS ZR/NB AFTER HE+ ION IRRADIATION

A.D. LOMYGIN[1], R.S. LAPTEV[1], D.G. KROTKEVICH[1], M.O. LIEDKE[2]

[1]Tomsk Polytechnic University, Russia, Tomsk
[2]Helmholtz Center Dresden-Rossendorf, Germany, Dresden
E-mail: lomyginanton141@gmail.com

Multilayer nanosized coatings with different crystal structures are considered as potential materials with high resistance to radiation defects, since vacancy-type defects and interstitial atoms recombine at the interfaces. Based on this concept, metals with different crystal structures (bcc, fcc and hcp) are considered for the fabrication of multilayer nanoscale coatings with high radiation resistance [1, 2].

The samples were analyzed using annihilation line Doppler broadening (DB) spectrometry using variable positron energy at the AIDA - Helmholtz Center Dresden-Rossendorf, HZDR. A monoenergetic positron beam 4 mm in diameter was used; the positron energy varied from 0.01 keV to 35 keV. Annihilation γ radiation was recorded by the HPGe detector with an energy resolution of 1.09 + 0.01 keV, interpolated for an energy of 511 keV. The obtained DB spectra were analyzed by estimating the parameters S and W of the annihilation line, as well as graphical representation of the R parameter as a function of S = f(W). The prepared samples were irradiated with He^+ ions using a PION-1M plasma ion source with a non-incandescent cathode. The energy of the accelerated ions was 25 keV. The irradiation time was chosen so as to cover a wide dose range from $3 \cdot 10^{16}$ to $3 \cdot 10^{17}$ ions/cm^2. During irradiation, the temperature of the samples did not exceed 200 °C.

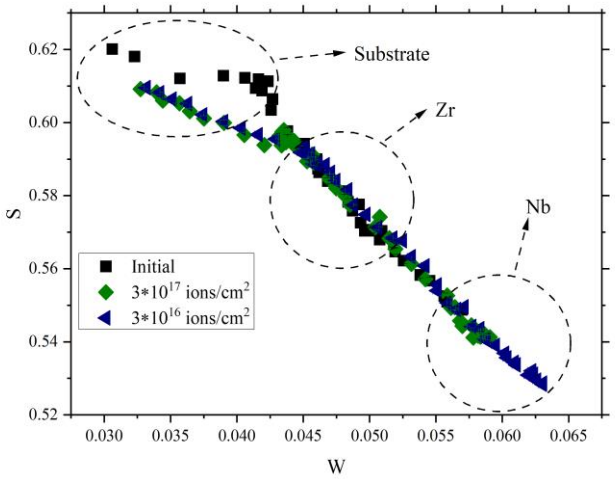

Fig. 1. Plot of the dependence of the S parameter on the W parameter for Zr/Nb NMCs with an individual layer thickness of 100 ± 10 nm and an irradiation dose range from $3 \cdot 10^{16}$ to $3 \cdot 10^{17}$ ions/cm^2

Fig. 1 shows the dependence of the S parameter on the W parameter of a Zr/Nb NMCs with a thickness of individual layers of 100 ± 10 nm and a range of irradiation doses from $3 \cdot 10^{16}$ to $3 \cdot 10^{17}$ ions/cm^2. A layer-by-layer analysis of positron annihilation in Zr/Nb NMCs showed that an increase in the dose of irradiation with He^+ ions does not lead to the formation of stable radiation defects. When the energy reaches 20 keV, the probability of positron annihilation in a single-crystal silicon substrate increases.

The research was supported by a grant from the Russian Science Foundation (project no. 20-79-10343).

REFERENCES

[1] Laptev R., Lomygin A., Krotkevich D., Syrtanov M., Kashkarov E., Bordulev Y., Siemek K., Kobets A. Effect of Proton Irradiation on the Defect Evolution of Zr/Nb Nanoscale Multilayers //Metals. – 2020. – Vol. 10. – №. 4. – Article number: 535. – P. 1–12.

[2] Laptev R., Svyatkin L., Krotkevich D., Stepanova E., Pushilina N., Lomygin A., Ognev S., Siemek K., Uglov V. First-Principles Calculations and Experimental Study of H+-Irradiated Zr/Nb Nanoscale Multilayer System //Metals. – 2021. – Vol. 11. – №. 4. – Article number: 627. – P. 1–17.

R4-O-039201

DEFECT-RELATED LUMINESCENCE IN $KLuP_2O_7$ DOPED WITH Pr^{3+} IONS AFTER IRRADIATION WITH FAST ELECTRONS AND NEUTRONS*

S.A. KISELEV[1], *V.A. PUSTOVAROV*[1], *M.O. PETROVA*[2]

[1]*Ural Federal University, Yekaterinburg, Russian Federation*
[2]*Joint Institute for Nuclear Research, Dubna, Russian Federation*

Praseodymium ions are recently paid attention due to perspective of their usage as impurity ions instead of Ce^{3+}. In comparison with impurity Ce^{3+} ions, praseodymium emission is located in higher energy region and has shorter lifetime (20-30 ns instead of 30-60) [1-3]. Compounds with Pr^{3+} ions impurity demonstrate three main channels of emission: interconfigurational *f–f*, intraconfigurational *d–f* transitions and defect-related luminescence. The latter act as competitive channel of charge carriers capture. With irradiation of scintillating materials in crystal lattice structural changes are observed. Their peculiarities depend on such features, as type, intensity and duration of the irradiation. Those changes influence on spectroscopic properties of compounds.

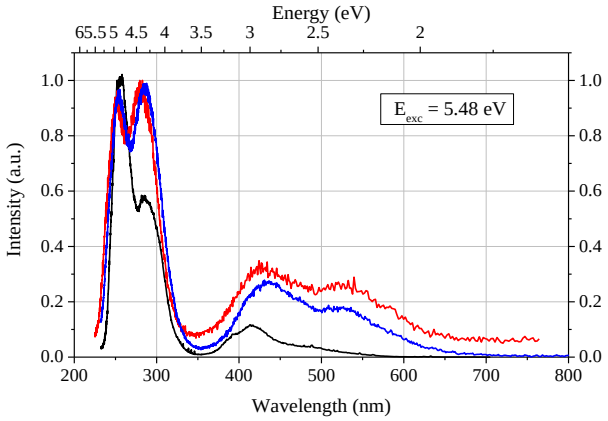

Fig.1. Photoluminescence spectra of $KLuP_2O_7:Pr^{3+}$ (1 %) upon UV excitation (E_{exc}), T = 295 K before (black) and after irradiation with 10 MeV electrons from LINAC (red), with neutrons (blue).

Crystalline powder $KLuP_2O_7:Pr^{3+}$ has been synthesized by a solid state reaction [4]. Luminescence spectroscopic properties upon UV-, X-ray and cathode-ray excitation have been previously studied in Refs. [4, 5]. These measurements approved promising characteristics of compound for scintillator applications.

To observe behavior of defect-related luminescence object was irradiated with electrons and neutrons. Fast electrons (E = 10 MeV) were obtained from linear electron accelerator in UrFU, Yekaterinburg. Fast neutrons (E > 1 MeV) flux was produced by pulse neutron reactor IBR-2 (FLNP JINR, Dubna). Both irradiation types cause defect formation inside lattice. Forming point defects is produced by impact mechanism – elastic collisions of particles with nucleus of lattice atoms. Redistribution of *d–f* transitions in 250-300 nm region is observed. In 450-550 nm region defect-relative radiative bands appear. These transitions are a sign of defects existing formed by radical groups of phosphorous and oxygen after interacting with irradiation particles.

REFERENCES

[1] M. Nikl, V.V. Laguta, A. Vedda, “Complex oxide scintillators: Material defects and scintillation performance,” Phys. Status Solidi (b), vol. 245, pp. 1701-1722, 2008.

[2] M. Nikl, H. Ogino, A. Yoshikawa, E. Mihokova, J. Pejchal, A. Beitlerova, A. Novoselov, T. Fukuda, “Fast 5d–4f luminescence of Pr^{3+} in Lu_2SiO_5 single crystal host,” Chem. Phys. Lett., vol. 410, pp. 218-221, 2005.

[3] A. Zych, M. de Lange, C. d. M. Donega, A. Meijerink, “Analysis of the radiative lifetime of Pr^{3+} *d-f* emission,” J. Appl. Phys., vol. 112, pp. 013536, 2012.

[4] M. Trevisani, K. Ivanovskikh, F. Piccinelli, M. Bettinelli, “Synchrotron Radiation Study of Interconfigurational 5*d*-4*f* Luminescence of Pr^{3+} in $KLuP_2O_7$,” Zeitschrift fur Naturforschung B, vol. 69, pp. 205-209, 2014.

[5] V.A. Pustovarov, K.V. Ivanovskikh, S.A. Kiselev, E.S. Trofimova, S. Omelkov, M. Bettinelli, “Testing performance of Pr^{3+}-doped $KLuP_2O_7$ upon UV-, sychrotron X-ray and cathode-ray excitation,” Opt. Mat., vol. 108, pp. 110234, 2020.

*The work was partially supported by the Ministry of Science and Higher Education of the Russian Federation through the basic part of the government mandate, project No. FEUZ-2020-0060.

R4-O-041301

ELECTRON PARAMAGNETIC RESONANCE AND THERMOLUMINESCENCE OF DEFECTS IN ZrO_2*

D.V. ANANCHENKO[1], S.V. NIKIFOROV[1], S.F. KONEV[1], K.V. SOBYANIN[1], Y.P. KASATKINA[1], A. DAULETBEKOVA[2]

[1]Ural Federal University, Ekaterinburg, Russia
[2]L.N. Gumilyov Eurasian National University, Nur-Sultan, Kazakhstan

Zirconium dioxide (ZrO_2) is a promising material for modern optoelectronics, photonics and luminescent dosimetry of ionizing radiation. The main types of paramagnetic defects in ZrO_2 are Zr^{3+} ions with g = 1.96-1.97 [1] and F^+-centers with g = 1.999-2.003 [1, 2]. However, thermal stability of these centers and their relation to thermoluminescent (TL) properties of the material have not been fully studied now.

The aim of this work is to study thermal stability of paramagnetic centers in monoclinic ZrO_2 and its relation to TL characteristics of this material.

ZrO_2 samples were made of nanopowders with particle sizes of 40-65 nm by using a method of uniaxial cold pressing under 1000 kgf/cm^2 pressure. A linear electron accelerator UELR-10-10C was used to irradiate the samples with an electron beam of 10 MeV energy and $2.9 \cdot 10^{14}$ cm^{-2} fluence. TL was measured in a linear heating mode at 2˚C/s. ELEXSYS 580 spectrometer was used to measure electron spin resonance (ESR) in X-band.

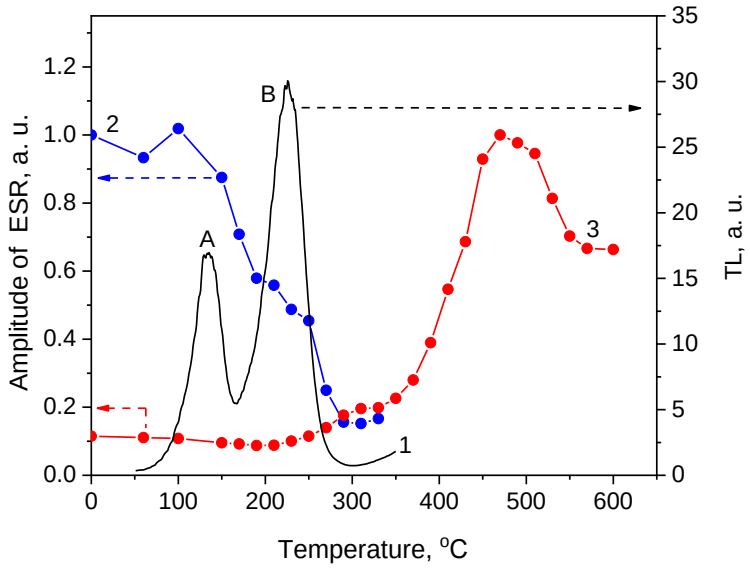

Fig.1. TL curve (1) and dependence of amplitude of ESR signals with g = 1.999 (2) and g = 1.965 (3) on ZrO_2 annealing temperature

It was found that exposure to electrons with 10 MeV energy results in TL peaks A at 135 ˚C and B at 225 ˚C (Figure 1). ESR spectra of the exposed samples feature signal I with g = 1.965, which is associated with the presence of Zr^{3+} ions in the samples; and signal II with g = 1.999, which is caused by formation of F^+-centers in the irradiated compacts. Signal I amplitude increases when the sample heating temperature grows from 250 up to 470 ˚C, and it becomes maximal at 470˚C. Further rising of temperature up to 600˚C decreases the amplitude of signal I by 35-40% from the maximum. The absence of any changes in ESR amplitude shows that Zr^{3+} does not participate in TL processes in the 50-350 ˚C temperature range.

The amplitude of signal II was found to decrease in the temperature range of TL peaks A and B. This can indicate destruction of F^+-centers due to trapping of charge carriers that were released from the traps associated with these TL peaks. The paper discusses mechanisms of changing concentrations of paramagnetic centers when the irradiated samples are annealed in the 50-600 ˚C temperature range.

REFERENCES

[1] C. Gionco, M. C. Paganini, E. Giamello, R. Burgess, C. Di Valentin, G. Pacchioni, “Paramagnetic defects in polycrystalline zirconia: an EPR and DFT study.” Chem. Mater., vol. 25, no. 11, pp. 2243-2253, 2013

[2] H. S. Lokesha, M. L. Chithambo, “A combined study of the thermoluminescence and electron paramagnetic resonance of point defects in ZrO_2: Er^{3+}”. *Radiat. Phys. Chem.*, vol. *172*, p. 108767, 2020

* The authors appreciate the Ministry of Education and Science of the Republic of Kazakhstan for grant AP09260057.

R4-O-042102

MICROSTRUCTURE AND MECHANICAL PROPERTIES RESPONSE OF ODS ALLOYS UNDER SWIFT HEAVY ION IRRADIATION*

E.A. KORNEEVA[1,2], A.S. SOHATSKY[1], V.A. SKURATOV[1,3,4], A.M. KORSUNSKY[5,6], A.I. SALIMON[5], E.S. STATNIK[5], P.A. SOMOV[5], I.N. KRUPATIN[5], T.N. VERSHININA[1]

[1] *Joint Institute for Nuclear Research, Dubna, Russia*
[2] *National University of Science and Technology NUST-MISiS, Moscow, Russia*
[3] *National Research Nuclear University MEPhI, Moscow, Russia*
[4] *Dubna State University, Dubna, Russia*
[5] *Skolkovo Institute of Science and Technology, Moscow, Russia*
[6] *University of Oxford, Oxford, United Kingdom*

Radiation tolerance of the perspective constructive materials for Generation IV nuclear reactors is one of the main research activities over the past years [1-3]. Special interest is dedicated to studies of the swift heavy ion (SHI) irradiation influence on the structure stability of fuel cladding materials that supposed to be in direct contact with fission fragments in reactor core. According to the previous research SHI irradiation is the only type of irradiation that can lead to significant changes in microstructure in dielectric materials down to complete amorphization [4-6].

In the present work ferritic ODS alloys reinforced by different nanosized particles based on yttrium oxides ($Y_2Ti_2O_7$, Y_2TiO_5, $Y_4Al_2O_9$) and carbides as well as nanopowders of the same composition as embedded nanoparticles were exposed to 1-3 MeV/amu Xe, Kr and Bi irradiation with different fluences. Post-irradiation microstructure examinations were made using transmission electron microscopy and X-ray diffraction. It was shown that SHI irradiation doesn't have crucial effect on metallic matrix and at the same time it leads to latent track formation of several nanometers in oxides and carbides. Starting from $2 \cdot 10^{12}$ cm^{-2} fluence, track overlapping takes place and with fluence increasing the phase transformation into amorphous state of the whole dielectric particles occurs. Mechanical properties of irradiated ODS alloys with crystalline, partially amorphous and completely amorphous particles were studied by nanoindentation and in-situ micropillar compression tests. Additional examinations were made on irradiated ferritic alloy without particles in order to estimate the possible influence on mechanical properties by irradiated ferritic matrix.

REFERENCES

[1] R. L. Klueh, A. T. Nelson, "Ferritic/martensitic steels for next-generation reactors," J. Nucl. Mater., vol. 371, no. 1-3, pp. 37-52, September 2007.

[2] S. Ukai, M. Fujiwara, "Perspective of ODS alloys application in nuclear environments," J. Nucl. Mater., vol. 307, pp. 749-757, December 2002.

[3] S. Xia, M. C. Gao, T. Yang, P. K. Liaw, Y. Zhang, "Phase stability and microstructures of high entropy alloys ion irradiated to high doses," J. Nucl. Mater., vol. 480, pp. 100-108, November 2016.

[4] M. Lang, R. Devanathan, M. Toulemonde, C. Trautmann, "Advances in understanding of swift heavy-ion tracks in complex ceramics," Curr. Opin. Solid State Mater. Sci., vol. 19, no. 1, pp. 39-48, February 2015.

[5] W. J. Weber, D. M. Duffy, L. Thomé, Y. Zhang, "The role of electronic energy loss in ion beam modification of materials," Curr. Opin. Solid State Mater. Sci., vol. 19, no. 1, pp. 1-11, February 2015.

[6] M.-L. Lescoat, I. Monnet, J. Ribis, P. Dubuisson, Y. de Carlan, J.-M. Costantini, J. Malaplate, "Amorphization of oxides in ODS materials under low and high energy ion irradiations," J. Nucl. Mater., vol. 417, no. 1-3, pp. 266-269, October 2011.

* This work was partially performed using the equipment of the Advanced Imaging Core Facility of Skolkovo Institute of Science and Technology.

R4-O-052401

INFLUENCE OF PROTON AND ELECTRON BEAMS OF DIFFERENT ENERGIES ON GRAPHENE STRUCTURES USED FOR TERAHERTZ APPLICATIONS *

K. BATRAKOV[1], *A. PADDUBSKAYA*[1], *N. VALYNETS*[1], *A. STEPANOV*[2], *I. EGOROV*[2], *G. REMNEV*[2], *S. MAKSIMENKO*[1]

[1]*Institute for Nuclear Problems of Belarusian State University, Bobruiskaya str. 11, 220006 Minsk, Belarus,*

[2]*Research and Production Laboratory "Pulse-Beam, Electric Discharge and Plasma Technologies", Tomsk, Polytechnic University, Lenin Ave, 30, 634050 Tomsk, Russia*

Graphene is one of the most promising 2D material for future development of nanoelectronic and nanophotonics. Its unique properties, such as high transparency, high carrier mobility, ballistic transport, thermal conductivity, make such material very attractive for space applications; in particular, for future development of THz devices working at geostationary orbit (GEO) [1]. Our theoretical and experimental findings [1] showed that graphene with the PMMA support can be used at GEO for over 10 years. However, interaction of charged particles by supported substance leads to decrease of its energy and the specific energy losses increase with particles energy decrease. Within this work, we investigate the influence of graphene interaction with charged particles of different energy, which in experiment can be regulated by the thickness of additional absorber (Fig. 1). The numerical modeling of irradiation of these graphene structures with radiation beam is performed. Purpose of these calculations is to prepare data and conditions for providing experiment on TEMP-4 ions setup with beam comprising carbon and hydrogen (70% and 30%, respectively) ions [2] and electron beam setups. For studying only protons influence of TEMP-4, additional absorber is placed before graphene structure, for example, PMMA layer with the thickness ≥ 1 μm provides carbon ions absorption, but protons pass through this layer, because energy losses are proportional to ion mass. Energy of protons which interact with graphene structure is regulated by thickness of absorber and can be approximately estimated using Bethe-Bloch energy loss per distance for protons, alpha particles and atomic ions. For exploring of electron beam influence, the much thicker absorbers (~ millimeter) should be used (Fig. 1a).

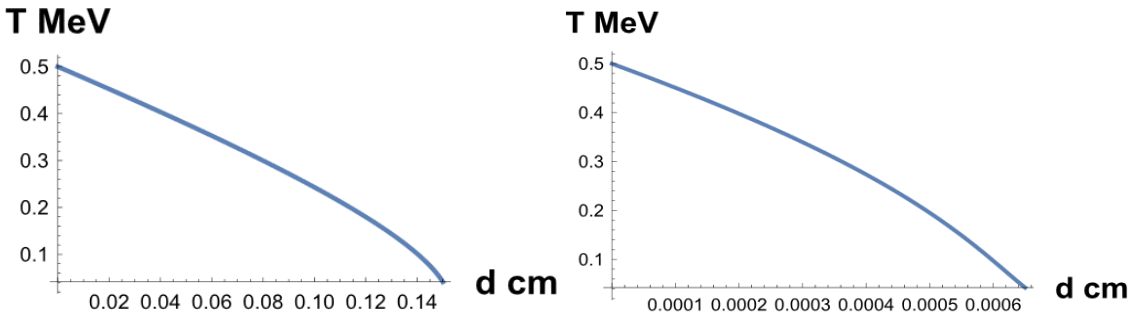

a b

Figure1. Dependence of particle energy (*T*) on the PMMA absorber thickness (*d*) for proton (1a) and electron (1b). Initial beam energy is 0.5 MeV.

[1] A. Paddubskaya, K. Batrakov, A. Khrushchinsky, S. Kuten, A. Plyushch, A. Stepanov, G. Remnev, V. Shvetsov, M. Baah, Yu. Svirko, P. Kuzhir, Outstanding Radiation Tolerance of Supported Graphene:Towards 2D Sensors for the Space Millimeter Radioastronomy, Nanomaterials 2021, 11, 170. https://dx.doi.org/10.3390/nano11010170

[2] Isakov, I.F.; Kolodii, V.N.; Opekunov, M.S.; Matvienko, V.M.; Pechenkin, S.A.; Remnev, G.E.; Usov, Y.P. Sources of high power ion beams for technological applications. Vacuum 1991, 42, 159–162.

* The work was supported by the Belarusian Republican Foundation for Fundamental Research N F21ARMG-006

R4-O-943601

MODELLING STUDY OF NUCLEAR REACTOR STRUCTURAL MATERIALS RADIATION DAMAGES BY USING ION BEAMS*

P.A. FEDIN[1], K.E. PRYANISHNIKOV[1,2], A.V. ZIIATDINOVA[1], A.V. KOZLOV[1], R.P. KUIBEDA[1], A.A NIKITIN[1], S.V. ROGOZHKIN[1,2], T.V. KULEVOY[1]

[1]NRC "Kurchatov institute", Moscow, Russia
[2]NRNU "MEPhI", Moscow, Russia

Ion accelerator facility is a powerful tool to simulate neutron irradiation effects in reactor materials. At the NRC "Kurchatov Institute" - ITEP the heavy-ion accelerator HIPr (heavy ion prototype) is used for the of radiation damage simulation in steels and alloys by ion beams [1-4]. Irradiations are carried out mainly with iron ions Fe^{2+} (5.6 MeV), but if necessary, beams of vanadium, tantalum, carbon and many other ions can be used. Irradiated specimens are investigated by atomic probe tomography and transmission electron microscopy (TEM). Helium and hydrogen ion beam implantation in heavy ion damaged area can be used to simulate transmutation effects occur in reactor materials [5]. This will allow modeling such an important process as radiation swelling of the material under the neutron radiation impact. Now work is underway to build a second beam line of the HIPr facility (see fig.1) for simultaneous sample irradiation by heavy ion and hydrogen/helium ion beams [6]. The descriptions of beam simulation experiments at ITEP on the HIPr facility and the on-going project of the second beam line for hydrogen/helium ion beams are reported.

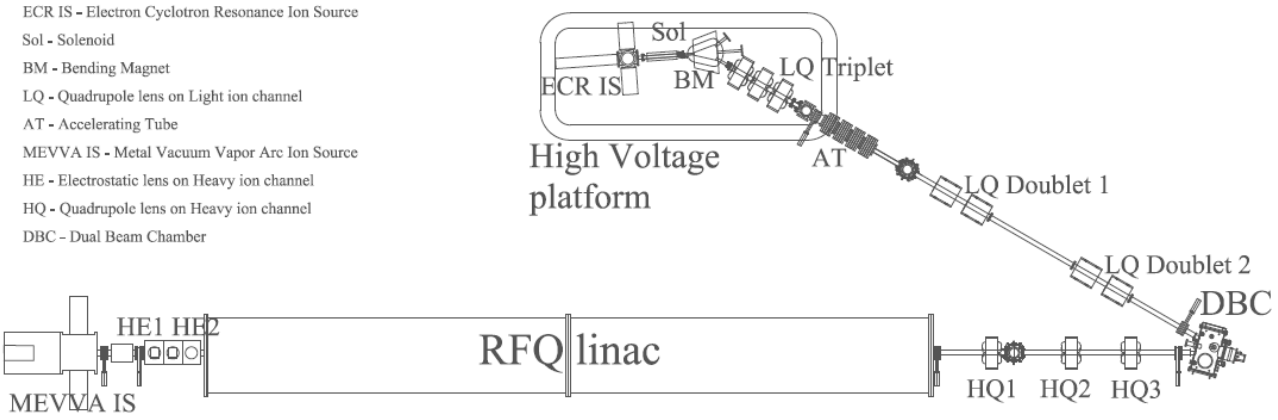

Fig.1. Layout of HIPr facility with designed second beam line of light ions.

REFERENCES

[1] Fedin P.A., Saratovskik M.S., Kuibeda R.P., Sitnikov A L, Kulevoy T.V.,Nikitin A.A., Rogozhkin S.V., "Simulation of irradiation effects with ions on the RFQ linac HIPr", Journal of Physics: Conference Series, 1115(3), 032026 2018.

[2] Rogozhkin S, Nikitin A, Orlov N, Bogachev A, Korchuganova O, Aleev A, Zaluzhnyi A, Kulevoy T, Linday R, Möslang A, Vladimirov P, "Evolution of microstructure in advanced ferritic-martensitic steels under irradiation: the origin of low temperature radiation embrittlement", MRS Advances, **2** 1143-1155, 2017

[3] Rogozhkin S, Schastlivaya I, Leonov V, Nikitin A, Orlov N, Kozodaev M, Vasiliev A, Orekhov A, "Study of nanostructure of experimental Ti–5Al–4V–2Zr alloy", Inorganic Materials: Applied Research **8** 848–860, 2017

[4] Rogozhkin S, Iskandarov N, Nikitin A, Khomich A, Khoroshilov V, Bogachev A, Lukyanchuk A, Raznitsyn O, Shutov A, Kulevoy T, Fedin P, Vasiliev A, Presnyakov M, Leontyeva-Smirnova M, Mozhanov E and Nikitina A, "Study of the Microscopic Origins of Radiation Hardening of Ferritic-Martensitic Steels RUSFER-EK-181 and ChS-139 in the Simulation Experiment with Heavy Ion Irradiation", Inorganic Materials: Applied Research **11** 359–365, 2020

[5] Marian J, Hoang T, Fluss M, Hsiung L "A review of helium–hydrogen synergistic effects in radiation damage observed in fusion energy steels and an interaction model to guide future understanding", J. Nucl. Mater. **462** 409–421, 2015

[6] Fedin P, Ziiatdinova A, Pryanishnikov K, Kuibeda R, Kulevoy T, Nikitin A, Rogozhkin S, "Requirements for the dual Fe + H/He beam at the accelerator hipr for simulation of neutron influence on nuclear reactor materials", J. Phys.: Conf. Ser. 1686 012073, 2020

* This work was supported by the Russian Science Foundation, project no. 22-29-01279. The equipment of the KAMIKS Shared Access Center (https://ckp-rf.ru/ckp/502001/) at the National Research Center "Kurchatov Institute" was used.

R4-P-001801

DOSE DEPOSITED DURING A RADIOLOGICAL EXAMINATIONS USING MONTE CARLO SIMULATION

O.EL BASRAOUI, O.EL BOUNAGUI, N. TAHIRI

Faculty of Sciences, Mohammed V University in Rabat, Morocco
elbounagui@gmail.com

In this study we have developed a program based on the Monte Carlo method to simulate the propagation of photons through living matter and subsequently calculate the absorbed dose taking into account the types of interactions of the photons with matter at lo energy .To complete this study, we adopted a cylindrical geometry to simulate the thorax of a child as a target organ by considering water as a material equivalent to biological tissues, and make a comparative study using the material composed of HCNO atoms. However, the results obtained by our program are in close agreement with the results given by the MCNP code.

R4-P-008501

RADIATION DEFECTS IN MgO SINGLE CRYSTALS IRRADIATED WITH SWIFT IONS*

G. BAUBEKOVA[1], R. ASSYLBAYEV[2], ZH. KARIPBAYEV[1], A. AKILBEKOV[1], A. LUSHCHIK[3]

[1]L.N. Gumilyov Eurasian National University, Munaitpassov Str. 5, 0100008 Nur-Sultan
[2]Pavlodar Pedagogical University Str. 64, 140000 Pavlodar
[3]Institute of Physics, University of Tartu, W. Ostwald Str. 1, 50411 Tartu, Estonis

Crystals of magnesium oxide and calcium fluoride are widely used and promising materials in various fields of science and technology. Magnesium oxide also has a wide range of uses. MgO crystals exhibit high resistance to irradiation and prolonged residence in a radiation medium. This property determines the prospects of MgO in nuclear applications, such as nuclear fuel, waste storage, fission reactor materials, and even as promising materials for diagnostic windows in future deuterium-tritium fusion reactors [1].

Highly pure MgO single crystals were irradiated with 0.23 GeV ^{132}Xe ions and Ar^{40} at fluences of $\Phi = 5\times10^{12}–3\times10^{14}$ ions/cm^2 at the DC-60 cyclotron in Nur-Sultan. The spectra of optical absorption were measured in a spectral region of 1.5-6.5 eV using a spectrometer СФ2000. The photoluminescence and excitation spectra were measured on a universal spectrofluorimeter CM2203 Solar. The luminescence spectra upon excitation by synchrotron radiation were measured at the MAX IV Lab synchrotron (Lund, Sweden).

Irradiation with ions creates many defects in the crystal, both in bulk and on surface. Induced defects form additional energy levels in the bandgap of the energy structure of crystal, which leads to its coloration and the appearance of radiation-induced optical absorption (RIOA). Therefore, one of the effective methods for studying radiation defect formation is optical absorption spectroscopy. By the area of the absorption band, we can talk about the relative concentration of defects responsible for this band.

The absorption spectrum contains a wide non-elementary band with a maximum at about 5 eV. In this area F and F^+ centers (oxygen vacancies with two and one captured electron, respectively, maxima at 4.92 and 5.03 eV, respectively [2]) are responsible for optical absorption. With an increase in the irradiation fluence, we see a noticeable increase in this structural absorption band. F_2 centers (two neighboring F centers, maximum at 3.48 eV [3]) are created in a very low concentration. In addition, the spectrum contains a weak band at about 2.17 eV, a detailed study of which is given in [1].

Upon excitation by photons with an energy of 5 eV (near the absorption band of F^+ centers), a broad non-elementary emission band at about 3.25 eV is observed in the spectrum. The main contribution to this structural emission band is made by F^+ centers (emission at 3.2 eV [4]). Upon excitation at a point of 5.4 eV, a shift of this emission band to the short-wavelength side of the spectrum takes place, where the emission of F_2 centers can contribute [3]. In the excitation spectra (curves 3-5, Figure 3), bands of F, F^+ and P centers are noticeable. The excitation band at 4.36 eV is presumably associated with iron ions, which are always present in MgO as a residual impurity.

Luminescence spectra were also measured for MgO crystals upon excitation by synchrotron radiation. It can be seen that for a sample irradiated up to a fluence of 10^{12} Xe/cm^2, when the energy of the exciting light is shifted to the long-wavelength side of the spectrum, the maximum of the intensity shifts to the short-wavelength side. Under exciting with 4.8 eV light where F^+ centers are excited more, the emission in longer wavelength side gives rise. Excitation at 5.75 eV, where the P centers are absorbed, gives an intense glow with a maximum of about 2.97 eV. For a sample irradiated up to fluence of 6.7×10^{13} Xe/cm^2, excitation at a point of 5.4 eV gives a luminescence of about 3.3 eV.

REFERENCES

[1] Baubekova G. et al. About complexity of the 2.16-eV absorption band in MgO crystals irradiated with swift Xe ions // Radiat. Meas. Pergamon, 2020. Vol. 135. P. 106379.
[2] Kappers L.A., Kroes R.L., Hensley E.B. F+ and F′ centers in magnesium oxide // Phys. Rev. B. 1970. Vol. 1, № 10. P. 4151–4157.
[3] O'Connell D.O., Henderson B., Bolton J.M. Uniaxial stress and polarisation studies of F2 centre luminescence in MgO // Solid State Commun. 1981. Vol. 38, № 4. P. 283–285.
[4] Chen Y., Kolopus J.L., Sibley W.A. Luminescence of the F+ Center in MgO // Phys. Rev. American Physical Society, 1969. Vol. 186, № 3. P. 865.

*This research has been/is funded by the Science Committee of the Ministry of Education and Science of the Republic of Kazakhstan Grant No. AP08052050 and Grant No. AP13067816.

R4-P-028603

SIMULATED RADIATION DAMAGE TO TUMOR CELLS ACCUMULATED BORON NITRIDE QUANTUM DOTS

ULADZISLAU KULIK[1], *TATSIANA KULAHAVA*[1], *LENA GOLUBEWA*[1,2], *MARINA DEMIDENKO*[1], *ALEKSANDR BUGAY*[3] *SERGEY MAKSIMENKO*[1]

[1]*Institute for Nuclear Problems of Belarusian State University, Minsk, Belarus*
[2]*State Research Institute Center for Physical Sciences and Technology, Vilnius, Lithuania*
[3]*Laboratory of Radiation Biology, JINR, Dubna, Russian Federation*

Boron neutron capture therapy (BNCT) is a promising non-surgical radiotherapy method for the treatment of invasive malignant tumors (primary brain tumors, recurrent head, and neck cancer, cutaneous and extracutaneous melanomas), which includes two stages: (i) a drug, containing the non-radioactive isotope boron-10 (^{10}B), is injected to the patient, where it localizes in the tumor, (ii) the patient is irradiated with epithermal neutrons. The absorption of neutrons by boron-10 causes the formation of alpha particles, nucleus of ^{7}Li and high-energy gamma quant. The effectiveness of BNCT depends mainly on the concentration of boron (approximately 10^9 atoms of ^{10}B per cell should be selectively delivered [1]) and its selective accumulation and distribution in tumor target cells. In the present study, a theoretical evaluation of the effectiveness of BNCT based on the use of boron nitride quantum dots (BNQDs) is carried out.

Simulation of the interaction of formed pairs of ions (Li, α-particle) with the cell components was performed by the Monte Carlo method implemented in the 'Stopping and Range of Ion in Matter' (SRIM) [2]. Several models of tumor cells with different nucleoplasmic ratios (a unified cell model, lymphoma, melanoma, squamous cell carcinoma) were considered. The focus of the study was the dependence of radiation damage to cells on the specific localization of BNQDs in different compartments: intercellular space, membrane, cytoplasm, nucleus.

As a result of modeling, the optimal localization of BNQD in tumor cells depending on the type of tumor was determined. Cell nuclei are the main target for BNCT as they are the storage of DNA. It was revealed that the most effective damage to the nucleus of a unified cell (Fig.1a) occurs in the case of localization of the BNQD in the cytoplasm of cells due to the energy release (Fig.1b-c). The same results were obtained for other cell types with small variations.

The obtained results indicate that the increased effectiveness of BNCT can be achieved by using BNQDs specifically functionalized to be accumulated in the cell cytoplasm, thus, providing the possibility to reduce the time of BNCT and radiation dose as well as improve the prognosis for recovery.

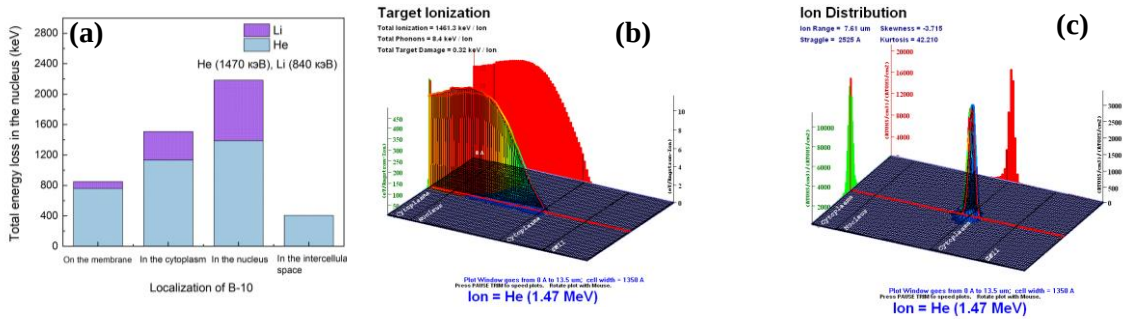

Fig. 1. Simulated radiation damage to tumor cells. **(a)** – the total energy loss on the ionization of the nucleus (violet and blue colors correspond to energy loss by Li ions and α-particles, respectively), **(b, c)** – Interaction of α-particles (1470 keV) with the cell during BNCT when BNQDs were localized in the cell cytoplasm: **(b)** – ionization of the target itself during the propagation of α-particles, **(c)** – final distribution of α-particles in the target.

REFERENCES

[1] Coderre J.A., Morris G.M. The radiation biology of boron neutron capture therapy // Radiation Research. 1999. Vol. 151, № 1. P. 1–18.
[2] Ziegler J. James Ziegler - SRIM & TRIM. 2017.

R4-P-033301

MECHANICAL STRESSES IN SILICON NITRIDE AND ALUMINA NITRIDE CERAMICS IRRADIATED WITH HIGH ENERGY IONS*

A. ZHUMAZHANOVA[1,2], A. MUTALI[1,2,3], A. IBRAYEVA[1,2,3], V. SKURATOV[2,4,5], A. DAULETBEKOVA[1], E. KORNEEVA[3], A. AKILBEKOV[1], M. ZDOROVETS[1,2,6]

[1] L.N. Gumilyov Eurasian National University, Nur-Sultan, Kazakhstan
[2] Astana Branch of the Institute of Nuclear Physics, Nur-Sultan, Kazakhstan
[3] G.N. Flerov Laboratory of Nuclear Reactions, Joint Institute for Nuclear Research, Dubna, Russia (
[4]National Research Nuclear University «MEPhI», Moscow, Russia
[5] University «Dubna», Dubna, Russia
[6] Ural Federal University, Yekaterinburg, Russia

Irradiation with heavy ions of 1-3 MeV/nucleon energies is characterized by pronounced inhomogeneous ionization and nuclear stopping profiles. As a result, the level of energy losses varies over a very wide range, which in own turn leads to a inhomogeneous spatial distribution of radiation damage and associated mechanical stresses. The range of ions with the above energies, depending on the density of the material, does not exceed several tens of microns. For energies of ~ 1 MeV/nucleon, which are of the greatest interest from a practical point of view for simulation of the fission fragments impact, this value is in the range from several microns to ~ 10 microns. Therefore, to get reliable information about stress profiles, it is necessary to use experimental methods with a spatial resolution of ~ 1 micron. Such accuracy can be achieved in techniques based on the use of the piezospectroscopic effect), which connect the spectral shift in optical absorption, luminescence, or Raman scattering spectra with the level of mechanical stresses [1,2].

In this work depth-resolved Raman spectroscopy technique was used to study the residual stress profiles in polycrystalline silicon and aluminum nitrides irradiated with Xe (167 MeV, 1×10^{11} cm^{-2} ÷ 4.87×10^{13} cm^{-2}) and Bi (710 MeV, 1×10^{11} cm^{-2} ÷ 1×10^{13} cm^{-2}) ions. It was shown that both compressive and tensile stress fields are formed in the irradiated specimen, separated by a buffer zone located at a depth coinciding with the thickness of layer, amorphized due to multiple overlapping of the track regions. Compressive stresses are registered in subsurface region, while at a greater depth, the tensile stresses are recorded and their level of reaches the maximum value in the end of ion range. The size of the amorphous layer was evaluated from the dose dependence of the FWHM of the dominant 204 cm^{-1} line in Raman spectra and scanning electron microscopy. In contrast to Si_3N_4, radiation-stimulated changes in mechanical stresses in AlN were within the measurement error throughout the entire thickness of the irradiated layer, except of the near-surface region. The observed effect is associated with the different structural sensitivity of silicon and aluminum nitrides to high-density ionization - the formation of amorphous latent tracks in Si_3N_4 and their absence in AlN.

REFERENCES

[1] Murari N. et al. Raman piezo-spectroscopic behavior of aluminum nitride //*Applied spectroscopy*. – 1997. –v. **51**. – pp. 1761-1765.

[2] Ma Q., Clarke D. R. Stress measurement in single-crystal and polycrystalline ceramics using their optical fluorescence //*Journal of the American Ceramic Society*. –1993. –v. **76**. – pp.1433-1440.

* The work was supported by grant of the Ministry of Education and Science of the Republic of Kazakhstan AP 08856368 «Radiation resistance of nitrides and carbides based ceramics against of impact of heavy ions with fission fragments energies».

R4-P-033601

MICROSTRUCTURAL STABILITY AND MECHANICAL PROPERTIES OF THE SYSTEM V-NB-TA-TI UNDER HELIUM ION IRRADIATION

A.E. RYSKULOV[1], M.M. BELOV[2], V.V. UGLOV[2], S.V. ZLOTSKI[2], K. JIN[3], I.A. IVANOV[1,4], A.L. KOZLOVSKIY[1,4], M.V. ZDOROVETS[1,4], A.E. KURAKHMEDOV[1], A.D. SAPAR[1], D.A. MUSTAFIN[1], Y.V. BIKHERT[1], T.A. KUZNETSOVA[5], V.A. LAPITSKAYA[5], A.V. KHABARAVA[5]

[1]*Institute of Nuclear Physics, Nur-Sultan, Kazakhstan*
[2]*Belarusian State University, Minsk, Belarus*
[3]*Beijing Institute of Technology, Beijing, China*
[4]*L.N. Gumilyov Eurasian National University, Nur-Sultan, Kazakhstan*
[5]*A.V. Luikov institute of Heat and Mass Transfer of the National Academy of Science of Belarus, Minsk, Belarus*

One of the promising areas of research in modern material science is the study of properties and methods for producing high-entropy alloys. High entropy alloys (HEAs) are composed of four or more metallic elements mixed in an equimolar or near equimolar ratio [1]. The introduction of near-equiatomic multicomponent single phase high entropy alloys has changed the conventional alloy design process in which only one or two principal elements determine the material primary properties. It is believed that maximizing the configuration entropy of high-entropy alloys promotes the formation of a single-phase disordered solid solution instead of the formation of complex intermetallic or second phases which might influence point defect recombination phenomena in irradiated materials by modifying the vacancy-interstitial recombination interaction distance, solute diffusivity, or other mechanisms, thereby producing different (superior or inferior) radiation stability compared to conventional single phase alloys [2, 3].

Multicomponent solid solutions based on V-Ti-Nb-Ta were synthesized using high-purity metals (>99.9%) by arc melting followed by homogenization. Then annealing was carried out for 24h and 72h at a temperature of 1150 ºC with cold rolling up to 85 % reduction in thickness. The samples were irradiated at room temperature with He^{2+} ions with an energy of 40 keV and a fluence of 2×10^{17} cm^{-2}.

The calculation of energy losses was carried out in the SRIM 2013 program using the Kinchin-Pease model. The maximum range of helium ions was 275–325 nm, with the maximum damage for vanadium at a depth of 160–170 nm, and for the VNbTaTi alloy, at 120–140 nm. The highest value of the damaging dose is 3.5–6.5 dpa, depending on the samples. The concentration of implanted He^{2+} ions does not exceed 17–23 at.%.

The X-ray diffraction analysis of initial samples showed that, regardless of the number of elements in the alloy, a single-phase solid solution with a BCC lattice is formed in all initial samples. The general view of the diffraction patterns (narrow and intense diffraction peaks) indicates a high crystallinity degree of the alloys; however, the shape of the diffraction lines (their asymmetry) is related to the possible both with the heterogeneity of the structure of the solid solution and for strongly deformed crystal lattices, which is characteristic of high-entropy alloys and is associated with the difference in the atomic radii of the selected elements. The lattice parameter for samples V, VNb, VNbTa, VNbTaTi was 0.3027 nm, 0.3177 nm, 0.3227 nm, 0.3234 nm, respectively. The results of energy dispersive analysis (EDX) confirm the formation of homogeneous equiatomic multicomponent solid solutions.

After irradiation with helium ions with at energy of 40 keV and a fluence of 2×10^{15} cm^{-2}, the uniformity of the distribution of elements and the phase composition of a multi-component solid solution based on V-Nb-Ti-Ta did not change, which is confirmed by the results of scanning electron microscopy and X-ray diffraction analysis. The diffraction pattern shows a more explicit asymmetry of the peaks and their shift towards smaller angles, which indicates the deformation of the crystal lattice caused by irradiation. Values of macro-deformation increased and amounted to 0.21%, 0.35%, 0.44%, 0.47% for V, VNb, VNbTa, VNbTaTi, respectively. The magnitude of the micro-deformation calculated by the Holder-Wagner method also increased with the number of elements in the system V-Nb-Ta-Ti, except pure vanadium and size of the coherent scattering regions decreased. The nano-hardness data of the initial and irradiated samples are compared with the results of micro- and macro-strain. In the work, we analyze in detail mechanisms of radiation resistance and the physical cause for this effect.

REFERENCES

[1] M.C. Troparevsky, J.R. Morris, M.Daene et al., "Beyond Atomic Sizes and Hume-Rothery Rules: Understanding and Predicting High-Entropy Alloys," JOM, vol.67, pp. 2350-2363, 2015.

[2] D.B. Miracle, O.N. Senkov, " A critical review of high entropy alloys and related concepts," Acta Materialia, vol.122, pp. 448-511, 2017.

[3] Ming-Hung Tsai, Jein-Wei Yeh, "High-Entropy Alloys: A Critical Review," Mater. Res. Lett., vol.2, pp. 107-123, 2014.

R4-P-050701

THE EFFECT OF ULTRAVIOLET RADIATION ON THE STRUCTURE AND PROPERTIES OF PENTAPHTHALIC PAINT COATINGS *

N.G. VALKO[1], D.I. BOGDEVICH[2], A.YU. IVANOV[3], N.S. RAGOZHKIN[4]

[1]Vice Dean of the Faculty of Physics and Technology ,Yanka Kupala State University of Grodno, Belarus
[2] Postgraduate student, Yanka Kupala State University of Grodno, Belarus
[3]Head of the Department of Theoretical Physics and Heat Engineering , Yanka Kupala State University of Grodno, Belarus
[4] Postgraduate student , Yanka Kupala State University of Grodno, Belarus

The work presents the results of the study of the effect of UV- radiation on a structure and properties of pentaphthalic paint coatings. The PF-115 pentaphthalic paint applied evenly onto 08 kp steel. Coatings were irradiated with the UV-rays (207 nm) during the curing process for 30 and 60 minutes [1, 2].

The impact of the effect of UV-radiation on the structure of pentaphthalic paint coatings was investigated by XRD method with help of a DRONE 3M diffractometer (CuKα)[3]. It was obtained that a degree of crystallinity of pentaphthalic coatings cured under the room temperature without irradiation is lower than a degree of crystallinity of coatings cured under irradiation by UV-rays. The results of the study are shown in Figure 1.

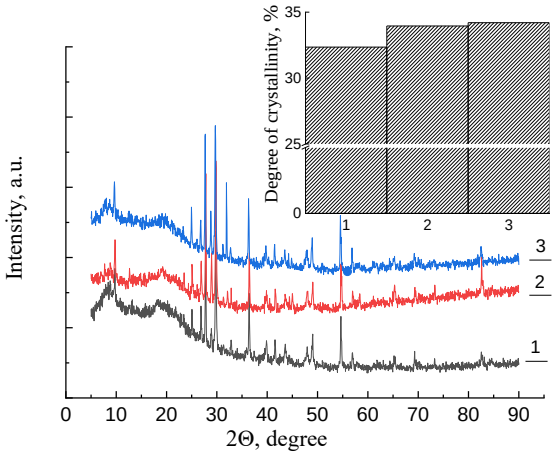

1 – curing without UV-effect; 2 – curing with UV radiation for 30 minutes; 3 – curing with UV radiation for 60 minutes

Fig.1. Dependence of the degree of crystallinity on the curing time by UV radiation

It has been established that curing of PF-115 pentaphthalic paint coatings under the UV rays (207 nm) leads to an increase in the degree of crystallinity of pentaphthalic paint coatings. In particular, the degree of crystallinity of the coating cured under natural conditions is 32,35 %, the degree of crystallinity of the coating cured under UV radiation for 60 minutes is 34,20 %. These features of increasing the degree of crystallinity indicate decreasing in the amorphousness of pentaphthalic coatings and an increase in polymerization. It has been found that an increase in the duration of irradiation contributes to an increase in the corrosion resistance and hardness of the coatings.

REFERENCES

[1] Valko, N. Structure and properties of paint coatings irradiated by ultraviolet rays / N.Valko, A. Hloba, A. Kasperovich // 7th International Congress on Energy Fluxes and Radiation Effects, Tomsk, 14-26 sept. 2020 / Tomsk Polytechnic University; ed.: G. Mesyats [et al.]. – Tomsk, 2020. – P. 1024-1027

[2] O.E. Babkin, Polymer coatings of UV curing: textbook.the manual. St. Petersburg. SPbGUKiT, 2012.

[3] D.I. Bogdevich, “The influence of ultraviolet radiation on the fine structure of alkyd coatings,” Condensed matter Physics: Materials of the XXX International Scientific and Practical Conf. of graduate students, undergraduates and students, Grodno, Belarus, pp. 15-16, 2022.

* The work was supported by the Ministry of Education of the Republic of Belarus.

R4-P-052701

MICROSTRUCTURE AND PHASE STATE OF A COMPOSITE BASED ON SILICON CARBIDE IRRADIATED WITH KRYPTON IONS

V.V. UGLOV[1], V.M. KHOLAD[1], P.S. GRINCHUK[2], M.V. KIYASHKO[2], I.A. IVANOV[3,4], A. L. KOZLOVSKIY[4], M.V. ZDOROVETS[3,4]

[1]*Belarusian State University, Minsk, Belarus*
[2]*A.V. Luikov institute of Heat and Mass Transfer of the National Academy of Science of Belarus, Minsk, Belarus*
[3]*L.N. Gumilyov Eurasian National University, Nur-sultan, Kazakhstan*
[4]*Institute of Nuclear Physics, Nur-sultan, Kazakhstan*

Due to its wide band gap, high thermal conductivity, good stability, high strength and radiation resistance, silicon carbide is a promising material for use as structural elements in thermonuclear reactors, fission reactors and gas-cooled fission reactors, as well as in the burial of radioactive nuclear waste. Title (EFRE Title style): 11pt, bold, roman, centered, all capitalized, first line indent 0 pt, spacing 6 pt before and 9 pt after, no word wrapping.

Ceramic SiC samples were obtained at IHMT NAS RB by binding two fractions of SiC powders M5 and M50 (grain size 5 microns and 50 microns, respectively) using a thermoplastic binder based on paraffin P-2 and subsequent silicification at a temperature of 1800 ° with and a pressure of 0.13 Pa. As a result, the final Si/SiC ceramics contain about 78% volume fraction SiC and less than 2% of single residual pores with a characteristic size of up to several microns. Before irradiation, the silicon carbide samples were mechanically polished. The samples were irradiated with Kr+ ions with an energy of 280 keV at RT at the DC-60 linear heavy ion accelerator (Institute of Nuclear Physics, Nur-Sultan, Kazakhstan). Irradiations with krypton ions were carried out with fluences 1×10^{13}, 1×10^{14}, 5×10^{15} sm^{-2}.

The study of the structural-phase state of the initial and irradiated SiC samples was carried out by X-ray diffraction analysis (XRD) and scanning electron microscopy (SEM).

The study of the structural-phase state of the initial samples showed that the samples are a composite: SiC-6H, Si and SiC-15R. The main phase is SiC-6H (~ 80%).

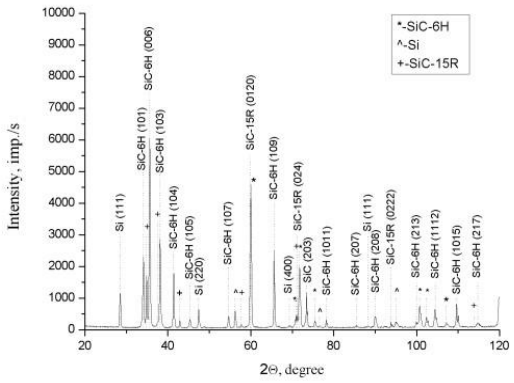

Fig. 1. XRD patterns of the initial SiC.

Irradiation with Kr^+ ions leads to a significant increase in lattice deformation, which is caused by the formation of radiation defects and their clusters. As the dose increases, the relative change in the lattice parameter a decreases, parameter c increases. Such a change in the crystal lattice occurs as a consequence of irradiation growth. This irradiation effect is characteristic of metals with a HCP, especially zirconium [1].

Analysis of the Raman spectra of samples irradiated at doses of 1×1013 and 1×1014 cm-2 showed that with increasing dose, the intensity and broadening of peaks decreases, which is associated with the disordering of the crystal structure, as well as the formation and accumulation of radiation defects in the SiC sample. At a dose of 5×1015 cm-2, there are no peaks of the first order of oscillations, what connected with amorphization of the SiC surface layer, which is also confirmed by the results of SEM.

REFERENCES

[1] Cluster dynamics modeling of irradiation growth in single crystal Zr/ Yang Li , Nasr Ghoniem // Journal of Nuclear Materials 540. – 2020. – 152312.

R4-P-052801

RADIATION STABILITY OF TIVNBTA HIGH ENTROPY ALLOY IRRADIATED BY HELIUM AND KRYPTON IONS

I.A. IVANOV[1,2], V.V. UGLOV[3], M.M. BELOV[3], S.V. ZLOTSKI[3], K. JIN[4], N.A. STEPANJUK[3], A.E. RYSKULOV[1], A.L. KOZLOVSKIY[1,2], M.V. KOLOBERDIN[1,2], A.E. KURAKHMEDOV[1], A.D. SAPAR[1]

[1]Institute of Nuclear Physics, Nur-Sultan, Kazakhstan
[2]L.N. Gumilyov Eurasian National University, Nur-sultan, Kazakhstan
[3]Belarusian State University, Minsk, Belarus
[4]Beijing Institute of Technology, Beijing, China

High-entropy alloys (HEAs) are a class of crystalline metallic material which does not have an unambiguously identifiable base element and is highly alloyed with multiple elements. Some HEAs have demonstrated the potential of exhibiting superior mechanical properties compared to conventional alloys [1]. It is believed that maximizing the configuration entropy of HEAs promotes the formation of a single-phase disordered solid solution instead of the formation of complex intermetallic or second phases; as a result, the alloy has a simple microstructure with improved properties compared to traditional alloys. Numerous studies have shown that high-entropy alloys have a high elastic limit, wear, creep, and thermal and radiation resistance [2]. Substantial results on the ion irradiation experiments, with both heavy ions and He ions, have demonstrated that controlling chemical complexity can delay the irradiation induced defect evolution, suppressing the void and He bubble formation, as well as the radiation-induced segregation [3]. The use of HEAs as structural materials under extreme environments has been proposed owing to their desirable mechanical properties and thermodynamic stability.

Multicomponent high entropy alloy TiVNbTa and medium entropy alloy TiVTa were synthesized using high-purity metals (>99.9%) by arc melting followed by homogenization. Then annealing was carried out for 24h and 72h at a temperature of 1150ºC with cold rolling up to 85 % reduction in thickness.

Ion implantation of alloys was carried out on a DC-60 heavy ion accelerator (Nur-Sultan) separately with He (40 keV, 2×10^{17} cm^{-2}) and Kr (280 keV, 5×10^{15} cm^{-2}) ions, as well as sequentially with helium and krypton ions.

The X-ray diffraction analysis showed that a single-phase solid solution with a BCC lattice is formed in all samples. The results of scanning electron microscopy and X-ray energy dispersive analysis confirm the formation of homogeneous equiatomic multicomponent solid solutions, the grain size in the VNbTiTa and TiVTa alloys was about 100-200 μm.

It was found that irradiation with helium and krypton ions did not lead to change in phase composition, microstructure and the uniformity of the elements distribution of the TiVNbTa and TiVTa alloys. No processes of radiation erosion (blistering or exfoliation) were revealed on the surface of the samples.

Irradiation with low-energy helium and krypton ions only leads to a change in internal stresses. Alloys TiVNbTa and TiVTa have compressive stresses of -0.40 and -0.57 GPa, respectively. Irradiation with helium ions leads to an increase in the level of compressive stresses to -0.64 and -0.94 GPa, and subsequent irradiation with krypton ions leads to a decrease in stresses to -0.49 and -0.63 GPa. CSS irradiation with only krypton ions reduces the stress level to -0.25 and -0.36 GPa.

The paper discusses the mechanisms of radiation stability of high-entropy alloy TiVNbTa and medium entropy alloy TiVTa, the influence of the type of ions on the formation of radiation defects, and their influence on the level of internal stresses.

REFERENCES

[1] B. Gludovatz, A. Hohenwarter, D. Catoor, E.H. Chang, E.P. George, R.O. Ritchie, «On the Brittle-to-Ductile Transition of the As-cast TiVNbTa Refractory High-entropy Alloy», Science (80-.), vol.345, Article Number 1153 LP, 2014.

[2] W. Zhang, P.K. Liaw, Y. Zhang, «High-entropy alumino-silicides: a novel class of high-entropy ceramics», Sci. China Mater., vol.61, Article Number 2, 2018.

[3] N. Jia, Y. Li, H. Huang et al., «Helium bubble formation in refractory single-phase concentrated solid solution alloys under MeV He ion irradiation», Journal of Nuclear Materials, vol.550, Article Number 152937, 2021.

R5-O-037102

NON-DESTRUCTIVE MEASUREMENT OF DETAILED TRANSVERSE BEAM DISTRIBUTION WITH THE USE OF AN IONIZATION MONITOR

TIMOSHENKO K.D., TETEREV YU.G., KRYLOV A.I., MITROFANOV S.V., ISSATOV A.

Joint Institute for Nuclear Research, Dubna, Russia

The constant monitoring of the uniformity of the density distribution of the flux of the accelerated particles is required in various applied fields as such as the studies of biological objects and of radiation resistance of electronic devices. The ionization monitor has been developed at FLNR JINR in order to make the non-destructive detailed high precision measurement of the transverse profile of a wide beam of accelerated particles. The monitor design is aimed at measuring the concentration of residual gas ions arising along on the beam path. The distribution of the ions is proportional to the distribution of the particle flux density. The ions are extracted from the beam region by a constant electric field larger than 0.2 kV/cm and then are accelerated by a sawtooth voltage with a frequency of 2 Hz. During the extraction the ions get the kinetic energy proportional to the distance traveled in a constant field and to the value of the subsequent accelerating voltage. The extracted ions enter two consecutive electrostatic analyzers separated by a plate with 1 mm slit. Ions can enter the second analyzer through this slit only if they were created in a narrow beam region, which position depends on the value of the sawtooth voltage. The monitor sensitivity is increased by MCP (Micro channel plate) placed after the analyzers. The collector divided into 31 strips is located after the MCP. The current from the strips is digitized by several ADC (Analog to digital converter) channels. The first coordinate of the ion formation position is determined by the number of the collector strip. The second coordinated is extracted from the value of the sawtooth voltage measured by another ADC. The number of employed ADCs allows every second measurement of a detailed two-dimensional distribution with 31x31 points on a beam cross section up to 45 mm in diameter. Because the ions of the residual gas are collected from the beam path 90 mm long, the sensitivity of the monitor is almost two orders of magnitude higher than the existing analogs [1, 2]. The monitor can also be used to measure the profile of secondary beams.

REFERENCES

[1] Poggi M., Mostert H. et al. Two-dimensional ionization beam profile measurement. // Proceedings of DIPAC, 2009, Basel, Switzerland.

[2] Гаврилов С. и др. Перспективы использования ионизационного монитора поперечного сечения пучка на ускорителях FRIB Michigan State University и У-70 ИФВЭ. Вопросы атомной науки и техники (Problems of atomic science and technology), 2012, т. 3(80), с. 19-23.

R5-P-003102

THE ELECTRON-OPTICAL SCHEME OF THE ENERGY ANALYZER OF SMALL-SIZED ELECTRON SPECTROMETER*

ZH.T. KAMBAROVA[1], *A.O. SAULEBEKOV*[2], *K.B. KOPBALINA*[3]

[1]*Buketov Karaganda University, Karaganda, Kazakhstan*
[2]*Lomonosov Moscow State University, Kazakhstan branch, Nur-Sultan, Kazakhstan*
[3]*Karaganda Technical University, Karaganda, Kazakhstan*

In this work, the calculation of the electron-optical scheme of the axially-symmetric electrostatic mirror-type energy analyzer based on a multipole electrode system is carried out. The field of the energy analyzer is designed as a superposition of the base cylindrical field and set of circular octupole coaxial with base field.

The authors of the work previously carried out the calculation and analysis of equipotential portraits of electrostatic octupole-cylindrical fields for different weight contributions of the cylindrical field and circular octupole in order to determine the electrode configuration of the energy analyzer [1].

The energy analyzer contains two coaxial electrodes: the inner electrode *1* has a cylindrical shape of radius r_0 and is under zero potential, the outer electrode *2* has a curvilinear profile and is under the deflecting potential U_0 (Fig. 1). A field that decelerates and deflects charged particles is created between the electrodes, which have the properties of an electrostatic mirror. The profile of the outer electrode *2* repeats the equipotential surface of the electrostatic octupole-cylindrical field.

The trajectory analysis of charged particles in field of the energy analyzer was performed on the basis of a numerical calculation method by using the CAE “Focus” software for numerical simulation of electron optics systems [2].

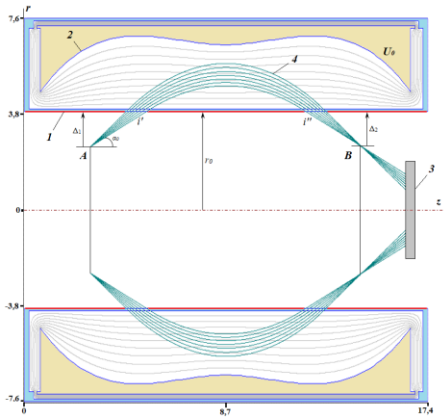

Fig.1. The electron-optical scheme of the energy analyzer: 1 - inner grounded cylindrical electrode, 2 - outer deflecting electrode, 3 - a position-sensitive detector, 4 - charged particle beam, *A* - ring source of charged particles, *B* - ring image, *i'* - entrance ring slit, *i''* - exit ring slit.

According to the scheme, the charged particles beam from the ring source *A* enters the analyzer field through the entrance slit *i'*, is reflected by the field, then returns to the zero potential region through the exit slit *i''* and is focused into the ring image *B*. Then the particles are registered by a position-sensitive detector *3*. Due to the curvilinear profile of the outer electrode *2*, the scheme provides a sharp 3rd-order angular focusing of charged particles near 36° with a divergence angle $\Delta\alpha=\pm6°$. The corpuscular-optical properties of the system are calculated. The energy analyzer is characterized by compactness, high focusing quality and energy resolution, and can be used to develop a small-sized highly sensitive electron spectrometer.

REFERENCES

[1] Zh.T. Kambarova, A.O. Saulebekov, K.B. Kopbalina, A.K. Tussupbekova, D.A. Saulebekova, “About the possibility of creating an efficient energy analyzer of charged particle beams based on axially-symmetrical octupole-cylindrical field,” Eurasian phys. tech. j., vol. 18, no. 2 (36), pp. 96-102, June 2021.

[2] A. Trubitsyn, E. Grachev, V. Gurov, I. Bochkov, V. Bochkov, "CAE "FOCUS" for modelling and simulating electron optics systems: Development and application," Proceedings of SPIE., vol. 10250, pp. 0V-1 – 0V-7, 2017.

* The work was supported by the Ministry of Education and Science of the Republic of Kazakhstan under grant No. AP09058188.

R5-P-003103

FEATURES OF SIMULATION OF CORPUSCULAR OPTICAL SYSTEMS FOR THE ANALYSIS OF CHARGED PARTICLE BEAMS*

A.O. SAULEBEKOV[1], ZH.T. KAMBAROVA[2], D.A. SAULEBEKOVA[3]

[1]Lomonosov Moscow State University, Kazakhstan branch, Nur-Sultan, Kazakhstan
[2]Buketov Karaganda University, Karaganda, Kazakhstan
[3]Institute Curie, Sorbonne University, Paris, France

The features of simulation of energy analyzers of charged particle beams are considered. Since the limits of energy change in the methods of secondary electron spectroscopy lie in the range from a few keV to eV, electrostatic systems are predominantly used as energy analyzers.

Basically, when modeling and calculating corpuscular-optical systems, two directions were used to improve energy resolution, arising from the following formula $R=(\Delta L/D)\cdot\Gamma$, where R, ΔL, D, Γ are energy resolution, linear image smearing, linear energy dispersion and linear magnification, respectively. The first direction of research is associated with a decrease of ΔL, that is, an improvement of the focusing quality of charged particles beam or an increase of angular focusing order. The second direction is associated with an increase of D. There is also a third direction associated with the coefficient Γ. It was rarely taken into account, this is due to the fact that for the most common cylindrical mirror analyzer $\Gamma=1$. The need to take into account Γ arose in the study of rough surfaces, for example, discontinuity surfaces by method of Auger electron spectroscopy. The small magnitude of Γ of the system preserves the "tuning to the focus" in a wide range of variations in the cavities depth and the asperities height of the rough surface.

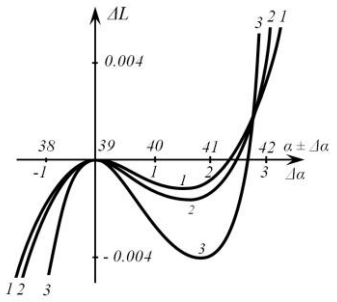

Fig.1. Aberration curves of a highly dispersive system for various parameters.

Let's consider one aspect concerning the first method. Decreasing ΔL improves the energy resolution, but decreases the luminosity of a device. This is primarily due to a decrease of the initial opening angle $\Delta\alpha$ of the charged particle beam. Information obtained from aberration curves can be useful. It can be seen from Fig.1, that the opening angle of the entrance beam can be taken from 38° to 41.5°. In this case, R=0.005% at luminosity 1.95% of 4π [1]. As another example, let's consider the electron-optical scheme of a hexapole-cylindrical analyzer corresponding to the following parameters: P=0.6 (reflection parameter relating the geometric and energy characteristics of the analyzer), $\alpha_0 = 43.742°$ (entrance angle of the axial trajectory into the analyzer field), $\Delta\alpha = \pm 8°$, D=1.7967, A_{III} =0.7340. The cubic aberration A_{III} in this scheme is not equal to zero, but it is small and at the same time has a maximum in the range of P. This means that the coefficient of spatial aberration of the next order A_{IV} at this point is equal to zero. This allows to conclude that the analyzer's angular focusing is close to ideal [2, 3]. The image smearing in a focus of an analyzer, caused by the angular divergence of a beam 16° in the axial plane, is determined by the cubic angular aberration $\Delta l = A_{III}\left(\Delta\alpha\right)^3$ and is equal to $\Delta l = 0.004$. Thus, a more detailed analysis of the aberration curves makes it possible to obtain a higher luminosity of the analyzer, while maintaining a high energy resolution.

REFERENCES

[1] V.V. Zashkvara, A.O. Saulebekov, L.S. Yurchak, A.I. Chasnikov, "Electron-optical properties of electrostatic spherical mirror and systems based on it," Journal of technical physics, vol., no. 6, pp.189-204, 1992. [in Russian]

[2] B.U. Ashimbaeva, K.Sh. Chokin, A.O. Saulebekov, Zh.T. Kambarova, "Modeling of electron-optical scheme of a hexapole-cylindrical analyzer," Applied physics, no. 2, pp. 45–48, 2012. [in Russian]

[3] V.S. Gurov, A.O. Saulebekov, A.A. Trubitsyn, Approximate-Analytical and Numerical Methods in the Design of Energy Analyzers, Advances in imaging and electron physics. Toulouse, France. - Academic Press is an imprint of Elsevier, vol.192, 224 p., 2015.

* The work was supported by the Ministry of Education and Science of the Republic of Kazakhstan under grant No. AP09058188.

R5-P-005901

DETERMINATION OF ARGON PLASMA PARAMETERS AND THEIR SPATIAL DISTRIBUTION IN DC MAGNETRON DISCHARGE BY MEANS OF OPTICAL EMISSION SPECTROSCOPY AND COLLISIONAL-RADIATIVE MODEL

S.V. SERUSHKIN

Bauman Moscow State Technical University, Moscow, Russia

The work describes determination results of magnetron plasma parameters, such as electron density and temperature, and their spatial distribution in axisymmetric DC magnetron discharge with argon pressure in the vacuum chamber $P = 2$ Pa. A specialized experimental-computational technique was developed and applied to investigate local emissive characteristics of argon discharge plasma.

For experimental part of the study, a diagnostic complex based on the AvaSpec-2048 spectrophotometer was used, which allows to record optical emission spectra (OES) from various areas of the discharge due to two-coordinate movement of the optical collimator in the plane perpendicular to the magnetron axis [1]. The obtained chordal distributions of the Ar atoms spectral lines intensities were recalculated into radial distributions in various discharge cross sections using the inverse integral Abel transform mathematical apparatus.

The method of determining magnetron plasma parameters: electron temperature and density, is based on minimization of difference between relative intensities of Ar spectral lines obtained by optical emission spectroscopy experiment at various discharge areas and calculated theoretically by some model (see Fig. 1 (a)). To obtain calculated population densities of excited states, a collisional-radiative model (CRM) for Ar atoms is used [2]. Electron energy distribution function for this model was considered to be both Maxwellian and non-Maxwellian [3, 4].

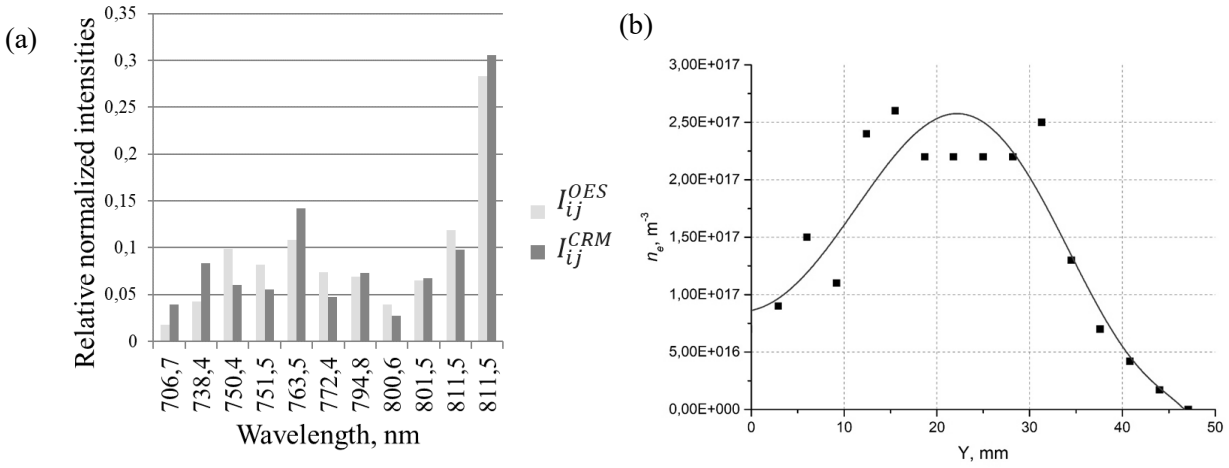

Fig.1 (a). Comparison between experimentally (OES) and theoretically (CRM) obtained Ar atoms spectral lines relative intensities, (b). Electron density radial distribution in axisymmetric magnetron discharge plasma with Ar pressure of 2 Pa.

The results obtained can be represented as radial distributions of plasma parameters. In particular, Fig. 2 (b) shows an example of the electron density distribution, which has a shape that correlates with the natural optical emission intensity distribution of an axisymmetric magnetron discharge with a dip near the axis and maxima in the region of the brightest glow.

REFERENCES

[1] V.M. Gradov, A.M. Zimin, S.V. Serushkin, I.A. Zemtsov, "Determination of spatial distributions of plasma parameters of a compact magnetron discharge," Physics of Atomic Nuclei, vol. 82, pp. 1376-1381, 2019.

[2] K.E. Evdokimov, M.E. Konischev, V.F. Pichugin, Z. Sun, "Study of argon ions density and electron temperature and density in magnetron plasma by optical emission spectroscopy and collisional-radiative model," Resource-Efficient Technologies, vol. 3, pp. 187–193, 2017.

[3] V.M. Donelly, "Plasma electron temperatures and electron energy distributions measured by trace rare gases optical emission spectroscopy", J. Phys. D 37 (2004) R217–R236 .

[4] X.-M. Zhu, Y.-K. Pu, Y. Celik, S. Siepa, E. Schungel, D. Luggenholscher, U. Czarnetzki, "Possibilities of determining non-Maxwellian EEDFs from the OES line-ratios in low-pressure capacitive and inductive plasmas containing argon and krypton," Plasma Sources Sci. Technol., vol. 21, 024003 (11 pp), 2012.

R5-P-022401

MODELLING AND EXPERIMENTAL MOSSBAUER SPECTRA OF SOLID SOLUTION FE(SN)

A.K. ZHUBAEV[1], G.A. RAKHMETOLLA[1], S.K. YEREZHEPOVA[1], YE.A. KANTARBAY[2]

[1]Zhubanov Aktobe Regional University, Aktobe, Kazakhstan
[2]International IT University, Almaty, Kazakhstan

The Fe-Sn binary system is characterized by the solubility of Tin in γFe and αFe, as well as the presence of regions of existence of various intermetallic compounds on the state diagram with an increase in temperature [1]. The solubility of Sn in α-Fe is maximal (9.2% at.) at 900°C and decreases to 3.2% at. Sn (at 600°C).

In a solid solution of α-Fe(Sn), there are 8 neighboring atoms in the nearest environment of the Fe atom. If we assume that Sn atoms are equally likely to replace the positions of Fe atoms from the nearest environment, then we can calculate the probability of the appearance of *m* Sn atoms in the nearest environment of the Fe atom using the binomial distribution

$$P(m; C_{Sn}) = \frac{8!}{m!(8-m)!} C_{Sn}^{m} (1 - C_{Sn})^{8-m}, \quad (1)$$

At the same time, each configuration of the nearest environment corresponds to its own partial spectrum. The substitution of an Iron atom for a Tin atom leads to a decrease in the hyperfine field. In [2], the changes in the hyperfine magnetic field and isomeric shift were determined when one Fe atom was mixed with an Sn atom in the first coordination sphere of an Iron atom in a solid solution at different impurity concentrations in the solution. There is a average decrease in the hyperfine field by 22.15 ±0.14 kOe.

Using the MSTools software package [3], the Mossbauer spectra of Fe nuclei were modeled according to the method [4] when the atoms of Iron atoms were replaced by impurity atoms. At the same time, the change ΔH=22 kOe is accepted. The relative intensities I(*m*) of all partial spectra were calculated for solid solutions of Fe-2.1% at Sn, Fe-2.5% at Sn, Fe-5% at Sn, Fe-7.8% at Sn. Using the technique [5], the Mossbauer spectra of a solution of α-Fe(Sn) with different concentrations of Sn atoms were modeled (Fig.1).

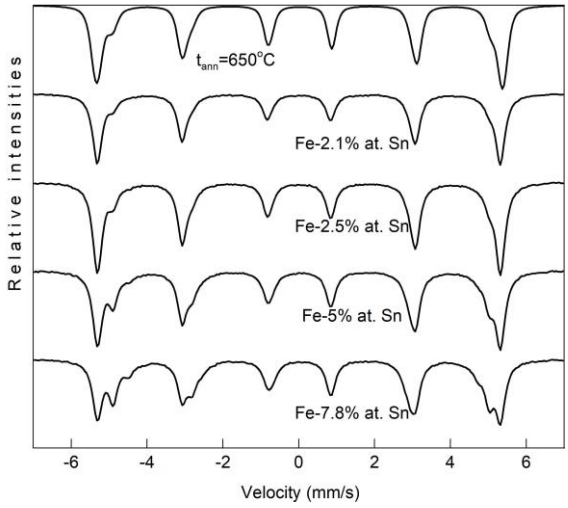

Fig.1. Comparison of the partial spectrum of a solid solution α-Fe(Sn) and the simulated spectra

Figure 1 shows the partial spectrum of the solid solution α-Fe(Sn) separated from the experimental spectrum of the layered system Sn(4 μm)-Fe(10 μm) after annealing at 650°C for 5 hours. Comparison of experimental spectra with simulated spectra shows a good correlation.

REFERENCES

[1] N.P. Lyakishev, Diagrams of the State of Double Metal Systems. Moscow: Mashinostroenie, 1997.
[2] I. Vincze, and A.T. Aldred, Phys. Rev. B, vol.9. no 9. p.3845, 1974.
[3] V.S. Rusakov, Mossbauer spectroscopy of locally inhomogeneous systems. Almaty, 2000.
[4] A.K. Zhubaev, T.S. Mukhanbetzhan and S.K. Yerezhepova, IOP Conf. Series: Journal of Physics: Conf. Series, 1281, 012097, 2019.
[5] A.K. Zhubaev, and B.Zh. Suleimanov, Izvesia vuzov. Fizika, vol.61, no 8/2, pp.151-154, 2018.

R5-P-031002

MODELING OF NEUTRONS GENERATION UNDER IRRADIATION WITH FAST ATOMS

A.I. PUSHKAREV, S.S. POLISADOV

Tomsk Polytechnic University, Tomsk, 634050 Russia

The results of modeling the neutron yield during irradiation of a TiD_2 target with deutron D^+ and deuterium atoms (D-D reaction) are presented. The neutron yield per deutron with energy E was calculated by the ratio for a thick target:

$$Y_{1D}(E) = A \int_0^{E_{max}} \frac{\sigma(E)}{dE/dx} dE, \; neutrons \qquad (1)$$

where A is the density of deuterium atoms in the target, cm^{-3}; σ(E) is the cross section of the D-D reaction, cm^2; dE/dx is the linear energy loss (LEL) of the deutron in the target, eV/cm.

Experimental values of the D-D reaction cross section [1] were used in the simulation, LEL of the deutron in the TiD_2 target was calculated using the SRIM program [2]. The results of the calculation of the LEL and the neutrons yield are shown in figure 1.

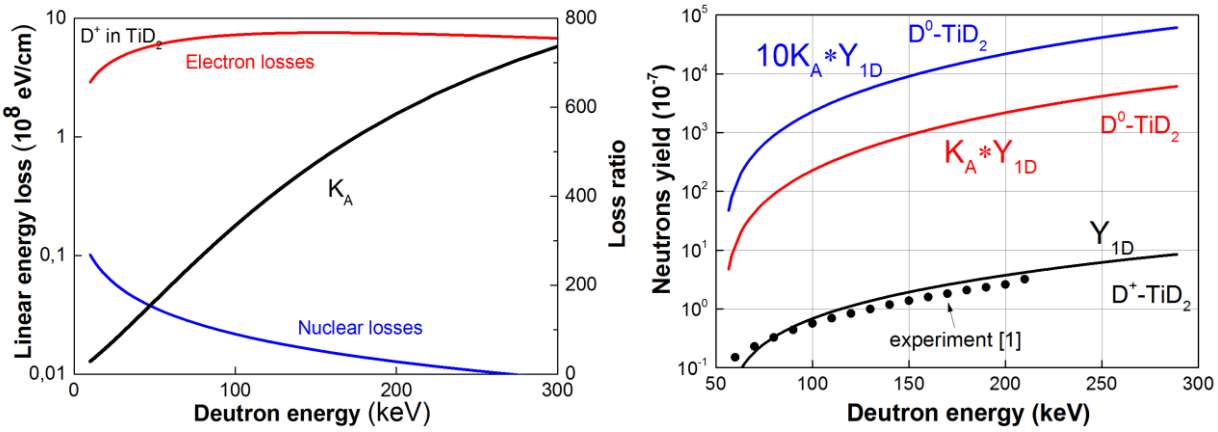

Fig.1. Dependence on the deutron energy of the LEL of the deutron in the TiD_2 target and the neutron yield per deutron in the D-D reaction

When ions are absorbed in a metal target, the main part of their energy is spent on interaction with the target electrons (electron losses), see Fig. 1. When the target is irradiated with deuterium atoms, the electronic losses are significantly less. To account for the increase in neutron yield when irradiated with deuterium atoms, we use the K_A coefficient in the Eq. (1), which takes into account the increase in the efficiency of kinetic energy transfer by an accelerated deuterium atom to the target atom (see figure 1):

$$K_A = \frac{(dE/dx)_{electr} + (dE/dx)_{nucl}}{(dE/dx)_{nucl}}, \qquad (2)$$

where $(dE/dx)_{electr}$ is the LEL of the deutron in the target when interacting with electrons (electron losses), $(dE/dx)_{nucl}$ is the LEL of the deutron in the target during elastic scattering (nuclear losses).

Figure 1 shows the results of calculating the neutron yield in the D-D reaction when irradiating a TiD_2 target with deuterium atoms.

The performed studies have shown that when the target is irradiated with fast deuterium atoms, the neutron yield can be significantly higher when irradiated with deuterons, due to the reduction of electronic losses. The TEMP-6 accelerator (300 keV, 150 ns) [3], when generating a pulsed beam of deuterium atoms, can form neutron pulses with an integral neutrons yield per pulse of $\approx 6 \cdot 10^{12}$ neutrons.

REFERENCES

[1]. A.S. Ganeev, ets. “The D-D reaction in the deutron energy range 100 - 1000 keV,” Atomnaya Energiya, 1957. Supplement Issue.5, p.26 (in Russian).
[2]. J.F. Ziegler - SRIM & TRIM. URL: http://www.srim.org/
[3]. A.I. Pushkarev, Yu.I Isakova. “A gigawatt power pulsed ion beam generator for industrial application,” Surface and Coatings Technology Vol. 228, Supplement 1, 15 August 2013, Pages S382–S384.

R5-P-046001

REACTIVITY OF SILVER AZIDE CRYSTALS IN A SPATIALLY INCREASING MAGNETIC FIELD

E.G. GAZENAUR, L.V. KUZMINA, MEHRUBONI DAVLATALII ABDUNAZAR, N.V. GAZENAUR

Kemerovo State University, Kemerovo, Russia

The use of magnetic field to initiate or stimulate a chemical reaction is especially relevant for highly sensitive materials, such as explosives.

The purpose of this work is to study the main regularities of the decomposition of silver azide crystals in a spatially increasing magnetic field, which can play a significant role in the search for unconventional ways to study of the mechanisms of solid-state reactions [1–3].

To solve the tasks set, the designs of magnetic systems and experimental cells were developed, as well as the optimal conditions for conducting experiments, namely, the field growth rate and exposure time, and the orientation of the crystal faces [4] relative of the lines of the magnetic field. The proposed design makes it possible to observe the release of gaseous decomposition products (nitrogen gas bubbles) during the action of a magnetic field and determine their release rate (outgas sing rate is the total volume of the released gas). The range of magnetic field inductions from 0.01 T to 0.3 T with inhomogeneity of magnetic field from 1.5 to 20 percent was studied.

It has been experimentally shown that in a non-uniform magnetic field, the decomposition reaction of silver azide crystals, which is detected by gas evolution, proceeds more intensively and starts earlier than in a uniform magnetic field, the inhomogeneity of which is not more than 1.5%. As can be seen from the graph in Figure 1, the rate of release of gaseous decomposition products depends on the inhomogeneity of the magnetic field created in the working volume of the magnetic system. The time of gas release is practically independent of the power characteristics of the magnetic field and inhomogeneity of here and is no more than 2 minutes.

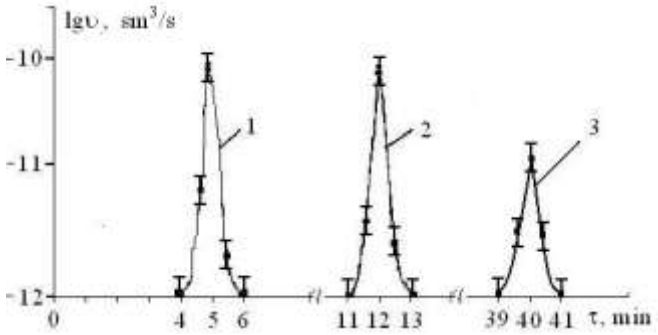

Fig.1. Dependences of the gas release rate in silver azide crystals on the time of exposure to magnetic field (average B=0.3 T) with inhomogeneity of magnetic fields in the working volume: 20% - curve 1; 10% - curve 2; 1.5% - curve 3.

In addition, experimental results show that, in an increasing magnetic field, features of the distribution of gaseous decomposition products over the crystal faces are observed. The gas is released mainly from the side faces of the crystal and partially from the developed face. If compared with the topography of gas release in a uniform magnetic field, it can be noted that the gas is released from the face of the crystal which is perpendicular of to the direction of the magnetic field induction line.

If we talk about the cause of the effect of a spatially growing magnetic field, then we can assume the appearance of an additional component of the Lorentz force, as a activity's result of which positive charge carriers (which are future reagents of a chemical reaction) are concentrated in the region of the crystal, which combined with magnetic field lines of higher density.

REFERENCES

[1] B.P. Aduev M.V. Anan'eva, A.A. Zvekov et al., "Miro-hotspot model for the laser initiation of explosive decomposition of energetic materials with melting taken into account," Combustion, Explosion, and Shock Waves, vol.50(6), Article Number 704-710, 2014.

[2] V.G. Kriger, A.V. Kalenskii, M.V. Anan'eva et al., "Determination of spatial characteristics of the chain reaction wave in silver azide," Russian Journal of Physical Chemistry., vol.8(4), Article Number 485-491, 2014.

[3] V.I. Korepanov, V.M. Lisitsyn, V.I Oleshko et al., "Kinetics and mechanism of explosive decomposition of heavy metal azides", Combustion, Explosion, and Shock Waves, vol.42(1), Article Number 94-106, 2006.

[4] F.I. Ivanov, L.B. Zuev and V.D. Maltsev, "Determination of spatial characteristics of the chain reaction wave in silver azide," Russ. J. Crystallogr., vol.28(1), Article Number 194-195, 1983.

R5-P-047801

ENSURING THE RADIATION SAFETY OF MEDICAL EXAMINATIONS WITH THE USE OF THERMOLUMINESCENT DOSIMETRY

N.L ALUKER [1], A.S. ARTAMONOV [2]

[1] Kemerovo State University, Kemerovo, Russia
Russia Federal Research Center of Coal and Coal Chemistry SB RAS, Kemerovo, Russia
[2] National Research Nuclear University MEPhI (Moscow Engineering Physics Institute),Moscow, Russia

Radiation diagnostics and therapy are the most effective, large-scale and dynamically developing branches of healthcare. More than 80% of all diagnoses are established with their help [1-3]. Reducing the doses of medical exposure of personnel and patients by only 10% in its effect is tantamount to the complete elimination of other artificial sources of radiation exposure to the population, including nuclear energy.

The main physical quantity that determines the degree of radiation exposure to the environment and humans is the absorbed dose of ionizing radiation. The concept of "absorbed dose" applies to any type of radiation, any irradiated material and the detector used for registration. However, it should be understood that the absorbed doses of different types of radiation in different materials at the same exposure doses can vary significantly, therefore, to measure them in a certain environment, it is necessary to use materials as detectors that are closest in their physicochemical characteristics to the parameters of the environment. [4-6]. An important condition for adequate dosimetry of different tissues is the thickness of the detector used and the cover layer.

Dosimetric control can allow the selection of optimal radiation regimens, reduce doses for medical staff working under x-ray control and patients due to improved technology of procedures. It is important to involve physicians – radiologists and radiologists in this activity. Currently, regulatory documents [3] offer them the use of various indirect methods of control.

The paper proposes the use of thermoluminescent detectors TLD-K (effective atomic number - Zeff is similar to bone tissue) to measure absorbed doses in the range from 0.1 mGy to 1 kGy [5,6]. A technique for dosimetric control of medical staff working under X-ray control and patients during diagnostic studies and X-ray therapy is proposed. The use of these highly sensitive detectors and micron-thick cover layers makes it possible to record doses, including those to the skin and cornea of the eyes, and to study their distribution [7].

Hydrophilic biocompatible and low toxicity microparticles of TLD-K detectors based on silicon oxide allow the detection of biochemical processes in vivo. At extreme doses, such as radiation treatment, every micron-sized detector particle can be detected [8].

REFERENCES

[1] Hygienic requirements for the design and operation of medical X-ray rooms and apparatus and for the conduct of X-ray examinations. SanPiN 2.6.1. 1192-2003. –M. Ministry of Health of Russia. 2003.

[2] Protection of the population in the appointment and conduct of X-ray diagnostic studies. Guidelines. February 6, 2004 No. 11-2/4-09.

[3] Guidelines for ensuring radiation safety. 2.6.1. Ionizing radiation. Radiation safety. Determination of individual effective doses of radiation exposure of patients during X-ray studies using dose-area product meters.

[4] Microdosimetry. Report 36 ICRU, M., Energoatomizdat, 1988, 193s.

[5] Aluker N. L. High-efficiency thermoluminescent detectors for measuring the absorbed ionizing radiation dose in the environment / N. L. Aluker, Ya. M. Suzdaltseva, M. E. Herrmann Dulepova, A.S. // Instruments and techniques of the experiment. 2016.59(5). pp. 733-739. ten.

[6] N. L. Aluker, A. S. Artamonov, and M. Herrmann Thermoluminescent Detectors of High-Density Ionizing Radiation Instruments and Experimental Techniques, 2021, Vol. 64, no. 3, pp. 437–443.

[7] Problems of eye lens dosimetry / S.I. Ivanov, S.V. Loginova, N.A. Akopova [et al.] // Medical Radiology and Radiation Safety. - 2014. - T. 59. - No. 4. - S. 67–72.

[8] GOST 34157-2017 Guidelines for dosimetry in food processing with electron beams and X-ray (bremsstrahlung) Standard Practice for Dosimetry in Electron Beam and X-Ray (Bremsstrahlung) Irradiation Facilities for Food Processing (as amended) INTERSTATE STANDARD ISS 67.040 Date introductions 2019-02-01

5th International Conference on New Materials and High Technologies

Chair	Alexey MARKOV	Tomsk Scientific Center SB RAS, Tomsk, Russia
Co-Chair	Yuri MAKSIMOV	Tomsk Scientific Center SB RAS, Tomsk, Russia
Program Chair	Alexey MARKOV	Tomsk Scientific Center SB RAS, Tomsk, Russia

Program Committee

Sergey ZELEPUGIN	Tomsk Scientific Center SB RAS, Tomsk, Russia
Alexander KIRDYASHKIN	Tomsk Scientific Center SB RAS, Tomsk, Russia
Mikhail SLOBODYAN	Tomsk Scientific Center SB RAS, Tomsk, Russia
Evgeniy LIPATOV	Institute of High Current Electronics, SB RAS, Tomsk, Russia

International Advisory Committee

Mikhail ALYMOV	Merzhanov Institute of Structural Macrokinetics and Materials Science, RAS, Chernogolovka, Moscow Region, Russia
Alexander BARDENSHTEIN	Danish Technological Institute, Taastrup, Danish
Massimiliano BESTETTI	Politecnico di Milano, Milan, Italy
Alexander KIRDYASHKIN	Tomsk Scientific Center, SB RAS, Tomsk, Russia
Irina KURZINA	National Research Tomsk Polytechnic University, Tomsk, Russia
Nikolay LYAKHOV	Institute of Solid State Chemistry and Mechanochemistry, SB RAS, Novosibirsk, Russia
Zulkhair MANSUROV	Institute of Combustion Problems, Almaty, Kazakhstan
Sergei MINAEV	Far Eastern Federal University, Vladivostok, Russia
Zbigniew WERNER	National Center for Nuclear Research, Otwock, Poland
Sergey ZELEPUGIN	Tomsk Scientific Center, SB RAS, Tomsk, Russia

Conference topics

N1 Nonisothermal synthesis, functional materials and coatings
N2 Combustion: fundamentals and applications
N3 Welding, surfacing and additive manufacturing
N4 Carbon materials in electronics and photonics

N1-O-007701

HIGH-CURRENT PULSED ELECTRON BEAMS FOR MODIFICATION OF THE SURFACE LAYER OF PARTS OF THE FLOW PART OF MODERN GTE

O. A. BYTCENKO [1]

[1] *Moscow Aviation Institute (National Research University), Moscow, Russian Federation*

In this paper, a generalizing analysis of the results of studies and tests concerning the modification of the surface layer of highly loaded parts of modern aircraft engines is carried out.

It is shown that a high-current pulsed electron beam is a reliable tool for improving the operational properties of the working blades of a gas turbine engine, and the data obtained allow us to consider the possibility of using HPEB irradiation in repair technology, as well as for leveling production defects.

In addition, the necessity of using irradiation with simultaneous exposure of a high-current pulsed electron beam on all surfaces of the sample is shown, which allows obtaining a high level of operational properties.

a b c

Fig.1 Topography of the turbine blade pen after various irradiation modes:
a) 28,4 J/cm^2,n=5; b) 34,6 J/cm^2,n=5; c) 44,4 J/cm^2,n=5.

REFERENCES

[1] Bytsenko O.A., Tishkov V.V., Steshenko I.G., Panov V.A., Markov A.B. “Structural and phase cnanges of the surface layres of heatresistant multicomponent coating of ion-plasma coating Ni-Cr-Al-Y after modification by high-current pulsed electron beams microsecond duration”,Periodico Tche Quimica. 2020. vol. 17. № 34. pp. 459-468.

[2] Teryaev D.A., Shulov V.A., Bytsenko O.A., Steshenko I.G. “Formaton of residual stresses in the surface layers of targets from heat-resistant titanium alloys by irradiation of high-current pulsed electron beams” In the collection: Journal of Physics: Conference Series. 2018. pp. 032-058.

[3] Shulov V.A., Engelko V.I., Gromov A.N. Influence of irradiation regimes by high-current pulsed electron beams on the process of crater formation on the surface of nickel alloy targets. Hardening Technologies and Coatings. 2013, №11 (107), pp.15-19.

[4] Bytsenko O.A., Filonova E.V., Markov A.B. The effect of intense beams on the surface layers of modern heat-resistant alloys with ion-plasma coatings of various compositions. London: Interaction of radiation with solid, 2015, pp.193-195.

[5] Bytsenko O.A., Filonova E.V., Markov A.B. High-current pulsed electron beams for surface engineering of ion-plasma coatings. News of materials science. Science and Technology, 2017, №2 (26), p.9.

[6] Bytsenko O.A., Grigorenko V.B., Lukina E.A. The development of methods of metallophysical research: methodological issues and practical significance. Aviation materials and technologies, 2017, S, ppю 498-515

[7] Bytsenko O.A., Filonova E.V., Markov A.B., Belova N.A. The effect of irradiation with high-current electron beams on the surface layers of modern heat-resistant nickel alloys with ion-plasma coatings of various compositions. Proceedings of VIAM. Electronic Journal, 2016, №6 (42). URL: http://viam-works.ru (17.07.2016). DOI: 10.18577/2307-6046-2016-0-6-10-10.

N1-O-010802

EFFECT OF MECHANOCHEMICAL ACTIVATION ON HIGH-TEMPERATURE SYNTHESIS AND PHASE FORMATION IN THE ZnO-MgO-Co_3O_4-$Mr(NO)_2 \cdot 6H_2O$-Al_2O_3-Al SYSTEM

O.V. LVOV, N.I. RADISHEVSKAYA, A.Yu. NAZAROVA

Tomsk Scientific Center of the SB RAS, Tomsk, Russia

Increased demand for inorganic pigments is due to their longer service life compared to organic pigments. Stable colors, chemical resistance to acids and alkalis, resistance to high temperatures, and environmental friendliness - these are the properties of spinels that are required for coloring ceramic and construction products, food ware, plastics, rubber, etc. Spinel pigments have also proven themselves for coloring polymers used for 3D-printing. Energy saving in the production of refractory materials is becoming increasingly important. There has been a growing interest in combining self-propagating high-temperature synthesis (SHS) and mechanochemical activation (MA) methods of initial reagents. This is due to the fact that the preliminary MA of powder reaction mixtures extends the combustion range for inorganic materials, reduces their initial ignition temperatures, and helps to achieve homogeneity of the final product [1].

Oxides of ZnO, MgO, Co_3O_4, Al_2O_3, magnesium nitrate $Mg(NO_3)_2 \cdot 6H_2O$, and Al powder (ASD-4) were used to obtain blue pigments in the system ZnO-MgO-Co_3O_4-$Mr(NO)_2 \cdot 6H_2O$-Al_2O_3-Al by SHS. Starting powders were mixed and subjected to MA in a M3 planetary ball mill (45 g acceleration) with 1 dm^3 steel drums using steel balls with a diameter of 7 mm. The mass of the powder mixture was 0.05 kg, and the ball-to-powder mass ratio was 4:1. Synthesis was conducted in a gradient furnace in the air at atmospheric pressure. The upper part of the samples, where the furnace temperature was maximum, was ignited. The heat transferred from the spiral initiated a chemical reaction, resulting in a combustion wave propagated from top to down. Temperature-time profiles during SHS of spinel were measured using a 100 μm diameter tungsten-rhenium thermocouple BP5-BP20 placed in the center of the samples.

The main SHS parameters (Fig. 1) and the composition of combustion products were studied as a function of MA time for the cobalt-containing reaction mixture.

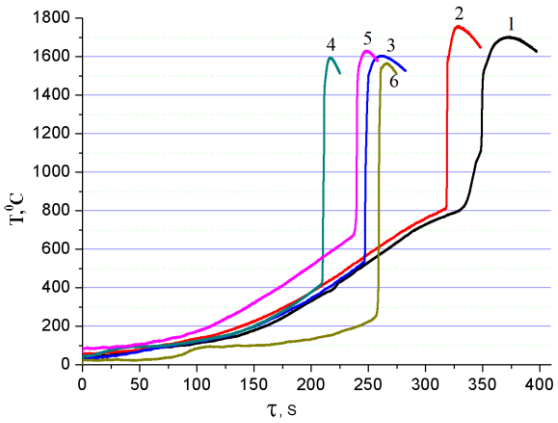

Fig. 1. Thermograms of SHS of blue pigment at different MA times, where (1) no MA, (2) 5 sec MA, (3) 30 sec MA, (4) 60 sec MA, (5) 90 sec MA, (6) 120 sec MA.

It was shown that an increase in the MA time leads to the change in the maximum combustion temperatures and the initial ignition temperatures, which depends on mixing, particle size and structural changes on the surface of starting components. IR spectroscopic analysis performed on a Nicolet 5700 FTIR spectrometer confirmed changes in the molecular structure of reactive compositions depending on the time of MA of a starting reaction mixture. Scanning electron microscopy (Philips SEM 515) showed the nuclei of a new phase (spinel) on the surface of Al_2O_3 particles, which influence the combustion process of the system. The MA of the starting reaction mixture improves the purity of pigment colors.

REFERENCES

[1] A.S. Rogachev, Mechanical activation of heterogeneous exothermic reactions in powder mixtures/RUSSIAN CHEMICAL REVIEWS (2019) V. 88, №9.-P.875-900; DOI 10.1070/RCR4884

N1-O-011003

DEVELOPMENT OF ZINC TIN OXIDE (ZTO) FILMS DEPOSITED BY SPRAY PYROLYSIS METHOD

A.A. REGER, K.A. BOLGARU, A.A. AKULINKIN

Tomsk Scientific Center SB RAS, 10/4 Akademicheskii Pr., Tomsk, 634055, Russian Federation, akulinkinalex@gmail.com, +7(3822)492294

ZTO has drawn great research interest due to its good characteristics such as high stability and attractive optical properties [1]. ZTO has been used in the fields of solar cell [2], lithium battery [3], gas sensor [4] and photocatalyst [5]. There are a number of methods for producing ZTO, such as spray pyrolysis, chemical vapor deposition, hydrothermal.

ZTO precursor solution was prepared by dissolving zinc acetate ($Zn(CH_3COO)_2 \cdot 2H_2O$) and tin chloride ($SnCl_4 \cdot 5H_2O$) in two solvents: ethanol and water (Zn/Sn ratio=2). The ZTO films are deposited onto the glass substrates using the spray pyrolysis method (Fig.1a), followed by annealing at 400 °C for 4 h in ambient air.

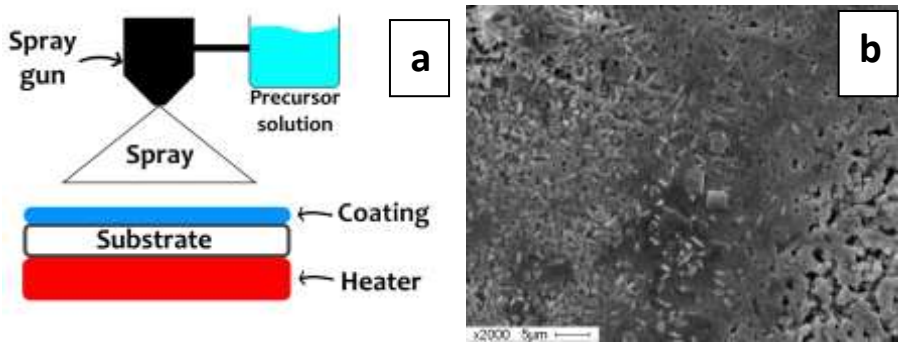

Fig.1. (a) Schematic view of the fabrication process of sprayed-coating, (b) SEM image of ZTO film

Microstructures of ZTO films having moderately packed grains with different grain sizes as shown in Fig. 1b. Increasing the substrate temperature, morphology of the samples becomes rougher. At lower substrate temperatures ZTO films show the particulate structure. In the film deposited at higher temperature the overgrown particles can be seen. The increase in the particle size with substrate temperature is due to the rapid formation of the grains due to the faster reaction rate at high temperature. The volatility of the solvent also affects the structure of the coating

REFERENCES

[1] G.Gnanamoorthy et. all, "Enhanced photocatalytic performance of $ZnSnO_3$/rGO nanocomposite", Chem. Phys. Lett., vol. 739, pp. 137050, 2020

[2] M. Tai et. all, "Ultrathin Zn_2SnO_4 (ZTO) passivated ZnO nanocone arrays for efficient and stable perovskite solar cells", Chem. Eng. J., vol. 361, pp. 60-66, 2019

[3] A. Ron et. all, "Hydrothermal synthesis of Zn_2SnO_4 as anode materials for Li-ion battery", J. Phys. Chem. B 110, pp. 14754–14760, 2006.

[4] V.V. Ganbavle et. all, "Development of Zn_2SnO_4 thin films deposited by spray pyrolysis method and their utility for NO_2 gas sensors at moderate operatingtemperature", J. Anal. Appl. Pyrolysis, vol. 107, pp. 233-241, 2014

[5] S. Silvestri et. all, "Degradation of methylene blue using Zn_2SnO_4 catalysts prepared with poreforming agents", Mater. Res. Bull., vol. 117, pp. 56-62, 2019

N1-O-015601

DEPOSITION OF HARD, WEAR- AND OXIDATION-RESISTANT COATINGS BY HIPIMS AND PCAE METHODS USING CERAMIC CATHODES: APPLICATION FEATURES AND MAIN ADVANTAGES*

PH.V. KIRYUKHANTSEV-KORNEEV, A.D. SYTCHENKO, E.A. LEVASHOV

National University of Science and Technology "MISIS", Moscow, Russia

Coatings based on refractory compounds of transition metals demonstrate high hardness, wear-, corrosion-, and oxidation resistance, good thermal stability. The use of high-power impulse magnetron sputtering (HIPIMS) methods for coating's deposition has a number of significant advantages, among which it can be noted: high adhesive strength and crack resistance of coatings, high density and low defectiveness, low surface roughness, high resistance to thermal shock, etc. The main effects are associated with an increase in the degree of ionization of the flow and an increase in the energy of the deposited particles. Another way to obtain a highly ionized flow is cathode-arc evaporation traditionally. However, when ceramic cathode materials evaporate, difficulties arise due to the high temperature gradient in the material, leading to rapid destruction of the cathode. The solution to this problem is the supply of energy in short pulses, which is implemented in the pulsed cathodic arc evaporation (PCAE) method.

Present work is devoted to the study of the deposition features and the identification of a positive effect on characteristics during deposition of coatings by these methods when using multicomponent ceramic cathodes. Cathodes were manufactured using self-propagating high-temperature synthesis (SHS).

The molybdenum silicide and zirconium boride targets as well as multicomponent MoSiB, MoHfSiB, MoZrSiB, MoSiB/Y, ZrMoSiB, ZrTaSiB SHS-electrodes were sputtered/evaporated in Ar, Ar-N_2, and Ar-C_2H_4 gas mixtures. Plasma diagnostics was performed by optical emission spectroscopy using Plasmascope (Horiba Jobin Yvon) unit. The metal and non-metal model materials (alumina, silicon) were used as the substrates. To evaluate the oxidation resistance and anti-diffusion properties the coatings were annealed in air or in vacuum at T=500-1700°C. The structure of as-deposited and annealed coatings was studied by X-ray diffraction, scanning and transmission electron microscopy, X-ray photoelectron spectroscopy, glow discharge optical emission spectroscopy, FTIR, and Raman spectroscopy. The samples were characterized using nanoindentation, impact-, RT/HT tribo- and scratch-testing.

The results obtained show that critical load of adhesive failure of HIPIMS coatings exceeded 70 N, whereas for samples deposited at direct current (DCMS), the values did not exceed 10 N. The highest level of mechanical properties was achieved for MoZrSiB coatings deposited at a frequency of 200 Hz. At the same time, for coatings obtained at a frequency of 50 Hz and annealed in vacuum at 1000°C, the maximum values were fixed at the level of 40 GPa due to self-hardening effect. The transition from DCMS to HIPIMS led to an increase in resistance to thermal cycling, as well as to thermal shocks, which was confirmed by experiments on heating followed by cooling in water. PCAE coatings based on MoSiB had satisfactory mechanical properties, however, the presence of a droplet phase significantly reduced oxidation resistance, the maximum operating temperatures did not exceed 900-1000°C. DCMS and HIPIMS coatings had high oxidation resistance at 1500-1700°C

Combination of relatively high mechanical properties, remarkable thermal stability, and oxidation resistance makes new materials promising candidates for protective coatings to be used in high-temperature applications.

REFERENCES

[1] Ph.V. Kiryukhantsev-Korneev et al. **Surf. Coat. Technol.** (2022) 128141
[2] Ph.V. Kiryukhantsev-Korneev et al. **Surf. Coat. Technol.** 403 (2020) 126373
[3] Ph.V. Kiryukhantsev-Korneev et al. **Corrosion Science** 123 (2017) 319–327

* The work was supported by the Russian Science Foundation (project No. 19-19-00117).

N1-O-016403

SYNTHESIS OF ZnO NANOPOWDER BY COMBUSTION OF ZINC NITRATE-GLYCINE GEL AND ITS PHOTOCATALYTIC ACTIVITY IN PHENOL DECOMPOSITION*

A.P. AMOSOV[1], V.A. NOVIKOV[1], E.M. KACHKIN[1], N.A. KRYUKOV[1], A.A. TITOV[1], I.M. SOSNIN[2], D.L. MERSON[2]

[1] Samara State Technical University, Samara, Russia
[2] Togliatti State University, Togliatti, Russia

Zinc oxide (*ZnO*) nanopowder exhibits significant photocatalytic activity during the decomposition of such a toxic water pollutant as phenol under the action of ultraviolet radiation and visible light without the formation of secondary toxic products [1]. In this paper, the possibility of using such a simple, energy-saving and high-performance method as the synthesis in gel combustion of reagents mixture of a self-sustaining exothermic redox reaction, in which the oxidizer is zinc nitrate $Zn(NO_3)_2$ and the fuel is glycine $C_2H_5NO_2$, for the production of *ZnO* nanopowder is considered [2, 3]. The equation of the redox reaction is:

$$Zn(NO_3)_2+\frac{10}{9}\varphi C_2H_5NO_2+\frac{5}{2}(\varphi-1)O_2=ZnO+\frac{25}{9}\varphi H_2O+\frac{20}{9}\varphi CO_2+(\frac{5}{9}\varphi+1)N_2,$$

where the dimensionless criterion φ, characterizing the ratio of fuel and oxidizer, shows that excess oxygen is released or, conversely, oxygen missing for complete oxidation of the elements is consumed from the surrounding gas environment during synthesis in combustion of the reagents gel. In this case , the gel of the reagents mixture can be formed in two ways: 1) from a mixture of aqueous solutions of reagents when heating and removing water at its boiling point (Solution Combustion Synthesis) or 2) when mixing dry reagents, accompanied by their spontaneous humidification from the ambient air due to hygroscopicity, and subsequent drying by heating at a temperature below the boiling point of water (Gel Combustion Synthesis) [2-4]. A theoretical and experimental study of the *ZnO* synthesis process has been carried out with a change in the values of the criterion φ in the range $0.25\leq\varphi\leq3$ with a step of 0.25.

Thermodynamic calculations using the THERMO computer program made it possible to determine the adiabatic temperatures and the equilibrium composition of the reaction products, to find the optimal values of the criterion $\varphi\approx1$ for the synthesis of pure *ZnO*. However, an experimental study when heating a vessel with an aqueous solution of reagents on an electric stove with an average surface temperature of 800 ^{o}C showed that after boiling water and gel formation at $0.5\leq\varphi\leq1.5$, the reaction takes place in a very fast volumetric combustion mode with a sharp ejection of the reacting mixture and reaction products from the vessel. With a reduced fuel content φ=0.25, the reaction proceeds in a flameless mode with smoke emission and partial product ejection, and with an increased fuel content $\varphi\geq1.75$, the reaction takes place in the form of slow smoldering without product ejection, but in both these cases, the combustion products contain a significant amount of free carbon: 6.45 wt.% at φ=0.25, 10 wt.% at φ=2 and 25.5 wt.% at φ=3. Calcination at 650 ^{o}C of these products reduces the impurity content of free carbon to 0.67 wt.% at φ=2, and 0.86 wt.% at φ=3. The average particle size of calcined powders found by the Scherer method is in the range from 30 to 35 nm. Similar results on the composition and structure of combustion products were obtained in the synthesis of *ZnO* by burning gel from mixtures of dry reagents, only here the delay time of combustion is much less (about 1 min) compared with burning gel from an aqueous solution of reagents (about 8 min).

The evaluation of the photocatalytic activity of synthesized *ZnO* during the decomposition of phenol under the action of ultraviolet radiation was carried out in an experiment with an initial concentration of phenol in water of 1 mg/l, a concentration of suspended zinc oxide particles of 1 g/ l, a wavelength of ultraviolet irradiation of 365 nm. After 4 hours of irradiation, the phenol concentration decreased by 18% in the case of non-calcined *ZnO* and by 92% in the case of calcined *ZnO*.

REFERENCES

[1] Ch.B. Ong, L.Yo. Ng, A.W. Mohammad, “A review of ZnO nanoparticles as solar photocatalysts: Synthesis, mechanisms and applications”, Renew. Sustain. Energy Rev., vol. 81, pp. 536–551, 2018.

[2] Ch.-Ch. Hwang, Ts.-Yu. Wu, “Synthesis and characterization of nanocrystalline ZnO powders by a novel combustion synthesis method”, Mater. Sci. Eng. B, vol. 111, pp. 197-206, 2004.

[3] N. Riahi-Noori, R. Sarraf-Mamoory, P. Alizadeh, “Synthesis of ZnO nano powder by a gel combustion method”, J. Ceram. Proc. Res., vol. 9, no. 3, pp. 246-249, 2008.

[4] A. Varma, A. Mukasyan, A. Rogachev, K. Manukyan, “Solution Combustion Synthesis of nanoscale materials”, *Chem. Rev.*, vol. 116, no. 23, pp. 14493–14586, 2016.

* The work was supported by the Russian Science Foundation under grant No. 22-29-00287.

N1-O-016405

APPLICATION OF Ti-NaN_3-NH_4Cl-C POWDER MIXTURE COMBUSTION FOR SYNTHESIS OF HIGHLY DISPERSED TiN-TiC CERAMIC COMPOSITION*

A.P. AMOSOV, Y.V. TITOVA, A.F. MINEKHANOVA, D.A. MAIDAN, A.V. SHOLOMOVA

Samara State Technical University, Samara, Russia

Due to the development of the aerospace, energy, chemical and automotive industries, the need for hard-to-process materials such as superalloys, hardened steel and ultra-high-strength steel is growing. There is also a growing demand for cutting tool materials with high performance characteristics. Due to its high hardness, excellent wear resistance, ceramic cutting tools are an ideal choice for high-speed cutting of hard-to-process materials.

Due to the high strength and poor thermal properties of ultrahigh-strength steels, high cutting temperatures, high-speed steel processing results in a strong hardening. Therefore, the desired ceramic tool materials must have exceptionally high hardness and significant wear resistance. Al_2O_3 and *TiN* microparticles and *TiC* nanoparticles have high hardness and good wear resistance, and *TiN* particles can inhibit the growth of Al_2O_3 micrograins. Meanwhile, *TiC* nanoparticles can reduce Al_2O_3 grains in size, which leads to an increase in the fracture toughness of ceramics [1].

A study of the effect of *TiN* additives on sintering, mechanical properties and microstructure of *TiC*-based materials showed that the introduction of *TiN* increased the relative density of *TiC* by about 1.5%, amounting to about 97%, Vickers hardness - 2750 HV, bending strength - 450 MPa [2]. However, such composites have a high cost and are difficult to manufacture, which is due to the high cost of ceramic nanopowders and the practical impossibility of their homogeneous mechanical mixing [3]. Therefore, chemical methods of direct synthesis of ceramic powders inside the desired composition from inexpensive starting reagents are preferred. Among chemical methods, a simple energy-saving method of self-propagating high-temperature synthesis (SHS) attracts much attention. In this paper, the use of azide SHS is investigated, in which sodium azide powder as a nitriding reagent and halide salts are used. The compositions of the initial powder mixtures for the synthesis of single-phase *TiN* and *TiC* are known, based on the analysis of which the following chemical reaction equations were used for the synthesis of a *TiN-TiC* composition with a molar phase ratio from 1:4 to 4:1:

$$2Ti + C + NaN_3 + NH_4Cl = TiN + TiC + NaCl + 1{,}5N_2 + 2H_2, \quad (1)$$

$$3Ti + 2C + NaN_3 + NH_4Cl = TiN + 2TiC + NaCl + 1{,}5N_2 + 2H_2, \quad (2)$$

$$5Ti + 4C + NaN_3 + NH_4Cl = TiN + 4TiC + NaCl + 1{,}5N_2 + 2H_2, \quad (3)$$

$$3Ti + C + NaN_3 + NH_4Cl = 2TiN + TiC + NaCl + N_2 + 2H_2, \quad (4)$$

$$5Ti + C + NaN_3 + NH_4Cl = 4TiN + TiC + NaCl + 2H_2. \quad (5)$$

The results of thermodynamic calculations of these reactions are obtained, according to which the adiabatic temperatures are high enough to realize a self-sustaining combustion regime, and the reaction products correspond to the right-hand sides of equations (1)-(5). The combustion temperatures and velocities, structure and phase composition of the combustion products were determined during the experimental study. The study of the microstructure showed that the synthesized composition consists of equiaxed *TiN* and *TiC* particles ranging in size from 100 to 350 nm.

Thus, the azide SHS method made it possible to prepare a promising *TiN-TiC* ceramic composition in one stage, and with a different ratio of target phases.

REFERENCES

[1] D. Wanga, Ch. Xuea, Y. Caoa, J. Zhao, “Microstructure design and preparation of Al_2O_3/TiC/TiN micro-nanocomposite ceramic tool materials based on properties prediction with finite element method”, Ceram. Int., vol. 44, pp. 5093-5101, 2018.

[2] Y. Pazhouhanfara, A. Sabahi Naminib, S.A. Delbarid, T.P. Nguyene, “Microstructural and mechanical characterization of spark plasma sintered TiC ceramics with TiN additive”, Ceram. Int., vol. 46, pp. 18924-18932, 2020.

[3] P. Palmero, “Structural ceramic nanocomposites: a review of properties and powders’ synthesis methods”, Nanomaterials, vol. 5, pp. 656-696, 2015.

* The work was carried out with the financial support of the Ministry of Science and Education of the Russian Federation within the framework of the basic part of the state assignment no. 0778-2020-0005.

N1-O-017703

METALLURGICAL PATTERNS OF THE IMPACT OF HIGH-CURRENT PULSED ELECTRON BEAMS ON METAL TARGETS*

A.B. MARKOV, M.S. SLOBODYAN

Tomsk Scientific Center of the Siberian Branch of the Russian Academy of Sciences, Tomsk, Russia

Electron-beam facilities are widely deployed for welding of various metals, alloys and steel in many industries since the middle of the 20th century. Nowadays, EB-based procedures are also being implemented for both additive manufacturing of metal products and final treatment of their surfaces. For the last-mentioned purpose, in addition to continuous wave EB irradiation, the low-energy high-current pulsed EB (LEHCPEB) processing has been suggested almost three decades ago. Principles of operation of pulsed EB accelerators have been proposed as early as the 1960s and developed in advanced facilities by now, which enable to treat surfaces and alloy them (with several components if necessary) in a single vacuum cycle. Many metals, ceramics, polymers, composites, semiconductors and glasses have been already modified and/or doped by this method. The research results on changes in their various functional properties have been published in several hundred papers (Figure 1), but have not comprehensively summarized yet. It should be noted that this huge amount of data is contradictory in many cases. Some authors have reported the formation of craters, cracks and pores in the modified surface layers in addition to quenching structures and great residual tensile stresses, while others have stated on dramatic improvement in their corrosion resistance. In order to shed light on real achievements, to realize the existing challenges for the wide industrial implementation of this surface treatment method, and to propose unified research methods, the authors have tried to critically summarize the metallurgical patterns of the process. In particular, LEHCPEB processing of aluminum, copper, magnesium, nickel, iron, titanium, zinc and their alloys, as well as steels of various grades have been considered. In addition, both high-entropy and hard alloys, NiTi compounds, as well as superalloys are in the scope of the review. Special attention is paid to alloying of the metal surfaces and the formation of surface alloys due to the preliminary deposition of coatings (including multicomponent ones) before LEHCPEB processing (in a single vacuum cycle). The authors have paid special attention to the need for improving the functional properties of the studied materials and the fundamental possibility of achieving this goal by LEHCPEB processing. For this purpose, typical operating conditions of the materials are shown along with their weldability, as one of the thoroughly studied key parameters that determine the possibility to be processed by such high-energy methods.

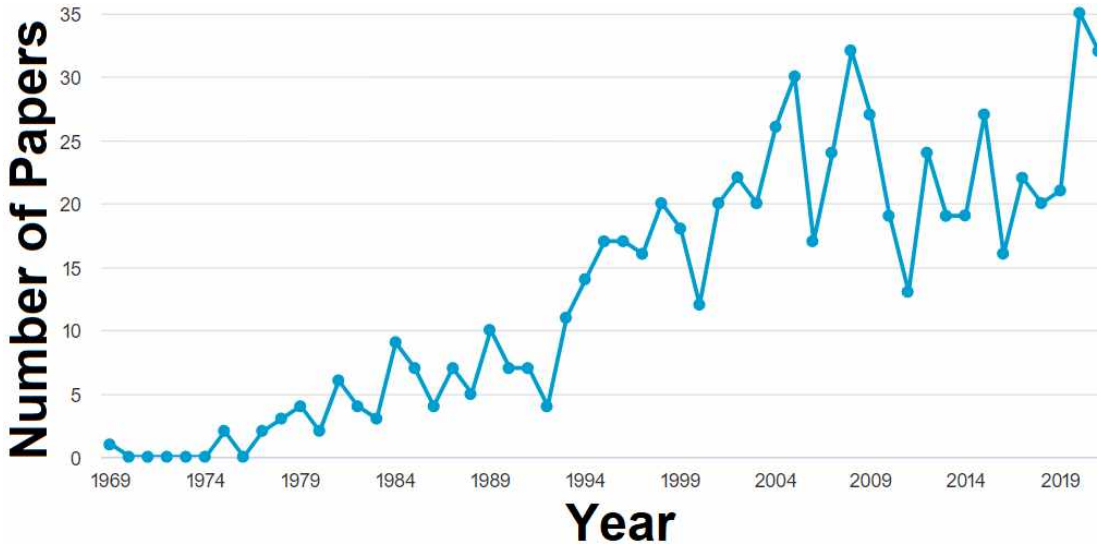

Fig.1. The dynamics of publication of research papers according to the Scopus database, which connected with the ‘pulsed electron beam processing’ keywords

* The work was supported by the Ministry of Science and Higher Education of the Russian Federation (project No FWRF-2021-0001).

N1-O-019801

FEATURES OF THE PLASMA-POLYMERIZED COATINGS CHEMICAL COMPOSITION FORMATION BY THE MONOMER INJECTION INTO DIFFERENT REGIONS OF A GLOW DISCHARGE *

D.A. ZUZA[1], *V.O. NEKHOROSHEV*[1], *I.A. KURZINA*[2], *A.V. BATRAKOV*[1]

[1]*Institute of High Current Electronics SB RAS, Tomsk, Russia*
[2]*Tomsk State University, Tomsk, Russia*

The polymerization of organic substances using gas discharge plasma is currently being actively studied, due to the fact that polymer coatings obtained by this method can be widely used. In particular, we have shown that such coatings can be used as protective dielectric layers for electronics [1, 2]. It is known that the chemical structure and composition of polymer coatings determine the physical and operational properties of coatings [3, 4]. Despite this, the mechanisms of plasma-chemical processes leading to the formation of the chemical structure of coatings have not been adequately studied [5].

In this paper, we consider the features of the formation of the chemical structure of polymeric organosilicon coatings deposited using a plasma-chemical reactor based on a low-pressure glow discharge in a carrier gas/monomer mixture flow. Plasma chemical reactor is a gas-discharge system containing two hollow coaxial electrodes. A DC source was used to ignite and maintain the discharge in the current range from 5 to 70 mA. [6]. Argon and hexamethyldisiloxane (HMDSO) were used as carrier gas and monomer, respectively. Argon at a flow rate of 230 mg/min was injected into the plasma-chemical reactor through the cathode hollow. HMDSO was mixed with argon and injected into the reactor through the cathode hollow (pre-mixing) or injected into the reactor into the region of the positive plasma column through the side tap of the plasma-chemical reactor (mixing in the region of the positive column).

The elemental composition and chemical structure of polymer coatings obtained with different supply of monomer to the plasma-chemical reactor are considered. The study of the chemical structure and composition of the coatings was carried out using infrared spectroscopy and X-ray photoelectron spectroscopy. It is shown that during premixing, the C/Si ratio changes from 1 to 7.5 with increasing discharge power. In the case when mixing occurs in the region of the positive column, the C/Si ratio corresponds to ~ 1, regardless of the variation in the discharge power. It has also been shown that 30-50% (depending on the power consumption of the discharge) of carbon atoms in coatings obtained using pre-mixing are subject to oxidation. The features of the chemical structure formation and composition of the obtained coatings can be explained by considering the differences in conditions in different regions of the glow discharge plasma. The mechanisms of plasma-chemical processes occurring in different regions of the glow discharge plasma are proposed. In particular, the formation of hydrogenated carbon in the cathode layers of the discharge, and the formation of mono- and bi-radicals in the positive column of the glow discharge are considered.

REFERENCES

[1] D. Zuza, A. Batrakov, V. Nekhoroshev, I. Kurzina and S. Popov, "Plasma-Assisted Deposition of Dielectric Conformal Coating Using Hexamethyldisiloxane as Precursor," *2020 7th International Congress on Energy Fluxes and Radiation Effects (EFRE)*, 2020, pp. 1132-1135.

[2] A. V. Batrakov, S. A. Popov, K. V. Karlik, E. L. Dubrovskaya, A. V. Schneider, I. Kurzina, S. B. Suntsov, A. V. Seloustev, A. A. Hvalko, "Suppression of Prebreakdown Emission Activity Inside the On-board Spacecraft Equipment by Local Polymerization in Discharge", *Proc. 28th Int. Symposium on Discharges and Electrical Insulation in Vacuum (ISDEIV)*, vol. 2, pp. 777-780, 2018

[3] G. Dakroub, T. Duguet, J. Esvan, C. Lacaze-Dufaure, S. Roualdes, V. Rouessac, "Comparative study of bulk and surface compositions of plasma polymerized organosilicon thin films," Surfaces and Interfaces, vol. 25, 101256, 2021.

[4] L. Kleines, S. Wilski, P. Alizadeh, J. Rubner, M. Wessling, C. Hopmann, R. Dahlmann, "Structure and gas separation properties of ultra-smooth PE-CVD silicon organic coated composite membranes," Surface and Coatings Technology, vol. 421, 127338, 2021.

[5] D. Hegemann, E. Bülbül, B. Hanselmann, U. Schütz, M. Amberg, S. Gaiser, "Plasma polymerization of hexamethyldisiloxane: Revisited," Plasma Process Polym., vol. 18, no. 2, 2000176, 2021.

[6] Korolev, Yu. D. , Nekhoroshev, V. O. ;Frants, O. B. ; Bolotov, A. V. ; Landl, N. V. "Power Supply for Generation of Low-Temperature Plasma Jets," Russian Physics Journal, vol. 62, no 11, pp. 2052-2058, 2020.

* This work was supported by the Ministry of Science and Higher Education of the Russian Federation (project No. FWRM-2021-0007).

N1-O-021003

NUMERICAL SIMULATION OF CHEMICAL REACTIONS IN POWDER MIXTURES TAKING INTO ACCOUNT MELTING

N.V. PAKHNUTOVA, R.O. CHEREPANOV, O.V. IVANOVA, S.A. ZELEPUGIN

Tomsk Scientific Center of the Siberian Branch of the Russian Academy of Sciences, Tomsk, Russia

This paper presents a numerical model of chemically reacting powders mixture under explosive loading conditions. Such mixtures make it possible to obtain homogeneous solid reaction products of high density and homogeneity.

The processes of elastic-plastic deformation of particles and diffusion processes are simulated based on the meshless method of smooth particles [1, 2]. To simulate the motion of the medium it is suggested to use a weak variational formulation of the equations of motion [3], which allows one to reduce requirements for order of spatial derivatives of the solution and ensures fulfillment of conservation laws.

Diffusion and heat conduction processes are also modelled by the meshless smooth particle method [4] with the use of Morris [5] and Schweiger [6] approximations. Under the conditions considered, the initiation of reaction takes place at the particle contact boundaries, resulting in temperature rise and melting of one of the mixture components, after which the flow of the molten component and diffusion in the melt starts to play an important role. A special feature of the approach is that SPH allows transition from the model of an elastic-plastic medium to a fluid medium without explicitly identifying the boundaries.

Numerical simulations show that two scenarios of reaction propagation are possible in such a reaction - when reaction initiation in the whole volume is carried out by a passing shockwave, and when shockwave initiation occurs in a limited volume of reacting materials [7], which causes their heating, and the heat released in this case is a factor of reaction propagation in the surrounding volume of the powders mixture. Assuming that reactions in powder mixtures occur at the solid-liquid interface, in the second case, the heat exchange conditions between the particles and the initial temperature may influence the final result of the reaction by influencing the wetting of the more refractory components of the mixture by the more fusible ones. The approach and numerical model proposed in this work allow us to investigate on a micro level the melting process of the fusible component of the mixture and its interaction with refractory components with account to heat transfer and diffusion of components in chemically reaction media.

REFERENCES

[1] J.W. Swegle, D.L. Hicks, S.W. Attaway, “Smoothed particle hydrodynamics stability analysis,” J. Comput. Phys., vol. 116, pp. 123–134, 1995.

[2] J. Monaghan, “Simulating free surface flows with SPH,” J. Comp. Phys., vol. 110, pp. 39–406, 1994.

[3] J. Bonet, S. Kulasegaram, M.X. Rodriguez-Paz, M. Profit, “Variational formulation for the smooth particle hydrodynamics (SPH) simulation of fluid and solid problems,” Computer Methods in Applied Mechanics and Engineering, vol 193 (12–14), pp. 1245–1256, 2004.

[4] J.K. Chen, J.E. Beraun, T.C. Carney, “A corrective smoothed particle method for boundary value problems in heat conduction,” Int J Numer Methods Eng, vol. 46(2), pp. 231–252, 1999.

[5] J.P. Morris, P.J. Fox, Y. Zhu, “Modelling low Reynolds number incompressible flows using SPH,” J. Comput. Phys., vol. 136, pp. 214–226, 1997.

[6] H.F. Schwaiger, "An implicit corrected SPH formulation for thermal diffusion with linear free surface boundary conditions," Int. J. Numer. Meth. Engng, vol 75, pp. 647–671, 2008.

[7] V.F. Tolkachev, O.V. Ivanova, S.A. Zelepugin, "Initiation and development of exothermic reactions during solid-phase synthesis under explosive loading," Thermal Science, vol. 23, pp. 505–511, 2019.

N1-O-025204

CORROSION PROPERTIES OF ZIRCONIUM IRRADIATED BY LOW-ENERGY HIGH-CURRENT ELECTRON BEAM*

E.A. PESTEREV, E.V. YAKOVLEV, M.S. SLOBODYAN, A.B. MARKOV, A.V. SOLOVYOV, V.I. PETROV

Tomsk Scientific Center of the Siberian Branch of the Russian Academy of Sciences, Tomsk, Russian Federation

Attractive properties, such as low neutron absorption, good corrosion resistance, and a satisfactory combination of ductility and strength, have made it possible to widely use Zr alloys in the chemical and nuclear industries [1–3]. To obtain optimal surface properties of Zr alloys, attempts were made to use various surface treatment methods, such as ion implantation [4], microarc oxidation [5], laser surface melting [6], etc.

As another method of material surface modification, low-energy high-current electron beam (LEHCEB) has attracted wide attention due to its great application potential and advantages [7]. When irradiated with LEHCEB, high energy can be released in the surface layer in a very short time and produce extremely fast heating, melting and even evaporation, then rapid cooling through the thermal conductivity of the sample. The dynamic stress fields caused by the rapid cooling process lead to intense modifications that can propagate in the material up to several tens of microns in depth. Accordingly, special modification effects can be achieved and, as a consequence, the corrosion properties of the material can be improved [8, 9].

Fig. 1,a shows the polarization curves in a 3.5% NaCl solution to compare the corrosion resistance between the original and irradiated samples. After LEHCEB irradiation, a wide area of primary passivity is visible, as well as an increase in the corrosion potential. Fig. 1, b also shows the SEM image of the Zr surface of the corrosion experiment. Pits with an interesting broken pattern appeared over the entire area of impact of the solution.

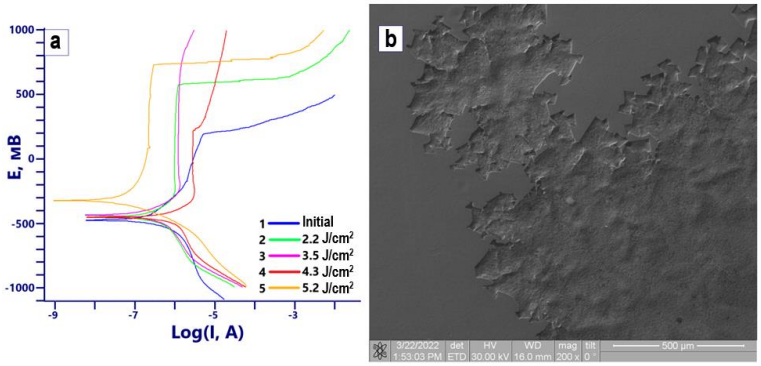

Fig. 1 – Potentiodynamic polarization curves (a) of Zr before and after irradiation with LEHCEB and SEM image (b) after the corrosion experiment.

REFERENCES

[1] S.J. Zinkle, G.S. Was, Materials challenges in nuclear energy / Zinkle S.J., Was G.S., // Acta Mater. 61 (2013) 735–758.

[2] M. Slobodyan High-energy surface processing of zirconium alloys for fuel claddings of water-cooled nuclear reactors // Nucl. Engin. and Design. 382 (2021) 111364

[3] J. Yang Review on chromium coated zirconium alloy accident tolerant fuel cladding / Yang J. [et al.] // Journal of Alloys and Compounds. 895 (2022) 162450

[4] D.Q. Peng Surface analysis and corrosion behavior of zirconium samples implanted with yttrium and lanthanum / Peng D.Q., Bai X.D., Chen B.S., // Surf. Coat. Technol. 190 (2005) 440–447.

[5] D.L. Zhang Microarc oxidation of zircaloy-4 / Zhang D.L. [et al.] // Rare Met. Mater. Eng. 32 (2003) 658–661.

[6] K.F. Amouzouvi Microstructural changes in laser hardened Zr-2.5Nb alloy / Amouzouvi K.F. [et al.] // Scripta Metall. Mater. 32 (1995) 289–294

[7] D.I. Proskurovsky Pulsed electron-beam technology for surface modification of metallic materials / Proskurovsky D.I. [et al.] // J. Vac. Sci. Technol., A 16 (1998) 2480–2488.

[8] S. Yang Microstructures and properties of zirconium-702 irradiated by high current pulsed electron beam / Yang S. [et al.] // Nucl. Instrum. Meth. Phys. Res. B 358 (2015) 151–159.

[9] В.П. Ротштейн Поверхностная модификация титанового сплава низкоэнергетическим сильноточным электронным пучком при повышенных начальных температурах / Ротштейн В.П. [и др.] // Физика и химия обработки материалов. – 2006. – С. 62-

* The work was supported by the Ministry of Science and Higher Education of the Russian Federation (project № FWRF-2021-0001).

N1-O-027801

SELF-POWERED PHOTODIODE BASED ON Ga_2O_3/N-GaAs STRUCTURES*

O. KISELEVA, A. TSYMBALOV, V. KALYGINA, A. ALMAEV

National Research Tomsk State University, Tomsk, Russia

The electrical and photoelectric characteristics of Ga_2O_3/n-GaAs structures obtained by RF-magnetron sputtering of a gallium oxide film on gallium arsenide epitaxial layers with an electron concentration of $N_d = 9.5 \cdot 10^{14}$ cm^{-3} are studied. The structures were annealed in argon for 30 minutes at a temperature of 900°C, after the deposition of the Ga_2O_3/n-GaAs oxide film.

Platinum contacts were deposited on the Ga_2O_3 surface and the rear side of the semiconductor substrate to measure the electrical characteristics. The contact to the semiconductor was deposited in the form of a continuous metal film, and the contact to gallium oxide was created by metal deposition through masks 1 mm in diameter. The area of the electrode to Ga_2O_3 (gate) was 1.04 cm^{-2}.

The dark current-voltage characteristics of the samples (I_D) are nonlinear and are determined by the polarity and magnitude of the gate potential. The rectification factor at voltages of ± 4 V is 10^3.

The forward current decreases, and the reverse current increases under UV exposure (Fig. 1). The most noticeable effect of radiation with λ = 254 nm is observed at low positive and negative voltages on the sample, in the vicinity of $U \approx 0$ V.

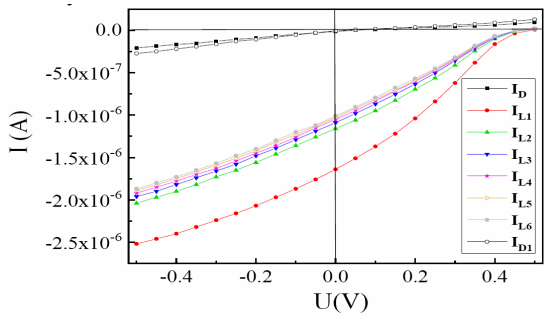

Fig.1. Current-voltage characteristics of the sample at positive and negative potentials on the gate: dark (I_D) and under exposure of radiation with λ = 254 nm (I_{L1}-I_{L6}).

The largest changes in the forward and reverse currents under UV radiation are observed at the first measurement of the detector (I_{L1}). A decrease in the photocurrent I_{ph} was found during subsequent measurements of the I-V characteristics under continuous exposure to UV radiation (Fig. 1, curves I_{L2}–I_{L6}).

The studied M/Ga_2O_3/n-GaAs structures reveal the properties of photodiodes. The reverse current increases by more than two orders of magnitude under UV radiation and voltage U = -0.012 V. It makes possible to use such structures as detectors of UV radiation in the wavelength range of 200–280 nm. The photocurrent is 1 μA at U = 0 V (Fig. 1).

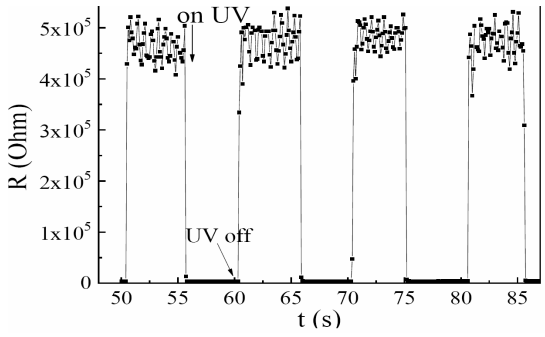

Fig.1. Time dependences of the change in the resistance of the M/Ga_2O_3/n-GaAs structure.

Measurements of the time dependences of the change in the conductivity of the samples upon turning on and off the radiation with λ = 254 nm showed that the response and recovery times do not exceed 1–2 seconds (Fig. 2).

* The work was supported by the Russian Science Foundation (grant no. 20-79-10043).

N1-O-028201

INVESTIGATION OF THE PHOTOCATALYTIC ACTIVITY AND RADIOPACITY OF NANOPOWDERS PRODUCED BY PULSED ELECTRON BEAM EVAPORATION IN VACUUM*

A.S. GERASIMOV[1,2], *A.S. CHEPUSOV*[2], *V.G. ILVES*[2], *O.A. SVETLOVA*[1,2], *S. YU. SOKOVNIN*[1,2]

[1]*Ural Federal University, Yekaterinburg, Russia*
[2]*Institute of Electrophysics, UB, RAS, Yekaterinburg, Russia*

Nanopowders (NP) are promising substances for use in the medical and pharmaceutical field due to antimicrobial, antitumor and other properties of their shell and bioinert core. Various methods of obtaining nanopowders can significantly affect their properties. Thus, bismuth and zirconium oxide nanopowders produced by the pulsed electron beam evaporation (PEBE) method showed high biological and photocatalytic activity [1].

In this work, were investigated the photocatalytic properties and radiopacity of titanium TiO_2 and zinc Zn-ZnO oxide nanopowders produced by the PEBE method in vacuum [2]. These compounds can be used as photocatalytic thin coatings, whose nanoparticles have antimicrobial properties [3]. The high atomic number of metals and high density of atoms per nanoparticle in these oxides makes them prospective for implementation as a contrast agent for computed tomography (CT).

The photocatalytic activity of examined NP at the concentration of 300 mcg/ml was evaluated in comparison with the decomposition of methyl violet (MV) in the medium under ultraviolet light irradiation. The rate of decomposition of MV from the time of exposure to UV radiation can be described by the linear equation $y=kx+b$, where the coefficient k is the rate of photodestruction. The higher the coefficient k, the faster the solution discolors [4]. The measurement of k is exemplified below.

Table 1 – The k coefficient values for TiO_2 and Zn-ZnO NP

Sample	Absolute value	Relative to MV
MV	-0,0053	1
TiO_2	-0,0078	1,47
Zn-ZnO	-0,0085	1,60

Both NP showed significant photocatalytic activity. However, it was found that zinc oxide has better photocatalytic properties compared to TiO_2 samples.

The radiopacity of NP was evaluated relative to commercial iodine CT contrast agent Ultravist®, by analogy with the work [5]. For the study were prepared solutions of 0.75% Na-Carboxymethylcellulose containing nanopowders in various concentrations. X-ray images of the samples were processed in the "ImageJ" software package. During the analysis, were calculated linear X-ray attenuation coefficients.

The highest attenuation coefficient was found in a sample of titanium oxide at a concentration of 12.5% and amounted to 70% relative to Ultravist®. At the same time, the ZnO-Zn sample did not show high radiopaque ability.

REFERENCES

[1] O.A. Svetlova, V.G. Ilves, S.YU.Sokovnin, "Investigation of biological and photocatalytic activity of multimodal nanopowders produced by pulsed electron beam evaporation in vacuum," J. Phys.: Conf. Ser., vol. 2064, no. 1, p. 012087, September 2021.

[2] Sokovnin S. Y., Il'ves V. G., Zuev M. G. "Production of complex metal oxide nanopowders using pulsed electron beam in low-pressure gas for biomaterials application," Engineering of Nanobiomaterials, vol. 2, pp. 29-75, Februrary 2016.

[3] Pang S. et al. "Multifunctional ZnO/TiO2 nanoarray composite coating with antibacterial activity, cytocompatibility and piezoelectricity," Ceramics International, vol. 45, no. 10, pp. 12663-12671, March 2019.

[4] Sokovnin S. Y. et al. "Investigation of biological and photocatalytic activity of nanopowders metal oxides with nanosized silver coating," J. Phys.: Conf. Ser., vol. 1954, no. 1, p. 012047, May 2021.

[5] Ghazanfari A. et al. "Synthesis, characterization, and X-ray attenuation properties of polyacrylic acid-coated ultrasmall heavy metal oxide (Bi2O3, Yb2O3, NaTaO3, Dy2O3, and Gd2O3) nanoparticles as potential CT contrast agents," Colloids and Surfaces A: Physicochemical and Engineering Aspects, vol. 576, no. 5, pp. 73-81, May 2019

* The work was supported by the RFBR and GACR under grant No. 20-58-26002

N1-O-028202

INVESTIGATION OF ANTIOXIDANT PROPERTIES OF CERIUM OXIDE NANOPOWDERS UNDER NANOSECOND BREMSSTRAHLUNG*

A.S. GERASIMOV[1,2], M.E. BALEZIN[2], V.G. ILVES[2], S. YU. SOKOVNIN[1,2]

[1]Ural Federal University, Yekaterinburg, 620002, Russia
[2]Institute of Electrophysics, UB, RAS, Yekaterinburg, Russia
e-mail: andrei.gerasimov@urfu.ru

Cerium oxide CeO_2 nanoparticles (CONP's) possess unique properties, among which is the ability to inhibit free radicals [1]. The antioxidant (AO) activity of CONP's has been well studied [1], however, a quantitative and comparative assessment of the antioxidant properties of these and other nanoparticles is difficult due to the imperfection of currently existing methods.

Various methods of obtaining nanopowders can significantly affect their properties. In this work, the AO properties of CONP's obtained by the pulsed electron beam evaporation (PEBE) method in vacuum were investigated [2]. The PEBE method enables to obtain CONP's with a high specific surface area (up to 190 m^2/g) [2] and a high content of Ce^{4+} (68%) [3], which ensures their high AO activity.

Quantitative assessment of AO properties was performed using a ferrous sulfate dosimeter (FSD). The principle of operation of FSD is based on the oxidation of trivalent iron Fe3+ by free radicals formed under the ionizing radiation. The AO ability of nanoparticles allows to change the amount of free radicals, which is expressed in a change in the absorbed dose.

For the analysis, CONP's were added to the FSD solution at a concentration of 100 mcg/ml. The obtained samples with and without CONP's were irradiated with bremsstrahlung at the URT-1M accelerator [4] (convector made of steel-3 with a thickness of 1 mm). After irradiation, the optical density of the samples was measured at a wavelength λ = 304 nm on a "5300UF Ekroschim" spectrophotometer. The measurement results are shown in Figure 1.

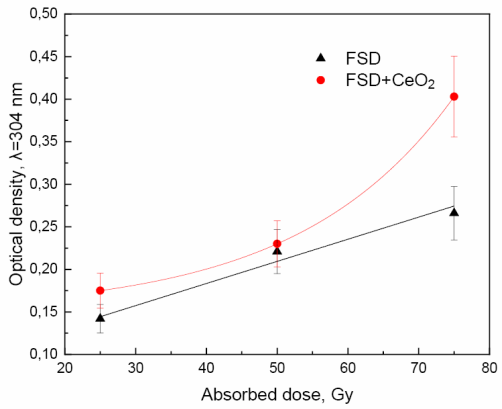

Fig.1. Dose dependance of optical density on wavelength 304 nm of FSD with and without nanoparticles.

The obtained results show that the addition of CONP's led to a violation of the linearity of the FSD, which indicates the operability of the proposed technique. However, it is necessary to clarify the effect with increased absorption of low-energy photons by heavy cerium atoms [5].

REFERENCES

[1] A. B. Shcherbakov et al. "Nanomaterials based on cerium dioxide: properties and prospects of use in biology and medicine," Biotechnologia acta, vol. 4, no 1, pp. 9–28, February 2011.

[2] V. G. Il'ves, S. Yu. Sokovnin "Production and studies of properties of nanopowders on the basis of CeO2," Nanotechnologies in Russia, vol. 7, iss. 5, pp. 213-226, May 2012.

[3] R. A. Vazirov et al. "Physicochemical characterization and antioxidant properties of cerium oxide nanoparticles," J. Phys: Conf. Ser., vol. 1115, no. 3, p. 032094, November 2018.

[4] S. Y. Sokovnin, M. E. Balezin "Repetitive nanosecond electron accelerators type URT-1 for radiation technology" Radiation Physics and Chemistry, vol. 144, pp. 265-270, March 2018.

[5] A. S. Gerasimov, R. A. Vazirov "Analytical calculation of dose change factor values for cerium, gold and hafnium oxide nanoparticles" AIP Conference Proceedings. – AIP Publishing LLC, vol. 2313, no. 1, p. 080010, December 2020.

* The work was supported by the RFBR and GACR No. 20-58-26002

N1-O-031401

THE EFFECT OF SEPARATING LAYER BETWEEN REACTING MEDIA AND MOLDING TEMPLATE ON THE POROUS STRUCTURE OF COMBUSTION SYNTHESIZED NI-AL INTERMETALLICS

N.S. PICHUGIN[1]

[1] *Tomsk Scientific Center SB RAS, Tomsk, Russian Federation*

This research focuses on identifying conditions under which porous intermetallics with a welded granular structure comprised of mm-sized spheroidal alloy elements can be directly obtained by combustion synthesis using μm-sized metal powders as starting reagents. The main question is whether the porous structure can be controlled by modifying the interface between the reacting mixture and the molding template with a separating layer. In the present work we consider the effect of two types of separating layers: (i) chemically inert having low thermal conductivity to suppress the heat loss rate, and (ii) chemically active to stimulate the eutectic melting of the reacting system.

85 wt% Ni + 15 wt% Al porous intermetallics were synthesized and examined. The green mixture was placed in a cylindrical molding tool made of stainless steel with inner diameter of 32 mm, wall thickness 3 mm, height 60 mm. The SHS was performed in the argon atmosphere with the initial preheating of 320 °C. Two types of separating layers between the reacting mixture and the molding template were considered: (i) chemically inert layers made on the surface of the template cavity via a dip-coating process using the water-based slurries of ceramic powders (Al_2O_3, SiO_2, ZrO_2, or porous mullite microspheres), and (ii) chemically active cellulose-based layers made of microcrystalline cellulose powder (dip-coating process) or rolled paper (CaO coated paper, 90 g/m^2, 70 μm thick).

Intermetallics synthesized without separating layer has a microporous crust over the exterior layer. We assumed that applying ceramic powder coating on the inner surface of the steel molding template should decrease the heat loss rate of reacting medium and suppress the crust formation. However, the experiments had shown that microporous crust remains almost unchanged even when a 1.5 mm thick coating from porous microspheres was used.

As for the cellulose-based layers, even a thin separating layer with a thickness of 70 μm suppresses the crust formation. The average size of alloy elements in the exterior layer of synthesized materials D_E increases with the thickness of separating layer h (Fig. 1a). This effect is presumably attributed to the chemical interaction of the cellulose with the reacting medium. The decomposition of cellulose mainly occurs at the temperature range of 280 – 400 °C and generates carbon-containing tar, char, and light gases in the preheating zone of the combustion wave. According to the Ni-C phase diagram (Fig. 1c), the melting temperature of nickel gradually decreases in the presence of carbon, attaining a minimum of 1326 °C for 0.5 wt% C [1]. Therefore, the coarsening mechanism suggested here is that products of cellulose pyrolysis saturate the reacting metals with carbon, leading to an increase in the volume of media that melts near the template surface, providing the coalescence of large droplets. Argument for coarsening effect of carbon is that the artificial addition of carbon black to the Ni-Al mixture of more than 0.3 wt% significantly increases the average size of alloy elements (Fig. 1b)

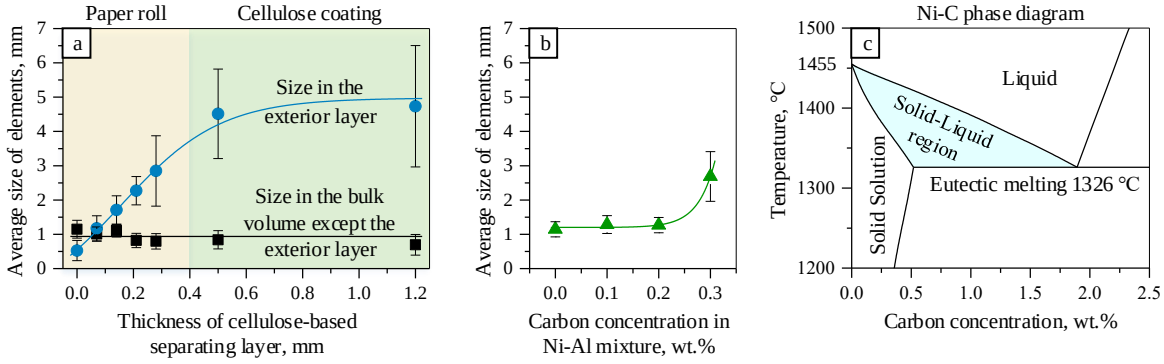

Fig.1. Average size of Ni-Al alloy elements versus the thickness of cellulose-based separating layers (a), and the concentration of carbon black in the Ni-Al reaction mixture (b). Ni-C phase diagram (c), adapted from [1].

REFERENCES

[1] M. Singleton and P. Nash, "The C-Ni (Carbon-Nickel) system," *Bull. Alloy Phase Diagrams*, vol. 10, no. 2, pp. 121–126, 1989.

N1-O-035703

FORMATION OF ALUMINUM MATRIX COMPOSITES CONTAINING Fe-BASED ALLOY@INTERMETALLIC CORE-SHELL REINFORCING STRUCTURES BY SPARK PLASMA SINTERING

V. I. KVASHNIN[1,2], *M. A. LEGAN*[1,2], *A. N. NOVOSELOV*[1], *A. V. UKHINA*[3], *D. V. DUDINA*[1,2,3], *K. GEORGARAKIS*[4], *G. Y. KOGA*[5]

[1] *Lavrentyev Institute of Hydrodynamics SB RAS, Novosibirsk, Russia*
[2] *Novosibirsk State Technical University, Russia*
[3] *Institute of Solid State Chemistry and Mechanochemistry SB RAS, Novosibirsk, Russia*
4 School of Aerospace, Transport and Manufacturing, Cranfield University, Cranfield, UK
[5] *Department of Materials Science and Engineering, Federal University of São Carlos, São Carlos, Brazil*

Aluminum matrix composites are a promising class of materials possessing a high strength to weight ratio, high corrosion and wear resistance and appreciable electrical conductivity. One of the modern trends in the AMC area is to avoid ceramic reinforcements and utilize alternative materials instead. These alternatives are metallic alloys (high-entropy alloys, quasicrystals or metallic glasses) [1-3]. This group of reinforcements should show better adhesion to the aluminum matrix than the ceramic particles due to the same nature of bonding (metallic bonding) in the metal-alloy systems.

In the present work, particles of $Fe_{66}Cr_{10}Nb_5B_{19}$ metallic glass <45 μm in size were used as a reinforcement for aluminum matrix composites. The choice of the reinforcement was dictated by the attractive properties of amorphous alloys – high hardness, strength, wear and corrosion resistance [4].

The sintering behavior of mixtures containing a crystalline or a glassy Fe-based alloy was first investigated to determine the influence of the crystalline state of the alloy on densification. Consolidation of the mixtures was carried out by heating under pressure above the glass transition temperature of the $Fe_{66}Cr_{10}Nb_5B_{19}$ alloy in a spark plasma sintering (SPS) facility. It was shown that the glassy state of the alloy is for beneficial for densification when particles of the alloy form chains.

The phase composition, microstructure and mechanical properties of composites produced from mixtures containing 20 vol.% and 50 vol.% of $Fe_{66}Cr_{10}Nb_5B_{19}$ by SPS at 540 °C and 570 °C were studied. Microstructure investigations together with the X-ray diffraction phase analysis revealed that a chemical reaction between matrix and the reinforcement occurs during sintering at 540 °C. The reaction products were observed at the Fe-based alloy/Al matrix interface and formed a shell. The thickness of the shell increased with increasing sintering temperature and soaking time. The shell was $Al_{13}Fe_4$ after SPS at 540 °C and a mixture of $Al_{13}Fe_4$ and Al_5Fe_2 after sintering at 570 °C. In these composites, the reinforcing role was played by Fe-based alloy@intermetallic core-shell structures.

Compression tests of the samples sintered from mixtures containing 20 vol.% $Fe_{66}Cr_{10}Nb_5B_{19}$ demonstrated that partial reaction between the components of the composite is beneficial for increasing its strength. Shells of small thickness helped increase the yield strength without deteriorating plasticity of the composite. The formation of thick shells led to a dramatic increase in compressive strength and limited the deformation at fracture of the composite to 2% [5].

REFERENCES

[1] W. Wolf, C. Bolfarini, C.S. Kiminami, W.J. Botta, “Recent developments on fabrication of Al-matrix composites reinforced with quasicrystals: From metastable to conventional processing”, Journal of Materials Research, Vol. 36, pp. 281-297, 2021.

[2] Y. Liu, J. Chen, X. Wang, T. Guo, J. Liu, “Significantly improving strength and plasticity of Al-based composites by in-situ formed AlCoCrFeNi core-shell structure”, Journal of Materials Research and Technology, Vol. 15, pp. 4117-4129, 2021.

[3] T. He, T. Lu, N. Ciftci, V. Uhlenwinkel, W. Chen, K. Nielsch, S. Scudino, “Interfacial characteristics and mechanical asymmetry in Al2024 matrix composites containing Fe-based metallic glass particles”, Materials Science & Engineering A, Vol. 793, 2020.

[4] J. Eckert, J. Das, S. Pauly, C. Duhamel, “Mechanical properties of bulk metallic glasses and composites”, J. Mater. Res., Vol. 22, no. 2, pp. 285-301, 2007.

[5] D.V. Dudina, B.B. Bokhonov, I.S. Batraev, V.I. Kvashnin, M.A. Legan, A.N. Novoselov, A.G. Anisimov, M.A. Esikov, A.V. Ukhina, A.A.Matvienko, K. Georgarakis, G.Y. Koga, A.M. Jorge, Jr., “Microstructure and Mechanical Properties of Composites Obtained by Spark Plasma Sintering of Al–$Fe_{66}Cr_{10}Nb_5B_{19}$ Metallic Glass Powder Mixtures”, Metals, Vol. 11. P. 1457, 2021.

* The work was partially supported by the Ministry of Science and Higher Education of the Russian Federation, project FWGG-2019-0003.

N1-O-038601

THE MECHANICAL RESPONCE OF TITANIUM ALLOYS TO DYNAMIC IMPACTS IN A WIDE TEMPERATURE RANGE*

V.A. SKRIPNYAK, V.V. SKRIPNYAK, K.V. IOHIM , E.G. SKRIPNYAK

National Research Tomsk State University, Tomsk, Russia

The titanium alloys applications in aerospace, medical, marine techniques, owing to its superior high strength-to-weight ratio, excellent corrosion resistance, and good formability. This work aimed to evaluate deformation and fracture of alpha and alpha+ beta titanium alloys under dynamic loading in temperature range from 77 K to 900 K.

The patterns of deformation and fracture of alloys during high-speed deformation at high and low initial temperatures were studied using numerical simulation of uniaxial tension of flat samples and loading of plates by plane shock waves. The response of titanium alloys to dynamic influences in a wide temperature range was described by a model of a damaged elastic viscoplastic medium. The constitutive equation takes into account the effect temperature on the flow stress, equivalent strain rate, accumulated equivalent plastic strain, pressure p, and average grain size d_g [1,2]. The macroscopic plastic flow stress was determined as the sum of the contributions of the stresses required to overcome the resistance to dislocation slip, resistance to twinning, and stresses from the inhomogeneity of the phase composition of the alloy.

The used Mie−Grüneisen equation of states takes into account the change in temperature during volumetric deformation. In this work the change in temperature due to the dissipative effect was calculated in adiabatic assumption:

$$T = T(\rho/\rho_0) + \int_0^{\varepsilon^p_{eq}} (\beta/\rho C_p)\sigma_{eq} d\varepsilon^p_{eq}, \quad (1)$$

where $T(\rho/\rho_0)$ is the temperature at volumetric strain, ρ is the mass density, and $\beta \sim 0.9$ is the parameter representing a fraction of plastic work converted into heat, σ_{eq} is the equivalent stress, ε^p_{eq} is the equivalent plastic strain.

The value of $T(\rho/\rho_0)$ calculated by the equation of states and energy conservation equation. This value is close to initial temperature of material at relatively low pressure. The accuracy of predicting the temperature rise under dynamic loadings depends on the adequacy of the description of the temperature dependence of specific heat. In this research the specific heat capacity C_p changes under dynamic loading was described by phenomenological relation. The constitutive relations have been implemented in the LS-DYNA explicit solver by writing a Fortran user-subroutine. Simulations of deformation and spall fracture of titanium plates under plane shock waves loadings were carried out using quadratic artificial viscosity, which does not introduce significant errors in determining the temperature increment during deformation in weak shock waves. The model was used for simulation of commercially pure titanium alloy, Ti-5Al-2.5 Sn, Ti-6Al-4V under uniaxial tension at strain rates from 0.1 to 1000 s^{-1}, and temperatures from 77 K to 900 K. The simulation results confirmed that strain hardening can be considered as a result of the simultaneous action of thermally activated dislocation mechanisms of plasticity and twinning, which weakly depends on temperature. The processes of spall fracture and mechanical response of titanium alloys under sub-microsecond shock pulse loading at temperatures of 103 K and 298 K at have been investigated.

The obtained results of spall fracture are consistent with the available experimental data. The calculated changes in the velocity of elastic precursors in Ti-6Al-4V plates good correlated with the experimental data at the specified initial temperatures. The calculation results showed that the damage growth rate increases in the spall zone with a decrease in the initial temperature. Spall fracture remains ductile in the considered temperature range, but a slight decrease in the effective spall strength is observed.

REFERENCES

[1] V.V. Skripnyak, A.A. Kozulyn, V.A. Skripnyak, "The influence of stress triaxiality on ductility of α titanium alloy in a wide range of strain rates", Mater. Phys. Mech. Vol. 42, 415-422, 2019.

[2] V.V. Skripnyak, V.A. Skripnyak, E.G. Skripnyak, "Ductility of titanium alloys in a wide range of strain rates". Paper presented at 6th International Conference Integrity-Reliability-Failure Lisbon/Portugal 22-26 July 2018. Editors J.F. Silva Gomes and S.A. Meguid Publ. INEGI/FEUP (2018); Paper REF: 7127 (2018)

* The work was supported by the Russian Science Foundation under grant No. 20-79-00102.

N1-O-038602

DYNAMIC FRACTURE OF HEXAGONAL CLOSE PACKED ALLOYS*

V.V. SKRIPNYAK, E.G. SKRIPNYAK, V.A. SKRIPNYAK

National Research Tomsk State University, Tomsk, Russia

Predictions of the mechanical behavior of metals and alloys with a hexagonal close-packed (HCP) lattice, under dynamic loadings are in demand in solving a wide range of applied problems.

This work aimed to study the processes of deformation, damage and ductile fracture of HCP alloys under dynamic influences. Based on the generalization of the obtained experimental data, a version of the model is proposed that allows to adequately describe the regularities of plastic deformation during tension, the formation of zones of localization of plastic shears and the development of damage and fracture in the range of strain rates from 10^{-3} to 10^{3} s^{-1} at the values of the triaxiality parameter of the stress state from 0.33 to 0.6 [1,2]. The model was used for 3D numerical modeling of uniaxial tension of specimens and spall fracture in Ti, Zr, Be, Hf plates under plane shock waves impacts. The influence of the damage parameter, the stress state triaxiality parameter on the flow stress is taken into constitutive equation.

The proposed constitutive equation takes into account the change in flow stress in wide range of a cumulative plastic strain, a homologous temperature, and the logarithm of the normalized equivalent strain rate. The modification damage equation makes it possible to describe the kinetics of the damage parameter D increasing at spall fracture as a result of nucleation, growth and coalescence of voids:

$$dD/dt = dD_1/dt + dD_2/dt, \quad (1)$$

where D is the damage parameter, D_1 is the constituent of D associated with damages caused by negative pressure, D_2 is the constituent of damages caused by voids evolution under repeated loading.

$$dD_1/dt = \alpha_1 \min[0, dp/dt]\, H(-p + p_c), \quad (2)$$

where $H(\cdot)$ is the Heaviside function, p is the pressure, α_1, and $p_c < 0$ are constants of the material.

$$dD_2/dt = [1/(\gamma_1 \cdot A \cdot \sqrt{2\pi})] \cdot \exp[-(\ln(A)/\gamma_1 \cdot \sqrt{2})\, 2], \quad (3)$$

where $A = \int_0^t \frac{W^e}{\beta_1 \exp\left(-\beta_2 W^p\right)\cdot(1-D)} \frac{dW^p}{dt}\, dt]$, β_1, β_2, γ_1, are constants of the material, W^e, and W^p are the specific internal energy, and the specific dissipated energy, respectively.

The processes of spall fracture and mechanical response of Ti, Zr, Be, Hf alloys under sub-microsecond shock pulse loading have been investigated by numerical simulations. The computer simulations were performed with the use of LS DYNA (ANSYS WB 15.2, ANSYS, Inc., Canonsburg, PA, USA) software.

The calculations were carried out using the second order accuracy finite-difference scheme. Computational domains were meshed with eight-node linear bricks and reduced integration together with hourglass control. The constitutive relations have been implemented in the LS-DYNA explicit solver by writing a Fortran user-subroutine. We adopted Becker's implicit return mapping algorithm for the Gurson-type yield potential. Employed algorithm provides accurate integration of the damage in shock impact problems where the loading direction can change significantly at a time step.

It was shown that parallel cracks oriented normal to the direction of impact are formed by damaged mesoscopic volumes.

Thus, the proposed constitutive equations and damage model make it possible to describe the main regularities of the mechanical behavior of a subgroup of HCP alloys with a lattice parameter ratio $c/a < 1.633$ in a wide range of strain rates and weak shock wave amplitudes.

REFERENCES

[1] V. V. Skripnyak, E. G. Skripnyak, V. A. Skripnyak, "Fracture of Titanium Alloys at High Strain Rates and under Stress Triaxiality", Metals, Vol. 10(3), 305, 2020.

[2] V.V. Skripnyak, A.A. Kozulyn, V.A. Skripnyak, "The influence of stress triaxiality on ductility of α titanium alloy in a wide range of strain rates", Mater. Phys. Mech. Vol. 42, 415-422, 2019.

* The work was supported by the Russian Science Foundation under grant 20-79-00102.

N1-O-039601

BEHAVIOR FEATURES OF THE METASTABLE $Fe_{13}Ga_9$ PHASE DURING HEATING OF NON-EQUILIBRIUM Fe-Ga ALLOYS WITH A HIGH CONTENT OF GALLIUM *

T.N. VERSHININA[1,2], *I.A. BOBRIKOV*[1,3], *S.V. SUMNIKOV*[1,3], *A.M. BALAGUROV*[1,3,4], *V.V. PALACHEVA*[3], *I.S. GOLOVIN*[3]

[1] *Joint Institute for Nuclear Research, Dubna, Russian Federation*
[2] *Dubna State University, Dubna, Russian Federation*
[3] *National University of Science and Technology "MISIS", Moscow, Russian Federation*
[4] *Lomonosov Moscow State University, Moscow, Russian Federation*

A surge of interest in Fe-xGa alloys occurred in the early 2000s after discovering increased values of the magnetostriction constant for x ≈ (17-19) and (26-27) at. % [1]. Therefore, the concentration range up to 30 at.% is considered in most works that studied the features of phase transitions between different structural states of Fe-Ga alloys. At the same time, the region of high concentrations of gallium (x > 30 at.%) has not yet been studied in sufficient depth.

Due to the fact that diffusion at low temperatures in alloys of the Fe-Ga system proceeds slowly, it is possible to fix non-equilibrium states during quenching from the high-temperature region. One of the phases that can be fixed in the 32.9-38.4 Ga alloys is $Fe_{13}Ga_9$ [2]. The stability of this phase under heating conditions and the features of phase transitions in alloys with high gallium content were studied by *in situ* real-time neutron diffraction. The high neutron penetration depth allows observation of bulk effects and exclusion of the influence of the surface layer (evaporation of gallium) and local inhomogeneities of the structure.

It was shown that in the studied Fe-Ga alloys with 32.9-38.4 Ga the metastable $Fe_{13}Ga_9$ phase presents in the as-cast state in different amounts. Content of $Fe_{13}Ga_9$ increases during heating and it is stable upon reaching ~550 °C. An example of such typical phase behavior for Fe-34.4Ga is shown in Figure 1. A detailed consideration of the phase transformations under the Fe-38.4Ga alloy heating was presented earlier in our paper [3].

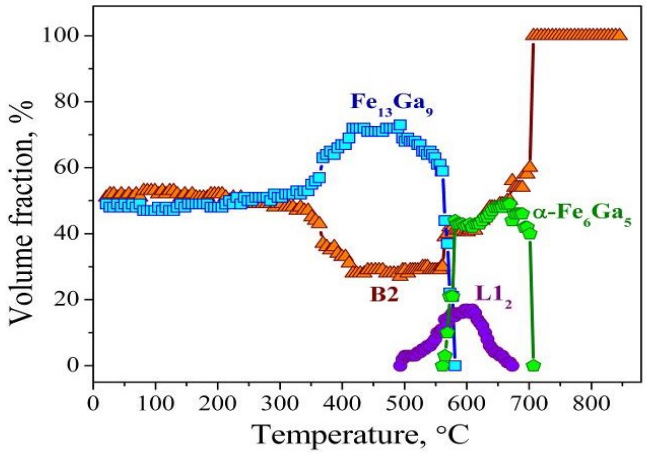

Fig. 1. Evolution of the phase composition of the Fe-34.4Ga alloy in the as-cast state upon heating to 880°C.

REFERENCES

[1] E.M. Summers, T.A. Lograsso, M. Wun-Fogle, "Magnetostriction of binary and ternary Fe-Ga alloys", J. Mater. Sci., vol. 42, pp. 9582-9594, August 2007.

[2] A. Leineweber, H. Becker, A.O. Boev, I.A. Bobrikov, A.M. Balagurov, I.S. Golovin, $Fe_{13}Ga_9$ intermetallic in bcc-base Fe-Ga alloy, Intermetallics, vol. 131, 107059, April 2021.

[3] Vershinina T.N., Bobrikov I.A., Sumnikov S.V., A.M. Balagurov, Mohamed A.K., Golovin I.S. "Structure evolution of as-cast metastable Fe-38Ga alloy towards equilibrium", J. Alloys Compd, vol. 889, 161782, December 2021.

* The work is supported by RSF (Russia) project № 22-42-04404

N1-O-041201

THE BROAD RANGE SPECTROSCOPY OF HYBRID PEROVSKITES $CH_3NH_3PBX_3$ (X=I, BR)*

V.E. ANIKEEVA[1,2], *O.I. SEMENOVA*[3], *M.N. POPOVA*[1], *K.N. BOLDYREV* [1,2]

[1] *Institute of Spectroscopy of the Russian Academy of Sciences, Troitsk, Russian Federation*
[2] *HSE University, Moscow, Russian Federation*
[3] *Institute of Semiconductor Physics, Siberian Branch of the Russian Academy of Sciences, Novosibirsk, Russian Federation*

Hybrid perovskites became one of the most popular functional materials in the field of photovoltaics. The complex structure of these compounds with the general formula ABX_3 (where A is molecular organic cation CH_3NH_3 or $CH(NH_2)_2$, B is cation of Pb or Sn, and X is halide anion I, Br, Cl) provides a number of unique optoelectronic properties such as long diffusion lengths [1], high carrier mobility [2] and optimal band gap for solar cells [3]. Many of transport properties are closely related to electron-phonon interactions and phonon spectra. Phonon modes in hybrid perovskites are distributed in three regions: vibrations of the lead halide inorganic cage and translational/librational modes of the CH_3NH_3 cation are distributed between ~15 and 100 cm^{-1} (0.45 – 3 THz), CH_3NH_3 rocking modes, C−N stretching, and CH_3 and NH_3 bending vibrations occupy the spectral interval 900 – 1600 cm^{-1}, while C−H and N−H stretching mode frequencies are between 3000 and 3200 cm^{-1} [4]. Moreover, depending on the temperature, there are three structural phases for $CH_3NH_3PbI_3$: cubic (T > 330 K), tetragonal (330 K < T < 160 K) and orthorhombic (T < 160 K); and four structural phases for $CH_3NH_3PbBr_3$: cubic (T > 236 K), tetragonal I (236 K < T < 155 K), tetragonal II (155 K < T < 149 K) and orthorhombic (T < 149 K).

In this work, high quality $CH_3NH_3PbI_3$ and $CH_3NH_3PbBr_3$ single crystals were studied by optical high-resolution spectroscopy in the wide frequency (15 – 19000 cm^{-1}) and temperature (5 – 300 K) ranges. The study in a wide frequency range made it possible to observe features at the temperatures of all phase transitions in both crystals as in the multiphonon absorption spectra and as near the fundamental absorption edge. So, for example, in Fig. 1 shows the temperature dependence of the shift of the peak position around 6010 cm^{-1} on cooling (blue) and heating (red) for $CH_3NH_3PbBr_3$. A sharp shift in position indicates a structural phase transition of the first order. Also the spectral changes appear at the T = 70 K, which correlate with the transition to the tunneling splitting. Several low-frequency modes predicted by calculations were experimentally observed for the first time in both $CH_3NH_3PbI_3$ [5] and $CH_3NH_3PbBr_3$.

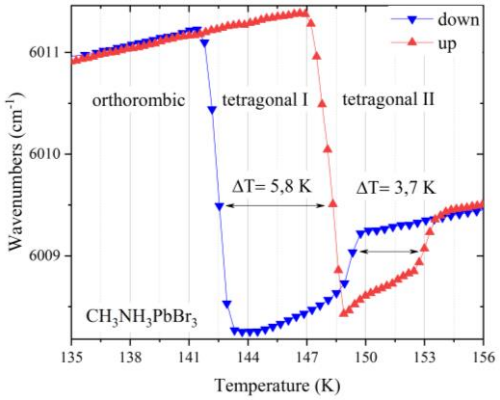

Fig.1. The hysteretic dependence of peak positions near 6010 cm^{-1} from temperature during phase transitions in $CH_3NH_3PbBr_3$ (blue– for cooling, red – for heating).

REFERENCES

[1] Q. Dong, Y. Fang, et al., "Electron-hole diffusion lengths > 175 μm in solution-grown $CH_3NH_3PbI_3$ single crystals," Science, vol. 347, no. 6225, pp. 967–970, February 2015.

[2] G. A. Elbaz, "Transport Phenomena in Lead Halide Perovskites and Layered Materials," Columbia University, 2017.

[3] D. I. Kim, J. W. Lee, R. H. Jeong, and J.-H. Boo, "A high-efficiency and stable perovskite solar cell fabricated in ambient air using a polyaniline passivation layer," Sci Rep, vol. 12, no. 1, Art. no. 1, January 2022.

[4] F. Brivio *et al.*, "Lattice dynamics and vibrational spectra of the orthorhombic, tetragonal, and cubic phases of methylammonium lead iodide," *Phys. Rev. B*, vol. 92, no. 14, p. 144308, Oct. 2015.

[5] K. N. Boldyrev, V. E. Anikeeva *et al.*, "Infrared Spectra of the $CH_3NH_3PbI_3$ Hybrid Perovskite: Signatures of Phase Transitions and of Organic Cation Dynamics," *J. Phys. Chem. C*, vol. 124, no. 42, pp. 23307–23316, Oct. 2020.

* The work was supported by the Russian Science Foundation (Grant No.19-72-10132).

N1-O-044001

MECHANOCHEMICAL SYNTHESIS OF COMPOSITES TUNGSTEN (MOLYBDENUM) - MAGNESIUM OXIDE*

T.A. UDALOVA[1,2], T.F. GRIGOREVA[1], S.V. VOSMERIKOV[1], E.T. DEVYATKINA[1], N.Z. LYAKHOV[1,3]

[1]Institute of solid state chemistry and mechanochemistry of the SB RAS, Novosibirsk, Russian
[2]Novosibirsk State Technical University, Novosibirsk, Russian
[3]Novosibirsk State University, Novosibirsk, Russian

Tungsten and molybdenum, possessing properties such as high T_{melt} and T_{boil}, density, hardness, low coefficient of linear thermal expansion and steam pressure, good electrical and thermal conductivity [1-2], finds application from metallurgy to electronics [3].

Mechanochemical reduction of metal oxides by an active metal magnesium leads to simultaneous grinding of the substance, acceleration of mass transfer, increase in the contact surface area, deformational mixing of mixture components and activation of their mechanochemical interaction. As a result, composites (Me/(MgO) are formed - powder mixtures of highly dispersed metal particles and active metal oxide.

Mechanochemical reduction of WO_3 (MoO_3) and $MgWO_4$ ($MgMoO_4$) with magnesium, proceeding with a high exothermic effect can be carried out in the process of only mechanical activation with the formation of a mechanochemical composites W(Mo)/MgO.

The goal of the work was to study the possibility of mechanochemical synthesis of magnesium wolframite (molybdate) from tungsten (molybdenum) and magnesium oxides, the formation of a W(Mo)/MgO composite during the mechanochemical reduction of WO_3 (MoO_3) and $MgWO_4$ ($MgMoO_4$) by magnesium, and the subsequent separation of highly dispersed tungsten (molybdenum) from MgO from the composites W(Mo)/MgO.

X-ray diffraction of $MgWO_4$ ($MgMoO_4$) mechanochemical reduction samples obtained with various stoichiometric compositions and mechanical activation modes showed that, with a ratio of $MgWO_4$ ($MgMoO_4$) : Mg = 1 : 3.1, the rotational speed of the vials around the common axis, the reduction is complete by 8 min with the formation W(Mo)/MgO composite. In the diffractograms of the samples of the mechanochemical reduction of magnesium wolframat (molybdate), only broadened reflections of MgO and W (Mo) recorded.

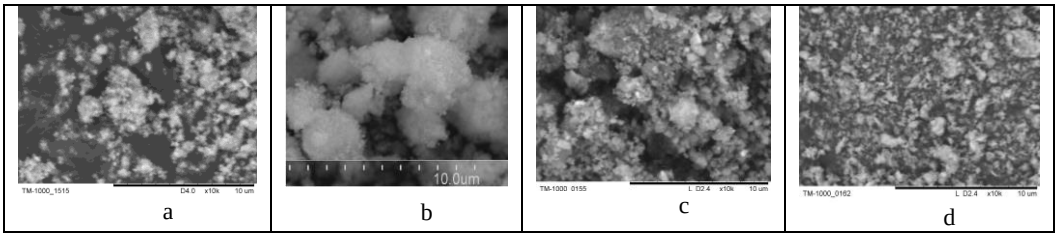

Fig.1. SEM: (a) W/MgO mechanocomposite; (b) highly dispersed W after acid treatment of mechanochemical composite W/MgO; (c) Mo/MgO mechanocomposite; (d) highly dispersed Mo after acid treatment of mechanochemical composite W/MgO, magnification 10000x.

Sequential treatment of W (Mo)/MgO composites with acid solutions leads to a product containing predominantly metallic tungsten (molybdenum). Particles of finely dispersed tungsten (molybdenum) have sizes of ~ 0.1 μm, aggregated into larger ones, with sizes of 2–4 μm.

REFERENCES

[1] Wang H., Fang Z.Z., Hwang K.S., Zhang H., Siddle D., Int. Journal of Refractory Metals & Hard Materials, 28 (2010) P. 312 – 316..
[2] Lassner E., Schubert W.D., Tungsten Properties, Chemistry, Technology of the Element, Alloys, and Chemical Compounds – Kluwer Academic, Plenum Publishers, New York, 1999.
[3] Schubert W.D., Lassner E. "Tungsten: properties chemistry technology of the element alloys and chemical compounds". N.Y.: Kluwer Academics, 1999, pp. 288.

* The work was supported by as part of the state task of ISSC SC RAS (project №. 121032500062-4) and as thematic plan TP - Chemistry and chemical technology -1_22.

N1-O-044004

MECHANOCHEMICAL SYNTHESIS OF NB/MGO COMPOSITE FROM MAGNESIUM NIOBATE MGNB2O6 AND NIOBIUM OXIDE NB2O5

T.A. UDALOVA[1,2], *T.F. GRIGOREVA*[1], *S.V. VOSMERIKOV*[1], *E.T. DEVYATKINA*[1], *N.Z. LYAKHOV*[1,3]

[1]*Institute of Solid State Chemistry and Mechanochemistry of the SB RAS, Novosibirsk, Russian*
[2]*Novosibirsk State Technical University, Novosibirsk, Russian*
[3]*Novosibirsk State University, Novosibirsk, Russian*

The growing demand for the production of modern materials based on highly dispersed metal powders necessitates the development of innovative "breakthrough" technologies for their creation. The main industrial methods for the production of niobium and its alloys are metal-thermal reduction of oxide compounds: aluminothermic, sodium-thermal, carbothermal from a mixture of Nb_2O_5 and soot. The reduction reactions of metal oxides that proceed with a large exothermic effect can be carried out in the process of mechanical activation alone.

Mechanical activation of solid mixtures of metal oxides with active metal leads to an increase in the contact surface area, acceleration of mass transfer, and, as a result, activation of their mechanochemical interaction with the formation of composites (Me/(Meact)xOy) - powder mixtures of highly dispersed particles of reduced metal and active metal oxide [1, 2]. As an active metal, it is possible to use various active metals Al, Zn, etc. To extract a reduced element from mechanochemical composites without disturbing its finely dispersed state, it is necessary to choose an active metal oxide solvent that would be simultaneously inert with respect to the reduced metal. The most promising active metal is magnesium, which, during mechanical activation, forms the MgO phase, which prevents significant sintering of mechanical activation products; when interacting with dilute solutions of HCl or H_2SO_4, magnesium oxide forms well-soluble compounds [3].

The aim of this work is to study the conditions of mechanochemical synthesis of magnesium niobate ($MgNb_2O_6$) and its reduction and simple niobium oxide (Nb_2O_5) by magnesium with the formation of Nb/MgO mechanocomposites for subsequent separation of finely dispersed niobium powder from such composites by the method of acid dissolution of magnesium oxide.

We propose a mechanochemical method for the synthesis of magnesium niobate by activation of mixtures of MgO with Nb_2O_5. It has been shown by X-ray phase analysis (XPA) that 8 min of activation of the corresponding oxides is sufficient for the formation of $MgNb_2O_6$ (with a strict stoichiometry of 1:1 and a drum rotation speed of 1000 rpm in a high-energy planetary mill). The diffraction patterns of the samples synthesized under such conditions by mechanochemical activation are in good agreement with the literature data.

Mechanochemically synthesized magnesium niobate was used for mechanochemical reduction with magnesium. From the results of X-ray phase analysis of the products of mechanochemical reduction of $MgNb_2O_6$ with magnesium, the optimal conditions for mechanical activation and the ratio of components of mixtures of $MgNb_2O_6$ with Mg were determined. It has been shown that at a speed of rotation of the drums around a common axis of 1000 rpm, mechanochemical redox reactions completed with the formation of Nb/MgO composites within an activation time of 8 min.

A study of the mechanochemical reduction of niobium oxide (Nb_2O_5) with magnesium showed that the formation of the Nb/MgO composite occurs at a ratio of Nb_2O_5 : Mg mixture components of 1:5.2 at a rotation speed of the drums about a common axis of 1000 rpm. for an activation time of 4 min.

The method presented by us makes it possible to obtain highly dispersed niobium powders by mechanochemical synthesis practically at room temperature with a high (97%) yield and the possibility of utilizing magnesium oxide by-product by known methods.

REFERENCES

[1] Urakaev F. H., Shevchenko V. S., Boldyrev V. V. // Doklady RAN. 2001.Vol. 377. No. 1. P. 69–71.T. V. Koval, Le Hu Dung, “Investigation of plasma generation and current transmission of an intense low-energy electron beam,” Izv. Vyssh. Uchebn. Zaved. Fiz., vol. 57, no. 3/2, pp. 118–121, March 2014.

[2] Grigoreva T. F., Barinova A. P., Lyakhov N. Z. Mechanochemical synthesis in metallic systems. Novosibirsk: Parallel, 2008. 310 p .

[3] Raschman P., Fedoroc¢ková A. // Hydrometallurgy. 2004 Vol. 71. P. 403–412.

* The work was supported by as part of the state task of ISSC SC RAS (project №. 121032500062-4) and as thematic plan TP - Chemistry and chemical technology -1_22.

N1-O-046701

PLASMA-SOLUTION SYNTHESIS OF A SOLID PHASE FROM SOLUTIONS OF IRON AND COBALT NITRATES OF VARIOUS CONCENTRATIONS*

K.V. SMIRNOVA[1], *D.A. SHUTOV*[1], *A.N. IVANOV*[1], *V.V. RYBKIN*[1]

[1]*Ivanovo State University of Chemistry and Technology, Ivanovo, Russia*

In recent years, magnetic nanoparticles (MNPs) have attracted a considerable amount of attention due to their special superparamagnetic (SPM) properties, high adsorption capacities and surface area to volume ratio. In particular, transition metal oxides with spinel structures commonly referred to as ferrite are among one of the most important MNPs. Based on their crystal structures and magnetic properties, ferrites are classified as spinel [1-2]. This is mainly due to their excellence magnetic properties, simple chemical composition, and wide applications in several areas, which include water and wastewater treatment, biomedical, catalyst and electronic device. There are a large number of different methods for obtaining spinels, one of the new and promising ones is the synthesis from a solution under the action of a low-temperature nonequilibrium plasma.

In this work, we used aqueous solutions of ferrum and cobalt nitrates (analytical grade) with a different concentration for each component (Table1). We describe the experimental setup used in the study in detail in [3]. External electrodes were made of titanium. The electrode-solution distance was 5 mm. The discharge current could vary within 30-70 mA. Obtaining and analysis of particles can be conventionally divided into two stages. First: plasma-solution synthesis (analysis of particles in solution and after drying); Second: calcination of the particles after drying and examination of the resulting oxides.

Table 1. Designation of samples depending on the initial concentration of the components.

Raw materials	**Fe2Co1**	**Fe1Co2**	**Fe2.5Co50**	**Fe3Co50**	**Fe5Co50**
$Fe(NO_3)_3$	3.3 mmol	1.7 mmol	2.5 mmol	3 mmol	5 mmol
$Co(NO_3)_2$	1.7 mmol	3.3 mmol	50 mmol	50 mmol	50 mmol

The average effective particle size was determined by dynamic light scattering (DLS) using a Photocor Compact-Z size analyzer (Photocor, Russia). Immediately after plasma treatment (50 mA, 10 minutes), particles of two characteristic sizes can be isolated in the solution. The first fraction: 92.91 nm and the second: 1.46 μm, while the zeta potential ζ= 24.76 mV.

X-ray phase analysis (XRD) (DRON 3M) of powders showed the presence of a large number of pronounced reflections, which indicates the crystallinity of the structure of the synthesized substances. Elemental analysis data (Aztec EDS, Oxford Instruments Ltd., England) showed that the synthesized powders after high temperature treatment have a complex composition as shown in Table 2.

Table 2. EDS analysis of the composition of the resulting powders.

Fe2Co1	**Fe1Co2**	**Fe2.5Co50**	**Fe3Co50**	**Fe5Co50**
$(Fe_2O_3)_{0,99}(CoO)_{0,01}$	$(Fe_2O_3)_{0,76}(CoO)_{0,24}$	$(Fe_2O_3)_{0,26}(CoO)_{0,74}$	$(Fe_2O_3)(CoO)$	$(Fe_2O_3)_{0,60}(CoO)_{0,40}$

We found that by varying the initial concentrations of the initial salts in the solution, it is possible to obtain spinels of a given composition. These materials are of great interest for various applications.

REFERENCES

[1] Ra'ul Valenzuela, "Novel applications of ferrites," Phys. Res. Int., pp. 1–9, 2012.

[2] G. Litsardakis, I. Manolakis, C. Serletis, K.G. Efthimiadis, "Effects of Gd substitution on the structural and magnetic properties of strontium hexaferrites," J. Magn. Magn. Mater., vol. 316, pp. 170–173, 2007.

[3] D. A. Shutov, K. V. Smirnova, M. V. Gromov, A. N. Ivanov, V. V. Rybkin, "Synthesis of CdO Ultradisperse Powders Using Atmospheric Pressure Glow Discharge in Contact With Solution and the Investigation of Intermediate Products," Plasma Chem. Plasma Process., 38(1) pp. 107-121, 2018.

*This work was supported by the Ministry of High Education and Science of the Russian Federation, project No FZZW-2020-0009. This work was supported by Russian Science Foundation № 22-22-00372 and in part by the grant of the Russian Federation President (MK-2607.2022.1.2).

N1-O-046702

SYNTHESIS OF ZINC DOPED WITH CADMIUM FROM NITRATE SOLUTIONS UNDER THE ACTION OF A GLOW DISCHARGE*

K.V. SMIRNOVA[1], *D.A. SHUTOV*[1], *A.N. IVANOV*[1], *V.V. RYBKIN*[1]

[1]*Ivanovo State University of Chemistry and Technology, Ivanovo, Russia*

Usually, oxides of zinc, cadmium, tin, and indium nanoparticles are used in microelectronics [1-2]. At the same time, doping of these oxides led to improved electrical conductivity without deteriorating their other properties of these materials. Zinc and cadmium, transition metals belonging to the same group of the periodic table. The study of the Cd – Zn – O system is of fundamental and practical interest, since this semiconductor material combines many useful characteristics of both Cd and Zn. Cadmium oxide is an n-type semiconductor with a band gap of 2.5 eV is widely used in optoelectronics. In turn, zinc oxide, a direct-gap semiconductor with a band gap of 3.3 eV, is used as sensor materials. There are a large number of different methods for obtaining nanoparticles; one of the new and promising is the synthesis based on the interaction of plasma with salt solutions.

In this work, we used aqueous solutions of zinc and cadmium nitrates (analytical grade) with a concentration of 50 mmol/l for each component. The experimental setup used in the study is described in detail by us in [3]. External electrodes were made of titanium. The electrode-solution distance was 5 mm. The discharge current could vary within 30-70 mA.

The kinetics of the formation of colloidal particles was investigated by the turbidimetric method. It turned out that the rate of formation increases with an increase in the discharge current from 30 to 70 mA. The results of the kinetic curve are shown in Figure 1. At concentrations of zinc and cadmium nitrates 50 mmol/l the rate constant of the process increases from $1.3 \cdot 10^{-3}$ to $12 \cdot 10^{-3}$ s^{-1}.

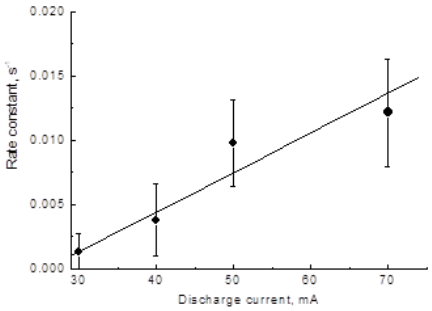

Fig.1. The dependence of the effective rate constant on the discharge current

Analysis of the results obtained by XRD and EDS analyzes showed that the resulting substance has a complex structure consisting of crystalline phases $Cd(NO_3)OH \cdot H_2O$, β and γ $Cd(OH)_2$, and for zinc - from $Zn(NO_3)OH \cdot H_2O$ and $Zn(OH)_2$. DSC analysis confirmed the data obtained by XRD analysis.

The sediment particles, as shown by SEM, have a spheroidal shape with a characteristic size of about 1 μm. Thermal decomposition of the resulting precipitate proceeds in several stages and ends at a temperature of ~300 °C. As a result of calcination, a mixture of crystalline zinc and cadmium oxides is formed. According to EDX data, at a molar ratio of 1:1 of zinc and cadmium in the initial solution, the obtained solid particles contain 8 mol% cadmium and 92% zinc.

REFERENCES

[1] W. U. Huynh, J. J. Dittmer and A. P. Alivisatos, “Hybrid Nanorod, Polymer Solar Cells,” Science, vol. 295, no. 5564, pp. 2425-2427, 2002.

[2] R. E. Bailey, A. M. Smith, and S. Nie, “Quantum dots in biology and medicine,” Physica E: Low-dimensional Systems and Nanostructures, pp.1-12, 2004.

[3] Shutov D.A. et al. // Plasma Chem Plasma Process, 2018, Vol. 38, P. 107. D. A. Shutov, K. V. Smirnova, M. V. Gromov, A. N. Ivanov, V. V. Rybkin, “Synthesis of CdO Ultradisperse Powders Using Atmospheric Pressure Glow Discharge in Contact With Solution and the Investigation of Intermediate Products,” Plasma Chem Plasma Process, 38(1): 107-121, 2018.

* This work was supported by the Ministry of High Education and Science of the Russian Federation, project No FZZW-2020-0009. This work was supported by Russian Science Foundation № 22-22-00372 and in part by the grant of the Russian Federation President (MK-2607.2022.1.2).

N1-O-049201

INVESTIGATION OF PROCESSES OCCURRING AT THE IRIDIUM/SILICON CARBIDE INTERFACE IN A WIDE TEMPERATURE RANGE*

M.A. GOLOSOV, A.V. UTKIN, V.V. LOZANOV, N.I. BAKLANOVA

Institute of Solid State Chemistry and Mechanochemistry SB RAS, Novosibirsk, Russian Federation

Silicon carbide, due to a combination of unique properties, is an integral component of high-temperature structural materials. However, the manufacture of products of complex shapes from SiC, due to its high hardness (9 – 9.5 according to Mohs), is a very laborious and difficult task. There is a concept of connecting two or more parts into one with the help of an intermediate metal layer. SiC-Me couples are currently developed for these purposes, where Ti, Mo, V, Cr, etc. act as the metal, and have insufficient oxidative stability and low impact strength, which is a consequence of the formation of a brittle carbide phase [1]. The use of iridium, a noble metal that does not form carbides and has an extremely high oxidative stability up to Tm (2446 °C), is the most promising approach to solving this problem [2]. The combination of components such as SiC and Ir is also of great interest in the fields of nuclear power, high temperature electronics and aerospace. Information on the Ir-SiC system is very scarce and contradictory [3,4,5], so there is a need to study the physicochemical processes that occur at the Ir/SiC interface.

The aim of this work is a physicochemical study of the interaction features at the Ir/SiC interface using diffusion couples in a wide temperature range. To achieve this goal, samples were obtained by heat treatment of diffusion couples of iridium - silicon carbide ceramics in the range of 1300 – 1800 °C and different holding times. The interaction products were studied by a complex of physicochemical methods of analysis, including XRD, SEM/EDX, TG-DTA, and Raman spectroscopy.

It has been established that the type of interaction changes with increasing temperature from solid-phase ($T \leq 1400°C$) to interaction involving the liquid phase ($T > 1400°C$), as evidenced by the presence of a drop-like layer. In the solid phase regime, the following sequence of phase layers is observed: SiC / IrSi+C / IrSi (without C) / Ir_3Si_2 / Eutectoid: «Ir_3Si_2+Ir_3Si» / Ir_3Si / Ir, which is consistent with the phase diagram of the Ir-Si system. It should be noted that the eutectoid layer was formed as a result of the decomposition of the Ir_2Si phase during cooling, according to the data of the Ir-Si phase diagram. Judging by the phase sizes and their dynamic growth, we can conclude that the diffusion of iridium atoms is much faster than the diffusion of silicon atoms. The dependence of the sizes of layers of product phases does not follow a parabolic law, from which we can conclude that under these conditions the reaction is controlled by kinetics. Based on the data obtained, an interaction model was proposed. The evolution of morphology during solid-state reaction and reaction with the participation of a liquid was also studied. Sequential alternation of dense IrSi bands and bands with a random distribution of IrSi and carbon grains was found. The band width of dense IrSi increases with distance from the reaction front. The degree of order and the size of carbon agglomerates increase with distance from the reaction front. For the first time, the values of CTE and microhardness of iridium silicides formed in the reaction were obtained. It was found that the microhardness of silicides is, on average, 2 times higher than the microhardness of iridium. The values of CTE and volumes of products do not differ much from the initial reagents.

The data obtained can be in demand in the fields of materials science related to the creation of products that are resistant to aggressive environments, high temperatures, abrasive wear, and high mechanical loads.

REFERENCES

[1] Guiwu Liu, Xiangzhao Zhang, Jian Yang, Gunjun Qiao, “Recent advances in joining of SiC-based materials (monolithic SiC and SiCf/SiC composites): Joining processes, joint strength, and interfacial behavior” // Journal of Advanced Ceramics. 2019. Vol. 8, № 1. P. 19–38.

[2] Wu W., Chen Z. Iridium Coating: Processes, Properties and Application. Part I // Johnson Matthey Technology Review. 2017. Vol. 61, № 1. P. 16–28.

[3] Strife J.R., Smeggil J.G., Worrell W.L. Reaction of Iradium with Metal Carbides in the Temperature Range of 1923 to 2400 K // Journal of the American Ceramic Society. 1990. Vol. 73, № 4. P. 838–845.

[4] Camarano A., Narciso J., Giuranno D. Solid state reactions between SiC and Ir // Journal of the European Ceramic Society. 2019. Vol. 39, № 14. P. 3959–3970.

[5] Golosov M.A., Lozanov V.V., Titov A.T., Baklanova N.I. Toward understanding the reaction between silicon carbide and iridium in a broad temperature range // Journal of the American Ceramic Society. 2021. Vol.104. Iss. 12. P.6653-6669

* The work was supported by a grant from the Russian Science Foundation № 18-19-00075.

N1-O-051401

THERMO-VISCO-ELASTIC MODEL OF POWDER LAYER MODIFICATION BY MOVING HEAT SOURCE *

A.G. KNYAZEVA

Institute of Strength Physics and Materials Science SB RAS, Tomsk, Russia

There are fundamentally different methods of synthesizing 3D material in powder technology. In one of them, the powder is preliminary sprayed on the surface to be treated and then the surface is scanned by laser radiation or an electron beam. In the other, the powder is fed directly into a melt bath, which is pre-formed in the area of a moving energy source. In either case, the powder undergoes a change from a solid state to a liquid state and back; the entire process is accompanied by a variety of physical and chemical phenomena. Before the planetary scale boom in additive technologies, similar methods were actively developed for coating and surface treatment of materials. In mathematical modeling of the accompanying phenomena, the problem arises of selecting or constructing a suitable model that adequately describes the behavior of the material in both the solid and liquid phases, as well as in the two-phase region. Related to this is the variety of modeling approaches. Numerous publications analyze purely thermophysical models for calculating temperature fields at different variants of the heat source setting; study the behavior of fine particles in the melt bath; describe powder melting and melt flow in the unmelted powder, including using filtration theory; analyze variants for calculating residual stresses, etc.

In spite of the fact that each of the approaches allows obtaining interesting results and studying a number of phenomena, the process of creating a new material in dynamics proves to be insufficiently studied.

The present work aims to compare two variants of the coupled model the treatment by moving heat source of powder layer placed on a substrate. The models are based on the Maxwell thermo-viscous-elastic medium model and considering melting: (A) under the condition of a single melting temperature, in the neighborhood of which the effective heat capacity and viscosity change and (B) under the condition of melting in a certain temperature interval, in which the effective heat capacity and viscosity depend on the fraction of the liquid phase. In any case, the rheological properties change from those of the liquid phase to those of the solid phase. The applicability of the Maxwell model and its generalizations to the description of the synthesis of new materials is shown, for example, in [1-4].

Different variants of the coupled model (with and without taking into account the heat release from possible chemical reactions) are of independent interest. The possibility of transition to a two-level coupled model, when melting and/ or chemical reactions are described within the framework of the mesolevel model (at the level of powder particles), is discussed.

REFERENCES

[1] A.G. Knyazeva and E.A.Dyukerev, "Model for the propagation of a stationary reaction front in a viscoelastic medium," Comb. Expl. And Shock waves., vol.36, No 4., P.452-461, 2000.

[2] A.G. Knyazeva and S.N.Sorokova, " Stability of the combustion wave in a viscoelastic medium to small one-dimensional perturbations Comb. Expl. And Shock waves., vol.42, No 4., P.411-420, 2006.

[3] N.K. Evstigneev and A.G. Knyazeva, " Selection of a rheological model to describe the synthesis of intermetallide combined with extrusion through a conical mold //Vestnik Perm GTU. Mechanika (in Russian), № 1., P. 59 – 71, 2010

[4] A Knyazeva, "Kinetics of powder layer shrinkage during electron-beam treatment", J. of Physics: Conf. Ser., vol. 754, Article Number 042009, 2016

* The work was performed according to the Government research assignment for ISPMS SB RAS, project FWRW-2022-0003.

N1-P-004601

THE EFFECT OF PRELIMINARY MECHANICAL ACTIVATION OF TITANIUM POWDER IN ARGON ON SUBSEQUENT ACTIVATION IN NITROGEN.

O.A.SHKODA

Tomsk Scientific Center of the Siberian Branch of the Russian Academy of Sciences, Tomsk, Russia.

Nitrides of refractory metals are of great interest for study due to their properties. They are widely used in engineering as various kinds of additives and coatings, as well as independent materials. Fine grinding of green materials is widely used for the synthesis of ceramic materials, while the rate of solid-phase reactions increases due to the "pumping" of excess elastic energy into the material and an increase in the surface area of the reagents. An important characteristic in these processes is the state of the grain surface of the components, which can change markedly due to the course of mechanochemical reactions involving the surrounding gas environment. The grinding of substances is used in production and is an important technological process. Most often, various kinds of mills are used as grinders, in which grinding is carried out with the help of grinding bodies located in the chamber together with the crushed powder.

In this paper, the regularities of the mechanical synthesis of titanium nitride during mechanical activation of titanium powder in a nitrogen atmosphere are investigated. Experimental studies of the mechanochemical synthesis of titanium nitride have revealed that mechanical activation intensifies chemical transformation in the Ti - N system, and the intermittent mode allows synthesizing the final product under "soft" controlled conditions without noticeable heat release [1].

In this paper, studies on the preliminary mechanical activation of titanium powder in argon were carried out in order to increase the defectiveness of the powder in advance. It was assumed that the pretreated powder would absorb nitrogen better.

Two series of experiments were carried out: in one, the mechanical activation time of titanium in argon changed (10 s, 30 s, 3 min, 5 min) with a constant time of 5 min mechanical activation of titanium in nitrogen. In the second series, the mechanical activation time of titanium in argon was unchanged for 10 min and the mechanical activation time of titanium in nitrogen (17, 25, 40 min) changed.

Titanium powder (TU 14-22-57-92) was ground and mechanically activated in an M-3 planetary mill in nitrogen (high grade, GOST 9293-74). The initial size of titanium particles did not exceed 100 μm.

The morphology and size of the powders were studied by scanning electron microscope (Philips SEM 515 with EDAX attachment and electronic focused ion beam system Quanta 200 3D). The phase composition of the final products was characterized by X-ray diffraction analysis DRON-UM1 (CuKα radiation).

The dependence of nitrogen assimilation by titanium, with the preliminary mechanically activated of titanium in argon, was investigated. Analysis of the data obtained from photo, X-ray and microanalysis showed that at short exposure times, preliminary mechanical activation in argon accelerates nitrogen absorption, and at large, it slows down.

This deceleration can be explained as follows: when activated for some time (activation time in argon plus activation time in nitrogen), all particles go into a nanostructured state and stop grinding, fresh surfaces disappear, nitrogen does not decompose and nitriding stops. Thus, the preliminary mechanical activation of titanium powder in argon reduces the time of effective activation in nitrogen, at which fresh surfaces are formed.

REFERENCES

[1] Oleg Lapshin, Olga Shkoda, Oksana Ivanova and Sergey Zelepugin, Discrete One-Stage Mechanochemical Synthesis of Titanium-Nitride in a High-Energy Mill, Metals 2021, 11, 1743. https://doi.org/10.3390/met11111743

N1-P-004602

SHS SYSTEM "TI-CO-N": THE MECHANISM OF PHASE FORMATION AND THE ROLE OF INTERMEDIATE PHASES*

O.A.SHKODA

Tomsk Scientific Center of the Siberian Branch of the Russian Academy of Sciences, Tomsk, Russia.

The self-propagating high-temperature synthesis (SHS) of the TI-Co-N system was investigated and the relationship of combustion parameters, the state diagram, the mechanism of phase formation and the role of intermediate phases of nitrides in this is found. Combustion system parameters were studied under various initial conditions that characterize the behavior of a high-temperature chemically active solid-liquid medium. The zone of chemical reactions for combustion is a solid-liquid melt, with nitrogen gas enters, corresponding to the melt solidus-liquidus (L-S) of the state diagram [1-6].

The purpose of the work is to clarify the mechanism of phase formation in the process of SHS, to find the relationship of the phase composition of the combustion product with the type of intermediate unstable nitrides formed in the combustion wave, and the diagram of the state of the system, with a change in various initial parameters.

The SHS of the samples was carried out in a constant pressure reactor in a nitrogen medium. The relative density varied from 0.22 to 0.38. The initial composition changed in the ratio: Co/Ti, wt. %. within the values of 5/50. The final and intermediate products were studied using RFA analysis and quenching. Changes in the concentration of the environment and the rate of combustion of samples were obtained by changing the initial parameters (initial concentration of substances, initial density of samples, diameter, height of samples, etc.).

Regardless of the initial composition, dispersion and density of the sample, the values of combustion parameters (combustion conversion, maximum burning temperature, amount of stoichiometric absorbed nitrogen) obtained in the experiment lie in the region between the S-L lines, i.e. in the region of solid-liquid suspension. SHS processes occur only in the solid-liquid melt L-S [7].

It is found that during the transition from "soludus" to "liquidus", the melting particles necessarily pass through the nanoscale. During the heating process, Co diffusely enters Ti and, Co into Ti. The incoming nitrogen interacts with these intermetallides by a catalytic mechanism. Titanium nitride is formed due to interaction with atomic N formed during the decay of Co nitride. As a result of the reaction, the final product consists of titanium nitride and an intermetallic matrix with a small amount of hardened cobalt nitrides. It is established that the amount of assimilated nitrogen forms integer atomic ratios with both Co and Ti. Thus, in the combustion wave, an intermediate, rapidly decaying nitride with a certain crystal lattice is formed, which can correspond only to the equilibrium nitride, according to the phase diagram. An invariant combining the experimental points is found, which is the atomic ratio of nitrogen and titanium in nitrides.

REFERENCES

[1] B.B.Khina, A.V.Belyaev, P.A. Vityaz', et al., Application of SHS for the production of porous powder permeable composite materials of titanium—Titanium nitride. Powder Metall Met Ceram 36, 298–302 (1997). https://doi.org/10.1007/BF02676221

[2] G.S.Oniashvili, Z.G.Aslamazashvili, G.V.Zakharov,. et al., SHS of fine-grained ceramics containing carbides, nitrides, and borides. Int. J Self-Propag. High-Temp. Synth. 22, 185–188 (2013). https://doi.org/10.3103/S106138621304002X

[3] A.S. Mukasyan, and I.P.Borovinskaya, Structure Formation in SHS Nitrides, Int. J. SHS, 1992, vol. 1, no. 1, pp. 55–63.

[4] L.G.Raskolenko, A.Y. Gerul'skii, Compounds WAl4, WAl3, W3Al7, and WAl2 and Al-W-N combustion products. Inorg Mater 44, 30–39 (2008). https://doi.org/10.1134/S0020168508010056

[5] N.V.Kruglova, L.G. Raskolenko, and Yu.M. Maksimov, Self-propagating High-Temperature Synthesis of Three-Component Systems Based on Titanium and Group III, VI, and VIII Metals with Nitrogen, Izv. Vyssh. Uchebn. Zaved., Tsvetn. Metall., 2002, no. 2, pp. 56–59.

[6] L.G. Raskolenko, O.A. Shkoda, The Dynamic Structure Plotting During Experimental Research Into The Behavior of Systems With Complex Organization, Eurasian Physical Technical Journal. Volume 7, No. 2(14), 2010, pp. 49 – 52

[7] O. A. Shkoda, SHS system "Ti-Co-N": relation between the combustion process and the phase diagram. PROCEEDINGS 7th International Congress on Energy Fluxes and Radiation Effects (EFRE 2020), DOI: 10.1109/EFRE47760.2020.9242011

*ACKNOWLEDGMENT: The blessed memory of Raskolenko Larisa G. whose ideas are the basis of this work. Thank you Peleneva Sofiya P. for helping with the experiments.

N1-P-010601

INTERACTION OF THE "FERROSILICON-ZIRCON-ALUMINIUM" MIXTURE WITH NITROGEN DURING SHS

O.G. KRYUKOVA

Tomsk Scientific Center of the Siberian Branch of the Russian Academy of Sciences, Tomsk, 634055, Russia

Si_3N_4 due to its properties (high hardness, heat resistance, mechanical strength) and composite materials based on it (Si_3N_4-SiC, Si_3N_4-TiN, Si_3N_4-BN, Si_3N_4-$MoSi_2$ etc.) are widely used in tool industry, mechanical engineering, chemistry, electrical and radio engineering [1-3]. Due to the covalent bonds, Si_3N_4 is a high-sintering material. Activating oxygen-containing additives (Al, Mg, REM oxides) are used to obtain high-density Si_3N_4 - based ceramics. Sintering activators also include ZrO_2. In this work, a new approach to the synthesis of Si_3N_4-based composite powders was proposed. It was proposed to nitride ferrosilicon (iron-silicon alloy) with natural oxides (zircon) by self-propagating high-temperature synthesis (SHS). The heat of the nitride formation reaction contributes to an endothermic process of zircon dissociation and the powder Si_3N_4-ZrO_2-Si_2N_2O-Fe is obtained without additional energy costs.

In [4] the effect of aluminum additives (1-10 wt%) on the phase composition of composite powders was reported using the "40 % ferrosilicon - 30 % nitrided ferrosilicon - 30 % zircon" mixture that was nitrided by SHS. It was found that the addition of 1% Al leads sharply decreases the Si_2N_2O phase content in the synthesized products, and a further increase in Al leads to the disappearance of Si_2N_2O. Addition of 6 % and more leads to the formation of ZrN phase in the burned samples, which is visually observed as separate areas of golden color. The addition of Al additives to the mixture leads to the formation of a solid solution based on Si_3N_4 in the final products. However, the mechanism of interaction of the mixture with nitrogen in the presence of aluminum during combustion remains unclear. This work is an ongoing research and devoted to the study of chemical transformations during nitriding of the mixture with aluminum additives (1 - 10 %) using the methods of isothermal synthesis and differential scanning calorimetry.

To study physicochemical processes occurring during nitriding of the mixture with Al, sample 1 (mixture + 6 % Al) and sample 2 (mixture + 10 % Al) were used. Nitriding of sample 1 under isothermal conditions showed a small amount of nitrogen in the products in the temperature range of 800 - 1000ºC with increasing the nitriding time (30 - 180 min). At temperatures above 1000ºC, the amount of nitrogen in the products increases. According to XRD data, AlN is formed in the products at 800ºC. At 900ºC, Si_3N_4 reflexes are observed in X-ray diffraction patterns, and ZrO_2 at 1000ºC. In the temperature range of 1000 - 1250ºC, the phase composition of the products is represented by β- Si_3N_4, ZrO_2. With increasing the nitriding time, the intensity of reflexes of these phases slightly increases. The synthesized products contain unreacted components of the mixture ($FeSi_2$, Si, Fe_xSi_y, $ZrSiO_4$). A similar pattern is observed during nitriding of sample 2 under isothermal conditions.

REFERENCES

[1] F.L. Riley “Silicon nitride and related materials,” *J. Am. Ceram. Soc.*, vol. 83, no. 2, pp. 245–265, 2004.
[2] Z. Gábrišová, P. Švec and A. Brusilová “Microstructure and selected properties of Si_3N_4 + SiC composite,” Manufact. Technol., vol. 20, no. 3, pp. 293–299, 2020.
[3] A.S. Lysenkov, K.A. Kim, Yu.F. Kargin, M.G. Frolova, D.D. Titov, S.N. Ivicheva, N.A. Ovsyannikov, A.A. Konovalov and S.N. Perevislov “Si_3N_4–TiN composites obtained by hot pressing of silicon nitride and titanium powders,” Inorg. Mater., vol. 56, pp. 309–320, 2020.
[4] O. G. Kryukova*a*, K. A. Bolgaru and A. N. Avramchik “Combustion of Ferrosilicon–Zircon Mixtures in Nitrogen Gas:Impact of Aluminum Additives,” Int. J. SHS, vol. 30, no. 4, pp. 236–240, 2021.

N1-P-010602

EFFECT OF THE ADDITION OF CARBON ON THE CALCIOTHERMIC REDUCTION OF ZrO_2 AND TiO_2 UNDER NITROGEN PRESSURE

B.SH. BRAVERMAN, A.N. AVRAMCHIK, O.G. KRYUKOVA, YU. M. MAKSIMOV

Tomsk Scientific Center of the SB RAS, Tomsk, Russia

The calciothermic reduction of metal oxides under nitrogen pressure is used to obtain refractory nitride powders, such as titanium and zirconium [1]. Carbonitrides of these metals are of interest for industrial applications and can be prepared by adding carbon to the TiO_2/ZrO_2 – Ca – N_2 system. The purpose of this work is to study the effect of carbon addition on the calciothermic reduction of ZrO_2 and TiO_2 under nitrogen pressure.

The important parameters of this process are the adiabatic temperature and the equilibrium composition of products. The TERRA software was used to calculate these parameters [2]. The objects of the study are systems TiO_2+X·C+N+Ca and ZrO_2+X·C+N+Ca where X is a dimensionless parameter expressing the ratio of the current and stoichiometric carbon content required for the synthesis of ZrC and TiC in the absence of nitrogen. The amount of calcium and N_2 pressure was also varied. Carbonitrides were identified by the possible formation of ZrC-ZrN and TiC-TiN solid solutions in the products. Figure 1 shows the calculated adiabatic combustion temperature of compositions as a function of the carbon content.

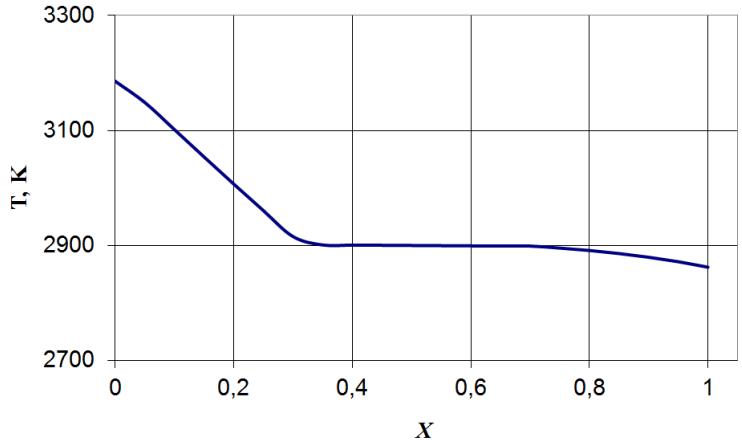

Fig.1. Adiabatic combustion temperature (T) of the TiO_2+X·C+N+Ca system as a function of carbon content (parameter X) at nitrogen pressure of 2 MPa and calcium excess of 10%.

Compositions without carbon have the maximum combustion temperature. The addition of carbon lowers the temperature. The plateau at T = 2900 K is due to the phase transition of CaO from liquid to solid state. Carbonitrides are formed in the products with any amount of carbon added. The formation of TiC and ZrC under equilibrium conditions is impossible. The resulting excess carbon interacts with excess calcium, forming CaC_2 carbide. Some carbon interacts with oxygen to produce CO. Increasing the pressure decreases the equilibrium CO content.

REFERENCES

1. Yu.M. Maksimov, A.N. Avramchik, B.Sh. Braverman, and A.M. Shulpekov, "Combustion of Thermite TiO_2/ZrO_2–Ca Mixtures in Nitrogen Gas", Int. J. Self-Prop. High-Temp. Synth., 2020, vol. 29, no. 1, pp. 31–35. https://doi.org/10.3103/S1061386220010069
2. B.G. Trusov, "Code System for Simulation of Phase and Chemical Equilibriums at Higher Temperatures", Engineering Journal: Science and Innovation, 2012, vol. 1, no. 1, pp. 240–249. DOI: 10.18698/2308-6033-2012-1-31 http://engjournal.ru/catalog/it/hidden/31.html http://engjournal.ru/articles/31/31.pdf

N1-P-010801

SYNTHESIS OF MANGANESE PIGMENTS BY THE SOLUTION COMBUSTION METHOD

O.V. LVOV, N.I. RADISHEVSKAYA, A.Yu. NAZAROVA, R.V. MININ

Tomsk Scientific Center of the SB RAS, Tomsk, Russia

Beige-brown cored pigments, the core of which is a mineral filler coated with solid solutions based on alumomagnesian and manganese spinels, were obtained by solution combustion synthesis (SCS). Solutions of magnesium, manganese, and aluminum nitrates were used as initial reagents, and the mineral marshalite (dusty quartz, a finely dispersed mineral filler) was used as a substrate. The quantitative composition of the starting components was determined from the pigment-to-marshalite ratio equal to 1:3.

Citrate-nitrate synthesis belongs to the solution combustion methods [1]. Active evolution of gases during combustion simplifies the formation of a finely dispersed product. Hydroxytricarboxylic acid citric acid $(NOOSSN)_2C(OH)SON$ was an energetic and gas-generating organic additive. The acidity of the solution was regulated with concentrated ammonia. White and beige-brown pigments were prepared by SCS using aluminomagnesian and manganese-containing spinels deposited on beige marshalite served as mineral. The use of mineral reduces the cost of the synthesized pigment considerably.

The final products were characterized by X-ray diffraction using the DRON-UM-1 diffractometer (filtered CuK_α-radiation) with an automated X-ray imaging system. Structural properties were studied using infrared spectroscopy in the 4000-400 cm^{-1} region (Nicolet 5700 FTIR spectrometer, KBr). The elemental composition of silicon and impurities present in marshalite was determined by atomic emission spectrometry using an ICAP 6300 Duo spectrometer (Thermo Scientific, UK). The microstructure of the samples was studied using a Philips SEM 515 scanning electron microscope.

Figure 1 shows the microphotographs of marshalite, white and chocolate pigments. As can be seen, the dispersion of pigments is determined by the size of marshalite particles covered by finely dispersed spinel particles.

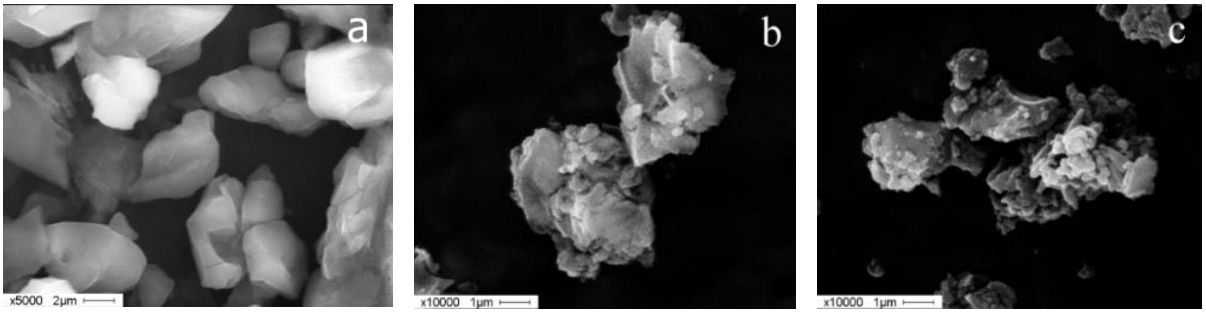

Fig. 1. Microphotographs of marshalite (a), white (b) and chocolate (c) pigments deposited on marshalite, (Philips SEM 515).

Thus, high-temperature spinel-based finely dispersed pigments deposited on marshalite and withstanding an annealing temperature of 1100°C were synthesized by the solution combustion method.

Acid synthesis, the absence of polynuclear complexes and ammonium salts leads to a less polymerized and viscous gel, which ensures its quasi-steady combustion.

The use of natural marshalite, as a substrate, reduces the cost of the pigments' production method.

This method is simple and easily scalable and can be used to produce multicomponent materials.

REFERENCES

[1] V.A. Zhuravlev, R.V. Minin., V.I. Itinb, I.Yu. Lilenko Structural parameters and magnetic properties of copper ferrite nanopowders obtained by the sol-gel combustion//Journal of Alloys and Compounds, 2017, №692.-C.705-712; doi: 10.1016/j.jallcom.2016.09.069.

N1-P-010901

NONISOTHERMIC SYNTHESIS OF TRIBOLOGICAL COMPOSITES BASED ON MAX PHASES AND ALMGB$_{14}$

O.K. LEPAKOVA, N.I. AFANAS'EV, R.V MININ

Tomsk Scientific Center of the SB RAS, Tomsk, Russia

Friction and wearing along with fatigue are the main causes of failure of mechanisms and parts. Development of new tribological materials with increased wear resistance at elevated temperatures, pressures and chemical environments is the urgent problem of materials science.

MAX phase composites have been actively studied as new antifriction materials, which due to their layered structure are considered to be promising tribological materials. The effect of addition of TiC, BN, and SiC to Ti_3SiC_2-based composites on tribological characteristics is investigated with the purpose of their use in high-temperature friction units and mechanical parts subjected to wear [1, 2]. Aluminum-magnesium boride $AlMgB_{14}$ is a chemical compound of aluminum, magnesium and boron characterized by high hardness (25-35 GPa), low density (2.66 g/cm^3), extremely low friction coefficient (0.04-0.05), and high plasticity index (H/E-0.14). High mechanical and, first of all, tribological characteristics open wide prospects for application as wear-resistant coatings, and also in the composition of composites.

The aim of this study was to obtain Ti3SiC_2-based composite with the addition of boride-aluminum-magnesium $AlMgB_{14}$ by SHS and study the effect of additives on the phase composition, microstructure and properties (primarily, tribological) of the synthesized composites.

In this work, composite materials were prepared by the SHS method using nanolaminate Ti-Si-C compounds with the addition of $AlMgB_{14}$, which expand the application field of antifriction materials due to their high resistance to chemical decomposition at elevated temperatures. Methods of obtaining ultradispersed superhard powders were developed. Physical and chemical mechanisms and control methods of SHS processes were established. The factors influencing the structure were investigated and the thermal resistance and physical and mechanical properties of synthesized materials were determined.

REFERENCES

[1] Yang, W. Gu, L. Pan, K. Song, X. Chen, T. Qiu, «Friction and Wear Properties of in situ (TiB_2 +TiC)/Ti_3SiC_2 Composites», Wear, vol.271, pp. 2940-2946, 2011.

[2] X.Shi, M.Wang, Z. Hu, W.Zhai, Q. Zhang, «Tribological Behavior of Ti_3SiC_2/(WC-10Co) Composites Prepared by Spark Plasma Sintering», Mater. Des., vol.45, pp. 179-189, 2013.

N1-P-015602

TEMPERATURE-INDUCED STRUCTURAL CHANGES IN PVD ZR-MO-SI-B FILMS: IN-SITU HRTEM INVESTIGATION *

PH.V. KIRYUKHANTSEV-KORNEEV[1], A.D. SYTCHENKO[1], P.A. LOGINOV[1], A.S. OREKHOV[2], E.A. LEVASHOV[1]

1- National University of Science and Technology "MISIS", Moscow, Russia
2- Federal Scientific Research Centre "Crystallography and Photonics", Russian Academy of Sciences, Moscow, Russia

Currently, much attention is being paid to the development of ZrB_2-based coatings for high-temperature applications. ZrB_2 coatings are rapidly oxidized at T >1100 ° C, therefore, to increase the oxidation resistance as well as strength and durability of ZrB_2, SiC, $TaSi_2$, $MoSi_2$, etc. are alloyed. A comparative study of alloyed coatings has shown that the addition of $MoSi_2$ increases the oxidation resistance of coatings by ~3 times compared with SiC and $TaSi_2$ additives. This work is devoted to a comprehensive study of Zr-Mo-Si-B coatings, including in-situ transmission electron microscopy (TEM) studies of the structure during heating up to 1000°C.

The coatings were deposited by magnetron sputtering in an Ar medium using ZrB_2-$MoSi_2$-MoB ceramic SHS target. The lamellae for TEM were manufactured by ion beam etching using FIB and PIPS II systems. In situ TEM studies of structural-phase transformations were carried out during step heating of lamellae in JEM-2100 microscope. The data obtained were analyzed in comparison with the results of the investigation of the coatings in the as-deposited state and after vacuum annealing at 200-1000°C. The comprehensive study also included the determination of the structure, phase composition, roughness, morphology of coatings by XPS, XRD, FTIR, SEM, and GDOES methods and mechanical properties by nanoindentation.

The results of the TEM show that the column structure of Zr-Mo-Si-B coatings was preserved up to 1000°C. Each columnar grain consisted of equiaxial subgrains. With an increase in temperature, subgrain growth occurred inside the columnar elements. It is important to note that the electronograms recorded at different temperatures are identical and indicate the presence of the h-ZrB_2 phase. The formation of additional crystalline phases was not detected. At the same time, it was revealed that heating led to a decrease in the interplane distance, probably due to the fact that the molybdenum and silicon atoms, leaving the h-ZrB_2 lattice, formed an amorphous $MoSi_x$ phase. Such a change in the composition of the main phase affects strongly on mechanical properties of the coating. At room temperature, the hardness was 39 GPa. Heating up to 200C and 400°C led to a drop in hardness, which can be associated with relaxation of internal stresses during heating. Hardness increased in the temperature diapason of 400-800°C. With and reaching a maximum of 38 GPa, apparently, occurred as a result of the redistribution of molybdenum and silicon atoms between the crystalline phase based on ZrB_2 and the amorphous phase. A further decrease in hardness in the 800-1000 °C area is probably due to an increase in grain size. It was also found that the developed coatings have high thermal stability of the structure and oxidation resistance at temperatures >1200°C.

REFERENCES

[1] Ph.V. Kiryukhantsev-Korneev et al. **Materials** 2021, 14, 1932
[2] Ph.V. Kiryukhantsev-Korneev et al. **Metals** 2021, 11, 1194

* This work was carried out with financial support from the Ministry of Science and Higher Education of the Russian Federation under the State Assignment (Project No. 0718-2020-0034).

N1-P-021004

MICROHARDNESS OF A DEFORMED COPPER SAMPLE WHEN IMPACTED ON A RIGID WALL

N.V. PAKHNUTOVA[1,2], *E.N. BOYANGIN*[1], *O.A. SHKODA*[1], *S.A. ZELEPUGIN*[1,2]

[1]*Tomsk Scientific Center of the Siberian Branch of the Russian Academy of Sciences, Tomsk, Russia*
[2]*National Research Tomsk State University, Tomsk, Russia*

One of the widely used method for evaluating the dynamic characteristics of metals and alloys is the Taylor impact test. This method relates the dynamic yield strength of a cylindrical sample material to its residual length after impact on a non-deformable target. Taylor impact test is commonly used to determine the yield strength [1-3] and select constitutive relations and constants in numerical simulations [2-4].

This paper presents the Taylor impact test conducted using a one-stage light-gas gun [5]. A copper cylinder (M1) with a length of 32 mm and a diameter of 7.8 mm was used as a sample. The mass of the sample was about 15 g. Throwing conditions were chosen to ensure that the velocity of the sample exiting the barrel ranged from 150 to 450 m/s. Samples after testing were cut into two parts along the axis of symmetry using a DK7732 CNC EDM Wire Cutting Machine. Microhardness of samples was determined on a PTM-3 hardness tester (GOST 9650-76) with a measurements error of 2%.

Figure 1 shows the microhardness measurements along the symmetry axis of a copper sample at different impact velocities.

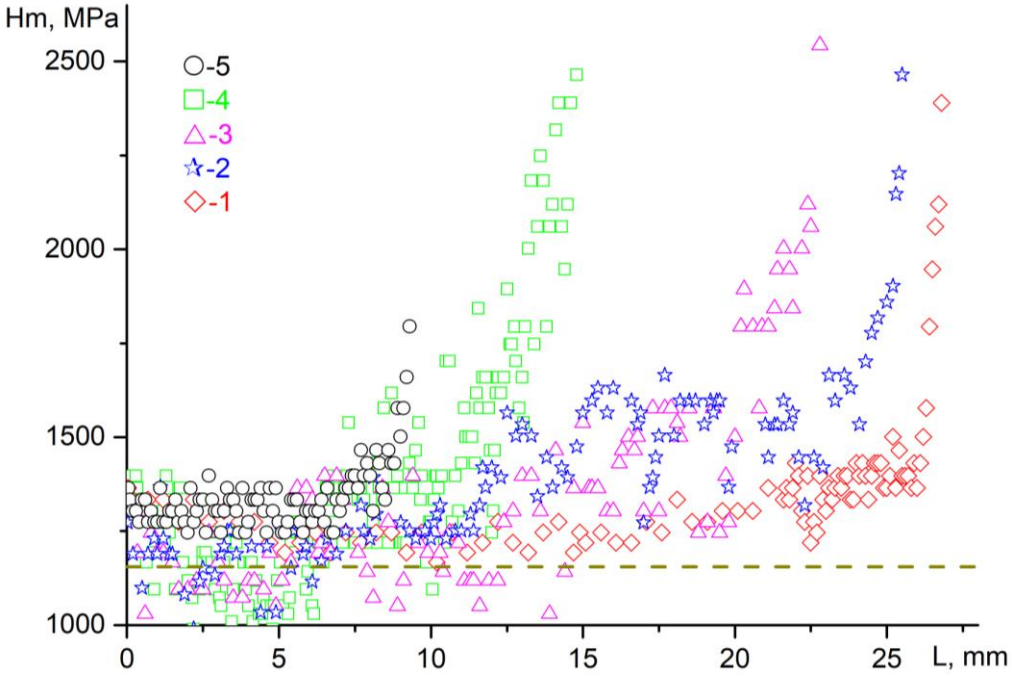

Fig.1. Distribution of microhardness along the axis of the samples at different impact velocities: (1) 162 m/s, (2) 167 m/s, (3) 225 m/s, (4) 316 m/s, (5) 416 m/s.

Non-linear changes in microhardness are observed along the sample axis after impact on the non-deformable target. For the starting sample, the average value of microhardness is 1155 MPa (Fig. 1, dashed line). The results in Fig. 1 show the higher microhardness at most points in the deformed state compared with the initial state.

REFERENCES

[1] A.N. Bogomolov, V.A. Gorel'skii, S.A. Zelepugin, I.E. Khorev “Behavior of bodies of revolution in dynamic contact with a rigid wall”, Journal of Applied Mechanics and Technical Physics, vol. 27, Issue 1, pp. 149-152, 1986. DOI: 10.1007/BF00911139.

[2] E. Włodarczyk, M. Sarzynski “Strain energy method for determining dynamic yield stress in Taylor’s test”, Engineering Transactions, vol. 65(3), p. 499–511, 2017.

[3] Y.V. Bayandin, D.A. Bilalov, S.V. Uvarov “Verification of wide-range constitutive relations for elastic-viscoplastic materials using taylor-hopkinson test”, Computational Continuum Mechanics, vol. 13(4), p. 449–458, 2021. DOI: 10.7242/1999-6691/2020.13.4.35.

[4] D.V. Yanov, A.S. Bodrov, N.V. Pakhnutova, S.A. Zelepugin “Simulation of dynamic channel-angular pressing of copper samples with allowance for experimental data of loading”, Vestnik Tomskogo gosudarstvennogo universiteta. Matematika i mekhanika [Tomsk State University Journal of Mathematics and Mechanics], vol. 60. pp. 141−151, 2019. DOI: 10.17223/19988621/60/11.

[5] Y.F. Khristenko, S.A. Zelepugin, A.V. Gerasimov “New light-gas guns for the high-velocity throwing of mechanical particles”, ARPN Journal of Engineering and Applied Sciences, vol. 12, no. 22. P, 2017. 6606-6610.

N1-P-024602

MORPHOLOGY OF CORUNDUM MICROSPHERES PRODUCED BY THE PLASMA METHOD*

V.V. SHEKHOVTSOV, R.E. GAFAROV, N.K. SKRIPNIKOVA, A.B. ULMASOV, O.A. KUNTS

Tomsk State University of Architecture and Building, TSUAB, Tomsk, Russia

Today, the relevance of corundum microspheres is due to their high-performance characteristics (high strength, melting point, wear resistance, etc.). The combination of these characteristics increases the demand in the industrial market. Thus, the search for new technological solutions for the efficient production of corundum microspheres from natural materials is topical. The high melting point of corundum (2345 K) imposes a number of restrictions on the use of classical heating sources. The most efficient and structurally simple are direct current electric arc plasmatron, which make it possible to realize a plasma flow with an average mass temperature of ≥ 5000 K [1–4].

This paper presents the results of experimental studies of obtaining corundum microspheres based on boehmite γ–AlO(OH) in a thermal plasma medium. It is expedient to evaluate the effectiveness of plasma exposure by the spheroidization of particles and the formation of a non-porous shell [5]. On Fig. 1 shows electronic images of three types of formed shells of corundum microspheres during plasma treatment.

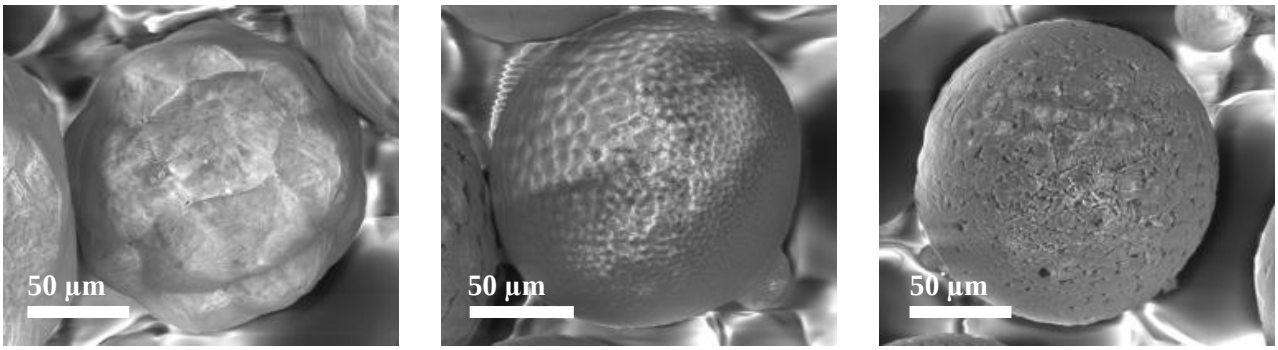

a *b* *c*

Fig.1. Surface morphology of microspheres based on boehmite.

The first type (Fig. 1, *a*) of the particle surface structure is characterized by the presence of acute-angled craters. Some craters are interconnected, the size of the craters is in the range of 2÷5 µm. The second type (Fig. 1, *b*) of the surface structure includes prismatic particles fused together with rounded corners 5–10 µm in size. The third view (Fig. 1, *c*) of the particle surface is presented as separate hilly layers. The different type of surface structure of particles obtained in a plasma flow is associated with the peculiarities of the preparation of agglomerated powders based on boehmite and is difficult to control during thermal treatment. According to the results of EDX spectrometry, no change in the elemental composition depending on the morphology of the obtained microspheres was found. The obtained energy spectra indicate that the composition contains a high content of aluminum (Al) – 67.42 wt. %. The content of oxygen (O) is fixed at around 29.66 wt. %. There are traces of silicon (Si) with a concentration of 2.92 wt. %.

REFERENCES

[1] V.A. Vlasov, V.V. Shekhovtsov, O.G. Volokitin, G.G. Volokitin, N.K. Skripnikova, A.A. Klopotov, "Physical processes of sio2 spherical particle formation in thermal plasma flow," Russian Physics Journal, vol. 61, no. 4, pp. 708–714, 2018.

[2] I.P. Gulyaev, O.P. Solonenko, "Simulation of the behavior of hollow ZrO2 particles in a plasma jet, taking into account their thermal expansion," Thermophysics and Aeromechanics, vol. 20, no. 6, pp. 789–802, 2013.

[3] Y.A. Abzaev, G.G. Volokitin, N.K. Skripnikova, O.G. Volokitin, V.V. Shekhovtsov, "Investigation of the melting of quartz sand by low–temperature plasma," Glass and Ceramics, vol. 72, no. 5–6, pp. 225–227, 2015.

[4] O.G. Volokitin, V.V. Shekhovtsov, "Prospects of application of low-temperature plasma in construction and architecture," Glass Physics and Chemistry, vol. 44, no. 3, pp. 251–253, 2018.

[5] E. Pfender, Y.C. Lee, "Particle dynamics and particle heat and mass transfer in thermal plasmas. Part I. The motion of a single particle without thermal effects," Plasma Chemistry. Plasma Processing. vol. 5, no. 3, pp. 211–237, 1985.

* The work was carried out with the support of the state task of the Ministry of Science and Higher Education of the Russian Federation FEMN–2020–0004 and grant President of the Russian Federation MK–66.2022.4.

N1-P-025205

COMPUTER SIMULATION OF THERMAL FIELDS OF THE MO-ZR SYSTEM FOR COATING FORMATION USING A LOW-ENERGY HIGH-CURRENT ELECTRON BEAM*

A.V. SOLOVYOV, A.B. MARKOV, E.A. PESTEREV, E.V. YAKOVLEV, V.I. PETROV

Tomsk Scientific Center of the Siberian Branch of the Russian Academy of Sciences, Tomsk, Russian Federation

Currently an important task is to achieve a more accident tolerant fuel (ATF) cladding that by virtue of its higher oxidation resistance would allow for increased coping times under a loss of coolant accident (LOCA) scenario [1]. One of the many ways to create ATF is to apply chromium-containing coatings using a low-energy high-current electron beam [2, 3]. Molybdenum is used as a barrier layer between zirconium and chrome-containing coatings [4]. For example, the FeCrAl alloy provides excellent oxidation resistance, but Fe forms eutectics with Zr at temperatures up to 1201 K, which leads to mutual diffusion and associated melting. Molybdenum is used as an interlayer coating due to its high melting point (2893 °C), low diffusion rate of Cr, Fe and Zr into Mo, and high eutectic points with Fe and Zr [5-8].

The report presents the results of computer calculations of the thermal fields of the Mo-Zr system for the formation of protective coatings. Melting thresholds for pure metals were calculated: Mo - 7.02 J/cm^2, Zr - 1.83 J/cm^2. The dependences of melting thresholds for the Mo-Zr system as a function of film thickness were calculated. For film thicknesses from 0.1 to 8 μm, the film melting threshold is higher than the substrate melting threshold. In this case, the Zr substrate melts first, followed by the Mo film. For film thicknesses above 8 μm, the film melting threshold is below the substrate melting threshold. In this case, the Mo film begins to melt first, then the Zr substrate. The threshold of Mo melting with increasing film thickness increases from 2.9 J/cm^2 (Mo film thickness is 0.1 μm) to 7.02 J/cm^2 according to the law close to the polynomial of the second degree. The Zr substrate melting threshold increases from 1.83 J/cm^2 (Mo film thickness is 0.1 μm) to infinity according to the law also close to the polynomial of the second degree. The dependences of the melt thickness on the NSEP energy density for the systems Mo(0.1)/Zr, Mo(0.25)/Zr, Mo(0.5)/Zr, Mo(1.0)/Zr are calculated. The dependences of the lifetime of the film and substrate melts on the NSEP energy density for the systems Mo(0.1)/Zr, Mo(0.25)/Zr, Mo(0.5)/Zr, Mo(1.0)/Zr are calculated. The optimum conditions for the synthesis of the surface Mo-Zr alloy have been determined.

REFERENCES

[1] B.A. Pint, K.A. Terrani, M.P. Brady, T. Cheng, J.R. “Keiser High temperature oxidation of fuel cladding candidate materials in steam–hydrogen environments,” J. Nucl. Mater., vol. 440, pp. 420-427, 2013.

[2] Markov A.B., Yakovlev E.V., Solovyov A.V., Pesterev E.A., Petrov V.I., Slobodyan M.S. “Formation of a Cr-Zr surface alloy using a low-energy high-current electron beam,” J. Phys. Conf. Ser., vol. 2064, 2021.

[3] Markov A.B., Solovyov A.V., Yakovlev E.V., Pesterev E.A., Petrov V.I., Slobodyan M.S. “Computer simulation of temperature fields in the Cr (film)-Zr (substrate) system during pulsed electron-beam irradiation,” J. Phys. Conf. Ser., vol. 2064, 2021.

[4] Yeom H., Maier B., Johnson G., Dabney T., Walters J., Sridharan K. “Development of cold spray process for oxidation-resistant FeCrAl and Mo diffusion barrier coatings on optimized ZIRLO,: Journal of Nuclear Materials,. vol. 507, pp. 306-315, 2018.

[5] J. Houserová, J. Vřešťál, M. Šob “Phase diagram calculations in the Co-Mo and Fe-Mo systems using first-principles results for the sigma phase,” Calphad Comput. Coupling Phase Diagrams Thermochem., vol. 29, pp. 133-139, 2005.

[6] M. Zinkevich, N. Mattern “Thermodynamic assessment of the Mo-Zr system,” J. Phase Equil., vol. 23, pp. 156-162, 2002.

[7] B. Cheng, Y.-J. Kim, P. Chou “Improving accident tolerance of nuclear fuel with coated Mo-alloy cladding,” Nucl. Eng. Technol, vol. 48, pp. 16-25, 2015.

[8] G. Neumann, C. Tuijn, Self-diffusion and Impurity Diffusion in Pure Metals: Handbook of Experimental Data. Elsevier, 2011.

* The work was supported by the Ministry of Science and Higher Education of the Russian Federation (project № FWRF-2021-0001).

N1-P-027501

ARC PLASMA SYNTHESIS OF IV-V GROUPS TRANSITION METALS HIGH-ENTROPY CARBIDES CUBIC PHASES[*]

A.A. GUMOVSKAYA, A.YA. PAK, ZH.S. BOLATOVA, P.V. POVALYAEV, R.D. GERASIMOV

National Research Tomsk Polytechnic University, Tomsk, Russian Federation

Carbides of transition metals of groups IV-V of the periodic table are usually superhard refractory compounds [1]. In the last 5–7 years, reports have appeared on the possibility of synthesizing single-phase multicomponent carbides containing 4–5 metals and carbon, and the proportion of each metal should be 5 – 35 % (atomic) [2]. Such materials are solid solutions with a cubic NaCl-type lattice and a high degree of configurational entropy; therefore, these crystalline phases are called “high-entropy” carbides (HEC) [3]. Many different combinations of the chemical composition of HEC (combinations of 4-5 elements from known transition metals, in particular, IV-V groups) give a hope for new results in the field of creating ultrahigh temperature ceramics materials. A number of HECs have already been synthesized; many of crystalline HEC phases have been theoretically predicted [4].

HEC synthesis requires high temperatures as well as high energy density. The most common approach to the synthesis of HEC is spark plasma sintering. The issue of developing simple and low-cost methods for obtaining HEC for rapid testing of hypotheses about the possibility of obtaining one or another hypothetical HEC phase is topical. The method of electric arc melting looks promising due to the possibility of achieving high temperatures high heating rates [5-6].

Our group had achieved some success in the field of synthesis of one of the most studied HEC phases TiZrNbHfTaC5 using the original plasma arc reactor [7-8]. In a series of experiments, the synthesis of a number of HECs was carried out using metal powders as raw material, as well as ultrafine carbon. The starting raw materials were mixed in a ball mill and processed by electric arc plasma in the volume of a hollow graphite cathode. In all cases, a cubic lattice of the NaCl-type is formed, which is confirmed by the results of X-ray diffractometry. The lattice parameters estimated from the XRD data are close to the known data on the HEC structure.

According to the scanning electron microscopy data and transmission electron microscopy, mapping of the chemical composition, it was found that in a number of experiments it is possible to achieve a uniform distribution of the chemical composition. This proves the possibility of obtaining HEC by the developed electric arc method. The disadvantage of the method used at the current research stage is the contamination of the synthesis product with anode erosion material (graphite). Further work will be aimed at increasing the concentration of the desired HEC phases, proving the possibility of obtaining HEC of various compositions by the claimed method, and studying the properties of the synthesized HEC.

REFERENCES

[1] E. Castle, T. Csanádi, S. Grasso, J. Dusza, M. Reece, Processing and Properties of High-Entropy Ultra-High Temperature Carbides, Nature, Scientific reports. vol.8, Article Number 8609, 2018.

[2] T. J. Harrington, Phase stability and mechanical properties of novel high entropy transition metal carbides, Acta Materialia. vol.166, p.271-280, 2019.

[3] E. Chicardi, Low temperature synthesis of an equiatomic $(TiZrHfVNb)C_5$ high entropy carbide by a mechanically-induced carbon diffusion route, Ceramics International. vol.45, p.21858–21863, 2019.

[4] K. Kaufmann, Discovery of high-entropy ceramics via machine learning, Nature, Computational materials. vol.6, Article Number 42, 2020.

[5] Z. Zhang, Arc melting: a novel method to prepare homogeneous solid solutions of transition metal carbides (Zr, Ta, Hf), Ceramics International. vol.45, p. 9316-9319, 2019.

[6] W. H. Kan, Precipitation of (Ti, Zr, Nb, Ta, Hf)C high entropy carbides in a steel matrix, Matrialia. vol.9, Article Number 100540, 2020.

[7] A.Ya. Pak, P.S. Grinchuk, A.A. Gumovskaya, Yu.Z. Vassilyeva, Synthesis of transition metal carbides and high-entropy carbide TiZrNbHfTaC5 in self-shielding DC arc discharge plasma, Ceramics International. vol.48, p. 3818-3825, 2022.

[8] A.Ya. Pak, G.Y. Mamontov, P.S. Grinchuk, Sposob polucheniya poroshka, soderzhashego odnofazniy vysokoentropiyniy karbid sostava Ti-Nb-Zr-Hf-Ta-C s cubicheskoy reshetkoy (Method for obtaining powder containing single-phase high-entropy carbide of composition Ti-Nb-Zr-Hf-Ta-C with a cubic lattice). RU 2746673 C1, 19.04.2021

[*] The research was funded by the Russian Science Foundation project [grant number 21-79-10030].

N1-P-032301

COMPOSITE STRUCTURES BASED ON POLYMERS, WITH THE ADDITION OF NANOMATERIALS

M.N. KOLCHEVSKAY[1], *F.F. KOMAROV*[1]

[1]*A.N.Sevchenko Institute of Applied Physical Problems of Belarusian State University, Minsk, Belarus*

To ensure the safe operation of electronic and optoelectronic systems, as well as optical devices under conditions of natural and artificial electromagnetic radiation (EMR), to eliminate electromagnetic interference, to ensure the electromagnetic compatibility of individual components of high-frequency equipment, composite materials based on polymer compositions with carbon nanotubes, graphene and other carbon nanomaterials. In these radio absorbing materials, in particular, multilayer broadband microwave absorbers based on composite materials, the principle of converting electromagnetic energy into heat is used. These materials should provide the necessary degree of attenuation of the EMR reflectivity of the near and far fields for various objects with different angles of incidence and polarization.

Products made of composites based on polymers filled with carbon nanomaterials have aroused great interest in recent years also as antireflection systems in the UV, visible, and IR ranges of the spectrum. The area of their application covers a wide range of products from spacecraft objects (solar cells, optoelectronic and optical systems), military equipment to household appliances. Thus, the topic of the work is relevant and timely.

Work has been carried out to create composites for the above purposes based on such polymers as polyurethane, epoxy resin and elastomer - Dimethylpolysiloxane compound "Silagery 8030" (Russia). Various types of multilayer carbon nanotubes and graphene produced by OOO NanoTechcenter (Tambov), as well as finely dispersed particles of metals and their oxides, were used as additives.

The experimental base of the laboratory of A.N. Sevchenko Institute of Applied Physical Problems of Belarusian State University provided a full scope of technological work, as well as studies of the composition, structure of composites, electrical and optical properties in a wide temperature and frequency ranges.

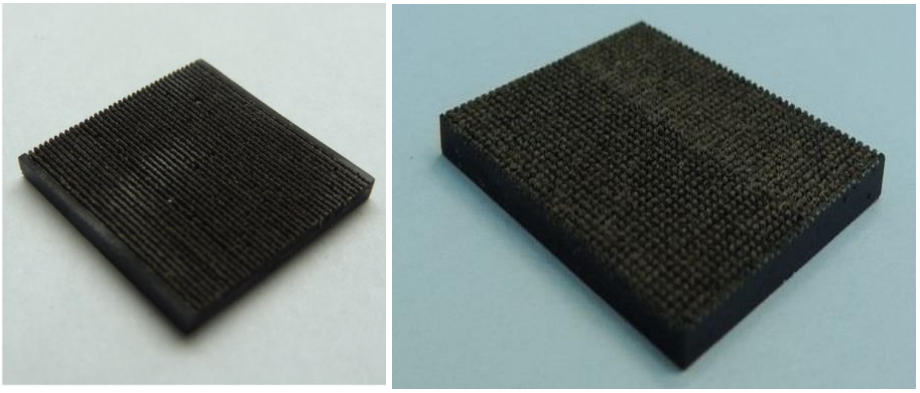

Fig.1. Samples of anti-reflection coatings with laser surface treatment.

The effect of composite's surface in the visual and near IR regions modification by to pulse laser treatment on light reflectivity has been studied. The possibility of creating innovative non-reflective surfaces of the composite samples in the visual and near-IR ranges is demonstrated.

REFERENCES

[1] J. Zhu, X. Yang, Z. Fu, C. Wang, W. Wu, L. Zhang. Facile fabrication of ultra-low density, high-surface-area, broadband antireflective carbon aerogels as ultra-black materials. J. Porous Mater, 2016, vol. 23, no. 5, pp. 1217 – 1225.

[2] Y. Lin, J. He. Recent progress in antireflection and self-cleaning technology – From surface engineering to functional surfaces. Progress in Materials Science, 2014, vol. 61, pp. 94 – 143.

[3] K. Amemiya, H. Koshikawa, T. Yamaki, Y. Maekawa, H. Shitomi, T. Numata, K. Kinoshita, M. Tanabe, D. Fukuda. Fabrication of hard-coated optical absorbers with microstructured surfaces using etched ion tracks: Toward broadband ultra-low reflectance. Nuclear Instruments and Methods in Physics Research B, 2015, vol. 356, pp. 154 – 159.

[4] S. Chuang, H. Chen, J. Shieh, C. Lin, C. Cheng, H. Liu, C. Yu. Nanoscale of biomimetic moth-eye structures exhibiting inverse polarization phenomena at the Brewster angle. Nanoscale, 2010, vol. 2, pp. 799 – 805.

[5] Y. Sun, J. Evans, F. Ding, N. Liu, Y. Zhang, S. He. Bendable, ultra-black absorber based on a graphite nanocone nanowire composite structure. Optics Express, 2015, vol. 23, no. 15, pp. 20115 – 20123.

N1-P-037501

EXTREME EFFECTS IN MAGNETIC FIELD LOCALIZATION AT DIELECTRIC MESOSCALE PARTICLES

I.V. MININ[1], *O.V.MININ*[1]

[1]*Tomsk Polytechnic University, Tomsk, Russia*

In optics, the weakly dissipating dielectric spheres permit to realize high-order Fano resonances associated with internal Mie modes [1,2] and the field structure has no WGM structure. These resonances for specific values of the Mie size parameter of dielectric sphere yield field-intensity enhancement factors about 10^4–10^9, at a unique arrangement of hotspots at the poles of the sphere, which can be directly obtained from analytical calculations based on Mie theory. These "super-resonances" (SR) [3] provide magnetic hot spot with giant magnetic fields, which is attractive for many applications [4-6]. This provides a new physical phenomenon to obtain extreme field localization with giant field enhancement, which is comparable to that for plasmonics. The disadvantages of high magnetic fields generation by SR's are strong sensitivity to the losses in the mesoscale particle material and Mie size parameter. Note that such a magnetic field is comparable with magnetic cumulative generators. For SR condition, the local ratio of wave vectors in singular points near the outer surface of a particle can reach $K_0/K_l \sim 10^2$, where K_0 is a wave-vector of incident wave [2]. So the giant magnetic fields can be created inside the dielectric particle due to creating subwavelength optical vortices with large phase gradients in the vicinity of singularities [2]. The new effect of a decrease in the size of the field localization (hotspots) down to less than the diffraction limit was found when small losses are introduced into the sphere material, which can be even less than in the ideal case of the particle material without losses [5].

Moreover, while spherical mesoscale dielectric particle shapes have only 2 degrees of freedom (Mie size parameter q and refractive index of the particle material), sphere with broken symmetry [7], composed of 2 different dielectrics, provide additional degrees of flexibility in electromagnetic response tuning to generate strong magnetic hot spots.

Our investigations shown that in the structures under consideration it is necessary to take into account the change in the refractive index of the environment (air), the structure of the material of the particle (different local density) and the value of the "roughness" of its surface.

REFERENCES

[1] Z. Wang, B. Luk'yanchuk, R. Paniagua-Dominguez, B. Yan, J. Monks, O. V. Minin, I. V. Minin, S. Huang, A. Fedyanin, **"**High Order Fano-Resonances and Extreme Effects in Field Localization," Proc. 9th Week of the young researcher, Quantum Sci.: Light-matter Interaction, Moscow, p.27, 2019.

[2] O.V.Minin and I.V.Minin, "Optical phenomena in mesoscale dielectric particles," Photonics, vol.8, no.12, 591, 2021.

[3] T. Hoang, Y. Duan, X. Chen, and G. Barbastathis, "Focusing and imaging in microsphere-based microscopy," Opt. Express, vol.23, no.9, 12337, 2015.

[4] Z. Wan, B. Luk'yanchuk, L. Yue, B. Yan, J. Monks, R. Dhama, O.V. Minin, I.V. Minin, S. Huang, A. Fedyanin, "High order Fano resonances and giant magnetic fields in dielectric microspheres," Sci. Rep. vol.9. 20293, 2019.

[5] L. Yue, Z. Wan, B. Yan, J. Monks, Y. Joya, R. Dhama, O.V. Minin, I.V. Minin, "Super-Enhancement Focusing of Teflon Spheres," Ann. Phys. vol. 532, 2000373, 2020.

[6] L. Yue, B. Yan, J. Monks, R. Dhama, C. Jiang, O.V. Minin, I.V. Minin, Z. Wan, "Full three-dimensional Poynting vector flow analysis of great field-intensity enhancement in specifically sized spherical-particles," Sci. Rep. vol.9, 20224, 2019.

[7] I.V. Minin, O.V. Minin, Y. Cao, B. Yan, Z. Wan, B. Luk'yanchuk, "Photonic lenses with whispering gallery waves at Janus particles," Opto-Electron Sci, vol.1, 210008, 2022.

N1-P-037601

SYNTHESIS OF MO-ZR SURFACE ALLOY BY USING A LOW-ENERGY HIGH-CURRENT ELECTRON BEAM *

E.V. YAKOVLEV, A.V. SOLOVYOV, V.I. PETROV, A.E. PESTEREV, A.B. MARKOV

Tomsk Scientific Center of the Siberian Branch of the Russian Academy of Sciences, Tomsk, Russian Federation

Zirconium-based alloys have served the nuclear industry for several decades due to their unique set of properties [1]. During normal operation, zirconium alloys form a protective layer of zirconium oxide that protects against corrosion. However, at high temperatures, which can occur under accident conditions, zirconium alloys exhibit poor oxidation kinetics [2, 3]. The developing concept of accident tolerant fuel (ATF) defines a several areas of research and development aimed at improving the safety of nuclear fuel during normal operation, transients and possible accident [3-5]. One of the areas of ATF is the development of protective coatings on the surface of zirconium [4, 5]. Coatings based on chromium are the most promising, since they meet the basic requirements for ATF coating materials for Zr fuel cladding. Chromium has a high melting point, high corrosion resistance in water and steam due to protective chromium scale, and a coefficient of thermal expansion similar to zirconium alloys [4, 5]. However, interdiffusion at the interface between the protective coating and the substrate is a serious problem. In addition, interdiffusion can degrade the adhesive properties of the coating, leading to the destruction or bulging of the coating. The easiest way to limit diffusion between the Cr coating and the Zr substrate is to add a diffusion barrier between the coating and the Zr substrate. Molybdenum is considered one of the most promising interlayer materials, as it exhibits good barrier properties, CTE close to Cr, high thermal conductivity, high melting point, and acceptable neutron cross section. Moreover, the potential eutectic phase Mo-Zr has a higher melting point (1550°C) compared to Cr-Zr (1330°C) [6, 7].

The aim of present work was to synthesize of Mo-Zr surface alloy using magnetron deposition of Mo films and consequent irradiation with a low-energy, high-current electron beam (LEHCEB).

The electron-beam machine “RITM-SP” with an explosive-emission cathode and a plasma-filled diode generating the LEHCEB was employed in the work [8]. This machine is equipped with a magnetron sputtering system enabling formation of multicomponent surface alloys. The surface alloy was formed by repeating the operations of deposition of the Mo film on the Zr substrate and following LEHCEB irradiation. The surface alloy was formed at different NEEP energy densities, which resulted in different melt thicknesses and, consequently, different elemental and structural-phase compositions of the surface layer.

The surface morphology, phase and elemental composition of the Mo-Zr surface alloys were analyzed, the microhardness and wear resistance were measured. For its characterization different techniques like SEM, XRD and others have been used. The elemental composition of both the surface and cross sections of the samples was analyzed by EDS analysis. The structure and properties of the synthesized Mo-Zr surface alloy was compared with witness-specimens, which is coatings but without LEHCEB treatment.

REFERENCES

[1] V. Azhazha, B. Borts, I. Butenko, V. Voevodin et al., Zirconium-Niobium alloys for NPP, Alushta, Ukraine, 2012.

[2] J.C. Brachet, E. Rouesne, J. Ribis et. al., "High temperature steam oxidation of chromium-coated zirconium-based alloys: Kinetics and process," Corros. Sci., vol. 167, Article Number 108537, 2020.

[3] K.A. Terrani, S.J. Zinkle, L.L. Snead, "Advanced oxidation-resistant iron-based alloys for LWR fuel cladding," J. Nucl. Mater. vol. 448, pp. 420–435, 2014.

[4] E. Kashkarov, B. Afornu, D. Sidelev et. al., "Recent advances in protective coatings for accident tolerant Zr-based fuel claddings," Coatings, vol. 11, Article Number 557, 2021.

[5] J.Yang, M. Steinbrück, C. Tang et. al., "Review on chromium coated zirconium alloy accident tolerant fuel cladding," J. Alloys and Comp., vol. 895, Article Number 162450, 2022.

[6] J. Houserová, J. Vřešťál, M. Šob "Phase diagram calculations in the Co-Mo and Fe-Mo systems using first-principles results for the sigma phase," Calphad Comput. Coupling Phase Diagrams Thermochem., vol. 29, pp. 133-139, 2005.

[7] B. Cheng, Y.-J. Kim, P. Chou "Improving accident tolerance of nuclear fuel with coated Mo-alloy cladding," Nucl. Eng. Technol, vol. 48, pp. 16-25, 2015.

[8] A.B Markov, A.V. Mikov, G.E. Ozu, A.G. Padei, Instrum. and Experim. Tech., vol. 54, pp. 862-866, 2011.

* The work was supported by the Ministry of Science and Higher Education of the Russian Federation (project № FWRF-2021-0001).

N1-P-037602

HEAT RESISTANCE OF ZIRCONIUM-CROMIUM SURFACE ALLOYS*

V.I. PETROV, A.B. MARKOV, A.V. SOLOVYOV, E.A. PESTEREV, E.V. YAKOVLEV

Tomsk Scientific Center of the Siberian Branch of the Russian Academy of Sciences, Tomsk, Russian Federation

The state of affairs in the field of technology for the production of zirconium and its alloys is studied in a row of monographs, books and reviews, starting from the second half of the 20th century, for example [1, 2]. The methods of their production, properties, advantages and disadvantages, and the impact on properties of certain alloying elements are described in this works. One of the main alloying elements for zirconium alloys is chromium (Cr).

This paper presents the results of testing the heat resistance of Cr-Zr surface alloys. Cr-Zr surface alloys are formed by deposition of Cr films onto Zr substrates, followed by pulsed melting with a low-energy high-current electron beam. A comparison is made with the heat resistance of a Cr magnetron coating on a Zr substrate.

The tests were carried out in a muffle furnace in an air atmosphere at a temperature of 953÷973 K. The heat resistance was evaluated by the weight gain of the samples, weighing was carried out after 1-3 hours. The duration of the tests was 10 hours.

The effect of treatment with a low-energy high-current electron beam on the heat resistance of zirconium was not revealed in the work.

It is shown in the work that in order to increase the heat resistance of Zr, it is necessary to form protective layers of pure chromium with a thickness of more than 2 μm.

REFERENCES

[1] B. Lustman, F. Kerze, The metallurgy of zirconium, New York, McGraw-Hill, 1955.

[2] Azevedo C.R.F. “Selection of fuel cladding material for nuclear fission reactors. Review”, Engineering Failure Analysis, vol.18, p.1943–1962, 2011

* The work was supported by the Ministry of Science and Higher Education of the Russian Federation (project № FWRF-2021-0001).

N1-P-040001

STRUCTURE FORMATION IN POWDER MATERIALS OF THE TI-AL-O SYSTEM UNDER REACTION SINTERING CONDITIONS*

ELENA N. KOROSTELEVA[1,2], IVAN O. NIKOLAEV[1]

[1] Institute Strength Physics and Materials Science SB RAS, Tomsk, Russia
[2]Tomsk Polytechnic University, Tomsk, Russia
rmkast97@gmail.com

Titanium-based composite powder materials are of great interest due to the unique properties resulting from the synergistic effect of combining the properties of structural elements. Despite a large number of studies in this area, the question of the influence of some complex components on the structural-phase composition and physical and mechanical characteristics of a titanium-based powder composite remains open. These components include oxides of both titanium itself and other metals (Al_2O_3, Fe_2O_3), with which titanium interacts well. In particular, the Al_2O_3 compound has temperature coefficients of linear expansion (TCLE) similar to titanium, which solves the problem of residual stresses during processing. In addition, the oxide phase in titanium composites can be present not only as an inert additive, but also participate in reduction reactions. This is especially important when considering the structure formation of a composite under conditions of nonequilibrium combined technologies associated with sintering and reduction reactions. The problem is aggravated by the lack of adequate models of technological joint processes of sintering and reduction, accompanied by complex physical and chemical phenomena in non-equilibrium conditions under high-energy exposure. The production process of composite materials and products under sintering conditions in various technological processes, including additive technologies, MIM, spark sintering, etc., consists of many interconnected physical and chemical phenomena (for example, the interaction of mass and heat transfer processes with a complex set of chemical reactions and the field of mechanical stresses generated by the change in composition). In this regard, the presented work allows us to expand the understanding of some points that are associated with the interaction of the components of titanium-based powder materials with oxide additives under reaction sintering conditions. In this work, we analyzed the results of reaction sintering of a titanium-based powder material containing aluminum and titanium dioxide as additives. Moreover, the ratio of titanium dioxide and aluminum was calculated in such a way as to ensure the expected reduction reaction (TiO_2 + Al) → (Al_2O_3 + Ti) and the volume of possible synthesized oxide should not exceed 10%. To assess the effect of the mixing procedure in the formation of the structural-phase state, powder mixtures were prepared in two ways. The first way is simple mixing of all components for 4 hours, followed by treatment in an activator for no more than 60 minutes. The second way is two-stage mixing, where first a mixture of aluminum and titanium dioxide was processed in an activator, then titanium powder was added, and mixing was continued in an axial mixer for 2 hours. Specimens with a residual porosity of 35-38% were pressed from the resulting mixtures for subsequent vacuum sintering under controlled heating conditions at a temperature of 1150°C with an exposure of 60 minutes. The sintering results showed that the mixing procedure is of great importance in realizing the reaction sintering and the reduction step. Preliminary mechanical activation of the pair (TiO_2 + Al) did not fully guarantee the implementation of the reduction reaction, and after subsequent sintering, the titanium-based solid-solution phase dominated in the structure, where aluminum and oxygen were actually dissolved. Residual aluminum was also observed in small amounts (no more than 1%). On the other hand, as a result of the simultaneous mixing of all components, the transition of TiO_2 to Ti_2O occurred against the background of the formation of Al_2O_3 and TiAl, which was insignificant in terms of volume. Thus, it was shown that the aluminothermic reduction reaction of titanium from TiO_2 does not go to completion, but stops at the intermediate stage TiO_2 → Ti_2O.

* This research was supported by the Russian Science Foundation (Grant No 22-13-20031).

N1-P-040401

THERMALLY CONNECTED SHS PROCESSES IN A LAYERED POWDER SYSTEM Ni + Al/PbO_2 + B + INERT

SHULPEKOV A.M. GABBASOV R.M.

Tomsk Scientific Center SB RAS

Thermally coupled SHS processes make it possible to expand the range of materials produced by the SHS method. So, for example, the use of external heating of a low-exothermic or endothermic mixture with the help of a highly exothermic mixture makes it possible to obtain such valuable materials as WC, CrAlC, TiNi, etc. The method does not require sophisticated equipment, energy costs are negligible. Another advantage of the method is the possibility of obtaining functionally gradient materials, such as layers of metals and ceramics with high heat resistance and resistance to thermal shocks.

The same method can be used to obtain multilayer coatings with different electrical conductivity in the layers. For example, if the lower layer is made dielectric and the upper layer is electrically conductive, then it will be possible to obtain flat electric heaters in one stage. Now this technology requires 6-8 stages with firing in high-temperature furnaces.

The work is devoted to the study of processes occurring in a two-layer powder system Ni + Al/PbO_2 + B + inert (glass + Al_2O_3). In which the Ni + Al mixture is a heat donor and serves to create an electrically conductive layer. A mixture of PbO_2 + B + inert (glass + Al_2O_3) serves as both an acceptor and a heat donor. By changing the content of the inert component, one can control the temperature in the layer and set the chemical composition of the glass obtained during the reactions, which serves as an insulator. The temperature can also be controlled by changing the thickness of the Ni + Al layer. Thus, it is possible to choose the conditions for obtaining a reliable coating with a minimum thickness.

To prepare the initial mixture (Ni + 31 wt. % Al), nickel PNK-L5 and aluminum ASD 4 were used. To obtain a dielectric coating, a mixture of PbO_2 , boron, Al_2O_3, and glass powders was used. In this case, a mixture of PbO_2 + B was prepared separately. The ratio of components was calculated in accordance with the reaction equation $PbO_2 + 2B = PbO + B_2O_3$. As well as a mixture of 50 wt. % Al_2O_3 and 50 wt. % glass powder. A mixture of powders in the form of a suspension in isopropanol was applied to ceramic (VK 1, 98 wt % Al_2O_3) or steel (St3) substrates through a stencil 0.5 thick; 1.1 and 1.6 mm.

The temperature and propagation velocity of the reaction front were determined by the tarmocouple method, using multichannel optical sensors, and a high-speed video camera. X-ray phase analysis was carried out on a portable RIKOR diffractometer provided by the Tomsk Common Use Center of the Siberian Branch of the Russian Academy of Sciences. The coating microstructure was studied using an Axiovert optical microscope (Karl Zeiss, Germany).

It has been established that an increase in the thickness of the Ni + Al layer leads to an increase in the temperature and velocity of the combustion wave front. A similar regularity is also observed with an increase in the content of the PbO_2 + B mixture in the lower layer. In addition, an increase in the content of the PbO_2 + B mixture in the lower layer leads to the expansion of the wave front in the Ni + Al layer due to heating from the exothermic reaction in the lower layer. An increase in the content of the PbO_2 + B mixture leads not only to the melting of glass particles and the formation of a glass-ceramic coating, but also to the chemcal interaction between the components of the mixture with the formation of a homogeneous glass coating. The microstructure of the fracture of the coating indicates the formation of two layers: the upper NiAl and the lower glass-ceramic, firmly bonded to each other.

Thus, in the course of the study, the possibility of obtaining a two-layer electrically conductive and dielectric coating by the SHS method was shown. The optimal ratios of the layer thicknesses and the composition of the powder mixture of the layers have been established. The addition of a PbO_2 + B mixture to the lower layer makes it possible to reduce the thickness of the NiAl layer and ensure the formation of a uniform dielectric coating.

N1-P-045101

ON THE MELTING THESHHOLDS OF FILM-SUBSTRATE SYSTEM IRRADIATED WITH A PULSED ELECTRON BEAM *

A.B. MARKOV, A.V. SOLOVYOV

Tomsk Scientific Center of the Siberian Branch of the Russian Academy of Sciences, Tomsk, Russian Federation

One of the most important predicted characteristics when modeling of temperature fields in targets irradiated with a pulsed electron beams is the melting threshold, i.e., the lowest value of the beam energy density at which the phase transformation of the material from the solid to the liquid phase occurs [1, 2]. For any homogeneous material, the melting threshold is a number. For the film-substrate system, this is already a functional dependence, since the film thickness *d* can vary (see Figure 1 [3]). It is clear that the substrate melting threshold gradually increases from the melting threshold of the homogeneous substrate material to infinity. The melting threshold of the film in the infinity tends to the melting threshold of the homogeneous film material. The relative positions of these curves can be different. They may [3] or may not [4] intersect, the melting threshold of the film may increase or decrease with increasing film thickness. All this depends on the ratio of the thermal properties of the film and substrate materials.

The paper analyzes the influence of the thermal properties of the film and substrate materials on the behavior of the functional dependence "melting threshold - film thickness" during irradiation with a LEHCEB. It is concluded that the key role in the behavior of dependences is played by the difference between the thermal conductivities of the film and substrate materials.

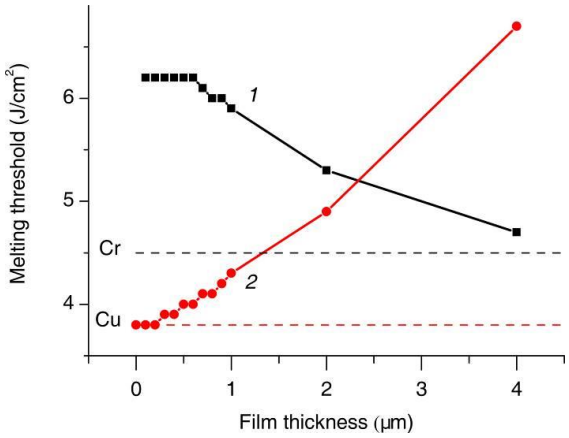

Fig.1. Melting thresholds of the film (1) and substrate (2) for the Cr (film)-Cu (substrate) system depending on the thickness of the Cr film.

REFERENCES

[1] A.B. Markov, V.P. Rotshtein, "The mechanism of increase of the thickness of the zone of thermal effect during pulse-periodic treatment of a target by an electron beam," High Temperature, vol. 38, pp.15-19, 2000.

[2] Markov A.B., Yakovlev E.V., Solovyov A.V., Pesterev E.A., Petrov V.I., Slobodyan M.S. "Formation of a Cr-Zr surface alloy using a low-energy high-current electron beam," J. Phys. Conf. Ser., vol. 2064, 2021.

[3] A.B. Markov, E.V. Yakovlev, D.A. Shepel', "Calculation of heat regimes for a Cr-Cu surface alloy formed with a low-energy high-current electron beam," J. Phys. Conf. Ser., vol. 1115, 2018.

[4] A.B. Markov, A.V. Solovyov, E.V. Yakovlev, E.A. Pesterev, V.I. Petrov, M.S. Slobodyan, "Computer simulation of temperature fields in the Cr (film)-Zr (substrate) system during pulsed electron-beam irradiation," J. Phys. Conf. Ser., vol. 2064, 2021.

* The work was supported by the Ministry of Science and Higher Education of the Russian Federation (project № FWRF-2021-0001).

N1-P-049501

INVESTIGATION OF THE INTERACTION OF TUNGSTEN BORIDE (W_2B) WITH IRIDIUM*

D.A. BANNYKH, A.V. UTKIN, V.V. LOZANOV, N.A. BAKLANOVA

[1]*Institute of Solid State Chemistry and Mechanochemistry SB RAS, Novosibirsk, Russia*

Interest in the study of ternary systems consisting of transition refractory metals and platinum group metals has grown significantly recently. Compounds in W-M-B systems (where M = platinum group metal) have a set of valuable properties, including high thermal and oxidative stability, high hardness, superconductivity, therefore they are in demand in various fields of modern materials science. Ternary boride systems based on tungsten and iridium are of particular interest, since iridium has a high melting point (2446 °C) and a low rate of recession in oxygen at temperatures above 2000 °C.

The aim of this work is a physicochemical study of the interaction of iridium and tungsten boride W2B in the temperature range of 1000 – 1600 °C.

To study the interaction, Ir/W_2B diffusion pairs and mixtures of iridium powder and W_2B were prepared in a molar ratio metals of 1:1 and 3:1, which were heated to a predetermined temperature in the range of 1000 – 1600 °C in an inert atmosphere. The phase and elemental composition, as well as the morphology of the products were studied using X-ray phase analysis and electron scanning microscopy at various accelerating voltages. This made it possible to identify both heavy (W and Ir) and light (B) elements.

Using XRD, it was found that the interaction between Ir and W2B becomes noticeable at 1100 °C, while $IrB_{1.1}$, intermetallic compound of variable composition WxIr1-x and unreacted initial phases were detected. With an increase in temperature to 1200 °C and above, phases W_xIr_{1-x} (x = 0.33), $W_2Ir_3B_{6-x}$, WB, IrB1.1 were detected in the products. In addition, reflexes are present in the radiographs that cannot be attributed to any known phase of the W-Ir-B system. The SEM/EDX data (Fig. 1) confirm the results of the XRD. In addition to the phases already mentioned, a double boride of the assumed composition $W_2Ir_5B_2$ was detected using SEM/EDX.

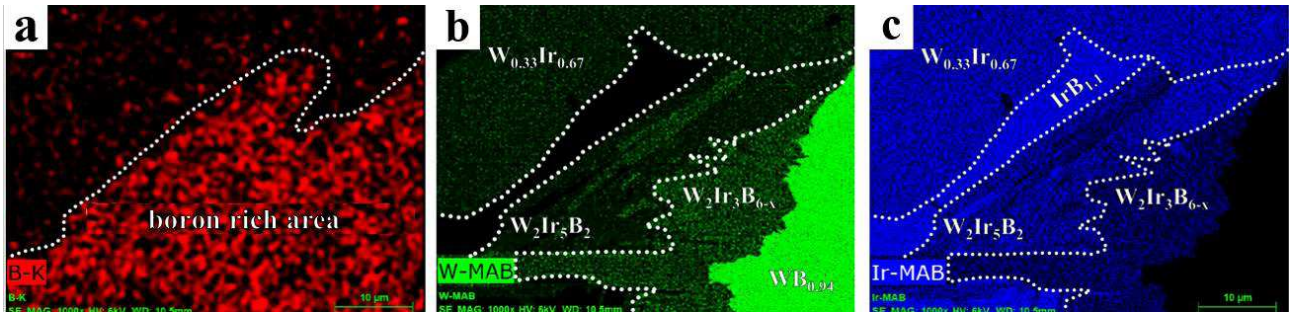

Fig.1. Mapping by cross–section elements of a powder mixture of iridium and tungsten boride (3:1) heated at 1600 °C: a – boron, b – tungsten, c – iridium.

Thus, it is established that the phase composition of the products of interaction of iridium with tungsten boride (W2B) depends on the ratio of components and temperature. At elevated temperatures in the W-Ir-B system, when W2B interacts with iridium, along with iridium boride ($IrB_{1.1}$) and intermetallic compound (W_xIr_{1-x}), WB and double borides are also formed.

* The work was supported by the Russian Science Foundation under grant No. № 18-19-00075.

N1-P-051402

BASIC MODELS OF PHASE FORMATION AT THE MESOLEVEL UNDER REACTIVE SINTERING OF TI-AL-FE2O3 POWDER MIXTURE*

A.G. KNYAZEVA, M.A. ANISIMOVA

Institute of Strength Physics and Materials Science SB RAS, Tomsk, Russia

Titanium-based composites are used in various industries due to their relatively low density, high strength and corrosion resistance. The possibility of using a large number of additional components in the form of both simple elements and compounds that significantly increase its functional and physical-mechanical characteristics is widely used. One of the possible options for the creation of composites based on titanium is the use of reaction sintering, in the course of which the strengthening phase in the form of oxides is directly synthesized. If for relatively simple binary systems like Ti+Al the situation with the limiting physical and chemical stages is relatively clear, then when adding third-grade powders to the mixture, options that are not obvious at first glance are possible. Thus, in the Ti+Al+Fe2O3 system, depending on the percentage of powders, mixing conditions, and heating, different variants of mesovolumes can be distinguished in which the sequence of reactions and accompanying phenomena will lead to different phase composition. To analyze possible variants of events in reaction sintering conditions based on literature data, the following phase-formation models are considered under varying temperature conditions:

Ti+Al (reactions in the melt).

Ti+Al (diffusion couple, constant temperature, solid-phase process).

Ti (melt)+Fe2O3 (solid).

Al (melt)+Fe2O3 (solid).

(Ti+Al) (melt)+Fe2O3 (solid).

The main stages which can be expected under the experimental conditions are established. Particular models with moving interfaces are analyzed and the regularities for different temperatures and different rates of their change are analyzed.

Variants of models of interaction of iron oxide particles with the melt, taking into account the role of wettability of the solid surface, are proposed.

* The work was supported by the Russian Science Foundation under grant No. 22-13-20031.

N1-P-052501

THIN NITROGEN-CONTAINING TITANIUM COATINGS FORMATION ON THE PLLA SCAFFOLDS SURFACE BY REACTIVE MAGNETRON SPUTTERING IN N_2 + Xe MIXTURES*

P.V. Maryin, S.I. Tverdokhlebov

Tomsk Polytechnic University, 30 Lenin Avenue, Tomsk, Russian Federation

For the bioresorbable scaffolds manufacture polymer of poly-L lactic acid (PLLA) [1] are widely used, which are currently one of the most promising biodegradable materials [2]. However, their use for tissue engineering applications is limited by high surface hydrophobicity, which prevents cell adhesion and proliferation. One of the most promising modifying method of PLLA scaffolds surface and give them a high free energy of the surface is to apply thin nitrogen-containing titanium coatings (TiN_xO_y) via PVD methods [3].

The reactive magnetron sputtering is the most universal method for TiN_xO_y coating depositions, since in wide range allows you to vary the composition of the operating gas, the target material, power on the power supply and other parameters. It is known that the working gas has a strong effect on the coefficient and sputtering rate, the ionization cross section, gas ionization energy and Penning effect [4]. Therefore, the use of jet and inert gases, as well as their mixtures, was the usual phenomenon for the formation of various TiN_xO_y coatings. On the other hand, the method of reactive magnetron sputtering allows you to process complex structures, such as polymer bioresorbisable PLLA scaffolds, as well as affect the sputtering rate and the chemical composition of the formed coatings

In this paper, the results of PLLA scaffolds surface modification the by the method of reactive magnetron sputtering of the titanium target in the presence of a mixture of reactive nitrogen (N2) gas with a working xenon (Xe) gas are presented. As a result of such a process of modification on the surface of the PLLA of scaffolds, a thin nitrogen-containing titanium coating, represented by oxide and titanium oxynitrides of various stoichiometry, is formed. The modification process does not significantly affect the morphology of PLLA scaffold, and an increase in the wettability of the surface is observed.

REFERENCES

[1] Nair l. S., Laurencin C. T. Biodegradable polymers as biomaterials //Progress in polymer science. – 2007. – т. 32. – №. 8-9. – с. 762-798.

[2] Nampoothiri K. M., Nair N. R., John R. P. An overview of the recent developments in polylactide (PLA) research //Bioresource technology. – 2010. – т. 101. – №. 22. – с. 8493-8501.

[3] Windecker S. et al. Randomized comparison of a titanium-nitride-oxide–coated stent with a stainless steel stent for coronary revascularization: the TiNOx trial //Circulation. – 2005. – т. 111. – №. 20. – с. 2617-2622.

[4] Petrov I. et al. Comparison of magnetron sputter deposition conditions in neon, argon, krypton, and xenon discharges //Journal of Vacuum Science & Technology a: vacuum, surfaces, and films. – 1993. – т. 11. – №. 5. – с. 2733-2741.

* This study was funded by the Russian Foundation for Basic Research (RFBR) according to the research project № 20-32-90133. This research was supported by the TPU development program - Priority 2030 (Project No. Priority-2030-NIP/IZ-011-0000-2022).

N1-P-910903

SYNTHESIS OF SINGLE-PHASE NIOBIUM SILICID $NBSI_2$ AND NB_5SI_3

V.G. SALAMATOV[2], O.K. LEPAKOVA [1], O. A.SHKODA[1], A.S. SHCHUKIN[2], I.D. KOVALEV[2]

[1] Tomsk Scientific Center of the Siberian Branch of the Russian Academy of Sciences, Tomsk, Russia,
[2]Merzhanov Institute of Structural Macrokinetics and Materials Science (ISMAN), Chernogolovka, Russia

Currently, silicides are widely used in various fields of science and technology for the implementation of special technological processes and the creation of materials with the necessary properties. Materials based on niobium silicides have been actively considered in recent years as a replacement for heat-resistant alloys in high-temperature structures, due to the highest melting temperatures and lower density than those of nickel-based heat-resistant alloys in aviation technology. Silicides were chosen as the main material for the blades of high-pressure turbines. There are attempts to use niobium–silicon-based composites for the production of additives for additive technologies. The niobium–silicon system is considered a low-energy system and it is considered impossible to carry out self-propagating high-temperature synthesis without any preliminary preparation in the form of separate heating or mechanical activation.

In this work, from powder mixtures Nb+37.7 wt. %Si ($NbSi_2$) and Nb+15.36 wt. % Si (Nb_5Si_3) cylindrical samples with a diameter of 12 mm, a weight of 5 g and a height of 14.5 and 11 mm, respectively, were formed by unilateral pressing. The initial reagents were powders Nb (particle size less than 40 microns) and Si (particle size less than 20 microns) with a frequency of at least 99.9%. Hollow cylinders with a diameter of 30 mm, a mass of 20 g and a height of 15 mm were formed from the powder mixture Ti+0.6 Si. Cylindrical holes with a diameter of 12.2 mm were formed along the axis of the samples, into which samples from a mixture of Nb and Si were placed. Control of the gorenje temperature Nb c Si used tungsten-rhenium thermocouples with a junction diameter of 100 microns. Thermocouples were placed to a depth of 3 mm from the lower end of the samples. The synthesis was carried out in an argon medium at a pressure of 1 atm. The initiation of gorenje samples from a mixture of Ti+ 0.6Si was carried out by a heated tungsten spiral from the upper end.

As a result of the experiments carried out, it was possible to carry out self-propagating high-temperature synthesis and obtain synthesized niobium silicides. The reaction products were easily daubed samples, the composition of which, according to X-ray phase and X-ray structural analysis, corresponds to single-phase products $NbSi_2$ and Nb_5Si_3 of hexagonal structure. The analysis of the structure by X-ray phase and microanalysis of the obtained products showed the formation of single-phase products $NbSi_2$ and Nb_5Si^3 hexagonal structure.

N1-P-925901

EFFECT OF MECHANOCHEMICAL SYNTHESIS CONDITIONS ON OBTAINING NANOSIZED MAGNETITE POWDERS

A.A. NEVMYVAKA, V.I. ITIN

Tomsk Scientific Center of the Siberian Branch of the Russian Academy of Sciences,
10/4 Akademichesky Pr., Tomsk, 634055, Russia

The paper investigates the possibility of synthesis of nanosized magnetite powder by mechanochemical activation without the addition of the inert diluent NaCl to the reaction mixture. Physical and chemical properties of the product obtained are also investigated.

Magnetite nanopowder was prepared according to the reaction:

$$FeSO_4 \cdot 7H_2O + 2FeCl_3 + 8NaOH = Fe_3O_4 + Na_2SO_4 + 6NaCl + 11H_2O$$

The synthesis was performed in an APF-3 planetary mill (60 g acceleration) with a steel ball (d=5 mm)-to-powder weight ratio equal to 20:1. Samples were obtained at activation times of 30 s, 1, 2.5 and 5 min. The phase composition, morphology, dispersion, and structure of the synthesized powders were studied by X-ray diffraction analysis, and their specific surface was measured. Intermediate compounds formed on the surface of the particles during the reaction were studied by infrared spectroscopy.

X-ray diffraction analysis of the powders showed the pronounced reflections of the reaction products (sodium chloride and Disodium tetraaquabis(sulfato)iron(II) [$FeNa_2(SO_4)_2(H_2O)_4$]) on the X-ray diffraction pattern after 30 s activation of the reaction mixture [1]. This confirms an exchange reaction in the activator, and one of the reaction products immediately crystallizes. According to the data obtained, the washing of powders after mechanical activation leads to the destruction of Disodium tetraaquabis(sulfato)iron(II) and the formation of magnetite and hematite phases. X-ray spectra show a certain amount of substance in the X-ray amorphous state.

The specific surface of magnetite powders changes nonlinearly with increasing the activation time (Table 1). During the first minute, the specific surface of the powder sharply increases up to 115 m^2/g and then decreases to 103 m^2/g. This fact is likely to be related to the processes of disordering and aggregation of particles in the milling device under intense plastic deformation (impact, friction). Further intense treatment leads to disaggregation of the powder and the increase in the specific surface at 5 min mechanical activation. As shown in [2], the specific surface of magnetite powder synthesized at 30 min activation is 150 m^2/g.

Table 1. Specific surface and average particle size of magnetite powders

$\tau_{activation}$	S_{spec}, m^2/g	D, nm
30 s	115	9.9
1 min	168	6.8
2.5 min	103	11.1
5 min	132	8.7

A comparison of the infrared spectra of magnetite powders synthesized at different activation times shows the presence of goethite (-FeOOH) on the surface, which is indirect evidence of the participation of crystallization water of the initial compound $FeSO_4 \cdot 7H_2O$ in the synthesis reaction.

The results show that a change in the synthesis procedure as compared to that presented in [2], namely, mechanochemical activation in the absence of the inert diluent NaCl, leads to obtaining magnetite nanoparticles with an average particle size of 8 nm with a large specific surface.

REFERENCES

[1] M. Hudak, J. Garcia Diaz and J. Kozisek, "Disodium tetraaquabis(sulfato)iron(II)", J. Acta Cryst. vol. E64, 10, 2008.

[2] O.G. Terekhova, V.I. Itin, A.A. Magaeva et al., Russ. J. Non-Ferr. Mater. vol.49, 2008.

N1-P-925902

MAGNETITE NANOPOWDERS AS A SORBENT FOR OIL EXTRACTION FROM THE WATER SURFACE

A.A. NEVMYVAKA, V.I. ITIN

*Tomsk Scientific Center of the Siberian Branch of the Russian Academy of Sciences,
10/4 Akademichesky Pr., Tomsk, 634055, Russia*

The paper discusses the application of magnetite nanopowders obtained by mechanochemical synthesis for sorption of oil spilled in water, in particular, the sorption of mineral oil (MBP grade, GOST 1805-76).

Mechanochemical synthesis of magnetite nanopowders was performed according to the reaction:

$$FeSO_4 \cdot 7H_2O + 2FeCl_3 \cdot 6H_2O + 8NaOH = Fe_3O_4 + Na_2SO_4 + 6NaCl + 23H_2O$$

Powders were synthesized in an AGO-3 planetary mill (60 g acceleration) for 30 min with a ratio of the reaction mixture to the inert component sodium chloride equal to 1:2.

The experimental procedure for studying the ability of magnetite nanopowders to sorb mineral oil on the water surface corresponds to [1]. Magnetite particles were removed from the surface using a magnet.

The gravimetric method and thermogravimetric studies were used to assess the ability of magnetite nanopowders to sorb mineral oil. The amount of oil was determined on VK-600 electronic scales with an accuracy of 0.01 g, measuring the mass of oil with pre-weighed magnetite nanopowder after its removal from the aqueous medium. It was found that the magnetite nanopowder sorb about 42 wt % of mineral oil.

According to thermogravimetry, magnetite nanopowders concentrate a significant amount of oil (Fig. 1). The oil combustion occurs in the range from 250 to 420 ^{0}C with intensive heat emission (exothermic peak at 379 ^{0}C). The exothermic effect in this temperature range corresponds to a large mass loss on the TG curve (Fig. 1), which determines the amount of oil retained by the nanopowder.

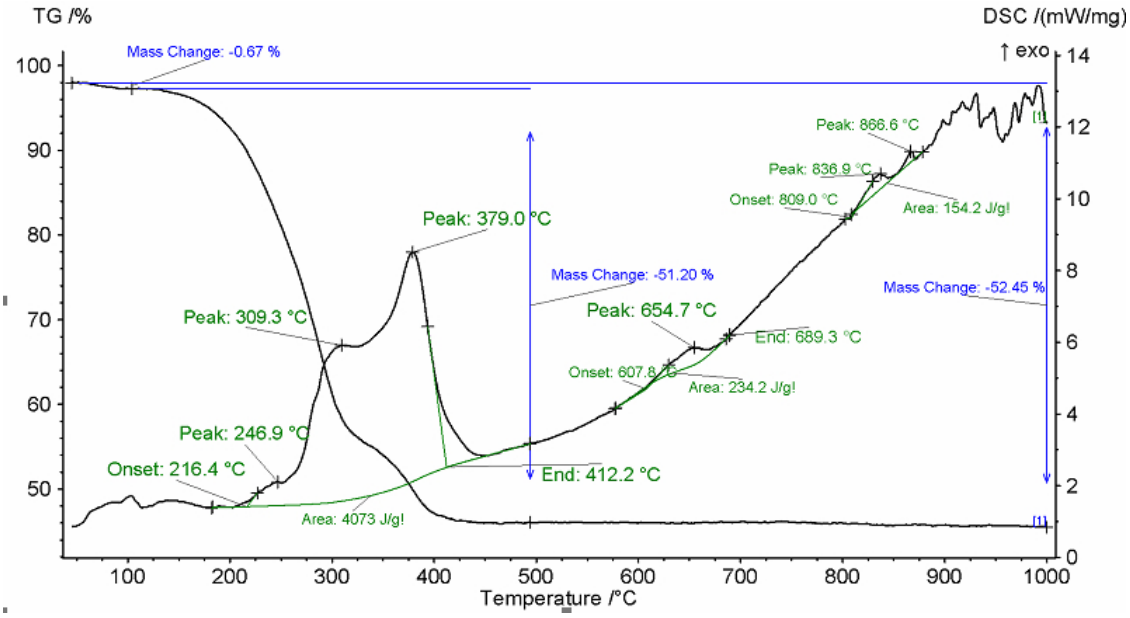

Figure 1. Thermogravimetric analysis of magnetite nanopowder with sorbed mineral oil.

The results showed the possibility of using ferrimagnetic nanopowders obtained by mechanochemical synthesis as materials for the sorption of oil products. It is known that for nanosized particles the surface area-to-volume ratio is very high, and the agglomeration process is thermodynamically favorable. It can be assumed that mineral oil is sorbed by weakly bonded agglomerates of magnetite particles with large porous space, which traps mineral oil under the action of capillary forces.

REFERENCES

V. Mironov, V. Zemchenkov, V. Lapkovskiy, Yu. Trays, V., Ecological Bulletin of Research Centers of the Black Sea Economic Cooperation, № 1. P. 32, 2013.

N1-P-953001

SYNCHROTRON X-RAY DIFFRACTION ANALYSIS OF STRUCTURAL AND PHASE EVOLUTION AT THE INTERFACE OF METALS1

K.I. EMURLAEV, I.A. BATAEV

Novosibirsk State Technical University, Novosibirsk, Russia

Wear processes are of special interest both in scientific and practical terms. This is due to the enormous energy costs of overcoming friction forces as well as the regular failure of products and friction units as a result of wear [1, 2]. The only way to avoid wear is to eliminate direct contact between the rubbing pair. For this purpose, lubricants are usually introduced into the friction units. However, they don't always completely eliminate the problem of wear during operation, since there may appear zones working under of boundary or even dry friction conditions. Therefore, understanding the processes of structural transformations that occur directly during friction is extremely important, especially if one consider that dry friction is an inevitable and even desirable phenomenon in a number of units, for instance, in braking systems.

Synchrotron X-ray diffraction technique is a promising way to analyze structural and phase transformations in materials. High brilliance of the synchrotron radiation, many orders of magnitude more than with X-rays produced in conventional X-ray tubes, provides a high spatio-temporal resolution and makes it possible to implement *in situ* or *operando* observation of changes in the structure and analyze local areas of the material surface under friction [3-5]. Recently, an *operando* approach to control the structure of materials has been proposed at Novosibirsk State Technical University (NSTU). The scheme of the experiment is shown in Figure 1 and described in [4, 5].

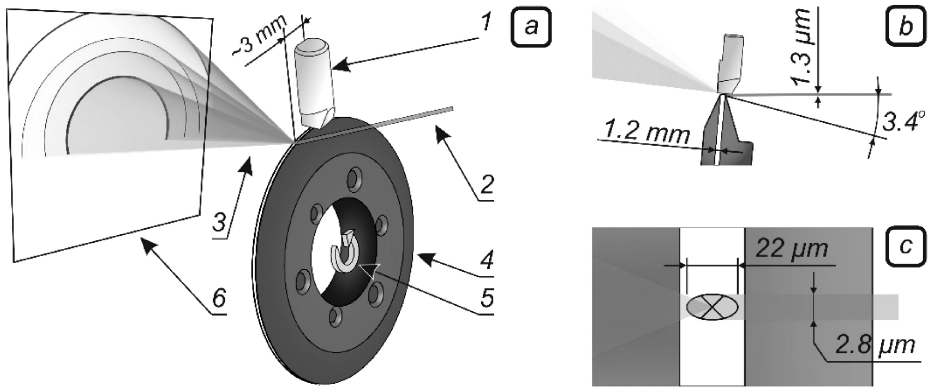

Fig.1. (a) The scheme of the *operando* observation of friction-induced structural changes using synchrotron X-ray diffraction: 1 – the pin; 2, 3 – the incident and diffracted radiation, respectively; 4 – the disk-like sample; 5 – the rotation direction; 6 – the flat detector; (b) the scheme of grazing incidence geometry; (c) the footprint of the beam on the work surface.

The results and features of the experiment will be presented during the report. The research was carried out at the ID13 beamline at the European Synchrotron Radiation Facility (France).

REFERENCES

K. Holmberg and A. Erdemir, "Global impact of friction on energy consumption, economy and environment," FME Trans., vol. 33, no. 3, pp. 181-185, March 2015.

K. Holmberg and A. Erdemir, "Influence of tribology on global energy consumption, costs and emissions," Friction, vol. 5, no. 3, pp. 263-284, September 2017 .

K. Yagi, Y. Ebisu, J. Sugimura, S. Kajita, T. Ohmori, A. Suzuki, "In Situ Observation of Wear Process Before and During Scuffing in Sliding Contact," Tribol. Lett., vol. 43, no. 3, pp. 361-368, June 2011 .

A.A. Bataev, V.G. Burov, A.A. Nikulina, I.A. Bataev, D. V. Lazurenko, A.I. Popelukh, D.A. Ivanov, "A Novel Device for Quasi In Situ Studies of Materials Microstructure during Friction," Mater. Perform. Charact., vol. 7, no. 3, pp. 20170065, March 2018 .

I.A. Bataev, D.V. Lazurenko, A.A. Bataev, V.G. Burov, I.V. Ivanov, K.I. Emurlaev, A.I. Smirnov, M. Rosenthal, M. Burghammer, D.A. Ivanov, K. Georgarakis, A.A. Ruktuev, T.S. Ogneva, A.M.J. Jorge, "A novel operando approach to analyze the structural evolution of metallic materials during friction with application of synchrotron radiation," Acta Mater., vol. 196, pp. 355-369, September 2020 .

1 The work was supported by Ministry of Science and Higher Education of the Russian Federation (project FSUN- 2020-0014 (2019-0931)). Structural research was conducted at NSTU Materials Research Center.

S4-O-038401

DEVELOPMENT OF MATERIAL BASED ON NANOSTRUCTURED Cu-Nb ALLOY FOR HIGH MAGNETIC FIELD COILS*

E.Yu. ZAYTSEV[1], *A.V. SPIRIN*[1], *V.I. KRUTIKOV*[1], *S.N. PARANIN*[1], *S.V. ZAYATS*[1], *A.S. KAIGORODOV*[1], *A.V. KEBETS*[2]

[1]*Institute of Electrophysics UB RAS, Ekaterinburg, Russia*
[2]*Physical-Technical Institute NASB, Minsk, Belarus*

The nanostructured Cu-Nb composite, characterized by high conductivity and tensile strength, is a candidate material for the development of tool coils (inductors) for magnetic pulse processing technologies exploiting high, 30–50 T, magnetic fields (HMF) of 10–100 μs in duration. Using it in the form of a wire, reliable 70 T multi-turn pulsed magnets of subsecond pulse duration are being developed [1], but it was not studied under the generation of microsecond HMFs due to the availability as a wire only. The aim of this work is to produce a material based on Cu-Nb alloy by powder approach, to study the effect of TiC addition on electrical, mechanical, structural properties and the behavior of the materials, including layered structures on their basis [2], under the generation of 40 T magnetic field as compared to commercial wire.

Cu-18% Nb commercial wire 0.15–0.18 mm in dia obtained by "melting and drawing" technique [3] (50% IACS, 1.57 GPa UTS, Nanoelectro LLC Company) was used as a raw material to obtain a powder with particles 20–64 μm in size by ball milling the wire in petrol. To form the layered structures with layers that differed in resistivity TiC was added to the base Cu-Nb powder (BP) in amount 10–20 vol.% through a ball milling. As-milled powders after vacuum annealing at 500°C were then pressed by magnetic pulsed compaction (MPC) in evacuated and preheated to 430°C mold at a pressure pulse of 1–1.3 GPa. Annealing in vacuum for 1 h at temperatures up to 850°C was performed to study its effect on materials density, conductivity, structural characteristics, and mechanical properties.

For testing the materials in HMFs, some samples of 32 mm in dia, including the sample with bi-layer structure (Fig. 1a), were cut into bars having a cross-section 2×8 mm close to that of commercial Cu-18%Nb multicore rectangular wire of the same manufacturer. It was done to compare the commercial and lab materials in close conditions. The bars cut of the pellets and commercial wire were the brazed parts of a duplex field shaper (DFS, Fig. 1b) which was placed inside a capacitor-driven single-turn inductor. The testing conditions were: peak magnetic field – 40 T, half-period – 15 μs, discharged peak current – 540 kA.

The results. Generally, the powder samples were more hardened and thermally stable then initial wire. Addition of TiC particles resulted in increasing both the composite microhardness and resistivity, and the lowering the tensile strength at the same time. As expected, the powder samples were inferior in some performance to commercial wire. However, such an approach is considered to be acceptable for producing the massive articles of complex shape like field shapers. Under the generation of 40 T magnetic field, the powder samples exhibited a comparable to commercial wire lifetime, about 100 pulses (Fig. 1c).

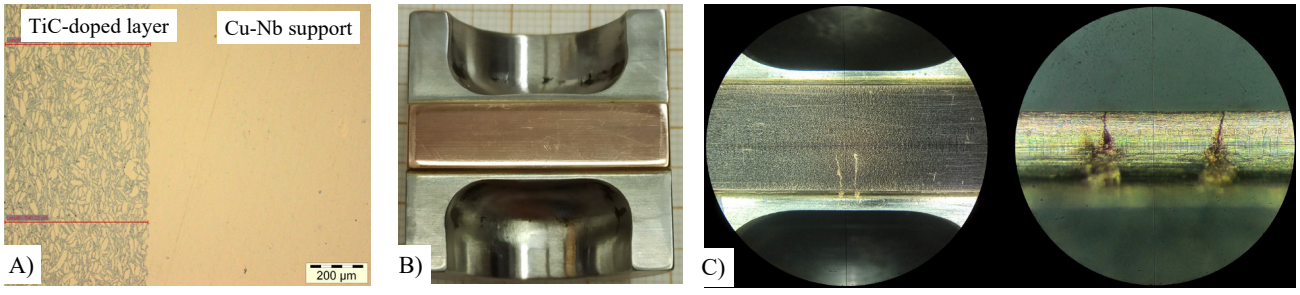

Fig. 1. Cross section of bi-layer structure (a), one part of duplex DFS with brazed sample (b), and (c) view of powder sample surface after 100 pulses of HMF (left – high-field working surface, right – side view)

REFERENCES

[1] A. Lagutin, K. Rosseel, F. Herlach1, J. Vanacken, Y. Bruynseraede, "Measurement Science and Technology Development of reliable 70 T pulsed magnets," Meas. Sci. Technol., vol. 14, no. 12, pp. 2144-2150, 2003.

[2] P. Russkikh, G. Boltachev, S. Paranin, A. Kebets, "Simulating the Conductor With a Nonuniform Resistance Under High-Pulsed Magnetic Fields," IEEE TRANS. PLASMA SCI., vol, 49, no. 9, pp. 2463-2469, 2021.

[3] A. Shikov, V. Pantsyrnyi, A. Vorobieva, N. Khlebova, A. Silaev, "High strength, high conductivity Cu–Nb based conductors with nanoscaled microstructure," Physica C, vol. 354, pp. 410-414, 2001.

* The work was partly supported by the RFBR and BRFFR, RFBR and ROSATOM grants (Nos. 20-58-00029, 20-21-00050).

N2-O-004301

LIFETIME ASSESSMENT OF RADIANT BURNERS MADE OF SHS-INTERMETALLICS*

A. MAZNOY

Tomsk Scientific Center SB RAS, 10/4 Akademicheskii pr., Tomsk, 634055, Russia, maznoy_a@mail.ru, +79234124765

During the last decade, thin-shell radiant burners [1] made of porous SHS-intermetallics [2] have been developing in TSC SB RAS. Low oxidation resistance is a barrier to the successful commercialization of the burners. My presentation will be focused on recent results and prospects for the high-temperature oxidation resistance of porous Ni-Al-Cr intermetallics. The first results have shown that porous SHS-intermetallics with spheroidal elements of 1-2 mm in diameter can work for one year or more at 1000-1100 °C (Fig.1).

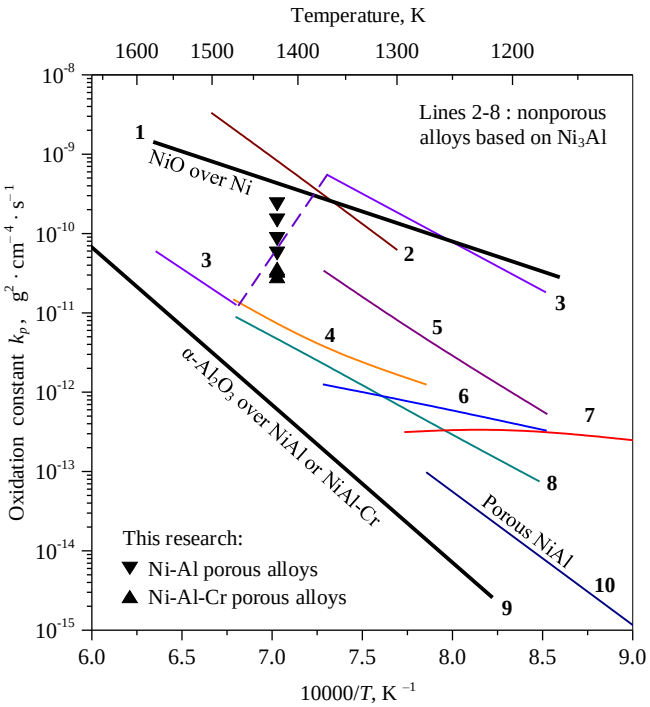

Fig.1. Arrhenius diagrams of k_p vs 10000/T for oxidation of SHS-porous alloys. Lines are literature data: 1 – NiO scale over Ni [3], 2 – pure Ni_3Al [4], 3 – Ni-11.8wt.%Al alloy [3], 4 – pure Ni_3Al [5], 5 – IC221M alloy (Ni_3Al + Cr-Zr-Mo-B) [6], 6 – nanocrystaline Ni_3Al made by MA & SPS [7], 7 – powder-metallurgical Ni_3Al [8], 8 – pure Ni_3Al [3], 9 – α-Al_2O_3 scale over B2-NiAl or NiAl-Cr [9], 10 – porous NiAl [10].

REFERENCES

[1] A. Maznoy, N. Pichugin, I. Yakovlev, R. Fursenko, D. Petrov, S.S. Shy, “Fuel Interchangeability for Lean Premixed Combustion in Cylindrical Radiant Burner Operated in the Internal Combustion Mode,” Appl. Therm. Eng. vol. 186, no. 115997. March 2021.

[2] A. Maznoy, A. Kirdyashkin, V. Kitler, N. Pichugin, V. Salamatov, K. Tcoi, “Self-propagating high-temperature synthesis of macroporous B2+$L1_2$ Ni-Al intermetallics used in cylindrical radiant burners,” J. Alloys Compd. vol. 792, pp. 561–573, July 2019.

[3] J.D. Kuenzly, D.L. Douglass, “The oxidation mechanism of Ni_3Al containing yttrium,“ vol. 8, pp. 139–178. June 1974.

[4] S. Taniguchi, T. Shibata, H. Tsuruoka, “Isothermal oxidation behavior of Ni_3Al-0.1B base alloys containing Ti, Zr, or Hf additions,“ Oxid. Met. 1986 261. vol. 26, pp. 1–17. August 1986.

[5] S.C. Choi, H.J. Cho, Y.J. Kim, D.B. Lee, “High-temperature oxidation behavior of pure Ni_3Al,“ Oxid. Met. vol. 46, pp. 51–72. August 1996.

[6] D.B. Lee, M.L. Santella, “High temperature oxidation of Ni_3Al alloy containing Cr, Zr, Mo, and B,“ Mater. Sci. Eng. A. vol. 374, pp. 217–223. June 2004.

[7] G. Cao, L. Geng, Z. Zheng, M. Naka, “The oxidation of nanocrystalline Ni3Al fabricated by mechanical alloying and spark plasma sintering,“ Intermetallics. vol. 15, pp. 1672–1677. December 2007.

[8] P. Pérez, J.L. González-Carrasco, P. Adeva, “Oxidation behavior of a Ni_3Al PM alloy,“ Oxid. Met. vol. 48, pp. 143–170. August 1997.

[9] M.W. Brumm, H.J. Grabke, “The oxidation behaviour of NiAl-I. Phase transformations in the alumina scale during oxidation of NiAl and NiAl-Cr alloys,“ Corros. Sci. vol. 33, pp. 1677–1690. November 1992.

[10] H.X. Dong, Y. Jiang, Y.H. He, J. Zou, N.P. Xu, B.Y. Huang, C.T. Liu, P.K. Liaw, “Oxidation behavior of porous NiAl prepared through reactive synthesis,“ Mater. Chem. Phys. vol. 122, pp. 417–423. August 2010.

* The research was funded by Russian Science Foundation (project № 21-79-10445).

N2-O-011002

OBTAINING OF B-SIALON BY SHS FROM ALUMINUM FERROSILICON WITH THE ADDITION OF MARSHALITE

A. A. REGER[1], *K. A. BOLGARU*[1], *A. A. AKULINKIN*[1]

[1]*Tomsk Scientific Center of the Siberian Branch of the Russian Academy of Sciences, Tomsk, Russia*

Sialon is a material with unique physical and chemical properties. This material due to its properties has a wide range of applications [1, 2]. Self-propagating high-temperature synthesis (SHS) is the appropriate method to produce sialon and materials based on it due to the short synthesis time, energy efficiency, environmental friendliness, and simple equipment [3, 4].

Despite the advantages of the SHS method, its application in industry was limited by the high cost of starting materials. The use of ferroalloys in SHS processes reduced the cost of the products obtained and shifted this method from the laboratory to the large-scale industrial level [5].

The goal of this work is to obtain a sialon-based material from a mixture of aluminum ferrosilicon - based powders and marshalite in the combustion mode.

In [1] it was shown that the optimal composition of aluminum ferrosilicon and marshalite is 90:10 wt. %. However, the products obtained by combustion of this composition, according to X-ray diffraction, contained iron silicide phases. The presence of silicidal phases indicates an incomplete nitriding reaction.

In order to increase the yield of sialonic phase in the synthesized products, pre-nitrated product and gasifying additive, ammonium fluoride, were added to the mixture of aluminum ferrosilicon and 10 wt. % marshalite. The addition of a pre-nitrated product up to 30 wt. % reduced the intensity of iron silicide reflexes (Fig. 1a). The addition of a pre-nitrated product more than 30 wt. % makes the combustion reaction impossible. After the addition of 1 wt. % ammonium fluoride, silicide phase reflexes are not observed (Fig. 1c). Figure 2 shows a picture of the nitrated sample.

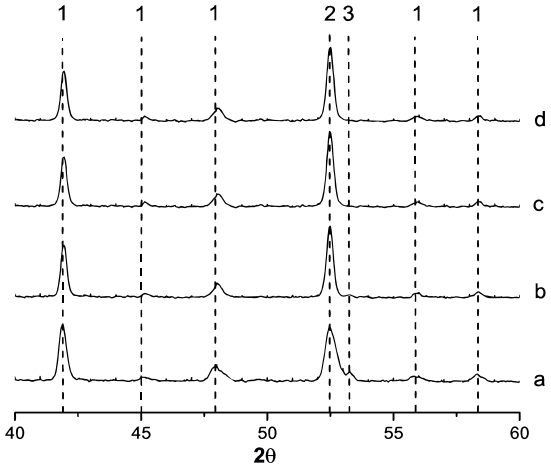

Fig.1. X-ray diffraction patterns of the mixture of aluminum ferrosilicon and marshalite with addition of nitrided product and NH_4F (**a**– 0**, b** – 0.5, **c** – 1, **d** – 1.5 мас. % NH_4F; 1 – β-SiAlON, 2 – α-Fe, 3 – Fe_xSi_y).

Fig.2. Picture of the nitrated mixture of aluminum ferrosilicon, marshalite, nitrated product, and ammonium fluoride.

Thus, the maximum yield of the sialon phase (87 wt%) was obtained from a mixture of powders based on aluminum ferrosilicon and marshalite by the SHS method.

REFERENCES

[1] K. A. Bolgaru, V. I. Vereshchagin, A. A. Reger, ”Combustion synthesis of SiAlON and nitride phases based on ferrosilicoaluminum with marshalite additives”, Refractories and Industrial Ceramics, vol. 61, 655-658, 2021.

[2] I. M. Low, Ceramic Matrix composites. Microstructure, Properties and Applications. Woodhead Publishing Ltd., 2006.

[3] Konstantin Bolgaru, Anton Reger, Vladimir Vereshchagin, Alexander Akulinkin “Combustion synthesis of porous ceramic β-Si3N4-based composites with the use of ferroalloys”, Ceramics International, vol. 47, 34765-34773, 2021.

[4] I.G. Gano, M. A Rodriguez, “Synthesis of β-Silicon nitride by SHS: fiber growth”, Scripta Mater., vol. 50, 383–386, 2004.

[5] Y.M. Maksimov, Industrial ferroalloys. Concise Encyclopedia of self-propagating high-temperature synthesis, 2017.

N2-O-023201

STRUCTURED MULTILAYERED COMPOSITE MATERIALS BY SHS METHOD: EXPERIMENTAL STUDY*

O.K. KAMYNINA[1], *S.G. VADCHENKO*[2], *I.D. KOVALEV*[2], *D.V. PROKHOROV*[1]

[1]*ISSP RAS, Chernogolovka, Russia*
[2]*ISMAN, Chernogolovka, Russia*

Design of materials that combine properties of ceramics and metals, such as hardness, strength, heat resistance, high-temperature strength, wear resistance, and ductility is a popular trend in materials research and design. Layered composite materials (cermets) that combine the properties of metals (ductility, heat resistance, and thermal conductivity) and ceramics (hardness, corrosion resistance, high-temperature strength, and low thermal conductivity) find wide application in different areas of aerospace industry, mechanical engineering, power engineering, etc. Meanwhile, the fabrication of multilayer composite materials encounters serious difficulties caused by strongly different mechanochemical parameters of metals and ceramics to be joined. Joining of metals with ceramic is a complicate issue due to strongly difficult physical properties of these dissimilar materials. The quality of joining is governed by the following two factors: (a) the fit of thermal expansion and (b) the formation of undesired interfacial layers [1]. The problem of joining dissimilar materials still remains to be of current importance despite of huge number of publications in the field.

Self-propagating high-temperature synthesis (SHS) is a advance technique for the synthesis of materials and deposition of coatings which is attractive due to a wide range of suitable reagents, relatively simple facilities, and high combustion temperatures developed during combustion reaction [2]. SHS method was found applicable to joining such dissimilar materials as ceramics, metals, and carbon materials [3].

In this work, we report on the SHS-assisted joining between Ti, Hf, Ta foils and ceramic layers SHS-produced in situ from reactive Ti–B, Ti–C, and Ti–Si tapes. According to [4], the reactive cold-rolled Ti–B tapes 100–300 μm thick are capable of rapid burning at a high rate of heat release. The choice of individual layers for compiling green sandwich-like multilayer assemblies was done with due regard for key thermophysical parameters of foils and rolled reactive tapes. The samples comprised of metal foils and reactive ceramic-generating tapes were ignited in a combustion chamber under Ar. The combustion process was monitored with set of thermocouples. Combustion-synthesized composites were characterized by SEM, EDX and XRD. Thermomechanical behavior of synthesized samples was determined by three-point loading at 25°C and 1100°C under Ar using a modified testing machine Instron-1195.

Lightweight Ti–Hf–ceramic and Ti–Hf–Ta–ceramic layered composite platelets 2–3 mm thick can be prepared via a short-term (around 0.2–0.6 s) combustion of preliminary sandwich-like stacks of metal foils and reactive tapes. Good joining of Ti with Hf and Ta was achieved due to SHS reactions in reactive tapes yielding ceramics and reaction heat. Layered composite material is formed as a result of mutual impregnation, interdiffusion, and chemical reactions. In contrast to the technique of ceramic–metal diffusion bonding, our combustion-aided process affords for joining dissimilar materials in short processing time without using complicate facilities. Good joining between metals and ceramics is reached due to the formation of interfacial layers in the form of cermets and eutectic solutions.

REFERENCES

[1] W. Wunderlich. “The atomic structure of metal/ceramic interfaces is the key issue for developing better properties”, Metals, vol. 4, no. 3, pp. 410–427, September 2014.

[2] E.A. Levashov, A.S. Mukasyan, A.S. Rogachev, D.V. Shtansky. “Self-propagating high-temperature synthesis of advanced materials and coatings”, Int. Mater. Rev., vol. 62, no. 4, pp. 203–239, February 2017.

[3] A.S. Rogachev, S.G. Vadchenko, A.A. Nepapushev, S.A. Rogachev, Yu.B. Scheck, A.S. Mukasyan. “Gasless reactive compositions for materials joining: An overview”, Adv. Eng. Mater., vol. 20, no. 8, pp. 1701044–1701044, August 2018.

[4] S.G. Vadchenko. “Dependence of the burning rates of tapes of Ti + xB mixtures on boron concentration”, Combust. Explos. Shock Waves, vol. 55, no. 2, pp. 177–183, March 2019.

* The work was supported by Russian Foundation of Basic Research (project no. 20-08-00594_a).

N2-O-023401

OSCILLATORY FLAME INSTABILITY IN POROUS MEDIA*

I.A. YAKOVLEV[1]

[1]Tomsk Scientific Center SB RAS, Tomsk, Russian Federation,

Porous media combustion (PMC) is of great interest for last decade due to specific advantages such as enhanced flammability range, low pollutant emission and improved flame stability in contrast to free-flame burners [1]. Global course to emission reduction of greenhouse gases and fuel saving prompts to use lean mixtures in burner devices down to lean limit. Intense heat recuperation in PMC allows extremely decrease fuel concentration in combustible mixture till $\varphi \approx 0.15$ [2]. However, some types of flame instabilities can develop under such conditions.

In this study a pore-scale numerical simulation of the flame behavior in two-dimensional randomly-backed bed of circle particles (7 mm in diameter) has been performed for methane-air mixture. The computational domain consisted of fluid and solid regions. Mathematical problem statement, based on the finite volume method, described the fluid flow in the interstitial space with chemical reaction, thermal conductivity of the solid particles as well as conjugate heat transfer and radiation. Full problem statement can be found in [3].

The combustion wave propagates upstream with velocity of ~0.01 mm/s. During that fragments of the flame front oscillates with frequency of ~50 Hz. Figure 1a shows the temperature contour at the case when the macroscopic wave reaches center section of the domain.

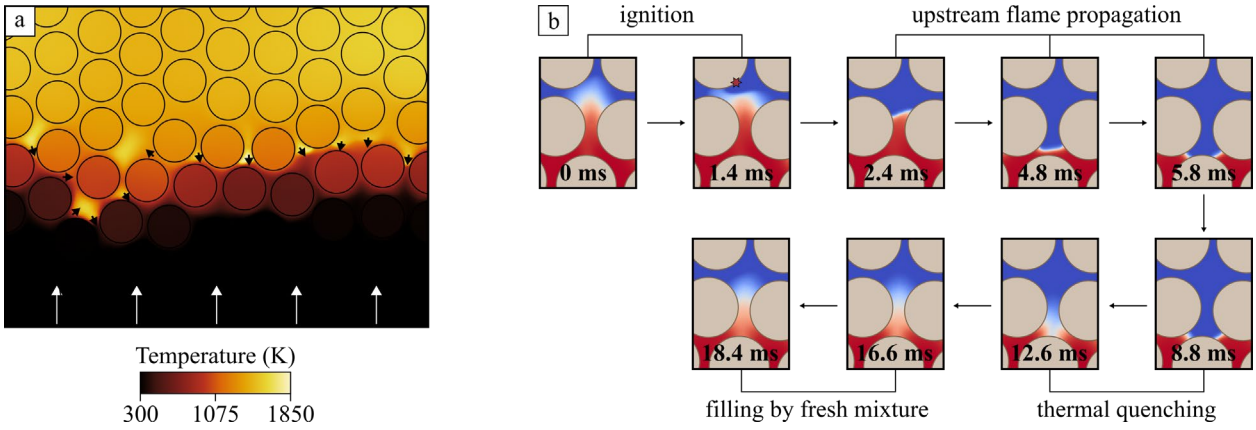

Fig.1. Temperature distribution (a) and flame front behavior in pore channel (b).

At pore scale the flame front propagation is a repeatable process of mixture ignition, upstream flame propagation, thermal quenching and filling the channel with fresh mixture. These stages are similar with the unstable flames with repetitive extinction and ignition (FREI), observed in microchannels with external heating [4]. Considering the significant tortuosity of the pore channels with temperature gradient as a result of heat recuperation mechanism, the mechanisms are identical. In contrast to straight channels that flame front fragments in adjacent connected channels can influence each other hydrodynamically (pulsations of the pressure and flow rate) and thermally. In microchannels some transitional regimes without full flame extinction have been observed. In this study small oscillations with frequency from 150–300 Hz have been predicted numerically for the case with small particles diameter of 1.5–2 mm.

REFERENCES

[1] J. L. Ellzey, E. L. Belmont, C. H. Smith, “Heat recirculating reactors: Fundamental research and applications,” Prog. Energy Combust. Sci., vol. 72, pp. 32–58, 2019.

[2] S. Zhdanok, L. A. Kennedy, G. Koester, “Superadiabatic combustion of methane air mixtures under filtration in a packed bed,” Combust. Flame, vol. 100, pp. 221–231, 1995.

[3] R. V. Fursenko, I. A. Yakovlev, E. S. Odintsov, S. D. Zambalov, S. S. Minaev, “Pore-scale flame dynamics in a one-layer porous burner,” Combust. Flame, vol. 235, article number 111711, 2022.

[4] K. Maruta, T. Kataoka, N.I. Kim, S. Minaev, R. Fursenko, “Characteristics of combustion in a narrow channel with a temperature gradient,” Proc. Combust. Inst., vol. 30, pp. 2429–2436, 2005.

* The work was supported by RFBR, project number 20-38-70119.

N2-O-024303

MATHEMATICAL MODELING OF UNSTATIONARY COMBUSTION OF GASLESS SYSTEMS WITH A CONVECTIVE FLOW OF THE MELT

O.V. LAPSHIN[1], V.G. PROKOF'EV[1,2]

[1]Tomsk Scientific Center, Russia
[2]Tomsk State University, Russia

One of the features of the synthesis of ceramic materials in the combustion mode of gasless powder compacts is the melting and spreading of one or more components of a heterogeneous system in a matrix of refractory components and reaction products [1]. The thermocapillary mechanism of melt flow is due to the action of surface tension forces in a porous medium. "Abnormal" dependences of the combustion rate on the particle size of titanium for Ti+Si and Ti+Fe powder systems have been experimentally obtained [2-3]. The convective mechanism of mixing of system components takes place along with a diffusion and capillary mass transfer. The melting of the reagent and the wetting of the refractory component of the mixture by the melt increases the heat release rate and raises the temperature in the combustion front.

In this work, we consider a combustion mathematical model for a binary mixture, one of the components of which is a fusible metal. Let a system under consideration be formed by three interpenetrating continua – high-melting reagent A, low-melting reagent B, and pores. The reaction scheme can be represented as $st_1 A(solid) + st_2 B(solid, liquid) = P(solid)$, where st_1 and st_2 stand for respective stoichiometric coefficients. The mathematical model of the combustion process is described in the work [4]. In this work, we take into account the change in the reaction rate with the appearance of a liquid phase.

The typical dynamics of porosity formation in non-stationary combustion mode is shown in Figure 1. The main goal of solving the problem was to calculate the burning rate of the binary mixture A + B, as the main integral characteristic of high-temperature synthesis.

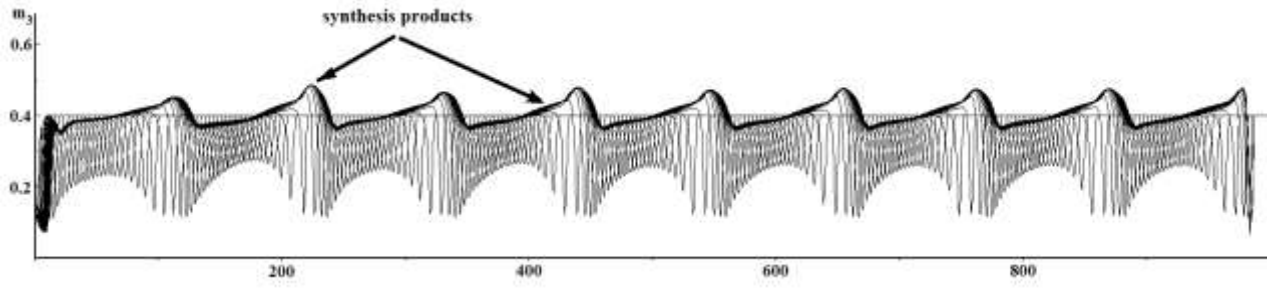

Fig.1. Distributions of porosity in non-stationary combustion mode with an excess of component B (initial porosity – m_0= 0.4).

The calculated dependences of the burning rate on the initial porosity are in qualitative agreement with the experimental data.

REFERENCES

[1] A.I. Kirdyashkin, V.D. Kitler, V.G. Salamatov, R.A. Yusupov, Yu.M. Maksimov, "Specific features of structural dynamics of high-temperature metallothermal processes with the FeO-Al-Al_2O_3 system as an example", Combust. Explos. Shock Waves., vol. 44, no. 1, pp. 71–75, 2008.

[2] Yu.M. Maksimov, A.I. Kirdyashkin, M.Kh. Ziatdinov, V.D. Kitler, "Interphase convection in the contact interaction of metals under non-isothermal conditions", Combust. Explos. Shock Waves., vol. 36, no. 4, pp. 462–469, 2000.

[3] A.I. Kirdyashkin, V.D. Kitler, V.G. Salamatov, R.A.Yusupov, Yu.M. Maksimov, 'Capillary hydrodynamic phenomena in gas-free combustion", Combust. Explos. Shock Waves., vol. 43, no. 6, pp. 645–653, 2007.

[4] O.V. Lapshin, V.G. Prokof'ev, "Combustion of gasless systems: thermocapillary convection of metal melt", Intern. J. of SHS, vol.30, no. 3, pp. 127-131, 2021.

N2-O-029001

A DEVOLATILIZATION PROCESS OF BROWN COAL DURING HEATING UNDER DIFFERENT CONDITIONS

A. PONOMAREVA[1,2], E. KOROSTYLEVA[1], V. SITNIKOVA[1]

[1] Saint-Petersburg National Research University of Information Technologies, Mechanics and Optics, Saint-Petersburg, Russia
[2]Far Eastern Federal University, Vladivostok, Russia

The devolatilization process is referred to the release of gaseous fuel components during heating of solid fuels. This process is a key characteristic of the combustion of solid fuels [1]. The volatiles burn much more rapidly than the remaining char particles and therefore are important for flame ignition and stability and play an important role in gas pollution formation. On the other hand, at the same time the water evaporation occurs that can delay the ignition of solid fuel [2]. Moreover, the devolatilization process determines how much char remains to be burned as well as the physical characteristics of the resulting char, with subsequent impacts on the char combustion properties [1]. In this work, the methods of infrared spectroscopy of disturbed total internal reflection were used to study the change in the chemical structure of fine particles of brown coal during heat treatment in an air atmosphere and with a limited presence of air. Deconvolution methods for the IR spectra of samples made it possible to clarify information on the structure and chemical bonds in brown coal, including in the range of O–H vibrations.

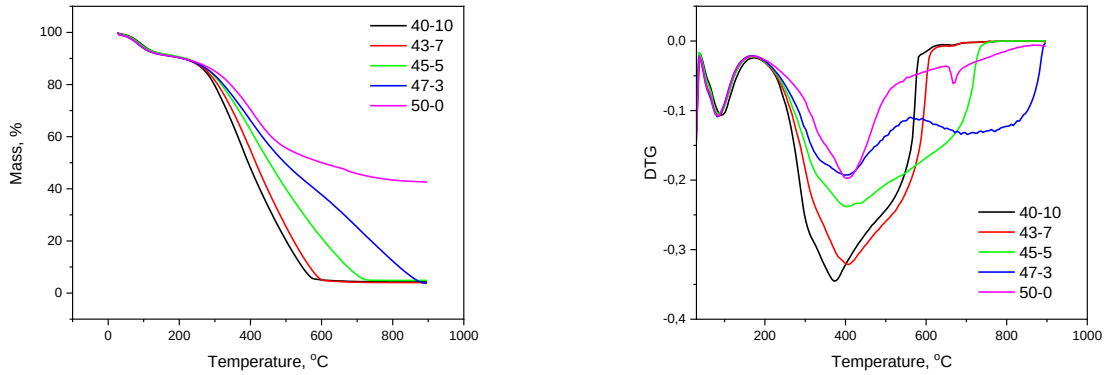

Fig.1. *TG and DTG curves of brown coal samples in nitrogen-oxygen atmosphere (Numbers indicate the nitrogen/oxygen flow rates.).*

Non-isothermal thermogravimetry (TG) was applied for determining chemical kinetic parameters in coal combustion. Activation energy and the pre-exponential factor were determined considering first order Arrhenius' kinetics. The pyrolysis experiments for coal samples were performed on Thermo-Gravimetric Analyzer (TG 209 F1 Libra, NETZSCH). In a typical run, 5±0.2 mg samples were used to carry out experiments at the heating rates of 10, 15, 20 K/min in the temperature range of 25°C to 900°C in a N_2 atmosphere (99.99% pure) at a constant flow rate of 50 mL/min. Before each experiment, the sample was further ground to a smaller size to eliminate the influence of thermal effects on the TG measurements. In the combustion experiments synthetic air atmospheres were used. To investigate the oxidation process, measurements were carried out in an air atmosphere with different oxygen contents (0, 6, 10, 14, and 20%) at a heating rate of 10 K/min and at a constant flow rate of 50 mL/min.

The study of changes in the chemical composition of coal particles during heat treatment is relevant and interesting for mathematical models' development to describe the combustion of organic solid-phase fuels and multifuels systems. Moreover, it could be useful for a deeper understanding of the conditions for fabricating coal-based sorbents with improved properties.

This work was supported financially by the Ministry of Science and Higher Education of the Russian Federation (project №075-15-2020-806).

REFERENCES

[1] I. Glassman, R. A.Yetter, N. G.Glumac, Combustion, fifth ed., Chapter 9 - Combustion of nonvolatile fuels, pp. 477-536, 2015.

[2] H. Zhu, K. Sheng, Y. Zhang, S. Fang, Y.Wu, "The stage analysis and countermeasures of coal spontaneous combustion based on "five stages" division", PLoS ONE 13(8): e0202724, 2018.

N2-O-031501

UTILIZATION OF SYNGAS-FUELED ROTARY ENGINE FOR REMOTE POWER GENERATION*

S.D. ZAMBALOV[1]

[1]*Tomsk Scientific Center SB RAS, Tomsk, Russian Federation*

Reciprocating internal combustion engines represent well-established technology of syngas utilization for decentralized energy generation [1,2]. In this study the possibilities of the rotary engine fueled by syngas, produced on a large scale from various feedstocks by mature technologies were investigated. The four technologies of syngas production were chosen in order to understand the suitability of syngas in rotary engines. The catalytic steam methane reforming (Syn 1) and non-catalytic partial oxidation (Syn 3) are considered since the natural gas is the dominant feedstock for the industrial production of syngas. The syngases produced from biomass (Syn 4) and coal (Syn 2) through gasification are also investigated. The three-dimensional simulation of working progress in the engine was based on the finite volume method.

The temperature distribution in combustion chamber for different fuels at stoichiometric conditions was shown in Fig. 1. The common complex structure with asymmetric large-scale vortex near to the side housing of the engine (green lines) can be revealed.

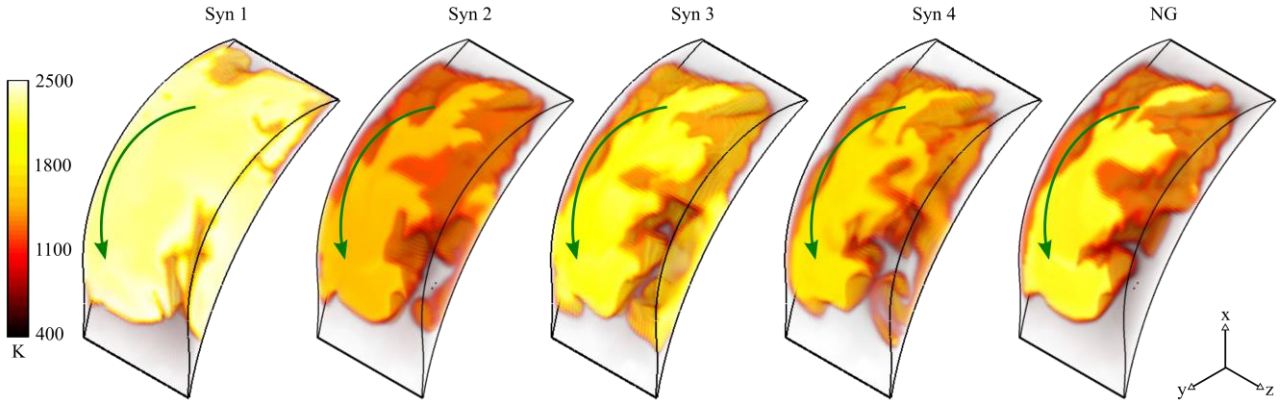

Fig.1. Temperature distributions in combustion chamber of rotary engine.

It was shown that employment of syngas in the energy sector could provide a solid basis for a circular self-sustaining economy and have important social and economic implications. The rotary engine with Syn 1 is expected to have high power characteristics due to high hydrogen concentration, as well as the possible NO_X emission due to high combustion temperature. The engine performance fueled by Syn 2 is expected lower in comparison with Syn 1 fueling as a consequence of lower hydrogen content. Also, the carbon dioxide dilution can result in high CO_2 emission compared to other syngas types. The syngases produced with an air gasifying agent are expected to provide similar power and emission characteristics. Nitrogen addition and lower H_2 concentration in syngas produced from natural gas by non-catalytic partial oxidation and syngas produced by biomass gasification have an inhibiting effect on efficiency with a drastic decrease at lean conditions.

The use of syngas in a rotary engine can be considered as a valid method of electricity, power and heat production. The choice of appropriate production technology depends on the local availability of resources without excessive transportation costs. Syngas power generation system can provide environmental sustainability to the industry and reduce the external demand of energy carriers. The results of this work can be useful for further optimization to work with various types of syngas.

REFERENCES

[1] M. Fiore, “Internal combustion engines powered by syngas: A review,” Appl. Energy, vol. 276, 2020.

[2] J. Arroyo, F. Moreno, M. Munoz, C. Monne, N. Bernal, “Combustion behavior of a spark ignition engine fueled with synthetic gases derived from biogas,” Fuel, vol. 177, 2014

* The work was supported by Russian Science Foundation according to the research project №21-79-00170, https://rscf.ru/en/project/21-79-00170/.

N2-O-031502

ANALYSIS OF COMBUSTION, PERFORMANCE AND EMISSIONS OF SYNGAS-FUELED ROTARY ENGINE WITH DUAL INJECTION*

S.D. ZAMBALOV[1]

[1]*Tomsk Scientific Center SB RAS, Tomsk, Russian Federation*

Synthesis gas (syngas) can be considered as a potential replacement of fossil fuels in transportation and energy production sector [1]. Reciprocating internal combustion engines represent well-known technology of syngas application. The promising technology for efficient utilization of syngas is dual injection that comprise advantages of port fuel injection and direct injection [2]. In this study syngas of 50% H_2: 50% CO_2 by volume is considered as a main fuel for rotary engine. The three-dimensional simulation of the air-fuel mixture formation and combustion processes in the rotary engine was based on the finite volume method.

The engine configuration with proposed fuel injection system was shown in Fig. 1. The location of the injector was adapted from research works devoted to investigation of the port fuel injections and direct injections in rotary engines [3,4]

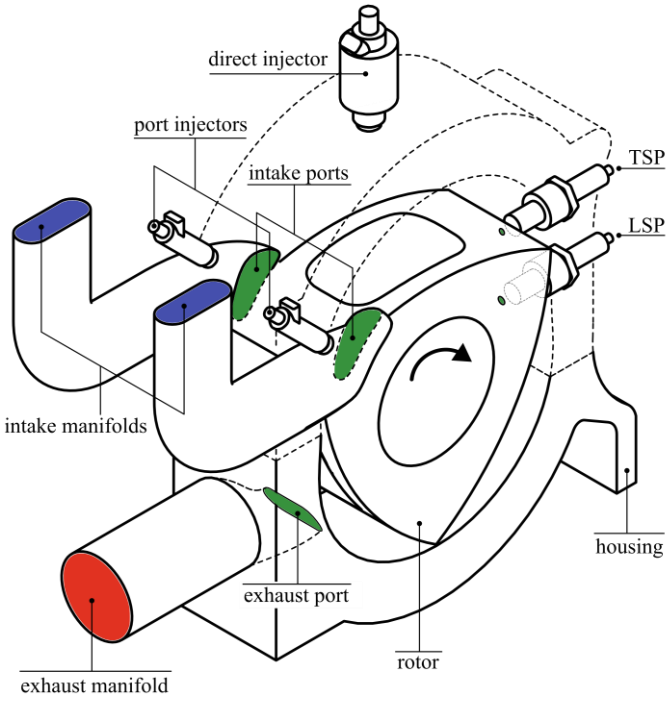

Fig.1. Rotary engine with dual injection system.

The use of dual injection system in a rotary engine can be considered as an effective and efficient method to use syngas in rotary engine with spark ignition. The dual injection technology provide flexibility in the control of air-fuel mixture formation process. The results of this work can be useful for further optimization of the rotary engine.

REFERENCES

[1] M. Fiore, “Internal combustion engines powered by syngas: A review,” Appl. Energy, vol. 276, 2020.

[2] Y. Huang, N. Surawski, Y. Zhuang, “Dual injection: An effective and efficient technology to use renewable fuels in spark-ignition engines,” Renewable and Sustainable Energy Reviews, vol. 143, 2021

[3] M. Ohkubo, S. Tashima, R. Shimizu “Developed Technologies of the New Rotary engine (Renesis),” SAE Technical Paper, vol. 1790, 2004

[4] Y. Hasegawa, K. Yamaguchi “An experimental investigation on air-fuel mixture formation inside a low-pressure direct injection stratified charge rotary engine,” SAE Technical Paper, vol. 930678, 1993

* The work was supported by Russian Science Foundation according to the research project №21-79-00170, https://rscf.ru/en/project/21-79-00170/.

EFFICIENT NUMERICAL METHOD TO INTEGRATE MULTI-WELL MASTER EQUATION FOR CHEMICAL RACTION RATES ESTIMATION*

VIATCHESLAV BYKOV[1] AND ANDREY KOKSHAROV[2]

[1]Karlsruhe Institute of Technology, Institute of Technical Thermodynamics, Engelbert-Arnold-Strasse 4, Geb.10.91, 76131 Karlsruhe, Germany
[2]German Aerospace Center (DLR), Stuttgart, Germany

Chemical Master Equation (CME) approach can be efficiently used to evaluate rate coefficients of elementary chemical reactions on the level of molecular dynamics [1]. However, conventional methods to handle this problem especially for multi-well systems remain rather empirical and are computationally demanding [2]. The conventional method leads to a coupled linear but highly dimensional systems of equations, which are employed to delineate estimations for elementary reactions rates [2,3].

In this study a quasi-spectral method to integrate single-, multi-well CMEs systems will be presented [3]. For given reactions system CMEs are integrated such that the evolution over the whole energy range of entire populations of the species involved can be determined. The latter can be used to define the rates of elementary reactions in a systematic manner. We present a method to estimate reaction rate constants by solving inverse problem for rates of a phenomenological model. The suggested approach is illustrated by the problem of the allene isomerization into propyne through cylcopropene. The comparison of the conventional method and the proposed method will be presented demonstrating performance and to validate the suggested approach to compute the chemical reaction rates.

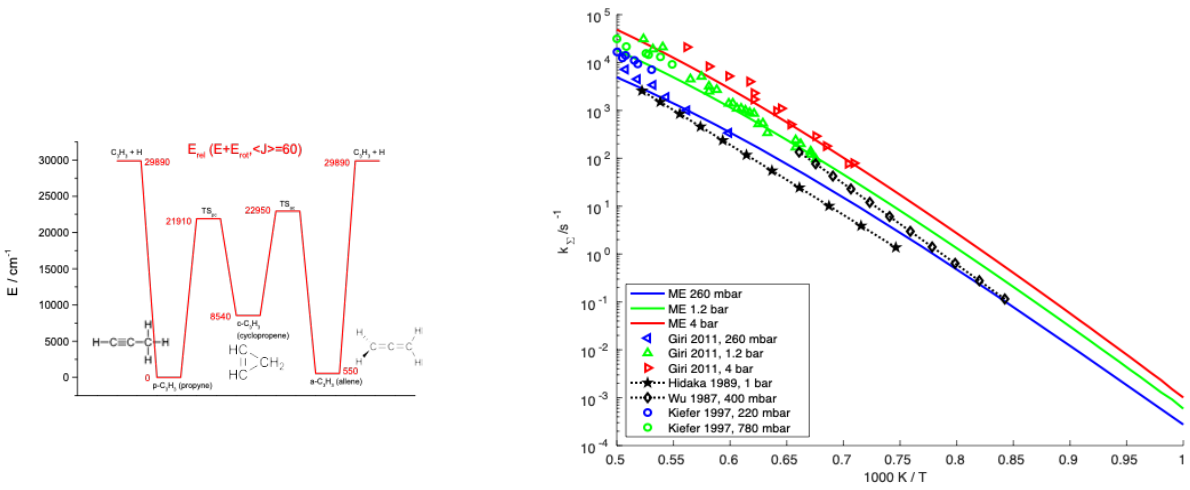

Fig.1. Left: Schematic potential energy diagram of the allene-propyne isomerization; Right: Comparison of the alyne decomposition rate for different pressures as function if the initial temperatures.

Figure 1 on the left shows schematically the energy wells for allene, propyne and cylcopropene correspondingly. The reaction rates are computed by using the detailed solution of the CME [3,4]. The detailed solution of the species population over energies evolving in time [4] is then used to estimate the kinetic parameters of the phenomenological model. The latter is applied to describe the concentration (mass of the population) evolving in time. This way the results of the detailed evolution are fitted to the mode which is based on the mass action and Arrhenius laws. The rates of these elementary reactions are compared to experiments and shown on the right of Fig. 1.

REFERENCES

[1] Gilbert, R. G.; Smith, S. C. Theory of Unimolecular and Recombination Reactions; Blackwell: Oxford, UK, 1990.

[2] Miller, J. A.; Klippenstein, S. J. J Phys Chem A, 110 (2006) 10528–10544.

[3] Kiefer, J. H., S. S. Kumaran und P. S. Mudipalli, Chemical physics letters, 224(1-2) (1994) 51–55.

[4] Koksharov et al, Quasi-Spectral Method for the Solution of the Master Equation for Unimolecular Reaction Systems, International Journal of Chemical Kinetics 50(5) (2018) 357-369.

* The work was supported by the DFG-TRR 150 project, project number: 237267381.

N2-O-038501

BEHAVIOR OF PREMIXED STRETCHED FLAMES IN PLANAR CHANNEL*

S.N. MOKRIN[1,2], V.V. GUBERNOV[2], S.S. MINAEV[2,3]

[1]Far Eastern Federal University, Vladivostok, Russia
[2]P.N. Lebedev Physical Institute RAS, Moscow, Russia
[3]Institute of Applied Mathematics FEB RAS, Vladivostok, Russia

Experimental studies of low stretched flames require the microgravity conditions due to the significant effect of natural convection on the flame. This restriction forces the use of expensive experimental facilities. In recent studies [1, 2], an experimental setup allowing to reduce the natural convection effect on flame was proposed and it makes possible study low stretched flames under normal gravity conditions. The countercurrent flames in these papers were stabilized inside a flat microchannel. In present study, we proposed an experimental setup to study a low stretched flame stabilized near heated wall. The aim of the work was to establish the effect of a heated wall on the normal speed and flame extinction limit.

A lean (ϕ=0.6 and ϕ=0.7) methane-air stretched flames were investigated in experiment. The stretch rate was determined as the ratio of fresh mixture velocity at the burner outlet to the distance from the edge of the burner and heated wall. The average temperature along the heated wall was 1000±20 K and 1200±25 K, respectively. Location of the flame front was determined by averaging of blue signal peaks along the flame front line at a distance of ±1 cm from the burner's symmetry axis. For each experimental point, five images were taken, the data from which were averaged and the corresponding errors were determined.

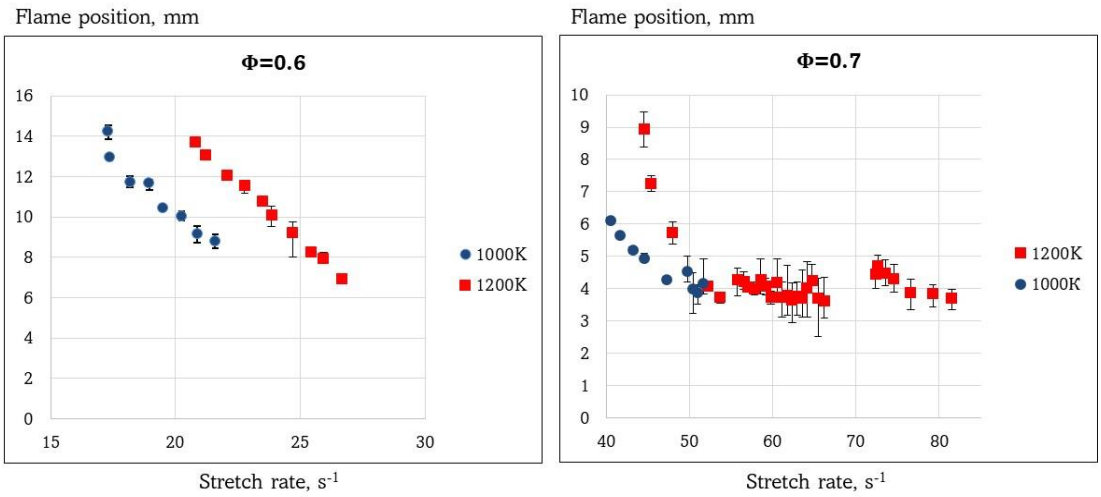

Fig.1. Dependency of flame location on stretch rate for different equivalence ratios and wall temperatures

Fig. 1 shows the dependences of flame front location on stretch rate obtained from the experiment. The experimental data clearly shows that a decreasing the wall temperature leads to a narrowing of the flame extinction limit. In addition, the experiment shows a significant difference from works [3, 4], in which the distance between the flames tended to zero and there was a critical value of stretch rate at which the flames collapsed. One of the explanations of this phenomena may be the fact that the selected wall temperatures were “relatively” low, and thus an additional heat loss from the reaction zone appeared in the system, which led to early quenching.

REFERENCES

[1] M.J. Lee et al, “Characteristics of opposed flow partially premixed flames in mesoscale channels at low strain rates”, Proceedings of the Combustion Institute, vol. 35 (3), pp. 3439–3446, 2015

[2] S. Mokrin et al, “Flammability limit of moderate- and low-stretched premixed flames stabilized in planar channel”, Combustion and Flame, vol. 185, pp. 261–264, 2017.

[3] K. Maruta et al, “Experimental study on methane-air premixed flame extinction at small stretch rates in microgravity”, Symposium (International) on Combustion, vol. 26, pp. 1283–1289, 1996.

[4] H. Guo et al, “Radiation Extinction Limit of Counterflow Premixed Lean Methane-Air Flames”, Combustion and Flame, vol. 109, pp. 639–646, 1997.

* The work was supported by the Russian Science Foundation (project #21-13-00434)

N2-O-040304

SHS OF POROUS NI-AL ALLOYS IN A REACTION MEDIUM WITH A FLUID-FORMING COMPONENT*

A.I. KIRDYASHKIN, V.D. KITLER, R.M. GABBASOV

Tomsk Scientific Center SB RAS, Tomsk, Russia

The SHS process is one of the most economical technologies for producing porous Ni-Al alloys with a wide range of phase composition ($NiAl \div Ni_3Al$) and transport pore size (0.01÷2mm). Such materials are of great practical interest when used in corrosion-resistant filters, catalysts, solid oxide fuel cells, and heat-resistant radiation burners. The synthesis of the most coarsely porous alloys is carried out in the presence of fluid-forming components of the reaction system, such as $CaCO_3$, $Ca(OH)_2$. Fluid formers (F) simultaneously act as a melting point for refractory oxide impurities and as a system gas source. The detailed mechanism of action of the F-components has not been fully elucidated.

In this work, a comprehensive study of the structural-thermal dynamics of the synthesis of materials during the propagation of the SHS wave in highly porous Ni-Al powder mixtures with an F-component was carried out. A wide range of experimental methods has been applied, including high-speed video filming with laser illumination, thermocouple and pyrometric measurements, quenching of reaction processes and physicochemical analysis of synthesis products.

Using the example of the compositions $(Ni+20wt\%Al)+xCaCO_3$, the main features of the reaction

* At x = 0, the formation of the target alloy proceeds through successive stages:

1 – nucleation of primary alloy particles (≈ 0.1 mm) by means of liquid-phase reaction coalescence of powder components in the fixed preheating layer of the mixture (≈ 0.2 mm);

2 - sintering of primary particles into a finely porous skeleton of the final product;

** At x > 0, the preheating layer of the powder mixture passes into a pseudo-boiling state and expands to 2 mm. Pseudo-boiling of the system is stimulated by the primary particles of the alloy, which are generated in the upper part of the layer, move deep into the mixture and cause thermal gasification of the F-component. The reason for particle motion is capillary drift associated with exothermic reactions on the particle surface. After incubation cycles lasting up to 1 s, explosive agglomeration of the mixture and primary particles periodically occurs with the formation of secondary alloy particles up to 2 mm in size. The latter are sintered into a large-pore skeleton. The internal structure of the material has characteristic cells formed by the boundaries of primary particles. In the course of explosive agglomeration, pulsed heating of particles is observed with the achievement of a temperature that can exceed the base combustion temperature by 250°C. With an increase in the concentration of the F-component and the initial porosity of the system, the amplitude of explosive heating and the size of the secondary particles of the alloy increase.

The data obtained expand the existing understanding of the mechanisms of SHS, as well as complement the ways to control and modify the properties of the synthesized alloys for practical applications.

* The work was supported by the Russian Science Foundation under grant No. 21-79-10445.

N2-O-040701

NUMERICAL STUDY OF THE FUEL DROPLETS EFFECT ON COMBUSTION PROCESSES UNDER CONDITIONS TYPICAL FOR HYBRID ROCKET ENGINES

V.A. KOSYAKOV[1,2], *R.V. FURSENKO*[1]

[1]Khristianovich Institute of Theoretical and Applied Mechanics SB RAS, Novosibirsk, Russia
[2]Novosibirsk State Technical University, Novosibirsk, Russia

The study of hybrid rocket engines in the era of orbital and suborbital flights has become more relevant than ever. This type of engines has several advantages over liquid and solid propellant rocket engines. The main disadvantage of such motors is their low specific thrust impulse. The usage of the low-melting fuels with low viscosity is considered as a promising way to solve this problem. In this case the fuel droplets from the liquid layer formed on the solid fuel surface are involved into the oxidizer stream due to the near wall shear layer instability [1,2]. In this work, the influence of the liquid fuel droplets on the combustion characteristics of a diffusion flame stabilized in the boundary layer of a high-speed oxidizer flow is studied. As a result of numerical simulations, two-dimensional distributions of characteristics were obtained of the oxidizer and gaseous fuel, droplet sizes and their number concentrations. Depending on the position of the droplet and its size, the local temperature near it decreases in the range from ≈50 K to ≈ 800 K (Fig.1).

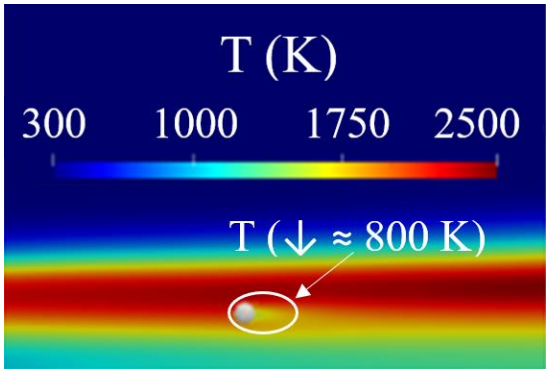

Fig.1. Two-dimensional temperature distribution. Initial droplet size 200 μm.

Depending on the size of the droplets, the characteristics of the system are changed. Thus, at small droplet sizes of ~50 μm, the liquid fuel evaporates completely. With an increase in the diameter of liquid fuel droplets, the evaporation fraction decreases and for droplets with a diameter of 100 μm, 150 μm, and 200 μm, it averages 0.9, 0.76, and 0.63, respectively.

If the ratio of the volume of droplets to the volume of gas in the system does not exceed 10^{-3}, then the quantitative concentration of droplets does not affect the fraction of droplet evaporation. For example, for 150 μm diameter droplets, the evaporation fraction for different number concentrations ranges from 0.76 to 0.77.

The effect of liquid fuel droplets on the diffusion flame stabilized in a boundary layer of a high-speed oxidizer flow consists in a local decrease of the gas temperature near the droplets, which also leads to a global decrease in the temperature of the flame front, as well as to its narrowing. An additional influx of gaseous fuel, as a result of droplet evaporation, leads to an increase in the gas temperature in the area under the flame front.

REFERENCES

[1] Giuseppe Leccese, Daniele Bianchi, Francesco Nasuti., “Modeling and Simulation of Paraffin–Based Hybrid Rocket Internal Ballistics”, AIAA Propulsion and Energy 2018.

[2] Giuseppe Leccese, Enrico Cavallini, Marco Pizzarelli., “State of Art and Current Challenges of the Paraffin–Based Hybrid Rocket Technology”, AIAA Propulsion and Energy 2019.

N2-O-042802

DIFFUSIVE-THERMAL INSTABILITIES OF THE BURNER STABILIZED METHANE-HYDROGEN AIR FLAMES

A.D. MOROSHKINA, V.V. MISLAVSKII, V.V. GUBERNOV

P.N. Lebedev Physical Institute RAS, Moscow, Russian Federation

In this work we report our recent results on the analysis of the diffusive-thermal instabilities of the burner stabilized methane-hydrogen-air flames The investigation is undertaken by means of (a) the direct numerical simulation of combustion wave dynamics by using the mathematical model with the detailed reaction mechanism and (b) experimental study of the chemiluminiscence and LIF of OH* radicals. The methodology is described in detail in [1,2]. The typical configuration used in experiments is shown in figure 1.

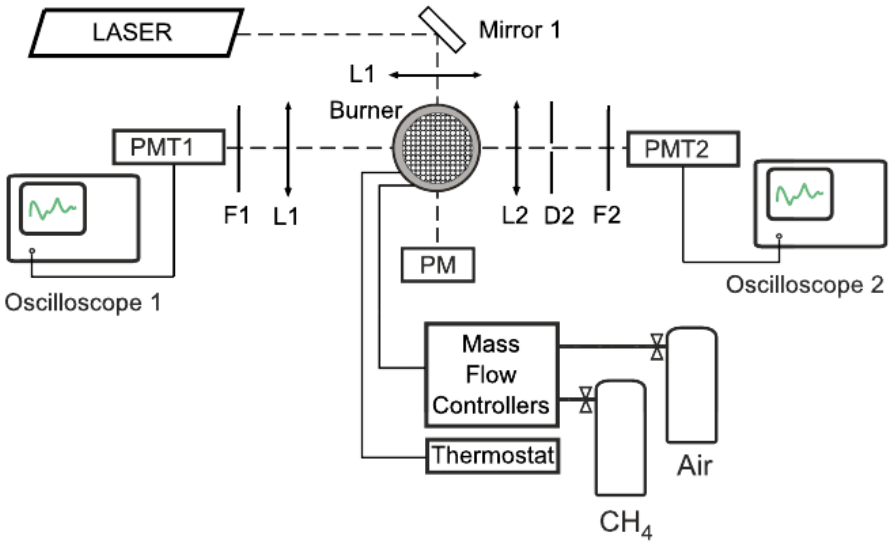

Fig. 1. The scheme of experimental setup.

The results obtained by various approaches are compared and it is demonstrated that the difference between the numerical data calculated with different reaction mechanisms is greater then the experimental uncertainty, demonstrating that the proposed technique can be used to verify the reaction mechanisms. The prospects of further work is discussed.

REFERENCES

[1] Mislavskii, V., Pestovskii, N., Tskhai, S., Kichatov, B., Gubernov, V., Bykov, V., & Maas, U. (2021). Diffusive-thermal pulsations of burner stabilized methane-air flames. *Combustion and Flame*, *234*, 111638.

[2] Nechipurenko, S., Miroshnichenko, T., Pestovskii, N., Tskhai, S., Kichatov, B., Gubernov, V., ... & Maas, U. (2020). Experimental observation of diffusive-thermal oscillations of burner stabilized methane-air flames. *Combustion and Flame*, *213*, 202-210.

N2-O-043901

DETERMINATION OF THE PARAMETERS OF GLOBAL CHEMICAL KINETICS MECHANISMS USING OPTIMIZATION METHODS

A.D. ZAKHAROV, R.V. FURSENKO

Khristianovich Institute of Theoretical and Applied Mechanics SB RAS, Novosibirsk, Russia

In the paper, an optimization approach to determining global chemical reaction rate constants is proposed. This method allows to select reaction rate parameters (i.e. activation energy, preexponential factor, etc.) on the basis of experimental data or simulations with detailed reaction mechanisms. Computer program implementing proposed method was developed and the features of the application and operation of the optimization approach were investigated.

Although the optimization method can be applied to any reacting system, in this paper the methane-air combustion is considered. Reaction mechanisms are compared by the laminar burning velocity of the premixed flames and the species concentration profiles of the counterflow diffusion flames. To determine the reaction rate constants of global mechanisms, we use an optimization algorithm, which consists in minimizing the deviation between the chosen flame characteristics obtained using a global mechanism and the reference values of these characteristics. Thus, in the case of one flame characteristic (e.g. laminar burning velocity) the following function is subject to minimization:

$$\mathrm{Err} = \sqrt{\sum_i^n (\mathrm{F_i} - \mathrm{F_{GRI-mech\ 3.0_i}})^2}\,, \qquad (1)$$

Where n is the number of different parameter values at which chosen characteristic was calculated, $\mathrm{F_i}$ and $\mathrm{F_{GRI-mech\ 3.0_i}}$ are the characteristic values for the i–th set of parameters calculated using global and detailed GRI-mech 3.0 [1] mechanisms, respectively.

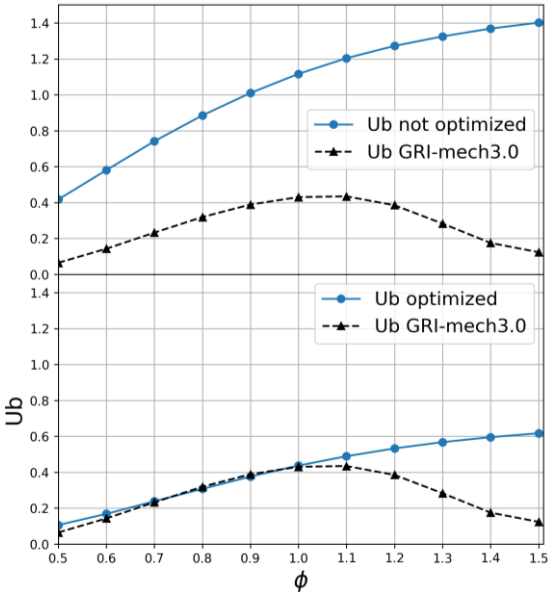

Fig.1. Normal flame velocity before (top) and after (bottom) optimization.

The figure shows a graph of Ub(ϕ), where Ub - laminar burning velocity, ϕ - equivalence ratio. The selected characteristic is calculated with the determined values of the activation energy and the pre-exponential factor in the Arrhenius equation. These parameters are optimized by the algorithm.

It can be concluded that optimization methods are applicable to solve the problems of determination of optimal reaction rate parameters of global mechanisms, providing the best fitting of chosen flame characteristic. Examples of optimization algorithm application for determination of reaction rate constants of one-, two- and four-step mechanisms are presented. The possibility of multi-aim parameters optimization by several characteristics was also investigated and confirmed. It was found that the solution does not have uniqueness, and this fact was confirmed using the brute force method.

REFERENCES

[1] G.P. Smith, D.M. Golden, M. Frenklach, et al. Available at http://www.me.berkeley.edu/gri_mech/.

N2-O-046501

NUMERICAL STUDY OF THE COMBUSTION FRONT PROPAGATION FEATURES IN GAS MIXTURES WITH LOW LEWIS NUMBERS*

E.V. SERESHCHENKO[1,2], *R.V. FURSENKO*[1], *S.S. MINAEV*[2]

[1]*Khristianovich Institute of Theoretical and Applied Mechanics SB RAS, Novosibirsk, Russia*
[2]*P.N. Lebedev Physical Institute RAS, Moscow, Russia*

In the last decade, there are a trend towards a transition to the ecofriendly technologies, more sparing to the environment. Examples of such promising technologies are the methods of lean hydrocarbon fuels burning and the transition to hydrogen power. Dilution of lean hydrocarbon fuels with hydrogen can increase flammability limits and efficiency, as well as reduce emissions. In this regard, the study of the combustion of lean gas mixtures with a low Lewis numbers is a relevant task.

The present study is devoted to a numerical study of the combustion front propagation dynamics of a premixed gas mixture in straight channels, as well as of a spherical diffusion flame in the framework of a three-dimensional reaction-diffusion models. In both cases, mixtures with a low Lewis numbers are considered. Numerical results shown that the combustion wave can be a continuous cellular front and sporadic flames (see Fig. 1). For the case of sporadic combustion wave consisting of sets of individual flame spots, a method for determining the propagation velocity of a flame front is proposed. The dependences of the propagation velocity of a sporadic combustion wave, the concentration of residual fuel, and the number of flame spots are obtained as functions of the channel size, mass flow rate, and radiative heat losses h. The continuous flame fronts are formed at small h whereas at large h it consists of separate cup-like flames.

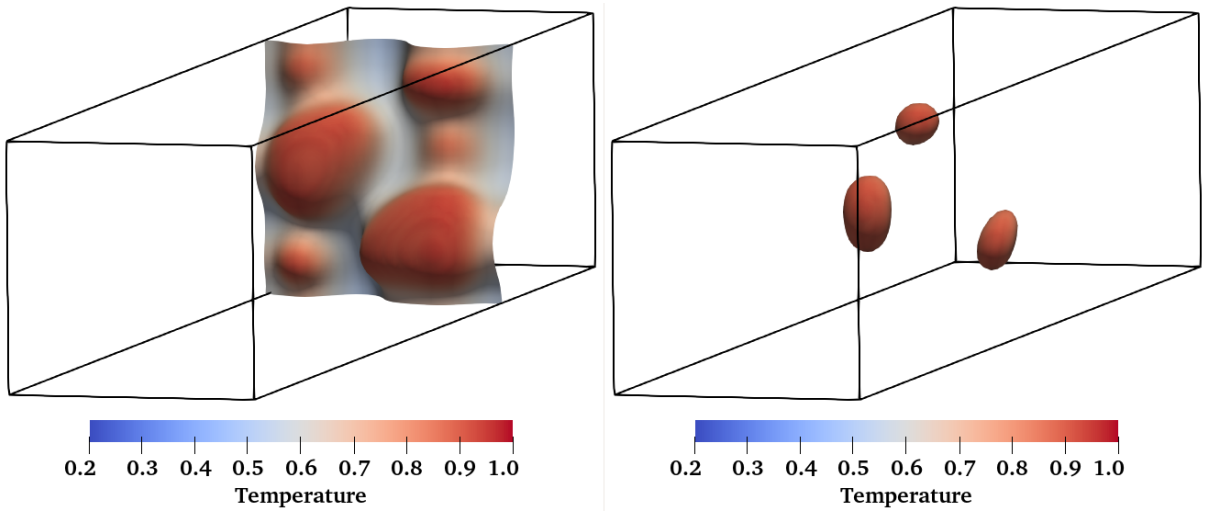

Fig.1. Isosurfaces of the concentration C=0.1 colored according to the gas temperature and illustrating the surface of the reaction front in straight channels: continuous cellular flame front (on the left) and sporadic combustion wave (on the right).

Analysis of the numerical results shown the existence of a special transverse channel size D^*, starting from which, as the channel size increases, the number of flame spots increases in proportion to the increase in the transverse channel size area. This critical diameter D^* is proportional to the radiative heat loss intensity h which is characterized by the mixture equivalence ratio. Thus, the presence of a universal size of flame spots is shown, which for its existence requires a certain area around it filled with a fresh mixture. It is also numerically shown that the dynamics of combustion wave does not depend on the geometry of the channel inlet section and is determined by its area. Solution of this fundamental problem is important for the development of eco-friendly lean gas combustion technologies and energy saving.

* The work was supported by the Russian Science Foundation (project no. 21-13-00434). The numerical simulations were carried out using the supercomputer facilities of the Equipment Sharing Center "Mechanics" of ITAM SB RAS.

N2-O-047301

NUMERICAL MODELING OF FILTRATION GAS COMBUSTION IN A CYLINDRICAL RADIATION BURNER WITH AXIAL GAS FLOW*

E.P. DATS[1,2], *S.S. MINAEV*[3]

[1]*Institute of Applied Mathematics FEB RAS, Vladivostok, Russia*
[2]*Vladivostok State University of Economics and Service, Vladivostok, Russia*
[3]*Far Eastern Federal University, Vladivostok, Russia*

The filtrational gas combustion in a chemically inert porous media allows create an intensive radiative heat fluxes compared with radiation from free flame. Other advantages of filtrational gas combustion burners over combustion systems with free flame are the higher burning rates, increased power dynamic range, extension of the lean flammability limits, and the low emissions of pollutants. The reviews on this interesting topic one can find in [1-8]. Extensive experimental and numerical works were carried out and are still underway, to explore the feasibility of porous burners with filtrational gas combustion for energy production and others applications. Porous radiation burners are promising for creating sources of thermal radiation with controlled power, spectrum and distribution of radiation density for contactless heating of workpieces or materials in industrial processes. The porous radiant burners potentially can be applied in those technical processes where electrical heat sources are used. It can significantly increase production efficiency due to the absence of the electricity generation stage from energy produced by combustion and the transmission electricity losses. Another advantage of porous radiant burners is the insensitivity to the electromagnetic interference and the absence of open flames, reduction of accidents when using lean mixtures, as well as stability of operation and protection from external influences, which is ensured by the gas combustion occurring inside the burner's porous body.

Combustion in a porous cylindrical tube with axial injection of combustible mixture was studied. This configuration can be potentially used as new type of heater for the contactless heating of materials in industrial processes. The material under treatment is placed inside the cylindrical porous tube and is heating by radiative flux from the cylindrical tube wall. The calculation of combustion in a porous cylindrical burner is carried out within the framework of a two-temperature thermo-diffusion model [1,3] taking into account the gas filtration effects described by Darcy's law. We represent combustion in a porous medium with a two-dimensional model that includes one-step Arrhenius type chemistry, radiative heat losses from the inner surface of hollow cylindrical burner, separate gas and solid energy equations and the transport of fuel concentration of the combustible lean mixture. Numerical modeling allowed to estimate the range of gas flow rates at which stable combustion regimes exist, to find the temperature distribution in the gas and the porous body, and to evaluate the radiation fluxes inside the reactor. It was shown that stable combustion can take place in a certain range of pressure drops and radiation heat losses on the inner surface. High levels of radiative heat fluxes and wide range of operation condition with stable combustion shown feasibility application of this type of porous burner for contactless treatment of different materials.

REFERENCES

[1] Howell J.R., Hall M.J., Ellzey J.L., Combustion of hydrocarbon fuels within porous inert media. Prog Energy Combust Sci 1996;22(2):121-145.

[2] Trimis D, Durst F. Combustion in a porous medium - advances and applications. Combust Sci Technol 1996;121(1-6):153-168.

[3] L. Kennedy, A. Fridman, A. Saveliev, Superadiabatic combustion in porous media: Wave propagation, instabilities, new type of chemical reactor, International Journal of Fluid Mechanics Research 22 (2) (1996) 1–26.

[4] Oliveria A.A.M., Kaviani M. Nonequilibrium in the transport of heat and reactants during combustion in porous media. Prog. Energy Combust Sci, 2001, 27, pp.523-545.

[5] Mohamad A.A. Combustion in porous media: fundamentals and applications. Transport phenomena in porous media III; 2005, pp. 287-304.

[6] Kamal M.M., Mohamad A.A. Combustion in porous media, a review. J Power Energy 2006, 220(5):487-508.

[7] Pantangi V.K., Mishra S.C. Combustion of gaseous hydrocarbon fuels within porous media - a review, Advances in Energy Research (AER - 2006), pp. 455-461.

[8] Wood S., Harris A.T. Porous burners for lean-burn applications. Prog. Energy Combust Sci. 2008; 34: 667-684.

* This work was financially supported by the Ministry of Science and Higher Education of the Russian Federation (project No. 075-15-2020-806).

N2-P-004302

AN ASSESSMENT OF THE SELF-ASPIRATING CONCEPT OF LEAN MIXTURE SUPPLY FOR RADIANT BURNERS OPERATING IN THE INTERNAL COMBUSTION MODE*

A. MAZNOY

Tomsk Scientific Center SB RAS, 10/4 Akademicheskii pr., Tomsk, 634055, Russia, maznoy_a@mail.ru, +79234124765

During the last decade, thin-shell radiant burners [1-3] made of porous SHS-intermetallics [4,5] have been developing in TSC SB RAS. There are exactly two options on how all the air needed for premixed lean combustion could inflow into the reaction zone: (*i*) the concept of forced air supply using an adjustable electrical blower, and (*ii*) the self-aspirating concept using a simple combination of single-hole nozzle injector and venturi-like mixing tube. The latter method is of interest because no electricity supply is required for IR heater operation. In the self-aspirating concept, the high-speed jet of fuel entrains the air directly into the burner by following the Bernoulli principle. A venturi geometry of pipe is required to mix a fuel jet with entrained air before the gas mixture reaches a combustion zone. Typically, a combination of proper nozzle parameters and geometry of venturi tube provides sufficient air-entrainment, especially at a low firing rate. However, this method of fresh mixture supply has never been described in the literature for radiant burners operated in the internal combustion mode. The experiments have proven that the self-aspirating approach is suitable for the lean combustion of LPG and natural gas (Fig.1). My presentation will be focused on the first results and prospects of applying the self-aspirating concept for radiant burners operated in the internal combustion mode.

Fig.1. Image of IR heater based on self-aspirated radiant burner operated in the internal combustion mode.

REFERENCES

[1] A. Maznoy, A. Kirdyashkin, S. Minaev, A. Markov, N. Pichugin, E. Yakovlev, "A study on the effects of porous structure on the environmental and radiative characteristics of cylindrical Ni-Al burners," Energy. vol. 160, pp. 399–409. October 2018.

[2] A. Maznoy, A. Kirdyashkin, N. Pichugin, S. Zambalov, D. Petrov, "Development of a new infrared heater based on an annular cylindrical radiant burner for direct heating applications," Energy. vol. 204, no. 117965. August 2020.

[3] A. Maznoy, N. Pichugin, I. Yakovlev, R. Fursenko, D. Petrov, S.S. Shy, "Fuel Interchangeability for Lean Premixed Combustion in Cylindrical Radiant Burner Operated in the Internal Combustion Mode," Appl. Therm. Eng. vol. 186, no. 115997. March 2021.

[4] A. Maznoy, A. Kirdyashkin, V. Kitler, N. Pichugin, V. Salamatov, K. Tcoi, "Self-propagating high-temperature synthesis of macroporous B2+$L1_2$ Ni-Al intermetallics used in cylindrical radiant burners," J. Alloys Compd. vol. 792, pp. 561–573, July 2019.

[5] N. Pichugin, A. Kirdyashkin, V. Kitler, A. Maznoy, "The effect of separating layer between reacting media and molding template on the porous structure of combustion synthesized Ni-Al intermetallics," Mater. Lett. vol. 314, no. 131854. May 2022.

* The research was funded by Tomsk Scientific Center

N2-P-024304

THERMAL EXPLOSION IN A 3NI+AL POWDER MIXTURE PRELIMINARY ACTIVATED IN A LOW-POWER MILL

O.V. LAPSHIN[1], E.N. BOYANGIN[1]

[1]Tomsk Scientific Center, Russia

Mechanical activation (MA) of a reaction system is an effective method to control a chemical transformation. Despite the long-term practical use of MA, the consistent study of mechanochemical reactions was developed only in the 20th century. The reason for this is the complexity of the phenomenon, the study of which requires knowledge of the physics, chemistry, and mechanics of condensed matter. Another reason is the lack of reliable and accurate tools and techniques for the direct study of chemical reactions under conditions of intense dynamic loads. Therefore, most of the current knowledge about mechanochemical reactions has been obtained indirectly. At present, the mechanical method of activation of chemical transformations is used to stimulate various solid-phase reactions [1–5].

In this work, experimental results are presented that reflect the effect of the parameters of preliminary MA on the temperature-time characteristics of the synthesis of the Ni_3Al intermetallic compound.

It is shown that preliminary MA promotes an increase in the reactivity of the mixture due to the formation of a developed interfacial surface in it and an increase in the reserve of excess energy contained in structural defects. It was also found that the mild conditions of MA of the initial powder mixture in a low-energy mill make it possible to avoid the effects of its deactivation.

REFERENCES

[1] L. Takacs, “The historical development of mechanochemistry”, Chem. Soc. Rev. vol. 42, 7649–7659, 2013.

[2] A.S. Rogachev, “Mechanical activation of heterogeneous exothermic reactions in powder mixtures”, Russ. Chem. Rev., vol. 88, (2019) 875–900, 2019.

[3] O.V. Lapshin, E.V. Boldyreva, V.V. Boldyrev, “Role of mixing and milling in mechanochemistry synthesis (review)”, Russ. J. Inorg. Chem., vol. 66, 433–453, 2021.

[4] B.S.B. Reddy, K. Das, S. Das, “A review on the synthesis of in situ aluminum based composites by thermal, mechanical, and mechanical-thermal activation of chemical reactions”, J. Mater. Sci., vol. 42, 9366–9378, 2007.

[5] F. Delogu, “Activation of self-sustaining high-temperature reactions by mechanical processing of Ti–C powder mixtures”, Scr. Mater., vol. 69 223–226, 2013.

N2-P-040305

FILTRATION COMBUSTION FURNACE FOR HEAT TREATMENT OF REFRACTORY CERAMICS*

R.M. GABBASOV, A.I. KIRDYASHKIN, V.D. KITLER

Tomsk Scientific Center SB RAS, Tomsk, Russia

At present, the development of high-temperature energy-efficient furnaces used for sintering operations is important to reduce the cost of production of products from refractory ceramic materials. In this work, the combustion of premixed fuel mixtures based on natural gas, air, and oxygen was experimentally studied in a prototype of a sintering furnace with the chamber of cylindrical shape which was filled with the packed bed of sphere ceramics. Temperature measurements were carried out using the thermocouple method and spectral pyrometry, which made it possible to provide an absolute error of less than 30 K. Combustion was studied in the range of specific natural gas flow rates from 7 to 107 nl•s $^{-1}$/m^2, fuel-to-oxidizer ratio from 0.40 to 3.30 , oxygen concentration in the oxidizer from 21 to 30 vol.%. In these ranges, temperature control is provided in the range of 1230 – 2220 K. The furnace allows the use of two combustion modes: (1) filtration combustion, when the narrow reaction front (combustion wave) freely propagates through the packed bed, (2) jet-stabilized combustion when the reaction front is aerodynamically stabilized by inlet nozzles used for supplying the fresh mixture into the packed bed. In the filtration combustion mode, the motion of the combustion wave was recorded at a speed of up to 0.1 mm/s in both upstream and downstream directions. The temperature of the packed bed increases with specific fuel consumption, and depends strongly non-linearly on the equivalence ratio. Forced gas-dynamic stabilization of the combustion wave near the flame trap makes it possible to increase the temperature of the packed bed by 100 – 300 K.

Test sintering of powder samples from magnesium oxide, aluminum oxide, and $MgAl_2O_4$ spinel was carried out at a temperature of 2170 K. It has been established that sintering in the filtration combustion mode is effective for obtaining products with a characteristic size of up to 10 mm. This sintering mode can be used to produce ceramic abrasive particles, thermal insulating fills, or catalyst carriers. The jet-stabilized combustion mode is effective for sintering large-format products, while immersing powder samples inside the porous inert media saves fuel twice as compared with free placement of the sample in the volume of the high-temperature furnace chamber. The new furnace based on the principles of combustion of gas mixtures in porous inert media will expand the range of technical devices for economical high-temperature sintering of ceramic materials.

N2-P-042902

MEASUREMENT OF ACTIVATION ENERGY OF METHANE-AIR MIXTURE BY THIN-FIBER PYROMETRY*

A.D. MOROSHKINA, V.V. GUBERNOV, V.V. MISLAVSKII

P.N. Lebedev Physical Institute RAS, Moscow, Russian Federation

In this work, activation energy measurements have been carried out for various methane-air mixtures by thin-fiber pyrometry. The experimental installation is a flat porous burner from which a gas mixture flows, a filament of silicon carbide (d=15μm) is placed parallel to the plane of the burner, and a thermal imager OPTRIS PI is used to detect the temperature of the gas. According to the formula [1]

$$M = A \exp\left(-\frac{E_a}{2RT}\right), \quad (1)$$

where M – gas flow rate which was measured by Bronkhost Elflow controllers, E_a – activation energy, T – gas temperature. The temperature of the filament T_f was recalculated to the gas temperature T_g according to the formula [2]

$$T_g = T_f + \frac{\varepsilon\sigma {T_f}^4}{h_c}, \quad (2)$$

where ε – emissivity, σ – Stefan-Boltzmann constant, h_c – the coefficient describing the heat exchange of the filament and the gas.

The results of the experiment are compared with the numerical calculation made within the detailed reaction mechanism model GRI3.0 [3], and they are found to agree within the measurement error.

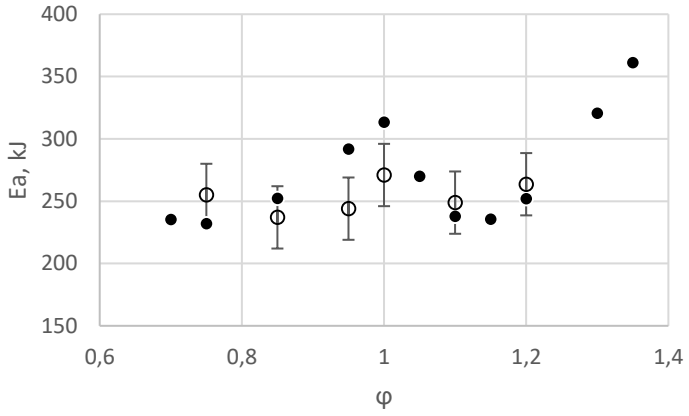

Fig.1. Activation energy for different concentrations of methane in the mixture. Black dots are numerical calculations, white dots are experimental data.

The data were also compared with the literature [4]. The prospects of further investigation are discussed.

REFERENCES

[1] Зельдович Я.Б., Баренблатт Г.И., Либрович В.Б., Г.М. Махвиладзе Г.М., Математическая теория горения и взрыва, М.: Наука, 1980
[2] Vilimpoc, LP Goss, B Sarka, “Spatial temperature-profile measurements by the thin-filament-pyrometry technique,” Optics letters, 1988 - osapublishing.org
[3] G.P. Smith, D.M. Golden, M. Frenklach, N.W. Moriarty, B. Eiteneer, M. Goldenberg, C.T. Bowman, R.K. Hanson, S. Song, W.C. Gardiner, Jr, V.V. Lissianski, Z. Qin, “Gri-mech 3.0,” 1999, http://www.sciencedirect.com/science/article/pii/001021809390078H
[4] RW Francisco Jr, AAM Oliveira, “Simultaneous measurement of the adiabatic flame velocity and overall activation energy using a flat flame burner and a flame asymptotic model,” Experimental Thermal and Fluid Science, 2018 - Elsevier

* This work was supported by RSF № 21-13-00434.

N3-O-004401

FINE STRUCTURE OF THE SUPERALLOY COMPONENTS FORMED BY ELECTRON BEAM ADDITIVE MANUFACTURING*

S.V. FORTUNA, D.A. GURIANOV, S.Y. NIKONOV

Institute of Strength Physics and Materials Science SB RAS, Tomsk, Russia

Superalloys of the second and subsequent generations [1] are used for manufacturing by casting with directed solidification of gas turbine engines working blades for aviation and power purposes [2]. At the same time, the currently widespread casting technologies with directional solidification are extremely resource-intensive in all practical aspects. Both in terms of the formation of a large proportion of virtually irrecoverable, or difficult to regenerate, waste of expensive materials. Also in terms of labor intensity with many technological transitions, equipment complexity, etc.

In the near future, the development of the potentialities of intensively developing additive technologies may allow reducing the technology of turbojet engine blades with a single-crystal microstructure to several operations [2].

An analysis of the results of studies carried out by the team of this work authors showed that in the process of electron-beam additive technology (EBAM) from filaments in the form of superalloy rods [3], it is possible to form products with a directed columnar microstructure [4]. In this case, directional solidification occur exclusively antiparallel to the direction of the temperature gradient. As a rule, with an increase in the height of the additive product it changes its direction from normal to the plane of the surface of the cooled substrate to the co-directional printing trajectory in layers. To control the structure of the material of an additive product, it is necessary to understand the principles of solidification under conditions, multidirectional components of heat removal, as well as various values of linear energy (energy input per unit length) [5].

This paper presents the results of a qualitative and quantitative analysis of the fine structure, phase composition, and morphology of the structural elements of a complexly alloyed superalloy containing rhenium in the cast state, as well as in the material of an additive product formed by the EBAM method.

REFERENCES

[1] P. Fernandez-Zelaia, O. D. Acevedo, M. M. Kirka, D. Leonard, S. Yoder, Y. Lee, “Creep Behavior of a High-γ′ Ni-Based Superalloy Fabricated via Electron Beam Melting,” Metall. Mater. Trans. A., vol. 52a., pp. 574-590, 2021.

[2] G. Liu, D. Du, K. Wang, Z. Pu, D. Zhang, B. Chang, “Microstructure and nanoindentation creep behavior of IC10 directionally solidified superalloy repaired by laser metal deposition,” Mater. Sci. Eng. A, vol. 808, 140911, 2021.

[3] S. V. Fortuna, D. A. Gurianov, P. S. Sokolov, A. S. Fortuna, “To the Method of Manufacturing Filaments for Electron-Beam Additive Technology from Casting and Hardly Deformable Metallic Materials, ” AIP Conf. Proc., vol. 2167, 020107, 2019.

[4] S.V. Fortuna, D.A. Gurianov, K.N. Kalashnikov, A.,V. Chumaevskii, Yu.P. Mironov, E.A. Kolubaev, “Directional Solidification of a Nickel-Based Superalloy Product Structure Fabricated on Stainless Steel Substrate by Electron Beam Additive Manufacturing,” Metall. Mater. Trans. A., vol. 52. no. 2, pp. 857-870, 2021.

[5] ISO 857-1:2002 Welding and Allied Processes—Vocabulary—Part 1: Metal Welding Processes.

* The investigation was supported by the Russian Science Foundation grant No. 22-22-00891, https://rscf.ru/en/project/22-22-00891/.

N3-O-006001

FORMATION OF BIMETALLIC PRODUCTS FROM NICKEL-BASED SUPERALLOY AND BRONZE BY WIRE-FEED ELECTRON BEAM ADDITIVE TECHNOLOGY *

D.A. GURIANOV, S.V. FORTUNA, S.YU. NIKONOV, A.V. CHUMAEVSKII, M.P. KALASHNIKOV

Institute of Strength Physics and Materials Science SB RAS, Tomsk, Russia

Investigations of methods for obtaining bimetallic and functionally graded materials remain an urgent task of the last decade [1]. Such materials are in demand in various industries from medicine to astronautics, when it is necessary to provide in a single product the properties characteristic of different materials. One of the ways to achieve this task is welding or another method of obtaining integral joints of dissimilar materials. However, this approach produces at least three different zones in the material: the base metal, the heat-affected zone and the fusion zone. These areas may differ in structural-phase composition and properties, which in turn leads to the formation of defects. Another way to obtain products from heterogeneous materials is the use of additive technologies. Since this approach involves growing the product layer-by-layer and each layer is periodically remelted and heat treated, the base metal area is absent as such, and most of the product is represented by the structure inherent in the heat affected area.

One striking example of the need to obtain products from dissimilar materials is a rocket engine, in which the key structural elements are the copper liner, which provides thermal properties, and its jacket of nickel alloy, which is responsible for the strength of the product [2].

In the present work the products in the form of walls from the nickel-based superalloy Udimet 500™ (wt.%: 53Ni - 18Cr - 18Co - 4.0Mo - 2.9Ti - 2.9Al - 0. 006B) and the heat-resistant bronze CuCr1 (wt.%: 0.08Fe - 0.7Cr - 99Cu - 0.3Zn) using wire-feed electron beam additive manufacturing (EBAM). These materials are heterogeneous but isomorphic, i.e., the matrix phase of each material has a FCC crystal lattice. In the course of the study, three strategies for printing bimetallic products were chosen. The first was at begin form a 3 cm high bronze wall and then deposit a 3 cm high nickel alloy wall on top of it. In the second approach, on the contrary, the nickel part was formed first and then the bronze part. In the third case, parallel formation of dissimilar materials took place: first a layer of nickel alloy was obtained and next to it a layer of bronze, then a second layer of nickel alloy and a second layer of bronze were deposited, and so on. General views of the obtained products are shown in Fig. 1.

Fig.1. Ni-Cu bimetallic products obtained by EBAM.

The product obtained by parallel formation of layers was found to be unsatisfactory because pores and voids up to 3 mm in size were present between the dissimilar materials. When forming a nickel wall and bronze on top of it, the bronze material spreads out excessively and loses its geometry, which is also a significant defect. And the most satisfactory was the product obtained using the first printing strategy. For example, no macro defects in the form of cracks and fractures were detected between the layers of nickel material and bronze. It is worth noting that in this work a sharp transition between heterogeneous materials was used in the formation of products. However, since nickel and copper have unlimited solubility with respect to each other, the formation of Ni-Cu solid solutions of different composition occurs throughout the first few layers of the nickel alloy, resulting in a gradient transition from one alloy to another.

REFERENCES

[1] Srinivasan Chandrasekaran, S. Hari, Murugaiyan Amirthalingam, "Functionally graded materials for marine risers by additive manufacturing for high-temperature applications: Experimental investigations," Structures, vol.35, pages 931-938, 2022.

[2] W.S. Loewenthal and D.L. Ellis, “Fabrication of GRCop-84 rocket thrust chambers,” Presentation at NASA Glenn Research Center, Cleveland, OH, January 12, 2006.

* The work was performed according to the Government research assignment for ISPMS SB RAS, project FWRW-2022-0004.

N3-O-007702

FORMATION OF RESIDUAL STRESSES IN THE SURFACE LAYERS OF CORROSION-RESISTANT STEEL SAMPLES AFTER IRRADIATION WITH HIGH-CURRENT PULSED ELECTRON BEAMS

O. A. BYTCENKO[1], *I.G. STESHENKO*[1,2]

[1]*Moscow Aviation Institute (National Research University), Moscow, Russian Federation*
[2]*Chernyshev Moscow Machine-Building Enterprise, Moscow, Russian Federation*

In this paper, the level of residual surface stresses of PH 15-5 steel samples manufactured using additive technology before and after heat treatment is analyzed. The research was carried out by layer-by-layer electrochemical etching of stressed metal layers from the sample surface. As a result of the tests, the parameters of the distribution of surface technological residual stresses of the 1st kind (sign, magnitude, depth of occurrence) were obtained.In addition, it is shown that irradiation with high-current and pulsed electron beams affects the level of surface residual stresses and depends on the presence of post-processing operations with or without machining after growing samples by selective laser melting.

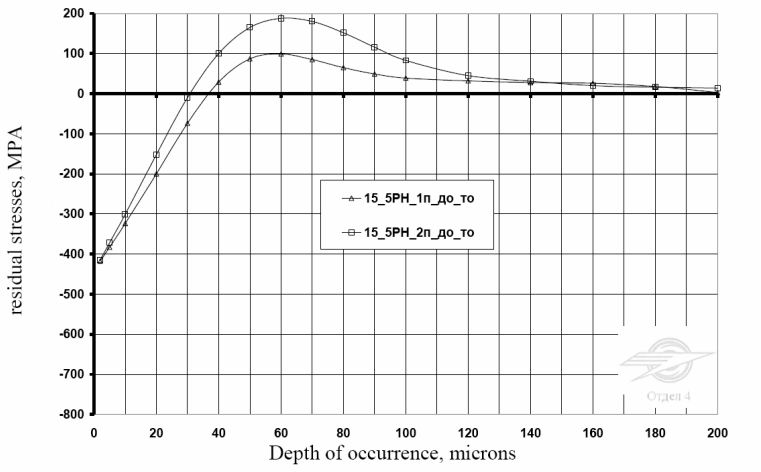

Fig.1. The level of residual stresses before heat treatment after milling.

REFERENCES

[1] Bytsenko O.A., Tishkov V.V., Steshenko I.G., Panov V.A., Markov A.B. “Structural and phase cnanges of the surface layres of heatresistant multicomponent coating of ion-plasma coating Ni-Cr-Al-Y after modification by high-current pulsed electron beams microsecond duration”,Periodico Tche Quimica. 2020. vol. 17. № 34. pp. 459-468.

[2] Teryaev D.A., Shulov V.A., Bytsenko O.A., Steshenko I.G. “Formaton of residual stresses in the surface layers of targets from heat-resistant titanium alloys by irradiation of high-current pulsed electron beams” In the collection: Journal of Physics: Conference Series. 2018. pp. 032-058.

[3] Shulov V.A., Engelko V.I., Gromov A.N. Influence of irradiation regimes by high-current pulsed electron beams on the process of crater formation on the surface of nickel alloy targets. Hardening Technologies and Coatings. 2013, №11 (107), pp.15-19.

[4] Bytsenko O.A., Filonova E.V., Markov A.B. The effect of intense beams on the surface layers of modern heat-resistant alloys with ion-plasma coatings of various compositions. London: Interaction of radiation with solid, 2015, pp.193-195.

[5] Bytsenko O.A., Filonova E.V., Markov A.B. High-current pulsed electron beams for surface engineering of ion-plasma coatings. News of materials science. Science and Technology, 2017, №2 (26), p.9.

[6] Bytsenko O.A., Grigorenko V.B., Lukina E.A. The development of methods of metallophysical research: methodological issues and practical significance. Aviation materials and technologies, 2017, S, ppю 498-515

[7] Bytsenko O.A., Filonova E.V., Markov A.B., Belova N.A. The effect of irradiation with high-current electron beams on the surface layers of modern heat-resistant nickel alloys with ion-plasma coatings of various compositions. Proceedings of VIAM. Electronic Journal, 2016, №6 (42). URL: http://viam-works.ru (17.07.2016). DOI: 10.18577/2307-6046-2016-0-6-10-10.

N3-O-014103

GEOPOLYMER CONCRETE FOR CONSTRUCTION 3D PRINTING

T.M. MUKHAMETKALIYEV [1, 2], V.A. KUTUGIN [1], V.I. VERESHAGIN[1], K.V. SKIRDIN [1], Md.H. ALI[2]

[1]Tomsk Polytechnic University, Tomsk, Russia
[2]Nazarbayev University, Nursultan, Kazakhstan

3D printing offers revolutionary prospects of "smart" technologies for the construction industry due to the following rationale. 3D printing, along with advances in Industry 4.0, has a high potential to lead to more efficient and sustainable construction because of the considerable advantages over conventional construction methods. Such advantages include formwork and mould-free manufacturing, increased geometrical freedom, improved safety in construction, reduction in construction waste, time, labour, and lower cost [1].

However, the introduction of 3DCP as a novel construction technology poses several challenges regarding material properties. Firstly, the printable material should be flowable enough to be pumped through the transporting system to the printing nozzle [2, 3]. Secondly, the printable material should secure quick structural build-up to retain the designed shape and to withstand its own weight as well as deposited layers on the top right after the extrusion [2-4]. Ordinary Portland cement (OPC) concrete to be printable requires a great number of additives, plasticizers, and stabilizing agents which increase its initial cost. Moreover, the production of OPC triggers stronger CO_2 emissions (8% of global CO_2 emissions) [5]. The global standards of the modern construction industry imply the commitments to abate greenhouse gas emissions and to decrease the energy-consuming process produced by OPC [5]. Therefore, current 3DCP technology needs to identify high-performing printable cementitious materials considering the need for controlled rheology, rapid hardening properties, and sustainable solutions.

Geopolymers have been introduced as a promising alternative to OPC with a staggering 90% lower CO_2 footprint. The distinctive advantage of a geopolymer over an OPC is that geopolymer cement can be synthesized at room temperature while OPC cement requires a four times higher amount of embodied energy for production [6]. Geopolymers are innovative solutions for industrial waste disposal of Russia and Kazakhstan's massive mining and metallurgical industries. The growing building industry in aforementioned countries has contributed to a rise in the production of construction materials by more than three times [7]. However, the implementation of industrial waste for the production of construction material remains negligibly low.

Several types of geopolymer concrete based on industrial by-products in Kazakhstan are already developed from fly ash, GGBS and kaolin clay. The compressive strength for the developed Fly-ash/slag and kaolin-based geopolymers is between 40-60 MPa (Fig. 1), flexural strength between 8-10 MPa, freeze-thaw resistance 400-500 cycles, water-resistance, W12-16, and higher depending on the mix.

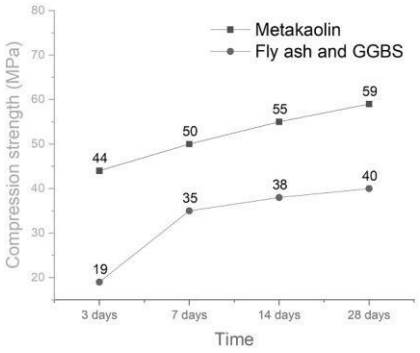

Fig.1. Compression strength of Fly-ash/GGBS geopolymer concrete and Kaolin based geopolymer concrete

REFERENCES

[1] Vantyghem, G., et al., 3D printing of a post-tensioned concrete girder designed by topology optimization. Automation in Construction, 2020. 112: p. 103084.

[2] Buswell, R.A., et al., 3D printing using concrete extrusion: A roadmap for research. Cement and Concrete Research, 2018. 112: p. 37-49.

[3] Khan, M.A., Mix suitable for concrete 3D printing: A review. Materials Today: Proceedings, 2020. 32: p. 831-837.

[4] Kristombu Baduge, S., et al., Improving performance of additive manufactured (3D printed) concrete: A review on material mix design, processing, interlayer bonding, and reinforcing methods. Structures, 2021. 29: p. 1597-1609.

[5] Worrell, E., et al., Carbon-dioxide emissions from the global cement industry. Annual Review of Energy and the Environment, 2001. 26(1): p. 303-329.

[6] Davidovits, J., Geopolymer Chemistry and Applications. Vol. 171. 2008.

[7] PrimeMinister.kz, Production Volume for Building Materials Increased 3 Times. Prime Minister Press Service of the Republic of Kazakhstan, 2020. https://primeminister.kz/ru/news/v-kazahstane-obemproizvodstva-stroitelnyh-materialov-uvelichilsya-v-33-raza-miir-rk-2161319 (accessed on 2 September 2021).

N3-O-017201

COMPARISON OF THE PRODUCTION OF SPHERICAL PARTICLES IN THE ELECTRIC EXPLOSION OF A WIRE AND A LOW-POWER DISCHARGE USING A LIQUID ANODE

BARYSHNIKOV YU.S., KURAKIN R.O., TVERDOKHLEBOV K.V., PONYAEV S.A.

Ioffe Physical-Technical Institute of the RAS, Saint-Petersburg, Russia

The work is devoted to the study of spherical particles produced by the methods of (i) electric explosion of wires (EEW) and (ii) a low-power discharge using a liquid anode (LA). The spherical particles themselves may be of practical interest for additive technologies and other applications. Currently, there are various methods for producing spherical particles [1], one of them is close to the liquid anode method, like the liquid cathode method, but has a higher discharge energy (electrical parameters of the described liquid cathode method [2]: 300-1000V, 100-300A).

The commonality of the processes of the presented methods is the expansion of metal droplets and their rapid cooling in the environment (Fig. 1). In the two methods under consideration, the main difference is the difference in the discharge currents, so for the EEW method the discharge current was tens of kiloamperes at a discharge voltage of kilovolts (current density up to 108 A/m), and for LA method 150-300V, currents up to 0.6A (current density up to 103 A/m). There was also a difference in the scheme of the experiment, with EEW, the conductor was placed between two brass rods, which were the electrodes of a high-voltage battery, and a pulsed current was passed through it, with an LA, the wire was periodically lowered into the liquid anode until the formation of metal expansion from the electrode.

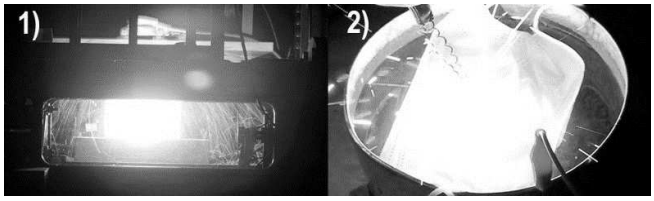

Fig.1. The process of scattering of metal droplets (sparks) during EEW(1) and LA(2).

In these processes, particles of an ideal spherical shape were mainly obtained (Fig. 2). But with EEW, more particles of non-ideal shape (with chips and deviations from sphericity) were obtained than with LA. On fig. 2 shows the results of experiments with a galvanized iron conductor, 0.8 mm in diameter, the electrolyte for LA was a solution of water with sodium chloride. The chemical composition of the particles in both cases was iron oxide.

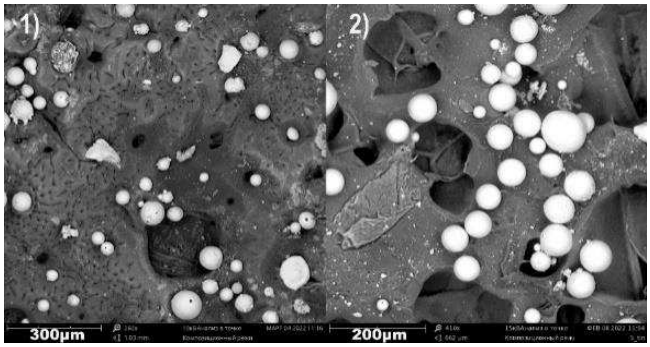

Fig.2. Spherical particles of iron oxide photographed through a Phenom ProX electron microscope obtained with EEW(1) and LA(2).

The diameter of the resulting spherical particles with EEW and LA is 15-150 μm, this range is of interest for use in additive technologies. From the point of view of practical implementation, the LA method seems to be simpler, not only in comparison with the EEW, but also with other currently existing methods for obtaining spherical particles. As part of experiments with the LA method, it has been shown that it can be used to obtain spherical particles from various materials, such as stainless steel, titanium, while for tungsten and copper, the results are currently unsatisfactory due to the presence of a large number of non-spherical particles.

REFERENCES

[1] Rodionov A. I., Efimochkin I. Yu., Buyakina A. A., Letnikov M. N. Spheroidization of metal powders (review) // Aviation materials and technologies. 2016 No. 1 P. 60–64

[2] R. N. Kashapov et al 2021 J. Phys.: Conf. Ser. 1923 012025 https://doi.org/10.1088/1742-6596/1923/1/012025

N3-O-020301

STUDY OF THE SURFACE PROPERTIES OF AM60B AND AZ91D MAGNESIUM ALLOYS COATED BY PVD WITH TITANIUM FILMS AND ALLOYED BY LEHCEB

CHIARA LETO[1], FEDERICO MORINI[1], ANDREA LUCCHINI HUSPEK[1], MASSIMILIANO BESTETTI[1,2]

[1]Politecnico di Milano, Department of Chemistry, Materials and Chemical Engineering "Giulio Natta", Milano, Italy
[2]Tomsk Polytechnic University, The Weinberg Research Center, Tomsk, Russia

Magnesium alloys combine useful properties such as low density (Mg 1.73 g/cm^3), excellent strength-to-weight ratio, relatively large thermal and electrical conductivities, satisfactory formability, and excellent biocompatibility. These properties make magnesium alloys among the most used light-weight materials for automotive, aerospace, consumer electronic and sport goods, and biomedical implants.

Magnesium has a very low standard reduction potential (-2.37 V vs SHE at 25°C) while commonly used magnesium alloys have corrosion potential E_{corr} in 1M NaCl aqueous solution at 25°C in the range between -1.7 and -1.6 V vs SCE. Their corrosion resistance is a still a technological problem, especially when magnesium alloys are in galvanic contact with other metals. Microgalvanic corrosion of magnesium alloys is also an intrinsic problem related to the presence of secondary more noble phases within the solid solution. Moreover, corrosion resistance is particularly poor when they are exposed to aggressive environments, such as chlorides electrolytes. The issue of microgalvanic corrosion in magnesium alloys has been already addressed by treating the surface of the AM60B and AZ91D alloys by means of the low energy high current electron beam technique (LEHCEB) able to dissolve the $Mg_{17}Al_{12}$ intermetallic compound into the solid solution matrix and to change the surface composition by preferentially evaporating Mg in respect to Al from the irradiated surface. [1]

Titanium has a positive effect on the corrosion resistance of magnesium alloys. Xu et al. co-deposited by magnetron sputtering Mg and Ti on glass slides with different compositions. Ti is a strong passivating element increasing the passivity of Mg as well and reducing its dissolution in saturated $Mg(OH)_2$ solutions with and without addition of NaCl. [2] According to Liu et al., gradient composition structures obtained by Ti implantation in AZ91 alloys greatly improves the corrosion resistance. [3] Song et al. deposited Mg-Ti alloys by RF magnetron sputtering on quartz plates, and they found that the passivity of Mg-Ti alloy was enhanced and the corrosion rate decreased with the increase of Ti content. [4]

In the present work we investigated the possibility to form surface alloys between titanium and the commercially used AM60B and AZ91D magnesium alloys by LEHCEB technique. A pretreatment with the LEHCEB was performed to prepare the surface of the alloys (15 kV, 10 pulses) and then thin films of Ti were deposited (100, 500 and 1000 nm) by DC magnetron sputtering. Surface alloying by LEHCEB between titanium films and AM60B and AZ91D alloys was investigated by varying the acceleration voltage (20 and 25 kV) and number of pulses (5 and 10).

The obtained surface alloys have been characterized in term of composition (EDS, XRD), morphology (SEM), Vickers instrumented microindentation and corrosion resistance.

REFERENCES

[1] F. Morini, M. Bestetti, S. Franz, A. Vicenzo, A. Markov, and E. Yakovlev, "Surface properties modification of magnesium alloys by low energy high current pulsed electron beam," Surface and Coatings Technology, vol. 420, pp. 127351, 2021.

[2] Z. Xu, G Song, D. Haddad, "Corrosion Performance of Mg-Ti Alloys Synthesized by Magnetron Sputtering", in: Sillekens WH, Agnew SR, Neelameggham NR, Mathaudhu SN (Eds.), Magnesium Technology 2011, Springer International Publishing, Cham, pp. 611-615, 2016.

[3] C. Liu, Y. Xin, X. Tian, J Zhao, PK Chu., "Corrosion resistance of titanium ion implanted AZ91 magnesium alloy", Journal of Vacuum Science & Technology, A. 25, pp. 334-339, 2007.

[4] G. Song, K.A. Unocic, H. Meyer, E. Cakmak, M.P. Brady, PE Gannon, et al. "The corrosion and passivity of sputtered Mg–Ti alloys", Corros.Sci., 104, pp. 36-46, 2016.

N3-O-020302

A NOVEL APPROACH TO REMOVE DLC COATING FROM CEMENTED CARBIDES TOOLS BY USING LOW-ENERGY HIGH-CURRENT ELECTRON BEAMS *

A. LUCCHINI HUSPEK,[1] MASSIMILIANO BESTETTI[1,2].

[1]Politecnico di Milano, Department of Chemistry, Materials and Chemical Engineering "Giulio Natta", Milano, Italy
[2]Tomsk Polytechnic University, The Weinberg Research Center, Tomsk, Russia

Deposition of carbon-based coatings, such as Diamond-Like Carbon, is a highly effective procedure to further increase the useful lifespan and the performance of hard metals tools. However, considering the harsh service conditions in which industrial utensils are employed, DLC coatings are subjected to wear and this affect in turn their efficiency and cutting ability [1,2].

For this reason, tool reconditioning aimed at the reuse of the Co-cemented carbide substrates would guarantee a remarkable cost reduction for industries and a lower consumption of raw materials. Consequently, a successful technique for DLC decoating is required, which would allow the WC-Co surface to be re-sharpened and coated again. Of course, the stripping process is deemed efficient only when the coating is fully removed without inflicting irreversible damages to the substrate. Even though DLC films have grown in popularity during the last decades, very little attention has been devoted to the issue of diamond-like carbon decoating. [3,4]

In the present work, a Low-Energy High-Current Electron Beam has been used to remove two different type of DLC coatings: a-C:H and Ta-C (both 1.5 µm thick). In between the DLC and the Cr adhesion layer (100 nm), a-C:H samples also presented a W-C:H transition layer (1.2 µm). Moreover, a preliminary analysis on bare WC-Co (Co wt.%: 2.0 ± 0.4) has been done to investigate the effects of LEHCEB on Co-cemented carbides. The entire experimental procedure was assisted by a detailed computational simulation to predict and better understand overall results.

The decoating process was done using a relatively low number of pulses, up to 20, with accelerating voltage of 20, 25 and 30 kV (associated energy density up to 5-6 J/cm^2). The aim was to find the minimum energy threshold for a complete and uniform cleaning of WC-Co surface. On the other hand, uncoated samples were treated with a higher number of pulses, up to 40, at 15, 20 and 25 kV in order to assess the beneficial or detrimental effects of a prolonged LEHCEB irradiation. At the end, a combination of the two aforementioned treatments has been used to study the influence of electron beam treatment on the adhesion of a new DLC coating on cleaned WC-Co substrates. Then, concerning computational models, calculations on Co binder and Cr adhesion layer were focused on solid-liquid transitions and melt state properties. Simulation of WC was concentrated on depth thermal profiles and thermal stresses while DLC a-C:H and Ta-C were simulated mainly to evaluate the evaporation threshold and ablation rate.

REFERENCES

[1] K. AL Mahmud, M. Kalam, H. Masjuki, H. Mobarak, N. Zulkifli, "An updated oberview of diamond-like carbon coating in tribology", Critical Reviews in Solid State and Materials Sciences, 2015

[2] R. Polini, M. Barletta, G. Rubino and S. Vesco, "Recent advances in the deposition of diamond coatings on Co-cemend tungsten carbides", Advances in Material Science and Engineering, 2012.

[3] T. Primus, J. Hlavinka, P. Zeman, J. Brajen, M. Sorm, A. Cermak, P. Kozmin, F. Holesovsky, "Investigation of multiparameter laser stripping of AlTiN and DLC C Coatings", Materials, 2021.

[4] A. Zivelonghi, L. Giorleo, M. Gelfi, E. Ceretti, G. La Vecchia, " Laser decoating of DLC films for tribological applications", The International Journal of Advanced Manufacturing Technology, 2017.

* The present work was realized with the financial support of Fondazione Cariplo – Circular economy 2020 "Cutting tools regeneration by means of innovative vacuum plasma technologies" a project in collaboration with Tomsk Polytechnic University.

N3-O-026802

PRODUCTIVITY OF ELECTRICAL DISCHARGE MACHINING ALUMINA USING SNO ASSISTING POWDER*

A.A. OKUNKOVA[1], *M.A. VOLOSOVA*[1], *K. HAMDY*[1,2], *S.V. FEDOROV*[1]

[1]*Moscow State University of Technology "STANKIN", Moscow, Russia*
[2] *Faculty of Engineering, Minia University, Minia, Egypt*

The issues of microtexturing of working surfaces of critical engineering products made of difficult-to-machine materials and composites, including those based on dielectric oxide and nitride ceramics, have been the subject of theoretical and experimental research by leading scientific groups. For the first time, a group of domestic scientists proposed a method for electrical discharge machining (EDM) of dielectric superhard materials in the mid-80s [1]. Since then, progress has been made in the field of surface modification of silicon nitride [2] and zirconium dioxide [3], while alumina remains a problematic material [4-5]. It is primarily due to the specific thermochemical properties of aluminum, which exhibits a high affinity for oxygen under normal conditions and forms dielectric compounds in the presence of hydrocarbons during the thermal decomposition of the oxide [6] such as Al_4C_3 (steady up to 1400 °C, but unstable to water, oxygen or hydrogen).

Using a nickel-chromium coating applied by the PVD method [7,8] with a thickness of 10 – 15 μm and a SnO suspension of various concentrations fed directly into the processing zone is proposed to solve the problem of alumina's low machinability. The nickel-chromium coating was chosen due to the known affinity of nickel for aluminum to form conductive bonds [9]. The band gap of optically white tin oxide determines the choice of this dielectric powder to assist electrical discharge machining of dielectric ceramics. An analysis of the processing performance of alumina using techniques was carried out in an aqueous medium in the range of electric current pulse lengths of 1.0 – 2.7 μs and a pulse frequency of 10 – 30 kHz.

A slot (kerf) in the dielectric ceramics to a depth of 49.74 – 95.20 μm was formed using a brass wire tool. Spectroscopy and scanning electron microscopy demonstrated the diffusion of the auxiliary electrode and assisting powder materials in the form of secondary material on the ceramic sample surfaces, which is explained by the predominant binding of Zn of brass to oxides and its precipitation [10]. In addition, there was a significant increase in the material removal rate at a particle concentration of 150 g/l for pulse frequency 25 – 30 kHz. The experiments proved the effectiveness of the proposed combined approach in machining alumina for a depth of up to 95.20 μm using a brass wire tool. The maximum material removal rate of 0.001 mm³/s and the minimum interelectrode gap correspond to stable processing and uniform density of electric discharges. It was achieved at an electric current pulse frequency of 30 kHz, the SnO-suspension concentration (granulometry - ⌀ 10 μm) 150 g/l water-based when using an assisted coating electrode of 10 – 15 μm. The obtained data indicate that the developed method is superior to analogs by 2.12 times.

REFERENCES

[1] S.V. Lukashenko, A.V. Kovtun, P.N. Dashuk, B.N. Sokolov, *Patent SU* 1542715, 1986.

[2] T. Tani, Y. Fukuzawa, N. Mohri, et al., "Machining phenomena in WEDM of insulating ceramics", J. Mater. Process. Tech., vol. 149, 124–128, 2004.

[3] G. Kucukturk, C. Cogun, "A New Method For Machining Of Electrically Nonconductive Workpieces Using Electric Discharge Machining Technique", Mach. Sci. Technol., vol. 14, 189–207, 2010.

[4] S. N. Grigoriev, M. P. Kozochkin, A. N. Porvatov, et al., "Electrical discharge machining of ceramic nanocomposites: Sublimation phenomena and adaptive control", Heliyon, vol. 5, e02629, 2019.

[5] S. N. Grigoriev, M. A. Volosova, A. A. Okunkova, et al., "Electrical Discharge Machining of Oxide Nanocomposite: Nanomodification of Surface and Subsurface Layers", J. Manuf. Mater. Process., vol. 4, 96, 2020.

[6] M. A. Volosova, A. A. Okunkova, S. V. Fedorov, et al., "Electrical Discharge Machining Non-Conductive Ceramics: Combination of Materials", Technologies, vol. 8, 32, 2020.

[7] V. V. Kuzin, S. N. Grigoriev, M. A. Volosova, "The role of the thermal factor in the wear mechanism of ceramic tools: Part 1. Macrolevel", J. Frict. Wear, vol. 35, 505–510, 2014.

[8] S. N. Grigoriev, A. A. Vereschaka, A. S. Vereschaka, A. A. Kutin, "Cutting tools made of layered composite ceramics with nano-scale multilayered coatings", Proc. CIRP, vol. 1, 301-306, 2012.

[9] S. N. Grigoriev, K. Hamdy, M. A. Volosova, A. A. Okunkova, S. V. Fedorov, "Electrical Discharge Machining of Oxide and Nitride Ceramics: A Review", Materials & Design, vol. 209, 109965, 2021.

[10] S. N. Grigoriev, M. A. Volosova, A. A. Okunkova, S. V. Fedorov, K. Hamdy, P.A. Podrabinnik, "Elemental and Thermochemical Analyses of Materials after Electrical Discharge Machining in Water: Focus on Ni and Zn", Materials, vol. 14, 3189, 2021.

* The work was supported by a grant of the Russian Science Foundation, project No. 21-19-00790.

N3-O-030101

FABRICATION OF PEEK-CF LAYERED COMPOSITES WITH THE USE OF ULTRASONIC WELDING MACHINE*

S.V. PANIN[1,2], *A.V.BYAKOV*[1], *V.O.ALEXENKO*[1], *D.G. DUSLOVICH*[1], *T. DEFAN*[2]

[1]*Institute of Strength Physics and Materials Sciences SB RAS, Tomsk, Russia*
[2] *National Research Tomsk Polytechnic University, Tomsk, Russia*

Application of ultrasonic (US) vibrations is one of the most spread methods for welding of thermoplastics. For doing so, high-frequency low-amplitude mechanical vibrations are applied to implement frictional heating of the contacting surfaces, which leads to their local melting and subsequent formation of a permanent joint. Ultrasonic welding allows joining both amorphous and semi-crystalline thermoplastic polymer materials without additional external heating [1, 2].

An advantage of the ultrasonic welding (USW) is a relatively high speed of joint formation process, since the welding proceeds during several thousand oscillatory cycles (from fractions to several seconds). In addition, mass production might be easily automated. Working frequencies of industrial technological US equipment vary from 10 to 75 kHz; however, the 20 +/- 4 kHz band is the most common operating frequency range. In doing so, the amplitude of the working tool vibration displacement ranges from 0.1 to 100 microns.

Recently, various aspects of fabricating laminated thermoplastic based composites with the use of ultrasonic welding equipment have been actively discussed in R&D literature. The relevance of this approach is motivated by a possibility of long-range products fabrication by serial ultrasound-assisted action onto joined layers (parts). It was shown that an efficient approach for US-assisted joining of thermoplastic layers is the use of intermediate (consumable) films (the so-called Energy Director - ED). During the US-vibration exposure, the latter melts and a dense interlayer is formed. In doing so, the lapped plates, as a rule, of the same materials are joined (connected). In addition to films from the same materials, the EDs are fabricated from ones with lower melting points. The ED thickness and porosity are variables; moreover, reinforcing particles and fibers are additionally loaded, etc. Professor Irene Fernandez Villegas from the Delft University of Technology should be refereed as one of the most successful researchers in this area [3].

However, besides joining plates of the same thermoplastic materials, the use of ultrasonic vibrations can be a way of forming layered (laminated) composites, containing layers of reinforcing fabrics. At present, such layered composites based on thermoplastic binders are manufactured mostly by hot pressing of sequentially laid layers of polymers (including films) and fabric [4]. However, the use of prepregs (reinforcing fabric in a binder) can allow the formation of layered composites using ultrasound technologies. This issue is currently just briefly studied in the relevant literature.

The paper is aimed at the study of lap joints formation of thermoplastic materials (in this case, high-strength polyetheretherketone - PEEK) reinforced with carbon fiber fabric with the use of an ultrasonic welding machine.

It was shown that ultrasonic welding of two PEEK plates without the use of the Energy Director did not ensure formation of a high strength lap joint. The introduction of the PEEK–CF prepreg layer between two PEEK plates did not stimulated the formation of a reliable lap joint with high LSS value. The reason was the low weight fraction of the binder in the prepreg (34%).

The formation of a multilayer (laminated) PEEK–CF–PEEK composite might be realized when a prepreg is used as a central layer, while PEEK–film Energy Directors are placed between joined plates. It was shown that a PEEK film with a thickness of 250 μm might be efficiently used. During the tensile test, fracture occurred along the base material, while the lap joint maintained its structural integrity.

REFERENCES

[1] J. A. Gallego-Juárez and K. F. Graff, Power Ultrasonics: Applications of High-Intensity Ultrasound (Elsevier, Amsterdam, 2015), pp 295–312.

[2] X. Sánchez-Sánchez, M. Hernández-Avila, L. E. Elizalde, O. Martínez, I. Ferrer, A. Elías-Zuñiga, Mater. Des. 132, 1–12 (2017).

[3] I. Fernandez Villegas, B. Valle Grande, H. E. N. Bersee, R. Benedictus, "A comparative evaluation between flat and traditional energy directors for ultrasonic welding of thermoplastic composites," in 16th European conference on composite materials-2014, Composite Interfaces 22, edited by F. Paris and A. Barroso (Taylor and Francis, London, UK, 2015), pp. 1–8.

[4] E. Tsiangou, S.Teixeira de Freitas, I. Fernandez Villegas, R, Benedictus, Compos. B. Eng. 173, 107014 (2019).

* The study was funded by Russian Science Foundation # 21-19-00741, https://rscf.ru/project/21-19-00741/».

N3-O-036403

COLD SPRAY METHOD FOR "ALUMINUM-ALUMINA-CNF" COMPOSITE PREPARATION*

A.YU. NALIVAIKO[1,2], D.YU. OZHERELKOV[1], S.V. CHERNYSHIKHIN[1], A.A. GROMOV[1,2]

[1] MISIS Catalysis Lab, National University of Science and Technology MISIS, Moscow, Russia
[2] Moscow Polytechnic University, Moscow, Russia

One of the possible approaches to enhance hardness of ductile aluminum alloys are different surface treatment, among them: laser welding deposition [1], thermal spraying [2], anodizing [3], and others. The cold spray method is a relatively new manufacturing process [4] during which particles do not reach the melting point and form a solid material due to the high kinetic energy of collision [5]. Present study is aimed to study the synthesized coatings from aluminum - alumina - carbon nanofibers (CNF) composite material using cold spray method. In our previous studies, binary composites (aluminum-carbon nanomaterial or alumina-carbon nanomaterial) were used while the present study considers a ternary system in the range of CNF concentrations of 0.5-1.5 wt. %. The investigation considers the process of preparation of the specified composite by ball milling as well as the process of synthesis of a solid object (coating) by cold spray method. It also should be noted that both the original aluminum powder and the substrate were made from the same alloy. Therefore, the present study is of high practical importance since the considered composites and synthesis regimes can be used to increase the surface properties of a particular aluminum alloy. Feedstock powder was prepared using planetary mill, that allowed a uniform distribution of CNFs on the aluminum particles' surface (see Figure 1).

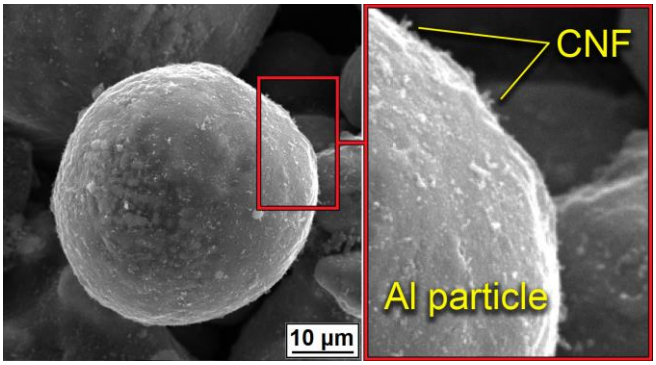

Fig.1. Distribution of CNF on the surface of Al powder after mixing.

The different combinations of hard alumina micron-sized particles and soft micron-sized aluminum particles as well as the hard nano-CNF lead to different morphology of the synthesized coatings. There are limits from both sides: low content of hard particles will not lead to sufficient improving of the surface mechanical properties, but too high content of alumina could not form the coating because of poor bonding and adhesion between brittle Al_2O_3 particles. The microstructure of samples synthesized by cold spray method are also affected by CNF content due to an increase in the bulk density of the feedstock powder, as well as high antifriction properties of carbon. CNF content of 1.5 wt. % led to 20 % increase in the microhardness of samples which is due to the mechanism of dispersive strengthening.

REFERENCES

[1] Y. Li, Y. Shi, "Microhardness, Wear Resistance, and Corrosion Resistance of AlxCrFeCoNiCu High-Entropy Alloy Coatings on Aluminum by Laser Cladding", Opt. Laser Technol., vol. 134, p. 106632, 2021.

[2] Y. Shin, Y. Ohmori, T. Morimoto, T. Kumai, A. Yanagida, "Formation of Nano-Microstructured Aluminum Alloy Film Using Thermal Spray Gun with Ultra Rapid Cooling", Mater. Trans., vol. 57, pp. 488–493, 2016.

[3] M. Gombár, A. Vagaská, J. Kmec, P. Michal, "Microhardness of the Coatings Created by Anodic Oxidation of Aluminum", Appl. Mech. Mater., vol. 308, pp. 95-100, 2013.

[4] R.N. Raoelison, Y. Xie, T. Sapanathan, M.P. Planche, R. Kromer, S. Costil, C. Langlade, "Cold Gas Dynamic Spray Technology: A Comprehensive Review of Processing Conditions for Various Technological Developments till to Date", Addit. Manuf., vol. 19, pp. 134-159, 2018.

[5] H. Assadi, F. Gärtner, T. Stoltenhoff, H. Kreye, "Bonding Mechanism in Cold Gas Spraying", Acta Mater., vol. 51, pp. 4379–4394, 2003.

* The work was supported by Russian Science Foundation (Project 21-79-10240).

N3-O-041902

DIFFUSION WELDING OF METALS WITH PRELOMINARY LASER TREATMENT OF WELDED SURFACES

A.V. LIUSHINSKII

LLC "Aviaspacetech", Moscow, Skolkovo, Russia

When implementing the technology of diffusion welding, there are applied various methods to intensify the process of formation of one-piece joints [1,2]. It is done in order to decrease a thermal deformation impact onto welded materials, to shorten the welding technology process cycle and to extend the nomenclature of welded materials.

The following items are used as the main methods [1,2]:

- interfacial layers made of metallic foils, sputtered and galvanic films, superdispersed metallic powders;
- cyclic changes of the process temperature and/or the welding pressure;
- directing some ultrasonic oscillations into the contact zone;
- placing the welded parts into an electrostatic field;
- preliminary impact of ionizing emission, neutron, α-particle, γ-ray and electron irradiation onto the welded surfaces.

In the recent years, the simplest in its performance technology and relevant with achieved results method has been the method of activation of the welded surfaces by the laser emission [3,5], especially when taking into account a relative cheapness of used equipment and technology processes applied to prepare and treat the surfaces.

There was explored a possibility to lower the diffusion welding process temperature T (at the same welding pressure P and delay time t) of welded specimens of stainless steel 12Kh18N10T (2X18H10T), the surfaces of which had preliminarily been under the laser treatment. When the laser treating, only the emission density E was changed in different modes (2.1 J/sm^2, 3.2 J/sm^2 and 4.3 J/sm^2, 220 μm spot diameter), and also the beam was scanned both in the same direction and in mutually perpendicular directions. The end faces of stainless steel specimens (30 mm height, 16 mm diameter) after a turning machining had Rz=1.2 μm. On completing the laser treatment, the Rz size of each specimen was measured by the "Profilograph – profilometer 252" instrument. The results demonstrated that as the E value increases, the height and form of microroughnesses change from 13.6 μm to 45.5 μm.

The carried out researches showed that the maximum strength of welded joints ($\sigma_в$ = 10.8 kgf/mm^2) belonged to the specimens having R_z = 45.5 μm with a conical form of microroughnesses with minimum angles of their apexes. The uniform strength of welded joints of steel 12Kh18N10T (12X18H10T) with the preliminary laser treatment of welded surfaces with the emission density of 4.3 J/sm^2 can be obtained at T= 950°C.

REFERENCES

[1] N.F. Kazakov. Diffusion weldung of materials. M.: Mashinostroyenie, 1976, 312 pages

[2] A.V. Liushinskii. Special methods of welding. M.: KNORUS, 2020, 208 pages

[3] V.N. Yelkin, T.V. Malinskiy, S.I. Mikolutskiy, R.R. Khasaya, Y,V. Khomich, V.A. Yamshchikov. Influence of the nanosecond laser pulse emission on the structure of surface of metallic alloys. "Физика и химия обработки материалов" ("Physics and chemistry of treatment of metals"), 2016, No.6, pp. 5-12.

[4] A.V. Liushinskii, V.N. Yelkin, V.N. Petrovskiy and others. Diffusion welding of metallic surfaces undergone a preliminary laser treatment. "Физика и химия обработки металлов" ("Physics and chemistry of treatment of metals"), 2021, №5, pp.22-29.

[5] A.V. Liushinskii. Influence of the laser treatment of welded surfaces on the properties of diffision welded joints. Сварочное производство (Welding production), 2022, No.4, pp.37-42.

N3-O-041903

DIFFUSION WELDING OF ALUMINOSILICATE GLASS S48-3 WITH MOLYBDENIC ALLOY TsM-2A

A.V. LIUSHINSKII

LLC "Aviaspacetech", Moscow, Skolkovo, Russia

Diffusion welding is the only bonding technology which allows obtaining qualitative one-piece joints of metallic materials with nonmetallic materials in various combinations [1,2]. In particular, it is applied to the bonding of aluminosilicate glass S48-3 (C48-3) and molybdenic alloy TsM-2A (ЦМ-2А), widely used in precision instrument-making industry, in electronic and electric devices.

The main requirements for such devices (besides achievements of the strength of joint at the level of the strength of bonded materials) are:

- provision of hermeticity of the joint at the level from $5 \cdot 10^{-12}$ $m^3 \cdot Pa/s$ to $1 \cdot 10^{-10}$ $m^3 \cdot Pa/s$ for all the operating period and also after thermocycling in the temperature range from minus 65°C to +55°C;
- value of residual thermal stress in the welded joint shall not be more than 10 MPa;
- parts after welding shall not have changes of their geometric sizes.

Diffusion welding of the parts made of the above materials may be carried out by two technology process schemes:

1. Bond the glass with the alloy directly to each other. In this case, the qualitative joint is formed at the temperature T > 700°C, which is close to the temperature of glass softening (T_s = 810°C). But even at a minimum force of squeeze (P = 0.5 kgf/mm^2), the glass begins to deform plastically.

2. Apply an interfacial layer of 0.1 mm thickness aluminum foil in order to lower the welding process temperature. At that, of course, in the zone of joining will form intermetallic compounds of the Al-Mo system. As the welding temperature increases, there also increases the formation speed and amount of intermetallic compounds in the welded joint. Microfractures and nonsolid areas appear in the zone of intermetallic compounds formation. They have a negative impact upon the hermeticity of joint.

Nevertheless, the diffusion welding mode with T=600°C, P>5 kgf/mm^2 and t=30 min provides fulfillment of the announced requirements. It is connected with the fact that the applied welding pressure deforms plastically the intermetallic compounds and provides seizing with the main material.

The same effect can be achieved if foils of titanium and aluminum are used as interfacial layers; at that, at first, a diffusion welding of the titanium foil with the molybdenic alloy is to be carried out, and then the aluminum foil is to be placed in between the welded titanium foil and the glass, and the diffusion welding is to be carried out with the above given parameters.

REFERENCES

[1] N.F. Kazakov. Diffusion weldung of materials. M.: Mashinostroyenie, 1976, 312 pages

[2] A.V. Liushinskii. Diffusion welding of heterogenious materials. M.: ITs "Academia", 2006, 208 pages.

[3] V.A. Bachin. Diffusion welding of glass and silicon with metalls / V.A. Bachin. – M.: Mashinostroyenie, 1986, 184 pages.

N3-O-042501

COMPOSITE MATERIAL OF THE Ti-Ta-Zr SYSTEM INTENDED TO WORK IN BOILING SULFURIC AND HYDROCHLORIC ACIDS*

V.V.Samoylenko[1], M.G.Golkovski[2], I.S. Ivanchik[1], I.K. Chakin[2], I.A. Polyakov[1]

[1]*Novosibirsk State Technical University, Novosibirsk, Russia.*
[2]*Budker Institute of Nuclear Physics, SB of RAS, Novosibirsk, Russia*

This study is a continuation of a series of works on the study of composite materials obtained by surfacing corrosion-resistant layers on a titanium base using an electron beam of the MeV range of electron energy released into the atmosphere. This method allows the surfacing of powder mixtures containing corrosion-resistant elements with very different melting points, in particular, from the series Ti, Ta, Nb, Zr, etc. Volumetric heating of the powder mixture of these elements makes it possible to avoid segregation during coating formation. The coating thickness is about 2 mm. As shown in previous publications [1,2], coatings of the Ti-Ta and Ti-Ta-Nb systems exhibit high resistance in especially aggressive corrosive environments, in particular, in concentrated (65%) boiling nitric acid. However, these coatings are not sufficiently stable in two other strong acids at boiling points: sulfuric and hydrochloric. Due to zirconium is more stable in mentioned acids than niobium, the including of it instead of niobium in the surfaced powder mixture allow to increase the corrosion resistance of surfaced layer [3, 4], but the resistance of it still quite not sufficient for industrial applications. Only a sharp increase in the alloying concentration in the Ti-Ta-Zr system made it possible to obtain an anti-corrosion layer that is quite efficient also in boiling sulfuric and hydrochloric acids. A high alloying concentration was achieved, in particular, due to the repeated surfacing of the initial powder mixture on the layer formed after the first surfacing. The composition of the deposited layer after the first surfacing was 31%Ta-12%Zr, Ti-rest, after the second - 48%Ta-20%Zr, Ti-rest.

The authors used a method of weight control for corrosion resistance characterization. A number of coatings with gradually increasing alloying levels were tested. The results for the layer with the highest concentration compared to the titanium substrate materials, pure zirconium and pure tantalum, taken in the form of plates are shown in the table blow.

Table. Corrosion resistance in the boiling acids of the most alloyed layer, titanium base material, commercially pure zirconium and tantalum, mm/year.

Sample composition	65% HNO_3	40% H_2SO_4	20% HCl
BT1-0	0.191	1980	389
48%Ta-20%Zr-32%Ti	0.006	0.071	0.191
Zr	0.001	0.016	0.41
Ta	0.000	0.001	0.000

Conclusion. The use of a mixture of zirconium and tantalum in the formation of an anti-corrosion coating makes it possible to obtain a protective coating with maximum alloying. The corrosion resistance of the resulting coating is enough to use it for operation in boiling sulfuric and hydrochloric acids with sufficiently high concentrations.

REFERENCES

[1] M. G. Golkovski, I. A. Bataev, A. A. Bataev, A. A. Ruktuev, T. V. Zhuravina, N. K. Kuksanov, R. A. Salimov, V. A. Bataev, Atmospheric electron-beam surface alloying of titanium with tantalum, Mater. Sci. Eng., A. 578 (2013) 310-317.

[2] A.A. Ruktuev, V.V. Samoylenko, M.G. Golkovski. Structure and corrosion resistance of Ti-Ta-Nb coatings obtained by electron beam cladding in the air-atmosphere. Applied Mechanics and Materials Vol. 682 (2014) pp 100-103. Trans Tech Publications, Switzerland, doi:10.4028/www.scientific.net/AMM.682.100.

[3] V.V. Samoylenko, T.S. Ogneva, I.A. Polyakov, I.S. Ivanchik, O.G. Lenivtseva, and O.E. Matts. Structure and properties of surface-alloyed layers formed by non-vacuum electron beam cladding of Ta and Zr powders on commercially pure titanium plates. AIP Conference Proceedings 1785, 040057 (2016); doi: 10.1063/1.496

[4] I.A. Polyakov, O.G. Lenivtseva, V.V. Samoylenko, M.G. Colkovski and I.S. Ivanchik. Corrosion resistance of Ti-Ta-Zr coatings in the Boiling Acid Solutions IOP conference series: material science and engineering, V 156 (2016) doi:10.1088/1757-899X/156/1/012023. http://iopscience.iop.org/article/10.1088/1757-899X/156/1/012023.

* The work was partially supported by the Russian Ministry of Education and Science under grant No. 14.604.21.0135.

N3-O-043502

EFFECT OF ELECTRON BEAM MELTING PROCESSING PARAMETERS ON PROPERTIES OF Ti-42Nb ALLOY PARTS

M. KOZADAEVA[1], *A.P. VOLKOVA*[1], *I.Y. GRUBOVA*[1], *A. KOPTYUG*[2], *M.A. SURMENEVA*[1], *R.A. SURMENEV*[1]

[1]*Physical Materials Science and Composite Materials Centre, Research School of Chemistry & Applied Biomedical Sciences, National Research Tomsk Polytechnic University, Tomsk, Russia*
[2]*Mid Sweden University, Östersund, Sweden*

Additive Manufacturing (AM) techniques allow producing metal implants with the suitable porosity, size, and complex geometric design. One of the most perspective powder bed AM techniques is Selective Electron Beam Melting (SEBM). Titanium and its alloys are widely used in bone replacement surgery due to their low weight, high strength, reduced elastic modulus and good biocompatibility [1]. However, the elastic modulus of most commonly used titanium alloys is still much higher than that of bone tissues causing a stress-shielding phenomenon, which can lead to implant loosening [2]. Niobium is a β-stabilizer of titanium and its addition reduces the elastic modulus of the alloys [3]. Compared to nickel Nb is a non-toxic biocompatible metal [3]. However, there are no established process settings for SEBM of Ti-Nb alloys, and corresponding parameters leading to adequate quality material should be selected for each material.

In this study several samples were manufactured using a pre-alloyed Ti-42 wt.% Nb powder in ARCAM A2 EBM machine (GE Additive, Mölndal, Sweden) to find a suitable processing parameter window. Processing regimes with raster type scanning, different currents and scanning speeds with the same target layer thickness of 100 μm and surface energy between 2.40 and 5.15 J/mm^2 were used (Tab.1).

Tab. 1. The EBM processing parameters for Ti-42 wt.% Nb alloy (Taniobis GmbH)

Sample Nr	Beam current, mA	Scanning speed, mm/s	Beam track spacing, L_{off}, mm		Beam power, W	Surface energy, E_{area}, J/mm^2
1	3.5	700	0.125		210	2.40
2	4	700	0.100		240	3.43
3	4	800	0.100		240	3.00
4	4	900	0.100		240	2.67
5	4-5	800	0.100		270	3.38
6	5	700	0.100		300	4.29
7	5	900	0.100		300	3.33
8	7.5	700	0.125		450	5.14

Regimes № 1, 4, 5, 6, 7 result in a lack of fusion between some of the consecutive layers, while regimes № 2, 3, 8 yielded samples with good layer-to-layer fusion. The presence of pores with 2-15 μm size is typical for all samples. Optical microphotographs after chemical etching in Kroll's solution at room temperature (1 ml 45 % HF, 3 ml 65 % HNO_3 and 46 ml H_2O) showed grains with 50-150 μm size. The shape of the grains corresponds to the β-phase [4]. Elongated grains of the lath α-phase were not detected.

The XRD patterns of the pre-alloyed Ti-42Nb precursor powder identified only the β-phase peaks (BCC structure, space group $Im\bar{3}m$). However, the XRD analysis of the samples as-manufactured by SEBM reveals that the alloys consist mainly of β-phase and a small amount of metastable α″-phase (orthorhombic structure, space group *Cmcm*). The martensitic α″-phase transformation has been identified in some previous studies of Ti-Nb alloys [4–6]. The α″-phase was most clearly detected in two samples, produced with a scanning speed of 700 mm/s and current of 4 and 7.5 mA. The appearance of the α-phase can be resulting from a slower cooling rate. The low scanning speed together with high surface energy results in a longer time melt-pool stays 'open' and a decreased cooling rate [5].

Authors acknowledge RSF grant no. 20-43-04430 for the financial support of the sample fabrication and investigation.

REFERENCES

1. M. Niinomi, "Wear Characteristics of Surface Oxidation Treated New Biomedical Beta-Type Titanium Alloy in Simulated Body Environment", Tesu-to-Hagane, vol. 88(9), pp. 567-574, 2002.

2. G. Ryan, A. Pandit, D.P. Apatsidis, "Fabrication methods of porous metals for use in orthopedic applications", Biomaterials, vol. 27, pp. 2651–2670, 2006.

3. M. Fischer, D. Joguet, G. Robin, "In situ elaboration of a binary Ti–26Nb alloy by selective laser melting of elemental titanium and niobium mixed powders", Mater Sci Eng C, vol. 62, pp. 852-859, 2016.

4. M.A. Surmeneva, D. Khrapov, A. Koptyug, "In situ synthesis of a binary Ti–10at% Nb alloy by electron beam melting using a mixture of elemental niobium and titanium powders", Journal of Materials Processing Technology. Elsevier Ltd, 2020. Vol. 282.

5. T. Kurzynowski. M. Madeja, R. Dziedzic, "The effect of EBM process parameters on porosity and microstructure of Ti-5Al-5Mo-5V-1Cr-1Fe alloy", Scanning. Hindawi Limited, 2019.

6. M. Bönisch, A. Panigrahi, M. Calin, "Thermal stability and latent heat of Nb–rich martensitic Ti-Nb alloys", Journal of Alloys and Compounds, vol. 697, pp. 300-309, 2017.

N3-O-044101

SINTERING OF COMPOSITE POWDER COMPACTS Ti_3AlC_2 / Cu*

M.G. KRINITCYN [1]

[1]*Institute of Strehngth Physics and Materials Science SB RAS, Tomsk, Russia*

Triple carbides and nitrides, called MAX phases, form a new class of materials that has very specific properties, combining the properties of both metal alloys and ceramic materials [1, 2]. One of the most promising MAX phases is formed in the Ti-Al-C system. The materials of this system can be used as materials with high strength and deformation resistance, including cyclic loading [3]. The chemical etching of aluminum results in the formation of so-called MXenes, which, due to their nanolaminate structure, can be used in including for storage of electrical energy or hydrogen [4, 5]. Composites "metal - Ti_3AlC_2" are promising materials that combine the advantages of the metal enhanced by the features of the MAX phase. In this work, we studied Ti_3AlC_2/Cu composites obtained by mixing Ti_3AlC_2 powders and copper nanopowder.

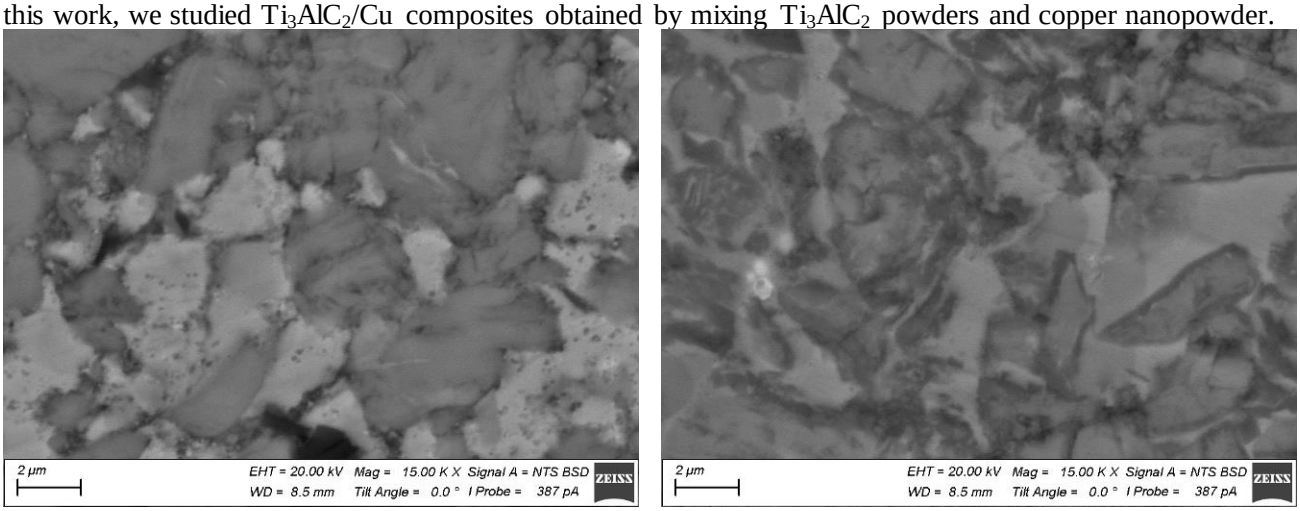

a b

Fig.1. SEM pictures of Ti_3AlC_2 / Cu powder composite cross-sections after sintering at 800 °C and 1050 °C

Bulk samples from the powder of the MAX phase Ti_3AlC_2 and Cu nanopowder were obtained by dry mixing and cold pressing with further vacuum sintering at different temperatures. A comprehensive structural-phase study was carried out using optical and electron microscopy techniques, as well as XRD and EDX analysis. This study allowed to describe the elemental and phase composition, as well as the morphology of both the initial powders and bulk samples.

It was found that the structure of the composites changes with an increase in the sintering temperature, and phase changes also occur: titanium carbide begins to form along the perimeter of the MAX-phase particles. In addition, the MAX phases begin to delaminate, which is clearly seen in the micrographs of the samples. The use of copper nanopowder provides a higher density of compacts and a larger contact surface between copper particles and the MAX phase compared to composites with copper micropowder.

REFERENCES

[1] Authors, “Article title,” Abbreviated Journal Title, vol. , no. , pp. , Month year .

[2] T. V. Koval, Le Hu Dung, “Investigation of plasma generation and current transmission of an intense low-energy electron beam,” Izv. Vyssh. Uchebn. Zaved. Fiz., vol. 57, no. 3/2, pp. 118–121, March 2014.

[3] L.P. Zharkova, I.V. Romanchenko, M.A. Bolshakov, V.V. Postov, “Mitochondrial respiration inhibition after exposure to UWB pulses as a possible mechanism of antitumor action,” J. Phys. Conf. Ser., vol. 830, 2017.

[4] Authors, Book Title, City: Publishing House, year.

[5] Y. Korolev and G. Mesyats, Physics of Pulsed Breakdown in Gases. Yekaterinburg: UrB RAS, 1998.

[6] Authors, “Article title,” Proc. Conf., City, Country, pp. , year.

[7] M.S. Vorobyov, V.F. Tarasenko, E.Kh. Baksht, A.V. Kozyrev, N.N. Koval, S.Yu. Doroshkevich, “Energy spectrum of an electron beam outputted into ambient air on an electron accelerator with a grid plasma cathode,” Proc. 20th Int. Conf. on High Current Electronics (ISHCE), Tomsk, Russia, pp. 209–213, 2018.

* The work was supported by a grant from the President of the Russian Federation for state support of young scientists No. MK-209.2022.4

N3-O-044102

SYNTHESIS AND SINTERING OF THE W / CU PSEUDOALLOY*

M.G. KRINITCYN [1], N.E. TOROPKOV [1], A.V. PERVIKOV [1], M.I. LERNER [1]

[1]Institute of Strength Physics and Materials Science SB RAS, Tomsk, Russia

Over the past decade, the development and synthesis of bimetallic nanomaterials has attracted much attention due to their functionality, mechanical properties, catalytic activity, and other characteristics compared to monometallic nanomaterials [1]. Alloys W - Cu are widely used for the manufacture of heavy-duty electrical contacts and electrodes [2]. Copper provides high conductivity, while tungsten provides mechanical strength, tribological resistance and hardness.

Recently, there has been increased interest in W-Cu pseudoalloys due to their excellent temperature control properties and high microwave absorption capacity. Due to the mutual insolubility of the elements, it is difficult to form microscale composites of this system by solid-phase and liquid-phase sintering, or the formed composites have anisotropy of properties. Obtaining a nanopowder in the process of explosion, and not from mixtures of powders, makes it possible to obtain a structure with a uniform distribution of elements over the volume, which leads to isotropy of properties at the microlevel [3].

In the present study, bimetallic nanoparticles were obtained by electric explosion of two wires, one of which is W and the other is Cu. Wires of a certain diameter were chosen, so that the Cu content did not exceed 30%. The synthesized powders were passivated in the atmosphere to reduce their pyrophoricity.

The powder is represented by both micro- and nanoparticles. In this case, the maximum size of microparticles is 10 μm, and the nanostructure as a whole is preserved. The study of the elemental composition shows the presence of tungsten and copper, the W:Cu ratio is 70:30 by weight. Oxygen is present in an amount of not more than 10 at.% on the surface of the particles. Its presence is associated with the passivation of the powder in air. The phase composition shows the presence of small amounts of tungsten oxide (identical to β-W), in addition to pure α-W and Cu.

The pressed W-Cu powders were sintered at different temperatures. Initially, the samples have high porosity, which is associated with poor compressibility of the powders. The porosity of raw samples is at the level of 16% and begins to decrease with an increase in the sintering temperature. Above 900°C, a sharp shrinkage of the sample occurs, associated with the approach to the melting point of copper (T_{melt} = 1085°C, T = 900°C = 0.83 T_{melt}). When Tm is reached, the density reaches 98% and further growth stops. The established sintering modes indicate the need for sintering at a temperature not lower than 950 °C to increase the density of the samples. The experimentally obtained behavior of W-Cu powder shrinkage during sintering as a function of temperature is confirmed by literature data on this system [4].

The microhardness (HV 0.5/10) of the samples after sintering at 1000°C is 2.2 ± 0.2 GPa. The hardness of the composite is 1.95 GPa calculated according to the rule of mixtures:

$$H = n_W H_W + n_{Cu} H_{Cu}$$

where H_W and H_{Cu} are the theoretical hardness of W and Cu, respectively, n_W and n_{Cu} are the proportional contents of W and Cu, respectively, $n_W + n_{Cu} = 1$). The hardness of the obtained samples is higher than expected due to the presence of dispersed particles W in the material. The particle size W does not change after sintering due to the relatively low temperature of the process.

REFERENCES

[1] Druzhinin A. V. et al. The effect of interface stress on the grain boundary grooving in nanomaterials: Application to the thermal degradation of Cu/W nano-multilayers //Scripta Materialia. – 2021. – Vol. 199. – No. 113866.

[2] Lungu M. V. Synthesis and processing techniques of tungsten copper composite powders for electrical contact materials (A Review) //Oriental Journal of Chemistry. – 2019. – Vol. 35. – No. 2. – P. 491.

[3] Hou C. et al. W–Cu composites with submicron-and nanostructures: progress and challenges //NPG Asia Materials. – 2019. – Vol. 11. – No. 1. – P. 1-20.

[4] Zhuo L. et al. Achieving both high conductivity and reliable high strength for W–Cu composite alloys using spherical initial powders //Vacuum. – 2020. – Vol. 181. – No. 109620.

* The study was supported by a grant from the Russian Science Foundation (project No. 21-79-30006)

N3-O-044301

SYNTHESIS OF TI-AU UNDER CONDITIONS OF ELECTRON BEAM WELDING

VASILIY KLIMENOV[1], MIKHAIL SLOBODYAN2[1,2], VASILIY FEDOROV[1] IRINA STRELKOVA[1], ANATOLIY KLOPOTOV[3], MARGARITA KHIMICH[4,5], SERGEY MATRENIN[1], DARYA SEMEYKINA[1]

[1]*National Research Tomsk Polytechnic University; 30, Lenin Avenue, Tomsk, 634050, Russia*
[2]*Tomsk Scientific Center of Siberian Branch of Russian Academy of Sciences; 10/4, Akademicheskii Prospekt, 634055, Russia*
[3] *Tomsk State University of Architecture and Building;2, Solyanaya Square, Tomsk, 634003, Russia*
[4] *Institute of Strength Physics and Materials Science of Siberian Branch of Russian Academy of Sciences; 2/4,Akademicheskii Prospekt, 634055, Russia*
[5] *National Research Tomsk State University; 36, Lenin Avenue, Tomsk, 634050, Russia*

Titanium is the most suitable material for many medical products, such as implants, endoprostheses, plates for osteosynthesis and cranioplasty of skulls, as well as various fasteners (bridges, staples, screws, etc.) in traumatology and dentistry due to its good combination of physical, mechanical and biomedical properties [1–4]. At the same time, improving both strength and corrosion resistance of such products is an urgent task nowadays [5, 6]. The fact is that commercially pure titanium (CP Ti) possesses advanced inert and biocompatible characteristics, but it has some disadvantages as well, including reduced deformability and insufficient wear resistance [7]. In addition, the high melting point and reactivity of titanium to oxygen and nitrogen complicate its processing and treatment for improving functional properties. Thus, alloying titanium with various metals is the common method for this purpose, but it has some limitations because of incompatibilities with human bodies that greatly narrow the range of possible compositions. So, despite the widespread use of such titanium alloys as the TiNi intermetallic compounds, possessing the shape memory effect, the Ti-6Al-4V alloy, characterized by improved strength characteristics, and the Ti-Nb ones with relatively low elastic modulus [5], there are some issues due to the presence of toxic Ni, Al, V and Nb as their components. Therefore, there is a huge interest in alloying titanium with noble metals (such as silver, gold and platinum) for some dental applications for many years despite their high cost [8–11]. In addition to being non-toxic, they can also have anti-microbial and anti-inflammatory effects on human bodies (silver, as an instance) [12–17]. It should be noted that both mechanical properties and corrosion resistance must be improved in these cases [13, 14, 16], which determine the reliability and durability of such implants or prostheses. Consequently, titanium biomedical alloys with noble metals (first of all, with gold) have been studied in sufficient detail [12–17]. The influence of the Ti-Au alloy compositions on their microstructure, forming phases and mechanical properties has been reported for a fairly wide range of gold concentrations (up to 40%, by weight as a rule) [13, 14, 16] and even from 0 up to 100% [17]. Typically, their phase compositions have been determined on the basis of both equilibrium Ti-Au state diagram (drawn by J.L. Murray [18]) and data, thermodynamically calculated using the CALPHAD method [19]. However, there are still some gaps in knowledge, which the authors of paper [17] have tried to fill by a detailed study of the Ti-Au alloys, connecting the phase diagram plots with Vickers hardness values. Two data arrays have been distinguished: high hardness levels of 6.50–7.80 GPa for the gold concentrations in the range of 22–34 wt.% and low ones of 2.64–2.83 GPa at its contents of 50–80 wt.%. The low hardness range is close to that for cast CP Ti, while the high hardness values are associated with the formation of the Ti3Au intermetallic compound. Respectively, these observed patterns enable to use microhardness tests as an express method for identifying the formation of the Ti3Au phase in the Ti-Au alloys.

REFERENCES

[1] C. Leyens, M. Peters, Titanium and Titanium Alloys. Fundamentals and Applications. Weinheim, WILEY- VCH Verlag GmbH & Co., 2003.

[2] F.H. Froes (Ed.), Titanium – Physical Metallurgy, Processing, and Applications. Materials Park, ASM International, 2015.

[3] J. Wataha, G. Schmalz, Dental Alloys. In: Biocompatibility of Dental Materials. Berlin, Springer, 2009. pp. 221–254. https://doi.org/10.1007/978-3-540-77782-3_8

[4] Q. Chen, G.A. Thouas, Metallic implant biomaterials, Materials Science and Engineering R: Reports 87 (2015) 1–57. https://doi.org/10.1016/j.mser.2014.10.001

[5] L.-C. Zhang, L.-Y. Chen, A review on biomedical titanium alloys: recent progress and prospect, Advanced Engineering Materials 21:4 (2019) 1801215. https://doi.org/10.1002/adem.201801215

[6] N. Eliaz, Corrosion of metallic biomaterials: a review, Materials 12:3 (2019) 407. https://doi.org/10.3390/ma12030407

N3-O-044801

INFLUENCE OF THE CURRENT PULSE SHAPE IN SMALL-SCALE RESISTANCE SPOT WELDING OF A NICKEL ALLOY ON ITS MICROSTRUCTURE-RELATED PROPERTIES OF THE JOINTS

S.E. BUTSYKIN[1,2], *M.A. ELKIN*[1,2], *V.A. KLIMENOV*[1], *M.S. SLOBODYAN*[3]

[1]*Tomsk Polytechnic University, Tomsk, Russia*
[2]*Research and Production Center 'Polyus', Tomsk, Russia*
[3]*Tomsk Scientific Center SB RAS, Tomsk, Russia*

The influence of various current pulse shapes in small-scale resistance spot welding of the nickel alloy plates 0.2 mm thick on its microstructure-related properties of the joints are presented. The first mode was a rectangular current pulse, the second one included the preheating stage, which was supplemented by a prolonged down slope in the third case (Fig. 1a).

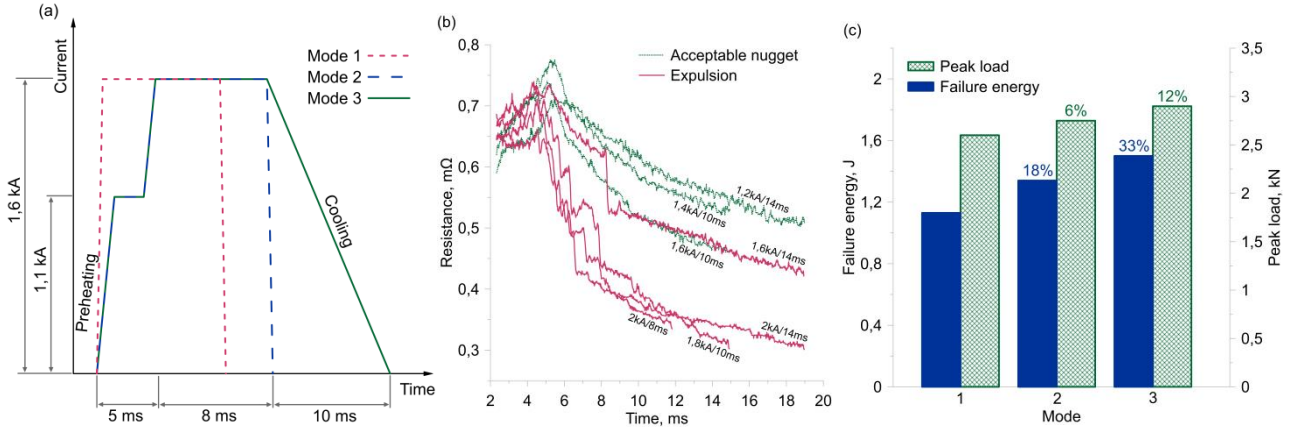

Fig.1. The welding current pulse shapes (a); sheet-to-sheet dynamic resistance curves (b); the corresponding tensile test results for the welded joints (c)

The mechanical properties of the welded joints were determined by tensile tests in accordance with [1, 2]. Vickers microhardness was measured along the diagonal axis of the nugget with a step between indentations of 50 μm. The microstructure was investigated using an optical microscope. Upon welding, the real current and voltage values were recorded using a digital oscilloscope.

Two types of the dynamic resistance curves were observed in the welding process (Fig. 1b). The optimal nugget sizes corresponded to a smooth decrease in the curves. Their sharp drop was recorded in the case of the metal expulsion. This result was consistent with the data reported by the authors [3], explained this phenomenon by the loss of the nugget material, shortening the current path.

The preheating stage stabilized heat input due to preliminary microroughness deformation and fracture of oxide films [4, 5], causing the sound weld and an increase in its failure energy by 18% (Fig. 1c). With a rectangular current pulse, cracks appeared in the cross section of the nugget. High cooling rates had inhibited volumetric diffusion that resulted in a non-equilibrium microstructure of the core metal. In this case, alloying elements were unevenly distributed in the nugget volume, affecting its tensile properties [6]. The prolonged down slope of the current pulse had reduced the solidification rate of the molten nugget metal. As a result, deviations of its final microhardness values from their average levels were reduced by about two times and the joint tensile strength was significantly improved.

REFERENCES

[1] B.D. Orlov, Control of spot and roller electric welding. Moscow: Engineering, 1973.

[2] M. Zhou et al, "Critical specimen sizes for tensile-shear testing of steel sheets," Welding journal, vol. 78, pp. 305–313, September 1999.

[3] W. Tan et al, "A study of dynamic resistance during small scale resistance spot welding of thin Ni sheets," Journal of physics D: Applied physics, vol. 37, pp. 1998-2008, June 2004.

[4] F.L. Jones, The Physics of Electrical Contacts. Oxford: Clarendon Press, 1957.

[5] V.V. Usov, Metallurgy of Electrical Contacts. Moscow: Gosenergoizdat, 1963.

[6] B.D. Orlov, Technology and equipment of contact welding. Moscow: Engineering, 1975.

N3-O-048801

MAGNETRON SPUTTERING AND LEHCEB SYNTHESIS OF TI-NB, TI-W AND TI-TA SURFACE ALLOYS FOR THE ENHANCEMENT OF MECHANICAL PROPERTIES AND WEAR RESISTANCE

FEDERICO MORINI[1], MASSIMILIANO BESTETTI[1,2], NORA LECIS[3], KARIM SALAHELDIN[3]

[1]Politecnico di Milano, Department of Chemistry, Materials and Chemical Engineering "Giulio Natta", Milano, Italy
[2]Tomsk Polytechnic University, The Weinberg Research Center, Tomsk, Russia
[3]Politecnico di Milano, Department of Mechanics, Milano, Italy

Titanium and its alloys are characterized by excellent mechanical and corrosion resistance properties that make them interesting for various applications such as in automotive and aerospace fields, and biomedical implants. [1] However, titanium is characterized by poor wear resistance restricting its application. There is the possibility to enhance such property by forming surface alloys of titanium with other metals.

By combining magnetron sputtering deposition and Low Energy High Current Electron Beam (LEHCEB) it is possible to produce surface alloys with improved properties, by keeping the bulk properties unaltered. In this way the outermost micrometric layer can be characterized by higher microhardness, lower elastic modulus and lower friction coefficient. [2, 3]

In the present work chemical etched and LEHCEB pretreated (20 kV and 5 pulses) c.p. Ti substrates were prepared, then thin films of Nb (100 nm), W (350 and 700 nm) or Ta (700 nm) were deposited by DC magnetron sputtering onto substrates. Finally, surface alloying was carried out by LEHCEB, by varying the acceleration voltage (25 and 30 kV) and the number of pulses (from 10 to 80), depending on the thermophysical properties of thin films metals.

The surface alloys were characterized in terms of chemical and phase composition. Mechanical properties (Vickers microhardness and elastic modulus) were investigated as well friction coefficient through wear resistance tests, both on treated and untreated samples.

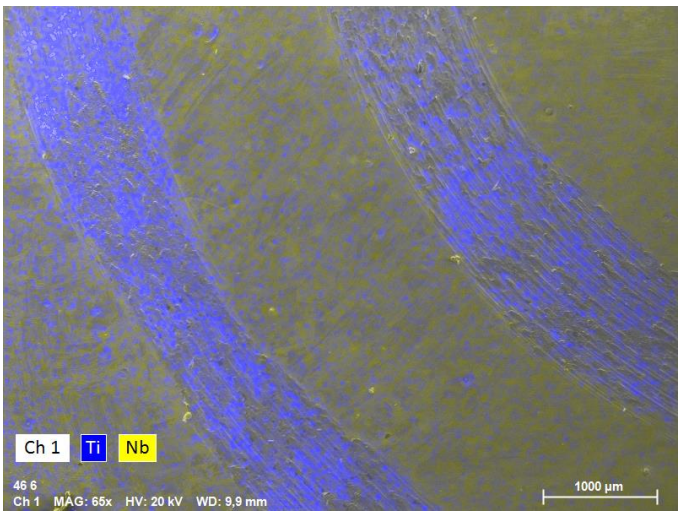

Fig.1. Surface EDS map of the Al_2O_3 ball trace left on Ti-Nb wear tests on sample synthetized with 100 nm of deposited Nb and LEHCEB alloyed at 25 kV with 10 pulses.

REFERENCES

[1] R. P. Kolli and A. Devaraj, "A review of metastable beta titanium alloys" Metals (Basel), vol. 8, no. 7, pp. 1–41, 2018

[2] J. X. Zou, K. M. Zhang, S. Z. Hao, C. Dong, and T. Grosdidier, "Mechanisms of hardening, wear and corrosion improvement of 316 L stainless steel by low energy high current pulsed electron beam surface treatment," Thin Solid Films, vol. 519, no. 4, pp. 1404–1415, 2010.

[3] F. Morini, M. Bestetti, S. Franz, A. Vicenzo, A. Markov, E. Yakovlev, "Synthesis and Characterization of Ti–Nb Alloy Films Obtained by Magnetron Sputtering and Low-Energy High-Current Electron Beam Treatment", Materials, vol. 14, 2021.

N3-O-051201

SYNTHESIS OF CU-NB ALLOYS BY LOW ENERGY HIGH CURRENT ELECTRON BEAM

LUCA MURACHELLI [1], MASSIMILIANO BESTETTI [1,2], ANTONELLO VICENZO [1], SILVIA FRANZ [1]

[1]Politecnico di Milano, Department of Chemistry, Materials and Chemical Engineering "Giulio Natta", Milano, Italy
[2]Tomsk Polytechnic University, The Weinberg Research Center, Tomsk, Russia

Copper-niobium alloys are of great interest in the fields of high deformability, high conductivity, strain hardening and superconducting alloys [1, 2]. Niobium, due to the very limited solubility in copper, exhibits strong tendency towards segregation, leading to the impossibility of proper production of single-phase Cu-Nb alloys via traditional methods [2]. On the other hand, Low Energy High Current Electron Beam (LEHCEB) gives the possibility to deliver enough energy in the form of electron beam pulses of microseconds, that allow melting and solidifying, at extremely high cooling rates layers, of few micrometres layers [3].

By combining in this way, elements are mixed together at the liquid state and the rapid solidification brings to the formation of non-equilibrium alloys [4]. This is an innovative route for vacuum surface treatment of materials. Coatings result being strongly adherent to substrates [5].

Cu-Nb surface alloys were realized by magnetron sputtering niobium thin films (thicknesses from 100 to 500 nm) onto commercially pure copper. Samples were then irradiated with three electron beam pulses at different accelerating voltages (from 15 to 30 kV, resulting in energy density between 1.64 and 5.56 J/cm^2). X-Ray Diffraction (XRD), surface topography and micro indentation data were used for characterization. Diffraction spectra highlighted non-equilibrium FCC solid solutions with 29.7 and 80.2 at % of copper, as well as BCC solid solutions with 77.3 and 47.4at% of niobium. Microhardness of Cu-Nb surface reached up to 450 HV, with a large increment with respect to copper substrate (120 HV).

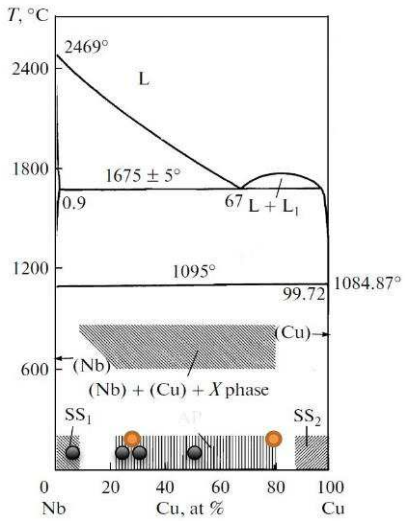

Fig.1. Non-equilibrium phase diagram of the niobium-copper system. At room temperature: SS1, solid solution of copper in niobium; SS2, solid solution of niobium in copper; central part, amorphous phase [6].

Superimposed: phases obtained via LEHCEB. Black dot for BCC Nb-based and orange dot for FCC Cu-based alloys.

REFERENCES

[1] C. C. Tsuei, Superconducting composite of copper and niobium - a metallurgical approach, Journal of Applied Physics, 1974, 45, pp. 1385 – 1388.

[2] R. Roberge, J. L. Fihey, Origin of Superconductivity in copper niobium alloys, Journal of Applied Physics, 1977, 48, pp. 1327 – 1331.

[3] V. Rotshtein, Y. Ivanov, A. Markov, Surface Treatment of Materials with Low-Energy High-Current Electron Beams in Materials Surface Processing by Direct Energy Techniques, Elsevier, 2006, pp. 205 – 240.

[4] C. Zhang et al., The microstructure and properties of tungsten alloying layer on copper by high-current pulse electron beam, Applied Surface Science, 2017, 422, pp. 582 – 590.

[5] A. B. Markov, E. V. Yakovlev, V. Petrov, Electron-Beam Technique for Forming HighConductivity and High-Adhesion Surface Alloy for Application in Microelectronics, Proceedings of 28th International Symposium on Discharges and Electrical Insulation in Vacuum, Greifswald, Germany, September 23 - 28, 2018, pp. 717 – 720.

[6] V. N. Volodin, Yu. Zh. Tuleushev, E. A. Zhakanbaev, Structure and Phase Composition of Niobium-Copper Deposited Films, X-Ray Synchrotron and Neutron Techniques in Journal of Surface Investigation, 2015, 9, 1, pp. 178 – 183.

N3-P-009202

MACRO- AND MICROSTRUCTURE OF THE SUPERALLOY COMPONENTS FORMED BY ELECTRON BEAM ADDITIVE MANUFACTURING*

S.Y. NIKONOV, S.V. FORTUNA, D.A. GURIANOV

Institute of Strength Physics and Materials Science SB RAS, Tomsk, Russia

Additive manufacturing processes are characterized by very high temperature gradients and crystallization rates. These conditions lead to the formation of microstructural elements of a smaller size than in conventional casting processes, a multiple or more times. As applied to nickel-based superalloys, this opens up potential opportunities for developing methods for forming parts of the hot path of gas turbine plants with improved performance [1]. However, the high cracking susceptibility of PH superalloys is a problem for additive products.

In the present work, additive products of a simplified form in the form of vertical walls from the second generation superalloy ZhS32 [2] were fabricated by means of electron beam additive manufacturing (EBAM). The influence of heat input [3] and the printing strategy on the given geometry of additive products, on the formation of macrodefects in the material of products, as well as on the sizes and morphology of microstructure elements was studied. The studies were carried out by means of optical and scanning electron microscopy.

As an example, Figure 1 shows images of the microstructure of superalloy ZhS32 in the initial (cast) state, as well as the material of an additive product formed from bars of the same alloy on a substrate of austenitic steel SS316. It is clearly seen that the microstructure of the material of the additive product is represented by colonies of dendrites. In this case, the axes of the first-order dendrites are predominantly oriented along the direction of additive growth of the product (building direction - BD in Figure 1b) with an inclination of approximately 30 degrees towards the 3D printing trajectory (scanning trajectory - ST in Figure 1b). Note that the average distance between the axes of the first-order dendrites λ_1 in the material of the additive product is about 33 μm, and in the cast state about 75 μm.

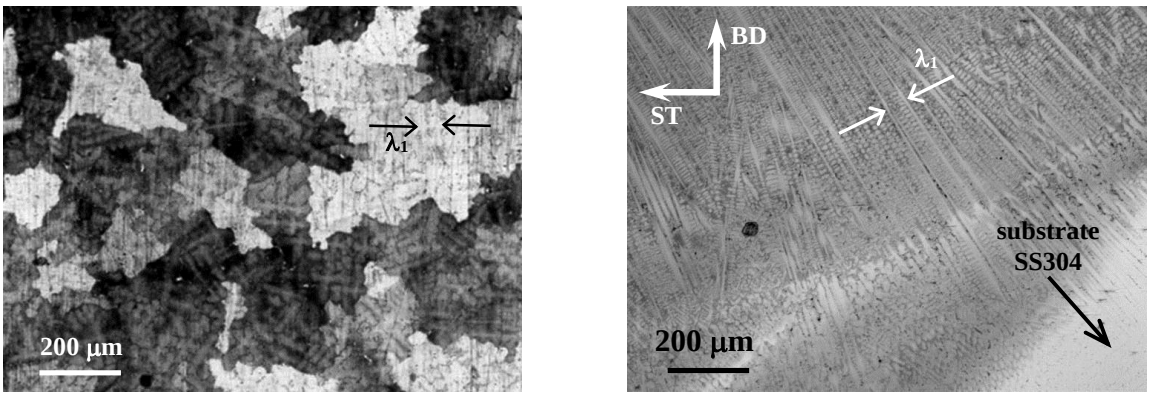

(a) (b)

Fig. 1. Microstructure of nickel-based superalloy ZhS32 in the as-cast state (a) and microstructure of material of product obtained by wire-feed EBAM (b)

REFERENCES

[1] G. Liu, D. Du, K. Wang, Z. Pu, D. Zhang, B. Chang, "Microstructure and nanoindentation creep behavior of IC10 directionally solidified superalloy repaired by laser metal deposition," Mater. Sci. Eng. A, vol. 808, 140911, 2021.

[2] P. Fernandez-Zelaia, O. D. Acevedo, M. M. Kirka, D. Leonard, S. Yoder, Y. Lee, "Creep Behavior of a High-γ′ Ni-Based Superalloy Fabricated via Electron Beam Melting," Metall. Mater. Trans. A., vol. 52a., pp. 574-590, 2021.

[3] ISO 857-1:2002 Welding and Allied Processes—Vocabulary—Part 1: Metal Welding Processes.

* The investigation was supported by the Russian Science Foundation grant No. 22-22-00891, https://rscf.ru/en/project/22-22-00891/.

N4-O-001201

NV-CENTERS LASER GENERATION IN DIAMOND*

D.E. GENIN[1,2], *A.D. SAVVIN*[1], *M.A. SHULEPOV*[1,2]

[1]*National Research Tomsk State University, Tomsk, Russia*
[2]*Institute of High Current Electronics SB RAS, Tomsk, Russia*

Diamond is a promising material for quantum electronics and photonics due to its unique properties: hardness, high thermal conductivity, big value of charge carrier mobility (for both electrons and holes), good radiation stability. Also diamond can contain colour centers that are supposed to be used as room-temperature qubits: NV, SiV, PbV, SnV etc., where V is a vacancy.

In process of quantum calculations we need laser radiation to perform initialization and reading operations. If qubits are the part of diamond lattice, it is convenient to use laser that is also based on diamond. In the future fully diamond-based quantum computer can be created.

In 2021 laser generation in diamond, containing NV-centers in the negative charge state (NV^-), was observed for the first time ever [1]. The pulse energy was estimated as 10 nJ, the linewidth was about 15 nm at half maximum. In the current work we tried to improve the results and define the optimal impurity-defect composition of diamond sample. We managed to obtain radiation with more narrow line (approximately 6 nm) and far bigger pulse energy – up to 50 μJ.

NV^--laser can be applied for operations with SiV qubits. In the future we plan to obtain laser generation on other centers, which will enable to operate NV^- qubits.

REFERENCES

[1] Savvin, A., Dormidonov, A., Smetanina, E. et al. “NV– diamond laser”, Nat Commun 12, 7118 (2021)

* The study was carried out on the state order of the Ministry of Science and Higher Education of the Russian Federation, project № 0721-2020-0048.

N4-O-009501

SYNTHETIC DIAMOND COLOR CENTERS IN QUANTUM INFORMATION TECHNOLOGIES*

E.I. LIPATOV[1,2]

[1]*Institute of High Current Electronics, Tomsk, Russian Federation*
[2]*Tomsk State University, Tomsk, Russian Federation*

Synthetic diamond is beginning to use in quantum technologies: sensing, computing and cryptography. The characteristics of diamond are such that they will allow diamond-based devices to operate at room and elevated temperatures, at high levels of radiation and in chemically aggressive environments. In addition to quantum technologies, diamond will get applications in radiation-resistant, high-temperature and power electronics and photonics.

Optically active centers in diamond containing a vacancy and impurity atoms (N, N_2, Si, Ge, etc.) are characterized by high photostability, absorption and luminescence spectra in the visible range, and characteristic luminescence times on the scale of tens of nanoseconds [1–3]. Most of the centers mentioned are relatively easy to create in a diamond sample in the process of diamond synthesis or during its post-growth radiation-thermal treatment.

The recent demonstration of laser radiation at NV centers under optical pumping [4] opens up wide opportunities for creating injection diamond lasers and then integrated diamond lasers based on photoactive color centers. This, in turn, will make it possible to create compact integrated quantum magnetic field sensors, quantum processors based on the spin states of NV centers in diamond, etc.

The report presents the results of studies of optical absorption, luminescence, excitation of spin states of photoactive centers, discusses the existing and possible applications of impurity-defect centers in diamond, photoactive in the green and red regions of the visible range, for problems of integrated optics, quantum communications and quantum computing.

REFERENCES

[1] I. A. Dobrinets, V. G. Vins, A. M. Zaitsev, “HPHT-Treated Diamonds,” Springer Series in Materials Science, vol. 181, pp.1-270, 2013.

[2] M. A. Lobaev, D. B. Radishev, S. A. Bogdanov, A. L. Vikharev, A. M. Gorbachev, V. A. Isaev, S. A. Kraev, A. I. Okhapkin, E. A. Arhipova, M. N. Drozdov, V. I. Shashkin, “Diamond p-i-n diode with nitrogen containing intrinsic region for the study of nitrogen-vacancy center electroluminescence,” Physica Status Solidi, vol. 14, no. 11, 2000347, 2020.

[3] S. Pezzagna, J. Meijer, “Quantum computer based on color centers in diamond,” Applied Physics Reviews, vol. 8, 011308, 2021.

[4] A. Savvin, A. Dormidonov, E. Smetanina, V. Mitrokhin, E. Lipatov, D. Genin, S. Potanin, A. Yelisseyev, V. Vins, “NV^- diamond laser,” Nature communications, vol. 12, 7118, 2021.

* The work was supported by the Ministry of Education and Science of Russian Federation (the state order, project No 0721-2020-0048).

N4-O-011102

EDGE CATHODOLUMINESCENCE IN DIAMOND IN TEMPERATURE RANGE FROM 70 TO 500 K*

V.S. RIPENKO[1,2], *A.G. BURACHENKO*[1,2], *A.S. POPOVA*[2], *D.A. PERESEDOVA*[2]

[1]*Institute of high current electronics SB RAS, Tomsk, Russia*
[2]*National research Tomsk state university, Tomsk, Russia*

Paper deals with the spectral study of the radiative recombination of free excitons in synthetic diamonds, irradiated by a beam of charged particles (electrons) in a temperature range from 70 to 500 K. This method of treatment is an example of nondestructive inspection technique of the crystal structure perfection of a synthetic sample. In addition, diamond, having a strong exciton cathodoluminescence, is a promising material for using it as a luminophore in a cathodoluminescent emitter.

There are relatively few works devoted to the study of diamond luminescence at elevated temperature. For example, authors of [1, 2] studied the glow of diamond samples at elevated temperatures with electroluminescence. In [3, 4] the temperature dependences of the cathodoluminescence peaks of free excitons in CVD diamonds was investigated. But we didn't found data on the behavior of luminescence at temperatures above 300 K.

In our work we used HTHP diamond samples for luminescence investigations. Figure 1 shows non typical dependence of exciton peak intensity at 235 nm from temperature.

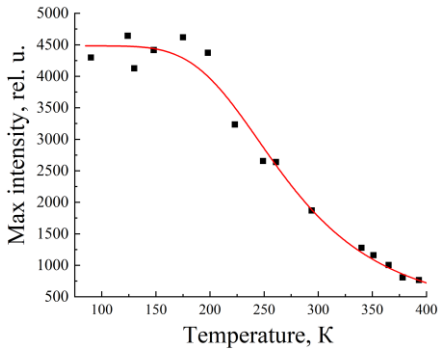

Fig.1. Dependence of excitonic peak intensity at 235 nm from temperature.

Knowledge and understanding of the behavior of exciton cathodoluminescence in diamond can become an impulse for the creation of a new type of ultraviolet emitter.

REFERENCES

[1] S. Lagomarsino et al. "Robust luminescence of the silicon-vacancy center in diamond at high temperatures, " AIP Advances., vol. 5, no. 12, pp. 127117, 2015.

[2] A.A. Melnikov, A.V. Denisenko, A.M. Zaitsev, A. Shulenkov, V.S. Varichenko, , A.R. Filipp, V.A. Dravin, H. Kanda, W.R. Fahrner "Electrical and optical properties of light-emitting p–i–n diodes on diamond, " Journal of applied physics., vol. 84, no. 11, pp. 6127-6134, 1998.

[3] Y. Chen, P. Jin, G. Zhou, M. Feng, F. Fu, J. Wu, Z. Wang "Investigation ofexcitonic recombination in single-crystal diamond with cathodoluminescence spectroscopy, " Journal of Luminescence, vol. 226, pp.117428, 2020.

[4] H.Watanabe, C.E. Nebel "Cathodoluminescence experiments on isotopic clean diamond with carbon isotopes ^{12}C and ^{13}C, " Diamond and Related Materials, vol. 4-5, pp. 511-514, 2008.

* The work was supported by the Russian Science Foundation (Grant No. 22-22-00984).

N4-O-011202

SUPERLUMINESCENCE OF NV CENTERS IN DIAMOND PUMPED BY THE SECOND HARMONIC OF A ND:YAG LASER *

D.E. GENIN[1], V.P. MIRONOV[1], E.N. TEL'MINOV[1], M.A. SHULEPOV[1,2]

[1]National Research Tomsk State University
[2]Institute of High Current Electronics SB RAS, Tomsk, Russia

In the light of the creation of a diamond laser [1], an urgent task is to determine the characteristics of diamonds in order to determine the range in which such lasers can be created not in isolated cases. This work is aimed at creating superluminescence in diamond under the action of optical pumping by the second harmonic of an ND:YAG laser (λ=532nm).

At a pump intensity above ~2.0 MW/cm^2 in the spectral region of 700–760 nm, against the background of the spontaneous luminescence spectrum, a nonlinear increase in intensity was detected in the HPHT diamond sample upon pulsed excitation by an ND:YAG laser, and with a further increase in the pump intensity, this band turns into an intense a peak with a maximum at about 718 nm. The FWHM of this peak increased from 13 to 19 nm as the pump intensity increased from 2.7 to 46 MW/cm^2. At high pump intensities, nonlinearities were found in the absorption and accumulation of NV centers in the excited state. Superluminescence was observed only in separate growth zones of the crystal.

The calculation of the position of the photoluminescence band, carried out taking into account the intrinsic absorption spectrum of the crystal, is close to the experimental one. On fig. 1 against the background of the absorption spectrum shows the calculated emission spectra calculated at inversion densities N*(cm^{-3}) = 1·10^{17}; 2·10^{17}; 2.5·10^{17}cm^{-3} and medium length 1 cm.

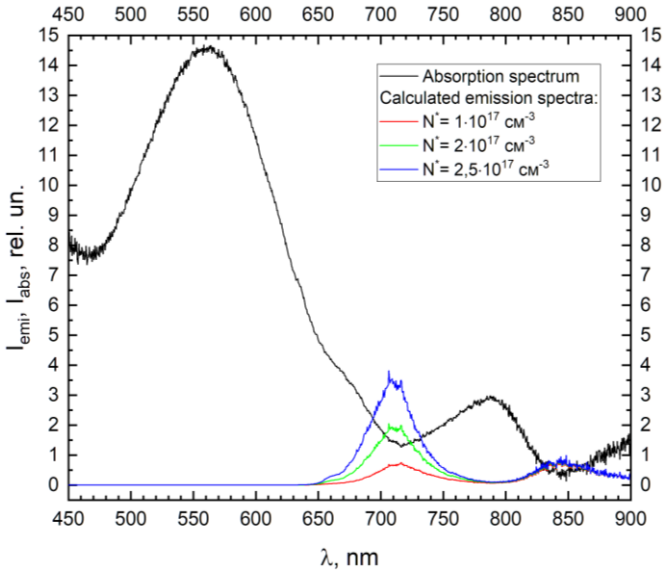

Fig.1. Absorption spectrum and calculated emission spectra.

REFERENCES

[1] Savvin, A., Dormidonov, A., Smetanina, E. et al. NV– diamond laser. Nat Commun 12, 7118 (2021). https://doi.org/10.1038/s41467-021-27470-7

* The study was carried out on the state order of the Ministry of Science and Higher Education of the Russian Federation, project No 072120200048.

N4-O-011801

CALCULATION OF ONE-DIMENSIONAL PHOTONIC CRYSTALS BASED ON DIAMOND

V. V. CHASHCHIN[1], *E. I. LIPATOV*[1,2]

[1]*National Research Tomsk State University, Tomsk, Russia*
[2]*Institute of High Current Electronics SB RAS, Tomsk, Russia*

Diamond is a very perspective material for photonic and optical applications due to its unique physical and chemical properties (e.g. high refractive index of diamond n=2.42). Despite the fact that doping with nitrogen doesn't have a strong effect on the refractive index of diamond, it nevertheless changes by ~1%, that gives us the opportunity to use a structure consisting of a set of diamond layers with and without substitutional nitrogen as a photonic crystal [1].

One-dimensional photonic crystal is a structure with periodic change of refractive indices in one direction [2]. In our work we have structure which consists of periodically alternating layers of undoped diamond and nitrogen-doped diamond layers. The main advantage of same structures is the ability to obtain almost 100% reflection in the range of the optical spectrum we are interested in. This property of one-dimensional photonic crystals makes them advantageous for use as laser resonators.

In this paper, we used the finite element method to calculate the parameters of a diamond-based one-dimensional photonic crystal of interest to us, including the values of the maximum possible reflection.

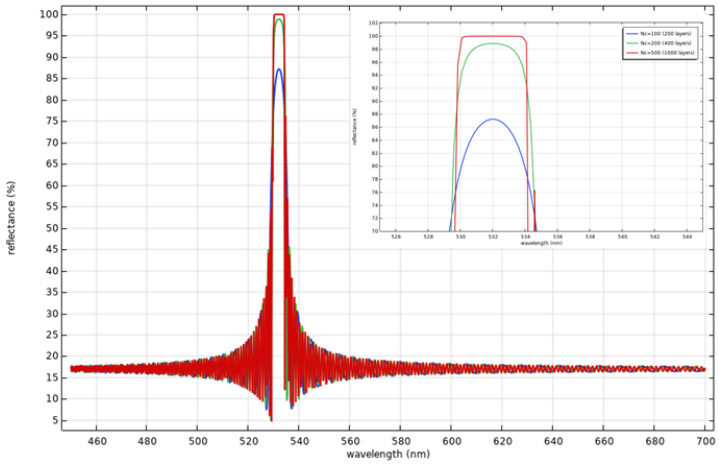

Fig. 1 Reflection from simulation

Fig. 1 shows a computed dependence graph of the reflection coefficient on the wavelength while different numbers of layers of the structure were used. The results were obtained for a different number of pairs (N=100, 200, 500) of nitrogen-doped diamond layers (n=2.39) and undoped diamond layers (n=2.42) for the wavelength of interest (λ=532 nm). When calculating the thicknesses of the layers the Wulff-Bragg's condition was used:

$$2 \cdot \Lambda = m \cdot \lambda,$$

where Λ – period of the one-dimensional photonic crystal, λ – central wavelength, m – integer.

REFERENCES

[1] Zaitsev A. M. Optical properties of diamond: a data handbook. – Springer Science & Business Media, 2013

[2] Krauss T. F., Richard M. Photonic crystals in the optical regime—past, present and future //Progress in Quantum electronics. – 1999. – Т. 23. – №. 2. – С. 51-96.

N4-O-014302

CHERENKOV RADIATION IN DIAMOND EXCITED BY ELECTRON BEAM WITH AN ENERGY OF TENS-HUNDREDS OF KEV IN A WIDE TEMPERATURE RANGE*

A.G. BURACHENKO[1,2], *V.S. RIPENKO*[1,2], *E.I. LIPATOV*[1,2], *K.P. ARTYOMOV*[1], *A.A. KRYLOV*[1]

[1] *High Current Electronics Institute SB RAS, Tomsk, Russia*
[2] *Tomsk State University, Tomsk, Russia*

Cherenkov detectors based on the Cherenkov effect are widely used to detect high-energy electron fluxes. Since Cherenkov radiation occurs only at a certain energy of a charged particle, then due to particles with energies less than this energy, radiation caused by luminescence can be detected. The parasitic contribution of luminescence to the signal of a Cherenkov detector can be especially noticeable also in the case of registration of electrons with an energy of tens to hundreds of keV. One of the promising areas of the Cherenkov detector application is thermonuclear installations, in which it is necessary to control high-energy electron fluxes from energies of tens to hundreds of keV, which can adversely affect the operation of a thermonuclear installation, up to its complete failure. Another promising area is the detection of charged particles fluxes of the solar wind in near-Earth outer space, due to which the electronic equipment of space vehicles can fail, which also entails huge financial costs. In both cases, the registration of electron fluxes must be carried out in a wide temperature range, which can reach above 500 K. Therefore, special requirements are imposed on the material of the Cherenkov detector radiator. One of the most suitable materials for a radiator, which has a high temperature and radiation resistance, as well as conductivity when excited by an electron beam, is diamond. In addition, diamond has a low Cherenkov radiation threshold (~ 50 keV), and transparency in the UV region of the spectrum (from 225 nm).

In this work, the impurity-defect composition of various samples of synthetic diamonds was studied by spectroscopic methods. Based on these studies, the most suitable samples for registration of Cherenkov radiation were selected. A chamber was made with an induction heating system and registration system of the spectral characteristics of diamond samples radiation. The study of the spectral characteristics radiation was carried out under the influence of an electron beam with an energy of tens-hundreds of keV on the RADAN-220 and NORA pulsers with a sealed-off electron tube IMA3-150E in a wide temperature range.

* The work was supported by the grant from the Russian Science Foundation, project № 22-22-00984

N4-O-037802

PROPERTIES OF ULTRANANOCRYSTALLINE DIAMOND GROWN UNDER DIFFERENT DEPOSITION CONDITIONS*

A.S. MITULINSKY[1], *S.A. LINNIK*[1], *S.P. ZENKIN*[1], *A.V. GAYDAYCHUK*[1]

[1]*Tomsk Polytechnic University, Tomsk, Russia*

Diamond films have many industrial applications due to the combination of unique physical and chemical properties. One important concern of diamond films deposition is achieving a good adhesion to the substrate, which depends on residual stresses in the film after deposition. Other important concerns of deposition are achieving good mechanical properties comparable with a single-crystal diamond, as well as fine structure and surface parameters. Ultrananocrystalline diamond (UNCD) films have a grain size in the range of 5–10 nm and smooth surface in comparison with micro- and nanocrystalline diamond films.

We synthesized UNCD films on Si substrates by hot filament chemical vapor deposition method with different methane concentrations (up to 24 vol. %) in the gas mixture and the deposition pressure at 20 Torr. To characterize obtained films we used Raman spectroscopy, XRD analysis, profilometer measurements, AFM to estimate surface roughness, nanoindentation tests were performed to obtain hardness and Young's modulus.

Figure 1 shows results of nanoindentation test and residual stress estimation.

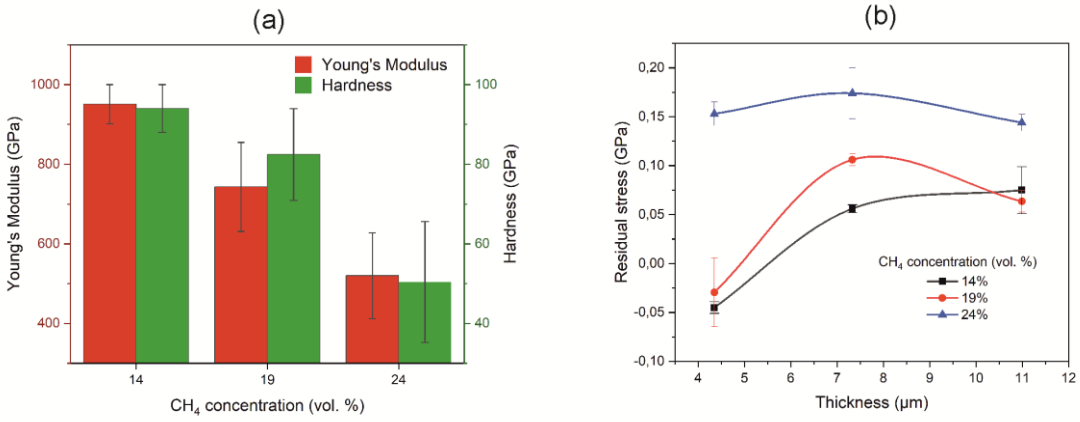

Fig.1. Data for (a) hardness and Young's modulus, and (b) residual stress.

Results from fig. 1. (a) shows that with increase in the methane concentration hardness and Young's modulus decrease. Young's modulus of a material correlates with a concentration of defects in it [1], and in this case grain boundary content acts as a defects. As can be seen from fig. 1 (b) with increase in the methane concentration, tensile stress increases. This is due to increase in non-diamond phase and grain boundary content, because accordingly to [2] increase in defect concentration leads to rise in tension stress.

This research is planned to be one in the series of works devoted to application of UNCD coatings for cutting tools.

REFERENCES

[1] K. K. Phani, "Elastic-constant-porosity relations for polycristalline thoria," Journal of Materials Science Letters. vol. 5, no. 7, pp. 747-70, July 1986.

[2] J. G. Kim, J. Yu, "Measurement of residual stress in diamond films obtained using chemical vapor deposition," Japanese Journal of Applied Physics, vol. 37, no. 7, pp. L890-893, July 1998.

* The work was supported by the grant of the Russian Science Foundation (project no. 21-79-10004). The CVD growth equipment was created with the support by Tomsk Polytechnic University development program.

N4-O-037903

LIGHT-INDUCED OPTICAL EFFECTS ON PHOSPHORUS AND BORON DOPED DIAMONDS*

K.N. BOLDYREV[1,*], YU.YU. DIHTYAR[1], V.N. DENISOV[2]

[1]Institute of spectroscopy, Russian Academy of Sciences, Troitsk, Moscow, Russia
[2]Technological Institute for Superhard and Novel Carbon Materials, Troitsk, Moscow, Russia

Diamond is a material with many unique properties suitable for the different applications from power electronics to quantum computing. It has an ultra-wide band gap (5.47 eV), high electron and hole mobility, high thermal conductivity, high reflectivity, transparency from RF to UV radiation, and has compelling potential advantages over the most known analogs, such as the narrow-bandgap silicon (Si), in radiation-resistant, high-power, and high-frequency electronics, as well as in deep-UV optoelectronics, synchrotron optics, quantum information, quantum sensing and extreme-environment applications [1]. As well a diamond is an excellent photoconductor, and this property can be used for UV detectors with ultra-high sensitivity [2]. It is known that p-type semiconducting diamond is synthesized by doping boron impurity. Phosphorus and nitrogen are impurities for n-type semiconducting diamond established at this moment. But nitrogen level is too deep in the bandgap for the applications (see figure), so phosphorus donor is the best candidate for the n-type diamond. P-donors in a diamond can be used for quantum computing, spin-to-photon conversion, photonic memory, integrated single-photon sources, and all-optical switches because of the read-in/read-out is in the optical region showing extremely high decoherence time up to hours [3]. Earlier studies of the photoconductivity of the phosphorus-doped diamond, which made it possible to register several electronic transitions near 600 meV [4]. These studies gave hope for the presence of photochromic effects in P-doped diamonds, by analogy with such effects in silicon [5]. In addition, based on such effects, it is possible to create a technique for the optical monitoring of the quality and concentration of doping [5,6].

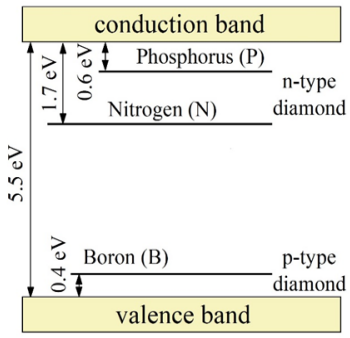

Fig.1. The energies of electroactive shallow impurities in the band gap of diamond.

In this work, we report the detail studies of the light-induced effects of the large-sized HPHT-grown high-quality P-, B- and N-doped single-crystal diamonds by the high-resolution spectroscopy. We found a significant light-induced effect on the electronic transitions of phosphorus and boron. A strong intensity measurement in the absorption spectra is observed under the influence of external optical radiation. In addition, there was a redistribution of intensities in the absorption region of boron and phosphorus, by analogy with the dopant of boron and phosphorus in silicon [5,6]. Based on this effect, a method is proposed for determining the real concentration of boron and phosphorus in a diamond.

REFERENCES

[1] J. Y. Tsao, S. Chowdhury, M. A. Hollis et al., “Ultrawide-Bandgap Semiconductors: Research Opportunities and Challenges”, Adv. Electron. Mater., vol. 4, p. 1600501, 2018.

[2] F. Hochedez, W. Schmutz, Y. Stockman et al., “LYRA, a Solar UV Radiometer on Proba 2”, Adv. Space Res., vol. 37, no. 2, p. 303-312, 2006.

[3] K. Saeedi, S. Simmons, J. Z. Salvail et al., “Room-temperature quantum bit storage exceeding 39 minutes using ionized donors in silicon-28” Science, vol. 342, p. 830, 2013.

[4] K. Haenen, K. Meykens, M. Nesladek et al., “Temperature dependent spectroscopic study of the electronic structure of phosphorus in n-type CVD diamond films”, Dia. and Rel. Mat., vol. 9, p. 952, 2000.

[5] “Test method for low temperature FT-IR analysis of single crystal silicon for III-V impurities”, SEMI MF 1630-0704, 2004.

[6] K.N. Boldyrev, N.Yu. Boldyrev, R.V. Kirillin, “Device for measuring doping impurities of Groups III and V in high-purity silicon by long-wavelength spectroscopy”, Bull. Russ. Acad. Sci. Phys., vol. 77., no. 12, p. 1420, 2013.

* A financial support by the Russian Science Foundation under Grant № 19-72-10132 is acknowledged.

N4-O-045401

FORMATION OF GE-V CENTERS IN VARIOUS CVD DIAMOND MATERIALS: SINGLE-CRYSTALS, POLYCRYSTALLINE FILMS AND NANOPARTICLES

V.S. SEDOV[1], A.K. MARTYANOV[1], A.S. ALTAKHOV[1], D.G. PASTERNAK[1], E.A. DOBRETSOVA[1], K.N. BOLDYREV[2]
[1]Prokhorov General Physics Institute of the Russian Academy of Sciences, Moscow, Russia
[2]Institute of Spectroscopy of the Russian Academy of Sciences, Troitsk, Russia

Germanium-Vacancy (Ge-V) color center in diamond possesses a narrow band photoluminescence (PL) emission in orange spectral range interesting as a single-photon source for quantum optical technologies and thermometry, therefore, the development of methods for controllable doping of diamond with Ge is of high importance for such applications [1,2].

Here, we report on the growth of various Ge-doped diamond materials using microwave plasma chemical vapor deposition (CVD, reactor ARDIS-100, 2.45 GHz) by adding the germane (GeH_4) gas to CH_4-H_2 mixtures. The obtained materials included epitaxial Ge-doped diamond layers, micro- and nanocrystalline diamond films (MCD and NCD, accordingly; see similar research for Si-V centers in [3]), and individual micro- and nanoparticles. The polycrystalline films and separate particles were deposited on Si and AlN substrates, the epitaxial diamond was grown on Ib and IIa HPHT diamond substrates. The results of our investigation of the Ge-V peak intensity at the wavelength of 602 nm in the PL spectra taken both at room and liquid helium (4 K) temperatures will be reported (for Ge-doped thick MCD film – see Fig. 1). The data on diamond morphology, growth rate, Raman spectra and Ge-V PL and optical absorption for all types of samples will be compared.

In summary, the *in situ* doping of diamond with Ge from GeH_4 gas added in microwave plasma is promising to be a convenient way to control Ge-V abundance and PL emission, similarly to the diamond doping from silane [3].

The work was supported by the Russian Science Foundation, Grant № 21-72-10153.

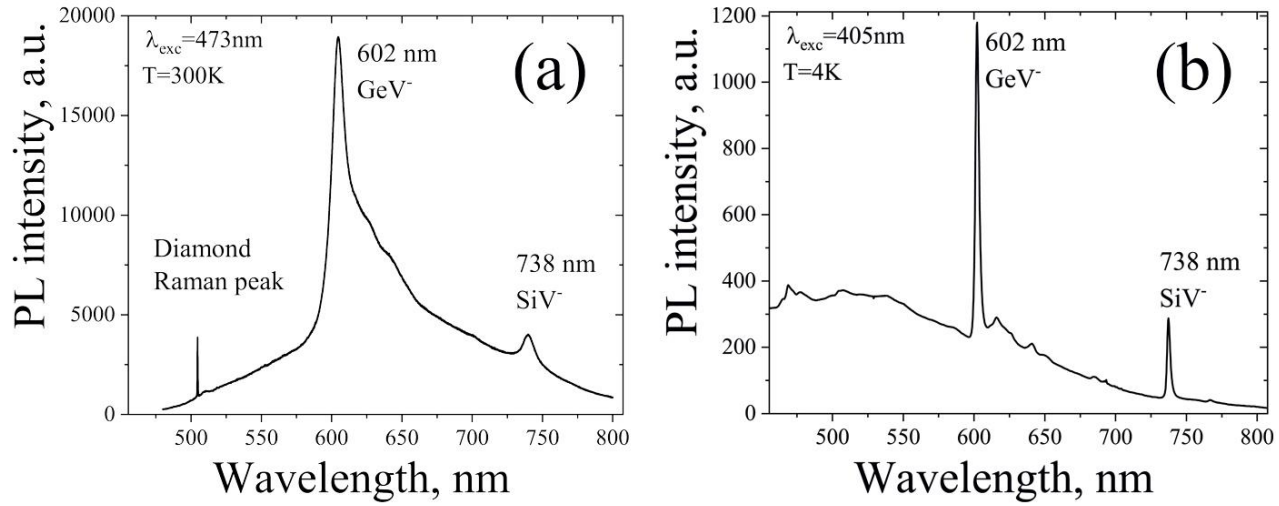

Fig.1. PL spectra of CVD-grown Ge-doped 100 μm thick MCD film at room temperature (a) and at 4 K (b).

REFERENCES

[1] Ralchenko V., et al. Bull. Lebedev Phys. Inst. 42 (2015), 165.
[2] Sedov, V., et al. Diam. Relat. Mater. 90 (2018), 47.
[3] Sedov, V., et al. Diam. Relat. Mater. 56 (2015), 23.

N4-O-045501

X-RAY AS A METHOD FOR MANIPULATION OF COLOR CENTERS CHARGE STATE IN DIAMONDS*

E.S. SEKTAROV[1, 2], V.S. SEDOV[3], K.N. BOLDYREV[1]

[1]Institute of spectroscopy, Russian Academy of Sciences, Troitsk, Moscow, Russia
[2]Department of Physics, National Research University Higher School of Economics, Moscow, Russia
[3]Prokhorov General Physics Institute, Russian Academy of Sciences, Moscow, Russia

Crystals with color centers are widely used in various fields of industry and science. They can be applied to optical quantum memory, quantum sensorics and quantum cryptography. Color centers are a defect in the crystal lattice that absorbs and/or radiates in the wavelength range outside the intrinsic absorption of the crystal.

In this work, we studied the charge states changing of color centers in diamond, such as nitrogen (NV), silicon (SiV), germanium-vacancy (GeV) centers, after their irradiation with X-rays.

The study of color centers in the X-rays was carried out on a Bruker IFS 125HR high-resolution Fourier spectrometer with a cryogenic attachment based on an X-ray tube BSV-30 with a copper anode, with a nominal power of 500 W and a characteristic radiation Cu Kα 8027 eV. The results of the research were absorption spectra obtained at a temperature of 5 K. The absorption method is a well-resolved structure of lines in the spectra, which makes it possible to quantify the concentration of color centers.

The obtained spectra illustrate that after X-ray exposure, the absorption line intensities change at wavelengths of 946 nm (SiV^0), 737 nm (SiV^-), 575 nm (NV^0), 637 nm (NV^-) and 602 nm (GeV^-), corresponding to color centers. In the sample with GeV, the appearance of new lines was observed, which can relate to GeV^0 and/or GeV^+ centers. A change in the SiV and NV centers was noted, the increase in the concentration of SiV^0 is proportional to the decrease in SiV^-. A more complex interaction is observed between NV^0 and NV^- because other charge states such as NV^+, NV^{2+} or unknown states may be involved in the process as the appearance of new lines after irradiation was found.

For samples with NV and SiV, changes in defect concentrations (x) were calculated using formula (1) from [1]. Calibration coefficients k_{zpl} are given in [1] for SiV and [2] for NV, the integral intensity I_{zpl} of absorption lines was calculated using the OPUS software.

$$I_{zpl} = k_{zpl} \cdot x\,, \tag{1}$$

The result of research demonstrates that X-rays radiation can control the charge states of color centers in diamonds.

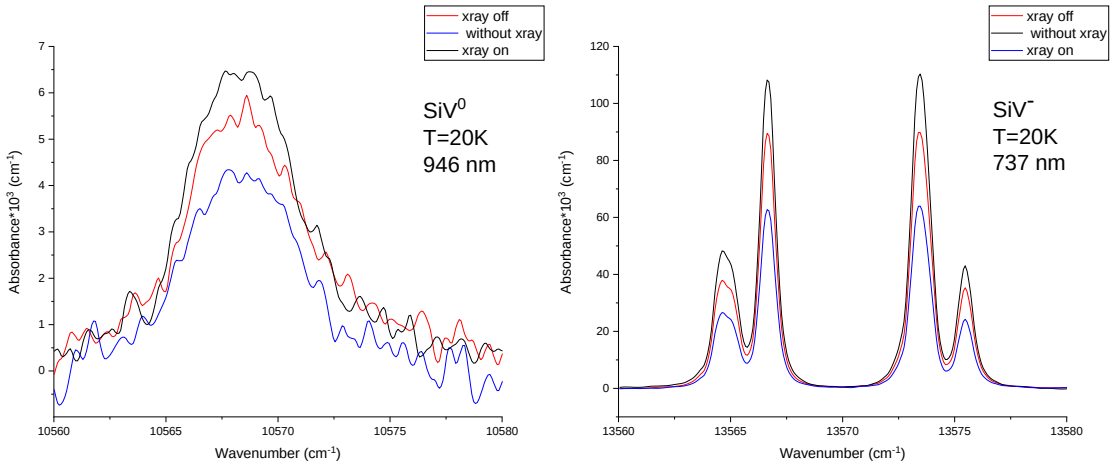

Fig.1. The changing of SiV^0 and SiV^- absorption spectra by X-Ray radiation.

REFERENCES

[1] U. D'Haenens-Johansson, A. Edmonds, M, Newton, J. Goss, P. Briddon, J. Baker, P. Martineau, R. Khan, D. Twitchen, S. Williams, "EPR of a defect in CVD diamond involving both silicon and hydrogen that shows preferential alignment," Phys. Rev. B., vol. 82, no. 15, October 2010.

[2] G. Davies, "Current problems in diamond: towards a quantitative understanding," Physic: Condensa. Matter, vol. 273, pp. 15–23, December 1999.

* The work was supported by the Russian Science Foundation (grant no. 19-72-10132).

N4-O-048303

EROSIONS MECHANISMS OF DIAMOND-LIKE CARBON COATINGS ON POLYIMIDE AND SILICON OXIDE SUBSTRATES BY INFLUENCE OF A PULSED GAS DISCHARGE

I.A. ZUR[1], *Y.E. SHMANAY*[1], *J.A. FEDOTOVA*[1], *G.E. REMNEV*[2], *S.A. MOVCHAN*[3]

[1]*Institute for Nuclear Problems of Belarusian State University, Minsk, Belarus*
[2]*Tomsk Polytechnic University, Tomsk, Russian Federation*
[3] *Joint Institute for Nuclear Research, Dubna, Russian Federation*

Progress in modern physics of elementary particles is largely due to the level of experimental capabilities of detectors. One of the main problems of gas-discharge detectors is the development of self-sustaining gas discharges. The purpose of this research is to determine the most probable mechanism of erosion of a diamond-like coating (DLC) of a flat anode by influence of a pulsed discharge in an $Ar_{90}(CO_2)_{10}$ gas.

The gas discharge was created by a pulsed voltage source with an output power of 0.8 MW at atmospheric pressure. Samples of two types were used: 1 – DLC_{pi} (polyimide substrate) with a thickness of 200 nm and 2 – DLC_{Si} (silicon substrate) with a thickness of 166 nm.

For DLC_{Si} samples was observed a through gas discharge with rounded damage of the coating (Fig.1a). For DLC_{pi} samples was observed a barrier gas discharge along the film-gas interface with oblong-shaped damage to the coating (Fig.1b).

Heating and subsequent erosion of the DLC film are caused by the radiation of the discharge plasma channel in the first case and ohmic heating due to an electron current in the second case. It has been established, that the main contribution to the erosion of the DLC film by influence of discharge is made by the peeling of the film from the substrate due to different expansion coefficients, however, such alternative mechanisms as a thermoelastic wave due to the heating of the plasma channel, sputtering of film atoms by gas ions, and sublimation of the coating were also considered.

The proposed mathematical model of erosion of a DLC coating under the influence of a barrier gas discharge is based on the non-stationary equations of deformation and thermal conductivity for a solid body was solved using the COMSOL Multiphysics package and predicts thermal stresses in the sample, induced by discharges of different power. Distribution of thermal stresses at different moments of time along the interface film and substrate is given on Fig.2.

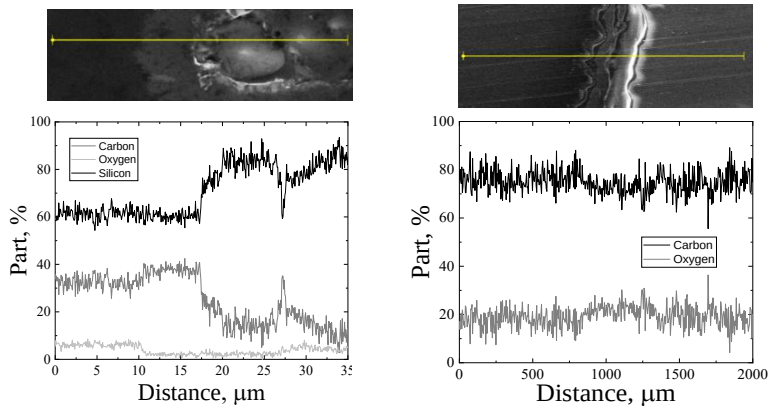

a) b)

Fig.1. Scanning electron microscopy (SEM) images with distributions of chemical elements along the scan line in the erosion zone after exposure to the plasma channel on DLC coatings on Pi (a) and Si/SiO_2 (b) substrates

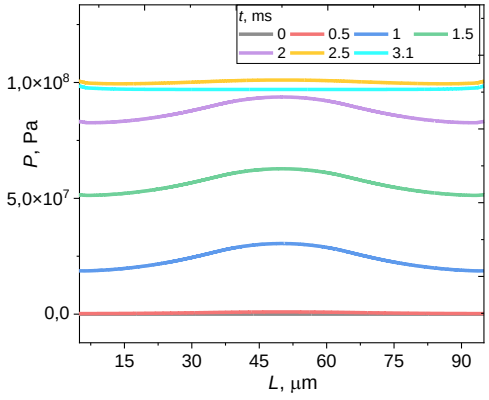

Fig.2. Distribution of thermal stresses at different moments of time along the interface between the film and the Pi substrate

Thus, it has been established that the main mechanism of erosion of a diamond-like coating by the influence of a pulsed barrier discharge is the peeling of the film from the substrate, and a numerical model has also been proposed that predicts the thermal stresses of the coating at specified discharge parameters.

The authors of the article would like to thank the Joint Institute for Nuclear Research for financial support. The work was performed under contract №08626319/201142470-74.

N4-O-050901

ATOMIC DEFECTS IN DIAMOND: PATTERNS OF FORMATION AND SUBSEQUENT TRANSFORMATION

VIKTOR VINS

VELMAN Ltd, Novosibirsk, Russian Federation

Representative collections of laboratory-grown (HPHT/CVD) and natural diamonds have been studied. Mechanisms installed:

- Generation and subsequent transformation of primary growth and radiation defects;
- Transformations of intrinsic and impurity structural defects during annealing of diamonds of different genesis in the stability fields of diamond and graphite.

Models for the transformation of atomic defects in the diamond structure are constructed, allowing to obtain promising environments for various ultra high tech applications.

N4-O-950601

EFFECT OF IRRADIATION AND HIGH TEMPERATURE ANNEALING WITHOUT STABILIZING PRESSURE ON THE OPTICAL PROPERTIES OF HPHT SYNTHETIC DIAMONDS

A. YELISSEYEV[1], *V. VINS*[2], *Z. URMANTSEVA*[2]

[1] *V. S. Sobolev Institute of Geology and Mineralogy SB RAS, Novosibirsk 630090 Russia*
[2] *Vellman Ltd, Novosibirsk 630058 Russia*

The most common way to control the state of impurity centers in diamonds for a certain high-tech application is ionizing irradiation followed by high-temperature annealing. Annealing at high pressure is usually used to prevent graphitization. But recently, much attention has been paid to annealing at normal (atmospheric) pressure, which reduces the risk of crystal destruction and simplifies (reduces the cost) of the equipment used.

The HPHT synthetic diamonds with nitrogen concentration ~300 ppm were grown in the Fe-Ni-C system. A 0.4 mm thick plate containing colorless area (octahedral sector, type Ia+Ib, with dominant nitrogen A-centers) and yellow areas (cubic sectors, type Ib, C-centers) was cut and polished. This plate was irradiated with fast 3 MeV electrons with dose up to 10^{18} e^-/cm^2 and heated at different temperatures (600, 900, 1200, 1500 and 1800°C) without stabilizing pressure. The changes in optical properties occurring during such processing were studied in detail using optical (absorption and luminescence) spectroscopy including absorption Fourier spectroscopy in the mid-IR. Attention was paid both to spatial distribution (mapping) and spectroscopic features.

It is shown that the color of the crystal at different stages is determined by vacancies, nitrogen (Si) and nitrogen-vacancy centers (NV, N_2V) in different charge states. The conditions of formation and the limits of stability of these defects during annealing are determined. The state of these defects, as well as of nickel and nitrogen-nickel centers, was monitored by photoluminescence (PL) spectra. The obtained data are compared with the available information on the HPHT annealing.

N4-P-011901

CATHODOLUMINESCENCE OF DIAMONDS WITH DIFFERENT IMPURITY-DEFECTIVE COMPOSITION*

D.A. PERESEDOVA[1], *V.S. RIPENKO*[1,2]

[1]*National research Tomsk state university, Tomsk, Russia*
[2]*Institute of high current electronics SB RAS, Tomsk, Russia*

Diamond is a promising semiconductor, so at the moment it is used in such area as medicine, construction, optics and electrical engineering [1].

Paper deals with the study of cathodoluminescence of impurity-defect centers in diamond. The samples were irradiated using electron beam generated by NORA type accelerator. At a short treatment time, this type of radiation is an example of nondestructive inspection technique of crystal structure perfection.

In this work, five samples of diamonds synthesized by the chemical vapor deposition (CVD) and high pressure, high temperature (HPHT) methods with different impurity defect compositions were used to study their cathodoluminescence. We registered spectra of samples cathodoluminescence in the temperature range from 72 K to 500 K, using optical spectrometers Ocean Optics HR2000 and HR4000, in the spectral range 200-1100 nm and 200-300 nm, respectively. For example, Fig. 1 shows the spectra of diamond at different temperatures.

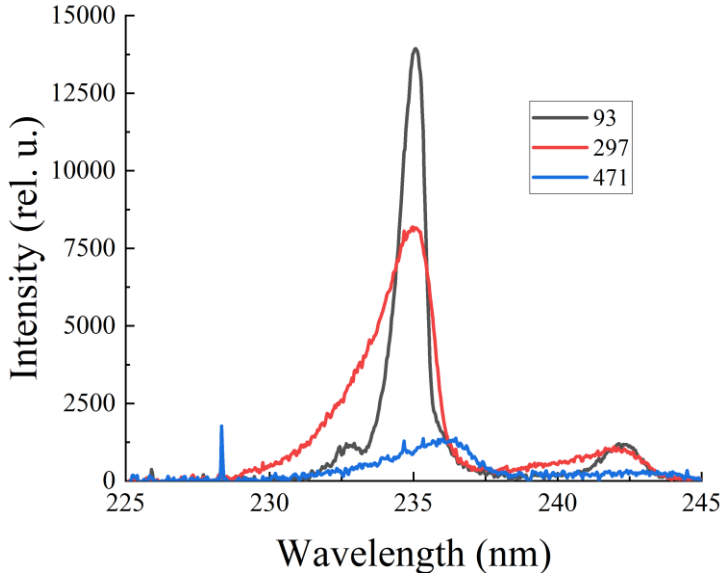

Fig. 1. Exciton cathodoluminescence spectra of pure (N<10 ppm) diamond at different temperatures.

The spectra of cathodoluminescence can be used to estimate not only quality of the crystal, but also the impurity-defective composition of test sample.

References

[1] R.A. Khmelnicky, N.Kh. Talipov, G.V. Chucheva, Synthetic diamond for electronics and optics. Izdatelstvo ICAR, 2017.

* The study was carried out on the state order of the Ministry of Science and Higher Education of the Russian Federation, project N◦ 0721-2020-0048.

N4-P-012901

CATHODOLUMINESCENCE AND RADIATION OF VAVILOV-CHERENKOV IN DIAMOND UNDER THE ACTION OF AN ELECTRON BEAM WITH AN ENERGY UP TO 300 KEV*

A.A. KRYLOV[1,2], *A.G. BURACHENKO*[1,2]

[1]*Institute of high current electronics SB RAS, Tomsk, Russia*
[2]*National research Tomsk state university, Tomsk, Russia*

Various detectors are used to register high-energy charged particles, among which a detector operating on the basis of the Cherenkov effect can be distinguished [1, 2]. Unlike other types of detectors, Cherenkov detectors (CD) have a number of advantages and are widely used in such fields of science and technology as high energy physics, astrophysics and nuclear physics. As a rule, CD is used to register charged particles, in particular electrons, with an energy of tens to hundreds of MeV and higher. At such electron energies, the luminescence level of the medium (radiator) in which the Cherenkov radiation (CR) occurs is small, and in most cases it can be ignored. However, there are areas of CD application where it is necessary to register electron fluxes with an energy of tens to hundreds of keV, for example, in controlled thermonuclear fusion installations of the tokamak type. It is also known that high temperatures are reached during the operation of the tokamak, which imposes restrictions on the choice of CD radiator material. One of the promising materials of the CD radiator used in tokamaks, which has high temperature and radiation resistance, is diamond. In addition, the diamond has a relatively low threshold energy of the occurrence of the CR ~ 50 keV due to the high refractive index (n = 2.42), as well as transparency in the UV region of the spectrum, where the intensity of the CR is maximum. However, when exposed to an electron beam with an energy of tens to hundreds of keV, cathodoluminescence (CL) may occur in the radiator material in addition to the CR which will distort the signal of the Cherenkov detector. Therefore, to register electron beams with an energy of tens to hundreds of keV, it is important to know the contribution of CL to the luminescence spectrum of the CD radiator material.

The aim of the work is to study the spectral characteristics of the radiation of diamond samples under the action of an electron beam with an energy of tens to hundreds of keV (up to 300 keV).

The excitation of the radiation of various diamond samples was carried out using a NORA generator with a soldered IMA3-150E electron tube. The energy spectrum of the electron beam for this generator was in the range of 30-300 keV.

The spectral characteristics of the luminescence of various diamond samples, as well as the impurity-defect composition of these samples were studied by Raman spectroscopy. As a result of these studies, diamond samples were selected that are most suitable for the registration of CR. The calculated CR spectra were compared with the obtained experimental luminescence spectra of diamond samples under the action of an electron beam with an energy of up to 300 keV.

It is shown that, when registering an CR in a diamond, it is necessary to take into account the contribution of CL to the signal of the Cherenkov detector when excited by an electron beam with an energy of up to 300 keV.

REFERENCES

[1] J. V. Jelly, Cherenkov radiation and its application, London: Pergamon Press, 1960.

[2] Bolotovskii B. M., “Vavilov–Cherenkov radiation: its discovery and application”, Physics-Uspekhi, vol. 55, no. 11, pp. 1099, 2009

* The work was supported by the grant from the Russian Science Foundation, project № 22-22-00984..

ABSORPTION SPECTRA OF SINTHETIC DIAMONDS IIA TYPE IN THE TEMPERATURE RANGE FROM 12K TO 460K *

A. S. POPOVA[1], *V. S. RIPENKO*[1,2]

[1]*National Research Tomsk State University, Tomsk, Russia*
[2]*Institute of High-Current Electronics SB RAS, Tomsk, Russia*

Paper is devoted to the calculation of synthetic HPHT diamonds absorption spectra obtained at temperatures from 12 to 460 K. Variouse methods for determining the band gap for synthetic samples at a temperature of 12 K are also considered. The methods discussed in this paper allow us to more accurately determine the band gap of diamonds.

We used 8 pure HPHT diamonds with concentration of N<10 ppm in our experiments. The transmission spectra of the samples were recorded on a helium cryostat at temperatures from 12 to 460 K by using optical spectrometer HR 4000 in spectral range 200-300 nm, and then the absorption values were calculated using following formula:

$$T(\lambda) = \frac{(1 - r(\lambda))^2 \cdot e^{-\alpha(\lambda)d}}{1 - r(\lambda)^2 \cdot e^{-2\alpha(\lambda)d}}, \quad (1)$$

where T(λ) is the transmission coefficient, r(λ) is the reflection coefficient from one face, and α(λ) is the absorption index. Transmission of samples was obtained from cryostat experiments; reflection coefficient was calculated from [2].

We consider 5 methods [1] for determining the band gap values. Figure 1 shows a graph of the obtained results.

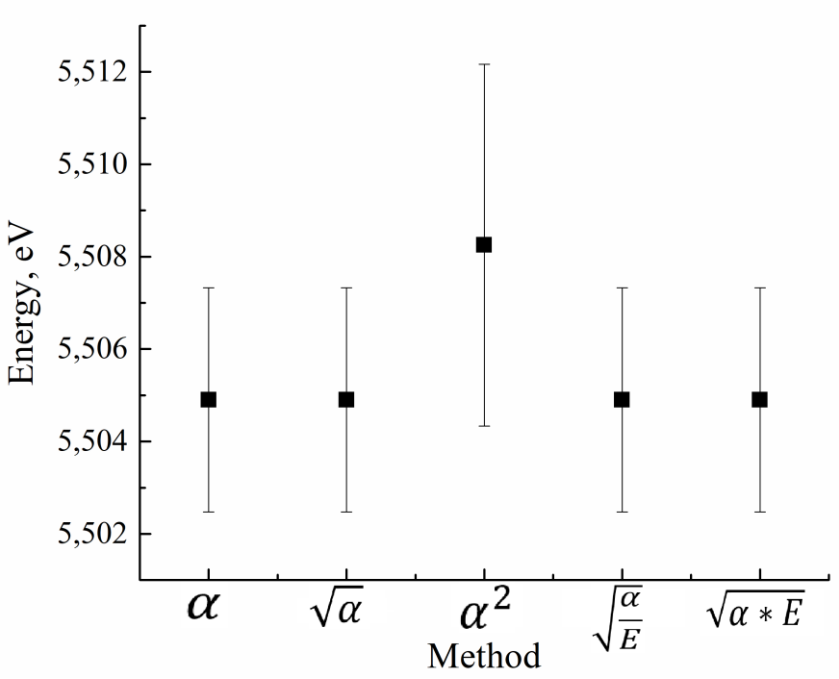

Fig.1. Energy of the band gap determined by various methods

The absorption spectra of pure diamonds (N<10 ppm) are obtained in the temperature range from 12K to 460K, and the band gap of such diamonds is determined to be 5.505 eV.

REFERENCES

[1] A.R. Zanatta "Revisiting the optical bandgap of semiconductors and the proposal of a unified methodology to its determination," Scientific Reports, vol 9, 11225, 2019.
[2] N.V. Novikova, Fizicheckie svoystva almaza: Spravochnik. Kiev: Naukova dumka, 1987.

* The study was carried out on the state order of the Ministry of Science and Higher Education of the Russian Federation, project N◦ 0721-2020-0048.

N4-P-014802

ELECTROLUMINESCENCE IN DIAMOND *

Z.I. BORODULIN [1], M.A. SHULEPOV [1, 2]

[1] National Research Tomsk State University, Tomsk, Russia
[2] Institute of High Current Electronics SB RAS, Tomsk, Russia

With the development of science in the field of quantum technologies, there was a need for a diamond laser. Recently, a diamond laser was invented with pumping from another laser [1]. The effect of electroluminescence will be useful when creating a diamond semiconductor laser and will facilitate its construction.

The paper presents the effect of electroluminescence at a voltage of up to 100 V and a current of up to 0.2 A with a frequency of 1 kHz. The experiment was carried out in geometry - the point is a plane. A negative charge was applied to the flat electrode and a positive charge was applied to the tip. Electroluminescence depends on the number of defects in the diamond structure. Since diamonds have sectoriality, the number of defects at different points differ. Therefore, electroluminescence does not occur at all points. When contacts come into contact with a diamond, a non-thermal glow occurs (Fig.1). Electroluminescence spectra were also taken.

Fig.1. Electroluminescence in diamond.

REFERENCES

[1] Savvin, A., Dormidonov, A., Smetanina, E. et al. NV– diamond laser. Nat Commun 12,7118, 2021. https://doi.org/10.1038/s41467-021-27470-7

* The study was carried out on the state order of the Ministry of Science and Higher Education of the Russian Federation, project No 072120200048.

TEMPERATURE DEPENDENCES OF ABSORPTION SPECTRA IN DIAMOND *

O.I. LYGA[1], *M.A. SHULEPOV*[1,2]

[1] *National Research Tomsk State University, Tomsk, Russia*
[2] *Institute of High Current Electronics, Tomsk, Russia*

Today, presence of diamonds as the main element in computing technologies and space industry plays an important role. In this regard, an urgent task is to create diamonds with identical properties. In this paper, we investigated changes of absorption spectra from temperature. The sample was placed in a vacuum chamber of cryostat on a substrate, which was cooled to 12 K and then heated to 470 K in 10 K increments.

When the temperature of the diamond changed, transmission spectra were recorded. Absorption spectra were calculated from the transmission spectra according to formula (1), and the temperature dependences of SiV-center phonon wing change were determined [1].

$$\alpha(E) = +\frac{1}{d}\ln\left[\frac{(1-R)^2}{2T} + \sqrt{\frac{(1-R)^4}{4T^2} + R^2}\right], \quad (1)$$

where d - thickness of diamond sample, T - transmission coefficient, R - reflection coefficient.

Figure 1 shows the absorption spectra of a diamond sample with SiV-centers at temperatures of 12 K, 300 K, 470 K, calculated by formula (1).

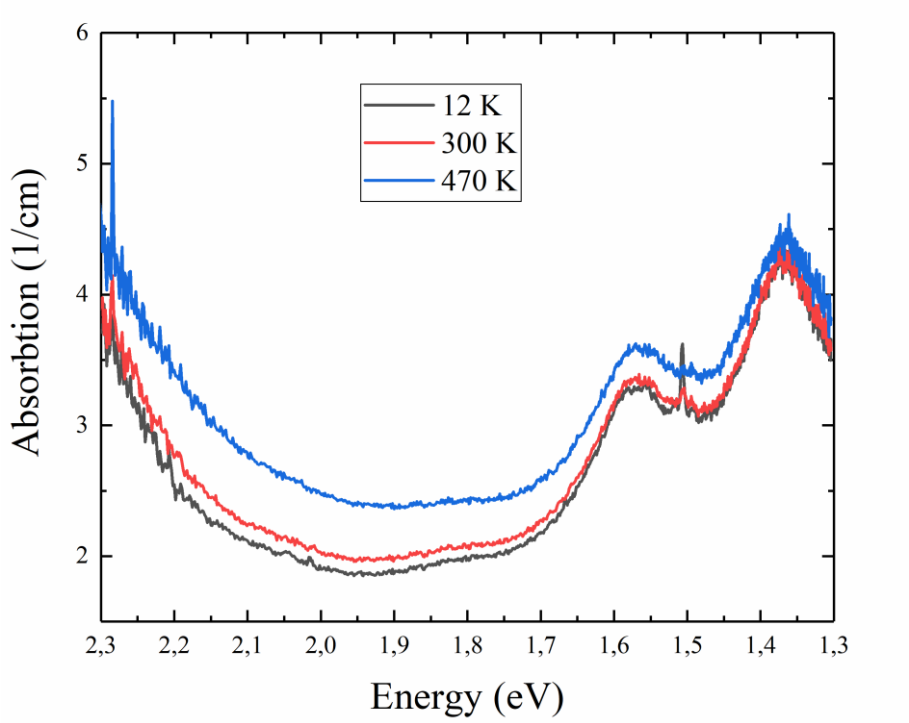

Fig.1. Absorption spectra of a diamond sample with SiV-centers at temperatures of 12 K, 300 K, 470 K.

REFERENCES

[1] A. R. Zanatta, “Revisiting the optical bandgap of semiconductors and the proposal of a unified methodology to its determination, ” Scientific Reports, vol. 9, 11225, August 2019.

* The study was carried out on the state order of the Ministry of Science and Higher Education of the Russian Federation, project No 072120200048.

N4-P-022002

NV^- CENTER EMULATION IN AN EXTERNAL MAGNETIC FIELD

A.V.KOZOREZ[1,3], *E.I. LIPATOV*[1,2]

[1]*Institute of High Current Electronics, Tomsk, Russian Federation*
[2]*Tomsk State University, Tomsk, Russian Federation*
[3]*Tomsk State Pedagogical University, Tomsk, Russian Federation*

An NV center is an impurity-defect complex in diamond, the electronic levels of which experience a fine splitting into spin states, which is caused by different mutual orientations of their half-integer spins. When a tetravalent carbon atom is replaced by pentavalent nitrogen, an additional electron appears in the lattice, and when a neighboring vacancy is formed, four more electrons are released. So, three valence electrons of the nitrogen atom are covalently bonded to nearby carbon atoms, two to the vacancy. Often these five electrons attached to the center are joined by a sixth electron from another nitrogen atom. Thus, the center can be either neutral or negatively charged. It should be noted that the paramagnetic ground state of a center with a strong electron spin polarization is inherent only in the NV^- form. The energy of the zero energy sublevel turns out to be less than the energies of sublevels -1 and 1 by 2.87 GHz. [1].

In total, there are 4 bonds between the vacancy and neighboring atoms (including a nitrogen one) located at an angle of 109.5° relative to each other [2]. Having the magnitude of the signal of optically detected magnetic resonance (ODMR), it is possible to reconstruct the vector of the external magnetic field, taking into account its projection angle on the bonds with the vacancy [3].

The work is devoted to emulating the correlation of a projection of magnetic field vector on axes of nitrogen-vacancy center in diamond lattice with frequencies of optically detected magnetic resonance (ODMR).

REFERENCES

[1] Tsukanov, A.V. “NV centers in diamond. Part I: general information, manufacturing technology, structure of the animal” / A.V. Tsukanov // Microelectronics. - 2012. - T. 41. - No. 2. - S. 104-119.

[2] E.P. Novokreshchenova, “Introduction to Crystal Chemistry of Semiconductors: Textbook”, Voronezh: FGBOU VPO "Voronezh State Technical University", 2012.

[3] Neumann, P. “Excited-state spectroscopy of single NV defects in diamond using optically detected magnetic resonance” // P. Neumann, R. Kolesov , V. Jacques, J. Beck, J. Tisler, A. Batalov, L. Rogers, N.B. Manson, G. Balasubramanian, F. Jelezko, J. Wrachtrup // New J. Phys. - 2009. - V. 11. - P. 013017.

N4-P-032302

PROCESS SIMULATION FORMATION OF ISOTROPIC SOLUTION OF CARBON NANOTUBES IN POLYMERS

M.N. KOLCHEVSKAY[1], *F.F. KOMAROV*[1]

[1]*A.N.Sevchenko Institute of Applied Physical Problems of Belarusian State University, Minsk, Belarus*

The use of carbon nanotubes (CNTs) as additives to the polymer matrix to create new functional composite materials is relevant. The potential for using CNTs as a builder is limited by the difficulties associated with uneven distribution of entangled CNTs during processing and poor interfacial interaction between CNTs and the polymer matrix. The nature of the uneven distribution problem for CNTs is different from that of other fillers such as spherical particles and carbon fibers because CNTs have a high aspect ratio (>1000) and therefore an extremely large surface area. In addition, commercialized CNTs are supplied in highly entangled structures, leading to dispersion difficulties.

The program "NanTu" has been developed to calculate the distribution of CNTs by linear dimensions in a polymer matrix depending on the intensity and duration of mechanical and ultrasonic mixing. The program sets the probability of destruction of CNTs depending on the length of the nanotube. The initial data for the program is the size distribution function of CNTs. The output of the program is the distribution function of CNTs from the processing time. The developed program is used to evaluate the behavior of CNTs in solution during dispersion and optimize the process of preparing composite materials. The obtained results of calculations make it possible to study various mechanisms of CNT destruction.

The algorithm of the program is as follows. At the first stage, the maximum and minimum lengths of nanotubes in solution are set, the length below which the nanotube does not break down, the range of sizes subject to destruction during processing, the discretization step of the nanotube sizes, and the size distribution function of the nanotubes.

At the second stage, the distribution function of nanotubes is calculated for one time interval of solution processing. Successive launches of the program calculate subsequent distribution functions of nanotubes at the following time intervals. The program calculates three types of graphs - the dependence of the mass on the length of nanotubes, the distribution of the probability of destruction and the size distribution of nanotubes (Fig. 1).

Figure shows the results of calculating the distribution of CNTs after three stages of processing 104 identical nanotubes 1 μm long. The resolution probability distribution function has a maximum in the middle of the nanotube. The calculation results show the presence of a maximum in the region of 500 nm, which slowly grows with increasing processing steps. This is due to the successive destruction of the initial nanotubes 1 μm long and the increase in the number of nanotubes of other sizes during processing.

The characteristics of composite materials significantly depend on the type and duration of preparation and processing. The developed software makes it possible to set the function of the probability of destruction of nanotubes, which will make it possible to create composite materials with desired properties.

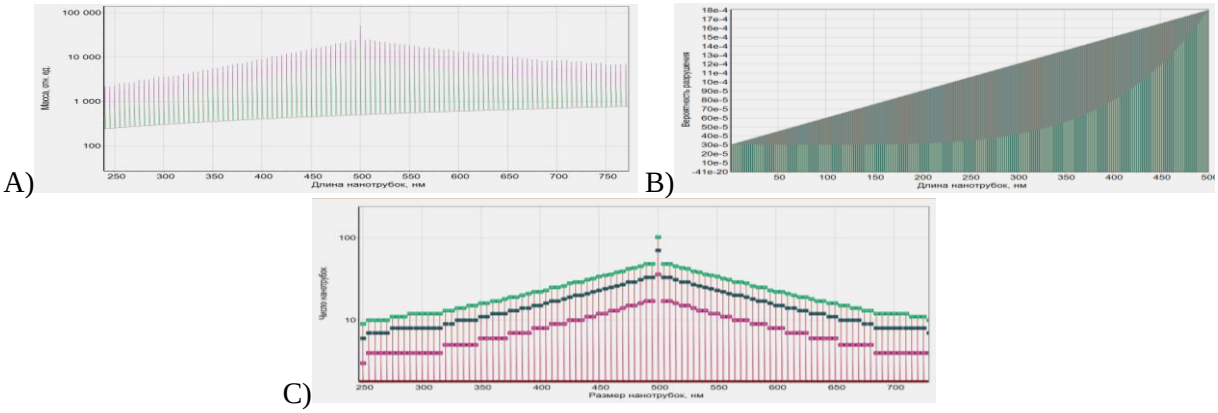

Fig.1. Graphs of the dependence of the mass on the length of nanotubes (A), the distribution of the probability of destruction (B), the size distribution of nanotubes (C).

REFERENCES

[1] Ma P.C., Siddiqui N.A., Marom G., Kim J.K. Dispersion and functionalization of carbon nanotubes for polymer-based nanocomposites: A review // Composite: Part A – 2010. – Vol. 41. P. 1345 – 1367.

N4-P-037904

SILICON AND CARBON ISOTOPE SHIFTS IN SIV^0 COLOR CENTER*

K.N. BOLDYREV[1], V.S. SEDOV[2]

[1]Institute of spectroscopy, Russian Academy of Sciences, Troitsk, Moscow, Russia
[2]Prokhorov General Physics Institute, Russian Academy of Sciences, Moscow, Russia

Studies of color centers, such as silicon vacancy (SiV) center in diamond are currently of high interest in view of applications in photonics, particularly, in quantum information technologies [1]. Changing the isotopes of impurities in crystals is a fruitful method of studying optically active defects. Particularly, analysis of phonon band positions in PL or absorption spectra, when isotope of diamond host lattice is changed, allows a discrimination of local vibration modes (LVM) and phonon modes. Collins et al.[2] observed isotope shifts for 12 different ZPL lines in 99% ^{13}C HPHT diamond and identified LVM for some of the defects.

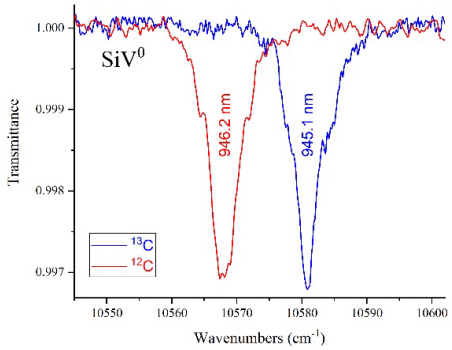

Fig.1. *Absorption spectra of SiV^0 center in diamonds enriched ^{12}C-^{13}C isotopes*

By playing with C and Si isotopes, it's possible to observe a frequency shift in SiV center, which indicates the relation between the lattice structure of SiV ceter and its PL. Such possibility is important for various applications, especially in the field of quantum technologies. Moreover, the use of isotopically pure materials makes it possible to obtain the narrowest lines of SiV color centers [3]. Previously, line shift was investigated for SiV$^-$ color centers in diamonds enriched both in ^{28}Si, ^{29}Si, and ^{30}Si isotopes [3] and in ^{12}C and ^{13}C isotopes [4].

Neutrally charged SiV^0 (946 nm) exhibits excellent spin properties, with spin-lattice relaxation times (T_1) approaching one minute and coherence times (T_2) approaching one second [5], as well as excellent optical properties, with approximately 90% of its emission into the zero-phonon line and near-transform limited optical linewidths [5]. In spite of significant activity on the study of color centers in isotopically modified diamond [6], no data on SiV^0 in ^{13}C diamond, as well enriched by different Si isotopes was reported so far. Here, we report on isotopic shift effects in SiV0 centers for both carbon and silicon atoms. The present work describes the MPCVD-growth of single-crystal diamond layers with engineered isotope compositions: (1) ^{12}C/^{13}C with natural Si content, (b) ^{28}Si/^{29}Si/^{30}Si with natural carbon content. The influence of isotope composition in these series of samples on SiV^0 peak will be reported. Specifically, a large isotopic shift for ^{12}C and ^{13}C diamonds was observed (Fig. 1), while for the change of silicon isotopes almost no significant shift was registered. Potentially, the obtained results will have an impact for the prospects of using SiV^0 centers in diamond as single-photon sources in quantum optical information technologies.

REFERENCES

[1] R. Evans, et al., "Photon-mediated interactions between quantum emitters in a diamond nanocavity", Science, vol. 362, p. 662, 2018.

[2] G. Davies, "Current problems in diamond: towards a quantitative understanding", Physica B: Cond. Matt., vol. 273, p. 15, 1999.

[3] V. Ralchenko, et al., "Monoisotopic Ensembles of Silicon-Vacancy Color Centers with Narrow-Line Luminescence in Homoepitaxial Diamond Layers Grown in H_2–CH_4–$^{[x]}$SiH4 Gas Mixtures (x = 28, 29, 30)", ACS Photonics, vol. 6, no. 1, pp. 66–72, 2019.

[4] V. Sedov, et al., "SiV Color Centers in Si-Doped Isotopically Enriched ^{12}C and ^{13}C CVD Diamonds", Phys. Status Solidi A, vol. 214, no. 11, p. 1700198, 2017.

[5] B. C. Rose, et al., "Observation of an environmentally insensitive solid-state spin defect in diamond", Science, vol. 361, pp. 60–63, 2018.

[6] A. Collins, et al., "Spectroscopic studies of carbon-13 synthetic diamond", J. Phys. C: Solid State Phys., vol. 21, p. 1363, 1988.

* The work was supported by the Russian Science Foundation (grant no. 21-72-10153).

N4-P-052901

DARK CURRENT BEHAVIOUR ANALYSIS FOR AVALANCHE PHOTODIODES *

R.M.H. DOUHAN[1], *A.P. KOKHANENKO*[1], *K.A. LOZOVOY*[1]

[1]*National Research Tomsk State University, Tomsk, Russian Federation*

In the last few decades the technologies to produce high quality semiconductors materials have rabidly improved as the demand on them has increased which led the scientists to pay more attention to these materials and their properties. One of the most advanced photodetectors nowadays is the avalanche photodiodes due to their high performance and their operating conditions [1].

Since the demonstration of molecular beam epitaxy which widened the ability to establish more applications based on semiconductor materials, and after the big success of QDIP for infrared detection, a lot of attention has been paid to the quantum discoveries, this has stimulated the development of avalanche photodiode and its ability for single photon detection [2]. Small-sized and high-performance photonic devices were recently integrated thanks to a monolithic integration approach. Such achievements were obtained with the help of two group-IV materials: silicon (Si) and germanium (Ge) [3]. The use of group-IV materials seems optimal for the future needs of monolithic chip integration [4].

An ideal APD should possess high avalanche gain, low dark current, small bias voltage, and detect high-speed optical signals of up to 100 Gbit/s. Ge-APDs based on metal semiconductor metal (MSM) structure feature high avalanche gain at low bias voltage and are compatible with semiconductor silicon transistor processes. However, such MSM schemes suffer from limited avalanche gain, large dark current, and reduced receiver sensitivity.

For Ge-APDs based on the separate absorption-charge-multiplication (SACM) structure, thanks to the confining carrier multiplication in intrinsic Si, devices benefit from low multiplication noise and impressive gain-bandwidth product (GBP) [5].

In this work, the avalanche photodiode were investigated, some calculations were done and highlighted. The results of these calculations will be shown and analyzed in order to widen our prospective in infrared detection area.

This work discusses the behavior of avalanche photodiodes under certain conditions and emphasizes the dark current characteristics. First, we comprehensively study the opto-electrical properties of avalanche multilayer photodiodes of germanium with silicon quantum dots then we analyze the results with a lot of consideration to the dark current characteristics in several modes and under different conditions and parameters.

REFERENCES

[1] Hongmei Liu, Jianqi Zhang “Performance investigations of quantum dot infrared photodetectors”, Infrared Physics & Technology, vol 55, pp. 320–325, 2012.

[2] Douhan R.M.H., Kokhanenko A.P., Lozovoy K.A., “Performance analysis of multilayer Ge/Si photodetector with quantum dots”, Proceedings of SPIE. vol. 12086. pp. 120861X-1-120861X-7, 2021

[3] zhnin I. I., Lozovoy K. A., Kokhanenko A. P., “Single photon avalanche diode detectors based on group IV materials”, Applied Nanoscience, vol. 12, pp. 253 263, 2022.

[4] Benedikovic D., Virot, L., Aubin, G., “28 Gbps silicon-germanium heterostructure avalanche photodetectors”, Proceedings of SPIE. vol. 11283, pp. 112830Y-10, 2020.

[5] Xiao Hu, Hongguang Zhang, Dingyi Wu, “High-performance germanium avalanche photodetector for 100 Gbit/s photonics receivers”, Optics Letters, vol. 46, pp. 3837-3840, 2021.

* The work was supported by Ministry of Science and Higher Education of the Russian Federation (state task No. 0721-2020-0048).

N4-P-955001

ESIGN AND DEVELOPMENT OF AN OPTICAL FIBER LASER SYSTEM FOR THE CONTROLLABLE PROCESS OF GRAPHENE OXIDE THIN FILMS*

D.L. CHESHEV, A. KAPUSCHAK, E.S. SHEREMET

National research Tomsk Polytechnic University, Tomsk, Russian Federation

Laser processing of thin films is a straightforward and suitable way to achieve new unexplored materials' properties and build various structures. Nowadays, a branch of nanomaterial science is strongly connected with laser processing techniques that include the application of continuous and pulsed lasers [1]. In terms of graphene oxide (GO), the laser processing method allows obtaining unique properties such as turning an insulating GO into conductive reduced GO via a reduction process, caused by local heating. Herein, laser irradiation also provides precise control of the parameters of the GO reduction process such as the power of the laser beam, power density, exposure time, and wavelength. That's why it is important to have an advanced laser system with a set of controllable parameters.

In this work, we design and develop an optical fiber laser system for the controllable process of graphene oxide thin films on a large scale. Our goal is to realize a system with switchable laser modules and an optical fiber delivery system to facilitate laser beam travel from the source to a sample. Moreover, we also aim to integrate a multifunctional detection system to control a set of parameters, such as laser beam profile, laser power, power distribution, and pulse duration.

REFERENCES

[1] Kumar R, Pérez del Pino A, Sahoo S, Singh RK, Tan WK, Kar KK, et al. Laser processing of graphene and related materials for energy storage: State of the art and future prospects. Prog Energy Combust Sci.; vol. 91: p. 100981,

* The work was supported by the Russian Science Foundation grant № 22-12-20027, https://rscf.ru/project/22-12-20027/ and the funding from the Tomsk region administration.

N4-P-955301

BIODEGRADABLE POLYMER/GRAPHENE OXIDE COMPOSITE FOR IN VIVO USE*

E.G. ABYZOVA, E.M. DOGADINA, E.N. BOLBASOV, E.V. PLOTNIKOV, R. RODRIGUEZ, E.S. SHEREMET

National Research Tomsk Polytechnic University, Tomsk, Russian Federation
abyzovaeg@gmail.com

Recently, there has been a growing need for the installation of implants to monitor particular processes, stimulate cell growth or activity, or replace tissues. The use of remote monitoring using biodegradable materials would facilitate the work of doctors, simplify the lives of patients, and also have a beneficial effect on the environment. Remote monitoring would allow monitoring of the tissues around the implant and the condition of the implant itself. Reduced graphene oxide (rGO) is one of the promising carbon materials due to its distinctive properties: low cost, ease of production, and high conductivity. It is proposed to create electronic components based on laser-reduced graphene oxide and biodegradable polymers for monitoring the state of the implant. The study of the properties of rGO on biodegradable polymers made it possible to select laser reduction parameters and select the PLLA polymer for further study. The mechanical stability test suggests the formation of a composite of rGO and polymers. After chemical exposure, a change in conductivity is observed. The samples were shown to be non-toxic for fibroblast, which means they were found to be suitable for subsequent studies. Further, the electrical characterization and approaches to creating the electronic components have been investigated. This work paves the way for the creation of composites based on graphene-like materials and polymers that would be suitable for implantable electronics.

* The work was supported by the Russian Science Foundation grant № 22-12-20027, https://rscf.ru/project/22-12-20027/, and the funding from the Tomsk region administration. Material selection has been performed in the framework of IEC\R2\202134.

C2-P-958101

ION-PLASMA NITRIDING IN THE GLOW DISCHARGE OF PLASTICALLY DEFORMED HSS M2 - EFFECT ON THE WEAR RESISTANCE OF THE SURFACE*

R.K. VAFIN[1], A.V. ASYLBAEV[1], D.V. MAMONTOV[1], I.D. SKLIZKOV[1]

Ufa State Aviation Technical University, Ufa, Russian Federation
[1] alexander.aslb@gmail.com

Ion-plasma nitriding is efficient and widely used technology that improves mechanical and performance properties of various structural materials [1, 2]. However, ion-plasma nitriding is a long process, which reduces its overall efficiency. Therefore, the intensification of ion nitriding seems a relevant task.

It is known that diffusion of atoms in metals is greatly influenced by various structural defects - with the structural defects increase, the diffusion rate in the metal increases [3]. However, along with structural defects, diffusion is also affected by the size of the metal grain: the finer the grain, the higher the diffusion rate [4, 5]. Therefore, to increase the diffusion rate in metals, methods of plastic deformation have recently become increasingly widespread.

This work is devoted to the study of the effect of plastic deformation during ion-plasma nitriding in the glow discharge on the wear resistance of the surface of HSS M2. The results of the study show that plastic deformation of the steel surface before ion-plasma nitriding increases the wear resistance of the surface of HSS M2 by 1.5 times compared to nitriding without magnetic field.

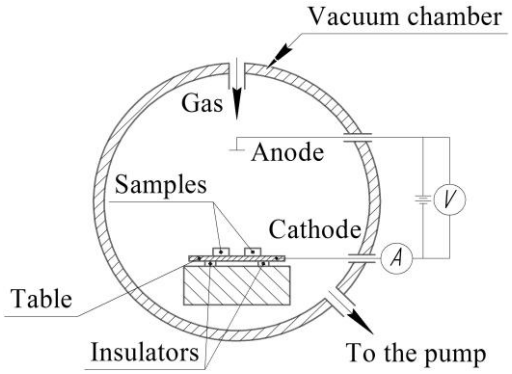

Fig.1. Process schemes ion-plasma nitriding in the glow discharge.

REFERENCES

[1] T. Bell, Y. Sun, “Low-temperature plasma nitriding and carburising of austenitic stainless steels,” Heat Treatment of metals, no. 3, pp. 57-64, 2002.

[2] N. Yasumaru, “Low-temperature ion nitriding of austenitic stainless steels,” Materials Transactions, JIM, vol. 39, no. 10, pp. 1046-1052, 1998.

[3] Bokshtejn B. S., Diffusion in metals, Moscow: Metallurgy, 1978.

[4] Valiev R. Z., Zhilyaev A. P. and Langdon T. G., Bulk nanostructured materials. Fundamental and Applications, Hoboken: Wiley/TMS, 2014.

[5] Valiev R. Z. and Aleksandrov I. V., Nanostrukturnye materialy, poluchennye intensivnoj plasticheskoj deformaciej, España: Universidad Complutense de Madrid, 2000.

* The work was supported by a grant in the form of subsidies in science from the budget of the Republic of Bashkortostan for state support of young scientists - postgraduate students and candidates of science (theme: AT-TM-04-21-GB).

Author Index

Scientific Edition

8th International Congress on Energy Fluxes and Radiation Effects (EFRE 2022)

Abstracts

Published in author's version

Typesetting Shklyaev Valery

Registered in TPU Publishing House
Available at the TPU corporate portal in full accordance with the quality of the given make up page

Publishing House
TOMSK POLYTECHNIC UNIVERSITY